


Jason A. Burdick
Robert L. Mauck
Editors

Biomaterials for Tissue Engineering Applications

A Review of the Past
and Future Trends

 SpringerWienNewYork

 SpringerWienNewYork

Jason A. Burdick • Robert L. Mauck
Editors

Biomaterials for Tissue Engineering Applications

A Review of the Past and Future Trends

SpringerWienNewYork

Prof. Dr. Jason A. Burdick
University of Pennsylvania
Dept. of Bioengineering
210 S. 33rd Street, 240 Skirkanich Hall
19104-6321 Philadelphia
Pennsylvania
USA
burdick2@seas.upenn.edu

Prof. Dr. Robert L. Mauck
University of Pennsylvania
Dept. of Orthopaedic Surgery
McKay Orthopaedic Research Laboratory
36th Street and Hamilton Walk
19104 Philadelphia Pennsylvania
USA
lemauck@mail.med.upenn.edu

This work is subject to copyright.

All rights are reserved, whether the whole or part of the material is concerned, specifically those of translation, reprinting, re-use of illustrations, broadcasting, reproduction by photocopying machines or similar means, and storage in data banks.

Product Liability: The publisher can give no guarantee for all the information contained in this book. The use of registered names, trademarks, etc. in this publication does not imply, even in the absence of a specific statement, that such names are exempt from the relevant protective laws and regulations and therefore free for general use.

© 2011 Springer-Verlag/Wien
Printed in Germany

SpringerWienNewYork is a part of Springer Science+Business Media
springer.at

Cover Illustration: Scanning electron microscopy image of articular chondrocytes interacting with the surface of a fibrous and biodegradable scaffold (courtesy of Dr. Brendon Baker)

Typesetting: SPI, Pondicherry, India

Printed on acid-free and chlorine-free bleached paper
SPIN: 12652570

With 62 Figures

ISBN 978-3-7091-0384-5 e-ISBN 978-3-7091-0385-2
DOI 10.1007/978-3-7091-0385-2
SpringerWienNewYork

Contents

1 Introduction	1
Jason A. Burdick and Robert L. Mauck	
Biomaterials Technologies for Tissue Engineering	
2 Hydrogels in Tissue Engineering	9
Sarah E. Grieshaber, Amit K. Jha, Alexandra J. E. Farran, and Xinqiao Jia	
3 Fibrous Scaffolds for Tissue Engineering	47
Wan-Ju Li and James A. Cooper Jr.	
4 Bioelastomers in Tissue Engineering	75
Zhengwei You and Yadong Wang	
5 Microscale Biomaterials for Tissue Engineering	119
Ian Wheeldon, Javier Fernandez, Hojae Bae, Hirokazu Kaji, and Ali Khademhosseini	
6 Micro and Nanotechnologies for Tissue Engineering	139
Nadeen O. Chahine and Pen-hsiu Grace Chao	
7 Bioceramics in Tissue Engineering	179
Yunzhi Yang, Yunqing Kang, Milan Sen, and Sangwon Park	
8 Natural Materials in Tissue Engineering Applications	209
Elyssa L. Monzack, Karien J. Rodriguez, Chloe M. McCoy, Xiaoxiao Gu, and Kristyn S. Masters	
9 Engineered Polypeptides for Tissue Engineering	243
Wei Shen	

Specific Applications in Tissue Engineering

- | | | |
|-----------|--|-----|
| 10 | Cartilage Engineering: Current Status and Future Trends | 279 |
| | Emily E. Coates and John P. Fisher | |
| 11 | Biomaterials for Regeneration of Tendons and Ligaments | 307 |
| | Taymour M. Hammoudi and Johnna S. Temenoff | |
| 12 | Materials for Bone Graft Substitutes and Osseous
Tissue Regeneration | 343 |
| | Steven B. Nicoll | |
| 13 | Fibrocartilage Tissue Engineering | 363 |
| | Christopher J. Hunter | |
| 14 | Liver Tissue Engineering | 389 |
| | Sihong Wang and Deepak Nagrath | |
| 15 | Cardiac Tissue Engineering | 421 |
| | Devang Odedra, Loraine Chiu, Lewis Reis, Fiona Rask,
Katherine Chiang, and Milica Radisic | |
| 16 | Biomaterials Approaches in Vascular Engineering: a Review of Past
and Future Trends | 457 |
| | Donny Hanjaya-Putra, Maureen Wanjare, and Sharon Gerech | |
| 17 | Neural Tissue Engineering | 489 |
| | Erin Lavik | |
| 18 | Controlling Stem Cells with Biomaterials | 511 |
| | Nivedita Sangaj and Shyni Varghese | |

Concepts in Biomaterial Translation and Product Development

- | | | |
|-----------|--|-----|
| 19 | Translation of New Tissue Engineering Materials to Clinical Application | 541 |
| | Benjamin A. Byers and Dolores Baksh | |
| | About the Editors | 563 |

Contributors

Hojae Bae Department of Medicine, Center for Biomedical Engineering, Brigham and Women's Hospital, Harvard Medical School, Boston, MA 02115, USA; Harvard-MIT Division of Health Sciences and Technology, Massachusetts Institute of Technology, Cambridge, MA 02139, USA

Dolores Baksh Research & Development, Organogenesis Inc., 150 Dan Road, Canton, MA 02021, USA, dbaksh@organo.com

Jason A. Burdick Department of Bioengineering, University of Pennsylvania, 240 Skirkanich Hall, Philadelphia, PA 19104, USA, Burdick2@seas.upenn.edu

Benjamin A. Byers New Product Development, DePuy Mitek a Johnson & Johnson Company, 325 Paramount Drive, Raynham, MA 02356, USA, bbyers@its.jnj.com

Nadeen O. Chahine Biomechanics & Bioengineering Laboratory, Feinstein Institute for Medical Research, North Shore LIJ Health System, 350 Community Drive, Manhasset, NY, 11030, USA, nchahine@nshs.edu

Pen-hsiu Grace Chao Institute of Biomedical Engineering, School of Engineering and School of Medicine, National Taiwan University, 503 Zhanshulou, 1 Section 4 Roosevelt Road, Taipei, Taiwan, pgchao@ntu.edu.tw

Katherine Chiang Department of Chemical Engineering and Applied Chemistry, Institute of Biomaterials and Biomedical Engineering, University of Toronto, Toronto, ON, Canada

Loraine Chiu Department of Chemical Engineering and Applied Chemistry, Institute of Biomaterials and Biomedical Engineering, University of Toronto, Toronto, ON, Canada

Emily E. Coates Fischell Department of Bioengineering, University of Maryland, 3238 Jeong H. Kim Building, College Park, MD 20742, USA

James A. Cooper Jr Department of Biomedical Engineering, Center for Biotechnology and Interdisciplinary Studies, Rensselaer Polytechnic Institute, Room 3139, 110 8th Street, Troy, NY 12180-3590, USA, coopej5@rpi.edu

Alexandra J. E. Farran Department of Materials Science and Engineering, Delaware Biotechnology Institute, University of Delaware, Newark, DE 19716, USA

Javier Fernandez Department of Medicine, Center for Biomedical Engineering, Brigham and Women's Hospital, Harvard Medical School, Boston, MA 02115, USA; Harvard-MIT Division of Health Sciences and Technology, Massachusetts Institute of Technology, Cambridge, MA 02139, USA

John P. Fisher Fischell Department of Bioengineering, University of Maryland, 3238 Jeong H. Kim Building, College Park, MD 20742, USA, jpfisher@umd.edu

Sharon Gerecht Department of Chemical and Biomolecular Engineering, Johns Hopkins Physical Science Oncology Center and Institute for NanoBioTechnology, Johns Hopkins University, Baltimore, MD 21218, USA, gerecht@jhu.edu

Sarah E. Grieshaber Department of Materials Science and Engineering, Delaware Biotechnology Institute, University of Delaware, Newark, DE 19716, USA

Xiaoxiao Gu Department of Biomedical Engineering, University of Wisconsin, Madison, WI 53706, USA

Taymour M. Hammoudi Department of Biomedical Engineering, Georgia Institute of Technology, Emory University School of Medicine, 313 Ferst Drive, Atlanta, GA 30332, USA, thammoudi3@gatech.edu

Donny Hanjaya-Putra Department of Chemical and Biomolecular Engineering, Johns Hopkins Physical Science Oncology Center and Institute for NanoBioTechnology, Johns Hopkins University, Baltimore, MD 21218, USA

Christopher J. Hunter Department of Mechanical & Manufacturing Engineering, Centre for Bioengineering Research & Education, McCaig Institute for Bone & Joint Health, University of Calgary, 2500 University Dr NW, Calgary, AB T2N 1N4, Canada, chunter@ucalgary.ca

Amit K. Jha Department of Materials Science and Engineering, Delaware Biotechnology Institute, University of Delaware, Newark, DE 19716, USA

Xinqiao Jia Department of Materials Science and Engineering, Delaware Biotechnology Institute, University of Delaware, Newark, DE 19716, USA, xjia@udel.edu

Hirokazu Kaji Department of Medicine, Center for Biomedical Engineering, Brigham and Women's Hospital, Harvard Medical School, Boston, MA 02115, USA; Harvard-MIT Division of Health Sciences and Technology, Massachusetts Institute of Technology, Cambridge, MA 02139, USA; Department of Bioengineering and Robotics of Graduate School of Engineering in Tohoku University, Sendai, Japan

Yunqing Kang Houston Biomaterials Research Center, Department of Restorative Dentistry and Biomaterials, The University of Texas Health Science Center at Houston, Houston, TX 77030, USA

Ali Khademhosseini Harvard-Massachusetts Institute of Technology Division of Health Sciences and Technology, Harvard Medical School/Brigham and Women's Hospital, 65 Landsdowne Street, Rm. 265, Cambridge, MA 02139, USA, alik@mit.edu

Erin Lavik Case Western Reserve University, Room 309 Wickenden Building, 10900 Euclid Avenue, Cleveland, OH 44106, USA, Erin.lavik@case.edu

Wan-Ju Li Department of Orthopedics and Rehabilitation, Department of Biomedical Engineering, University of Wisconsin-Madison, 1111 Highland Avenue, WIMR 5051, Madison, WI 53705, USA, li@ortho.wisc.edu

Kristyn S. Masters Department of Biomedical Engineering, University of Wisconsin, 1550 Engineering Drive, #2152, Madison, WI 53706, USA, kmasters@wisc.edu

Robert L. Mauck Departments of Orthopaedic Surgery and Bioengineering, University of Pennsylvania, Philadelphia, PA 19104, USA, lemauck@mail.med.upenn.edu

Chloe M. McCoy Department of Biomedical Engineering, University of Wisconsin, Madison, WI 53706, USA

Elyssa L. Monzack Department of Biomedical Engineering, University of Wisconsin, Madison, WI 53706, USA

Deepak Nagrath Department of Chemical and Biomolecular Engineering, MS-362, Rice University, P.O. Box 1892, Houston, TX 77251-1892, USA, deepak.nagrath@rice.edu

Steven Nicoll Department of Biomedical Engineering, The City College of New York, 160 Convent Avenue, Steinman Hall, T-431, New York, NY 10031, USA, snicoll@ccny.cuny.edu

Devang Odedra Department of Chemical Engineering and Applied Chemistry, Institute of Biomaterials and Biomedical Engineering, University of Toronto, Toronto, ON, Canada

Sangwon Park Department of Prosthodontics, School of Dentistry, Chonnam National University, Gwangju 504-190, South Korea

Milica Radisic Department of Chemical Engineering and Applied Chemistry, Institute of Biomaterials and Biomedical Engineering, University of Toronto, 164 College Street, Room 407, Toronto, ON M5S 3G9, Canada, m.radisic@utoronto.ca

Fiona Rask Department of Chemical Engineering and Applied Chemistry, Institute of Biomaterials and Biomedical Engineering, University of Toronto, Toronto, ON, Canada

Lewis Reis Department of Chemical Engineering and Applied Chemistry, Institute of Biomaterials and Biomedical Engineering, University of Toronto, Toronto, ON, Canada

Karien J. Rodriguez Department of Biomedical Engineering, University of Wisconsin, Madison, WI, 53706, USA

Nivedita Sangaj Department of Bioengineering, University of California, San Diego, 9500 Gilman Drive, La Jolla, CA, 92093, USA, svarghese@ucsd.edu

Milan Sen Department of Orthopedic Surgery, The University of Texas Health Science Center at Houston, Houston, TX, 77030, USA

Wei Shen Department of Biomedical Engineering, University of Minnesota, 7-118 Haselmo Hall, Minneapolis, MN, 55455, USA, Shenx104@umn.edu

Johnna S. Temenoff Department of Biomedical Engineering, Georgia Institute of Technology, Emory University School of Medicine, 313 Ferst Drive, Atlanta, GA, 30332, USA, johnna.temenoff@bme.gatech.edu

Shyni Varghese Department of Bioengineering, University of California, San Diego, 9500 Gilman Drive, La Jolla, CA, 92093, USA, svarghese@ucsd.edu

Sihong Wang Department of Biomedical Engineering, The City College of New York, Steinman Hall, T-434, New York, NY, 10031, USA, shwang@ccny.cuny.edu

Yadong Wang Bioengineering and the McGowan Institute, University of Pittsburgh, 300 Technology Drive, Pittsburgh, PA, 15219, USA, yaw20@pitt.edu

Maureen Wanjare Department of Chemical and Biomolecular Engineering, Johns Hopkins Physical Science Oncology Center and Institute for NanoBioTechnology, Johns Hopkins University, Baltimore, MD, 21218, USA

Ian Wheeldon Department of Medicine, Center for Biomedical Engineering, Brigham and Women's Hospital, Harvard Medical School, Boston, MA, 02115, USA; Harvard-MIT Division of Health Sciences and Technology, Massachusetts Institute of Technology, Cambridge, MA, 02139, USA

Yunzhi Yang Houston Biomaterials Research Center, Department of Restorative Dentistry and Biomaterials, The University of Texas Health Science Center at Houston, Houston, TX, 77030, USA, Yunzhi.yang@uth.tmc.edu

Zhengwei You Bioengineering and the McGowan Institute, University of Pittsburgh, 300 Technology Drive, Pittsburgh, PA, 15219, USA

Jason A. Burdick and Robert L. Mauck

Contents

1.1 Overview and Intent of the Book

When approached to put together this compilation on recent advances on the material component of tissue engineering, we first asked ourselves whether there was a need for another book in this field. Tissue engineering books abound; however, a review of the existing literature soon made clear that no other work exists that focuses specifically on the material aspects of tissue engineering science and the approach that we and others use within our own research. Namely, we operate under the principle that rational material design, directed and informed by native tissue structure and function, will enhance the generation of engineered constructs with functional utility. Moreover, as advances are being made in this arena at an exceedingly rapid pace, it is important to routinely update the field. To address this important need, we asked several emerging experts, who we thought may contribute a fresh perspective on this topic, to contribute reviews on past and current work on a range of materials and the formation of engineered tissues from these materials. Further, we asked that each contributor provide their own opinion on the new directions that the field is taking, so as to identify the emerging consensus areas of focus for the future.

This book is divided into three main sections. The first section focuses on a variety of types of materials, including hydrogels, fibrous materials, ceramics, elastomers, micro- and nanotechnology, natural materials, and polypeptides. These topics cover the main types and classes of biomaterials that are being investigated for engineering a range of tissues. The chapters provide basic background on each material type, as well as a review of how these materials have been implemented into tissue engineering constructs and/or products. The second section focuses on the biomaterial component in the engineering of specific

J.A. Burdick (✉)

Department of Bioengineering, University of Pennsylvania, Philadelphia, PA 19104, USA
e-mail: burdick2@seas.upenn.edu

1 tissues such as cartilage, tendon/ligament, bone, fibrocartilage, liver, cardiac muscle, vascular structures, and neural tissues. This section also addresses aspects of how biomaterial design may be utilized to control stem cell fate. Within these chapters, specific criteria in biomaterial development are addressed, and materials that have been investigated to engineer the respective tissues are reviewed. The final section addresses the translation of these new tissues to the clinic, and issues that must be considered in this process.

1.2 A Brief Overview of Tissue Engineering

In developing this book, we formulated our own perspective on the progress of the general field of tissue engineering and the direction that this field is taking. To begin, this field was defined nearly 20 years ago, when Langer and Vacanti published a seminal article describing the process of tissue engineering [1], in which biological and engineering principles are harnessed to assemble cells, biomolecules, and scaffolding to repair or grow new tissues. At the time, the concept of de novo creation of tissues in the laboratory may have sounded far-fetched or perhaps Frankenstein-like. However, landmark studies soon followed; for example, the growth of a human-shaped ear on the back of a mouse excited and directed a new way of thinking towards the regeneration of entire tissues [2]. Rapidly, new synthetic materials were generated and fabrication processes developed to support the production of these neo-tissues.

Despite this excitement and activity, and significant public and private investment, clinical advances in tissue engineering have moved much slower than many had envisioned [3, 4]. Regardless, some recent clinical successes have been reported; engineered skin for burn victims and treatment of diabetic ulcers [5], implantation of an engineered trachea in a woman with a failing airway [6], cartilage therapies used clinically or in clinical trials [7], and implantation of engineered bladders in patients with spina bifida [8]. It is interesting to note that, despite our intense focus on developing synthetic scaffolds, and except for a composite system in the bladder device, these successes have all been realized using scaffolds derived from native tissues, either collagen alone or decellularized extracellular matrix (ECM).

Natural materials, by their very composition, and with a millennia of fine-tuning, possess precisely those features that are necessary to enable robust tissue growth and remodeling. Indeed, properties such as adhesion, catabolism, and growth factor retention, may underlie some of the recent success in their clinical application. The processing of natural matrices typically involves removal of antigenicity and decellularization, essentially stripping the native tissue of some of the complexity to produce a base material that will not provoke an adverse response when implanted.

With this in mind, it is important to consider if synthetic materials will actually find utility in tissue engineering approaches. We believe there is a place for these synthetic systems, but that insight from the natural ECM can be applied to advance and direct sophisticated material design. One important area is in cases where tailored mechanics are needed and cannot be met with ECM-derived materials. Also, the engineering of more complex tissues (e.g., myocardium and neural tissues) that exhibit organized heterogeneity and

multiple cell types may not be achieved without added complexity. For these situations, it may be more appropriate to build up a synthetic system with the appropriate user-orchestrated biological signals, rather than breaking down a native tissue into basic biological components.

As a field, biomaterials scientists increasingly appreciate the complexity of the underlying biology of tissue formation and healing, and are considering how a range of cues from the local microenvironment (including mechanics, topography, and chemistry), and their sequence of presentation, may influence the decision of a cell to expand, migrate, or differentiate [9]. It is clear (as evidenced from many chapters within this work) that scaffold design is increasing in complexity and becoming “smarter” with this knowledge. Traditionally, synthetic scaffolds were designed as a structural component with features of degradation times, stability, and toxicity considered. However, the emerging trend is to incorporate some biological sophistication into scaffolds, introduce those cues that are necessary and sufficient to promote regeneration, and better understand how these features engender more active and instructive scaffolds [10]. Advances in chemical and fabrication methodologies have provided additional tunability to scaffold design, such as multiple degradation mechanisms under independent control [11], incorporating features that would not be possible in native tissue matrices.

One example of this is with hydrogels (water-swollen polymer networks) that maintain cells in an important 3-dimensional context and may possess tissue-like properties [12]. The evolution of hydrogels has transitioned from purely synthetic materials to covalent appending of appropriate signals through advanced chemistry or through hybrid synthetic/natural systems. For instance, hydrogels based on the natural ECM, including with hyaluronic acid, are being used to direct the fate of stem cells through their chemistry [13]. Several groups have also modulated mesenchymal stem cell phenotypic transitions by incorporating biologic moieties into otherwise inert hydrogel backbones [14]. Engineered polypeptide and protein hydrogels introduce another level of complexity and can be designed with a range of properties and signals [15].

A recent report demonstrated new photolabile chemistry within hydrogels that can be used to impart control over material properties and biological cues in space (with masks or lasers) or in time (with intermittent light exposure) [16]. The power of this technology is the precision that is possible using light for material manipulation. Beyond molecular interactions, the ability of a scaffold to guide direction-dependent tissue formation may be critical. Engelmayr et al. [17] designed scaffolds with unique accordion-like structures, to replicate key anisotropic features of the native myocardium. Others have designed synthetic nanofiber-based scaffolds that direct tissue anisotropy [18], have dynamic material and degradation profiles [19], and recapitulate complex native tissue hierarchies [20].

These examples illustrate the increasing sophistication in scaffold design, particularly when compared to early tissue engineering scaffolds. These new materials have significant potential for regenerative therapies and are already providing insight into how cells interact with their microenvironment and how native tissues form and function. Their successful application may depend on the degree to which they are able to recapitulate key features of native tissue, while preserving their material flexibility such that modification can further optimize tissue growth. Beyond their efficacy, it is also important to consider therapies that will actually be used by surgeons, whose costs will be considered worthwhile, and that are

1 clinically superior to current alternatives. Additional hurdles for synthetics relate to intellectual property and regulatory considerations, the first of which may limit widespread application of new materials and encourage the development of “better mousetraps” to circumvent prior art, and the second of which will slow the transition of new materials to clinical application. As antibiotic development has advanced from simple anti-microbial sulfa drugs to extensive current options, so too might the development of materials for tissue engineering lead to more desirable and clinically useful therapies. Let’s hope the transition in this case is timely.

1.3 Closing Thoughts

This book represents a careful review of the necessary aspects related to biomaterial design, and reviews past research in the field and new technologies for future implementation. We hope that this book will excite the current and next generation of researchers in this field to further expand the complexity of biomaterials in tissue engineering. We also hope that this work will be a resource for the field, and will further advance tissue engineered products towards clinical realization for the restoration of damaged and diseased tissues and organs.

References

1. Langer R, Vacanti JP. Tissue engineering. *Science* 1993 May 14;260(5110):920–926.
2. Griffith LG, Naughton G. Tissue engineering – current challenges and expanding opportunities. *Science* 2002 Feb 8;295(5557):1009–1014.
3. Lysaght MJ, Hazlehurst AL. Tissue engineering: the end of the beginning. *Tissue Eng* 2004 Jan–Feb;10(1–2):309–320.
4. Lysaght MJ, Jaklenec A, Deweerd E. Great expectations: private sector activity in tissue engineering, regenerative medicine, and stem cell therapeutics. *Tissue Eng Part A* 2008 Feb;14(2):305–315.
5. Khademhosseini A, Vacanti JP, Langer R. Progress in tissue engineering. *Sci Am* 2009 May;300(5):64–71.
6. Macchiarini P, Jungebluth P, Go T, Asnaghi MA, Rees LE, Cogan TA, et al. Clinical transplantation of a tissue-engineered airway. *Lancet* 2008 Dec 13;372(9655):2023–2030.
7. Klein J. Chemistry Repair or replacement – a joint perspective. *Science* 2009 Jan 2;323(5910):47–48.
8. Atala A, Bauer SB, Soker S, Yoo JJ, Retik AB. Tissue-engineered autologous bladders for patients needing cystoplasty. *Lancet* 2006 Apr 15;367(9518):1241–1246.
9. Discher DE, Mooney DJ, Zandstra PW. Growth factors, matrices, and forces combine and control stem cells. *Science* 2009 Jun 26;324(5935):1673–1677.
10. Lutolf MP, Hubbell JA. Synthetic biomaterials as instructive extracellular microenvironments for morphogenesis in tissue engineering. *Nat Biotechnol* 2005 Jan;23(1):47–55.
11. Sahoo S, Chung C, Khetan S, Burdick JA. Hydrolytically degradable hyaluronic acid hydrogels with controlled temporal structures. *Biomacromolecules* 2008 Apr;9(4):1088–1092.

12. Cushing MC, Anseth KS. Materials science. Hydrogel cell cultures. *Science* 2007 May 25;316(5828):1133–1134.
13. Gerecht S, Burdick JA, Ferreira LS, Townsend SA, Langer R, Vunjak-Novakovic G. Hyaluronic acid hydrogel for controlled self-renewal and differentiation of human embryonic stem cells. *Proc Natl Acad Sci U S A* 2007 Jul 3;104(27):11298–11303.
14. Lee HJ, Yu C, Chansakul T, Hwang NS, Varghese S, Yu SM, et al. Enhanced chondrogenesis of mesenchymal stem cells in collagen mimetic peptide-mediated microenvironment. *Tissue Eng Part A* 2008 Nov;14(11):1843–1851.
15. Shen W, Zhang K, Kornfield JA, Tirrell DA. Tuning the erosion rate of artificial protein hydrogels through control of network topology. *Nat Mater* 2006 Feb;5(2):153–158.
16. Kloxin AM, Kasko AM, Salinas CN, Anseth KS. Photodegradable hydrogels for dynamic tuning of physical and chemical properties. *Science* 2009 Apr 3;324(5923):59–63.
17. Engelmayer GC, Jr., Cheng M, Bettinger CJ, Borenstein JT, Langer R, Freed LE. Accordion-like honeycombs for tissue engineering of cardiac anisotropy. *Nat Mater* 2008 Dec;7(12):1003–1010.
18. Li WJ, Mauck RL, Cooper JA, Yuan X, Tuan RS. Engineering controllable anisotropy in electrospun biodegradable nanofibrous scaffolds for musculoskeletal tissue engineering. *J Biomech* 2007;40(8):1686–1693.
19. Baker BM, Nerurkar NL, Burdick JA, Elliott DM, Mauck RL. Fabrication and modeling of dynamic multipolymer nanofibrous scaffolds. *J Biomech Eng* 2009 Oct;131(10):101012.
20. Nerurkar NL, Baker BM, Sen S, Wible EE, Elliott DM, Mauck RL. Nanofibrous biologic laminates replicate the form and function of the annulus fibrosus. *Nat Mater* 2009 Dec;8(12):986–992.

Part I

**Biomaterials Technologies for
Tissue Engineering**

Contents

2.1	Introduction	11
2.2	Basic Concepts	12
2.3	Hydrogel Synthesis	12
2.3.1	Chemical Crosslinking	12
2.3.2	Physical Crosslinking	21
2.4	Modulating Hydrogel Microstructure and Mechanical Properties	26
2.4.1	Modulating Hydrogel Microstructure	26
2.4.2	Engineering Hydrogels with Robust Mechanical Properties	28
2.5	Biodegradable and Bioactive Hydrogels	31
2.5.1	Biodegradable Hydrogels	31
2.5.2	Engineering Bioactive Hydrogels	33
2.6	Conclusion and Future Directions	36
	References	37

Abstract The successful engineering of synthetic hydrogels that exhibit key features of the natural extracellular matrices has led to significant advances in the field of tissue engineering. Various chemical and physical approaches have been developed for hydrogel synthesis. While the chemical methods rely on the presence of readily addressable functional groups for the formation of covalent bonds at the crosslinking points, the physical approaches utilize weak and reversible interactions for gelation purposes. In many cases, physical gels need to be covalently stabilized for their long term applications in tissue engineering. Over the past decade, hydrogels have evolved from passive scaffolding materials to bioactive and cell-responsive matrices that play a defining role in the regulation of cellular functions and tissue growth. Novel hydrogels with tunable microstructures, mechanical properties, and degradation rates have been engineered. Biological motifs or soluble factors have been successfully incorporated in the hydrogel matrices to allow for a higher level of cell-matrix communication. These synthesis methods have resulted in the production of a wide variety of functional

X. Jia (✉)

Department of Materials Science and Engineering, Delaware Biotechnology Institute, University of Delaware, Newark, DE 19716, USA
e-mail: xjia@udel.edu

hydrogels that support the growth of many different tissue types. The development of the next generation biomimetic hydrogels relies on parallel advancements in materials chemistry, cell biology and developmental biology.

Keywords Bioactive • Covalent crosslinking • Extracellular matrix • Growth factors • Hierarchical • Hydrogels • Mechanical properties • Networks • Physical crosslinking • Structure • Tissue engineering

Abbreviations

ADH	Adipic acid dihydrazide
BMP-2	Bone morphogenic protein 2
CD	Cyclodextrin
CryoSEM	Cryogenic scanning electron microscopy
DXN	Doubly crosslinked network
ECM	Extracellular matrix
EDC	<i>N,N</i> -(3-dimethylaminopropyl)- <i>N</i> -ethyl carbodiimide
ELP	Elastin-like polypeptide
Fmoc	Fluorenylmethoxycarbonyl
GAG	Glycosaminoglycan
HA	Hyaluronic acid
HBGF	Heparin binding growth factor
HBP	Heparin-binding peptide
HGP	Hydrogel particle
HGP-P ₁	Perlecan domain I conjugated hydrogel particles
HMDI	1,6-hexamethylene diisocyanate
HRP	Horse radish peroxidase
HSPG	Heparan sulfate proteoglycan
IGF	Insulin-like growth factor
MMP	Matrix metalloproteinase
OPF	Oligo[poly(ethylene glycol) fumarate]
OTMC	Oligo (trimethylene carbonate)
PCL	Poly(ϵ -caprolactone)
PDLA	Poly(D-lactide)
PEG	Poly(ethylene glycol)
PEGDA	Poly(ethylene glycol) diacrylate
PGA	Poly(glycolic acid)
PLA	Poly(lactic acid)
PLGA	Poly(lactic-co-glycolic acid)
PLLA	Poly(L-lactide)
PlnDI	Domain I of perlecan
PMAA	Poly(methacrylic acid)

PAA	Poly(acrylic acid)
PPF	Poly(propylene fumarate)
PVA	Poly(vinyl alcohol)
PVFF	Porcine vocal fold fibroblast
RGD	Arginine-Glycine-Aspartic acid
SEM	Scanning electron microscopy
sGAG	Synthetic glycosaminoglycan
TGF	Transforming growth factor

2.1 Introduction

The goal of tissue engineering is to replace or regenerate the normal biological functions of the tissues or organs via the rational combination of cells, biomimetic matrices, biological signals and biophysical cues. Whereas *in vivo* tissue engineering takes advantage of the body's own healing power and utilizes scaffolding materials to recruit endogenous cells for tissue repair, *in vitro* tissue engineering relies on the ability of engineers to re-create the microenvironment *ex vivo* for the generation of tissue-like constructs that can be implanted. Although the cells ultimately are the true “engineers”, the importance of the scaffolding materials cannot be neglected. Polymeric scaffolds are not simply physical templates, rather they are designed to actively regulate cell functions and promote tissue growth by presenting specific cell recognition sites and signaling molecules in a temporal and spatial fashion [1, 2].

Hydrogels are the most attractive tissue engineering scaffolds due to their structural and functional similarities to the natural extracellular matrices (ECM). Hydrogels are defined as interconnected networks of macroscopic dimensions, consisting of hydrophilic (or amphiphilic) building blocks that are rendered insoluble due to the presence of crosslinks. Hydrogels can be formed from soluble monomers, multifunctional polymers (macromers), or insoluble, microscopic entities such as nanofibrils and nano- or micro-particles. Crosslinks, whether chemical or physical in nature, are junction points where more than two polymeric chains or microscopic objects cross over.

In general, hydrogels to be used as the transient artificial ECM for tissue engineering should (1) be biocompatible and biodegradable; (2) allow for the free diffusion of nutrients and metabolites; (3) be able to provide mechanical support and effectively transmit forces from the environment to the growing tissue over a prolonged period of time and (4) present biological cues in a spatial and temporal fashion [3, 4]. In this chapter, we discuss how hydrogels are synthesized, how their intrinsic properties are modulated and how they can be made biodegradable and bioactive. When rationally designed and properly processed, hydrogels have the potential to provide cells with a biologically relevant microenvironment that fosters cell proliferation, migration and ECM production, ultimately leading to the growth of functional tissues.

2.2 Basic Concepts

Hydrogels are created through a crosslinking process, during which the subunits, or the constituent building blocks, bond, associate or entangle with each other, ultimately forming a network of macroscopic dimensions where all the subunits are interconnected. Several distinct levels of crosslinking can be observed during the gelation process. Initially, the subunits grow and branch out, but remain soluble or dispersible. As the crosslinking continues, clusters form, and the size of the clusters increases. Eventually, the structure becomes infinite in size and a gel point is reached where all the subunits are linked to each other at multiple points. The presence of crosslinks ensures the structural and mechanical integrity of the hydrogels and prevents them from dissolution when exposed to an aqueous environment [5].

Hydrogels are inherently heterogeneous, containing solid-rich regions distributed within a liquid environment. Water in hydrogels can be free to diffuse in and out of the matrix, or be loosely bound or tightly associated to the network. Hydrogels are solid-like since they exhibit an infinite viscosity, defined shape and modulus. Hydrogels are also liquid-like. Solute molecules can diffuse freely through the matrix so long as their sizes do not exceed the average mesh size of the network and no specific interactions exist between the solute and the hydrogel building blocks. Depending on the chemical composition and the method of crosslinking, hydrogels vary in their morphology, mesh size, viscoelasticity, degradation behaviors and biological activities.

2.3 Hydrogel Synthesis

2.3.1 Chemical Crosslinking

Ideally, chemical methods adopted for hydrogel synthesis should be efficient, high-yielding and functional group-tolerant. The reactions should occur under mild conditions with minimal by-products. Crosslinking reagents must contain at least two functional groups and should share common solvents with the polymer precursors to ensure accessibility of the functional groups. As the crosslinking reaction proceeds, the solution viscosity increases, and the diffusivity of the polymeric species decreases. Consequently, 100% functional group consumption is not possible. Ideally, the residual, un-reacted functional groups should not react with the biological entities, including electrolytes, proteins and cells. Certain by-products from the chemical process can be physically trapped in the hydrogels and be released later on when cells are present, causing toxicity. Therefore, long-term biocompatibility has to be considered when new crosslinking chemistry is introduced. Depending on the particular crosslinking chemistry applied, one can synthesize the hydrogels first and then process them into the desired geometry and porosity. Cells can

be subsequently introduced to the pre-existing scaffolds for both in vivo and in vitro tissue engineering purposes. Alternatively, cells can be included during the gelation process and be entrapped within the cage established by the polymeric chains.

2.3.1.1

Covalent Crosslinking via Vinyl Groups

Radical polymerization is the most widely used method for synthesizing covalently crosslinked hydrogels using monomers containing vinyl groups along with multifunctional crosslinkers [6]. Alternatively, macromonomers can be prepared by modifying the end groups or the repeating units of the prepolymers with (meth)acrylic acid or its derivatives (Fig. 2.1a). Radicals can be generated via the reaction between the oxidation (typically a persulfate) and reducing reagents (such as ascorbate, *N,N,N',N'*-tetramethyl ethylenediamine or metabisulfite) in aqueous media at ambient temperature. Photoinitiators, such as 2,2-dimethoxy-2-phenylacetophenone (Irgacure 651), 2-hydroxy-1-[4-(hydroxyethoxy) phenyl]-2-methyl-propanone (Darocur 2959) and Eosin Y, photolytically decompose to generate free radicals [7].

Once generated, radicals immediately participate in subsequent propagation and crosslinking reactions through the vinyl groups. The monomer reactivity ratio needs to be taken into account when designing radically crosslinked hydrogels using monomers and macromers with different vinyl groups [7]. Radically crosslinked hydrogels have been prepared from a variety of monomer/polymer sources, including (meth)acrylic acid, 2-hydroxyethyl methacrylate, *N*-vinylpyrrolidone, *N*-isopropylacrylamide, dextran, hyaluronic acid (HA), (hydroxyethyl)starch, poly(vinyl alcohol) (PVA), oligo[poly(ethylene glycol) fumarate] (OPF) and poly(ethylene glycol) (PEG). If the initiator and the wavelength of the light are carefully tuned, photocrosslinking allows for in situ cell encapsulation in a spatial and temporal fashion with minimal DNA damage and cell toxicity [8].

2.3.1.2

Covalent Crosslinking via Carboxylate Groups

In the presence of an appropriate activating reagent, such as *N,N*-(3-dimethylaminopropyl)-*N*-ethyl carbodiimide (EDC), polymers carrying carboxylic acid groups can be crosslinked by amine-presenting molecules, forming amide bonds at the crosslinking points. Reaction of carboxylic acids with EDC involves the formation of an unstable *O*-acylisourea intermediate that has the tendency to rearrange to a more stable, unreactive *N*-acylurea [9, 10]. However, if bicarbodiimide is used, this undesirable rearrangement reaction can still lead to hydrogel formation. [11] On the other hand, rescuing the active intermediate by 1-hydroxybenzotriazole or *N*-hydroxysuccinimide (NHS) allows the coupling reaction between $-NH_2$ and $-COOH$ to occur in water (Fig. 2.1a). The slow reaction kinetics, combined with the need for activating reagents and the generation of small molecule leaving groups, makes this type of chemistry unsuitable for in situ cell encapsulation. Nevertheless, gelatin/chondroitin hydrogels, crosslinked by EDC/NHS and impregnated in Dacron, have

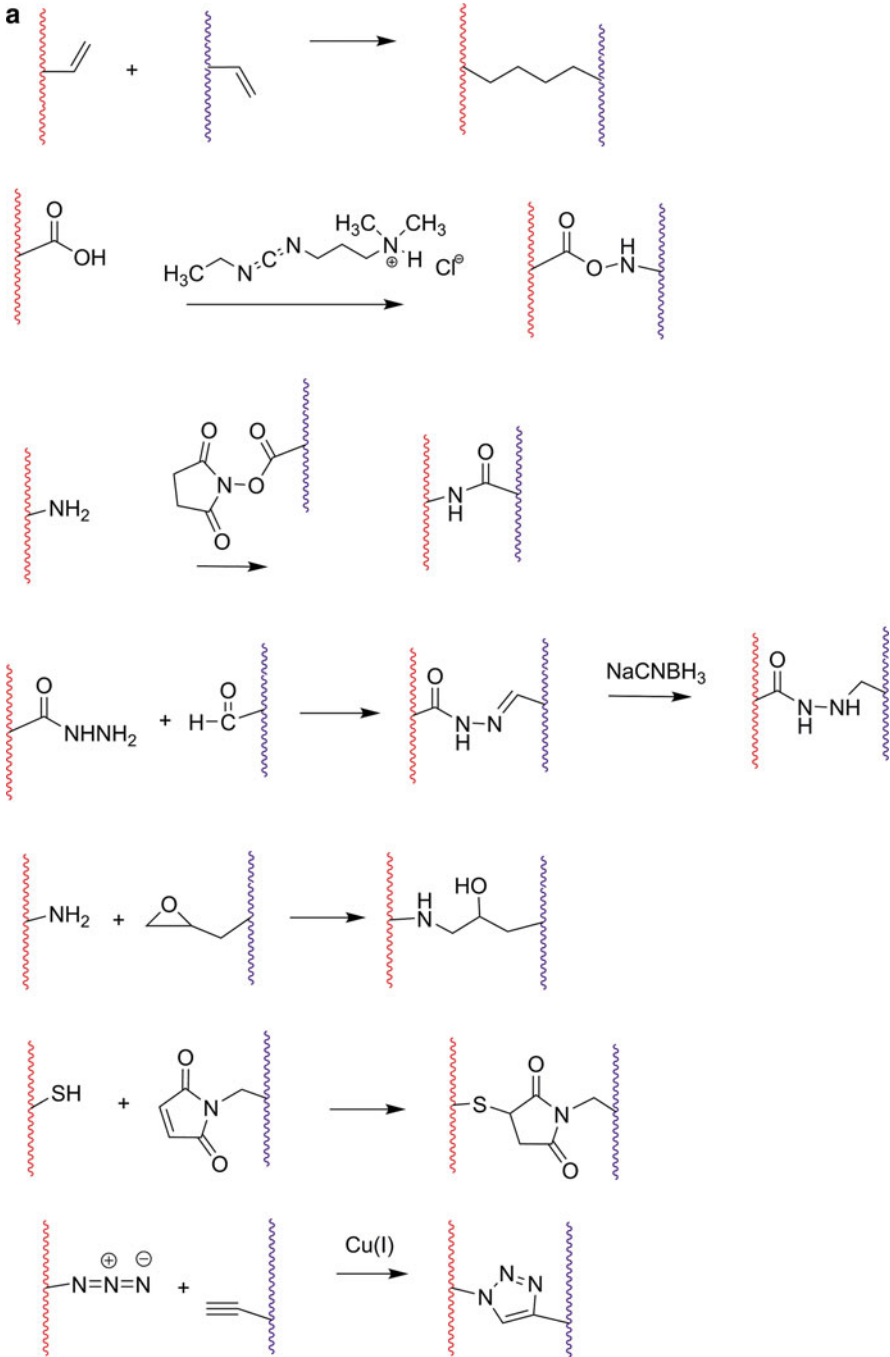


Fig. 2.1 (continued)

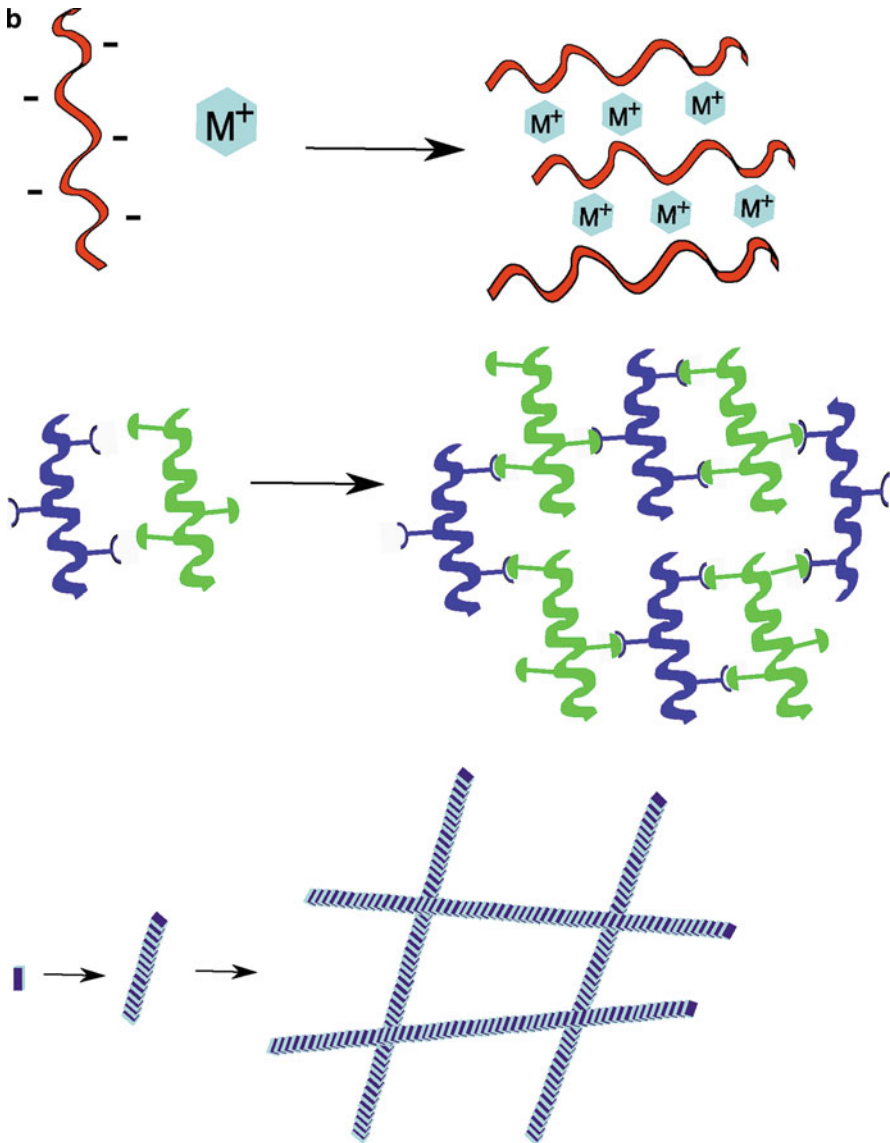


Fig. 2.1 Overview of chemical (a) and physical (b) approaches for hydrogel synthesis. Hydrogels can be synthesized by covalent crosslinking using readily addressable functional groups as the reactive handles. Physical crosslinking can be established by weak secondary forces, molecular self-assembly or biological recognition events

2 been shown to induce a mild tissue reaction when implanted in subcutaneous pockets in rats [12].

The carbodiimide chemistry has been frequently employed to stabilize reconstituted collagen gels by the coupling reaction between the carboxylic acid groups (in glutamic acid and aspartic acid residues) and lysine amines, forming zero length crosslinks. This method has been successfully applied to fabricate transparent, robust hydrogels as corneal substitutes [13]. Instead of using lysine amines, Duan et al. utilized polypropyleneimine octaamine dendrimers as effective collagen crosslinkers. Compared to the zero length crosslinking, the resulting hydrogels had a lower water uptake and were more resistant to denaturation and enzymatic degradation [14].

2.3.1.3

Covalent Crosslinking via Amino Groups

Polymers containing amine groups can react with various electron deficient groups including isocyanates, isothiocyanates, epoxides, anhydrides and NHS-esters (Fig. 2.1a) to form crosslinked hydrogels [15]. For example, multiblock hybrid copolymers consisting of alternating lysine-containing peptide and PEG segments were crosslinked by 1,6-hexamethylene diisocyanate (HMDI) in DMSO to afford elastomeric hydrogels [16]. HMDI, in conjunction with high pressure CO₂, produced crosslinked, highly porous α -elastin hydrogel scaffolds [17]. Crosslinked chitosan films were obtained in a mixed solvent using a water-soluble, protected isocyanate, hexamethylene-1,6-di-(aminocarboxysulfonate), via the formation of a urea linkage [18]. It is worth emphasizing that isocyanates can react with various functional groups in proteins such as lysine, cysteine, and histidine, although the relative reactivity varies [19].

In addition to EDC-activated carboxylates, amine derivatives can react with carbonyl groups, such as aldehydes (or ketones) to form a Schiff base. Schiff bases formed between primary amines and aldehydes, also known as imines, lack the adjacent resonance structure that stabilizes the C=N bond, and therefore are hydrolytically unstable. Sodium cyanoborohydride (NaBH₃CN) can be used to reduce the unstable double bond to a stable C–N single bond [15]. This addition/reduction reaction has been utilized for the covalent crosslinking of recombinant human collagen type III using synthetic glycosaminoglycan (sGAG) mimetics [20]. Crosslinking occurs between the lysine amines in collagen and the ring-opened aldose form of galactose (aldehyde) in sGAG. The resulting composite gels were shown to be less susceptible to collagenase-induced biodegradation than the control gels crosslinked by EDC/NHS.

Glutaraldehyde has been widely applied to stabilize protein-based hydrogels in the absence of the reducing agent, although the chemistry involved has been largely ignored. The expected reaction between the aldehyde and the amino groups leads to a reversible Schiff base that does not contribute significantly to the overall crosslinking. In fact, glutaraldehyde is known to undergo polymerization by aldol condensation to give rise to polymers with α,β -unsaturated aldehydes at neutral or slightly alkaline pH. Subsequent nucleophilic addition of amines to the unsaturated C=C bonds creates a stably crosslinked

collagen gel [21]. Although glutaraldehyde is an effective protein crosslinker, severe toxicity has been observed from glutaraldehyde-crosslinked hydrogels [10].

Hydrazides are a unique class of compounds containing an N–N bond with an acyl substituent. Having lower pKa values than amines, hydrazides are more nucleophilic under neutral or acidic conditions. Hydrazides are capable of undergoing facile reactions with all amine-reactive molecules. Furthermore, hydrazides react rapidly with aldehydes (or ketones) to form hydrazone linkages that are significantly more stable than the corresponding imine bonds. For example, hydrazide-derivitized HA has been crosslinked by *bis*-NHS-esters, glutaraldehyde or NaIO₄-oxidized HA to form bulk gels with high water content [10, 22, 23]. The rapid gelation kinetics and the biocompatibility of the hydrazone chemistry (Fig. 2.1a) allow for in situ encapsulation and 3D culture of non-adherent, prostate cancer cells [24]. The same chemistry, when conducted within the water/mineral oil inverse emulsion droplets stabilized by Span 80, afforded HA-based hydrogel particles with an average diameter of 10 μm [25].

Although hydrazone linkages are more stable than imine bonds, in aqueous solution, they are still hydrolyzable and rapidly exchange with a hydrazide under acidic conditions. Mooney and coworkers [26] generated covalently crosslinked alginate gels using oxidized alginate and adipic acid dihydrazide (ADH). The hydrazone linkage is degradable in aqueous media and the degradation behavior generally depends on the cross-linking density. Interestingly, hydrogels with many dangling single-end molecules showed retarded degradation behavior irrespective of their low initial modulus and low degree of cross-linking density due potentially to re-crosslinking of dangling single-end molecules during degradation. The mechanical properties and degradation time can be decoupled by utilizing partially bound crosslinking molecules that are capable of reversibly crosslinking the polymer to form the hydrogel.

Finally, amines can undergo quantitative reactions with phosphine derivatives that contain hydroxy-methyl group substitutions, forming stable secondary or tertiary amines. Recombinantly expressed elastin-like polypeptides (ELPs) comprised of crosslinkable, hydrophobic ELP blocks with periodic lysine residues and aliphatic, hydrophilic ELP blocks with no crosslinking sites were covalently crosslinked with hydroxymethylphosphine in aqueous solution. Rapid crosslinking was observed within several minutes under physiological conditions. The biocompatible nature of the chemistry allowed for fibroblasts to be embedded in the gels during the cross-linking process [27]. A similar approach was employed to prepare elastomeric hydrogels based on resilin-like polypeptides [28]. Although stable in aqueous solutions, these phosphine derivatives are susceptible to oxidation to form the uncreative, phosphine oxide derivatives [29].

2.3.1.4

Covalent Crosslinking via Hydroxyl Groups

Hydroxyl groups, when activated by *N,N'*-carbonyl diimidazole (CDI), *N*-hydroxysuccinimidyl chloroformate or *N,N'*-disuccinimidyl carbonate, react with amines to form a stable urethane bond. Owing to the susceptibility of the activating reagents to hydrolysis, cross-linking reactions are usually carried out in organic solvents. In addition, hydroxyls can react

2 with isocyanate, epoxide (Fig. 2.1a) and vinyl sulfone derivatives to form urethane or ether linkages. For example, HA can be crosslinked by ethylene glycol diglycidyl ether in ethanolic NaOH solution at 60°C to afford a hydrogel with high water content and inflammation-dependent degradation properties. HA has also been crosslinked by divinyl sulfone in alkaline medium via the reaction of the vinyl groups with the hydroxyl groups [30, 31]. Polyrotaxane-based hydrogels were formed by the reaction between the CDI-activated hydroxyls of α -cyclodextrins (α -CDs) and PEG-diamine. The polyrotaxane was composed of a PEG chain threaded with many α -CDs and capped with bulky groups via ester linkages [32].

The low reactivity of the hydroxyl groups has motivated researchers to convert them into chemoselective moieties for rapid hydrogel formation in the presence of cells. Ossipov et al. reported straightforward approaches for introducing different types of the chemoselective functionalities, including thiols, amines, aminoxy, hydrazide, methacrylate, or maleimide, into PVA at low degrees (3%). The PVA derivatives were proven to be effective crosslinkers [33].

2.3.1.5

Covalent Crosslinking via Sulfhydryl Groups

Sulfhydryl groups have been extensively investigated for bioconjugation purposes due to the presence of cysteine in various macromolecules. Alternatively, cysteine residues can be readily incorporated in peptides either by solid phase peptide synthesis or genetic engineering. In synthetic polymers, sulfhydryl groups can be introduced using heterodifunctional reagents or protected cysteine derivatives. Sulfhydryl groups are capable of undergoing rapid and efficient addition reactions with α,β -unsaturated carbonyls, such as maleimide derivatives (Fig. 2.1a), vinyl sulfones, and acryloyl derivatives, forming stable thioester bonds without creating any by-products [29]. These reactions represent one particular class of Michael addition reactions. Maleimide reactions have been widely explored for hydrogel formation in the pH range of 6.5–7.5 where the reaction of the maleimides with sulfhydryls proceeds at a rate 1,000 times greater than its reaction with amines. Vinyl sulfone groups can be used to crosslink thiol containing polymers in aqueous solution at slightly alkaline pH. Derivatives of acrylic acid also are able to participate in Michael addition reactions, although the rate is slower than that of maleimides. Sulfhydryl groups can dimerize to form disulfide bonds. This reaction is typically much slower than Michael addition reactions, and oxidation reagents, such as O₂ or H₂O₂, have been introduced to accelerate the reactions [34]. To avoid this undesirable reaction, trace amounts of reducing agents, such as *tris*(2-carboxyethyl)phosphine or dithiothreitol, can be included in the reaction mixture.

The Michael addition reaction has gained increasing popularity as a standard method for in situ cell encapsulation and 3D culture of mammalian cells. Typically, telechelic, multifunctional polymers carrying Michael addition acceptors (α,β -unsaturated carbonyls) are allowed to react with polymers or peptides with multiple sulfhydryl groups under physiological conditions. Inclusion of biologically active peptide motifs into the hydrogels permits cell-responsive matrices to be custom engineered (see below). Realizing the ability of acrylates to participate in both Michael addition reactions and radical polymerization, Burdick and

coworkers created a novel process to provide gel environments that are either permissive or inhibitory to cellular spreading. Specifically, acrylated HA was first crosslinked with an addition reaction using a metalloproteinase (MMP)-cleavable peptide containing thiol groups. When an adhesive peptide was also coupled to the network, this environment permitted the spreading of encapsulated human mesenchymal stem cells. The introduction of a second network via a photoinitiated radical mechanism created covalent barriers that rendered the matrix non-adhesive. The directionality of photochemistry allowed for cell spreading to be spatially controlled [35].

Another important class of reaction involving sulfhydryl groups is the so-called thiol-ene chemistry. Discovered in 1905, the thiol-ene addition reaction has been extensively explored in coating, printing, adhesive and imaging technologies. Thiol-ene polymerization proceeds via a free-radical, step-growth mechanism involving multifunctional thiol and ene (vinyl) monomers. Radicals, commonly generated through a photoinitiation process, abstract hydrogen atoms from a thiol monomer, creating thiyl radicals which can either propagate through a carbon-carbon double bond or terminate by coupling. The subsequent propagation-chain transfer events lead to polymer formation. Competing reactions exist when electron-deficient vinyl monomers (such as acrylate-based monomers) are used, in which case chain growth homopolymerization dominates with a preferential consumption of the acrylate monomers. Conjugated double bonds copolymerize very slowly with thiols, whereas mercaptopropionate esters polymerize faster than mercaptoacetate esters, which in turn react more quickly than simple alkyl thiols [36].

When adapted to hydrogel synthesis, the thiol-ene reaction leads to rapid and efficient crosslinking. Similar to photoinitiated radical polymerization, thiol-ene chemistry allows for spatial and temporal control of the polymerization. The step-growth mechanism ensures a delayed gelation at high monomer conversion, potentially giving rise to more homogeneous network structures. Unlike traditional radical chain mechanisms, thiol-ene polymerization cannot be quenched or significantly affected by O₂ [36, 37]. The versatility of the thiol-ene reaction permits biological species to be readily incorporated into the hydrogel formulation. The mild reaction conditions and rapid gelation are suitable for in situ cell encapsulation. Thiol-ene chemistry has been extensively investigated for the formation of PEG-based hydrogels [38, 39].

2.3.1.6

Covalent Crosslinking Using Orthogonal Click Chemistry

The Cu(I)-catalyzed Huisgen 1,3-dipolar cycloaddition reaction between azide and terminal alkyne moieties has proven to be an efficient method for bioconjugation and polymer synthesis [40]. Known as Orthogonal Click Chemistry, this reaction proceeds rapidly with close to 100% yield, forming a stable triazole ring without any byproducts. The orthogonal nature of this reaction ensures the absence of cross-reactions with other functional groups. The instability of Cu(I) requires it to be generated in situ by the reduction of Cu(II) with ascorbic acid. Hawker and coworkers [41] reported the preparation of well-defined PEG-based hydrogels using alkyne-terminated and azide-terminated star PEG (Fig. 2.1a). They suggest that the resulting gels have improved mechanical properties compared to their

2 homologues produced by free radical photocrosslinking. When an azide-functionalized RGD peptide was included, cell-adhesive “Click Gels” were obtained [42]. Similarly, PVA [43] or polysaccharide-based [44] hydrogels were synthesized using the prepolymers partially derivatized with azide and alkyne groups. The toxicity of the catalyst renders such reactions undesirable for in situ cell encapsulation. The residual Cu (I) trapped in the gels during the synthesis needs to be extracted thoroughly before the gels can be used for cell culture.

The thermodynamic barrier for alkyne-azide cycloaddition in the absence of a copper catalyst can be overcome by introducing ring strain. Hence, azide and cyclooctyne derivatives undergo rapid cycloaddition reactions under physiological conditions in the absence of auxiliary reagents [45, 46]. Taking advantage of this chemistry, Johnson et al. [47] prepared photodegradable networks with well-defined structures and tunable gelation times using bifunctional, fluorinated cyclooctynes for in situ “click” crosslinking of azide-terminated photodegradable star polymers. More recently, Anseth and coworkers successfully encapsulated 3T3 fibroblasts in PEG/peptide “Click” hydrogels with minimum cell death. Subsequently, thiol-ene photocoupling chemistry was introduced that enabled patterning of biological functionalities within the gel in real time and with micrometer scale resolution. This material system enabled researchers to tailor independently the biophysical and biochemical properties of the cell culture microenvironments in situ [48].

2.3.1.7

Other Chemical Crosslinking Methods

Other less explored chemical approaches for hydrogel synthesis include the Diels-Alder reaction, aryl azide-based photochemical reactions, Staudinger ligation and Native Chemical Ligation. The Diels-Alder reaction involves the covalent coupling of a diene with an alkene to form a 6-membered ring product in the absence of initiator or catalyst. Under different conditions, the Diels-Alder adduct can be decomposed to the starting species via a retro-Diels-Alder reaction. Electron-withdrawing substituents on the alkene and the electron-donating groups on the diene are important for increasing reaction rates [15]. When properly modified with furan and maleimide groups, polyoxazoline [49] and poly(acrylamide)/PEG-based [50] thermoreversible hydrogels can be synthesized. Another type of photochemistry that has been employed for hydrogel synthesis relies on the presence of aryl azide derivatives that form short-lived nitrenes upon photolysis. Nitrenes subsequently undergo ring expansion reactions or non-specific insertions with polymeric species [29] to form covalently crosslinked hydrogel networks [51]. This chemistry, however, is mechanistically different from the photocrosslinking discussed above.

Two bioorthogonal chemistries that have been widely used for bioconjugation purposes are Staudinger ligation and native chemical ligation. Staudinger ligation refers to the amide bond formation between an azide and a phosphine derivative containing a neighboring electrophilic group. This reaction is chemoselective, biocompatible and does not require any catalyst, and thereby is well suited for selective chemical transformations within a cellular context [52]. Staudinger ligation has been explored for the covalent stabilization of ionically crosslinked alginate hydrogels using azide functionalized alginate and 1-methyl-2-diphenylphosphinoterephthalate-terminated, telechelic PEG [53]. In native chemical ligation,

a peptide having a C-terminal thioester reacts with an N-terminal cysteine residue in another peptide to undergo a transthioesterification reaction, resulting in the formation of the neighboring α -amine group on cysteine. A subsequent nucleophilic attack of the electron-rich nitrogen in the ester carbonyl results in an S–N shift, forming a native amide bond. This reaction proceeds at physiological pH under mild conditions without any additional additives. Recently, native chemical ligation has been explored to create covalently crosslinked hydrogels [54] using macromonomers of four-armed PEG with either thioester or N-terminal cysteine peptides. Mixing the respective macromonomer solutions results in rapid gelation within minutes. The thiol functional groups regenerated after the crosslinking were utilized as the reactive handles for bioconjugation with a maleimide-GRGDSPG-NH₂ peptide [55]. A similar strategy has been applied to prepare anti-inflammatory hydrogels supporting islet cell survival in the presence of diffusible pro-inflammatory cytokines [56].

Enzymes can be employed to catalyze various reactions with high efficiency and minimal toxicity. The action of enzymes requires very specific substrates, thus it is orthogonal and specific. Enzyme-catalyzed reactions occur at physiological conditions, and are therefore suitable for cell encapsulation. Transglutaminase (also known as Factor XIII), when activated by thrombin and Ca²⁺ to factor XIIIa during the blood coagulation cascade, is capable of catalyzing covalent crosslinks between the ϵ -amine group of lysine side chains and the γ -glutamyl side chain of glutamine residues. When transglutaminase substrates were incorporated into synthetic or peptidic building blocks, rapid gelation in the presence of the enzyme and its cofactor, Ca²⁺ ions, was observed [57–59].

Horse radish peroxidase (HRP) catalyzes the oxidative coupling of neighbouring tyrosine in the presence of H₂O₂ to form dityrosine. Lee et al. created an enzymatically-crosslinked HA hydrogel with tunable mechanical strength and gelation rate by mixing [60] an HA-tyramine conjugate with HRP in the presence of H₂O₂. The HRP-catalyzed hydrogelation of a saccharide-peptide alternating copolymer was reported by Guan and coworkers. The polymers are composed of alternating galactaric acid and lysine on the backbone, with tyrosine grafted onto the side chain as a handle for enzymatic reaction [61]. The resulting hydrogels are degradable under simulated physiological conditions and exhibit minimal cytotoxicity on dermal fibroblasts and PC-12 cells. Enzyme-catalyzed gelation reactions usually result in heterogeneous hydrogels with low mechanical strength due to the low conversion imposed by the inability of enzymes to diffuse readily during the gelation process [62].

2.3.2

Physical Crosslinking

Hydrogels can also be prepared via physical means (Fig. 2.1b) in the absence of crosslinking reagents. Traditionally, crosslinking is initiated by isolated non-covalent interactions such as ionic interaction, hydrophobic association, H-bonding, crystallization, stereocomplexation or host-guest inclusion complexation. On the other hand, molecular self-assembly requires the interplay of multiple physical interactions that contribute synergistically to the overall

2 integrity of the gels. Finally, biological motifs involved in specific protein/protein associations and protein/carbohydrate interactions have been incorporated in synthetic hydrogels for crosslinking purposes. Compared to the covalently crosslinked hydrogels, physical crosslinking, in general, affords highly versatile, dynamic and responsive hydrogel materials. Due to the low stability and mechanical strength, covalent crosslinking can be introduced during or after the physical assembly to stabilize the network structure.

2.3.2.1

Traditional Physical Crosslinking

Ionic crosslinking (Fig. 2.1b) occurs when multivalent ions form charge complexes with polyelectrolytes. Both naturally occurring and synthetic polyelectrolytes have been ionically crosslinked. For example, alginate is capable of forming ionically-crosslinked hydrogels by divalent calcium ions at room temperature under physiological conditions in the presence of living cells or biomacromolecules. Islet cells [63] and endostatin-transfected cells [64] have been successfully encapsulated in ionically-crosslinked alginate beads for immunoisolation purposes. High molecular weight HA has been crosslinked by Fe^{3+} to form hydrogel films for the prevention of post-surgical adhesions [31]. Chitosan has been ionically crosslinked by glycerol-phosphate disodium salts at elevated temperature [65]. Dextran microspheres coated with anionic and cationic polymers exhibit spontaneous gelation upon mixing due to ionic complex formation between the oppositely charged microparticles [66]. Ionically-crosslinked hydrogels suffer from low stability; degradation occurs when ionic species in the cell culture media or in the extracellular fluid bind competitively with the gel components [67].

Advances in controlled polymerization techniques have allowed for amphiphilic block copolymers with well-defined molecular architecture, controlled molecular weight and narrow polydispersity to be readily synthesized [68–71]. Under appropriate conditions, these block copolymers can assemble into hydrogels in aqueous solutions with aggregated hydrophobic segments surrounded by hydrophilic shells that bridge between neighboring hydrophobic clusters [72]. The gelation temperature depends on the polymer concentration, the relative length of the hydrophobic and hydrophilic blocks, and the chemical structure and molecular architecture of the polymer [67]. While PEG or poly(acrylic acid) (PAA) are commonly used as the hydrophilic block, the hydrophobic block varies from polyesters [poly(lactic-co-glycolic acid) (PLGA), poly(ϵ -caprolactone) (PCL), poly(propylene fumarate)], polyether [poly(propylene oxide)], polyisobutylene, poly(γ -benzyl L-glutamate), poly(*N*-isopropylacrylamide), polyurethanes and poly(organophosphazene). Similar to ionically-crosslinked hydrogels, hydrophobically-associated hydrogels suffer from weak mechanical strength and rapid dissociation [73].

Gelation can be induced by crystallization and/or H-bonding interaction. For example, PVA, when subjected to repeating freeze-thawing cycles, forms a relatively strong and elastic gel by the formation of small crystallites that serve as physical junctions. The crystallites formed in PVA gels are strengthened by H-bonding between the hydroxyls. The properties of the gel depend on the PVA molecular weight, the PVA concentration, the

temperature and time of the freezing and the numbers of the cycles. PVA hydrogels with anisotropic stiffness mimicking the aorta were created via the application of thermal cycling and external strain [74].

H-bonding can be established between the carboxyls in PAA or poly(methacrylic acid) (PMAA) and oxygen in PEG. In the case of PMAA, hydrophobic interactions also play a role. The deprotected carboxylic acid is not an H-bonding donor. Therefore, when the media pH is altered, these gels may dissociate [75, 76]. When polymers containing multiple stereoisomeric units are mixed, stereocomplexation leads to physical gels. Classical examples are polymers based on PEG-b-poly(L-lactide) and PEG-b-poly(D-lactide) [77]. Physical gels can be formed via specific host-guest inclusion mechanisms.

Host-guest inclusion complexation has been exploited for hydrogel formation. Formation of inclusion complexes between adamantane or cholesterol with β -CD has been frequently exploited for the assembly of polymeric networks owing to their high binding constants. Typically, β -CD and adamantane (or cholesterol) are separately coupled to the synthetic polymer repeating units or to the termini and gelation is induced via simple mixing of the complementary solutions under appropriate conditions [78]. The physical nature of the networks render them sensitive to external stimuli, such as mechanical forces, temperature, and the addition of competitive inclusion complex forming molecules.

2.3.2.2

Physical Crosslinking by Molecular Self-Assembly

Molecular self-assembly refers to the ordered arrangement of molecular species into well-defined nanostructures with tunable macroscopic properties via a process that involves concerted action of weak and non-covalent interactions [79]. Molecular self-assembly is emerging as a promising new route to engineer hydrogel matrices (Fig. 2.1b) that provide cells with more physiologically relevant microenvironments. Due to their strong tendency to associate, peptides with specific motifs or sequences have been investigated for gelation purposes.

Aromatic fluorenylmethoxycarbonyl (Fmoc)-dipeptides can self-assemble to form nanofibrous matrices. Gelation occurs through the formation of antiparallel β -sheets that are stabilized by the fluorenyl groups by aromatic interactions (π - π stacking). By including the RGD peptide in the modular mixture, cell adhesive hydrogels can be engineered [80]. The low solubility of these peptides in aqueous solution requires that the peptides be solubilized in organic solvent and self-assembly be induced by solvent exchange. Masking tyrosine with phosphate groups rendered the peptide water-soluble and the self-assembly process was by triggered by enzymatic dephosphorylation. By controlling the levels of calcium and phosphate ions associated with the supramolecular structure, mineralized hydrogels of variable hardness can be prepared in the form of hybrid composites comprising interconnecting networks of calcified nanofilaments [81]. However, the complexity of the system and co-existences of several processes, including enzymatic reactions, peptide association and mineralization, may limit the practical application of such materials in tissue engineering.

A 15 amino acid-long, facially amphiphilic peptide has been commercialized as PuraMatrixTM by BD Bioscience as 3D matrices for cell culture. This peptide contains

2 alternating hydrophilic and hydrophobic amino acid residues. The hydrophilic residues, in turn, alternate between being positively and negatively charged. Several physical mechanisms, including ionic interactions, H-bonding and hydrophobic interactions, synergistically contribute to the self-assembly process. Upon exposure to cell culture media, the peptide self-assembles into β -sheets that further stack to form double-walled nanoribbons. Physical entanglement of the nanoribbons gives rise to macroscopic gels. The resulting hydrogels contain nanofibers of 7–10 nm in diameter, and 50–400 nm sized nanopores, closely mimicking the morphological characteristics of natural ECM. Despite their low mechanical strength, these hydrogels have been shown to support the growth of a wide spectrum of mammalian cells [82], maintain the functions of differentiated neural cells [83] and chondrocytes [84] and promote the differentiation of liver progenitor cells [85].

Separately, peptide amphiphiles containing a hydrophobic alkyl tail and a hydrophilic oligopeptide head were shown to assemble into cylindrical nanofibers with defined fibril diameters. Self-assembly is driven by the hydrophobic interaction between the hydrophobic tails and the H-bonding interaction between the amino acid residues. Liquid-to-gel transformation was induced by fibril entanglement. Covalent coupling between neighboring cysteine residues was introduced to stabilize the resulting fibrous structures [86–88]. Peptide sequences that facilitate mineralization and foster cell adhesion can be readily incorporated in these amphiphilic molecules without compromising their assembly potential. More importantly, the density of the bioactive epitope can be modulated via peptide design. These peptide amphiphiles can assemble into stable hydrogels under physiological conditions, allowing cells to be encapsulated in a 3D nanofibrous matrix. Rapid, selective differentiation of neural progenitor cells into neurons was achieved through the amplification of the bioactive epitope to cells by the assembled nanofibers [89].

A higher level of organizational control was demonstrated using a de novo designed peptide that forms a pH-responsive self-assembled β -hairpin [90]. The sequence consists of alternating hydrophobic (valine) and hydrophilic (lysine) residues of high β -sheet propensity flanking a four-residue segment incorporated to promote the formation of a type II β -turn. Hydrogelation proceeds through peptide intramolecular folding into β -hairpins and concomitant self-assembly into branched clusters of well-defined (uniform, 3 nm cross section), semiflexible, β -sheet-rich nanofibrils [91, 92]. Due to the non-covalent nature of the hydrogel, it is responsive to external stimuli, including addition of salt, pH and temperature changes and mechanical shear [93], making it an ideal matrix for in situ cell encapsulation. The hydrogel construct has been shown to be non-toxic and cytocompatible [94]. Interestingly, this class of hydrogels fosters the attachment and proliferation of mammalian cells [94], yet effectively inhibits and kills bacteria [95] on contact, demonstrating the versatility of the hydrogels.

Genetically engineered protein polymers composed of tandemly repeated silk-like (GAGAGS) and elastin-like (GVGVP) amino acid blocks can self-assemble to form elastic gels. Hydrogels form due to the crystallization of the silk-like segments through the formation of aligned H-bonded β -strands [96]. The non-covalent nature of the gelation ensures safe inclusion of bioactive molecules during the gelation process. The periodic inclusion of elastin-like blocks imparts flexibility to the matrix. These hydrogels are shown to be biocompatible and biodegradable [97].

The hydrogels described above rely predominantly on the presence of β -sheet structure. Noteworthy, self-assembled hydrogels have also been obtained from linear peptides with purely α -helical structures. The peptide sequences can be engineered to alter the underlying mechanism of gelation and, consequently, the hydrogel properties [98]. Hierarchical α -helical structures such as coiled-coils have also been exploited for gelation purposes. Coiled-coil motifs are comprised of left-handed superhelices of several right-handed α -helices, and are characterized by a hydrophilic and a hydrophobic side due to a typical repeating sequence of amino acids with different polarity.

Tirrell and coworkers [99] created artificial proteins consisting of terminal leucine zipper domains flanking a central, flexible, water-soluble polyelectrolyte segment. The polypeptide undergoes reversible gelation in response to changes in pH or temperature. Formation of coiled-coil aggregates of the terminal domains in near-neutral aqueous solutions triggers formation of a 3D polymer network, with the polyelectrolyte segment retaining solvent and preventing precipitation of the chain. Dissociation of the coiled-coil aggregates through elevation of pH or temperature causes dissolution of the gel and a return to the viscous behavior that is characteristic of polymer solutions. The rapid erosion of these hydrogels, however, limits their potential application. By harnessing the selective molecular recognition, discrete aggregation number and orientational discrimination of coiled-coil protein domains [100], the erosion rate can be tuned over several orders of magnitude in these artificial protein hydrogels. The coiled-coil motifs, in conjunction with a metal chelating mechanism, have been incorporated into poly(*N*-(2-hydroxypropyl) methacrylamide) for the assembly of thermal-responsive physical gels [101–103].

2.3.2.3

Physical Crosslinking by Recognition Events

Biological recognition events can be introduced to synthetic polymers to induce physical gelation via specific and reversible protein/protein and protein/carbohydrate interactions. The ability of an antigen to recognize a specific antibody provides the basis for the fabrication of antigen-sensitive hydrogels (Fig. 2.1b). A polyacrylamide-based, semi-interpenetrating network was synthesized by redox-initiated radical polymerization/crosslinking of *N*-succinimidyl acrylate-functionalized antibodies and antigens, along with acrylamide monomer and *N,N'*-methylenebis(acrylamide). In this system, the covalently crosslinked polyacrylamide establishes the major framework that is further reinforced by the antigen/antibody interaction. Reversible swelling/deswelling was observed upon alternating exposure of the hydrogel to antigen-containing and antigen-free solutions. Such a system holds potential for controlled release of biomolecules in response to specific antigens [104].

Protein/polysaccharide affinity interactions have also been exploited for the formation of highly responsive hydrogels. Heparin is a highly negatively charged GAG comprised of variably sulfated disaccharides of iduronic acid and glucosamine and is capable of mediation of binding to many proteins [105, 106], including antithrombin III and growth factors. Viscoelastic hydrogel materials can be generated by mixing heparin with vinyl sulfone-functionalized star PEGs that contain cysteine-equipped, heparin-binding peptides (HBP) [107]. Owing to the inferior mechanical properties of these initial materials, additional,

2 covalent, crosslinks comprising *bis*-cysteine-functionalized peptides were incorporated into the PEG-based hydrogels [108]. The dually-crosslinked gels showed temperature- and frequency-dependence of their viscoelastic properties. Similarly, direct mixing of star PEGs that have been modified with low molecular weight heparin and HBPs results in soft hydrogels with growth factor binding capacity [109, 110]. Replacing HBPs with vascular endothelial growth factor (VEGF) permits the formation of hydrogels that selectively erode in the presence of the VEGFR-2 receptor [111].

2.4 Modulating Hydrogel Microstructure and Mechanical Properties

2.4.1 Modulating Hydrogel Microstructure

It is well known that the structural characteristics of hydrogels, such as the mesh size and the matrix morphology, have profound effects on cellular functions including cell migration, proliferation, phenotype and metabolism [112]. Traditional hydrogels are macroscopic gels consisting of nanoscale pores [113, 114] defined by the soluble polymer precursors that are randomly interconnected, lacking the structural complexity and functional diversity seen in the natural ECM. On the other hand, the natural ECM has to be able to accommodate cells that are typically $\sim 10\ \mu\text{m}$ in size, yet exhibit features at all length scales from the macro down to the molecular to allow cells to respond, maintain and remodel their environment as they go through various cell cycles and different stages of development [112].

Intrigued by the multiple levels of matrix organization in the natural biological system, researchers started to develop methodologies to create more complex and information-rich hydrogels. As discussed above, molecular self-assembly has emerged as a bottom-up technology that has the potential to recapitulate the hierarchical organization found in the natural ECM. We have discussed several elegant examples of hierarchically-assembled peptide gels above (Fig. 2.2a). Alternatively, nanostructured hydrogels have been prepared using hydrogel particles of nano or micron size as the building blocks or crosslinkers instead of linear or branched soluble polymer precursors used in the preparation of traditional hydrogels [62, 115]. Using HA as the starting material, Jia and coworkers have created a new class of hydrogels with HA hydrogel particles (HGP) embedded in and covalently crosslinked to a secondary network that is also HA-based [25, 30, 116]. Nanoporous HA HGPs were synthesized by an inverse emulsion crosslinking technique. Doubly crosslinked networks (DXNs) were obtained by covalent crosslinking of HA HGPs with a water-soluble, secondary crosslinker. Structural analysis [117] of the DXNs by cryogenic scanning electron microscopy (cryoSEM) and neutron scattering techniques revealed the presence of a hierarchical structure with densely crosslinked, nanoporous HGPs interconnected to a loose secondary network that exhibited porosity at the micron size range. A close inspection of the cryoSEM image (Fig. 2.2b) for DXNs indicates a diffuse interphase between individual HGPs and the secondary matrix, which proves that the secondary network originates from the particle surface. As a result, the secondary

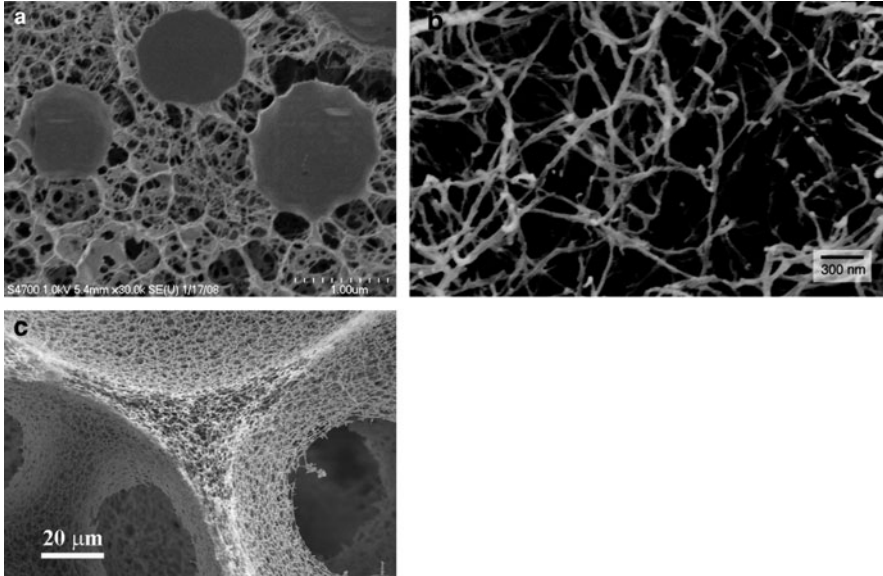


Fig. 2.2 Representative SEM images of synthetic hydrogels. (a) CryoSEM image of HA-based, doubly crosslinked networks [117]. Copyright permission from American Chemical Society. (b) SEM image of an IKVAV nanofiber network formed by adding cell media to a peptide amphiphile aqueous solution [89]. Copyright permission from American Association for the Advancement of Science. (c) SEM image of nanofibrous gelatin scaffold [122]. Copyright permission from Elsevier Science Ltd

network can exert mechanical constraints on the hydrogel particles, leading to the deformation of HGPs through the covalent linkages between the secondary network and the HGP surface. These novel HA based hydrogels are promising ECM mimetics for cartilage tissue regeneration.

Rather than altering the dimension of the hydrogel building blocks, hierarchically structured hydrogels with optimal environments for cell adhesion, proliferation, differentiation and neotissue formation can be induced by careful employment of novel processing conditions. Macroporous hydrogel scaffolds have been created by employing a variety of processing techniques, such as salt leaching, gas foaming, freeze drying, colloidal templating, and phase separation [17, 118–121]. Combining a thermally induced phase separation technique with a porogen-leaching process, Ma and coworkers [122] created macroporous gelatin scaffolds containing nanofibrous structures of the same chemical makeup. Systematic variation of the processing parameters permits control over the fiber diameter, fiber length, surface area, porosity, pore size, inter-pore connectivity, pore wall architecture, and mechanical properties of the nanofibrous gelatin scaffolds (Fig. 2.2c). The resulting scaffolds possess high surface areas ($>32 \text{ m}^2/\text{g}$), high porosities ($>96\%$), well-connected macropores, and nanofibrous pore wall structures. Compared to commercial gelatin foam (Gelfoam®), these scaffolds showed much better dimensional stability in a tissue culture environment.

2.4.2

Engineering Hydrogels with Robust Mechanical Properties

In addition to matrix architecture, abundant evidence suggests that mechanical signals have profound effects on cellular functions including growth, differentiation, apoptosis, motility, and gene expression [123]. Furthermore, cells are known to preferentially differentiate on artificial extracellular matrices that have mechanical stiffness similar to that of their natural tissues [124, 125]. These discoveries underscore the importance of engineering hydrogel matrices with high strength and appropriate elasticity in order to maintain the desired cell phenotype and to effectively transmit the external mechanical forces to the encapsulated cells [126, 127]. Unfortunately, traditional hydrogels usually exhibit slow responses and inferior mechanical properties. The presence of network defects, such as dangling chain ends and loops, compromises the overall mechanical integrity of the hydrogels. The uncontrolled and inefficient chemical methods, combined with the increase in the viscosity of the reaction media, give rise to variations in molecular weight between crosslinks (M_c) and a random distribution of crosslinking points in the network. These problems are further compounded by possible phase separation during the reaction [128, 129].

Due to their high water content, low density of polymer chains, and small friction between the chains, hydrogels are mechanically weak. Theoretically, a hydrogel matrix can be reinforced by hard and stiff inorganic nanoparticles [130]. By homogeneously dispersing exfoliated inorganic clay particles and initiating polymerization from their surfaces [131, 132], Gong et al. have constructed nanocomposite gels with unprecedented mechanical strength. In these composite hydrogels, neighboring clay sheets act as multifunctional crosslinking agents for the polymers in the absence of organic crosslinkers. The gels must be formed by initiating polymerization from the clay surface, resulting in the flexible polymer chains with a random coil conformation connecting the clay and filling the space between the clay sheets. With a monomer:water ratio of 0.1, the nanocomposite gels have an elastic modulus of about 10^4 Pa, and can be stretched to about ten times their original length. The unique properties were attributed to the reduced fluctuation in the crosslinking density of the gels and the cooperativity of the polymer chains connecting the same clays [132].

If efficient energy dissipation mechanisms can be introduced, hydrogels with robust mechanical properties can be obtained. Taking advantage of host-guest inclusion complexation, highly water-absorbent and remarkably stretchable hydrogels have been prepared. The basic building blocks of the hydrogels are polyrotaxane consisting of PEG chains threaded with multiple CD molecules and end-capped with bulky functional groups. Intermolecular crosslinking between the threaded CDs created figure-eight crosslinks that can slide along the PEG chains. The resulting gels are referred to as topographical gels. In traditional chemical gels, tension is distributed unevenly among the polymer chains, causing chain scission to occur gradually. Such tension can be released in topographical gels through the sliding of the polymer chains by figure-eight crosslinks [132, 133].

Alternatively, double network gels consist of two interpenetrating polymer networks: one made of highly cross-linked rigid polymers and the other of loosely cross-linked flexible polymers. Such double network gels, containing about 90 wt% water, possess both hardness (elastic modulus of 0.3 MPa) and toughness (fracture stress of 10 MPa). The loosely crosslinked network entangled around the densely crosslinked first network

effectively absorbs the elastic energy around the crack either by viscous dissipation or by large deformation of the polymer chains, preventing the crack growth to a macroscopic level [131, 132, 134]. Recent work by the same group showed that by entrapping ionically-crosslinked, highly ordered, anisotropic poly(2,2'-disulfonyl-4,4'-benzidine terephthalamide) in an interpenetrating, radically-crosslinked poly(acrylamide) network, the resulting hydrogels can be extended to >2,200% its original length [135]. Although these hydrogels exhibit unprecedented mechanical strength, their utility in tissue engineering has not been realized yet.

By carefully balancing the hydrophobicity/hydrophilicity of the hydrogel network and the molecular weight between crosslinks, mechanically tough and biodegradable hydrogels were developed from triblocks comprising a long PEG (PEG20, 20,000 g/mol) center block flanked with short trimethylene carbonate (OTMC, total of 650 g/mol) segments. Both ends of the block copolymer were methacrylated for photocrosslinking purposes [136]. The presence of long flexible chains between the crosslinking points is believed to allow the hydrogels to undergo deformation upon stress and the incorporation of short, hydrophobic OTMC blocks was found to enhance the overall mechanical properties (compressive modulus, fracture stress, toughness) of these hydrogels without compromising the swelling ratio and ability to deform under stress before breakage with near-complete recovery. Hydrogels synthesized from block copolymers with the same PEG center block but more OTMC segments were found to be brittle under the same experimental conditions. Such observations underscore the importance of fine-tuning the network parameters for the attainment of desirable hydrogel mechanical properties.

The approaches discussed above rely on the microscopic level manipulation of hydrogel compositions. Our group has developed elastomeric hydrogels by mimicking the molecular architecture and mechanical properties of natural elastin. Elastin achieves its excellent mechanical properties through a multiblock copolypeptide structure composed largely of two types of short segments that alternate along the polypeptide chain: highly flexible hydrophobic segments composed of VPGVG repeats, with many transient structures that can easily change their conformation when stretched; and alanine- and lysine- rich α -helical segments, which form crosslinks between adjacent molecules via the action of lysyl oxidase in the ECM [137]. The elasticity of the protein has been discussed primarily in terms of dominant entropic components [138, 139] and the main models of elastin's elasticity share the perspective that either chain entropy or internal chain dynamics are at least in part at the origin of the elasticity [140–142].

Our strategy involves the synthesis of multiblock hybrid polymers consisting of flexible synthetic polymers alternating with alanine-rich, lysine containing peptides that are the structural component of the hydrophilic crosslinking domains of natural elastin (Fig. 2.3a) [16]. Specifically, multiblock elastin mimetic hybrid polymers were synthesized via a condensation polymerization approach employing orthogonal click chemistry using azide-functionalized, telechelic PEG and alkyne-terminated peptides $[X(AKAAAKA)_2X]$, X: propargyl glycine, A: alanine, K: lysine] as the macromonomers. Covalent crosslinking of the resulting multiblock copolymers by HMDI was achieved universally through the lysine side chains of the peptide domain to form urea linkages. Compared to the dry samples, the fully swollen hybrid hydrogels are softer and more compressible, consistent with results observed for natural elastin [143]. Moreover, the hybrid hydrogels exhibit

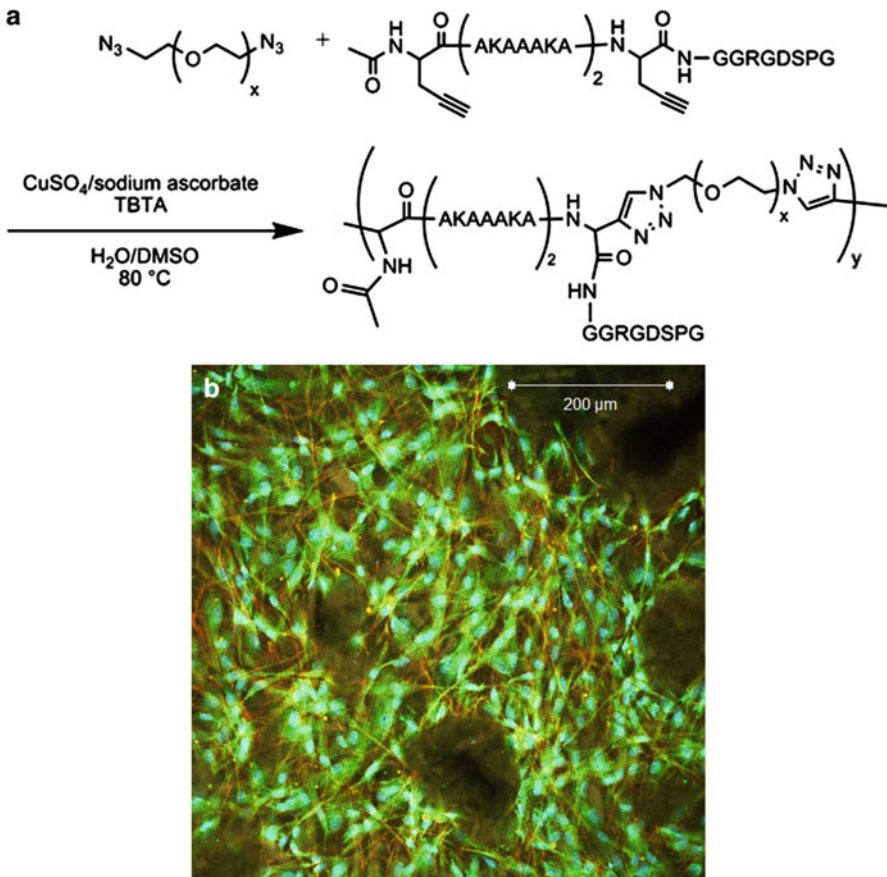


Fig. 2.3 Covalent crosslinking of RGD-containing, hybrid multiblock copolymers afforded cell-adhesive, elastomeric matrices. Unpublished results from the Jia/Kiick Groups. **(a)**. Synthesis of RGD-containing, multiblock, hybrid copolymer via Cu(I) catalyzed alkyne-azide cycloaddition. **(b)**. Immunostaining of neonatal foreskin fibroblasts cultured on the RGD-containing, covalently crosslinked, elastin mimetic hybrid hydrogels. Cells were cultured in serum-free media for 24 h. Nuclei, F-actin and vinculin were stained *blue*, *red* and *green*, respectively

similar compressive properties to a hydrophobic polyurethane elastomer (Tecoflex SG80A) widely used for tissue engineering applications. The elastin mimetic hybrid hydrogels are capable of rapid recovery from mechanical stress, as evidenced by the remarkable overlapping loading-unloading curves in the cyclic compression tests. To promote integrin-mediated cell adhesion to these gels, fibronectin-derived GRGDSP domains have been included in the peptide building blocks. Human neonatal foreskin fibroblasts (hNFF) are able to attach and proliferate readily on RGD-containing, *bis*(sulfosuccinimidyl) suberate (BS^3)-crosslinked hybrid copolymers (Fig. 2.3b). The modular nature of the design, coupled with the chemical nature of the synthesis, will permit facile adjustment of mechanical, morphological and biological properties of the resulting polymers.

2.5 Biodegradable and Bioactive Hydrogels

2.5.1 Biodegradable Hydrogels

For use as tissue engineering scaffolds, hydrogel degradation needs to be fine tuned to meet the ever-evolving needs of the cells. Matrix degradation inevitably results in alteration of the average mesh size and the swelling level, as well as the matrix viscoelasticity. On the one hand, the increased mesh size facilitates the diffusion of macromolecules and migration of the cells. On the other hand, the mechanical properties of the degrading hydrogel decrease significantly if cells residing in the matrix have not produced their own matrix components. Ideally, the degradation of the synthetic matrix should mirror the deposition of the native ECM proteins so that the physical properties of the matrix remain unchanged during the initial period of culture. Various functional groups or biological motifs have been incorporated in the hydrogel formulation, rendering the resulting matrices degradable by mild chemical and/or enzymatic processes [144].

2.5.1.1 Hydrolytically Degradable Hydrogels

Typically, synthetic hydrogels can be made biodegradable by introducing hydrolytically labile groups such as ester bonds or cyclic acetal linkages [7, 145, 146]. Hydrogels formed by photopolymerization of PEG di(meth)acrylate are non-degradable within the typical timescale of cell culture experiments, but can be rendered degradable by introducing oligo poly(esters), such as poly(lactic acid) (PLA), poly(glycolic acid) (PGA) or PCL to a PEG center block prior to the coupling of (meth)acrylate groups. By varying the composition and the length of the hydrolyzable blocks, the degradation rate can be tailored [147]. Taking advantage of the neighboring group participation-assisted hydrolysis, the degradation rate of PEG-peptide hydrogels, synthesized via a Michael addition reaction between 4-arm PEG-acrylate and cysteine-bearing peptides, was systematically modulated by tailoring the amino acid composition [148]. Installing fumaric acid to the repeating units of synthetic polymers provides unique opportunities to modulate the degradation and bioactivity of the hydrogels. While the ester bonds can be hydrolytically degraded, the abundant unsaturated double bonds facilitate crosslinking as well as bioconjugation. Bioactive and biodegradable hydrogels with varying stiffnesses have been engineered from fumarate-containing macromers.[149]

Hydrogels containing oligoesters degrade into acidic byproducts that accumulate in tissues, provoking an inflammatory response and altering scaffold degradation kinetics. To address this concern, a novel class of hydrogels containing cyclic acetal moieties in the crosslinking points was developed [145]. The hydrolysis products are neutral hydroxyl and carbonyl-terminated compounds that do not lead to significant changes in the solution/tissue pH values. Minimal inflammatory response was observed when this type of hydrogels was used in vivo to repair bone defects.

2.5.1.2

Externally Degradable Hydrogels

The degradation mechanisms described above are passive in that the hydrolysis of esters or acetals is induced non-specifically by water. One of the desirable features of synthetic hydrogel matrices is a user-controllable composition that would permit rapid recovery of viable cells under mild, non-enzymatic conditions. To this end, Prestwich and colleagues synthesized PEG-diacrylate-based crosslinkers containing disulfide linkages for covalent crosslinking of [150] thiol-modified HA and gelatin macromonomers in the presence of cells. Such a matrix permits in situ encapsulation and 3D expansion of a variety of cells. Hydrogels can be readily dissociated using the thiol-disulfide exchange reaction in the presence of *N*-acetyl-cysteine or glutathione, releasing the encapsulated cells in high yield and with high viability. Such a system is promising as a 3D platform for expanding cells in a physiologically relevant microenvironment.

Alternatively, photocrosslinked, PEG-based hydrogels were rendered photolytically degradable by incorporating a photolabile nitrobenzyl ether-derived moiety [151]. Post gelation control of the gel properties was demonstrated to introduce temporal changes, creation of arbitrarily shaped features, and on-demand pendant functionality release. Using laser rastering with a single- or two-photon laser scanning microscope, 3D channels were created in the presence of cells. Photodegradation at predetermined locales within the gels led to the deprivation of cell adhesive modalities and allowed cell migration to occur, inducing chondrogenic differentiation of encapsulated stem cells. The ability to manipulate material properties or chemistry in real time in a spatial manner provides dynamic environments to regulate cellular functions.

2.5.1.3

Enzymatically Degradable Hydrogels

A more biomimetic approach for hydrogel degradation relies on the enzymes secreted by the cells, including the cysteine and serine proteases and matrix metalloproteinases (MMPs), all of which target specific cleavage sites on ECM proteins and proteoglycans. MMP-cleavable peptide sequences have been identified and incorporated as crosslinking motifs in synthetic hydrogels to enable cell-mediated proteolysis. Hydrogel materials that were not sensitive to hydrolytic cleavage, but were susceptible to enzymatic degradation have been developed by Hubbell and co-workers [152, 153]. In their early studies, peptide-PEG-peptide triblock copolymers were synthesized and end-functionalized with acrylate groups to allow for UV-initiated photocrosslinking. The peptide sequences incorporated were potential collagenase or plasmin substrates. The resulting hydrogels were degraded under the action of the target enzyme but remained stable in the presence of the other enzyme [154]. Using vinyl sulfone-terminated multiarm PEG macromers and a cysteine-terminated MMP substrate as the crosslinker (Fig. 2.4) [155, 156], Lutolf et al. synthesized enzymatically-degradable hydrogels that have gained increasing popularity among researchers as 3D culture platforms. If a cell adhesive peptide is included, the resulting

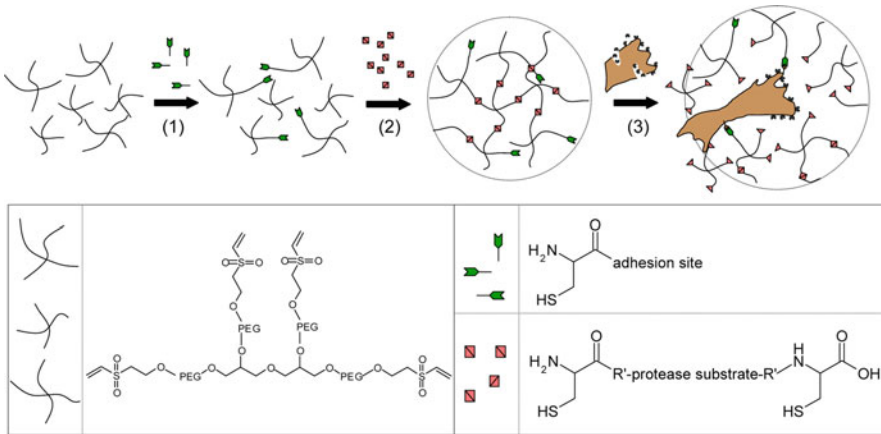


Fig. 2.4 Cell-responsive hydrogel matrices were synthesized by a two-step process using Michael type addition reaction. In the first step, vinyl sulfone-functionalized multiarm PEGs were allowed to react with mono-cysteine adhesion peptides. Subsequent reaction with *bis*-cysteine MMP substrate peptides led to the formation of elastic gels in the presence of cells. This type of hydrogel allows for cell-mediated local matrix remodeling [156]. Copyright permission from Wiley Interscience

gels allow for cell attachment and migration through a cell-mediated matrix remodeling process (see below).

Combining cell-mediated matrix remodeling with careful selection of chemical composition of the hydrogels, cellular functions can be, in turn, modulated by the enzymatic breakdown products. For example, hydrogels containing polyphosphoesters can be degraded both hydrolytically and enzymatically by alkaline phosphatase, a naturally abundant enzyme in bone matrix, and its level of expression directly correlated to the activity of osteoblasts [157, 158]. Due to their natural origin, the breakdown products of the phosphoesters are capable of binding calcium ions to induce matrix calcification, thereby recapitulating the natural event during bone formation. Finally, the ability of the calcified scaffolds to sequester cell-secreted proteins, such as osteopontin, makes this class of hydrogels attractive candidates for bone tissue engineering [159].

2.5.2

Engineering Bioactive Hydrogels

2.5.2.1

Bioactive Hydrogels with Immobilized Biological Motifs

As discussed above, tissue engineering scaffolds are designed to serve as provisional matrices for cells to proliferate, organize and perform normal cellular functions. Ideal synthetic matrices should provide an instructive microenvironment that responds to changes in cell cycles [160]. Due to their hydrophilic nature, most synthetic hydrogels exhibit minimal protein adsorption, preventing direct cell/matrix interactions. In order to design hydrogels that mediate cell attachment, integrin binding sites such as RGD peptides, alone

2 or in conjunction with other cell-binding motifs, have been incorporated [161, 162]. Unfortunately, while hydrogels modified with adhesion peptides allow cell adhesion on 2D hydrogel surfaces, adaptation of these hydrogels into 3D culture has been unsuccessful. In fact, the RGD-modified PEG gels did not seem to support sustained cell attachment and cell viability in 3D. Compared to the 2D asymmetrical substrate lying underneath them, cells in 3D are subjected to the same environment in all directions. When entrapped during the encapsulation process, cells naturally maintain the round-shape morphology, and the very small pore size and inherent non-degradability of the PEG-based cross-links prevent further spreading and migration of these cells.

A further improvement in cell-matrix interaction has been demonstrated by integrating the invasive characteristics of native ECM into the synthetic hydrogels. Using Michael-type addition reactions, RGD peptides and MMP substrates were conjugated into the PEG-based hydrogels. The resulting hydrogels contain MMP peptides bridging adjacent PEG and RGD peptides dangling from the network. The crosslinking chemistry allows for cells to be entrapped in 3D biomimetic matrices. The matrix was degradable and invasive by cells via cell-secreted MMPs, thus the properties of the matrix were directly controlled by cell cycles (Fig. 2.4). Further, primary human fibroblasts were demonstrated to proteolytically invade these networks, a process that depended on MMP substrate activity, adhesion ligand concentration and network crosslinking density [152, 155, 156]. By systematic modulation of matrix elasticity, MMP-sensitivity and the concentration of a matrix-bound RGDSP peptide, mature cardiac cells could be obtained from pluripotent cardio progenitors [163].

To further enhance the complexity of the hybrid hydrogel matrices, artificial proteins containing the repeating amino acid sequences based on fibrinogen and anti-thrombin III, comprising an RGD integrin-binding motif, two plasmin degradation sites, and a heparin-binding site was created by recombinant DNA methods and chemically grafted with PEG diacrylate (PEGDA). Subsequent photopolymerization of the macromers yielded protein-graft-PEG hydrogels. With initial Young's moduli up to 3.5 kPa, these hydrogels are (1) cell adhesive, both on 2D and in 3D; (2) cell invasive, via cell secreted serineprotease; and (3) capable of binding heparin [164]. Alternatively, researchers resort to intact proteins for enhanced biological functions. PEG-fibrinogen or PEG-fibronectin hydrogels, first described by Seliktar [165] and colleagues, were shown to support the attachment and proliferation of smooth muscle cells [166], chondrocytes [167], cardiomyocytes [168] and dorsal root ganglion in 3D [169]. PEGylation of fibrinogen or fibronectin gave rise to photocrosslinkable proteins that can be copolymerized with varying amounts of PEGDA to form 3D hybrid hydrogels in the presence of UV irradiation [170]. The addition of fibrinogen or fibronectin into this system provided an opportunity for both cell adhesion and cell-mediated degradation and remodeling of the original gels with time. The mechanical properties of PEG-fibrinogen gels can be readily tuned to match that of the targeted tissues [168]. Although hybrid protein-containing hydrogels are promising candidates for use as 3D matrices for tissue engineering, it is difficult to obtain a large quantity of pure and well-defined proteins for structure-function assessment. Chemical modification of large proteins is not trivial either.

In addition to proteins, natural ECM also contains GAGs that are not just space fillers; they perform a wide spectrum of biological functions. Their incorporation into the aforementioned synthetic matrices can further enhance their overall bioactivities. HA is an

essential ECM component that not only modulates cellular adhesion, signaling, differentiation and motility, but also plays a key role in natural wound healing, morphogenesis and cancer metastasis [171]. HA-based hydrogels have become increasingly popular as controlled release devices [172, 173] and tissue engineering matrices [24, 174–177]. Prestwich and coworkers have developed modular and hybrid hydrogels for 3D cell culture, with the goal of replicating the complexity of the native ECM environment with the minimum number of components necessary to allow cells to rebuild and replicate a given tissue. These semi-synthetic ECMs are based on HA derivatives as the matrix, modified gelatin for cell attachment, and PEGDA for stability and enhanced crosslinking kinetics. These covalently crosslinked, biodegradable hydrogels are suitable for 3D culture of primary and stem cells *in vitro*, and for tissue formation *in vivo*. The synthetic ECMs can be engineered to provide appropriate biological cues needed to recapitulate the complexity of a given ECM environment [178, 179]. Using chemically derivatized HA as the constituent building blocks, we have synthesized HA/collagen composite hydrogels composed of immature collagen fibrils interpenetrated in an amorphous, covalently crosslinked HA matrix. Porcine vocal fold fibroblasts (PVFFs) encapsulated in the matrix adopted a fibroblastic morphology and expressed genes related to important ECM proteins. PVFFs not only proliferate within the matrix but also actively remodel its viscoelasticity to an end value close to that of a mature vocal fold lamina propria [180].

2.5.2.2

Bioactive Hydrogels with Soluble Growth Factors

The development of biomimetic hydrogel matrices with spatial and temporal presentation of biochemical cues may lead to novel multifunctional platforms able to control and guide the tissue regeneration processes [181]. Unlike macroscopic, bulk hydrogel matrices, particle-based systems offer versatility to tailor the release rate and bioavailability by changing the particle composition, hydrophilicity, average particle mesh size and the overall particle size and morphology [182, 183]. In the absence of covalent coupling or physical associations between the carriers and the proteins, initial burst followed by minimum release afterwards is frequently encountered. In the native ECM, growth factors are stored as an intact, latent complex through their specific binding to ECM molecules including heparan sulfate proteoglycans (HSPGs). HSPGs, alone or through their specific binding with heparin binding growth factors, effectively modulate cellular growth, development, angiogenesis, and tissue regeneration [184].

To emulate this feature *in vitro*, Jia and colleagues [185] covalently immobilized domain I of perlecan (PlnDI), an important HSPG expressed in many ECM and basement membranes, to HA HGP through a flexible PEG linker. Compared to HGPs without PlnDI, PlnDI conjugated HGPs (HGP-P₁) exhibited significantly (higher bone morphogenic protein 2) BMP-2 binding capacity and distinctly different BMP-2 release kinetics. Heparitinase treatment increased the amount of BMP-2 released from HGP-P₁, confirming the HS-dependent BMP-2 binding. While BMP-2 was released from HGPs with a distinct burst release followed by a minimal cumulative release, its release from HGP-P₁ exhibited a minimal burst release followed by linear release kinetics over 15 days. The bioactivity of the

2 hydrogel particles was evaluated using micromass culture of multipotent mesenchymal stem cells (MSCs), and the chondrogenic differentiation was assessed by the production of glycosaminoglycan, aggrecan and collagen type II. Our results revealed that BMP-2 loaded HGP-P₁ stimulates more robust cartilage-specific ECM production as compared to BMP-2 loaded HGP, due to the ability of HGP-P₁ to potentiate BMP-2 and modulate its release with near zero-order release kinetics.

Alternatively, the therapeutic potential of growth factor cytokines can be maximized by embedding growth factor-loaded particles in a hydrogel matrix [67]. If compatible hydrogel particles, rather than hydrophobic particles, are used, these composite matrices can provide defined biological cues for tissue repair, functional angiogenesis and stem cell differentiation [186]. Using glutaraldehyde-crosslinked gelatin HGPs loaded with various growth factors, the Mikos group has demonstrated the applicability of the composite hydrogels for cartilage tissue engineering [187]. In most cases, the matrix is based on radically cross-linked OPF that is hydrolytically degradable. This technology was extended to the dual delivery of IGF-1 (insulin-like growth factor) and TGF- β 1 (transforming growth factor) by loading these growth factors into either the OPF hydrogel phase or gelatin microparticle phase of composites [188]. Release profiles were successfully manipulated by altering the phase of growth factor loading and microparticle crosslinking extent [189]. Compared to hydrogels without the HGPs, constructs containing TGF- β 1 loaded HGPs induced better chondrocyte attachment, increased the construct cellularity and maintained cell phenotype [190].

2.6 Conclusion and Future Directions

This chapter highlights the chemical and physical methods employed for hydrogel synthesis and new strategies for fine-tuning hydrogel properties, including structural characteristics, mechanical strength and biological activities. Over the past few decades, hydrogel biomaterials have evolved from passive supporting scaffolds with simple chemical composition and inferior mechanical properties to interactive matrices that are capable of providing cells with biochemical and biomechanical cues. As insight continues to be gleaned from developmental biology and other biology disciplines, more intelligent and complex hydrogel materials will likely emerge as conducive matrices for tissue repair and regeneration [1, 116, 191].

Inspirations drawn from nature have motivated researchers to develop biocompatible and biodegradable hydrogels whose materials properties and biological responses can be readily tailored for specific tissues. Strikingly, natural ECM exhibits a high degree of functional complexity, yet it is relatively simply in composition. Nature modulates the mechanical and biological properties of tissues by subtle adjustments of its composition, yet a perceivable alteration of its micro- or nano- scale organization. Its hierarchical organizations allow the matrix to take a variety of forms in different tissues and at different stages of development in the same tissue. Furthermore, biological assemblies are dynamic entities whose transitions may include the disassembly and re-assembly of some of the

subunits to accomplish local and global conformation changes. Many biological molecules exhibit distinctly different biological functions depending on whether they are in folded or unfolded states, assembled into filaments or disassembled as the monomeric units, intact or degraded. Recapitulating such responsive characteristics will likely lead to the generation of robust, dynamic and information-rich hydrogels that provide guidance cues to the embedded cells.

As the choice of the building blocks for the construction of hydrogels continues to expand, more advanced hydrogel synthesis techniques need to be developed to accommodate the ever-increasing need to build more complex hydrogels. Recent advancements in organic chemistry and polymer synthesis suggest that the preparation of well-defined polymers and nanostructure materials is possible and materials scientists are uniquely positioned to take this challenge to develop the next generation of hydrogels that are compositionally simple but functionally diverse.

Acknowledgements We acknowledge funding from the US National Institutes of Health (National Institute on Deafness and Other Communication Disorders) and the US National Science Foundation (Division of Materials Research, Biomaterials Program).

References

1. Place ES, Evans ND, Stevens MM. Complexity in biomaterials for tissue engineering. *Nat Mater* 2009;8:457–70.
2. Langer R, Vacanti JP. Tissue engineering. *Science* 1993;260:920–6.
3. Langer R, Tirrell DA. Designing materials for biology and medicine. *Nature* 2004;428:487–92.
4. Lutolf MP, Gilbert PM, Blau HM. Designing materials to direct stem-cell fate. *Nature* 2009;462:433–41.
5. Bohidar HB, Dubin P, Osade Y. *Polymer Gels: Fundamentals and Applications* (ACS Symposium Series). Washington, DC: American Chemical Society; 2003.
6. Odian G. *Principles of Polymerization*. 4th ed. Hoboken, NJ: John Wiley & Sons, Inc.; 2004.
7. Ifkovits JL, Burdick JA. Review: Photopolymerizable and degradable biomaterials for tissue engineering applications. *Tissue Eng* 2007;13:2369–85.
8. Bryant SJ, Nuttelman CR, Anseth KS. Cytocompatibility of UV and visible light photoinitiating systems on cultured NIH/3T3 fibroblasts in vitro. *J Biomater Sci Polym Ed* 2000;11:439–57.
9. Williams A, Ibrahim IT. Carbodiimide chemistry – recent advances. *Chem Rev* 1981;81:589–636.
10. Bulpitt P, Aeschlimann D. New strategy for chemical modification of hyaluronic acid: Preparation of functionalized derivatives and their use in the formation of novel biocompatible hydrogels. *J Biomed Mater Res* 1999;47:152–69.
11. Kuo JW, Swann DA, Prestwich GD. Chemical modification of hyaluronic-acid by carbodiimides. *Bioconjugate Chem* 1991;2:232–41.
12. Kuijpers AJ, van Wachem PB, van Luyn MJA, Brouwer LA, Engbers GHM, Krijgsveld J, et al. In vitro and in vivo evaluation of gelatin-chondroitin sulphate hydrogels for controlled release of antibacterial proteins. *Biomaterials* 2000;21:1763–72.
13. Liu W, Merrett K, Griffith M, Fagerholm P, Dravida S, Heyne B, et al. Recombinant human collagen for tissue engineered corneal substitutes. *Biomaterials* 2008;29:1147–58.

14. Duan X, Sheardown H. Crosslinking of collagen with dendrimers. *J Biomed Mater Res A* 2005;75A:510–8.
15. March J. *Advanced Organic Chemistry*. 4th ed. New York, NY: John Wiley & Sons, Inc.; 1992.
16. Grieshaber SE, Farran AJE, Lin-Gibson S, Kiick KL, Jia XQ. Synthesis and characterization of Elastin-Mimetic hybrid polymers with multiblock, alternating molecular architecture and elastomeric properties. *Macromolecules* 2009;42:2532–41.
17. Annabi N, Mithieux SM, Boughton EA, Ruys AJ, Weiss AS, Dehghani F. Synthesis of highly porous crosslinked elastin hydrogels and their interaction with fibroblasts in vitro. *Biomaterials* 2009;30:4550–7.
18. Welsh ER, Price RR. Chitosan cross-linking with a water-soluble, blocked diisocyanate. 2. Solvates and hydrogels. *Biomacromolecules* 2003;4:1357–61.
19. Nowatzki PJ, Tirrell DA. Physical properties of artificial extracellular matrix protein films prepared by isocyanate crosslinking. *Biomaterials* 2004;25:1261–7.
20. Merrett K, Liu WG, Mitra D, Camm KD, McLaughlin CR, Liu YW, et al. Synthetic neoglycopolymer-recombinant human collagen hybrids as biomimetic crosslinking agents in corneal tissue engineering. *Biomaterials* 2009;30:5403–8.
21. Richards FM, Knowles JR. Glutaraldehyde as a protein cross-linking reagent. *J Mol Biol* 1968;37:231–3.
22. Jia XQ, Colombo G, Padera R, Langer R, Kohane DS. Prolongation of sciatic nerve blockade by in situ cross-linked hyaluronic acid. *Biomaterials* 2004;25:4797–804.
23. Luo Y, Kirker KR, Prestwich GD. Cross-linked hyaluronic acid hydrogel films: new biomaterials for drug delivery. *J Control Release* 2000;69:169–84.
24. Gurski LA, Jha AK, Zhang C, Jia XQ, Farach-Carson MC. Hyaluronic acid-based hydrogels as 3D matrices for in vitro evaluation of chemotherapeutic drugs using poorly adherent prostate cancer cells. *Biomaterials* 2009;30:6076–85.
25. Jia XQ, Yeo Y, Clifton RJ, Jiao T, Kohane DS, Kobler JB, et al. Hyaluronic acid-based microgels and microgel networks for vocal fold regeneration. *Biomacromolecules* 2006;7:3336–44.
26. Lee KY, Bouhadir KH, Mooney DJ. Degradation behavior of covalently cross-linked poly (aldehyde guluronate) hydrogels. *Macromolecules* 2000;33:97–101.
27. Lim DW, Nettles DL, Setton LA, Chilkoti A. In situ cross-linking of elastin-like polypeptide block copolymers for tissue repair. *Biomacromolecules* 2008;9:222–30.
28. Charati MB, Ifkovits JL, Burdick JA, Linhardt JG, Kiick KL. Hydrophilic elastomeric biomaterials based on resilin-like polypeptides. *Soft Matter* 2009;5:3412–6.
29. Hermanson GT. *Bioconjugate Techniques*. 2nd ed. London, UK: Elsevier Inc; 2008.
30. Sahiner N, Jha AK, Nguyen D, Jia XQ. Fabrication and characterization of cross-linkable hydrogel particles based on hyaluronic acid: potential application in vocal fold regeneration. *J Biomater Sci Polym Ed* 2008;19:223–43.
31. Shu XZ, Prestwich GD. *Therapeutic Biomaterials from Chemically Modified Hyaluronan*. In: Garg HG, Hales CA, editors. *Chemistry and biology of hyaluronan*. 1st ed. Oxford: Elsevier Ltd.; 2004. p. 475–504.
32. Ichi T, Watanabe J, Ooya T, Yui N. Controllable erosion time and profile in poly(ethylene glycol) hydrogels by supramolecular structure of hydrolyzable polyrotaxane. *Biomacromolecules* 2001;2:204–10.
33. Ossipov DA, Piskounova S, Hilborn J. Poly(vinyl alcohol) cross-linkers for in vivo injectable hydrogels. *Macromolecules* 2008;41:3971–82.
34. Liu YC, Shu XZ, Prestwich GD. Biocompatibility and stability of disulfide-crosslinked hyaluronan films. *Biomaterials* 2005;26:4737–46.
35. Khetan S, Katz JS, Burdick JA. Sequential crosslinking to control cellular spreading in 3-dimensional hydrogels. *Soft Matter* 2009;5:1601–6.

36. Hoyle CE, Lee TY, Roper T. Thiol-enes: Chemistry of the past with promise for the future. *J Polym Sci Pol Chem* 2004;42:5301–38.
37. Cramer NB, Bowman CN. Kinetics of thiol-ene and thiol-acrylate photopolymerizations with real-time Fourier transform infrared. *J Polym Sci Pol Chem* 2001;39:3311–9.
38. Aimetti AA, Machen AJ, Anseth KS. Poly(ethylene glycol) hydrogels formed by thiol-ene photopolymerization for enzyme-responsive protein delivery. *Biomaterials* 2009;30:6048–54.
39. Salinas CN, Cole BB, Kasko AM, Anseth KS. Chondrogenic differentiation potential of human mesenchymal stem cells photoencapsulated within poly(ethylene glycol)-arginine-glycine-aspartic acid-serine thiol-methacrylate mixed-mode networks. *Tissue Eng* 2007;13:1025–34.
40. Kolb HC, Finn MG, Sharpless KB. Click chemistry: Diverse chemical function from a few good reactions. *Angew Chem Int Ed Engl* 2001;40:2004–21.
41. Malkoch M, Vestberg R, Gupta N, Mespouille L, Dubois P, Mason AF, et al. Synthesis of well-defined hydrogel networks using Click chemistry. *Chem Commun* 2006:2774–6.
42. Liu SQ, Ee PLR, Ke CY, Hedrick JL, Yang YY. Biodegradable poly(ethylene glycol)-peptide hydrogels with well-defined structure and properties for cell delivery. *Biomaterials* 2009;30:1453–61.
43. Ossipov DA, Hilborn J. Poly(vinyl alcohol)-based hydrogels formed by “click chemistry”. *Macromolecules* 2006;39:1709–18.
44. Crescenzi V, Cornelio L, Di Meo C, Nardecchia S, Lamanna R. Novel hydrogels via click chemistry: Synthesis and potential biomedical applications. *Biomacromolecules* 2007;8:1844–50.
45. Agard NJ, Prescher JA, Bertozzi CR. A strain-promoted [3+2] azide-alkyne cycloaddition for covalent modification of biomolecules in living systems. *J Am Chem Soc* 2004;126:15046–7.
46. Prescher JA, Bertozzi CR. Chemistry in living systems. *Nat Chem Biol* 2005;1:13–21.
47. Johnson JA, Baskin JM, Bertozzi CR, Koberstein JT, Turro NJ. Copper-free click chemistry for the in situ crosslinking of photodegradable star polymers. *Chem Commun* 2008:3064–6.
48. DeForest CA, Polizzotti BD, Anseth KS. Sequential click reactions for synthesizing and patterning three-dimensional cell microenvironments. *Nat Mater* 2009;8:659–64.
49. Chujo Y, Sada K, Saegusa T. A novel nonionic hydrogel from 2-methyl-2-oxazoline. 4. Reversible gelation of polyoxazline by means of diels-alder reaction. *Macromolecules* 1990;23:2636–41.
50. Wei HL, Yang Z, Zheng LM, Shen YM. Thermosensitive hydrogels synthesized by fast Diels-Alder reaction in water. *Polymer* 2009;50:2836–40.
51. Yeo Y, Geng WL, Ito T, Kohane DS, Burdick JA, Radisic M. Photocrosslinkable hydrogel for myocyte cell culture and injection. *J Biomed Mater Res Part B* 2007;81B:312–22.
52. Saxon E, Bertozzi CR. Cell surface engineering by a modified Staudinger reaction. *Science* 2000;287:2007–10.
53. Gattas-Asfura KM, Stabler CL. Chemoselective cross-linking and functionalization of alginate via staudinger ligation. *Biomacromolecules* 2009;10:3122–9.
54. Dawson PE, Muir TW, Clarklewis I, Kent SBH. Synthesis of proteins by native chemical ligation. *Science* 1994;266:776–9.
55. Hu BH, Su J, Messersmith PB. Hydrogels cross-linked by native chemical ligation. *Biomacromolecules* 2009;10:2194–200.
56. Su J, Hu BH, Lowe WL, Kaufman DB, Messersmith PB. Anti-inflammatory peptide-functionalized hydrogels for insulin-secreting cell encapsulation. *Biomaterials* 2010;31:308–14.
57. Ehrbar M, Rizzi SC, Schoenmakers RG, San Miguel B, Hubbell JA, Weber FE, et al. Biomolecular hydrogels formed and degraded via site-specific enzymatic reactions. *Biomacromolecules* 2007;8:3000–7.
58. Sanborn TJ, Messersmith PB, Barron AE. In situ crosslinking of a biomimetic peptide-PEG hydrogel via thermally triggered activation of factor XIII. *Biomaterials* 2002;23:2703–10.

59. Sperinde JJ, Griffith LG. Synthesis and characterization of enzymatically-cross-linked poly (ethylene glycol) hydrogels. *Macromolecules* 1997;30:5255–64.
60. Lee F, Chung JE, Kurisawa M. An injectable enzymatically crosslinked hyaluronic acid-tyramine hydrogel system with independent tuning of mechanical strength and gelation rate. *Soft Matter* 2008;4:880–7.
61. Liao SW, Yu TB, Guan ZB. De novo design of saccharide-peptide hydrogels as synthetic scaffolds for tailored cell responses. *J Am Chem Soc* 2009;131:17638–46.
62. Gan TT, Zhang YJ, Guan Y. In situ gelation of P(NIPAM-HEMA) microgel dispersion and its applications as injectable 3D cell scaffold. *Biomacromolecules* 2009;10:1410–5.
63. Chaikof EL. Engineering and material considerations in islet cell transplantation. *Annu Rev Biomed Eng* 1999;1:103–27.
64. Read TA, Sorensen DR, Mahesparan R, Enger PO, Timpl R, Olsen BR, et al. Local endostatin treatment of gliomas administered by microencapsulated producer cells. *Nat Biotechnol* 2001; 19:29–34.
65. Cho MH, Kim KS, Ahn HH, Kim MS, Kim SH, Khang G, et al. Chitosan gel as an in situ-forming scaffold for rat bone marrow mesenchymal stem cells in vivo. *Tissue Eng* 2008; 14:1099–108.
66. Van Tomme SR, van Steenberghe MJ, De Smedt SC, van Nostrum CF, Hennink WE. Self-gelling hydrogels based on oppositely charged dextran microspheres. *Biomaterials* 2005; 26:2129–35.
67. Hoare TR, Kohane DS. Hydrogels in drug delivery: Progress and challenges. *Polymer* 2008; 49:1993–2007.
68. Mespouille L, Hedrick JL, Dubois P. Expanding the role of chemistry to produce new amphiphilic polymer (co)networks. *Soft Matter* 2009;5:4878–92.
69. Braunecker WA, Matyjaszewski K. Controlled/living radical polymerization: Features, developments, and perspectives. *Prog Polym Sci* 2007;32:93–146.
70. Hawker CJ, Wooley KL. The convergence of synthetic organic and polymer chemistries. *Science* 2005;309:1200–5.
71. Albertsson AC, Varma IK. Recent developments in ring opening polymerization of lactones for biomedical applications. *Biomacromolecules* 2003;4:1466–86.
72. Hennink WE, van Nostrum CF. Novel crosslinking methods to design hydrogels. *Adv Drug Deliver Rev* 2002;54:13–36.
73. He CL, Kim SW, Lee DS. In situ gelling stimuli-sensitive block copolymer hydrogels for drug delivery. *J Control Release* 2008;127:189–207.
74. Millon LE, Mohammadi H, Wan WK. Anisotropic polyvinyl alcohol hydrogel for cardiovascular applications. *J Biomed Mater Res Part B* 2006;79B:305–11.
75. Yoshihito O. Equilibrium study of polymer-polymer complexation of poly(methacrylic acid) and poly(acrylic acid) with complementary polymers through cooperative hydrogen bonding. *J Polym Sci Pol Chem* 1979;17:3485–98.
76. Haglund BO, Joshi R, Himmelstein KJ. An in situ gelling system for parenteral delivery. *J Control Release* 1996;41:229–35.
77. Fujiwara T, Mukose T, Yamaoka T, Yamane H, Sakurai S, Kimura Y. Novel thermo-responsive formation of a hydrogel by stereo-complexation between PLLA-PEG-PLLA and PDLA-PEG-PDLA block copolymers. *Macromol Biosci* 2001;1:204–8.
78. Koopmans C, Ritter H. Formation of physical hydrogels via Host-guest interactions of β -cyclodextrin polymers and copolymers bearing adamantyl groups. *Macromolecules* 2008; 41:7418–22.
79. Ulijn RV, Smith AM. Designing peptide based nanomaterials. *Chem Soc Rev* 2008;37: 664–75.
80. Orbach R, Adler-Abramovich L, Zigerson S, Mironi-Harpaz I, Seliktar D, Gazit E. Self-assembled Fmoc-peptides as a platform for the formation of nanostructures and hydrogels. *Biomacromolecules* 2009;10:2646–51.

81. Schnepf ZAC, Gonzalez-McQuire R, Mann S. Hybrid biocomposites based on calcium phosphate mineralization of self-assembled supramolecular hydrogels. *Adv Mater* 2006; 18:1869–72.
82. Zhang S, Holmes TC, DiPersio CM, Hynes RO, Su X, Rich A. Self-complementary oligopeptide matrices support mammalian cell attachment. *Biomaterials* 1995;16:1385–93.
83. Holmes TC, de Lacalle S, Su X, Liu GS, Rich A, Zhang SG. Extensive neurite outgrowth and active synapse formation on self-assembling peptide scaffolds. *Proc Natl Acad Sci USA* 2000; 97:6728–33.
84. Kisiday J, Jin M, Kurtz B, Hung H, Semino C, Zhang S, et al. Self-assembling peptide hydrogel fosters chondrocyte extracellular matrix production and cell division: implications for cartilage tissue repair. *Proc Natl Acad Sci USA* 2002;99:9996–10001.
85. Semino CE, Merok JR, Crane GG, Panagiotakos G, Zhang SG. Functional differentiation of hepatocyte-like spheroid structures from putative liver progenitor cells in three-dimensional peptide scaffolds. *Differentiation* 2003;71:262–70.
86. Hartgerink JD, Beniash E, Stupp SI. Self-assembly and mineralization of peptide-amphiphile nanofibers. *Science* 2001;294:1684–8.
87. Hartgerink JD, Beniash E, Stupp SI. Peptide-amphiphile nanofibers: A versatile scaffold for the preparation of self-assembling materials. *Proc Natl Acad Sci USA* 2002;99:5133–8.
88. Stupp SI, Donners J, Li LS, Mata A. Expanding frontiers in biomaterials. *MRS Bulletin* 2005; 30:864–73.
89. Silva GA, Czeisler C, Niece KL, Beniash E, Harrington DA, Kessler JA, et al. Selective differentiation of neural progenitor cells by high-epitope density nanofibers. *Science* 2004; 303:1352–5.
90. Schneider JP, Pochan DJ, Ozbas B, Rajagopal K, Pakstis L, Kretsinger J. Responsive hydrogels from the intramolecular folding and self-assembly of a designed peptide. *J Am Chem Soc* 2002;124:15030–7.
91. Ozbas B, Rajagopal K, Schneider JP, Pochan DJ. Semiflexible chain networks formed via self-assembly of beta-hairpin molecules. *Phys Rev Lett* 2004;93:268106.
92. Yucel T, Micklitsch CM, Schneider JP, Pochan DJ. Direct observation of early-time hydrogelation in beta-hairpin peptide self-assembly. *Macromolecules* 2008;41:5763–72.
93. Ozbas B, Kretsinger J, Rajagopal K, Schneider JP, Pochan DJ. Salt-triggered peptide folding and consequent self-assembly into hydrogels with tunable modulus. *Macromolecules* 2004; 37:7331–7.
94. Kretsinger JK, Haines LA, Ozbas B, Pochan DJ, Schneider JP. Cytocompatibility of self-assembled [beta]-hairpin peptide hydrogel surfaces. *Biomaterials* 2005;26:5177–86.
95. Salick DA, Kretsinger JK, Pochan DJ, Schneider JP. Inherent antibacterial activity of a peptide-based beta-hairpin hydrogel. *J Am Chem Soc* 2007;129:14793–9.
96. Megeed Z, Cappello J, Ghandehari H. Genetically engineered silk-elastinlike protein polymers for controlled drug delivery. *Adv Drug Deliver Rev* 2002;54:1075–91.
97. Haider M, Cappello J, Ghandehari H, Leong KW. In vitro chondrogenesis of mesenchymal stem cells in recombinant silk-elastinlike hydrogels. *Pharm Res* 2008;25:692–9.
98. Banwell EF, Abelardo ES, Adams DJ, Birchall MA, Corrigan A, Donald AM, et al. Rational design and application of responsive alpha-helical peptide hydrogels. *Nat Mater* 2009;8: 596–600.
99. Petka WA, Harden JL, McGrath KP, Wirtz D, Tirrell DA. Reversible hydrogels from self-assembling artificial proteins. *Science* 1998;281:389–92.
100. Shen W, Zhang KC, Kornfield JA, Tirrell DA. Tuning the erosion rate of artificial protein hydrogels through control of network topology. *Nat Mater* 2006;5:153–8.
101. Kopecek J. Smart and genetically engineered biomaterials and drug delivery systems. *Eur J Pharm Sci* 2003;20:1–16.
102. Kopecek J. Hydrogel biomaterials: A smart future? *Biomaterials* 2007;28:5185–92.

103. Wang C, Stewart RJ, Kopecek J. Hybrid hydrogels assembled from synthetic polymers and coiled-coil protein domains. *Nature* 1999;397:417–20.
104. Miyata T, Asami N, Uragami T. A reversibly antigen-responsive hydrogel. *Nature* 1999;399:766–9.
105. Capila I, Linhardt RJ. Heparin-protein interactions. *Angew Chem Int Ed* 2002;41:390–412.
106. Fromm JR, Hileman RE, Caldwell EEO, Weiler JM, Linhardt RJ. Pattern and spacing of basic amino acids in heparin binding sites. *Arch Biochem Biophys* 1997;343:92–100.
107. Seal BL, Panitch A. Physical polymer matrices based on affinity interactions between peptides and polysaccharides. *Biomacromolecules* 2003;4:1572–82.
108. Seal BL, Panitch A. Viscoelastic behavior of environmentally sensitive biomimetic polymer matrices. *Macromolecules* 2006;39:2268–74.
109. Yamaguchi N, Kiick KL. Polysaccharide-poly(ethylene glycol) star copolymer as a scaffold for the production of bioactive hydrogels. *Biomacromolecules* 2005;6:1921–30.
110. Zhang L, Furst EM, Kiick KL. Assembly of hydrogels with controlled protein delivery profiles via the use of peptide-polysaccharide interactions. *J Control Release* 2006;114:130–42.
111. Yamaguchi N, Zhang L, Chae BS, Palla CS, Furst EM, Kiick KL. Growth factor mediated assembly of cell receptor-responsive hydrogels. *J Am Chem Soc* 2007;129:3040–1.
112. Stevens MM, George JH. Exploring and engineering the cell surface interface. *Science* 2005;310:1135–8.
113. Kong HJ, Alsberg E, Kaigler D, Lee KY, Mooney DJ. Controlling degradation of hydrogels via the size of cross-linked junctions. *Adv Mater* 2004;16:1917–21.
114. Freudenberg U, Hermann A, Welzel PB, Stirl K, Schwarz SC, Grimmer M, et al. A star-PEG-heparin hydrogel platform to aid cell replacement therapies for neurodegenerative diseases. *Biomaterials* 2009;30:5049–60.
115. Bencherif SA, Siegwart DJ, Srinivasan A, Horkay F, Hollinger JO, Washburn NR, et al. Nanostructured hybrid hydrogels prepared by a combination of atom transfer radical polymerization and free radical polymerization. *Biomaterials* 2009;30:5270–8.
116. Jia XQ, Kiick KL. Hybrid multicomponent hydrogels for tissue engineering. *Macromol Biosci* 2009;9:140–56.
117. Jha AK, Hule RA, Jiao T, Teller SS, Clifton RJ, Duncan RL, et al. Structural analysis and mechanical characterization of hyaluronic acid-based doubly cross-linked networks. *Macromolecules* 2009;42:537–46.
118. Huang T, Xu HG, Jiao KX, Zhu LP, Brown HR, Wang HL. A novel hydrogel with high mechanical strength: A macromolecular microsphere composite hydrogel. *Adv Mater* 2007;19:1622–6.
119. Martin L, Alonso M, Girotti A, Arias FJ, Rodriguez-Cabello JC. Synthesis and characterization of macroporous thermosensitive hydrogels from recombinant elastin-like polymers. *Biomacromolecules* 2009;10:3015–22.
120. Keskar V, Marion NW, Mao JJ, Gemeinhart RA. In vitro evaluation of macroporous hydrogels to facilitate stem cell infiltration, growth, and mineralization. *Tissue Eng A* 2009;15:1695–707.
121. Plieva FM, Ekstrom P, Galaev IY, Mattiasson B. Monolithic cryogels with open porous structure and unique double-continuous macroporous networks. *Soft Matter* 2008;4:2418–28.
122. Liu XH, Ma PX. Phase separation, pore structure, and properties of nanofibrous gelatin scaffolds. *Biomaterials* 2009;30:4094–103.
123. Chicurel ME, Chen CS, Ingber DE. Cellular control lies in the balance of forces. *Curr Opin Cell Biol* 1998;10:232–9.
124. Discher DE, Janmey P, Wang Y-L. Tissue cells feel and respond to the stiffness of their substrate. *Science* 2005;310:1139–43.

125. Engler AJ, Griffin MA, Sen S, Bonnetmann CG, Sweeney HL, Discher DE. Myotubes differentiate optimally on substrates with tissue-like stiffness: pathological implications for soft or stiff microenvironments. *J Cell Biol* 2004;166:877–87.
126. Ingber DE. Cellular mechanotransduction: putting all the pieces together again. *FASEB J* 2006;20:811–27.
127. Kung C. A possible unifying principle for mechanosensation. *Nature* 2005;436:647–54.
128. Kopecek J. Hydrogels: From soft contact lenses and implants to self-assembled nanomaterials. *J Polym Sci Pol Chem* 2009;47:5929–46.
129. Smith KE, Parks SS, Hyjek MA, Downey SE, Gall K. The effect of the glass transition temperature on the toughness of photopolymerizable (meth)acrylate networks under physiological conditions. *Polymer* 2009;50:5112–23.
130. Haraguchi K, Farnworth R, Ohbayashi A, Takehisa T. Compositional effects on mechanical properties of nanocomposite hydrogels composed of poly(*N,N*-dimethylacrylamide) and clay. *Macromolecules* 2003;36:5732–41.
131. Gong JP, Katsuyama Y, Kurokawa T, Osada Y. Double-network hydrogels with extremely high mechanical strength. *Adv Mater* 2003;15:1155–8.
132. Tanaka Y, Gong JP, Osada Y. Novel hydrogels with excellent mechanical performance. *Prog Polym Sci* 2005;30:1–9.
133. Okumura Y, Ito K. The polyrotaxane gel: A topological gel by figure-of-eight cross-links. *Adv Mater* 2001;13:485–7.
134. Osada Y, Gong JP. Soft and wet materials: Polymer gels. *Adv Mater* 1998;10:827–37.
135. Yang W, Furukawa H, Gong JP. Highly extensible double-network gels with self-assembling anisotropic structure. *Adv Mater* 2008;20:4499–503.
136. Zhang C, Aung A, Liao LQ, Varghese S. A novel single precursor-based biodegradable hydrogel with enhanced mechanical properties. *Soft Matter* 2009;5:3831–4.
137. Vrhovski B, Weiss AS. Biochemistry of tropoelastin. *Eur J Biochem* 1998;258:1–18.
138. Aaron BB, Gosline JM. Elastin as a random-network elastomer – a mechanical and optical analysis of single elastin fibers. *Biopolymers* 1981;20:1247–60.
139. Fleming WW, Sullivan CE, Torchia DA. Characterization of molecular motions in C¹³-labeled aortic elastin by C¹²-H¹ magnetic double resonance. *Biopolymers* 1980;19:597–617.
140. Gosline JM. Hydrophobic interaction and a model for elasticity of elastin. *Biopolymers* 1978;17:677–95.
141. Tamburro AM, Guantieri V. Classical and fractal description of elastin structure. In: Rossi C, Tiezzi E, editors. Amsterdam: Elsevier; 1991. p. 391.
142. Urry DW, Hugel T, Seitz M, Gaub HE, Sheiba L, Dea J, et al. Elastin: A representative ideal protein elastomer. *Philos Trans R Soc Lond B Biol Sci* 2002;357:169–84.
143. Lillie MA, Gosline JM. The effects of hydration on the dynamic mechanical properties of elastin. *Biopolymers* 1990;29:1147–60.
144. Eglin D, Mortisen D, Alini M. Degradation of synthetic polymeric scaffolds for bone and cartilage tissue repairs. *Soft Matter* 2009;5:938–47.
145. Falco EE, Patel M, Fisher JP. Recent developments in cyclic acetal biomaterials for tissue engineering applications. *Pharm Res* 2008;25:2348–56.
146. Kim JK, Lee KW, Hefferan TE, Currier BL, Yaszemski MJ, Lu LC. Synthesis and evaluation of novel biodegradable hydrogels based on poly(ethylene glycol) and sebacic acid as tissue engineering scaffolds. *Biomacromolecules* 2008;9:149–57.
147. Benoit DSW, Durney AR, Anseth KS. Manipulations in hydrogel degradation behavior enhance osteoblast function and mineralized tissue formation. *Tissue Eng* 2006;12:1663–73.
148. Jo YS, Gantz J, Hubbell JA, Lutolf MP. Tailoring hydrogel degradation and drug release via neighboring amino acid controlled ester hydrolysis. *Soft Matter* 2009;5:440–6.
149. Kasper FK, Tanahashi K, Fisher JP, Mikos AG. Synthesis of poly(propylene fumarate). *Nat Protoc* 2009;4:518–25.

150. Zhang JX, Skardal A, Prestwich GD. Engineered extracellular matrices with cleavable cross-linkers for cell expansion and easy cell recovery. *Biomaterials* 2008;29:4521–31.
151. Kloxin AM, Kasko AM, Salinas CN, Anseth KS. Photodegradable hydrogels for dynamic tuning of physical and chemical properties. *Science* 2009;324:59–63.
152. Lutolf MP, Hubbell JA. Synthesis and physicochemical characterization of end-linked poly(ethylene glycol)-co-peptide hydrogels formed by Michael-type addition. *Biomacromolecules* 2003;4:713–22.
153. Sakiyama-Elbert SE, Hubbell JA. Functional biomaterials: Design of novel biomaterials. *Annu Rev Mater Res* 2001;31:183–201.
154. West JL, Hubbell JA. Polymeric biomaterials with degradation sites for proteases involved in cell migration. *Macromolecules* 1999;32:241–4.
155. Lutolf MP, Lauer-Fields JL, Schmoekel HG, Metters AT, Weber FE, Fields GB, et al. Synthetic matrix metalloproteinase-sensitive hydrogels for the conduction of tissue regeneration: Engineering cell-invasion characteristics. *Proc Natl Acad Sci USA* 2003;100:5413–8.
156. Lutolf MP, Raeber GP, Zisch AH, Tirelli N, Hubbell JA. Cell-responsive synthetic hydrogels. *Adv Mater* 2003;15:888–92.
157. Li Q, Wang J, Shahani S, Sun DDN, Sharma B, Elisseeff JH, et al. Biodegradable and photocrosslinkable polyphosphoester hydrogel. *Biomaterials* 2006;27:1027–34.
158. Wachiralarpphaithoon C, Iwasaki Y, Akiyoshi K. Enzyme-degradable phosphorylcholine porous hydrogels cross-linked with polyphosphoesters for cell matrices. *Biomaterials* 2007;28:984–93.
159. Wang DA, Williams CG, Yang F, Cher N, Lee H, Elisseeff JH. Bioresponsive phosphoester hydrogels for bone tissue engineering. *Tissue Eng* 2005;11:201–13.
160. Lutolf MP, Hubbell JA. Synthetic biomaterials as instructive extracellular microenvironments for morphogenesis in tissue engineering. *Nat Biotechnol* 2005;23:47–55.
161. Gullberg D, Ekblom P. Extracellular matrix and its receptors during development. *Int J Dev Biol* 1995;39:845–54.
162. Hersel U, Dahmen C, Kessler H. RGD modified polymers: Biomaterials for stimulated cell adhesion and beyond. *Biomaterials* 2003;24:4385–415.
163. Kraehenbuehl TP, Zammaretti P, Van der Vlies AJ, Schoenmakers RG, Lutolf MP, Jaconi ME, et al. Three-dimensional extracellular matrix-directed cardioprogenitor differentiation: Systematic modulation of a synthetic cell-responsive PEG-hydrogel. *Biomaterials* 2008;29:2757–66.
164. Halstenberg S, Panitch A, Rizzi S, Hall H, Hubbell JA. Biologically engineered protein-graft-poly(ethylene glycol) hydrogels: A cell adhesive and plasm in-degradable biosynthetic material for tissue repair. *Biomacromolecules* 2002;3:710–23.
165. Gonen-Wadmany M, Oss-Ronen L, Seliktar D. Protein-polymer conjugates for forming photopolymerizable biomimetic hydrogels for tissue engineering. *Biomaterials* 2007;28:3876–86.
166. Peyton SR, Kim PD, Ghajar CM, Seliktar D, Putnam AJ. The effects of matrix stiffness and RhoA on the phenotypic plasticity of smooth muscle cells in a 3-D biosynthetic hydrogel system. *Biomaterials* 2008;29:2597–607.
167. Schmidt O, Mizrahi J, Elisseeff J, Seliktar D. Immobilized fibrinogen in PEG hydrogels does not improve chondrocyte-mediated matrix deposition in response to mechanical stimulation. *Biotechnol Bioeng* 2006;95:1061–9.
168. Shapira-Schweitzer K, Seliktar D. Matrix stiffness affects spontaneous contraction of cardiomyocytes cultured within a PEGylated fibrinogen biomaterial. *Acta Biomater* 2007;3:33–41.
169. Sarig-Nadir O, Seliktar D. Compositional alterations of fibrin-based materials for regulating in vitro neural outgrowth. *Tissue Eng A* 2008;14:401–11.

170. Dikovskiy D, Bianco-Peled H, Seliktar D. The effect of structural alterations of PEG-fibrinogen hydrogel scaffolds on 3-D cellular morphology and cellular migration. *Biomaterials* 2006; 27:1496–506.
171. Laurent TCE. *The Chemistry, Biology, and Medical Applications of Hyaluronan and its Derivatives*. Miami: Portland Press; 1998.
172. Leach JB, Schmidt CE. Characterization of protein release from photocrosslinkable hyaluronic acid-polyethylene glycol hydrogel tissue engineering scaffolds. *Biomaterials* 2005; 26:125–35.
173. Varghese OP, Sun WL, Hilborn J, Ossipov DA. In situ cross-linkable high molecular weight hyaluronan-bisphosphonate conjugate for localized delivery and cell-specific targeting: A hydrogel linked prodrug approach. *J Am Chem Soc* 2009;131:8781–3.
174. Gerecht S, Burdick JA, Ferreira LS, Townsend SA, Langer R, Vunjak-Novakovic G. Hyaluronic acid hydrogel for controlled self-renewal and differentiation of human embryonic stem cells. *Proc Natl Acad Sci USA* 2007;104:11298–303.
175. Chung C, Beecham M, Mauck RL, Burdick JA. The influence of degradation characteristics of hyaluronic acid hydrogels on in vitro neocartilage formation by mesenchymal stem cells. *Biomaterials* 2009;30:4287–96.
176. Jia XQ, Burdick JA, Kobler J, Clifton RJ, Rosowski JJ, Zeitels SM, et al. Synthesis and characterization of in situ cross-linkable hyaluronic acid-based hydrogels with potential application for vocal fold regeneration. *Macromolecules* 2004;37:3239–48.
177. Masters KS, Shah DN, Leinwand LA, Anseth KS. Crosslinked hyaluronan scaffolds as a biologically active carrier for valvular interstitial cells. *Biomaterials* 2005;26:2517–25.
178. Cai S, Liu Y, Zheng Shu X, Prestwich GD. Injectable glycosaminoglycan hydrogels for controlled release of human basic fibroblast growth factor. *Biomaterials* 2005;26:6054–67.
179. Serban MA, Prestwich GD. Synthesis of hyaluronan haloacetates and biology of novel cross-linker-free synthetic extracellular matrix hydrogels. *Biomacromolecules* 2007;8:2821–8.
180. Farran AJE, Teller SS, Jha AK, Hule R, Jiao T, Clifton RJ, et al. Three Dimensional culture of vocal fold fibroblasts: Effects of matrix composition and microstructure on cellular functions. *Tissue Eng Epub ahead of print*; PMID: 20064012.
181. Biondi M, Ungaro F, Quaglia F, Netti PA. Controlled drug delivery in tissue engineering. *Adv Drug Deliv Rev* 2008;60:229–42.
182. Oh JK, Drumright R, Siegwart DJ, Matyjaszewski K. The development of microgels/nanogels for drug delivery applications. *Prog Polym Sci* 2008;33:448–77.
183. Goldberg M, Langer R, Jia XQ. Nanostructured materials for applications in drug delivery and tissue engineering. *J Biomater Sci Polym Ed* 2007;18:241–68.
184. Farach-Carson MC, Hecht JT, Carson DD. Heparan sulfate proteoglycans: key players in cartilage biology. *Crit Rev Eukaryot Gene Expr* 2005;15:29–48.
185. Jha AK, Yang WD, Kirn-Safran CB, Farach-Carson MC, Jia XQ. Perlecan domain I-conjugated, hyaluronic acid-based hydrogel particles for enhanced chondrogenic differentiation via BMP-2 release. *Biomaterials* 2009;30:6964–75.
186. Norton LW, Tegnell E, Toporek SS, Reichert WM. In vitro characterization of vascular endothelial growth factor and dexamethasone releasing hydrogels for implantable probe coatings. *Biomaterials* 2005;26:3285–97.
187. Holland TA, Tabata Y, Mikos AG. In vitro release of transforming growth factor-beta 1 from gelatin microparticles encapsulated in biodegradable, injectable oligo(poly(ethylene glycol) fumarate) hydrogels. *J Control Release* 2003;91:299–313.
188. Holland TA, Tabata Y, Mikos AG. Dual growth factor delivery from degradable oligo(poly(ethylene glycol) fumarate) hydrogel scaffolds for cartilage tissue engineering. *J Control Release* 2005;101:111–25.

189. Holland TA, Bodde EWH, Baggett LS, Tabata Y, Mikos AG, Jansen JA. Osteochondral repair in the rabbit model utilizing bilayered, degradable oligo(poly(ethylene glycol) fumarate) hydrogel scaffolds. *J Biomed Mater Res A* 2005;75A:156–67.
190. Park H, Temenoff JS, Holland TA, Tabata Y, Mikos AG. Delivery of TGF-beta 1 and chondrocytes via injectable, biodegradable hydrogels for cartilage tissue engineering applications. *Biomaterials* 2005;26:7095–103.
191. Huebsch N, Mooney DJ. Inspiration and application in the evolution of biomaterials. *Nature* 2009;462:426–32.

Wan-Ju Li and James A. Cooper Jr.

Contents

3.1	Introduction	48
3.2	Rationale for Using Fibers as a Scaffolding Material	49
3.2.1	Favorable Structural Properties	49
3.2.2	Imitation of Extracellular Matrix	49
3.2.3	Structural and Property Versatility	50
3.3	Microfibrous Scaffolds	50
3.3.1	Fabrication	50
3.3.2	Biomedical Applications	54
3.4	Nanofibrous Scaffolds	57
3.4.1	Fabrication	58
3.5	The Electrospinning Technique	60
3.5.1	Setup	60
3.5.2	Fabrication and Properties of Electrospun Nanofibrous Scaffolds	61
3.5.3	Biological Enhancement with Nanofibrous Scaffold	63
3.5.4	Biomaterials for Nanofibrous Scaffolds	64
3.5.5	Comparison Between Microfibrous and Nanofibrous Scaffolds	65
3.5.6	Nanofibrous Scaffolds for Tissue Engineering Applications	66
3.6	Future Directions	68
	References	69

Abstract Fibers are a continuous material structure that have an extremely high ratio of length to width, and are particularly suitable for fabrication into biomaterial scaffolds for tissue engineering since fibrous structures can morphologically resemble extracellular matrix components in tissues. In addition, fibers can be collected and processed into complex fibrous networks using conventional textile techniques, such as knitting, weaving,

W.-J. Li (✉)

Department of Orthopedics and Rehabilitation, University of Wisconsin-Madison, 1111 Highland Ave., WIMR 5051, Madison, WI 53705, USA
e-mail: li@ortho.wisc.edu

J.A. Cooper Jr.

Department of Biomedical Engineering, Rensselaer Polytechnic Institute, 110 8th Street, Center for Biotechnology and Interdisciplinary Studies, Room 3139, Troy, NY 12180, USA
e-mail: coopej5@rpi.edu

3 or braiding, to create three-dimensional (3D) structures with improved structural and mechanical properties. Recently, there is a growing interest in using nanofabrication techniques to fabricate nanometer-sized fibers for tissue engineering. Nano-sized fibers exhibit enhanced physical and biological properties that are favorable for effective biomaterial scaffolds, compared to micro-sized fibers. While great progress using fibrous scaffolds to grow various human tissues has been made, it is important for scaffold-based tissue engineering to develop the next generation “smart” scaffolds capable of promoting cell-matrix interactions through a bio-inspired surface, and inducing favorable biological activity via controlled release of incorporated biological molecules.

Keywords Microfiber • Nanofiber • Scaffold • Tissue engineering

3.1 Introduction

The use of fibrous biomaterials date back to the ancient Egyptians and American Indians. These biomaterials were among the earliest materials processed in ancient times into textile structures for medical devices, such as bandages and sutures [1–3]. The Egyptians used fibers to draw wounds together, and the American Indians used horse hair, cotton and leather for the same purpose [1–3]. Fibrous biomaterials with the versatility of being fabricated into structures with unique hierarchical architectures have been extensively used in medical applications during modern times. Specifically, over the past few decades with the advent of polymer and fiber processing technologies, fibrous biomaterials have met with success in wound healing, implantation, and tissue engineering.

Fibers are a continuous material structure that have an extremely high ratio of length to width. Fibers can be made of continuous or short-length monofilaments and multifilaments. Filaments are the basic unit of fibrous biomaterials, and are usually circular in shape but can be in other extruded shapes as well. The filaments can be natural or synthetic polymers, degradable or non-degradable. Once the fibers are formed of filaments, they can be processed into textile structures for various biomedical applications.

Textile processing techniques allow fibers to be fabricated into more complex fibrous structures. Two-dimensional (2D) and 3D textiles are made by interlacing, intertwining or interlooping fibers. By fabricating textiles with various arrangements of fiber architecture, the structure can have a wide range of pore sizes and geometries, and structural properties. Textiles can be fabricated into 3D structures with knitted, woven, non-woven, felted, plaited, and braided fibers. The 3D textiles are porous structures that have been shown to support tissue ingrowth in tissue engineering and regeneration applications. For example, tendon and ligament prostheses are usually made of flexible textile structures that consist of woven or braided microfibers. These textile structures are usually highly porous, which helps the transportation of oxygen and nutrients throughout the structure for cell growth, and allows the regeneration of a new tissue between the pores. Physically, the structures composed of the well-integrated fiber network are able to handle the biomechanical demand for ligaments and tendons.

This chapter is focused on discussing the importance of using fibrous structures as tissue engineered scaffolds, introducing two types of fibrous biomaterial matrices, microfibrinous and nanofibrous scaffolds, comparing their potential of biological regulation, and finally discussing the scaffold fabrication methods, properties, and biomedical applications.

3.2

Rationale for Using Fibers as a Scaffolding Material

3.2.1

Favorable Structural Properties

For tissue engineering applications, a biomaterial scaffold made of a biodegradable polymer should be a 3D, porous structure that functions to accommodate cells and support tissue mechanics. In the past few years, many different structured scaffolds have been developed to culture cells for various types of tissue engineering applications [4]. These 3D, porous scaffolds, including sphere-, sponge-, gel-, and fiber-based structures produced by different fabrication approaches have a wide spectrum of properties owing to their distinct structural architecture. Among these structures, fibers are particularly suitable for being fabricated into biomaterial scaffolds since fibrous structures can morphologically resemble collagen fibers that are the major extracellular matrix (ECM) component in tissues. In addition, fibers can be fabricated into different lengths, diameters, and shapes to meet specific requirements of scaffolds for various tissue engineering applications. For example, emerging nanofabrication techniques, such as electrospinning, have been used to produce nanometer-scaled fibers dimensionally similar to collagen fibrils, whereas conventional fiber spinning techniques are utilized to produce larger, micrometer-sized fibers [5]. In addition, scaffolds made of fibers are predisposed to have a larger surface area, as compared to other structured scaffolds, and the availability of a larger surface can be beneficial to accommodate more cells in the scaffold. In general, fibrous scaffolds are highly porous and pores in the structure are well interconnected. These structural properties make fibrous scaffolds favorable for tissue engineering.

3.2.2

Imitation of Extracellular Matrix

Collagen is the most abundant protein that provides the structural framework of many tissues in our body and holds responsibility for shape and biomechanical properties, such as tensile properties. There are 27 different collagens that have been identified in vertebrates and each of them has its unique biochemical composition and structural feature [6]. Among all of the distinct collagens, collagen type I is the most plentiful collagen and can be found in bone, dermis, tendon, ligament, cornea, and most other tissues. Structurally, a micrometer-sized collagen type I fiber is a hierarchical macromolecule assembled of nanometer-sized collagen fibrils, and each collagen fibril is composed of procollagens, a triple helix

3 structure formed of two $\alpha 1(I)$ and one $\alpha 2(I)$ polypeptides [7]. Previous experimental results showed that the average diameter of a collagen type I fibril was around 100 nm [8], and with the fibrils assembling into a collagen fiber, the average diameter of the collagen fiber could range from 1 to 100 μm [9]. Notably, the hierarchical structure of a collagen fiber that is assembled of multiple smaller fibrils can effectively strengthen tensile properties of the fiber, which is important for collagen fibers to successfully carry out the mechanical role in tissues with high mechanical demand, such as tendon or ligament. The tensile modulus increases from collagen fibers (54 ± 25 MPa) to tendon tissue (1390 ± 53 MPa) with the level of structural complexity [9]. Artificial fibers fabricated by the emerging nanofabrication technique have been shown to morphologically and mechanically resemble native collagen fibrils. For example, ultra-fine fibers, both synthetic and natural, with the diameter of a few to several hundreds nanometers can be fabricated to imitate the size of collagen fibrils. Mechanical properties of the nano-sized fibers comparable with those of native collagen fibrils can be tailored with careful selection of materials and fabrication approaches [10]. With the capability of closely imitating natural ECM morphology, fiber is a suitable material form for scaffold fabrication.

3.2.3

Structural and Property Versatility

Another advantage of using fibers as a tissue engineered scaffold is that fibers can be collected and processed into a complex structure using conventional textile techniques, such as knitting, weaving, or braiding. These techniques integrate linear, individual fibers into a fibrous network to create a 2D or 3D fabric with improved structural and mechanical properties. Depending on the type of technique used to process fibers, the fabrics have distinct fibrous structures and properties. Interestingly, the finished textile structure often features enhanced macroscopic properties, such as improved mechanical properties [11], while still retaining microscopic properties of the composing fibers, such as fiber texture. For example, fibers (primary structure) can be collected and made into a fiber bundle known as a yarn (secondary structure), and the multiple yarns can be weaved, knitted, or braided into woven structures (tertiary structure) (Fig. 3.1). The braided fabric may be ideal as a tissue engineered scaffold because it has the microscopic fiber texture that may be favorably recognized by cells as collagen fibers, and also features a hierarchical fibrous structure as a tissue scaffold mimic, providing sufficient mechanical strength through the fiber integration approach.

3.3

Microfibrous Scaffolds

3.3.1

Fabrication

Microfibers used in medical textile applications are made from natural polymers, such as silk, chitosan, alginate, cotton, wool and collagen, and synthetic polymers include

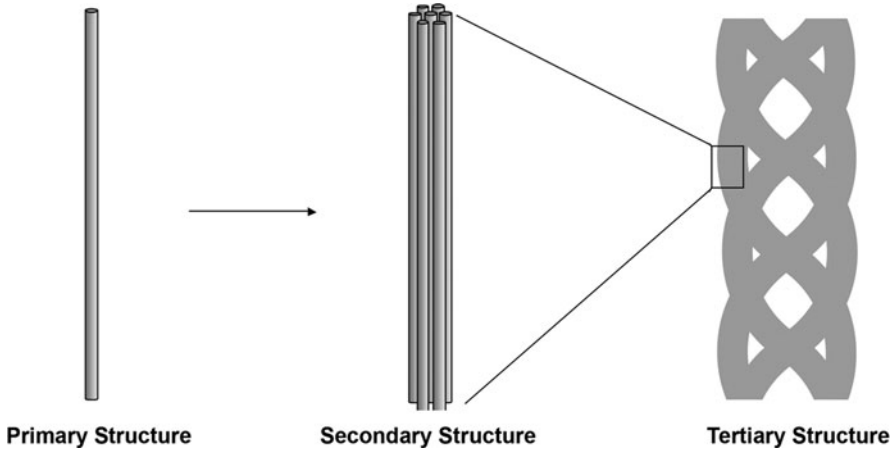


Fig. 3.1 Illustration of the hierarchical structure of a braided fibrous material. The tertiary structure of a braided fibrous material is composed of the secondary structure of fiber bundles that is made of the primary structure of fibers

non-biodegradable polymers, such as polyethylene, polypropylene, polytetrafluoroethylene, nylon, aramids and polyethylene terephthalate, as well as biodegradable polymers, such as polyglycolide (PGA), polylactide-co-glycolide (PLGA), polylactide (PLA), poly(p-dioxanone), and poly(alkylene oxalates). Examples of techniques used to process the raw material into microfibers which can be handled and fabricated into scaffolds are extrusion, fiber spinning, rapid prototyping, and various textile processing techniques [3, 12].

3.3.1.1

Polymer Extrusion

Polymer extrusion is a fabrication process based on the ability of the material to undergo a plastic deformation. A screw moves within a heated chamber that is filled with pellets of the polymer causing them to melt and mix into a continuous stock. This stock fluid is viscous and is fed through an orifice and cooled by air or water to solidify the shape of the polymer. The extrusion method is used to make polymeric fibers which can then be used to fabricate particular scaffolds.

3.3.1.2

Fiber Spinning

Another technique used to produce microfibrillar materials is called fiber spinning. Fiber spinning is a modification of the extrusion process in which the molten polymer is pumped through a spinneret which is usually a plate with many holes to form single fibers upon cooling. The strength and size of these fibers during fabrication can be tailored by drawing

and applying tension on the fibers along its main extruding axis. Fibers made through the fiber spinning process have been used to fabricate vascular, ligament, and tendon grafts. In addition, these fibers have been used to make microfibrinous scaffolds to provide cells with 3D topography by weaving, knitting, and braiding. These microfibrinous scaffolds are fabricated with desired porosity for tissue ingrowth depending on the diameter and packing density of the fibers.

3.3.1.3

Rapid Prototyping

Most recently, rapid prototyping has been used to produce ordered 3D structures that possess an intricate network of fibers and interconnected pores. The fabrication of tissue engineered fibrous scaffolds begins with generating a mold with the architecture identical to a target tissue scanned by magnetic resonance imaging (MRI) or computed tomography (CT). These models are then used with rapid prototyping techniques, such as stereolithography, fused deposition modeling (FDM- extrusion process), 3D printing (3-DP-inkjet printing process), laminated object manufacturing (LOM), and selective laser sintering (SLS), to produce layered laminated fibrous structures [3, 12, 13]. The thickness of the layers is hundreds of microns after the polymer fibers are deposited on an x-y base platform in multiple layers. The development of fibrous scaffolds by these methods has been used to investigate bone tissue engineering.

3.3.1.4

Various Textile Processing Techniques

The fabrication of textile structures of knitted, woven, non-woven and braids provide the options which can be used to develop fibrous scaffolds. These techniques commonly used in textile industry are considered a post-fabrication process to manipulate fibers to produce 3D fibrous scaffolds with different structures and properties.

Knitted fabrics are interlooped structures wherein the knitting loops are either produced by the introduction of the knitting yarn in the cross machine direction (weft knit), or along the machine direction (warp knit), producing a large number of stitch geometries. A wide range of pore geometries can be generated by controlling the stitch (loop) density [14]. The maximum fiber packing density of knitted structures is lower than that of the woven fabrics because of interloped nature. The high level of conformability and porosity of weft knitted fabrics make them ideal candidates for vascular implants [15, 16].

Woven fabrics are fabricated by interlacing yarns and there are hundreds of possible woven fabric combinations. The fiber orientation of woven fabrics can be divided into biaxial and triaxial woven structures. Biaxial weaves consist of 0° and 90° yarns interlaced in various repeating patterns [14], whereas the triaxial weave is the $90 \pm 60^\circ$ hexagonal yarn orientation in one plane, resulting in a high level of in-plane shear resistance. High levels of isotropy and dimensional stability can be achieved with triaxial weave at a very low fiber volume fraction [14].

Nonwoven textiles are manufactured by a process of direct conversion of fibers to fabrics. The two major classes of nonwovens are chemically and mechanically bonded, the mechanically bonded systems tend to be high bulk, thick and nonporous. The chemically bonded nonwovens tend to be more paper-like, thin, low bulk and less porous. As a result, the mechanically bonded nonwovens are more permeable, extensible, and compressible, and have higher extensibility than chemically bonded nonwovens [14].

Braids are textile structures produced by intertwining two or more yarns together. The braiding process is one of the oldest technologies known to man, which includes hair, rope, and art forms of ancient civilizations. In the eighteenth century, braiding turned from an art to a scientific technology when Weber-Partenheimer developed the first braiding machine [17]. Braiding technology is used in many critical applications due to its structural integrity, durability, design flexibility, and precision [17, 18]. Braided fabrics can be formed into a flat or tubular shape. The biasing of the interlacing yarns can make them conformable, shear resistant and tolerant to impact damage (3D braid) [17–21]. The geometric parameters which determine the shape and fiber architecture of braids include braiding angle distribution, yarn volume fraction, and if a mandrel is used, coverage factors. The braiding angle can range from 5° to 85° theoretically, but because of geometric limitations of yarn jamming, the braiding angle depends on yarn size and mandrel diameter, as presented by Ko [21]. These parameters also include the number of carriers and braiding yarn width. Braids have been used in medical applications such as sutures and ligaments because of their high level of torsional stability. Braid geometry is defined by the braiding angle, which is half the angle of the intertwining between yarn systems with respect to the braiding direction [17, 18]. Tightness of the braid is represented by the frequency of intertwining. The distance between intertwining points is known as the pick spacing. The basic formation technique of braiding is the intertwining of yarn carriers on a track plate through position displacement. The carriers control the tension of the braiding yarns and they are attached to a forming point to control the dimension and shape. A braided structure with two braiding yarns in the thickness is considered 2D braiding. Three-dimensional braiding is when three or more braiding yarns in the thickness of the fabric are used to form an integral braided structure. Three-dimensional braids for composites were first developed in the late 1960's during the development of a multidirectional reinforced composite for aerospace applications [17, 18, 21]. The 3D braided structure is a 3D network of continuous, yarn bundles with a fibrous architecture oriented in various directions. The internal structure of the 3D braid is characterized by continuous fibers oriented and integrated in three or more directions. These braids have more than three yarn bundle diameters in the through-thickness direction that enable it to be distinguished from the 2D braided structures that gain thickness through intertwining multiple layers of fabric together. The 3D braiding system can produce thin and thick structures in a wide variety of shapes through the selection of yarn bundle sizes and braided architecture.

There are two types of braiding looms used in 3D braiding, circular machines for hollow shapes and rectangular machines for solid rectangular shapes. Studies have explored braided structures toward the formation of 3D braided structures to replace anterior cruciate ligaments [16, 22–24]. The 3D braided composites like other traditional 2D braided composites have mechanical properties that are dependent on fiber orientation and volume fraction. Theoretically, it has been determined that the maximum fiber volume fraction or

volume of fiber packing in a 3D braided composite is approximately 68% without distortion [19, 21]. The theoretical braiding angle of 55° or larger is greater than the experimental braiding angle because the theoretical angle does not take into account the physical properties of the fiber such as flexibility. It has been shown that the tensile strength and modulus of the 3D braid composites tend to increase as fiber bundle size increases. This is due to the relationship between fiber bundles and fiber orientation. For example, the use of large fiber bundle sizes can produce lower crimp or lower fiber angles that correspond to higher strength and modulus. The circular braids are usually higher in tensile strength and modulus compared to rectangular braids due to the straight configuration of their longitudinal yarns, whereas rectangular braids have crimps in their longitudinal yarns [21].

Previous ligament prostheses have been made of flexible composites consisting of fibers that have been woven or braided into structures. These composite structures as tissue prostheses have problems of poor tissue integration, poor abrasion resistance and fatigue failure [25]. On the other hand, 3D braided structures can overcome some of these problems through the development of an interconnected network of porous structures that help the transportation of oxygen and nutrients throughout the implant site. The flexible, porous 3D braids allow the regeneration of new tissue between the pores and serve as scaffolds for cell proliferation. These 3D fibrous braids must also handle the biomechanical stresses of ligaments. Moreover these 3D braided structures are suitable for this application because they are more durable to fatigue and impact resistance, compared to 2D braided composites. This gives the 3D braided structures high damage resistance during the initial implantation period as the body adjusts to the implant. Therefore, the circular and rectangular 3D braiding processes mentioned above would be beneficial to the construction of an artificial ligament replacement. The 3D braids have sufficient strength and high flexibility in the longitudinal direction and are able to reduce or prevent the damage that normally causes severe fragmentation in other braided structures placed in the body [25].

3.3.2

Biomedical Applications

Fibrous biomaterials are used externally and internally for medical applications. External applications of woven and nonwoven textiles include wound dressings, surgical garments, sheets, and adhesive tapes. Internal applications are primarily used in wound repair and soft tissue replacements [3, 12, 15, 16].

3.3.2.1

Wound Healing

Fibrous biomaterials for surgical applications include sutures to close wounds and fabrics for wound dressings and soft tissue support. Sutures are available as monofilaments and multifilament braids and used to provide a sufficient level of strength to close wound or compress blood vessels in order to stop bleeding. Sutures can be composed of biodegradable PGA or nondegradable polypropylene. In the case of soft tissue support interwoven

patches can be used to allow platelets and clotting factors to adhere over areas of bleeding. Medical textiles made of fibrous materials are also used in reconstructive surgery as implants. For example, hernia mesh made of polypropylene and PLA have been used to reinforce the muscles in the abdomen for hernia repair [26–28].

3.3.2.2

Cardiovascular Implant

Cardiovascular applications of fibrous biomaterials include vascular grafts, prosthetic heart valves, and heart assist devices. Voorhees and associates first postulated to replace diseased blood vessels with synthetic grafts [29]. This study led to the use of Dacron (polyethylene terephthalate) and expanded (polytetrafluoroethylene (ePTFE)) grafts in cardiovascular surgery [30]. Dacron and ePTFE have been successful for large diameter blood vessel replacement but smaller vessel grafts developed with these materials have the problems of thrombosis. Tissue engineered vascular grafts have been fabricated from novel bioabsorbable polymers (PGA/poly-4-hydroxybutyrate) and sequentially seeded with bovine vascular myofibroblasts and endothelial cells [31]. In this particular study, the mechanical properties of pulsed vascular grafts comprised supra-physiological burst strength and suture retention strength appropriate for surgical implantation. It demonstrates the feasibility of tissue engineering of viable, surgically implantable small caliber vascular grafts and the important effect of a biomimetic in vitro environment on tissue maturation and ECM formation [31]. Studies by Niklason and associates have also shown the effectiveness of pulsatile flow conditions using biodegradable polymeric meshes for vascular grafts [32]. Developing cardiovascular implants with favorable porosity, hemocompatibility, and mechanical compliance, is a challenge but can be achieved using fibrous composite scaffolds. The proper selection of biodegradable fibrous materials will allow the development of functional tissue engineered cardiovascular scaffolds by providing a proper environment for cells to differentiate and regenerate the tissue.

3.3.2.3

Musculoskeletal Tissue Engineering

Fibrous porous mats have been used as scaffolds for tissue ingrowth and stabilization for orthopaedic, reconstructive and maxillofacial surgeries. Musculoskeletal applications of fibrous scaffolds have been focused on skin, cartilage, tendon, rotator cuff, muscle, and ligament [33]. In general, fibrous scaffolds must follow the same requirements of tissue engineering scaffolds: being biodegradable to allow for tissue regeneration, being porous to maintain space for tissue ingrowth and nutrient transport, supporting cell adhesion so that cells can attach and proliferate, supplying signaling factors to guide and regulate the cells in the regenerated tissue, and lastly being the load bearer in mechanically active sites.

An excellent example of a fibrous scaffold that meets these requirements during regeneration is the ligament replacement. Scaffolds used for the ligament regeneration

require high tensile strength and adequate elasticity to handle the cyclic loading and contraction. The scaffold must also transfer the biodynamic stresses to the neo-ligament tissue so that no stress shielding occurs. In previous studies, it has been shown that fibrous biomaterial and scaffolds are critical to the success or failure of the ligament replacement [22, 24, 25]. Analysis of failed fibrous scaffolds for ligament replacement by Guidion and associates has shown how important scaffold design and material properties are for tissue infiltration and regeneration of ligament [25]. In other studies by Cooper and associates, the design of fibrous scaffolds was described and ligament regeneration was assessed in a rabbit model using a ED braided fibrous scaffold [24, 33–36]. In Fig. 3.2, a scanning electron microphotograph is shown as an example that illustrates the interwoven yarns form a 3D rectangular braided structure. In 3D braiding, pores are created in the space between the intertoven yarns in an orderly orientation with a braiding angle. In Fig. 3.3, a photograph of a 3D braided scaffold designed as a ligament replacement for a rabbit model is shown. The center of the replacement has an open porous structure to allow for anterior cruciate ligament replacement and tissue ingrowth for regeneration. The ends of the fibrous scaffold have a tighter braiding angle to handle the rigors of fixation within the bone tunnel and to allow for bone tissue ingrowth after the ligament replacement is implanted.

Fibrous scaffolds have also been used in the regeneration of cartilage tissue. Previous studies have used nonwoven mesh scaffolds of PGA fibers to produce cartilage *in vitro* [36, 37]. Currently, Moutos and associates have developed a microscaled 3D weaving technique to produce anisotropic 3D woven structures for novel composite scaffolds that are infiltrated with a chondrocyte–hydrogel mixture to create cartilage tissue constructs [38]. Briefly, these scaffolds showed mechanical properties of the same order as native articular cartilage. These scaffolds show the unique potential of fibrous structures for load-bearing immediately after the implantation *in vivo* with biological support for cell-based tissue

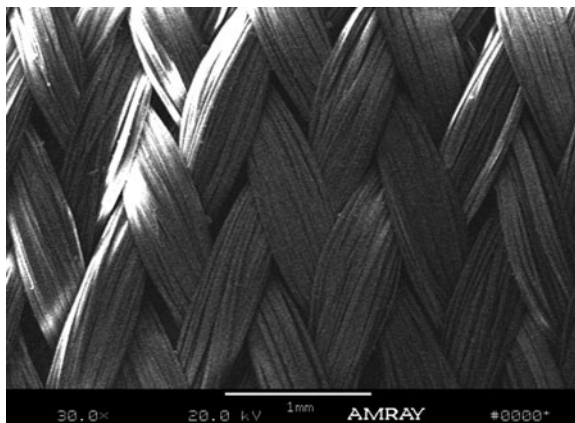


Fig. 3.2 Scanning electron photomicrograph of the surface yarns of a poly(lactide) 4×12 three-dimensional rectangular braid



Fig. 3.3 A photograph of a poly lactide, three-dimensional 5×5 square braid developed for ligament regeneration research in an in vivo rabbit model study; open structure substitute for intra-articular anterior cruciate ligament and tighter braided edge region for bone tunnel fixation

regeneration without requiring cultivation in vitro [12, 38]. Therefore, the development of fibrous scaffolds with the functional mechanical compliance can lead the success tissue engineered scaffolds that require less pre-conditioning before implantation.

3.4 Nanofibrous Scaffolds

In recent years, there is a growing interest in using nanofabrication techniques to fabricate nanometer-sized fibers for tissue engineering. The upward trend can be found from the increasing number of scientific publications containing the keywords “nanofiber” and “tissue engineering” when performing the PubMed search; the number increases from 5 to 149 during the first decade of the 2000s. With the properties of high porosity, variable pore-size distribution, high surface area-to-volume ratio, and morphological similarity to natural collagen fibrils, nanofibrous scaffolds are promising in enhancing biologically favorable cell-matrix interactions [5]. It is anticipated that the growing interest of using nanofibrous scaffolds for tissue engineering will continue and more breakthrough findings will be revealed.

A number of techniques based on different physics principles have been developed to fabricate structures comprising nanometer-sized fibers. These techniques including but not limited to phase separation [39], self-assembly [40], and electrospinning [41], use either the bottom-up (i.e., materials are assembled molecule by molecule) or top-down (i.e., materials are broken down into their respective components) approach to fabricate the ultra-fine fibers. Nanofibrous structures fabricated by different techniques have distinct fiber morphologies and mechanical properties that can be used for meeting the specific needs of various engineered tissues.

3.4.1

Fabrication

3.4.1.1

Phase Separation

Phase separation is a relatively simple technique that uses the principle of thermally induced phase separation to fabricate nanofibrous scaffolds. In the process, the polymer is dissolved in a solvent, and then the resulting polymer solution is quenched to form two phases, a polymer-rich and a polymer-lean solvent phase. The solvent in the polymer-lean solvent phase is then removed by sublimation, extraction, or evaporation, leaving the polymer-rich phase behind and forming a porous polymeric scaffold. Depending on the type of solvent and polymer, the quenching temperature, and the concentration of polymer solution used in the fabrication process, the morphology of structure and the diameter of nanofiber can be greatly affected. For example, Zhang et al. fabricated poly(L-lactic acid) (PLLA) nanofibrous scaffolds from 1 to 5% (W/V) PLLA/Tetrahydrofuran (THF) solutions [42]. The diameters of nanofibers in the nanofibrous scaffolds are in the range of 50–500 nm, but the 1% PLLA scaffold was more porous and less strong than the 5% one. Interestingly, though phase separation-fabricated nanofibrous scaffolds feature the high porosity of 98%, pore space between nanofibers are relatively small for cells to migrate through. An alternative approach has been introduced to increase pore size of the scaffold by adding porogens, such as sugar, salt particles, or paraffin spheres, into the polymer solution before the fabrication [39]. The phase separation approach can create both micro- and nano-architecture in nanofibrous scaffolds for enhancing even cell distribution and efficient mass transport.

Phase separation-fabricated nanofibrous scaffolds have been seeded with the MC3T3-E1 mouse osteoblasts for potential bone tissue engineering applications [43]. The research results show that PLLA nanofibrous scaffolds significantly enhance expression of bone markers, such as osteocalcin, bone sialoprotein, and alkaline phosphatase, compared to PLLA films, suggesting that the architectural feature of a nanofibrous scaffold affects cell activities and phase separation-fabricated nanofibrous scaffolds are promising for bone tissue engineering.

3.4.1.2

Self-Assembly

Self-assembly is a process in which molecules are spontaneously organized into an aggregate with a well-defined structure. Many biological molecules in our body tend to use the mechanism to stabilize their structure, prevent degradation, or form a structure required for specific biological activities. For example, lipid molecules can spontaneously aggregate into micelles in an aqueous solution. Recently, the principle of self-assembly has been applied to fabricate nanometer-sized fibers using synthesized molecules with the well-defined chemistry for applications of 3D culture or tissue engineered scaffolds [44]. The most extensively investigated molecules are oligopeptides with complementary positive- and negative-charged, and hydrophilic and hydrophobic residues. When

dissolved in an aqueous solution, the charge-complementary oligopeptides spontaneously assemble into a macrostructure forming a nanofiber [45]. Compared to the phase separation technique that is based on a top-down approach, self-assembly uses a bottom-up approach to fabricate nanofibers. Giving that nanofibers are formed by the different mechanisms, scaffolds fabricated using the two techniques have distinct physical and chemical properties. For example, scaffolds made of self-assembly nanofibers are in a gel-form whereas those made of phase separation nanofibers are in a dehydrated-form.

The self-assembly process forming nanofibers can be best described as a process similar to putting pieces of Legos together into a large assembly. In the assembly process, the molecular Legos, oligopeptides, are self-assembled via weak, non-covalent bonds, i.e., ionic bonds, hydrophobic interactions, van der Waals interactions, and water-mediated hydrogen bonds [44]. To date, much of the work on self-assembly in tissue engineering has been focused on the fabrication of 3D nanofibrous scaffolds using amphiphilic peptides. One of the samples is the commercially available product, Pur-aMatrix. This product uses 16 amino acid oligopeptides with positive- and negative-charged, and hydrophilic and hydrophobic residues in an aqueous solution to form self-assembled β -sheet structured nanofibers, and these assembled nanofibers with the diameters ranging from 10 to 15 nm form a fiber network that is capable of retaining a large volume of water, creating a hydrogel scaffold. One of the advantages of using the self-assembly technique to fabricate nanofibers is that the physical properties of nanofibers, such as diameter, length, and stiffness, can be tailored through the control of oligopeptide composition and chemistry. For biochemical properties, the amino acid residues can be chemically modified by grafting bioactive moieties to enhance biological activities. Arginine-glycine-aspartic acid (RGD) peptides were included in amphiphilic peptides [45], and the functionalized nanofiber significantly enhanced the attachment, proliferation, and osteogenesis of mesenchymal stem cells (MSCs) [46]. Another advantage is that the self-assembled nanofibrous scaffold is particularly suitable for *in vivo* use, since self-assembly can be carried out in physiological media, thus avoiding the use of organic solvents to reduce cytotoxicity.

Self-assembled nanofibrous scaffolds closely mimicking natural ECM have been used in neural, bone, cartilage, and blood vessel tissue engineering, as well as wound repair [47]. For cartilage tissue engineering, self-assembly peptides were mixed with bovine chondrocytes before the peptides assemble into nanofibers, forming a solidified cell-hydrogel in culture medium. The approach of seeding cells in the self-assembly nanofibrous scaffold effectively overcomes the common problem of uneven cell distribution in a scaffold. In addition, bovine chondrocytes encapsulated within the self-assembly peptide scaffold retained their morphology and expressed cartilaginous ECM rich in proteoglycans and collagen type II, biochemical markers of phenotypic chondrocytes [48]. The self-assembly-fabricated nanofibrous scaffold formed a nanofibrous network embedded in a hydrogel, recapitulating the microenvironment in native cartilage. In a wound repair study, self-assembly peptides combined with epidermal growth factor (EGF) as a wound dressing were applied onto wound created in skin-equivalent culture to encourage epithelial cell repopulation [49]. Compared to the group using the self-assembly peptide without EGF or the control group without scaffolds, the EGF included-self-assembly peptide effectively accelerated the process of wound healing.

3.4.1.3

Electrospinning

Electrospinning is the most commonly used technique for fabrication of nanofibrous scaffolds because the fabrication setup is relatively simple and can be easily modified to produce fibrous structures with different fiber architectures. In addition, there are many polymer selections available for electrospinning to produce nanofibrous scaffolds with specific structural or mechanical properties for various tissue engineering applications. Practically, the production of electrospun nanofiber can be scaled up; the electrospinning technique is suitable for a small quantity of fiber production for laboratory research use, as well as mass production for industry needs. With all the aforementioned advantages, the electrospinning technique has been extensively developed and many sophisticated fabrication setups have been introduced to precisely and effectively electrospin nanofibrous scaffolds in the past few years. The following sections will detail the setup and control of electrospinning, properties and characterization of electrospun nanofibers, and tissue engineering applications of nanofibrous scaffolds.

3.5

The Electrospinning Technique

Fiber formation in the process of electrospinning is similar to that in the electrospray phenomenon first described by Lord Rayleigh in 1882 [50]. During the electrospraying process, Rayleigh discovered that, when passing through a voltage gradient, a highly charged droplet would break down into smaller droplets and spray, in response to the Coulombic repulsive force. After his pioneering study, many researchers further investigated electrospraying of aqueous solutions or dilute polymer solutions, and these seminal studies laid the foundation for the development of electrospinning. In 1934, Formhals electrospun fine fibers from a cellulose acetate solution and was granted with a series of U.S. patents based on the technique [51]. In the past few decades, the development of electrospinning was primarily focused on textile or filter applications. Until recently, the surging interest in nanostructured biomaterials has engendered renewed attention to this convenient, economical technique that would allow engineers to produce collagen-imitating nanofibers for biomaterial applications.

3.5.1

Setup

The electrospinning apparatus consists of three key components: a high-voltage power supply, a polymer solution reservoir (e.g., a syringe, with a small diameter needle) with or without a flow control pump, and a conductive fiber-collecting surface [52]. The high-voltage power supply with multiple independent outputs is capable of providing up to 50-kV DC power for each output. The polymer reservoir composed of a syringe and a metal needle is used to store

dissolved polymer solution and is connected to a power supply for electrospinning. To precisely control the amount of the polymer solution consumption during electrospinning, a flow control pump can be used to regulate the polymer flow rate. The fiber-collecting surface should be conductive and can be either a stationary plate or a rotary platform for collecting non-woven or aligned fibers, respectively.

To initiate fiber formation in electrospinning, a polymer solution prepared from a selected polymer dissolved in an appropriate solvent is loaded into the polymer reservoir, and applied with an optimal working voltage. The surface charge on a polymer droplet, extruded by the pump and/or gravity force and formed at the tip of the needle, increases with the applied voltage. Once the surface charge overcomes the surface tension of the polymer droplet, a polymer jet is initiated and travels in the electrostatic field. During the polymer jet traveling to the collecting surface, the charge density increases while the solvent in the polymer jet is evaporated, creating repulsive forces to split the polymer jet into multiple smaller jets. The same splitting process repeatedly occurs to the smaller jets, eventually forming layer-by-layer ultra-fine fibers deposited on the collecting surface, which can be collected as a 3D porous fibrous structure.

The physics of the fiber formation during electrospinning is complex and the mechanism by which nanofibers are formed has yet to be completely elucidated. Although a number of studies have investigated the mechanism of fiber formation in order to reproducibly control the properties of nanofibrous structures, such as fiber or pore size, little theoretical clarity has been achieved. Indeed, it has been technically challenging to control how fibers are electrospun. During the electrospinning process, both extrinsic factors and intrinsic parameters affect the structural morphology of nanofibers, and some of these factors are inter-dependent [53]. Specifically, extrinsic factors, such as environmental humidity and temperature, and intrinsic parameters, including applied voltage, working distance, and conductivity and viscosity of the polymer solution, need to be optimized to produce uniform nanofibers [41]. In general, the extrinsic factors are well controlled in the laboratory environment whereas the control of the intrinsic parameters is critical to nanofiber properties.

3.5.2

Fabrication and Properties of Electrospun Nanofibrous Scaffolds

Structural properties of electrospun nanofibrous scaffolds are affected by the fabrication parameters and setup of electrospinning. Fabrication parameters, such as polymer solution viscosity and conductivity, applied voltage, and working distance, can control microstructural properties of electrospun nanofibrous scaffolds, including fiber diameter and interfiber pore size, whereas setup of the electrospinning apparatus can determine macrostructural properties of the scaffolds, such as fiber alignment.

3.5.2.1

Microstructural Control

Polymer solution viscosity, directly proportional to the concentration of a polymer solution, is the most critical parameter controlling nanofiber morphology and diameter. To form

uniform nanofibers, the solution viscosity should be controlled in a specific range, and the range is polymer and solvent type-dependent [54, 55]. In addition, the polymer solution viscosity in the range is directly associated with the diameter of electrospun nanofibers. Recent studies conducted by Deitzel et al. [56] and Demir et al. [57] have shown that a more viscous polymer solution resulted in larger fibers. The conductivity of a polymer solution affected by the polymer and solvent type, and the availability of ionizable salts controls nanofiber morphology and diameter as well. A highly conductive polymer solution carries more electric charges to generate a stronger repulsive force, facilitating the formation of bead-free, uniform fibers during the electrospinning process. To enhance the conductivity of a polymer solution, a dipolar aprotic solvent, such as N,N-Dimethylformamide, is added to synthetic biodegradable polymer solutions [58]. Another working approach to increase polymer solution conductivity is to add salts, such as benzyl triethylammonium chloride [59] or sodium chloride [60]. The increased conductivity can effectively reduce fiber diameter and enhance fiber uniformity.

An applied voltage imparting charge to the polymer droplet is the driving force to spin fibers. A working distance is defined as the distance between the tip of syringe and the fiber collecting surface, together with an applied voltage, can control structural properties of nanofibers. Demir et al. have showed that when a higher voltage was applied, more polymer was ejected to form larger fibers [57].

3.5.2.2

Macrostructural Control

While the microstructure is defined by the physical structure of fibers and pores, the macrostructure of a nanofibrous scaffold is defined by the architecture of randomly-oriented or aligned fiber.

Nonwoven, Randomly-Oriented Nanofiber

Upon ejection from the nozzle of a needle, a polymer jet travels spirally in the space between the needle tip and the fiber-collecting surface. The jet path is a complicated three-dimensional curve and thus nanofibers are deposited on the target platform in a random manner, resulting in a non-woven fibrous mat composed of nanofibers oriented equally in every direction, and polygonal, interconnected pores of various sizes formed between nanofibers. The homogeneous nanofibrous structure with randomly-oriented nanofibers has isotropic properties.

Aligned Nanofiber

The approach for aligning nanofibers is based on an as-spun fiber-assembly method, which uses either electrodes [61] or a rotary collector, such as a rotary disc [62] or shaft [63], to align electrospun nanofibers. With the approach using electrodes, a fiber collector

consisting of two rectangular conductive electrodes is placed on a highly insulating substrate with a space gap [61]. Electrospun nanofibers are attracted by and uniaxially deposited on the electrodes across the gap. Fiber alignment is affected by the amount of charges on the nanofibers; increasing charges on the nanofibers improves fiber alignment. Altering the pattern of the electrode array can change the orientation of uniaxial nanofibers and fabricate aligned nanofibers with a complicated pattern.

Another approach, commonly used to align nanofibers, is to use a high-speed rotator to collect and align electrospun nanofibers. Theron et al. utilized a rotary disc as a fiber collector to electrically and mechanically align nanofibers [62]. As an electrode, the sharp edge of the disc accumulated charges to attract positively-charged nanofibers. Mechanically, the rotary sharp edge acts as a continuously moving, charged band that forces nanofibers to align on a limited strip surface and wind around the circumference of the disc. To collect more aligned nanofibers for a larger and thicker nanofibrous mat, the disc can be replaced by a drum or a shaft with a large surface area. Several studies have shown that nanofiber alignment is highly dependent on the rotation speed of the disc, drum or shaft; fiber alignment increases with the rotation speed of the collecting surface [63]. An aligned fibrous structure with the fibers oriented in one direction is shown to possess anisotropic mechanical properties. The structure possesses preferentially enhanced mechanical properties, such as tensile modulus and strength, along with the fiber direction. The anisotropic mechanical properties are correlated with the percentage of fiber alignment.

3.5.3

Biological Enhancement with Nanofibrous Scaffold

Cell adhesion is the first cellular event to take place after cells are seeded onto a biomaterial surface; other cell activities, such as cell migration, proliferation, and differentiation, take place only after cells are securely adhered. A previous study showed that when cultured with cells, synthetic polymeric biomaterials attract plasma/serum proteins to the surface for cell adhesion [64]. The nanofibrous scaffold with a high surface-area-to-volume ratio adsorbed approximately four times as much serum proteins, such as fibronectin and vitronectin, compared to the scaffold with solid pore walls. Although the mechanism by which the nanofibrous scaffold acts as a selective substrate is not yet known, it is clear that nanofibers enhance adsorption of cell adhesion molecules.

The unique feature of 3D ultra-fine fibers of nanofibrous scaffolds has been shown to play a direct and/or indirect role in the regulation of cellular activities. The structural feature and the increased adsorption of cell adhesion molecules are able to effectively promote *in vivo*-like 3D matrix adhesion for cultured cells, and activate the down-stream cell signaling pathway. Schindler et al. demonstrate that cells cultured on a nanofiber surface have a less defined pattern of punctate vinculin and decreased focal adhesion kinase (FAK) at the edge of lamellipodia [65]. The decrease of FAK at the adhesion site is a characteristic of a cell with *in vivo*-like 3D matrix adhesion, suggesting that cells cultured in nanofibrous culture may be able to recapitulate cell-matrix interactions in the *in vivo* cellular microenvironment. Studies have shown that nanofibrous scaffolds regulate the family of Rho GTPases, Rho, Rac, and Cdc42, to control cell morphology and cytoskeletal organization [66]. Specifically, cells

cultured on a nanofibrous surface extensively activate Rac, and the activated Rac is found to accumulate at the lamellipodial edge, intracellular vesicles, and dorsal membrane ruffles. The activation of Rho and Cdc42 is not as significant as that of Rac but both GTPases are mildly elevated in nanofibrous culture. The finding suggests that nanofibrous scaffolds are capable of providing spatial cues to activate intracellular signaling pathways to regulate cell activities.

Nanofibrous scaffolds have been shown to support re-differentiation of chondrocytes *in vitro* [67]. In this study, chondrocytes are seeded onto nanofibrous scaffolds, or on standard tissue culture polystyrene as a control substrate. Gene expression analysis shows that chondrocytes seeded on nanofibrous scaffolds continuously maintain their cartilage specific ECM genes. In addition to maintaining chondrocytic phenotype, nanofibrous scaffold also supports cellular proliferation. These results indicate that biological activities of chondrocytes are crucially dependent on the architecture of scaffolds, and that the nanofibrous scaffold acts as a biologically preferred scaffold for proliferation and maintenance of chondrocytic phenotype.

A nanofibrous structure resembling a basement membrane matrix has been used to culture embryonic stem cells [68], and the results show that significantly larger colonies of undifferentiated cells and enhanced proliferation are found in nanofibrous scaffolds, compared to the control film, suggesting that physical cues from the unique geometry of the nanofibrous surface regulate stem cell activities. It has also been reported that nanofibrous scaffolds support multi-potential differentiation of MSCs [69]. MSCs from bone marrow differentiate into adipocytes, chondrocytes, and osteoblasts in nanofibrous scaffolds.

3.5.4

Biomaterials for Nanofibrous Scaffolds

A variety of biomaterials, including non-biodegradable and biodegradable polymers, have been successfully electrospun into nanofibers. Non-biodegradable polymers as scaffold materials are utilized for tissues requiring mechanical stability. However, their long-lasting nature may interfere with tissue turnover and remodeling. On the other hand, the degradation characteristic of biodegradable polymers is favorable to tissue engineering. To date, more than one hundred different biodegradable polymers, including natural and synthetic, have been fabricated and evaluated for different tissue-engineering applications [41].

Natural polymers are used to fabricate nanofibrous scaffolds because their bioactive molecules, such as peptides and polysaccharides, can be easily recognized by cells. Electrospun nanofibrous scaffolds prepared from protein-based polymers, such as collagen [70], gelatin [71], elastin [72], silk fibroin [73], and fibrinogen [74], or from carbohydrate-based polymers, such as chitin [75], chitosan [76], and hyaluronic acid [77], have been successfully fabricated and evaluated for various tissue applications. However, without proper crosslinking, natural polymer-based electrospun nanofibers are prone to rapid degradation, significantly limiting their applications as scaffolds. On the other hand, synthetic polymers can be tailored to have desired material properties, such as improved mechanical strength and programmed degradation profile, and are commonly used to fabricate nanofibrous scaffolds. The polymers include but are not limited to poly(α -hydroxy esters) [78], such as PLA, PGA poly(glycolic acid), PLGA, and poly(ϵ -caprolactone)

(PCL), and poly(3-hydroxybutyrate-co-3-hydroxyvalerate) [59]. Among these polymers, the commercially available, FDA-approved, poly(α -hydroxy ester) family is the commonly used polymer for electrospinning. In the past few years, the properties of poly(α -hydroxy ester) nanofibrous scaffolds have been extensively studied. In general, synthetic polymer-based nanofibrous scaffolds are able to satisfactorily meet the requirements of tissue engineered scaffolds, though the drawback is that electrospun synthetic nanofibers lack natural molecules for cells to recognize.

To fabricate nanofibers with favorable properties from both natural and synthetic polymers, for example, a nanofibrous scaffold with improved mechanical strength and enhanced bioactivity, a polymer blend composed of multiple natural or synthetic polymers has been introduced for electrospinning. The blended-polymer nanofibrous scaffolds are able to retain the properties of each composing polymer. One of the samples is to electrospin a multiple natural polymer blend into a nanofiber mixture to closely mimic native ECM. Specifically, many tissues contain both collagen and elastin fibers that are frequently subjected to tensile and elastic loading, respectively. Nanofibrous scaffolds composed of collagen types I and III, and elastin have been fabricated to replicate native ECM of blood vessels [72]. Besides the natural-natural blend, a synthetic-synthetic blend is commonly used to fabricate nanofibrous scaffolds. With the combination properties of PLA being biodegradable but hydrophobic, and poly(ethylene glycol) (PEG) being hydrophilic but non-biodegradable, the resultant PLA/PEG-blended nanofibrous scaffold is more hydrophilic than a PLA-alone scaffold and more biodegradable than a PEG-alone scaffold [79]. In addition, the combination properties can be programmed by changing the ratio of the two polymers. Finally, electrospinning a natural and synthetic polymer mixture can make nanofibers with both natural and synthetic polymer properties [71]. However, this is challenging since the solvent choices suitable for both polymers are limited; natural polymers are required to be dissolved in an aqueous solution that is not compatible with a majority of organic solvents. A possible alternative is to use synthetic polymers that can be dissolved in aqueous solutions with natural polymers. Poly(ethylene oxide) (PEO) is one of the polymers that can be dissolved in water and commonly used to blend with other natural polymers. A study shows that the chitosan/PEO blend has improved conductivity, surface tension, and viscosity, favorable for the formation of smaller, uniform nanofibers, compared to a pure chitosan or PEO solution [80]. Furthermore, a large portion of natural polymers by themselves cannot be electrospun into uniform nanofibers, PEO can function as an “electrospinning-driving” polymer to facilitate nanofiber formation.

3.5.5

Comparison Between Microfibrous and Nanofibrous Scaffolds

Fibrous scaffolds, regardless of their compositions, can be grouped into two categories, microfibrous and nanofibrous scaffolds, simply based on the size of fibers (Fig. 3.4). The two groups of fibrous scaffolds have been independently evaluated *in vitro* or *in vivo* for potential scaffold applications, and the results are generally promising. However, study being focused on the comparison between microfibrous and nanofibrous scaffolds would be

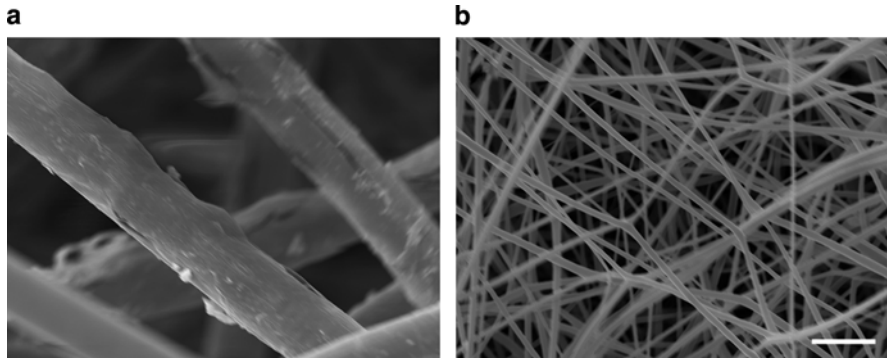


Fig. 3.4 SEM micrographs of poly(L-lactic acid) fibers. Nonwoven fibrous structures are formed of micro-sized fibers with the approximate diameter of 15 μm (a), or nano-sized fibers with the approximate diameter of 900 nm (b). Bar, 10 μm

useful to biomaterial scientists or tissue engineers who intend to use fibrous scaffolds in tissue engineering.

Several groups have reported their study results of comparing microfibrillar and nanofibrillar scaffolds. One such study evaluates the fiber-size effect on biological activities of chondrocytes by culturing the cells in PLLA microfibrillar and nanofibrillar scaffolds [81]. The results show that chondrocytes seeded in microfibrillar scaffolds express dedifferentiated, fibroblast-like morphology, whereas chondrocytes seeded in nanofibrillar scaffolds maintain chondrocyte-like morphology. Cell activities, such as proliferation and ECM production, are enhanced in nanofibrillar scaffolds, compared to microfibrillar scaffolds. The findings suggest that the nanofibrillar scaffold may be a more biologically favorable scaffold for tissue engineering. Another group also reports a similar conclusion that nanofibers outperform microfibers in regulating neural stem cell activity [82], in which they compare cell response to 300 nm nanofibers and 1.5 μm microfibers. The results show that a larger percentage of neural stem cells cultured in nanofibrillar scaffolds exhibit neuron-like morphology than in microfibrillar scaffolds. The average neurite length of neural stem cells with nanofibers is significantly longer than that of the cells with microfibers, suggesting that nanofibers may enhance the neurite outgrowth.

3.5.6

Nanofibrillar Scaffolds for Tissue Engineering Applications

Electrospun nanofibrillar scaffolds made of natural, synthetic, or both polymers have been extensively investigated for various tissue engineering applications that include almost every tissue in the body [41]. Among these applications, musculoskeletal, cardiovascular, skin, and neural tissue engineering have been particularly focused in the past few years. In this section, only musculoskeletal tissue engineering will be discussed, as an example to illustrate the development of nanofibrillar scaffolds for tissue engineering.

Musculoskeletal tissue engineering includes bone, cartilage, muscle, ligament, and tendon, and the ECM composition and structure of each tissue are different from each other and contribute to distinct physiological properties. For example, bone is a hard, solid connective tissue that provides structural protection to the body, whereas ligament is a soft and flexible tissue that transmits forces and stabilizes joints. To meet the functional requirements, nanofibrous scaffolds with different physical and chemical properties have been fabricated for various tissue engineering applications. Cells used in bone tissue engineering include osteoblasts, osteoprogenitor cells, and MSCs. MSCs are a promising cell type for bone tissue engineering because of their extensive expandability and multipotential differentiation capabilities [83]. Yoshimoto et al. report that PCL nanofibrous scaffolds seeded with rat bone marrow-derived MSCs successfully turn into bone in a bioreactor [84]. PCL nanofibrous scaffolds promote MSCs to differentiate into osteoblast-like cells producing collagen type I and minerals. A further assessment of bone formation *in vivo* by Shin et al. shows that new osseous matrix is deposited throughout the cellular nanofibrous scaffolds, forming a white, stiff bone in a rat model [85]. To actively induce bone formation, osteo-conductive hydroxyapatite [86] or osteo-inductive demineralized bone powder [87] has been co-electrospun with PCL to fabricate a composite nanofibrous scaffold. The addition of hydroxyapatite or bone powder effectively increases mineralization of cellular nanofibrous scaffolds, and also enhances compressive properties of the scaffold. Composite nanofibrous scaffolds containing nanofibers and calcium minerals seem promising for bone tissue engineering.

Cartilage is a specialized tissue and its primary function is to mechanically protect joints from compressive impact. The superior compression-resisting capability of cartilage is primarily defined by a large portion of ECM macromolecules and water in the tissue. Therefore, scaffolds for cartilage tissue engineering should be able to induce cells to actively produce quality ECM for demanding mechanical needs. Li et al. show that chondrocytes seeded in PCL nanofibrous scaffolds express cartilage-specific ECM genes, collagen types II and IX, aggrecan, and COMP [67]. Notably, the nanofibrous scaffolds induce cells to express collagen type IIB gene, a spliced variant transcript, suggesting the scaffold is able to promote the phenotype of mature chondrocytes phenotype. Chondrocytes in the nanofibrous scaffold exhibit round shaped, phenotypic morphology. In another study, the same group compares chondrogenic activities of MSCs in PCL nanofibrous scaffolds to those in gold-standard high-density cell pellets [88]. The level of chondrogenesis in the MSC-laden nanofibrous scaffolds is comparable to that in MSC pellets, suggesting that the nanofibrous scaffold as an effective 3D structure supports MSC chondrogenesis. The results show that the nanofibrous scaffold can be a biologically favorable scaffold for cartilage tissue engineering.

Skeletal muscle is composed of bundles of highly oriented and dense muscle fibers, each representing a multinucleated cell derived from myoblasts. Therefore, to enhance the biological activity of tissue engineered muscle, it would be important to use a scaffold with the structure to actively direct cell morphology and orientation. Aligned nanofibrous scaffolds with nanofibers imitating the architecture of skeletal muscle ECM has been shown to be promising for skeletal muscle tissue engineering. Choi et al. compare the biological response of human skeletal muscle cells in aligned and randomly oriented PCL/collagen nanofibrous scaffolds [89]. The cell morphology is greatly affected by the fiber structure;

cells are uniformly elongated and oriented with the fiber direction in the aligned nanofibrous scaffold whereas the cells are not specifically oriented in the non-aligned nanofibrous scaffold. Moreover, the aligned nanofibrous structure promotes skeletal muscle cells to fuse into myotubes, and the length of myotubes in the aligned nanofibrous scaffold is more than two times that in the randomly oriented nanofibrous scaffolds, suggesting aligned nanofibers enhance muscle cell maturation.

Ligament is a slightly elastic connective tissue and tough fibrous band that provides stability to joints. Similar to the cells and ECM in skeletal muscle, ligament cells and ECM are also aligned uniformly in a specific direction. The study investigating the effects of fiber alignment on human ligament fibroblasts (HLFs) and ECM in PU nanofibrous scaffolds shows that HLFs cultured on aligned nanofibers are spindle-shaped and oriented with the nanofiber direction, whereas the cells on non-aligned nanofibers have no specific directionality [90]. In addition, after 7 days of culture, HLFs on aligned nanofibers show significantly increased collagen synthesis, compared to those on non-aligned fibers. Cell attachment and proliferation in the nanofibrous scaffolds are greatly enhanced than those on the casted membranes. The results suggest that aligned electrospun nanofibers capable of regulating ligament fibroblast morphology and ECM production are promising for ligament tissue engineering.

3.6 Future Directions

The future direction is to develop the next generation “smart” fibrous scaffold, which should be made of materials with a biomimetic structure and a bio-inspired, functionalized surface to support favorable cell-matrix interactions and should have the capacity to release biomolecules in a controlled manner to actively instruct cell behavior and facilitate tissue regeneration.

Nano-scaled fibers structurally mimicking natural ECM have been shown to effectively enhance biological activity. However, nanofibers fabricated of synthetic polymers lack the bioactive surface chemistry for favorable biological activity. To improve bioactivity, nanofibrous scaffolds can be grafted with bioactive molecules to functionalize the scaffold surfaces. Indeed, there have been a few experimental attempts to functionalize nanofibrous scaffolds with cell adhesion peptides, such as RGD, to improve cell attachment, and these studies show promising results of enhanced cell activity [91]. As a result, the further studies should be focused on functionalizing nanofibrous scaffolds by chemically modifying or grafting the surface with bioactive molecules to instruct favorable cell activity.

Other future studies may include fabrication of fibrous scaffolds with the capability of controlled release of molecules, such as growth factors, that act to enhance biological activity. Giving delivery of bioactive molecules can be achieved via biodegradation of scaffolds, and the release kinetics of the target molecules is associated with the characteristic of the polymer property. Theoretically, with differential degradation properties, multiple biodegradable polymers in a scaffold can degrade at different times, the scaffold is capable of sequentially releasing various growth factors to maximize biological effects. Using this

approach, it is possible to fabricate “smart” nanofibrous scaffolds with the capability of controlled release of multiple growth factors. In addition, the “smart” nanofibrous scaffolds should be able to protect the delivered molecules from denaturation and maintain their biological activities, giving many conventional nanofiber fabrication methods are likely to harm biological activities of the incorporated molecules. To overcome this problem, many research groups have developed dual-structured scaffolds that embed with microparticles for encapsulating growth factors to protect the bioactivities of the delivered molecules [92, 93].

A “smart” nanofibrous scaffolds capable of promoting cell-matrix interaction through a bio-inspired surface, and inducing favorable biological activity via controlled release of incorporated biological molecules would be important for scaffold-based tissue engineering.

References

1. Wesolow A, Snyder RW, Textiles. In: von Recum AF, editor. *Handbook of Biomaterials Evaluation: Scientific, Technical, and Clinical Testing of Implant Materials*. New York: Macmillan, 1986. p. 79–97.
2. Casey DJ, Lewis OG, Absorbable and Nonabsorbable Sutures. In: von Recum AF, editor. *Handbook of Biomaterials Evaluation: Scientific, Technical, and Clinical Testing of Implant Materials*. New York: Macmillan, 1986. p. 86–94.
3. Shalaby SW, Fabrics. In: Ratner BD, Hoffman AS, Shoen FJ, Lemons JE, editors. *Biomaterials Science: An Introduction to Materials in Medicine*. 2nd ed. Boston: Elsevier Academic Press, 2004. p. 118–124.
4. Moroni L, de Wijn JR, van Blitterswijk CA. Integrating novel technologies to fabricate smart scaffolds. *J Biomater Sci Polym Ed* 2008;19:543–572.
5. Li WJ, Laurencin CT, Caterson EJ, Tuan RS, Ko FK. Electrospun nanofibrous structure: a novel scaffold for tissue engineering. *J Biomed Mater Res* 2002;60:613–621.
6. von der Mark K, Structure, Biosynthesis, and Gene Regulation of Collagens in Cartilage and Bone. In: Seibel MJ, Robins SP, Bilezikian JP, editors. *Dynamics of Bone and Cartilage Metabolism*. San Diego: Academic Press, 1999. p. 3–29.
7. Kuivaniemi H, Tromp G, Chu ML, Prockop DJ. Structure of a full-length cDNA clone for the prepro alpha 2(I) chain of human type I procollagen. Comparison with the chicken gene confirms unusual patterns of gene conservation. *Biochem J* 1988;252:633–640.
8. Minary-Jolandan M, Yu MF. Nanoscale characterization of isolated individual type I collagen fibrils: polarization and piezoelectricity. *Nanotechnology* 2009;20:85706.
9. An KN, Sun YL, Luo ZP. Flexibility of type I collagen and mechanical property of connective tissue. *Biorheology* 2004;41:239–246.
10. Yang L, Fitie CF, van der Werf KO, Bennink ML, Dijkstra PJ, Feijen J. Mechanical properties of single electrospun collagen type I fibers. *Biomaterials* 2008;29:955–962.
11. Ide A, Sakane M, Chen G, Shimojo H, Ushida T, et al. Collagen hybridization with poly L-lactic acid braid promotes ligament cell migration. *Mater Sci Eng C* 2001;17:95–99.
12. Ko FK, Fabrics. In: Wnek GE, Bowlin GL, editors. *Encyclopedia of Biomaterials and Biomedical Engineering*. New York: Marcel Dekker, 2004. p. 583–602.
13. Jacobs PF. Stereolithography and other RP&M technologies: from rapid prototyping to rapid tooling. Dearborn, Mich. New York: Society of Manufacturing Engineers in cooperation with the Rapid Prototyping Association of SME; New York, NY: ASME Press, 1996.

14. Hatch KL. Textile Science. New York: West Publishing Co., 1993. p. 318–370.
15. Wollina U, Heide M, Muller-Litz W, Obenauf D, Ash J. Functional textiles in prevention of chronic wounds, wound healing and tissue engineering. *Curr Probl Dermatol* 2003;31:82–97.
16. Tuzlakoglu K, Reis RL. Biodegradable polymeric fiber structures in tissue engineering. *Tissue Eng Part B Rev* 2009;15:17–27.
17. Ko FK, Pastore CM, Head AA. *Atkins and Pearce Handbook of Industrial Braiding*. Covington: Atkins and Pearce, Inc., 1989.
18. Ko FK. Braiding. In: *Engineered Materials Handbook, Volume 1, Composites*. Metals Park, OH: ASM International, 1987. p. 519–528
19. Ko FK. Preform fiber architecture for ceramic-matrix composites. *Ceram Bull* 1989;68:401–414.
20. Ko FK, Soebroto HB, Lei C. 3-D Net Shaped Composites by the 2-Step Braiding Process. The 33rd International SAMPE Symposium; 1988 3/7/1988: SAMPE; 1988. p. 912–921.
21. Ko FK, Pastore CM, Structure and Properties of an Integrated 3-D Fabric for Structural Composites. In: Vinson J, Taya M, editors. *Recent Advances in Composites in the U.S. and Japan*. Philadelphia, PA: American Society for Testing and Materials, 1985.
22. Duval N, Chaput C, A Classification of Prosthetic Ligament Failures. In: Yahia LH, editor. *Ligaments and Ligamentoplasties*. Berlin: Springer, 1997. p. 167–191.
23. Lu HH, Cooper JA, Jr., Manuel S, Freeman JW, Attawia MA, Ko FK, et al. Anterior cruciate ligament regeneration using braided biodegradable scaffolds: in vitro optimization studies. *Biomaterials* 2005;26:4805–4816.
24. Cooper JA, Lu HH, Ko FK, Freeman JW, Laurencin CT. Fiber-based tissue-engineered scaffold for ligament replacement: design considerations and in vitro evaluation. *Biomaterials* 2005;26:1523–1532.
25. Guidoin MF, Marois Y, Bejui J, Poddevin N, King MW, Guidoin R. Analysis of retrieved polymer fiber based replacements for the ACL. *Biomaterials* 2000;21:2461–2474.
26. King MW, Soares MB, Guidoin R, The Chemical, Physical and Structural Properties of Synthetic Biomaterials used in Hernia Repair. In: Bendavid R, editor. *Prostheses and Abdominal Wall Hernias*. Austin: Landes, 1994. p. 191–206.
27. Klinge U, Klosterhalfen B, Muller M, Anurov M, Ottinger A, Schumpelick V. Influence of polyglactin-coating on functional and morphological parameters of polypropylene-mesh modifications for abdominal wall repair. *Biomaterials* 1999;20:613–623.
28. Marois Y, Cadi R, Gourdon J, Fatouraee N, King MW, Zhang Z, et al. Biostability, inflammatory response, and healing characteristics of a fluoropassivated polyester-knit mesh in the repair of experimental abdominal hernias. *Artif Organs* 2000;24:533–543.
29. Voorhees AB, Jr., Jaretzki A, 3rd, Blakemore AH. The use of tubes constructed from vinyon “N” cloth in bridging arterial defects. *Ann Surg* 1952;135:332–336.
30. Szilagyi DE, Elliott JP, Jr., Smith RF, Reddy DJ, McPharlin M. A thirty-year survey of the reconstructive surgical treatment of aortoiliac occlusive disease. *J Vasc Surg* 1986;3:421–436.
31. Hoerstrup SP, Zund G, Sodian R, Schnell AM, Grunenfelder J, Turina MI. Tissue engineering of small caliber vascular grafts. *Eur J Cardiothorac Surg* 2001;20:164–169.
32. Niklason LE, Gao J, Abbott WM, Hirschi KK, Houser S, Marini R, et al. Functional arteries grown in vitro. *Science* 1999;284:489–493.
33. Laurencin CT, Khan Y, Kofron M, El-Amin S, Botchwey E, Yu X, et al. The ABJS Nicolas Andry Award: tissue engineering of bone and ligament: a 15-year perspective. *Clin Orthop Relat Res* 2006;447:221–236.
34. Cooper JA, Jr., Bailey LO, Carter JN, Castiglioni CE, Kofron MD, Ko FK, et al. Evaluation of the anterior cruciate ligament, medial collateral ligament, achilles tendon and patellar tendon as cell sources for tissue-engineered ligament. *Biomaterials* 2006;27:2747–2754.
35. Cooper JA, Jr., Sahota JS, Gorum WJ, 2nd, Carter J, Doty SB, Laurencin CT. Biomimetic tissue-engineered anterior cruciate ligament replacement. *Proc Natl Acad Sci USA* 2007; 104:3049–3054.

36. Lu L, Zhu X, Pederson LG, Jabbari E, Currier B, O'Driscoll S, et al. Effects of dynamic fluid pressure on chondrocytes cultured in biodegradable poly(glycolic acid) fibrous scaffolds. *Tissue Eng* 2005;11:1852–1859.
37. Freed LE, Vunjak-Novakovic G, Biron RJ, Eagles DB, Lesnoy DC, Barlow SK, et al. Biodegradable polymer scaffolds for tissue engineering. *Biotechnology (N Y)* 1994;12:689–693.
38. Moutos FT, Freed LE, Guilak F. A biomimetic three-dimensional woven composite scaffold for functional tissue engineering of cartilage. *Nat Mater* 2007;6:162–167.
39. Smith LA, Ma PX. Nano-fibrous scaffolds for tissue engineering. *Colloids Surf B Biointerfaces* 2004;39:125–131.
40. Zhang S. Designer self-assembling Peptide nanofiber scaffolds for study of 3-d cell biology and beyond. *Adv Cancer Res* 2008;99:335–362.
41. Sill TJ, von Recum HA. Electrospinning: applications in drug delivery and tissue engineering. *Biomaterials* 2008;29:1989–2006.
42. Zhang R, Ma PX. Synthetic nano-fibrillar extracellular matrices with predesigned macroporous architectures. *J Biomed Mater Res* 2000;52:430–438.
43. Hu J, Liu X, Ma PX. Induction of osteoblast differentiation phenotype on poly(L-lactic acid) nanofibrous matrix. *Biomaterials* 2008;29:3815–3821.
44. Zhang S. Fabrication of novel biomaterials through molecular self-assembly. *Nat Biotechnol* 2003;21:1171–1178.
45. Hartgerink JD, Beniash E, Stupp SI. Self-assembly and mineralization of peptide-amphiphile nanofibers. *Science* 2001;294:1684–1688.
46. Hosseinkhani H, Hosseinkhani M, Tian F, Kobayashi H, Tabata Y. Osteogenic differentiation of mesenchymal stem cells in self-assembled peptide-amphiphile nanofibers. *Biomaterials* 2006;27:4079–4086.
47. Semino CE. Self-assembling peptides: from bio-inspired materials to bone regeneration. *J Dent Res* 2008;87:606–616.
48. Kisiday J, Jin M, Kurz B, Hung H, Semino C, Zhang S, et al. Self-assembling peptide hydrogel fosters chondrocyte extracellular matrix production and cell division: implications for cartilage tissue repair. *Proc Natl Acad Sci USA* 2002;99:9996–10001.
49. Schneider A, Garlick JA, Egles C. Self-assembling peptide nanofiber scaffolds accelerate wound healing. *PLoS One* 2008;3:e1410.
50. Rayleigh JWG. *Lond Edinburgh Dublin Phil Mag* 1882;14:184.
51. Formhals A. US Patent No. 1,975,504, 1934.
52. Li WJ, Tuan RS. Fabrication and application of nanofibrous scaffolds in tissue engineering. *Curr Protoc Cell Biol* 2009;Chapter 25:Unit 25.2.
53. Doshi J, Reneker DH. Electrospinning process and applications of electrospun fibers. *J Electrostat* 1995;35:151–160.
54. Fong H, Chun I, Reneker DH. Beaded nanofibers formed during electrospinning. *Polymer* 1999;40:4585–4592.
55. Liu HQ, Hsieh YL. Ultrafine fibrous cellulose membranes from electrospinning of cellulose acetate. *J Polym Sci B Polym Phys* 2002;40:2119–2129.
56. Deitzel JM, Kleinmeyer J, Harris D, Tan NCB. The effect of processing variables on the morphology of electrospun nanofibers and textiles. *Polymer* 2001;42:261–272.
57. Demir MM, Yilgor I, Yilgor E, Erman B. Electrospinning of polyurethane fibers. *Polymer* 2002;43:3303–3309.
58. Lee KH, Kim HY, Khil MS, Ra YM, Lee DR. Characterization of nano-structured poly(ϵ -caprolactone) nonwoven mats via electrospinning. *Polymer* 2003;44:1287–1294.
59. Choi JS, Lee SW, Jeong L, Bae SH, Min BC, Youk JH, et al. Effect of organosoluble salts on the nanofibrous structure of electrospun poly(3-hydroxybutyrate-co-3-hydroxyvalerate). *Int J Biol Macromol* 2004;34:249–256.

- 3
60. Zong X, Kim K, Fang D, Ran S, Hsiao BS, Chu B. Structure and process relationship of electrospun bioabsorbable nanofiber membranes. *Polymer* 2002;43:4403–4412.
 61. Li D, Ouyang G, McCann JT, Xia Y. Collecting electrospun nanofibers with patterned electrodes. *Nano Lett* 2005;5:913–916.
 62. Theron A, Zussman E, Yarin AL. Electrostatic field-assisted alignment of electrospun nanofibres. *Nanotechnology* 2001;12:384–390.
 63. Li WJ, Mauck RL, Cooper JA, Yuan X, Tuan RS. Engineering controllable anisotropy in electrospun biodegradable nanofibrous scaffolds for musculoskeletal tissue engineering. *J Biomech* 2007;40:1686–1693.
 64. Woo KM, Chen VJ, Ma PX. Nano-fibrous scaffolding architecture selectively enhances protein adsorption contributing to cell attachment. *J Biomed Mater Res A* 2003;67:531–537.
 65. Schindler M, Ahmed I, Kamal J, Nur EKA, Grafe TH, Young CH, et al. A synthetic nanofibrillar matrix promotes *in vivo*-like organization and morphogenesis for cells in culture. *Biomaterials* 2005;26:5624–5631.
 66. Nur EKA, Ahmed I, Kamal J, Schindler M, Meiners S. Three dimensional nanofibrillar surfaces induce activation of Rac. *Biochem Biophys Res Commun* 2005;331:428–434.
 67. Li WJ, Danielson KG, Alexander PG, Tuan RS. Biological response of chondrocytes cultured in three-dimensional nanofibrous poly(epsilon-caprolactone) scaffolds. *J Biomed Mater Res A* 2003;67:1105–1114.
 68. Nur EKA, Ahmed I, Kamal J, Schindler M, Meiners S. Three-dimensional nanofibrillar surfaces promote self-renewal in mouse embryonic stem cells. *Stem Cells* 2006;24:426–433.
 69. Li WJ, Tuli R, Huang X, Laquerriere P, Tuan RS. Multilineage differentiation of human mesenchymal stem cells in a three-dimensional nanofibrous scaffold. *Biomaterials* 2005;26:5158–5166.
 70. Rho KS, Jeong L, Lee G, Seo BM, Park YJ, Hong SD, et al. Electrospinning of collagen nanofibers: effects on the behavior of normal human keratinocytes and early-stage wound healing. *Biomaterials* 2006;27:1452–1461.
 71. Zhang Y, Ouyang H, Lim CT, Ramakrishna S, Huang ZM. Electrospinning of gelatin fibers and gelatin/PCL composite fibrous scaffolds. *J Biomed Mater Res B Appl Biomater* 2005;72:156–165.
 72. Boland ED, Matthews JA, Pawlowski KJ, Simpson DG, Wnek GE, Bowlin GL. Electrospinning collagen and elastin: preliminary vascular tissue engineering. *Front Biosci* 2004;9:1422–1432.
 73. Min BM, Lee G, Kim SH, Nam YS, Lee TS, Park WH. Electrospinning of silk fibroin nanofibers and its effect on the adhesion and spreading of normal human keratinocytes and fibroblasts *in vitro*. *Biomaterials* 2004;25:1289–1297.
 74. McManus MC, Boland ED, Simpson DG, Barnes CP, Bowlin GL. Electrospun fibrinogen: feasibility as a tissue engineering scaffold in a rat cell culture model. *J Biomed Mater Res A* 2007;81:299–309.
 75. Noh HK, Lee SW, Kim JM, Oh JE, Kim KH, Chung CP, et al. Electrospinning of chitin nanofibers: degradation behavior and cellular response to normal human keratinocytes and fibroblasts. *Biomaterials* 2006;27:3934–3944.
 76. Subramanian A, Lin HY, Vu D, Larsen G. Synthesis and evaluation of scaffolds prepared from chitosan fibers for potential use in cartilage tissue engineering. *Biomed Sci Instrum* 2004;40:117–122.
 77. Um IC, Fang D, Hsiao BS, Okamoto A, Chu B. Electro-spinning and electro-blowing of hyaluronic acid. *Biomacromolecules* 2004;5:1428–1436.
 78. Li WJ, Cooper JA, Jr, Mauck RL, Tuan RS. Fabrication and characterization of six electrospun poly(alpha-hydroxy ester)-based fibrous scaffolds for tissue engineering applications. *Acta Biomater* 2006;2:377–385.

79. Zong X, Li S, Chen E, Garlick B, Kim KS, Fang D, et al. Prevention of postsurgery-induced abdominal adhesions by electrospun bioabsorbable nanofibrous poly(lactide-co-glycolide)-based membranes. *Ann Surg* 2004;240:910–915.
80. Duan B, Dong C, Yuan X, Yao K. Electrospinning of chitosan solutions in acetic acid with poly(ethylene oxide). *J Biomater Sci Polym Ed* 2004;15:797–811.
81. Elisseeff J, Anseth K, Sims D, McIntosh W, Randolph M, Yaremchuk M, et al. Transdermal photopolymerization of poly(ethylene oxide)-based injectable hydrogels for tissue-engineered cartilage. *Plast Reconstr Surg* 1999;104:1014–1022.
82. Yang F, Murugan R, Wang S, Ramakrishna S. Electrospinning of nano/micro scale poly(L-lactic acid) aligned fibers and their potential in neural tissue engineering. *Biomaterials* 2005;26:2603–2610.
83. Pittenger MF, Mackay AM, Beck SC, Jaiswal RK, Douglas R, Mosca JD, et al. Multilineage potential of adult human mesenchymal stem cells. *Science* 1999;284:143–147.
84. Yoshimoto H, Shin YM, Terai H, Vacanti JP. A biodegradable nanofiber scaffold by electrospinning and its potential for bone tissue engineering. *Biomaterials* 2003;24:2077–2082.
85. Shin M, Yoshimoto H, Vacanti JP. In vivo bone tissue engineering using mesenchymal stem cells on a novel electrospun nanofibrous scaffold. *Tissue Eng* 2004;10:33–41.
86. Venugopal J, Low S, Choon AT, Sampath Kumar TS, Ramakrishna S. Mineralization of osteoblasts with electrospun collagen/hydroxyapatite nanofibers. *J Mater Sci Mater Med* 2008;19:2039–2046.
87. Ko EK, Jeong SI, Rim NG, Lee YM, Shin H, Lee BK. In vitro osteogenic differentiation of human mesenchymal stem cells and in vivo bone formation in composite nanofiber meshes. *Tissue Eng A* 2008;14:2105–2119.
88. Li WJ, Tuli R, Okafor C, Derfoul A, Danielson KG, Hall DJ, et al. A three-dimensional nanofibrous scaffold for cartilage tissue engineering using human mesenchymal stem cells. *Biomaterials* 2005;26:599–609.
89. Choi JS, Lee SJ, Christ GJ, Atala A, Yoo JJ. The influence of electrospun aligned poly(epsilon-caprolactone)/collagen nanofiber meshes on the formation of self-aligned skeletal muscle myotubes. *Biomaterials* 2008;29:2899–2906.
90. Lee CH, Shin HJ, Cho IH, Kang YM, Kim IA, Park KD, et al. Nanofiber alignment and direction of mechanical strain affect the ECM production of human ACL fibroblast. *Biomaterials* 2005;26:1261–1270.
91. Kim TG, Park TG. Biomimicking extracellular matrix: cell adhesive RGD peptide modified electrospun poly(D,L-lactic-co-glycolic acid) nanofiber mesh. *Tissue Eng* 2006;12:221–233.
92. Qi H, Hu P, Xu J, Wang A. Encapsulation of drug reservoirs in fibers by emulsion electrospinning: morphology characterization and preliminary release assessment. *Biomacromolecules* 2006;7:2327–2330.
93. Xie J, Tan RS, Wang CH. Biodegradable microparticles and fiber fabrics for sustained delivery of cisplatin to treat C6 glioma in vitro. *J Biomed Mater Res A* 2008;85:897–908.

Zhengwei You and Yadong Wang

Contents

4.1	Introduction	76
4.1.1	Matrix Elasticity Impacts Cell and Tissue Function	76
4.1.2	Mechanical Stimulation Affects Cell and Tissue Development	77
4.1.3	Elastic Materials are Important Scaffold Materials for Tissue Engineering	79
4.2	Designing Bioelastomers for Tissue Engineering	79
4.2.1	Important Considerations in Bioelastomer Design	79
4.2.2	Current State of Bioelastomers	80
4.3	Recent Progress of Synthetic Bioelastomers	81
4.3.1	Polyurethanes	82
4.3.2	Other Thermoplastic Bioelastomers	91
4.3.3	Poly(glycerol sebacate)	97
4.3.4	Other Thermoset Bioelastomers	103
4.4	Future Directions	108
	References	109

Abstract The rapid progress in cell and developmental biology has clearly revealed that substrate elasticity and mechanical stimulation significantly affect cell function and tissue development. Further, many engineered soft-tissue constructs such as vascular grafts, cardiac patches, and cartilage are implanted in a mechanically dynamic environment, thus successful implants must sustain and recover from various deformations without mechanical irritations to surrounding tissues. Ideal scaffolds for these tissue engineering applications would be made of biodegradable elastomers with properties that resemble those of the extracellular matrix, providing a biomimetic mechanical environment and mechanical stimulation to cells and tissues. However, traditional biodegradable scaffold materials such as polylactide, polyglycolide, and poly(lactide-co-glycolide) are stiff and are subjected to plastic deformation and failure under cyclic strain. Consequently, for the past decade, many novel bioelastomers have been developed and extensively investigated for

Y. Wang (✉)

The McGowan Institute, University of Pittsburgh, 300 Technology Drive, Pittsburgh, PA 15219, USA

e-mail: yaw20@pitt.edu

applications in tissue engineering. Both thermoplastic elastomers such as polyurethane, poly(ϵ -caprolactone) copolyester, poly(ether ester) and thermoset elastomers such as cross-linked polyesters have been developed and evaluated to engineer various tissues such as heart muscle and valves, blood vessels, skin, and cartilage. This chapter will cover representative bioelastomers and their applications in tissue engineering to highlight recent advances in this area.

Keywords Bioelastomers • Cardiovascular tissue • Elasticity • Mechanical stimulation • Poly(glycerol sebacate) • Polyurethane • Soft tissues

4.1 Introduction

Since the pioneering concept of reconstructing tissue using cell-seeded scaffolds was proposed two decades ago [1], the field of tissue engineering has quickly caught the attention of scientists and the general public and transformed the landscape of medicine, giving rise to regenerative medicine. There are still many challenges facing tissue engineering, one of which is the relative narrow choices of biomaterials compared with the huge variety of matrix materials in the native tissues. Many grafts fail partly due to mechanical-property mismatch between native and engineered tissues [2]. Recently, the progress in cell and developmental biology has provided new insights for more rational design of scaffold materials for tissue engineering. It has become clear that substrate elasticity and mechanical stimulation significantly affect cell functions and tissue development [3]. Thus elastomeric materials are recognized as an important class of scaffold materials for tissue engineering.

4.1.1 Matrix Elasticity Impacts Cell and Tissue Function

Substrate mechanical properties profoundly impact cell and tissue functions [4–6]. Elasticity is an important mechanical property for many tissues and organs (Table 4.1) [7]. Niche elasticity greatly influences many cell behaviors such as cytoskeleton organization, cell adhesion, spreading, and differentiation, especially in soft tissues [5, 6, 8]. For example, Neurons show greater proliferation on softer substrates that mechanically resemble the brain [9]. Myotubes differentiate optimally on substrate with muscle-like elasticity [10]. Polyacrylamide gels with varying elasticity direct human mesenchymal stem cell differentiation: gel elasticity similar to that of muscle, brain, and bone tissues results in myoblasts, neurons, and osteoblasts, respectively (Fig. 4.1) [11]. Substrate elasticity also influences communication between neighboring endothelial cells fostering tissue formation, where elastomeric substrates encourage sustained contacts, while stiffer substrates induce migratory

Table 4.1 Mechanical properties of selected human tissues

	Modulus E (MPa)	Maximal strength σ (MPa)	Maximal strain ϵ (%)	Testing method	References
Spinal cord	0.089	–	–	Tension	[7]
Thyroid	0.009	–	–	Compression	[7]
Liver	0.64	–	–	Compression	[7]
Mammary gland	0.16	–	–	Compression	[7]
Relaxed smooth muscle	0.006	–	300	Tension	[13]
Contracted smooth muscle	0.01	–	300	Tension	[13]
Myocardium	0.02–0.5	0.003–0.015	–	Tension	[14]
Carotid artery	0.084	–	–	Radial distension	[15]
Bladder	0.25	0.27	69	Tension	[16]
Aortic valve leaflet (circumferential)	15.6	2.6	21.9	Tension	[17]
Aortic valve leaflet (radial)	2.0	0.42	29.8	Tension	[17]
Pericardium	20.4	2.51	34.9	Tension	[18]
Cortical artery	21.42	4.14	145	Tension	[19]
Cortical vein	3.41	1.39	193	Tension	[19]
Cartilage	0.7–15.3	3.7–10.5	–	Tension	[20]
Ligament	65–541	13–46	–	Tension	[20]
Tendon	143–2,310	24–112	–	Tension	[20]

responses [12]. In summary, the elasticity of the cellular microenvironment plays an important role in morphogenesis and regeneration of tissues [3–5].

4.1.2

Mechanical Stimulation Affects Cell and Tissue Development

Mechanical stimulation is increasingly recognized as a major factor in determining cell morphology and function [21]. Mechanical cues from the cellular microenvironment govern cellular processes such as adhesion, spreading, and cytoskeletal remodeling [6]. Specific mechanical stimulations impact the functionality of various cell types including cardiovascular, lung, and bone cells, adult and embryonic mesenchymal progenitor cells, and embryonic stem cells [22]. Mechanical interactions between cells and the extracellular matrix (ECM) play a crucial role in the morphogenesis and function of tissues [3]. In view of this, mechanical stimulation has been applied to tissue engineered constructs to promote desirable tissue development [23]. Studies show that mechanical stimulations including

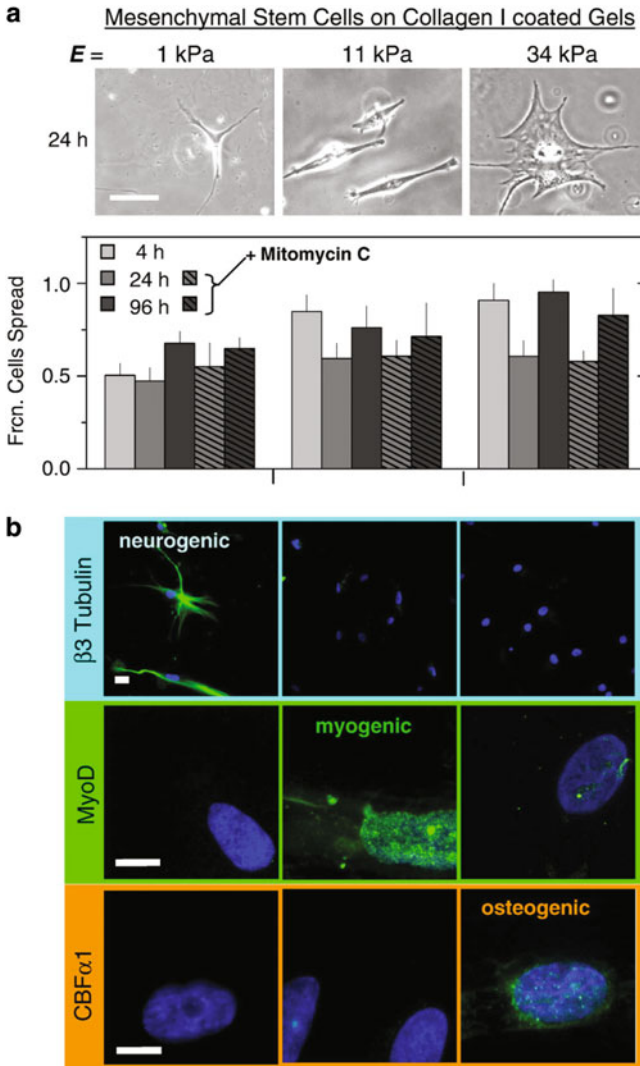


Fig. 4.1 Mesenchymal stem cell (MSC) differentiation on elastic substrates. **(a)** Morphology of naive, low passage MSCs (*upper panel*) 24 h after plating on PA gels of different stiffness closely matches that of cell lineages found within each microenvironment. Naive MSCs are initially small and round but a dominant fraction indicated here (*lower panel*) develops increasingly branched, spindle, or polygonal shapes within days of plating when grown on matrices with respective elasticities of 1 kPa, 11 kPa, and 34 kPa. Results for mitomycin C treated cells are shown with diagonally-hatched bars. Scale bar is 20 μm . **(b)** Differentiation of MSCs directed by substrate elasticity elucidated by key marker proteins. The neuronal cytoskeletal marker $\beta 3$ tubulin is expressed in branches of initially naive MSCs (>75%) and only on soft, neurogenic matrices (*first row*). The muscle transcription factor MyoD is up-regulated and nuclear localized only in MSCs on myogenic matrices (*second row*). The osteoblast transcription factor $CBF\alpha 1$ is likewise expressed only on stiff osteogenic substrates (*third row*). Scale bar is 5 μm (Reprinted by permission from [5]. Copyright 2007, Elsevier B.V.)

shear stress, cyclic strain (uniaxial or biaxial), scaffold fixation, and static and dynamic loading can control both cell behaviors during tissue formation and overall properties of the resultant engineered tissue [22–24].

4.1.3

Elastic Materials are Important Scaffold Materials for Tissue Engineering

The above findings in biology and tissue engineering indicate that elastomeric scaffolds are ideal to engineer elastic and mechanically active tissues such as lung, bladder, and cardiovascular tissues. An elastomer with mechanical properties matching the native tissue will produce a biomimetic environment for cell growth and tissue development. An elastomer will also effectively transmit the mechanical stimulation to the adhered cells and promote tissue morphogenesis. Further, elastomers can recover from cyclic deformations, making them suitable for mechanically dynamic culture in vitro and implantation at mechanically dynamic sites. Upon implantation, an elastomer with tissue-mimetic mechanical properties will fulfill similar mechanical functions of the target tissue before construct maturation, with minimal mechanical irritation to the host tissue. For elastic tissues such as pulmonary tissues, elastomeric scaffolds are even more critical. In summary, elastomeric biomaterials (bioelastomers) are an important class of scaffold materials and further innovations in bioelastomers will lead to more exciting breakthroughs in tissue engineering.

4.2

Designing Bioelastomers for Tissue Engineering

Elastomers are polymeric networks that have long and highly flexible polymer chains with high mobility that can rapidly reconfigure upon applied stresses. Thus, elastomers can withstand large deformations. The crosslinking between the polymer chains provides necessary mechanical strength, resisting unrestricted sliding between chains and ensuring reversible recovery from deformation upon removal of the external stress. The combination of these two properties makes the polymeric network elastomeric. To be useful in tissue engineering, an elastomer also needs to be biocompatible and biodegradable. In this section we will discuss common requirements for bioelastomer design and provide an overview of current bioelastomers.

4.2.1

Important Considerations in Bioelastomer Design

Many factors influence a bioelastomer's performance in a particular tissue engineering application. This section examines some of the critical parameters in bioelastomer design.

4.2.1.1

Mechanical Properties

Most bioelastomers are designed to resemble the mechanical properties of the target tissue [25]. Since the mechanical properties of native tissues vary in a wide range (Table 4.1) [7], the mechanical properties of bioelastomers should be tailored according to the specific application. Many different factors impact a bioelastomer's mechanical properties, such as chain length, crosslink density, and the nature of the chain and crosslink. We will discuss these in the following sections according to the types of bioelastomers.

4.2.1.2

Biodegradability

It is generally accepted that the degradation rate of a scaffold should match the regeneration rate of the tissue. Thus, a bioelastomer should be designed to degrade at a rate matching the neo-tissue growth at the site of implantation. Further, a bioelastomer ideally degrades by surface erosion to preserve bulk integrity and provide sufficient elastic support within the defect until the regenerated tissue becomes load-bearing. Surface erosion leads to a linear degradation profile of mass loss, retention of mechanical properties, and preservation of geometric integrity. The degradation rate can be modulated by several parameters: the nature of the labile bonds such as hydrolytic or enzymatic degradation, the amount of labile bonds, the surface and bulk hydrophilicity, and the presence and amount of crystalline, glassy, or amorphous segments. We will discuss these in the following sections in more details.

Other desirable characteristics of a scaffold material include biocompatibility of the bioelastomer and its degradation products, cell-philicity (promoting cell adhesion, immigration, proliferation, and differentiation), availability (easy preparation and low cost), and processability (easy fabrication to desired scaffold). It should be noted that many material properties are inter-related and the change of one property often affects certain other properties. For example, increasing crosslink density can enhance mechanical strength, but may also reduce the maximal strain and slow degradation. In addition, the mechanical properties will inevitably alter with degradation, so modulation of the degradation rate should consider the change of mechanical properties during degradation. For practical applications, global consideration and balance between various properties are necessary.

4.2.2

Current State of Bioelastomers

The growing interest and rapid development of bioelastomers are primarily driven by the need of a better scaffold material for cardiovascular tissue engineering. To engineer cardiac tissue, traditional biodegradable polymers such as polyglycolide (PGA), polylactide (PLA),

and their copolymer poly(lactide-*co*-glycolide)(PLGA) may not be ideal because of their stiffness [14, 26]. The PLGA family of polymers are stiff and brittle with a tensile modulus $E > 1.4$ GPa [20], which is much stiffer than most soft tissues (Table 4.1). Their elasticity is very limited, usually failing at low strain (maximal strain $\epsilon < 20\%$) with plastic deformation under stress [14, 20, 27]. Bioelastomers can be classified into three categories: (1) elastin-like polypeptides produced by protein engineering [28–30]; (2) polyhydroxyalkanoates produced by fermentation [31–33]; and (3) chemically synthesized bioelastomers. In this chapter, we will focus on synthetic bioelastomers, which experienced great progress throughout the last decade. The advantages of synthetic materials includes: (1) a wide range of mechanical, degradation, and bioactive properties that provide flexible material choices; (2) precise control of the polymeric structure, which results in tailored material properties; (3) good reproducibility; (4) easy purification and well defined compositions that greatly reduce concerns of disease transmission and endotoxin contamination. The exciting progress of chemically synthesized bioelastomers has enabled new methods of tissue engineering and greatly impacted soft tissue regeneration. We will discuss these in detail in Sect. 4.3. For the first two classes of bioelastomers please refer to the other chapters within this book and relevant reviews [28–33].

4.3 Recent Progress of Synthetic Bioelastomers

There are two types of synthetic bioelastomers: thermoplastic, which is physically crosslinked, and thermoset, which is chemically crosslinked. Both can be further classified into different subcategories. We will discuss thermoplastic bioelastomers first, then thermoset bioelastomers. The following sections will be organized according to the chemical structure of bioelastomers.

Thermoplastic Bioelastomers

Thermoplastic bioelastomers are physically crosslinked, which endow them both advantages and disadvantages. Individual physical crosslinks are weak, however, a high molecular weight (MW) thermoplastic bioelastomer may possess high amounts of physical crosslinking, thus the overall crosslink strength can be very high, leading to high mechanical strength. A thermoplastic material can be easily fabricated by solution or melt processing. However, their weak physical crosslinking can result in creep upon long-term or cyclic mechanical deformation. Thermoplastic bioelastomers have heterogeneous structures including both amorphous (providing flexibility) and crystalline or glassy regions (providing physical crosslinking), generally leading to heterogeneous degradation. As a result, they often lose mechanical strength and crack at early stages of degradation. Polyurethane, the most widely used thermoplastic bioelastomer, will be discussed in Sect. 4.3.1, followed by other thermoplastic bioelastomers in Sect. 4.3.2.

4.3.1 Polyurethanes

4.3.1.1

Introduction

Brief History

Polyurethane (PU) has a long history and is one of the most important elastomers. PU was discovered in the 1930s and was introduced to the biomedical field in the 1960s [34, 35]. Due to its superior mechanical strength and elastomeric properties, PUs have become one of the most popular synthetic materials in biomedical applications today [36, 37]. Traditionally, PUs are used for long-term implanted medical devices. However, the biostability of PUs has raised concerns about the safety of enduring implants containing PUs since the 1970s [38–40]. PUs degrade in vivo and produce toxic, carcinogenic, and mutagenic aromatic diamines [41]. Biomer[®], the first biomedical PUs product for cardiovascular applications had to be withdrawn in 1991 due to its degradation in vivo [42]. Accordingly, extensive research was employed to determine the biodegradability properties of PUs in order to improve their biostability [43]. On the other hand, this observation opens the door for PUs in a brand-new area, tissue engineering, where controlled degradation is required. From the 1990s, biodegradable PUs have been widely investigated and developed to be one of the most robust biodegradable biomaterials in regenerative medicine [42]. Further, advanced research has also greatly improved the biocompatibility of PUs. Here, we will review recent advancements of PU bioelastomers used in soft tissue engineering. For more thorough reviews of PUs, the readers are directed to several excellent articles [36, 37, 42].

Structure and Synthesis

Since thermoplastic PUs are much more commonly used as bioelastomers in tissue engineering than thermoset PUs, the following discussion will focus on thermoplastic PUs. Thermoset PUs will be briefly covered in Sect. 4.3.1.3. Typically, thermoplastic PUs comprise three units: macrodiol (MW from 600 to 4,000 Da), diisocyanate, and chain extender (MW from 61 to 400 Da) [34]. Macrodiol reacts with excessive diisocyanate to produce polyurethane prepolymer terminated by the isocyanate group $-N=C=O$. To accelerate the reaction, urethane catalysts such as $Sn(OOct)_2$, and elevated temperatures (60–90°C) may be used [42, 44]. The oligomeric prepolymer is connected by chain extender diamine or diol, resulting in thermoplastic PUs. Thermoplastic PUs are segmented copolymers. The multiblock structure of this phase-separated system endows PUs' elastomeric properties. The diisocyanate and chain extender comprise the hard segment, which is either glassy or crystalline at the use temperature to provide physical crosslinking to resist flow when stress is applied to the material. Extensive hydrogen bonding in the hard segments of adjacent polymer chains also significantly contributes to the strength of physical crosslinking [45, 46]. Macrodiol comprises the soft segment, which is amorphous or semicrystalline and flexible. The soft segments account for most of the elastic properties of

Table 4.2 Blocks for polyurethane synthesis

Function	Chemical name (abbreviation)	References
Diisocyanate	Butylene-1,4-diisocyanate (BDI)	[44, 47–61]
Diisocyanate	Lysine ester diisocyanate (LDI)	[62–71]
Diisocyanate	Hexamethylene-1,6-diisocyanate (HDI)	[70, 72–76]
Diisocyanate	4,4'-diphenylmethane diisocyanate (MDI)	[77–81]
Macrodiol	Polycaprolactone diol (PCL)	[44, 47–56, 58–81]
Macrodiol	Poly(ethylene oxide) (PEO)	[44, 50, 51, 57, 62–64, 72, 73, 75]
Macrodiol	Poly(propylene oxide) (PPO)	[57]
Macrodiol	Poly(trimethylene carbonate) (PTMC)	[57]
Chain extender	Lysine ethyl ester (Lys)	[47]
Chain extender	1,4-cyclohexanedimethanol L-phenylalanine diester (Phe)	[62–69]
Chain extender	Putrescine (P)	[44, 47–50, 52–54, 57–61]
Chain extender	Ala-Ala-Lys(AAK)	[51, 55, 56]
Chain extender	1,3-diaminopropane (1,3-DAP)	[77, 78, 80, 81]
Chain extender	Butanediol (BD)	[71, 73, 79]
Chain extender	2, 2'-(methylimino)diethanol (MIDE)	[79]
Chain extender	Saccharine (isosorbide) diol	[74]
Chain extender	2-hydroxyethyl 2-hydroxypropanoate (LAEG)	[70]
Chain extender	Ethylene glycol (EG)	[70]

the PUs. Some common macrodiols, diisocyanates, and chain extenders included in this review are listed in Table 4.2. The resultant PUs with their mechanical and degradation properties are listed in Table 4.3. We use PU(x/y/z) to represent PU made from macrodiol x, diisocyanate y, and chain extender z. There are relative few diisocyanates that have been used to prepare PUs, partly because of the difficulty of synthesis. The most widely used chain extenders are linear low molecular weight diols and diamines. Normally, macrodiols are hydroxyl-terminated aliphatic polyesters such as polycaprolactone (PCL) diol, and polyethers such as poly(ethylene oxide) (PEO). Mixtures of polyester and polyether are also used to yield useful combination properties.

Mechanical Properties

Mechanical properties of PUs can be varied in a wide range via adjusting multiple factors such as composition, relative content and molecular weight of each segment and the whole polymer (Table 4.3). The amount and stability of the hard segment principally determine the strength and stiffness of PUs [46, 79]. It was reported that urea bonds in the hard domain led to 3D hydrogen bonding, resulting in extremely strong hard domain cohesion while urethane carbonyls were not hydrogen bonded [45, 46]. Therefore, PUs prepared from diamine chain extender had a stronger mechanical profile than similar PUs prepared from

Table 4.3 Mechanical and degradation properties of selected polyurethanes

PU ^a	<i>E</i> (MPa)	σ (MPa)	ϵ (%)	Degradation ^b time, mass loss	References
PCL/BDI/Lys	14–38	9.2–13	841–895	56 d, 30–60%	[47–49]
PCL/BDI/P	54–78	25–29	660–686	56 d, ~5%	[47–50, 52–54, 61, 68, 69]
PEO-co-PCL/BDI/P	4.6–75	8–20	325–560	56 d, 10–30%	[44, 50]
PEO-co-PCL/BDI/AAK	–	15–20	670–890	56 d, 12–17%	[51]
PCL/BDI/AAK	–	28	830	56 d, 18%–35% ^c	[51, 55, 56]
PEO-co-PTMC/BDI/P	3.5	1.8	53	56 d, ~26% ^c	[57]
PPO-co-PEO-co-PTMC/BDI/P	5.5–7.4	8.1–17.9	363–711	42 d, 32%	[57]
PCL/LDI/Phe	6.6–81.9	12.5–30.8	618–682	42 d, 2–6%	[62, 63, 68, 69]
PEO-co-PCL/LDI/Phe	49–105	6–26	510–726	28 d, 2–8% ^d	[62–64]
PCL/MDI/BD	–	63.8	797	28 d, 0.7–3% ^e	[79]
PCL/MDI/MIDE	–	40.9	756	14 d, 5–25% ^f	[79]
PEO-co-PCL/HDI/BD	30.8	3.64	>500	20 d, 16%	[79]
PCL/LDI/LAEG	2.09–4.03	1.05–3.55	979–1,165	20 d, 58%	[73]
PCL/LDI/EG	4.2–11.2	1.02–4.74	263–1,519	–	[70]
PCL/HDI/LAEG	17.04	6.2	923	365 d, ~25–80%	[70]
PCL/HDI/EG	21.12	29.0	1084	365 d, ~0–6.6%	[70]
				365 d, ~4%	[70]
				365 d, 0%	[70]

E: Young's modulus, ϵ : Maximal strain, σ : Tensile strength

^aThe content of different units may vary, please refer to the references

^bPBS, 37°C unless otherwise noted

^c0.3 mg/ml elastase, 37°C

^dChymotrypsin solution, 37°C

^eTris buffer solution (0.036 M Tris with 0.045 M CaCl₂ and 0.02% NaN₃, pH 8.0)

^fTris-buffered saline (TBS, 0.05 M Tris, 0.1 M NaCl, pH 7.4), 37°C

diol chain extenders [45, 46]. An increase of the hard segment content usually enhances the mechanical strength to yield a stronger but stiffer elastomer with lower maximal strain [77]. Because the availability of diisocyanate is relative limited, the soft segments are more often varied to modulate the properties of PUs. The hard segment content can be increased by decreasing the MW of the macrodiol or the relative feed ratio of macrodiol to diisocyanate and chain extender.

The structure of the soft segment also affects the mechanical properties of PUs. For example, PCL and PEO are two commonly used macrodiols. PUs prepared from PCL are relative strong, elastomeric materials which range from completely amorphous to semicrystalline and PUs prepared from PEO are generally weak, tacky amorphous materials [62]. PU using PCL as the soft segment are normally stronger with higher tensile strength than similar PUs with PEO and PCL copolymer as the soft segment [50, 51, 64]. Increasing PCL segment length increases the tensile strength, modulus, and maximal elongation, because of facilitating phase separation and soft segment crystallinity [62]. In contrast, increasing PEO segment length decreases the tensile strength [51, 64]. Other structures such as poly(trimethylene carbonate) (PTMC) and poly(propylene oxide) (PPO) are also used as soft segments to modulate the properties of PUs [57]. Replacing PEO with the similar length PEO–PPO–PEO resulted in higher mechanical strength and maximal strain [57]. Increasing PTMC length significantly increased the tensile strength, maximal strain, and Young's modulus [57].

Biodegradability

Biodegradability of PUs can be varied by selection of different hard and soft segments, and their relative content (Table 4.3). Hard segments in traditional PUs for long-term implantation applications are typically synthesized from aromatic diisocyanate, which are normally biostable [43]. In contrast, degradable PUs are usually made from aliphatic diisocyanate such as Butylene-1,4-diisocyanate (BDI) and Hexamethylene-1,6-diisocyanate (HDI). Also, enzymatically degradable Lysine ester diisocyanate (LDI) has been introduced to further adjust the degradation of hard segments [62–64].

More typically, soft segments are used to modulate the degradation rate of PUs [43]. Normally, increasing the length and hydrophilicity of soft segments will increase the degradation [47, 77]. The degradation rate greatly enhances when PPO is replaced by hydrophilic PEO [57]. Combining different soft segments is an effective strategy to improve the overall properties. For example, combining PEO and PCL can take advantage of the two soft segments on mechanical integrity and the degradation rates [44, 64]. Increasing PEO length or decreasing PCL length increases water absorption and biodegradation rate likely due to increased hydrophilicity and decreased crystallinity [44, 64].

In addition, structural variations of the chain extender are employed to modulate the degradation properties. Using substrates of enzymatic degradation in the chain extender is also an efficient way to increase degradation. Phenylalanine derived diamine chain extender 1,4-cyclohexanedimethanol *L*-phenylalanine diester (Phe) has been investigated for a long time [63]. This extender results in increased susceptibility to enzyme-mediated, but not buffer-mediated, erosion in comparison to the control PU [63]. PUs using putrescine as the chain extender only displayed a little mass loss during an 8-week period in vitro [47].

However, when putrescine was replaced by lysine derived diamine, a considerable and continuous mass loss was observed [47]. Recently, tripeptide based diamine AAK (Table 4.2) was introduced as a chain extender to endow the resultant PUs predefined elastase sensitivity [51, 55]. As expected, their degradation in elastase solution was significantly higher than in PBS [51]. Scaffolds made of AAK containing PUs were completely absorbed 8 weeks post-subcutaneous implantation in rats, much faster than similar PUs without AAK units [55]. Desaminotyrosine tyrosyl hexyl ester is another amino acid based chain extender, which also makes corresponding PUs more susceptible to enzymatic degradation [72]. Introducing hydrophilic units to chain extender also leads to faster degradation. Hydrolyzable chain extenders based on DL-lactic acid and ethylene glycol accelerates hard segment degradation [70]. Mass loss of these PUs is directly proportional to hard segment weight percentage, suggesting that the hard segment is susceptible to degradation. Comparing the PUs made from 2,2'-(methylimino)diethanol (MIDE) and BD as chain extenders, the former has a 4–10 times faster degradation rate than the latter due to greater hydrophilicity of MIDE [79]. Recently, amphiphilic multiblock PUs with ammonium cationic groups in the chain extender were synthesized and showed much faster degradation than control PUs [71].

Biocompatibility

Traditional aromatic PUs may produce toxic degradation products, however, many aliphatic biodegradable PUs and several in the 4,4'-diphenylmethane diisocyanate (MDI) family have been created and shown to be nontoxic for both the polymers and their degradation products (most PUs listed in Table 4.3 are biocompatible). So far, most of them have only been tested in vitro and more in vivo evaluation is necessary to determine the interactions between tissue and PUs biomaterials.

4.3.1.2

Applications

Due to their excellent mechanical properties, good processability, and tunable structures, PUs have been extensively applied in tissue engineering, particularly in soft tissue engineering.

Scaffold Fabrication

Thermoplastic PUs can be processed easily and there are various methods that are amendable to fabricate PU scaffolds. Thermally induced phase separation has been employed to fabricate PU(PEO-co-PCL/BDI/P) and PU(PCL/BDI/P) into microfibrinous scaffolds [50]. The pore size, morphology (several μm to 150 μm), and porosity (80–97%) can be modulated by polymer solution concentration and quenching temperature. Maximal strain of the resultant PU scaffolds is 214% and higher with a tensile strength of approximately

1.0 MPa. Both scaffolds support smooth muscle cell (SMC) adhesion and growth with more extensive growth in the PEO containing PUs because of its increased hydrophilicity and faster degradation rate. By controlling the heat transfer direction, oriented PU scaffolds with anisotropic mechanical properties can be produced [55]. PU scaffolds with basic fibroblast growth factor release are also fabricated by this method [54]. The resultant scaffolds have tensile strengths of 0.25–2.8 MPa and elongations at break of 81–443%.

Electrospinning of PUs has been extensively explored. Electrospinning PU(PCL/LDI/Phe) yields a nanofibrous scaffold with an ultimate tensile stress of 1.33 MPa and tensile strain of 78.6% [69]. To improve the cytophilicity of PU scaffolds, *co*-electrospinning of PU (PCL/BDI/P) and Type I collagen or urinary bladder matrix was performed to fabricate hybrid fibrous scaffolds [48, 49]. The resultant scaffolds showed moderate mechanical properties and significantly enhanced the ability to promote SMC adhesion and growth [48, 49]. Further, controlled electrospinning of PU(PCL/BDI/P) can produce a mechanically anisotropic scaffold, which closely resembles the native pulmonary heart valve leaflet [52]. This study provided a practical strategy to fabricate tissue engineering scaffolds mimicking the mechanical anisotropy of native tissues. Recently, IGF delivery was also built into electrospun elastase-sensitive PU(PCL/BDI/AAK) to provide an anisotropic scaffold with the ability to improve mesenchymal stem cell survival and orientation [56]. Moreover, a *co*-electrospinning technology was established to micro-integrate SMCs into PU fibrous matrixes [53]. The resultant constructs show high cell survival, strong, flexible and anisotropic mechanical properties with tensile strengths ranging from 2.0 to 6.5 MPa, and maximal strains from 850 to 1,700%. This provides a novel fabrication method for elastic tissue mimetics with high cell density.

In addition, the good processing capability of PU makes it a suitable material amendable to advanced fabrication methods. For example, a low-temperature deposition rapid prototyping technique can process PU(PCL/PEO/HDI) into an advanced scaffold with various internal channels and micro-pores, a promising scaffold for vascular tissue engineering [73].

Applications in Cardiovascular Tissues

PUs are highly pliable and very suitable to fabricate scaffolds for cardiovascular tissue engineering. PU(PCL/BDI/P) is one of the most extensively investigated PUs in tissue engineering. To improve cell adhesion, a well established surface modification method – radio-frequency glow discharge followed by the coupling of Arg-Gly-Asp-Ser [47] was used. The modified PU(PCL/BDI/P) enhanced human endothelial cells adhesion by nearly twofold, better than tissue culture treated polystyrene (TCPS) [47]. This method was also employed to modify other PU surfaces [44, 51, 57]. Anisotropic ECM and alignment of cardiomyocytes are unique properties of heart tissue. To mimic this character, electrospinning was employed to process PU(PCL/BDI/P) into aligned microfibers [68]. *In vitro*, the anisotropic PU(PCL/BDI/P) fibrous scaffold yielded highly oriented cardiomyocyte groupings and more mature cells than unaligned controls. *In vivo* evaluation of PU(PCL/BDI/P) scaffold as a biodegradable patch to repair cardiac tissue defects was performed using a surgical defect in the right ventricular outflow tract of adult rats as the animal model [59]. In contrast to PTFE patches, fibroblasts impregnated PU(PCL/BDI/P) patches within 4 weeks.

Complete endothelialization was observed within 12 weeks with a moderate inflammatory reaction and no thrombus. PU(PCL/BDI/P) elastic patches were applied to subacute infarcts in the rat model [60]. After 8 weeks of implantation, the patch was largely resorbed and the left ventricular wall was thicker than the infarction control. The patch promotes the formation of contractile smooth muscle cells, cardiac remodeling, and the improvement of contractile function. This approach provides a potential alternative to cellular cardiomyoplasty or larger ventricular restraint devices for cardiac repair.

The potential of PU(PCL/BDI/P) scaffolds in tissue engineered vascular grafts has also been examined. A novel rotational vacuum seeding technique was used to rapidly and evenly seed muscle-derived stem cells into the tubular PU scaffolds (Fig. 4.2) [61, 82]. The stem cells remained viable and proliferated, and the cell phenotype was intact in vitro for 7 days. Recently, phospholipid-containing polymer poly(2-methacryloyloxyethyl phosphorylcholine-co-methacryloyloxyethyl butylurethane) was blended with PU(PCL/BDI/P) to produce a scaffold that was both non-thrombogenic and with mechanical properties appropriate for vascular tissue. The resultant conduits showed reduced thrombogenicity and greater patency when implanted in a rat abdominal aorta for 8 weeks [58].

Other PUs are also employed for cardiovascular regeneration. PU(PCL/LDI/Phe) is one of the first biodegradable PUs used in tissue engineering. Its potential to serve as cardiac grafts to replace damaged cardiac tissue has been evaluated by culture of embryonic stem cell-derived cardiomyocytes on PU films [65]. Laminin or collagen IV coatings on the PU films promoted preferential cell attachment and yielded a greater number of contracting films with fully contractile myocytes compared to controls after 30 days culture [65]. Further investigation of the behavior of cardiomyocytes seeded on different porous PU (PCL/LDI/Phe) scaffolds reveals that the material macrostructure does not directly effect the functionality of cells [66]. Cell seeded PU(PCL/MDI/1,3-DAP) constructs are being investigated for myocardial repair in vivo [80, 81]. Highly porous PU scaffolds were seeded by rat skeletal myoblasts and implanted on infarcted hearts in Lewis rats [81]. Laminin coating promoted the highest cell attachment. After 4 weeks, numerous myoblasts penetrated throughout the scaffolds without any apparent inflammatory reaction [80]. However, no cell differentiation and migration, and no neovessels were observed [80]. In addition, this PU scaffold based cell delivery did not increase the functional benefit when compared to direct injection of myoblasts [81]. Therefore, further studies are required to determine the efficiency of this therapeutic approach. PU(PCL/HDI/PEO) is evaluated for tissue engineered vascular grafts in vivo [75]. Tri-layer tubular scaffolds (6-mm i.d., 4 cm long) with PU(PCL/HDI/PEO) sandwiched by PLA were seeded by bone marrow stromal cells and cultured for 7 days to produce small diameter vascular constructs. The constructs implanted in canine abdominal aorta exhibited good biocompatibility, long term patency, and remodeling ability up to 24 weeks.

Applications in Other Tissues

PUs have been found to be useful for anterior cruciate ligament regeneration. To identify a suitable PU for anterior cruciate ligament tissue engineering, a series of PUs made from PCL, MDI, and various aliphatic diamines as chain extenders were investigated [77]. It was

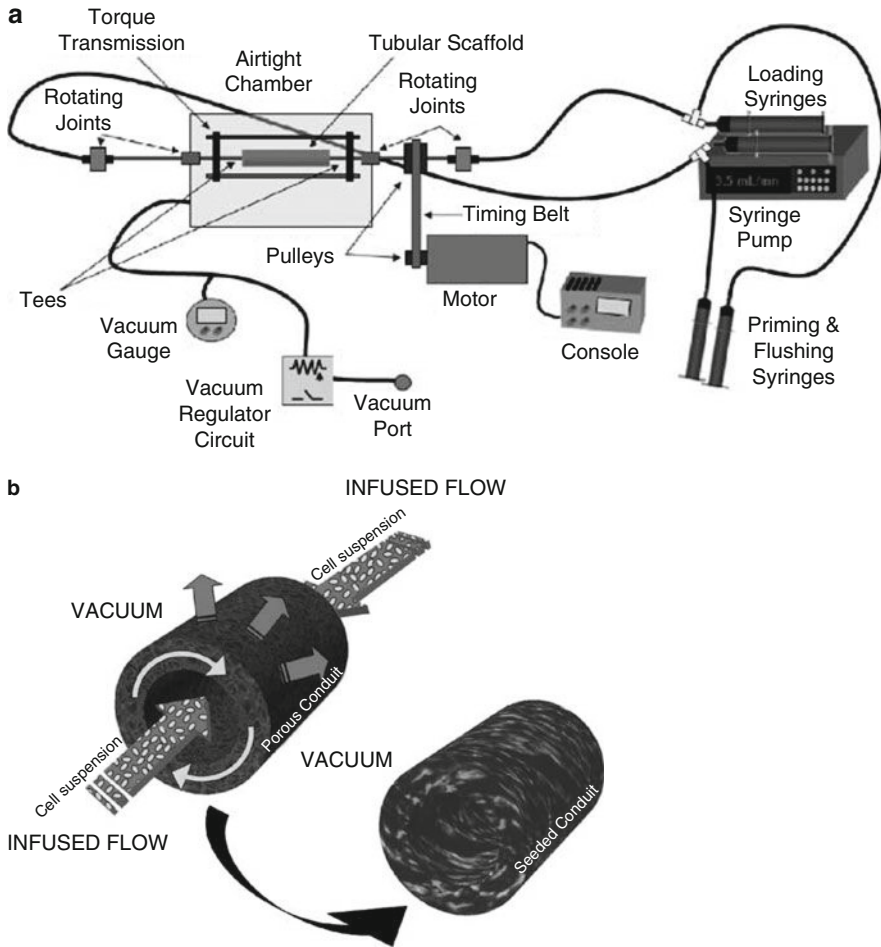


Fig. 4.2 (a) Schematic of the seeding device. A cell suspension is infused intraluminally into both ends of a PU(PCL/BDI/P) porous tubular scaffold by means of a syringe pump. Applied vacuum in the chamber fosters the radial exudation of the liquid phase of the cell suspension across the thickness of the polymer. An electrical motor rotates the construct, promoting a homogeneous distribution of cells around the circumference. (b) Operating principle of the seeding technique. A transmural flow is induced by an external vacuum and intraluminal infusion of a cell suspension. The porous nature of the scaffold allows for the liquid phase to exude through while the particulate (e.g., cells, microspheres) become entrapped in the pores. Rotation is employed to yield a uniform circumferential seeding distribution (Reprinted by permission from [82]. Copyright 2006, Elsevier Ltd.)

found that PU(PCL/MDI/1,3-DAP) using PCL($M_n = 530$ Da) has a relative high tensile strength and modulus, and low degradation rate to maintain sufficiently high mechanical strength during degradation. The mechanical properties of the PU band approach those of the normal human anterior cruciate ligament. PU (PCL/MDI/1,3-DAP) bands show good

biocompatibility *in vivo* and ingrowth of connective tissue was detected over a 24-month implantation in both rabbits and minipigs [78].

Recently, PU(HDI/PCL/isosorbide diol) was used for cartilage regeneration [74]. The PU was fabricated as microporous membranes with different pores size ($<5\ \mu\text{m}$, $10\text{--}20\ \mu\text{m}$, $40\text{--}60\ \mu\text{m}$). Compared with PLA membranes (pores size from 10 to $70\ \mu\text{m}$), all PU membranes promote similar cell proliferation. Cells growing in PU membranes with pore sizes of less than $5\ \mu\text{m}$ and $10\text{--}20\ \mu\text{m}$ produced more matrix than those in PLA membranes in the first 10 days, while PU membranes with pore size from 40 to $60\ \mu\text{m}$ lagged behind PLA. In addition, the resilient biomechanical profile of PU membranes is believed to facilitate mechanical loading and cartilage regeneration. This study provides a potential flap substitute and a chondrocyte carrier for cartilage repair.

4.3.1.3

Crosslinked Polyurethanes

Besides thermoplastic PUs, thermoset PUs have also been used in tissue engineering. Although most of them are designed for bone regeneration, the basic design principles should be applicable to soft tissue engineering as well [42]. Certain thermoset PUs have interesting features such as injectability and *in situ* gas foaming capability. Therefore, we will discuss some recent examples of thermoset PUs. All of them are crosslinked network containing urethane bonds.

The common method to obtain thermoset PUs is polycondensation of polyisocyanate, polyol, or/and polyamine with at least one reactant containing more than two functionalities. Similar to crosslinked polyester bioelastomers (see sections 4.3.3 and 4.3.4), the properties of resultant PU bioelastomers can be modulated by selection of different monomers and varying their ratios, but the residual isocyanate groups might be toxic. Thus, the purification should be thorough to completely remove all the isocyanate groups. One example is LDI-glucose PUs [83]. Using a two-step polymerization, porous scaffolds can be readily prepared by simple addition of water during crosslinking of prepolymer prepared from LDI and glucose. The mechanism is that water reacts with the isocyanate group of the prepolymer to yield an unstable carbamic acid, which then decomposes to an amine group while liberating carbon dioxide as a porogen to form the foam structure. The pores are interconnected with sizes between 20 and $1,000\ \mu\text{m}$. Although the mechanical properties were not reported, the authors stated that by control over the feed ratio of LDI and glucose the resultant PU matrix could be hard or soft and pliable. The resultant PUs show a moderate *in vitro* degradation rate with 67.7% mass loss in PBS at 37°C in 60 days. Lysine and glucose are identified to be the degradation products, which don't markedly change the pH of the solution. However, the PUs degraded *in vivo* three times faster than *in vitro*, as evidenced by subcutaneous implantation in rats. The implants are not immunogenic and induce a minimal foreign body reaction.

Recently, the *in situ* gelling system comprising poly(ϵ -caprolactone-*co*-glycolide) triol and HDI was employed as an injectable growth factor delivery system for wound healing [84]. Platelet-derived growth factor was added to the system as a lyophilized powder to retain its bioactivity. The release of growth factor lasts up to 21 days *in vitro* after an initial burst. When implanted in rat skin excisional wounds, PU scaffolds with growth factor

promoted better wound healing than blank PU controls. New granulation tissue forms as early as day 3 and complete healing with reepithelization occurs at day 14. This presents a novel injectable local delivery system for tissue regeneration.

Another route to obtain crosslinked PU networks was reported recently [85]. Poly (hexamethylene carbonate) diol reacts with 2 equivalents of LDI to produce a diisocyanate intermediate, which is treated with 2-hydroxyethyl methacrylate to provide a divinyl oligomer. The cross-linker was synthesized using 2.01:1.00 molar ratio of 2-hydroxyethyl methacrylate and LDI. Benzoyl peroxide initiating radical copolymerization of divinyl oligomer, methacrylic acid, methyl methacrylate, and cross-linker in the presence of NaHCO_3 particles as porogen produces the degradable PU porous scaffolds. As expected, increasing cross-linker concentration leads to an increase of the Young's modulus (from 0.5 to 21 MPa) and a decrease of elongation at yield (from 45 to 5%). In vitro, these PU scaffolds support the adhesion and growth of A10 vascular SMCs.

4.3.2

Other Thermoplastic Bioelastomers

4.3.2.1

Copolymers of PLA, PGA, PCL

Introduction

The good biocompatibility of PLA, PGA, and PCL has been recognized for a long time [86, 87]. Therefore, they are often the first choice for building blocks for new biomaterials. Although PLA, PGA, and their copolymer PLGA have been widely used in tissue engineering [20, 27], the stiffness mismatches with the elastomeric ECM of soft tissues and their plasticity will lead to permanent deformations when implanted in a mechanically dynamic environment [14]. Also, PLA and PGA possess a relatively high rate of degradation. PCL is another US Food and Drug Administration (FDA) approved polyester and has also been widely used in biomedical engineering [20, 88]. PCL is relative flexible with a semicrystalline structure. However, due to its hydrophobicity, PCL degrades very slowly (normally more than 2 years) and is unsuitable for many tissue engineering applications [20]. To retain their biocompatibility and integrate their advantages to improve the overall performance, the copolymers using PLA/PGA/PLGA as hard segment and PCL as soft segment have been extensively investigated. By controlling the composition, a series of thermoplastic bioelastomers with suitable mechanical and degradation characteristics have been produced and evaluated for tissue engineering applications.

Poly(glycolide-*co*- ϵ -caprolactone) (PGCL) is synthesized by random copolymerization of glycolide and ϵ -caprolactone at 170°C using $\text{Sn}(\text{Oct})_2$ as the catalyst [89]. The porous PGCL and PLGA scaffolds are fabricated by a solvent casting/particulate leaching method and their mechanical properties are compared. PGCL scaffolds exhibit much better elasticity than PLGA scaffolds. The maximal strain of PGCL scaffolds are up to 250% higher than the ones of PLGA scaffolds (10–15%). In addition, PGCL scaffolds show a robust ability to resist deformation. They recover well from large elongation (96% recovery after 230%

strain) and long-time cyclic deformation (4% residual extension after cyclic elongation of 20% for 6 days). In contrast, PLGA scaffolds only can recover 85% at applied strain of 3%. Subcutaneous implantation of smooth muscle cell-seeded constructs in nude mice confirms the *in vivo* biocompatibility of PGCL scaffolds. Smooth muscle tissue forms in the scaffold within 3 weeks. *In vitro* degradation of PGCL scaffolds is estimated in PBS at 37°C: mass loss of 3% and 50% are found after 2 and 6 weeks, respectively.

Poly(lactide-*co*- ϵ -caprolactone) (PLCL) is synthesized by Sn(Oct)₂ catalyzing random copolymerization of L-lactide and ϵ -caprolactone at 170°C using 1,6-hexanediol as initiator [90]. Porous PLCL scaffolds fabricated by solvent casting/particulate leaching method also exhibit good elasticity. They can be easily twisted and bended, while PLGA is broken. Even for highly porous scaffolds (90 wt% salt), it can be extended to 200%, displays 100% recovery from near 100% strain, and withstands cyclic mechanical strain up to 2 weeks without any deformation. *In vitro* SMC culture shows that cell adhesion and proliferation are enhanced with pore size and porosity. The *in vivo* biocompatibility was confirmed by subcutaneous implantation of PLCL scaffolds in nude mice for 8 weeks [91]. At the same time, the *in vivo* degradation behavior was investigated. The subcutaneously implanted PLCL scaffolds lost 19% mass over 15 weeks. The caprolactone segments degraded faster than lactide segments due to their different amorphous (PCL unit) and crystalline (LA unit) morphology [91].

Applications

Highly elastic PLCL provides a suitable substrate for engineering vascular tissue under mechanically dynamic conditions. Porous tubular PLCL scaffolds seeded with SMCs are cultured in pulsatile perfusion bioreactors for up to 8 weeks [92]. Compared to static culture, the pulsatile strain and shear stress are found to enhance the SMC's proliferation and collagen production. Importantly, the mechano-active condition significantly facilitates cell alignment and retention of differentiated cell phenotype. To further improve the performance of PLCL scaffolds, the researchers fabricated a tubular fibrous PLCL scaffold using a novel gel-spinning process [93]. The resultant PLCL scaffolds display much better mechanical properties than extruded PLCL scaffolds: 5 times higher tensile strength (2.77 vs. 0.57 MPa), 4.8 times higher Young's modulus (0.925 vs. 0.192 MPa), and greater maximal strain (540% vs. 421%). Further, gel-spun scaffolds markedly enhanced cell seeding efficiency and proliferation. To prevent intimal hyperplasia of tissue engineered PLCL vascular grafts, the endothelialization of PLCL scaffold was performed [94]. A PLCL nanofibrous mesh with a porosity of 64–67% was fabricated by electrospinning. Its mechanical testing displayed a suitable tensile strength (6.3 MPa) in the range of native coronary artery (1.40–11.4 MPa) and greater maximal elongation (175%) than native coronary artery (45–99%). To enhance the endothelialization, the scaffolds were treated by plasma and coated with collagen. It was found that collagen coated scaffolds promoted human coronary artery endothelial cell attachment, viability, and phenotypic maintenance better than uncoated ones.

In addition, PLCL is fabricated to thin films to serve as a delivery matrix of adipose tissue derived stem cells to treat abdominal aortic aneurysms [95]. The tensile strength of 250- μ m-thick films is 8.55 MPa and its maximal elongation is up to 854%, which can impart implanted

PLCL sufficient strength to withstand aortic pressures. The films showed a moderate degradation rate with 50% mass loss in 6 month in vitro, which will provide sufficient time for tissue ingrowth. Stem cells adhered to PLCL films, firmly resisting a wide range of physiologic shear stresses. Fibronectin coating further increased the cell viability on the films.

Most excitedly, tissue-engineered grafts made from PLCL seeded with autologous bone marrow cells have already been clinically evaluated for cardiac repair in 42 patients (ages from 1 to 24 years) [96, 97] (Fig. 4.3). All grafts are patent to a maximum follow-up of 32 months. No complications such as thrombosis, stenosis, or obstruction were observed. In addition, the diameter of the grafts increased with time ($110\% \pm 7\%$ of the implanted size). These results are quite encouraging and demonstrate the feasibility of tissue-engineered grafts for pediatric cardiovascular surgery.

Because of the toughness of PLCL, its potential for engineering relative hard tissue was also investigated. PLCL sponges with various porosities (71–86%) were fabricated by solvent casting/salt leaching method. The compression, creep, and stress relaxation tests of these scaffolds and rabbit articular cartilage show similar profiles, indicating their potential in cartilage tissue engineering [98].

4.3.2.2

Poly(ether ester)

Introduction

Poly (ether ester)s are well known thermoplastic elastomers [34]. They consist of amorphous polyethers as soft segments and crystalline polyesters as hard segments. Their mechanical and degradation properties can be modulated in a wide range, via varying structure and ratio of the segments. Among them, poly(ethylene oxide)/poly(butylene terephthalate) (PEO/PBT) is FDA approved, commercially available (polyActive[®]), and widely used in biomedical engineering. PEO/PBT copolymer is typically synthesized via melt polycondensation of dimethyl terephthalate, PEO, and 1,4-butanediol under high vacuum and temperature using a titanium catalyst. The copolymers are normally abbreviated as aPEObPBTc, where a, b, c are the MW of PEO, the weight% of PEO-terephthalate, and the weight% PBT, respectively.

By varying the feed ratio of PEO to 1,4-butanediol and the MW of the PEO, a series of polymers with diverse mechanical and degradation properties can be obtained. Mechanical testing of 1000PEO72PBT28, 1000PEO55PBT45, 1000PEO30PBT70, 300PEO67PBT33 displays tensile strengths from 8 to 23 MPa and maximal elongation from 500 to 1,300%. It is concluded that the mechanical properties are influenced by the phase separation, which is enhanced by increasing the MW of PEO or the PBT content [99]. A degradation study of 300PEO69PBT31, 1000PEO69PBT31, and 1000PEO61PBT39 in PBS at 37°C traced by intrinsic viscosity and mechanical properties shows totally different degradation profiles. No obvious degradation of 300PEO69PBT31 is observed after 24 weeks. However, 1000PEO69PBT31 loses all of its mechanical strength within 12 weeks [99]. It is concluded that high content of PEO leads to faster degradation of PEO/PBT. The in vivo degradation of PEO/PBT is also investigated [100]. All the copolymers involved: 1000PEO71PBT29,

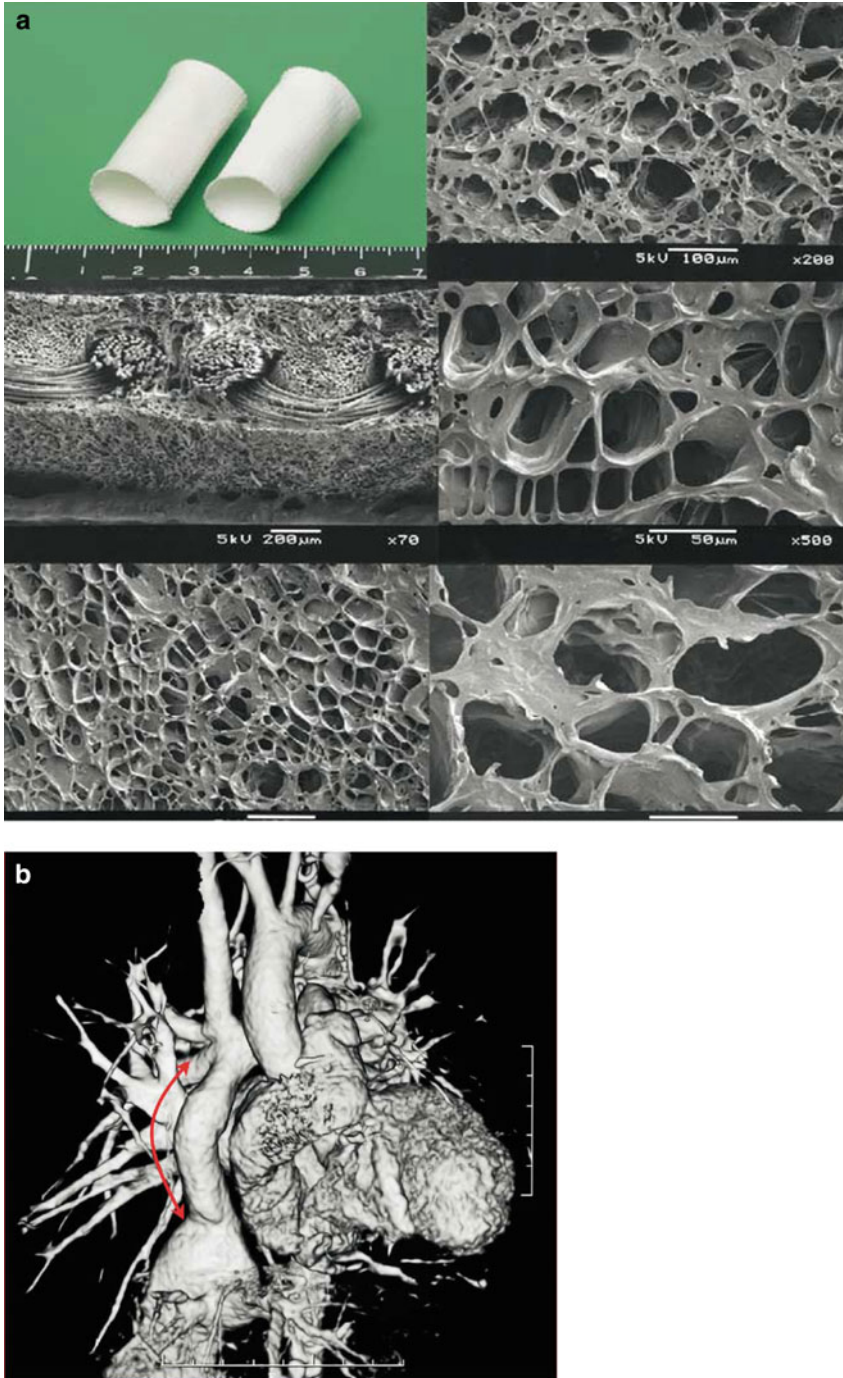


Fig. 4.3 (a) Macroscopic view of biodegradable scaffolds and scanning electromicroscopic findings of polymer scaffolds. *Upper left*, Macroscopic finding; 18 mm in diameter. Copolymer of L-lactide and ϵ -caprolactone synthesized by ring-opening polymerization, with weight composition ratio of L-lactide and ϵ -caprolactone at 50:50. Polymeric woven scaffold reinforced with PGA mesh.

300PEO65PBT35, 300PEO50PBT50 exhibit slow degradation when implanted subcutaneously in rats. The last two only degrade moderately after 6 months. Same as in vitro, a higher PEO content induces faster degradation. In addition, soluble PEO and insoluble PEOT/PBT fraction are identified as the degradation products.

The biocompatibility of PEO/PBT polymer has been well documented. Recent in vivo biocompatibility of porous PEO/PBT scaffolds made of various compositions: 300PEO55PBT45, 300PEO70PBT30, 1000PEO70PBT30, 4000PEO55PBT45, and 2000PEO80PBT20 were systematically evaluated via subcutaneous implantation in minipigs [101]. No wound edema, skin irritation, chronic inflammation, localized tissue necrosis, and granuloma formation was observed in the implants. The rate and extent of polymeric fragmentation associated with the hydrophilicity of the copolymers seem to be the determining factor of success of soft tissue augmentation.

Applications

Here we will introduce a few recent applications of PEO/PBT in tissue engineering. For a more complete review on PEO/PBT, readers are referred to a recent review [102].

PEO/PBT has been extensively investigated for dermal tissue regeneration. Porous scaffolds made of 300PEO55PBT45 were employed to construct a human skin substitute [103]. Human dermal fibroblasts were found to grow well and express ECM consisting of collagen types I and III in PEO/PBT porous scaffold for 21 days culture in vitro. The combination of dynamic seeding and static cultivation was identified to be the most effective method. In another relative study, PEO55PBT45 with various PEO molecular weights (300–4,000 Da) was used [104]. Fibroblasts were cultured in scaffolds for 3 weeks followed by seeding with human keratinocytes. Both cells grew well and led to a multi-layered epithelium with a morphology corresponding to that of the native epidermis. Although there are still some defects of the tissue engineered dermal construct, it provides a potential treatment of large full-thickness skin defects and chronic wounds, avoiding use of large size autologous skin.

Recently, PEO/PBT was also studied for cartilage tissue engineering [105]. Two types of porous 300PEO55PBT45 scaffolds with porosity from 75% to 80% were fabricated by compression-molding/particulate-leaching and 3D fiber deposition. Articular chondrocytes were seeded and tissue formation was evaluated. Although there is no evidence of cartilage-like tissue formation in vitro, 3D fiber deposition PEO/PBT scaffolds significantly increased glycosaminoglycans/DNA considerably better than compression-molding/particulate-leaching ones following subcutaneous implantation. Softer scaffolds made of 1000PEO70PBT30 yielded better results [106]. After implantation in rabbit osteochondral defects for 12 weeks, cartilage-like tissue formed in 1000PEO70PBT30 scaffolds on top of trabecular bone, whereas

← **Fig. 4.3** (continued) Bars represent 200 μm (middle left), 100 μm (lower left, upper right), and 50 μm (middle right, lower right). **(b)** Three-dimensional computed tomographic image of patient's heart 12 months after implantation of autologous bone marrow cells seeded with above PLCL polymeric graft. Arrow indicates location of tissue-engineered conduits (Reprinted by permission from [97]. Copyright 2005, the American Association for Thoracic surgery)

4 the tissue within the 300PEO55PBT45 scaffolds consisted predominantly of trabecular bone. O'Driscoll scores for 1000PEO70PBT30 scaffolds are significantly better than 1000PEO70PBT30 scaffolds and untreated osteochondral defects. This study reveals that the biomechanical and biochemical properties of the scaffold play an important role by themselves, and can affect the healing response of osteochondral defects. PEO/PBT scaffolds with low mechanical properties are superior in engineering cartilage tissue in vivo.

4.3.2.3

Poly(trimethylene carbonate) and Copolymers

PTMC based copolymers is another group of bioelastomers recently studied for tissue engineering application. It is reported that high molecular weight (with M_n above 200,000 Da) PTMC prepared by the ring opening polymerization of trimethylene carbonate is totally amorphous with a low glass transition temperature ($<-17^\circ\text{C}$) and exhibits some rubbery properties at room temperature [107]. But without crosslinking, PTMC cannot recover well from large deformations (yield strain $\varepsilon_{\text{yield}} = 120\text{--}150\%$, yield strength $\delta_{\text{yield}} = 2.1\text{--}2.3$ MPa) and suffers marked creep, and thus is not suitable for practical application as an bioelastomer. Therefore, second segments such PCL or PLA are introduced to provide sufficient physical crosslinking to resist chain flow.

First, poly(trimethylene carbonate-*co*- ε -caprolactone) copolymers were investigated [108]. Addition of PCL reduces both $\varepsilon_{\text{yield}}$ and δ_{yield} when the TMC content is higher than 25 mol%. Further reducing TMC content to 14 mol% causes crystals to form at room temperature and $\varepsilon_{\text{yield}}$ to decrease to 13%. Overall, there were little benefit in introducing PCL to PTMC. Later researchers turned to poly(trimethylene carbonate-*co*-D,L-lactide) copolymers [109]. Better bioelastomers are obtained with $\varepsilon_{\text{yield}}$ of 300% and δ_{yield} of 2 MPa when the TMC content is 72 mol%. Both poly(trimethylene carbonate-*co*- ε -caprolactone) and poly(trimethylene carbonate-*co*-D,L-lactide) exhibit mild inflammatory responses when implanted subcutaneously in rats for 1 year [110]. PTMCs degrade via surface erosion by enzyme mediated processes in vivo, which is advantageous because it leads to a linear decrease of their physical and mechanical properties [110]. However PTMC degradation is hard to predict, since contradictory results are reported [111]. Although the material properties of PTMC based copolymers have been extensively investigated, its usefulness in tissue engineering has not been reported.

4.3.2.4

Poly(ester amide)

Poly(ester amide) is another family of thermoplastic bioelastomers. Generally, polyamide segments are employed as the hard phase. The crystallinity and the strong hydrogen bonding between the amide bonds of individual chains serve as physical crosslinking to impart the segmented polymer mechanical strength. On the other hand, flexible polyester segments are employed as the soft phase to convey elasticity to the polymer. In addition, polyesters are superior in solubility, and hydrolytic susceptibility, and thus can be designed

to modulate the processability and degradability of resultant polymers [112]. Relative to other bioelastomers, reports on poly(ester amide) in tissue engineering are limited. A recent example is introduced here.

A segmented poly(ester amide) with a soft block based on 1,4-butanediol and dimethyl adipate and a hard block based on dimethyl adipate, ϵ -caprolactone, and 1,4-diaminobutane was developed [113]. It was synthesized by two-step polycondensation of dimethyl adipate, 1,4-butanediol and N,N' - α,ω -alkanediyl-bis[6-hydroxy-hexanamide] (bisamide-diol) catalyzed by tetrabutyl(orthotitanate). Polymers with 25 and 50 mol% of amide content supported fibroblast growth in vitro and led to a mild foreign-body reaction upon subcutaneous implantation. Tensile testing shows that they are relatively hard bioelastomers. Young's modulus (from 150 to 313 MPa) and tensile strength (δ_{yield} from 8 to 14 MPa, δ_{break} from 21 to 25 MPa) increased with the increasing amide content, with similar maximal strain (745% and 775%). Complete degradation of these polymers in vitro (PBS, 37°C) occurs in 7 months. In vivo, only 2.5% mass loss of the polymer with 50% amide content was found after 42 days of subcutaneous implantation. In addition, either segment can also be incorporated to modulate the properties [114].

Thermoset Bioelastomers

Thermoset bioelastomers are covalently crosslinked, which is stronger than physical crosslinks. They usually have good mechanical stability, suitable for applications in a mechanically dynamic environment. Very importantly, their amorphous structure is more homogeneous and often leads to a more uniform degradation with good retention of structural and mechanical integrity during degradation. The last fabrication step of thermoset elastomer is curing, an irreversible step that locks the polymer in its final shape. One drawback of a thermoset polymer is that the curing step may not be compatible with certain biomolecules. Another drawback of thermoset elastomer is that the curing step may pose a challenge in material processing. Poly(glycerol sebacate) (PGS), a representative thermoset bioelastomer will be discussed in Sect. 4.3.3, followed by other thermoset bioelastomers in Sect. 4.3.4.

4.3.3

Poly(glycerol sebacate)

4.3.3.1

Introduction

Design and Structure

Current interest in thermoset bioelastomers for tissue engineering is largely driven by soft-tissue, especially cardiovascular tissue engineering. A novel thermoset bioelastomer, poly(glycerol sebacate) (PGS) was created specifically for implantation in dynamic mechanical environments such as the cardiovascular system [115]. The rationale of this bioelastomer is to create a biodegradable analog to vulcanized rubber. The covalent crosslinking creates a 3D

network of random coils, which resembles the structure of vulcanized rubber and gives this polymeric network rubber-like elasticity. Hydrogen bonding interactions are designed into the polymeric network to further modulate the mechanical properties of PGS. Such a strategy to achieve tough and elastic materials is also inspired by naturally biological elastomeric systems. For example, collagen and elastin, the major fibrous protein components of ECM are crosslinked. Both covalent crosslinking and the hydrogen bonding interactions likely contribute to their mechanical strength. Different from nondegradable elastomers, PGS is constructed by hydrolysable ester bonds, which are expected to degrade in the physiological environment with minimal differences in degradation caused by variance in enzyme levels. To increase biocompatibility, the elastomer is made from endogenous building blocks: glycerol and sebacic acid. The former is the basic building block for lipids. The latter is the natural metabolic intermediate in ω -oxidation of medium- to long-chain fatty acids. The FDA has approved glycerol and polymers containing sebacic acid for medical applications. Therefore, the potential degradation products of PGS are nontoxic.

Synthesis and Mechanical Properties

PGS is synthesized by a two-step polycondensation [115]. First, equimolar amounts of glycerol and sebacic acid react at 120°C under argon for 24 h to furnish an uncrosslinked prepolymer. The prepolymer is easily processed into various shapes, because it melts into liquid and dissolves in common organic solvents such as 1,3-dioxane, tetrahydrofuran, ethanol, isopropanol, and *N,N*-dimethylformamide. Further curing of prepolymer in a vacuum oven at 120°C and 40 mTorr produces the PGS bioelastomer. Tensile test shows that PGS has elastomeric properties that resemble cured natural rubber with a Young's modulus of 0.282 ± 0.0250 MPa. The ultimate tensile stress and strain are at least 0.5 MPa and $267 \pm 59.4\%$ respectively. The mechanical properties of PGS are similar to those of soft tissues (Table 4.1) [116].

Degradability

PGS shows a linear *in vivo* degradation profile with preservation of geometry and retention of mechanical strength, both are critical parameters for applications in tissue engineering [117]. PGS implants maintain their integrity and no cracks form in the implant. However, apparent cracks in PLGA are observable starting at 7 days post-implantation and continue to develop throughout the implantation period [117]. The mass and compression modulus of PGS implants decrease nearly linearly, with a steady increase of degree of swelling throughout the 35-day study. In contrast, PLGA implants lose their mechanical strength greatly (98%) within 7 days and show a sharp decrease in mass and accelerated water uptake after 14 days. These findings indicate that the degradation mechanisms of PGS (surface erosion) and PLGA (bulk erosion) are different. In addition, PGS shows a different degradation rate *in vitro* and *in vivo*. It loses $17 \pm 6\%$ mass when agitated in PBS solution at 37°C for 60 days, whereas PGS implants are totally absorbed at this point. The difference is most likely due to the presence of enzymes and macrophage mediated degradation *in vivo*.

In addition, multiple research groups have demonstrated that the mechanical and degradation properties of PGS can be easily tailored in a wide range by varying the curing temperature, time, and feed ratio of sebacic acid and glycerol [14, 118–120].

Biocompatibility

PGS shows excellent in vitro and in vivo biocompatibility [115]. The in vitro biocompatibility is evaluated by culture of NIH 3T3 fibroblast cells on the surface of the polymer. The cells adhere well and show normal morphology, with higher growth rate than those on PLGA. The in vivo biocompatibility is evaluated by subcutaneous implantation in Sprague-Dawley rats. Similar to former reports, fibrous capsules (thick avascular collagen layer) surrounding PLGA implants develop within 14 days and remain approximately 140 μm in thickness. In contrast, only 45 μm thick fibrous capsules around PGS implants appear at 35 days and are highly vascularized. At 60 days, the PGS implants are completely absorbed without formation of granulation or scar tissue, and the implantation site is restored to its normal histologic architecture. Overall, PGS is at least as biocompatible as PLGA.

4.3.3.2

Applications

Because PGS is easy to synthesize and has good biocompatibility, tunable mechanical and degradation properties, it has been widely used in tissue engineering, drug delivery [121] and anti-adhesion in abdominal surgeries [122]. Herein, we will focus on its applications in soft tissue engineering.

Scaffold Fabrication

Various types of PGS scaffolds have been fabricated. Photolithographical tools have been used to produce a capillary network of PGS [123]. Human umbilical vein endothelial cells adhere well on these micro-channels. Under flow culture conditions, the cells proliferate and partly approach confluence within 14 days, and remain viable up to at least 4 weeks. Specifically tailored microfabrication processes produce microfluidic PGS scaffolds [124] and scaffolds that can provide contact guidance [125]. Hepatocytes (cell line) can be cultured in microfluidic PGS scaffolds with long-term perfusion. This method can lead to vascularized liver constructs, which may be integrated with the patient's existing vasculature in order to restore organ function. An improved solvent casting/salt leaching method produced porous PGS scaffolds with approximately 90% porosity, extensive micropores, good pore interconnectivity, and uniform scaffold thickness [126, 127]. Fibroblasts adhered and proliferated well within these scaffolds and formed 3D tissue-engineered constructs within 8 days. Recently, an elegant coaxial core/shell electrospinning scheme is reported that uses polylactide as the shell material to fabricate a nanofibrous PGS scaffold. The mechanical

properties of the scaffolds resembles that of elastin [128]. The scaffold possesses excellent cytocompatibility, as demonstrated by culture of human microvascular endothelial cells.

Applications in Cardiovascular Tissue

PGS sustains and recovers well from cyclic deformation, making it suitable as scaffold material in the cardiovascular system. Development of small-diameter arterial grafts with long-term patency is still a major challenge in tissue engineering. Previous investigations using stiff materials such as PLA and PGA always lead to very high collagen content and superb burst pressures, but have low elastin expression and compliance mismatch. Compliance mismatch is known to cause intimal hyperplasia and ultimately graft occlusion in vascular grafts. It is hypothesized that engineering small arteries on elastomeric scaffolds under dynamic mechanical stimulation will result in strong and compliant arterial constructs. Accordingly, seamless tubular highly porous PGS scaffolds are fabricated and employed in the engineering of small arteries [127, 129–131]. Primary baboon endothelial progenitor cells and baboon SMCs adhere and proliferate well in PGS scaffolds. The cells exhibit normal morphologic and phenotypic properties, and synthesize a significant amount of ECM within 15 days [129]. Using a pulsatile flow system at physiologic pressure and co-culture of endothelial progenitor cells and SMCs, the constructs of PGS scaffolds co-express elastin and collagen, leading to highly compliant and distensible engineered blood vessels, demonstrating that elastin synthesis and compliance matching are feasible in blood vessel tissue engineering [130]. Further comparison of constructs created from PGS and PLGA scaffolds cultured with SMCs under identical conditions demonstrates that: (1) substrate stiffness directly affects in vitro tissue development and mechanical properties; (2) elastic materials greatly facilitate crosslinked elastin expression and lead to engineered arterial tissues with physiologic compliance after only 10 days of culture [131].

Another important application of PGS is in tissue engineering of cardiac tissues [132–135]. The mechanical properties of PGS can be readily modulated to match those of myocardial tissues [14]. A highly porous PGS scaffold with parallel channels is successfully fabricated, which mimics the capillary network in native myocardium [132]. In contrast, the attempt to fabricate channeled scaffold using collagen fails due to the inferior mechanical properties of collagen [134]. Co-culture of cardiac fibroblasts and cardiomyocytes in a perfusion bioreactor with oxygen carriers yields contractile constructs within 11 days [134]. In vivo, cell-free PGS scaffolds are vascularized after implantation in a rat infarcted myocardium model for 2 weeks [134]. Recently, a PGS scaffold with an accordion-like honeycomb microstructure was created (Fig. 4.4) [135]. Its stiffness is well controlled by curing time and closely matches the mechanical properties of native adult rat right ventricular myocardium. Further, it integrates anisotropy into scaffold materials, which guides neonatal rat cardiomyocyte orientation in the constructs. This exciting development of PGS scaffolds overcomes principal structural-mechanical limitations of isotropic scaffolds and paves a new way towards advanced tissue-engineering scaffolds tailored for tissue-specific regeneration. In addition, PGS scaffold precoated by proteins increases cellularity, enhances ECM protein production and modulates the differentiation of endothelial progenitor cells [136]. It provides a promising scaffold for tissue engineering of heart valves.

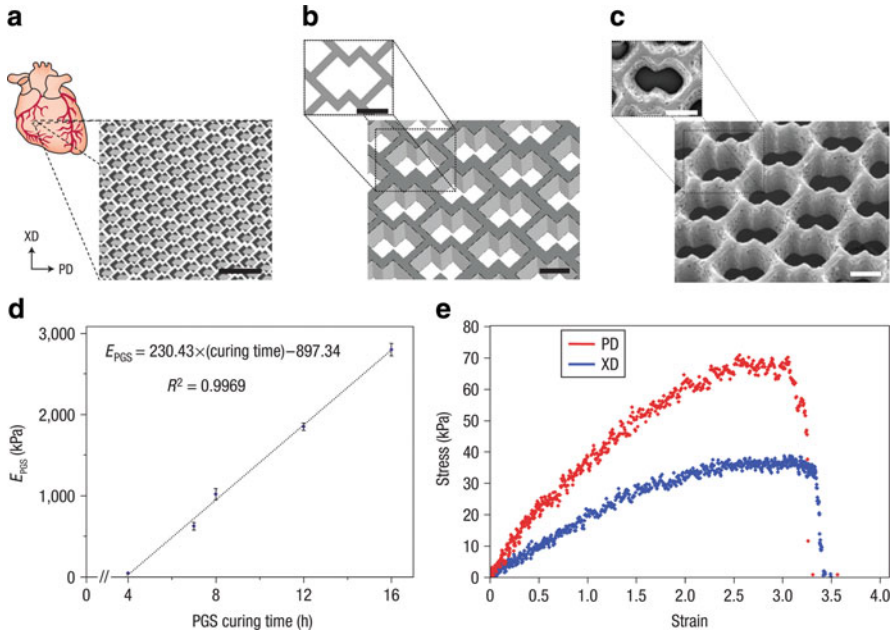


Fig. 4.4 Accordion-like honeycomb scaffolds yield anisotropic mechanical properties similar to native myocardium. **(a, b)** Schematic diagrams illustrating the accordion-like honeycomb design constructed by two overlapping $200 \times 200 \mu\text{m}$ squares rotated 45° (*diamonds*). Preferred (PD) and orthogonal cross-preferred (XD) material directions, respectively, corresponding to circumferential and longitudinal axes of the heart, are indicated. Scale bars: 1 mm **(a)** and $200 \mu\text{m}$ **(b)**. **(c)** Scanning electron micrographs demonstrating the fidelity of excimer laser microablation in rendering an accordion-like honeycomb design in PGS. Scale bars: $200 \mu\text{m}$. **(d)** PGS curing time was systematically varied, yielding a linear dependence of PGS effective stiffness (E_{PGS}) on curing time within the tested range. **(e)** Representative uniaxial stress–strain plots for accordion-like honeycomb scaffolds with cultured neonatal rat heart cells (scaffolds were fabricated from PGS membranes cured for 7.5 h at 160°C ; neonatal rat heart cells were cultured for 1 week) (Reprinted by permission from [135]. Copyright 2008, Nature Publishing Group)

Applications in Nervous Tissue

PGS has been also demonstrated to be a promising scaffold material for nerve regeneration [137]. The *in vitro* and *in vivo* neural biocompatibility of PGS have been systematically evaluated. Primary Schwann cells show similar attachment rate and metabolic activity on both PGS and PLGA surfaces *in vitro*. The cells on PGS have a higher proliferation rate and lower apoptotic activity than those on PLGA. *In vivo* implantation juxtaposed to the sciatic nerve reveals that PGS causes a significantly lower chronic inflammatory response than PLGA, probably because its degradation proceeds by surface erosion with low swelling. A recent study investigates microfabricated PGS porous scaffold for retinal progenitor cell (RPC) grafting. The scaffold has a Young's modulus of $1.66 \pm 0.23 \text{ MPa}$ and a maximal strain of $113 \pm 22\%$ [138]. These mechanical properties more closely resemble those of

4 retinal tissue (Young's modulus of 0.1 MPa and maximal strain of 83%) than the traditional PLA/PLGA blend (Young's modulus of 9.0 ± 1.7 MPa and maximal strain of 9%) used for RPCs delivery. In vitro study reveals that RPCs adhere and proliferate well in the PGS scaffold, and show a trend towards differentiation. Subretinal transplantations demonstrate long-term RPC survival and high levels of RPC migration into host retinal tissue [139].

4.3.3.3

Improvement

Poly(glycerol sebacate) Acrylate

Curing of PGS is typically performed at high temperature and high vacuum for 1–2 days. The procedure is relatively long and the conditions are too harsh for biomolecules such as proteins. Acrylation of PGS leads to poly(glycerol sebacate) acrylate (PGSA) with photocrosslinkable double bonds [140]. Varying the degree of acrylation and copolymerization with PEO modulates the mechanical properties of PGSA bioelastomers over a wide range: Young's modulus from 0.05 to 20 MPa, tensile strength from 0.05 to 0.89 MPa, and maximal strain from 4% to 189%. At the same time, the degradation rate and swelling ratio in an aqueous environment can also be varied. By adding nonreactive glycerol during polymerization, a porous PGSA scaffold is fabricated that is capable of encapsulating cells in situ [141]. The encapsulated neuroblastoma and human embryonic stem cells adhere into the matrix and grow well. The neuroblastoma cells form matrix fibrils and tissue, and embryonic stem cells differentiate to form 3D tissue mimetic structures within 7 days. Subcutaneous transplantation demonstrate the in vivo biocompatibilities of PGSA scaffolds and their ability to promote tissue ingrowth [141]. Recently, PGSA is fabricated to fibrous scaffolds via electrospinning using gelatin as a carrier polymer [142]. The resultant scaffolds show diverse mechanical (Young's modulus from ~ 0.06 to 1 MPa) and degradation properties (~ 45 –70% mass loss by 12 weeks). In vitro evaluation using mesenchymal stem cells demonstrates their cytocompatibility. In vivo evaluation using an acute myocardial infarction rat model reveals a diverse host response, depending on the PGS macromer acrylation and the scaffold thickness.

Poly(sebacoyl diglyceride)

PGS and later developed crosslinked polyester bioelastomers are typically synthesized by random polycondensation [115, 143–147]. This method produces prepolymers with relatively low molecular weight, high polydispersity index, undefined branched structure, and are prone to premature crosslinking. All of these issues compromise the mechanical properties of the bioelastomer and impede their further modification. To overcome these limitations, a novel synthetic strategy has been developed to prepare poly(sebacoyl diglyceride) (PSeD) bearing free hydroxyl groups by an epoxide ring opening reaction between diglycidyl sebacate and sebacic acid [148]. PSeD can be viewed as a linear subset of PGS. MTT assay using nonimmortalized Baboon SMCs (TCPS as a control) and subcutaneous

implantation in Sprague Dawley rats (PLGA as a control) demonstrate that PSeD retains the favorable in vitro and in vivo biocompatibility of PGS. The distinct synthetic method imparts PSeD several superior advantages over PGS prepolymer: better defined structure with more free $-OH$ groups and higher linearity (10% vs. 55% branching); higher molecular weight (M_n 16.6 kDa vs. 9.0 kDa); narrower polydispersity index (2.5 vs. 9.3); and longer shelf time (>1 year vs. <3 months). Crosslinking PSeD with sebacic acid yields a much tougher and more elastic elastomer than cured PGS: 5 times higher Young's modulus (1.57 ± 0.48 vs. 0.282 ± 0.025 MPa), more than 3 times higher tensile strength (1.83 ± 0.06 vs. 0.5 MPa), and greater maximal strain ($409 \pm 29\%$ vs. $267 \pm 59.4\%$). In addition, the cyclic tensile test reveals the PSeD's ability to recover well from cyclic deformations. The feasibility of functionalization of PSeD is demonstrated by ready glycation and maleic esterification. This versatile synthetic strategy is also applicable to other diepoxides and diacids, which will lead to diverse biodegradable and biofunctionalized bioelastomers with a variety of mechanical and physiochemical properties.

4.3.4

Other Thermoset Bioelastomers

4.3.4.1

Crosslinked Polyester Bioelastomers Prepared by Polycondensation

Introduction

Invention and successful applications of PGS in biomedical engineering have led to the development of many other crosslinked polyester bioelastomers. Following the design principles of PGS, these bioelastomers are typically synthesized from nontoxic polyacids and polyols by polycondensation to increase biocompatibility. Polyester based network with various predetermined structures and controlled crosslinking imparts them tunable mechanical properties and biodegradability. Some representative examples of these crosslinked polyester bioelastomers are listed in Table 4.4. For more structural variations, readers are directed to relevant reviews [13, 88].

By varying the compositions and curing conditions, mechanical and degradation properties of crosslinked polyester bioelastomers can be modulated in a wide range (Table 4.4): from very soft relative weak to very strong relative hard materials [149], from very fast degradation [149] to almost inertness [147]. First, different compositions will directly affect the properties of these bioelastomers. Normally, hydrophobic structures will impede the water uptake and slow the degradation. But for mechanical properties, so far, it is hard to tell which one is better. Secondly, for fixed compositions, closer content of reactive functionalities in reactors such as hydroxyl and carboxylic acid groups, higher curing temperature, and longer curing time normally will induce higher crosslinking density and result in an increase of the Young's modulus and ultimate tensile strength, but decrease of the maximal strain and degradation rate. For practical applications, mechanical, degradation, and other properties should be considered together. For example, from a biocompatibility standpoint, generally water soluble monomers are preferable, since they will be easy to remove from the body after degradation. But, too

Table 4.4 Selected examples of crosslinked polyester bioelastomers

Materials	Curing conditions	E (MPa)	σ (MPa)	ε (%)	Degradation ^a time, mass loss	References
POC	12°C, 2 Pa, 1 d	2.84	3.62	253	3 d, ~90% ^b	[143, 151]
POC	120°C, 2 Pa, 3 d	4.69	5.34	160	3 d, ~15%	[143, 151]
POC	120°C, 2 Pa, 6 d	6.44	5.80	117	–	[143, 151]
POC	80°C, 14 d	2.66	–	265	–	[143]
POC	80°C, 2 d	1.38	1.64	–	28 d, ~23% 12 h, ~95% ^b	[151]
POC	80°C, 4 d	1.85	2.93	367	–	[151]
PHC	80°C, 2 d	–	–	–	12 h, ~95% ^b	[151]
PHC	80°C, 4 d	12.08	5.99	389	–	[151]
PDC	80°C, 2 d	–	–	–	12 h, ~85% ^b	[151]
PDC	80°C, 4 d	1.92	3.49	338	–	[151]
PDDC	80°C, 2 d	–	–	–	12 h, ~25% ^b	[151]
PDDC	80°C, 4 d	1.60	6.19	502	–	[151]
POCM	80°C, 4 d	13.98	9.76	386	–	[151]
POCM	80°C, 2 d	8.1	5.6	–	28 d, ~70%	[151]
POCM	80°C, 4 d	13.98	9.76	386	–	
PDDCM	80°C, 4 d	4.30	11.15	445	–	[151]
PXS 1:1	120°C, 2 Pa, 4 d	0.82	0.61	205.16	105 d, 1.78% 49 d, 100% ^c	[145, 147]
PXS 1:2	120°C, 2 Pa, 4 d	5.33	1.43	33.12	105 d, 1.88%; 196 d, 23.3% ^c	[145, 147]
PSS 1:1	120°C, 2 Pa, 5 d	0.37	0.57	192.24	105 d, 15.66% 84 d, 100% ^c	[147]
PSS 1:2	120°C, 2 Pa, 4 d	2.67	1.16	65.94	105 d, 5.57%	[147]
PMS 1:1	140°C, 2 Pa, 5 d	2.21	0.79	50.54	105 d, 21.90%	[147]
PMS 1:2	140°C, 2 Pa, 5 d	12.82	3.32	44.99	105 d, 9.00%	[147]
PMtS 1:4	150°C, 2 Pa, 5 d	378.0	17.64	10.90	105 d, 0.76%	[147]
2DAHP-1G	170°C, 50 mTorr, 24 h	2.45	1.33	92	42 d, 97.0% ^d	[146]
2DAHP-1G	170°C, 50 mTorr, 48 h	4.34	1.69	64	42 d, 44.3% ^d 140 d, 12.9% ^c	[146]
2DAHP-1T	170°C, 50 mTorr, 24 h	1.45	0.39	60	42 d, 70.4% ^d	[146]
2DAHP-1T	170°C, 50 mTorr, 48 h	1.48	0.24	21	42 d, 42.8% ^d 140 d, 13.0% ^c	[146]
CUPE0.6	80°C, 2 d	2.99	16.02	252.37	56 d, 16%	[150]
CUPE0.9	80°C, 2 d	5.84	32.10	278.24	56 d, ~15%	[150]
CUPE1.2	80°C, 2 d	29.82	33.35	260.87	56 d, 8.13%	[150]
CUPE1.2	80°C, 1 d	4.84	28.75	265.43	–	[150]
CUPE0.6	80°C, 1 d	2.53	15.62	291.26	–	[150]
PPCLM300	120°C, 1 d	–	1.26	72.70	70 d, ~66%	[152]
PPCLM300	120°C, 3 d	–	8.18	123.12	70 d, ~45%	[152]
PPCLM300	120°C, 5 d	–	15.19	172.37	70 d, ~30%	[152]
PPCLM900	120°C, 1 d	–	0.32	204.18	70 d, 23.1%	[152]
PPCLM900	120°C, 3 d	–	0.63	49.03	70 d, ~12%	[152]

(continued)

Table 4.4 (continued)

Materials	Curing conditions	E (MPa)	σ (MPa)	ε (%)	Degradation ^a time, mass loss	References
PPCLM900	120°C, 5 d	–	0.70	30.97	70 d, 10.51%	[152]
PBa	60°C, 7 d	1.95	1.0	583	2 d, 100%	[149]
PHa	60°C, 7 d	0.1	0.3	395	4 d, 100%	[149]
PGa	90°C, 2 d	459.4	9.3	121	3 d, 100%	[149]
PBa	90°C, 2 d	161.3	4.7	418	7 d, 100%	[149]
PHa	90°C, 2 d	2.5	2.1	176	14 d, 100%	[149]
PGa	120°C, 1 d	499.7	16.7	43	8 d, 100%	[149]
PBa	120°C, 1 d	381.9	8.1	95	17 d, 100%	[149]
PHa	120°C, 1 d	657.4	30.8	22	28 d, 100%	[149]
PHa	120°C, 6 h	0.1	0.2	379	4 d, 100%	[149]
PHa	120°C, 12 h	1.3	1.2	151	12 d, 100%	[149]
PHa	120°C, 8 h	4.2	2.2	200	13 d, 100%	[149]
PGSL	140°C, 40 m Torr, 30 h	2.94	0.15	133	30 d, ~17%	[153]
PGSC4/4/1	120°C, 8 h	1.03	0.76	106	28 d, ~23%	[154, 155]
PGSC4/4/1	120°C, 10 h	1.43	0.84	86	28 d, ~20%	[155]
PGSC4/4/1	120°C, 12 h	2.07	0.97	65	28 d, ~16%	[154, 155]
PGSC4/4/1	120°C, 14 h	3.26	1.46	62	28 d, ~12.5%	[154, 155]
PGSC4/4/0.6	120°C, 12 h	0.61	0.63	170	28 d, ~17%	[154]
PGSC4/4/0.6	120°C, 16 h	1.55	0.80	78	–	[154]
PGSC4/4/0.6	120°C, 18 h	2.23	0.86	51	28 d, ~15%	[154]

E Young's modulus, ε Maximal strain, σ Tensile strength, *POC* Poly(1,8-octanediol-*co*-citrate), *PHC* Poly(1,6-hexanediol-*co*-citrate), *PDC* Poly(1,10-decanediol-*co*-citrate), *PDDC* Poly(1,12-dodecanediol-*co*-citrate), *POCM* Poly[1,8-octanediol(90%)-*co*-*N*-methyl-diethanolamine-*co*-citrate], *PDDCM* Poly[1,12-dodecanediol(90%)-*co*-*N*-methyl-diethanolamine-*co*-citrate], *PXS a/b* Poly(xylylitol sebacate), $M_{xylylitol}/M_{sebacic\ acid} = a/b$, *PSS a/b* Poly(sorbitol sebacate), $M_{sorbitol}/M_{sebacic\ acid} = a/b$, *PMS a/b* Poly(mannitol sebacate), $M_{mannitol}/M_{sebacic\ acid} = a/b$, *PMtS a/b* Poly(maltitol sebacate), $M_{maltitol}/M_{sebacic\ acid} = a/b$, *2DAHPIG* Poly(1,3-diamino-2-hydroxy-propane-*co*-glycerol sebacate), *2DAHPIT* Poly(1,3-diamino-2-hydroxy-propane-*co*-threitol sebacate), *CUPEa* Crosslinked urethane-doped polyesters, $M_{pre-POC}/M_{HDI} = 1/a$, *PPCLMa* Poly(polycaprolactone triol malate), *Mn(PCL) = a*, *PBa* Poly(1,2,4-butanetriol $\dot{\alpha}$ -ketoglutarate), *PHa* Poly(1,2,6-hexanetriol $\dot{\alpha}$ -ketoglutarate), *PGa* Poly(glycerol $\dot{\alpha}$ -ketoglutarate), *PGSL* Poly(glycerol-sebacate-lactic acid), *PGSCa/b/c* poly(glycerol-sebacate-citrate), $M_{glycerol}/M_{sebacic\ acid}/M_{citric\ acid} = a/b/c$

^aPBS, 37°C unless otherwise noted

^b0.1 M NaOH, 37°C

^cIn vivo degradation (subcutaneous implantation in rat)

^dNaOAc buffer, 37°C

hydrophilic of a monomer will lead to water soluble prepolymers, such as poly(xylitol-citrate) and result in very weak hydrogel rather than the desired bioelastomer after crosslinking [145]. Recently, besides polyols and polyacids, some other monomers such as amino alcohol [146] and other crosslinking reagents such as diisocyanate [150] have also been used to provide more choices to control the properties of resultant bioelastomers.

Applications

Some of the above bioelastomers have been investigated for tissue engineering applications. Recent examples are introduced below. POC (Table 4.4) has been fabricated to porous scaffolds [156, 157]. Their mechanical properties are varied by porosity [157]. The culture of human aortic SMCs, endothelial cells, and mouse cardiac muscle cell line HL-1 in the scaffolds demonstrate their preliminary potential for cardiovascular tissue engineering. In addition, porous POC scaffolds have also been tested for cartilage tissue engineering [158]. Articular chondrocytes from bovine knee grow well in the scaffolds and secrete detectable levels of glycosaminoglycans and collagen. The produced POC-chondrocyte construct showed much higher Young's modulus than cell-free POC scaffold.

A biphasic elastic scaffold based on PPCLM (Table 4.4) has been fabricated for annulus fibrous tissue regeneration [152]. Porous PPCLM foams seeded with rabbit chondrocytes (inner phase) are rolled over and inserted into a ring-shaped demineralized bone matrix gelatin (outer phase) to produce a structurally and elastically mimetic construct of annulus fibrous tissue. The resultant biphasic scaffold shows moderate tensile strength (3.37 MPa) close to that of normal rabbit annulus fibrous (6.95 MPa). Chondrocytes proliferate and penetrate the inside of the scaffold after 4 weeks of in vitro culture. Subcutaneous implantation demonstrates that there is no obvious inflammatory response up to 8 weeks. In-growth of surrounding tissues is observed at 2, 4, and 8 weeks. This study indicates that PPCLM biphasic scaffolds are promising candidates for annulus fibrous regeneration.

Recently, poly(ester amide)s, 2DAH-1G and 2DAH-1T (Table 4.4) have been fabricated into a collagen-mimetic scaffold [159]. Replica-molding creates nanotopographic features in the scaffolds, which enhances initial attachment, spreading, and adhesion of primary rat hepatocytes with reduction of liver-specific cell function including albumin secretion and urea synthesis. A similar trend was observed in hepatocytes cultured on collagen substrates. This study provides promising engineered substrates that may function as synthetic collagen analogs.

Advantages of Polycondensation Strategy

Compared with other strategies to produce bioelastomers for tissue engineering, the polycondensation strategy described here has several unique advantages.

1. Feasible and versatile synthesis: The synthetic strategy is very flexible and can provide a wide range of products with tunable mechanical, physical, and biological properties. At the same time, the chemistry involved is simple. No catalyst is needed. Normally

residual catalyst may introduce toxicity. The synthetic bioelastomers are ready to use without purification.

2. Excellent properties: The polyester based structure with well defined hydrolytic degradation provides predicted degradation byproducts and good biocompatibility can be expected with proper design. Compared to physically crosslinked thermoplastic bioelastomers, these thermoset bioelastomers are covalently crosslinked and are more resilient to creeping. More importantly, degradation studies revealed that these bioelastomers normally degrade via surface erosion, which leads to geometrical integrity and linear loss of mass and mechanical properties [117, 153, 160]. Both are critical properties for in vivo application.
3. Functionalizability: The bioelastomers synthesized by this method typically contain many unreacted functional groups such as hydroxyl, amine, and carboxylic acid groups, which enable further biofunctionalization. Although undefined presentation of functional groups are not ideal for practical modification, employment of novel synthetic strategies has been shown to yield a much more defined structure with free functional groups, which will better realize this potential [148]. Through the newly developed biofunctionalizable platform, special biochemical cues such as peptides can be readily introduced to control cell-material interactions.

In summary, numerous bioelastomers have been developed by polycondensation, and some of the newer ones have not been widely investigated. More investigations are needed to realize their potential in tissue engineering.

4.3.4.2

Thermoset Bioelastomers Prepared by Ring-Opening Polymerization

Besides polycondensation, another route to prepare thermoset bioelastomers is crosslinking multi-arm star-shaped biodegradable prepolymers, which are typically synthesized by ring-opening polymerization (ROP) using polyols as initiators [13]. Some of the most commonly used monomers for ROP include glycolides, lactides, ϵ -caprolactone, and trimethylene carbonate. ROP are normally performed as bulk polymerization in the melt using organo-metallic compounds such as stannous 2-ethylhexanoate (SnOEt_2) as the catalyst under high temperature (90–180°C). Varying the prepolymer MW and the compositions provides a family of bioelastomers with diverse mechanical and degradation properties. Compared to polycondensation, the ROP can be better controlled, but it needs strict reaction conditions and the residual metal catalyst will lead to potential toxicity. Unlike the ones prepared by polycondensation of multi-functional monomers, the bioelastomers produced by ROP normally lack functional groups. This makes them difficult to be biofunctionalized, and the unmodified polymer may have poor affinity to cells [161]. Compared to polycondensation, this method is still in the early stage and has not been well studied in tissue engineering. Yet, this class of polymer may be useful in certain biomedical applications. A representative example is used to highlight the development in this area.

Crosslinked ω, ω, ω -triacylate [*star*-poly(ϵ -caprolactone-*co*-D,L-lactide)] (ASCP) is one of the first examples of this type of bioelastomer being studied for tissue engineering [162].

The prepolymer SCP is prepared by ROP of lactide and ϵ -caprolactone initiated by glycerol. Acrylation of SCP using acryloyl chloride reaction followed by UV-crosslinking produces final bioelastomers. Various crosslinked ASCPs with different MWs of prepolymer are synthesized ($M_{nSCP} = 1,250, 2,700, 7,800, 11,900$). All of them show low glass-transition temperature from -6 to -8°C . As expected, increasing the prepolymer MW increases the tensile strengths and Young's modulus, while decreasing maximal strains. The *in vitro* degradation in PBS at 37°C for 12 weeks shows relative little mass loss, from 18 to 35%, with little dimensional change. It is found that bioelastomers prepared from lower MW prepolymer degrades faster. The mechanical strength decreases greatly during degradation with little change of maximal strain. *In vivo* degradation by subcutaneous implantation in rats reveals a similarly linear degradation pattern of ASCP ($M_{nSCP} = 1,250$) with high crosslink density via surface erosion during 12 weeks period [163]. However, the ASCP ($M_{nSCP} = 7,800$) with low crosslink density exhibits bulk erosion with initially slow degradation followed by a noticeable loss of mechanical strength after 4 weeks. To improve the cell adhesion on the bioelastomers, the peptide GRGDS is incorporated by using acryloyl-PEO-GRGDS during photocrosslinking [161]. It is revealed that introduction of GRGDS improves both cell adhesion and proliferation, with more marked effects on the high crosslink density ASCPs. In addition, SCP is also crosslinked by copolymerization with different ratios of ϵ -caprolactone and a crosslinking monomer, 2,2-*bis*(ϵ -caprolactone-4-yl)-propane[164]. The resultant polymers displays a low glass transition temperature (-32°C). Mechanical testing shows tunable Young's module (0.55–1.55 MPa), tensile strength (0.21–0.60 MPa), and maximal strain (65–154%). *In vitro* degradation in PBS reveals a logarithmic fashion of tensile strength with time.

4.4 Future Directions

Although remarkable progress has been made already, bioelastomers are still in its early stage. Much work remains to develop them into more useful and versatile scaffold materials.

Current bioelastomers are still oversimplified mimetics of elastic ECM molecules. Most of them are designed to match special mechanical parameters of native tissue such as modulus or strength. But most tissues possess complex viscoelastic, anisotropic, and non-linear mechanical properties that may even vary with age and location [25, 165]. For example, articular cartilage exhibits appreciable viscoelasticity [166] and depth-dependant modulus, as well as around two orders of magnitude difference in tensile and compressive moduli [167]. Further, its modulus significantly varies with strain [168, 169]. To better mimic these complexities of native tissues, advanced material synthetic strategies, such as fiber reinforcement and 3D woven composite materials [170] and sophisticated fabrication methods such as excimer laser microablation [135] may be very useful [2].

Recently, mechanical control has been shown to profoundly affect cell and tissue behaviors [3]. It should also be noticed that biochemical regulation on cell and tissue function is also very important [171]. A single factor is not enough to fully optimize cell and tissue development [172]. For example mesenchymal stem cells show better

differentiation upon the cooperative effects of matrix elasticity and soluble induction factors than single mechanical effect, indicating that both mechanical and chemical cues are critical for cell differentiation [11]. Therefore, combining biochemical cues and bioelastomers may lead to a unique ensemble of biological and mechanical regulations, which can lead to better material performance in tissue regeneration.

Advanced material development will further increase the value of bioelastomers. For example, shape-memory polymers are a special family of elastomers [173]. As a smart material, the device made from shape-memory polymer can be fabricated to a small, rigid, easy handling state during implantation at room temperature for minimally invasive surgical procedures, and deploy automatically to become soft and elastic at body temperature to serve as an ideal compliant material for soft tissue. According to this design, shape-memory polymer has already shown some optimistic biomedical applications such as biodegradable sutures, actuators, catheters, and smart stents [174–176]. However, their potential in tissue engineering has yet been explored [174, 177]. More recently, self-healing elastomers have been created [178, 179]. It may be fabricated into smart scaffolds that can self-heal during degradation and provide a constant mechanical support.

The progress of cell and developmental biology will continue to guide the design of bioelastomers. We expect that advancements in bioelastomer development will greatly contribute to realization of the promise of tissue engineering in the not too distant future.

References

1. Langer R, Vacanti JP. Tissue engineering. *Science* 1993;260(5110):920–926.
2. Freed LE, Engelmayr GC, Borenstein JT, Moutos FT, Guilak F. Advanced material strategies for tissue engineering scaffolds. *Adv Mater* 2009;21(32–33):3410–3418.
3. Ghosh K, Ingber DE. Micromechanical control of cell and tissue development: implications for tissue engineering. *Adv Drug Deliv Rev* 2007;59(13):1306–1318.
4. Mitragotri S, Lahann J. Physical approaches to biomaterial design. *Nat Mater* 2009;8(1):15–23.
5. Rehfeldt F, Engler AJ, Eckhardt A, Ahmed F, Discher DE. Cell responses to the mechanochemical microenvironment – implications for regenerative medicine and drug delivery. *Adv Drug Deliv Rev* 2007;59(13):1329–1339.
6. Discher DE, Janmey P, Wang YL. Tissue cells feel and respond to the stiffness of their substrate. *Science* 2005;310(5751):1139–1143.
7. Levental I, Georges PC, Janmey PA. Soft biological materials and their impact on cell function. *Soft Matter* 2007;3(3):299–306.
8. Lutolf MP, Gilbert PM, Blau HM. Designing materials to direct stem-cell fate. *Nature* 2009;462(7272):433–441.
9. Engler AJ, Griffin MA, Sen S, Bonnetmann CG, Sweeney HL, Discher DE. Myotubes differentiate optimally on substrates with tissue-like stiffness: pathological implications for soft or stiff microenvironments. *J Cell Biol* 2004;166(6):877–887.
10. Griffin MA, Sen S, Sweeney HL, Discher DE. Adhesion-contractile balance in myocyte differentiation. *J Cell Sci* 2004;117(Pt 24):5855–5863.
11. Engler AJ, Sen S, Sweeney HL, Discher DE. Matrix elasticity directs stem cell lineage specification. *Cell* 2006;126(4):677–689.

12. Reinhart-King CA, Dembo M, Hammer DA. Cell-cell mechanical communication through compliant substrates. *Biophys J* 2008;95(12):6044–6051.
13. Amsden B. Curable, biodegradable elastomers: emerging biomaterials for drug delivery and tissue engineering. *Soft Matter* 2007;3(11):1335–1348.
14. Chen QZ, Bismarck A, Hansen U, Junaid S, Tran MQ, Harding SE, Ali NN, Boccaccini AR. Characterisation of a soft elastomer poly(glycerol sebacate) designed to match the mechanical properties of myocardial tissue. *Biomaterials* 2008;29(1):47–57.
15. Gupta BS, Kasyanov VA. Biomechanics of human common carotid artery and design of novel hybrid textile compliant vascular grafts. *J Biomed Mater Res* 1997;34(3):341–349.
16. Dahms SE, Piechota HJ, Dahiya R, Lue TF, Tanagho EA. Composition and biomechanical properties of the bladder acellular matrix graft: comparative analysis in rat, pig and human. *Br J Urol* 1998;82(3):411–419.
17. Balguid A, Rubbens MP, Mol A, Bank RA, Bogers AJ, van Kats JP, de Mol BA, Baaijens FP, Bouten CV. The role of collagen cross-links in biomechanical behavior of human aortic heart valve leaflets – relevance for tissue engineering. *Tissue Eng* 2007;13(7):1501–1511.
18. Lee JM, Boughner DR. Mechanical properties of human pericardium. Differences in viscoelastic response when compared with canine pericardium. *Circ Res* 1985;57(3):475–481.
19. Monson KL, Goldsmith W, Barbaro NM, Manley GT. Axial mechanical properties of fresh human cerebral blood vessels. *J Biomech Eng* 2003;125(2):288–294.
20. Yang SF, Leong KF, Du ZH, Chua CK. The design of scaffolds for use in tissue engineering. Part 1. Traditional factors. *Tissue Eng* 2001;7(6):679–689.
21. Janmey PA, McCulloch CA. Cell mechanics: integrating cell responses to mechanical stimuli. *Annu Rev Biomed Eng* 2007;9:1–34.
22. Dado D, Levenberg S. Cell-scaffold mechanical interplay within engineered tissue. *Semin Cell Dev Biol* 2009;20(6):656–664.
23. Bilodeau K, Mantovani D. Bioreactors for tissue engineering: focus on mechanical constraints. A comparative review. *Tissue Eng* 2006;12(8):2367–2383.
24. Zimmermann WH, Cesnjevar R. Cardiac tissue engineering: implications for pediatric heart surgery. *Pediatr Cardiol* 2009;30(5):716–723.
25. Hollister SJ. Scaffold design and manufacturing: from concept to clinic. *Adv Mater* 2009;21(32–33):3330–3342.
26. Zimmermann WH. Tissue engineering polymers flex their muscles. *Nat Mater* 2008;7(12):932–933.
27. Lavik E, Langer R. Tissue engineering: current state and perspectives. *Appl Microbiol Biotechnol* 2004;65(1):1–8.
28. Chow D, Nunalee ML, Lim DW, Simnick AJ, Chilkoti A. Peptide-based biopolymers in biomedicine and biotechnology. *Mater Sci Eng R Rep* 2008;62(4):125–155.
29. van Hest JCM, Tirrell DA. Protein-based materials, toward a new level of structural control. *Chem Commun* 2001;(19):1897–1904.
30. Daamen WF, Veerkamp JH, van Hest JCM, van Kuppevelt TH. Elastin as a biomaterial for tissue engineering. *Biomaterials* 2007;28(30):4378–4398.
31. Martin DP, Williams SF. Medical applications of poly-4-hydroxybutyrate: a strong flexible absorbable biomaterial. *Biochem Eng J* 2003;16(2):97–105.
32. Chen GQ, Wu Q. The application of polyhydroxyalkanoates as tissue engineering materials. *Biomaterials* 2005;26(33):6565–6578.
33. Malafaya PB, Silva GA, Reis RL. Natural-origin polymers as carriers and scaffolds for biomolecules and cell delivery in tissue engineering applications. *Adv Drug Del Rev* 2007;59(4–5):207–233.
34. Drobny JG. Handbook of thermoplastic elastomers. Norwich, NY: PDL(Plastics Design Library)/William Andrew Pub., 2007.
35. Boretos JW, Pierce WS. Segmented polyurethane: a new elastomer for biomedical applications. *Science* 1967;158(807):1481–1482.

36. Zdrachala RJ, Zdrachala IJ. Biomedical applications of polyurethanes: a review of past promises, present realities, and a vibrant future. *J Biomater Appl* 1999;14(1):67–90.
37. Burke A, Hasirci N. Polyurethanes in biomedical applications. *Adv Exp Med Biol* 2004; 553:83–101.
38. Wagner H, Beller FK, Pfautsch M. Electron and light microscopy examination of capsules around breast implants. *Plast Reconstr Surg* 1977;60(1):49–55.
39. Bucky LP, Ehrlich HP, Sohoni S, May JW, Jr. The capsule quality of saline-filled smooth silicone, textured silicone, and polyurethane implants in rabbits: a long-term study. *Plast Reconstr Surg* 1994;93(6):1123–1131; discussion 1132–1133.
40. Slade CL, Peterson HD. Disappearance of the polyurethane cover of the Ashley Natural Y prosthesis. *Plast Reconstr Surg* 1982;70(3):379–383.
41. Szycher M, Siciliano AA. An assessment of 2,4 TDA formation from Surgitek polyurethane foam under simulated physiological conditions. *J Biomater Appl* 1991;5(4):323–336.
42. Guelcher SA. Biodegradable polyurethanes: synthesis and applications in regenerative medicine. *Tissue Eng Part B Rev* 2008;14(1):3–17.
43. Santerre JP, Woodhouse K, Laroche G, Labow RS. Understanding the biodegradation of polyurethanes: from classical implants to tissue engineering materials. *Biomaterials* 2005; 26(35):7457–7470.
44. Guan JJ, Sacks MS, Beckman EJ, Wagner WR. Biodegradable poly(ether ester urethane)urea elastomers based on poly(ether ester) triblock copolymers and putrescine: synthesis, characterization and cytocompatibility. *Biomaterials* 2004;25(1):85–96.
45. Sung CSP, Smith TW, Sung NH. Properties of segmented polyether poly(urethaneureas) based on 2,4-toluene diisocyanate. 2. Infrared and mechanical studies. *Macromolecules* 1980;13(1): 117–121.
46. Wang CB, Cooper SL. Morphology and properties of segmented polyether polyurethaneureas. *Macromolecules* 1983;16(5):775–786.
47. Guan JJ, Sacks MS, Beckman EJ, Wagner WR. Synthesis, characterization, and cytocompatibility of elastomeric, biodegradable poly(ester-urethane)ureas based on poly(caprolactone) and putrescine. *J Biomed Mater Res* 2002;61(3):493–503.
48. Stankus JJ, Guan JJ, Wagner WR. Fabrication of biodegradable elastomeric scaffolds with sub-micron morphologies. *J Biomed Mater Res A* 2004;70A(4):603–614.
49. Stankus JJ, Freytes DO, Badylak SF, Wagner WR. Hybrid nanofibrous scaffolds from electrospinning of a synthetic biodegradable elastomer and urinary bladder matrix. *J Biomater Sci Polym Ed* 2008;19(5):635–652.
50. Guan JJ, Fujimoto KL, Sacks MS, Wagner WR. Preparation and characterization of highly porous, biodegradable polyurethane scaffolds for soft tissue applications. *Biomaterials* 2005; 26(18):3961–3971.
51. Guan JJ, Wagner WR. Synthesis, characterization and cytocompatibility of polyurethaneurea elastomers with designed elastase sensitivity. *Biomacromolecules* 2005;6(5):2833–2842.
52. Courtney T, Sacks MS, Stankus J, Guan J, Wagner WR. Design and analysis of tissue engineering scaffolds that mimic soft tissue mechanical anisotropy. *Biomaterials* 2006; 27(19):3631–3638.
53. Stankus JJ, Guan JJ, Fujimoto K, Wagner WR. Microintegrating smooth muscle cells into a biodegradable, elastomeric fiber matrix. *Biomaterials* 2006;27(5):735–744.
54. Guan J, Stankus JJ, Wagner WR. Biodegradable elastomeric scaffolds with basic fibroblast growth factor release. *J Control Release* 2007;120(1–2):70–78.
55. Guan J, Fujimoto KL, Wagner WR. Elastase-sensitive elastomeric scaffolds with variable anisotropy for soft tissue engineering. *Pharm Res* 2008;25(10):2400–2412.
56. Wang F, Li ZQ, Tamama K, Sen CK, Guan JJ. Fabrication and characterization of pro-survival growth factor releasing, anisotropic scaffolds for enhanced mesenchymal stem cell survival/growth and orientation. *Biomacromolecules* 2009;10(9):2609–2618.

57. Wang F, Li ZQ, Lannutti JL, Wagner WR, Guan JJ. Synthesis, characterization and surface modification of low moduli poly(ether carbonate urethane)ureas for soft tissue engineering. *Acta Biomater* 2009;5(8):2901–2912.
58. Hong Y, Ye SH, Nieponice A, Soletti L, Vorp DA, Wagner WR. A small diameter, fibrous vascular conduit generated from a poly(ester urethane)urea and phospholipid polymer blend. *Biomaterials* 2009;30(13):2457–2467.
59. Fujimoto KL, Guan JJ, Oshima H, Sakai T, Wagner WR. In vivo evaluation of a porous, elastic, biodegradable patch for reconstructive cardiac procedures. *Ann Thorac Surg* 2007;83(2):648–654.
60. Fujimoto KL, Tobita K, Merryman WD, Guan JJ, Momoi N, Stolz DB, Sacks MS, Keller BB, Wagner WR. An elastic, biodegradable cardiac patch induces contractile smooth muscle and improves cardiac remodeling and function in subacute myocardial infarction. *J Am Coll Cardiol* 2007;49(23):2292–2300.
61. Nieponice A, Soletti L, Guan JJ, Deasy BM, Huard J, Wagner WR, Vorp DA. Development of a tissue-engineered vascular graft combining a biodegradable scaffold, muscle-derived stem cells and a rotational vacuum seeding technique. *Biomaterials* 2008;29(7):825–833.
62. Skarja GA, Woodhouse KA. Structure-property relationships of degradable polyurethane elastomers containing an amino acid-based chain extender. *J Appl Polym Sci* 2000;75(12):1522–1534.
63. Skarja GA, Woodhouse KA. In vitro degradation and erosion of degradable, segmented polyurethanes containing an amino acid-based chain extender. *J Biomater Sci Polym Ed* 2001;12(8):851–873.
64. Fromstein JD, Woodhouse KA. Elastomeric biodegradable polyurethane blends for soft tissue applications. *J Biomater Sci Polym Ed* 2002;13(4):391–406.
65. Alperin C, Zandstra PW, Woodhouse KA. Polyurethane films seeded with embryonic stem cell-derived cardiomyocytes for use in cardiac tissue engineering applications. *Biomaterials* 2005;26(35):7377–7386.
66. Fromstein JD, Zandstra PW, Alperin C, Rockwood D, Rabolt JF, Woodhouse KA. Seeding bioreactor-produced embryonic stem cell-derived cardiomyocytes on different porous, degradable, polyurethane scaffolds reveals the effect of scaffold architecture on cell morphology. *Tissue Eng Part A* 2008;14(3):369–378.
67. McDevitt TC, Woodhouse KA, Hauschka SD, Murry CE, Stayton PS. Spatially organized layers of cardiomyocytes on biodegradable polyurethane films for myocardial repair. *J Biomed Mater Res A* 2003;66A(3):586–595.
68. Rockwood DN, Akins RE, Parrag IC, Woodhouse KA, Rabolt JF. Culture on electrospun polyurethane scaffolds decreases atrial natriuretic peptide expression by cardiomyocytes in vitro. *Biomaterials* 2008;29(36):4783–4791.
69. Rockwood DN, Woodhouse KA, Fromstein JD, Chase DB, Rabolt JF. Characterization of biodegradable polyurethane microfibers for tissue engineering. *J Biomater Sci Polym Ed* 2007;18(6):743–758.
70. Tatoi L, Moore TG, Adhikari R, Malherbe F, Jayasekara R, Griffiths I, Gunatillake PA. Thermoplastic biodegradable polyurethanes: the effect of chain extender structure on properties and in-vitro degradation. *Biomaterials* 2007;28(36):5407–5417.
71. Ding MM, Li JH, Fu XT, Zhou J, Tan H, Gu Q, Fu Q. Synthesis, degradation, and cytotoxicity of multiblock poly(epsilon-caprolactone urethane)s containing Gemini quaternary ammonium cationic groups. *Biomacromolecules* 2009;10(10):2857–2865.
72. Sarkar D, Lopina ST. Oxidative and enzymatic degradations of L-tyrosine based polyurethanes. *Polym Degrad Stab* 2007;92(11):1994–2004.
73. Xu W, Wang XH, Yan YN, Zhang RJ. Rapid prototyping of polyurethane for the creation of vascular systems. *J Bioact Compat Polym* 2008;23(2):103–114.

74. Chia SL, Gorna K, Gogolewski S, Alini M. Biodegradable elastomeric polyurethane membranes as chondrocyte carriers for cartilage repair. *Tissue Eng* 2006;12(7):1945–1953.
75. Zhang L, Zhou JY, Lu QP, Wei YJ, Hu SS. A novel small-diameter vascular graft: in vivo behavior of biodegradable three-layered tubular scaffolds. *Biotechnol Bioeng* 2008;99(4):1007–1015.
76. Laschke MW, Strohe A, Scheuer C, Eglin D, Verrier S, Alini M, Pohlemann T, Menger MD. In vivo biocompatibility and vascularization of biodegradable porous polyurethane scaffolds for tissue engineering. *Acta Biomater* 2009;5(6):1991–2001.
77. Gisselbalt K, Edberg B, Flodin P. Synthesis and properties of degradable poly(urethane urea)s to be used for ligament reconstructions. *Biomacromolecules* 2002;3(5):951–958.
78. Liljensten E, Gisselbalt K, Edberg B, Bertilsson H, Flodin P, Nilsson A, Lindahl A, Peterson L. Studies of polyurethane urea bands for ACL reconstruction. *J Mater Sci Mater Med* 2002;13(4):351–359.
79. Zhang CH, Zhang N, Wen XJ. Improving the elasticity and cytophilicity of biodegradable polyurethane by changing chain extender. *J Biomed Mater Res B Appl Biomater* 2006;79B(2):335–344.
80. Siepe M, Giraud MN, Liljensten E, Nydegger U, Menasche P, Carrel T, Tevæarai HT. Construction of skeletal myoblast-based polyurethane scaffolds for myocardial repair. *Artif Organs* 2007;31(6):425–433.
81. Siepe M, Giraud MN, Pavlovic M, Recepto C, Beyersdorf F, Menasche P, Carrel T, Tevæarai HT. Myoblast-seeded biodegradable scaffolds to prevent post-myocardial infarction evolution toward heart failure. *J Thorac Cardiovasc Surg* 2006;132(1):124–131.
82. Soletti L, Nieponice A, Guan JJ, Stankus JJ, Wagner WR, Vorp DA. A seeding device for tissue engineered tubular structures. *Biomaterials* 2006;27(28):4863–4870.
83. Zhang JY, Beckman EJ, Hu J, Yang GG, Agarwal S, Hollinger JO. Synthesis, biodegradability, and biocompatibility of lysine diisocyanate-glucose polymers. *Tissue Eng* 2002;8(5):771–785.
84. Li B, Davidson JM, Guelcher SA. The effect of the local delivery of platelet-derived growth factor from reactive two-component polyurethane scaffolds on the healing in rat skin excisional wounds. *Biomaterials* 2009;30(20):3486–3494.
85. Sharifpoor S, Labow RS, Santerre JP. Synthesis and characterization of degradable polar hydrophobic ionic polyurethane scaffolds for vascular tissue engineering applications. *Biomacromolecules* 2009;10(10):2729–2739.
86. Hollinger JO. Preliminary report on the osteogenic potential of a biodegradable copolymer of polylactide (PLA) and polyglycolide (PGA). *J Biomed Mater Res* 1983;17(1):71–82.
87. Pitt CG, Gratzl MM, Kimmel GL, Surlis J, Schindler A. Aliphatic polyesters II. The degradation of poly (DL-lactide), poly (epsilon-caprolactone), and their copolymers in vivo. *Biomaterials* 1981;2(4):215–220.
88. Barrett DG, Yousaf MN. Design and Applications of biodegradable polyester tissue scaffolds based on endogenous monomers found in human metabolism. *Molecules* 2009;14(10):4022–4050.
89. Lee SH, Kim BS, Kim SH, Choi SW, Jeong SI, Kwon IK, Kang SW, Nikolovski J, Mooney DJ, Han YK, Kim YH. Elastic biodegradable poly(glycolide-co-caprolactone) scaffold for tissue engineering. *J Biomed Mater Res A* 2003;66A(1):29–37.
90. Jeong SI, Kim SH, Kim YH, Jung Y, Kwon JH, Kim BS, Lee YM. Manufacture of elastic biodegradable PLCL scaffolds for mechano-active vascular tissue engineering. *J Biomater Sci Polym Ed* 2004;15(5):645–660.
91. Jeong SI, Kim BS, Kang SW, Kwon JH, Lee YM, Kim SH, Kim YH. In vivo biocompatibility and degradation behavior of elastic poly(L-lactide-co-epsilon-caprolactone) scaffolds. *Biomaterials* 2004;25(28):5939–5946.
92. Jeong SI, Kwon JH, Lim JI, Cho SW, Jung YM, Sung WJ, Kim SH, Kim YH, Lee YM, Kim BS, Choi CY, Kim SJ. Mechano-active tissue engineering of vascular smooth muscle using

- pulsatile perfusion bioreactors and elastic PLCL scaffolds. *Biomaterials* 2005;26(12):1405–1411.
93. Kim SH, Kwon JH, Chung MS, Chung E, Jung Y, Kim SH, Kim YH. Fabrication of a new tubular fibrous PLCL scaffold for vascular tissue engineering. *J Biomater Sci Polym Ed* 2006;17(12):1359–1374.
 94. He W, Ma ZW, Yong T, Teo WE, Ramakrishna S. Fabrication of collagen-coated biodegradable polymer nanofiber mesh and its potential for endothelial cells growth. *Biomaterials* 2005;26(36):7606–7615.
 95. Burks CA, Bundy K, Fotuhi P, Alt E. Characterization of 75 : 25 poly(l-lactide-co-epsilon-caprolactone) thin films for the endoluminal delivery of adipose-derived stem cells to abdominal aortic aneurysms. *Tissue Eng* 2006;12(9):2591–2600.
 96. Matsumura G, Hibino N, Ikada Y, Kurosawa H, Shin'oka T. Successful application of tissue engineered vascular autografts: clinical experience. *Biomaterials* 2003;24(13):2303–2308.
 97. Shin'oka T, Matsumura G, Hibino N, Naito Y, Watanabe M, Konuma T, Sakamoto T, Nagatsu M, Kurosawa H. Midterm clinical result of tissue-engineered vascular autografts seeded with autologous bone marrow cells. *J Thorac Cardiovasc Surg* 2005;129(6):1330–1338.
 98. Xie J, Ihara M, Jung Y, Kwon IK, Kim SH, Kim YH, Matsuda T. Mechano-active scaffold design based on microporous poly(L-lactide-co-epsilon-caprolactone) for articular cartilage tissue engineering: dependence of porosity on compression force-applied mechanical behaviors. *Tissue Eng* 2006;12(3):449–458.
 99. Deschamps AA, Grijpma DW, Feijen J. Poly(ethylene oxide)/poly(butylene terephthalate) segmented block copolymers: the effect of copolymer composition on physical properties and degradation behavior. *Polymer* 2001;42(23):9335–9345.
 100. Deschamps AA, van Apeldoorn AA, Hayen H, de Bruijn JD, Karst U, Grijpma DW, Feijen J. In vivo and in vitro degradation of poly(ether ester) block copolymers based on poly(ethylene glycol) and poly(butylene terephthalate). *Biomaterials* 2004;25(2):247–258.
 101. Lamme EN, Druce D, Pieper J, May PS, Kaim P, Jacobsen F, Steinau HU, Steinstraesser L. Long-term evaluation of porous PEGT/PBT implants for soft tissue augmentation. *J Biomater Appl* 2008;22(4):309–335.
 102. Shi R, Chen DF, Liu QY, Wu Y, Xu XC, Zhang LQ, Tian W. Recent advances in synthetic bioelastomers. *Int J Mol Sci* 2009;10(10):4223–4256.
 103. Xiao YL, Riesle J, Van Blitterswijk CA. Static and dynamic fibroblast seeding and cultivation in porous PEO/PBT scaffolds. *J Mater Sci Mater Med* 1999;10(12):773–777.
 104. van Dorp AGM, Verhoeven MCH, Koerten HK, van Blitterswijk CA, Ponec M. Bilayered biodegradable poly(ethylene glycol)/poly(butylene terephthalate) copolymer (polyactive (TM)) as substrate for human fibroblasts and keratinocytes. *J Biomed Mater Res* 1999;47(3):292–300.
 105. Malda J, Woodfield TBF, van der Vloodt F, Wilson C, Martens DE, Tramper J, van Blitterswijk CA, Riesle J. The effect of PEGT/PBT scaffold architecture on the composition of tissue engineered cartilage. *Biomaterials* 2005;26(1):63–72.
 106. Jansen EJP, Pieper J, Gijbels MJJ, Guldemond NA, Riesle J, Van Rhijn LW, Bulstra SK, Kuijter R. PEOT/PBT based scaffolds with low mechanical properties improve cartilage repair tissue formation in osteochondral defects. *J Biomed Mater Res A* 2009;89A(2):444–452.
 107. Pego AP, Grijpma DW, Feijen J. Enhanced mechanical properties of 1,3-trimethylene carbonate polymers and networks. *Polymer* 2003;44(21):6495–6504.
 108. Pego AP, Poot AA, Grijpma DW, Feijen J. Copolymers of trimethylene carbonate and epsilon-caprolactone for porous nerve guides: synthesis and properties. *J Biomater Sci Polym Ed* 2001;12(1):35–53.
 109. Pego AP, Poot AA, Grijpma DW, Feijen J. Physical properties of high molecular weight 1,3-trimethylene carbonate and D,L-lactide copolymers. *J Mater Sci Mater Med* 2003;14(9):767–773.

110. Pego AP, Van Luyn MJA, Brouwer LA, van Wachem PB, Poot AA, Grijpma DW, Feijen J. In vivo behavior of poly(1,3-trimethylene carbonate) and copolymers of 1,3-trimethylene carbonate with D,L-lactide or epsilon-caprolactone: degradation and tissue response. *J Biomed Mater Res A* 2003;67A(3):1044–1054.
111. Zhang Z, Kuijjer R, Bulstra SK, Grijpma DW, Feijen J. The in vivo and in vitro degradation behavior of poly(trimethylene carbonate). *Biomaterials* 2006;27(9):1741–1748.
112. Edlund U, Albertsson AC. Polyesters based on diacid monomers. *Adv Drug Deliv Rev* 2003;55(4):585–609.
113. Lips PAM, van Luyn MJA, Chiellini F, Brouwer LA, Velthoen IW, Dijkstra PJ, Feijen J. Biocompatibility and degradation of aliphatic segmented poly(ester amide)s: in vitro and in vivo evaluation. *J Biomed Mater Res A* 2006;76A(4):699–710.
114. Deschamps AA, van Apeldoorn AA, de Bruijn JD, Grijpma DW, Feijen J. Poly(ether ester amide)s for tissue engineering. *Biomaterials* 2003;24(15):2643–2652.
115. Wang YD, Ameer GA, Sheppard BJ, Langer R. A tough biodegradable elastomer. *Nat Biotechnol* 2002;20(6):602–606.
116. Lee MC, Haut RC. Strain rate effects on tensile failure properties of the common carotid artery and jugular vein of ferrets. *J Biomech* 1992;25(8):925–927.
117. Wang YD, Kim YM, Langer R. In vivo degradation characteristics of poly(glycerol sebacate). *J Biomed Mater Res A* 2003;66A(1):192–197.
118. Liu QY, Tian M, Shi R, Zhang LQ, Chen DF, Tian W. Structure and properties of thermoplastic poly(glycerol sebacate) elastomers originating from prepolymers with different molecular weights. *J Appl Polym Sci* 2007;104(2):1131–1137.
119. Liu QY, Tian M, Ding T, Shi R, Zhang LQ. Preparation and characterization of a biodegradable polyester elastomer with thermal processing abilities. *J Appl Polym Sci* 2005;98(5):2033–2041.
120. Pomerantseva I, Krebs N, Hart A, Neville CM, Huang AY, Sundback CA. Degradation behavior of poly(glycerol sebacate). *J Biomed Mater Res A* 2009;91A(4):1038–1047.
121. Sun ZJ, Chen C, Sun MZ, Ai CH, Lu XL, Zheng YF, Yang BF, Dong DL. The application of poly (glycerol-sebacate) as biodegradable drug carrier. *Biomaterials* 2009;30(28):5209–5214.
122. Pryor HI, O'Doherty E, Hart A, Owens G, Hoganson D, Vacanti JP, Masiakos PT, Sundback CA. Poly(glycerol sebacate) films prevent postoperative adhesions and allow laparoscopic placement. *Surgery* 2009;146(3):490–497.
123. Fidkowski C, Kaazempur-Mofrad MR, Borenstein J, Vacanti JP, Langer R, Wang YD. Endothelialized microvasculature based on a biodegradable elastomer. *Tissue Eng* 2005; 11(1–2):302–309.
124. Bettinger CJ, Weinberg EJ, Kulig KM, Vacanti JP, Wang YD, Borenstein JT, Langer R. Three-dimensional microfluidic tissue-engineering scaffolds using a flexible biodegradable polymer. *Adv Mater* 2006;18(2):165–169.
125. Bettinger CJ, Orrick B, Misra A, Langer R, Borenstein JT. Micro fabrication of poly (glycerol-sebacate) for contact guidance applications. *Biomaterials* 2006;27(12):2558–2565.
126. Gao J, Crapo PM, Wang YD. Macroporous elastomeric scaffolds with extensive micropores for soft tissue engineering. *Tissue Eng* 2006;12(4):917–925.
127. Crapo PM, Gao J, Wang YD. Seamless tubular poly(glycerol sebacate) scaffolds: high-yield fabrication and potential applications. *J Biomed Mater Res A* 2008;86A(2):354–363.
128. Yi F, Lavan DA. Poly(glycerol sebacate) nanofiber scaffolds by core/shell electrospinning. *Macromol Biosci* 2008;8(9):803–806.
129. Gao J, Ensley AE, Nerem RM, Wang YD. Poly(glycerol sebacate) supports the proliferation and phenotypic protein expression of primary baboon vascular cells. *J Biomed Mater Res A* 2007;83A(4):1070–1075.
130. Gao J, Crapo P, Nerern R, Wang YD. Co-expression of elastin and collagen leads to highly compliant engineered blood vessels. *J Biomed Mater Res A* 2008;85A(4):1120–1128.

131. Crapo PM, Wang Y. Physiologic compliance in engineered small-diameter arterial constructs based on an elastomeric substrate. *Biomaterials* 2010;31(7):1626–1635.
132. Radisic M, Park H, Chen F, Salazar-Lazzaro JE, Wang YD, Dennis R, Langer R, Freed LE, Vunjak-Novakovic G. Biomimetic approach to cardiac tissue engineering: oxygen carriers and channeled scaffolds. *Tissue Eng* 2006;12(8):2077–2091.
133. Radisic M, Marsano A, Maidhof R, Wang Y, Vunjak-Novakovic G. Cardiac tissue engineering using perfusion bioreactor systems. *Nat Protoc* 2008;3(4):719–738.
134. Radisic M, Park H, Martens TP, Salazar-Lazaro JE, Geng WL, Wang YD, Langer R, Freed LE, Vunjak-Novakovic G. Pre-treatment of synthetic elastomeric scaffolds by cardiac fibroblasts improves engineered heart tissue. *J Biomed Mater Res A* 2008;86A(3):713–724.
135. Engelmayer GC, Cheng MY, Bettinger CJ, Borenstein JT, Langer R, Freed LE. Accordion-like honeycombs for tissue engineering of cardiac anisotropy. *Nat Mater* 2008;7(12):1003–1010.
136. Sales VL, Engelmayer GC, Johnson JA, Gao J, Wang YD, Sacks MS, Mayer JE. Protein precoating of elastomeric tissue-engineering scaffolds increased cellularity, enhanced extracellular matrix protein production, and differentially regulated the phenotypes of circulating endothelial progenitor cells. *Circulation* 2007;116(11):155–163.
137. Sundback CA, Shyu JY, Wang YD, Faquin WC, Langer RS, Vacanti JP, Hadlock TA. Biocompatibility analysis of poly(glycerol sebacate) as a nerve guide material. *Biomaterials* 2005;26(27):5454–5464.
138. Neeley WL, Redenti S, Klassen H, Tao S, Desai T, Young MJ, Langer R. A microfabricated scaffold for retinal progenitor cell grafting. *Biomaterials* 2008;29(4):418–426.
139. Redenti S, Neeley WL, Rompani S, Saigal S, Yang J, Klassen H, Langer R, Young MJ. Engineering retinal progenitor cell and scrollable poly(glycerol-sebacate) composites for expansion and subretinal transplantation. *Biomaterials* 2009;30(20):3405–3414.
140. Nijst CLE, Bruggeman JP, Karp JM, Ferreira L, Zumbuehl A, Bettinger CJ, Langer R. Synthesis and characterization of photocurable elastomers from poly(glycerol-co-sebacate). *Biomacromolecules* 2007;8(10):3067–3073.
141. Gerecht S, Townsend SA, Pressler H, Zhu H, Nijst CLE, Bruggeman JP, Nichol JW, Langer R. A porous photocurable elastomer for cell encapsulation and culture. *Biomaterials* 2007;28:4826–4835.
142. Ifkovits JL, Devlin JJ, Eng G, Martens TP, Vunjak-Novakovic G, Burdick JA. Biodegradable fibrous scaffolds with tunable properties formed from photo-cross-linkable poly(glycerol sebacate). *ACS ACS Appl Mater Interfaces* 2009;1(9):1878–1886.
143. Yang J, Webb AR, Ameer GA. Novel citric acid-based biodegradable elastomers for tissue engineering. *Adv Mater* 2004;16(6):511–516.
144. Nijst CLE, Bruggeman JP, Karp JM, Ferreira L, Zumbuehl A, Bettinger CJ, Langer R. Synthesis and characterization of photocurable elastomers from poly(glycerol-co-sebacate). *Biomacromolecules* 2007;8:3067–3073.
145. Bruggeman JP, Bettinger CJ, Nijst CLE, Kohane DS, Langer R. Biodegradable xylitol-based polymers. *Adv Mater* 2008;20(10):1922–1927.
146. Bettinger CJ, Bruggeman JP, Borenstein JT, Langer RS. Amino alcohol-based degradable poly(ester amide) elastomers. *Biomaterials* 2008;29(15):2315–2325.
147. Bruggeman JP, de Bruin BJ, Bettinger CJ, Langer R. Biodegradable poly(polyol sebacate) polymers. *Biomaterials* 2008;29(36):4726–4735.
148. You Z, Cao H, Gao J, Shin PH, Day BW, Wang Y. A functionalizable polyester with free hydroxyl groups and tunable physiochemical and biological properties. *Biomaterials* 2010;31(12):3129–3138.
149. Barrett DG, Yousaf MN. Poly(triol alpha-ketoglutarate) as biodegradable, chemoselective, and mechanically tunable elastomers. *Macromolecules* 2008;41(17):6347–6352.

150. Dey J, Xu H, Shen JH, Thevenot P, Gondi SR, Nguyen KT, Sumerlin BS, Tang LP, Yang J. Development of biodegradable crosslinked urethane-doped polyester elastomers. *Biomaterials* 2008;29(35):4637–4649.
151. Yang J, Webb AR, Pickerill SJ, Hageman G, Ameer GA. Synthesis and evaluation of poly (diol citrate) biodegradable elastomers. *Biomaterials* 2006;27(9):1889–1898.
152. Wan YQ, Feng G, Shen FH, Laurencin CT, Li XD. Biphasic scaffold for annulus fibrosus tissue regeneration. *Biomaterials* 2008;29(6):643–652.
153. Sun ZJ, Wu L, Lu XL, Meng ZX, Zheng YF, Dong DL. The characterization of mechanical and surface properties of poly (glycerol-sebacate-lactic acid) during degradation in phosphate buffered saline. *Appl Surf Sci* 2008;255(2):350–352.
154. Liu QY, Tan TW, Weng JY, Zhang LQ. Study on the control of the compositions and properties of a biodegradable polyester elastomer. *Biomed Mater* 2009;4(2):9.
155. Liu QY, Wu SZ, Tan TW, Weng JY, Zhang LQ, Liu L, Tian W, Chen DF. Preparation and properties of a novel biodegradable polyester elastomer with functional groups. *J Biomater Sci Polym Ed* 2009;20(11):1567–1578.
156. Yang J, Motlagh D, Webb AR, Ameer GA. Novel biphasic elastomeric scaffold for small-diameter blood vessel tissue engineering. *Tissue Eng* 2005;11(11–12):1876–1886.
157. Hidalgo-Bastida LA, Barry JJA, Everitt NM, Rose FRAJ, Buttery LD, Hall IP, Claycomb WC, Shakesheff KM. Cell adhesion and mechanical properties of a flexible scaffold for cardiac tissue engineering. *Acta Biomater* 2007;3(4):457–462.
158. Kang Y, Yang J, Khan S, Anissian L, Ameer GA. A new biodegradable polyester elastomer for cartilage tissue engineering. *J Biomed Mater Res A* 2006;77A(2):331–339.
159. Bettinger CJ, Kulig KM, Vacanti JP, Langer R, Borenstein JT. Nanofabricated collagen-inspired synthetic elastomers for primary rat hepatocyte culture. *Tissue Eng Part A* 2009;15(6):1321–1329.
160. Sun ZJ, Wu L, Huang W, Zhang XL, Lu XL, Zheng YF, Yang BF, Dong DL. The influence of lactic on the properties of poly (glycerol-sebacate-lactic acid). *Mater Sci Eng C Biomim Supramol Syst* 2009;29(1):178–182.
161. Ilagan BG, Amsden BG. Surface modifications of photocrosslinked biodegradable elastomers and their influence on smooth muscle cell adhesion and proliferation. *Acta Biomater* 2009;5(7):2429–2440.
162. Amsden BG, Misra G, Gu F, Younes HM. Synthesis and characterization of a photo-cross-linked biodegradable elastomer. *Biomacromolecules* 2004;5(6):2479–2486.
163. Amsden BG, Tse MY, Turner ND, Knight DK, Pang SC. In vivo degradation behavior of photo-cross-linked star-poly(epsilon-caprolactone-co-D,L-lactide) elastomers. *Biomacromolecules* 2006;7(1):365–372.
164. Younes HM, Bravo-Grimaldo E, Amsden BG. Synthesis, characterization and in vitro degradation of a biodegradable elastomer. *Biomaterials* 2004;25(22):5261–5269.
165. Butler DL, Goldstein SA, Guilak F. Functional tissue engineering: the role of biomechanics. *J Biomech Eng* 2000;122(6):570–575.
166. Mow VC, Kuei SC, Lai WM, Armstrong CG. Biphasic creep and stress relaxation of articular cartilage in compression? Theory and experiments. *J Biomech Eng* 1980;102(1):73–84.
167. Huang CY, Stankiewicz A, Ateshian GA, Mow VC. Anisotropy, inhomogeneity, and tension-compression nonlinearity of human glenohumeral cartilage in finite deformation. *J Biomech* 2005;38(4):799–809.
168. Ateshian GA, Warden WH, Kim JJ, Grelsamer RP, Mow VC. Finite deformation biphasic material properties of bovine articular cartilage from confined compression experiments. *J Biomech* 1997;30(11–12):1157–1164.
169. Lai WM, Mow VC. Drag-induced compression of articular cartilage during a permeation experiment. *Biorheology* 1980;17(1–2):111–123.

- 4
170. Moutos FT, Guilak F. Composite scaffolds for cartilage tissue engineering. *Biorheology* 2008; 45(3–4):501–512.
 171. Lutolf MP, Hubbell JA. Synthetic biomaterials as instructive extracellular microenvironments for morphogenesis in tissue engineering. *Nat Biotechnol* 2005;23(1):47–55.
 172. Place ES, Evans ND, Stevens MM. Complexity in biomaterials for tissue engineering. *Nat Mater* 2009;8(6):457–470.
 173. Mather PT, Luo XF, Rousseau IA. Shape memory polymer research. *Annu Rev Mat Res* 2009; 39:445–471.
 174. Sokolowski W, Metcalfe A, Hayashi S, Yahia L, Raymond J. Medical applications of shape memory polymers. *Biomed Mater* 2007;2(1):S23–S27.
 175. Liu C, Qin H, Mather PT. Review of progress in shape-memory polymers. *J Mater Chem* 2007;17(16):1543–1558.
 176. Langer R, Tirrell DA. Designing materials for biology and medicine. *Nature* 2004; 428(6982): 487–492.
 177. Zheng XT, Zhou SB, Yu XJ, Li XH, Feng B, Qu SX, Weng J. Effect of in vitro degradation of poly(D,L-lactide)/beta-tricalcium composite on its shape-memory properties. *J Biomed Mater Res B Appl Biomater* 2008;86B(1):170–180.
 178. Cordier P, Tournilhac F, Soulie-Ziakovic C, Leibler L. Self-healing and thermoreversible rubber from supramolecular assembly. *Nature* 2008;451(7181):977–980.
 179. Greef TFA, Meijer EW. Materials science – supramolecular polymers. *Nature* 2008; 453(7192):171–173.

Microscale Biomaterials for Tissue Engineering 5

Ian Wheeldon, Javier Fernandez, Hojae Bae, Hirokazu Kaji,
and Ali Khademhosseini

Contents

5.1	Introduction	120
5.2	Microscale Technologies for Engineering Biomaterials and the Cell Microenvironment	121
5.2.1	Photolithography	122
5.2.2	Soft Lithography	122
5.2.3	Microfluidics	123
5.2.4	Robotic Spotting and Printing	124
5.2.5	Other Microscale Techniques	124
5.3	Microscale Engineering of the Cell Microenvironment	124
5.3.1	Cell Patterning and Controlling Cell–Cell Contacts	125
5.3.2	Controlling Tissue Microarchitecture	126
5.3.3	Cell-Soluble Factor Interactions	128
5.4	High Throughput and Combinatorial Investigations of the Cell Microenvironment	129
5.4.1	High Throughput Synthesis and Screening of Cell Microenvironments	129
5.4.2	Microfluidics for High Throughput Investigations of the Cell Microenvironment	130
5.5	Future Directions	131
	References	133

Abstract Microscale and high throughput technologies are powerful tools for addressing many of the challenges in the field of tissue engineering. In this chapter, we present an overview of these technologies and their applications in controlling the cellular microenvironment for tissue engineering applications. We focus on concepts and techniques that can be used to create two- and three-dimensional tissue engineering substrates and scaffolds. Common to these techniques is the ability to control one or more aspects of the cellular microenvironment, including chemical and mechanical cues, cell–cell, cell–matrix,

A. Khademhosseini (✉)

Department of Medicine, Center for Biomedical Engineering, Brigham and Women’s Hospital, Harvard Medical School, Boston, MA 02115, USA

and

Harvard-MIT Division of Health Sciences and Technology, Massachusetts Institute of Technology, Cambridge, Massachusetts 02139

e-mail: alik@rics.bwh.harvard.edu

and cell-soluble factor interactions. We also discuss recent developments in high throughput techniques that are used to explore the vast number of combinations of factors that comprise the cellular microenvironment.

Keywords Cellular microenvironment • High throughput arrays • Microfabrication • Stem cells

5.1 Introduction

Cellular behavior and the development of tissues and organs occur in response to precise sets of environmental cues. These cues can include interactions with neighbouring cells, ligand binding from molecular signalling, and interactions with the surrounding extracellular matrix (ECM) [1]. These cues and signalling events occur at the micro- and nanometer length scales, the sum of which defines the cellular microenvironment. The successful production of *in vitro* tissue constructs requires the recapitulation of *in vivo* microenvironmental factors [2]. It is here that the fields of microscale technologies and tissue engineering intersect [3]. Microscale technologies, some of which have been developed in microelectronics and micro-electro-mechanical systems (MEMS) can control material features from $<1\ \mu\text{m}$ to $>1\ \text{cm}$, thus providing unprecedented control over the interface between cells and substrate and the surrounding environment [4]. In addition, the biological, chemical, and mechanical properties of biomaterials can also be tuned to further control the cellular microenvironment.

The cellular microenvironment is comprised of, cell–cell, cell–ECM, and cell-soluble factor interactions. Microscale technologies have been used to control each of these interactions. For example, microengineered wells are used to control cell aggregate size [5, 6]; microcontact printing of cell adhesion proteins is used to control the shape of adhered cells [7–9]; soft lithography techniques can be used to pattern co-cultures [10]; photocross-linkable hydrogels are used to create cell-laden microgels [11]; microfluidic devices are used to create complex soluble factor gradients [12]; and porous scaffolds are used to provide a three-dimensional (3D) environment for cells to reorganize [13].

In tissue engineering, creating an environment with the appropriate biological and mechanical cues is essential. The ideal tissue engineering scaffold must: (1) match the biological and mechanical requirements of the desired tissue construct; (2) be able to support the desired cell types; and (3) be manufacturable. Microscale processing and fabrication impose certain material property criteria on biomaterials, and often the challenge in microscale tissue engineering is balancing the microscale processing criteria with the desired material properties with respect to the cell culture.

The experimental challenge that tissue engineers face is not only to develop technologies to control the cellular microenvironment but also, to investigate the vast number of possible combinations of different interactions. It is here that technologies such as robotic spotting have begun to make significant advancements [14, 15]. With these methods, researchers

have been able to synthesize and screen biomaterials in a combinatorial manner [16] and investigate combinations of soluble factors and cell–matrix interactions [17, 18].

Over the past decade, the number of fabrication techniques specifically designed for tissue engineering applications has grown considerably. In a number of cases those techniques have been adapted, sometimes with considerable modifications, from the microelectronics industry. Additionally, there has been significant efforts toward the development of microscale fabrication techniques that specifically address challenges in bio- and tissue engineering applications. Microfabrication techniques can be classified into two main groups: (1) techniques for the fabrication of planar, or two-dimensional (2D), surfaces; and (2) techniques for the fabrication of 3D scaffolds. Patterning of surfaces with bioactivity or biological functionalities allows for control over the interface between substrate material and cellular actions, i.e., surfaces are modified to interact with cells in a specific and controllable manner.

In this chapter, we discuss the concepts and techniques that are currently used to fabricate 2D and 3D microscale features for *in vitro* tissue engineering applications. We focus on those techniques that have been used to control different aspects of the cell microenvironment, including soft lithography, photolithography, and microfluidics. We also discuss robotic spotting techniques that have been used to create microarrays of biomaterials for the combinatorial and high throughput investigation of the cellular microenvironment. Furthermore, we highlight pertinent examples from the scientific literature that demonstrate the success of microscale and high throughput technologies in the field of tissue engineering.

5.2

Microscale Technologies for Engineering Biomaterials and the Cell Microenvironment

Some of the first applications of microscale technologies in biotechnology and tissue engineering were based on surface modification techniques [4, 9]. Since these initial experiments, it has become well established that techniques such as photolithography and soft lithography are able to produce substrates with microscale features that may be useful for biological applications. A great deal of insight into cell biology, bioengineering and tissue engineering has come from investigating the interactions between cells and substrates; however, the complexities of biological systems often extend to a third spatial dimension [19–21]. Fidelity in mimicking the *in vivo* microenvironment has been the driving force behind microengineering and fabrication of microscale systems with 3D structures. Mimicking complex microarchitectures of native tissues also poses a significant challenge. With techniques such as photolithography, micromolding and microfluidics, researchers have begun to study cell biology in ways that were previously not possible. Robotic printing technologies have also recently been used to synthesize and screen biomaterials [16, 17].

Here, we discuss some of the most common techniques that are used to microengineer biomaterials and engineer the cell microenvironment, including photolithography, soft lithography, and microfluidics. We also describe technologies used to create microscale systems for the high throughput and combinatorial investigation of the cell microenvironment, such as

robotic printing, and microfluidics. Many of these techniques are not mutually exclusive, and often two or more techniques can be used together to produce the desired result.

5.2.1

Photolithography

Initially developed for the microelectronics industry, photolithography is used in biological applications and tissue engineering to pattern substrates with chemical and biological functionalities. Photolithography is broadly defined as the selective modification of a photosensitive surface by illumination through a photomask. The result is selective surface modifications corresponding to the pattern of exposed and masked areas. Subsequent steps can be used to selectively modify the patterned surface.

The resulting microscale patterns of chemical functionalities can be used to pattern cells by selective control of the positioning of adhesion proteins [22]. For example, proteins can be covalently bound to surfaces modified with monolayers of alkanethiol, alkaneamino, or other alkane chains with terminal functional groups. Protein patterns can also be created by selective photoablation of proteins adsorbed on silicon or glass surfaces. It is also possible to create microscale patterns of encapsulating cells in patterns of photocrosslinkable materials.

Similarly, arrays of immobilized DNA have also been created [23]. These patterning and arraying technologies have been used extensively in the early high throughput screening technologies, where protein and DNA arrays were created to explore protein ligand and DNA hybridization events in a high throughput manner [24]. While photolithography has been quite successful in biological studies and tissue engineering devices, it is limited to widespread use due to the need for expensive clean room facilities and high equipment costs. An alternate strategy is soft lithography.

5.2.2

Soft Lithography

The microscale fabrication techniques that have been borrowed from the microelectronics industry have been highly successful, but there are several techniques that have been specifically developed for use in chemistry and biology. The most common, and perhaps the most successful, is the family of tools described as soft lithography. The soft lithography techniques stand out as collectively they provide a simple, inexpensive, and reliable option for researchers to produce substrates with microscale chemical, biological, and topographical features [4, 25].

Soft lithography involves the use of an elastomeric material to transfer and replicate patterns of topography and chemical surface modifications with features down to several hundreds of nanometers to a surface of interest. Patterns are first generated on a silicon wafer and then replicated onto an elastomeric mold or stamp. Molds can be used to create microscale topographies or microscale structures made of a moldable biomaterial. Stamps

can be used to transfer patterns of different solutions or “inks”, and elastomeric structures can be used to make microfluidic devices.

Poly(dimethyl siloxane) (PDMS) is often the material of choice in soft lithography as it is soft and flexible, transparent to visible and UV light, permeable to oxygen, inexpensive, unreactive, suitable for cell cultures, and the prepolymer is easy to handle and prepare. A solid PDMS mold or stamp is prepared by mixing the prepolymer solution with a curing agent. The mixture must be well mixed and air bubbles removed before pouring the unset mixture onto the template, or into the master mold.

Replica molding and microcontact printing are techniques within the soft lithography family that have become well established in the biological and tissue engineering fields. Both use an elastomeric mold, usually PDMS, with a topography and shape replicated from a patterned template. The template is often a silicon wafer, but can also be other templating materials. The elastomer is peeled away from the template after crosslinking resulting in a negative replica of the template.

In microcontact printing a solution or “ink” is transferred from an elastomeric mold to a substrate. The solution is often a mixture of protein(s) or small molecules, and is only transferred at the interface(s) that make contact [4, 9]. Thus, a replica pattern of the mold of ink is produced on the target substrate. Microcontact printing has been used to create microscale patterns of biocompatible polymers including PEG, and cell adhesion proteins including collagen and fibronectin, among others. Replica molding is mainly used for the fabrication of microcontact printing stamps and the production of microscale structures for microfluidic devices, but, it can also be used to create structures to impose geometric constraints in tissue cultures.

5.2.3

Microfluidics

PDMS molds fabricated by replica molding can be used to create microfluidic channels by placing the mold onto a glass substrate. Such microfluidic devices are used in many different applications, and are discussed here as they have been used to create microscale patterns of surface modification in a similar manner as described in the above section on soft lithography [26, 27]. PDMS microfluidic channels are also used to selectively deliver cells and small molecules to substrates or to form topographies at the interface between two reactive fluids [28]. Microfluidic devices can also be used to generate gradients either on surfaces or with soluble factors [29, 30].

In addition to creating soluble factor gradients and surface patterns, microfluidic systems have emerged as a useful option to provide controlled fluid flow to microscale cell cultures. There are a number of examples of microfluidic bioreactors, these types of applications are reviewed elsewhere [31, 32]. Microfluidic bioreactors have been used to investigate cell responses to shear stress and pulsatile flows, as well as being used to mimic vasculature [3, 33]. Generally, these applications are limited to planar systems, as thick 3D structures with intricate microchannels made from biocompatible materials have proven difficult to produce.

5.2.4

Robotic Spotting and Printing

Robotic spotting technologies have been widely used to produce DNA and protein microarrays. DNA arrays are commonly used for genomic analysis and quantitative gene-expression measurement [34], and microarrayed proteins are used to screen protein–ligand interactions in a high throughput manner [35]. Protein and DNA microarrays are reviewed in detail elsewhere [23, 36–38]. Here, we will describe spotting technologies that have been used to create biomaterial microarrays, and protein arrays for investigating cell–ECM interactions [16, 17]. Additionally, there have been attempts to use robotic spotting techniques to create arrays of 3D cell-laden microgels [39].

Microarray technologies print nano-liter sized spots by dipping pins into the solutions of interest and spotting the solution onto a suitably modified substrate. To fabricate DNA microarrays the solutions contain probe DNA, whereas in the case of synthetic biomaterial microarrays the solutions are prepolymer solutions. Slots in the pins are filled by capillary action, and spots are printed as the filled pins come in contact with the substrate. Spot size is dependent on the diameter of the pins as well as the solution viscosity and composition. With robotic manipulators, microarrays of thousands of individual spots can be produced on a single glass slide. With pin heads containing as many as 96 pins, tens of thousands of spots can be generated quickly. The time required to create microarrays is, in part, dependent on the complexity of microarrayer, with some models capable of printing 60 slides each with 10,000 individual spots in a few hours.

5.2.5

Other Microscale Techniques

There are several other microscale technologies that have been used to fabricate tissue engineering constructs and to create tools for investigating the cellular microenvironment. For example, bioprinting, the freeform fabrication of synthetic and natural polymers with incorporated growth factors, proteins, and living cells, has been used to create 3D scaffolds with complex architectures [40, 41]. There has also been much effort focused on the development of microfibrinous and microporous scaffolds [42, 43]. Additionally, advancements to the basic set of soft lithography techniques has led to the development of new microscale patterning techniques such as simultaneous chemical and topography transfer [44, 45]. Finally, control of chemical and physical properties and features is possible with layer-by-layer assembly [46].

5.3

Microscale Engineering of the Cell Microenvironment

Microscale technologies are potentially powerful tools in solving a number of challenges in the field of tissue engineering. This section highlights some recent advances in microscale technologies for creating and controlling the cellular microenvironment, and for

investigating and directing cellular behavior. Many of the examples discussed here use a combination of the microscale fabrication concepts and technologies described in Sect. 5.2. In doing so, these studies produce new cell-materials composites, as well as techniques to control cell-microenvironment interactions.

5.3.1

Cell Patterning and Controlling Cell–Cell Contacts

Surface patterning of cell adhesion molecules is a highly successful means of investigating cell patterns and controlling cell–ECM interactions, cell shape, and cell–cell contacts. Often, cell adhesion molecules are patterned by microcontact printing and photolithography. These patterns are used to control the spatial organization and positioning of a single or multiple cell types.

Cells adhere onto micropatterned substrates and align to the shape of the underlying adhesive region. For example, Chen et al. demonstrated that the change of cell shapes influences proliferation and apoptosis [47]. It has also been demonstrated that cell shape can control stem cell differentiation. In one example, mesenchymal stem cells were shown to differentiate into osteoblasts when cultured on large adhesive islands and adipocytes when cultured on small islands [48]. In another example, micropatterns of fibronectin and laminin were used to pattern cardiovascular smooth and striated muscle cells, and measure the contractility of the engineered tissue-like constructs [49]. By using specific micropatterns and statistical analysis of cell compartment positions, They et al. demonstrated that ECM geometry determines the orientation of cell polarity axes [50]. For more examples of micropatterning technologies for regulating cell behavior the reader is directed to other reviews [51–53].

Microscale technologies have also been used to create micropatterned co-cultures. For example, micropatterning and layer-by-layer techniques have been combined to create co-cultures of hepatocytes and fibroblasts with ECM proteins [54, 55]. Chien et al. created co-cultures on multilayer micropatterned films of poly(acrylic acid) (PAA) conjugated with 4-azidoaniline and PAA/polyacrylamide (PAM) multilayer films [56]. Microfabricated stencils have also been used to control cell–cell interactions. To this end, Jinno et al. used microscale stencils made from paralyene-C to create dynamic co-cultures [10]. This technique was used to investigate temporal changes in co-cultures of murine embryonic cells with other cell types.

Microwell arrays are also emerging as important tools for controlling cell microenvironments *in vitro*. Microwell arrays have been fabricated from many types of materials including glass, polymers or silicon and have been shown to be useful for various cell culture applications. Microwell arrays have also been used to investigate the dynamics of individual stem cell fate decisions in a high-throughput manner. In one study, an automated microscope was used to track the proliferation and death of individual neural progenitor cells cultured within microwells over several days, to generate clonally-derived information of cellular kinetics and cell fate decisions [57].

Microwell arrays can also be readily used to produce cell aggregates, such as embryonic bodies (EBs), of controlled sizes and shapes. These cultures have shown that the size of EBs influences stem cell self-renewal and differentiation (Fig. 5.1). For instance, it has been demonstrated that larger EBs preferentially undergo cardiac differentiation, whereas smaller

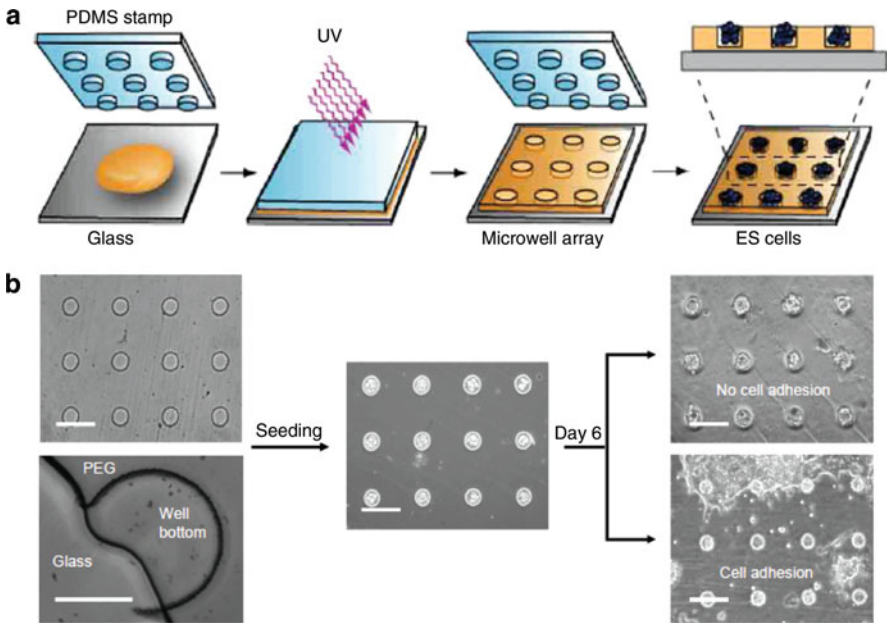


Fig. 5.1 Soft lithography approach to creating hydrogel microstructures for culturing cell aggregates of controlled sizes. **(a)** Schematic representation of the micromolding process to generate a PEG microwell array from a photocrosslinkable PEG-DA prepolymer solution. PEG was molded using a PDMS stamp followed by UV photocrosslinking. The cross-sectional image shows a microwell array loaded with ES cells. **(b)** Phase contrast images show a 50 μm microwell before and after seeding. Higher magnification of a 175 μm microwell that was cut vertically shows that the entire microwell surface was made of PEG. Embryonic stem cell aggregates grew until constrained by the size of the well, yielding a culture of homogeneously size aggregates. Reproduced with permission [5]

ones result in endothelial-like cells [58]. In addition, microwell cell culture provides quasi-3D single cell microenvironments that mimic essential features of the native 3D extracellular milieu by functionalizing the inner surface of microwells with ECM molecules [59, 60]. These studies will help to understand differences in cell behavior between 2- and 3D cultures.

5.3.2

Controlling Tissue Microarchitecture

The fabrication of biomimetic tissue microarchitecture may be an important factor for engineering functionalized tissues, and scaffolds and hydrogels that provide structural support and biochemical cues for cell attachment, spreading, proliferation, and differentiation are essential to the success of these technologies. A promising technique for the construction of 3D engineered tissues is the encapsulation of cells in hydrogels. In

comparison to prefabricated scaffolds, cells can be entrapped or encapsulated inside a hydrogel scaffold during fabrication. Hydrogels are ideal for encapsulating cells as they are highly hydrated and can provide an environment similar to that of native tissues.

In combination with soft lithography or photolithography techniques, it is possible to create microscale hydrogels with controlled shapes and sizes. Control of the size and shape of hydrogels and cell-laden hydrogels opens many possible applications for the construction of tissue-like structures with controlled tissue architecture and control over the cell-micro-environment interactions.

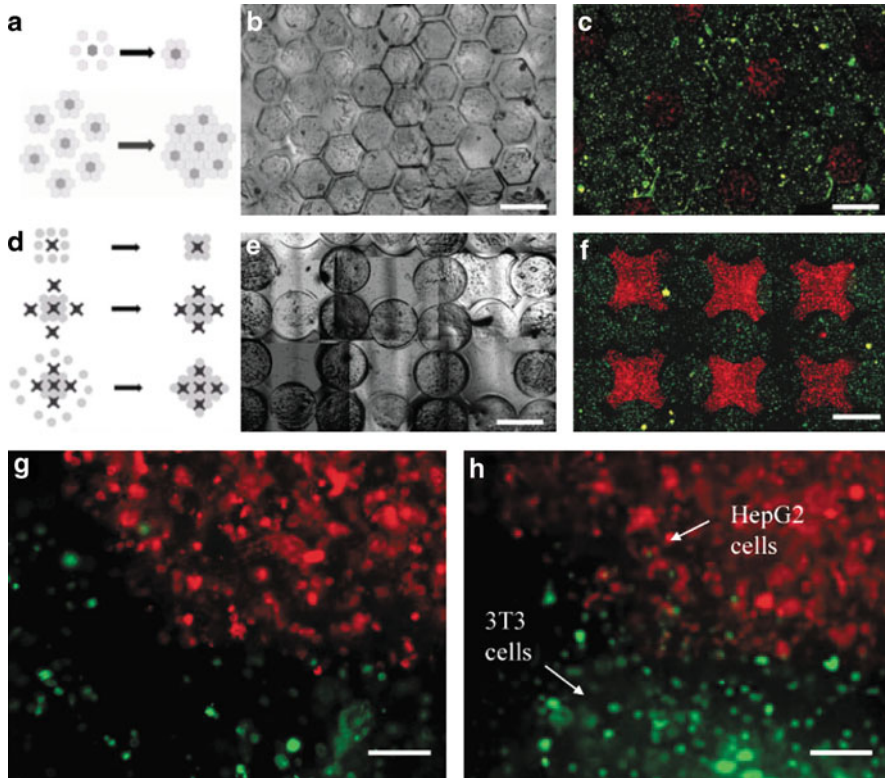


Fig. 5.2 Assemblies of cell-laden microgel structures. Microgels are produced by photolithography and assembled at an air-liquid interface. Schematic representations of co-culture microgels (a) and assemblies of microgels (d). Phase contrast (b) and fluorescence (c) images of assemblies of microgels. Phase contrast (e) and fluorescence (f) images of lock-and-key complex microgel building blocks with controlled co-culture conditions. The scale bar is 1 mm. The interface between microgels of containing 3T3 fibroblasts (green) and HepG2 cells (red) after 1 day (g) and 7 days (h). The scale bar in (g), (h) is 100 μm . and fluorescence (b) images of the microgel assemblies with the red-labeled cells (encapsulated in microgels) and green-labeled cells (encapsulated in bulk hydrogel). Morphology and viability staining of the cell-laden microgel before assembly (c, d) and after assembly in patterned bulk hydrogel (e, f). Scale bars for (b, c, e, f) are 400 μm . Reproduced with permission [65]

A number of studies have demonstrated microgels made from various types of synthetic polymers, such as poly(ethylene glycol) (PEG), and their applicability for cell encapsulation [61–63]. Shape controlled cell-laden microgels can be created by various means such as micromolding and photolithography to mimic tissue units. These tissue units may be assembled in an emerging technique called “*bottom-up*” tissue assembly and may be a promising approach for creating tissues from smaller building blocks [64–66]. These microgels, that are on the order of the few tens to hundreds of micrometers, can be assembled to form large surfaces and 3D structures with high precision in the geometry and the position of the sub-units (Fig. 5.2).

Multi-layered photolithography can also be used to create 3D tissue-like structures [62, 67]. An interesting example of this technique is the fabrication of an artificial 3D network of hepatocytes encapsulated in PEG. Hepatocytes in these structures remain metabolically active cells for days, demonstrating the possibility of long term applications of the encapsulated cells.

5.3.3

Cell-Soluble Factor Interactions

Microfluidic technologies have been used in a number of different applications for studying different aspects of cell biology such as the effects of shear flow and concentration gradients on cells, as well as high throughput screening. Microfluidic systems have also been used to control the spatial and temporal presentation of soluble factors to cellular and subcellular structures, thus allowing for the investigation of activated biochemical signalling pathways in response to soluble stimuli [68, 69]. An active area for using microfluidics in regenerative medicine is to direct the differentiation of stem cells. For example, microfluidic systems can be used to study embryonic stem (ES) cells within microbioreactors [70]. Microreactors enable biological processes to be carried out under tightly controlled (oxygen, nutrients, or other molecular and physical regulatory factors) conditions and minimize batch to batch variability [71].

Gradients of soluble factors play important roles in a number of physiological processes, and a number of microfluidic designs have been developed to create stable gradients to study these processes. In one example, microfluidic devices were used to create and dynamically control chemical gradients to investigate the biological mechanisms responsible for the recruitment of neutrophils to injured, and infected areas [72]. Oxygen gradients have been created for the study of oxygen-induced migration of olfactory sensing in *Caenorhabditis elegans* [73]. Microfluidic systems have also been used to create in vitro models of hepatic zones. In this example, a perfusable microfluidic bioreactor was used to create physiological oxygen gradients in hepatocyte and non-parenchymal cell co-cultures to study drug induced hepatotoxicity [74].

Multilayer soft lithography, an extension of the soft lithography paradigm, has been used to fabricate 3D microfluidic structures. These structures are fabricated by assembling separate layers of PDMS membranes produced by replica molding [75]. The chips fabricated by multilayer soft lithography can be used to fabricate micromechanical valves that prevent cross contamination or leakage between steps of the processes [76] and has been used for protein crystallization [77], nanoliter-volume PCR [78], microfabricated fluorescence

activated cell sorting (μ FACS) [79] and single-cell enzyme screening [80]. Moreover, multi-layer soft lithographic methods can also be used to fabricate microfluidic channels and scaffolds for tissue engineering in a convenient, rapid and inexpensive manner [4, 81].

5.4 High Throughput and Combinatorial Investigations of the Cell Microenvironment

Microscale technologies can also be used to miniaturize traditional experimentation and enable high throughput microarrays and microfluidic systems. These techniques can be used to perform thousands of tests in parallel and have become important tools in drug discovery and other relevant fields [82, 83]. Microarray technologies can also be used to investigate combinatorial microenvironments, and the high throughput screening of cell–ECM, cell–cell, and cell-soluble factor interactions. In this section, we review examples of microscale technologies used to investigate combinatorial microenvironments, and the high throughput synthesis and screening of biomaterials for tissue engineering applications.

5.4.1 High Throughput Synthesis and Screening of Cell Microenvironments

High throughput arrays are promising tools to test the effect of large combinatorial libraries of biomaterials, environmental stimuli and chemicals on cell behavior. A broad range of different molecules including small molecules, polymers, antibodies and other proteins can be arrayed using robotic spotting technology or soft lithography [84]. In general, to perform an assay, cells are seeded uniformly across the entire array and analyzed collectively using appropriate detection methods. For example, a microarray-based gene expression system in which cells are cultured on a glass slide with different DNAs printed in defined locations has been developed [85]. This work demonstrates that thousands of different nucleic acid sequences can be transfected into cells in parallel, and that the outcomes of these transfections can be analyzed in a high throughput manner. The platform has also been extended to RNA-mediated interference (RNAi) [86].

In another example, a microarray composed of different synthetic polymers was developed to investigate the response of ES cells to various extracellular signals [16]. In this approach, thousands of synthesized polymeric materials were printed on a slide and the effect on the differentiation of human ES cells was evaluated (Fig. 5.3).

Microarrays have also been used to investigate the effects of ECM components on stem cell differentiation. In one approach, arrays of micropatterned combinations of ECM proteins were used to investigate ES cell differentiation and to study the maintenance of primary rat hepatocytes during *in vitro* cell culture [17, 18]. Using a similar method, arrays of ECM proteins and Wnt signalling molecules were created to study the role of modulating the ECM environment on hepatic stellate cells [87]. Technologies for investigating 3D cell cultures in microarray format have also been developed. Arrays of murine ES cells encapsulated in alginate hydrogels have been created to study stem cell-soluble factor interactions in a 3D environment [88].

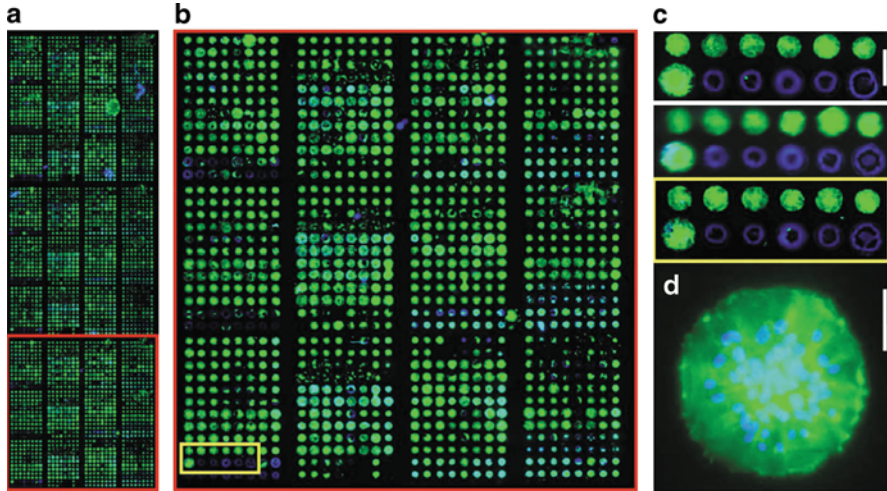


Fig. 5.3 Human mesenchymal stem cells (hMSCs) grown on polymer microarrays. (a–c) hMSCs were cultured on a polymer microarray and stained for actin (*green*; 500 μm scale bar). (d) High magnification images of a polymer spot with hMSC cells, stained with actin (*green*) and DNA/nucleus (*blue*; 100 μm scale bar). Reproduced with permission [103]

Elucidation of the mechanisms responsible for the observed cellular behavior in combinatorial ECM and biomaterials arrays requires rigorous characterization of the arrayed systems. To this end, there have been many efforts in creating high throughput chemical and physical analyses including, high throughput chemical surface characterizations, and nanomechanical measurements. In one example, Tweedie et al. developed a nanomechanical-profiling approach to analyze biomaterial arrays. An array of 1,700 individual photopolymerizable polymers was synthesized and the mechanical properties of each polymer was investigated by an automated nanomechanical screening system [89]. A similar library of photocrosslinkable polymer was characterized by time-of-flight secondary ion mass spectrometry, X-ray photoelectron spectroscopy, and water contact angle in a high throughput manner [90].

5.4.2

Microfluidics for High Throughput Investigations of the Cell Microenvironment

Microfluidics is a versatile technology that has been used to precisely control spatiotemporal aspects of the soluble cellular microenvironment. With simple microfluidic devices researchers have been able to create chemical gradients, control transient stimuli, and create changes in the soluble environment over time. Cell arrays are powerful platforms for high throughput screening of cell–matrix and cell–cell interactions, and in combination with microfluidics, cell arrays can also be used to investigate cell–soluble interactions in a high throughput manner.

Microfluidics can also be used to create cell arrays by manipulating cell location with controlled fluid flows. For example, high-density arrays of single cells isolated in a purely

hydrodynamic fashion have been developed [91], and multiple cell types have been selectively docked in microwells within microchannels [28]. In the latter approach, reversible sealing of a PDMS mold was used to immobilize a series of microchannel patterns on the microwells to enable sequential delivery of fluids to each microwell.

Gradient-generating microfluidic devices have been used for real time monitoring of cell behavior including migration, proliferation, differentiation and apoptosis [92]. For example, a cell array, with an integrated concentration gradient generator has been developed for long term monitoring of cell growth and proliferation [93]. In another example, a microfluidic device with a gradient generation component was developed for pharmacological gradient profiling [94]. Using this device, drug streams were held at different concentrations and voltage-gate K^+ ion channels were screened using scanning probe measurements. Gradient generation permits many soluble factor conditions to be analyzed in a combinatorial fashion and is well suited for high throughput assays in which a large number of conditions need to be screened in parallel.

High throughput microfluidic systems can significantly increase the efficiency of drug target selection, lead compound generation and identification by offering parallel experimentation and reduced reagent consumption. For example, Thorsen et al. developed a high throughput microfluidic chip which integrated 1,000 valves with 256 individual chambers [80]. Using a similar device, different cell types were screened against a number of different toxins in parallel [95].

The merging of cell microarrays and microfluidics has led to the creation of screening methods that can systematically vary one or more parameters, temporally and spatially, across the cell microarray. In one example, the activation of transcription factor NF- κ B across a microarray of HeLa S3 cells was monitored in real-time in response to varying concentrations of the cytokine TNF α [96]. In another example, a strategy was developed to simultaneously create different dynamic soluble microenvironments across a cell array [97]. Microfluidic channels upstream of the cell array were used to generate different temporal profiles of soluble factors, the effects of which were monitored by fluorescence in cell lines with specific gene reporters.

Microfluidic strategies have also proven useful in optimizing stem cell culture conditions. In a fully automated cell culture screening system, 96 independent culture chambers were provided unique culture media compositions and feeding schedules (Fig. 5.4) [98]. The device was used to quantify effects of transient stimulation schedules on the osteogenic differentiation of human mesenchymal stem cells. A similar strategy has been developed for studying stem cell cultures in 3D microenvironments [99]. In this approach, individually addressable cultures of murine embryonic fibroblasts embedded in 3D Matrigel were subject to dynamic soluble microenvironments. This system also allows for the study of culture-to-culture communication of diffusable factors.

5.5 Future Directions

The development of new microscale techniques has led to dramatic enhancements in the ability to study biological systems at the micrometer length scale. In particular, there has been much success in using microscale technologies to control the cellular microenvironment,

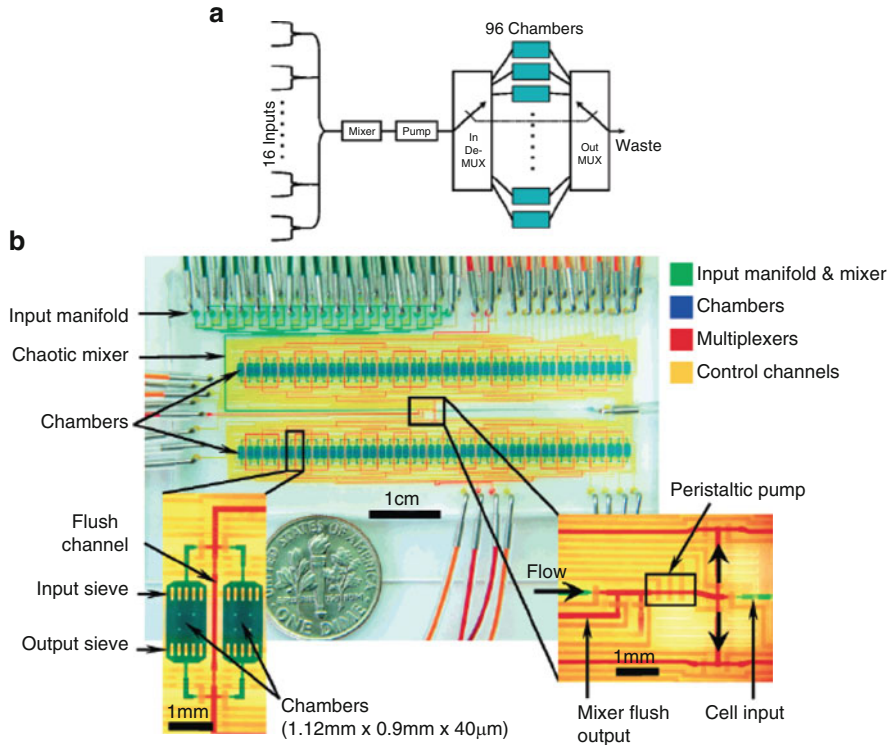


Fig. 5.4 A Microfluidic device for screening cell culture conditions. **(a)** A simplified schematic diagram of the fluidic path in the device (MUX, multiplexer). **(b)** Photograph of a microfluidic culture device with the channels filled with colored water so that different parts of the device can be seen. *Left inset:* higher magnification images of two culture chambers. *Right inset:* higher magnification image of the input multiplexer [98]

and to investigate cellular responses to changes in the cellular microenvironment. However, there is still much work to be accomplished at the intersection of microfabrication and cell biology. The field of tissue engineering will benefit from new microscale technologies that can control different aspects of 3D microenvironments. The main challenge that microscale technologies can help address is the recapitulation of the *in vivo* microenvironment, *in vitro*.

One of the major experimental challenges in investigating the cell microenvironment is the vast number of possible combinations of different factors and interactions. Many cues and biological signalling events during development are context dependent [100, 101], and basic cell behaviors, such as migration, are drastically different under 2- and 3D environments [102]. Thorough investigation of cell behaviors *in vitro*, and the ability to determine mechanisms for the observed cell behaviors requires microscale technologies with fine control over the engineered cellular microenvironment.

Techniques to create microarrays of 3D microgels for the investigation of cell–materials interactions will be of great utility in tissue engineering. Such techniques face a number of technical challenges including the creation of combinatorial experiments with cell-laden scaffolds and the high throughput screening of outcomes in 3D. Additionally, the high throughput analysis of arrays of cell aggregates, and the analysis of combinatorial material arrays with cell aggregates will be of great use in studying cell-microenvironment interactions in 3D environments. We also envision that further merging of microfluidics with biomaterials arrays will produce new technologies to investigate combinatorial materials and soluble factor experiments.

ES cells and induced pluripotent stem cells have enormous potential in regenerative medicine and tissue engineering. One of the major limitations to the widespread use of stem cells as a cell source in tissue engineering is the lack of the ability to precisely direct their differentiation. We envision many new microscale technologies to address this challenge. For example, it might be possible to direct cell fate with patterns of signaling molecules. Patterning of cues and developmental signals could direct stem cell cultures to differentiation in a spatially organized manner. In this way, mimics of native tissue structures could be produced.

In the past decade there have been many successes in the development of microscale technologies for controlling the cellular microenvironment. These successes have led to the advancement of tissue engineering, and have helped push the field of tissue engineering closer to clinical therapies. The future holds great promise for the continuing success of the existing and as-of-yet developed microscale technologies.

Acknowledgements This chapter was supported by the National Institutes of Health (EB007249; DE019024; HL092836), National Science Foundation (DMR0847287), the institute for Soldier Nanotechnology, and the US Army Corps of Engineers. H.K. acknowledges support from JSPS Fellowship for Research Abroad.

References

1. Langer R, Vacanti JP. Tissue engineering. *Science* 1993;260(5110):920–926.
2. Lutolf MP, Hubbell JA. Synthetic biomaterials as instructive extracellular microenvironments for morphogenesis in tissue engineering. *Nature Biotechnology* 2005;23(1):47–55.
3. Khademhosseini A, Langer R, Borenstein J, Vacanti JP. Microscale technologies for tissue engineering and biology. *Proceedings of the National Academy of Sciences of the United States of America* 2006;103(8):2480–2487.
4. Whitesides GM, Ostuni E, Takayama S, Jiang XY, Ingber DE. Soft lithography in biology and biochemistry. *Annual Review of Biomedical Engineering* 2001;3:335–373.
5. Moeller HC, Mian MK, Shrivastava S, Chung BG, Khademhosseini A. A microwell array system for stem cell culture. *Biomaterials* 2008;29(6):752–763.
6. Karp JM, Yeh J, Eng G, Fukuda J, Blumling J, Suh KY, et al. Controlling size, shape and homogeneity of embryoid bodies using poly(ethylene glycol) microwells. *Lab on a Chip* 2007;7(6):786–794.
7. Ostuni E, Chen CS, Ingber DE, Whitesides GM. Selective deposition of proteins and cells in arrays of microwells. *Langmuir* 2001;17(9):2828–2834.

8. Ostuni E, Yan L, Whitesides GM. The interaction of proteins and cells with self-assembled monolayers of alkanethiolates on gold and silver. *Colloids and Surfaces. B, Biointerfaces* 1999;15(1):3–30.
9. Kane RS, Takayama S, Ostuni E, Ingber DE, Whitesides GM. Patterning proteins and cells using soft lithography. *Biomaterials* 1999;20(23–24):2363–2376.
10. Jinno S, Moeller HC, Chen CL, Rajalingam B, Chung BG, Dokmeci MR, et al. Macrofabricated multilayer parylene-C stencils for the generation of patterned dynamic co-cultures. *Journal of Biomedical Materials Research. Part A* 2008;86A(1):278–288.
11. Ling Y, Rubin J, Deng Y, Huang C, Demirci U, Karp JM, et al. A cell-laden microfluidic hydrogel. *Lab on a Chip* 2007;7(6):756–762.
12. Dertinger SKW, Jiang XY, Li ZY, Murthy VN, Whitesides GM. Gradients of substrate-bound laminin orient axonal specification of neurons. *Proceedings of the National Academy of Sciences of the United States of America* 2002;99(20):12542–12547.
13. Park JH, Chung BG, Lee WG, Kim J, Brigham MD, Shim J, et al. Microporous cell-laden hydrogels for engineered tissue constructs. *Biotechnology and Bioengineering* 2010; 106(1): 138–148
14. Hook AL, Anderson DG, Langer R, Williams P, Davies MC, Alexander MR. High throughput methods applied in biomaterial development and discovery. *Biomaterials* 2010;31(2): 187–198.
15. Peters A, Brey DM, Burdick JA. High-throughput and combinatorial technologies for tissue engineering applications. *Tissue Engineering. Part B: Reviews* 2009;15(3):225–239.
16. Anderson DG, Levenberg S, Langer R. Nanoliter-scale synthesis of arrayed biomaterials and application to human embryonic stem cells. *Nature Biotechnology* 2004;22(7):863–866.
17. Flaim CJ, Chien S, Bhatia SN. An extracellular matrix microarray for probing cellular differentiation. *Nature Methods* 2005;2(2):119–125.
18. Flaim CJ, Teng D, Chien S, Bhatia SN. Combinatorial signaling microenvironments for studying stem cell fate. *Stem Cells and Development* 2008;17(1):29–39.
19. Cukierman E, Pankov R, Stevens DR, Yamada KM. Taking cell–matrix adhesions to the third dimension. *Science* 2001;294(5547):1708–1712.
20. Doyle AD, Wang FW, Matsumoto K, Yamada KM. One-dimensional topography underlies three-dimensional fibrillar cell migration. *The Journal of Cell Biology* 2009;184(4):481–490.
21. Stevens MM, George JH. Exploring and engineering the cell surface interface. *Science* 2005;310(5751):1135–1138.
22. Blawas AS, Reichert WM. Protein patterning. *Biomaterials* 1998;19(7–9):595–609.
23. Barbulovic-Nad I, Lucente M, Sun Y, Zhang MJ, Wheeler AR, Bussmann M. Bio-microarray fabrication techniques – a review. *Critical Reviews in Biotechnology* 2006;26(4):237–259.
24. Bertone P, Snyder M. Advances in functional protein microarray technology. 15th Biennial Conference on Methods in Protein Structure Analysis; 2004 Aug 29–Sep 02; Seattle, WA: Blackwell Publishing; 2004. p. 5400–5411.
25. Xia YN, Whitesides GM. Soft lithography. *Angewandte Chemie (International edition)* 1998; 37(5):551–575.
26. Takayama S, Ostuni E, LeDuc P, Naruse K, Ingber DE, Whitesides GM. Laminar flows – subcellular positioning of small molecules. *Nature* 2001;411(6841):1016.
27. Takayama S, Ostuni E, Qian XP, McDonald JC, Jiang XY, LeDuc P, et al. Topographical micropatterning of poly(dimethylsiloxane) using laminar flows of liquids in capillaries. *Advanced Materials* 2001;13(8):570–574.
28. Khademhosseini A, Yeh J, Eng G, Karp J, Kaji H, Borenstein J, et al. Cell docking inside microwells within reversibly sealed microfluidic channels for fabricating multiphenotype cell arrays. *Lab on a Chip* 2005;5(12):1380–1386.
29. Rhee SW, Taylor AM, Tu CH, Cribbs DH, Cotman CW, Jeon NL. Patterned cell culture inside microfluidic devices. *Lab on a Chip* 2005;5(1):102–107.

30. Khademhosseini A, Bettinger C, Karp JM, Yeh J, Ling YB, Borenstein J, et al. Interplay of biomaterials and micro-scale technologies for advancing biomedical applications. *Journal of Biomaterials Science, Polymer Edition* 2006;17(11):1221–1240.
31. Khetani SR, Bhatia SN. Engineering tissues for in vitro applications. *Current Opinion in Biotechnology* 2006;17(5):524–531.
32. Micheletti M, Lye GJ. Microscale bioprocess optimisation. *Current Opinion in Biotechnology* 2006;17(6):611–618.
33. Portner R, Nagel-Heyer S, Goepfert C, Adamietz P, Meenen NM. Bioreactor design for tissue engineering. *Journal of Bioscience and Bioengineering* 2005;100(3):235–245.
34. Auburn RP, Kreil DP, Meadows LA, Fischer B, Matilla SS, Russell S. Robotic spotting of cDNA and oligonucleotide microarrays. *Trends in Biotechnology* 2005;23(7):374–379.
35. MacBeath G, Schreiber SL. Printing proteins as microarrays for high-throughput function determination. *Science* 2000;289(5485):1760–1763.
36. Mirzabekov A, Kolchinsky A. Emerging array-based technologies in proteomics. *Current Opinion in Chemical Biology* 2002;6(1):70–75.
37. Rusmini F, Zhong ZY, Feijen J. Protein immobilization strategies for protein biochips. *Biomacromolecules* 2007;8(6):1775–1789.
38. Wilson DS, Nock S. Functional protein microarrays. *Current Opinion in Chemical Biology* 2002;6(1):81–85.
39. Lee MY, Kumar RA, Sukumaran SM, Hogg MG, Clark DS, Dordick JS. Three-dimensional cellular microarray for high-throughput toxicology assays. *Proceedings of the National Academy of Sciences of the United States of America* 2008;105(1):59–63.
40. Xu F, et al. A droplet-based building block approach for bladder smooth muscle cell (SMC) proliferation. *Biofabrication* 2010;2(1):014105.
41. Khalil S, Sun W. Bioprinting endothelial cells with alginate for 3D tissue constructs. [Journal of Biomechanical Engineering-Transactions on ASME](#) 2009;131(11):8.
42. Lannutti J, Reneker D, Ma T, Tomasko D, Farson DF. Electrospinning for tissue engineering scaffolds. *Materials Science & Engineering C-Biomimetic and Supramolecular Systems* 2007;27(3):504–509.
43. Chen GP, Ushida T, Tateishi T. Scaffold design for tissue engineering. *Macromolecular Bioscience* 2002;2(2):67–77.
44. Quist AP, Pavlovic E, Oscarsson S. Recent advances in microcontact printing. *Analytical and Bioanalytical Chemistry* 2005;381(3):591–600.
45. Perl A, Reinhoudt DN, Huskens J. Microcontact printing: limitations and achievements. *Advanced Materials* 2009;21(22):2257–2268.
46. Hammond PT. Form and function in multilayer assembly: new applications at the nanoscale. *Advanced Materials* 2004;16(15):1271–1293.
47. Chen CS, Mrksich M, Huang S, Whitesides GM, Ingber DE. Geometric control of cell life and death. *Science* 1997;276(5317):1425–1428.
48. McBeath R, Pirone DM, Nelson CM, Bhadriraju K, Chen CS. Cell shape, cytoskeletal tension, and RhoA regulate stem cell lineage commitment. *Developmental Cell* 2004;6(4):483–495.
49. Alford PW, Feinberg AW, Sheehy SP, Parker KK. Biohybrid thin films for measuring contractility in engineered cardiovascular muscle. *Biomaterials* 2010;31(13):3613–3621.
50. They M, Racine V, Piel M, Pepin A, Dimitrov A, Chen Y, et al. Anisotropy of cell adhesive microenvironment governs cell internal organization and orientation of polarity. *Proceedings of the National Academy of Sciences of the United States of America* 2006;103(52):19771–19776.
51. Falconnet D, Csucs G, Grandin HM, Textor M. Surface engineering approaches to micro-pattern surfaces for cell-based assays. *Biomaterials* 2006;27(16):3044–3063.
52. Fink J, They M, Azioune A, Dupont R, Chatelain F, Bornens M, et al. Comparative study and improvement of current cell micro-patterning techniques. *Lab on a Chip* 2007;7(6):672–680.

53. Folch A, Toner M. Microengineering of cellular interactions. *Annual Review of Biomedical Engineering* 2000;2:227–256.
54. Khademhosseini A, Suh KY, Yang JM, Eng G, Yeh J, Levenberg S, et al. Layer-by-layer deposition of hyaluronic acid and poly-L-lysine for patterned cell co-cultures. *Biomaterials* 2004;25(17):3583–3592.
55. Fukuda J, Khademhosseini A, Yeh J, Eng G, Cheng JJ, Farokhzad OC, et al. Micropatterned cell co-cultures using layer-by-layer deposition of extracellular matrix components. *Biomaterials* 2006;27(8):1479–1486.
56. Chien HW, Chang TY, Tsai WB. Spatial control of cellular adhesion using photo-crosslinked micropatterned polyelectrolyte multilayer films. *Biomaterials* 2009;30(12):2209–2218.
57. Chin VI, Taupin P, Sanga S, Scheel J, Gage FH, Bhatia SN. Microfabricated platform for studying stem cell fates. *Biotechnology and Bioengineering* 2004;88(3):399–415.
58. Hwang YS, Chung BG, Ortmann D, Hattori N, Moeller HC, Khademhosseini A. Microwell-mediated control of embryoid body size regulates embryonic stem cell fate via differential expression of WNT5a and WNT11. *Proceedings of the National Academy of Sciences of the United States of America* 2009;106(40):16978–16983.
59. Ochsner M, Dusseiller MR, Grandin HM, Luna-Morris S, Textor M, Vogel V, et al. Microwell arrays for 3D shape control and high resolution analysis of single cells. *Lab on a Chip* 2007;7(8):1074–1077.
60. Dusseiller MR, Schlaepfer D, Koch M, Kroschewski R, Textor M. An inverted microcontact printing method on topographically structured polystyrene chips for arrayed micro-3-D culturing of single cells. *Biomaterials* 2005;26(29):5917–5925.
61. Koh WG, Revzin A, Pishko MV. Poly(ethylene glycol) hydrogel microstructures encapsulating living cells. *Langmuir* 2002;18(7):2459–2462.
62. Liu VA, Bhatia SN. Three-dimensional photopatterning of hydrogels containing living cells. *Biomedical Microdevices* 2002;4(4):257–266.
63. Peppas NA, Hilt JZ, Khademhosseini A, Langer R. Hydrogels in biology and medicine: from molecular principles to bionanotechnology. *Advanced Materials* 2006;18(11):1345–1360.
64. Mironov V, Boland T, Trusk T, Forgacs G, Markwald RR. Organ printing: computer-aided jet-based 3D tissue engineering. *Trends in Biotechnology* 2003;21(4):157–161.
65. Zamanian B, Masaeli M, Nichol JW, Khabiry M, Hancock MJ, Bae H, et al. Interface-directed self-assembly of cell-laden microgels. *Small* 2010;6(8):937–944.
66. Du Y, Lo E, Vidula MK, Khabiry M, Khademhosseini A. Method of bottom-up directed assembly of cell-laden microgels. *Cellular and Molecular Bioengineering* 2008;1(2–3):157–162.
67. Tsang VL, Chen AA, Cho LM, Jadin KD, Sah RL, DeLong S, et al. Fabrication of 3D hepatic tissues by additive photopatterning of cellular hydrogels. *The FASEB Journal* 2007;21(3):790–801.
68. Lucchetta EM, Lee JH, Fu LA, Patel NH, Ismagilov RF. Dynamics of *Drosophila* embryonic patterning network perturbed in space and time using microfluidics. *Nature* 2005;434(7037):1134–1138.
69. Sawano A, Takayama S, Matsuda M, Miyawaki A. Lateral propagation of EGF signaling after local stimulation is dependent on receptor density. *Developmental Cell* 2002;3(2):245–257.
70. Wobus AM, Boheler KR. Embryonic stem cells: prospects for developmental biology and cell therapy. *Physiological Reviews* 2005;85(2):635–678.
71. Burdick JA, Vunjak-Novakovic G. Engineered microenvironments for controlled stem cell differentiation. *Tissue Engineering. Part A* 2009;15(2):205–219.
72. Irimia D, Liu SY, Tharp WG, Samadani A, Toner M, Poznansky MC. Microfluidic system for measuring neutrophil migratory responses to fast switches of chemical gradients. *Lab on a Chip* 2006;6(2):191–198.

73. Gray JM, Karow DS, Lu H, Chang AJ, Chang JS, Ellis RE, et al. Oxygen sensation and social feeding mediated by a *C-elegans* guanylate cyclase homologue. *Nature* 2004;430(6997):317–322.
74. Allen JW, Khetani SR, Bhatia SN. In vitro zonation and toxicity in a hepatocyte bioreactor. *Toxicological Sciences* 2005;84(1):110–119.
75. Unger MA, Chou HP, Thorsen T, Scherer A, Quake SR. Monolithic microfabricated valves and pumps by multilayer soft lithography. *Science* 2000;288(5463):113–116.
76. Hong JW, Studer V, Hang G, Anderson WF, Quake SR. A nanoliter-scale nucleic acid processor with parallel architecture. *Nature Biotechnology* 2004;22(4):435–439.
77. Hansen CL, Skordalakes E, Berger JM, Quake SR. A robust and scalable microfluidic metering method that allows protein crystal growth by free interface diffusion. *Proceedings of the National Academy of Sciences of the United States of America* 2002;99(26):16531–16536.
78. Liu J, Enzelberger M, Quake S. A nanoliter rotary device for polymerase chain reaction. *Electrophoresis* 2002;23(10):1531–1536.
79. Fu AY, Chou HP, Spence C, Arnold FH, Quake SR. An integrated microfabricated cell sorter. *Analytical Chemistry* 2002;74(11):2451–2457.
80. Thorsen T, Maerkl SJ, Quake SR. Microfluidic large-scale integration. *Science* 2002;298(5593):580–584.
81. Walker GM, Zeringue HC, Beebe DJ. Microenvironment design considerations for cellular scale studies. *Lab on a Chip* 2004;4(2):91–97.
82. Fernandes TG, Diogo MM, Clark DS, Dordick JS, Cabral JMS. High-throughput cellular microarray platforms: applications in drug discovery, toxicology and stem cell research. *Trends in Biotechnology* 2009;27(6):342–349.
83. Hong J, Edel JB, de Mello AJ. Micro- and nanofluidic systems for high-throughput biological screening. *Drug Discovery Today* 2009;14(3–4):134–146.
84. Howbrook DN, van der Valk AM, O’Shaughnessy MC, Sarker DK, Baker SC, Lloyd AW. Developments in microarray technologies. *Drug Discovery Today* 2003;8(14):642–651.
85. Ziauddin J, Sabatini DM. Microarrays of cells expressing defined cDNAs. *Nature* 2001;411(6833):107–110.
86. Sharma S, Rao A. RNAi screening: tips and techniques. *Nature Immunology* 2009;10(8):799–804.
87. Brafman DA, de Minicis S, Seki E, Shah KD, Teng DY, Brenner D, et al. Investigating the role of the extracellular environment in modulating hepatic stellate cell biology with arrayed combinatorial microenvironments. *Integrative Biology* 2009;1(8–9):513–524.
88. Fernandes TG, Kwon S-J, Bale SS, Lee M-Y, Diogo MM, Clark DS, et al. Three-dimensional cell culture microarray for high-throughput studies of stem cell fate. *Biotechnology and Bioengineering* 2010;106(1):106–118.
89. Tweedie CA, Anderson DG, Langer R, Van Vliet KJ. Combinatorial material mechanics: high-throughput polymer synthesis and nanomechanical screening. *Advanced Materials* 2005;17(21):2599–2604.
90. Urquhart AJ, Anderson DG, Taylor M, Alexander MR, Langer R, Davies MC. High throughput surface characterisation of a combinatorial material library. *Advanced Materials* 2007;19(18):2486–2491.
91. Di Carlo D, Wu LY, Lee LP. Dynamic single cell culture array. *Lab on a Chip* 2006;6(11):1445–1449.
92. Singh M, Berklund C, Detamore MS. Strategies and applications for incorporating physical and chemical signal gradients in tissue engineering. *Tissue Engineering Part B-Reviews* 2008;14(4):341–366.
93. Hung PJ, Lee PJ, Sabounchi P, Aghdam N, Lin R, Lee LP. A novel high aspect ratio microfluidic design to provide a stable and uniform microenvironment for cell growth in a high throughput mammalian cell culture array. *Lab on a Chip* 2005;5(1):44–48.

- 5
94. Pihl J, Sinclair J, Sahlin E, Karlsson M, Petterson F, Olofsson J, et al. Microfluidic gradient-generating device for pharmacological profiling. *Analytical Chemistry* 2005;77(13):3897–3903.
 95. Wang ZH, Kim MC, Marquez M, Thorsen T. High-density microfluidic arrays for cell cytotoxicity analysis. *Lab on a Chip* 2007;7(6):740–745.
 96. Thompson DM, King KR, Wieder KJ, Toner M, Yarmush ML, Jayaraman A. Dynamic gene expression profiling using a microfabricated living cell array. *Analytical Chemistry* 2004; 76(14):4098–4103.
 97. Kim L, Vahey MD, Lee HY, Voldman J. Microfluidic arrays for logarithmically perfused embryonic stem cell culture. *Lab on a Chip* 2006;6(3):394–406.
 98. Gomez-Sjoberg R, Leyrat AA, Pirone DM, Chen CS, Quake SR. Versatile, fully automated, microfluidic cell culture system. *Analytical Chemistry* 2007;79(22):8557–8563.
 99. Lii J, Hsu W-J, Parsa H, Das A, Rouse R, Sia SK. Real-time microfluidic system for studying mammalian cells in 3D microenvironments. *Analytical Chemistry* 2008;80(10):3640–3647.
 100. Armant DR. Blastocysts don't go it alone. Extrinsic signals fine-tune the intrinsic developmental program of trophoblast cells. *Developmental Biology* 2005;280(2):260–280.
 101. Veeman MT, Axelrod JD, Moon RT. A second canon: functions and mechanisms of beta-catenin-independent wnt signaling. *Developmental Cell* 2003;5(3):367–377.
 102. Dong H, Hartgerink JD. Short homodimeric and heterodimeric coiled coils. *Biomacromolecules* 2006;7(3):691–695.
 103. Anderson DG, Putnam D, Lavik EB, Mahmood TA, Langer R. Biomaterial microarrays: rapid, microscale screening of polymer-cell interaction. *Biomaterials* 2005;26(23):4892–4897.

Contents

6.1	Introduction	140
6.2	Creation of Micro- and Nano Features on 2D Substrates	141
6.2.1	Substrate Modification	142
6.2.2	Surface Patterning	142
6.2.3	Soft Lithography	142
6.2.4	Micro Contact Printing (μ CP)	144
6.2.5	Micro and Nano Fluidics	144
6.3	Cellular Interactions with 2D Micro and Nano Patterns	144
6.3.1	Mechanism of Cell–Matrix Interactions	145
6.3.2	Changes in Morphology	146
6.3.3	Effect on Migration	148
6.3.4	Cellular Proliferation	148
6.3.5	Phenotype	149
6.4	Nanomaterials and Synthesis	150
6.4.1	Nanofibers	150
6.4.2	Nanotubes	154
6.4.3	Functionalized Nanomaterials	157
6.5	Interfacing Cells with Nanomaterials	158
6.5.1	Bone Tissue Engineering	160
6.5.2	Articular Cartilage Tissue Engineering	162
6.5.3	Fibrocartilaginous Tissues (Meniscus and Intervertebral Disc)	163
6.5.4	Tendon/Ligament Tissue Engineering	164
6.5.5	Neural and Muscular Tissue Engineering	166
6.6	Future Directions	167
	References	169

Abstract Nanotechnology has enabled the creation of novel structures or devices with organization and structure at the molecular and atomic scale. Nano-dimensions impart distinctive properties compared to micron sized materials. In this chapter, we will review techniques for creation of micron and nanometer features on 2D substrates and 3D

N.O. Chahine (✉)

Biomechanics and Bioengineering Laboratory, Feinstein Institute for Medical Research, North Shore LIJ Health System, 350 Community Drive, Manhasset, NY 11030, USA
e-mail: nchahine@nshs.edu

nanomaterials which have been used in tissue engineering applications. In the first half, we will review the latest advances in custom designed micro- and nano-substrates to enhance the phenotypic expressions of cells and mechanisms behind changes in cell behaviors. In the second half, we will focus on nanomaterials and discuss recent developments in both design and applications for tissue engineering and mechanisms behind cellular interactions with nanomaterials. In addition, an examination of the effects of nanomaterials on biocompatibility and cytotoxicity will be presented. Specific applications of nanomaterials in tissue engineering of connective, neural, muscular and boney tissue will also be examined.

Keywords Biocompatibility • Cell–matrix interactions • Electrospinning • Microfabrication • Nanotechnology • Nanotubes • Surface modifications • Tissue engineering

6.1 Introduction

Micro and nanomaterials are materials with dimensions or morphological features on the order of the micrometer ($1 \mu\text{m} = 1 \times 10^{-6} \text{ m}$) and nanometer ($1 \text{ nm} = 1 \times 10^{-9} \text{ m}$), respectively. By definition, the nanoscale is defined as smaller than a one tenth of a micrometer ($0.1 \mu\text{m}$ or 100 nm) in at least one dimension though this term is sometimes also used for materials in the submicron scale ($<1 \mu\text{m}$). The scaling down of material dimension and features to the nanoscale imparts unique properties on cells and tissues. Materials engineered to be in this size range can exhibit novel or enhanced properties, especially in defining the interaction between cells and their surrounding matrices.

Nanotechnology has enabled the creation of novel structures or devices with organization and structure at the molecular and atomic scale. The dimensions of nanomaterials are comparable to that of biological molecules such as proteins and DNA, forcing nanomaterials to be the physical interface between biology and material science. Nano-dimensions impart distinctive properties compared to micron sized materials. Some of these properties exhibited include a high surface area to volume ratio and tunable optical emission and super paramagnetic behavior, which can be successfully exploited for a variety of health care applications ranging from drug delivery to biosensors. Nanotechnology applications have spurred bio-inspired nanodevices and materials which can be used for applications such as drug delivery [1], molecular or optical imaging, sensors etc. Though the use of nanoparticles for drug delivery (e.g. in cancer treatment) or nanostructures for enhanced imaging demonstrate the significant potential of nanotechnology applications in medicine, these types of nanodevices are outside the scope of this chapter.

Nanotechnology can also be used to reproduce cellular building blocks or molecular design principles by means of highly organized structures that mimic the natural structure of biological tissues, or extracellular matrix (ECM). This enables the creation of 2D and 3D substrates with specific topographical, morphological and chemical characteristics utilized

to direct the functionality of cells grown on these substrates. In addition, 3D porous scaffolds from singular nanofibers, nanotubes and other nanomaterials have been developed and cultured in the presence of cells in order to generate replacement tissues. The development of porous nanomaterial-based scaffolds for tissue engineering provides a cellular environment which best mimics the native ECM of connective tissues and an opportunity for cells to interact with the ECM.

Cells in their native environment reside in a social context where they interact with other cells and their ECM. ECM composition and quantity varies greatly with different tissues. With a variety of matrix proteins, such as fibronectin and proteoglycans, the ECM provides a mechanical, biochemical, and topographical environment (Fig. 6.2a). In the bone marrow cavity, the ECM is believed to provide a stem cell ‘niche’ where the mechanical and topographical features present a 3D physical environment that combines with biochemistry to direct stem cell fate [2]. One of the most abundant ECM proteins is type I collagen. Type I collagen is a fibrillar protein abundant in skin, bone, cornea, blood vessel and other connective tissues. The triple helix structure of collagen, formed by two $\alpha 1$ and one $\alpha 2$ polypeptides, can be linked to other helices to form fibrils and fibers. Depending on tissue type, these fiber diameters can range from 31 nm in the cornea to 4 μm in the alveoli [3, 4]. Collagen fibril size and spacing can influence a number of physical properties such as transparency of the cornea and mechanical properties of alveoli [4, 5]. Furthermore, collagen fiber size has been shown to modulate the osteoblastic MG61 cell migration and morphology [6]. This structure-function relationship of the ECM is not well understood *in vivo* but a variety of methods have been employed to recapitulate the *in situ* environment. With the advance of microfabrication and nanotechnology, much research has generated significant progress in this area. We will describe the application of micro and nanofabrication on understanding cellular interactions with ECM and materials.

In this chapter, we will review techniques for creation of micron and nanometer features on 2D substrates and 3D nanomaterials which have been used in tissue engineering applications. In the first half, we will review the latest advances in custom designed micro- and nano-substrates to study mechanisms behind changes in cell behaviors and enhanced phenotypic expressions. In the second half, we will focus on nanomaterials and discuss recent developments in both design and applications for tissue engineering and mechanisms behind cellular interactions with nanomaterials. In addition, an examination of the effects of nanomaterials on biocompatibility and cytotoxicity will be presented. Specific applications of nanomaterials in tissue engineering of connective, neural, muscular and boney tissue will also be examined.

6.2

Creation of Micro- and Nano Features on 2D Substrates

Richard Feynman’s seminal lecture in 1959, “There is plenty of room at the bottom”, sparked the revolution of nanotechnology [7]. Most of these microfabrication techniques were originally developed in the field of microelectronics for the fabrication of integrated circuits. With the rapid expansion of the electronics field (and market), a paradigm shift in

new methodology has revolutionized the world of engineering. Toward the end of the twentieth century, scientists started adapting microfabrication technology developed and refined in the electronics field and applying them to the study of biology and medicine. Microfabrication is a collection of techniques, some of which originated from ancient concepts in the case of lithography. We will focus on two dimensional surface modifications in the first part of the chapter. In the context of studying cell/cell or cell/matrix interactions, microfabrication often involves the following components (see also schematics in Fig. 6.1).

6.2.1

Substrate Modification

Microfabricated devices often are formed over a support substrate. Substrate materials such as silicon wafers, quartz or glass are often used and modifications are made to the substrate in layers via thin film deposition, sputtering or spin coating. The purpose of these films varies with different applications. For instance, in addition to structural elements, conductive materials can be deposited on silicon substrates to serve as detection electrodes or provide electrical potentials. Chemical modifications can also be made to the substrate surface to change its biological activities by modifying surface charge, hydrophobicity, or adding adhesive proteins to promote cell adhesion. Self assembly monolayers (SAMs), highly ordered molecular assemblies formed by chemisorption of functionalized molecules, are often employed to modify substrate surface chemical properties (Fig. 6.1a) [8].

6.2.2

Surface Patterning

Depending on scale or application, a variety of methods are used to create structures with the substrate or deposited layers. Photolithography, usually via UV light, can be used to create patterns in the micrometer scale while electron beam (e-beam) can be used for smaller features. Photolithography procedures are much like that of film development, including the terminology. A mask is generated with the desired pattern (image) using a high resolution printer and a thin layer of the photo- (or e-beam) reactive polymer is deposited onto the substrate to “detect” the pattern. This polymer, photoresist, can then be *exposed* with the light source and *developed* to reveal the pattern. The resist layer can serve as a shield to protect the substrate from etching procedures or can themselves serve as structures.

6.2.3

Soft Lithography

George Whitesides’ group at Harvard University spearheaded the use of elastic silicon polymers to replicate the microfabricated structure (master) made by photolithography [9]. The “soft” is represented by the use of elastomeric materials that conform to the master

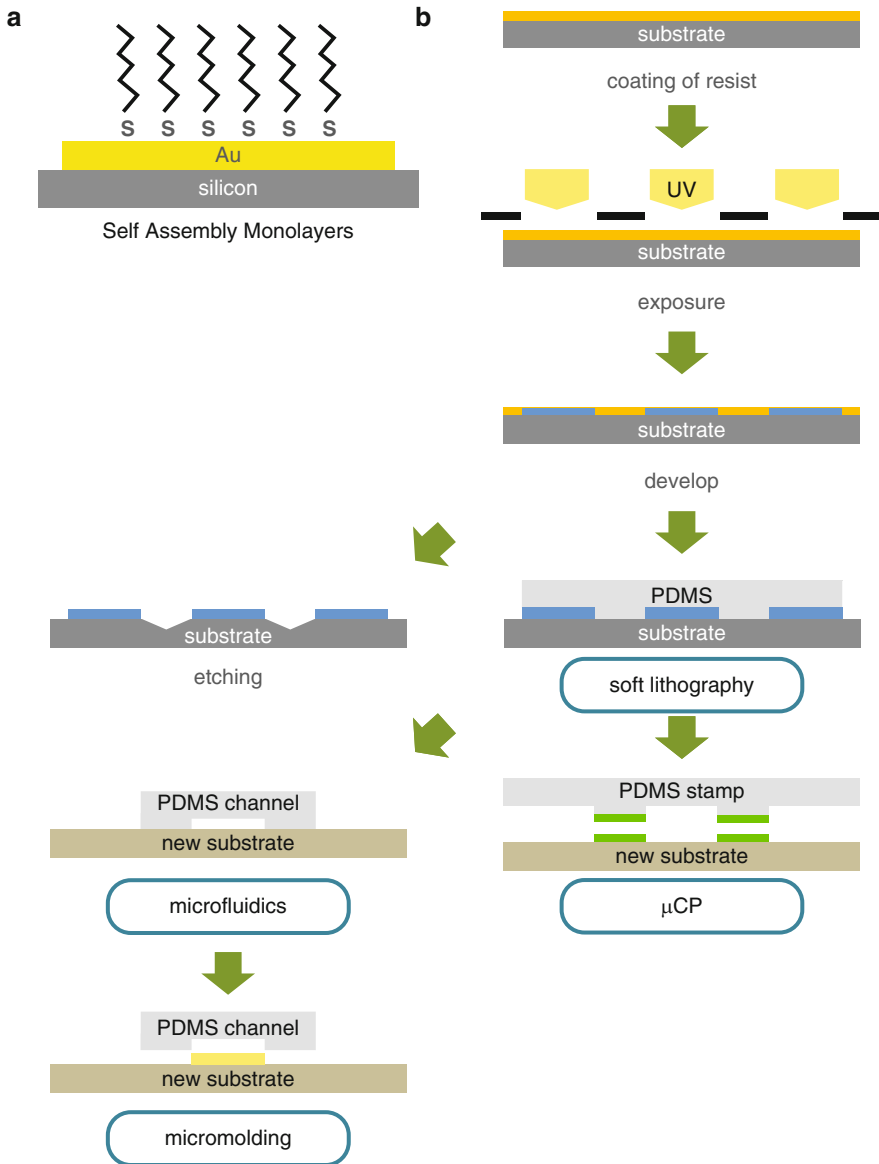


Fig. 6.1 Microfabrication Techniques. (a) Illustration of self assembly monolayers (SAMs). (b) Schematic of the microfabrication process and application

features or the substrate. Soft lithography is low cost and has many applications described in the following sections (see Fig. 6.1b). One of the most used materials for soft lithography is polydimethylsiloxane (PDMS), which offers high structural fidelity, transparency, chemical inertness and gas permeability.

6.2.4

Micro Contact Printing (μ CP)

μ CP takes advantage of the conformative nature of the molded PDMS to create a replicated pattern on a substrate, often times via self assembly monolayers. An “ink” of desired molecules such as the adhesion protein fibronectin can be printed onto the substrate with high geometric precision to generate a chemical pattern. The substrate surface can be prepared in advance with SAMs for covalent binding to the “ink”, providing a long-lasting modification. Alternatively, non-specific binding to the substrate can also be achieved just by stamping to an untreated clean glass slide. An often used application is to create cell adhesive and nonadhesive zones on a substrate to study the effect of cell shape, size, or receptor clustering [10, 11].

6.2.5

Micro and Nano Fluidics

Patterns generated on the silicon master with resist can be designed as a series of connected lines. The replica molded PDMS would then be shaped into a flow system, creating a variety of flow patterns. Due to the size scale, fluids flowing in the channels are microliter in volume, hence termed “micro-fluidic”. For the same reason, the flow patterns generated in these channels are laminar flows with minimal mixing, thus allowing precise control of fluid composition and location. A famous study illustrated that a microfluidic device can deliver two fluorescent markers on either side of the cell without perturbing the other side (Fig. 6.2b, [12]). Microfluidics can also be used to create 3D patterns with materials not compatible with the aforementioned harsh microfabrication procedures. Biological molecules such as proteins and hyaluronan can be introduced into the channels and form hydrogels by changing their pH values or adding polymerizing initiators. Replica molding can also be achieved by compressing the microfabricated stamp into a soft material before it solidifies.

6.3

Cellular Interactions with 2D Micro and Nano Patterns

As early as 1911, Ross Harrison noted that cells growing on spider webs spread and align according to the shape of the underlying fibers and identified it as stereotropism [13]. This behavior is now often termed contact guidance, coined by Paul Weiss circa 1934 [14], and describes the cell behavior and morphology change in response to surface geometry or topography. Microfabrication techniques have enabled many studies investigating micro- or nano-scale topographies, most of which are groove patterns. Cellular responses to these patterns include changes in adhesion, spreading, migration, gene expression, proliferation, and stem cell lineage commitments.

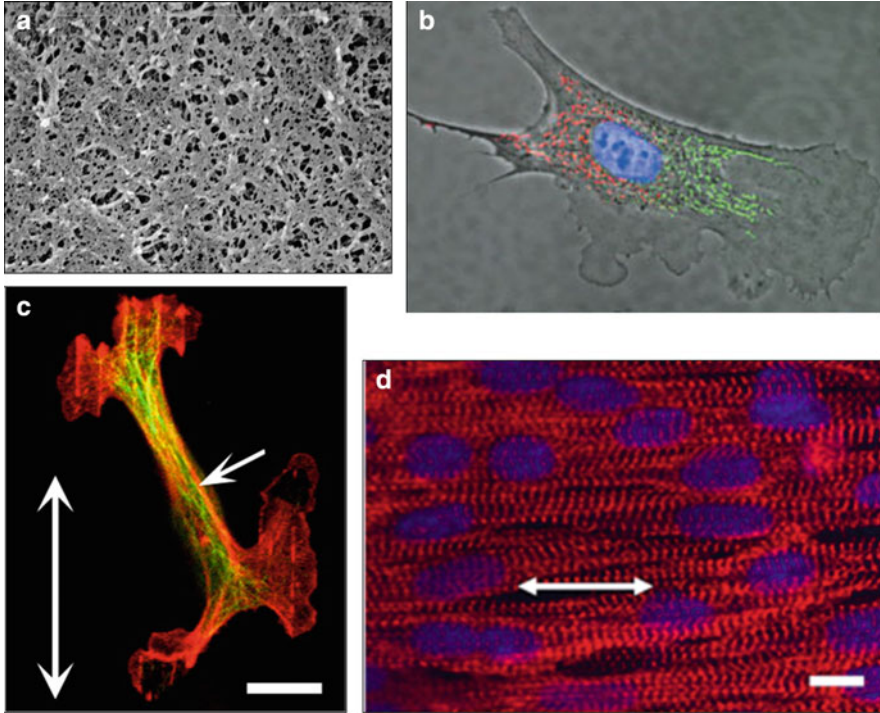


Fig. 6.2 (a) Scanning electron microscopy (SEM) image of macaque monkey corneal epithelial basement membrane (Reprinted from [180] with permission from Elsevier). Scale bar equals 500 nm. (b) Fluorescence images of a single cell after treatment of green and red mitotracker dyes on either side (Reprinted from [12] with permission from Macmillan Publishers Ltd, © 2001). (c) Fluorescence images of corneal epithelial cells on microgrooves 130 nm deep and 2 μm wide, as indicated with the double-headed arrow. The actin cytoskeleton is represented in *green* and microtubule is shown in *red*. *Arrow* indicates thick actin band parallel to the long axis of cell. Scale bar equals 10 μm . (Reprinted from [20] with permission from Elsevier). (d) Sarcomeric α -actinin organization of neonatal rat cardiomyocytes cultured on nano-patterned substrate with 400 nm wide ridges on a 800 nm pitch (Reprinted from [59] with permission from National Academy of Sciences)

6.3.1

Mechanism of Cell–Matrix Interactions

How do the cells sense the extracellular environment, especially topography? It is believed that cells extend filopodia (or microspikes, a thin club-like cellular extension composed mostly of actin cytoskeleton and plasma membrane) to sense and find new attachment sites [15]. This “sensation” comes from changes in cytoskeleton tension when the filopodia forms new contacts at the leading edge [16]. On micro- or nano-patterned surfaces, cells appear to increase their filopodia extensions, which may increase the cell’s perception of the surrounding topography [15, 17]. Dalton and coworkers hypothesized that filopodia

extension is obstructed with the ridge wall [18]. Using microfabricated grooves, Teixeira and colleagues found filopodia extension is often bent at the point of contact with the substrate and hence is confined to align with the microgrooves [19, 20]. Similar to the actin network, focal adhesion is also confined to the topographic pattern, thus preventing lateral spreading and results in anisotropic cellular extension and preferential spreading along the pattern direction [19]. In addition to the actin cytoskeleton, microtubule also reorganizes and aligns with the microenvironment [21, 22]. Studies by Oakley and Brunette found in gingival ligament fibroblasts, microtubule extension may precede actin filaments [21]. While different cell types and substrate geometry were used with the previously mentioned studies, it is in general believed that microtubules, actin filaments, and focal adhesions act in concert to align along the discontinuous surfaces (edges, Fig. 6.2c). Additionally, treatment of cytoskeleton inhibitors such as cytochalasin D and colcemid do not completely abolish the cell alignment response, suggesting alternative mechanisms might be involved [23, 24].

In addition to topographical cues, other factors are also known to align, direct and change cell behaviors. Vascular endothelial cells align perpendicular to cyclic strain, however, substrates with parallel-oriented microgrooves limit their response to applied cyclic strain [25]. Chemotaxis directionality is also modulated by the underlying topography [26]. Intriguingly, while 3T3 fibroblast migration is influenced by both topography and substrate stiffness, the cancer fibroblastic cells (SaI/N) do not respond to substrate stiffness [27], which may be related to the loss of anchorage dependence discussed earlier. In another example, applied direct current (DC) electric field (EF) directs corneal epithelial cell migration toward the cathode. When the microgroove pattern is parallel to the applied EF, these two factors act synergistically and increase directed cell migration. When the microgroove pattern is orthogonal to the applied EF, however, corneal epithelial cells appear to “choose” one or the other cue. Some migrate vertically along microgrooves and others migrate across the microgrooves towards the cathode [28]. Since these two cues act through two different signaling pathways (EF-cdc42, microgrooves-rho), the authors suggested a rho/cdc42 switch mechanism to sort contradicting cues. In neonatal cardiomyocytes, applied alternating pulsatile EFs appear to have a lesser effect on cell alignment direction than the topographical cues [29]. On chemically and topographically patterned surfaces (both in the μm scale), baby hamster kidney (BHK) cells were found to align preferentially to the chemical pattern and osteoblast-like cells (MC3T3) were found to align preferentially to the topographical pattern [30, 31]. As no governing principle can be easily elucidated from these results, more detailed investigations into cell and pattern specificity are needed to determine the interaction between topography and other polarizing cues.

6.3.2

Changes in Morphology

Cell morphology is intimately related to cell attachment, cytoskeleton organization, and phenotype. Cell attachment to the substrate is mediated through focal adhesion complexes which are transmembrane clusters of cell surface receptors, intracellular cytoskeleton and signal transduction proteins. A major family of cell surface receptors for the ECM is integrin. When in contact with appropriate ligands (usually inclusive of the RGD peptide

sequence), integrin molecules cluster and recruit associating proteins to form the focal adhesion complex. Integrin clustering also requires external ligand clusters in the nano-scale. Using a synthetic polymer-linking method, Maheshwari and coworkers presented 1, 5, or 9 RGD peptides on a single polymer and varied their density on substrates [32]. At the same overall RGD density, murine NR6 fibroblasts exhibited migration speeds almost an order of magnitude faster on the 9 RGD-cluster surfaces than the 5 or single RGD clusters. Cell-substrate adhesion strength follows similar trends. Bigger clusters also resulted in more stress fibers. Individual cluster size is a few tens of nanometers while cluster spacing is from tens to hundreds of nanometers. These findings suggest that cell attachment formation, cytoskeleton organization and migration are dependent on local spatial presentation of the RGD sequence. Formation of these adhesion complexes can modulate cell phenotype. While many studies have incorporated the RGD sequence to enhance cell adhesion to materials, other cofactors can further modulate cell behavior and phenotype. In the case of osteogenesis, presentation of the RGD peptide with the synergy site PHSRN leads to increases in ECM production and alkaline phosphatase production [33].

On patterned surfaces, nano-grooves have been found to enhance cell attachment in general. Endothelial cells have been found to have greater adhesion and coverage on aligned nanometer-scaled patterns compared with larger micrometer-scale patterns, or controls consisting of random nano-structured surface features [34, 35]. Human corneal epithelial cells exhibited the highest adhesion strength on features of 400 nm pitch size (~220 nm ridge, ~180 nm groove) where focal adhesion complexes are mostly confined to a single ridge surface. In a few instances, however, focal adhesions can spread across the groove and span a 330 nm gap. The enhanced adhesion strengths of nanotopography are lost when feature pitch size exceeds 4,000 nm [36]. This result is believed to arise from the similarity of the microgroove size with natural ECM topography. On micropits or microposts, small attachment footprints are in general correlated with decreased attachment strength [15, 37].

An apparent morphology difference on microfabricated surfaces is the cell shape change. On microgrooves, the majority of cell types exhibit contact guidance and align parallel to the pattern direction (Fig. 6.2c [20]). Interestingly, Rajnicek and coworkers found that rat hippocampal neurites grow parallel to microgrooves when the feature size is large and align perpendicular to the smaller and shallower patterns [38]. This differential response is believed to involve calcium signaling [23]. Similar phenomenon has also been observed in corneal epithelial cells [39]. Feature size also has an effect on cell shape. Loesberg and coworkers generated microgrooves of 1:1 pitch ratio (ridge:groove), ranging from 40 to 1,000 nm in pitch and depths from 4 to 40 nm. Rat dermal fibroblasts aligned to all pitch sizes but only with groove depths of 35 nm or above [40]. Using patterns featuring consistent ridge width and groove depth (1 μm and 400 nm, respectively) and a gradient of groove widths (1–9.1 μm , with 0.1 μm increment), Kim and colleagues found stronger alignment and elongation of NIH 3T3 fibroblasts on denser patterns [41]. When compared with the attachment strength results, 4,000 nm pitch sized patterns were found to illicit human corneal epithelial cell alignment, yet had no effect on cell attachment strength [36]. Upon closer inspection, cell alignment to groove patterns is coordinated with cytoskeleton organization parallel to the alignment direction. Both microtubule and actin cytoskeleton are involved in the alignment response. When feature sizes are smaller than 500 nm,

interestingly, microtubules appear to be required to align human gingival fibroblasts [22]. On micropits or microposts, no apparent alignment behavior can be observed, although some report has suggested that cells can sense symmetry in the topography [15].

6.3.3

Effect on Migration

With varied cell attachment and alignment, one can imagine that the cell migration behavior is also modulated on the micro-patterned surfaces. On microgrooves, cells mostly exhibited migration preferentially along the alignment direction [18, 28]. Migration on the groove width gradient revealed a biphasic response where migration speed is the highest in medium groove density [41]. Microtubule organizing centers (MTOCs) of smooth muscle cells have been shown to polarize according to groove pattern directions, suggesting it is the geometric constraint of surface topography that dictates cell migration direction, rather than a precise cellular migratory function in the leading region [42]. Two dimensional fibronectin patterns generated by μ CP also revealed similar polarization of MTOCs and Golgi complexes [43]. Rho activities may also be involved in contact guidance migration in corneal epithelial cells [28]. On microposts, 3T3 fibroblasts demonstrated persistent migration and responded to the micropost rigidity change [27]. More studies are needed to better understand cell behaviors on micropit and micropost patterns and the mechanisms behind them.

6.3.4

Cellular Proliferation

Other than some exceptions, the majority of metazoan cells require attachment to a solid substrate to survive. This phenomenon is called anchorage dependence. Many transformed cells lose this dependence and it is one mechanism of metastasis. Cell attachment to the substrate initiates a series of events, including the previously mentioned focal adhesion complex formation and cytoskeleton organization. In conjunction with mitogens, the cellular structural change can regulate cell cycle progression, hence modulating cell proliferation [44]. Furthermore, Chen and coworkers demonstrated that cell size, independent of attachment area, can influence cell fate of apoptosis or DNA replication [45]. This effect is mediated by cell tension and modulations in cell tension can change cell proliferation rate in single cell or monolayers [46]. Changes in cell attachment and cytoskeleton organization can therefore modulate cell proliferation. In human embryonic stem cells, microgrooves with pitch size of 1,200 nm suppressed proliferation when compared with flat surfaces [47]. In human embryonic kidney cells (HEK-293), however, microgrooves enhance cell proliferation [48]. Similarly, nanotubular titanium has been shown to provide a favorable template for proliferation and osteoblastic function (bone matrix deposition) compared to cells grown on flat titanium surfaces [49, 50]. This variation in response may be due to phenotypic differences in cell properties and their abilities to sense and respond to the extracellular mechanical environment [51], which will be further elaborated in the following section.

6.3.5 Phenotype

In addition to chemical components, physical factors in the environment have been known to modulate cell phenotype. Substrate elasticity, for example, can influence stem cell differentiation lineage [52]. Cell morphology has also been demonstrated elegantly by McBeath and coworkers to determine mesenchymal stem cell (MSC) differentiation between adipogenesis and osteogenesis [53]. In turn, mechanical properties of the cell change with differentiation, hence changing their response to the extracellular stimulation [51]. It is therefore feasible to imagine that cells with different phenotype would respond differently to similar physical environments. Fibroblasts have been known to increase fibronectin production and assembly when cultured on microgrooves [54]. A few tissue specific examples will be discussed here.

Osteogenesis has been widely studied regarding surface roughness and cell phenotypic changes since it is of great interest for orthopaedic and dental implant compatibility and adaptation. Groessner-Schreiber and Tuan demonstrated as early as 1992 that chick embryonic calvarial osteoblasts responded to rough-textured and porous-coated titanium surfaces with increased attachment, matrix production and mineralization compared to smooth surfaces [55]. More recently, Mathew Dalby's group showed that human osteoblasts exhibited different focal adhesion behavior on substrates with different sizes and topographies [56]. Additionally, using stro-1 enriched human MSCs, they revealed the different substrate topographies activated different canonical signal transduction pathways. In a separate study, human MSC elongation, stress fiber formation, and gene expression of bone phenotypic markers were found on aligned TiO₂ nanotubes of larger feature sizes (70 or 100 nm compared to 30 or 50 nm) without soluble osteogenic factors [57]. Moreover, Dalby's group demonstrated that using the same sized micropit features, pattern symmetry and disorder can significantly alter MSC osteogenesis [58]. A biphasic response to the degree of disorder was observed in osteogenic potential without chemical stimulation. Compared to the highly organized or totally random features, higher phenotypic expression was found on "nanodisplaced topography", where the micropits were displaced randomly by up to 50 nm on both axes from their position in a true square array. These studies suggest that topographical cues play a distinct differentiation role independent of chemical factors.

In addition to orthopaedic applications, the myogenic phenotype can also benefit from topographical patterning. Nanoscale microgrooves on polyethylene glycol (PEG) hydrogels facilitated rat neonatal cardiomyocyte alignment and phenotypic expression of the cell junction protein connexin 43 and sarcomeric organization (Fig. 6.2d, [59]). These improvements resulted in enhanced functionality of the resulting myofibers in terms of contractility and electrophysiology. In the micron scale, chemical or topographical patterning have also generated similar results [60, 61]. Similar to muscle, neural tissues are composed of highly organized networks. Embryonic rat hippocampal cells were found to have enhanced polarization on polypyrrole surfaces with microgrooves at 1 and 2 μm widths. Wider grooves generated significantly more polarized cells, although no differences were observed for axon length [62]. When applied with the neurogenic factor retinoic acid, microgroove patterns can even induce transdifferentiation of human MSCs into neuronal lineage, especially when the groove width is in the nano-scale (350 nm compared with 1 and 10 μm) [63].

With advances of nano- and micro-fabrication technology and knowledge in cell biology, we are gaining momentum in the understanding of cell and microenvironment interactions. Based on these findings, 3D materials designed for optimized tissue regeneration and growth will be discussed in the following sections.

6.4 Nanomaterials and Synthesis

6.4.1 Nanofibers

In tissue engineering, nanofibers, nanotubes or composite nanomaterials have been used as porous 3D scaffolds for engineering various tissues such as skin, blood vessels, nerve, tendon, bone and cartilage. Nanofibers, solid fibers with diameters on the order of 1–100 nm, have high surface-area-to-volume ratio, resulting in highly porous scaffolds with exceptional mechanical properties. These scaffolds offer a wide variety of topographical features that encourage cell adhesion and proliferation. It is possible to fabricate fibers in the diameter range of ~3 nm up to 5 μm (though submicron diameters more strongly adhere to the nanofiber definition) and several meters in length. Certain nanofiber matrices are morphologically similar to natural ECM, mimicking the ultrafine continuous fibers, high surface-to-volume ratio, high porosity and variable pore-size distribution. In addition, nanofiber matrices as tissue engineering scaffolds provide interconnected highly porous structures to facilitate cellular migration and transport of nutrients and metabolic wastes for neo-tissue formation.

Many techniques have been utilized for the fabrication of nanofibers, and the most widely and successfully applied technique is electrospinning. Other techniques such as template synthesis, drawing, and interfacial polymerization have also been utilized in nanomaterial production, though with less emphasis on biodegradable polymers. Other successful techniques in creating nanofibrous tissue engineering structures include self assembly and phase separation.

6.4.1.1 Electrospinning

Electrospinning provides a versatile and rapid method to fabricate nanofibrous scaffolds allowing for the engineering of fibers at the nanometer diameter. In electrospinning, a high voltage electric potential is applied to a droplet of polymer solution from a syringe or capillary tube, and when the applied electric potential overcomes the surface tension, the polymer jet is ejected (Fig. 6.3a) [64–67]. The jet travels rapidly to the collector under the influence of an applied electrical field and the infinitely long fiber collects in the form of a non-woven web as the jet dries (Fig. 6.3b). In order to minimize the instability due to the repulsive electrostatic forces, the jet elongates to undergo large amounts of plastic

stretching, resulting in ultra-thin fibers [64, 65, 68]. Several other factors affect the jet stability and thus the diameter of the resulting fibers, such as polymer concentration, viscosity, working distance between spinneret and collector, surface tension, temperature, and vapor pressure (Table 6.1) [68–71].

Electrospun fibers can be collected on various types of collectors. Fibers spun onto a stationary collector, consisting of a grounded conductive substrate, result in a random web of nanofibers [64–67]. When rotation is introduced to the target collector, the fibers are deposited in alignment on a rotating drum or dual rings [72–74]. The gap method has also been used to create alignment of fibers, where a split electrode consisting of two conductive substrates separated by a void gap results in the deposition of aligned nanofibers across from the gap [75]. This method essentially provides preferential direction for electrostatic forces to control the motion of the fibers. In these cases directional scaffolds can be produced where the fibers are highly aligned, which may be useful to replicate the ECM for specific tissues such as tendons, where fibrils are aligned to a similar degree.

While electrospinning requires specialized equipment, its adaptability to various polymer solutions and ease of control has propelled it to be the most widely used nanofiber production technique. Polymer solutions composed of synthetic polymers such as poly(glycolic acid) (PGA), poly(L-lactic acid) (PLLA), poly(DL-lactide-co-glycolide) (PLGA), poly(ethylene oxide) (PEO), poly(*ε*-caprolactone) (PCL), poly(dimethylsiloxane) (PDMS), poly(ester urethane)urea (PEUU) and many others have all been used for nanofiber electrospinning. In addition, natural polymers such as collagen, silk fibroin, chitin, elastin, and fibrinogen have also been used in electrospinning applications yielding controlled nanofibrous scaffolds [76].

6.4.1.2

Self Assembly

Self-assembly involves the spontaneous organization of individual components into an ordered and stable structure with preprogrammed non-covalent bonds [76–79]. While a common natural process responsible for several essential biological components (nucleic acid synthesis, protein synthesis, and energy transduction), self-assembly is a rather complex process that is limited to only a select few polymer configurations (diblock copolymers, triblock copolymers, triblocks from peptide-amphiphile, and dendrimers) [76, 80]. Peptide-amphiphiles (PA) are the most common of these polymers for the production of nanoscale fibers [77, 81]. Hartgerink et al have shown that PAs can form nanofiber cylindrical micelles due to their cone shape and amphiphilic nature [77, 81]. The nanofibers are approximately 5–8 nm in diameter and over 1 μm in length (Fig. 6.3c). Nanofiber forming PAs are designed to have five key structural features. They include: long alkyl tail that conveys hydrophobic characteristics to the molecule; four consecutive cysteine residues that form disulfide bonds to polymerize the structure; a linker region containing three glycine residues to provide the hydrophilic head group the flexibility from the rigid cross-linked regions; a phosphorylated serine residue that interacts strongly with calcium ions and helps to direct mineralization; and Arg-Gly-Asp (RGD), a cell adhesion ligand. The cysteine, phosphorylated serine and RGD sequence are specific characteristics of the

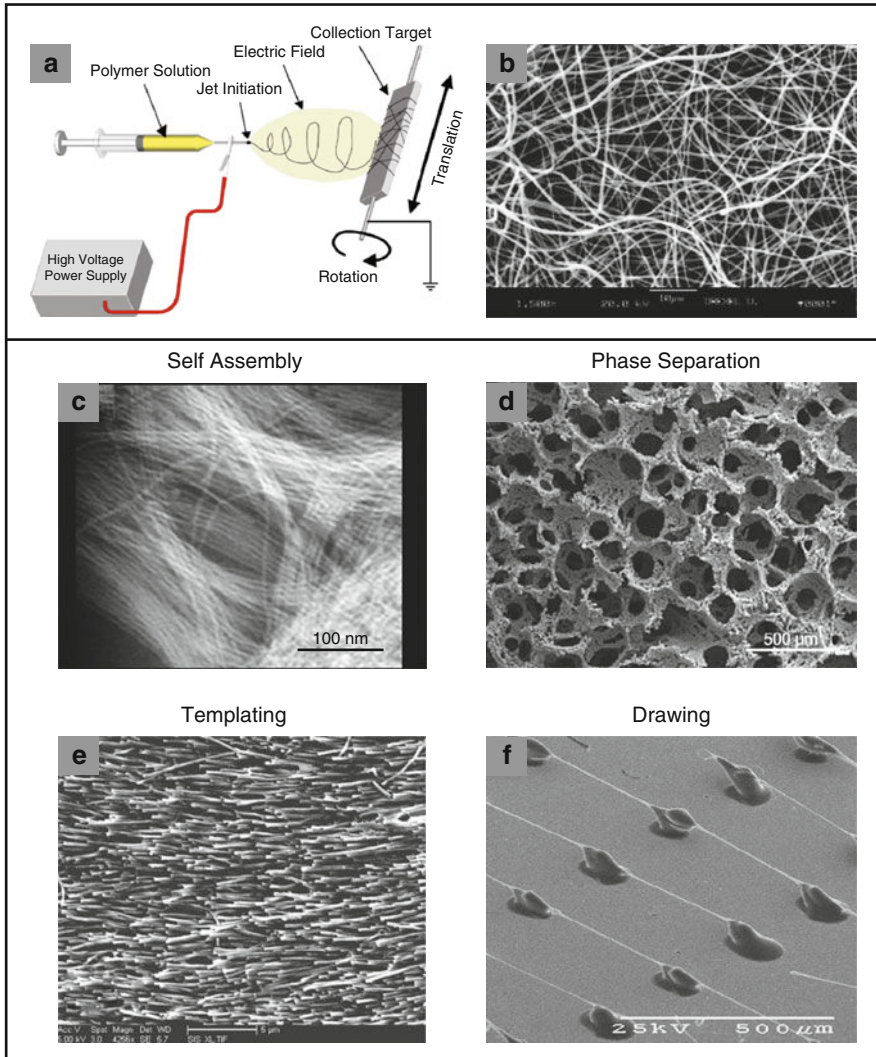


Fig. 6.3 (a) Schematic of the electrospinning process to illustrate the basic phenomena and process components (Reprinted from [76] with permission from Elsevier, © 2007). (b) Nonwoven electrospun PLGA nanofibers (Reprinted from [181], © 2002 John Wiley & Sons). (c) Nanofibers created through acid induced self-assembly of two different molecules with the same peptide sequence (Reprinted from [81], © 2002 with permission from the National Academy of Sciences). (d) Nanofibrous PLLA matrix created through phase separation with paraffin spheres (Reprinted from [182], © 2004, with permission from Elsevier). (e) Nanostructures made from biodegradable polymer, PCL, by bringing porous template in contact with the polymer melt (Reprinted from [85], © 2007 American Chemical Society). (f) Continuously drawn array of fibers on a silicon substrate (Reprinted from [86], © 2006 American Institute of Physics)

Table 6.1 Factors in polymer solution or electrospinning instrumentation that result in smaller fiber diameters

	Lower values lead to smaller fiber diameter	Higher values lead to smaller fiber diameter	Ambiguous/ unknown correlation	References
Viscosity	X			[160–174]
Concentration	X			[160–174]
Conductivity		X		[164–168, 171, 173]
Flow rate	X			[161, 162, 169, 175, 176]
Surface tension			X	[161, 162, 170, 174]
Voltage			X	[164, 168, 170, 173, 177]
Ambient temperature		X		[163, 178, 179]

peptide portion of the PA [76, 77, 81]. When the PAs are in this form, the amphiphile molecules are perpendicular to the nanofibers with the hydrophobic portion in the interior and the hydrophilic part on the surface. This is different from the natural collagen matrix, in which collagen molecules align parallel to each other [76, 79, 82].

Other self-assembly methods include divalent ion induced self-assembly (addition of Ca^{2+} ions to cause gelation of the solution) and drying on surfaces (simply allowing the pH 8 water solution to dry on a surface) [77–79, 81, 82]. While each of the self-assembly techniques successfully yields nanofibers that are consistently on the small end of the natural ECM scale, the complexity of the procedure and the low productivity of the method limit it as a large-scale tissue engineering option.

6.4.1.3

Phase Separation

Phase separation is a process that separates a polymer solution into a polymer-rich component and a solvent-rich component. Phase separation has been used to produce nanofibrous, 3D scaffolds whose macroporous architecture can be tailored to individual tissue types. This is achieved with use of a water-soluble porogen material (e.g. sugar, inorganic salt, paraffin spheres) that is fabricated into 3D negative replicas of the desired macroporous architectures. Next, a polymer solution is cast over the porogen assembly in a mold, and is thermally phase-separated to form nanofibrous matrices (Fig. 6.3d). The porogen material is then leached out with water to finally form the synthetic nanofibrous extracellular matrices with predesigned macroporous architectures. In this way, synthetic polymer matrices are created with architectural features at several levels, including the anatomical shape of the matrix, macroporous elements (100 μm to mm), interfiber distance (microns), and the diameter of the fibers (50–500 nm) [76, 78–80, 82]. This technique provides a significant amount of control in tailoring both the pore sizes and interconnectivity by altering the concentration, size, and geometry of the porogens [76, 78].

Unlike self-assembly, phase separation is a simple technique that does not require much specialized equipment. However, this method is limited to being effective with only a select number of polymers and is strictly a laboratory scale technique at this point [80].

6.4.1.4

Templating

Another method for achieving control of the hierarchical structure of the nanostructured surface is templating. This method entails synthesis of the desired material within the pores of a nano-porous membrane (Fig. 6.3e) [83]. Because the membranes contain cylindrical pores of uniform diameter, nanocylinders of the desired material are obtained in which the dimensions can be directed by the size of membrane pores [83]. Depending on the material and the chemistry of the pore wall, this cylinder may be solid (a nanofiber) or hollow (a nanotube). This “template” method has been used to prepare nondegradable polymers, metals, semiconductors, and other materials on a nanometer scale.

For tissue engineering applications, the creation of nano-engineered structures from biodegradable polymers enhances the potential success of the material after implantation. PCL nanofibers have been fabricated by the extrusion of a precursor solution through a template into a solidifying solvent under pressure utilizing custom instrumentation [84]. Template synthesis has also been used to form oriented nanowire and nanofiber arrays from biodegradable polymers without the use of organic solvents or pressure assistance [85]. This resulted in a fast and inexpensive method for creating biodegradable nanowires and fibers for tissue regeneration.

6.4.1.5

Drawing

Using drawing techniques, polymeric nanofibers are formed by drawing and solidifying a viscous liquid polymer solution through a glass micropipette. By controlling the drawing parameters, this method is able to form networks of suspended fibers having amorphous internal structure and uniform diameters from micrometers down to sub-50-nm for different molecular weights [80, 86]. Briefly, a micropipette is used to suspend polymer fibers on a substrate. The substrate is first raised until it comes into contact with the polymer droplet, and then the stage is moved along a predetermined trajectory with a constant speed while forming the solid polymer fiber by the evaporation of the solvent. The fiber is suspended by contacting the substrate with the pipette (Fig. 6.3f).

6.4.2

Nanotubes

Nanotubes are hollow cylinders that are nanometers in diameter and possess single or multiple walls (SWNT and MWNT, respectively). Nanotubes are typically made of one element,

normally carbon, and possess a broad range of electronic, thermal, and structural properties that change depending on the structure of nanotube (i.e. diameter, length, and chirality).

Since their discovery in 1991 by Iijima [87], carbon nanotubes (CNTs) have been exploited and evaluated for various applications. It has been of immense interest to apply these nanotubes to improve human health and disease treatment because of their attractive chemical, electrical, and mechanical properties. Currently, the majority of studies on CNT's biological applications revolve around the biosensor development in which the CNTs are integrated with biomolecules such as proteins, nucleic acids or carbohydrates and used as a sensor for ultrasensitive disease diagnosis [88, 89]. In addition, considerable efforts have been made to utilize CNTs as biocompatible carriers or biomaterials for tissue regeneration and in vivo gene and drug delivery. CNTs are one of the strongest materials ever reported [90], making it an attractive material for reinforcement of polymers for tissue engineering applications. Typically, reinforcement is achieved by incorporating nanotubes into polymers and hydrogels for use as composite scaffold in tissue engineering (Fig. 6.4a). Nanocomposites are composed of one or more nanoparticle components, where ultra-fine solid particles such as nanospheres or nanocrystals are dispersed into a micron or sub-micron sized mixture.

Carbon nanotubes are synthesized either with arc-discharge, laser ablation or most commonly chemical vapor deposition (CVD). Arc discharge is the classical synthesis method used by Iijima when CNTs were discovered. Arc-discharge and laser ablation are currently the principal methods for obtaining small quantities of high quality CNTs. However, the inherent design of these systems poses limitations to the large-scale production of CNTs. In addition, both methods result in highly tangled forms of CNTs, mixed with unwanted forms of carbon and/or metal species. The CNTs thus produced are difficult to purify, manipulate, and assemble for building nanotube-device architectures for practical applications [91].

6.4.2.1

Arc Discharge

The arc discharge method creates CNTs through arc-vaporization of two carbon rods placed end to end, separated by approximately 1 mm, in an enclosure that is usually filled with inert gas at low pressure. A direct current of 50–100 A, driven by a potential difference of approximately 20 V, creates a high temperature discharge between the two electrodes. The discharge vaporizes the surface of one of the carbon electrodes, and forms a small rod-shaped deposit on the other electrode. The resulting product is a complex mixture of components that requires further purification to separate the CNTs from the soot and the residual catalytic metals present in the crude product.

6.4.2.2

Laser Ablation

Nobel Laureate Robert Smalley synthesized CNTs using a dual-pulsed laser, achieving high yields of purity [92, 93]. Samples were prepared by laser vaporization of graphite rods with

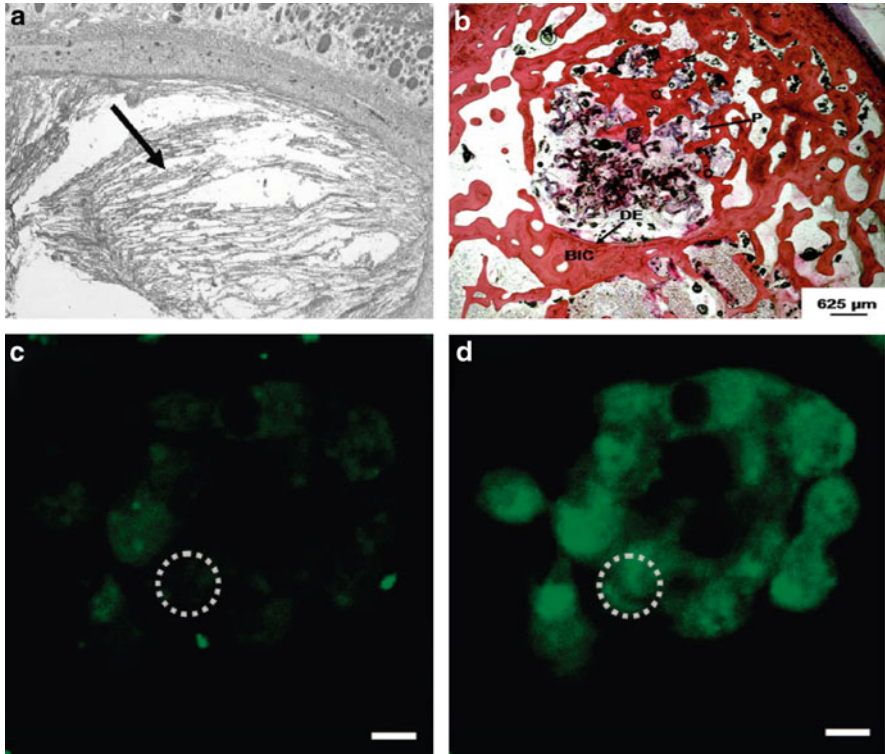


Fig. 6.4 (a) Light microscopic views of CNT-alginate composite after subcutaneous implantation (Reprinted from [98], © 2006 J-STAGE). (b), CNT-PFF scaffold after 12 weeks implantation in femoral condyle defect (Reprinted from [124], © 2008, with permission from Elsevier). (c) Confocal image of a neural stem cell clusters cultured on CNT substrate before start of stimulation and (d) during electrical stimulation. Increased calcium signaling (*green*) confirms the CNTs role in creating a neural network (Reprinted from [155], © 2009 American Chemical Society)

a 50:50 catalyst mixture of cobalt and nickel at 1,200°C in flowing argon, followed by heat treatment in a vacuum at 1,000°C to remove the C60 and other fullerenes. The initial laser vaporization pulse was followed by a second pulse, to vaporize the target more uniformly. The use of two successive laser pulses minimizes the amount of carbon deposited as soot. The second laser pulse breaks up the larger particles ablated by the first one, and feeds them into the growing nanotube structure. The material produced by this method appears as a mat of “ropes”, 10–20 nm in diameter and up to 100 μm or more in length. Each rope is found to consist primarily of a bundle of single walled nanotubes, aligned along a common axis. By varying the growth temperature, the catalyst composition, and other process parameters, the average nanotube diameter and size distribution can be varied.

6.4.2.3

Chemical Vapor Deposition

Chemical vapor deposition of hydrocarbons over a metal catalyst is a classical method that has been used to produce various carbon materials such as carbon fibers and filaments for over twenty years. Large amounts of CNTs can be formed by catalytic CVD. There are two steps to the CVD technique: catalyst preparation and the actual reaction. Metal catalysts can be prepared as a patterned substrate, resulting in mats of CNTs on a surface. Alternatively, decomposition of metallo-organic compounds can be performed within the reactor, without the use of a substrate, resulting in floating catalyst and subsequent synthesis. The actual CNT synthesis is initiated from nucleation sites in the catalysts with the introduction of a gaseous carbon feed stock, typically at temperatures between 500 and 1,000°C. Many parameters affect the outcome of the CVD synthesis, including catalyst material, gas, temperature, flow-rate and synthesis time. The versatility of the CVD technique further enables CNTs to be synthesized for a wide range of end-use applications, including patterned CNTs on substrates, which cannot be manufactured using the arc-discharge or laser ablation techniques.

6.4.3

Functionalized Nanomaterials

A common strategy in tissue engineering is surface functionalization, where the surface of a nanomaterial is chemically modified, adding functional groups that enhance the physical or biological performance of the material. CNTs are inherently hydrophobic when utilized in the “as-produced” form, a condition which must be overcome in order to suspend CNTs in water or ionic rich buffers. The most popular strategy for improving the solubility of CNTs is by surface coating the nanotubes with functional groups. Functionalization of carbon nanotubes is considered as an essential step to enable their manipulation and application in potential end-use products. Acid reflux of SWNT or MWNTs have been widely used to attach carboxyl groups to the surface of CNTs (e.g. SWNT-COOH) [94–96]. These carboxylated nanotubes can be further derivatized to covalently link the CNTs with other polymers (e.g. PEG), effectively increasing the CNT’s solubility and biocompatibility [94–96]. Alternatively, further functionalization of carboxylated nanotubes with biological molecules can be simply achieved using aqueous carbodiimide chemistry, yielding a versatile way to use CNTs for drug delivery and specifications in tissue engineering.

Many studies have examined the effects of surface functionalization of CNTs on cellular responses in 2D and 3D (e.g. [97–99]). Most recently, a study by Webster and colleagues developed an RGDSK (Arg-Gly-Asp-Ser-Lys) modified rosette nanotube (RNT) hydrogel composite for bone repair [100]. Results showed that the modified nanotube hydrogel caused around a 200% increase in osteoblast adhesion, mediated by increased fibronectin adsorption, compared to hydrogel controls. This supports the notion that both surface chemistry and biomimetic nanoscale properties contribute to the cell-favorable environment [100]. It has been suggested that the tubular shape of CNTs and differing chemical reactivity

of the ends versus the sidewalls can be used to conjugate two different functional groups in each location. This would represent a significant advantage of CNTs in drug delivery over spherical nanoparticles [101].

Electrospun synthetic fibers can also be functionalized either by post processing or by incorporating bioactive factors into the spinning solution, though both processes are generally more complex than functionalization of CNTs. In an effort to promote neuronal growth on nanofibers, Koh et al coupled laminin to PLLA nanofibers using blended electrospinning [102]. Using post-processing techniques, Park et al. treated electrospun nanofibers with oxygen plasma to graft acrylic acid (AA) onto the nanofibers [103]. The properties of the grafted fibers were significantly different from those of the unmodified nanofibrous scaffolds. Fibroblasts seeded on the scaffolds spread over a larger surface area on the AA-grafted surface as compared to the unmodified PGA, PLLA and PLGA nanofibrous scaffolds. Cultured for up to 6 days, the fibroblast proliferation was also found to be much better on the surface-modified nanofibrous scaffolds [103]. In another study, PCL nanofibers were coated with gelatin through layer-by-layer self-assembly, followed by functionalization with a uniform coating of bonelike calcium phosphate [104]. It was found that the incorporation of gelatin promoted nucleation and growth of calcium phosphate, promoting a bone-like extracellular environment. Pre-osteoblastic cells attached, spread, and proliferated significantly more on the mineralized scaffolds than on the pristine fibrous scaffolds after 7 days in culture.

Surface modification of natural polymers has also been explored. In a recent study, BMP-2 was immobilized directly on a chitosan nanofibrous membrane, providing a bioactive surface that can enhance bone-regeneration capacity [105]. The BMP-2-conjugated surface increased osteoblastic cell attachment in a dose-dependent manner. The surface modified chitosan membrane also significantly promoted cell proliferation, alkaline phosphatase activity, and calcium deposition when compared to BMP-2-adsorbed membrane. These findings indicate that the stable localization of BMP-2 on nanofibrous membranes is more osteoinductive than having the soluble growth factor present in the local microenvironment of the cells [105].

6.5 Interfacing Cells with Nanomaterials

Although the promise of tissue engineering is rapidly reaching reality, challenges remain, particularly in creating constructs that more closely replicate the complex architecture and distribution of native tissues. The cytotoxicity and long-term impact of nanomaterials on human health is an area of great interest as the use of nanomaterials in biomedical applications heightens.

A number of studies have been specifically interested in examining the biocompatibility of CNTs on cells. The majority of these studies examine the toxicological response of cells in 2D cultures (i.e. on plated cell lines or primary cells). One mechanism by which CNTs interact with cell is by acting as molecular transporters of proteins and other nutrients in and

out of cells (e.g. [106]). Nanotoxicology is a large field of research that examines the signaling pathways and mechanisms leading to toxic effects or interactions between cells and nanomaterials. A number of studies have explored this avenue of research with various cell types; the outcome of most of these studies have also been summarized in several review articles (e.g. [107–110]). Unfortunately, findings from the field of CNT-induced toxicology has been full of contradictions, with some studies indicating CNTs as highly toxic and others showing lack of any toxic effects. For example, treatment of the HEK 293 cells with SWNTs has been shown to result in reduction in cell viability that is time and dose dependent [111]. Studies using MWNTs on mouse embryonic stem cells (ESC) revealed that the CNTs can accumulate and induce apoptosis and activate tumor suppressor protein p53 within 2 h of exposure. Where as, experiments performed on the HL-60 cells revealed that SWNTs up to 25 $\mu\text{g}/\text{mL}$ have no effect on cell proliferation and viability if the cells are exposed to CNTs for a short time period such as 2 h [112]. Similarly, chondrocytes exposed to SWNTs for longer durations (up to 2 weeks) were able to maintain 80% viability in the presence of SWNTs at dose of 10 $\mu\text{g}/\text{ml}$ [113].

The discrepancy in the cytotoxicity/biocompatibility studies of CNTs are in part due to variable factors such as the size, solubility, surface functionalization, concentration and exposure time of CNTs used in these studies. Another potential reason for the varied responses may stem from the effects of oxidative stress on each cell type. Nanoparticles can create reactive forms of oxygen that can damage cells, and cells can defend themselves by producing anti-oxidants when they encounter low concentrations of nanoparticles [114]. However, each cell type's response to this oxidative damage may vary, providing a more cellular based mechanism for the variability in responses of cells to nanoparticle toxicity.

It is important to note that most 2D studies are rarely translatable to 3D systems. For example, several studies have explored the effects of nanosurfaces and nano-topographies on cell attachment in 2D. The outcomes of these studies also vary based on the type of nanomaterial and the type of cells examined. For example, in one study nano-sized carbon nanofibers were found to promote osteoblast (bone cell) adhesion, while fibroblasts (skin cells), chondrocytes (cartilage cells) and smooth muscle cells showed decreased adhesion [115]. These types of findings are relevant for the comparative analysis of different cells on a single type of material. However, for tissue engineering applications, these findings from 2D are limited in translation into 3D. Typically, optimization of dosages, culture durations and cellular responses in 2D provide a starting point for optimization of the response of cells in 3D. The presence of cell–matrix interaction in 3D causes cells to respond differently because the omnipresence of ECM around the cell alters the cells' morphology, adhesion, and metabolism. Consequently, there is a need for specific exploration and optimization of both the cytotoxic potential as well as growth conditions of cells on nanomaterial scaffolds, directly in the 3D environment and material of choice. The use of 3D nanomaterial networks for tissue engineering is a very novel approach and likely path toward success of replacement tissues. In the following sections, the use of nanomaterials in specific applications for bone, cartilage, and neural tissue engineering are addressed.

6.5.1

Bone Tissue Engineering

In order to assess how bone substitute materials determine bone formation *in vivo*, it is useful to understand the mechanisms of the material surface/tissue interaction on a cellular level. Artificial materials are used in two applications, as surface biomaterials (e.g. implant surface) or as porous scaffolds for osteoblasts in tissue engineering. Recently, many efforts have been undertaken to improve bone regeneration by the use of nano material surfaces. Surface properties as well as biophysical constraints at the biomaterial surface, are of major importance since these features will direct cell responses. Studies on osteoblast cell reactivity towards nanomaterials will have to focus on the different steps of protein and cell reactions towards defined surface properties at micro and nano scales.

Relying on natural materials inherent to bone, porous bone tissue engineering scaffolds have been fabricated using hydroxyapatite (HA), a major mineral component and essential ingredient of normal bone. Sintered scaffolds of nano-HA powder (20 nm average particle size) or micro-HA powder (10 μm average particle size) were created and cultured with osteoblasts. Greater cell numbers were found on nano-HA scaffolds compared with similarly processed micro-HA scaffolds 5 days after seeding, though cell attachment did not appear to be greater on the nano HA scaffolds [116]. Similarly, a highly porous nano-HA/chitosan composite scaffold was developed, where nano-HA particles were dispersed within a porous chitosan scaffolds [117]. Nano-HA particles were found to bind to the chitosan scaffolds very well, limiting the migration of nano-HA particles into the bordering regions of the surrounding tissues. This composite also showed better biocompatibility than pure chitosan scaffolds [117]. These results suggest that the nano-HA scaffolds may serve as a good 3D substrate for cell attachment and migration in bone tissue engineering.

Applications of synthetic nanomaterials for bone tissue engineering were initially carried out using electrospun nanofibers. In studies from Vacanti and colleagues, microporous, non-woven PCL nanofibers were electrospun into scaffolds and were seeded with marrow-derived mesenchymal stem cells (MSCs) from neonatal rats [118, 119]. The cell-polymer constructs were cultured with osteogenic supplements in a rotating bioreactor up to 4 weeks. Penetration of cells and abundant extracellular matrix were observed in the cell-polymer constructs after 1 week, and surfaces were covered with cell multilayers at 4 weeks. Results also indicate that significant matrix mineralization and collagen type I deposition was present throughout the construct after 4 weeks [119]. *In vivo* studies in rats with similar constructs showed that implantation of the nanofibrous PCL constructs after the 4-week *in vitro* conditioning protocol lead to successful growth of boney tissue in the omenta of rats [118]. After explantation, the constructs were found to be rigid and having a bone-like appearance. Multi-layers of osteoblasts, some osteocyte-like cells, and a woven bone-like appearance were observed throughout the constructs [118]. These studies established the ability to develop bone grafts on electrospun nanofibrous scaffolds *in vivo*, however the implantation of [95] these constructs in non-musculoskeletal (i.e. non-load-bearing) organs limits the extrapolation of these findings to potential success of constructs in a bone defect model.

While early success with nanofibers was seen for bone tissue engineering, a significant effort has been dedicated toward the use of nanotubes in boney tissue regeneration.

Developing biocompatible scaffold materials that can support the growth and proliferation of osteoblasts and thereby increment to replace boney tissues still remains a major challenge for biomedical engineers. Currently, most artificial bone scaffolds are relatively weaker than natural bone. CNTs have been utilized in various techniques for bone repair and tissue engineering, because of the inherent mechanical strength of CNTs [110].

In studies by Haddon and coworkers, the effects of CNTs were examined on bone formation and bone cell viability [96, 120]. Neutral CNTs (SWNTs and SWNTs functionalized with PEG) were found to support the greatest amount of cell viability after 5 days. SWNTs coated with carboxylic acid (COOH) or poly(aminobenzene sulfonic acid) (PABS) had a net surface charge, which resulted in less cell growth than neutral SWNTs. Interestingly, glass surfaces coated with SWNTs functionalized with phosphonates or with PABS were found to induce bone formation and mineralization. A film coating of SWNTs on a glass substrate resulted in HA nucleation and crystallization that was well-aligned, reaching up to 3 μm in thickness after 14 days of mineralization [96, 120]. In addition, it was found that the presence of CNTs in the scaffold improved cell adhesion, which is crucial for cell growth, proliferation, differentiation, and migration within the scaffold.

In a different approach, CNTs have been used in bone engineering to enhance the mechanical properties of some biomaterials that are currently used in bone regeneration. For example, polymethyl methacrylate (PMMA) is a common polymer material for bone cement and dental prostheses. It has been found that the properties of bone cement are improved by incorporating CNTs into the PMMA polymer [121]. The mechanical properties of the PMMA with MWNT (0–10%wt) was found to enhance the static and fatigue mechanical properties of the bone cement compared to polymer only controls. The authors also discovered that the augmentation of the bone cement with the nanotubes offers thermal benefits and improves the longevity of the implants [110, 121].

In several studies by Mikos and colleagues, SWNTs have also been incorporated into biodegradable polymers for their use in tissue engineering [122–124]. SWNTs and functionalized SWNTs (F-SWNTs) were combined with the polymer poly(propylene fumarate) (PPF) to examine the effect of the nanocomposite on rheological, electrical and mechanical properties of the polymer. Cross-linked nanocomposites with F-SWNTs were superior to those with unmodified SWNTs in terms of their mechanical properties. Nanocomposites with 0.1% wt F-SWNTs resulted in a three-fold increase in both compressive modulus and flexural modulus and a two-fold increase in both compressive offset yield strength and flexural strength when compared to pure PPF networks. In comparison, the addition of 0.1% wt unfunctionalized SWNTs resulted in only 37% mechanical reinforcement. These extraordinary mechanical enhancements indicated strong SWNT-polymer interactions and increased cross-linking densities, resulting in effective load transfer during mechanical testing [123]. In follow up studies, it was also shown that these reinforced porous biodegradable scaffolds are biocompatible up to 12 weeks post implantation in a rabbit femoral condyle (Fig. 6.4b) [122, 124]. The nanocomposite scaffolds exhibited favorable responses *in vivo*, where a greater amount of boney ingrowth was seen in nanocomposite scaffolds vs. control (polymer only) scaffolds. In addition, results suggest that nanocomposite scaffolds may play a role in activating osteogenesis *in vivo*. With the enhanced mechanical properties

and growth capabilities, these SWNT/polymer nanocomposites hold significant implications for the fabrication of bone tissue engineering scaffolds [122, 124].

The high surface to volume ratio of nanomaterials is hypothesized to affect the behavior of cells *in vivo*, where increased surface areas result in increased surface adhesion with the underlying substrate. However, other studies suggest that CNTs increase the surface roughness of composite materials, and may be responsible for the increase in the osteoblastic cell proliferation and differentiation [125, 126]. This increase in surface roughness is thought to result in higher adsorption of proteins like fibronectin on the composite surface, thus enhancing cellular adhesion [125, 126].

While the majority of nanotube bone studies employ SWNTs, implantation of MWNTs into mouse skull subperiosteum and tibial bones was also investigated. This study found that the MWNTs did not cause any major inflammatory reaction compared to graphite particles [127]. MWNTs did not inhibit bone repair during the 4-week period, and the nanotubes became integrated into the boney matrix. Interestingly, incorporation of BMP-2 with the MWNTs implanted into the bone was found to accelerate new bone formation [127]. This study highlights the inherent advantages of using CNTs in bone repair, where the nanotubes act as material for mechanical reinforcement, cellular stimulus, and potentially for drug delivery.

6.5.2

Articular Cartilage Tissue Engineering

One of the major limitations in cartilage tissue engineering has been the relatively weak mechanical properties of engineered scaffolds. Constructs with too weak of mechanical properties are likely to be crushed inside the joint post implantation. Many efforts in the use of nanomaterials for cartilage tissue engineering have focused on the improvement or reinforcement of mechanical properties of scaffolds for the successful implantation inside the joint. In a composite approach, nano-HA was utilized to reinforce poly(vinyl alcohol) gel (nano-HA/PVA gel) for use as articular cartilage repair biomaterial [128]. The results showed that both storage modulus and loss modulus were dependent on the content of the nano-HA, with peak values obtained for 6% nano-HA content. In another composite scaffold, nano-HA was incorporated into a polyamide (PA66) composite, yielding anisotropic properties both in morphology and mechanical behavior [129]. A novel thermally induced phase separation technique was used to generate these orientation-structured scaffolds for cartilage tissue engineering, with the aim of replicating the anisotropic structure and mechanical properties of native cartilage. The morphological study proved that the nanoHA/PA66 scaffolds exhibited directional architecture with high porosity (80–85%) and pore size ranging from 200 to 500 μm . In addition, increase in the nano-HA content yielded improvement in anisotropic morphology. The compressive mechanical properties were also found to be 50% greater in the longitudinal direction compared to the transverse direction, mimicking the mechanical relationship of anisotropic cartilage in compression [129].

In a recent study, the safety and regenerative potential of a nanocomposite scaffold was examined in an osteochondral defect model in sheep [130]. A multilayer gradient

nano-composite scaffold was created by nucleating collagen fibrils with nano HA particles. The scaffolds were implanted into the defect site either alone or after culturing with autologous chondrocytes *in vitro*. Histologic and gross evaluation of specimens showed good integration of the chondral surface, and good bone regeneration was seen in the scaffold containing groups relative to empty defect group. Neo formed hyaline cartilage was found in the scaffold filled defects, though no appreciable enhancement was seen in the cell-seeded group over the cell-free group. These results demonstrate that this nanocomposite scaffold was successful at inducing hyaline cartilage repair by recruiting local cells into the defect region and providing a substrate for successful growth and differentiation [130].

Chondrocytes cultured on electrospun PCL nanofibers have been shown to maintain their phenotype expressing cartilage-specific extracellular matrix genes, including collagen types II and IX, aggrecan, and cartilage oligomeric matrix protein [131, 132]. In addition to differentiated chondrocytes, MSCs have also been cultured on fibers because of their ability to differentiate into multiple cell lineages. Li and colleagues have shown that MSCs cultured on electrospun PCL fibers in the presence of TGF- β 1 differentiated to a chondrocytic phenotype, as indicated by chondrocyte-specific gene expression and protein synthesis [131, 132]. In addition, aligned fibers were also created to mimic the anisotropic morphology and biomechanics of cartilage in tension [133]. Highly oriented fibers (94% fiber alignment) were produced with a rotating target, yielding significantly higher tensile properties in fiber-aligned direction vs. the unaligned control. When seeded with cells, the fiber alignment was found to direct the cell orientation as well as the actin organization, yielding controlled anisotropy in the fibrous ultra structure and the cellular morphology [133].

Carbon nanotube hydrogel composites have been most widely used for the creation of engineered bone replacement. A study by Chahine and colleagues incorporated SWNTs into agarose hydrogels which were then cast with primary chondrocytes [134, 135]. Results indicate that SWNTs coated with carboxyl group (COOH) or PEG used in composite constructs allowed chondrocytes to maintain viability up to 28 days. In addition, matrix production of proteoglycans and collagen increased in cells cultured in CNT containing constructs vs. control. Expression of tumor protein 53 (p53) for potential carcinogenesis revealed no significant changes due to presence of SWNT up to 28 days in culture [136]. It is hypothesized that nano-composite hydrogels more closely resemble the morphology (size and organization) of the endogenous extracellular matrix than control hydrogels, which is critical for defining the cell–matrix interaction in a successful tissue regeneration process.

6.5.3

Fibrocartilaginous Tissues (Meniscus and Intervertebral Disc)

Fibrocartilaginous tissues are also load-bearing and pose the same level of complexity in engineering a tissue replacement as bone and cartilage, particular when considering the complex geometry and ultrastructure of the meniscus. In a study by Mauck and colleagues, biodegradable nanofibrous scaffolds were used for growth of meniscal fibrochondrocytes or MSCs [137]. Aligned and unaligned scaffolds were examined, yielding comparable amounts of matrix protein. Interestingly though, a significantly larger increase in mechanical properties was observed for the aligned scaffolds. MSC also yielded greater

amounts of matrix proteins and demonstrated comparable increases in mechanical properties, thereby confirming the utility of MSCs for meniscus tissue engineering [137]. When similar constructs were seeded with human meniscal fibroblasts, increases in biochemical content and mechanical properties were observed. In scaffolds seeded with particularly robust cells, construct tensile moduli approached maxima of ~ 40 MPa over the 10-week culture period, reaching values comparable to native healthy human meniscus [138].

Intervertebral disc (IVD) is also a fibrocartilagenous tissue, providing cushioning and support in the spine. The IVD is composed of three distinctive anatomical and functional structures, the nucleus pulposus (NP), annulus fibrosus (AF), and the vertebral end-plates (EP). Both the NP and EP tissues are rich in proteoglycans (PG), with EP closely resembling articular cartilage. The AF has high collagen content and its radially oriented fibers resemble other fibrocartilagenous tissues such as the meniscus. In an anatomically mimetic approach, a recent study developed a biphasic composite from an electrospun, biodegradable nanofibrous scaffold enveloping a hyaluronic acid hydrogel center [139]. These constructs architecturally resemble a native IVD, with an outer AF-like region and inner NP-like region. The constructs were seeded with MSCs and cultured up to 28 days in the presence of TGF- β . This study serves as a proof-of-concept that anatomically shaped IVD tissue constructs can be created from nanomaterial scaffolds for potential use in disc replacement.

Current approaches for tissue engineering of IVD have focused on the creation of a replacement tissue of a singular tissue type. In a recent study, a novel strategy for AF tissue engineering that replicates the natural hierarchy with anisotropic nanofibrous laminates was developed [140]. Bi-lamellar tissue constructs were formed first as single lamellar tissues from aligned nanofibrous scaffolds seeded with MSCs, then coupled into bilayers after 2 weeks of *in vitro* culture. The bilayers were oriented either in parallel or opposing fiber alignment relative to the long axis of the scaffold. After 10 weeks in culture, results indicate that these scaffolds directed the deposition of an organized, collagen-rich extracellular matrix that mimicked the angle-ply, multi-lamellar architecture of native AF. In addition, the engineered tissue achieved mechanical properties comparable to the native tissue. Interestingly, using these novel constructs, new mechanisms of tensile reinforcement were identified [140].

The effect of surface charge has been explored in stimulating cell synthesis. Cervical spine human AF cells have been seeded onto a nanofiber surface of randomly oriented electrospun polyamide nanofibers with a neutral or positive charge [141]. Results indicate that cells on the charged nanofiber surface deposited greater amounts of chondroitin sulfate than of type II collagen, compared to cells grown on a neutral surface. Cell proliferation did not differ among treatment groups, suggesting that the positive charge significantly increased total proteoglycan production. These findings point to the need for systematic scaling up of tissue regeneration efforts by adding levels of complexity in trying to replicate the native IVD [141].

6.5.4

Tendon/Ligament Tissue Engineering

Ligaments are fibrous bands or sheets of connective tissue, comprised of attenuated collagenous fibers, linking two or more bones. Ligaments are composed of densely packed

collagen fibers, thus native ligaments lend themselves well for tissue engineering applications with nanomaterials, especially nanofibers.

Lee et al. used a rotating cylindrical target to align electrospun polyurethane nanofibers for ligament tissue engineering. When cultured with human ligament fibroblasts, the cells became spindle-shaped and oriented in the direction of the nanofibers. In addition, significantly more collagen was synthesized on aligned nanofiber sheets compared to randomly oriented fibers. When mechanical strain was applied to the scaffolds, fibroblasts were found to be more sensitive to strain in the longitudinal direction than in transverse direction [142]. Similarly, Dalton et al. used yarns produced by the collection of nanofibers between dual rings as potential scaffolds for tissue engineering of tendons and muscles [143].

Lu and colleagues have designed a PLGA nanofiber-based scaffold for rotator cuff tendon tissue engineering, aiming to improve the attachment, alignment, gene expression, and matrix elaboration of human rotator cuff fibroblasts [144]. It was observed that rotator cuff fibroblasts cultured on the aligned scaffolds attached along the nanofiber long axis, and this was associated with a distinct integrin expression profile. In addition, physiologically relevant mechanical properties were attained for the aligned nanofiber scaffolds, compared to the unaligned [144].

In another composite effort, a tissue regeneration membrane was created by electrospinning a suspension consisting of PLLA, MWNTs and hydroxyapatite [145]. MWNTs/HA nanoparticles were uniformly dispersed in the membranes, and were found to enhance the adhesion and proliferation of periodontal ligament cells by 30%. Additionally, the membrane was found to inhibit the adhesion and proliferation of gingival epithelial cells by 30%, compared with the control group. In vivo, this new type of membrane shows excellent dual biological functions when implanted in murine muscles [145].

Knitted scaffolds have been proven to favor deposition of collagenous connective tissue matrix, which is crucial for tendon/ligament reconstruction. But cell seeding of such scaffolds often requires a gel system, which is unstable in a dynamic situation, especially in the knee joint. A study by Sahoo et al. developed a novel, biodegradable nano-microfibrous polymer scaffold by electrospinning PLGA nanofibers onto a knitted PLGA scaffold in order to provide a large biomimetic surface for cell attachment [146]. Porcine bone marrow stromal cells were incorporated by either pipetting a cell suspension directly on scaffold surface (direct), or by pipetting cells suspended in fibrin gel (immobilized). The increased surface for cell attachment when using direct suspension resulted in improved cell seeding and promoted cell proliferation, function, and differentiation over the immobilized cell technique [146]. This technique increased the surface area and reduced the pore size of the knitted scaffold, thereby eliminating the need of cell delivery by fibrin gel.

Collagen, a prominent biopolymer, is used extensively for tissue engineering applications, because its signature biological and physico-chemical properties are retained in *in vitro* preparations. While electrospinning of collagen nanofibers appears to be the most faithful biomimetic approach for tissue engineering of ligaments and tendons, recent studies have suggested that the properties of collagen as a leading natural biomaterial are lost when it is electro-spun into nanofibers out of fluoroalcohol solvents [147]. The resultant nano-scaffolds appear to lack the unique ultra-structural axial periodicity that confirms proper triple-helical structure of collagen. They were also characterized by low denaturation temperatures, similar to those obtained from gelatin preparations. This study concluded

that electrospinning of collagen out of fluoroalcohols solvents appears to defeat its purpose, namely to create biomimetic scaffolds emulating the collagen structure and function of the extracellular matrix [147].

Silk, another naturally occurring polymer, has been used clinically as sutures for centuries. Silk is composed of a filament core protein, termed fibroin, and a glue-like coating consisting of sericin proteins. In recent years, silk fibroin has been increasingly studied for new biomedical applications due to the biocompatibility, slow degradability and remarkable mechanical properties of the material [148]. Silk fibroin has been shown to support stem cell adhesion, proliferation, and differentiation *in vitro* and promote tissue repair *in vivo*. Nanofibrous silk based scaffolds can be prepared by electrospinning silk fibroin solution. Studies have shown that non-woven silk fibroin nanofibrous mats support the attachment, spreading and proliferation of human bone marrow stromal cells and fibroblasts *in vitro* [149]. Moreover, the *in vivo* biocompatibility of silk fibroin non-woven nanofiber membranes/nets was examined in repair of critical-sized calvarial bone defects in a rabbit model. The membranes were able to enhance bone formation over 12 weeks with no evidence of inflammatory reactions, further expanding the versatility of silk fibroins in micro and nano fiber based tissue engineering of soft and hard connective tissues [150].

6.5.5

Neural and Muscular Tissue Engineering

The requirements for neural and muscular tissue engineering are significantly different than that of connective tissues, including bone. Electronically capable materials, such as CNTs, have played an important role in neural tissue engineering. While nanofibrous scaffolds have been used for creation of conduits for neural growth or as substrates for muscular growth, a significant effort has focused on the effect of electronically conductive CNTs on cellular growth, differentiation and electrical excitability.

CNTs are attractive for use in fiber-reinforced composite materials due to their very high aspect ratio and mechanical properties. However for muscle regeneration, the electrical properties of CNTs can also be utilized for growth and stimulation of excitable tissues. Stegemann and colleagues created a composite comprising type-I collagen embedded with SWNTs that were seeded with smooth muscle cells [151]. Cell viability in all constructs was consistently above 85% after 3 and 7 days in culture. In a follow up study, SWNT-collagen composites were examined for their electrical properties [152]. Electrical conductivity of the constructs varied from 3 to 7 mS/cm, and increased in a SWNT dose dependent manner. These findings demonstrate that the electrical conductivity of cell-seeded collagen gels can be increased through the incorporation of carbon nanotubes. Protein-SWNT composite materials may have important application in tissue engineering, as well as substrates to study electrical stimulation of cells, and as transducers for biosensors [152].

Nanotubes grown in an array can be used to form neural networks when cells are cultured on top. Rat cortical tissue was cultured on a nanopatterned substrate containing carbon nanotubes. Neuronal cells became self-organized into networks with the island of CNTs. These CNT and cell interactions created an ordered and compact wired network.

Scanning electron microscopy of neuronal networks on CNT templates clearly reveal preferential adhesion of neurons and glia cells to the CNT-coated regions. In addition, the geometry of the ordered networks was dictated by the arrangement of the CNT islands [153]. In a separate study, neurons grown on CNTs were shown to have higher frequency of spontaneous postsynaptic currents, with no observable change in other electrophysiological characteristics [154]. This difference was attributed to the electrical conductivity of the substrate. Thus, CNTs can be used as structural support and as an electrically excitable substrate for neural applications. A more elegant approach was recently presented for integration of CNTs networks with neurons for implantation. A layer-by-layer composite was assembled from SWNTs and laminin, which is an essential part of ECM [155]. Laminin-SWNT thin films were found to be conducive to neuronal differentiation and suitable for their successful excitation. Extensive formation of a functional neural network was evident as indicated by the presence of synaptic connections and action potential propagation through the SWNT substrate (Fig. 6.4c, d). These results indicate that the protein-SWNT composite can serve as a material foundation of neural electrodes with chemical structure better adapted with long-term integration with the neural tissue [155].

From a biological perspective, CNTs have been shown to influence the cellular response (i.e. proliferation and metabolic activity) of various cell types grown with CNTs. However a recent study has revealed that a 2D thin film scaffold composed of biocompatible polymer grafted CNTs can selectively differentiate human embryonic stem cells into neuron cells while maintaining excellent cell viability. The surface analysis and cell adhesion studies suggested that CNT-based surfaces can enhance protein adsorption and cell attachment. This finding indicates that CNT-based materials are candidates for embryonic stem cell neural differentiation [156].

6.6 Future Directions

While nanomaterial based scaffolds show promise for creating biocompatible, cell based, mechanically viable scaffolds and tissue replacements, limitations exist for advancing this technology from the lab bench to more clinically relevant conditions.

One of the hallmark features of a biologically based replacement strategy is the potential for the engineered tissue to self-maintain in long term implantation through balanced metabolism. However, the incorporation of cells into nano scaffolds is limited mostly by the dense structure of the tissue. Recent efforts have examined ways to improve cell infiltration. Cells can be electrosprayed into the electrospinning polymer to enhance cell encapsulation and infiltration into the materials. Wagner and colleagues electrosprayed vascular smooth muscle cells (SMCs) concurrently with electrospinning PEUU [157]. This process increased cell seeding by 30%, did not diminish cell viability, and the SMCs spread and proliferated similar to control unprocessed cells. Using another novel method, a coaxial needle arrangement was used to drive a concentrated living cell suspension through the inner needle along with a medical-grade PDMS through the outer needle [158]. Using this technique, conditions under which the finest cell-containing microthreads have been

formed. These electrospun cell-fiber composite were cultured and found to be viable with no evidence of having incurred cellular damage during the nanofabrication process. Alternatively, it is possible to improve cell infiltration by increasing the pore size of the nanofibrous scaffold. Baker et al. co-electrospun PEO (a water-soluble polymer) with PCL nanofibers to form composite fiber-aligned scaffolds [159]. The selective removal of sacrificial PEO fibers resulted in increased porosity and improved infiltration of MSCs after 3 weeks in culture. These findings indicate that cell infiltration can be expedited in dense fibrous assemblies with the removal of sacrificial fibers, while maintaining alignment of the primary (PCL) nanofibers for continuous mechanical support [159].

While much scientific effort has been dedicated to examining the role of a single parameter on cellular responses (e.g. fiber diameter, surface coatings, alignment etc), the current body of scientific investigations are in need of systemic approaches to examining how changes in multiple parameters affect cellular behavior. Interactions among multiple parameters (e.g. pore size, alignment, effect of pre-condition in bioreactors etc) will help optimize conditions for achieving tissue-specific conditions. Moreover, incorporation of the biological complexity seen in native tissues is vital for the success of nanomaterials in vivo. For example, while many studies have focused on optimizing nanomaterial conditions for osteoblast growth, few studies have examined the effect of 3D nanomaterials on osteoclast and osteocyte behavior, two major cellular components of bone. In order for a nanomaterials based approach to succeed in bone replacement, the interaction of and between all 3 boney cell types must be examined and optimized prior to in vivo implantation.

Examination of interacting factors can also assist in elucidating mechanisms by which cells and scaffolds interact. For example, several studies have indicated that engineered constructs with comparable protein content can possess differing mechanical properties. This difference is inherently due to cell-induced changes in the ultra-structure of the nano-scaffolds. Some studies have indicated that cellular attachment and protein synthesis results in reinforcement of the nano scaffold in a fiber orientation dependent manner. These mechanisms are vital for tissue engineering and for understanding the behavior and organization of healthy native tissues. Consequently, the use of nanomaterials in building up replacement tissues can provide a step-by-step approach at recapitulating the complexity of native connective tissue, while examining how the addition of each step influences the mechanical or biological behavior of the entire composite.

Biocompatibility and cytotoxicity of nanomaterials is an area of great importance for tissue replacement strategy. Due to their size, nanoparticles are more easily taken up by the human body and can cross biological membranes, cells, tissues and organs more efficiently than larger microparticles. Once in the blood stream, nanomaterials can be transported around the body and can be taken up by organs and tissues including the brain, heart, liver, kidneys, spleen, bone marrow and nervous system. Consequently, the impact of implanting nanomaterials based scaffolds in the human body requires very complex analysis of particulate matter collecting in the various organs. While nanomaterial based medical devices or scaffolds require FDA review and approval, a number of nanomaterial consumer products have been released to market without explicit review of their nanotechnology impact on health outcomes. Currently, the FDA treats nanomaterials no differently than bulk material composed of the same ingredient. Several FDA regulated products employ nanotechnology, such as cosmetics and sunscreens, where nanoparticles are used to increase

the stability or modify the release of active ingredients. The interest in incorporating nanomaterials in drug, medical, food, and cosmetic industries has forged the effort for creation of the U.S. Nanotechnology Task Force. This task force is charged with determining regulatory approaches that encourage the continued development of innovative, safe, and effective FDA-regulated products that use nanotechnology materials. Future guidelines by this and other governmental agencies will shed light on the future implications of nanomaterial production and use in products for human consumption, including tissue engineered scaffolds.

Acknowledgements The author's acknowledge the support of funding from the National Science Council (NSC) 97-2221-E002-214 (PGC), 98-2221-E-002-158 (PGC), National Taiwan University 98R0702 (PGC), Department of Neurosurgery (NOC) and Feinstein Institute for Medical Research (NOC) at North Shore LIJ Health system.

References

1. Hadjiargyrou M and Chiu JB, Enhanced composite electrospun nanofiber scaffolds for use in drug delivery. *Expert Opin Drug Deliv* 2008; 5(10): p. 1093–106.
2. Scadden D, The stem-cell niche as an entity of action. *Nat Mater* 2006; 441(7097): p. 1075–9.
3. Matsuda M, Fung YC, and Sobin SS, Collagen and elastin fibers in human pulmonary alveolar mouths and ducts. *J Appl Physiol* 1987; 63(3): p. 1185–94.
4. Meek KM and Boote C, The organization of collagen in the corneal stroma. *Exp Eye Res* 2004; 78(3): p. 503–12.
5. Christiansen DL, Huang EK, and Silver FH, Assembly of type I collagen: fusion of fibril subunits and the influence of fibril diameter on mechanical properties. *Matrix Biol* 2000; 19(5): p. 409–20.
6. Hsu YM, Chen CN, Chiu JJ, Chang SH, and Wang YJ, The effects of fiber size on MG63 cells cultured with collagen based matrices. *J Biomed Mater Res B Appl Biomater* 2009; 91(2): p. 737–45.
7. Feynman R, There's Plenty of Room at the Bottom. 1959. California Institute of Technology, Engineering and Sciences. Feb 1960. <http://pr.caltech.edu/periodicals/EandS/>.
8. Yan L, Huck W, and Whitesides GM, Self-assembled monolayers (SAMS) and synthesis of planar micro- and nanostructures. *J Macromol Sci Polym Rev* 2004; C44(2): p. 175–206.
9. Xia Y, Whitesides G, Soft lithography. *Angew Chem Int Ed Engl* 1998; 37(5): p. 550–75.
10. Chen CS, Mrksich M, Huang S, Whitesides GM, and Ingber DE, Micropatterned surfaces for control of cell shape, position, and function. *Biotechnol Prog* 1998; 14(3): p. 356–63.
11. Shen K, Thomas VK, Dustin ML, and Kam LC, Micropatterning of costimulatory ligands enhances CD4+ T cell function. *Proc Natl Acad Sci USA* 2008; 105(22): p. 7791–6.
12. Takayama S, Ostuni E, LeDuc P, Naruse K, Ingber DE, and Whitesides GM, Laminar flows: subcellular positioning of small molecules. *Nat Mater* 2001; 411(6841): p. 1016.
13. Harrison RG, On the stereotropism of embryonic cells. *Science* 1911; 34(870): p. 279–81.
14. Weiss P, In vitro experiments on the factors determining the course of the outgrowing nerve fiber. *J Exp Zool* 1934; 68(3): p. 393–448.
15. Curtis ASG, Gadegaard N, Dalby MJ, Riehle MO, Wilkinson CDW, and Aitchison G, Cells react to nanoscale order and symmetry in their surroundings. *IEEE Trans Nanobioscience* 2004; 3(1): p. 61–5.

16. Chan CE and Odde DJ, Traction dynamics of filopodia on compliant substrates. *Science* 2008; 322(5908): p. 1687–91.
17. Dalby MJ, Riehle MO, Johnstone HJ, Affrossman S, and Curtis AS, Polymer-demixed nanotopography: control of fibroblast spreading and proliferation. *Tissue Eng* 2002; 8(6): p. 1099–108.
18. Dalton BA, Walboomers XF, Dziegielewski M, Evans MD, Taylor S, Jansen JA, and Steele JG, Modulation of epithelial tissue and cell migration by microgrooves. *J Biomed Mater Res* 2001; 56(2): p. 195–207.
19. Teixeira AI, Abrams GA, Bertics PJ, Murphy CJ, and Nealey PF, Epithelial contact guidance on well-defined micro- and nanostructured substrates. *J Cell Sci* 2003; 116(Pt 10): p. 1881–92.
20. Rajniecek AM, Foubister LE, and McCaig CD, Alignment of corneal and lens epithelial cells by co-operative effects of substratum topography and DC electric fields. *Biomaterials* 2008; 29(13): p. 2082–95.
21. Oakley C and Brunette DM, The sequence of alignment of microtubules, focal contacts and actin filaments in fibroblasts spreading on smooth and grooved titanium substrata. *J Cell Sci* 1993; 106(Pt 1): p. 343–54.
22. Oakley C, Jaeger N, and Brunette DM, Sensitivity of fibroblasts and their cytoskeletons to substratum topographies: topographic guidance and topographic compensation by micromachined grooves of different dimensions. *Exp Cell Res* 1997; 234(2): p. 413–24.
23. Rajniecek A and McCaig C, Guidance of CNS growth cones by substratum grooves and ridges: effects of inhibitors of the cytoskeleton, calcium channels and signal transduction pathways. *J Cell Sci* 1997; 110(Pt23): p. 2915–24.
24. Wojciak-Stothard B, Curtis AS, Monaghan W, McGrath M, Sommer I, and Wilkinson CD, Role of the cytoskeleton in the reaction of fibroblasts to multiple grooved substrata. *Cell Motil Cytoskeleton* 1995; 31(2): p. 147–58.
25. Houtchens GR, Foster MD, Desai TA, Morgan EF, and Wong JY, Combined effects of microtopography and cyclic strain on vascular smooth muscle cell orientation. *J Biomech* 2008; 41(4): p. 762–9.
26. Lee EJ, Hwang CM, Baek DH, and Lee SH, Fabrication of microfluidic system for the assessment of cell migration on 3D micropatterned substrates. *Conf Proc IEEE Eng Med Biol Soc* 2009; 1: p. 6034–7.
27. Tzvetkova-Chevolleau T, Stephanou A, Fuard D, Ohayon J, Schiavone P, and Tracqui P, The motility of normal and cancer cells in response to the combined influence of the substrate rigidity and anisotropic microstructure. *Biomaterials* 2008; 29(10): p. 1541–51.
28. Rajniecek AM, Foubister L, and McCaig CD, Prioritising guidance cues: Directional migration induced by substratum contours and electrical gradients is controlled by a rho/cdc42 switch. *Dev Biol* 2007; 312(1): p. 448–60.
29. Au HHT, Cui B, Chu ZE, Veres T, and Radisic M, Cell culture chips for simultaneous application of topographical and electrical cues enhance phenotype of cardiomyocytes. *Lab Chip* 2009; 9(4): p. 564–75.
30. Britland S, Morgan H, Wojciak-Stodart B, Riehle M, Curtis A, and Wilkinson C, Synergistic and hierarchical adhesive and topographic guidance of BHK cells. *Exp Cell Res* 1996; 228(2): p. 313–25.
31. Charest JL, Eliason MT, Garcia AJ, and King WP, Combined microscale mechanical topography and chemical patterns on polymer cell culture substrates. *Biomaterials* 2006; 27(11): p. 2487–94.
32. Maheshwari G, Brown G, Lauffenburger DA, Wells A, and Griffith LG, Cell adhesion and motility depend on nanoscale RGD clustering. *J Cell Sci* 2000; 113(Pt 10): p. 1677–86.
33. Benoit DS and Anseth KS, The effect on osteoblast function of colocalized RGD and PHSRN epitopes on PEG surfaces. *Biomaterials* 2005; 26(25): p. 5209–20.

34. Balasundaram G and Webster TJ, Nanotechnology and biomaterials for orthopedic medical applications. *Nanomedicine* 2006; 1(2): p. 169–76.
35. Lu J, Rao MP, Macdonald NC, Khang D, and Webster TJ, Improved endothelial cell adhesion and proliferation on patterned titanium surfaces with rationally designed, micrometer to nanometer features. *Acta Biomater* 2008; 4(1): p. 192–201.
36. Karuri NW, Liliensiek S, Teixeira AI, Abrams G, Campbell S, Nealey PF, and Murphy CJ, Biological length scale topography enhances cell-substratum adhesion of human corneal epithelial cells. *J Cell Sci* 2004; 117(Pt 15): p. 3153–64.
37. Curtis AS, Casey B, Gallagher JO, Pasqui D, Wood MA, and Wilkinson CD, Substratum nanotopography and the adhesion of biological cells. Are symmetry or regularity of nanotopography important? *Biophys Chem* 2001; 94(3): p. 275–83.
38. Rajniecek A, Britland S, and McCaig C, Contact guidance of CNS neurites on grooved quartz: influence of groove dimensions, neuronal age and cell type. *J Cell Sci* 1997; 110(Pt 23): p. 2905–13.
39. Teixeira AI, McKie GA, Foley JD, Bertics PJ, Nealey PF, and Murphy CJ, The effect of environmental factors on the response of human corneal epithelial cells to nanoscale substrate topography. *Biomaterials* 2006; 27(21): p. 3945–54.
40. Loesberg WA, te Riet J, van Delft FCMJM, Schon P, Figdor CG, Speller S, et al., The threshold at which substrate nanogroove dimensions may influence fibroblast alignment and adhesion. *Biomaterials* 2007; 28(27): p. 3944–51.
41. Kim DH, Han K, Gupta K, Kwon KW, Suh KY, and Levchenko A, Mechanosensitivity of fibroblast cell shape and movement to anisotropic substratum topography gradients. *Biomaterials* 2009; 30(29): p. 5433–44.
42. Yim EK, Reano RM, Pang SW, Yee AF, Chen CS, and Leong KW, Nanopattern-induced changes in morphology and motility of smooth muscle cells. *Biomaterials* 2005; 26(26): p. 5405–13.
43. Pouthas F, Girard P, Lecaudey V, Ly TB, Gilmour D, Boulin C, Pepperkok R, and Reynaud EG, In migrating cells, the Golgi complex and the position of the centrosome depend on geometrical constraints of the substratum. *J Cell Sci* 2008; 121(Pt 14): p. 2406–14.
44. Assoian RK and Zhu X, Cell anchorage and the cytoskeleton as partners in growth factor dependent cell cycle progression. *Curr Opin Cell Biol* 1997; 9(1): p. 93–8.
45. Chen CS, Mrksich M, Huang S, Whitesides GM, and Ingber DE, Geometric control of cell life and death. *Science* 1997; 276(5317): p. 1425–8.
46. Nelson CM, Jean RP, Tan JL, Liu WF, Sniadecki NJ, Spector AA, and Chen CS, Emergent patterns of growth controlled by multicellular form and mechanics. *Proc Natl Acad Sci USA* 2005; 102(33): p. 11594–9.
47. Gerecht S, Bettinger CJ, Zhang Z, Borenstein JT, Vunjak-Novakovic G, and Langer R, The effect of actin disrupting agents on contact guidance of human embryonic stem cells. *Biomaterials* 2007; 28(28): p. 4068–77.
48. Rebollar E, Frischauf I, Olbrich M, Peterbauer T, Hering S, Preiner J, Hinterdorfer P, Romanin C, and Heitz J, Proliferation of aligned mammalian cells on laser-nanostructured polystyrene. *Biomaterials* 2008; 29(12): p. 1796–806.
49. Popat KC, Eltgroth M, Latempa TJ, Grimes CA, and Desai TA, Decreased *Staphylococcus* epidermis adhesion and increased osteoblast functionality on antibiotic-loaded titania nanotubes. *Biomaterials* 2007; 28(32): p. 4880–8.
50. Popat KC, Leoni L, Grimes CA, and Desai TA, Influence of engineered titania nanotubular surfaces on bone cells. *Biomaterials* 2007; 28(21): p. 3188–97.
51. Chowdhury F, Na S, Li D, Poh YC, Tanaka TS, Wang F, and Wang N, Material properties of the cell dictate stress-induced spreading and differentiation in embryonic stem cells. *Nat Mater* 2009; 9(1): p. 82–8.

52. Engler AJ, Sen S, Sweeney HL, and Discher DE, Matrix elasticity directs stem cell lineage specification. *Cell* 2006; 126(4): p. 677–89.
53. McBeath R, Pirone DM, Nelson CM, Bhadriraju K, and Chen CS, Cell shape, cytoskeletal tension, and RhoA regulate stem cell lineage commitment. *Dev Cell* 2004; 6(4): p. 483–95.
54. Chou L, Firth JD, Uitto VJ, and Brunette DM, Substratum surface topography alters cell shape and regulates fibronectin mRNA level, mRNA stability, secretion and assembly in human fibroblasts. *J Cell Sci* 1995; 108 (4): p. 1563–73.
55. Groessner-Schreiber B and Tuan RS, Enhanced extracellular matrix production and mineralization by osteoblasts cultured on titanium surfaces in vitro. *J Cell Sci* 1992; 101(Pt 1): p. 209–17.
56. Biggs MJ, Richards RG, Gadegaard N, McMurray RJ, Affrossman S, Wilkinson CD, Oreffo RO, and Dalby MJ, Interactions with nanoscale topography: adhesion quantification and signal transduction in cells of osteogenic and multipotent lineage. *J Biomed Mater Res A* 2009; 91(1): p. 195–208.
57. Oh S, Brammer KS, Li YS, Teng D, Engler AJ, Chien S, and Jin S, Stem cell fate dictated solely by altered nanotube dimension. *Proc Natl Acad Sci USA* 2009; 106(7): p. 2130–5.
58. Dalby MJ, Gadegaard N, Tare R, Andar A, Riehle MO, Herzyk P, et al., The control of human mesenchymal cell differentiation using nanoscale symmetry and disorder. *Nat Mater* 2007; 6(12): p. 997–1003.
59. Kim DH, Lipke EA, Kim P, Cheong R, Thompson S, Delannoy M, Suh KY, Tung L, and Levchenko A, Nanoscale cues regulate the structure and function of macroscopic cardiac tissue constructs. *Proc Natl Acad Sci USA* 2010; 107(2): p. 565–70.
60. Cimetta E, Pizzato S, Bollini S, Serena E, De Coppi P, and Elvassore N, Production of arrays of cardiac and skeletal muscle myofibers by micropatterning techniques on a soft substrate. *Biomed Microdevices* 2009; 11(2): p. 389–400.
61. Khademhosseini A, Eng G, Yeh J, Kucharczyk PA, Langer R, Vunjak-Novakovic G, and Radisic M, Microfluidic patterning for fabrication of contractile cardiac organoids. *Biomed Microdevices* 2007; 9(2): p. 149–57.
62. Gomez N, Lee JY, Nickels JD, and Schmidt CE, Micropatterned polypyrrole: a combination of electrical and topographical characteristics for the stimulation of cells. *Adv Funct Mater* 2007; 17(10): p. 1645–53.
63. Yim EKF, Pang S, and Leong KW, Synthetic nanostructures inducing differentiation of human mesenchymal stem cells into neuronal lineage. *Exp Cell Res* 2007; 313(9): p. 1820–9.
64. Hohman M, Shin M, Rutledge G, and Brenner M, Electrospinning and electrically forced jets: I. Stability theory. *Phys Fluids* 2001; 13: p. 2201–20.
65. Hohman M, Shin M, Rutledge G, and Brenner M, Electrospinning and electrically forced jets: II. Applications. *Phys Fluids* 2001; 13: p. 2221–36.
66. Reneker D, Yarin A, Fong H, and Koombhongse S, Bending instability of electrically charged liquid jets of polymer solutions in electrospinning. *J Appl Phys* 2000; 87: p. 4531–47.
67. Yarin AL, Koombhongse S, Reneker DH, Bending instability in electrospinning of nanofibers. *J Appl Phys* 2001; 89: p. 3018–26.
68. Kumbhar SG, James R, Nukavarapu SP, and Laurencin CT, Electrospun nanofiber scaffolds: engineering soft tissues. *Biomed Mater* 2008; 3(3): p. 034002.
69. Burger C, Hsiao BS, and Chu B, Nanofibrous materials and their applications. *Annu Rev Mater Res* 2006; 36: p. 333–68.
70. Chew SY, Wen Y, Dzenis Y, and Leong KW, The role of electrospinning in the emerging field of nanomedicine. *Curr Pharm Des* 2006; 12(36): p. 4751–70.
71. Liao S, Li B, Ma Z, Wei H, Chan C, and Ramakrishna S, Biomimetic electrospun nanofibers for tissue regeneration. *Biomed Mater* 2006; 1(3): p. R45–53.
72. Katti DS, Robinson KW, Ko FK, and Laurencin CT, Bioresorbable nanofiber-based systems for wound healing and drug delivery: optimization of fabrication parameters. *J Biomed Mater Res B Appl Biomater* 2004; 70(2): p. 286–96.

73. Theron A, Zussman E, and Yarin AL, Electrostatic field-assisted alignment of electrospun nanofibres. *Nanotechnology* 2001; 12: p. 384–90.
74. Zhang Q, Chang Z, Zhu M, Mo X, and Chen D, Electrospun carbon nanotube composite nanofibres with uniaxially aligned arrays. *Nanotechnology* 2007; 18(11): p. 5611–6.
75. Li D, Ouyang G, McCann JT, and Xia Y, Collecting electrospun nanofibers with patterned electrodes. *Nano Lett* 2005; 5(5): p. 913–6.
76. Barnes CP, Sell SA, Boland ED, Simpson DG, and Bowlin GL, Nanofiber technology: designing the next generation of tissue engineering scaffolds. *Adv Drug Deliv Rev* 2007; 59(14): p. 1413–33.
77. Hartgerink JD, Beniash E, and Stupp SI, Self-assembly and mineralization of peptide-amphiphile nanofibers. *Science* 2001; 294(5547): p. 1684–8.
78. Zhang S, Fabrication of novel biomaterials through molecular self-assembly. *Nat Biotechnol* 2003; 21(10): p. 1171–8.
79. Smith LA and Ma PX, Nano-fibrous scaffolds for tissue engineering. *Colloids Surf B Biointerfaces* 2004; 39(3): p. 125–31.
80. Jayaraman K, Kotaki M, Zhang Y, Mo X, and Ramakrishna S, Recent advances in polymer nanofibers. *J Nanosci Nanotechnol* 2004; 4(1–2): p. 52–65.
81. Hartgerink JD, Beniash E, and Stupp SI, Peptide-amphiphile nanofibers: a versatile scaffold for the preparation of self-assembling materials. *Proc Natl Acad Sci USA* 2002; 99(8): p. 5133–8.
82. Ma Z, Kotaki M, Inai R, and Ramakrishna S, Potential of nanofiber matrix as tissue-engineering scaffolds. *Tissue Eng* 2005; 11(1–2): p. 101–9.
83. Martin CR, Nanomaterials: a membrane-based synthetic approach. *Science* 1994; 266(5193): p. 1961–6.
84. Chen Y, Zhang LN, Lu XY, Zhao N, and Xu J, Morphology and Crystalline structure of poly (ϵ -caprolactone) nanofiber via porous aluminium oxide template. *Macromol Mater Eng* 2006; 291(9): p. 1098.
85. Tao SL and Desai TA, Aligned arrays of biodegradable poly(ϵ -caprolactone) nanowires and nanofibers by template synthesis. *Nano Lett* 2007; 7(6): p. 1463–8.
86. Nain AS, Wong JC, Amon C, and Sitti M, Drawing suspended polymer micro-/nanofibers using glass micropipettes. *Appl Phys Lett* 2006; 89(18): p. 183105.
87. Iijima S, Helical microtubules of graphitic carbon. *Nature* 1991; 354(6348): p. 56–8.
88. Cui DX, Advances and prospects on biomolecules functionalized carbon nanotubes. *J Nanosci Nanotechnol* 2007; 7(4–5): p. 1298–314.
89. Veetil JV and Ye KM, Development of immunosensors using carbon nanotubes. *Biotechnol Prog* 2007; 23(3): p. 517–31.
90. Yu MF, Lourie O, Dyer MJ, Moloni K, Kelly TF, and Ruoff RS, Strength and breaking mechanism of multiwalled carbon nanotubes under tensile load. *Science* 2000; 287(5453): p. 637–40.
91. Wilson M, Kannangara K, Smith G, Simmons M, and Raguse B, *Nanotechnology: basic science and emerging technologies*. 2002. Chapman and Hall/CRC, Sydney, AU.
92. Guo T, Nikolaev P, Thess A, Colbert DT, and Smalley RE, Catalytic growth of single-walled nanotubes by laser vaporization. *Chem Phys Lett* 1995; 243(1–2): p. 49–54.
93. Guo T, Nikolaev P, Rinzler AG, Tomanek D, Colbert DT, and Smalley RE, Self-assembly of tubular fullerenes. *J Phys Chem* 1995; 99(27): p. 10694–7.
94. Zhang YC, Broekhuis AA, Stuart MCA, Landaluce TF, Fausti D, Rudolf P, and Picchioni F, Cross-linking of multiwalled carbon nanotubes with polymeric amines. *Macromolecules* 2008; 41(16): p. 6141–6.
95. Zhao B, Hu H, and Haddon RC, Synthesis and properties of a water-soluble single-walled carbon nanotube-poly(m-aminobenzene sulfonic acid) graft copolymer. *Adv Funct Mater* 2004; 14(1): p. 71–6.

96. Zhao B, Hu H, Yu A, Perea D, and Haddon RC, Synthesis and characterization of water soluble single-walled carbon nanotube graft copolymers. *J Am Chem Soc* 2005; 127(22): p. 8197–203.
97. Nimmagadda A, Thurston K, Nollert MU, and McFetridge PSF, Chemical modification of SWNT alters in vitro cell-SWNT interactions. *J Biomed Mater Res A* 2006; 76A(3): p. 614–25.
98. Kawaguchi M, Fukushima T, Hayakawa T, Nakashima N, Inoue Y, Takeda S, Okamura K, and Taniguchi K, Preparation of carbon nanotube-alginate nanocomposite gel for tissue engineering. *Dent Mater J* 2006; 25(4): p. 719–25.
99. Crouzier T, Nimmagadda A, Nollert MU, and McFetridge PS, Modification of single walled carbon nanotube surface chemistry to improve aqueous solubility and enhance cellular interactions. *Langmuir* 2008; 24(22): p. 13173–81.
100. Zhang L, Rakotondradany F, Myles AJ, Fenniri H, and Webster TJ, Arginine-glycine-aspartic acid modified rosette nanotube-hydrogel composites for bone tissue engineering. *Biomaterials* 2009; 30(7): p. 1309–20.
101. Harrison BS and Atala A, Carbon nanotube applications for tissue engineering. *Biomaterials* 2007; 28(2): p. 344–53.
102. Koh HS, Yong T, Chan CK, and Ramakrishna S, Enhancement of neurite outgrowth using nano-structured scaffolds coupled with laminin. *Biomaterials* 2008; 29(26): p. 3574–82.
103. Park K, Ju YM, Son JS, Ahn KD, and Han DK, Surface modification of biodegradable electrospun nanofiber scaffolds and their interaction with fibroblasts. *J Biomater Sci Polym Ed* 2007; 18(4): p. 369–82.
104. Li XR, Xie JW, Yuan XY, and Xia YN, Coating electrospun poly(epsilon-caprolactone) fibers with gelatin and calcium phosphate and their use as biomimetic scaffolds for bone tissue engineering. *Langmuir* 2008; 24(24): p. 14145–50.
105. Park YJ, Kim KH, Lee JY, Ku Y, Lee SJ, Min BM, and Chung CP, Immobilization of bone morphogenetic protein-2 on a nanofibrous chitosan membrane for enhanced guided bone regeneration. *Biotechnol Appl Biochem* 2006; 43: p. 17–24.
106. Guo L, Von Dem Bussche A, Buechner M, Yan A, Kane AB, and Hurt RH, Adsorption of essential micronutrients by carbon nanotubes and the implications for nanotoxicity testing. *Small* 2008; 4(6): p. 721–7.
107. Hurt RH, Monthieux M, and Kane A, Toxicology of carbon nanomaterials: Status, trends, and perspectives on the special issue. *Carbon* 2006; 44(6): p. 1028–33.
108. Smart SK, Cassady AI, Lu GQ, and Martin DJ, The biocompatibility of carbon nanotubes. *Carbon* 2006; 44(6): p. 1034–47.
109. Fiorito S, Serafino A, Andreola F, Togna A, and Togna G, Toxicity and biocompatibility of carbon nanoparticles. *J Nanosci Nanotechnol* 2006; 6(3): p. 591–9.
110. Veetil JV and Ye K, Tailored carbon nanotubes for tissue engineering applications. *Biotechnol Prog* 2009; 25(3): p. 709–21.
111. Cui DX, Tian FR, Ozkan CS, Wang M, and Gao HJ, Effect of single wall carbon nanotubes on human HEK293 cells. *Toxicol Lett* 2005; 155(1): p. 73–85.
112. Kam NW, O'Connell M, Wisdom JA, and Dai H, Carbon nanotubes as multifunctional biological transporters and near-infrared agents for selective cancer cell destruction. *Proc Natl Acad Sci USA* 2005; 102(33): p. 11600–5.
113. Chahine NO, Collette NM, Bahadori S, and Loots GG. Biocompatibility of Carbon Nanotubes for Chondrocyte Growth. in *Transactions of the Orthopedic Research Society*. 2008. San Francisco, CA.
114. Nel A, Xia T, Madler L, and Li N, Toxic potential of materials at the nanolevel. *Science* 2006; 311(5761): p. 622–7.
115. Price RL, Waid MC, Haberstroh KM, and Webster TJ, Selective bone cell adhesion on formulations containing carbon nanofibers. *Biomaterials* 2003; 24(11): p. 1877–87.

116. Smith IO, McCabe LR, and Baumann MJ, MC3T3-E1 osteoblast attachment and proliferation on porous hydroxyapatite scaffolds fabricated with nanophase powder. *Int J Nanomedicine* 2006; 1(2): p. 189–94.
117. Kong L, Gao Y, Cao W, Gong Y, Zhao N, and Zhang X, Preparation and characterization of nano-hydroxyapatite/chitosan composite scaffolds. *J Biomed Mater Res A* 2005; 75(2): p. 275–82.
118. Shin M, Yoshimoto H, and Vacanti JP, In vivo bone tissue engineering using mesenchymal stem cells on a novel electrospun nanofibrous scaffold. *Tissue Eng* 2004; 10(1–2): p. 33–41.
119. Yoshimoto H, Shin YM, Terai H, and Vacanti JP, A biodegradable nanofiber scaffold by electrospinning and its potential for bone tissue engineering. *Biomaterials* 2003; 24(12): p. 2077–82.
120. Zanello LP, Zhao B, Hu H, and Haddon RC, Bone cell proliferation on carbon nanotubes. *Nano Lett* 2006; 6(3): p. 562–7.
121. Marrs B, Andrews R, Rantell T, and Pienkowski D, Augmentation of acrylic bone cement with multiwall carbon nanotubes. *J Biomed Mater Res A* 2006; 77(2): p. 269–76.
122. Shi X, Sitharaman B, Pham QP, Spicer PP, Hudson JL, Wilson LJ, Tour JM, Raphael RM, and Mikos AG, In vitro cytotoxicity of single-walled carbon nanotube/biodegradable polymer nanocomposites. *J Biomed Mater Res A* 2008; 86(3): p. 813–23.
123. Shi XF, Hudson JL, Spicer PP, Tour JM, Krishnamoorti R, and Mikos AG, Rheological behaviour and mechanical characterization of injectable poly(propylene fumarate)/single-walled carbon nanotube composites for bone tissue engineering. *Nanotechnology* 2005; 16(7): p. S531–8.
124. Sitharaman B, Shi X, Walboomers XF, Liao H, Cuijpers V, Wilson LJ, Mikos AG, and Jansen JA, In vivo biocompatibility of ultra-short single-walled carbon nanotube/biodegradable polymer nanocomposites for bone tissue engineering. *Bone* 2008; 43(2): p. 362–70.
125. Hatano K, Inoue H, Kojo T, Matsunaga T, Tsujisawa T, Uchiyama C, and Uchida Y, Effect of surface roughness on proliferation and alkaline phosphatase expression of rat calvarial cells cultured on polystyrene. *Bone* 1999; 25(4): p. 439–45.
126. Khang D, Kim SY, Liu-Snyder P, Palmore GT, Durbin SM, and Webster TJ, Enhanced fibronectin adsorption on carbon nanotube/poly(carbonate) urethane: independent role of surface nano-roughness and associated surface energy. *Biomaterials* 2007; 28(32): p. 4756–68.
127. Usui Y, Aoki K, Narita N, Murakami N, Nakamura I, Nakamura K, Ishigaki N, Yamazaki H, Horiuchi H, Kato H, Taruta S, Kim YA, Endo M, and Saito N, Carbon nanotubes with high bone-tissue compatibility and bone-formation acceleration effects. *Small* 2008; 4(2): p. 240–6.
128. Pan YS, Xiong DS, and Gao F, Viscoelastic behavior of nano-hydroxyapatite reinforced poly(vinyl alcohol) gel biocomposites as an articular cartilage. *J Mater Sci Mater Med* 2008; 19(5): p. 1963–9.
129. Wang H, Zuo Y, Zou Q, Cheng L, Huang D, Wang L, and Li YB, Nano-hydroxyapatite/polyamide66 composite tissue-engineering scaffolds with anisotropy in morphology and mechanical behaviors. *J Polym Sci A Polym Chem* 2009; 47(3): p. 658–69.
130. Kon E, Delcogliano M, Filardo G, Fini M, Giavaresi G, Francioli S, Martin I, Pressato D, Arcangeli E, Quarto R, Sandri M, and Marcacci M, Orderly Osteochondral Regeneration in a Sheep Model Using a Novel Nano-Composite Multilayered Biomaterial. *J Orthop Res* 2010; 28(1): p. 116–24.
131. Li WJ, Danielson KG, Alexander PG, and Tuan RS, Biological response of chondrocytes cultured in three-dimensional nanofibrous poly(epsilon-caprolactone) scaffolds. *J Biomed Mater Res A* 2003; 67A(4): p. 1105–14.
132. Li WJ, Mauck RL, and Tuan RS, Electrospun nanofibrous scaffolds: production, characterization, and applications for tissue engineering and drug delivery. *J Biomed Nanotechnol* 2005; 1(3): p. 259–75.
133. Li WJ, Mauck RL, Cooper JA, Yuan XN, and Tuan RS, Engineering controllable anisotropy in electrospun biodegradable nanofibrous scaffolds for musculoskeletal tissue engineering. *J Biomech* 2007; 40(8): p. 1686–93.

134. Chahine NO, Collette NM, Thompson H, and Loots GG. Applications of Carbon Nanotubes in Cartilage Tissue Engineering. in *5th International Meeting on Cell Therapy, Bioengineering and Regenerative Medicine*. 2008. Nancy, France.
135. Chahine NO, Collette NM, Thompson H, and Loots GG. Applications of Carbon Nanotubes in Cartilage Tissue Engineering. in *Advances in Bioengineering ASME*. 2008. Marco Island, FL.
136. Chahine N, Genetos D, Thomas C, and Loots G. Effect of Carbon Nanotubes on the Gene Expression of Chondrocytes in Agarose Constructs. in *Orthopedic Research Society*. 2010. New Orleans, LA.
137. Baker BM and Mauck RL, The effect of nanofiber alignment on the maturation of engineered meniscus constructs. *Biomaterials* 2007; 28(11): p. 1967–77.
138. Baker BM, Nathan AS, Huffman GR, and Mauck RL, Tissue engineering with meniscus cells derived from surgical debris. *Osteoarthritis Cartilage* 2009; 17(3): p. 336–45.
139. Nesti LJ, Li WJ, Shanti RM, Jiang YJ, Jackson W, Freedman BA, Kuklo TR, Giuliani JR, and Tuan RS, Intervertebral disc tissue engineering using a novel hyaluronic acid-nanofibrous scaffold (HANFS) amalgam. *Tissue Eng Part A* 2008; 14(9): p. 1527–37.
140. Nerurkar NL, Baker BM, Sen S, Wible EE, Elliott DM, and Mauck RL, Nanofibrous biologic laminates replicate the form and function of the annulus fibrosus. *Nat Mater* 2009; 8(12): p. 986–92.
141. Gruber HE, Hoelscher G, Ingram JA, and Hanley EN, Culture of human anulus fibrosus cells on polyamide nanofibers extracellular matrix production. *Spine* 2009; 34(1): p. 4–9.
142. Lee CH, Shin HJ, Cho IH, Kang YM, Kim IA, Park KD, and Shin JW, Nanofiber alignment and direction of mechanical strain affect the ECM production of human ACL fibroblast. *Biomaterials* 2005; 26(11): p. 1261–70.
143. Dalton PD, Klee D, and Moller M, Electrospinning with dual collection rings. *Polymer* 2005; 46(3): p. 611–4.
144. Moffat KL, Kwei AS, Spalazzi JP, Doty SB, Levine WN, and Lu HH, Novel nanofiber-based scaffold for rotator cuff repair and augmentation. *Tissue Eng Part A* 2009; 15(1): p. 115–26.
145. Mei F, Zhong JS, Yang XP, Ouyang XY, Zhang S, Hu XY, Ma Q, Lu JG, Ryu S, and Deng XL, Improved biological characteristics of poly(L-lactic acid) electrospun membrane by incorporation of multiwalled carbon nanotubes/hydroxyapatite nanoparticles. *Biomacromolecules* 2007; 8(12): p. 3729–35.
146. Sahoo S, Ouyang H, Goh JCH, Tay TE, and Toh SL, Characterization of a novel polymeric scaffold for potential application in tendon/ligament tissue engineering. *Tissue Eng* 2006; 12(1): p. 91–9.
147. Zeugolis DI, Khew ST, Yew ESY, Ekaputra AK, Tong YW, Yung LYL, Hutmacher DW, Sheppard C, and Raghunath M, Electro-spinning of pure collagen nano-fibres – just an expensive way to make gelatin? *Biomaterials* 2008; 29(15): p. 2293–305.
148. Wang YZ, Kim HJ, Vunjak-Novakovic G, and Kaplan DL, Stem cell-based tissue engineering with silk biomaterials. *Biomaterials* 2006; 27(36): p. 6064–82.
149. Min BM, Lee G, Kim SH, Nam YS, Lee TS, and Park WH, Electrospinning of silk fibroin nanofibers and its effect on the adhesion and spreading of normal human keratinocytes and fibroblasts in vitro. *Biomaterials* 2004; 25(7–8): p. 1289–97.
150. Kim KH, Jeong L, Park HN, Shin SY, Park WH, Lee SC, Kim TI, Park YJ, Seol YJ, Lee YM, Ku Y, Rhyu IC, Han SB, and Chung CP, Biological efficacy of silk fibroin nanofiber membranes for guided bone regeneration. *J Biotechnol* 2005; 120(3): p. 327–39.
151. MacDonald RA, Laurenzi BF, Viswanathan G, Ajayan PM, and Stegemann JP, Collagen-carbon nanotube composite materials as scaffolds in tissue engineering. *J Biomed Mater Res A* 2005; 74(3): p. 489–96.
152. MacDonald RA, Voge CM, Kariolis M, and Stegemann JP, Carbon nanotubes increase the electrical conductivity of fibroblast-seeded collagen hydrogels. *Acta Biomater* 2008; 4(6): p. 1583–92.

153. Gabay T, Jakobs E, Ben-Jacob E, and Hanein Y, Engineered self-organization of neural networks using carbon nanotube clusters. *Phys A Stat Mech Appl* 2005; 350(2–4): p. 611–21.
154. Lovat V, Pantarotto D, Lagostena L, Cacciari B, Grandolfo M, Righi M, Spalluto G, Prato M, and Ballerini L, Carbon nanotube substrates boost neuronal electrical signaling. *Nano Lett* 2005; 5(6): p. 1107–10.
155. Kam NW, Jan E, and Kotov NA, Electrical stimulation of neural stem cells mediated by humanized carbon nanotube composite made with extracellular matrix protein. *Nano Lett* 2009; 9(1): p. 273–8.
156. Chao TI, Xiang S, Chen CS, Chin WC, Nelson AJ, Wang C, and Lu J, Carbon nanotubes promote neuron differentiation from human embryonic stem cells. *Biochem Biophys Res Commun* 2009; 384(4): p. 426–30.
157. Stankus JJ, Guan J, Fujimoto K, and Wagner WR, Microintegrating smooth muscle cells into a biodegradable, elastomeric fiber matrix. *Biomaterials* 2006; 27(5): p. 735–44.
158. Townsend-Nicholson A and Jayasinghe SN, Cell electrospinning: a unique biotechnique for encapsulating living organisms for generating active biological microthreads/scaffolds. *Bio-macromolecules* 2006; 7(12): p. 3364–9.
159. Baker BM, Gee AO, Metter RB, Nathan AS, Marklein RA, Burdick JA, and Mauck RL, The potential to improve cell infiltration in composite fiber-aligned electrospun scaffolds by the selective removal of sacrificial fibers. *Biomaterials* 2008; 29(15): p. 2348–58.
160. Ki CS, Baek DH, Gang KD, Lee KH, Um IC, and Park YH, Characterization of gelatin nanofiber prepared from gelatin-formic acid solution. *Polymer* 2005; 46(14): p. 5094–102.
161. Zuo WW, Zhu MF, Yang W, Yu H, Chen YM, and Zhang Y, Experimental study on relationship between jet instability and formation of beaded fibers during electrospinning. *Polym Eng Sci* 2005; 45(5): p. 704–9.
162. Zhang CX, Yuan XY, Wu LL, Han Y, and Sheng J, Study on morphology of electrospun poly (vinyl alcohol) mats. *Eur Polym J* 2005; 41(3): p. 423–32.
163. Mit-uppatham C, Nithitanakul M, and Supaphol P, Ultrathin electrospun polyamide-6 fibers: Effect of solution conditions on morphology and average fiber diameter. *Macromol Chem Phys* 2004; 205(17): p. 2327–38.
164. Chen H and Hsieh YL, Ultrafine hydrogel fibers with dual temperature- and pH-responsive swelling behaviors. *J Polym Sci A Polym Chem* 2004; 42(24): p. 6331–9.
165. Jiang HL, Fang DF, Hsiao BS, Chu B, and Chen WL, Optimization and characterization of dextran membranes prepared by electrospinning. *Biomacromolecules* 2004; 5(2): p. 326–33.
166. Koski A, Yim K, and Shivkumar S, Effect of molecular weight on fibrous PVA produced by electrospinning. *Mater Lett* 2004; 58(3–4): p. 493–97.
167. Ryu YJ, Kim HY, Lee KH, Park HC, and Lee DR, Transport properties of electrospun nylon 6 nonwoven mats. *Eur Polym J* 2003; 39(9): p. 1883–9.
168. Jun Z, Hou HQ, Schaper A, Wendorff JH, and Greiner A, Poly-L-lactide nanofibers by electrospinning – influence of solution viscosity and electrical conductivity on fiber diameter and fiber morphology. *E-Polymers* 2003.
169. Zong XH, Kim K, Fang DF, Ran SF, Hsiao BS, and Chu B, Structure and process relationship of electrospun bioabsorbable nanofiber membranes. *Polymer* 2002; 43(16): p. 4403–12.
170. Demir MM, Yilgor I, Yilgor E, and Erman B, Electrospinning of polyurethane fibers. *Polymer* 2002; 43(11): p. 3303–9.
171. Huang L, Nagapudi K, Apkarian RP, and Chaikof EL, Engineered collagen-PEO nanofibers and fabrics. *J Biomater Sci Polym Ed* 2001; 12(9): p. 979–93.
172. Deitzel JM, Kleinmeyer J, Harris D, and Tan NCB, The effect of processing variables on the morphology of electrospun nanofibers and textiles. *Polymer* 2001; 42(1): p. 261–72.
173. Buchko CJ, Chen LC, Shen Y, and Martin DC, Processing and microstructural characterization of porous biocompatible protein polymer thin films. *Polymer* 1999; 40(26): p. 7397–407.

174. Fong H, Chun I, and Reneker DH, Beaded nanofibers formed during electrospinning. *Polymer* 1999; 40(16): p. 4585–92.
175. Wannatong L, Sirivat A, and Supaphol P, Effects of solvents on electrospun polymeric fibers: preliminary study on polystyrene. *Polym Int* 2004; 53(11): p. 1851–9.
176. Yuan XY, Zhang YY, Dong CH, and Sheng J, Morphology of ultrafine polysulfone fibers prepared by electrospinning. *Polym Int* 2004; 53(11): p. 1704–10.
177. Kim HS, Kim K, Jin HJ, and Chin IJ, Morphological characterization of electrospun nanofibrous membranes of biodegradable poly(L-lactide) and poly(lactide-co-glycolide). *Macromol Symp* 2005; 224: p. 145–54.
178. Casper CL, Stephens JS, Tassi NG, Chase DB, and Rabolt JF, Controlling surface morphology of electrospun polystyrene fibers: Effect of humidity and molecular weight in the electrospinning process. *Macromolecules* 2004; 37(2): p. 573–8.
179. Reneker DH and Chun I, Nanometre diameter fibres of polymer, produced by electrospinning. *Nanotechnology* 1996; 7(3): p. 216–23.
180. Abrams GA, Goodman SL, Nealey PF, Franco M, and Murphy CJ, Nanoscale topography of the basement membrane underlying the corneal epithelium of the rhesus macaque. *Cell Tissue Res* 2000; 299(1): p. 39–46.
181. Li WJ, Laurencin CT, Cateson EJ, Tuan RS, and Ko FK, Electrospun nanofibrous structure: A novel scaffold for tissue engineering. *J Biomed Mater Res* 2002; 60(4): p. 613–21.
182. Chen VJ and Ma PX, Nano-fibrous poly(L-lactic acid) scaffolds with interconnected spherical macropores. *Biomaterials* 2004; 25(11): p. 2065–73.

Contents

7.1	Introduction	180
7.2	Classification of Bioceramics	181
7.2.1	Bioinert Ceramics	181
7.2.2	Glass-Ceramic and Bioactive Glass	184
7.2.3	Calcium Phosphate Bioceramics	186
7.3	Applications of Calcium Phosphate Ceramics	190
7.3.1	Bioactive Cement	190
7.3.2	Porous Bioceramic Scaffolds for Bone Tissue Engineering	192
7.3.3	Ceramic-Based Composite Scaffold for Tissue Engineering and Drug Delivery	193
7.4	Bioceramics for Cancer Therapy	197
7.4.1	Bioceramics for Radiation Therapy	197
7.4.2	Bioceramics for Hyperthermia Therapy for Cancer	197
7.5	Bioceramics for Dental Application	198
7.6	Future Trends	199
	References	200

Abstract This chapter is focused on the classification of bioceramics and their medical applications. Alumina, zirconia or alumina–zirconia-based composite bioinert ceramics are currently used as femoral heads, acetabular cups for hip replacement, and dental implants. Nano-structured bioinert ceramics with significantly improved toughness and stability are desirable for future clinical needs. Bioactive glass and calcium phosphates are being investigated as bone fillers, bone cements, coatings, and scaffolds for bone repair and regeneration. Cell-laden biodegradable bioceramic/biopolymer hybrid composites mimicking the bony hierarchical structure present the desired properties for bone substitution and tissue engineering and are creating a new generation of regeneration materials. Bioceramics for dental and cancer treatment are also introduced in this chapter. Further challenges in bioceramic scaffold fabrication for tissue engineering are also discussed.

Y. Yang (✉)

Houston Biomaterials Research Center, Department of Restorative Dentistry and Biomaterials, University of Texas Health Science Center at Houston, 6516 M.D. Anderson Blvd., D 4.133, Houston, TX 77030, USA

e-mail: yunzhi.yang@uth.tmc.edu

Keywords Bioactive glass • Bioinert ceramic • Bone tissue engineering • Calcium phosphate • Scaffold

7.1 Introduction

Ceramics, considered to be the oldest materials used by humans, have progressively been used for electronic, optical, energy-related, and medical applications. Applications of ceramics in medical fields have advanced significantly in the past few decades.

Biomaterials are defined as substances, other than drugs, that can be used to treat, augment, replace, or repair any tissue or organ of the body *in vivo* for any period of time. When biomaterials are implanted into the body, two factors will determine the fate of the biomaterials. One is tissue response to the biomaterials, i.e. physico-chemical properties, cytotoxicity, and chemical compositions. The other is the change in biomaterial properties after implantation, i.e. body fluid erosion, and enzyme degradation. Bioceramics is a large class of inorganic nonmetallic materials. It is widely used in repairing and replacing skeletal and hard tissues such as hip-joints, teeth, and bone due to its antimicrobial activity and resistance to pH change, acid and base solutions, and high temperatures. At the same time, bioceramics generally show better tissue responses than polymers or metals. Most bioceramics do not release their components into the human body unless they are designed to be bioresorbable. Therefore, bioceramics do not generate a foreign body response and are biocompatible to cells. Besides these safety features, a very important and useful feature of bioceramics such as apatite is their ability to bond with the bone. Apart from apatite, bioactive glass and bioactive glass ceramics can also bind directly with the bone.

Bioceramic materials generally include ceramics, bioglasses, and glass-ceramics. Over the past 50 years, advances in many specialties of bioceramics such as alumina, zirconia, hydroxyapatite, tricalcium phosphates, and bioactive glasses have made significant contributions to the development of the modern health care industry and have improved the quality of human life [1]. These ceramics are able to replace or restore various damaged bone tissue systems, due to their compositional similarity with the mineral phase of bone. Currently, bioceramics are primarily applied in the hip joint, knee joint, elbow joint, humerus, chest connection pin, teeth root, auditory ossicles and cranial bones.

The clinical use of bioceramics in dentistry started in the late eighteenth century with the use of porcelain in crowns. Since the late nineteenth century, plaster of paris, or gypsum, began to be used in orthopedics [2]. With the advancement of high-tech ceramic technology, more and more bioceramics were applied into the medical field since the twentieth century. The calcium phosphate family of ceramics was extensively used in bone defects and alumina (Al_2O_3), zirconia, and alumina–zirconia composite ceramics began to be used in hip joints [3].

In general, we classify bioceramics into two families: bioinert and bioactive ceramics. Their classification depends on whether the ceramic can directly form an integration at the interface between the bone and the ceramic. When a bioinert material is implanted into the

body, soft tissue interplay can happen, preventing the new bone from ingrowing to form a bond. However, for bioactive ceramics, ingrowth of new bone can often be achieved. Therefore, the “bioinert” ceramics used in hip joint prostheses or knee joint replacement are often coated with bioactive ceramics in order to better form integrations and to prevent aseptic implant loosening. The applications of bioceramics have evolved in many fields today, and research into further bioceramic development is also progressing at a fast pace. Therefore, it is not possible to exhaustively review all of the latest research and applications of bioceramics in this chapter. We will first briefly introduce previous work on bioceramics, and then intensively review the current and ongoing research in this area by presenting bioceramic classifications, applications, synthesis methods, and clinical developments.

7.2

Classification of Bioceramics

7.2.1

Bioinert Ceramics

Nearly inert bioceramics refers to the kinds of ceramics with stable physicochemical properties and good biocompatibility. High density, high strength alumina and zirconia are often considered bioinert ceramics. Due to their excellent corrosion resistance, high wear resistance, and good biocompatibility [4, 5], the major application of alumina or zirconia is in total hip joint and knee replacements.

7.2.1.1

Alumina

Alumina (Al_2O_3) is a representative bioinert ceramic. Alumina has been widely used in load-bearing artificial joints (hip joints, knee joints, finger joints), artificial bone, dental implants, artificial auditory ossicles and orthopedic surgery since the 1970s when Boutin introduced alumina into the artificial femur head [4].

Although there are several crystal systems of Al_2O_3 , the alumina used for bioceramics is $\alpha\text{-Al}_2\text{O}_3$, which is the most stable form. The crystalline structure of $\alpha\text{-Al}_2\text{O}_3$ is rhombohedral. Alumina is extremely stable in the human body and cannot be dissolved by strong acids or bases. Alumina has been widely used in the acetabulum and femur head and articulations digitorum manus. Alumina are attractive materials because of their high hardness, low wear rates and excellent biocompatibility, which make alumina an alternative to the common metal femoral heads articulating against an acetabular cup of polyethylene or to metal–metal bearing devices [6–8]. Klaus Jahnke reported the excellent tolerance of bioinert aluminium oxide ceramics after it was implanted into the middle ear for over 4 years. When he implanted alumina into an ossicular chain reconstruction, they observed no foreign body reactions within several weeks. They designed two types of angled implants to prevent the endplate of the implant from turning outwards when the eardrum

7 is retracted. This problem would result in an interference with the blood supply to the tympanic membrane [9].

Most total hip joints are composed of ultra-high molecular weight polyethylene (UHMWPE) and metal. However, the interaction between the UHMWPE and metal pair produces wear debris or releases metal particles, which may accumulate and cause a biological response [10]. The wear debris [11–14] leads to osteolysis and eventual loosening of the prosthesis [15–18]. This aseptic loosening failure of joint prostheses results in serious orthopaedic problems, thus affecting the long-term success of total hip arthroplasty (THA) [19–22]. Consequently, the reduction of the amount of polyethylene debris and metal particles due to wear becomes significantly important for the long term success of THA [23]. There has been increased interest in the development and use of low wearing components that exhibit negligible amounts of ion release as alternatives for hip prostheses. Thus, ceramic-on-ceramic THA has gained attention in the field of orthopaedic implants.

Since the 1990s, approximately 3.5 million alumina components and more than 600,000 zirconia femoral heads have successfully been placed into patients worldwide. However, due to the intrinsic brittleness and slow crack growth of ceramic materials [24, 25], significant *in vivo* implantation failures are frequently reported [26–29]. When these materials were first pioneered, the fracture rate was quite high (up to 13% for some versions), mainly for alumina–alumina pairs. It is worth noting that this ceramic breakage rate in total hip prostheses varies in the literature from 0.2% to 3.5% [30, 31]. A recent compilation of cases indicates that the *in vivo* failure rate (number of fractures/number of implanted heads) reported by the producer of BioloX[®] alumina has been below 0.01% for the past 10 years [32]. Even so, it is necessary to improve the reliability of implanted alumina ceramics.

7.2.1.2

Zirconia

In addition to the alumina ceramics discussed above, zirconia ceramics are also used for femoral heads in total hip arthroplasty. This is because zirconia ceramics are superior to alumina ceramics in terms of mechanical strength and fracture toughness. Zirconia has three variants: monoclinic, tetragonal, and cubic crystal structures. Monoclinic is the stable phase at low temperatures, but the tetragonal phase is always formed prior to the monoclinic phase during phase transformation. The enhancement of toughness results from the phase transformation toughening and microcrack propagation resistance. Transformation of metastable tetragonal grains to the monoclinic phase is accompanied by volume expansion, which induces compressive stress that hinders the crack from continuing. However, large volume variations from their phase transformation results in many cracks that may significantly decrease the mechanical properties of the material. Therefore, partially stabilized zirconia is suitable for use in biomedical applications with the requirement of mechanical strength. At present, meta-stabilized zirconia as a structural ceramic became a popular alternative to alumina due to its higher fracture toughness and strength [33], which actually opened a new way to design implant ceramics with high toughness.

A typical partially stabilized zirconia example is yttria stabilized zirconia. Yttria added to ZrO_2 stabilizes the tetragonal or cubic phase and prevents those phases from transforming to the monoclinic structure. Yttria-stabilized zirconia orthopedic implants have the largest value of fracture toughness. Static and fatigue strengths for zirconia femoral heads have been found to satisfy clinical requirements [34]. Application of zirconia also reduces frictional torque and the level of polyethylene debris production [35]. The wear performance has been shown to be superior even to alumina [36]. However, due to zirconia's meta-stability, some cases reported that aging happened in the presence of water when implanted *in vivo* [37]. This aging process results from the phase transformation at the surface from tetragonal to monoclinic transformation triggered by water molecules, which leads to surface roughening and micro-cracking [38]. Therefore, these femoral heads may undergo slow degradation during long-term implantation in the human body, which would be pronounced after several years [39, 40].

7.2.1.3

Zirconia–Alumina

Although zirconia ceramics have certain advantages on the toughness fracture and have good mechanical properties, long term aging *in vivo* after implantation is still a major concern for medical use. The presence of water could promote tetragonal to monoclinic transformation in zirconia. Chevalier et al. [38, 41] performed a detailed analysis of the aging mechanism. It is likely that the oxygen of environmental water penetrates into vacancy sites of the zirconia and hydrogen is placed on adjacent interstitial sites. Oxygen vacancies in the zirconia affect the water diffusion rate, which results in volume instability of surface grains and micro-cracking [42]. Based on stabilization mechanisms, minimizing the quantity of oxygen vacancies in the zirconia is feasible and necessary in order to address this issue. Meta-stabilizing zirconia with yttria reduces the oxygen vacancy and diffusion of water radicals into the zirconia lattice, which prevents the propagation of the transformation of zirconia grains from one grain to another. Some efforts have been dedicated to develop this kind of zirconia–alumina composite to reduce aging issues of zirconia [43, 44]. A potential solution is to develop a zirconia-based alumina ceramic, combining the enhanced toughness of zirconia and the surface degradation resistance of alumina when implanted *in vivo*.

Metal-doped zirconia is being developed today and may be widely used in the clinic in the future. The addition of dopants is believed to stabilize the tetragonal or cubic zirconia phase [45, 46]. It has been reported that CeO_2 -doped zirconia presents superior mechanical properties, owing to the mechanism of phase transformation [47], ferroelastic domain switching [48] and shape memory behavior [49]. Nawa et al. [50] developed a Ce-TZP/ Al_2O_3 nanocomposite that exhibits extremely high resistance to low-temperature degradation, excellent biocompatibility and high wear resistance. Ceria-stabilized zirconia–alumina nanocomposites offer superior properties compared to conventional yttria stabilized zirconia [51]. The homogeneous dispersion of a nanoscale alumina phase in the Ce-TZP matrix increases the strength of the material without affecting the fracture toughness. The homogeneous dispersion suppresses grain growth and increases the hardness, elastic modulus and

hydrothermal stability of the tetragonal zirconia, which suggests that the addition of 10 mol % CeO₂ and 30 vol.% of Al₂O₃ to the zirconia matrix would be applicable in dental restorations [52].

Besides the addition of yttria, or ceria, other metal oxide dopants such as MgO, calcia, and even a combination of them could be added to stabilize the ZrO₂ in the tetragonal and/or cubic forms at room temperature. Wu and Brook [53] found that high density and small grain size could be achieved with the use of multiple additives, i.e. CaO (or Y₂O₃) together with MgO. Brito-Chaparro recently added heat-treated MgO powders as a stabilizer to micron ZrO₂ powders to increase both hardness and fracture toughness [54]. Actually, Mg-PSZ has been developed for femoral heads in total hip replacements. Therefore, the aging-resistant doped zirconia ceramics such as Mg-PSZ, Ce-TZP or combined metal dopants will be highly competitive in future joint or dental applications.

7.2.1.4

Carbonaceous Materials

Carbonaceous materials, including low-temperature isotropic pyrolytic carbon (LTIC), graphite, and diamond-like carbon (DLC), have been extensively used in artificial heart valves due to their good bio- and hemo-compatible nature. LTIC is the most widely used material. DLC is a potential substitute due to its good biocompatibility and mechanical properties. DLC has been widely investigated as coatings in the optics, magnetic media, semiconductor and biomedical field. As we discussed above, metallic implants release metal ions and wear debris into the surrounding tissue, which can lead to osteolysis and aseptic loosening-related failure of the implant. Coating the implants with protective DLC films, which can reduce corrosion and wear, may prevent or alleviate the problems described above and may extend the life-time of implants to the benefit of the patients. DLC, due to chemical inertness, corrosion and wear resistance, appears to be an ideal material for such purposes [55, 56].

7.2.2

Glass-Ceramic and Bioactive Glass

Bioactive glass and glass ceramic contain rich CaO and P₂O₅ contents. One representative is the bioglass 45S5 developed by Larry Hench in 1968 [57], which is composed of Na₂O 24.5, CaO 24.5, SiO₂ 45, and P₂O₅ 6.0wt%. This kind of glass-ceramic is mainly based on a SiO₂-CaO-Na₂O-P₂O₅ system, which is widely used in head and throat surgery in the form of middle ear devices and implants for the orbital floor. It has been reported that some bioactive glass and glass-ceramics can directly bond to bone as well as soft tissue. These bioglass and glass-ceramics have become known as bioactive materials. It is worth noting that a simple in vitro method has been developed to study whether these glasses have bioactivity and predict how they will react inside the body. In this method, a testing material is soaked in a simulated body fluid (SBF) that contains the same ions as present in the body fluid, and the evolution process of apatite layer formation on the testing material is

evaluated. Accordingly, the bioactivity of a material is defined as its ability to support apatite formation on the testing material. It is this simple way that enables us to investigate the possible *in vivo* behavior of the glass-ceramic *in vitro*. Hench [58] described the staged process. One important feature is that $\equiv\text{Si}-\text{OH}$ groups form in the initial kinetic reaction followed by a SiO_2 gel layer precipitated on the surface of the glass. An amorphous calcium phosphate then precipitates, which leads to the formation of hydroxycarbonate apatite. It is believed that forming bone-like apatite *in vitro* is critical because apatite is the dominant inorganic phase of hard tissue. Thus, bone-like apatite formation indicates good osteoconductivity in biomaterials. In fact, the non-apatite bioglass and glass ceramic materials exhibiting *in vitro* apatite formation in SBF has correlated with the ability to bond directly with bone *in vivo*. Therefore, it has been hypothesized that the precipitation of apatite in SBF *in vitro* can be used as an indicator to predict its excellent bioactivity *in vivo*. Yet, there are many factors correlating with the bone formation ability of bioceramics *in vivo*. Furthermore, more experiments are needed to improve the prediction of the bone-bonding ability of bioglass or glass-ceramic when implanted.

Many bioactive silica glasses are based on 45S5. During the early 1970s, Bromer et al. [59] developed bioactive glass-ceramics from a $\text{SiO}_2\text{-CaO-P}_2\text{O}_5$ system upon which various glass-ceramics were further developed. The bioactive behavior of this type of glass-ceramic has been successfully tested by Gross and Strunz [60]. These glass-ceramics have been used in middle ear surgery. Kokubo [61] developed an apatite-wollastonite glass-ceramic with the composition of 34 wt% SiO_2 , 44.7 CaO, 4.6 MgO, 16.2 P_2O_5 , and 0.5 CaF_2 . After heat treatment of the glass powder at 900°C , X-ray diffraction indicated that approximately 38 wt% apatite and 24 wt% wollastonite were present in the approximately 28 wt% residual glassy matrix phase. Therefore, this glass-ceramic is called A-W bioactive glass. After immersing this bioactive glass, Kokubo et al. did not observe the formation of an SiO_2 gel layer, as was the case with the bioactive glass from the $\text{SiO}_2\text{-CaO-Na}_2\text{O-P}_2\text{O}_5$ system. However, he found that the $\equiv\text{Si}-\text{OH}$ groups on the surface of the glass-ceramic would be favorable for apatite nucleation.

A glass-ceramic with this type of microstructure has favorable mechanical properties. It is possible that the specific microstructure of glass ceramics reinforces the mechanical properties of the whole piece with a bending strength of 215 MPa and compressive strength of 1,080 MPa [61], which is suitable for load-bearing implants [62].

In vivo experiments indicated that there would be bone bonding formation at the interface of bioglass and tissue. To understand the interface behavior mechanism, Hench immersed 45S5 bioglass into a low concentration collagen suspension. As a control, normal glass was also immersed in the same suspension. After 10 days, collagen grew into the inner surface layer of the bioglass. However, the collagen on the normal glass was easily washed away, suggesting the absence of weak bonding between normal glass and bioactive ingredients [63]. In addition, osteoblasts grew well on the surface of the bioglass. From the transmission electron microscope (TEM) observation, it was evident that there were connections between the cell layer and bioglass.

The development of bioglass ceramics in dental implants has achieved significant success over the last few years. Bioglass is widely used and is very promising for dental applications due to two reasons. First, chemical bonding between bioglass and surrounding bone tissues can be formed. Second, its elastic modulus matches more closely the elasticity

7 of the surrounding bone tissues, which is an important property, thus reducing the possible risk of bone resorption [64].

Current research and development of bioactive glass and glass-ceramic are concentrated on enduing the glass-ceramic with new functions besides bioactivity. Researchers [65, 66] added some magnetic materials such as magnetite (Fe_3O_4) into glass-ceramics to design magnetic bioactive glasses and glass ceramics. When this type of glass-ceramic is implanted, the implants fulfill two functions simultaneously, which are to regenerate bone and to treat osseous tumors. This kind of anti-cancer function can be realized through hyperthermia treatment when heating tumors up to around 43°C . Under this temperature, the malignant cells are selectively destroyed, whereas the healthy ones only undergo small and/or reversible damage [65, 66].

7.2.3

Calcium Phosphate Bioceramics

Calcium phosphate bioceramics currently constitute a major family of inorganic materials in a number of biomedical applications such as orthopedic reconstruction, dentistry and drug delivery because they exhibit considerably improved biological affinity and activity to surrounding host tissues when implanted, compared to currently existing synthetic materials. Specifically, hydroxyapatite (HA) and beta-tricalcium phosphate (β -TCP) were developed as bioceramics in the early 1980s and nowadays are the most common calcium phosphates used in clinical settings [67–69].

Natural bone typically consists of 25% water, 15% organic materials (mainly collagen) and 60% inorganic mineral phases. The inorganic mineral phases consist primarily of calcium-deficient carbonate hydroxyapatite. Hence, in the past 30–40 years, much attention had been paid to the use of calcium phosphates as bone substitute biomaterials. Many methods have been utilized to synthesize all kinds of calcium phosphates. Table 7.1 summarizes the various forms of calcium phosphates currently used in the biomedical field. Different phases are used in different applications depending upon whether a resorbable or bioactive material is desired.

Among these calcium phosphates, research is focused on apatites. Driessens [99] stated that calcium phosphates with a Ca/P ratio of less than 1 are not suitable for biological implantation, but if the ratio is higher than 1.67, the resorption rate dramatically decreases. The synthesis of this calcium phosphate is primarily based on an aqueous precipitation route. Aqueous precipitation is mainly performed by a reaction between a calcium salt and an alkaline phosphate. Other routes include solid-phase processing, hydrolysis and hydrothermal synthesis.

Among different forms of calcium phosphates, particular attention has been paid to tricalcium phosphate ($\text{Ca}_3(\text{PO}_4)_2$, TCP) and hydroxyapatite ($\text{Ca}_{10}(\text{PO}_4)_6(\text{OH})_2$, HA) due to their outstanding biocompatibility and osteoconduction. As a result, these materials have been widely used in medical applications. HA and β -TCP are generally used as bulk materials and as components of bioactive cements. Monocalcium phosphate monohydrate, dicalcium phosphate anhydrous, dicalcium phosphate dihydrate, α -TCP, and tetracalcium phosphate are used only as components of bioactive cements.

Table 7.1 Various calcium phosphates with their respective Ca/P atomic ratios

Ca/P ratio	Formula	Chemical name	Acronym	References
2.0	$\text{Ca}_4\text{P}_2\text{O}_9$	Tetracalcium phosphate	TTCP	[70–74]
1.67	$\text{Ca}_{10}(\text{PO}_4)_6(\text{OH})_2$	Hydroxyapatite	HA	[75, 76]
<1.67	$\text{Ca}_{10-x}\text{H}_x(\text{PO}_4)_6(\text{OH})_2$	Amorphous calcium phosphate	ACP	[77–79]
1.50	$\text{Ca}_3(\text{PO}_4)_2(\alpha\beta\gamma)$	Tricalcium phosphate	TCP($\alpha\beta\gamma$)	[80–83]
1.33	$\text{Ca}_8\text{H}_2(\text{PO}_4)_6 \cdot 5\text{H}_2\text{O}$	Octacalcium phosphate	OCP	[84–86]
1.0	$\text{CaHPO}_4 \cdot 2\text{H}_2\text{O}$	Dicalcium phosphate dihydrate	DCPD	[87, 88]
1.0	CaHPO_4	Dicalcium phosphate	DCP	[70, 88]
1.0	$\text{Ca}_2\text{P}_2\text{O}_7(\alpha\beta\gamma)$	Calcium pyrophosphate ($\alpha\beta\gamma$)	CPP	[89–92]
1.0	$\text{Ca}_2\text{P}_2\text{O}_7 \cdot 2\text{H}_2\text{O}$	Calcium pyrophosphate dihydrate	CPPD	[89–92]
0.7	$\text{Ca}_7(\text{P}_5\text{O}_{16})_2$	Heptacalcium phosphate	HCP	[93, 94]
0.67	$\text{Ca}_4\text{H}_2\text{P}_6\text{O}_{20}$	Tetracalcium dihydrate phosphate	TDHP	[74]
0.5	$\text{Ca}(\text{H}_2\text{PO}_4)_2 \cdot \text{H}_2\text{O}$	Monocalcium phosphate monohydrate	MCPM	[95–97]
0.5	$\text{Ca}(\text{PO}_3)_2(\alpha\beta\gamma)$	Calcium metaphosphate	CMP($\alpha\beta\gamma$)	[98]

7.2.3.1

Hydroxyapatite

Hydroxyapatite [$(\text{Ca}_{10}(\text{PO}_4)_6(\text{OH})_2)$, HA] bioactive ceramics have been widely used in various bone repairs and as coatings for metallic prostheses to improve their biological properties as powders or in particulate forms [100]. HA possesses a hexagonal structure with a $\text{P6}_3/\text{m}$ spacer group and cell dimensions $a = b = 9.42 \text{ \AA}$, and $c = 6.88 \text{ \AA}$, where $\text{P6}_3/\text{m}$ refers to a space group with a sixfold symmetry axis with a threefold helix and a microplane [101]. It has an exact stoichiometric Ca/P ratio of 1.67 and is chemically very similar to mineralized human bone [102]. It has high thermodynamical stability under physiological conditions and can form bone bonding at the interface between materials and tissue. However, in spite of its chemical similarities to bone, the mechanical performance of synthetic HA is very poor compared to natural bone. The structure of natural bone comprises of three-dimensional extracellular matrices, on which nano-inorganic phase precipitates. These inorganic phases are composed of nanocrystalline HA and other trace inorganic salts. To improve the mechanical properties of HA ceramics, much attention has been paid to synthesize nano-scale HA powders. It is believed that nano-HA has the potential to improve mechanical and biological properties in bone regeneration.

Many nanoparticle processing methods have been developed and used to synthesize HA nanoscale powders. These methods include sol–gel synthesis [36–40], co-precipitation [42], hydrothermal reaction [103], microemulsion syntheses [104] and mechanochemical synthesis [105]. Wang et al. [106] used a sol–gel method with phosphoric pentoxide (P_2O_5) and

7 calcium nitrate tetrahydrate as starting materials and gelled for 1 h at 60°C. After drying, the gel was sintered at 600–700°C and HA powder of 10–15 nm was obtained. This technique was simpler and faster than other sol–gel methods because it did not require control over pH or long hydrolysis times. Shih et al. [107] synthesized nano-sized hydroxyapatite (HA) powders from dicalcium phosphate dihydrate ($\text{CaHPO}_4 \cdot 2\text{H}_2\text{O}$, DCPD) and CaCO_3 using the hydrolysis of DCPD and CaCO_3 with 2.5 M NaOH solution at 75°C for 1 h. The only product synthesized from DCPD was HA, and the crystallinity of the HA was improved by increasing the annealing temperature. Guo et al. [108] successfully synthesized HA nanoparticles of 10–30 nm diameters by reverse microemulsion (aqueous solution/mixed TX-100 and Tween 80/mixed n-butanol and n-hexanol/cyclohexane) at room temperature. Compared to the conventional direct precipitation method, the reverse microemulsion route allowed for better control in particle size and a lower degree of particle agglomeration.

Due to the brittleness of calcium phosphate, the clinical application of bulk HA is largely limited to non-load bearing parts of the skeleton. Therefore, much interest has been focused on the use of HA coatings on metallic implant substrates. The other main reason that HA can be applied in coating metallic substrates for the hip joint head is that HA can directly form bone-bonding, which can not only prevent the release of metallic ions and wear debris but also enhance bone integration. Many advanced techniques are available for the deposition of calcium phosphate coatings, including sol–gel routes, electrochemical routes, biomimeticity, and sputtering, but the most popular commercial routes involve plasma spraying. In plasma spraying, HA powder is suspended in the carrier gas and fed into the plasma where it can be fired at a substrate. In this process, many of variable parameters influence the properties of coating, including coating thickness, crystallinity, and adhesive strength, which further affect the tissue response to the calcium phosphate coating.

7.2.3.2

Tricalcium Phosphate

β -tricalcium phosphates [$\beta\text{-Ca}_3(\text{PO}_4)_2$] (β -TCP) are widely applied in biomedical fields because of their biocompatibility and osteoconductivity. Tricalcium phosphate has been proven to be resorbable in vivo with new bone growth, replacing implanted TCP [109]. The resorption rate of calcium phosphate is considered to be related with the Ca/P ratio. The rate of dissolution increases with decreasing calcium-to-phosphorous ratios. Therefore, the dissolution rate of calcium phosphate decreases in the following order [110]: crystalline HA \ll β -TCP \ll α -TCP \ll amorphous HA.

Tricalcium phosphate has four forms, including α -TCP, β -TCP, γ -TCP and super α -TCP. The γ -TCP polymorph is a high-pressure phase and the super α -TCP is only observed at approximately 1,500°C. Therefore, only β -TCP and α -TCP are the most frequently observed polymorphs in bioceramics. The β -TCP polymorph transforms to α -TCP at around 1,120°C and 1,290°C. The α -TCP polymorph phase is stable in the range of 700–1,200°C. However, due to the quick resorption rate, very little attention has been paid to α -TCP in the biomedical field. This disadvantage limits its application in the medical field. β -TCP is essentially a slowly degrading bioresorbable calcium phosphate ceramic and has been used as bone and tooth implant material because of its

excellent biocompatibility, osteoinductivity, bioresorbability and safety in living tissues [111]. X-ray patterns have indicated that β -TCP has a pure hexagonal crystal structure. It is reported that the resorbability of β -TCP in vivo might be strongly related to the characterization and stability of the β -TCP structure [74].

The control of morphology and particle size of β -TCP powders becomes important in applications preparing scaffolds with high mechanical properties. Nano-sized calcium phosphate powders with appropriate stoichiometry, high purity and crystallinity are investigated due to their enhanced densification, osseointegrative, and bioactive properties. Many methods have been developed to prepare nano-scale β -TCP powder, such as sol-gel [113], hydrothermal, microemulsion, gas phase reactions and precipitation [114]. Among these methods, the sol-gel approach has received more attention because of well-known inherent advantages such as homogeneous molecular mixing, low processing temperature and its ability to generate nanocrystalline powders, bulk amorphous monolithic solids and thin films [115].

Conventionally, β -TCP powders are synthesized via solid-state [116] and wet-chemical methods [117]. A simple route for synthesizing nano-sized β -TCP at room temperature has been developed in methanol solvent. Nano-sized β -TCP phases around 50 nm in diameter can be readily synthesized at room temperature [102]. Sanosh et al. used a simple sol-gel route to prepare β -TCP nano-powders with 80 nm diameters using calcium nitrate and potassium dihydrogenphosphate as calcium and phosphorus precursors, respectively [113]. β -TCP was also prepared by a wet precipitation procedure from an aqueous solution of $\text{Ca}(\text{NO}_3)_2$ and NaH_2PO_4 and calcined at $1,150^\circ\text{C}$, the nano particle size of β -TCP can be used as bone substitutes after grinding and sieving to obtain the desired particle size.

Because of its degradation characteristics, β -TCP is regarded as an ideal material for bone substitutes that should degrade when new bone tissue infiltrates. These properties give β -TCP an edge over other biomedical materials when it comes to resorbability and replacement of the implanted TCP in vivo by the new bone tissue. Its excellent biocompatibility makes it a good candidate for making scaffolds because it allows bone regeneration and growth. Several β -TCP ceramics are commercially available, such as Orthograft[®] (Miter Inc.) and Osferion[®] (Olympus, Japan). When Osferion was implanted, β -TCP began to degrade and change in morphology at the bone defect site two months after the operation. New bone formation was seen at the periosteum. Eighteen months after operation, β -TCP was completely resorbed and replaced with new bone [118]. This result indicated the good bone formation ability of β -TCP ceramics.

7.2.3.3

Biphasic Calcium Phosphate

A combination of HA and β -TCP presents a new type of bioceramics, the biphasic calcium phosphate (BCP) [119]. The resorption rate of HA in physiological environments is very low while β -TCP has a relatively fast dissolution profile. The dissolution rate can be controlled by adjusting the ratio between HA and β -TCP due to the different resorption rate of HA and β -TCP [120]. Selecting the appropriate blend of both calcium phosphates, the mixture gradually dissolves in the physiological environment, releasing Ca^{2+} and PO_4^{3-}

7 ions and inducing bioactive behavior. Also, the mechanical properties of the BCP mixture were shown to be higher than those of the single phases [121].

Very few established methods exist for biphasic nano-composite synthesis and BCP. However, there are many different individual approaches for HA and β -TCP synthesis. Since BCP is the composite of HAP and β -TCP, its chemical properties are determined by the ratio of HAP to β -TCP. Avijit Kumar Guha et al. used a PVA mediated method to synthesize CaP bioceramic nanoparticles carried out to produce three different biphasic compositions having HA/ β -TCP ratios with 50:50, 55:45 and 60:40 respectively. They found that the biphasic system facilitates a series of signaling cascades in osteoblast division and differentiation. Samples having 50% HA and 50% β -TCP seem to be best for optimal mesenchymal cell attachment and proliferation [122]. Physical mixtures of HA and β -TCP cannot achieve the homogenous mixture of both and attain the expected properties. To obtain a more homogeneous BCP, other methods employ calcium-deficient apatite and its transformation to BCP upon sintering. N. Rameshbabu et al. used microwave heat treatment of CDHAs with different Ca/P molar ratios to prepare nanostructured BCPs with the desired HA/TCP ratio. They demonstrated the usefulness of microwave heat treatment to prepare nanostructured BCP ceramics. It is possible to finely tune the solubility as well as the biological lifetime of the BCPs by varying the HA/ β -TCP ratios [123]. Yamada et al. [124] prepared a BCP with various HA/ β -TCP ratios by calcining calcium-deficient apatite with different Ca/P ratios at 950°C for 2 h. The calcium-deficient apatite was prepared by an aqueous precipitation or hydrolysis of various calcium phosphate compounds. Obviously, the final HA/ β -TCP ratio in BCP depends on the preparation parameters, such as the pH value and the concentration of the hydrolysis agent. Bouler et al. [125] reported that the final HA/ β -TCP ratio was greatly affected by NaOH concentration and DCPD/solution volume ratio by the hydrolysis method.

7.3 Applications of Calcium Phosphate Ceramics

7.3.1 Bioactive Cement

Bioactive cements are important not only for the reconstruction of bone defects but also for the fixation of medical devices to osseous tissue. Cement originates from inorganic materials that harden during the setting period. It is often applied in the industrial field. Some biocompatible organic polymers have also been used in the medical field, such as poly (methyl methacrylate) (PMMA). However, unlike PMMA cements, calcium phosphate cements do not harden through a polymerization reaction and only a small amount of heat is released. In addition, the volume of CPC stays almost constant during the setting reaction. This kind of bioactive cement includes calcium phosphate bone cements and bioactive glass cements.

7.3.1.1

Calcium Phosphate Bone Cements

Calcium phosphate bone cements first appeared in literature during the 1980s. These materials offer the potential for in situ molding and injectability. Monma and Kanazawa [126] found that α -TCP was set to form calcium-deficient HA with a Ca/P molar ratio of 1.5 when α -TCP was hydrated in water at 60–100°C and at a pH between 8.1 and 11.4. Chow reported that a mixture of tetracalcium phosphate (TTCP) and dicalcium phosphate anhydrous (DCPA) or its dihydrate (DCPD) sets to form apatite in a much shorter period, 30–60 min at physiological temperature [127].

Calcium phosphate bone cements usually consist of one or more starting calcium phosphate powders and an aqueous solution, which are mixed together to form a paste that sets at room and body temperature. Upon mixing, the calcium phosphate powders dissolve and precipitate into a less soluble calcium phosphate. During the precipitation reaction, the calcium phosphate crystals grow and become entangled, thus providing a mechanical rigidity to the cement. There are three different endproducts of calcium phosphate precipitate [128]: apatite, brushite (DCPD), and amorphous calcium phosphate (ACP). The ACP cement will rapidly convert into apatite. Therefore, there are two categories of cement: (1) apatite CPC and (2) brushite CPC.

Since bone cement is a paste before setting, it can be conveniently injected from a syringe and filled directly into a bone defect. There are many factors affecting the injectability of the cement, such as the powder-to-liquid ratio, the type and concentration of gelling agent, the particle size of the powder and so on. If the powder is in a small spherical form, the injectability will be significantly improved [129, 130]. After setting, most CPCs have a tensile strength of 1–10 MPa, whereas the compression strength varies from 10 to 100 MPa. Therefore, CPCs can only be used in combination with metal implants or in low or non-load bearing applications. Most commercial products have a porosity of around 50 vol%. The pore size is close to 1 μm . Thus, the pores are too small to allow fast bone ingrowth and the CPC degrades layer-by-layer.

7.3.1.2

Bioactive Glass Cement

The development of bioactive glass bone cements is another research area in the medical field. These cements can be prepared using bioactive glass powders. The bioactive glass cement mainly consists of Ca–Mg–Si–P glass elements. Several studies have proven that bioactive glasses which contained SiO_2 , Na_2O , CaO and P_2O_5 are able to bond to bone through a Ca–P-rich layer as a result of a biological response at the tissue-material interface [131]. These bioactive glass cements can be injected into a surgical site or molded into putty and placed directly into the surgical site. The bioactive cement has been used in 30 clinical cases at Kyoto University to fix hip prostheses since 1993 [118]. Results were quite satisfactory and no adverse effects occurred. However, the clinical application is still limited because of its poor ductility and high rigidity.

7.3.2

7.3.2 Porous Bioceramic Scaffolds for Bone Tissue Engineering

Bioceramics are available in various physical forms – particles or blocks; dense or porous. There is a great need in clinics to develop bone tissue-engineering scaffolds and bone filler materials that can be used in the reconstruction of large orthopaedic defects and for the fixation of orthopaedic implants. The bone has excellent regenerative ability. Therefore, bone defects can be rectified by supplying the void space with bioresorbable ceramics to induce bone tissue regeneration. Bone tissue engineering aims to use the scaffold to either induce the formation of bone from surrounding tissue or to act as a carrier or template for implanted bone cells or other biomolecular agents. A porous scaffold will act as a temporary matrix for cell proliferation and extracellular matrix deposition. Moreover, it would also act as a template for the vascularization of neo-tissue and act as a biomolecular reservoir for releasing growth factors in the regenerative process [132].

Scaffolds must possess open pores. It is ideal for a scaffold to have a fully interconnected porous structure with large surface area to volume ratios, which will allow cell in-growth and nutrient transport. Porosity and interconnectivity are very critical for new bony tissue formation. However, there is always a tradeoff between the porosity needed for bone ingrowth and the mechanical properties of the scaffold for handling and initial support after implantation. Therefore, a particular effort should be made to balance the porosity of a scaffold with the need for mechanical properties when implanted in the specific site.

Diverse techniques have been used to build porous ceramic scaffolds for tissue engineering. Saiz et al. used a replica template of polymer sponges to prepare porous HA scaffolds. This method involves the infiltration of a polymer sponge with ceramic slurry until the inner polymer walls are completely coated by the ceramic powders. Subsequently, the green body is fired to remove the polymer and form a ceramic skeleton that is strengthened by sintering at high temperature. The prepared scaffold exhibits a microstructure consisting of round interconnected alveoli around 100–200 μm wide [133].

Bohner used calcium phosphate emulsions to synthesize β -TCP macroporous scaffolds, leading to reproducible and controlled structures. The macropore size can be easily modified by adjusting the emulsifier concentration without modifying the total pore volume and microporosity. The mean diameters of the macropores range from 150 to 1,220 μm [134]. Deville reported that freeze casting was used to synthesize porous hydroxyapatite scaffolds with unusually high compressive strengths, e.g. up to 145 MPa for 47% porosity and 65 MPa for 56% porosity, which may be appropriate for some load-bearing applications. They investigated various parameters affecting porosity and compressive strength, including the initial slurry concentration, freezing rate, and sintering conditions [135]. However, most of the parameters offer only a very limited control of the porosity and are not suited for the fabrication of materials with complex shapes. Franco et al. [136] reported the preparation of ceramic-based inks for robotic-assisted deposition (robocasting) using Pluronic F-127 solutions. They used direct write assembly of calcium phosphate scaffolds using a water-based hydrogel. This method can be used to prepare HA, β -TCP and biphasic (HA/ β -TCP) scaffolds. This method encompasses a flexible fabrication technology that is able to tailor the scaffold chemistry and architecture for specific applications.

In order to achieve a structure similar to natural bone, extensive efforts have been made with encouraging results, including the various methods mentioned above in the development of highly porous scaffolds for bone regeneration. Although these efforts have been made, all porous ceramic scaffold materials have a common limitation: the inherent tradeoff between strength and porosity. Recently in our lab, we developed a new template-casting method that can be used to prepare completely interconnected, macroporous biodegradable β -tricalcium phosphate (β -TCP) scaffolds. One representative macroporous scaffold with interconnected pores is shown in Fig. 7.1. The TCP scaffolds of high porosity (80%) also exhibited high compressive strength (9.3 MPa) [137]. In addition, the architecture and chemistry of the scaffolds can be fully manipulated by varying the design of the templates and casting materials. Four types of macroporous scaffolds with different pore sizes and pore arrangements are demonstrated in Fig. 7.2. Furthermore, the template-casting method allows us to manipulate the porosity across the synthetic scaffold. A long-bone-like scaffold consists of a relatively dense peripheral zone and central porous zone and is shown in Fig. 7.3. The porous central area of the scaffold mimics the cancellous in porosity (approximately 73% porosity). The relatively dense peripheral area of the scaffold mimics the cortical bone in porosity (approximately 20% porosity). Moreover, the scaffolds prepared in our lab exhibit a mechanical strength equivalent to cortical bone [138] (Fig. 7.4). By means of optimizing electrical, physical, chemical, and biological guidance cues of the scaffold in a graded design, the scaffolds can be customized to patients' needs.

7.3.3

Ceramic-Based Composite Scaffold for Tissue Engineering and Drug Delivery

In bone tissue engineering research, cells and growth factors may need to be introduced into the scaffold to expedite tissue ingrowth and regeneration. However, cell proliferation is often encountered with difficulties due to a limited supply of nutrients at the center of the implants.

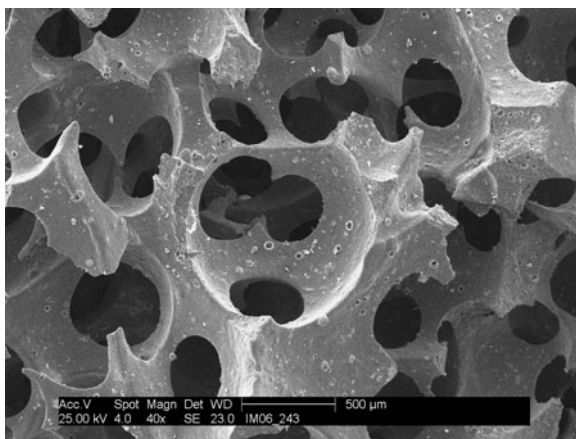


Fig. 7.1 SEM morphology of the scaffold prepared by the template-casting method

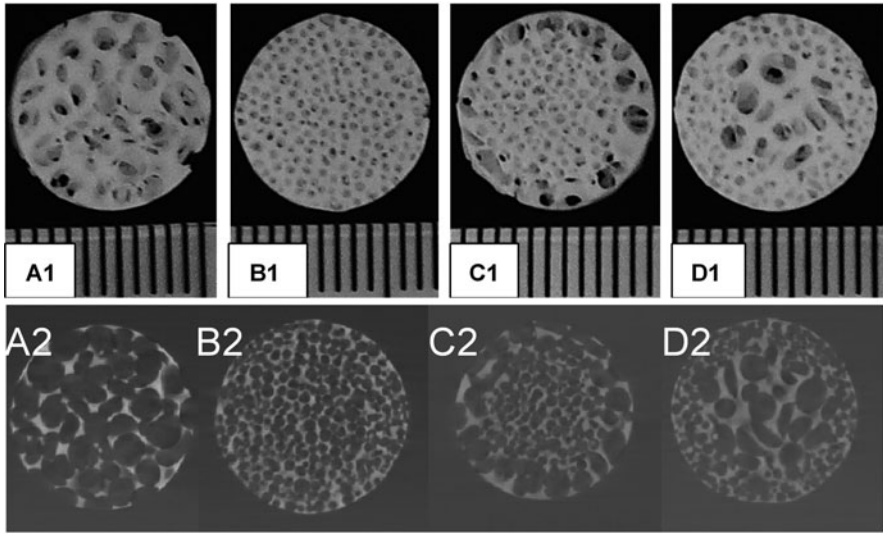


Fig. 7.2 Representative 3D digital images (A1, B1, C1 and D1) and 2D Micro CT images (A2, B2, C2 and D2) of the biodegradable β -TCP scaffolds by a template-casting method. (a) is the scaffolds with uniform big pores; (b) is the scaffolds with uniform small pores; (c) is the FGS with central small pores and peripheral big pores; (d) is the FGS with central big pores and peripheral small pores

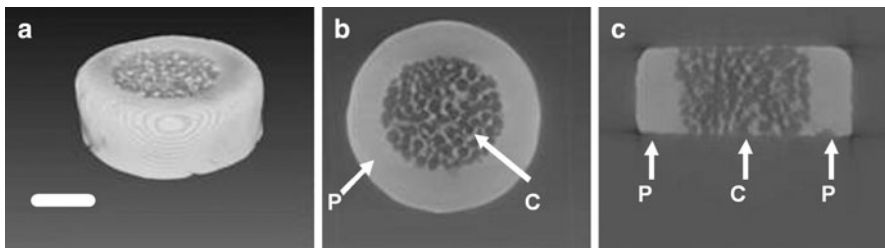


Fig. 7.3 Micro CT images of a long-bone-like β -TCP graded scaffold with Peripheral dense zone (P) and Central porous zone (C) with 600–800 μm pore size. (a) 3D image; (b) coronal view of 2D image; (c) Sagittal view of 2D image. Bar = 2 mm

Currently in bone tissue engineering, growth factors such as bone morphogenic protein-2 (BMP-2), basic fibroblast growth factor (bFGF), transforming growth factor (TGF- β), and vascular endothelial growth factor (VEGF) are commonly introduced into scaffolds due to their osteoinductive and vascularization properties. Ceramics have a high affinity for drugs and growth factors. Therefore, scaffolds can load these proteins just by physical absorption from a growth-factor containing solution. Due to the high affinity of CaP ceramics for proteins, ceramics can retain a high percentage of drug loading. However, sintered CaP ceramics often have low resorbability due to its crystalline architecture. The release pattern of protein from the loaded ceramics consists of an initial burst release followed by a specific

release dependent on the material or drug. Guicheux et al. [139] reported a rapid release within the first 48 h, followed by a slow sustained release of human growth hormone from a macroporous BCP ceramic loaded with 5 μg of drugs. Different release profiles and efficiencies depend on the type of growth factor and topomorphology of the ceramics. In one experiment in our lab, we loaded 10 μg BMP-2 into β -TCP scaffolds with different pore sizes and arrangements and implanted the BMP-2 impregnated β -TCP scaffolds subcutaneously. At one month after implantation, we evaluated the BMP-2 induced ectopic bone formation by histomorphometry. There were 4 types of scaffolds shown in Fig. 7.2. Scaffold A was a scaffold with uniform 600–800 μm big pores; Scaffold B was a scaffold with uniform 350–500 μm pores; Scaffold C was a graded scaffold with central 350–500 μm pores and peripheral 600–800 μm pores; Scaffold D was a graded scaffold with central 600–800 μm pores and peripheral 350–500 μm pores. Table 7.2 lists the histomorphometrical results of bone formation. The graded scaffolds with central 600–800 μm pores and peripheral 350–500 μm pores exhibited significantly greater bone formation compared to those uniform scaffolds with 600–800 μm pores ($P = 0.04089$) and those graded scaffolds with central 350–500 μm pores and peripheral 600–800 μm pores ($P = 0.03345$). The uniform scaffolds with 350–500 μm pores exhibited no significantly different bone formation compared to those with 600–800 μm pores ($P = 0.53853$) and those graded scaffolds with central 350–500 μm pores and peripheral 600–800 μm pores ($P = 0.69125$). This

Fig. 7.4 Compressive strength of human cortical bone, and bone-like β -TCP graded scaffolds with central 73% porosity and peripheral 20% porosity

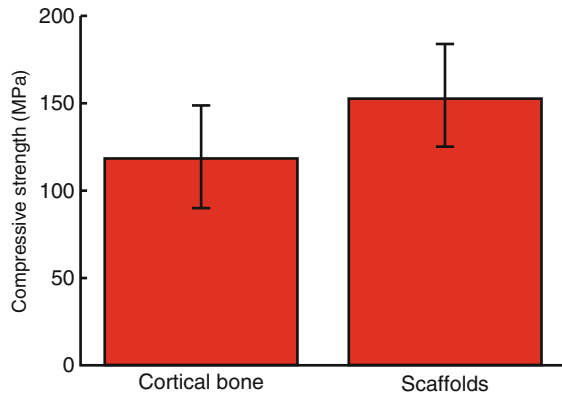


Table 7.2 Histomorphometrical analysis results of BMP-2 induced ectopic bone formation in porous β -TCP scaffolds at one month after implantation

Scaffolds	Bone formation (%)
Scaffolds A	13.20 \pm 3.88 ^a
Scaffolds B	8.62 \pm 11.30
Graded scaffolds C	11.62 \pm 4.55 ^b
Graded scaffolds D	21.86 \pm 3.21 ^{a,b}

Note: a and b indicate significant differences ($p < 0.05$)

study has suggested that the pore arrangement and pore size do affect the release profiles of BMP-2, leading to varied bone formation. Further studies will be needed to verify the results and search for specific mechanisms.

Although ceramics have been widely used in the field of dentistry and orthopedics, there are some concerns with the ceramic scaffold, such as the relatively slow degradability of the material, low tensile strength and brittleness. More and more attention has been paid to composite scaffolds that imitate the natural structure of bone. The addition of polymer could provide the opportunity to change the degradability and physical/chemical properties of ceramics. There are several biodegradable and biocompatible polymers applied in tissue engineering and in drug delivery systems.

Poly(α -hydroxy ester)-based polymers such as polylactic acid (PLA), polyglycolic acid (PGA), poly-(lactic-co-glycolic) acid (PLGA) and poly- ϵ -caprolactone (PCL) have been well studied in drug delivery systems. The degradation rate of polymers can be tailored by changing the molecular weight, polymerization degree, and lactic/glycolic-ratio in the case of PLGA, thus modulating the release profile of drugs if they are used to deliver drugs. The degradation of this ester-backbone type polymer occurs through a hydrolysis reaction. Generally, glycolic acid residue degrades faster than polylactic acid. Therefore, the degradation rate of this type of polymer is in the following order: $PGA > PLGA > PLA > PCL$. To obtain different release profiles of drugs, different molecular weights of different polymers can be chosen. Acid degradation products of polymers might result in aseptic inflammation of tissues and the products' hydrophobicity can significantly affect cells penetrating into the scaffolds. Therefore, a well-defined polymer/bioceramic composite scaffold should combine the advantages of the two biomaterials. Extensive studies are focusing on combining HA, TCP and BCP as ceramic components in a PLLA, PLGA or PCL matrix to obtain altered degradation properties and mechanical properties. Navarro et al. [140] made a glass-ceramic particle/PLA scaffold by homogeneously mixing a glass-ceramic into a PLA solution, after which NaCl particles were added to create macroporosity in the scaffold. Zhang et al. [141] prepared highly porous composites (85.1–95.6%) of HA and PLLA/PLGA by solid–liquid phase separation and solvent sublimation of a polymer/HAP mixture in dioxane/water. Ambrosio et al. [142] prepared macroporous scaffolds by sintering composite CaP/PLGA microspheres where the CaP-phase was trapped inside the microspheres. Lee et al. [143] added TCP particles to chitosan sponges by freeze-drying and crosslinking a mixture of a chitosan solution and TCP. These scaffolds can load drugs by immersion into a drug-containing solution. The scaffold would release the drugs through an initial burst release, followed by a slow release rate. A PLGA polymeric system with VEGF was coated with bioactive glass, resulting in additive bone healing effects in a rat critical-sized defect [144]. These results outline a promising approach to enhance bone healing in hypovascularized defects.

Porous blocks of calcium hydroxyapatite have been studied as delivery systems for the sustained release of antibiotics. The bactericidal activity of the drug has not been affected by its incorporation in the ceramic devices. Kim et al. [145] loaded tetracycline hydrochloride into HA-polycaprolactone composites with 87% porosity. In vitro release indicated a 7-day duration of release. Beta tricalcium phosphate beads carrying gentamicin and vancomycin have been studied as a resorbable bone substitute in rabbits induced with osteomyelitis. Ciprofloxacin-loaded tricalcium phosphate ceramic capsules exhibited long-term release of the antibiotic and showed good biocompatibility and degraded gradually in in vitro studies

[146]. Antibiotic-impregnated hydroxyapatite has also been used to treat patients with chronic osteomyelitis after removing necrotic tissue [147]. These studies show that bioceramics have immense potential for delivering drugs in tissue engineering.

7.4 Bioceramics for Cancer Therapy

7.4.1 Bioceramics for Radiation Therapy

Radiation therapy is used for cancer treatment. However, a drawback to this method is that normal cells are exposed undesirably to radiation. Other methods such as chemotherapy and immunotherapy do not have this drawback. It is obviously desirable therefore to develop a treatment for cancer that can destroy only the cancer cells and allow normal tissue to regenerate after treatment. In radiation therapy, an insufficient dose of radiation is often received by the cancer, which is especially true for deep-seated cancers, while healthy tissue is harmed by irradiation. However, ceramic microspheres may potentially solve this problem. It has been reported that 20–30 μm diameter $17\text{Y}_2\text{O}_3\text{--}19\text{Al}_2\text{O}_3\text{--}64\text{SiO}_2$ (mol%) glass microspheres are useful for the in situ irradiation of cancers, since Yttrium-89 (^{89}Y) is radioactivated by neutrons to radiate β -rays, which has half-life of 64.1 h. When injected in the target organ of the cancer, they become trapped inside small blood vessels in the tumors and block the nutritional supply to the tumor, thus providing a large localized dose of β -rays in tumors. However, since the yttrium content of the glass in the microspheres is only 17 mol%, the dose of β -rays from these glass microspheres is not enough. Fortunately, Kawashita et al. used a high-frequency induction thermal plasma flame method to fabricate cubic Y_2O_3 microspheres 20–30 μm in diameter to increase the yttrium content in the microspheres [148]. Simultaneously, they prepared microspheres composed mainly of YPO_4 crystals with some accompanying Y_2O_3 crystals in the plasma flame technique. Although both the Y_2O_3 and YPO_4 microspheres showed high chemical durability in saline solutions buffered at $\text{pH} = 6$ and 7, the use of Y_2O_3 microspheres for radiation therapy is yet to be approved for clinical use.

7.4.2 Bioceramics for Hyperthermia Therapy for Cancer

Magnetic induction hyperthermia is a technique for destroying cancer cells with the use of a magnetic field. Hyperthermia treatment of cancer consists of heating tumors up to temperatures between 43 and 47°C. This method aims to heat-destroy cancer cells by increasing the temperature, but at the same time, this method could potentially damage normal cells too if the high temperature is not localized within the tumor. The main drawback of hyperthermia is the difficulty of reaching and controlling those temperatures at the tumor site. For this reason, this treatment is difficult to use for deep-seated tumors from the clinical point of view. This therapy will be effective in combination with conventional cancer therapies such

as chemotherapy and radiotherapy. Ruiz-Hernández synthesized a biphasic material from mixtures of a magnetic glass ceramic and a bioactive sol-gel glass [149]. Preliminary heating tests have shown that the magnetic glass ceramic content under consideration was sufficient to reach hyperthermia temperature ranges for hyperthermia treatment of bone tumors. Presently, a number of ferromagnetic glass ceramic systems have been developed for this purpose, such as $\text{FeO-Fe}_2\text{O}_3\text{-CaO-SiO}_2$, $\text{ZnO-Fe}_2\text{O}_3\text{-CaO-SiO}_2$, $\text{SiO}_2\text{-Na}_2\text{O-CaO-P}_2\text{O}_5\text{-FeO-Fe}_2\text{O}_3$, $\text{Li}_2\text{O-MnO}_2\text{-CaO-P}_2\text{O}_5\text{-SiO}_2$, $\text{Fe}_2\text{O}_3\text{-CaO-ZnO-SiO}_2\text{-B}_2\text{O}_3$, magnetite/hydroxyapatite composite. However, further studies are yet to be performed for the clinical application [150].

7.5 Bioceramics for Dental Application

Ceramics have been widely used in dentistry. They are the key materials for dental restorations due to their ability to mimic the optical characteristics of enamel and dentin, their aesthetics, chemical inertness and biocompatibility. Ceramics used in dentistry include feldspathic porcelain, glass-ceramics, glass-infiltrated alumina, and zirconia. However, only feldspathic porcelains are currently used to approximate the appearance and functioning of natural teeth either as a veneer for metal-ceramic or full ceramic restorations and are used in direct contact against opposing teeth during oral functions [151]. Dental porcelain has been used as artificial porcelain teeth in complete or partial dentures, porcelain crowns or inlays, and dental cement. Interest in inlay and veneer porcelain materials have developed as a result of increased demand for aesthetic restorations.

There are two restoration systems for the dental material: full-ceramic and metal-ceramic systems. Full-ceramic systems can provide a better esthetic result than metal-ceramics for a wider range of patients because a wide range of translucency–opacity can be achieved with commercially available ceramic systems. The primary advantage to using a full-ceramic restoration is increased translucency correlated with improved esthetics. The opaque porcelain masking a metal substrate reflects light and decreases translucency. The advantages of metal-ceramic systems lie in their predictable structural performance and their versatility. The structural performance of metal-ceramic systems remains far better than that of any all-ceramic system. However, in the metal-ceramic system, the mismatch of thermal expansion coefficients of the porcelain and the alloy is a major issue. In this system, the ceramic is fused on the metallic substrate or metal crown. The porcelain is bonded to a metal crown by firing. Good adhesion depends on the interface bond strength between metal and ceramic, which is an important factor on the adhesion. However, there are also other factors that determine the bond strength between metal and ceramic. The important point about this ceramic-fused-metal system is that fused porcelain should wet the alloy surface. To match the thermal expansion coefficient of porcelain and alloy, sodium and potassium oxides are added into the ceramic powder to increase the thermal expansion coefficient, as the metal usually has a larger thermal expansion coefficient than that of the porcelain.

Dental ceramics that best mimic the optical properties of enamel and dentin are predominantly glassy materials. To improve mechanical properties, filler particles are often added

to the base glass composition. Adding the filler ceramic particles can also control optical effects such as opalescence, color, and opacity. The first fillers to be used in dental ceramics contained particles of a crystalline mineral called leucite, which is used in relatively low concentrations in porcelains for metal-ceramic systems and in higher concentrations as a strengthening filler in numerous all-ceramic systems. This filler was added to create porcelains that could be successfully fired onto metal substructures. Improved strength will be achieved by mechanically mixing crystalline filler particles into glass before firing so that the appropriate fillers are uniformly dispersed. Most highly esthetic ceramics are filled glass composites based on aluminosilicate glasses derived from mined feldspathic minerals [152].

The demands for tooth-colored restorations and the availability of new types of dental ceramics have driven increased use of ceramic materials in a variety of restorative situations. New ceramic materials have been used both as high strength core materials and as veneers. New stable glass ceramics, heat-pressed glass ceramics, and machinable glass ceramics are also used in dentistry. These bring in the need for further studies and clinical observations in order to apply these materials in the proper manner.

7.6 Future Trends

In the past few decades, bioceramics have been increasingly used in clinical applications due to their quality of disease treatment and excellent biocompatibility. Bioceramics as bulk materials have mainly been used in non-load bearing anatomical sites. However, the intrinsic brittleness of bioactive glasses and calcium phosphates impairs their clinical use in load-bearing applications and makes it difficult for surgeons to handle. Therefore, the mechanical performance of existing bioactive ceramics would have to be improved in order to satisfy the clinical setting needs. In order to achieve less brittle bone substitutes, it is necessary to incorporate tougher materials, for example, polyester polymers to the ceramic matrix. Such a combination would take advantage of the stiffness and toughness of polymers and ceramics since the natural bone consists of the mineralized collagen fibril, an organic–inorganic composite. However, the natural bone is a highly organized composite with a sophisticated hierarchical structure. A large effort needed for developing this organic–inorganic composite system with biomimetic hierarchical structure and enhanced functionality before successful clinical use. This effort can be made through a polymer matrix approach [153–155] or ceramic-based strategy [156, 157]. Some studies have attempted a biomimetic approach, mimicking the natural structure of bone. However, neither self-assembled mineralized collagen (bottom-up) [158] nor a structure made of sintered ceramic with polymer (top-down) [159] offer the structural features of bone that is “brick-and-mortar” [160] with a complex structure of apatite and collagen.

In addition to the high mechanical strength of bioceramics for easy handling and load-bearing applications, its workability is also very important since surgeons often need to shape the bioceramics during surgery. Unfortunately, the workability of bioceramics is low due to low flexibility. Moreover, shaping the bioceramics may affect their reliability.

Therefore, the toughness of bioceramics would also need to be improved in order to successfully applied in the medical field.

Bioinert ceramics aim at restoring function by providing a mechanical substitute to natural bone and joints. Second generation bioactive ceramics are aimed just at bone repair by improving biomineralization. Therefore, bioceramics scaffolds in tissue engineering should possess properties that would provide an adequate signal to guide and accelerate bone cells and stem cells to perform their regeneration processes in vivo. An ideal scaffold should be able to sustain mechanical loading and also transmit signals to the cells [2]. It is not clear whether there is a certain signal pathway involving the bone mineral in collagen [161]. For bone and teeth tissue engineering, further effort needs to be made to better understand the fundamentals of bone response to specific signals in tissue repair and regeneration processes. It is only then that we will be able to design and develop better bioceramics in the future.

Acknowledgments We would like to acknowledge the grant support from the Wallace H. Coulter Foundation, the March of Dimes Birth Defect Foundation, the Airlift Research Foundation, DOD W81XWH-10-1-0966, and NIH R01AR057837.

References

1. Kalita SJ, Bhardwaj A, Bhatt HA. Nanocrystalline calcium phosphate ceramics in biomedical engineering. *Mater Sci Eng C* 2007;27:441–49.
2. Chevalier J, Gremillard L. Ceramics for medical applications: A picture for the next 20 years. *J Eur Ceram Soc* 2009;29:1245–55.
3. Rieger W. Ceramics in orthopedics – 30 years of evolution and experience, in World tribology forum in arthroplasty, C Rieker, S Oberholzer and U Wyss, eds. Hans Huber Verlag, Bern, Suisse, 2001
4. Miller JA, Talton JD, Bhatia S. Total hip replacement: metal-on-metal systems. In *Clinical performance of Skeletal Prostheses*, LL Hench and J Wilson, eds. Chapman and Hall, London, 1996, pp. 41–56.
5. Hulbert S. The use of alumina and zirconia in surgical implants, in *An introduction to bioceramics*, LL Hench and Wilson J, eds. World Scientific, Singapore, 1993, pp. 125–38
6. Schmalzried TP, Kwong LM, Jasty M, et al. The mechanism of loosening of cemented acetabular components in total hip arthroplasty. Analysis of specimens retrieved at autopsy. *Clin Orthop* 1992;274:60–78.
7. Schmalzried TP, Guttman D, Grecula M, Amstutz HC. The relationship between the design, position and articular wear of acetabular components inserted without cement and the development of pelvic osteolysis. *J Bone Joint Surg* 1994;76A:677–88.
8. Manley MT, Serekian P. Wear debris. *Clin Orthop Related Res* 1994;298:137–46.
9. Jahnke K, Plester D, Heimke G. Experiences with Al₂O₃-ceramic middle ear implants, *Biomaterials* 1983; 4:137–8.
10. Boutin P, Christel P, Dorlot J-M, Meunier A, de Roquancourt A, Blanquaert D, Herman S, Sedel L, Witvoet J. The use of dense alumina–alumina ceramic combination in total hip replacement. *J Biomed Mater Res* 1988;22:1203–32.
11. Campbell P, Doorn P, Dorey F, Amstutz H. Wear and morphology of ultra-high molecular weight polyethylene wear particles from total hip replacements. *Proc Inst Mech Eng H* 1996;210:167–74.

12. Goodman S, Aspenberg P, Song Y, Knoblich G, Huie P, Regula D, Lidgren L. Tissue ingrowth and differentiation in the boneharvest chamber in the presence of cobalt chromium alloy and high density polyethylene particles. *J Bone Joint Surg* 1995;77A:1025–35.
13. Howie DW, Vernon-Roberts B, Oakshott R, Manthey B. A rat model of resorption of bone at the cement–bone interface in the presence of polyethylene wear particles. *J Bone Joint Surg* 1988;70A:257–63.
14. Willert HG, Semlitsch M. Reactions of the articular capsule to wear products of artificial joint prostheses. *J Biomed Mater Res* 1977;11:157–64.
15. Schmalzried TP, Jasty M, Harris WH. Periprosthetic bone loss in total hip arthroplasty: polyethylene wear debris and the concept of the effective joint space. *J Bone Joint Surg* 1992;74A: 849–63.
16. Amstutz HC, Campbell P, Kossovsky N, Clarke IC. Mechanism and clinical significance of wear debris-induced osteolysis. *Clin Orthop* 1992;276:7–18.
17. Murray DW, Rushton N. Macrophages stimulate bone resorption when they phagocytose particles. *J Bone Joint Surg* 1990;72B:988–92.
18. Jiranek WA, Machado M, Jasty M. Production of cytokines around loosened cemented acetabular components. Analysis with immunohistochemical techniques and in situ hybridization. *J Bone Joint Surg* 1993;75A:863–79.
19. Hamadouche M, Boutin P, Daussange J, Bolander ME, Sedel L. Alumina-on-alumina total hip arthroplasty: a minimum 18.5-years follow-up study. *J Bone Joint Surg Am* 2002;84:69–77.
20. Yoo JJ, Kim YM, Yoon KS, Koo KH, Song WS, Kim HJ. Alumina-on-alumina total hip arthroplasty a five-year minimum follow-up study. *J Bone Joint Surg Am* 2005;87:530–5.
21. Dorlot JM. Long-term effects of alumina components in total hip prostheses. *Clin Orthop Relat Res* 1992;282:47–52.
22. Catelas I, Petit A, Marchand R, Zukor DJ, Yahia L, Huk OL. Cytotoxicity and macrophage cytokine release induced by ceramic and polyethylene particles in vitro. *J Bone Joint Surg Br* 1999; 81:516–21.
23. Villermaux F. Zirconia-alumina as the new generation of ceramic-ceramic THR: wear performance evaluation including extreme life conditions. Proceedings of 6th World Biomaterials Congress, Workshop on Zirconia Femoral Heads for Total Hip Prostheses, Kamuela, Hawaii, USA: Society for Biomaterials, 2000
24. Lawn B. Fracture of brittle solids, Cambridge solid state science series 2nd ed. UK: Cambridge university press, 1993:378
25. Campbell P, Shen FW, McKellop H. Biologic and tribologic considerations of alternative bearing surfaces. *Clin Orthop* 2004;418:98–111
26. Heros R, Willmann G. Ceramics in total hip arthroplasty: history, mechanical properties, clinical results and current manufacturing state of the art *Semin Arthroplasty* 1998; 9:114–22.
27. Yoon TR, Rowe SM, Jung ST, Seon KJ, Maloney WJ. Osteolysis in association with a total hip arthroplasty with ceramic bearing surfaces, *J Bone Joint Surg* 1998;80A:1459–68.
28. Mahoney OM, Dimon III JH. Unsatisfactory results with a ceramic total hip prosthesis. *J Bone Joint Surg* 1990;72A:663–671
29. Wirganowicz PZ, Thomas BJ. Massive osteolysis after ceramic on ceramic total hip arthroplasty. *Clin Orthop Relat Res* 1997;338:100–4.
30. Garcia-Cimbrello E, Martinez-Sayanes JM, Minuesa A, Munuera L. Mittelmeier ceramic-on-ceramic hip prosthesis after 10 years. *J Arthroplasty* 1996;11:773–81.
31. Mittelmeier H, Heisel J. Sixteen-years' experience with ceramic hip prostheses. *Clin Orthop* 1992;282:64–72.
32. Willmann G. Ceramic femoral head retrieval data, *Clin Orthop* 2000;379:173–7.
33. Piconi C, Maccauro G. Zirconia as a ceramic biomaterial: a review. *Biomaterials* 1999;20:1–25.

34. Nasser S, Campbell PA, Kilgus D, Kossovsky N, Amstutz HC. Cementless total joint arthroplasty prostheses with titanium–alloy articular surfaces. A human retrieval analysis. *Clin Orthop Relat Res* 1990; 261:171–85.
35. Sabokbar A, Fujikawa Y, Murray DW, Athanasou NA. Bisphosphonates in bone cement inhibit PMMA particle induced bone resorption. *Ann Rheum Dis* 1998;57:614–8.
36. Ingham E, Green TR, Stone MH, Kowalski R, Watkins N, Fisher J. Production of TNF-alpha and bone resorbing activity by macrophages in response to different types of bone cement particles. *Biomaterials* 2000; 21: 1005–13.
37. Horowitz SM, Purdon MA. Mediator interactions in macrophage/particulate bone resorption. *J Biomed Mater Res* 1995;29:477–84.
38. Chevalier J. What future for zirconia as a biomaterial? *Biomaterials* 2006;27:535–43.
39. Gowen M, Wood DD, Ihrie EJ, McGuire MK, Russell RG. An interleukin 1 like factor stimulates bone resorption in vitro. *Nature* 1983;306:378–80.
40. Bertolini DR, Nedwin GE, Bringman TS, Smith DD, Mundy GR. Stimulation of bone resorption and inhibition of bone formation in vitro by human tumor necrosis factors. *Nature* 1986;319:516–18.
41. Chevalier J, Gremillard L, Deville S. Low-temperature degradation of zirconia and implications for biomedical implants. *Annu Rev Mater Res* 2007;37:1–32.
42. Schubert H, Frey F. Stability of Y-TZP during hydrothermal treatment: neutron experiments and stability considerations. *J Eur Ceram Soc* 2005;25:1597–602.
43. Affatato S, Goldoni M, Testoni M, Toni A. Mixed-oxides prosthetic ceramic ball heads Part 3: effect of the ZrO₂ fraction on the wear of ceramic on ceramic hip joint prostheses. A long-term in vitro wear study. *Biomaterials* 2001; 22:717–23.
44. De Aza AH, Chevalier J, Fantozzi G, Schehl M, Torrecillas R. Crack growth resistance of alumina, zirconia and zirconia toughened alumina ceramics for joint prostheses. *Biomaterials* 2002; 23:937–45.
45. Fabris S, Paxton AT, Finnis MW. A stabilization mechanism of zirconia based on oxygen vacancies only. *Acta Mater* 2002;50:5171–8.
46. Tsipas SA. Effect of dopants on the phase stability of zirconia-based plasma sprayed thermal barrier coatings. *J Eur Ceramic Soc* 2010;30:61–72.
47. Porter DL, Heuer AH. Mechanism of toughening partially stabilized zirconia PSZ. *J Am Ceram Soc* 1977; 60:183–4.
48. Virkar AV, Matsumoto RLK. Ferroelastic domain switching as a toughening mechanism in tetragonal zirconia. *J Am Ceram Soc* 1986;69:224–6.
49. Mehta K, Virkar AV. Fracture mechanisms in ferroelectric-ferroelastic lead zirconate titanate Zr:Ti = 054:046; *Ceramics*. *J Am Ceram Soc* 1990;73:567–74.
50. Nawa M, Nakamoto S, Sekino T, Niihara K. Tough and strong Ce-TZP/Alumina nanocomposites doped with titania. *Ceram Int* 1998;24:497–506
51. Fischer J, Stawarczyk B, Trottmann A, Hämmerle CHF. Impact of thermal properties of veneering ceramics on the fracture load of layered Ce-TZP/A nanocomposite frameworks. *Dent Mater* 2009;25:326–30.
52. Fischer J, Stawarczyk B. Compatibility of machined Ce-TZP/Al₂O₃ nanocomposite and a veneering ceramic. *Dent Mater* 2007;23:1500–5.
53. WU S, Brook RJ. Sintering additives for zirconia ceramics. *Trans J Br Ceram Soc* 1983; 82:260–4.
54. Brito-Chaparro JA, Aguilar-Elguezabal A, Echeberria J, Bocanegra-Bernal MH. Using high-purity MgO nanopowder as a stabilizer in two different particle size monoclinic ZrO₂: its influence on the fracture toughness. *Mater Chem Phys* 2009;114:407–14.
55. Yang Y, Liu Y, Park S, Kim H, Lee K, Koh J, Nanoscale bioactive surfaces and endosseous implantology, in *Nanoscience in Biomedicine*, D Shi, ed. Tsinghua University Press, Beijing and Springer-Verlag GmbH, Berlin, Heidelberg, 2009, pp. 428–50

56. Yang Y, Ran J, Zheng C. Preparation of DLC/stainless steel gradient film materials using magnetron sputtering plasma method, in 13th International symposium on plasma chemistry, symposium proceedings, C Wu, ed. Peking University Press, Beijing, China, III, 1997, pp. 1232–7.
57. Hench LL. Bioceramic. *J Am Ceram Soc* 1998;81:1705–28.
58. Hench LL. Bioceramics: from concept to clinic. *J Am Ceram Soc* 1991;74:1487–510.
59. Bromer H, Deutscher K, Blencke B, Pfeil E, Strunz V. Properties of the bioactive implant materials ‘Ceravital’. *Sci Ceram* 1977;9:219–25.
60. Gross UM, Strunz V. The anchoring of glass ceramics of different solubility in the femur of the rat. *J Biomed Mater Res* 1980;14:607–18.
61. Kokubo T, Shigematsu M, Nagashima Y, Tashiro M, Nakamura T, Yamamuro T. Apatite- and wollastonite-containing glass-ceramics for prosthetic applications. *Bull Inst Chem Res Kyoto Univ* 1982;60:260–8.
62. Gil-Albarova J, Salinas A, Bueno-Lozano AL, Romn J, Aldini-Nicolo N, García-Barea A, Giavaresi G, Fini M, Giardini R, Vallet-Regí M. The in vivo behaviour of a sol–gel glass and a glass-ceramic during critical diaphyseal bone defects healing. *Biomaterials* 2005;26:4374–82.
63. Rehman I, Hench LL, Bonfield W, Smith R. Analysis of surface layers on bioactive glasses. *Biomaterials* 1994;15:865–70.
64. Gheysen G, Ducheyne P, Hench LL, de Meester P. Bioglass composites: a potential material for dental application. *Biomaterials* 1983;4:81–4.
65. Arcos D, del Real RP, Vallet-Regí M. A novel bioactive and magnetic biphasic material. *Biomaterials* 2002;23:2151–8.
66. Ruiz E, Serrano MC, Arcos D, Vallet-Regí M. Glass-glass ceramic thermoseeds for hyperthermic treatment of bone tumors. *J Biomed Mater Res* 2006;79A:533–43.
67. Jarcho M. Calcium phosphate as biomaterials Properties and applications. *Dent Clin North Am* 1986;30:25–48.
68. Kent JN, Quinn JH, Zide MF, Finge IM, Jarcho M, Rothstein SS. Correction of alveolar ridge deficiencies with nonresorbable hydroxylapatite. *J Am Dent Assoc* 1982;105:993–1001.
69. Jarcho M. Calcium phosphate ceramics as hard tissue prosthetic. *Clin Orthop* 1981;157:259–60.
70. Wang JC, Ko CL, Hung CC, Tyan YC, Lai CH, Chen WC, Wang CK. Deriving fast setting properties of tetracalcium phosphate/dicalcium phosphate anhydrous bone cement with nanocrystallites on the reactant surfaces. *J Dent* 2010;38:158–65.
71. Tsai CH, Lin RM, Ju CP, Lin JHC. Bioresorption behavior of tetracalcium phosphate-derived calcium phosphate cement implanted in femur of rabbits. *Biomaterials* 2008;29:984–93.
72. Chow LC, Markovic M, Frukhtbeyn SA, Takagi S. Hydrolysis of tetracalcium phosphate under a near-constant-composition condition – effects of pH and particle size. *Biomaterials* 2005;26:393–401.
73. Guo DG, Xu KW, Han Y. Influence of cooling modes on purity of solid-state synthesized tetracalcium phosphate. *Mater Sci Eng B* 2005;116:175–81.
74. Blom EJ, Klein-Nulend J, Wolke JGC, Kurashina K, van Waas MAJ, Burger EH. Transforming growth factor- β 1 incorporation in an α -tricalcium phosphate/dicalcium phosphate dihydrate/tetracalcium phosphate monoxide cement: release characteristics and physicochemical properties. *Biomaterials* 2002;23:1261–8.
75. Tami AE, Leitner MM, Baucke MG, Mueller TL, Harry van Lenthe G, Müller Rh, Ito K. Hydroxyapatite particles maintain peri-implant bone mantle during osseointegration in osteoporotic bone. *Bone* 2009; 45:1117–24.
76. Sanosh KP, Chu MC, Balakrishnan A, Lee YJ, Kim TN, Cho SJ. Synthesis of nano hydroxyapatite powder that simulate teeth particle morphology and composition. *Curr Appl Phys* 2009;9:1459–62.

77. Langhorst SE, O'Donnell JNR, Skrtic D. In vitro remineralization of enamel by polymeric amorphous calcium phosphate composite: Quantitative microradiographic study. *Dent Mater* 2009;25:884–91.
78. Beniash E, Metzler RA, Lam RSK, Gilbert PUPA. Transient amorphous calcium phosphate in forming enamel. *J Struct Biol* 2009;166:133–43.
79. Maciejewski M, Brunner TJ, Loher SF, Stark WJ, Baiker A. Phase transitions in amorphous calcium phosphates with different Ca/P ratios. *Thermochim Acta* 2008;468:75–80.
80. Sanosh KP, Chu M-C, Balakrishnan A, Kim TN, Cho S-J. Sol-gel synthesis of pure nano sized β -tricalcium phosphate crystalline powders. *Curr Appl Phys* 2010;10:68–71.
81. Bohner M, Luginbühl R, Reber C, Doebelin N, Baroud G, Conforto E. A physical approach to modify the hydraulic reactivity of α -tricalcium phosphate powder. *Acta Biomater* 2009;5:3524–35.
82. Le Huec JC, Clément D, Aunoble S, Tournier C, Harmand MF. A brief summary of 15 years of research on beta-tricalcium phosphates. *SAS J* 2009;3:112–3.
83. Park YM, Ryu SC, Yoon SY, Stevens R, Park HC. Preparation of whisker-shaped hydroxyapatite/ β -tricalcium phosphate composite. *Mater Chem Phys* 2008;109:440–7.
84. Ishihara S, Matsumoto T, Onoki T, Sohmura T, Nakahira A. New concept bioceramics composed of octacalcium phosphate OCP; and dicarboxylic acid-intercalated OCP via hydrothermal hot-pressing. *Mater Sci Eng C* 2009;29:1885–8.
85. Arellano-Jiménez MJ, García-García R, Reyes-Gasga J. Synthesis and hydrolysis of octacalcium phosphate and its characterization by electron microscopy and X-ray diffraction. *J Phys Chem Solids* 2009;70:390–5.
86. Dekker RJ, de Bruijn JD, Stigter M, Barrere F, Layrolle P, van Blitterswijk CA. Bone tissue engineering on amorphous carbonated apatite and crystalline octacalcium phosphate-coated titanium discs. *Biomaterials* 2005;26:5231–9.
87. Oliveira C, Ferreira A, Rocha F. Dicalcium phosphate dihydrate precipitation: characterization and crystal growth. *Chem Eng Res Des* 2007;85:1655–61.
88. Xu JW, Butler IS, Gilson DFR. FT-Raman and high-pressure infrared spectroscopic studies of dicalcium phosphate dihydrate $\text{CaHPO}_4 \cdot 2\text{H}_2\text{O}$; and anhydrous dicalcium phosphate CaHPO_4 . *Spectrochim Acta A Mol Biomol Spectrosc* 1999;55:2801–9.
89. El Kady AM, Mohamed KR, El-Bassyouni GT. Fabrication, characterization and bioactivity evaluation of calcium pyrophosphate/polymeric biocomposites. *Ceram Int* 2009;35:2933–42.
90. Nicholas BD, Smith II JL, Kellman RM. Calcium pyrophosphate deposition of the temporomandibular joint with massive bony erosion. *J Oral Maxillofac Surg* 2007;65:2086–9.
91. Kasuga T. Bioactive calcium pyrophosphate glasses and glass-ceramics. *Acta Biomater* 2005;1:55–64.
92. Tudan C, Jackson JK, Higo TT, Hampong M, Pelech SL, Burt HM. Calcium pyrophosphate dihydrate crystal associated induction of neutrophil activation and repression of TNF- α -induced apoptosis is mediated by the p38 MAP kinase. *Cell Signal* 2004;16:211–21.
93. Vallet-Regí M, González-Calbet JM. Calcium phosphates as substitution of bone tissues. *Prog Solid State Chem* 2004;32:1–31.
94. Schmitz JP, Hollinger JO, Milam SB. Reconstruction of bone using calcium phosphate bone cements: a critical review. *J Oral Maxillofac Surg* 1999;57:1122–6.
95. Xu JW, Gilson DFR, Butler IS. FT-Raman and high-pressure FT-infrared spectroscopic investigation of monocalcium phosphate monohydrate, $\text{CaH}_2\text{PO}_4 \cdot 2\text{H}_2\text{O}$. *Spectrochim Acta A Mol Biomol Spectrosc* 1998;54:1869–78.
96. Jinawath S, Pongkao D, Suchanek W, Yoshimura M. Hydrothermal synthesis of monetite and hydroxyapatite from monocalcium phosphate monohydrate. *Int J Inorg Mater* 2001;3:997–1001.

97. Huan ZG, Chang J. Novel bioactive composite bone cements based on the β -tricalcium phosphate–monocalcium phosphate monohydrate composite cement system. *Acta Biomater* 2009;5:1253–64.
98. Jung Y, Kim SS, Kim YH, Kim SH, Kim BS, Kim S, Choi CY, Kim SH. A polylactic acid/calcium metaphosphate composite for bone tissue engineering. *Biomaterials* 2005;26:6314–22
99. Driessens FCM. Formation and stability of calcium phosphate in relation to the phase composition of the mineral in calcified tissue, in *Bioceramics of Calcium phosphate*, K DeGroot, ed. KCRC Press, Boca Raton, Florida, 1983
100. Liu DM, Troczynski T, Seng WJT. Water-based sol–gel synthesis of hydroxyapatite: process development. *Biomaterials* 2001;22:1721–30.
101. De Groot K, Klein CPAT, Wolke JGC, Blicek-Hogervorst JMA. Chemistry of calcium phosphate bioceramics, *CRC Handbook of Bioactive Ceramics, Calcium Phosphate and Hydroxylapatite Ceramics*, vol II. CRC press, Boca Raton, FL, 1990
102. Bow JS, Liou SC, Chen SY. Structural characterization of room-temperature synthesized nano-sized β -tricalcium phosphate. *Biomaterials* 2004;25:3155–61.
103. Liu HS, Chin TS, Lai LS, Chiu SY, Chung KH, Chang CS, Liu MT. Hydroxyapatite synthesized by a simplified hydrothermal method. *Ceram Int* 1997;23:19–25.
104. Lim GK, Wang J, Ng SC, Chew CH, Gan LM. Processing of hydroxyapatite via microemulsion and emulsion routes. *Biomaterials* 1997;18:1433–9.
105. Suchanek WL, Shuk P, Byrappa K, Riman RE, TenHuisen KS, Janas VF, Mechanochemical–hydrothermal synthesis of carbonated apatite powders at room temperature. *Biomaterials* 2002;23:699–710.
106. Wang F, Li MS, Lu YP, Qi YX. A simple sol–gel technique for preparing hydroxyapatite nanopowders. *Mater Lett* 2005;59:916–9.
107. Shih W, Chen YF, Wang MC, Hon MH. Crystal growth and morphology of the nano-sized hydroxyapatite powders synthesized from $\text{CaHPO}_4 \cdot 2\text{H}_2\text{O}$ and CaCO_3 by hydrolysis method. *J Cryst Growth* 2004;270:211–8.
108. Guo GS, Sun YX, Wang ZH, Guo HY. Preparation of hydroxyapatite nanoparticles by reverse microemulsion. *Ceram Int* 2005;31:869–72.
109. Gibson IR, Rehman I, Best SM, Bonfield W. Characterization of the transformation from calcium-deficient apatite to beta-tricalcium phosphate. *J Mater Sci Mater Med* 2000;12:799–804.
110. Oonishi H, Kushitani S, Iwaki H. Comparative bone formation in several kinds of bioceramic granules, in *Eighth international symposium on ceramics in medicine*, J Wilson, LL Hench, D Greenspan eds. Tokyo, Japan: Elsevier Science Ltd, 1995, pp. 137–144.
111. Kivrak N, Tas AC. Synthesis of calcium hydroxyapatite-tricalcium phosphate composite bioceramic powders and their sintering behavior. *J Am Ceram Soc* 1998;81:2245–52.
112. Okazaki M, Sato M. Computer graphics of hydroxyapatite and β -tricalcium phosphate. *Biomaterials* 1990;11:573–78.
113. Sanosh KP, Min-Cheol Chu, Balakrishnan A, Kim TN, Cho SJ. Sol–gel synthesis of pure nano sized β -tricalcium phosphate crystalline powders. *Curr Appl Phys* 2010;10:68–71.
114. Lin K, Chang J, Lu J, Wu W, Zeng Y. Properties of β - $\text{Ca}_3\text{PO}_4 \cdot 2$ bioceramics prepared using nano-size powders. *Ceram Int* 2007;33:979–85.
115. Dean-Mo L, Troczynski T, Tseng WJ. Water-based sol–gel synthesis of hydroxyapatite: process development. *Biomaterials* 2001;22:1721–30.
116. Pan Y, Huang JL, Shao CY. Preparation of β -TCP with high thermal stability by solid reaction routs. *J Mater Sci* 2003;38:1049–56.
117. Liou SC, Chen SY. Transformation mechanism of different chemically precipitated apatitic precursors into β -tricalcium phosphate upon calcinations. *Biomaterials* 2002;23:4541–7.
118. Ishikawa K, Matsuya S, *Bioceramics*. *Compr Struct Integr* 2007;9:169–214.

- 7
119. LeGeros RZ, Lin S, Rohanizadeh R, Mijares D, LeGeros JP. Biphasic calcium phosphate bioceramics: preparation, properties and applications. *J Mater Sci Mater Med* 2003;14: 201–9.
 120. Yamada S, Heymann D, Boulter JM, Duculsi G. Osteoclastic resorption of calcium phosphate ceramics with different hydroxyapatite/ β -tricalcium phosphate ratios. *Biomaterials* 1997;18:1037–41.
 121. Ruseska G, Fidanceska E, Bossert J. Mechanical and thermalexpansion characteristics of $\text{Ca}_{10}\text{PO}_4\text{OH};_2\text{-Ca}_3\text{PO}_4\text{;}_2$. *Sci Sintering* 38 2006;245–54.
 122. Guha AK, Singh S, Kumaresan R, Nayar S, Sinha A. Mesenchymal cell response to nanosized biphasic calcium phosphate composites. *Colloids Surf B Biointerfaces* 2009;73:146–51.
 123. Rameshbabu N, Prasad Rao K. Microwave synthesis, characterization and in-vitro evaluation of nanostructured biphasic calcium phosphates. *Curr Appl Phys* 2009;9:S29–S31.
 124. Yamada S, Heymann D, Boulter JM, Duculsi G. Osteoclastic resorption of biphasic calcium phosphate ceramic in vitro. *J Biomed Mater Res* 1997;37:346–52.
 125. Boulter JM, LeGeros RZ, Duculsi G. Biphasic calcium phosphates: influence of three synthesis parameters on the HA/ β -TCP ratio. *J Biomed Mater Res* 2000;51:680–84.
 126. Monma H, Ueno S, Kanazawa TT. Properties of hydroxyapatite prepared by the hydrolysis of tricalcium phosphate. *J Chem Tech Biotechnol* 1981;31:15–24.
 127. Takagi S, Chow LC, Ishikawa K. Formation of hydroxyapatite in new calcium phosphate cements. *Biomaterials* 1998;19:1593–9.
 128. Bohner M. Calcium phosphatem ceramic. *Injury* 2000;1:S-D37–47.
 129. Ueyama Y, Ishikawa K, Mano T, Koyama T, Matsumura T, Suzuki K. Initial tissue response to anti-washout apatite cement in the rat palatal region: comparison with conventional apatite cement. *J Biomed Mater Res* 2001;55:652–60.
 130. Yuasa T, Miyamoto Y, Ishikawa K, Takechi M, Nagayama M, Suzuki K. In vitro resorption of three apatite cements with osteoclasts. *J Biomed Mater Res* 2001;54:344–50.
 131. Hench LL, Spinter RJ, Allen WC, Greenlee JTK. Bonding mechanisms at the interface of ceramic prosthetic materials. *J Biomed Mater Res* 1971;2:117–41.
 132. Langer R, Vacanti JP. Tissue engineering. *Science* 1993;260:920–26.
 133. Saiz E, Gremillard L, Menendez G, Miranda P, Gryn K, Tomsia AP. Preparation of porous hydroxyapatite scaffolds. *Mat Sci Eng C Bio* 2007;S27:546–50.
 134. Bohner M, Hvan Lenthe G, Grunenfelder S, Hirsiger W, Evison R, Muller R. Synthesis and characterization of porous beta-tricalcium phosphate blocks. *Biomaterials* 2005;26:6099–105.
 135. Deville S, Saiz E, Tomsia AP. Freeze casting of hydroxyapatite scaffolds for bone tissue engineering. *Biomaterials* 2006;27:5480–9.
 136. Franco J, Hunger P, Launey ME, Tomsia AP, Saiz E. Direct write assembly of calcium phosphate scaffolds using a water-based hydrogel. *Acta Biomater* 2010;6:218–28.
 137. Liu YX, Kim JH, Young D, Kim SW, Nishimoto SK, Yang YZ. Novel template-casting technique for fabricating β -tricalcium phosphate scaffolds with high interconnectivity and mechanical strength and in vitro cell responses. *J Biomed Mater Res A* 2010;92A:997–1006.
 138. An YH, Friedman RJ. Animal models of bone defect repair. Boca Raton, FL: CRC Press LLC, 1999, pp. 241–60.
 139. Guicheux J, Gauthier O, Aguado E, Heymann D, Pilet P, Couillard S, Faivre A, Duculsi G. Growth hormone-loaded macroporous calcium phosphate ceramic: in vitro biopharmaceutical characterization and preliminary in vivo study. *J Biomed Mater Res* 1998;40:560–6.
 140. Navarro M, Ginebra MP, Planell JA, Zepetelli S, Ambrosio L. Development and cell response of a new biodegradable composite scaffold for guided bone regeneration. *J Mater Sci Mater Med* 2004;15:419–22.
 141. Zhang R, Ma PX. Poly α -hydroxyl acids/hydroxyapatite porous composites for bone–tissue engineering I Preparation and morphology. *J Biomed Mater Res* 1999;44:446–55.

142. Ambrosio AMA, Sahota JS, Khan Y, Laurencin CT. A novel amorphous calcium phosphate polymer ceramic for bone repair: I synthesis and characterization. *J Biomed Mater Res B Appl Biomater* 2001;58:295–301.
143. Lee YM, Park YJ, Lee SJ, Ku Y, Han SB, Choi SM, Klokkevold PR, Chung CP. Tissue engineered bone formation using chitosan/tricalcium phosphate sponges. *J Periodontol* 2000;71:410–17.
144. Leach JK, Kaigler D, Wang Z, Krebsbach PH, Mooney DJ. Coating of VEGF-releasing scaffolds with bioactive glass for angiogenesis and bone regeneration. *Biomaterials* 2006;27:3249–55.
145. Kim HW, Knowles JC, Kim HE. Hydroxyapatite/polyε-caprolactone; composite coatings on hydroxyapatite porous bone scaffold for drug delivery. *Biomaterials* 2004;25:1279–87.
146. Wu H, Zheng O, Du J, Yan Y, Liu C. New drug delivery system ciprofloxacin/tricalcium phosphate delivery capsule CTDC; and its in vitro drug release pattern. *J Tongji Med Univ* 1997;17:160–4.
147. Yamashita Y, Uchida A, Yamakawa T, Shinto Y, Araki N, Kato K. Treatment of chronic osteomyelitis using calcium hydroxyapatite ceramic implants impregnated with antibiotic. *Int Orthop* 1998;22:247–51.
148. Erbe EM, Day DE. Chemical durability of $Y_2O_3-Al_2O_3-SiO_2$ glasses for the in vivo delivery of beta radiation. *J Biomed Mater Res* 1987;27:1301–8.
149. Ruiz-Hernandez E, Serrano MC, Arcos D, Vallet-Regí M. Glass-glass ceramic thermoseeds for hyperthermic treatment of bone tumors. *J Biomed Mater Res A* 2006; 79:533–43.
150. SSAqlain A, Hashmi MU, Alam S, Shamim A. Magnetic and bioactivity evaluation of ferrimagnetic $ZnFe_2O_4$ containing glass ceramics for the hyperthermia treatment of cancer. *J Magnet and Magnetic Mater* 2010;322:375–81.
151. Yu HY, Cai ZB, Ren PD, Zhu MH, Zhou ZR. Friction and wear behavior of dental feldspathic porcelain. *Wear* 2006;261:611–21.
152. Kelly JR. Dental ceramics: current thinking and trends. *Dent Clin North Am* 2004;48:513–30.
153. JBlaker J, Maquet V, Jérôme R, Boccaccini AR, Nazhat SN. Mechanical properties of highly porous PDLA/Bioglass® composite foams as scaffolds for bone tissue engineering. *Acta Biomater* 2005;1:643–52.
154. Hasegawa S, Tamura J, Neo M, Goto K, Shikinami Y, Saito M, Kita M, Nakamura T. In vivo evaluation of a porous hydroxyapatite/poly-dl-lactide composite for use as a bone substitute. *J Biomed Mater Res* 2005;75A:567–79.
155. Niemelä T, Niiranen H, Kellomäki M, Törmälä P. Self-reinforced composites of bioabsorbable polymer and bioactive glass with different bioactive glass contents Part I Initial mechanical properties and bioactivity. *Acta Biomater* 2005;1:235–42.
156. Abdala AA, Milius DL, Adamson DH, Aksay IAA, Prud'homme RK. Inspired by abalone shell: strengthening of porous ceramics with polymers. *Polym Mater Sci Eng* 2004;90:384–5.
157. Peroglio M, Gremillard L, Chevalier J, Chazeau L, Gauthier C, Hamaide T. Toughening of bio-ceramics scaffolds by polymer coating. *J Eur Ceram Soc* 2007;27:2679–85.
158. Cui FZ, Li Y, Ge J. Self-assembly of mineralized collagen composites. *Mater Sci Eng R* 2007; R57:1–27.
159. Chen QZ, Boccaccini AR. Poly(D,L-lactic acid) coated 45S5 Bioglass®-based scaffolds: processing and characterization. *J Biomed Mater Res A* 2006;77A:445–57.
160. Munch E, Launey ME, Alsem DH, Saiz E, Tomsia AP, Ritchie RO. Tough, bio-inspired hybrid materials. *Science* 2008;322:1516–20.
161. Vallet-Regí M. Evolution of bioceramics within the field of biomaterials. *C R Chimie* 2010;13:174–85.

Elyssa L. Monzack, Karien J. Rodriguez, Chloe M. McCoy, Xiaoxiao Gu,
and Kristyn S. Masters

Contents

8.1	Introduction	210
8.2	Concepts in Material Development	210
8.2.1	Collagen and Gelatin	212
8.2.2	Fibrin	213
8.2.3	Elastin	214
8.2.4	Hyaluronic Acid	215
8.2.5	Silk	216
8.2.6	Alginate	217
8.2.7	Chitosan	219
8.3	Review of Previous Work	220
8.3.1	Collagen and Gelatin	220
8.3.2	Fibrin	223
8.3.3	Silk	224
8.3.4	Elastin	225
8.3.5	Hyaluronic Acid	227
8.3.6	Alginate	229
8.3.7	Chitosan	230
8.4	Future Directions	232
	References	233

Abstract Materials derived from natural sources are used extensively in tissue engineering. Consisting of proteins, polysaccharides, or ceramics, these materials may be harvested from a wide range of sources and possess an equally wide range of physical and biological properties. This chapter focuses upon seven of these materials, namely collagen, fibrin, elastin, hyaluronic acid, alginate, chitosan, and silk. These materials are first discussed with respect to their intrinsic features that are relevant to tissue engineering, such as structure, source, degradation, mechanics, immunogenicity, and recognition by cells. This is followed by a review of techniques for derivatizing natural materials, forming scaffolds, and tailoring these scaffolds, accompanied by select examples of how these natural materials have been

K.S. Masters (✉)

Department of Biomedical Engineering, University of Wisconsin, 1550 Engineering Drive, #2152,
Madison, WI 53706, USA
e-mail: kmasters@wisc.edu

used in tissue engineering applications. While natural materials possess many characteristics that render them attractive for use in tissue engineering, they are also accompanied by some unique challenges; both of these features are highlighted in this chapter.

Keywords Chemical modification • Extracellular matrix • Polysaccharides • Scaffold fabrication

8.1 Introduction

The majority of the initial documented instances of modern tissue engineering involved the use of biomaterials derived from natural sources [1]. In 1979, Drs. John Burke and Ioannis Yannas described the use of modified collagen-glycosaminoglycan scaffolds to form an artificial skin substitute [2]. Meanwhile, also in 1979, Dr. Eugene Bell documented the contraction of collagen gels by fibroblasts [3] and later expanded this work to smooth muscle cells to develop an early version of a tissue-engineered vascular graft [4].

Although other natural materials are relative newcomers to the field of tissue engineering, they have often seen use as biomaterials or in various medical applications for decades. For instance, fibrin patches were used during World War I to stop bleeding, and then soon employed as a biological adhesive by the 1940s [5]. The use of silk as a suture material dates back centuries [6], while coral was first investigated as a bone graft material in the 1970s [7].

The sources and characteristics of these natural materials cover a wide spectrum, as illustrated in Fig. 8.1. They may be derived from our own bodies, or may come from insects, marine life, or plants. They may be isolated from their source in the form of a chain of simple polysaccharides, or they may already be fully-formed porous scaffolds. Their physical forms may range from elastic hydrogels to brittle ceramics, and their degradation can span anywhere from hours to years.

It should be no surprise that such a diversity of materials would find use in the equally diverse field of tissue engineering, where applications span tissues with wide-ranging needs and characteristics. In the following sections, we will discuss some of these biomaterials, first reviewing their origins and properties, and then briefly delving into their current and future use in tissue engineering.

8.2 Concepts in Material Development

Numerous considerations contribute to the selection or design of a biomaterial for use in any given tissue engineering application. Whether natural or synthetic, the material must conform to the specifications of the application, possessing the mechanical properties, pore structure, degradation time, and other characteristics that yield the desirable tissue repair outcomes. However, the use of natural materials is often accompanied by unique obstacles that are not commonly a concern with synthetic materials.

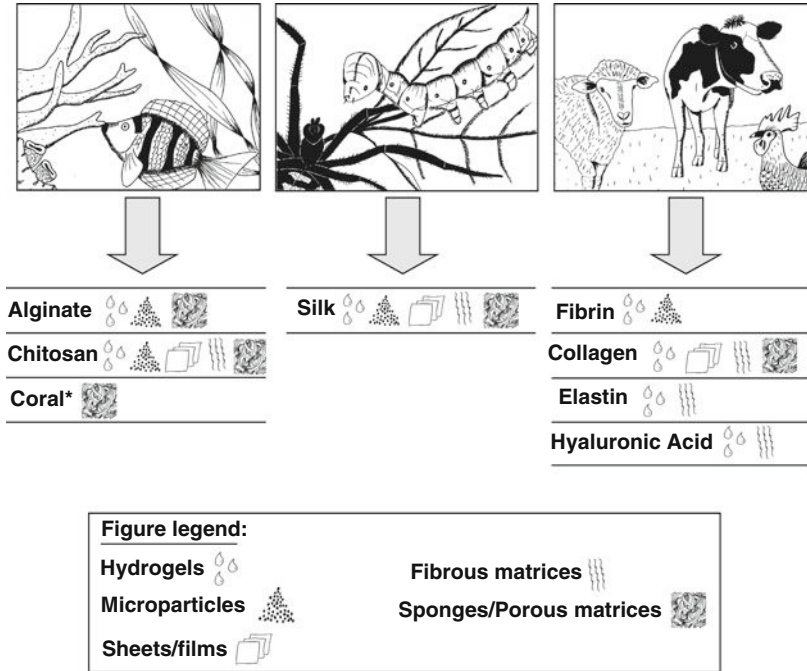


Fig. 8.1 Natural materials can be derived from a range of sources, including marine organisms, insects, birds, and mammals. As indicated by the illustrated legend next to each material, these materials can be fabricated into numerous types of scaffolds for use in tissue engineering applications. The indicated scaffold types represent those most commonly explored for tissue engineering applications and do not encompass the full range of processing options available for each material. *Coral is a ceramic natural material that is discussed in a separate chapter which focuses exclusively on ceramics. (Original artwork by E.L. Monzack)

While natural materials possess attractive biological properties, they are often more difficult to chemically or physically modify than synthetic materials. A reduced ability to tailor the structures of these materials can introduce challenges in achieving prospective design of biomaterials for tissue engineering applications. Many advances have been made in designing modification techniques for natural materials, although the range of applications of some natural materials remains restricted by their inherent structural limitations.

Another unique challenge in the use of natural materials is the availability of the material source. Derived from the natural world, these materials are sometimes limited in supply or synthesized by mechanisms that are difficult to maintain in a production environment or scale-up for commercial use. Ease of production can be further complicated by the greater likelihood of batch-to-batch variability experienced with biologically-derived polymers. Moreover, even in instances where source availability and production capacity obstacles have been overcome, such as material derivation from other mammals, disease transmission and immunogenicity often remain a concern.

However, the intrinsic bioactivity of many natural materials frequently offsets the aforementioned challenges. Unlike synthetic materials, which, in general, are biologically

passive, many natural materials possess sequences that are specifically recognized by cells and tissues in the body. The complexity of these interactions and the manner in which they regulate tissue repair and function is not completely understood, and can therefore not yet be fully mimicked through the use of synthetic materials. Moreover, most natural materials are readily degradable via native physiological mechanisms, a characteristic which facilitates tissue growth, repair, and integration. The enzymatic degradation of many natural materials can enable tissue growth and scaffold degradation to occur on similar time scales, leading to improved tissue regeneration.

In the following paragraphs, we discuss seven types of natural materials used in tissue engineering applications, focusing upon their native functions in nature and their characteristics as biomaterials. For each material, we discuss several attributes that are of particular interest in material selection for tissue engineering, namely source, structure, degradation, immunogenicity, mechanics, and recognition by cells. Section 8.3 will focus upon the creation of scaffolds from these materials and their implementation in various tissue engineering applications.

8.2.1

Collagen and Gelatin

Collagen is the most abundant protein in humans, accounting for nearly one third of all proteins in the body [8]. Its primary function is to maintain the structural integrity of the extracellular matrix (ECM) in body tissues [9–11]. In addition to playing a structural role in the ECM, collagen also interacts directly with the extracellular environment by influencing cellular adhesion, growth, and differentiation, responding to soluble factors during tissue remodelling and repair, and participating in wound healing processes and platelet aggregation [12, 13]. Because collagen plays such a dominant role in maintaining ECM integrity, it is a popular choice for tissue engineering applications that aim to restore structure and remodelling potential to tissue defects [13].

The primary structure of collagen is a polypeptide consisting of repeating Gly-X-Y residues, where X and Y are typically proline or hydroxyproline [11, 12, 14]. The rigid ring structures of proline and hydroxyproline amino acids contribute to the local secondary configuration of collagen, and the repeated triplet sequence adds stability to the overall polypeptide chain. This amino acid pattern allows for the formation of the molecular subunit tropocollagen, which consists of a unique tertiary conformation of three collagen chains held together in a triple helix by hydrogen bonds [8, 12]. The three polypeptide sequences in tropocollagen are termed α -chains and may exist as homotrimers or heterotrimers depending on the specific α -chain combinations [12]. Different combinations of chains result in different types of collagen specified for different functions in the body [15, 16]. There are 28 distinct types of collagen molecules identified to date [15], with types I, II, III, and IV being the most researched [11]. Type I is predominantly found in skin, tendon and bone and is the most widely used type of collagen in tissue engineering [17]. Type II is predominantly found in cartilage and intervertebral disks, type III forms reticular fibers and strengthens blood vessel walls, intestine, and uterus, and the nonfibrillar Type IV is found in basement membranes between epithelial and mesodermal tissues [16, 18]. The quaternary structure of collagen involves multiple triple helices packed into a microfibril lattice which

swells and shrinks substantially in response to changes in hydration. Changes in the pH of a collagen suspension can selectively and reversibly abolish this quaternary structure, while still preserving the triple helical structure [19].

Native collagen is normally degraded *in vivo* by mammalian collagenases into an N-terminal fragment and a C-terminal fragment [20]. These fragments are then spontaneously denatured to polypeptides that assume a random coil configuration referred to as gelatin [21]. Under physiological conditions, gelatin is further cleaved to oligopeptides. Synthetically, gelatin is generated by the denaturation of animal-derived collagen in the presence of a dilute acid [11]. Gelatin shares hemostatic properties with its precursor collagen, lacks significant antigenicity, and is easily crosslinked to form hydrogels that are capable of substantial swelling in aqueous environments [11, 21]. Uniquely, the processing of gelatin can be altered to produce products with varying isoelectric points which is useful for forming polyelectrolyte complexes with other polymers [11, 21]. These material characteristics make gelatin a prime candidate for tissue engineering and drug delivery applications where mechanical strength is not a priority and biodegradability is desired [11].

Collagen is a highly cell-adhesive protein, containing multiple discrete peptide sequences that are recognized by integrin receptors on the cell surface. Adhesion to collagen I in its native conformation is RGD-independent, with cells binding via $\alpha_1\beta_1$, $\alpha_{10}\beta_1$, $\alpha_{11}\beta_1$, and $\alpha_2\beta_1$ integrins, where the latter recognizes the collagen-specific DGEA sequence [22]. However, partial denaturation of collagen I reveals cryptic RGD motifs that can be recognized by $\alpha_5\beta_1$ and α_v -containing integrin receptors (i.e., $\alpha_v\beta_1$, $\alpha_v\beta_3$) [23, 24], thereby leading to significant differences in cell behavior depending upon the use of either native or denatured collagen substrates [25].

Commercial sources of collagen type I are most often derived from rat tail, bovine dermis, human placenta, or recombinant techniques. While animal-derived collagen can elicit immunogenic responses in recipients, the overall immunogenicity of this protein is considered relatively low due to its high sequence conservation across species as well as the low production of antibodies against collagen [26]. In general, most of the collagen sequential determinants are effectively protected by the collagen triple helix, with some determinants lying exposed on the non-helical ends of the collagen molecule. Therefore, when collagen is reduced to gelatin by collagenases, its sequential determinants are exposed for the brief period before gelatin itself is cleaved [26]. Thus, maintaining the tertiary triple helix during collagen processing can help minimize the exposure of these sequential determinants and reduce the amount of immunogenic response to the material.

8.2.2

Fibrin

The fibrillar protein fibrin plays a critical role in numerous physiological events, including blood clotting, inflammation, and wound healing. The glycoprotein fibrinogen and the enzyme thrombin are essential for the formation of fibrin, with calcium ions serving as key cofactors in the conversion of fibrinogen into fibrin. Fibrinogen is a hexameric glycoprotein composed of two sets of three different chains ($A\alpha$, $B\beta$, and γ), linked to

each other by disulfide bonds [27]. Thrombin (factor IIa) is a serine protease that is activated from its inactive form by factor Xa, in the presence of factor V [28]. In order to convert fibrinogen into fibrin, the activated thrombin cleaves two small peptides (fibrinopeptides A and B) from the amino-terminal ends of the α - and β -chains of fibrinogen, thus forming fibrin monomers that join together to form long fibrin strands via end-to-end polymerization that self-associate and precipitate [27]. Further crosslinking of the fibrin matrix may be achieved via factor XIIIa. Factor XIIIa is a transglutaminase activated by thrombin that covalently crosslinks the α - and γ -chains of the fibrin monomers by catalyzing reactions between lysine and glutamine residues. This additional crosslinking forms polymers between the fibrin chains, which can further stabilize the resulting fibrin material and impart greater mechanical strength and resistance to proteolysis [29].

In vivo, fibrin acts primarily as a provisional matrix often produced as a result of injury, and is ultimately replaced by other ECM components. Degradation of fibrin can be rapid and is accomplished via the proteolytic enzyme plasmin. Fibrin is one of the few biomaterials that can be derived from an autologous source. Fibrinogen and thrombin can be isolated from the blood plasma of the patient, avoiding complications such as disease transmission or immunogenicity [30]. With respect to tissue engineering, another attractive feature of fibrin is its ability to support cell adhesion, proliferation, and angiogenesis. The most established method of cell adhesion to fibrin occurs via interaction of the AGDV peptide on the γ -chains of fibrin with the $\alpha_{IIb}\beta_3$ integrin receptors on platelets [31]. RGD peptide sequences located on the α -chains of fibrin bind to several different integrin receptors on cell membranes [32, 33]. In addition to RGD, other adhesive peptides are believed to exist in fibrin(ogen), although their sequences have yet to be determined [32]. Commercial preparations of fibrinogen frequently contain other plasma proteins such as fibronectin, which also provide numerous cell adhesion moieties.

The interaction of fibrin with the $\alpha_v\beta_3$ receptor on endothelial cells is considered particularly crucial in the ability of fibrin to support or promote angiogenesis [34]. Moreover, fibrin possesses sites that recognize and bind certain growth factors, further contributing to the promotion of angiogenesis. Specifically, both basic fibroblast growth factor (bFGF) [35, 36] and vascular endothelial growth factor (VEGF) [37] bind to fibrinogen and fibrin with high affinity. These growth factors are pro-angiogenic and work in concert with endothelial cell binding to the $\alpha_v\beta_3$ integrin to promote vascularization, which is of critical importance for many tissue engineering strategies.

8.2.3

Elastin

Elastin is a highly hydrophobic ECM protein rich in glycine, proline, valine, and alanine that is found in almost all vertebrate animals and plays a critical role in the function of numerous tissues [38]. Elastin is the major component of elastic fibers (>90%), with microfibrils consisting of various acidic glycoproteins comprising the remaining component of the fibers [39]. Tropoelastin, the soluble elastin monomer, is synthesized in the rough endoplasmic reticulum and then secreted into the extracellular space where it first

goes through coacervation, followed by crosslinking at lysine residues by the copper-requiring enzyme lysyl oxidase to form the insoluble polymer elastin [38–41]. Deposition of elastin into the extracellular matrix is guided by the aforementioned glycoprotein microfibrils, which serve as a scaffold for polymer alignment [40].

Elastin imparts elastic recoil and resilience to many body tissues such as large arterial blood vessels, elastic ligaments, lungs, and skin [41]. Depending upon the source, it may have a half-life of several decades and can withstand millions of cycles of extension and recoil without failure [42, 43]. Natural degradation of insoluble elastin can occur enzymatically via elastases and certain elastolytic matrix metalloproteinases, although the turnover rate of elastin remains very slow [38]. In addition to its role in providing macroscale structural integrity and elastic recoil, elastin also participates in the regulation of cell function, as elastin and elastin-derived peptides play a role in the proliferation, migration, differentiation and chemotaxis of various cell types [41, 44]. Elastin can control various cell functions via interaction with the $\alpha_v\beta_3$ integrin receptor as well as the non-integrin elastin-laminin receptor [45, 46].

Commercial sources of elastin commonly use bovine neck ligament as the elastin source, although elastin is also isolated from the lung, skin, or aorta of numerous mammals including humans, rats, rabbits, cows, mice, and pigs. As discussed further in Section 8.3, incorporation of elastin into biomaterials is usually accomplished using α -elastin, a soluble derivative of elastin, or recombinant elastin-derived polypeptides. Soluble α -elastin is achieved via hydrolysis of insoluble elastin in hot oxalic acid, followed by separation of coacervated α -elastin from the soluble β -elastin [47]. The resulting α -elastin is comprised of partially-crosslinked peptides with a wide range of molecular weights, but this soluble elastin product retains the basic amino acid structure of insoluble elastin and remains easier to isolate than tropoelastin [38]. Elastin-like polypeptides (ELPs) are synthetic structures that retain physical and mechanical properties similar to that of native elastin, in addition to supporting cell growth [48–50]. ELPs have also demonstrated excellent biocompatibility, with the human body unable to differentiate ELPs from endogenous elastin [51].

8.2.4

Hyaluronic Acid

Hyaluronic acid (HA), also known as hyaluronan, is a negatively charged, linear polysaccharide composed of N-acetylglucosamine and glucuronic acid that is found in all body tissues. Although HA is part of the glycosaminoglycan (GAG) family, it is non-sulfated and synthesized by HA synthases at the inner wall of the plasma membrane, rather than in the Golgi apparatus [52, 53]. After synthesis, HA is transported to the ECM without any further modifications. Furthermore, in contrast to other GAGs, HA has a high molecular mass, with disaccharide chains reaching up to several million Daltons [54], and it is not bound to a core protein. HA is readily soluble in water, and solutions of HA are highly viscoelastic [55].

Proteins and proteoglycans that exhibit binding interactions with HA are termed hyaladherins, and are further subdivided into matrix and cell-surface hyaladherins. Matrix

hyaladherins include the proteoglycans aggrecan and versican [56], while the most widely studied cell-surface hyaladherins are the hyaluronan receptor CD44 and the receptor for hyaluronic acid mediated motility (RHAMM or CD168) via which HA can regulate many cellular processes, such as proliferation and migration, in a molecular weight-dependent fashion [57, 58]. The ability of HA alone to support cell adhesion and spreading is cell type-dependent [55, 59].

In mammals, three types of enzymes may participate in the enzymatic degradation of HA: hyaluronidase, β -D-glucuronidase, and β -N-acetyl-hexosaminidase. The in vivo half-life of unmodified HA can be short, ranging from a few minutes in the blood to hours or days in skin and joints [60, 61]. The degradation behavior of HA is particularly important with respect to its biological functions, as the cellular response to HA varies with HA molecular weight. For instance, HA degradation products that are 4–20 disaccharides in length exhibit angiogenic properties [62], stimulating capillary growth, endothelial cell proliferation and migration, and tube formation [55]. Conversely, high molecular weight HA can actually inhibit angiogenic processes.

Although HA is widely known to provide tissue structure in cartilage and cushioning properties in joints, it also plays an important role in numerous other tissues, including the lung, kidney, brain, and heart valves [57]. HA possesses many properties that render it attractive for tissue engineering applications. Commercially, HA is readily available from several sources, including rooster comb extracts, human umbilical cords, and bacterial cultures [63], and is considered to be non-immunogenic [55]. As noted above, HA also regulates several biological processes that are of particular importance in tissue engineering, such as angiogenesis. HA inhibits the adhesion and aggregation of platelets, and these non-thrombogenic properties are highly desirable for blood-contacting biomaterial applications. Moreover, HA-rich matrices are involved in the morphogenesis of many tissues, so HA may be used as a scaffold in tissue engineering applications in an effort to mimic the native environment during organ/tissue development. In wound healing, the presence of a HA-rich matrix has been linked to a decrease in scarring [64]. Due to its polyionic structure, HA is also able to scavenge free radicals, and this action can mediate inflammation by imparting an antioxidant effect [64]. Lastly, as discussed in Sect. 8.3, HA can endure numerous types of chemical modifications to its structure in order to enable the development of diverse material structures.

8.2.5

Silk

Silks are protein polymers whose composition, structure, and properties are highly dependent upon their source. Although the *Bombyx mori* silkworm is the most common source of silk for biomaterial applications due to the silkworm's facile domestication and production abilities [65], it does not comprise the only natural source of silk. Aside from the silkworm, several other insects and animals produce silk, including honeybees, wasps, and ants [66], as well as mussels [67] and spiders (specifically, *Nephila clavipes*). With respect to tissue engineering applications, the prevalence of spider-derived silk closely follows that of silkworm silk, although the lower silk production capacity of spiders and challenges in

maintaining spider colonies offer significant obstacles to using this source [65, 68]. The following paragraphs will focus on the properties of silkworm and spider silk with respect to their biomaterial applications.

Silkworm silk is composed of a heavy (325 kDa) and light (25 kDa) chain of core proteins called fibroins, which are coated by sericin, a collection of sticky, glue-like proteins. Sericin maintains the physical structure of the fibroins in silkworm silk only and is generally absent in spider silk [69]. The presence of sericin is a critical issue in the use of silk as a biomaterial, as sericin has been associated with hypersensitivity reactions and poor biocompatibility; once the sericin has been removed, the immune response becomes similar to that found with other common biomaterials [69]. Silk is degradable over time periods of several months in vivo, primarily via proteolytic activity mediated by a foreign body response. However, the exact time course for degradation depends upon numerous factors, including the site of implantation, the mechanical properties of that site, the processing conditions of the silk, and the physical characteristics of the silk scaffold (i.e., porosity, roughness, type of scaffold structure) [69, 70]. Enzymes such as chymotrypsin, actinase, and carboxylase are also able to degrade silk proteins [70].

Fibroins from both *B. mori* (silkworm) and *N. clavipes* (spider) are natural block copolymers, with both hydrophobic and hydrophilic blocks. The hydrophobic blocks are composed of mostly repetitive amino acid sequences, while the sequences of the hydrophilic blocks tend to be more complex. Together, the combination of the hydrophobic and hydrophilic regions is what gives rise to the unique mechanical properties of silk, which include extreme strength (elastic modulus of 5–17 GPa), toughness, elasticity, and compression resistance [69, 71]. The ultimate tensile strength of silk ranges from approximately 500–900 MPa and is highly dependent on the hydrophobic regions, which tend to form β -sheets or crystals [65, 71]. However, the heavy and light chain structure of silkworm silk tends to form a weaker and less extensible fiber when compared to the dragline silk of spiders [68]. Also, *B. mori* produces only one type of silk, while a single spider is capable of producing eight different types of silk. In general, dragline silk, originating from the spider's Major Ampullate silk gland, has garnered the most attention with respect to mechanics, as it can absorb more energy preceding rupture than almost any common material [72].

8.2.6

Alginate

Alginic acid, also known as algin or alginate, is found in the cell walls of brown algae such as *Macrocystis pyrifera* (California), *Ascophyllum nodosum* (North Atlantic), and various types of *Laminaria* (North Atlantic). As shown in Fig. 8.2, alginate is a linear, unbranched block copolymer composed of variable ratios of 1–4 linked β -D-mannuronic acid (M) and α -L-guluronic acid (G) [73]. The copolymer blocks are either similar (i.e., MMMM or GGGG) or strictly alternating (i.e., GMGM), where the relative amount of the blocks and the M/G ratio are dependent upon the origin of the alginate [74]. In algae, alginate is present as the sodium, calcium, or magnesium salts of alginic acid. Because only the sodium salt is soluble in aqueous solution, alginate extraction processes generally focus on conversion of alginate salts to sodium alginate, removal of seaweed residues, and subsequent recovery of

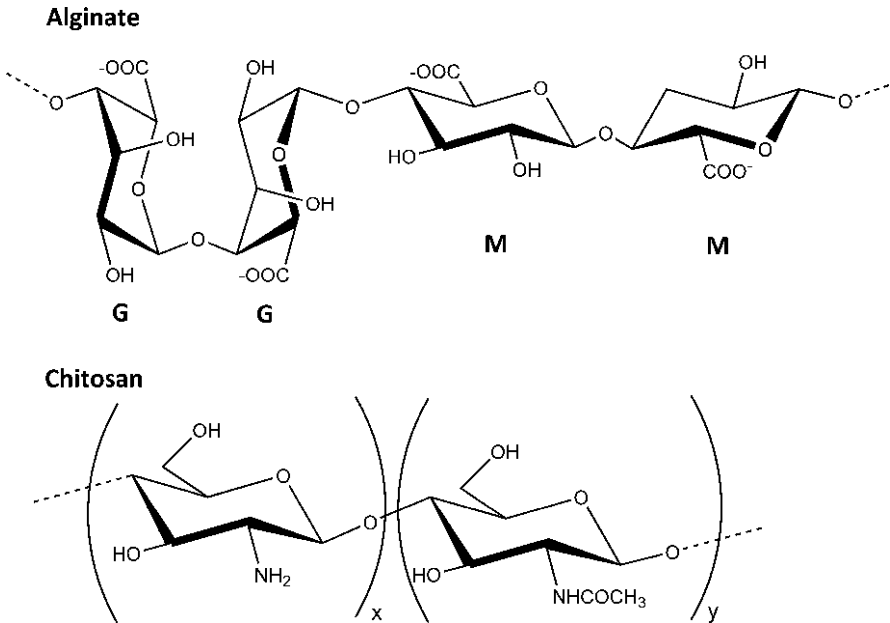


Fig. 8.2 *Top*: Chemical structure of alginate, a linear, unbranched block copolymer composed of variable ratios of 1-4 linked β -D-mannuronic acid (M) and α -L-guluronic acid (G). Alginate gelation occurs upon interaction of divalent cations (i.e., Ca^{2+}) with the carboxylic acid groups of two G blocks on adjacent polymer chains. *Bottom*: Chemical structure of chitosan, a linear polysaccharide composed of *N*-glucosamine and *N*-acetyl-glucosamine units linked by β (1-4) glycosidic bonds. The percentage of (x) units is known as the degree of deacetylation, where chitosan is composed predominantly of (x) units, while chitin is composed predominantly of (y) units

the sodium alginate from the aqueous solution via a variety of methods [75]. The molecular weight of sodium alginate is normally in the range of 50–100,000 Da.

Alginate is commonly used in paper manufacturing processes, pharmaceutical preparation, the food industry, and culinary arts. Its biocompatibility, abundance, low cost, and mild crosslinking mechanism have also led to the use of alginate in biomaterial and tissue engineering applications [76]. One highly attractive quality of alginate is its ability to rapidly form hydrogels upon exposure to divalent cations such as Ca^{2+} . These cations interact with the carboxylic acid groups on two G blocks on adjacent polymer chains, leading to the formation of a gel network. Because this network crosslinking is achieved simply with the addition of calcium, gelation can easily occur in the presence of cells or sensitive biomolecules. The block structure of the alginate strongly affects the physical properties of the resultant gels. For instance, because of the diaxial links found in guluronic acid residues, G blocks tend to be stiffer than M or alternating GM blocks [77]. These trends translate to species-dependent alginate properties, as *Ascophyllum* species tend to have a high M content, leading to the formation of softer gels, while sources such as *Laminaria hyperborea* tend to have a higher G content, yielding more rigid gels [74, 78].

Unlike many of the natural materials discussed in this chapter, however, alginate does not possess bioactive sequences that are recognized by cells or tissues. Thus, alginate is considered relatively inert, as cells do not readily adhere to unmodified alginate materials [76]. With respect to degradation, mammals cannot enzymatically degrade alginate chains; this task is accomplished by alginate lyases, which are found in algae, marine invertebrates, and marine and terrestrial microorganisms [79]. However, crosslinked alginate materials can be degraded by displacement of the crosslinking ions by chelating agents (such as citrate or EDTA) or by partial oxidation of alginate chains, resulting in increased susceptibility to hydrolysis [80].

8.2.7

Chitosan

Chitin, derived from the exoskeletons of crustaceans such as crab and shrimp, is the second most abundant natural polymer in the world after cellulose. N-deacetylation of the chitin molecule yields chitosan, a linear polysaccharide composed of *N*-glucosamine and *N*-acetyl-glucosamine units linked by $\beta(1-4)$ glycosidic bonds (Fig. 8.2). The glucosamine and *N*-acetyl-glucosamine units can be randomly or block distributed in the copolymer chain, with the glucosamine content referred to as the degree of deacetylation (DD) [81]. The properties of chitosan chains depend upon the source and the preparation procedure, with the molecular weight ranging from 50 to 1,000 kDa, and the DD ranging from 30 to 95% [81, 82]. Chitosan is normally insoluble in neutral or basic solutions, but soluble in dilute acids (pH < 6.0), as protonation of its amine groups facilitates the molecule's dissolution [81]. Moreover, the abundant hydroxyl and amino groups in chitosan provide reactive sites that allow for modification of the chitosan structure and characteristics.

The polycationic nature of chitosan has several biological consequences that are useful for tissue engineering applications. Unmodified chitosan does not contain elements that are specifically recognized by cellular receptors and does not support cell adhesion. However, chitosan's cationic chains can complex with several types of negatively-charged biomolecules or with DNA, yielding opportunities to enhance the biological activity of the chitosan scaffold or to protect molecules such as DNA from heat inactivation and nuclease degradation [83]. Anionic glycosaminoglycans such as heparin form ionic complexes with chitosan, thereby imparting upon the chitosan material the ability to bind heparin-binding proteins such as basic fibroblast growth factor [84], which plays an active role in the growth of many tissues. Chemical modification of chitosan can also provide alternative mechanisms for binding biomolecules to the chitosan structure [85], and will be discussed in Sect. 8.3. Interestingly, the cationic structure of chitosan may also be responsible for the unique antimicrobial properties of chitosan [81, 86], as the interaction of the cationic amino groups with the anionic microbial wall can suppress bacterial biosynthesis or disrupt mass transport across the cell wall. Chitosan confers antimicrobial activity across fungi as well as a broad spectrum of bacteria [81, 86].

In general, chitosan elicits a minimal foreign body reaction, with little or no fibrous encapsulation [82]. In fact, the interaction of chitosan oligosaccharides with immune cells may stimulate helpful wound healing processes such as cell proliferation and enhanced angiogenesis [81, 87]. In vivo, chitosan degrades by enzymatic hydrolysis. Lysozyme is the

primary enzyme responsible for degradation, as it hydrolyzes the acetylated residues, yielding chitosan oligosaccharides of varying lengths. The degradation time for chitosan ranges from weeks to months, with a strong dependence upon the DD of the chitosan. Highly deacetylated forms (>85% DD) exhibit the slowest degradation, whereas chains with a lower DD degrade more rapidly [81].

8.3 Review of Previous Work

Each tissue engineering application requires unique scaffold specifications in order to facilitate tissue repair or regeneration. Properties outlined in the previous section, such as material source, structure, degradation mechanism, and interaction with cells, can inform the selection of appropriate materials for a certain application. Moreover, these properties also affect the processing techniques that can be used with each material to yield scaffolds that possess different physical forms. As shown in Fig. 8.1, scaffolds may exist in many physical forms, ranging from hydrogels to microparticles to fibrous matrices. The select scaffold forms depicted in Fig. 8.1 represent those most commonly used specifically for tissue engineering applications of each material.

Tailoring of biomaterial properties is a critical step to achieve environments that are optimized for tissue growth and repair. The pore size, swelling, degradation rate, mechanics, fabrication mechanism, and bioactivity of scaffolds must be tailored to conform to the specifications of the desired tissue engineering application. Rarely do the intrinsic properties of an individual native biomaterial exactly match the properties needed for a certain tissue engineering application. Alteration of these features can require chemical or biological modification of the base material, adjustments to processing techniques, or copolymerization with other materials. The routes that may be taken to achieve such modifications vary with the type of material, with each material presenting unique advantages and challenges.

Thus, in this section, we focus on reviewing previous work in biomaterial modification and scaffold creation for the seven natural materials introduced earlier in this chapter. The following paragraphs concentrate on the types of scaffolds that may be created using each material and methods for tailoring the physical or biological properties of these scaffolds, with a few brief examples of how these materials have been used in tissue engineering applications (summarized in Fig. 8.3). The second section of this book describes the use of biomaterials in specific tissue engineering applications in greater detail.

8.3.1 Collagen and Gelatin

Collagen is a popular choice for medical applications, primarily due to its overall favorable properties of enzymatic degradability, general biocompatibility, versatile processing, and ability to be crosslinked [11]. It is because of these attributes that collagen has been used in

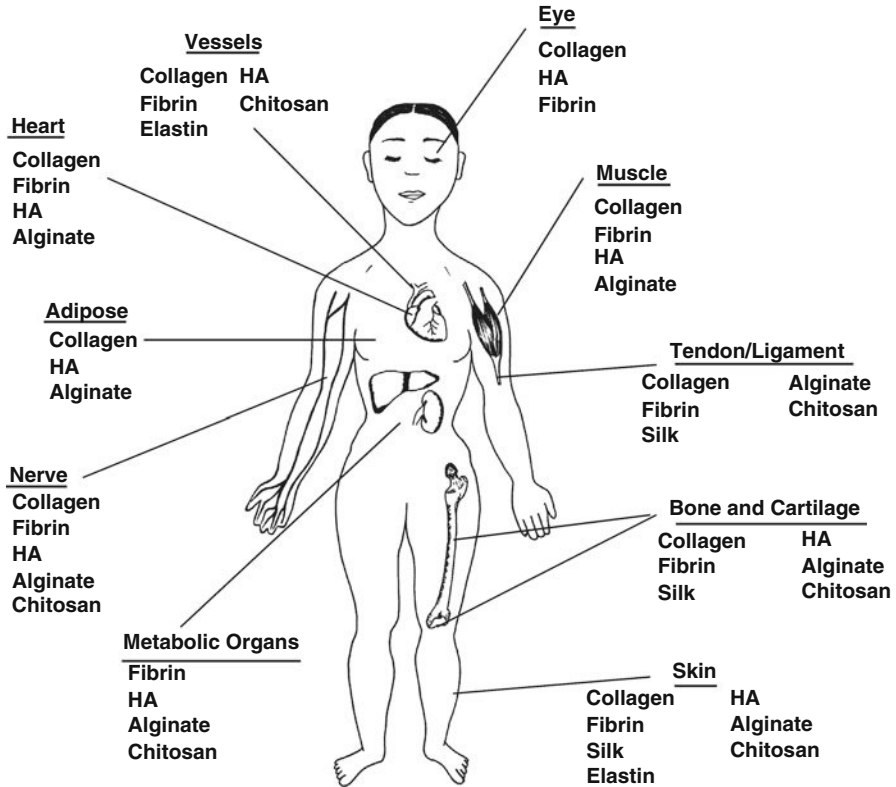


Fig. 8.3 Natural materials have numerous tissue engineering applications, ranging from structural to metabolic organs. This illustration depicts some of the more prevalent tissue engineering applications of the seven materials discussed in this chapter. (Original artwork by E.L. Monzack)

numerous forms for many different tissue engineering applications within the body (Fig. 8.3). Clinically, both animal- and human-derived collagens are FDA-approved for use as filler material in cosmetic procedures (i.e., Zyplast, Cosmoderm) and in dermal wound or burn dressings (i.e., Integra, Apligraf). Yet, some continuing concerns with the use of collagen as a biomaterial include its high cost of purification, potential for immunogenicity, transmission of animal-borne diseases, and product homogeneity for mass production and quality control of manufactured products [88, 89]. However, the use of recombinant collagens and gelatins in lieu of animal-derived collagen can eliminate many of the concerns of antigenicity and disease transmission associated with animal-derived collagen [18, 88, 89] and offer a scalable solution for the limited availability of the protein [12].

Processing of collagen biomaterials can be loosely classified into physical or chemical methods. The physical methods include drying, aging, emulsification, heating, or irradiating with UV or gamma rays [14, 90]. Each processing method produces unique mechanical and chemical properties in the collagen material. For example, one commonly used method of

inducing pore formation in collagen sponge constructs is by sublimation of a frozen suspension under a low-temperature vacuum [91]. This method allows for wide variation in pore structure based on the specific conditions of ice nucleation and growth. Freezing temperature is directly proportional to the average pore diameter, while the magnitude of the heat flux vector affects the orientation of pore channels [16, 91]. A porous collagen construct offers several biomaterial advantages including increased overall surface area and increased entry of cells and soluble factors into the material.

Collagen can also be formed into sponges, membranes, films, gels, and fibers using combinations of physical and chemical methods [14]. Fibrous collagen scaffolds are typically made by extracting insoluble fibers from native collagen matrices and reassembling them into a new biomaterial construct, while collagen hydrogels are simply made by adjusting purified fibrillar collagen solutions to a physiologic temperature and pH [12]. The resulting non-axial aligned fibers form a gel that can absorb large amounts of fluid which is advantageous for cell infiltration and microenvironment control [12].

Chemical modification of collagen has historically been performed via reaction with chromic acid or aldehyde fixation, both of which result in firm covalent crosslinks [14]. In tissue engineering, aldehyde fixation has been mainly used to increase the *in vivo* longevity and prolong the degradation time of collagen-based tissue implants. In addition, aldehyde fixation has also been shown to minimize the immune response to collagen implants and thus is an attractive method for use with materials made with animal-derived collagen [26]. Another effective technique for reducing collagen degradation *in vivo* is through dehydrative crosslinking which causes both collagen and gelatin to become insoluble through the introduction of interchain peptide bonds [92]. This is best accomplished by heating the collagen or gelatin suspension to temperatures in excess of 37°C, after decreasing the initial moisture content to prevent reversible melting of the helical structure by the high heat.

Because collagen can be converted to gelatin by heating above the helix-coil transition temperature (approximately 37°C for bovine collagen) it is important to consider this possibility within the context of the final desired product when processing a collagen-based biomaterial [16]. Unintentional conversion of collagen to gelatin can affect the degradation rate of the overall biomaterial *in vivo*, as gelatin degrades much more rapidly than collagen. To ensure quality control, infrared spectroscopic assays have been developed that assess gelatin content of collagen based on helical marker bands in the mid- and far infrared range [93].

The use of collagen as a scaffold biomaterial is accomplished through two main approaches, often termed top-down and bottom-up approaches [12]. In the top-down approach, the collagen matrix of an explanted tissue sample that exhibits a desired architecture is treated to remove all non-collagenous components and to strengthen the remaining collagen scaffold for further modification into a collagen heterograft [12, 14]. Examples of collagen-based explants first processed and then used as biomaterials include sutures (catgut is still used today [11]), blood vessels, porcine heart valves, and tendon cadaver-derived collagen scaffolds have been successfully implemented as dermal dressings for burn wounds due to their metabolically stable structure and ability to dynamically improve cellular adhesion and proliferation [11]. Further material modifications can also be used to better tailor a collagen matrix to a specific clinical requirement. Many collagen-based materials approved by the FDA, such as Integra, Apligraf, and Orcel, successfully combine

a collagen matrix with growth factors, small peptides (such as RGD) [94], cell seeding, and glycosaminoglycans to accelerate wound healing as skin substitutes [11].

The bottom-up approach starts with purified and solubilized collagen and crosslinks or re-forms the solution into a functional shape or scaffold which can then be further modified with cells or other molecules to form a reconstituted collagen construct [12]. The cell adhesive properties of collagen also make it useful for surface immobilization on scaffolds intended for cellular contact that may require bulk properties not provided by a collagen-based foundation [9]. Benefits of the bottom-up approach include a defined structure, ability to standardize side groups, ease of mass production, and many options for final product form such as fibers, membranes, gels, or sponges. Since collagen mainly provides structural support in its native environment, its ability to withstand tensile loads is often useful for applications which require structural integrity, such as tissue engineered bone, skin, and tendons [10, 11]. The FDA has approved many of these materials, such as a collagen and hydroxyapatite/tricalcium phosphate combination blend for use as a bone graft substitute [11]. Moreover, the use of collagen in tissue engineering is not confined to the aforementioned tissues, as collagen scaffolds can also support the repair or regeneration of nerve, cardiac, cornea, and vascular structures [15].

8.3.2

Fibrin

Clinically, fibrin has been widely used as a hemostatic agent or sealant in various surgical procedures. Numerous fibrin-based sealants, such as Tisseel, Evicel, and Crosseal, are FDA-approved for clinical use. In tissue engineering, fibrin is most often used in the form of hydrogels or fibrin glue. The ability to isolate fibrin scaffold components from an autologous source as well as the ability of fibrin to promote cell adhesion and angiogenesis supports its use as a scaffold material in tissue engineering, although the weak mechanical properties and rapid degradation of fibrin materials can introduce challenges in tissue engineering applications.

While the natural biodegradability of fibrin often serves as an advantage of these materials in tissue engineering, the rapid speed of this degradation has been considered a drawback. Several techniques have emerged to prolong the lifetime of fibrin matrices. As noted earlier, crosslinking via factor XIIIa can improve the resistance of fibrin to proteolysis; chemical crosslinkers such as genipin can also reinforce this effect [95]. Photochemical crosslinking of fibrinogen via the formation of dityrosine bonds has also been performed using ruthenium II trisbipyridyl chloride [96], resulting in materials with improved mechanics. The inhibition of proteolytic enzymes may also be used to address the issue of fibrin's rapid degradation. Proteolysis inhibitors such as aprotinin, or fibrinolysis inhibitors such as tranexamic acid or ϵ -aminocaproic acid, can also slow the degradation of fibrin scaffolds [97, 98], and may be delivered in tissue engineering applications in order to retain the fibrin structure for the length of time needed for effective tissue repair. The fabrication of fibrin microbeads via the delivery of concentrated fibrinogen and thrombin into a heated oil emulsion (75–80°C) and subsequent crosslinking with factor XIIIa has also been shown to

slow the fibrin degradation rate. These microbeads have exhibited particular promise for the culture and growth of mesenchymal stem cells [32].

The physical properties of fibrin scaffolds may also be controlled by varying the ionic strength and concentration of the fibrinogen and thrombin components. Although an increase in fibrinogen concentration leads to an increase in the number of fiber bundles, it is accompanied by a decrease in the average fiber bundle thickness, a decrease in scaffold compaction in the presence of cells, and an overall decrease in mechanical strength [99, 100]. Increased concentrations of thrombin and calcium had similar effects, with each factor decreasing both compaction and mechanical strength [100, 101]. Other methods of addressing the mechanical and degradation challenges associated with fibrin include the creation of composite materials, wherein fibrin is combined with other natural or synthetic polymers. For example, both the degradation and mechanical properties of fibrin-based scaffolds have been tailored through combination with collagen [102], polyurethane, polycaprolactone, and polyethylene glycol [103].

Both fibrin hydrogels and fibrin glue are formed via the cleavage of fibrinogen by thrombin in the presence of calcium and aqueous solution, with glue being distinguished from hydrogels by the presence of numerous other plasma proteins and enzymes, a faster gelation time, and generally higher protein concentration, with accompanying lower water content [30]. Fibrin glue is frequently delivered via a double-barrel syringe or a two-unit spray system, and its application can be performed concomitantly with delivery of cells. Both fibrin glue and fibrin hydrogels have been used as scaffolds for numerous tissue engineering applications, including bone, adipose, cardiac, cartilage, liver, muscle, nerve, tendon, eye, blood vessel, and skin tissues [32, 103]. Vascular tissue engineering has been a particular focus for fibrin materials due to the vascular-appropriate mechanics of fibrin scaffolds as well as their ability to support the growth of both smooth muscle and endothelial cells [104, 105]. Due to the natural role of fibrin as a provisional matrix during dermal wound healing, fibrin scaffolds have also been used extensively in skin tissue engineering, supporting the growth of keratinocytes and dermal fibroblasts, enhancing cellular motility, and acting as a carrier for the delivery of exogenous growth factors [106].

8.3.3

Silk

The ability of silk to support cell adhesion and growth, in addition to its good oxygen and water permeability, slow degradation, low immunogenicity, and high tensile strength, render it an attractive biomaterial for tissue engineering applications. Silk is also a versatile biomaterial matrix with respect to processing, as it can be formed into many structures, including films, fibers, microcapsules, hydrogels, and sponges. These scaffolds can be processed from concentrated silk fibroin solutions that consist of silk dissolved in appropriate solvents such as formic acid, calcium nitrate, hexafluoroisopropanol, ionic liquids or lithium salts [65].

Films made from silkworm silk have been found to support cell functions in both human and animal cell lines, with silk from wild silkworms outperforming that obtained from domestic silkworms due to the presence of the RGD peptide in the wild silkworm silk [71].

Films have also been made from genetically engineered spider silk, and these recombinant silk films have been successful in rivaling the properties of native spider silk. Films fabricated from silkworm silk support cell attachment, growth, and cell morphology similar to that seen on collagen films, but the slow degradation of silk compared to collagen has been an advantage for use in applications such as cartilage tissue engineering [107].

The surfaces of silk films can also be modified with RGD or growth factors to enhance material bioactivity. For instance, RGD coating of silk films promoted the production of mineralized matrix by osteoblasts [108]. Meanwhile, culture of mesenchymal stem cells on RGD-coupled recombinant spider silk matrices supported their differentiation into osteogenic cells [109]. The addition of biomolecules such as parathyroid hormone [108] or bone morphogenetic proteins (BMPs) [110] to silk matrices can further moderate cell functions or induce osteogenesis. Silk films have also shown promise as wound dressings, stimulating improved epidermal and collagen regeneration in comparison to traditional dressings [111].

Fibrous matrices can be formed from silk proteins via electrospinning, extrusion, or microfluidic approaches [65]. Fibrous silk matrices may hold particular promise for tissue engineering of ligaments. Consisting of a dense, cable-like structure, the anterior cruciate ligament (ACL) is the most commonly injured ligament [71]; repair of severe ACL tears requires surgical intervention, and synthetic ACL replacements are accompanied by several limitations [71]. When cabled into multi-corded, wire-rope matrices, the silk cable matrix has shown similar mechanical properties to the native human ACL and retains good mechanical properties following *in vivo* implantation [112]. Silk matrices have also supported the differentiation of adult mesenchymal stem cells into ligament-specific cells [69, 113], which can be enhanced through the use of a mechanical bioreactor [71, 114].

Silkworm silk and recombinant spider silk have been successfully transformed into hydrogel networks, with both silkworm and spider silk exhibiting promise for cartilage tissue engineering through their support of chondrocyte growth [65, 71, 107, 115]. Hydrogels from silkworm silk have also been explored for their potential in repairing cancellous (spongy) bone defects in rabbit models [116].

Lastly, silk-based porous matrices can be formed through additional techniques such as salt leaching, gas-foaming, and freeze-drying [51]. These methods yield scaffolds with porosity and mechanical properties that can be controlled by the silk fibroin concentration, freezing temperature, or particle size of the salt used in leaching processes [51]. Spongy porous matrices have also been made without freeze-drying or the aid of other materials by freezing and thawing an aqueous solution of silk fibroin in the presence of a small amount of water-miscible organic solvents [117].

8.3.4

Elastin

Tissue elasticity is of extreme importance for proper function of the cardiovascular and pulmonary systems. Failures in elastin synthesis or elastin insufficiencies can result in the development of clinical syndromes and in some cases can be lethal [118, 119]. Thus, the

importance of elastin in tissue function, combined with difficulties in achieving endogenous elastin production by engineered tissues [120], as well as its durability and low turnover rate, has stimulated the development of elastin-based scaffolds. The primary drawbacks to the use of elastin as a biomaterial are its complex purification, insolubility, and tendency to calcify upon implantation [121]. However, both recombinant techniques and fragmentation of elastin can yield products that retain the attractive physical properties of elastin while overcoming some of its challenges. Several elastin-based scaffold structures have been developed in recent years, although their implementation in tissue engineering applications has thus far been limited.

Recombinant tropoelastin has been used to create synthetic elastin with properties very similar to the native protein. This synthetic elastin supported cellular growth in both in vitro and in vivo studies [48]. Tropoelastin has also been used for the creation of elastin-like polymers. These polymers exhibit elastin-like mechanical performance, are biocompatible, and can be enhanced by coupling biological molecules that add functionality. The most common of these polymers are elastin-like polypeptides (ELPs). These peptides are composed of a repeat of the amino acid sequence of the tropoelastin molecule (Val-Pro-Gly-X-Gly) that can be manipulated by adding any amino acid (except proline) at the “X” site, leading to a temperature, pH, or electrochemical potential-dependent molecule [122]. These peptides can be controlled to self assemble in vitro [123], and have been used for various applications, including the creation of hydrogels and nanoparticles [122, 124]. Hydrogels constructed from ELPs have successfully supported the function of mature chondrocytes [125] as well as the chondrogenic differentiation of adipose-derived stem cells [126] in the absence of chondrogenic differentiation medium.

Soluble α -elastin, an elastin derivative that is isolated following acid hydrolysis of insoluble elastin, has been used as a scaffold surface coating and in the development of elastin scaffolds [120, 127]. Elastin-based scaffolds have been created by the reaction of α -elastin with a diepoxy crosslinker, where the physical scaffold properties, such as swelling, mechanics, and enzymatic degradation rate, can be controlled via adjustments to the pH of the reaction with the crosslinker [120]. These scaffolds supported the culture of vascular smooth muscle cells, and show promise for use in tissue engineering applications. A glutaraldehyde crosslinker, combined with exposure to pressurized carbon dioxide, has also been used to create highly porous α -elastin hydrogels [128] that support the attachment and growth of dermal fibroblasts. The creation and optimization of α -elastin-based scaffolds remains an emerging area, and the immunogenicity of these materials has yet to be determined [120].

Elastin has also been combined with other natural or synthetic molecules for the development of elastin-based copolymers. For instance, although electrospun scaffolds can be fabricated from tropoelastin or α -elastin alone [129], blending elastin with other polymers during electrospinning may be a preferred approach, as it improves the structural integrity of the scaffold [130]. Thus, to facilitate the formation of elastin-based electrospun scaffolds, elastin has been combined with various crosslinker molecules, other natural materials, and synthetic polymers such as polydioxanone [130]. Of particular relevance to vascular tissue engineering is the formation of elastin-collagen scaffolds, which have exhibited favorable mechanical properties and support the growth of vascular cells [131, 132].

8.3.5

Hyaluronic Acid

Hyaluronic acid is not only an important molecule in the body's extracellular matrix, but also a powerful molecule with respect to the development of tissue engineering scaffolds. HA is capable of regulating many cell functions, and it can be chemically modified for controlled degradation and stability [133]. Due to its highly negative charge, HA forms a coil-like structure in aqueous solutions, entrapping water within its structure and expanding in volume up to 1,000 times [60]; this unique property is desirable for the development of hydrogels [60]. Many variations of HA are FDA-approved for a range of clinical uses, such as Restylane and Juvederm as cosmetic fillers, Healon for ophthalmic procedures, Synvisc-One and Orthovisc for osteoarthritis, and Hyalofill wound dressings for dermal wound healing. With the exception of Hyalofill, which consists of a scaffold composed of esterified HA, all of these products are delivered in the form of a viscous HA-based injection [134–136]. As a result of the attractive biological and physical features of HA-based materials, HA scaffolds have been used extensively in tissue engineering for applications that include bone, cartilage, liver, cardiac, vocal fold, vascular, dermal, ophthalmic, and nerve repair and regeneration [63].

To effectively achieve material modification with HA or its incorporation into a polymer scaffold, the HA molecule is often modified via chemical derivatization and/or crosslinking with different molecules (Fig. 8.4) [133]. By performing these modifications, it is possible to tailor the mechanics and degradation rate of HA while maintaining its biological properties. In addition, the HA molecule can be modified to add more biological functionality via coupling of different biological moieties, cytokines, or therapeutic drugs [137]. The principal targets for the chemical modification of HA are the carboxylic acid, hydroxyl groups, or the acetamido group (Fig. 8.4). Examples of derivatization methods include: (1) esterification of the carboxyl or hydroxyl groups with an alcohol [138], (2) the use of carbodiimide compounds to modify the carboxylic groups [139], (3) sulfation of the hydroxyl groups with a sulfur trioxide-pyridine complex [140], and (4) oxidation of the hydroxyl groups with sodium periodate [141]. HA molecules derivatized in these manners may be directly used as scaffolds, as in the case of Hyaff scaffolds, which consist of esterified HA, or may be subsequently crosslinked via mechanisms discussed below.

Modified HA molecules are frequently crosslinked to form hydrogels. The degradation, mechanics, and other physical properties of crosslinked HA hydrogels may be controlled by the extent of crosslinker modification, the HA concentration, and the HA molecular weight. Thus, the mechanical properties of these hydrogels can vary from viscous-pourable gels to rigid and brittle gels, depending on the type and density of crosslinking. Different crosslinking methods that react with the hydroxyl groups have been explored such as the use of divinyl sulfone in an alkaline environment (creating Hylan-B gels) [55] or the use of glutaraldehyde [142]. Crosslinking methods that involve reaction with the carboxyl moiety of HA include the use of chelating metals to obtain a metal cation-mediated crosslink [143], and the use of carbodiimide in aqueous solution [144]. Formation of hydrogel scaffolds via photocrosslinking mechanisms has the advantages of allowing spatial and temporal control over the hydrogel structure and can be achieved via the addition of methacrylate groups to the HA molecule [145, 146]. Moreover, crosslinking via photo-initiated mechanisms

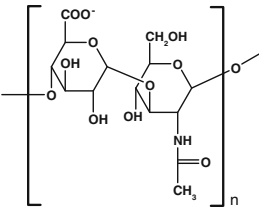
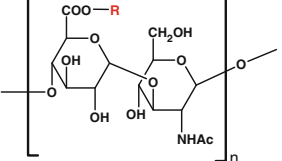
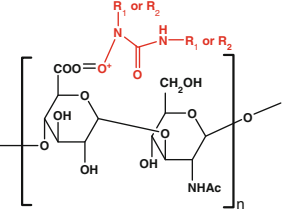
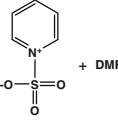
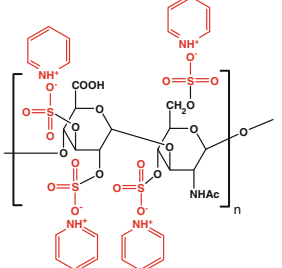
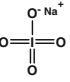
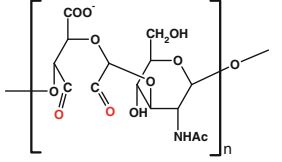
HA Molecule		
		
Type of Modification	Modified HA	Applications/Benefits
<p>Esterification At the carboxyl or hydroxyl groups with an alcohol</p> <p>$R-OH$</p>		<ul style="list-style-type: none"> • Degree of esterification regulates size of hydrophobic patches • Improves mechanical strength • Decreases susceptibility to enzymatic degradation
<p>Carbodiimide Reaction At the carboxyl groups</p> <p>$R_1N=C=NR_2$</p>		<ul style="list-style-type: none"> • Reaction can be done in aqueous solutions • Allows hydrazide coupling, facilitating incorporation of other biological molecules or crosslinking agents
<p>Sulfation At the hydroxyl groups</p> <p>e.g. Sulfur trioxide-pyridine complex</p>  <p>+ DMF</p>		<ul style="list-style-type: none"> • Degree of sulfation can be easily controlled • Modified structure has heparin-like activity • Resistant to enzymatic degradation • Anticoagulant property depends on the degree of sulfation
<p>Oxidation At the hydroxyl groups</p> <p>e.g. Sodium periodate</p> 		<ul style="list-style-type: none"> • Sodium periodate acts only on vicinal hydroxyl groups • Modified molecule can couple with primary amines and allow incorporation of crosslinkers or biological molecules

Fig. 8.4 Chemical modifications of hyaluronic acid (HA) enable the creation of a wide range of HA derivatives with varying functionalities. These modified HA molecules may be used to form crosslinked scaffolds or to alter the physical or biological characteristics of HA-based materials

enables the encapsulation of cells during gelation. Derivatized crosslinker molecules may also be reacted with HA in order to further enhance the range of properties that can be achieved with HA scaffolds. For instance, use of a crosslinker that possesses both a methacrylate moiety and lactic acid groups can impart hydrolytic degradability upon the HA scaffold [147]. The combination of hydrolytic with enzymatic degradation allows further tailoring of scaffold properties and can facilitate more uniform extracellular matrix deposition by encapsulated cells [147].

HA is also commonly copolymerized with other materials in order to combine the attractive biological properties of HA with the mechanics and prolonged degradation of other biological or synthetic materials. For instance, methacrylated HA may be combined with methacrylated or acrylated polyethylene glycol (PEG) to yield photocrosslinked scaffold networks that possess improved mechanical performance compared to HA alone, but are enzymatically degradable, unlike PEG alone [59]. Crosslinking of adipic dihydrazide-modified HA with PEG-dialdehyde yields degradable hydrogel matrices that accelerate the healing of full thickness dermal wounds [148].

Fibrous HA scaffolds are available in the form of Hyaff, which has been used as the primary structure for an FDA-approved dermal wound dressing (Hyalofill), and may also be used in tissue engineering to support the growth of various cell types. Hyaff scaffolds have proven to be permissive environments for the growth of chondrocytes and support the culture of mesenchymal stem cells [149] and their differentiation into chondrocytes and osteoblasts [150]. Electrospinning techniques may also be used to create nanofibrous HA scaffolds, although the high viscosity of HA in aqueous solutions and its water-retention ability can complicate the electrospinning process [151]. However, electrospinning challenges can also be overcome by combining HA with other materials, such as gelatin [152], or by incorporating photocrosslinking techniques in addition to other components [153].

8.3.6 Alginate

The abundance, relatively low cost, good biocompatibility, and simple gelation mechanism of alginate are attributes that render this material attractive for tissue engineering, with its primary drawback being its poorly regulated degradation. Sufficient purification of alginate and removal of contaminants from the raw source also remains a problem in some instances [154]. Alginate is most often used as a hydrogel in tissue engineering, although it can also be formed into fibrous meshes via electrospinning [151] or porous scaffolds via freeze-drying techniques [155].

As noted earlier, alginate hydrogels are formed from aqueous solutions of alginate in the presence of divalent cations such as Ca^{2+} , Mg^{2+} , Ba^{2+} , and Sr^{2+} [156]. This mild gelation mechanism facilitates the entrapment of cells during the gelation process, a feature which is often beneficial in tissue engineering. Delivery of droplets of alginate solution into a calcium-containing solution can be used as a facile and rapid method of forming alginate microcapsules, which may be used for drug delivery or cell encapsulation.

Different cation sources can be used to control the gelation time of alginate, as well as the physical properties of the alginate hydrogel. For instance, the rapid gelation obtained

through use of CaCl_2 or CaSO_4 can lead to heterogeneity in the alginate properties and structure, while use of CaCO_3 , which is less soluble in water, can allow for more homogeneous distribution of calcium ions throughout the alginate solution prior to gelation [157]. The use of CaCO_3 is accompanied by the addition of D-glucono- δ -lactone, whose hydrolysis facilitates the liberation of Ca^{2+} ions from CaCO_3 . By combining these different calcium sources, the gelation time, uniformity, and mechanics of alginate gels can be tailored to meet desired specifications for various tissue engineering applications [157].

Covalent crosslinking of alginate has also been achieved via a variety of mechanisms. The addition of methacrylate groups to alginate yields a material whose crosslinking is light-initiated and whose mechanics and degradation can be tailored through variations in the extent of methacrylation [158]. Various diamines and dihydrazides can also be coupled to alginate via carbodiimide chemistry and act as covalent crosslinkers to tailor gel properties [76, 159].

The mechanical properties of alginate hydrogels may also be controlled by altering the alginate concentration, calcium concentration, and alginate molecular weight, with higher values for any of these variables leading to stiffer gels. Although an increase in alginate concentration can lead to an undesirable increase in solution viscosity prior to gelation, this obstacle can be overcome through manipulations of the alginate MW and MW distribution [76]. Temperature also affects gelation rate, with lower temperatures leading to slower gelation and subsequently improved mechanical properties [160].

Alginate gels, microcapsules, and porous scaffolds have been used in the engineering of numerous tissues, including bone, cartilage, liver, skin, nerve, heart, pancreas, and ovarian follicle development [51, 76, 161]. Although native alginate does not support significant cell attachment, alginate is amenable to modification with cell adhesion peptide sequences, most commonly RGD [162]. Compared to unmodified alginate gels, RGD-modified alginate gels significantly enhance *in vivo* bone formation by transplanted osteoblasts, and co-transplantation of chondrocytes with osteoblasts in these gels leads to self-organization of the cells into structures resembling growth plates [163]. Alginate scaffolds and microcapsules have been used extensively in metabolic applications, such as liver and pancreas tissue engineering. These applications often make use of alginate's ability to form strong complexes with cationic compounds, where the coating of alginate microcapsules with poly-L-lysine can help to stabilize the microcapsule, as well as tailor the molecular weight cut-off of the structure in order to immunogenically isolate the encapsulated cells [154]. Alginate scaffolds have supported the differentiation of hepatic progenitor cells [164], as well as the maintenance of critical liver functions of mature hepatocytes [165].

8.3.7

Chitosan

The abundance, biocompatibility, degradability, chemical versatility, and hemostatic and anti-bacterial properties of chitosan have generated extensive interest in this material and its derivatives for biomaterial and tissue engineering applications [83, 166]. Chitosan is considered to be structurally similar to native glycosaminoglycans, and this property is thought to impart enhanced bioactivity upon chitosan-based materials [51]. The primary

drawback associated with the use of chitosan in tissue engineering scaffolds has been its limited solubility, although numerous techniques have been developed to address this challenge.

Containing several reactive as well as ionic moieties, chitosan is highly amenable to modification, yielding many possibilities for tailoring the mechanical and biological properties of the chitosan molecule and chitosan-based scaffolds. The majority of chemical modifications to the chitosan molecule focus upon improving its solubility or bioactivity. One of the most common water-soluble chitosan derivatives is *N*-carboxymethylchitosan, formed through reaction with chloroacetic acid in an alcohol solvent [85]. Reaction with succinic anhydride also produces a water-soluble derivative, *N*-succinylchitosan [85]. Modification of chitosan with cell-recognized sugars addresses both the solubility and bioactivity issues facing chitosan [85]. Various reaction mechanisms can be used to form sugar-bound chitosans such as galactosylated chitosan, which support hepatocyte culture [167], or mannosylated chitosan, which is specifically recognized by antigen-presenting cells [168]. Lastly, sulfonation of either the amino or hydroxyl groups of chitosan yields a polymer that bears a close structural resemblance to heparin [85].

As noted earlier, the cationic nature of chitosan also enables pH-dependent electrostatic interactions with anionic glycosaminoglycans such as heparin, which, in turn, binds numerous heparin-binding proteins. Thus, an assortment of biologically active molecules can be indirectly bound to chitosan scaffolds through heparin intermediates [83]. Although chitosan can indirectly bind molecules such as cytokines and growth factors, the base chitosan material still lacks the ability to directly support cell adhesion. To address this challenge, grafting of peptides such as RGD, YIGSR, and IKVAV onto chitosan materials has been achieved via photochemical methods or carbodiimide chemistry to yield structures that support the attachment and growth of cells [81, 169, 170].

Chitosan can be processed to form fibers, sponges, membranes, beads, and hydrogels [81, 82, 85]. Chitosan sponges with interconnected pore structures can be fabricated via freeze-drying techniques or a technique known as “internal bubbling process”, which involves the addition of CaCO_3 to chitosan solutions [81]. As with other types of porous structures, the mechanical properties of these scaffolds are dependent upon the pore size and orientation, and the pore structure can be tailored via changes in the processing condition, such as the rate of temperature decrease in freeze-drying techniques. Chitosan sponges have found wide use in tissue engineering applications, most predominantly in dermal wound healing, which takes advantage of the intrinsic properties of chitosan that promote healing [81, 166]. Chitosan hydrogels are also commonly formed for tissue engineering applications, with gelation of chitosan or its derivatives being possible through numerous physical or chemical methods, including covalent bonding using crosslinkers, ionic interactions, hydrogen bonding, and hydrophobic interactions [171]. The ability of chitosan to bind native GAGs has made chitosan-based hydrogels particularly attractive for cartilage tissue engineering [81, 172]. Other tissue engineering applications of chitosan, chitosan derivatives, and blends of chitosan with other materials include bone, nerve, liver, and vascular tissue engineering [81].

The insolubility of chitosan in neutral and alkaline solutions can occasionally be used as an advantage in its processing, as viscous solutions of chitosan can be extruded and gelled in high pH solutions to form gel fibers that are subsequently drawn and dried [173]. Fibrous

chitosan scaffolds have also been produced via electrospinning processes, although the polycationic nature and solubility restrictions of this molecule introduce significant challenges in achieving electrospun fibrous chitosan structures [151]. However, blending of chitosan with other polymers or the use of derivatized chitosans, such as hexanoyl chitosan, quaternized chitosan, and *N*-carboxyethylchitosan, yields more favorable electrospinning results [151] that are currently being explored for various tissue engineering applications.

8.4

Future Directions

The successful development of appropriate tissue engineering scaffold environments will ultimately require the combination of multiple features and functionalities in order to mimic the highly complex native structures that best support tissue repair and regeneration. Thus, although this chapter has focused upon individual natural materials, there exist innumerable possibilities for combining these materials with other natural or synthetic polymers and biomolecules to yield multi-functional materials that are tailored to meet the needs of specific tissue engineering applications. The use of genetically-engineered natural materials also holds promise for the creation of more complex, tailored scaffolds. Many natural materials can be created via recombinant techniques, and genetic manipulation may allow researchers to create structures that possess features such as decreased immunogenicity, increased bioactivity, or improved mechanical strength.

The body's ECM is composed of numerous components, and one example of achieving a higher degree of tissue engineering scaffold complexity using natural materials is the use of whole ECM structures derived from native tissues. Although decellularized tissues have been used for decades as allografts and xenografts, recent prominent successes in recovering tissue function following recellularization of these structures has focused greater attention on their use as tissue engineering scaffold materials. Notably, one group has demonstrated the decellularization of entire rat hearts, followed by their recellularization with neonatal cardiomyocytes and subsequent resumption of contraction and macroscopic beating [174]. Recellularization of decellularized tissues has also yielded impressive results in urologic and reproductive tissue engineering, where physiologically functional penile reconstruction was achieved *in vivo* in a rabbit model [175]. A variation on this approach is the decellularization and subsequent homogenization of native myocardial ECM, followed by its resolubilization to yield an injectable material that forms nanofibrous gels with a complex ECM structure [176]. Although these methods harvest the ECM from *in vivo* sources, there is also the possibility to harvest complex ECM compositions and structures from *in vitro* sources. ECM produced by planar cultures of cells may be combined with separate scaffold structures [177], or the 3-D matrix produced by engineered tissues *in vitro* may be decellularized to leave an ECM scaffold structure that may be recellularized at a later time using the patient's own cells in order to create an autologous graft.

Approaches that use complex ECM structures can be used not only as a stand-alone method for creating engineered tissues, but may also be combined with the derivatization or modification techniques discussed throughout this chapter, or these scaffolds may act as

a template for the de novo construction of scaffolds from many of the individual components discussed herein. Ongoing and future research is addressing the many challenges that face this area, such as scaffold/tissue availability and reproducibility, cell sourcing, tissue processing conditions, scaffold delivery mechanisms, and scaffold characterization.

Acknowledgements The authors acknowledge funding from the NSF and NIH (K.S.M.), the Translational Cardiovascular Sciences Training Program (E.L.M. and K.J.R.), the Biotechnology Training Program (C.M.M.) and the Graduate Engineering Research Scholars Program (K.J.R.).

References

1. C.A. Vacanti, History of tissue engineering and a glimpse into its future, *Tissue Eng* **12** (2006), pp. 1137–1142.
2. I.V. Yannas, J.F. Burke, P.L. Gordon, C. Huang, and R.H. Rubenstein, Design of an artificial skin. II. Control of chemical composition, *J Biomed Mater Res* **14** (1980), pp. 107–132.
3. E. Bell, B. Ivarsson, and C. Merrill, Production of a tissue-like structure by contraction of collagen lattices by human fibroblasts of different proliferative potential in vitro, *Proc Natl Acad Sci U S A* **76** (1979), pp. 1274–1278.
4. C.B. Weinberg, and E. Bell, A blood vessel model constructed from collagen and cultured vascular cells, *Science* **231** (1986), pp. 397–400.
5. M. Radosevich, H.I. Goubran, and T. Burnouf, Fibrin sealant: scientific rationale, production methods, properties, and current clinical use, *Vox Sang* **72** (1997), pp. 133–143.
6. W. Halsted, The employment of fine silk in preference to catgut and the advantage of transfixing tissues and vessels in controlling hemorrhage, *Ann Surg* **16** (1892), pp. 505.
7. C. Demers, C.R. Hamdy, K. Corsi, F. Chellat, M. Tabrizian, and L. Yahia, Natural coral exoskeleton as a bone graft substitute: a review, *Biomed Mater Eng* **12** (2002), pp. 15–35.
8. K.P. Rao, Recent developments of collagen-based materials for medical applications and drug delivery systems, *J Biomater Sci Polym Ed* **7** (1995), pp. 623–645.
9. H.J. Chung, and T.G. Park, Surface engineered and drug releasing pre-fabricated scaffolds for tissue engineering, *Adv Drug Deliv Rev* **59** (2007), pp. 249–262.
10. A.D. Metcalfe, and M.W. Ferguson, Tissue engineering of replacement skin: the crossroads of biomaterials, wound healing, embryonic development, stem cells and regeneration, *J R Soc Interface* **4** (2007), pp. 413–437.
11. L.S. Nair, and C.T. Laurencin, Polymers as biomaterials for tissue engineering and controlled drug delivery, *Adv Biochem Eng Biotechnol* **102** (2006), pp. 47–90.
12. R.A. Brown, and J.B. Phillips, Cell responses to biomimetic protein scaffolds used in tissue repair and engineering, *Int Rev Cytol* **262** (2007), pp. 75–150.
13. M. Mian, F. Beghe, and E. Mian, Collagen as a pharmacological approach in wound healing, *Int J Tissue React* **14 Suppl** (1992), pp. 1–9.
14. K.H. Stenzel, T. Miyata, and A.L. Rubin, Collagen as a biomaterial, *Annu Rev Biophys Bioeng* **3** (1974), pp. 231–253.
15. L. Cen, W. Liu, L. Cui, W. Zhang, and Y. Cao, Collagen tissue engineering: development of novel biomaterials and applications, *Pediatr Res* **63** (2008), pp. 492–496.
16. I.V. Yannas. Natural Materials. In: B.D. Ratner, A.S. Hoffman, F.J. Shoen, J.E. Lemons, editors. Biomaterials Science. San Diego, CA: Elsevier Academic Press; (2004)
17. K.S. Masters, and W.L. Murphy. Tissue Engineering. In: J.G. Webster, editor. Encyclopedia of Medical Devices and Instrumentation: John Wiley & Sons, Inc.; (2006), p. 379–395.

18. J.A. Ramshaw, Y.Y. Peng, V. Glattauer, and J.A. Werkmeister, Collagens as biomaterials, *J Mater Sci Mater Med* **20 Suppl 1** (2009), pp. S3–S8.
19. B. Brodsky, and J.A. Ramshaw, The collagen triple-helix structure, *Matrix Biol* **15** (1997), pp. 545–554.
20. H. Birkedal-Hansen, W.G. Moore, M.K. Bodden, L.J. Windsor, B. Birkedal-Hansen, A. DeCarlo, et al., Matrix metalloproteinases: a review, *Crit Rev Oral Biol Med* **4** (1993), pp. 197–250.
21. S. Young, M. Wong, Y. Tabata, and A.G. Mikos, Gelatin as a delivery vehicle for the controlled release of bioactive molecules, *J Control Release* **109** (2005), pp. 256–274.
22. D.J. White, S. Puranen, M.S. Johnson, and J. Heino, The collagen receptor subfamily of the integrins, *Int J Biochem Cell Biol* **36** (2004), pp. 1405–1410.
23. A.V. Taubenberger, M.A. Woodruff, H. Bai, D.J. Muller, and D.W. Huttmacher, The effect of unlocking RGD-motifs in collagen I on pre-osteoblast adhesion and differentiation, *Biomaterials* **31** (2010), pp. 2827–2835.
24. D. Gullberg, K.R. Gehlsen, D.C. Turner, K. Ahlen, L.S. Zijenah, M.J. Barnes, et al., Analysis of alpha 1 beta 1, alpha 2 beta 1 and alpha 3 beta 1 integrins in cell–collagen interactions: identification of conformation dependent alpha 1 beta 1 binding sites in collagen type I, *Embo J* **11** (1992), pp. 3865–3873.
25. J.R. Mauney, V. Volloch, and D.L. Kaplan, Matrix-mediated retention of adipogenic differentiation potential by human adult bone marrow-derived mesenchymal stem cells during ex vivo expansion, *Biomaterials* **26** (2005), pp. 6167–6175.
26. A.K. Lynn, I.V. Yannas, and W. Bonfield, Antigenicity and immunogenicity of collagen, *J Biomed Mater Res B Appl Biomater* **71** (2004), pp. 343–354.
27. M.W. Mosesson, Fibrinogen and fibrin structure and functions, *J Thromb Haemost* **3** (2005), pp. 1894–1904.
28. K. Suzuki, B. Dahlback, and J. Stenflo, Thrombin-catalyzed activation of human coagulation factor V, *J Biol Chem* **257** (1982), pp. 6556–6564.
29. P.A. Janmey, J.P. Winer, and J.W. Weisel, Fibrin gels and their clinical and bioengineering applications, *J R Soc Interface* **6** (2009), pp. 1–10.
30. C. Buchta, H.C. Hedrich, M. Macher, P. Hocker, and H. Redl, Biochemical characterization of autologous fibrin sealants produced by CryoSeal and Vivostat in comparison to the homologous fibrin sealant product Tissucol/Tisseel, *Biomaterials* **26** (2005), pp. 6233–6241.
31. J.J. Calvete, Structures of integrin domains and concerted conformational changes in the bidirectional signaling mechanism of alphaIIb beta3, *Exp Biol Med (Maywood)* **229** (2004), pp. 732–744.
32. R. Gorodetsky, The use of fibrin based matrices and fibrin microbeads (FMB) for cell based tissue regeneration, *Expert Opin Biol Ther* **8** (2008), pp. 1831–1846.
33. K. Suehiro, J. Mizuguchi, K. Nishiyama, S. Iwanaga, D.H. Farrell, and S. Ohtaki, Fibrinogen binds to integrin alpha(5)beta(1) via the carboxyl-terminal RGD site of the Aalpha-chain, *J Biochem* **128** (2000), pp. 705–710.
34. R.E. Nisato, J.C. Tille, A. Jonczyk, S.L. Goodman, and M.S. Pepper, alphav beta 3 and alphav beta 5 integrin antagonists inhibit angiogenesis in vitro, *Angiogenesis* **6** (2003), pp. 105–119.
35. A. Sahni, T. Odrljic, and C.W. Francis, Binding of basic fibroblast growth factor to fibrinogen and fibrin, *J Biol Chem* **273** (1998), pp. 7554–7559.
36. A. Sahni, and C.W. Francis, Stimulation of endothelial cell proliferation by FGF-2 in the presence of fibrinogen requires alphavbeta3, *Blood* **104** (2004), pp. 3635–3641.
37. A. Sahni, and C.W. Francis, Vascular endothelial growth factor binds to fibrinogen and fibrin and stimulates endothelial cell proliferation, *Blood* **96** (2000), pp. 3772–3778.
38. B. Vrhovski, and A.S. Weiss, Biochemistry of tropoelastin, *Eur J Biochem* **258** (1998), pp. 1–18.
39. J. Rosenbloom, W.R. Abrams, and R. Mecham, Extracellular matrix 4: the elastic fiber, *Faseb J* **7** (1993), pp. 1208–1218.

40. J.E. Wagenseil, and R.P. Mecham, New insights into elastic fiber assembly, *Birth Defects Res C Embryo Today* **81** (2007), pp. 229–240.
41. S.M. Mithieux, and A.S. Weiss, Elastin, *Adv Protein Chem* **70** (2005), pp. 437–461.
42. E. Petersen, F. Wagberg, and K.A. Angquist, Serum concentrations of elastin-derived peptides in patients with specific manifestations of atherosclerotic disease, *Eur J Vasc Endovasc Surg* **24** (2002), pp. 440–444.
43. F.W. Keeley, C.M. Bellingham, and K.A. Woodhouse, Elastin as a self-organizing biomaterial: use of recombinantly expressed human elastin polypeptides as a model for investigations of structure and self-assembly of elastin, *Philos Trans R Soc Lond B Biol Sci* **357** (2002), pp. 185–189.
44. W.F. Daamen, J.H. Veerkamp, J.C. van Hest, and T.H. van Kuppevelt, Elastin as a biomaterial for tissue engineering, *Biomaterials* **28** (2007), pp. 4378–4398.
45. A. Hinek, D.S. Wrenn, R.P. Mecham, and S.H. Barondes, The elastin receptor: a galactoside-binding protein, *Science* **239** (1988), pp. 1539–1541.
46. U.R. Rodgers, and A.S. Weiss, Integrin alpha v beta 3 binds a unique non-RGD site near the C-terminus of human tropoelastin, *Biochimie* **86** (2004), pp. 173–178.
47. S.M. Partridge, H.F. Davis, and G.S. Adair, The chemistry of connective tissues. 2. Soluble proteins derived from partial hydrolysis of elastin, *Biochem J* **61** (1955), pp. 11–21.
48. S.M. Mithieux, J.E. Rasko, and A.S. Weiss, Synthetic elastin hydrogels derived from massive elastic assemblies of self-organized human protein monomers, *Biomaterials* **25** (2004), pp. 4921–4927.
49. L. Nivison-Smith, J. Rnjak, and A.S. Weiss, Synthetic human elastin microfibers: Stable cross-linked tropoelastin and cell interactive constructs for tissue engineering applications, *Acta Biomater* **6** (2010), pp. 354–359.
50. J. Rnjak, Z. Li, P.K. Maitz, S.G. Wise, and A.S. Weiss, Primary human dermal fibroblast interactions with open weave three-dimensional scaffolds prepared from synthetic human elastin, *Biomaterials* **30** (2009), pp. 6469–6477.
51. M. Gomes, H. Azevedo, P. Malafaya, S. Silva, J. Oliveira, G. Silva, et al. Natural polymers in tissue engineering applications. In: C. van Blitterswijk, editor. *Tissue Engineering*. London, UK: Elsevier Inc.; (2008)
52. P. Prehm, Hyaluronate is synthesized at plasma membranes, *Biochem J* **220** (1984), pp. 597–600.
53. P.H. Weigel, V.C. Hascall, and M. Tammi, Hyaluronan synthases, *J Biol Chem* **272** (1997), pp. 13997–14000.
54. T.C. Laurent, U.B. Laurent, and J.R. Fraser, The structure and function of hyaluronan: an overview, *Immunol Cell Biol* **74** (1996), pp. A1–A7.
55. J. Baier Leach, and C.E. Schmidt. Hyaluronan. In: G.E. Wnek, G.L. Bowlin, editors. *Encyclopedia of Biomaterials and Biomedical Engineering*. New York, NY: Marcel Dekker, Inc.; (2004), p. 779–789.
56. C.B. Knudson, and W. Knudson, Hyaluronan-binding proteins in development, tissue homeostasis, and disease, *FASEB J* **7** (1993), pp. 1233–1241.
57. E.A. Turley, P.W. Noble, and L.Y. Bourguignon, Signaling properties of hyaluronan receptors, *J Biol Chem* **277** (2002), pp. 4589–4592.
58. D.C. West, and S. Kumar, The effect of hyaluronate and its oligosaccharides on endothelial cell proliferation and monolayer integrity, *Exp Cell Res* **183** (1989), pp. 179–196.
59. K.S. Masters, D.N. Shah, L.A. Leinwand, and K.S. Anseth, Crosslinked hyaluronan scaffolds as a biologically active carrier for valvular interstitial cells, *Biomaterials* **26** (2005), pp. 2517–2525.
60. T.C. Laurent, and J.R. Fraser, Hyaluronan, *FASEB J* **6** (1992), pp. 2397–2404.
61. J.R. Fraser, T.C. Laurent, and U.B. Laurent, Hyaluronan: its nature, distribution, functions and turnover, *J Intern Med* **242** (1997), pp. 27–33.
62. D.C. West, and S. Kumar, Hyaluronan and angiogenesis, *Ciba Found Symp* **143** (1989), pp. 187–201; discussion 201–207, 281–285.

63. D.D. Allison, and K.J. Grande-Allen, Review. Hyaluronan: a powerful tissue engineering tool, *Tissue Eng* **12** (2006), pp. 2131–2140.
64. W.Y. Chen, and G. Abatangelo, Functions of hyaluronan in wound repair, *Wound Repair Regen* **7** (1999), pp. 79–89.
65. J.A. Kluge, O. Rabotyagova, G.G. Leisk, and D.L. Kaplan, Spider silks and their applications, *Trends Biotechnol* **26** (2008), pp. 244–251.
66. T.D. Sutherland, S. Weisman, H.E. Trueman, A. Sriskantha, J.W. Trueman, and V.S. Haritos, Conservation of essential design features in coiled coil silks, *Mol Biol Evol* **24** (2007), pp. 2424–2432.
67. E. Carrington, Along the silk road, spiders make way for mussels, *Trends Biotechnol* **26** (2008), pp. 55–57.
68. L. Romer, and T. Scheibel, The elaborate structure of spider silk: structure and function of a natural high performance fiber, *Prion* **2** (2008), pp. 154–161.
69. G.H. Altman, F. Diaz, C. Jakuba, T. Calabro, R.L. Horan, J. Chen, et al., Silk-based biomaterials, *Biomaterials* **24** (2003), pp. 401–416.
70. Y. Cao, and B. Wang, Biodegradation of silk biomaterials, *Int J Mol Sci* **10** (2009), pp. 1514–1524.
71. Y. Wang, H.J. Kim, G. Vunjak-Novakovic, and D.L. Kaplan, Stem cell-based tissue engineering with silk biomaterials, *Biomaterials* **27** (2006), pp. 6064–6082.
72. R.V. Lewis, Spider silk: ancient ideas for new biomaterials, *Chem Rev* **106** (2006), pp. 3762–3774.
73. K.I. Draget, and C. Taylor, Chemical, physical and biological properties of alginates and their biomedical implications, *Food Hydrocoll* **25** (2011), pp. 251–256.
74. O. Smidsrød, and K.I. Draget, Chemistry and physical properties of alginates, *Carbohydr Eur* **14** (1996), pp. 6–13.
75. P.H. Calumpong, P.A. Maypa, and M. Magbanua, Population and alginate yield and quality of four *Sargassum* species in Negros Island, central Philippines, *Hydrobiologia* **398** (1999), pp. 211–215.
76. A.D. Augst, H.J. Kong, and D.J. Mooney, Alginate hydrogels as biomaterials, *Macromol Biosci* **6** (2006), pp. 623–633.
77. O. Smidsrod, and G. Skjak-Braek, Alginate as immobilization matrix for cells, *Trends Biotechnol* **8** (1990), pp. 71–78.
78. A. Martinsen, G. Skjak-Braek, and O. Smidsrod, Alginate as immobilization material: I. Correlation between chemical and physical properties of alginate gel beads, *Biotechnol Bioeng* **33** (1989), pp. 79–89.
79. T.Y. Wong, L.A. Preston, and N.L. Schiller, ALGINATE LYASE: review of major sources and enzyme characteristics, structure-function analysis, biological roles, and applications, *Annu Rev Microbiol* **54** (2000), pp. 289–340.
80. K.H. Bouhadir, K.Y. Lee, E. Alsberg, K.L. Damm, K.W. Anderson, and D.J. Mooney, Degradation of partially oxidized alginate and its potential application for tissue engineering, *Biotechnol Prog* **17** (2001), pp. 945–950.
81. I.Y. Kim, S.J. Seo, H.S. Moon, M.K. Yoo, I.Y. Park, B.C. Kim, et al., Chitosan and its derivatives for tissue engineering applications, *Biotechnol Adv* **26** (2008), pp. 1–21.
82. D.W. Hutmacher, J.C. Goh, and S.H. Teoh, An introduction to biodegradable materials for tissue engineering applications, *Ann Acad Med Singapore* **30** (2001), pp. 183–191.
83. T. Jiang, S.G. Kumbar, L.S. Nair, and C.T. Laurencin, Biologically active chitosan systems for tissue engineering and regenerative medicine, *Curr Top Med Chem* **8** (2008), pp. 354–364.
84. Y.C. Ho, F.L. Mi, H.W. Sung, and P.L. Kuo, Heparin-functionalized chitosan-alginate scaffolds for controlled release of growth factor, *Int J Pharm* **376** (2009), pp. 69–75.
85. G.G. d'Ayala, M. Malinconico, and P. Laurienzo, Marine derived polysaccharides for biomedical applications: chemical modification approaches, *Molecules* **13** (2008), pp. 2069–2106.
86. M. Ganan, A.V. Carrascosa, and A.J. Martinez-Rodriguez, Antimicrobial activity of chitosan against *Campylobacter* spp. and other microorganisms and its mechanism of action, *J Food Prot* **72** (2009), pp. 1735–1738.

87. A.K. Singla, and M. Chawla, Chitosan: some pharmaceutical and biological aspects – an update, *J Pharm Pharmacol* **53** (2001), pp. 1047–1067.
88. D. Olsen, C. Yang, M. Bodo, R. Chang, S. Leigh, J. Baez, et al., Recombinant collagen and gelatin for drug delivery, *Adv Drug Deliv Rev* **55** (2003), pp. 1547–1567.
89. C. Yang, P.J. Hillas, J.A. Baez, M. Nokelainen, J. Balan, J. Tang, et al., The application of recombinant human collagen in tissue engineering, *BioDrugs* **18** (2004), pp. 103–119.
90. A. Khademhosseini, and R. Langer, Microengineered hydrogels for tissue engineering, *Biomaterials* **28** (2007), pp. 5087–5092.
91. H. Schoof, J. Apel, I. Heschel, and G. Rau, Control of pore structure and size in freeze-dried collagen sponges, *J Biomed Mater Res* **58** (2001), pp. 352–357.
92. K. Weadock, R.M. Olson, and F.H. Silver, Evaluation of collagen crosslinking techniques, *Biomater Med Devices Artif Organs* **11** (1983), pp. 293–318.
93. L. Gonzalez, and T. Wess, Use of attenuated total reflection-Fourier transform infrared spectroscopy to measure collagen degradation in historical parchments, *Appl Spectrosc* **62** (2008), pp. 1108–1114.
94. U. Hersel, C. Dahmen, and H. Kessler, RGD modified polymers: biomaterials for stimulated cell adhesion and beyond, *Biomaterials* **24** (2003), pp. 4385–4415.
95. E.V. Dare, M. Griffith, P. Poitras, J.A. Kaupp, S.D. Waldman, D.J. Carlsson, et al., Genipin cross-linked fibrin hydrogels for in vitro human articular cartilage tissue-engineered regeneration, *Cells Tissues Organs* **190** (2009), pp. 313–325.
96. C.M. Elvin, S.J. Danon, A.G. Brownlee, J.F. White, M. Hickey, N.E. Liyou, et al., Evaluation of photo-crosslinked fibrinogen as a rapid and strong tissue adhesive, *J Biomed Mater Res A* **93** (2010), pp. 687–695.
97. E.D. Grassl, T.R. Oegema, and R.T. Tranquillo, Fibrin as an alternative biopolymer to type-I collagen for the fabrication of a media equivalent, *J Biomed Mater Res* **60** (2002), pp. 607–612.
98. E. Cholewinski, M. Dietrich, T.C. Flanagan, T. Schmitz-Rode, and S. Jockenhoevel, Tranexamic acid – an alternative to aprotinin in fibrin-based cardiovascular tissue engineering, *Tissue Eng Part A* **15** (2009), pp. 3645–3653.
99. C.B. Herbert, C. Nagaswami, G.D. Bittner, J.A. Hubbell, and J.W. Weisel, Effects of fibrin micromorphology on neurite growth from dorsal root ganglia cultured in three-dimensional fibrin gels, *J Biomed Mater Res* **40** (1998), pp. 551–559.
100. L. Yao, D.D. Swartz, S.F. Gugino, J.A. Russell, and S.T. Andreadis, Fibrin-based tissue-engineered blood vessels: differential effects of biomaterial and culture parameters on mechanical strength and vascular reactivity, *Tissue Eng* **11** (2005), pp. 991–1003.
101. S.L. Rowe, S. Lee, and J.P. Stegemann, Influence of thrombin concentration on the mechanical and morphological properties of cell-seeded fibrin hydrogels, *Acta Biomater* **3** (2007), pp. 59–67.
102. S.L. Rowe, and J.P. Stegemann, Interpenetrating collagen-fibrin composite matrices with varying protein contents and ratios, *Biomacromolecules* **7** (2006), pp. 2942–2948.
103. T.A. Ahmed, E.V. Dare, and M. Hincke, Fibrin: a versatile scaffold for tissue engineering applications, *Tissue Eng Part B Rev* **14** (2008), pp. 199–215.
104. B.C. Isenberg, C. Williams, and R.T. Tranquillo, Small-diameter artificial arteries engineered in vitro, *Circ Res* **98** (2006), pp. 25–35.
105. F.M. Shaikh, A. Callanan, E.G. Kavanagh, P.E. Burke, P.A. Grace, and T.M. McGloughlin, Fibrin: a natural biodegradable scaffold in vascular tissue engineering, *Cells Tissues Organs* **188** (2008), pp. 333–346.
106. L.J. Currie, J.R. Sharpe, and R. Martin, The use of fibrin glue in skin grafts and tissue-engineered skin replacements: a review, *Plast Reconstr Surg* **108** (2001), pp. 1713–1726.
107. A.C. MacIntosh, V.R. Kearns, A. Crawford, and P.V. Hatton, Skeletal tissue engineering using silk biomaterials, *J Tissue Eng Regen Med* **2** (2008), pp. 71–80.

108. S. Sofia, M.B. McCarthy, G. Gronowicz, and D.L. Kaplan, Functionalized silk-based biomaterials for bone formation, *J Biomed Mater Res* **54** (2001), pp. 139–148.
109. E. Bini, C.W. Foo, J. Huang, V. Karageorgiou, B. Kitchel, and D.L. Kaplan, RGD-functionalized bioengineered spider dragline silk biomaterial, *Biomacromolecules* **7** (2006), pp. 3139–3145.
110. C. Kirker-Head, V. Karageorgiou, S. Hofmann, R. Fajardo, O. Betz, H.P. Merkle, et al., BMP-silk composite matrices heal critically sized femoral defects, *Bone* **41** (2007), pp. 247–255.
111. A. Sugihara, K. Sugiura, H. Morita, T. Ninagawa, K. Tubouchi, R. Tobe, et al., Promotive effects of a silk film on epidermal recovery from full-thickness skin wounds, *Proc Soc Exp Biol Med* **225** (2000), pp. 58–64.
112. H. Fan, H. Liu, S.L. Toh, and J.C. Goh, Anterior cruciate ligament regeneration using mesenchymal stem cells and silk scaffold in large animal model, *Biomaterials* **30** (2009), pp. 4967–4977.
113. H. Liu, H. Fan, S.L. Toh, and J.C. Goh, A comparison of rabbit mesenchymal stem cells and anterior cruciate ligament fibroblasts responses on combined silk scaffolds, *Biomaterials* **29** (2008), pp. 1443–1453.
114. F.A. Petrigliano, D.R. McAllister, and B.M. Wu, Tissue engineering for anterior cruciate ligament reconstruction: a review of current strategies, *Arthroscopy* **22** (2006), pp. 441–451.
115. Y. Wang, D.J. Blasioli, H.J. Kim, H.S. Kim, and D.L. Kaplan, Cartilage tissue engineering with silk scaffolds and human articular chondrocytes, *Biomaterials* **27** (2006), pp. 4434–4442.
116. M. Fini, A. Motta, P. Torricelli, G. Giavaresi, N. Nicoli Aldini, M. Tschon, et al., The healing of confined critical size cancellous defects in the presence of silk fibroin hydrogel, *Biomaterials* **26** (2005), pp. 3527–3536.
117. Y. Tamada, New process to form a silk fibroin porous 3-D structure, *Biomacromolecules* **6** (2005), pp. 3100–3106.
118. B.S. Brooke, A. Bayes-Genis, and D.Y. Li, New insights into elastin and vascular disease, *Trends Cardiovasc Med* **13** (2003), pp. 176–181.
119. W. Shi, S. Bellussi, and D. Warburton, Lung development and adult lung diseases, *Chest* **132** (2007), pp. 651–656.
120. J.B. Leach, J.B. Wolinsky, P.J. Stone, and J.Y. Wong, Crosslinked alpha-elastin biomaterials: towards a processable elastin mimetic scaffold, *Acta Biomater* **1** (2005), pp. 155–164.
121. W.F. Daamen, S.T. Nillesen, T. Hafmans, J.H. Veerkamp, M.J. van Luyn, and T.H. van Kuppevelt, Tissue response of defined collagen-elastin scaffolds in young and adult rats with special attention to calcification, *Biomaterials* **26** (2005), pp. 81–92.
122. K. Trabbic-Carlson, L.A. Setton, and A. Chilkoti, Swelling and mechanical behaviors of chemically cross-linked hydrogels of elastin-like polypeptides, *Biomacromolecules* **4** (2003), pp. 572–580.
123. F.J. Arias, V. Reboto, S. Martin, I. Lopez, and J.C. Rodriguez-Cabello, Tailored recombinant elastin-like polymers for advanced biomedical and nano(bio)technological applications, *Bio-technol Lett* **28** (2006), pp. 687–695.
124. Y. Wu, J.A. MacKay, J.R. McDaniel, A. Chilkoti, and R.L. Clark, Fabrication of elastin-like polypeptide nanoparticles for drug delivery by electrospraying, *Biomacromolecules* **10** (2009), pp. 19–24.
125. H. Betre, L.A. Setton, D.E. Meyer, and A. Chilkoti, Characterization of a genetically engineered elastin-like polypeptide for cartilaginous tissue repair, *Biomacromolecules* **3** (2002), pp. 910–916.
126. H. Betre, S.R. Ong, F. Guilak, A. Chilkoti, B. Fermor, and L.A. Setton, Chondrocytic differentiation of human adipose-derived adult stem cells in elastin-like polypeptide, *Biomaterials* **27** (2006), pp. 91–99.
127. S. Ito, S. Ishimaru, and S.E. Wilson, Effect of coacervated alpha-elastin on proliferation of vascular smooth muscle and endothelial cells, *Angiology* **49** (1998), pp. 289–297.

128. N. Annabi, S.M. Mithieux, A.S. Weiss, and F. Dehghani, The fabrication of elastin-based hydrogels using high pressure CO₂, *Biomaterials* **30** (2009), pp. 1–7.
129. M. Li, M.J. Mondrinos, M.R. Gandhi, F.K. Ko, A.S. Weiss, and P.I. Leikes, Electrospun protein fibers as matrices for tissue engineering, *Biomaterials* **26** (2005), pp. 5999–6008.
130. S.A. Sell, M.J. McClure, K. Garg, P.S. Wolfe, and G.L. Bowlin, Electrospinning of collagen/biopolymers for regenerative medicine and cardiovascular tissue engineering, *Adv Drug Deliv Rev* **61** (2009), pp. 1007–1019.
131. L. Buttafoco, N.G. Kolkman, P. Engbers-Buijtenhuijs, A.A. Poot, P.J. Dijkstra, I. Vermes, et al., Electrospinning of collagen and elastin for tissue engineering applications, *Biomaterials* **27** (2006), pp. 724–734.
132. E.D. Boland, J.A. Matthews, K.J. Pawlowski, D.G. Simpson, G.E. Wnek, and G.L. Bowlin, Electrospinning collagen and elastin: preliminary vascular tissue engineering, *Front Biosci* **9** (2004), pp. 1422–1432.
133. G.D. Prestwich, and J.W. Kuo, Chemically-modified HA for therapy and regenerative medicine, *Curr Pharm Biotechnol* **9** (2008), pp. 242–245.
134. K.L. Beasley, M.A. Weiss, and R.A. Weiss, Hyaluronic acid fillers: a comprehensive review, *Facial Plast Surg* **25** (2009), pp. 86–94.
135. N. Bellamy, J. Campbell, V. Robinson, T. Gee, R. Bourne, and G. Wells, Viscosupplementation for the treatment of osteoarthritis of the knee, *Cochrane Database Syst Rev* (2006), pp. CD005321.
136. V. Colletta, D. Dioguardi, A. Di Lonardo, G. Maggio, and F. Torasso, A trial to assess the efficacy and tolerability of Hyalofill-F in non-healing venous leg ulcers, *J Wound Care* **12** (2003), pp. 357–360.
137. G.D. Prestwich, D.M. Marecek, J.F. Marecek, K.P. Vercruyse, and M.R. Ziebell, Controlled chemical modification of hyaluronic acid: synthesis, applications, and biodegradation of hydrazide derivatives, *J Control Release* **53** (1998), pp. 93–103.
138. D. Campoccia, P. Doherty, M. Radice, P. Brun, G. Abatangelo, and D.F. Williams, Semi-synthetic resorbable materials from hyaluronan esterification, *Biomaterials* **19** (1998), pp. 2101–2127.
139. J.W. Kuo, D.A. Swann, and G.D. Prestwich, Chemical modification of hyaluronic acid by carbodiimides, *Bioconjug Chem* **2** (1991), pp. 232–241.
140. A. Magnani, A. Albanese, S. Lamponi, and R. Barbucci, Blood-interaction performance of differently sulphated hyaluronic acids, *Thromb Res* **81** (1996), pp. 383–395.
141. X. Jia, J. Burdick, J. Kobler, R. Clifton, J. Rosowski, S. Zeitels, et al., Synthesis and characterization of in situ cross-linkable hyaluronic acid-based hydrogels with potential application for vocal fold regeneration, *Macromolecules* **37** (2004), pp. 3239–3248.
142. K. Tomihata, and Y. Ikada, Crosslinking of hyaluronic acid with glutaraldehyde, *J Polym Sci A Polym Chem* **35** (1997), pp. 3553–3559.
143. T. Miyazaki, C. Yomota, and S. Okada, Development and release characterization of hyaluronan-doxycycline gels based on metal coordination, *J Control Release* **76** (2001), pp. 337–347.
144. K. Tomihata, and Y. Ikada, Crosslinking of hyaluronic acid with water-soluble carbodiimide, *J Biomed Mater Res* **37** (1997), pp. 243–251.
145. K.A. Smeds, A. Pfister-Serres, D. Miki, K. Dastgheib, M. Inoue, D.L. Hatchell, et al., Photocrosslinkable polysaccharides for in situ hydrogel formation, *J Biomed Mater Res* **54** (2001), pp. 115–121.
146. J. Baier Leach, K.A. Bivens, C.W. Patrick, Jr., and C.E. Schmidt, Photocrosslinked hyaluronic acid hydrogels: natural, biodegradable tissue engineering scaffolds, *Biotechnol Bioeng* **82** (2003), pp. 578–589.
147. S. Sahoo, C. Chung, S. Khetan, and J.A. Burdick, Hydrolytically degradable hyaluronic acid hydrogels with controlled temporal structures, *Biomacromolecules* **9** (2008), pp. 1088–1092.

148. K.R. Kirker, Y. Luo, J.H. Nielson, J. Shelby, and G.D. Prestwich, Glycosaminoglycan hydrogel films as bio-interactive dressings for wound healing, *Biomaterials* **23** (2002), pp. 3661–3671.
149. B. Grigolo, G. Lisignoli, G. Desando, C. Cavallo, E. Marconi, M. Tschon, et al., Osteoarthritis treated with mesenchymal stem cells on hyaluronan-based scaffold in rabbit, *Tissue Eng Part C Methods* **15** (2009), pp. 647–658.
150. L.A. Solchaga, J.E. Dennis, V.M. Goldberg, and A.I. Caplan, Hyaluronic acid-based polymers as cell carriers for tissue-engineered repair of bone and cartilage, *J Orthop Res* **17** (1999), pp. 205–213.
151. K.Y. Lee, L. Jeong, Y.O. Kang, S.J. Lee, and W.H. Park, Electrospinning of polysaccharides for regenerative medicine, *Adv Drug Deliv Rev* **61** (2009), pp. 1020–1032.
152. J. Li, A. He, J. Zheng, and C.C. Han, Gelatin and gelatin-hyaluronic acid nanofibrous membranes produced by electrospinning of their aqueous solutions, *Biomacromolecules* **7** (2006), pp. 2243–2247.
153. J.L. Ifkovits, H.G. Sundararaghavan, and J.A. Burdick, Electrospinning fibrous polymer scaffolds for tissue engineering and cell culture, *J Vis Exp* **32** (2009), <http://www.jove.com/index/Details.stp?ID=1589>, doi: 10.3791/1589.
154. G. Orive, S.K. Tam, J.L. Pedraz, and J.P. Halle, Biocompatibility of alginate-poly-L-lysine microcapsules for cell therapy, *Biomaterials* **27** (2006), pp. 3691–3700.
155. L. Shapiro, and S. Cohen, Novel alginate sponges for cell culture and transplantation, *Biomaterials* **18** (1997), pp. 583–590.
156. K. Draget, K. Ostgaard, and O. Smidsrod, Homogeneous alginate gels – a technical approach, *Carbohydr Polym* **14** (1990), pp. 159–178.
157. C.K. Kuo, and P.X. Ma, Ionically crosslinked alginate hydrogels as scaffolds for tissue engineering: part 1. Structure, gelation rate and mechanical properties, *Biomaterials* **22** (2001), pp. 511–521.
158. O. Jeon, K.H. Bouhadir, J.M. Mansour, and E. Alsberg, Photocrosslinked alginate hydrogels with tunable biodegradation rates and mechanical properties, *Biomaterials* **30** (2009), pp. 2724–2734.
159. K. Lee, K. Bouhadir, and D. Mooney, Degradation behavior of covalently cross-linked poly (aldehyde guluronate) hydrogels, *Macromolecules* **33** (2000), pp. 97–101.
160. J.L. Drury, R.G. Dennis, and D.J. Mooney, The tensile properties of alginate hydrogels, *Biomaterials* **25** (2004), pp. 3187–3199.
161. E.R. West, L.D. Shea, and T.K. Woodruff, Engineering the follicle microenvironment, *Semin Reprod Med* **25** (2007), pp. 287–299.
162. J.A. Rowley, G. Madlambayan, and D.J. Mooney, Alginate hydrogels as synthetic extracellular matrix materials, *Biomaterials* **20** (1999), pp. 45–53.
163. E. Alsberg, K.W. Anderson, A. Albeiruti, J.A. Rowley, and D.J. Mooney, Engineering growing tissues, *Proc Natl Acad Sci U S A* **99** (2002), pp. 12025–12030.
164. N. Cheng, E. Wauthier, and L.M. Reid, Mature human hepatocytes from ex vivo differentiation of alginate-encapsulated hepatoblasts, *Tissue Eng Part A* **14** (2008), pp. 1–7.
165. M. Dvir-Ginzberg, I. Gamlieli-Bonshtein, R. Agbaria, and S. Cohen, Liver tissue engineering within alginate scaffolds: effects of cell-seeding density on hepatocyte viability, morphology, and function, *Tissue Eng* **9** (2003), pp. 757–766.
166. C. Shi, Y. Zhu, X. Ran, M. Wang, Y. Su, and T. Cheng, Therapeutic potential of chitosan and its derivatives in regenerative medicine, *J Surg Res* **133** (2006), pp. 185–192.
167. I.K. Park, J. Yang, H.J. Jeong, H.S. Bom, I. Harada, T. Akaike, et al., Galactosylated chitosan as a synthetic extracellular matrix for hepatocytes attachment, *Biomaterials* **24** (2003), pp. 2331–2337.
168. T.H. Kim, J.W. Nah, M.H. Cho, T.G. Park, and C.S. Cho, Receptor-mediated gene delivery into antigen presenting cells using mannosylated chitosan/DNA nanoparticles, *J Nanosci Nanotechnol* **6** (2006), pp. 2796–2803.

169. M. Suzuki, S. Itoh, I. Yamaguchi, K. Takakuda, H. Kobayashi, K. Shinomiya, et al., Tendon chitosan tubes covalently coupled with synthesized laminin peptides facilitate nerve regeneration in vivo, *J Neurosci Res* **72** (2003), pp. 646–659.
170. M.H. Ho, D.M. Wang, H.J. Hsieh, H.C. Liu, T.Y. Hsien, J.Y. Lai, et al., Preparation and characterization of RGD-immobilized chitosan scaffolds, *Biomaterials* **26** (2005), pp. 3197–3206.
171. Z.M. Wu, X.G. Zhang, C. Zheng, C.X. Li, S.M. Zhang, R.N. Dong, et al., Disulfide-cross-linked chitosan hydrogel for cell viability and controlled protein release, *Eur J Pharm Sci* **37** (2009), pp. 198–206.
172. D.L. Nettles, S.H. Elder, and J.A. Gilbert, Potential use of chitosan as a cell scaffold material for cartilage tissue engineering, *Tissue Eng* **8** (2002), pp. 1009–1016.
173. S. Hirano, Chitin biotechnology applications, *Biotechnol Annu Rev* **2** (1996), pp. 237–258.
174. H.C. Ott, T.S. Matthiesen, S.K. Goh, L.D. Black, S.M. Kren, T.I. Netoff, et al., Perfusion-decellularized matrix: using nature's platform to engineer a bioartificial heart, *Nat Med* **14** (2008), pp. 213–221.
175. K.L. Chen, D. Eberli, J.J. Yoo, and A. Atala, Regenerative Medicine Special Feature: Bioengineered corporal tissue for structural and functional restoration of the penis, *Proc Natl Acad Sci U S A* **107** (2010), pp. 3346–3350.
176. J.M. Singelyn, J.A. DeQuach, S.B. Seif-Naraghi, R.B. Littlefield, P.J. Schup-Magoffin, and K. L. Christman, Naturally derived myocardial matrix as an injectable scaffold for cardiac tissue engineering, *Biomaterials* **30** (2009), pp. 5409–5416.
177. K. Narayanan, K.J. Leck, S. Gao, and A.C. Wan, Three-dimensional reconstituted extracellular matrix scaffolds for tissue engineering, *Biomaterials* **30** (2009), pp. 4309–4317.

Wei Shen

Contents

9.1	Introduction	244
9.2	Concepts in Material Development	245
9.3	Review of Previous Work	248
9.3.1	Collagen-Inspired Polypeptide Materials	248
9.3.2	Elastin-Inspired Polypeptide Materials	251
9.3.3	Silk-Inspired Polypeptide Materials	255
9.3.4	Polypeptide Materials Self-Assembled Through α -Helical Domains	258
9.3.5	Bioactive and Dynamic Materials	261
9.3.6	Biosynthetic Incorporation of Non-natural Amino Acid Analogs for Engineering Polypeptide Materials	265
9.4	Future Directions	267
	References	269

Abstract Engineered polypeptides have emerged as attractive materials to construct artificial extracellular matrices (ECMs) in tissue engineering. These materials offer advantages over conventional synthetic materials in recapitulating essential characteristics of complex and dynamic native ECMs, which is one of the key requirements for successful tissue engineering, because proteins are major players in providing structural support, cell adhesion, and signal regulation in native ECMs. The structures and functions of these proteins and their domains, as well as those of de novo designed polypeptide domains having self-assembly and molecular recognition abilities, can be combined in engineered polypeptides in a modular manner to yield multifunctional, bioactive materials to mimic native ECMs and optimize tissue engineering outcomes. Engineered polypeptides can be synthesized both chemically and biosynthetically. In recent years, the biosynthetic methodology has received increasing attention because the advances in molecular biology and protein engineering have expanded its capacity. Biosynthetic preparation allows polypeptide materials to be genetically engineered in a modular manner and the resulting polymers have absolutely uniform sequence, composition, molecular weight, and consequently higher order

W. Shen

Department of Biomedical Engineering, University of Minnesota, Minneapolis, MN 55455, USA
e-mail: shenx104@umn.edu

9 structures and functions. These properties not only allow us to engineer novel multifunctional materials to elicit desired cell responses toward functional tissue regeneration, but also offer the opportunity to create well-controlled and tunable systems for systematic studies to enhance our understanding of the relationships among extracellular microenvironments, cell behavior and fate selection, and tissue assembly. Such understanding will provide valuable guidelines for design of future generations of artificial ECMs. In this chapter, engineered polypeptides that have been used or have the potential to be used in tissue engineering will be discussed with an emphasis placed on their molecular design as well as examples of their use in tissue engineering studies.

Keywords Biomimetic materials • Genetic engineering • Non-natural amino acids • Polypeptide-based polymers • Protein engineering • Self-assembly

9.1 Introduction

Materials constructed from engineered polypeptides have emerged as attractive artificial extracellular matrices (ECMs) for regeneration of functional tissues and organs. Since proteins are important components in native ECMs, artificial ECMs created from properly engineered polypeptide-based materials can potentially provide cells with microenvironments similar to their native counterparts. Native ECM proteins not only provide structural support and cell adhesion function, but also define many essential biochemical and physical cues to regulate cell proliferation, differentiation, migration, and fate selection during developmental and physiological processes. The success of tissue engineering to a large extent relies on whether artificial ECMs can mimic the structural, adhesive, and regulatory properties of their native counterparts. Conventional materials have limited ability to mimic native ECMs for optimization of tissue engineering outcomes. In contrast, essential biochemical and physical properties of ECMs can be readily and precisely engineered in polypeptide-based materials because of their similar molecular nature to that of native ECM proteins and the high-fidelity, modular biosynthetic approaches available for their preparation. The great potential of engineered polypeptides to recapitulate essential characteristics of *in vivo* extracellular microenvironments through rationally designed molecular structures, properties, and functions, combined with the possibility to prepare these materials in large scale owing to the advances in molecular biology and chemical synthesis, makes them increasingly attractive in tissue engineering. The modular and precise nature of these materials also provide unique opportunities to create well-controlled tunable systems that allow systematic study of the relationships among microenvironments, cell behavior, and tissue assembly, the understanding of which could provide guidelines for design of future generations of artificial ECMs.

This chapter will provide an overview of engineered polypeptide materials that have been used or have the potential to be used as artificial ECMs in tissue engineering. The emphasis will be placed on their molecular design along with examples of their applications

in tissue engineering studies. Polypeptide-based materials inspired by natural structural proteins such as collagens, elastins, and silks as well as other naturally occurring or de novo designed self-assembling domains such as coiled-coils will be summarized. Engineering of bioactive and dynamic materials desirable for tissue engineering applications by harnessing bioactivities and molecular recognition of polypeptides will be discussed. Recently developed technologies for biosynthetic incorporation of non-natural amino acid analogs, which are expected to provide new avenues to expand the scope of bioactive, multifunctional polypeptide materials, will also be included. Materials self-assembled from small peptide molecules such as peptide amphiphiles are also attractive and promising candidates for artificial ECMs in tissue engineering [1, 2], but they are not part of the scope of this chapter (please refer Chaps. 2 and 3 for more information on this topic).

9.2 Concepts in Material Development

Numerous naturally occurring or de novo designed proteins, polypeptide domains, or peptide motifs provide immense inspiration for molecular design of a wide variety of structural, bioactive, multifunctional, and intelligent materials that exhibit desired properties for tissue engineering (Fig. 9.1). These properties are often difficult to achieve or control with conventional synthetic polymers. One function that artificial ECMs need to perform is to provide structural and mechanical support. Polypeptide-based structural materials have been designed by using consensus peptide sequences derived from naturally occurring structural proteins such as collagens, elastins, and silks as building blocks. Most of these building blocks can form higher order structures, such as triple-helices and β -sheets, and self-assemble to result in physically cross-linked networks or fibers that further form three-dimensional (3D) supramolecular structures. Other self-assembling domains, such as coiled-coils, have also been introduced into polypeptide-based polymers to yield fibers and networks that can provide structural support in tissue engineering. In addition to self-assembly, other molecular mechanisms that nature uses to build structural materials, such as covalent cross-linking, have been mimicked in polypeptide-based materials as well. For example, lysine residues have been genetically introduced in elastin-like-polypeptides (ELPs) with absolute precision regarding their density and positions along the polypeptide backbone, mimicking the lysine-rich segments in tropoelastins (elastin precursors) that allow covalent cross-linking to result in mature elastins.

Artificial ECMs are expected to mediate cell adhesion and present a wide range of bioactivities to regulate cell behavior and fate selection in addition to providing structural support. Spatial and temporal control of these bioactivities is desirable to closely mimic the complex and dynamic in vivo extracellular microenvironments. Artificial ECMs should also be biodegradable, because the purpose of their use is to provide temporal mechanical support and define extracellular microenvironments for regeneration and remodeling rather than to retain these materials permanently. Polypeptide-based materials are particularly suitable for molecular engineering to satisfy these multiple requirements for artificial ECMs because native ECMs perform these functions through (poly)peptide domains and motifs,

(A) Polypeptide materials inspired by structural proteins and self-assembling domains

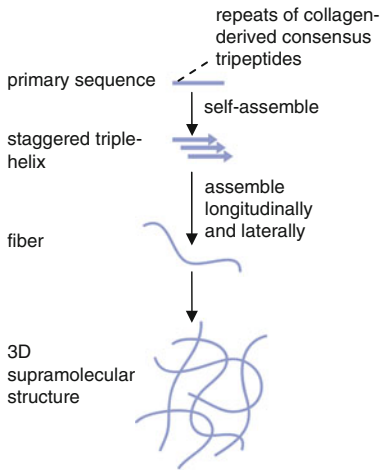
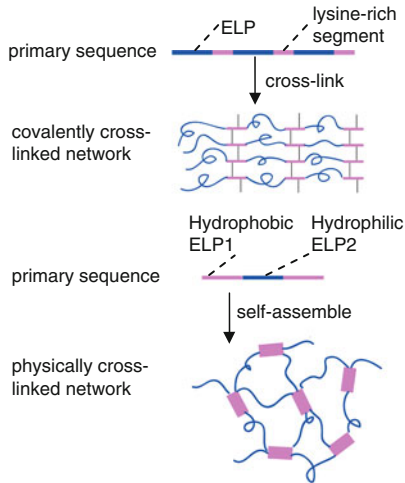
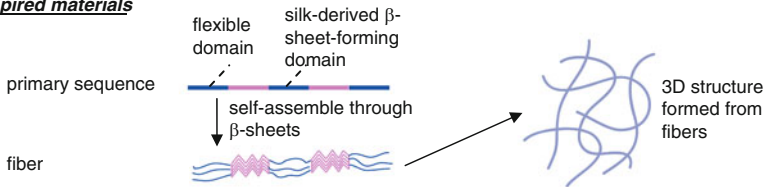
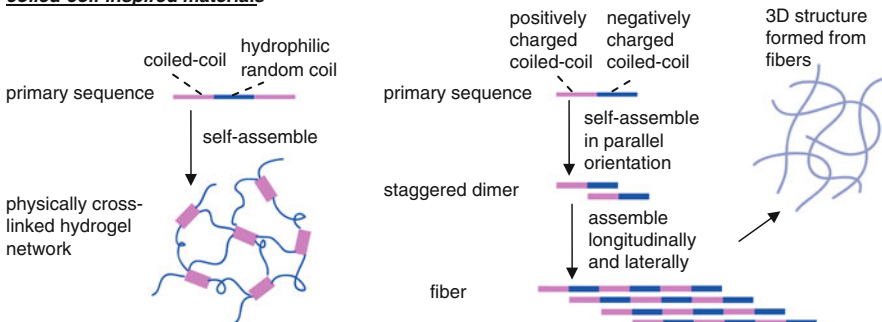
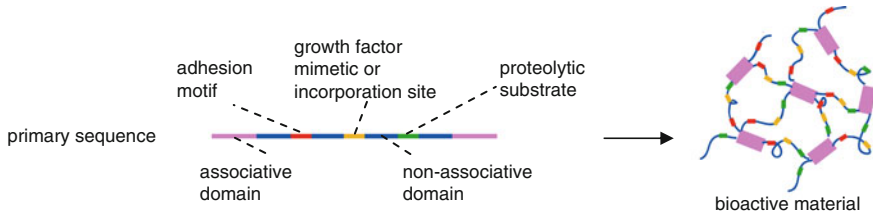
collagen-inspired materials***elastin-inspired materials******silk-inspired materials******coiled-coil-inspired materials***

Fig. 9.1 (continued)

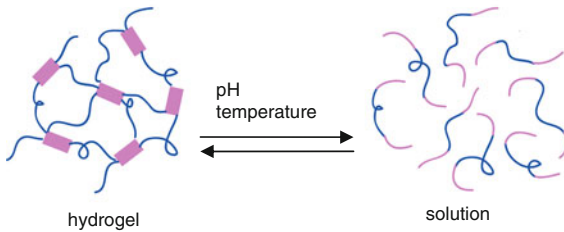
which can be rationally selected and readily combined on the molecular level in engineered polypeptides to yield multifunctional, bioactive materials. For example, cell adhesion peptide ligands and proteolytic peptide substrates derived from natural ECM proteins such as fibronectin and collagen have been incorporated into polypeptide materials on the

(B) Bioactive materials incorporating adhesive, regulatory, and degradable peptide stretches



(C) Materials incorporating intelligent features of proteins

Reversible materials constructed by protein domains exhibiting a stimuli-responsive conformational change and subsequent alteration in their self-assembly ability



Dynamic materials constructed by protein domains exhibiting stimuli-responsive conformational change and consequent alteration in their size

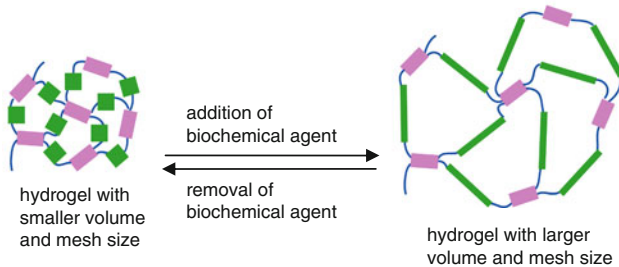


Fig. 9.1 Molecular design of polypeptide materials by exploiting naturally occurring or de novo designed proteins, polypeptide domains, and peptide motifs as building blocks to confer structural, bioactive, and intelligent functions

genetic level to confer cell adhesion properties and biodegradability. Growth factors and their mimetics can be either directly introduced into polypeptide backbones or attached to residues carefully engineered to permit orthogonal modification. In addition, many polypeptide domains have intelligent features: they have molecular recognition ability and undergo conformational changes in response to microenvironmental changes in pH, temperature, and biochemical components. The consequent alteration in their self-assembly capacity and/or size results in stimuli-responsive, reversible, and dynamic materials that may offer unique opportunities to better mimic *in vivo* extracellular microenvironments.

Molecularly designed polypeptide materials can be synthesized both chemically and biosynthetically. The biosynthetic methodology, in which the genes encoding the designed

polypeptides are created through recombinant DNA technology and the polypeptide polymers are expressed in biological hosts, is particularly attractive because it offers several advantages. The high fidelity of biosynthesis apparatus assures that biosynthesized polypeptide molecules are absolutely uniform in molecular weight, composition, sequence, and consequently higher-order structures and functionalities. Such a high level of precision in control of molecular structure and material properties has not been surpassed by chemical synthesis approaches. In addition, the modular nature of genetic engineering allows building blocks conferring distinct properties to be combined readily in a systematic manner to generate tailored, multifunctional materials. These modularly engineered and precisely controlled materials allow systematic investigation of the relationships among microenvironments, cell behavior, and tissue products, providing valuable guidelines for design of future generations of artificial ECMs.

The recent advances in biosynthetic incorporation of non-natural amino acid analogs into protein polymers have further expanded the scope of protein engineering and offered new opportunities to create novel polypeptide-based materials for biomedical applications, including tissue engineering. Some incorporated analogs can optimize the physical properties and self-assembly capacity of polypeptide domains. Some can introduce chemical functionalities not present in natural amino acids to enable orthogonal chemical modifications, which is particularly useful for creating hybrid materials composed of both polypeptides and conventional synthetic polymers, and for modifying polypeptide materials with small moieties or other polypeptides to introduce additional properties.

9.3

Review of Previous Work

9.3.1

Collagen-Inspired Polypeptide Materials

Collagens are a major ECM component in connective tissues, where they not only provide mechanical support, but also regulate a variety of cellular events, including cell adhesion, migration, proliferation, differentiation, and survival. Use of collagen-based materials as artificial ECMs can be traced back to the first generation of tissue-engineered skin substitutes, in which animal-derived type I collagen served as a scaffold. Since then, animal-derived type I collagen has been used in a wide variety of tissue engineering applications. However, animal-derived materials have drawbacks such as batch-to-batch variations, the risk of transmission of infectious diseases, and difficulties in modifying and precisely controlling material properties. In addition, even though more than 20 types of native collagens have been identified and proven to play distinct critical roles during natural tissue development and regeneration processes, collagens other than type I have not been widely used in tissue engineering because their presence in natural sources is not as abundant as that of type I collagen and isolation in large quantities is difficult. All of these limitations of naturally-derived collagens can be circumvented by engineered polypeptides that recapitulate the essential structures and properties of native collagens.

Native collagens are characterized by the consensus tripeptide sequence GXY, in which the X and Y positions are commonly occupied by proline and post-translationally modified hydroxyproline. This feature of the primary sequence allows interchain hydrogen bonding between hydroxyproline and glycine, providing the primary driving force for the assembly of closely packed triple-helices, a structural hallmark of collagens [3]. Collagen-inspired polypeptides composed of either collagen-derived domains or tandem repeats of the collagen-derived consensus tripeptide GXY have been designed and synthesized. Both chemical and biosynthetic methods have been successfully used to produce these engineered polypeptides. In recent years, the significant progress made in molecular biology has expanded the capacity of biosynthetic approaches, making them increasingly attractive. Collagen-inspired polypeptides containing hydroxyproline have been biosynthesized in a variety of expression systems, including bacteria [4], insect cells [5], yeast [6, 7], mammalian cells [8], and transgenic plants [9, 10], silkworms [11], or mice [12].

Polypeptides composed of various domains derived from human collagen II have been recombinantly engineered and used in cartilage tissue engineering [13, 14]. One polypeptide comprises a central segment consisting of three tandem repeats of the D4 domain (residues 703–936), which has the biological activity to support chondrocyte spreading and migration, and one D1 and one D0.4 terminal domain, which facilitate protein folding. The recombinant polypeptide was expressed in HT-1080 cells. The resulting product folded into collagen-like triple-helices. When coated on 3D fibrous scaffolds made of polyglycolic acid, this recombinant polypeptide performed better than the wild-type collagen II in enhancing seeding efficiency and subsequent invasion of chondrocytes. The resulting tissue engineered constructs had higher cell density and more efficient biosynthesis of cartilage ECMs.

In addition to collagen-derived domains, the collagen-derived consensus tripeptide sequences have also been used as building elements to construct polypeptides that recapitulate the essential structures and properties of collagens. The collagen-like polypeptides consisting of tandem repeats of the consensus tripeptide sequences form triple-helical structure and even long collagen-like fibrils and 3D supramolecular structures. Long fibrils and 3D structures form either from collagen-like polypeptides having high molecular weight or from short triple-helices through further longitudinal and lateral assembly. The molecular structures of these polypeptides are rationally designed to provide the driving forces, including hydrogen bonding, electrostatic interactions, hydrophobic interactions, metal ion chelation, and covalent bonding, for triple-helix formation and further longitudinal and lateral association.

Large collagen-like polypeptides have been synthesized chemically through the EDC coupling chemistry and native chemical ligation. Polymerization of the tripeptide monomer PHypG (Hyp: hydroxyproline) in the presence of 1-ethyl-3-(3-dimethyl-aminopropyl)-carbodiimide hydrochloride (EDC) yielded poly(PHypG) with a molecular weight greater than 10^4 Da [15]. This synthetic polypeptide formed stable triple-helical structures and was processed into 3D sponges through freeze-drying. When implanted subcutaneously in the dorsal area of rats, these sponges did not invoke adverse tissue reactions. Materials fabricated from this polypeptide were softer and less adhesive than those from bovine type I atelocollagen, but they degraded at a comparable rate. These properties led to their superior performance in promoting *in vivo* dermal epithelialization of a full-thickness

9 wound. An alternative chemical approach to synthesizing large collagen-like polypeptides is native chemical ligation [16]. Peptides containing 10 tripeptide motifs (most of them are PHypG), one N-terminal cysteine, and one C-terminal thioester were prepared using solid-phase peptide synthesis. These peptides underwent selective head-to-tail native chemical ligation under mild aqueous conditions and yielded large collagen-like polypeptides exhibiting triple-helical structures.

Long collagen-like fibrils have also been obtained from shorter polypeptides that are carefully designed to form triple-helices that can further assemble longitudinally. One strategy is to create staggered triple-helices by introducing interchain disulfide bridges [17, 18]. Cysteine residues were introduced to the chosen X and Y positions of a collagen-like polypeptide consisting of tandem repeats of GHyp to result in one biscysteinyll chain and two different monocysteinyll chains. Staggered triple-helices formed when the monocysteinyll chains were allowed to react with the biscysteinyll chain in a regioselective manner sequentially by selectively activating and protecting the cysteine residues in the biscysteinyll chain. This molecular design prevented intramolecular association and promoted intermolecular triple-helix formation. The resulting staggered triple-helices had self-complementary cohesive ends and were able to assemble longitudinally into long fibrils and further into 3D hydrogels.

Longitudinal assembly of short triple-helices can also be driven by electrostatic interactions [19]. A polypeptide having the (PRG)₄(PHypG)₄(EHypG)₄ sequence formed triple-helices characterized by a hydrophobic central region flanked by a positively charged N-terminal region and a negatively charged C-terminal region. The complementary electrostatic interactions between adjacent triple-helices led to staggered arrangement of the charged regions and drove longitudinal assembly of the helices into long fibrils and a 3D supramolecular architecture.

Interchain aromatic-stacking and hydrophobic interactions have also been used as driving forces to stabilize triple-helices and promote their supramolecular assembly [20]. Hydrophobic aromatic groups L-phenylalanine and L-pentafluorophenylalanine were placed at the two termini of collagen-like polypeptides consisting of tandem repeats of GHyp. Interchain aromatic-stacking and hydrophobic interactions provided by these groups stabilized the triple-helical structure and further drove head-to-tail assembly of these helices into long fibrils. These materials were able to induce platelet aggregation, which is a characteristic activity of type I collagen.

Molecular engineering of collagen-like polypeptides also led to materials assembled in response to external stimuli. A collagen-like polypeptide containing three metal-binding units, including an N-terminal nitrilotriacetic acid unit, a C-terminal 2-histidine sequence, and a bipyridyl moiety at the central position, was engineered to yield collagen-like hydrogels that formed in response to the trigger of metal ion chelation [21]. In the presence of metal ions such as Ni^{II}, Co^{II}, and Zn^{II}, the polypeptide self-assembled into stable triple-helices and further underwent head-to-tail ligation to form long fibrils and 3D hydrogels. HeLa cells encapsulated in these hydrogels were surrounded by a fibrous network and remained viable, suggesting that these 3D networks could potentially be used as artificial ECMs in tissue engineering.

Careful design of the sequences of collagen-like polypeptides can result in stable triple-helices even in the absence of hydroxyproline residues. Polypeptides having

the (GER)₁₅GPCCG, (GPP)₃GPRGEKGERGPR(GPP)₃GPCCG, and [GERGDLGPQ-GIAGQRGVV(GER)₃GAS]₈GPPGPCCGGG sequences, respectively, were prepared through either biosynthesis or solid-phase synthesis [22, 23]. The peptide motif GPCCG, which is derived from the C-terminus of type III collagen, was placed at the C-termini of these polypeptides to form disulfide knots. The GER motif was introduced to provide interchain electrostatic interactions; and the GPP motif was included to provide hydrophobic interactions. These interchain hydrophobic interactions, electrostatic interactions, and covalent disulfide bonds provided driving forces for the hydroxyproline-lacking polypeptides to assemble into stable triple-helices and even into microfibrillar structures, though the mechanism underlying the assembly was not completely clear. Since the GER tripeptide is a cell adhesion motif existing in many native collagens, these engineered polypeptide materials exhibited cell adhesion activity.

Copolypeptides consisting of collagenous blocks were engineered to form hydrogels [24]. Triblock copolypeptides comprising two self-assembling proline-rich endblocks and a hydrophilic random coil midblock were designed. The endblocks had the (PGP)₉ sequence, which was able to form trimers at physiological temperature and provide junction points for hydrogel networks; the midblock had the amino acid composition of a collagenous molecule, but the sequence was purposely scrambled so that it did not form triple-helices and only performed the function of retaining water in the networks. The hydrogels self-assembled from these polypeptides in aqueous solutions exhibited many hallmark properties of traditional collagenous materials.

9.3.2

Elastin-Inspired Polypeptide Materials

Elastins are another type of important structural proteins in native ECMs. Elastins are rich in elastic tissues and organs, such as blood vessels, skin, and lung [25]. Native elastins are converted from their precursors, tropoelastins, which are composed of alternating hydrophobic domains and lysine-rich crosslinking domains [26]. The lysine residues in tropoelastins are cross-linked through the mediation of lysyl oxidase, yielding mature elastins. Mature elastins are highly elastic because of their hydrophobic and cross-linked nature [25, 27]. In addition to high elasticity, the coacervation behavior, an entropy-driven phenomenon in which the polymer chains adopt more ordered structure with increasing temperature, is another characteristic property of elastins [28]. Elastins not only provide mechanical support for tissues, but also have biochemical activities to regulate important biological events ranging from ECM synthesis to cell proliferation, differentiation, and migration through their interactions with elastin–laminin receptors on cell surfaces [29, 30].

As important native ECM proteins, elastins are attractive biomaterials for constructing artificial ECMs in tissue engineering. But use of animal-derived elastins in tissue engineering is impractical, because they are limited in quantity and purity. In addition, batch-to-batch variations, the risk of diseases transmission, and difficulties in modifying and controlling material properties have all directed the interest toward engineered elastin or elastin-like polypeptides, which are expected to address the limitations associated with animal-derived elastins.

Recombinant tropoelastin and polypeptides composed of tropoelastin fragments have been biosynthesized in bacterial and mammalian expression systems. The lysine residues in these engineered proteins allowed them to be cross-linked by bifunctional, amine-reactive chemical reagents or through the lysyl-oxidase-mediated reaction [31]. The Young's modulus of the resulting materials ranged from 220 to 400 kPa. The recombinant tropoelastin coated on polymeric scaffolds enhanced attachment of both endothelial and smooth muscle cells, suggesting their potential use in small-diameter vascular graft engineering. The polypeptides consisting of tropoelastin fragments were coated on polyurethane catheters and significantly reduced thrombosis and increased catheter patency [32]. These studies show that recombinantly engineered tropoelastin-based proteins are potentially valuable materials for vascular tissue engineering.

Artificial elastin-like polypeptides (ELPs) that are designed according to short consensus pentapeptide sequences in elastins have also been prepared, extensively examined, and used in a variety of tissue engineering studies, including cardiovascular, musculoskeletal, and ocular surface tissue engineering as well as cell sheet engineering. ELPs comprise repeats of the elastin-derived pentapeptide sequence VPGXG, in which the guest residue X can be any amino acid residue except proline [33]. These engineered polypeptides display many important properties of native elastins, such as high elasticity and the coacervation behavior. ELPs have inverse temperature phase transition (or lower critical solution temperature LCST) phenomenon: they are soluble when the temperature is below the phase transition temperature T_t and aggregate when the temperature is increased to above T_t . T_t can be rationally engineered on the molecular level through the choice of the amino acid residue on the X position: T_t decreases with increasing hydrophobicity of this residue [34]. ELPs have been synthesized both chemically and biosynthetically in high yields [35, 36]. The biosynthetic approach has attracted increasing attention in recent years owing to the reasons discussed in Sect. 9.2 of this chapter. ELPs are not cytotoxic and exhibit good biocompatibility as revealed from animal studies [37, 38].

Chemically cross-linkable ELPs have been genetically engineered by including lysine residues, mimicking the composition of tropoelastins [39–47]. In most cases chemical cross-linking reactions occur between the primary amine of the lysine residue and an amine-reactive group in a selected bifunctional or trifunctional reagent, such as glutaraldehyde, disuccinimidyl glutarate, isocyanate, bis(sulfosuccinimidyl) suberate, disuccinimidyl suberate, and *tris*-succinimidyl aminotriacetate. The mechanical properties of chemically cross-linked ELP materials can be systematically tuned in a wide range by varying their molecular characteristics at the genetic level. In particular, the number of lysine residues and their positions along the polypeptide backbone can be tailored to modulate the cross-linking density and consequently the mechanical properties. The reported Young's modulus of chemically cross-linked ELP materials spans the whole range of values for native elastin (0.3–0.6 MPa) [41]. In addition to mechanical properties, biological properties of these ELP materials can also be precisely controlled at the genetic level. Fibronectin-derived cell adhesion motifs, RGD and REDV, have been incorporated to promote adhesion of endothelial cells [39, 41, 47]. These bioactive ELP materials have great potential in small-diameter vascular graft engineering because they not only possess mechanical properties comparable to those of native vessels but also allow endothelial cells to adhere and form a monolayer, which can prevent thrombosis.

To avoid the use of chemical cross-linking reagents during material processing, physically cross-linkable block ELPs have been developed [48–50]. Most chemical cross-linking reagents are toxic and cannot be removed completely after material processing, and the residual reagents may cause detrimental effects in tissue engineering applications. Physically cross-linkable triblock ELP copolypeptides consisting of two hydrophobic terminal ELP blocks and a hydrophilic midblock were engineered. The hydrophobicity/hydrophilicity of each block was tailored by careful choice of the residue on the guest position of each pentapeptide. Above the phase transition temperature of the endblocks, these polypeptides self-assembled into hydrogels in aqueous solutions [50]. They could also be dissolved in an organic solvent and cast into films [48, 49]. Mechanical properties of the resulting materials were controlled by engineering the molecular structure of the block copolypeptides (such as the sequence and size of each block) and selection of processing conditions (such as solvent and temperature). A young's modulus as high as 87 MPa has been reported for films prepared through solvent-casting.

In situ forming materials that change from liquid to semi-solid state under physiologically compatible conditions are particularly attractive for tissue engineering applications. These materials allow cells and sensitive biological factors to be uniformly encapsulated; they are injectable for minimally invasive delivery; and they can match the shape of defects perfectly. Physically cross-linkable triblock ELPs that exhibit liquid behavior at lower temperatures and self-assemble into hydrogels at 37°C represent one type of in situ forming ELP materials. Un-cross-linked coacervates, which form above phase transition temperature T_t , can be viewed as in situ forming ELP materials as well, and have been used for cell encapsulation in cartilage tissue engineering [51, 52]. An ELP having a T_t of 35°C was engineered by introducing V, G, and A residues at a 5:3:2 ratio to the guest positions in the [VPGXG]₉₀ polypeptide. This T_t , which lies between room temperature and body temperature, allowed cells to be suspended in a liquid precursor at room temperature and encapsulated in a coacervate upon a temperature raise to 37°C. The complex shear modulus of the coacervate was ca. 80 Pa, greater than that of the liquid precursor by 3 orders of magnitude. Chondrocytes encapsulated in this coacervate maintained a rounded morphology and chondrocytic phenotype, with characteristic cartilage matrix molecules (sulfated glycosaminoglycans and collagen) deposited at high levels. Human adipose-derived stem cells encapsulated in this coacervate underwent chondrocytic differentiation, even in the absence of chondrogenic supplements such as dexamethasone and TGF- β [52]. These studies suggest that ELP-based materials promote chondrogenesis of encapsulated chondrocytes or stem cells and have great potential for cartilage tissue repair.

ELP coacervates have proven to provide favorable chondrogenic environments, but their modulus and mechanical integrity are insufficient to support functional cartilage repair. Covalently cross-linked in situ forming ELP materials are expected to have enhanced mechanical properties compared to coacervates. One strategy to prepare such materials is to use tissue transglutaminase (tTG), which catalyzes covalent bond formation between glutamine residues and primary amines under physiologically compatible conditions [53]. Enzyme-mediated reactions regulate many aspects of matrix processing in vivo, and are attractive choices for modification of artificial ECMs in the presence of cells. Two ELPs, one having lysine K residues and the other having glutamine Q residues, were genetically engineered. When they were mixed at an equimolar ratio, gelation occurred in the presence

of tTG under physiological conditions. A complex shear modulus of 280 Pa was obtained, which was significantly greater than that of un-cross-linked coacervates. Chondrocytes encapsulated in these in situ forming ELP hydrogels remained viable and rounded. Their chondrocytic phenotype was maintained as indicated by the significant accumulation of sulfated glycosaminoglycans and type II collagen.

ELP hydrogels chemically cross-linked through the mediation of tTG have much higher modulus than un-cross-linked coacervates, but their modulus is still inadequate compared to that of native cartilage. To further improve mechanical properties of in situ forming ELP materials, a biologically benign, amine-reactive cross-linker β -[tris(hydroxymethyl) phosphino] propionic acid (betaine) (THPP) was used [54–56]. Addition of THPP in the solution of an ELP consisting of 144 repeats of (VPGXG)₉, in which the 9 guest positions were occupied by K, F, and V residues (1:1:7), at an equimolar ratio of THPP and lysine resulted in gelation within 5 min. Systematic modulation of the lysine density along the ELP backbone resulted in hydrogels exhibiting complex shear modulus in the range between 5.8 and 45.8 kPa, which was greater than that of un-cross-linked coacervates by 3 orders of magnitude. An in vitro study showed that fibroblasts survived the encapsulation process. When ELP hydrogels cross-linked by THPP were implanted in goats for cartilage repair, they supported the infiltration of cells and deposition of cartilage matrix. One drawback of these materials revealed from the in vivo study is their rapid degradation, which needs to be addressed through further research.

(Meth)acrylate-containing polymers are photo-cross-linkable under biologically benign conditions and therefore have been widely used for in situ cell encapsulation. A methacrylate-functionalized ELP has been prepared through modification of lysine residues with methacrylic anhydride. The modified ELP was processed into fibers through electrospinning and light irradiation, with the resulting products having diameters ranging from 300 nm to 1.5 μm [57]. These fibers can serve as preformed scaffolds for tissue engineering. Although the purpose of ELP modification in this study was to fabricate fibers, the methacrylate-functionalized ELP could potentially be used as photo-responsive in situ forming materials for cell encapsulation.

ELPs have been coated on surfaces and evaluated for their use in tissue engineering. A recombinant ELP containing the cell adhesion CS5 domain was coated on glass surfaces and examined for its potential for ocular surface tissue engineering [58]. Significant enhancement in adhesion and proliferation of conjunctival epithelial cells, but not fibroblasts, was observed on ELP-coated substrates compared to control substrates. Conjunctival epithelial cells maintained their differentiated phenotype. This preliminary study suggests that ELPs have the potential to serve as artificial ocular surface ECMs to promote tissue regeneration for vision restoration.

The LCST behavior of ELPs has been exploited to engineer cell sheets, which could be transplanted to repair tissues. In one study, an ELP having the sequence of (GVGVP)₂₈₈ was coated on the surface of tissue culture plates to further allow immobilization of an RGD-containing ELP at 37°C [59]. In another study, an RGD-containing ELP, [(GVGVP)₁₀GVGVPRGDS(PGVGVP)₁₀]₁₈, was directly coated on tissue culture plastics [60]. These ELP-modified surfaces were hydrophobic and presented the cell adhesion RGD motif at 37°C, allowing cells, including human amniotic epithelial and mesenchymal cells, to grow into monolayers. The cell sheets were harvested by reducing the temperature

to lower values, at which the ELPs became hydrophilic and non-associative. Cell detachment resulted from a combination of the hydrophilic nature of ELPs, the detachment or shielding of RGD, and changes in cellular metabolic activity at low temperature. These engineered cell sheets could allow transplantation with well-controlled size and location.

9.3.3

Silk-Inspired Polypeptide Materials

Silk-inspired polypeptides are another type of materials that have attracted considerable attention in tissue engineering. Naturally occurring silk proteins are derived from silkworms and spiders. They are not native to the human or animal body, but these fibrous structural proteins have exceptional mechanical properties and exhibit high biocompatibility, making them attractive as potential artificial ECMs [61–68]. Naturally-derived silk proteins have been reconstituted and processed into a variety of forms to support regeneration of bone, ligaments, cartilage, skin, and nerve fibers. However, these materials have several limitations. For example, they often contain residual impurities that cause adverse immune responses, even though the silk fibers themselves are immunologically inert [61]. Additionally, obtaining large quantities of spider silks, which have better mechanical properties than silkworm silks, is difficult. These problems can be addressed by developing engineered polypeptides that possess the essential structures and properties of silks. The engineering approach also allows versatile combination of intrinsic properties of silks, such as extraordinary mechanical properties, and additional functionalities tailored for tissue engineering requirements, such as cell adhesion and biodegradation. The advances in molecular biology have allowed recombinant silk proteins and silk-like polypeptides to be genetically engineered and biosynthetically produced in high yields in a variety of host systems, including bacteria [69], yeast [70], insect cells [71], mammalian cells [72], and transgenic plants [73]. Such synthesis ability makes it possible to use recombinantly produced silk-inspired polypeptides as artificial ECMs in tissue engineering.

The exceptional mechanical properties of silks, such as high tensile strength and toughness, are conferred by their primary sequences and secondary structures. Silk proteins comprise repetitive and alternating hydrophobic and hydrophilic domains. The alanine or alanine-glycine rich hydrophobic domains assemble into β -sheets and form crystalline regions through hydrophobic interactions and hydrogen bonding to provide high tensile strength; the less ordered hydrophilic domains provide elasticity and increase toughness [74, 75]. Recombinant polypeptides composed of consensus units derived from silkworm and spider silks have been genetically engineered, biosynthesized, and processed into fibers, films, foams, and hydrogels that can be potentially used as scaffolds in tissue engineering. Since spider silks have extraordinary mechanical properties, the consensus units derived from the Major Spidroin dragline types I and II of *N. clavipes* spiders (MaSp1 and MaSp2) and from the major ampullate silks of *Araneus diadematus* spiders (ADF-3 and ADF-4) have attracted considerable interest [76].

Molecular engineering approaches allow incorporation of cell adhesion motifs, which do not exist in natural silks, into silk-based polypeptides. Introduction of the cell adhesion property in artificial ECMs is essential in tissue engineering, because most tissues include

anchorage-dependent cells whose adhesion to ECMs modulates their spreading, migration, proliferation, differentiation, and survival, and consequently tissue engineering outcomes. The cell adhesion motifs RGD and GER, which are derived from natural ECM proteins fibronectin and collagen, have been genetically incorporated into recombinant silk-like polypeptides [77, 78]. The materials constructed from these polypeptides significantly enhanced cell adhesion. Adhesive peptides derived from other sources have also been used. A genetically engineered polypeptide combining the silk-like peptide (GAGAGS)₃ and the adhesive sequence, AKPSYPPTYK, derived from mussel-adhesive proteins supported the adhesion of neonatal normal human dermal fibroblasts [79].

A novel chimeric protein combining a recombinant silk-like polypeptide and the C-terminal portion of rat dentin matrix protein 1 (CDMP1), which plays an important role in regulating nucleation and growth of hydroxyapatite in bone *in vivo*, has been genetically engineered for bone regeneration [80]. The silk-like polypeptide in the chimeric protein contained repeats of a consensus sequence derived from spider silk protein MaSp1 and retained its ability to self-assemble and form crystalline regions. The CDMP1 domain retained its mineralization-inducing ability. Films fabricated from this chimeric protein induced the formation of osteoconductive calcium hydroxyapatite in the presence of simulated body fluids (Fig. 9.2). This novel polypeptide material has great potential as an artificial ECM for bone regeneration.

In addition to incorporation of cell adhesion and other bioactive domains/motifs, another consideration in the molecular design of silk-based materials is to improve their mechanical properties, which currently cannot match those of native silks. A MaSp1-based silk-like polypeptide was further engineered to selectively replace a dipeptide AA with CC [81]. The introduced intermolecular disulfide bridges resulted in an approximately 50% increase in the tensile modulus. In another study, recombinant silk-like polypeptides composed of an elastic motif, either the (GPGGA)₄ or the [(GPGGY)(GPGGS)]₂ peptide derived from the flagelliform protein, and an alanine-rich strength motif, the GGPSGPGS(A)₈ peptide derived from the dragline silk MaSp2 protein, were genetically engineered [82]. It was found that the choice of the fifth and tenth amino acid residues in the elastic motif had a profound impact on the β -sheet structure of the alanine-rich motif and consequently the mechanical properties of the polypeptide materials. Polypeptides having tyrosine and serine residues on these positions had a more stable β -sheet structure of the alanine-rich segments and higher tensile strength and toughness than those having alanine residues on these positions, probably because tyrosine and serine provided hydrogen bonding interactions to facilitate β -sheet formation. These results encourage further rational design on the molecular level to improve mechanical properties of engineered silk-like polypeptide materials.

Silk-based polypeptides have also been engineered on the molecular level to improve their compatibility with aqueous-phase processing, which is desirable for tissue engineering applications because potential detrimental effects of residual organic solvents can be avoided. Most silk-based polypeptides have poor aqueous solubility and have to be dissolved in organic solvents for material processing. In contrast, highly concentrated aqueous solutions of silk proteins can be maintained *in vivo*, where β -sheet assembly is tightly regulated through various chemical and mechanical mechanisms [74]. To mimic such exquisite control of β -sheet assembly and improve aqueous solubility, a redox-responsive

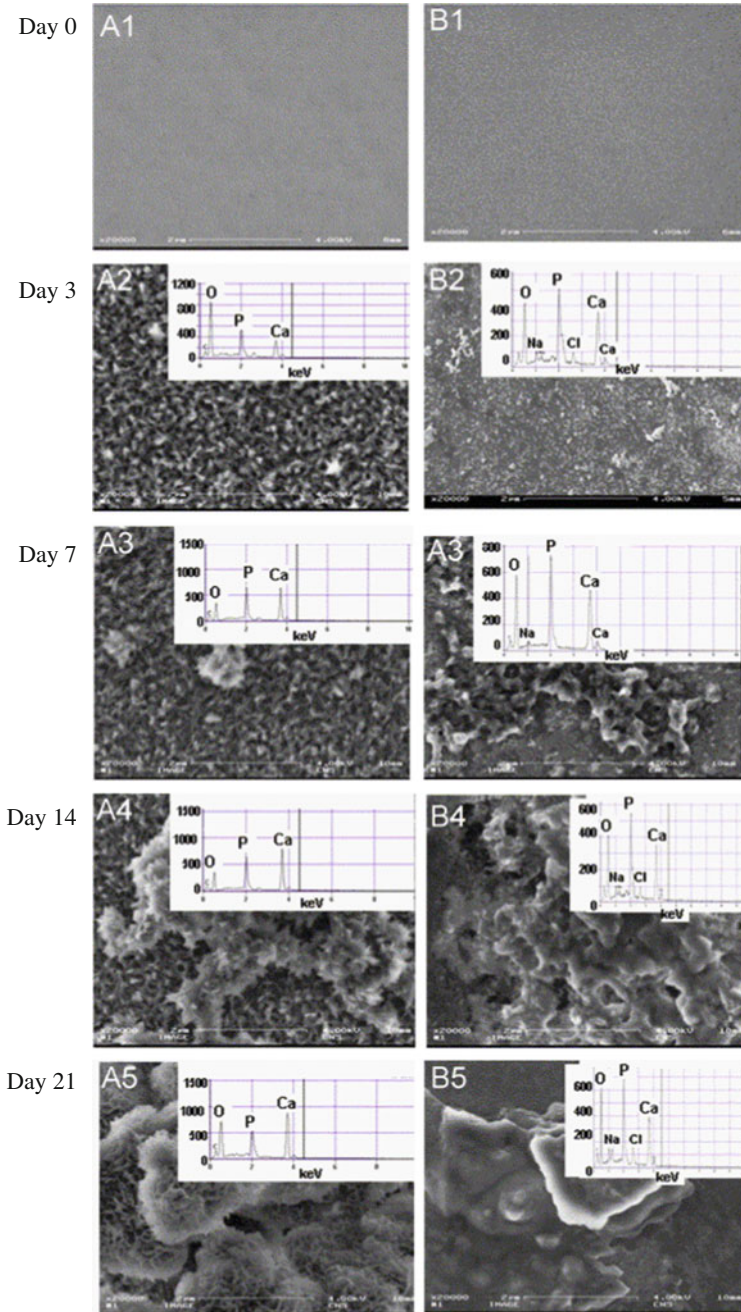


Fig. 9.2 Surface morphologies and the composition of the mineral deposition on the surfaces of recombinant spider silk films soaked in simulated body fluids for various periods of time. (A1)–(A5) Silk-like polypeptide fused with CDMP1. (B1)–(B5) Silk-like polypeptide with no CDMP1. At 21 days, the Ca/P ratio of the CDMP1-containing films was very close to the stoichiometric Ca/P ratio of hydroxyapatite (1.67). Reprinted with permission from ref. [80]. Copyright 2007 Elsevier

silk-like polypeptide was produced by introducing methionine residues to flank the hydrophobic AAAAAA motif [83, 84]. Under oxidizing conditions, this polypeptide had high aqueous solubility because the sulfoxides oxidized from the methionine residues interfered with hydrophobic interactions and prevented β -sheet assembly. Subsequent reduction of the oxidized methionine residues induced β -sheet assembly. In an alternative strategy, a peptide substrate for the cyclic AMP-dependent protein kinase, RGYSLG, was introduced into a silk-like polypeptide [85]. The phosphorylated serine residues inhibited hydrophobic interactions and β -sheet assembly, leading to high aqueous solubility. Assembly of β -sheets could be triggered by enzyme-mediated dephosphorylation.

Block copolypeptides composed of silk-like and elastin-like polypeptides have been recombinantly engineered and successfully expressed in various hosts. These silk-elastin-like protein polymers (SELPs) have high aqueous solubility and can be processed in the aqueous phase. SELPs have combined properties of silk-inspired and elastin-inspired polypeptides. The silk-like blocks provide high tensile strength and the elastin-like blocks confer high elasticity. In addition, elastin-like blocks exhibiting temperature-responsive phase transitions near physiological conditions can yield stimuli-responsive and in situ forming SELP materials, which are potentially useful for cell encapsulation in 3D tissue engineering. A recombinant SELP undergoing a temperature-responsive sol-to-gel transition near 37°C was engineered [86]. Human mesenchymal stem cells were encapsulated in this material and cultured in chondrogenic medium for 4 weeks. Chondrocytic differentiation was clearly observed, as indicated by accumulation of cartilage matrix sulfated glycosaminoglycans and collagen II.

9.3.4

Polypeptide Materials Self-Assembled Through α -Helical Domains

The α -helical structure is one of the most common secondary structures in proteins. Numerous natural or de novo designed α -helices have been used as building blocks to construct novel biomaterials. These self-assembling domains not only provide mechanical strength for materials, but also confer intelligent features through their stimuli-responsive molecular recognition. Coiled-coils, the α -helices that self-assemble and wrap around each other to form superhelical bundles, have attracted considerable attention in biomaterials engineering. The primary sequences of coiled-coils are characterized by periodic repeats of the heptad *abcdefg*, in which the *a* and *d* positions are occupied by hydrophobic residues and the *e* and *g* positions are occupied by charged residues [87, 88]. Under native conditions, coiled-coils adopt an α -helical secondary structure in which the hydrophobic residues are aligned on a hydrophobic interface. Interstrand hydrophobic interactions provide the primary driving force for self-assembly; and electrostatic interactions between charged residues regulate the specificity and stability of molecular association. The hydrophilic residues on the *b*, *c*, *f* sites are positioned at the exterior surface of assembled bundles and are exposed to the aqueous environment. An extensively studied family of coiled-coils is the leucine zipper family. The *a* and *d* positions in leucine zipper domains are mainly occupied by leucine residues [87, 88].

The self-assembly capacity of coiled-coils has been harnessed to construct hydrogels. A triblock copolypeptide consisting of two identical terminal leucine zipper domains flanking a hydrophilic polyelectrolyte segment was genetically engineered [89]. The leucine zipper was de novo designed, comprising six heptads in which the residues on the *a* and *d* positions were selected according to the *Jun* oncogene product. In aqueous solution and near neutral pH, the leucine zipper domains associated into tetramers to provide junction points; and the polyelectrolyte domain allowed water retention. The resulting 3D hydrogel networks were reversible in response to changes in pH and temperature, depending on whether the leucine zipper domains were folded or denatured. The network structure and material properties were further engineered by harnessing selective molecular recognition among distinct coiled-coils. When one terminal leucine zipper in the polypeptide described above was replaced with another coiled-coil that did not associate with the leucine zipper at the other terminus, intramolecular association was suppressed and the cross-linking density in the network increased. The resulting hydrogels exhibited increased stiffness and significantly reduced surface erosion rate [90].

Coiled-coils have also been used as associative domains to construct hybrid hydrogels consisting of both polypeptides and traditional synthetic polymers. When a linear hydrophilic copolymer of *N*-(2-hydroxypropyl)-methacrylamide (HPMA) was decorated with pendant metal-chelating iminodiacetate- Ni^{2+} ligands and mixed with histidine-tagged tetrameric or dimeric coiled-coils, highly swollen hydrogels formed through the interactions between the histidine tag and the iminodiacetate- Ni^{2+} ligand [91]. Coiled-coil bundles served as multifunctional cross-linkers in these hydrogels. In another molecular design, a pair of coiled-coils that possessed opposite charges and could heterodimerize in the antiparallel orientation were used to functionalize a linear hydrophilic copolymer of HPMA, respectively [92]. When the two modified polymers were mixed in PBS at neutral pH, heterodimerization of the coiled-coils directed in situ formation of hydrogels at a polymer concentration as low as 0.1 wt%. The coiled-coils heterodimerizing in the antiparallel orientation were chosen purposely to reduce the steric hindrance during the self-assembling process. These in situ forming hydrogels can be potentially used as artificial ECMs in tissue engineering.

Most hydrogels assembled through coiled-coils have not been tested for their immunological compatibility. To prepare materials that do not elicit adverse immune responses in tissue engineering applications, a coiled-coil derived from human fibrin, the provisional scaffold during natural wound healing processes, was used as a starting domain for rational modification [93]. The solvent-exposed residues on the *b*, *c*, *f* positions were left intact so that the assembled coiled-coil bundles would have the similar surface and biocompatibility as their natural counterparts. But the residues buried in the hydrophobic core were replaced with more hydrophobic residues to provide a stronger driving force for the assembly of coiled-coil bundles. The improved stability of the coiled-coil bundles was expected to enhance the mechanical properties of hydrogels when these bundles served as junction points in networks. This engineered coiled-coil was conjugated to the two ends of a poly(ethylene glycol) (PEG) chain and the resulting triblock hybrid polymer formed hydrogels under physiological conditions. Further studies are needed to determine whether these hydrogels exhibit a low level of or no immunogenicity as designed originally.

Rationally designed coiled-coil polypeptides can self-assemble into fibrous materials as well. Two complementary coiled-coils were designed to form staggered heterodimers having sticky ends for longitudinal assembly [94]. To guide the formation of staggered heterodimers, two molecular characteristics were introduced: lysine residues were included in the N-terminal half and glutamic acid residues were included in the C-terminal half of each polypeptide to promote the formation of staggered heterodimers through electrostatic interactions; a single asparagine residue was placed at a different *a* site in each polypeptide to foster parallel heterodimeric association directed by hydrogen bonding between asparagine residues, and the parallel orientation facilitates the formation of staggered heterodimers. The resulting staggered heterodimers possessed sticky overhangs that had complementary charges and the propensity to form a coiled-coil structure, and therefore they assembled longitudinally into fibrils several hundred micrometers long. These fibrils further associated laterally to form thicker fibers owing to the periodic and alternating charged patches on the surface. To make these fibrous materials more suitable for tissue engineering applications, further molecular engineering was performed [95]. In one improved molecular design, two acidic aspartic acid residues were placed in consecutive *b* sites in one polypeptide and two basic arginine residues were placed in consecutive *c* sites in the other polypeptide. The additional charges introduced through these residues enhanced fibril–fibril interactions and lateral assembly, leading to thicker fibers having higher mechanical strength. Another improvement was made by introducing an extra heptad into each polypeptide to increase hydrophobic overlap between the two heterodimerizing polypeptides. The resulting fibrous structure exhibited enhanced stability under physiological conditions. To demonstrate that bioactive functionalities can be incorporated into these fibrous materials, a lysine residue at the solvent-exposed *f* position was modified to introduce two small-molecule baits, biotin and the FLAG tag (DYKDDDDK), respectively [96]. The modification did not affect the structure and assembly of the polypeptides. The incorporated biotin and FLAG tag were presented on the surface of fibers and exposed to the solution phase, as indicated by their ability to capture streptavidin and anti-FLAG antibody, respectively, from the solution.

Self-assembling α -helical domains other than coiled-coils have also been used as building blocks to engineer novel biomaterials for tissue engineering applications. Hydrogel-forming diblock copolypeptides consisting of a hydrophobic α -helical domain and a hydrophilic polyelectrolyte domain were designed and chemically synthesized [97–99]. The α -helical domain was poly(L-leucine) and the polyelectrolyte domain was poly(L-lysine) or poly(L-glutamic acid). Both domains were indispensable for hydrogel formation, and their molecular characteristics determined the properties of resulting hydrogels. The helical conformation of the hydrophobic segment was essential for the gel-forming ability: when this segment had 10 leucine residues and was too short to form a complete α -helical structure, hydrogels did not form; when it comprised more than 20 leucine residues and adopted a complete α -helical structure, hydrogels formed. The minimum gelation concentration decreased and the hydrogel stiffness increased with the increasing length of the poly-leucine segment. The polyelectrolyte domain was also critical for hydrogel formation. It served two important roles: its hydrophilic nature facilitated water retention; and it provided electrostatic repulsion so that the α -helical domain did not assemble into

2-dimensional sheets. The presence of the polyelectrolyte domain forced the sheets assembled from the α -helical domain to twist into fibrillar tapes to minimize energy, resulting in 3D hydrogels [100]. The gel-forming ability and the hydrogel stiffness increased significantly with the increasing length of the polyelectrolyte segment. The hydrogels assembled from these diblock copolypeptides had good biocompatibility, as revealed from both *in vitro* and *in vivo* studies. They exhibited no cytotoxicity toward 3T3 fibroblasts *in vitro* [98]. When the hydrogels having similar stiffness as brain tissue were injected into mouse forebrain, they stimulated the same degree of gliosis, inflammation, and toxicity as a physiological saline control [101]. In-growth of blood vessels, glial cells, and nerve fibers were observed for several formulations. Cell infiltration appeared to be dependent on the amino acid compositions of the polypeptides: hydrogels formed from 2% E₁₈₀L₂₀ showed significantly higher potency in enhancing cell infiltration than those formed from 3% K₁₈₀L₂₀. The results suggest that these hydrogels are promising artificial ECM materials for tissue repair in the central nervous system.

9.3.5

Bioactive and Dynamic Materials

Polypeptide-based materials are attractive in tissue engineering because polypeptide domains and motifs not only can serve as structural building blocks to provide mechanical strength, but also offer numerous possibilities to create novel bioactive and dynamic materials. The success of tissue engineering relies on our ability to mimic *in vivo* extracellular microenvironments, which are complex and dynamic, with all the physical and biochemical signals tightly regulated at the right level, place, and time. Using engineered biomaterials to define artificial extracellular microenvironments is an important strategy in tissue engineering. However, currently available biomaterials provide a limited ability to recapitulate the essential characteristics of natural extracellular microenvironments. For example, it remains a challenge to engineer temporally regulated extracellular microenvironments. Polypeptide-based materials have advantages over conventional synthetic polymers in engineering bioactive and dynamic materials, because naturally occurring proteins perform a wide variety of functions ranging from providing adhesive and bioactive moieties to presenting, sensing, and responding to signals. Their ability to perform complex and smart functions is conferred by precisely-controlled and stimuli-responsive structures and biomolecular recognition. Engineered polypeptide materials inspired by the proteins that construct the molecular apparatus in natural biological systems can recapitulate these remarkable structural and functional features, allowing us to create artificial extracellular microenvironments that closely mimic their natural counterparts.

A variety of polypeptide-based bioactive materials have been constructed and used for tissue engineering applications. Engineered polypeptides containing cell adhesion motifs have been developed, as discussed in previous sections of this chapter. These materials are bioactive because the adhesion motifs, such as RGD and GER, not only allow cells to attach, but also play important roles in regulating intracellular signaling [102]. Cell adhesion through these motifs has profound influences on cell spreading, migration,

proliferation, differentiation, and survival, regulated through various biochemical, physical, and mechanical mechanisms. Polypeptide materials exhibiting other bioactivities have also been engineered. The chimera composed of a silk-like polypeptide and a CDMP1 domain (discussed in Sect. 9.3.3) is one example [80]. Polypeptides are important building elements in engineering bioactive materials presenting immobilized signaling molecules. A recombinantly engineered chimeric protein composed of EGF and an acidic coiled-coil was efficiently grafted on a surface functionalized with a basic coiled-coil that heterodimerized with the acidic coiled-coil [103, 104]. Such surface-immobilized EGF stimulated phosphorylation of the EGF receptor in cells plated on the surface more efficiently than randomly immobilized EGF, probably because the EGF immobilized through coiled-coil heterodimerization was oriented more properly. When the basic coiled-coil used to functionalize the surface was also fused to EGF, heterodimerization of coiled-coils led to the formation of dimeric EGF. This material enhanced the expansion efficiency of neural stem cells [105].

Controlled release of bioactive agents, such as soluble growth factors and the genes encoding bioactive proteins, is an important strategy to improve tissue engineering outcomes. The release of bioactive agents encapsulated in artificial ECMs can be controlled through tuning the ECM structures and properties. One advantage of polypeptide-based artificial ECMs is that their structures and properties can be precisely and systematically engineered. Therefore, polypeptide materials have a great potential to serve a dual role of artificial ECM and controlled release system in tissue engineering. The release rate of agents encapsulated in silk-elastinlike polypeptide hydrogels was examined to evaluate the potential of these materials for such use [106]. It was found that the release rate can be tuned through the control of the molecular structures of the polypeptides and consequently the microstructure and swelling behavior of the hydrogels. Polypeptide materials have also been rationally engineered for gene delivery [107, 108]. These recombinant polypeptides include lysine residues to condense DNA and histidine residues to promote endosomal escape of internalized DNA. In some cases nuclear localization sequence peptides are also incorporated to enhance transfection efficiency. The transfection efficiency mediated by these polypeptide materials is comparable or superior to that mediated by polyethylenimine (PEI). In contrast to PEI, which has high cytotoxicity, these polypeptide-based gene delivery agents exhibit minimal toxic effects.

Polypeptide-based hydrogels having enzymatic activities have been engineered. Two genetically engineered polypeptides formed bioelectrocatalytic hydrogels [109]. One was a triblock polypeptide consisting of two terminal leucine zipper domains and a random coil hydrophilic midblock. This polypeptide also contained a histidine tag on which a redox moiety, an osmium *bis*-bipyridine complex, was attached to confer electron-conducting functionality. The other polypeptide was a chimera consisting of a polyphenol oxidase, a hydrophilic random coil, and a leucine zipper. When these two polypeptides were mixed, self-assembly of the leucine zipper domains resulted in hydrogel networks in which polyphenol oxidase was attached to the physical junction points. The polyphenol oxidase in these hydrogels retained its enzymatic activity and was able to catalyze the reduction of dioxygen to water. In the presence of oxygen, a catalytic current was generated in polarized hydrogels. These hydrogels were not designed specifically for tissue engineering

applications, but the method could be readily adapted to engineer artificial ECM materials that need certain enzymatic activities.

Peptide substrates for proteolytic cleavage can be readily incorporated into polypeptide-based materials to make them biodegradable. Degradable materials are desirable in tissue engineering, because the aim of using artificial ECMs is to provide temporal mechanical support and define extracellular microenvironments to guide tissue regeneration and remodeling rather than to retain these materials permanently. A polypeptide containing a plasmin degradation site derived from human fibrinogen, a matrix metalloproteinase (MMP) cleavage site derived from human collagen, a cell adhesion RGD motif, and three cysteine residues was genetically engineered [110, 111]. This polypeptide reacted with a PEG having two terminal vinyl sulfone groups through a Michael-type addition reaction to yield in situ forming hybrid hydrogels. These hydrogels were degradable through the mediation of cell-secreted plasmin and MMP. When a hybrid hydrogel encapsulating bone morphogenetic protein-2 was implanted into a critical-sized defect in a rat calvarial defect model, cell infiltration and bone regeneration was observed. In contrast, a nondegradable control hydrogel having no proteolytic sites remained intact and did not support 3D bone regeneration.

Dynamic hydrogels that sense biochemical components in solutions and convert these signals into reversible changes in material properties have been engineered by incorporating calmodulin (CaM) into 3D networks. CaM adopts an extended, dumbbell-shaped conformation upon binding Ca^{2+} , and such conformation permits further binding with other ligands (such as trifluoperazine, phenothiazine, and some peptides) and the second binding event results in a collapsed conformation. The conformational changes associated with these molecular binding events are large and reversible. CaM and its ligand phenothiazine were both incorporated into a polymeric hydrogel as pendant moieties [112]. In the presence of Ca^{2+} , CaM sequentially bound to Ca^{2+} and phenothiazine and underwent conformational changes. The resulting hydrogels exhibited increased cross-linking density, reduced volume, and reduced permeability to vitamin B12. Removal of Ca^{2+} by a chelating reagent allowed the material properties to recover. In another molecular design strategy, CaM was genetically modified so that the tyrosine residues at positions 34 and 110, which were 50 Å apart in the extended conformation and 15 Å apart in the collapsed conformation, were replaced with cysteine residues. The modified CaM was allowed to react with an acrylate-terminated, four-arm PEG through a Michael-type addition reaction between thiol and acrylate, yielding hydrogels [113, 114]. Alternatively, the modified CaM was conjugated with PEG-diacrylate (PEGDA) in large excess of PEGDA, resulting in an acrylate-terminated PEG-CaM-PEG conjugate that could be photo-cross-linked into hydrogels upon exposure to long wavelength ultraviolet light [115]. The CaM incorporated in the hydrogel networks functioned normally: in the presence of both Ca^{2+} and a second binding ligand, the hydrogel volume decreased significantly; removal of Ca^{2+} by a chelating reagent allowed the volume to recover. The ability of the photo-cross-linked dynamic hydrogels to control the release of vascular endothelial growth factors (VEGF) in response to a biochemical ligand trifluoperazine (TFP) was demonstrated [116]. The conformational change of CaM induced by TFP caused a collapse in hydrogel volume, increasing the release of encapsulated VEGF (Fig. 9.3). Genetically engineered

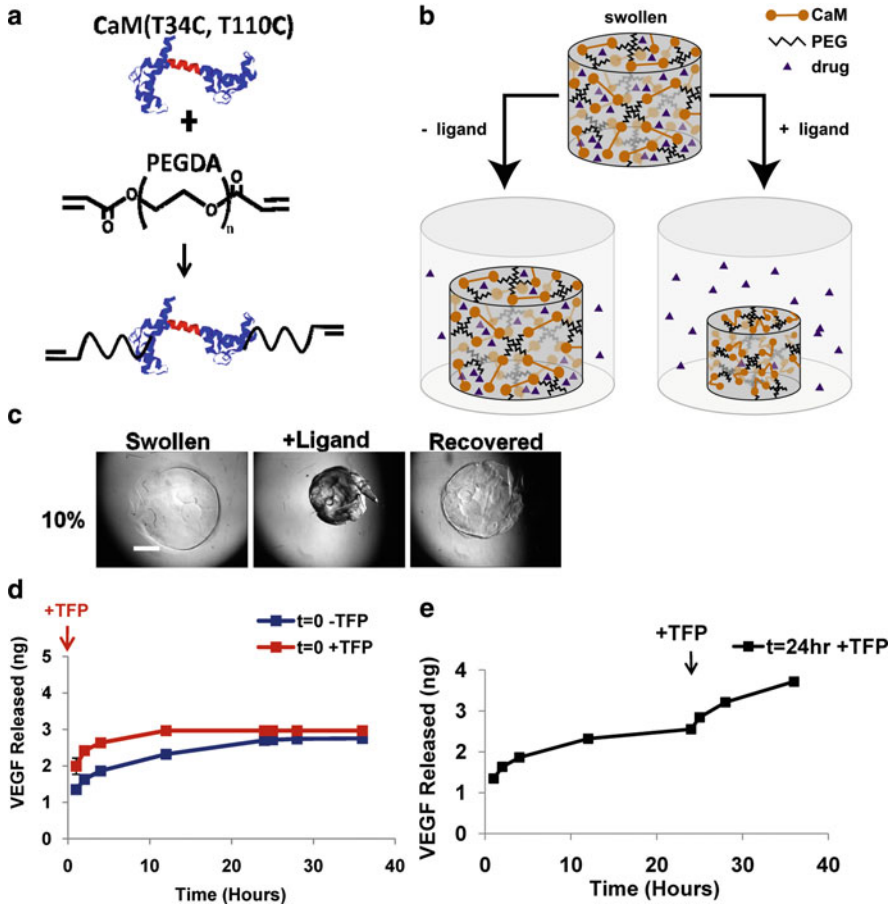


Fig. 9.3 Modulation of growth factor release from calmodulin-containing dynamic hydrogels. (a) Schematic illustration of the hydrogel-forming polymer. (b) Schematic illustration of ligand-responsive release of encapsulated drugs. (c) A hydrogel in its swollen, collapsed, and recovered state. (d and e) Regulation of VEGF release by addition of ligand trifluoperazine. Reprinted with permission from [116]. Copyright 2009 The Royal Society of Chemistry

triblock copolypeptides composed of CaM and associative polypeptide domains were also used to construct CaM-containing hydrogels [117]. These entirely polypeptide-based materials offer additional advantages of having precisely-controlled structure and properties. These dynamic hydrogels, either hybrid or purely polypeptide-based, have not been used in tissue engineering except the study on regulation of VEGF release. But the success of engineering such ligand-responsive dynamic hydrogels demonstrated the great potential of exploiting the intelligent molecular properties of natural proteins and their domains to create novel dynamic materials.

9.3.6

Biosynthetic Incorporation of Non-natural Amino Acid Analogs for Engineering Polypeptide Materials

The recent advances in biosynthetic incorporation of non-natural amino acid analogs have expanded our ability to engineer polypeptide-based materials. A variety of amino acid analogs having characteristics and functionalities that do not exist in the 20 canonical amino acids have been introduced into polypeptide chains either globally or at specific single or multiple sites during biosynthesis. The resulting polypeptides exhibit novel physical and chemical properties that cannot be conferred by natural amino acids. Various strategies have been used to incorporate these analogs. Some methods simply involve replacement of a natural amino acid with an analog in the culture medium and using an auxotrophic expression strain that does not synthesize that natural amino acid [118, 119]. Some methods require manipulation of the aminoacyl tRNA synthetase in the expression host, including over-expression of the wild-type synthetase or introduction of an engineered mutant synthetase that has an altered binding pocket and allows more efficient incorporation of the analog [120].

Fluorinated amino acid analogs of hydrophobic residues, such as 5,5,5-trifluoroleucine, hexafluoroleucine, 5,5,5-trifluoroisoleucine, 4,4,4-trifluorovaline, and fluoroproline, were incorporated into recombinant coiled-coils and elastin-like polypeptides in bacterial expression hosts [121–125]. The physical properties of these biosynthesized polypeptides were modified as compared to their counterparts composed of only natural amino acids. Introduction of hyperhydrophobic analogs to the *a* and/or *d* positions of coiled-coils resulted in an increased driving force for self-assembly, and the self-assembled structures exhibited enhanced stability against thermal and chemical denaturation [121–123]. Incorporation of fluoroproline into ELPs resulted in a shift in the inverse phase transition temperature [124, 125]. Coiled-coils and ELPs are both important building blocks to engineer hydrogels and fibrous materials that can potentially be used as artificial ECMs. The ability to incorporate hyperhydrophobic analogs and modify the physical properties and assembly behavior of these polypeptides may offer opportunities to engineer novel materials having improved properties for tissue engineering applications.

Physical properties other than structural and mechanical properties can also be engineered through incorporation of non-natural amino acid analogs. A polypeptide-based polythiophene was synthesized by incorporating a thiophene-containing phenylalanine analog, 3-thienylalanine, to substitute the phenylalanine residues in a silk-mimetic polypeptide [(AG)₃GF]₁₃ [126]. Polythiophenes are extensively studied conducting polymers that have a wide range of applications. The polypeptide-based polythiophene prepared through biosynthesis has potential applications in repairing and regenerating damaged neural and cardiac tissues.

Incorporation of non-natural amino acid analogs not only allows the physical properties of polypeptide materials to be engineered, but also provides the opportunity to introduce a variety of chemical functionalities to enable orthogonal chemical reaction and modification. Preparation of bioactive materials to elicit specific cell responses in tissue engineering often involves protein modification. Site-specific modification of proteins consisting of only natural amino acids is difficult, and non-specific side reactions sometimes compromise

protein structures and functions. Versatile chemical functionalities introduced through non-natural amino acid analogs enable orthogonal chemical modifications that allow protein structures and functions to remain intact, opening a new avenue to engineer novel bioactive and functional materials.

Analogs containing an alkyne or azide group are particularly attractive, because these functional groups allow azide-alkyne cycloaddition click chemistry and Staudinger ligation, which are orthogonal to natural amino acids and can be performed under physiologically compatible conditions and even in living systems. The alkyne-bearing *p*-ethynylphenylalanine was successfully incorporated to the sites encoded for phenylalanine when proteins were expressed in a phenylalanine auxotrophic *E. coli* strain that over-expressed the A294G mutant of phenylalanyl-tRNA synthetase, which had an enlarged binding pocket [120, 127]. Incorporation of *p*-ethynylphenylalanine was detected by azidocoumarin dye through Cu(I)-catalyzed azide-alkyne cycloaddition. The azide-bearing azidohomoalanine (AHA, a methionine surrogate) was also successfully incorporated to substitute methionine residues with high efficiency [119, 128, 129]. Protein expression was performed in methionine auxotrophic *E. coli* hosts that produced endogenous or over-expressed methionine-tRNA synthetase. When the model protein DHFR was expressed in medium supplemented with AHA and depleted with methionine, 95% of methionine residues were substituted with AHA even with the endogenous level of methionine-tRNA synthetase [119]. The resulting azide-containing DHFR was modified by a triarylphosphine-FLAG conjugate through Staudinger ligation, as revealed by the detection with anti-FLAG antibody. AHA was also incorporated into an outer membrane protein of *E. coli*, which displayed azide moieties at the cell surface and were selectively labeled by alkyne-containing reagents through azide-alkyne cycloaddition chemistry [130].

The photoreactive analog *p*-azidophenylalanine (*p*N3Phe) was incorporated into recombinant polypeptides to substitute phenylalanine and produce materials that allowed modification or processing through photoreactions [120, 131–133]. Protein expression was performed in a phenylalanine auxotrophic *E. coli* strain that over-expressed the A294G mutant of phenylalanyl-tRNA synthetase. Incorporation of *p*N3Phe in an ELP containing repeats of (VPGVG)₂VPGFG(VPGVG)₂ and the fibronectin-derived CS5 cell adhesion motif resulted in a photo-cross-linkable ELP, which could potentially be processed into vascular graft materials [131, 132] (Fig. 9.4). The elastic modulus of the films photo-cross-linked from this polypeptide could be controlled in the range of 0.14–1.39 MPa through tuning the analog substitution level during biosynthesis and/or the light irradiation time during the photo-cross-linking process. The possibility to prepare a film having step gradients of stiffness from this polypeptide was demonstrated by irradiating different portions of a polypeptide solution for different periods of time [132]. This *p*N3Phe-containing ELP was also micropatterned on surfaces using a photolithographic method and the resulting substrates allowed cell adhesion at selective locations to create cell arrays [131]. Incorporation of *p*N3Phe was also performed for a diblock copolypeptide consisting of an ELP sequence [(VPGVG)₂VPGFG(VPGVG)₂]₅ and an acidic coiled-coil domain [133]. The resulting polypeptide was spin-coated on a hydrophobic surface above the phase transition temperature of the ELP to allow its adhesion to the surface through hydrophobic interaction. This physical interaction

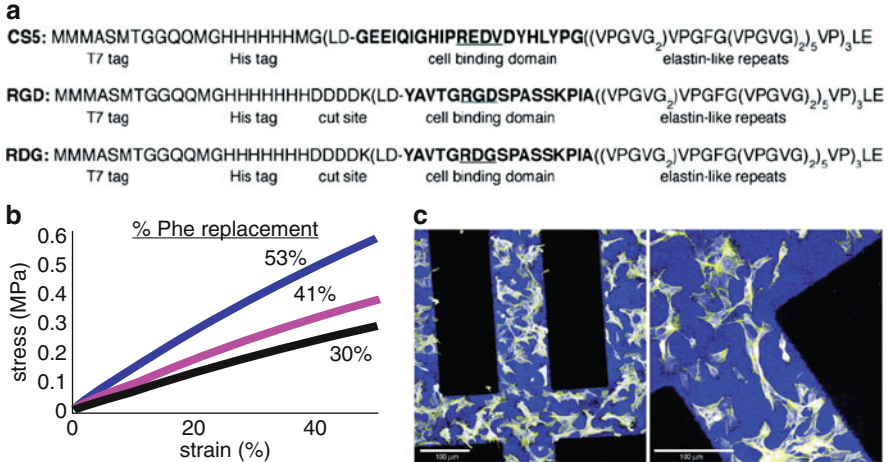


Fig. 9.4 Preparation of photoreactive elastin-like polypeptide materials through incorporation of non-natural amino acid analog *p*-azidophenylalanine. (a) Primary sequences of ELPs. (b) Uniaxial tensile tests revealing the correlation between the elastic modulus of irradiated mold-cast films and the level of analog substitution. (c) Confocal microscopy of fibroblasts attached to photolithographically micropatterned RGD-containing ELP. Reprinted with permission from [131]. Copyright 2007 American Chemical Society

brought the photoreactive *p*N3Phe close to the surface, and subsequent UV irradiation resulted in covalent immobilization of the polypeptide. The acidic coiled-coil domain in the immobilized polypeptide was able to selectively capture molecules tagged with a complementary basic coiled-coil from solution through coiled-coil heterodimerization.

9.4 Future Directions

Engineered polypeptide materials have unique properties that allow creation of well-controlled and biomimetic artificial ECMs, providing many opportunities to advance the field of tissue engineering in both fundamental studies and technological developments. Numerous naturally occurring and de novo designed protein and peptide domains/motifs provide a tool box from which building blocks can be selected and combined to engineer multifunctional biomaterials that enhance specific biological responses and tissue regeneration. The high degree of modularity of design and synthesis of these materials and the high fidelity of biosynthetic apparatus allow systematic and precise control of their biochemical and physical properties. Despite the great potential, the area of using engineered polypeptides as artificial ECMs in tissue engineering is still at a young stage. The full potential of

these materials has yet to be realized; many challenges need to be addressed. It is expected that the tunable, modular, and precisely-controllable nature of these materials will allow them to continue to make contributions in enabling systematic studies to enhance our understanding of cell behavior and fate selection in response to their microenvironments. Such understanding will provide valuable guidelines for the design of future generations of artificial ECMs to improve tissue engineering outcomes. It is also expected that more novel materials will be developed by harnessing diverse, bioactive, and smart proteins and protein domains that perform important and intelligent functions in biological systems and by utilizing new technologies in protein engineering such as biosynthetic incorporation of non-natural amino acid analogs. These novel materials will provide opportunities to more closely mimic the complex and dynamic *in vivo* extracellular microenvironments than currently available technologies. It is envisioned that the use of engineered polypeptide materials in tissue engineered products for *in vitro* applications, such as drug screening, will not encounter insurmountable barriers. However, many challenges need to be addressed before these materials can be used in implantable tissue engineered products. To date, engineered polypeptides have been used in *in vitro* studies and preclinical animal studies. No engineered polypeptides have been used in implantable commercial products. One important issue that remains largely unexplored or inconclusive for most engineered polypeptides is whether these materials elicit adverse immunogenic responses and what are the potential strategies to address this if it is indeed a problem. In addition, further improvement in synthesis yields, reduction in cost, and enhancement in the stability and shelf-life of polypeptide materials are other issues that need to be solved for successful use of these materials in commercial products.

Amino acids

A	Alanine
C	Cysteine
D	Aspartic acid
E	Glutamic acid
F	Phenyl alanine
G	Glycine
I	Isoleucine
K	Lysine
L	Leucine
P	Proline
Q	Glutamine
R	Arginine
S	Serine
V	Valine
Y	Tyrosine
T	Threonine
Hyp	Hydroxyproline

References

1. Silva GA, Czeisler C, Niece KL, Beniash E, Harrington DA, Kessler JA, Stupp SI. Selective differentiation of neural progenitor cells by high-epitope density nanofibers. *Science* 2004;303:1352–1355.
2. Zhang SG. Fabrication of novel biomaterials through molecular self-assembly. *Nat Biotechnol* 2003;21:1171–1178.
3. Bella J, Eaton M, Brodsky B, Berman HM. Crystal-structure and molecular-structure of a collagen-like peptide at 1.9-angstrom resolution. *Science* 1994;266:75–81.
4. Buechter DD, Paoletta DN, Leslie BS, Brown MS, Mehos KA, Gruskin EA. Co-translational incorporation of trans-4-hydroxyproline into recombinant proteins in bacteria. *J Biol Chem* 2003;278:645–650.
5. Myllyharju J, Lamberg A, Notbohm H, Fietzek PP, Pihlajaniemi T, Kivirikko KI. Expression of wild-type and modified pro alpha chains of human type I procollagen in insect cells leads to the formation of stable [alpha 1(I)](2)alpha 2(I) collagen heterotrimers and [alpha 1(I)](3) homotrimers but not [alpha 2(I)](3) homotrimers. *J Biol Chem* 1997;272:21824–21830.
6. Toman PD, Chisholm G, McMullin H, Gieren LM, Olsen DR, Kovach RJ, Leigh SD, Fong BE, Chang R, Daniels GA, Berg RA, Hitzeman RA. Production of recombinant human type I procollagen trimers using a four-gene expression system in the yeast *Saccharomyces cerevisiae*. *J Biol Chem* 2000;275:23303–23309.
7. Pakkanen O, Hamalainen ER, Kivirikko KI, Myllyharju J. Assembly of stable human type I and III collagen molecules from hydroxylated recombinant chains in the yeast *Pichia pastoris* – Effect of an engineered C-terminal oligomerization domain foldon. *J Biol Chem* 2003;278:32478–32483.
8. Chen M, Costa FK, Lindvay CR, Han YP, Woodley DT. The recombinant expression of full-length type VII collagen and characterization of molecular mechanisms underlying dystrophic epidermolysis bullosa. *J Biol Chem* 2002;277:2118–2124.
9. Stein H, Wilensky M, Tsafirir Y, Rosenthal M, Amir R, Avraham T, Ofir K, Dgany O, Yayon A, Shoseyov O. Production of bioactive, post-translationally modified, heterotrimeric, human recombinant type-I collagen in transgenic tobacco. *Biomacromolecules* 2009;10:2640–2645.
10. Merle C, Perret S, Lacour T, Jonval V, Hudaverdian S, Garrone R, Ruggiero F, Theisen M. Hydroxylated human homotrimeric collagen I in *Agrobacterium tumefaciens*-mediated transient expression and in transgenic tobacco plant. *FEBS Lett* 2002;515:114–118.
11. Tomita M, Munetsuna H, Sato T, Adachi T, Hino R, Hayashi M, Shimizu K, Nakamura N, Tamura T, Yoshizato K. Transgenic silkworms produce recombinant human type III procollagen in cocoons. *Nat Biotechnol* 2003;21:52–56.
12. Toman PD, Pieper F, Sakai N, Karatzas C, Platenburg E, de Wit I, Samuel C, Dekker A, Daniels GA, Berg RA, Platenburg GJ. Production of recombinant human type I procollagen homotrimer in the mammary gland of transgenic mice. *Transgenic Res* 1999;8:415–427.
13. Fertala A, Han WB, Ko FK. Mapping critical sites in collagen II for rational design of gene-engineered proteins for cell-supporting materials. *J Biomed Mater Res* 2001;57:48–58.
14. Ito H, Stepleski A, Alabyeva T, Fertala A. Testing the utility of rationally engineered recombinant collagen-like proteins for applications in tissue engineering. *J Biomed Mater Res A* 2006;76A:551–560.
15. Tanihara M, Kajiwara K, Ida K, Suzuki Y, Kamitakahara M, Ogata S. The biodegradability of poly(Pro-Hyp-Gly) synthetic polypeptide and the promotion of a dermal wound epithelialization using a poly(Pro-Hyp-Gly) sponge. *J Biomed Mater Res A* 2008;85A:133–139.
16. Paramonov SE, Gauba V, Hartgerink JD. Synthesis of collagen-like peptide polymers by native chemical ligation. *Macromolecules* 2005;38:7555–7561.

17. Yamazaki CM, Asada S, Kitagawa K, Koide T. Artificial collagen gels via self-assembly of de novo designed peptides. *Biopolymers* 2008;90:816–823.
18. Koide T, Homma DL, Asada S, Kitagawa K. Self-complementary peptides for the formation of collagen-like triple helical supramolecules. *Bioorg Med Chem Lett* 2005;15:5230–5233.
19. Rele S, Song Y, Apkarian RP, Qu Z, Conticello VP, Chaikof EL. D-periodic collagen-mimetic microfibers. *J Am Chem Soc* 2007;129:14780–14787.
20. Cejas MA, Kinnney WA, Chen C, Vinter JG, Almond HR, Balss KM, Maryanoff CA, Schmidt U, Breslav M, Mahan A, Lacy E, Maryanoff BE. Thrombogenic collagen-mimetic peptides: Self-assembly of triple helix-based fibrils driven by hydrophobic interactions. *Proc Natl Acad Sci U S A* 2008;105:8513–8518.
21. Pires MM, Przybyla DE, Chmielewski J. A metal-collagen peptide framework for three-dimensional cell culture. *Angew Chem Int Ed Engl* 2009;48:7813–7817.
22. Krishna OD, Kiick KL. Supramolecular assembly of electrostatically stabilized, hydroxyproline-lacking collagen-mimetic peptides. *Biomacromolecules* 2009;10:2626–2631.
23. Yao JM, Yanagisawa S, Asakura T. Design, expression and characterization of collagen-like proteins based on the cell adhesive and crosslinking sequences derived from native collagens. *J Biochem* 2004;136:643–649.
24. Werten MWT, Teles H, Moers APHA, Wolbert EJH, Sprakel J, Eggink G, de Wolf FA. Precision gels from collagen-inspired triblock copolymers. *Biomacromolecules* 2009;10:1106–1113.
25. Debelle L, Alix AJP. The structures of elastins and their function. *Biochimie* 1999;81:981–994.
26. Vrhovski B, Weiss AS. Biochemistry of tropoelastin. *Eur J Biochem* 1998;258:1–18.
27. Li B, Daggett V. Molecular basis for the extensibility of elastin. *J Muscle Res Cell Motil* 2002;23:561–573.
28. Urry DW. Molecular Mechanisms of elastin coacervation and coacervate calcification. *Faraday Discuss* 1976;61:205–212.
29. Grosso LE, Scott M. Pgaipg, a repeated hexapeptide of bovine tropoelastin, is a ligand for the 67-Kda bovine elastin receptor. *Matrix* 1993;13:157–164.
30. Mochizuki S, Brassart B, Hinek A. Signaling pathways transduced through the elastin receptor facilitate proliferation of arterial smooth muscle cells. *J Biol Chem* 2002;277:44854–44863.
31. Stephan S, Ball SG, Williamson M, Bax DV, Lomas A, Shuttleworth CA, Kielty CM. Cell-matrix biology in vascular tissue engineering. *J Anat* 2006;209:495–502.
32. Woodhouse KA, Klement P, Chen V, Gorbet MB, Keeley FW, Stahl R, Fromstein JD, Bellingham CM. Investigation of recombinant human elastin polypeptides as non-thrombogenic coatings. *Biomaterials* 2004;25:4543–4553.
33. Urry DW. Physical chemistry of biological free energy transduction as demonstrated by elastic protein-based polymers. *J Phys Chem B* 1997;101:11007–11028.
34. Urry DW, Luan CH, Parker TM, Gowda DC, Prasad KU, Reid MC, Safavy A. Temperature of polypeptide inverse temperature transition depends on mean residue hydrophobicity. *J Am Chem Soc* 1991;113:4346–4348.
35. Urry DW, Trapane TL, Sugano H, Prasad KU. Sequential polypeptides of elastin – Cyclic conformational correlates of the linear polypentapeptide. *J Am Chem Soc* 1981;103:2080–2089.
36. Mcpherson DT, Morrow C, Minehan DS, Wu JG, Hunter E, Urry DW. Production and purification of a recombinant elastomeric polypeptide, G-(Vpgvg)19-Vpgv, from *Escherichia coli*. *Biotechnol Prog* 1992;8:347–352.
37. Urry DW, Parker TM, Reid MC, Gowda DC. Biocompatibility of the bioelastic materials, poly(gvgvp) and its gamma-irradiation cross-linked matrix – Summary of generic biological test-results. *J Bioact Compat Polym* 1991;6:263–282.

38. Urry DW, Pattanaik A, Xu J, Woods TC, McPherson DT, Parker TM. Elastic protein-based polymers in soft tissue augmentation and generation. *J Biomater Sci Polym Ed* 1998;9:1015–1048.
39. Heilshorn SC, Liu JC, Tirrell DA. Cell-binding domain context affects cell behavior on engineered proteins. *Biomacromolecules* 2005;6:318–323.
40. Martino M, Tamburro AM. Chemical synthesis of cross-linked poly(KGGVG), an elastin-like biopolymer. *Biopolymers* 2001;59:29–37.
41. Welsh ER, Tirrell DA. Engineering the extracellular matrix: A novel approach to polymeric biomaterials. I. Control of the physical properties of artificial protein matrices designed to support adhesion of vascular endothelial cells. *Biomacromolecules* 2000;1:23–30.
42. Huang L, McMillan RA, Apkarian RP, Pourdeyhimi B, Conticello VP, Chaikof EL. Generation of synthetic elastin-mimetic small diameter fibers and fiber networks. *Macromolecules* 2000;33:2989–2997.
43. Di Zio K, Tirrell DA. Mechanical properties of artificial protein matrices engineered for control of cell and tissue behavior. *Macromolecules* 2003;36:1553–1558.
44. Nowatzki PJ, Tirrell DA. Physical properties of artificial extracellular matrix protein films prepared by isocyanate crosslinking. *Biomaterials* 2004;25:1261–1267.
45. McMillan RA, Lee TAT, Conticello VP. Rapid assembly of synthetic genes encoding protein polymers. *Macromolecules* 1999;32:3643–3648.
46. Trabbic-Carlson K, Setton LA, Chilkoti A. Swelling and mechanical behaviors of chemically cross-linked hydrogels of elastin-like polypeptides. *Biomacromolecules* 2003;4:572–580.
47. Liu JC, Heilshorn SC, Tirrell DA. Comparative cell response to artificial extracellular matrix proteins containing the RGD and CS5 cell-binding domains. *Biomacromolecules* 2004;5:497–504.
48. Wu X, Sallach RE, Caves JM, Conticello VP, Chaikof EL. Deformation responses of a physically cross-linked high molecular weight elastin-like protein polymer. *Biomacromolecules* 2008;9:1787–1794.
49. Wu XY, Sallach R, Haller CA, Caves JA, Nagapudi K, Conticello VP, Levenston ME, Chaikof EL. Alterations in physical cross-linking modulate mechanical properties of two-phase protein polymer networks. *Biomacromolecules* 2005;6:3037–3044.
50. Wright ER, McMillan RA, Cooper A, Apkarian RP, Conticello VP. Thermoplastic elastomer hydrogels via self-assembly of an elastin-mimetic triblock polypeptide. *Adv Funct Mater* 2002;12:149–154.
51. Betre H, Setton LA, Meyer DE, Chilkoti A. Characterization of a genetically engineered elastin-like polypeptide for cartilaginous tissue repair. *Biomacromolecules* 2002;3:910–916.
52. Betre H, Ong SR, Guilak F, Chilkoti A, Fermor B, Setton LA. Chondrocytic differentiation of human adipose-derived adult stem cells in elastin-like polypeptide. *Biomaterials* 2006;27:91–99.
53. McHale MK, Setton LA, Chilkoti A. Synthesis and in vitro evaluation of enzymatically cross-linked elastin-like polypeptide gels for cartilaginous tissue repair. *Tissue Eng* 2005;11:1768–1779.
54. Lim DW, Nettles DL, Setton LA, Chilkoti A. Rapid cross-linking of elastin-like polypeptides with (hydroxymethyl)phosphines in aqueous solution. *Biomacromolecules* 2007;8:1463–1470.
55. Nettles DL, Kitaoka K, Hanson NA, Flahiff CM, Mata BA, Hsu EW, Chilkoti A, Setton LA. In situ crosslinking elastin-like polypeptide gels for application to articular cartilage repair in a goat osteochondral defect model. *Tissue Eng Part A* 2008;14:1133–1140.
56. Lim DW, Nettles DL, Setton LA, Chilkoti A. In situ cross-linking of elastin-like polypeptide block copolymers for tissue repair. *Biomacromolecules* 2008;9:222–230.
57. Nagapudi K, Brinkman WT, Leisen JE, Huang L, McMillan RA, Apkarian RP, Conticello VP, Chaikof EL. Photomediated solid-state cross-linking of an elastin-mimetic recombinant protein polymer. *Macromolecules* 2002;35:1730–1737.

- 9
58. Martinez-Osorio H, Juarez-Campo M, Diebold Y, Girotti A, Alonso M, Javier Arias F, Rodriguez-Cabello JC, Garcia-Vazquez C, Calonge M. Genetically engineered elastin-like polymer as a substratum to culture cells from the ocular surface. *Curr Eye Res* 2009;34:48–56.
 59. Mie M, Mizushima Y, Kobatake E. Novel extracellular matrix for cell sheet recovery using genetically engineered elastin-like protein. *J Biomed Mater Res B Appl Biomater* 2008;86B:283–290.
 60. Zhang HL, Iwama M, Akaïke T, Urry DW, Pattanaik A, Parker TM, Konishi I, Nikaido T. Human amniotic cell sheet harvest using a novel temperature-responsive culture surface coated with protein-based polymer. *Tissue Eng* 2006;12:391–401.
 61. Altman GH, Diaz F, Jakuba C, Calabro T, Horan RL, Chen JS, Lu H, Richmond J, Kaplan DL. Silk-based biomaterials. *Biomaterials* 2003;24:401–416.
 62. Santin M, Motta A, Freddi G, Cannas M. In vitro evaluation of the inflammatory potential of the silk fibroin. *J Biomed Mater Res* 1999;46:382–389.
 63. Altman GH, Horan RL, Lu HH, Moreau J, Martin I, Richmond JC, Kaplan DL. Silk matrix for tissue engineered anterior cruciate ligaments. *Biomaterials* 2002;23:4131–4141.
 64. Sofia S, McCarthy MB, Gronowicz G, Kaplan DL. Functionalized silk-based biomaterials for bone formation. *J Biomed Mater Res* 2001;54:139–148.
 65. Dal Pra I, Petrini P, Charini A, Bozzini S, Fare S, Armato U. Silk fibroin-coated three-dimensional polyurethane scaffolds for tissue engineering: Interactions with normal human fibroblasts. *Tissue Eng* 2003;9:1113–1121.
 66. Meinel L, Hofmann S, Karageorgiou V, Zichner L, Langer R, Kaplan D, Vunjak-Novakovic G. Engineering cartilage-like tissue using human mesenchymal stem cells and silk protein scaffolds. *Biotechnol Bioeng* 2004;88:379–391.
 67. Sugihara A, Sugiura K, Morita H, Ninagawa T, Tubouchi K, Tobe R, Izumiya M, Horio T, Abraham NG, Ikehara S. Promotive effects of a silk film on epidermal recovery from full-thickness skin wounds. *Proc Soc Exp Biol Med* 2000;225:58–64.
 68. Allmeling C, Jokuszies A, Reimers K, Kall S, Vogt PM. Use of spider silk fibres as an innovative material in a biocompatible artificial nerve conduit. *J Cell Mol Med* 2006;10:770–777.
 69. Fahnstock SR, Irwin SL. Synthetic spider dragline silk proteins and their production in *Escherichia coli*. *Appl Microbiol Biotechnol* 1997;47:23–32.
 70. Fahnstock SR, Bedzyk LA. Production of synthetic spider dragline silk protein in *Pichia pastoris*. *Appl Microbiol Biotechnol* 1997;47:33–39.
 71. Miao Y, Zhang Y, Nakagaki K, Zhao T, Zhao A, Meng Y, Nakagaki M, Park EY, Maenaka K. Expression of spider flagelliform silk protein in *Bombyx mori* cell line by a novel Bac-to-Bac/BmNPV baculovirus expression system. *Appl Microbiol Biotechnol* 2006;71:192–199.
 72. Lazaris A, Arcidiacono S, Huang Y, Zhou JF, Duguay F, Chretien N, Welsh EA, Soares JW, Karatzas CN. Spider silk fibers spun from soluble recombinant silk produced in mammalian cells. *Science* 2002;295:472–476.
 73. Scheller J, Guhrs KH, Grosse F, Conrad U. Production of spider silk proteins in tobacco and potato. *Nat Biotechnol* 2001;19:573–577.
 74. Vollrath F, Knight DP. Liquid crystalline spinning of spider silk. *Nature* 2001;410:541–548.
 75. Jin HJ, Kaplan DL. Mechanism of silk processing in insects and spiders. *Nature* 2003;424:1057–1061.
 76. Huang J, Foo CWP, Kaplan DL. Biosynthesis and applications of silk-like and collagen-like proteins. *Polym Rev* 2007;47:29–62.
 77. Bini E, Foo CWP, Huang J, Karageorgiou V, Kitchel B, Kaplan DL. RGD-functionalized bioengineered spider dragline silk biomaterial. *Biomacromolecules* 2006;7:3139–3145.
 78. Yanagisawa S, Zhu Z, Kobayashi I, Uchino K, Tamada Y, Tamura T, Asakura T. Improving cell-adhesive properties of recombinant *Bombyx mori* silk by incorporation of collagen or fibronectin derived peptides produced by transgenic silkworms. *Biomacromolecules* 2007;8:3487–3492.

79. Yang M, Yamauchi K, Kurokawa M, Asakura T. Design of silk-like biomaterials inspired by mussel-adhesive protein. *Tissue Eng* 2007;13:2941–2947.
80. Huang J, Wong C, George A, Kaplan DL. The effect of genetically engineered spider silk-dentin matrix protein 1 chimeric protein on hydroxyapatite nucleation. *Biomaterials* 2007;28:2358–2367.
81. Grip S, Johansson J, Hedhammar M. Engineered disulfides improve mechanical properties of recombinant spider silk. *Protein Sci* 2009;18:1012–1022.
82. Teule F, Furin WA, Cooper AR, Duncan JR, Lewis RV. Modifications of spider silk sequences in an attempt to control the mechanical properties of the synthetic fibers. *J Mater Sci* 2007;42:8974–8985.
83. Szela S, Avtges P, Valluzzi R, Winkler S, Wilson D, Kirschner D, Kaplan DL. Reduction-oxidation control of beta-sheet assembly in genetically engineered silk. *Biomacromolecules* 2000;1:534–542.
84. Valluzzi R, Szela S, Avtges P, Kirschner D, Kaplan D. Methionine redox controlled crystallization of biosynthetic silk spidroin. *J Phys Chem B* 1999;103:11382–11392.
85. Winkler S, Wilson D, Kaplan DL. Controlling beta-sheet assembly in genetically engineered silk by enzymatic phosphorylation/dephosphorylation. *Biochemistry (N Y)* 2000;39:12739–12746.
86. Haider M, Cappello J, Ghandehari H, Leong KW. In vitro chondrogenesis of mesenchymal stem cells in recombinant silk-elastinlike hydrogels. *Pharm Res* 2008;25:692–699.
87. Oshea EK, Klemm JD, Kim PS, Alber T. X-ray structure of the Gcn4 leucine zipper, a 2-stranded, parallel coiled coil. *Science* 1991;254:539–544.
88. Oshea EK, Rutkowski R, Kim PS. Evidence that the leucine zipper is a coiled coil. *Science* 1989;243:538–542.
89. Petka WA, Harden JL, McGrath KP, Wirtz D, Tirrell DA. Reversible hydrogels from self-assembling artificial proteins. *Science* 1998;281:389–392.
90. Shen W, Zhang KC, Kornfield JA, Tirrell DA. Tuning the erosion rate of artificial protein hydrogels through control of network topology. *Nat Mater* 2006;5:153–158.
91. Wang C, Stewart RJ, Kopecek J. Hybrid hydrogels assembled from synthetic polymers and coiled-coil protein domains. *Nature* 1999;397:417–420.
92. Yang JY, Xu CY, Wang C, Kopecek J. Refolding hydrogels self-assembled from *N*-(2-hydroxypropyl)methacrylamide graft copolymers by antiparallel coiled-coil formation. *Biomacromolecules* 2006;7:1187–1195.
93. Jing P, Rudra JS, Herr AB, Collier JH. Self-assembling peptide-polymer hydrogels designed from the coiled coil region of fibrin. *Biomacromolecules* 2008;9:2438–2446.
94. Pandya MJ, Spooner GM, Sunde M, Thorpe JR, Rodger A, Woolfson DN. Sticky-end assembly of a designed peptide fiber provides insight into protein fibrillogenesis. *Biochemistry (N Y)* 2000;39:8728–8734.
95. Smith AM, Banwell EF, Edwards WR, Pandya MJ, Woolfson DN. Engineering increased stability into self-assembled protein fibers. *Adv Funct Mater* 2006;16:1022–1030.
96. Ryadnov MG, Woolfson DN. Fiber recruiting peptides: Noncovalent decoration of an engineered protein scaffold. *J Am Chem Soc* 2004;126:7454–7455.
97. Nowak AP, Breedveld V, Pakstis L, Ozbas B, Pine DJ, Pochan D, Deming TJ. Rapidly recovering hydrogel scaffolds from self-assembling diblock copolypeptide amphiphiles. *Nature* 2002;417:424–428.
98. Pakstis LM, Ozbas B, Hales KD, Nowak AP, Deming TJ, Pochan D. Effect of chemistry and morphology on the biofunctionality of self-assembling diblock copolypeptide hydrogels. *Biomacromolecules* 2004;5:312–318.
99. Nowak AP, Breedveld V, Pine DJ, Deming TJ. Unusual salt stability in highly charged diblock co-polypeptide hydrogels. *J Am Chem Soc* 2003;125:15666–15670.

100. Deming TJ. Polypeptide hydrogels via a unique assembly mechanism. *Soft Matter* 2005; 1:28–35.
101. Yang C, Song B, Ao Y, Nowak AP, Abelowitz RB, Korsak RA, Havton LA, Deming TJ, Sofroniew MV. Biocompatibility of amphiphilic diblock copolypeptide hydrogels in the central nervous system. *Biomaterials* 2009;30:2881–2898.
102. Giancotti FG, Ruoslahti E. Transduction – Integrin signaling. *Science* 1999;285:1028–1032.
103. Le PU, Lenferink AEG, Pinard M, Baardsnes J, Massie B, O'Connor-McCourt MD. *Escherichia coli* expression and refolding of E/K-coil-tagged EGF generates fully bioactive EGF for diverse applications. *Protein Expr Purif* 2009;64:108–117.
104. Boucher C, St-Laurent G, Loignon M, Jolicoeur M, De Crescenzo G, Durocher Y. The bioactivity and receptor affinity of recombinant tagged EGF designed for tissue engineering applications is defined by the nature and position of the tags. *Tissue Eng Part A* 2008;14:2069–2077.
105. Nakaji-Hirabayashi T, Kato K, Iwata H. Surface-anchoring of spontaneously dimerized epidermal growth factor for highly selective expansion of neural stem cells. *Bioconjug Chem* 2009;20:102–110.
106. Cappello J, Crissman JW, Crissman M, Ferrari FA, Textor G, Wallis O, Whitley JR, Zhou X, Burman D, Aukerman L, Stedronsky ER. In-situ self-assembling protein polymer gel systems for administration, delivery, and release of drugs. *J Control Release* 1998;53:105–117.
107. Manickam DS, Oupicky D. Multiblock reducible copolypeptides containing histidine-rich and nuclear localization sequences for gene delivery. *Bioconjug Chem* 2006;17:1395–1403.
108. Chen DJ, Majors BS, Zelikin A, Putnam D. Structure-function relationships of gene delivery vectors in a limited polycation library. *J Control Release* 2005;103:273–283.
109. Wheelton IR, Gallaway JW, Barton SC, Banta S. Bioelectrocatalytic hydrogels from electron-conducting metallopolypeptides coassembled with bifunctional enzymatic building blocks. *Proc Natl Acad Sci U S A* 2008;105:15275–15280.
110. Rizzi SC, Hubbell JA. Recombinant protein-co-PEG networks as cell-adhesive and proteolytically degradable hydrogel matrixes. Part I: Development and physicochemical characteristics. *Biomacromolecules* 2005;6:1226–1238.
111. Rizzi SC, Ehrbar M, Halstenberg S, Raeber GP, Schmoekel HG, Hagenmueller H, Mueller R, Weber FE, Hubbell JA. Recombinant protein-co-PEG networks as cell-adhesive and proteolytically degradable hydrogel matrixes. Part II: Biofunctional characteristics. *Biomacromolecules* 2006;7:3019–3029.
112. Ehrick JD, Deo SK, Browning TW, Bachas LG, Madou MJ, Daunert S. Genetically engineered protein in hydrogels tailors stimuli-responsive characteristics. *Nat Mater* 2005;4:298–302.
113. Murphy WL, Dillmore WS, Modica J, Mrksich M. Dynamic hydrogels: Translating a protein conformational change into macroscopic motion. *Angew Chem Int Ed Engl* 2007;46:3066–3069.
114. Sui Z, King WJ, Murphy WL. Dynamic materials based on a protein conformational change. *Adv Mater* 2007;19:3377–3380.
115. Sui Z, King WJ, Murphy WL. Protein-based hydrogels with tunable dynamic responses. *Adv Funct Mater* 2008;18:1824–1831.
116. King WJ, Mohammed JS, Murphy WL. Modulating growth factor release from hydrogels via a protein conformational change. *Soft Matter* 2009;5:2399–2406.
117. Topp S, Prasad V, Cianci GC, Weeks ER, Gallivan JP. A genetic toolbox for creating reversible Ca²⁺-sensitive materials. *J Am Chem Soc* 2006;128:13994–13995.
118. Kiick KL, van Hest JCM, Tirrell DA. Expanding the scope of protein biosynthesis by altering the methionyl-tRNA synthetase activity of a bacterial expression host. *Angew Chem Int Ed Engl* 2000;39:2148–2152.

119. Kiick KL, Saxon E, Tirrell DA, Bertozzi CR. Incorporation of azides into recombinant proteins for chemoselective modification by the Staudinger ligation. *Proc Natl Acad Sci U S A* 2002;99:19–24.
120. Kirshenbaum K, Carrico IS, Tirrell DA. Biosynthesis of proteins incorporating a versatile set of phenylalanine analogues. *Chembiochem* 2002;3:235–237.
121. Tang Y, Ghirlanda G, Petka WA, Nakajima T, DeGrado WF, Tirrell DA. Fluorinated coiled-coil proteins prepared in vivo display enhanced thermal and chemical stability. *Angew Chem Int Ed Engl* 2001;40:1494–1496.
122. Son S, Caglar Tanrikulu I, Tirrell DA. Stabilization of bzip peptides through incorporation of fluorinated aliphatic residues. *Chembiochem* 2006;7:1251–1257.
123. Montclare JK, Son S, Clark GA, Kumar K, Tirrell DA. Biosynthesis and stability of coiled-coil peptides containing (2S,4R)-5,5,5-trifluoroleucine and (2S,4S)-5,5,5-trifluoroleucine. *Chembiochem* 2009;10:84–86.
124. Kim W, McMillan RA, Snyder JP, Conticello VP. A stereoelectronic effect on turn formation due to proline substitution in elastin-mimetic polypeptides. *J Am Chem Soc* 2005;127:18121–18132.
125. Kim WY, George A, Evans M, Conticello VP. Cotranslational incorporation of a structurally diverse series of proline analogues in an *Escherichia coli* expression system. *Chembiochem* 2004;5:928–936.
126. Kothakota S, Mason TL, Tirrell DA, Fournier MJ. Biosynthesis of a periodic protein containing 3-thienylalanine – A Step toward genetically-engineered conducting polymers. *J Am Chem Soc* 1995;117:536–537.
127. Beatty KE, Xie F, Wang Q, Tirrell DA. Selective dye-labeling of newly synthesized proteins in bacterial cells. *J Am Chem Soc* 2005;127:14150–14151.
128. Link AJ, Vink MKS, Tirrell DA. Preparation of the functionalizable methionine surrogate azidohomoalanine via copper-catalyzed diazo transfer. *Nat Protoc* 2007;2:1879–1883.
129. van Hest JCM, Kiick KL, Tirrell DA. Efficient incorporation of unsaturated methionine analogues into proteins in vivo. *J Am Chem Soc* 2000;122:1282–1288.
130. Link AJ, Vink MKS, Tirrell DA. Presentation and detection of azide functionality in bacterial cell surface proteins. *J Am Chem Soc* 2004;126:10598–10602.
131. Carrico IS, Maskarinec SA, Heilshorn SC, Mock ML, Liu JC, Nowatzki PJ, Franck C, Ravichandran G, Tirrell DA. Lithographic patterning of photoreactive cell-adhesive proteins. *J Am Chem Soc* 2007;129:4874–4875.
132. Nowatzki PJ, Franck C, Maskarinec SA, Ravichandran G, Tirrell DA. Mechanically tunable thin films of photosensitive artificial proteins: Preparation and characterization by nanoindentation. *Macromolecules* 2008;41:1839–1845.
133. Zhang KC, Diehl MR, Tirrell DA. Artificial polypeptide scaffold for protein immobilization. *J Am Chem Soc* 2005;127:10136–10137.

Part II

Specific Applications in Tissue Engineering

Contents

10.1	Cartilage Tissue: Structure, Function, and Disease	280
10.1.1	Cellular and Extracellular Matrix Components	280
10.1.2	Proper Tissue Function and Response to Stress	282
10.1.3	Aged and Damaged Tissue	284
10.1.4	Need for Repair and Regeneration Strategies	285
10.2	Current Standards of Care and Limitations	286
10.2.1	Current Treatments in Cartilage Repair	286
10.2.2	Limitations of Current Standard Practices and Need for Engineering Approaches	289
10.3	Cartilage Engineering	290
10.3.1	Requirements of an Engineered Construct	290
10.3.2	Biomaterials and Cells for Cartilage Engineering	291
10.3.3	Engineered Constructs in Clinical Trials and Early Applications	294
10.3.4	Current Research Efforts	296
10.4	Future Directions	298
10.4.1	Zonal Cartilage Engineering	298
10.4.2	Stem Cells	299
10.4.3	Dynamic Culture Systems	300
	References	301

Abstract Articular cartilage provides the surface of articulating joints with frictionless movement while absorbing loading forces. The tissue's extracellular matrix (ECM) is comprised mainly of type II collagen and proteoglycans which are maintained by chondrocytes, the resident cell population. Cartilage is a structurally complex tissue, with zones that exhibit different cell morphologies and extracellular matrix structure depending on distance from the articulating surface. The tissue is both alymphatic and avascular. All nutrient, oxygen, and waste exchange occurs through diffusion. This, along with low cell density and proliferation, contributes to the tissue's limited ability to repair ECM damage. The high number of people suffering from arthritis has led to a plethora of cartilage

J.P. Fisher (✉)

Fischell Department of Bioengineering, University of Maryland, 3238 Jeong H. Kim Building, College Park, MD 20742, USA
e-mail: jpfisher@umd.edu

10 engineering research. Recent efforts have focused on aiding the body in cartilage restoration through both cell-based and acellular biomaterials. A variety of synthetic and natural polymers have been created for this purpose, each with their benefits and drawbacks. To date, an ideal biomaterial has yet to be created that can optimally repair or regenerate damaged cartilage. Here we highlight current biomaterial trends in cartilage engineering and examine future directions within the field.

Keywords Biomaterials • Cartilage engineering • Cartilage physiology • Cartilage repair

10.1 Cartilage Tissue: Structure, Function, and Disease

10.1.1 Cellular and Extracellular Matrix Components

Articular cartilage, typically 2–5 mm thick, is found on the surface of articulating joints throughout the body. Articular cartilage, along with the synovial fluid found inside the joint, provides frictionless movement between bones and absorbs loads during motion. The tissue is maintained by chondrocytes, which is the resident cell population. Chondrocytes are responsible for providing a balance between matrix synthesis and matrix breakdown, a process which is disrupted during disease or injury. The tissue is sparsely populated with cells; comprising less than 5% of the tissue volume [1]. Cartilage also lacks a lymphatic system, nerve fibers, or blood supply. As a result, all nutrient and waste exchange must occur through diffusion from the synovial fluid. Low cell density and the limited exchange of both waste and nutrients both play key roles in the limited ability of cartilage tissue to repair itself once injured.

10.1.1.1 Composition

Approximately 95% cartilage tissue is comprised of its extracellular matrix (ECM) – which the cells sustain. The ECM is a dense collagen and proteoglycan interconnected structure. Chondrocytes are linked to the ECM through cell-surface binding proteins. These connections allow cells to respond to the mechanical forces felt within the ECM [2, 3].

Approximately 10–20% of the wet weight of the tissue is collagen. The collagen network is comprised mainly of type II collagen fibers; up to 90% of the total collagen content is type II collagen which is crosslinked by covalent bonds throughout the tissue. The type II collagen fiber is a triple helix of identical polypeptide $\alpha_1(\text{II})$ chains, approximately 300 nm in length. Minor collagen types make up the rest of the tissue's collagen content and include collagen type IX, XI, and X. Each type of collagen has a

different function within the ECM. Type IX collagen is a short fibrillar collagen that helps connect the type II collagen network to proteoglycans. Type XI collagen is also a fiber formed with three distinct α -chains. Type XI forms co-polymers with type II collagen and acts to regulate fibril diameter, form bridges between fibrils, and even crosslinks to itself to increase the mechanical stability of the ECM. Type X collagen is a short helix molecule produced only by hypertrophic cells in the calcified tissue which divides articular cartilage from the underlying subchondral bone [1, 3–5].

In addition to collagen, the cartilage ECM is comprised of minor and major proteoglycans. Minor proteoglycans within the ECM include decorin, biglycan, and fibromodulin. These small proteoglycans bind to other molecules and help stabilize the overall matrix structure. Aggrecan is the major proteoglycan in the ECM. Aggrecan contains many branched glycosaminoglycans (GAGs) – primarily keratan sulfate (KS) and chondroitin sulfate (CS). The densely packed GAGs branch off of a central aggrecan backbone and give the molecule a molecular weight of 250,000 Da. Each molecule contains about 100 CS chains and 60 KS chains, and repeating sulfate groups in both give each aggrecan molecule a large negative charge [1, 2, 4].

The aggrecan molecule is bound to a long unbranched hyaluronic acid (HA) chain via a link protein. Hyaluronic acid is a polysaccharide chain with an average molecular weight of several million Daltons, with the addition of many aggrecan molecules linked to this backbone the aggregate molecular weight can reach up to several hundred million Daltons. The networks of HA chains linked to aggrecan molecules are entrapped within the collagen network to give cartilage an intricately organized ECM structure [1, 2, 5].

The complex ECM is maintained by the chondrocyte cell population. Chondrocytes have limited cell-to-cell communication, and as a result each cell acts as somewhat of an individual – maintaining only the tissue immediately surrounding it. Cells receive information through both mechanical forces and interactions with growth factors and cytokines. The ECM directly surrounding a cell is called the pericellular or lacunar matrix. This area contains an abundance of proteoglycans and few collagen fibers. Directly outside this region is the territorial or capsular matrix – which encapsulates the cell or a group of cells. The chondrocyte exists in a low oxygen environment, and as a result its metabolism is driven by anaerobic pathways, mainly glycolysis. Although chondrocytes produce ECM components, they usually do not divide past adolescence. Low cell density and division both contribute to the tissue's limited repair capability [6–8].

10.1.1.2

Structure

In addition to cellular components and a complex extracellular matrix articular cartilage also contains three distinct zones. Each zone has a distinct cellular phenotype and ECM organization. The superficial, or tangential zone, contains the articulating surface of the joint and extends to about 10% of the total tissue depth. The middle, or transitional zone, comprises approximately the middle 70% of the tissue depth and is followed by the deep, or

10 basal, zone which is the bottom 20% of articular cartilage. Below the deep zone lies the tidemark – below which the tissue becomes calcified and eventually turns into subchondral bone. The calcified zone contains few blood vessels and effectively blocks the diffusion of nutrients and waste between the subchondral bone and the deep zone of the articular cartilage [4, 9, 10].

The superficial zone is marked by cells and collagen fibers that are oriented parallel to the articulating surface. These cells are smaller than those of the other zones, thin, and disc shaped. The cell density is the highest in this zone, however the proteoglycan content is the lowest. The water content of the superficial zone is the lowest, with approximately 65% of the total water weight of cartilage found in the lower two zones [2, 11, 12]. The densely packed collagen fibers are small in diameter and packed in bundles parallel to the articulating surface. The tight organization of the superficial layer is thought to act as a boundary to block any large, unwanted molecules from the synovial fluid [13]. The superficial zone cells are the only cells to secrete superficial zone protein; a lubricating protein secreted into the synovial fluid [14].

The middle zone contains larger and more rounded chondrocytes. The cells, along with the collagen fibers are randomly oriented and can often be found in clusters. Middle zone chondrocytes produce higher levels of proteoglycans than superficial cells, and the cellular density here is lower than in the superficial zone [11, 15].

Deep zone cells are oval in shape, and the cells along with collagen fibers are oriented in vertical columns perpendicular to the articulating surface. The deep zone cells produces elevated levels of collagen and proteoglycans compared to the superficial cells. This zone also has a lower cell density, approximately one third of that of the superficial zone. Figure 10.1 shows histological staining for primary bovine chondrocytes isolated from the three tissue zones [2, 11].

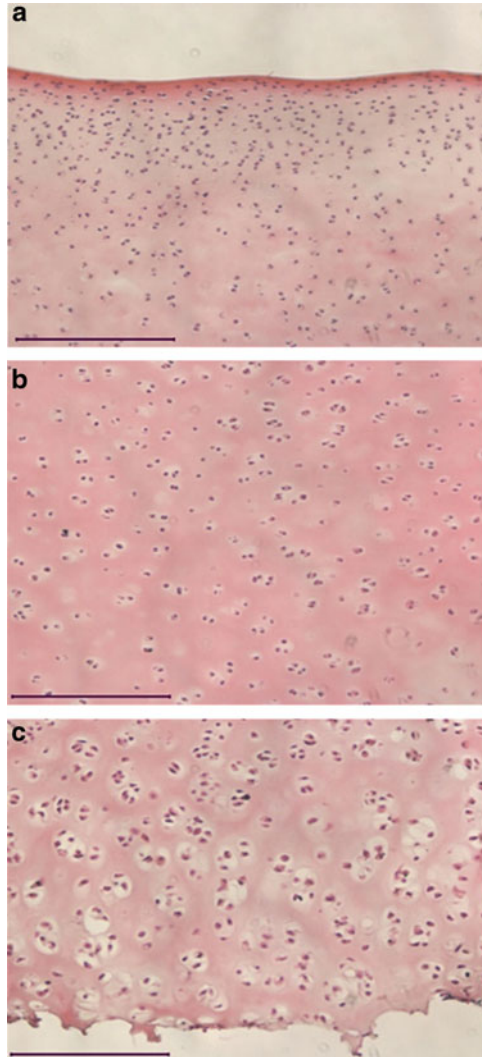
10.1.2

Proper Tissue Function and Response to Stress

Cartilage can withstand large numbers of repetitive strains over many years. For the tissue to function properly many critical biological relationships must remain in balance. Some key processes include the metabolic activity of the chondrocytes (the balance between matrix synthesis and breakdown), proper cell secretion and concentration of hormones, production of growth factors and cytokines, and proper distribution of mechanical loading by the ECM.

The integrity of the proteoglycan and collagen networks are critical for proper function of cartilage tissue. The collagen network provides tensile strength, and the proteoglycans are critical for resisting compressive loading. The net negative charges on each proteoglycan, from the presence of the GAG groups, give the tissue a high osmolality. Negative charges attract cations, which further raises the osmolality, which in turn increase water uptake. The result is a high osmotic tissue pressure (350–450 mOsm), however the strong type II collagen matrix prevents the tissue from swelling. High osmotic pressure results in cartilage tissue being approximately 70% water [2, 16, 17].

Fig. 10.1 Hematoxylin and eosin (H&E) staining of cells isolation from (a) superficial, (b) middle, and (c) deep zones of bovine articular cartilage. Cell nuclei are stained *dark violet*, cell cytoplasm are stained *light pink*, and extracellular matrix is stained slightly *darker pink*. Scale bars all 100 μm



During joint loading this high tissue pressure resists load and deformation, however a small amount of water is pushed outside the tissue into the joint. Here, this liquid helps to further resist friction and assists in the smooth motion of the joint. In addition, this liquid absorbs nutrients in the synovial cavity, and when the load is released the liquid flows back into the tissue and delivers these nutrients. As a result, dynamic loading stimulates matrix production and is dependent on the amplitude and frequency of the load. Conversely, static loading decreases the synthesis of certain matrix proteins. Therefore, just as proper tissue structure is necessary for loading mechanics, healthy loading is also necessary for proper tissue homeostasis [2, 16, 17].

10.1.3

Aged and Damaged Tissue

The natural aging process leaves cartilage less robust and with lower tensile strength as early as the third decade of life. With age the metabolic activity of the chondrocytes is altered; their ability to respond to growth factors and cytokines decreases. Compromised mechanical properties and decreased activity of the chondrocytes leaves aged tissue more susceptible to damage [13, 18].

Cartilage tissue can become damaged due to diseases such as arthritis or trauma which results tissue injury. The limited cell population and reliance on diffusion for nutrients and waste exchange make it difficult for chondrocytes to restore a damaged ECM. In unhealthy tissue the balance between matrix production and breakdown is disrupted and a cycle of tissue degradation ensues. Even minor tissue injuries usually do not fully repair, and leave the cartilage more susceptible to the onset of disease [2, 19].

10.1.3.1

Disease

Arthritis is marked by degradation of cartilage and subchondral bone tissue which results in joint pain and loss of motion. Arthritis can be divided into two major classes: inflammatory rheumatoid arthritis (RA) and non-inflammatory osteoarthritis (OA). In both cases the complex structure and biochemistry of the tissue becomes disrupted. OA is much more common, and affects a large percentage of the elderly population. In fact, about two out of three people over the age of 65 show radiographic signs of OA [20]. In both diseases enzymes such as matrix metalloproteinases (MMPs) cleave the bonds that hold the matrix together. Inflammatory rheumatoid arthritis is an autoimmune disease, while osteoarthritis is marked by degeneration of cartilage tissue. Due to its prevalence in society OA disease and repair strategies will be discussed [6].

There is no uniform appearance or single pathogenic mechanism that marks OA. It can present itself in a variety of appearances and is caused by a number of different factors. Causes can include genetic defects, extended joint overloading or overuse, or joint misalignment. OA can also onset as a result of trauma which results in direct injury to the joint or surrounding ligaments. OA can potentially affect any articulating joint, and is classified by pain, motion or gait problems, loss of ECM molecules into synovial fluid, loss of joint cartilage, and tissue remodeling in the subchondral bone. Factors such as alcohol abuse, obesity, and diabetes increase the risk for onset of OA [1, 3, 18].

Loss of integrity of the type II collagen network is an early ECM change during OA. An increase in osmotic pressure results in swelling which causes proteoglycans to escape. A reduction in the proteoglycan concentration lowers the tissue's osmotic pressure, which compromises its ability to resist loading. Once the process of matrix degradation has begun it accelerates due to the tissues inherent limited ability to self-repair [2, 21].

Disruption in production of ECM components, signaling molecules, and cytokines is also observed during disease [21]. In an attempt to combat matrix breakdown elevated levels of minor proteoglycans are usually observed in the early stages of osteoarthritis. Type

X collagen, usually only found in the calcified zone, can be found throughout the various zones of articular cartilage with the progression of disease. Elevated levels of enzymes such as MMPs cleave critical bonds in the collagen and proteoglycan matrices. Chondrocytes begin producing a meta-stable form of type II collagen (type IIa collagen), which is degraded before it can be functionally incorporated into the matrix [2, 13, 18].

Eventually the tissue becomes fragmented, with damaged areas alongside remaining healthy tissue. Failed repair events are noticeable throughout the tissue in the form of local accumulation of ECM precursor molecules (such as procollagen peptides), clumps of chondrocytes entrapped by bundles of minor collagens, and chondrocyte dedifferentiation. Damaged cartilage is heterogeneous, and can manifest itself in a variety of structural disruptions. Loss of tissue height from the superficial and middle zones is a common manifestation of OA [1, 3, 13, 18].

In the late states of the disease functional cartilage is gone, and areas of exposed bone-plate can be observed. Cracks in the subchondral plate and formation of subchondral bone cysts also occur. Gradually, bone marrow will make its way to the region and a layer of mechanically sub-optimal fibrocartilage will replace the once healthy cartilage tissue [1, 3, 13].

10.1.3.2

Trauma

Trauma can occur due to a single excessive load, or repetitive joint overloading. Tissue damage can occur in the form of a microfracture, where the damage to the articular surface is not visible, or it can occur in the form of a visible tissue disruption of variable length. If the damage penetrates through the tidemark and into the subchondral bone it is called an osteochondral fracture [2]. Unfortunately, defects rarely repair themselves and only continue to grow worse with age. Most significant injuries to articular cartilage will result in the eventual onset of OA. The healing potential and severity of disease are dependent on the size and location of injury, as well as patient health and age [19].

10.1.4

Need for Repair and Regeneration Strategies

Many obstacles make treating arthritis and cartilage injuries challenging. For one, it is difficult to repair a tissue lacking intrinsic repair mechanisms. Turnover in matrix proteins is relatively low even in healthy tissue, in fact the half life of collagen and proteoglycans are approximately 100 and 3–24 years respectively [22]. Additionally, there is no single reason or way tissue degradation occurs – making treatment options hard to identify. Pain medication given to arthritic patients may relieve pain, but it does nothing to stop the tissue erosion cycle. Some pain medications – such as non-steroidal anti-inflammatory drugs (NSAIDS) – are even thought to hurt matrix production. Furthermore, therapies that target cell populations will be ineffective if the cells have already become phenotypically unstable and entered hypertrophy or fibroblastic lineages [3]. Currently, engineered cartilage therapies are not standard practice in treating cartilage defects. Standard of care still involves non-surgical

interventions, or traditional surgical techniques. While these treatment methods have had some successes, they have several key disadvantages in restoring healthy tissue.

10.2

Current Standards of Care and Limitations

10.2.1

Current Treatments in Cartilage Repair

To date there are many approaches for treatment of cartilage defects and OA, however an ideal method is yet to be developed. The field has received much research attention, and many new products are in various stages of clinical trials. Despite this, there is a fairly limited range of treatments that are available on large scale. The estimated cost of OA and cartilage defects in the United States is between 10 [20] and 65 [23] billion dollars annually between loss of working days and medical treatments. Furthermore, more than one in eight Americans over the age of 25 are thought to be affected with some form of the disease [24].

The main symptoms of OA are joint pain and loss of function. However, the disconnect often observed between radiographic evidence of cartilage damage and experienced pain presents a major challenge in patient care. In fact, more than half of patients with severe radiographic evidence of OA report no pain [20]. The heterogeneity of the disease both in its physical manifestations and in symptoms reported by patients make it hard to classify, treat, and prevent.

The American College of Rheumatology (ACR), European League Against Rheumatism (EULAR), and the Osteoarthritis Research Society International (OARSI) all recommend the following progression of treatments: non-pharmacological, pharmacological, and finally surgery. Patients should only move to the next treatment if the methods they are using are ineffective and pain persists [20, 25].

10.2.1.1

Non-surgical

Non-pharmacological treatments include: weight reduction if necessary, education and self management, physical therapy, aerobics, muscle strengthening, and acupuncture. Generally, light exercise helps to reduce pain. If none of these methods are successful pharmacological treatments should be used.

Drug administration can be divided into two groups: pain-reducing agents, and therapeutic agents. Pain reducing agents are used simply to manage patient pain in order to improve functionality. Therapeutic agents also help to relieve pain and additionally aim to stop matrix degradation and slow down disease progression.

The first line of pain-reducing agents are acetaminophen, NSAIDs, and cyclooxygenase-2 (Cox-2) inhibitors. Acetaminophen is safe for long-term use in small doses however, it is relatively weak and can have adverse effects on the liver. While NSAIDs and Cox-2 inhibitors

are anti-inflammatory drugs, they are used in OA management for their pain-relieving properties. If inflammation due to arthritis is present their use will be more effective. Neither should be used long-term or in high doses, as they can have adverse cardiovascular effects. Patients at risk for gastrointestinal complications should avoid NSAIDs and use a Cox-2 inhibitor, but both should be used in as low doses as possible [20, 25].

More severe pain or flare-ups can be treated with corticosteroid injections or even opioids. Injections should be limited to every 3–4 months as they can have adverse metabolic effects and provide only short-term relief [26]. Opioids, which are effective pain relievers should be used in low doses and only for severe cases [20, 25].

Therapeutic drugs which aim to retard matrix erosion include glucosamines, chondroitin sulfate, S-adenosylmethionine (SAM), and hyaluronic acid. Glucosamines are thought to have structural remodeling potential, but clinically have varying results. They are available in either chloride or sulfate formulations, and after absorption are converted to salts. It is recommended that patients try glucosamines for a few months and discontinue if no benefits are observed. They have almost no side effects. Chondroitin sulfate, SAM, and hyaluronic acid also have varying clinical reports success. SAM may increase GAG production in chondrocytes, and has been reported to decrease pain – but this may be due to the drug's anti-depressant effects. Hyaluronic acid injections are reported to decrease pain and improve functionality but are not effective in severe cases of matrix degradation or limb misalignment. Rarely are adverse effects observed, but pain and infection at the injection site has been reported [20, 25, 27].

Several new compounds are in various stages of research investigation including inhibitors of MMPs, a new class of drugs called disease-modifying osteoarthritis drugs (DMOAD), and the use of growth factors [25]. However, there is currently no ideal drug, or cocktail of drugs for relieving pain, improving functionality, and stopping or reversing matrix destruction. The diverse nature of OA makes a single optimal treatment path difficult to identify.

10.2.1.2

Surgical

When non-pharmacological and pharmacological treatment methods prove ineffective the next step is surgical intervention. Surgical procedures can be broadly grouped into two classes: non-regenerative treatments and tissue replacement/regenerative treatments. Non-regenerative treatments aim to physically alter or remove the problem joint while regenerative treatments attempt to replace or regenerate the damaged tissue.

Non-regenerative

Non-regenerative procedures include osteotomy, arthrodesis, and arthroplasty. Osteotomy is usually performed for joint misalignment and involves the removal of bone to redistribute loads to areas of healthy cartilage. Risk factors include hemorrhage, inflammation, and nerve damage. Arthroplasty refers to total joint replacement and is reserved for the most

10 severe cases when all other treatments have failed. Although this is a fairly common surgery in the United States there is still a relatively large complication rate of 5.5%, most of which is associated with post-operative infection. Arthrodesis is the induction of bone formation between two bones to immobilize a joint. This is usually performed on the small joints present in the hands and feet [25, 28].

Tissue Replacement/Regenerative

Traditionally surgery has been used as a last resort option. However, one of the biggest risk factors for developing OA is the presence of cartilage defects. If these defects can be treated early and successfully with regenerative therapies, onset of disease may be slowed. Regenerative and replacement techniques can be subdivided into three groups: bone marrow stimulation techniques, osteochondral transfer or grafts, and cell-based therapies [25, 29].

Bone Marrow Stimulation

The most common marrow stimulation procedure is microfracture. During this operation micro-penetration of the subchondral bone plate fills the cartilage defect with blood cells that contain a population of mesenchymal stem cells (MSCs). MSCs can differentiate into chondrocytes, among other cell types. The result of MSCs populating the cartilage defect is the formation of fibro-cartilage tissue containing varying amounts of type II collagen. The procedure has several advantages and drawbacks. Advantages include limited invasiveness, low tissue morbidity, short recovery time, and cost-effectiveness. The greatest level of success is observed in young, athletic patients with early intervention. Drawbacks include formation of tissue lacking structure and function of healthy cartilage. The fibro-cartilage layer provides limited load-bearing capacity, is often much thinner than native tissue, does not fully integrate with surrounding tissue, and often includes overgrowth of the subchondral bone. A technique called enhanced microfracture attempts to address these drawbacks by including growth factors which induce chondrogenesis of the MSC populations [19, 25, 29, 30].

Osteochondral Transfer/Grafts

Osteochondral transfer includes both autografts and allografts. Autografts involve harvesting cartilage tissue from areas of low loading and transplanting to defects in weight bearing sites. There are several drawbacks of this procedures including difficulty in restoring proper joint architecture, pressure build up due to incongruity of restored surfaces, donor site morbidity, lack of integration of grafted tissue, and altered joint mechanics and load bearing capability. Allografts have the advantage of no donor site morbidity, however all the same disadvantages exists, plus potential immune response and transmission of disease [31].

The most modern form of the osteochondral graft is a procedure called mosaicplasty. This uses several small grafts to fill a single defect. Mosaicplasty treatment is most successful in patients under 50 with no joint misalignment [19, 25].

Cell-Based Therapies

The first cell based therapy introduced was autologous chondrocyte implantation (ACI) in 1994. It has been used ever since with considerable success reported. The procedure has two steps. First, chondrocytes are harvested from the patient, isolated, and expanded in vitro culture. Next, the expanded cell population is injected into a chondral defect. Despite positive surgical outcomes the procedure has many disadvantages. Donor site morbidity, the need for a second surgery, dislocation of cells implanted to defect, extended recovery, loss of chondrocyte phenotype in monolayer, and the formation of fibrous repair tissue are all limitations of the procedure [19, 22, 25, 29, 30].

A more advanced form of ACI, characterized chondrocyte implantation, uses the same procedure but during in vitro culture identifies cells with genetic markers that indicate high levels of matrix production. This technique has limited approval in Europe and has not yet been approved in the United States [29].

10.2.2

Limitations of Current Standard Practices and Need for Engineering Approaches

Despite the disadvantages of each, microfracture and mosaicplasty are currently the most popular choice of surgical interventions for repair of cartilage defects [29]. The ACI procedure is also popular, despite its challenges and potential complications [32]. The current standard of care treatments for cartilage defects and osteoarthritis leave much to be desired. There is no current treatment capable of thoroughly repairing cartilage defects and regenerating tissue that demonstrates chemical and physical properties similar to native cartilage. Tissue that is regenerated using current surgical methods is, at best, fibro-cartilage repair tissue that provides limited load-bearing capabilities and as a result will degrade over time [22, 25, 29, 30].

The primary challenge of tissue engineering solutions is to regenerate cartilage tissue with composition, structure, and function comparable to that of native tissue. Tissue engineering can be defined as the interactions between biomaterials, growth factors, and cells to regenerate functional tissue. A major challenge for engineering articular cartilage is obtaining a sufficiently large chondrocyte population that is phenotypically stable and has not begun to de-differentiate down a fibroblastic lineage [32]. Many research efforts have investigated the ideal biomaterial to maintain a healthy and productive chondrocyte population. Due to these efforts the field has grown considerably over the last decade. While current treatments do not usually involve tissue engineering approaches there are many products both abroad and in the United State in various stages of clinical trials. These new technologies may soon change the standard of cartilage repair procedures [22, 29, 31].

10.3 Cartilage Engineering

10.3.1 Requirements of an Engineered Construct

A tissue engineering scaffold can be seeded with a desired cell population and implanted into a defect site. The scaffold provides both mechanical support and a three-dimensional environment for cells to attach and proliferate. The cell population will produce extracellular matrix components which will infiltrate the scaffold material and surrounding tissue. Slowly the scaffold material will degrade – leaving only cells and native tissue. There are many materials used for the scaffold component of an engineered construct. Scaffolds can be made out of naturally or synthetically derived components. The majority of cartilage scaffolds contain building blocks of either proteins or polysaccharides. Scaffolds can also come in a variety of physical forms, such as foams, viscous liquids, hydrogels, and porous matrices.

10.3.1.1 Required and Desired Construct Properties

Fundamental requirements of all cartilage engineering scaffolds are: lack of immune response and inflammation, adhesion of chondrocytes, maintenance of the chondrocytes phenotype, and initial mechanical stability within the defect. Beyond these requirements there are many desirable, but not necessarily imperative, properties of a scaffold. These include: permeability to allow diffusion of signaling molecules and nutrients, adhesion to the defect site, controlled release of growth factors, injectable, minimally invasive, and biodegradable to allow growth of new ECM tissue to eventually fill the defect site [32–34].

Depending on the nature of the defect the desired properties of the scaffold may change. An osteochondral defect which penetrates the subchondral bone will be repaired differently than a chondral defect. Depending on the location and size of the chondral defect it may be repaired with different approaches as well. For example, a scaffold for an osteochondral defect may be biphasic – with a region for repair of the bone tissue and region for repair of the cartilage tissue. If the bone marrow has been penetrated and is entering the defect site this will also have to be addressed. Perhaps the bone marrow will be contained to the bone tissue, or factors to induce chondrogenesis of the cell populations in the marrow will be added to the scaffold. Additionally, the source of cells could even change depending on the size and location of a chondral defect. If the defect is on the surface of the articulating surface, a population of superficial cell may be harvested for the cellular component of the scaffold. Similarly, deep zone chondrocytes maybe be harvested if the defect lies in the deep zone of chondral tissue. Because the structure and function of cartilage tissue varies throughout its depth and location, engineering approaches must be able to tackle a broad array of defects.

10.3.1.2

Current Model for Engineering Cartilage

There are two major approaches to cartilage tissue engineering. The first approach is to culture cells with or without growth factors *in vitro* for a brief period of time and then implant the construct into the defect site. This method allows the cells to mature and become active inside the body, where they will hopefully start production of a healthy ECM. The second, and more popular model, involves a much longer *in vitro* culture period before implantation. This allows the ECM to build up before the construct enters the defect site, with the intention of providing mechanical support immediately upon implantation. If the scaffold is mechanically and biologically mature and functional before introduction to the defect it will have a greater chance of remaining so while supporting loading regions. In both cases the model includes gradual resorption of the biomaterial as the ECM is produced, as well as integration of the new ECM with the surrounding native tissue [17, 25].

An ideal current model for tissue engineering articular cartilage involves a multi-step procedure. First, an autologous cell population is obtained from the patient, either from cartilage tissue or tissue containing a population of MSCs (such as adipose tissue or bone marrow). Next, these cells are multiplied in monolayer culture, and then transferred to three dimensional culture on the scaffold material to help maintain the chondrocyte phenotype and re-differentiate cells if necessary. The scaffold is cultured for as long as desired, and then implanted into the defect site [17, 32, 35].

Tissue engineering efforts focus on treating cartilage defects that can lead to OA, as designing a scaffold for treatment of advanced stages of cartilage disease is very difficult. Through early intervention and treatment ideally the onset of OA can be delayed or avoided all together.

10.3.2

Biomaterials and Cells for Cartilage Engineering

Many materials have been developed for tissue engineering efforts. Among these there is a large range of chemical components, mechanical strengths, structure, surface topography, and biochemical properties. No ideal scaffold material has been developed, and each group of materials has their advantages and disadvantages. The major goal of the scaffold should be to ensure the retention of chondrocyte phenotype and provide mechanical stability. Hydrogels have received considerable attention in this area as they have properties similar to native tissue [17, 32, 35]. Table 10.1 includes a summary of materials that have been used in clinical or research settings for cartilage tissue engineering.

10.3.2.1

Scaffolds

Poly (L-lactic acid) (PLLA), poly(glycolic acid) (PGA), and the copolymer poly(lactic-co-glycolic acid) (PLGA) are some of the most popular synthetic materials investigated

Table 10.1 Materials that have been used in cartilage engineering efforts in either clinical or research settings

Materials used in cartilage engineering			
Naturally derived	Reference	Synthetically derived	References
Fibrin	[43, 47, 48, 92]	Poly(lactic acid)	[53, 93]
Collagen	[44–46]	Poly(glycolic acid)	[50–53, 94]
Chondroitin sulphate	[46, 95]	Co-polymers of poly(lactic acid) and poly(glycolic acid)	[53, 96]
Alginate	[38–42, 48, 63, 70]	Poly(ethylene oxide)	[58, 59]
Agarose	[68, 71, 84]	Poly(ethylene glycol)	[54–57]
Silk	[97–99]	Ceramics	[100, 101]
Chitosan	[97, 102, 103]	Pluronic copolymer of poly(ethylene oxide) and poly(propylene oxide)	[103, 104]
Hyaluronic acid	[42, 75, 104]	Poly(urethane)	[92]
Cellulose	[105]	Poly(hydroxybutyrate)	[106, 107]
Gelatin	[108]	Poly(ethylene-terephthalate)	[109]
		Poly(tetrafluoroethylene)	[110]
		Poly(1,9-octanediol citrate)	[111, 112]
		Poly(caprolactone)	[113, 114]
		Poly(ether ester) co-polymer	[115]
		Carbon fiber	[116, 117]
		Calcium phosphate	[118]
		Poly(methacrylates)	[119, 120]

for cartilage engineering. Synthetic polymers usually have an open lattice and high porosity which is good for exchange of nutrients and molecules. Their degradation rates can be tailored through composition, and chondrocytes have been shown to adhere and maintain their signature rounded morphology on these materials. Animal models show some preliminary success with synthetic materials, but due to their limitations human trial data is largely unavailable. Some key limitations include: difficulty to mold into complex shapes, hydrophobic – which generally means poor cell attachment and the need for very large chondrocytes populations, invasive implantation, and a strong foreign body reaction [22, 33–35].

Naturally derived materials provide the advantages of usually being biocompatible and biodegradable. Due to its prevalence in the ECM collagen is one of the most popular natural biomaterials for cartilage regeneration. Porous collagen sponges have been made with and without GAGs and growth factors and show good cell attachment and maintenance of cellular phenotype. However, in some cases they have been shown to cause a foreign body reaction which interferes with tissue integration. Additionally, any porous natural material would also have to be delivered through an invasive open surgery [22, 34, 35].

Hydrogels are popular in cartilage engineering due to their similarities to native tissue. Hydrogels are water-swollen polymer networks that can be chemically modified by crosslinks to form mechanically stable shapes. They are made by mixing a soluble polymer (natural or synthetic) in water and adding a crosslinking agent. They can be injectable and molded into desired shapes during gelation. This provides the potential for non-invasive delivery to a defect site. Their porosity can be adjusted by the network density, and their high water content and elastic properties make them similar to native tissue. Chondrocytes show strong attachment and retention of their phenotype in most hydrogels. Some natural hydrogels include alginate, agarose, chitosan, and fibrin. The main drawbacks of these materials include their lack of mechanical strength and difficulty controlling properties such as degradation rate. Synthetic hydrogels allow for somewhat more control over properties such as degradation rate. Some synthetic hydrogels used in cartilage engineering include: poly (ethylene oxide) (PEO), poly (propylene oxide) (PPO), poly (vinyl alcohol) (PVA), and poly(ethylene glycol)(PEG). Synthetic hydrogels often have more limited cell attachment properties than their naturally-derived counterparts. Limitations of both natural and synthetic hydrogels include cellular encapsulation and formation of a uniform gel. Injection provides challenges in controlling gelation rate, and difficulty controlling the homogeneity of the formed gel. The use of photocrosslinking has been shown to provide more uniform gelation as the entire hydrogel crosslinks simultaneously upon ultraviolet light exposure [8, 22, 33, 35, 36].

10.3.2.2

Cell Source

A major obstacle in tissue engineering articular cartilage is obtaining a sufficiently large, and phenotypically stable autologous cell population. Donor site morbidity makes a large cartilage harvest impractical and even dangerous. The low number of harvested chondrocytes creates the need for expansion culture in monolayer. Although chondrocytes maintain their phenotype better in three-dimensional culture their proliferation rates are much higher in monolayer. Monolayer culture causes chondrocytes to flatten, losing their rounded morphology and become more fibroblastic in nature. Three-dimensional culture following monolayer helps to re-differentiate the cells, however this process is relatively inefficient and the native phenotype is never fully restored. Quality and health of the harvested chondrocytes is also an issue of concern. Currently the mechanisms at play during chondrocyte differentiation and re-differentiation are not fully understood. Without this understanding the process will be difficult to control [22, 25, 32].

Using MSC populations on their own or mixed with autologous chondrocytes can reduce the need for the invasive harvest procedure, however the optimal conditions for chondrogenesis of a MSC are yet to be fully understood. Furthermore, bone marrow harvest of MSC populations is also an invasive procedure. The easiest place to harvest MSC is adipose tissue, where low donor site morbidity exists. However, MSCs derived from adipose tissue may be more difficult to differentiate into chondrocytes than those derived from bone marrow [17, 22, 25, 32].

10.3.3

Engineered Constructs in Clinical Trials and Early Applications

Many new products have entered clinical trials or are already commercially available. Most of these products seek to improve the traditional surgical treatment through tissue engineering strategies. The majority of these clinical trials and products are not yet available in the United States and statistics on their long-term success in humans do not yet exist [29].

10.3.3.1

Marrow Stimulation Techniques

A process called scaffold-guided microfracture uses a scaffold to help the bone marrow stay within the defect site following microfracture. The following products utilize this idea: BST-CarGel (Biosyntech Inc., Laval, Quebec, Canada), ChonDux (Biomet, Inc, Warsaw, Indiana), and Gelrin C (Regentis, Haifa, Israel). BST-CarGel is a biodegradable and injectable chitosan-glycerol phosphate based hydrogel. ChonDux is an injectable poly(ethylene glycol) hydrogel that contains an adhesive to stick to the defect site. Gelrin-C is a degradable and injectable copolymer of denatured fibrogen and poly(ethylene glycol) [29, 30].

10.3.3.2

Osteochondral Grafts

Scaffolds used in the place of tissue grafts can provide many benefits. Advantages include: biodegradability for new tissue to take its place, cost-effective, time-efficient, single procedure, no donor site morbidity, and the potential to include cell therapies. A drawback of using a substitute for a graft tissue, is of course, the lack of autologous, living tissue. Other potential complications include wear debris, inflammation, and friction between implanted material and tissue. Products developed for this use include: BST CarGel, Gelrin C, Salucartilage (Salumedica, Smyrna, GA), Chondromimetic (Ortho-mimetics, Cambridge, UK), TruFit Plug (OsteoBiologics/Smith & Nephew, Andover, MA), and OrthoGlide (Advanced Bio-Surfaces, Minnetonka, MN). SaluCartilage is another biodegradable and injectable hydrogel that solidifies *in vivo*. Chondromimetic is a dual-layer porous implant that has regions with properties similar to both subchondral bone and cartilage tissue. Tru-Fit and OrthoGlide are cylindrical-shaped polymers used for filling in circular drill holes where a defect site would lie [29].

10.3.3.3

Cell-Based Therapies

The matrix-induced autologous chondrocyte implantation is very similar to the traditional ACI procedure, with the addition of a degradable matrix to support the transplanted chondrocytes until they form their own matrix. This helps keep the transplanted cells in

the defect and provides much needed mechanical support. There is potential for growth factor incorporation to the scaffolds to aid in ECM production and retention of chondrocyte phenotype [29]. Developed products include: Carticel (Genzyme Inc, Cambridge, MA), ChondroGide (Geistlich Biomaterials, Wolhausen, Switzerland), CaRes (Anthro-Kinetics, Essingen, Germany), Hyalograft-C (Fidia Advanced Biopolymers, Abano Terma, Italy), and Neocart (Histogenics, Waltham, MA). Carticel and Chondrogide are porcine-derived type I and type II collagen matrices, CaRes is a type I collagen matrix, Hyalograft-C is a hyaluronic acid based scaffold, and Neocart is made of a bovine collagen matrix [22, 29, 37].

Fibrin based scaffolds are being developed on which minced harvested cartilage tissue is placed. The construct is then implanted into the defect site. A process called “neocartilage implantation” is also being developed during which harvested cells are grown in a scaffold in a dynamic culture system to produce and ECM. The ECM is then isolated and implanted into a cartilage defect [29]. Table 10.2 lists product information for commercially developed cartilage engineering products.

Table 10.2 Cartilage tissue engineering products developed for commercial use

Commercial products in cartilage tissue engineering		
Product name	Company	Website
BST-CarGel	Biosyntech Inc., Laval, Quebec, Canada	http://www.biosyntech.com
ChonDux	Biomet Inc., Warsaw, IN, USA	http://www.biomet.com
Gelrin C	Regentis, Haifa, Israel	http://www.regentis.co.il
Salucartilage	SaluMedica, Smyrna, GA, USA	http://www.salumedia.com
Chondromimetic	Orthomimetics, Cambridge, UK	http://www.orthomimetics.com
TrueFit Plug	OsteoBiologics/Smith & Nephew, Andover, MA, USA	http://www.global.smith-nephew.com
OrthoGlide	Advanced Biosurfaces, Minnetonka, MN, USA	http://www.advbiosurf.com
Carticel	Genzyme Inc, Cambridge, MA, USA	http://www.genzyme.com
ChondroGide	Geistlich Biomaterials, Wolhausen, Switzerland	http://www.geistlich.ch
CaRes	Anthro Kinetics, Essingen, Germany	http://www.arthro-kinetics.com
Hyalograft-C	Fidia Advanced Biopolymers, Abano Terma, Italy	http://www.fidiapharma.com
NeoCart, VeriCart	Histogenics, Waltham, MA, USA	http://www.histogenics.com

10.3.4

Current Research Efforts

The development of cartilage tissue engineering products has been the result of decades of research efforts that span many natural and synthetic scaffold materials. Although not all of these materials have developed into usable constructs this research has, and continues to, contribute to the current understanding and knowledge base within the field.

10.3.4.1

Natural Scaffolds

Some of the most popular natural scaffolds used in cartilage engineering research include alginate, fibrin, agarose, hyaluronic acid, chitosan, and type I and II collagens. Studies using alginate, collagens, and fibrin are highlighted due to their prevalence in the literature.

Early studies using alginate to encapsulate chondrocytes were performed in the late 1980s, these studies demonstrated retention of the chondrocyte phenotype and proliferation of chondrocytes seeded in three-dimensions [38]. Following studies have established that chondrocytes remain phenotypically active and proliferate within alginate, even up to even 8 months in culture [39–42]. Markers for phenotype retention include gene expression or biochemical presence of ECM components such as type II collagen, aggrecan, and GAGs. High gene expression of type I collagen indicates cells have started to differentiate to a more fibroblastic lineage. Alginate has been investigated for its potential in re-differentiating cells that have started down a fibroblastic lineage due to expansion in monolayer. Results show encapsulation in alginate can aid in re-differentiating cells to express higher levels of matrix proteins and lower levels of type I collagen following two-dimensional culture [40]. Despite maintaining a healthy chondrocyte population alginate's drawbacks include limited mechanical stability and biodegradation [43].

Studies using both type I and type II collagen matrices have also shown support of chondrocyte proliferation and maintenance of phenotype [44–46]. The incorporation of glycosaminoglycans, such as chondroitin sulfate, within the collagen scaffold have shown to further improve expression of matrix proteins [44, 46]. Additionally, mechanical loading of chondrocytes seeded on collagen scaffolds has been shown to alter cellular gene expression [45]. Collagen scaffolds are biodegradable, however they can be expensive and fairly difficult to produce.

Fibrin glue is made by mixing fibrinogen and thrombin to form a biodegradable, injectable material. It has been studied and classified for mixing with chondrocytes and injecting into cartilage defect sites. Animal trials with this method show significant wound healing and integration with native tissue [43]. Fibrin biodegradation can be tailored and it can be mixed with other polymers to improve its relatively weak mechanical strength. Various models of fibrin-alginate scaffolds have been show to support proliferation and the chondrocyte phenotype [47, 48].

10.3.4.2

Synthetic Scaffolds

Popular synthetically derived materials used in cartilage research include poly(glycolic acid) (PGA), poly(lactic acid) (PLA), poly(lactic-co-glycolic acid) (PLGA), poly(caprolactone) (PCL), and poly(ethylene glycol) (PEG). As a result of their prevalence in the literature, efforts using PGA and PEG will be covered in more detail.

PGA is an alpha polyester that degrades within months into products the body can readily absorb, making it biocompatible. As it degrades a loss of mechanical strength is observed, however in vitro culture and formation of ECM may strengthen its mechanical properties [49]. PGA scaffolds for cartilage engineering are usually made in the form of porous meshes that allow for nutrient and molecule transfer. Production of GAGs, aggrecan, and type II collagen are all observed in chondrocytes cultured in vitro for up to 40 days on PGA scaffolds [50, 51]. Porous PGA scaffolds seeded with bone marrow stromal cells and implanted subcutaneously into mice show formation of mature cartilage after 8 weeks [52]. PLA is another alpha polyester with similar mechanical and biological properties shown to support chondrocyte adherence and proliferation. A copolymer of PGA and PLA (PLGA), whose properties are similar and proportional to the proportion of each polymer, is also used in cartilage engineering efforts [49, 53].

PEG can be formed in to an injectable hydrogel with properties similar to native cartilage tissue. It is biocompatible, but not biodegradable on its own. Therefore, it must be copolymerized to achieve in vivo degradation. PEG-based polymers can be photopolymerized with addition of a photoinitiator. In this model the polymer and cell solution would be injected to the defect site as a liquid to fill the exact shape of the defect, the polymer would then be photocrosslinked forming a solid matrix. Copolymers of PEG and PLA as well as PEG and poly(vinyl alcohol) are biodegradable and promote chondrocyte adhesion and matrix molecule production [54–56]. Additionally, incorporation of matrix molecules such as chondroitin sulfate has been shown to increase mechanical properties as well as gene expression of matrix molecules [57]. Poly(ethylene oxide) (PEO), a higher molecular weight form of PEG, has also been photopolymerized into hydrogels for cartilage applications. PEO-based research shows that cells remain viable and produce significant levels of GAG and collagen in vitro during encapsulation in hydrogel scaffolds [58]. Copolymers with PEG have also shown favorable mechanical and biochemical properties and chondrocyte activity [59].

10.3.4.3

Growth Factors

Growth factors known to promote chondrocyte activity are often incorporated into scaffolds, or delivered to culture media to stimulate the cell population. Although many studies have investigated growth factor use, many of their effects – both alone and in combination – remain to be fully understood. The most prominent growth factors used in cartilage engineering studies include; insulin-like growth factor – I (IGF-I), basic fibroblast growth factor (bFGF), and transforming growth factor- β 1 (TGF- β 1) [5, 60–63]. All of these have demonstrated anabolic cellular effects and increased production of matrix molecules.

Although the effects of these factors are generally understood, the ideal combination of growth factors and delivery mechanism remains to be established.

10.4 Future Directions

Many advances have been made over the past few decades in understanding cartilage engineering, however major hurdles still exist within the field. Cell source, maintenance of the chondrocyte phenotype *in vitro*, and recreation of tissue with the structure and properties of native cartilage are today's major challenges. Research which address these challenges include zonal cartilage engineering, the use of stem cells, and utilization of dynamic *in vitro* culture systems. Together these fields are likely to have a major impact on cartilage regeneration in coming years.

10.4.1 Zonal Cartilage Engineering

Recreation of the zonal complexities present in native cartilage tissue has become a focus of many cartilage engineering efforts. Initial studies, and most currently available engineering solutions, attempt to remodel cartilage as a homogenous tissue. As the cellular and structural differences between cartilage zones are more fully understood, the need to recreate this complex tissue architecture is becoming more apparent. Articular cartilage is intricately organized and heterogeneous. It is unlikely that a homogenous tissue, based on a homogenous scaffold, can functionally replace this structure. Furthermore, it is likely that through formation of zonal organization there will be better integration with host tissue, and a more fluid transmission of stress between native and novel cartilage. Depth dependent variations in scaffold design (pore size, porosity, mechanical properties, and addition of growth factors, etc.) and the origin of the seeded cells (super zone, middle zone, or deep zone) can be used as tools in designing zonal scaffolds [33, 64].

While there is no current model for regenerating zonally organized tissue *in vitro*, several studies have attempted to establish the difference in phenotype between zonal cell populations and create culture systems which more closely mimic the native environment. These studies are paving the way for biomaterials which will help to restore defects in a zone-specific manner. For example, research has shown the shear modulus to vary by up two orders of magnitude through the depth of a single articular cartilage sample [65]. Additionally, studies show differences in matrix deposition, morphology, and gene expression between cultured populations isolated from distinct cartilage zones [66, 67]. Further studies have developed layered culture systems based on materials such as PEG, PEO, agarose, and alginate [15, 68–70]. These studies show both depth-dependent mechanical properties of the scaffolds and changes in metabolic activity of subpopulations cultured in layers [15, 71]. The continuation of such studies and the development of zonally-engineered cartilage tissue could potentially be very influential the next generation of cartilage repair solutions.

10.4.2

Stem Cells

A major challenge in cartilage engineering is obtaining a sufficiently large chondrocyte population to seed onto the scaffold material. Both maintaining the chondrocyte phenotype during culture and injury at the harvest site are significant challenges in this approach. An alternative to autologous chondrocytes harvest is the use of MSCs. MSC use also has significant challenges that are yet to be met. Harvesting the MSC population is the first challenge. The most classified and understood MSC population lies in bone marrow. However, bone marrow harvest is both painful and a potentially risky procedure. Adipose tissue also contains a MSC population and is much easier to harvest, however it is more challenging to induce chondrogenesis in adipose-derived MSCs. Other tissues with MSC populations include the synovial membrane, muscle, periostium, and umbilical cord [22, 72]. Once harvested, the next major challenge is inducing chondrogenesis in the stem cells. Various growth factors have been identified and studied for inducing the chondrocyte phenotype, however an ideal growth factor or combination is yet to be discovered. Furthermore, *in vitro* culture often leads to production of fibro-cartilage features and hypertrophy in the stem cell population [22, 72]. Current animal and human models that have used MSCs for cartilage repair have shown mixed results, often plagued by fibro-cartilage formation [17, 72, 73].

A biomaterial and proper incorporation or delivery of growth factors is needed which successfully differentiates MSCs into healthy articular chondrocytes. Several attempts to design such scaffold have been met with preliminary success. PEG based hydrogels with decorin moieties are reported to promote *in vitro* chondrogenesis of MSCs, marked by deposition of ECM components such as type II collagen and aggrecan [74]. Additionally, PEO based hydrogels with hyaluronic acid and TGF- β 3 are reported to induce chondrogenesis of MSC in *in vivo* animal models [75]. The future of MSCs in cartilage engineering will rely on development of a practical harvest method and production of a reliable chondrocyte phenotype. Eliminating the need for harmful autologous chondrocyte harvests will be a significant advance for cell-based cartilage engineering strategies.

Embryonic stem cells for cartilage engineering have recently received considerable attention, and may hold promise for the future. These cells have the advantage of large cell source numbers and the ability to proliferate significantly. Their drawbacks include potential immune response, and differentiation challenges [73]. Animal models show varying reports of success depending on where the embryonic stem cells are injected. Mouse models show chondral defects treated with undifferentiated embryonic stem cells result in the formations of teratomas. However, embryonic stem cells injected to osteochondral defects in the same animal model show restoration of healthy tissue [76, 77]. Control of the differentiation process to form functional chondrocytes is essential to establish for the use of embryonic stem cells. Studies report chondrogenesis of embryonic stem cells through the use of growth factors such as bone morphogenic proteins, transforming growth factor- β 1, and insulin-like growth factor-1 [78–80]. Additional studies have investigated the differentiation of embryonic stem cells to mesenchymal-

10 like stem cells and have reported success [81, 82]. The ability of these cells to undergo chondrogenesis has been studied using a modified PEG-based hydrogel. Results indicate promise for the use of embryonic stem cells in cartilage tissue engineering [82]. While these studies indicate great potential for chondrogenesis of embryonic stem cells, research in this field has yet to establish precise cellular mechanisms at work during this process.

Induced pluripotent stem cells may also hold promise for cartilage regeneration. Advantages of induced pluripotent stem cell use include production of an autologous cell population and elimination of harmful cartilage or bone marrow harvests [83]. However, there is limited research investigating the chondrogenic potential of these cells. Use of induced pluripotent stem cells in cartilage engineering will require research efforts to clearly establish differentiation parameters.

10.4.3

Dynamic Culture Systems

Healthy loading is essential for the maintenance of cartilage in the body. To understand the important relationship between loading and chondrocyte metabolism many studies have investigated the effects of both static and cyclic loading on chondrocyte activity. Reports show mixed inhibitory and stimulative effects depending on load magnitude, size, and which zone the chondrocytes originated from [84–86]. To create a culture system which mimics the dynamic *in vivo* environment many groups have designed bioreactor systems. Culturing engineered cartilage scaffolds in dynamic bioreactor systems is not the current standard, but this model holds great promise for maintaining healthier, and more phenotypically stable cell populations *in vitro*.

Results from bioreactor studies show increases in production of ECM molecules, cell proliferation, and mechanical properties [87, 88]. For example, PGA scaffolds in a perfusion system showed increases in both DNA and GAG content compared to controls [89]. Chondrocytes in PEG-based hydrogels exposed to dynamic laminar fluid flow showed increased levels of GAG and collagen production and better mechanical properties compared to controls [90, 91]. Studies have also added growth factors to dynamic culture conditions and observed even more favorable outcomes [60, 62]. The ideal combination of scaffold material, growth factors, and dynamic culture system are yet to be established for *in vitro* culture. Understanding how these factors work together to affect the chondrocyte phenotype is essential for the success of cartilage engineering strategies. Successful three-dimensional scaffold culture will create a plethora of stable chondrocytes producing ECM that can then be transplanted into cartilage defects. Current research strategies need to establish these culture conditions for practical implementation of engineering solutions.

Acknowledgements This work was supported by the National Science Foundation (CAREER Award to John P. Fisher #0448684), Arthritis Foundation (Arthritis Investigator Award to John P. Fisher), and the State of Maryland, Maryland Stem Cell Research Fund.

References

1. McDevitt, C.A., *Biochemistry of articular cartilage. Nature of proteoglycans and collagen of articular cartilage and their role in ageing and in osteoarthritis*. Ann Rheum Dis, 1973. **32** (4): p. 364–78.
2. Ulrich-Vinther, M., et al., *Articular cartilage biology*. J Am Acad Orthop Surg, 2003. **11**(6): p. 421–30.
3. Mollenhauer, J.A., *Perspectives on articular cartilage biology and osteoarthritis*. Injury, 2008. **39**(Suppl 1): p. S5–12.
4. Kuettner, K.E., *Biochemistry of articular cartilage in health and disease*. Clin Biochem, 1992. **25**(3): p. 155–63.
5. Yoon, D.M. and J.P. Fisher, *Chondrocyte signaling and artificial matrices for articular cartilage engineering*. Adv Exp Med Biol, 2006. **585**: p. 67–86.
6. Archer, C.W. and P. Francis-West, *The chondrocyte*. Int J Biochem Cell Biol, 2003. **35**(4): p. 401–4.
7. Lin, Z., et al., *The chondrocyte: biology and clinical application*. Tissue Eng, 2006. **12**(7): p. 1971–84.
8. Elisseeff, J.H., et al., *Biological response of chondrocytes to hydrogels*. Ann N Y Acad Sci, 2002. **961**: p. 118–22.
9. Wong, M., et al., *Zone-specific cell biosynthetic activity in mature bovine articular cartilage: a new method using confocal microscopic stereology and quantitative autoradiography*. J Orthop Res, 1996. **14**(3): p. 424–32.
10. Jiang, J., et al., *Interaction between zonal populations of articular chondrocytes suppresses chondrocyte mineralization and this process is mediated by PTHrP*. Osteoarthritis Cartilage, 2008. **16**(1): p. 70–82.
11. Aydelotte, M.B., R.R. Greenhill, and K.E. Kuettner, *Differences between sub-populations of cultured bovine articular chondrocytes. II. Proteoglycan metabolism*. Connect Tissue Res, 1988. **18**(3): p. 223–34.
12. Aydelotte, M.B. and K.E. Kuettner, *Differences between sub-populations of cultured bovine articular chondrocytes. I. Morphology and cartilage matrix production*. Connect Tissue Res, 1988. **18**(3): p. 205–22.
13. Huber, M., S. Trattng, and F. Lintner, *Anatomy, biochemistry, and physiology of articular cartilage*. Invest Radiol, 2000. **35**(10): p. 573–80.
14. Khalafi, A., et al., *Increased accumulation of superficial zone protein (SZP) in articular cartilage in response to bone morphogenetic protein-7 and growth factors*. J Orthop Res, 2007. **25**(3): p. 293–303.
15. Kim, T.K., et al., *Experimental model for cartilage tissue engineering to regenerate the zonal organization of articular cartilage*. Osteoarthritis Cartilage, 2003. **11**(9): p. 653–64.
16. Lu, X.L. and V.C. Mow, *Biomechanics of articular cartilage and determination of material properties*. Med Sci Sports Exerc, 2008. **40**(2): p. 193–9.
17. Chen, F.H., K.T. Rousche, and R.S. Tuan, *Technology insight: adult stem cells in cartilage regeneration and tissue engineering*. Nat Clin Pract Rheumatol, 2006. **2**(7): p. 373–82.
18. Abramson, S.B. and M. Attur, *Developments in the scientific understanding of osteoarthritis*. Arthritis Res Ther, 2009. **11**(3): p. 227.
19. Cancedda, R., et al., *Tissue engineering and cell therapy of cartilage and bone*. Matrix Biol, 2003. **22**(1): p. 81–91.
20. Bliddal, H. and R. Christensen, *The treatment and prevention of knee osteoarthritis: a tool for clinical decision-making*. Expert Opin Pharmacother, 2009. **10**(11): p. 1793–804.

21. Borrelli, J., Jr. and W.M. Ricci, *Acute effects of cartilage impact*. Clin Orthop Relat Res, 2004. (423): p. 33–9.
22. Vinatier, C., et al., *Cartilage tissue engineering: towards a biomaterial-assisted mesenchymal stem cell therapy*. Curr Stem Cell Res Ther, 2009. **4**(4): p. 318–29.
23. Jackson, D.W., T.M. Simon, and H.M. Aberman, *Symptomatic articular cartilage degeneration: the impact in the new millennium*. Clin Orthop Relat Res, 2001. (391 Suppl): p. S14–25.
24. Lawrence, R.C., et al., *Estimates of the prevalence of arthritis and other rheumatic conditions in the United States. Part II*. Arthritis Rheum, 2008. **58**(1): p. 26–35.
25. Clouet, J., et al., *From osteoarthritis treatments to future regenerative therapies for cartilage*. Drug Discov Today, 2009. **14**(19–20): p. 913–25.
26. Hepper, C.T., et al., *The efficacy and duration of intra-articular corticosteroid injection for knee osteoarthritis: a systematic review of level I studies*. J Am Acad Orthop Surg, 2009. **17** (10): p. 638–46.
27. Rainsford, K.D., *Importance of pharmaceutical composition and evidence from clinical trials and pharmacological studies in determining effectiveness of chondroitin sulphate and other glycosaminoglycans: a critique*. J Pharm Pharmacol, 2009. **61**(10): p. 1263–70.
28. Martinez de Aragon, J.S., et al., *Early outcomes of pyrolytic carbon hemiarthroplasty for the treatment of trapezial-metacarpal arthritis*. J Hand Surg Am, 2009. **34**(2): p. 205–12.
29. Clair, B.L., A.R. Johnson, and T. Howard, *Cartilage repair: current and emerging options in treatment*. Foot Ankle Spec, 2009. **2**(4): p. 179–88.
30. Richter, W., *Mesenchymal stem cells and cartilage in situ regeneration*. J Intern Med, 2009. **266**(4): p. 390–405.
31. Torun Kose, G. and V. Hasirci, *Cartilage tissue engineering*. Adv Exp Med Biol, 2004. **553**: p. 317–29.
32. Pelttari, K., A. Wixmerten, and I. Martin, *Do we really need cartilage tissue engineering?* Swiss Med Wkly, 2009. **139**(41–42): p. 602–9.
33. Sharma, B. and J.H. Elisseeff, *Engineering structurally organized cartilage and bone tissues*. Ann Biomed Eng, 2004. **32**(1): p. 148–59.
34. Stoop, R., *Smart biomaterials for tissue engineering of cartilage*. Injury, 2008. **39**(Suppl 1): p. S77–87.
35. Randolph, M.A., K. Anseth, and M.J. Yaremchuk, *Tissue engineering of cartilage*. Clin Plast Surg, 2003. **30**(4): p. 519–37.
36. Elisseeff, J., *Hydrogels: structure starts to gel*. Nat Mater, 2008. **7**(4): p. 271–3.
37. Kreuz, P.C., et al., *Treatment of focal degenerative cartilage defects with polymer-based autologous chondrocyte grafts: four-year clinical results*. Arthritis Res Ther, 2009. **11**(2): p. R33.
38. Guo, J.F., G.W. Jourdian, and D.K. MacCallum, *Culture and growth characteristics of chondrocytes encapsulated in alginate beads*. Connect Tissue Res, 1989. **19**(2–4): p. 277–97.
39. Hauselmann, H.J., et al., *Phenotypic stability of bovine articular chondrocytes after long-term culture in alginate beads*. J Cell Sci, 1994. **107**(Pt 1): p. 17–27.
40. Murphy, C.L. and A. Sambanis, *Effect of oxygen tension and alginate encapsulation on restoration of the differentiated phenotype of passaged chondrocytes*. Tissue Eng, 2001. **7**(6): p. 791–803.
41. Yoon, D.M., et al., *Effect of construct properties on encapsulated chondrocyte expression of insulin-like growth factor-1*. Biomaterials, 2007. **28**(2): p. 299–306.
42. Yoon, D.M., et al., *Addition of hyaluronic acid to alginate embedded chondrocytes interferes with insulin-like growth factor-1 signaling in vitro and in vivo*. Tissue Eng Part A, 2009. **15** (11): p. 3449–59.
43. Peretti, G.M., et al., *Review of injectable cartilage engineering using fibrin gel in mice and swine models*. Tissue Eng, 2006. **12**(5): p. 1151–68.

44. Lee, C.R., et al., *Articular cartilage chondrocytes in type I and type II collagen-GAG matrices exhibit contractile behavior in vitro*. *Tissue Eng*, 2000. **6**(5): p. 555–65.
45. Hunter, C.J., et al., *Mechanical compression alters gene expression and extracellular matrix synthesis by chondrocytes cultured in collagen I gels*. *Biomaterials*, 2002. **23**(4): p. 1249–59.
46. van Susanto, J.L.C., et al., *Linkage of chondroitin-sulfate to type I collagen scaffolds stimulates the bioactivity of seeded chondrocytes in vitro*. *Biomaterials*, 2001. **22**(17): p. 2359–69.
47. Perka, C., et al., *The use of fibrin beads for tissue engineering and subsequential transplantation*. *Tissue Eng*, 2001. **7**(3): p. 359–61.
48. Almqvist, K.F., et al., *Culture of chondrocytes in alginate surrounded by fibrin gel: characteristics of the cells over a period of eight weeks*. *Ann Rheum Dis*, 2001. **60**(8): p. 781–90.
49. Middleton, J.C. and A.J. Tipton, *Synthetic biodegradable polymers as orthopedic devices*. *Biomaterials*, 2000. **21**(23): p. 2335–46.
50. Grande, D.A., et al., *Evaluation of matrix scaffolds for tissue engineering of articular cartilage grafts*. *J Biomed Mater Res*, 1997. **34**(2): p. 211–20.
51. Freed, L.E., et al., *Chondrogenesis in a cell-polymer-bioreactor system*. *Exp Cell Res*, 1998. **240**(1): p. 58–65.
52. Zhu, L., et al., *Engineered cartilage with internal porous high-density polyethylene support from bone marrow stromal cells: a preliminary study in nude mice*. *Br J Oral Maxillofac Surg*, 2010. **48**(6): p. 462–5.
53. Ishaug-Riley, S.L., et al., *Human articular chondrocyte adhesion and proliferation on synthetic biodegradable polymer films*. *Biomaterials*, 1999. **20**(23–24): p. 2245–56.
54. Bryant, S.J., et al., *Encapsulating chondrocytes in degrading PEG hydrogels with high modulus: engineering gel structural changes to facilitate cartilaginous tissue production*. *Biotechnol Bioeng*, 2004. **86**(7): p. 747–55.
55. Martens, P.J., S.J. Bryant, and K.S. Anseth, *Tailoring the degradation of hydrogels formed from multivinyl poly(ethylene glycol) and poly(vinyl alcohol) macromers for cartilage tissue engineering*. *Biomacromolecules*, 2003. **4**(2): p. 283–92.
56. Rice, M.A. and K.S. Anseth, *Encapsulating chondrocytes in copolymer gels: bimodal degradation kinetics influence cell phenotype and extracellular matrix development*. *J Biomed Mater Res A*, 2004. **70**(4): p. 560–8.
57. Bryant, S.J., J.A. Arthur, and K.S. Anseth, *Incorporation of tissue-specific molecules alters chondrocyte metabolism and gene expression in photocrosslinked hydrogels*. *Acta Biomater*, 2005. **1**(2): p. 243–52.
58. Bryant, S.J. and K.S. Anseth, *The effects of scaffold thickness on tissue engineered cartilage in photocrosslinked poly(ethylene oxide) hydrogels*. *Biomaterials*, 2001. **22**(6): p. 619–26.
59. Elisseff, J., et al., *Photoencapsulation of chondrocytes in poly(ethylene oxide)-based semi-interpenetrating networks*. *J Biomed Mater Res*, 2000. **51**(2): p. 164–71.
60. Gooch, K.J., et al., *IGF-I and mechanical environment interact to modulate engineered cartilage development*. *Biochem Biophys Res Commun*, 2001. **286**(5): p. 909–15.
61. Darling, E.M. and K.A. Athanasiou, *Growth factor impact on articular cartilage subpopulations*. *Cell Tissue Res*, 2005. **322**(3): p. 463–73.
62. Koay, E.J., G. Ofek, and K.A. Athanasiou, *Effects of TGF-beta1 and IGF-I on the compressibility, biomechanics, and strain-dependent recovery behavior of single chondrocytes*. *J Biomech*, 2008. **41**(5): p. 1044–52.
63. Yoon, D.M. and J.P. Fisher, *Effects of exogenous IGF-I delivery on the early expression of IGF-I signaling molecules by alginate embedded chondrocytes*. *Tissue Eng Part A*, 2008. **14**(7): p. 1263–73.
64. Klein, T.J., et al., *Tissue engineering of articular cartilage with biomimetic zones*. *Tissue Eng Part B Rev*, 2009. **15**(2): p. 143–57.
65. Buckley, M.R., et al., *Mapping the depth dependence of shear properties in articular cartilage*. *J Biomech*, 2008. **41**(11): p. 2430–7.

66. Hidaka, C., et al., *Maturation differences in superficial and deep zone articular chondrocytes*. *Cell Tissue Res*, 2006. **323**(1): p. 127–35.
67. Siczkowski, M. and F.M. Watt, *Subpopulations of chondrocytes from different zones of pig articular cartilage. Isolation, growth and proteoglycan synthesis in culture*. *J Cell Sci*, 1990. **97**(Pt 2): p. 349–60.
68. Ng, K.W., et al., *A layered agarose approach to fabricate depth-dependent inhomogeneity in chondrocyte-seeded constructs*. *J Orthop Res*, 2005. **23**(1): p. 134–41.
69. Sharma, B., et al., *Designing zonal organization into tissue-engineered cartilage*. *Tissue Eng*, 2007. **13**(2): p. 405–14.
70. Gleghorn, J.P., et al., *Adhesive properties of laminated alginate gels for tissue engineering of layered structures*. *J Biomed Mater Res A*, 2008. **85**(3): p. 611–8.
71. Ng, K.W., G.A. Ateshian, and C.T. Hung, *Zonal chondrocytes seeded in a layered agarose hydrogel create engineered cartilage with depth-dependent cellular and mechanical inhomogeneity*. *Tissue Eng Part A*, 2009. **15**(9): p. 2315–24.
72. Pelttari, K., E. Steck, and W. Richter, *The use of mesenchymal stem cells for chondrogenesis*. *Injury*, 2008. **39**(Suppl 1): p. S58–65.
73. Hwang, N.S. and J. Elisseeff, *Application of stem cells for articular cartilage regeneration*. *J Knee Surg*, 2009. **22**(1): p. 60–71.
74. Salinas, C.N. and K.S. Anseth, *Decorin moieties tethered into PEG networks induce chondrogenesis of human mesenchymal stem cells*. *J Biomed Mater Res A*, 2009. **90**(2): p. 456–64.
75. Sharma, B., et al., *In vivo chondrogenesis of mesenchymal stem cells in a photopolymerized hydrogel*. *Plast Reconstr Surg*, 2007. **119**(1): p. 112–20.
76. Wakitani, S., et al., *Embryonic stem cells injected into the mouse knee joint form teratomas and subsequently destroy the joint*. *Rheumatology (Oxford)*, 2003. **42**(1): p. 162–5.
77. Wakitani, S., et al., *Embryonic stem cells form articular cartilage, not teratomas, in osteochondral defects of rat joints*. *Cell Transplant*, 2004. **13**(4): p. 331–6.
78. Kramer, J., et al., *Embryonic stem cell-derived chondrogenic differentiation in vitro: activation by BMP-2 and BMP-4*. *Mech Dev*, 2000. **92**(2): p. 193–205.
79. Koay, E.J., G.M. Hoben, and K.A. Athanasiou, *Tissue engineering with chondrogenically differentiated human embryonic stem cells*. *Stem Cells*, 2007. **25**(9): p. 2183–90.
80. Nakayama, N., et al., *Macroscopic cartilage formation with embryonic stem-cell-derived mesodermal progenitor cells*. *J Cell Sci*, 2003. **116**(Pt 10): p. 2015–28.
81. Olivier, E.N., A.C. Rybicki, and E.E. Bouhassira, *Differentiation of human embryonic stem cells into bipotent mesenchymal stem cells*. *Stem Cells*, 2006. **24**(8): p. 1914–22.
82. Hwang, N.S., et al., *Chondrogenic differentiation of human embryonic stem cell-derived cells in arginine-glycine-aspartate-modified hydrogels*. *Tissue Eng*, 2006. **12**(9): p. 2695–706.
83. Takahashi, K. and S. Yamanaka, *Induction of pluripotent stem cells from mouse embryonic and adult fibroblast cultures by defined factors*. *Cell*, 2006. **126**(4): p. 663–76.
84. Lee, D.A., et al., *Response of chondrocyte subpopulations cultured within unloaded and loaded agarose*. *J Orthop Res*, 1998. **16**(6): p. 726–33.
85. Vanderploeg, E.J., C.G. Wilson, and M.E. Levenston, *Articular chondrocytes derived from distinct tissue zones differentially respond to in vitro oscillatory tensile loading*. *Osteoarthritis Cartilage*, 2008. **16**(10): p. 1228–36.
86. Lane Smith, R., et al., *Effects of shear stress on articular chondrocyte metabolism*. *Biorheology*, 2000. **37**(1–2): p. 95–107.
87. Li, Z., et al., *Different response of articular chondrocyte subpopulations to surface motion*. *Osteoarthritis Cartilage*, 2007. **15**(9): p. 1034–41.
88. Preiss-Bloom, O., et al., *Real-time monitoring of force response measured in mechanically stimulated tissue-engineered cartilage*. *Artif Organs*, 2009. **33**(4): p. 318–27.
89. Davissou, T., R.L. Sah, and A. Ratcliffe, *Perfusion increases cell content and matrix synthesis in chondrocyte three-dimensional cultures*. *Tissue Eng*, 2002. **8**(5): p. 807–16.

90. Vunjak-Novakovic, G., et al., *Bioreactor cultivation conditions modulate the composition and mechanical properties of tissue-engineered cartilage*. J Orthop Res, 1999. **17**(1): p. 130–8.
91. Cooper, J.A., Jr., et al., *Encapsulated chondrocyte response in a pulsatile flow bioreactor*. Acta Biomater, 2007. **3**(1): p. 13–21.
92. Lee, C.R., et al., *Fibrin-polyurethane composites for articular cartilage tissue engineering: a preliminary analysis*. Tissue Eng, 2005. **11**(9–10): p. 1562–73.
93. Zeltinger, J., et al., *Effect of pore size and void fraction on cellular adhesion, proliferation, and matrix deposition*. Tissue Eng, 2001. **7**(5): p. 557–72.
94. Erggelet, C., et al., *Regeneration of ovine articular cartilage defects by cell-free polymer-based implants*. Biomaterials, 2007. **28**(36): p. 5570–80.
95. Wang, D.A., et al., *Multifunctional chondroitin sulphate for cartilage tissue-biomaterial integration*. Nat Mater, 2007. **6**(5): p. 385–92.
96. Mercier, N.R., et al., *Poly(lactide-co-glycolide) microspheres as a moldable scaffold for cartilage tissue engineering*. Biomaterials, 2005. **26**(14): p. 1945–52.
97. Silva, S.S., et al., *Novel genipin-cross-linked chitosan/silk fibroin sponges for cartilage engineering strategies*. Biomacromolecules, 2008. **9**(10): p. 2764–74.
98. Gellynck, K., et al., *Silkworm and spider silk scaffolds for chondrocyte support*. J Mater Sci Mater Med, 2008. **19**(11): p. 3399–409.
99. Wang, Y., et al., *Cartilage tissue engineering with silk scaffolds and human articular chondrocytes*. Biomaterials, 2006. **27**(25): p. 4434–42.
100. Ito, Y., et al., *Transplantation of tissue-engineered osteochondral plug using cultured chondrocytes and interconnected porous calcium hydroxyapatite ceramic cylindrical plugs to treat osteochondral defects in a rabbit model*. Artif Organs, 2008. **32**(1): p. 36–44.
101. Wiegandt, K., et al., *In vitro generation of cartilage-carrier-constructs on hydroxylapatite ceramics with different surface structures*. Open Biomed Eng J, 2008. **2**: p. 64–70.
102. Hao, T., et al., *The support of matrix accumulation and the promotion of sheep articular cartilage defects repair in vivo by chitosan hydrogels*. Osteoarthritis Cartilage, 2010. **18**(2): p. 257–65.
103. Park, K.M., et al., *Thermosensitive chitosan-Pluronic hydrogel as an injectable cell delivery carrier for cartilage regeneration*. Acta Biomater, 2009. **5**(6): p. 1956–65.
104. Lee, H. and T.G. Park, *Photo-crosslinkable, biomimetic, and thermo-sensitive pluronic grafted hyaluronic acid copolymers for injectable delivery of chondrocytes*. J Biomed Mater Res A, 2009. **88**(3): p. 797–806.
105. Vinatier, C., et al., *An injectable cellulose-based hydrogel for the transfer of autologous nasal chondrocytes in articular cartilage defects*. Biotechnol Bioeng, 2009. **102**(4): p. 1259–67.
106. Deng, Y., et al., *Poly(hydroxybutyrate-co-hydroxyhexanoate) promoted production of extracellular matrix of articular cartilage chondrocytes in vitro*. Biomaterials, 2003. **24**(23): p. 4273–81.
107. Wang, Y., et al., *Evaluation of three-dimensional scaffolds prepared from poly(3-hydroxybutyrate-co-3-hydroxyhexanoate) for growth of allogeneic chondrocytes for cartilage repair in rabbits*. Biomaterials, 2008. **29**(19): p. 2858–68.
108. Hu, X., et al., *Gelatin hydrogel prepared by photo-initiated polymerization and loaded with TGF-beta1 for cartilage tissue engineering*. Macromol Biosci, 2009. **9**(12): p. 1194–201.
109. Barbucci, R., et al., *Proliferative and re-differentiative effects of photo-immobilized micro-patterned hyaluronan surfaces on chondrocyte cells*. Biomaterials, 2005. **26**(36): p. 7596–605.
110. Jian-Wei, X., et al., *Producing a flexible tissue-engineered cartilage framework using expanded polytetrafluoroethylene membrane as a pseudoperichondrium*. Plast Reconstr Surg, 2005. **116**(2): p. 577–89.
111. Jeong, C.G. and S.J. Hollister, *Mechanical, permeability, and degradation properties of 3D designed poly(1,8 octanediol-co-citrate) scaffolds for soft tissue engineering*. J Biomed Mater Res B Appl Biomater, 2010. **93**(1): p. 141–9.

- 10
112. Kang, Y., et al., *A new biodegradable polyester elastomer for cartilage tissue engineering*. J Biomed Mater Res A, 2006. **77**(2): p. 331–9.
 113. Li, W.J., et al., *Evaluation of articular cartilage repair using biodegradable nanofibrous scaffolds in a swine model: a pilot study*. J Tissue Eng Regen Med, 2009. **3**(1): p. 1–10.
 114. Thorvaldsson, A., et al., *Electrospinning of highly porous scaffolds for cartilage regeneration*. Biomacromolecules, 2008. **9**(3): p. 1044–9.
 115. Mahmood, T.A., et al., *Tissue engineering of bovine articular cartilage within porous poly (ether ester) copolymer scaffolds with different structures*. Tissue Eng, 2005. **11**(7–8): p. 1244–53.
 116. Brittberg, M., et al., *Rabbit articular cartilage defects treated with autologous cultured chondrocytes*. Clin Orthop Relat Res, 1996. (326): p. 270–83.
 117. Curtin, W., et al., *The chondrogenic potential of carbon fiber and carbon fiber periosteum implants: an ultrastructural study in the rabbit*. Osteoarthritis Cartilage, 1994. **2**(4): p. 253–8.
 118. Petersen, J.P., et al., *Long term results after implantation of tissue engineered cartilage for the treatment of osteochondral lesions in a minipig model*. J Mater Sci Mater Med, 2008. **19**(5): p. 2029–38.
 119. Hutcheon, G.A., S. Downes, and M.C. Davies, *Interactions of chondrocytes with methacrylate copolymers*. J Mater Sci Mater Med, 1998. **9**(12): p. 815–8.
 120. Barry, J.J., et al., *Porous methacrylate scaffolds: supercritical fluid fabrication and in vitro chondrocyte responses*. Biomaterials, 2004. **25**(17): p. 3559–68.

Contents

11.1	Introduction	308
11.2	Tissue Overview and Requirements	309
11.2.1	Physiology and Mechanical Properties	309
11.2.2	Structure	311
11.2.3	Interfaces with Other Orthopaedic Tissues	315
11.2.4	Injury and Repair	317
11.3	Current Techniques for Reconstruction and Tissue Engineering	318
11.3.1	Current Surgical Management and Reconstruction of Tendons and Ligaments	318
11.3.2	Biomaterials for Tissue Engineering of Tendons and Ligaments	319
11.4	Conclusions and Future Work	329
	References	331

Abstract Ligaments and tendons play an important role in mediating normal movement and stability of joints in the musculoskeletal system, and their inability to undergo endogenous repair following injury leads to significant joint instability, injury of other tissues, and the development of degenerative joint disease. To restore their normal structure and function and address these clinical challenges, biomaterial scaffolds are being developed that incorporate cellular, morphogenetic, and mechanical cues into defined architectures that may be implanted as part of regenerative medicine therapies. This chapter explores the field of biomaterials for regeneration of tendons and ligaments with an emphasis on: (1) native tissue structure, function, mechanical properties, and interfaces with other orthopaedic tissues; (2) mechanisms of injury, healing responses, and limitations of current clinical approaches for repair; and (3) contemporary biomaterials-based approaches for tissue engineering of tendons and ligaments, including cell types used, design strategies, and results of their application in vitro and in vivo. Several challenges remain in achieving a successful biomaterial for tendon/ligament regeneration, yet significant design and

J.S. Temenoff (✉)

Wallace H. Coulter Department of Biomedical Engineering, Georgia Institute of Technology, Emory University School of Medicine, 313 Ferst Drive, Atlanta, GA 30332, USA
e-mail: johnna.temenoff@bme.gatech.edu

engineering improvements have continued to enhance their functional sophistication and hold much promise for future tissue engineering strategies.

Keywords Biomaterials • Ligament • Tendon • Tissue engineering

11.1 Introduction

Ligaments and tendons are dense bands of parallel fibers of connective tissue that play an important role in mediating normal movement and stability of joints in the musculoskeletal system. Injury to these structures is relatively common, requiring medical attention for over 800,000 people per year [1], and can cause significant joint instability that could lead to injury of other tissues and the development of degenerative joint disease [2]. Due to their avascularity and low cellularity, injured tendons and ligaments undergo a sub-optimal healing response that is unable to adequately regenerate normal tissue function and mechanical properties [1–4]. The development of a plethora of suturing techniques and the employment of grafted tissue have enjoyed limited success in repairing injured tendons and ligaments, often resulting in poor healing, significant donor site morbidity, and insufficient mechanical properties that may lead to graft failure [1, 3–5]. For these reasons, considerable efforts have been aimed at the design and implementation of novel biomaterials for tendon and ligament tissue engineering. Tissue engineering is an interdisciplinary approach that often combines biomaterial scaffolds with cells, growth factors or other biological stimuli to regenerate damaged or lost tissue [6, 7].

In working to heal injured tissues and restore joints to their normal function, understanding normal tendon and ligament biochemistry and physiological attributes is vital. Tendon and ligament structure is complex and serves to determine the mechanical function of the tissue. A complete knowledge of tendon/ligament biochemical composition, micro- and macro-architecture, and the interplay between structure and mechanical properties will aid in generating design parameters and evaluation criteria for novel biomaterials used in tendon/ligament tissue engineering. Successful biomaterials for use as tendon or ligament replacements should possess similar structural and mechanical properties to native tissue, allowing the tissue to function normally under various loading regimes and avoid mechanical failure.

Additionally, the success of biomaterials used for tendon/ligament tissue engineering relies on familiarity with normal processes of injury and healing. Multiple factors influence tendon/ligament injury and repair, including location of the injury within the tissue and in the joint capsule, size, and blood supply of oxygen and nutrients. Together, these variables may necessitate a variety of tissue engineering approaches. This requires an integral understanding of tendon and ligament healing mechanisms in response to different injuries. Such factors must also be carefully considered in the context of biocompatibility, integration, and degradation of the biomaterials applied.

This chapter will begin with an overview of tendon and ligament biochemical composition and architecture, with emphasis on their relationships with mechanical properties and integration with adjacent tissues in the joint. It will address mechanisms of injury, associated healing responses, and current reconstruction techniques with their associated limitations. This will provide context for addressing successes and limitations of contemporary biomaterials-based approaches for tissue engineering of tendons and ligaments. This chapter will review cell types used, current design strategies, and results of *in vitro* and *in vivo* applications for tendon/ligament biomaterials. It will conclude with remaining challenges and new frontiers in biomaterials for tendon and ligament tissue engineering.

11.2 Tissue Overview and Requirements

Current and future tissue engineering and regenerative medicine approaches to address tendon/ligament injury rely heavily on knowledge regarding structure-function relationships of these tissues. This section will review the macroscopic and microscopic architecture, cellular composition, and mechanical properties of tendons and ligaments and briefly examine their injury and repair.

11.2.1 Physiology and Mechanical Properties

Understanding how tendon and ligament tissue are structured and mechanically loaded is central to designing and engineering tendon/ligament tissue. Proper function of replacement tissue relies on recapitulating the mechanical strength of tendon/ligament tissue, which is derived from its intricate structure (see Sect. 11.2.2). A thorough understanding of this structure-function relationship is important when determining the design parameters for tissue engineering.

Tendons and ligaments share very similar biochemical compositions and structural characteristics, yet they have different functions. Tendons serve as an intermediate connecting muscle to bone, transmitting muscle generated loads and thereby enabling movement of a musculoskeletal joint through muscle contraction and relaxation [8]. Tendons are designed to withstand large tensile loads imparted by the musculoskeletal components that they join together. Typically these forces are generated during active motion in a direction along the long axis of the tendon. In the case of the Achilles tendon that joins the muscles of the calf with the calcaneus (heel), tensile forces may approach as much as 9 kN – equivalent to 12.5 times average body weight [9, 10].

Ligaments, in contrast, are short bands of fibrous tissue that connect one bone with another. In conjunction with skeletal geometry and the dynamic environment imposed by muscles and their tendons, ligaments limit and guide joint motion and provide integrity and stability to the joint [8]. They also comprise bands of fibrous tissue that lend support to solid

internal organs [8, 11]. Perhaps the most cited example of a joint stabilizing ligament is the anterior cruciate ligament (ACL), which preserves knee joint kinematics by preventing anterior sliding of the femur against the tibia. Much like their tendinous counterparts, ligaments must also resist large tensile forces. Additionally, ligaments experience torsional loads that result in twisting of fiber bundles, a more complex loading regime that increases the difficulty in designing an appropriate biomaterial. As an example, the ACL physiologically experiences forces ranging from 67 N while climbing stairs to 630 N while jogging [12], and may withstand a tensile load of up to 1.7 kN before failing [13].

Tendon and ligament share similar mechanical properties (Fig. 11.1). The stress-strain curve for tendon and ligament has an initial nonlinear toe region where the tendon experiences up to 1.5–3.0% strain under low stress [14, 15]. The existence of a toe region likely results from the extension of the “crimp” pattern in collagen fibers. Crimp represents a wavy (sinusoidal) pattern in collagen fiber alignment that extends and straightens in response to sudden tendon elongation, providing a buffer against fiber damage and acting as a shock absorber in response to tensile load [8, 16]. Crimp pattern geometry varies in different types of tendon and ligament tissue, and these differences affect the mechanical

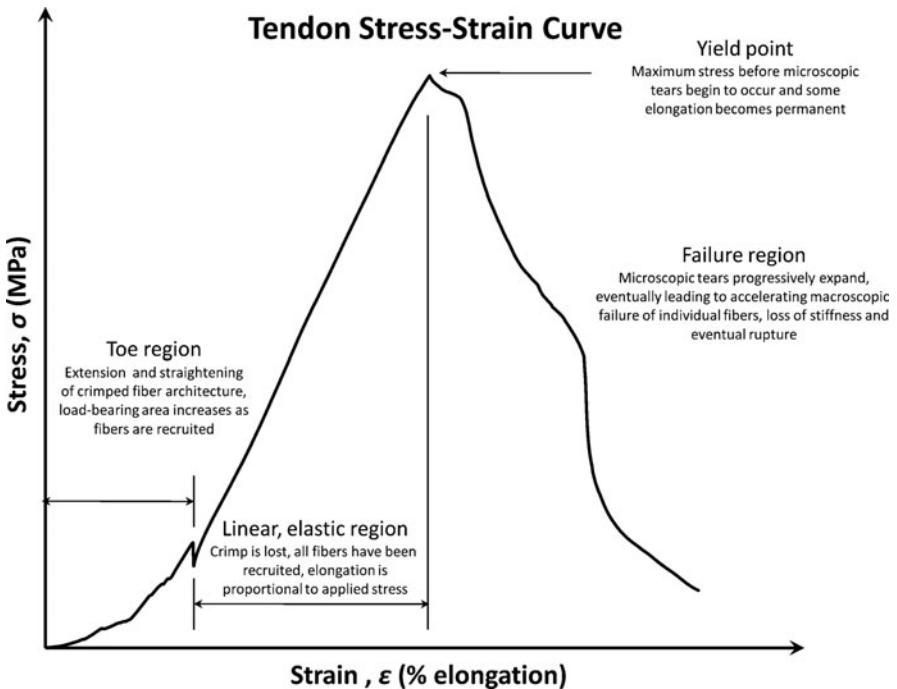


Fig. 11.1 Typical stress-strain curve for bovine patellar tendon depicting (1) a toe region corresponding to progressive fiber recruitment and crimp straightening, (2) a linear elastic region corresponding to stretching of collagen molecules in direct proportion to applied stress, (3) a yield point at which further deformation becomes permanent due to formation of microscopic tears, and (4) a failure region illustrating progressive collagen fiber tearing, loss of tendon stiffness, and eventual rupture (Graph courtesy of Dr. Yongzhi Qiu).

properties of the tendon [15, 16]. Following the toe region is a linear elastic region, where the tissue loses its crimp pattern and elongates proportionally to the stress applied. The elastic modulus generally lies between 1–2 GPa for most tendons and ligaments [14]. The yield point of tendon and ligament is reached when strain ranges from 5 to 7% [14, 15]. At this point, some of the elongation of tendon/ligament tissue becomes permanent as microscopic tearing of the fibers occurs, eventually resulting in macroscopic failure at 12–15% strain [14, 15]. Further strain inevitably results in tissue rupture. Overall, the tensile strength of tendon and ligament ranges from 50–150 MPa [14].

Tendon and ligament are viscoelastic tissues that experience creep, strain-relaxation and hysteresis in the stress-strain curve. Creep is defined as the increase in strain over time in a material from the initial elastic strain when the material is subjected to a constant load [16]. Stress-relaxation refers to the behavior of stress reaching a peak and then decreasing or relaxing over time under a fixed level of strain [14]. Both creep and stress-relaxation are time-dependent viscoelastic properties. Viscoelastic materials also exhibit hysteresis in the stress-strain curve, a phenomenon in which the unloading curve is lower than the loading curve that occurs due to a loss of energy in the loading process [14]. At low strain rates, viscoelastic materials absorb more energy but are less effective at transferring force, making them deform more at lower strain rates and less at higher strain rates [15]. The viscoelastic properties that are characteristic of tendons and ligaments may be derived from interactions between water and multiple extracellular matrix (ECM) molecules including collagens, proteoglycans, non-collagenous glycoproteins, elastin, and glycosaminoglycans (see Sect. 11.2.2.2).

11.2.2

Structure

As evidenced by the variation in the maximum loads to failure and stiffnesses discussed above, tendons and ligaments vary in their mechanical properties considerably depending on their location, function, and mechanical inputs [14, 17, 18]. This variation correlates strongly with the structural differences seen between each of these tissues [17]. Successful tissue engineering of a tendon or ligament must recapitulate these mechanical properties as closely as possible. Any deviation in these viscoelastic properties may result in inappropriate functionality and/or eventual mechanical failure. Thus, a thorough understanding of the structural basis underlying these mechanical properties is warranted.

Tendons and ligaments are both comprised of cells and extracellular matrix organized in a hierarchical architecture [15, 19]. Fibrils are the smallest structural unit (10–500 nm in diameter) and contain bundles of aligned collagen made from crosslinked triple-helical tropocollagen polypeptides. Fibrils are assembled into fibers (1–20 μm) surrounding the resident fibroblasts of the tissue and bound by endotenons/endoligaments, a thin layer of fascia that serves as a conduit for nerves, blood vessels and lymphatics. Fiber bundles are packaged into subfascicles and fascicles (20–200 μm) that are histologically characterized by a straight, parallel pattern or a planar or helical crimp pattern depending on their location in the tendon or ligament. Bundles of fascicles are ensheathed and surrounded by the epitenon/epiligament that serves as another conduit for blood vessels, lymphatics, and

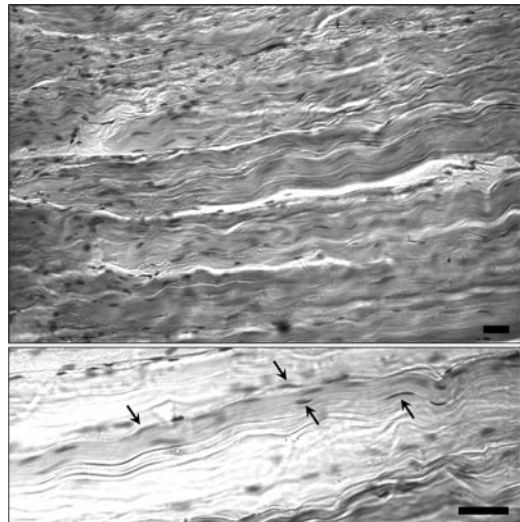
nerves. Tendons and ligaments may additionally be surrounded by a paratenon or synovial sheath, a condensation of connective tissue surrounding a tendon that reduces friction with adjacent tissue [20].

11.2.2.1

Cells

Fibroblasts are the most common cell type found in tendons and ligaments and are present in the fascicles and surrounding connective tissue sheaths (Fig. 11.2). Other cell types, including endothelial cells, synovial cells, and chondrocytes are also present in small quantities. The presence of cells is relatively scant compared with the amount of ECM present; cells occupy only 20% of the overall tendon volume [21]. They are typically arranged in elongated fashion in parallel with collagen fibers. In longitudinal histological sections, these fibroblasts have spindle-shaped, darkly staining nuclei and poorly staining cytoplasm (Fig. 11.2) [8, 20]. In transverse sections, the nuclei appear stellate and barely visible cytoplasmic processes extend around bundles of neighboring collagen fibers [20]. These processes extend laterally around collagen fibers and make contact with neighboring fibroblasts via gap junctions that facilitate intercellular communication through connexins 32 and 43 [20, 22]. Fibroblasts also bind to each other via adherens junctions and are linked mechanically with each other via longitudinally running actin stress fibers associated with these junctions [23]. Fibroblasts predominate in primordial tendon and ligament tissues, prior to the formation of dense collagen fibrils, and are thus responsible for synthesizing, excreting, and organizing components of the ECM (e.g., collagens, elastin, fibronectin, and proteoglycans) [15, 20]. Mechanical activation of tendon/ligament fibroblasts leads to upregulation of junctional components such as N-cadherin and vinculin as

Fig. 11.2 Longitudinal histological section of tendon tissue illustrating collagen fibers closely packed together in a “crimp” pattern (*top*) and the close apposition and conformation of spindle-shaped fibroblasts (*arrows*) embedded within the fibrous matrix (*bottom*). Scale bar = 50 μm (Histological images courtesy of Derek M. Doroski).



well as the cytoskeletal stress fiber component tropomyosin [24]. This suggests that these cells are able to adapt and respond to mechanical loads through changes in gene expression and ECM protein synthesis. Fibroblasts are recruited during injury and repair processes to synthesize and deposit collagen and other ECM components [2, 15]. They are also able to recruit other reparative and inflammatory cells through the release of chemotactic and endogenous growth factors [25], aiding in the coordination of remodeling and repair during wound healing [15, 26].

11.2.2.2

Extracellular Matrix

Tendons and ligaments are comprised of 89–94% of ECM components (collagen, proteoglycans, and elastin) by dry weight [15, 27], and water makes up 60–80% of total wet weight [8, 15, 27]. Tendon and ligament ECM represents a complex mixture of collagen fibers, elastin, glycoproteins, and proteoglycans. As discussed in this section, each component possesses a defined set of interactions with other components and serves a specific, important role in imparting unique mechanical properties to tendon/ligament tissue.

Collagen

Fibrillar collagen is by far the most abundant protein in tendons, accounting for approximately 75–85% of their dry weight [14, 15, 27]. Of the various types of collagens, collagen type I is the most abundant and is responsible for 60% of tendon dry mass and 95% of total collagen content in tendons [15]. Ligaments have similar collagen content to tendons (70–80% of ligament dry mass), and collagen type I comprises approximately 90% of total collagen content in ligaments. Collagen type I triple-helical strands pack together side-by-side to form collagen fibrils of 50–200 nm in diameter, and these fiber strands are offset from each other by one-quarter of their length to form striations that are visible in electron micrographs [8].

Of the remaining collagen content, collagen types III and V are the most prevalent. Collagen type III is primarily located in the endotenon/endoligament and epitenon/epiligament [15] as well as the attachment zones [15, 28]. It forms smaller and less organized collagen fibrils that may result in decreased mechanical strength and increase pliability of tendons and ligaments [15, 28]. Additionally, most of the newly synthesized collagen in the early phase of tendon/ligament healing is collagen type III [2]. Collagen type V regulates fibril growth and is intercalated into the core of collagen type I [15]. Collagen types II, VI, IX, X, and XI are all present in trace quantities in tendons and ligaments at their fibrocartiliginous insertion sites, where they assist in reducing stress concentration at the hard tissue interface (See Sect. 11.2.3.1) [29].

Elastin

Elastin comprises approximately 2% of tendon/ligament dry weight and forms elastic fibers with collagen type I and other microfibrillar proteins such as fibrillin [30, 31]. Elastin is an

11 insoluble globular protein that assumes a complex coiled arrangement when unstressed and stretches out to a more ordered form when stressed. Thus, as a component of elastic fibers, elastin is purported to play a role in recovery of collagen fibril crimp structure following applied strain [15, 32].

Noncollagenous Glycoproteins

Tendons and ligaments contain additional glycoproteins, primarily fibronectin and tenascin-C [15]. Fibronectin is typically found in small quantities in association with the surfaces of collagen fibrils [15, 33, 34]. Its synthesis and deposition are increased in response to injury and it serves as a provisional matrix foundation that is remodeled by fibroblasts in the deposition of more mature matrices [15, 34, 35]. Fibronectin contains binding sites for a multitude of ECM molecules such as collagen, proteoglycans, fibrin, tenascin-C, and other fibronectin molecules [36, 37]. In addition, several of its binding motifs interact with cell surface receptors such as integrins and syndecans. Together these interactions are necessary for collagen fibril assembly *in vivo*, providing a crucial role for this glycoprotein in the development of tendons and ligaments despite its relatively low presence compared with other ECM proteins [36]. Tenascin-C is purported to contribute to ECM assembly and mechanical stability through its interaction with collagen fibrils [38]. Its synthesis is upregulated in response to mechanical stress or growth factors such as TGF- β , and it appears to have an inhibitory effect on cell adhesion by blocking interaction with β_1 -integrin [39–41].

Proteoglycans

Proteoglycans make up relatively small quantities of tendon and ligament matrix (1–5% of dry weight), and their quantity varies depending on the location and function of the tissue [15, 20, 42, 43]. Despite their relatively small quantity, proteoglycans are soluble macromolecules that associated with much of the water in tendon/ligament tissue. Together, they provide lubrication and spacing that are crucial to the gliding of fibers as they cross over each other in tendon and ligament tissue [20]. Decorin, a small leucine-rich proteoglycan (36 kDa molecular weight), is the most abundant proteoglycan in ligament, and there are lower levels of biglycan and large aggregating proteoglycans, versican and aggrecan [42, 44, 45]. These proteoglycans are segregated within different regions of tendon and ligament, correlating with the mechanical forces that each region experiences. Decorin plays an important role in the organization of microfibrillar networks containing collagen type VI, fibrillin, and tropoelastin as well as collagen fiber networks [42, 43]. It is predominantly localized to tensile regions of tendons and ligaments. By facilitating fibrillar slippage during deformation [46] and inhibiting the formation of large collagen fibrils [43, 47], decorin allows for adaptation of the tissue under tension and improves tensile strength. Biglycan, another small leucine-rich proteoglycan, is also present in tensile regions of tendons and ligaments and plays a role in collagen fiber maturation [47]. Conversely, aggrecan possesses more than 100 chondroitin sulfate and keratan sulfate glycoaminoglycan chains protruding

laterally from a large core protein, similar to a bottle brush. This structure makes it among the largest of the proteoglycans present in tendons and ligaments (~220 kDa), and the numerous glycosaminoglycan side chains impart high anionic charge to attract water [42, 43]. Aggrecan is abundant in cartilaginous tissue due to its ability to hold water and enhance compressive stiffness, and this property correlates with its presence in fibrocartilaginous regions of tendon and ligament at their insertion sites with bone (see Sect. 11.2.3.1) [42, 43, 47]. The presence of versican, another large aggregating proteoglycan (~265–370 kDa), leads to expansion of ECM and to increased viscoelasticity of pericellular matrix that supports cell-shape changes necessary for cell proliferation and migration [47].

11.2.3

Interfaces with Other Orthopaedic Tissues

Two particular regions of interest exist at the proximal and distal ends of tendons and ligaments. These interfacial regions differ substantially in their cellular and ECM composition. Fibrous tissue-bone interfaces (entheses) and muscle-tendon interfaces (myotendinous junctions) exhibit distinct and important physiological roles and they serve to illustrate challenges in integrating biomaterials with native tissue. Tendon and ligament tissue interfaces provide transitional zones between tissues of different biochemical and mechanical properties, serving an important role in transitioning mechanical loads between disparate tissues. Tissue engineering of these interfaces or successful integration of biomaterials at their interfaces with surrounding tissues is critical to successfully regenerating tendon and ligament function.

11.2.3.1

Fibrous Tissue-Bone Interfaces

The attachment of tendons and ligaments to bone can occur via fibrocartilaginous (direct) or fibrous (indirect) entheses (Fig. 11.3). Fibrocartilaginous interfaces are typically encountered at the joint surfaces of long bones or among the short bones of the wrist and ankle, while fibrous interfaces typically occur on the shafts of long bones [20, 48]. The former contains four zones of tissue: dense fibrous connective tissue with typical fibroblasts, zones of uncalcified and calcified fibrocartilage that contain fibrocartilage cells rather than fibroblasts, and calcified bone characterized by osteocytes [4, 49, 50]. Fibrous interfaces, however, contain fibroblasts and collagen fibers (Sharpey's fibers) that extend directly into the bone at acute angles [4, 49]. Functionally, fibrocartilage cells at the tendon/ligament-bone interface secrete an ECM rich in aggrecan and collagen type II. Both molecules are typically found in articular cartilage and enable significant resistance to compression. This tolerance to compression enables fibrocartilage to dissipate stress at the tendon/ligament-bone interface, ensuring that deformation of collagen fibers during movement occurs gradually and is not concentrated at the bony interface [50].

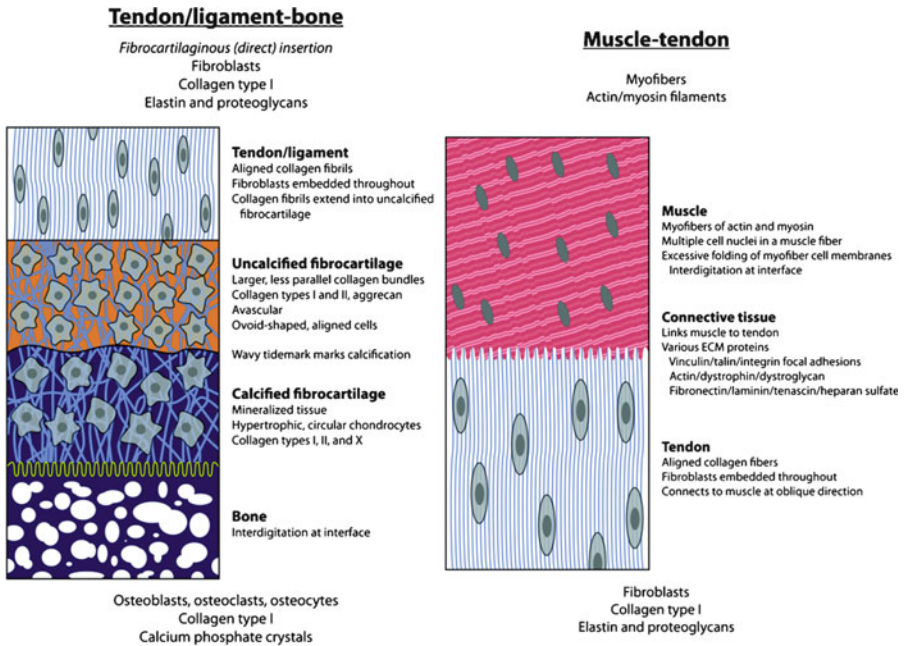


Fig. 11.3 A schematic depicting biomolecular and cellular architecture of fibrous tissue-bone interfaces (entheses, *left*) and myotendinous junctions (*right*). Each complex interfacial region exhibits graded matrix composition, progressive transitions and overlaps of tissue zones, and intercalating extracellular matrix with multiple cell types that facilitates load transfer between tissues of dramatically different material properties. *Colors* correspond to different tissue compositions: *light blue fibers* = collagen; *dark blue* = mineralized matrix; *orange* = presence of aggrecan; *red* = interconnected myofibers (Reprinted from [49] with permission).

Thus, fibrocartilaginous interfaces operate as transitional zones between tissues of drastically different mechanical properties.

11.2.3.2

Muscle-Tendon Interfaces

Major structural specialization occurs at myotendinous junctions with respect to both cells and ECM (Fig. 11.3). Cell membranes of myofibers are highly infolded to increase the contact surface area with tendon ECM by tenfold [49, 51, 52]. This serves to ensure that loaded junctions are primarily experiencing shear rather than tensile stresses and is significant because cell-cell junctions at this interface generally remain intact more easily under shear than in tension [20]. Additionally, infolding distributes the imparted stress over a broader area to minimize the risk of tearing [49]. The integrity of the myotendinous junction is largely dependent on the attachment of terminal myofibrils with muscle cell membrane proteins and the attachment of these to collagen fibers in the tendon. Thus, force transmission

ultimately relies on transmembrane associations between myofiber actin filaments and type I collagen fibers. This is achieved via multiple assembled focal adhesion complexes that link myofiber cytoskeletons to binding motifs in the tendon ECM [49, 53]. Within the tendinous portion of this interface, fibronectin, laminin, tenascin-C, and heparan sulfate proteoglycans have all been uniquely localized and may affect junctional mechanical properties [20].

11.2.4

Injury and Repair

A wide variety of tendon/ligament injuries are possible within and around the joint capsule. Understanding these different injuries and how the body responds to them is critical when designing tissue engineering approaches for tendon/ligament injury since different types of injury may require different solutions. Biomaterial properties and target parameters such as biocompatibility, degradation properties, and rate of construct integration are all informed by an understanding of natural tendon/ligament repair and healing.

Tendon and ligament injuries may occur when a joint, such as the knee, experiences rapid twisting, excessive force, or direct trauma. Injury can be classified as either acute or chronic injury, and as either direct or indirect. An acute, direct injury may result from contusion, non-penetrating blunt impact from motor accidents and sports injuries, or laceration [26]. Acute, direct injuries often result in rupture or tearing of the tendon or ligament. For ligaments, this is the most common mechanism of injury and occurs in varying clinical degrees [3, 54]. First-degree sprains involve tearing of a minimum number of fibers in less than one third of the ligament resulting in no increase in joint laxity. Second-degree sprains involve tearing of more ligamentous fibers in one third to two thirds of with a small increase in laxity. Third-degree sprains and ruptures involve greater than two thirds of the ligament with demonstrable laxity in the joint.

In contrast to direct injuries, indirect injuries often result from acute tensile overload or chronic overuse that results in repetitive microtrauma [26, 27]. The term “overuse” implies repetitive stretching of a tendon below its failure threshold to a point at which tendon tissue can no longer endure further tension. In tendon, tensile overload and chronic overuse injuries often result in injury to either the myotendinous junction or the osteotendinous junction, because the healthy tendon midsubstance can generally withstand larger tensile loads than the muscle-tendon or bone-tendon interfaces [26, 27, 55]. When overuse injury occurs at the tendon-bone junction, this is termed enthesopathy. Its features include metabolic activation of tendons at the insertion site, loosening of collagen fiber bundles, accumulation of lipids, and microcalcification [15, 56]. When overuse microinjuries do occur in the tendon midsubstance, they may not progress to rupture or tearing, generally resulting in a degenerative condition known as tendinopathy [15, 57].

With regard to repair, tendon and ligament are largely acellular and poorly vascularized tissues and have a poor healing capacity [3, 5, 26, 58]. Tendon and ligament healing can be described in stages: inflammation, cellular proliferation and ECM production, and remodeling [3–5, 27]. During the inflammatory stage, fluid accumulation occurs in the injured tendon/ligament and surrounding tissue immediately after injury and throughout the next 72 h [3, 5].

Rupture of surrounding blood vessels results in hematoma formation that includes platelet aggregation and degranulation [3, 26]. Activated platelets at the wound site release a host of growth factors and vasodilators, and mast cells release pro-inflammatory cytokines [3, 5, 26]. This plethora of chemotactic factors causes inflammatory cells including monocytes, leukocytes, and macrophages to migrate to the injury site [5]. These cells function to remove necrotic tissue and debris through phagocytosis, break down the clot, aid in recruitment of fibroblasts to the site of injury, and promote angiogenesis [26, 59, 60]. Overall, inflammation results in a general increase in water, cells, and provisional matrix in the form of fibronectin, glycosaminoglycans and collagen type III to stabilize the new ECM production [26].

Following the inflammatory stage, significant cellular proliferation and matrix repair occur in the second stage of tendon and ligament healing. Large numbers of fibroblasts are present and form disorganized vascular granulation tissue, while the presence of macrophages and mast cells diminishes [5, 26, 27]. At this point, fibroblasts proliferate to their maximum levels during the healing process, and they synthesize collagen type III in significantly larger quantities than collagen type I. Collagen type III is thought to be of particular use in the early repair process because of its ability to form rapid cross-links that stabilize the repair site [61]. Subsequently, the collagen type III is eventually turned over to collagen type I, conferring additional strength and stiffness to the repair site [26, 62]. Proliferation and ECM repair continues for approximately 6 weeks [3, 5].

During the remodeling stage, which may last for several months, the new ECM matures into slightly disorganized hypercellular tissue [5]. In this stage, fibroblasts undergo decreased growth, ECM synthesis slows, and collagen fibers are oriented longitudinally with the long axis of the tendon/ligament [4, 26]. The collagen type III to type I ratio returns to normal levels observed in intact tissue, and the amounts of collagen cross-links, glycosaminoglycans, water, and DNA content approach those of normal tissue [26]. However, lack of organization and difference in crimp pattern in the newly formed tissue often results in inferior mechanical properties compared to pre-injury levels [4, 5, 27], suggesting that normal physiological healing responses are insufficient in regenerating normal tissue function.

11.3

Current Techniques for Reconstruction and Tissue Engineering

11.3.1

Current Surgical Management and Reconstruction of Tendons and Ligaments

Current procedures of tendon/ligament replacement are able to restore locomotion to a substantial degree, yet they do not replicate full joint function. Surgical techniques that employ grafts and sutures or screws have experienced problems with prolonged mechanical strength, eventual fatigue and wear, donor-site morbidity, and infection [3–5, 26]. The use of grafts also presents challenges with proper fixation of the tissue to the bone tunnel for a mechanically stable, biologically viable connection interface that recapitulates the

properties discussed previously. These limitations demonstrate the need for tissue engineering alternatives for treatment of tendon/ligament injury.

When the normal repair process for tendons and ligaments fails to produce adequate healing, a surgical procedure is usually necessary to reconstruct the injured tissue. This surgery is performed as soon as possible following injury to achieve an optimal outcome. Sutures may be applied to reattach minor tendon and ligament tears, though sutured tissue often heals poorly and is unable to replicate the strength required of native tendon/ligament, resulting in failure [26]. For this reason, tissue grafts are often required.

Autografts, in which grafted tissue is acquired from the injured patient, remain the current standard procedure for tendon/ligament replacement [63–65]. Because of their size, strength, and availability, autografts consisting of the central or medial third of patellar tendon, together with the corresponding bony insertion sites, have been widely used for reconstruction of the anterior cruciate ligament [63–65]. This bone-patellar tendon-bone graft is anchored through a bone tunnel that is drilled through the tibia, drawn across knee, and anchored into a tunnel drilled through the femur. The bone or soft tissue of the graft is fed through the bone tunnel and may be secured into place using a variety of methods, including staples or interference screws [66]. Comparable results have also been achieved using a quadrupled hamstring graft [66, 67]. Autografts promote cell proliferation and new tissue growth, and they initially offer good mechanical strength [4, 5, 66]. However, despite their good tensile strength, ACL autografts fail to convey proper stabilization the knee under torsional loads [4]. Moreover, revascularization of grafted tissue *in vivo*, a requirement for the long term success of these grafts, remains an elusive goal [4, 66]. Because these autografts are acquired from the injured patient, a limited supply of donor tissue is available and additional intraoperative procedures are required for tissue harvest. This often results in donor site morbidity, including pain, decreased motion, muscle atrophy, and tendonitis [5, 58, 66–68].

Allografts present another option for tendon/ligament replacement in which graft material is removed from a cadaver and usually frozen [58, 67]. ACL allografts most often involve cadaver patellar tendon, hamstring tendon, or Achilles tendon [5, 67]. Reconstruction with allograft offers a major advantage of eliminating donor-site morbidity, allowing less postoperative pain and faster rehabilitation. Additionally, they appear to offer similar mechanical strength, cellular proliferation, and new tissue growth [5, 26, 66]. However, allograft carries the disadvantages of the potential for disease transmission and limited availability [5, 67–69]. In addition, concerns about slower integration with host tissue and possible immunogenicity have been raised in association with allograft [5, 67, 70].

11.3.2

Biomaterials for Tissue Engineering of Tendons and Ligaments

Given the drawbacks discussed regarding auto- and allograft treatments for tendon and ligament injury, increasing efforts have been made to engineer novel biomaterials for tissue engineering approaches to regenerating tendon and ligament tissue. The following section will address both natural and synthetic biomaterials and their fabrication, together with cell types employed and the results of *in vitro* and *in vivo* evaluations.

11.3.2.1

Cell Types Used in Combination with Biomaterials

Several cell types have been investigated for use in conjunction with biomaterials for tissue engineering of tendons and ligaments. Reparative cells may be recruited from host tissue through their attachment and integration with the implanted biomaterial, or these cells may be seeded in tissue engineered constructs with some level of conditioning prior to implantation. Seeded cells may also interact with native cells via soluble signals or cell–cell contacts, and may be additionally affected by the structural properties of the biomaterial and imposed mechanical forces. Ideally, the cell type selected for study should work effectively in concert with the biomaterial employed to allow survival, proliferation, and excretion of appropriate ECM to restore normal tendon/ligament function or regenerate new functional tissue.

Fibroblasts derived from tendons and ligaments are commonly used in evaluating the efficacy of biomaterials, stemming from the fact that they are the predominant cell type found in native tissue. They serve an integral role in facilitating organization and maintenance of ECM, particularly with respect to the collagen fibers that provide tendon/ligament tissue with its substantial mechanical strength [20]. Fibroblasts are readily incorporated into most scaffolds where they are able to adhere and proliferate [31, 71–74] as well as secrete ECM components such as collagens I and III and proteoglycans (see Sects. 11.3.2.3–11.3.2.4) [31, 71, 74–77]. These cells also respond to mechanical stimuli through their alterations in cell orientation and increased matrix deposition [39, 76, 78–82]. Fibroblasts also undergo cell migration and infiltration into implanted scaffolds [83–85]. A significant drawback with the use of tendon/ligament fibroblasts is the need for an autogenous cell source to avoid eliciting a host immune response. As evidenced from current autograft approaches for tendon/ligament reconstruction, harvesting fibroblasts from patient tendons and ligaments is invasive and would result in significant donor site morbidity, making them difficult to obtain [58].

Dermal fibroblasts present a feasible alternative to tendon/ligament fibroblasts since they are more readily available through a simple skin biopsy, though this still may result in some morbidity to the patient. In comparison with tendon/ligament fibroblasts, dermal fibroblasts may be more amenable to culture and scale up due to their more rapid proliferation and also show no detrimental effects when re-implanted *in vivo* [86–88]. Behaviorally, dermal fibroblasts adhere and proliferate in similar ways to many biomaterials and appear to synthesize many of the same ECM components (see Sects. 11.3.2.3–11.3.2.5) [89–92]. Their ultimate viability as a suitable source for tendon/ligament tissue engineering still remains an open question since these cells are not derived from the tissue for which they are being applied and therefore may not behave in the same way as fibroblasts from native tendon/ligament tissue for long-term tissue replacement.

Another potential cell source that has been widely applied in biomaterial approaches for tendon/ligament tissue engineering is marrow stromal cells or mesenchymal stem cells (MSCs). These bone marrow-derived cells are multipotent cells that can differentiate along several mesenchymal lineage pathways, culminating in the formation of bone, cartilage, muscle, marrow stroma, tendon and ligament, fat, and other connective tissues [93]. Though not as widely available as dermal fibroblasts, these cells are more readily accessible than tendon/ligament fibroblasts through a simple, minimally invasive needle aspiration. MSCs offer enormous potential as an autologous cell source, obviating the need for additional

surgeries required by current autograft procedures and circumventing immune rejection [58]. New evidence suggests that MSCs also secrete immunomodulatory factors and may in fact be immune-privileged [94], suggesting that allogeneic MSCs could be used in potential tendon/ligament tissue regeneration therapies. Additionally, they have been demonstrated to aid in repair of injured tissue [95, 96]. Like tendon/ligament and dermal fibroblasts, MSCs adhere to and proliferate on a variety of scaffold materials, and are capable of producing many of the same ECM molecules critical to native tendon and ligament (see Sects. 11.3.2.3–11.3.2.5) [96–100]. A host of growth factors and mechanical stimuli play a role in MSC maintenance and differentiation. Growth factors may be combined or delivered sequentially in order to elicit MSC differentiation. TGF- β , FGF-2, EGF, and IGF-2 each may enhance MSC proliferation and induce synthesis of numerous ECM components reminiscent of tendons and ligaments [101–104]. Independent of growth factor application, MSCs have been differentiated under cyclic strain regimens into fibroblast-like cells that are prone to expansion and tendon/ligament ECM production [71, 97, 105, 106]. Differentiation of MSCs has additionally been shown to be dependent on matrix stiffness [107]. Loading and matrix stiffness could be sensed through a variety of mechanotransduction mechanisms by affecting cell shape, protein unfolding, matrix orientation and porosity, ligand presentation, and other undetermined factors [108–110].

Several other sources of stem cells have been recently discovered that may be applied to the engineering of tendons and ligaments. MSCs may be differentiated from human embryonic stem cells and then differentiated again to promote tendon regeneration [111]. However, MSCs still are not bound by the same ethical concerns as embryonic stem cells. Alternatively, ligaments and tendons themselves may contain a population of progenitor cells that have multilineage potential [112–115], though they have yet to be fully characterized and employed with biomaterials for tissue engineering purposes.

11.3.2.2

Scaffold Design

A number of design requirements exist for the development of a suitable scaffold for tendon/ligament tissue engineering [11]. The material should be biocompatible, eliciting an appropriate immune response when implanted into the injury site while simultaneously promoting tissue formation and providing a therapeutic benefit. After fabrication, the scaffold should possess sufficient void space to allow proper nutrient delivery and waste removal to the seeded or infiltrating cell population [58, 116]. This porosity may also be utilized to promote tissue ingrowth through cellular proliferation and ECM production that may enable integration of the scaffold with the host tissue and strengthen it to withstand normal physiologic loads and deformations [5, 58, 116, 117]. Architectural properties should mimic those of native tendon and ligament, necessitating the development of anisotropic scaffolds and aligned matrices to optimize response to tensile loads. Sufficient mechanical properties including elastic modulus, toughness, and ultimate strength should also be designed into the material to lessen the chance of failure [2, 4, 5, 15, 58]. Ultimately, the scaffolding material or the neo-tissue that replaces it should have mechanical properties similar to that of native tendon or ligament to restore normal physiologic function and to prevent stress-shielding of newly developed tissue [2, 4, 5, 15, 58].

11 Biodegradability is also a feature of numerous scaffolds utilized for tendon/ligament tissue engineering, enabling the integration of host tissue and the eventual replacement of the scaffold with regenerated tissue. To retain stable tissue functionality and mechanical properties without stress-shielding, generally the construct degradation should be engineered to occur at a similar rate to the formation of new tissue [5, 11, 58]. As a consequence of these design criteria, a wide variety of natural and synthetic materials have been considered as scaffold materials for tendon/ligament tissue engineering.

11.3.2.3

Scaffold Fabrication Techniques

A number of scaffolds currently being studied for these applications are derived from polymers, both natural and synthetic, since they offer elastic or viscoelastic properties and can be strengthened through a number of synthesis and processing techniques [58, 68, 96, 116, 118–124]. Polymers may be assembled into porous scaffolds, extruded or electrospun into fibers, and can be used as components of composite materials [116, 121–124].

Several techniques exist for engineering porosity into materials for use as tissue engineering scaffolds. The most common of these involve particle leaching and replica molding [125–128]. Particle leaching relies on mixing a solubilized scaffold precursor material in either an aqueous or organic phase with particles of predetermined size and shape that are soluble only in the opposite phase. Once the scaffold is cured around the particles, then a solvent is added to extract or leach the particles out of the scaffold leaving behind a porous architecture [125–127, 129]. An additional method for generating porous scaffold architecture involves the use of solid free-form fabrication/rapid prototyping combined with computational topology design. These techniques include stereolithographic polymerization of liquid precursor, selective laser sintering of powdered materials, three-dimensional printing, or nozzle-based systems [116, 130, 131]. Stereolithography is an additive manufacturing process using a vat of liquid, light-curable photopolymer resin and a laser to build parts layer-by-layer through a computer-controlled tracing process. Selective laser sintering is an additive manufacturing technique that employs a laser to fuse small particles of plastic, metal, ceramic, or glass powders into a desired 3-dimensional scaffold. Three-dimensional printing involves directed deposition of a fine powder or liquid photopolymer by a movable printhead that is subsequently bonded using a printed adhesive or ultraviolet light mounted on the same printhead. Nozzle-based systems process the base material either thermally or chemically as it is extruded through a nozzle as part of a computer-aided additive manufacturing technique. Porous architectures are also achieved during fabrication and assembly of fibrous scaffolds as a result of inter-fiber spacing [121–124].

A variety of methods are available for producing fibers from synthetic and natural materials, including drawing, template synthesis, thermally induced phase separation, molecular self-assembly, and electrospinning [123]. Drawing is a gravity-driven extrusion process that produces a fiber from a polymer melt, while template synthesis is a replica-molding based approach. Template synthesis results from deposition of precursor material into a nanoporous mold where it preferentially nucleates and grows on the pore walls, resulting in tubules after

short times and fibers after long times. The major disadvantage of these techniques is their lack of scalability [132–134]. Thermally induced phase separation is accomplished by freeze-drying a polymer solution to extract solvent, leaving behind a highly porous fiber matrix. This technique allows the use of simple equipment and the mechanical properties of the resulting fiber matrices may be varied by changing the polymer composition [135]. However, it is limited to specific polymers and does not offer scalability or control over fiber dimensions [123]. Molecular self-assembly, commonly used in the synthesis of collagen fiber-based matrices, involves the autonomous organization of macromolecules into patterns or structures without human intervention. This technique creates smaller nanofibers of a 1–50 nm in diameter and a few microns in length, but there is little spatial control of fiber dimensions and the process is also not amenable to scalability [74, 86, 95, 96, 136].

Electrospinning thus remains the most popular current technique for production of nanofibrous matrices because it is a continuous and scalable process, is cost effective compared to other existing methods, and allows fabrication of fiber diameters ranging from nanometers to microns in random or aligned fashions [31, 75, 76, 82, 123]. The principle of electrospinning is to use an electric field to draw polymer solution or melt from an orifice to a collector. High voltages generate sufficient surface charge to overcome the surface tension in a suspended drop of the polymer fluid. The diameters of the electrospun fibers are at least one order of magnitude smaller than those made by conventional extrusion techniques. Electrospinning, however, is currently limited to synthetic polymers, may involve toxic solvents, and requires excessive tuning of multiple parameters such as polymer physical properties, solution properties, electrical potential, ambient parameters, and collector plate positioning and motion [123].

11.3.2.4

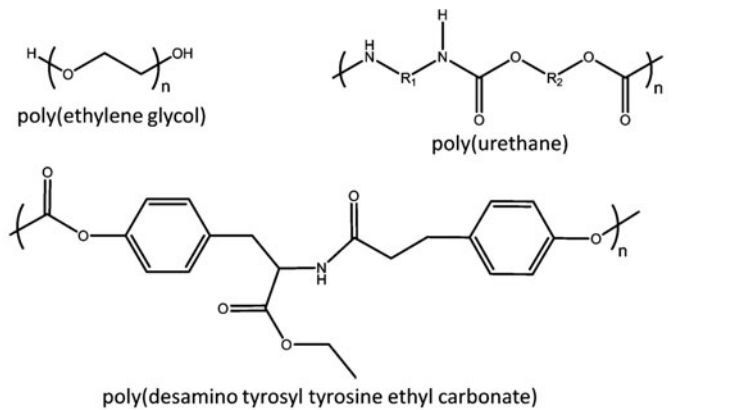
Types and Applications of Biomaterial Scaffolds

Biomaterials may be designed for tendon/ligament tissue engineering using synthetically and/or naturally derived materials [137–142]. Synthetic materials are readily derived from monomeric precursors and are easily amenable to many of the fabrication and processing techniques outlined above. Depending on the chemical structure, physical properties such as size and shape, and assembly techniques, synthetic polymers may be tuned to have a variety of mechanical properties and degradation characteristics. However, synthetic materials and their degradation or wear products may potentially elicit an inappropriate host response through their immunogenicity, toxicity, or poor clearance. Naturally derived materials are generally non-immunogenic, non-toxic, and readily degraded and cleared due to their normal presence in human tissues. Their biochemical composition mimics that of native tissue and provides architectures and signaling characteristics that are more easily recognized by native cells and more directly influences their responses. However, natural materials exist in relative scarcity when compared with synthetic materials because they must be harvested from biological specimens, and their acquisition typically requires destructive means that affect their physical and biochemical characteristics. Both synthetic and natural materials therefore possess advantages that merit their

examination and usefulness as scaffolds for tendon/ligament tissue engineering and will be examined in the subsequent section.

Synthetic Scaffolds

Several synthetic polymeric scaffolds have been evaluated for their potential use in tendon/ligament tissue engineering and regeneration (Fig. 11.4). In early attempts for tendon/ligament replacement, synthetic graft materials were employed as prosthetic devices using poly(tetrafluoroethylene), poly(propylene), poly(ethylene terephthalate), and carbon fibers [5, 21, 58, 68]. These materials enjoyed limited success as replacements due to their ability to initially restore function, yet they failed to provide a lasting benefit due to their inability to recapitulate the biomechanical properties of the original tissue [5, 14, 21, 68]. These materials were designed to be inert grafts and thus failed to properly integrate with host tissue via graft fixation and cellular/tissue infiltration [21, 58]. Additionally these graft materials also displayed poor mechanical and tribological properties, including fatigue, creep, permanent deformation, stress-shielding, abrasive wear and degradation, axial splitting, and low extensibility [14, 21, 58, 68].



Poly(esters):

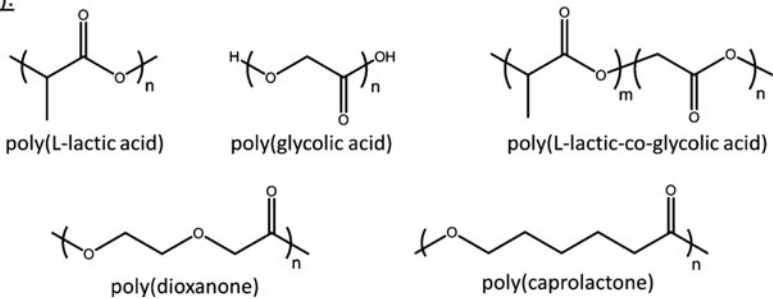


Fig. 11.4 Chemical composition of synthetic polymers employed as biomaterial scaffolds for tendon/ligament tissue engineering

While prosthetics and synthetic augmentation devices resulted in numerous failures and have since been taken off the market, they still proved instructive in designing a second generation of biomaterials specifically used for tissue engineering approaches. Counter to using “inert” materials, these next-generation biomaterials have high initial strength and are designed to gradually transfer the load-bearing responsibilities to maturing tissue containing autogenous cells and ingrown tissue through their degradability. The bulk of currently used materials include poly(urethanes) and poly(esters). Other less widely used synthetic scaffolds include poly(desaminotyrosyltyrosine ethyl carbonate) (poly (DTE carbonate)), and poly(dioxanone) [21].

Poly(urethanes) are a heterogeneous group of polymers of organic units joined by carbamate linkages (Fig. 11.4). They have dynamically tunable physical and mechanical properties covering a wide range of stiffnesses, densities, and porosities, may be fabricated into scaffolds for tissue engineering using a variety of processes, and can have tunable degradation characteristics [143]. Typical polyurethanes exhibit low stiffness characteristics (2–140 MPa) and ultimate tensile strengths (7–40 MPa), but are able to undergo significant elongation at break (>100%) [143]. Porous poly(urethane) scaffolds seeded with fibroblasts have demonstrated increased cell proliferation, matrix accumulation, and elastic modulus following a cyclic strain regimen [144]. A porous poly(carbonate)-poly(urethane) patch without seeded cells demonstrated significant tissue ingrowth when implanted in a rat supraspinatus tendon defect [145]. When seeded with fibroblasts, these constructs increased elastic modulus following sub-physiological cyclic strain regimens [81]. Electrospun poly(urethane) fibrous scaffolds have been used in combination with seeded cells for *in vitro* studies. Human ligament fibroblasts cultured on poly(urethane) nanofibers demonstrated a spindle shaped morphology oriented along the axis of strain and showed enhanced deposition of collagen [82]. Bone marrow stromal cells seeded onto aligned electrospun poly(urethane) assumed a more spindle-shaped morphology, were oriented parallel to the direction of sub-micron fiber alignment, and demonstrated upregulated collagen type I, decorin, and tenomodulin expression [146]. While exhibiting good cytocompatibility, poly(urethanes) that are rendered biodegradable through chemical modification may still release potentially toxic degradation products and are not able to maintain robust mechanical properties similar to native tendon/ligament upon degradation [143].

Poly(esters), another widely used tendon/ligament scaffold material, are a class of polymers that contain ester functional groups in their main chains. While simple poly(ester) fibers do not possess the desired mechanical properties alone, these materials are easily processed into braids and woven matrices that initially enhance mechanical strength to levels comparable to tendon/ligament tissue [121]. Several classes of poly(esters) have been used for a tendon/ligament scaffold material. Due to their chemical structure, poly(esters) are hydrolytically degradable via their ester bonds leaving byproducts that are either inert or metabolically removed. Polymer degradation varies with environmental pH, composition, cross-linking density, and hydrophilicity [147]. The most commonly used poly(esters) for tendon/ligament tissue engineering are poly(α -hydroxyesters), including poly(L-lactic acid) (PLLA), poly(glycolic acid) (PGA), and poly(L-lactic-co-glycolic acid) (PLGA). When used for tendon/ligament regeneration, these scaffolds are commonly used in a fibrous form that is further processed to form higher-ordered structures such as sheets [31, 75, 76, 89], woven or knitted meshes [148–150], and braids [83, 84, 151–155]. Fibroblasts cultured on PGA [31, 89] or

11 PLGA [75, 76] revealed that cell alignment, distribution, and matrix deposition conformed with fiber alignment and that mechanical properties increased upon application of cyclic mechanical strain. Knitted PLLA scaffolds seeded with MSCs upregulated collagen I, tenascin C, decorin, integrins, and matrix metalloproteinases after two weeks in culture [148, 150], and this effect was enhanced in the presence of TGF- β , PDGF-BB, and BMP-13 [148]. Braided PLGA scaffolds exhibit viscoelastic properties and enhanced mechanical strength that is enhanced by twisting the fibers when compared with the above scaffolds. The large interfiber pore diameter (100–200 μm) allows significant collagen deposition around PLGA fibers throughout the center of the construct, both in vitro when seeded with tendon/ligament fibroblasts and in vivo when implanted in a rabbit model for ACL reconstruction, though integration in the bone tunnel has not yet been demonstrated [83, 84, 151–153]. When braided scaffolds were seeded with bone marrow stromal cells under static loading conditions or with the addition of TGF- β and GDF-5, cells remained viable showed significant deposition of collagen both in vitro and in vivo [154–156]. A wide range of degradation profiles and mechanical properties are achievable with poly(esters) depending on fiber diameter, architecture, and blending techniques. However, a suitable material that retains mechanical properties of tendon/ligament during degradation and replacement by growth of new tissue remains to be found [121].

Natural Scaffolds

Given that tendon and ligament tissue are primarily composed of ECM containing collagen type I, assemblies of collagen type I fibers have been widely explored as a natural, two- or three-dimensional matrix for tendon and ligament tissue engineering. Early approaches for generating collagen based gels relied on spontaneous fibrillization of collagen type I to generate a three-dimensional, porous scaffold of randomly oriented collagen fibers [74, 86, 95, 136]. Mechanical properties of these collagen fiber matrices without cells possessed sub-optimal mechanical properties when compared with native tendon ligament tissue, including an elastic modulus of 2–40 MPa and an ultimate tensile strength below 10 MPa [46]. When seeded with tendon fibroblasts [74] or MSCs [136], the gels underwent significant in vitro cell-mediated contraction in a dose-dependent response and aligned in the direction of the isotropic collagen fibrils. MSC-collagen composites deployed in a patellar tendon defect hastened the development of higher maximum stresses and moduli, yet these values were still significantly less than that of native patellar tendon [95]. The mechanical properties of these gels may be further augmented by the mechanical stimulation of cell-seeded collagen constructs [79, 80, 97, 157–166]. Several studies have shown that MSC-seeded porous collagen sponges generate aligned collagen fibers under cyclic tensile strain that in turn increased gel stiffness and tensile strength over non-strained controls both in vitro and in vivo [158–160, 163–166]. MSCs in these sponges demonstrated increased ECM gene expression and protein deposition during in vitro culture and in vivo implantation for patellar and Achilles tendon repair [158–160]. This effect is also observed for fibroblasts [79, 80, 97, 157] and may be mediated through a combination of growth factor signaling [161] and mechanosensation via integrins [80]. Alternatively, aligned collagen fibers may be fabricated using extrusion, electrochemical or microfluidic

methods in the absence of tensile strain and crosslinked using chemical, physical, or biological means to enhance their mechanical properties and direct cellular migration and infiltration of the scaffold [87, 88, 90, 91, 132–134, 167]. Collagen matrices do present some drawbacks that are potentially prohibitive to their more widespread use. Purified collagen derived from animal tissues must be processed to remove foreign antigens and potential donor pathogens to reduce immunogenicity, which is currently detrimental to its mechanical strength and only alleviated by non-physiological crosslinking methods [121]. Crosslinked collagen matrices still retain insufficient mechanical properties, with an elastic modulus of only 400–800 MPa and an ultimate tensile strength under 80 MPa [46]. Collagen also undergoes relatively fast *in vivo* degradation and loss of its mechanical strength [121, 168].

Alternatively, cells encased within or seeded on various provisional matrices found during tissue development and wound healing have been used for tendon/ligament tissue engineering with the hope that seeded cells or native cells encountered *in vivo* will further remodel the provisional matrix. Fibrin matrix crosslinked with thrombin and containing bone marrow stromal cells resulted in upregulated collagen I gene expression, increased collagen deposition, increased collagen fibril diameter, and enhanced mechanical properties when compared with fibrin matrix alone in a rat patellar tendon defect [169, 170]. When combined with platelets and collagen, fibrin scaffolds have induced infiltration, proliferation, and collagen deposition of fibroblasts from injured ACL *in vitro* and enhanced mechanical properties of the injured ACL when compared to untreated control *in vivo* [85, 171–173]. Like collagen matrices however, these matrices are still unable to achieve desired mechanical properties (elastic modulus in the kPa range) and may require mechanical conditioning or additional modifications to architecture and biochemistry to render them appropriate functional replacements [121, 168].

Another natural scaffold for tendon-ligament tissue engineering is silk, a protein fiber derived from cocoons of the silkworm *Bombyx mori* [71, 98, 101–106, 118, 174–179]. Silk fibers have a triangular cross section with rounded corners, 5–10 μm wide and are composed primarily of a fibroin heavy-chain that is configured in beta sheets [180]. Of the fibrous scaffolds discussed, silk represents the strongest with an elastic modulus (~ 10 GPa), ultimate tensile strength (740 MPa), and failure strain (20%) greater than that of native tendon tissue [118, 181]. Silk scaffolds are also biocompatible and promote cell adhesion, proliferation, and ECM deposition. Silk demonstrates high linear stiffness; however, orienting fibers in parallel fails to replicate the mechanical properties of tendon [58]. Compared with other biodegradable scaffolds, silk degradation occurs at a relatively slow rate *in vivo*, with a reduction in its tensile strength after 1 year and complete degradation after 2 years [118]. Arrangement of silk fibers in a wire-rope significantly enhances tensile strength and achieves similar mechanical properties to those of native ligament. This silk scaffold was shown to support MSC attachment and spreading, proliferation, and tendon/ligament ECM deposition after two weeks of *in vitro* culture [71, 98, 101–106, 118]. A microporous silk sponge encasing a braided silk cord and seeded with MSCs has also been used for *in vivo* studies in small and large animal models of ACL repair. This approach has met with some success in producing ECM and showed some histological evidence of integration with host tissue [174, 175, 177–179]. Despite its numerous advantages outlined here and elsewhere, silk does present some concerns with adequate removal of contaminating proteins,

extremely slow degradation kinetics of water-insoluble β -sheets, and potential immunogenicity since it is not a native protein in humans [118, 121].

Composite Scaffolds

In addition to the use of scaffolds comprised of single materials, several natural and synthetic composite scaffolds have been recently developed for tendon/ligament tissue engineering. Natural composite scaffolds comprise a group of de-cellularized tissues with the intention for use as an allograft or xenograft approach. Synthetic composites tend to be multiphasic, utilizing one or more fabrication techniques and composed of two or more materials. Together, these scaffolds are primarily intended to supply a more complex environment with a variety of size scales and scaffold configurations for enhanced integration with surrounding tissue and to improve the mechanical properties of the engineered tissue beyond that of single materials.

Natural, de-cellularized matrices contain complex mixtures of ECM components derived from donor tissue. The composition of these tissues is not well-characterized, though they present a feasible alternative since they may be acquired from cadaveric donors of the same species. De-cellularization of these matrices renders them with a reduced risk of graft rejection and disease transmission. Additionally, these matrices retain a similar structural composition of the targeted tissue and allow re-cellularization with host cells. The most common of these are acellular tendon or ligament allografts [92, 182–189]. Detergent treatments yield effectively de-cellularized matrices, yet cellular infiltration requires modification of the porosity of the matrix through mechanical or enzymatic disruption that adversely affects mechanical properties [183, 184, 186–189]. By contrast, small intestinal submucosa has been applied as a decellularized sheet that wraps around a tendon or ligament defect and allowed greater cellular infiltration and deposition of ECM when compared with untreated or autograft controls [190–193]. However, these matrices display poor mechanical properties in comparison with native tendon and ligament [194, 195] and also illicit a significant host inflammatory response [190, 193, 196]. Acellular dermal matrices and human umbilical veins also offer similar biochemical composition to tendon/ligament, allow cellular infiltration, and exhibit a minimal inflammatory response, but have an order of magnitude lower elastic modulus than native tissue [197–201].

Several natural and synthetic materials have been used in combination to synergistically combine the positive aspects of the individual materials themselves. Numerous groups have combined fibrous scaffolds with hydrogels to allow homogeneous cell seeding of fibrous scaffolds, facilitate alignment of cells and matrix within gel systems, enable mechanical reinforcement of the gel scaffold, and enable controlled delivery of bioactive factors via the hydrogel [202–204]. A silk cable-reinforced gelatin/silk fibroin scaffold enabled homogeneous seeding of MSCs that in turn proliferated, differentiated into fibroblast-like cells, and secreted ligament ECM components in response to fibroblast-conditioned medium [202]. A composite scaffold containing aligned, electrospun poly(ϵ -caprolactone-co-D,L-lactide) fibers embedded in a photocrosslinked N-methacrylated glycol chitosan hydrogel enabled deposition of ECM along the fibrous portions of the scaffold by ligament fibroblasts [203]. A braided PLLA scaffold incorporated with a gelatin hydrogel for controlled release of

bFGF and wrapped with a collagen membrane has been used in a rabbit ACL reconstruction model and showed enhanced mechanical strength, collagen deposition, vascularization, and increased mineralized matrix deposition in the bone tunnel when compared with PLLA alone [204].

Additional groups have investigated the use of composite materials for engineering tendon/ligament-bone interfaces. A stratified scaffold has been implemented using three distinct yet continuous phases has been fabricated using a series of knitted meshes and sintered microspheres [205, 206]. Each phase is designed to mimic a particular region of tissue in the interface: (1) a soft tissue phase consisting of sintered poly(glactin) 10:90 knitted mesh sheets seeded with fibroblasts, (2) an intermediate phase consisting of PLGA microspheres seeded with chondrocytes or left empty for generating a fibrocartilaginous region, and (3) a hard tissue phase consisting of composite microspheres with a 4:1 ratio of PLGA and bioactive glass seeded with osteoblasts. This tri-phasic scaffold supported cell proliferation, migration and phenotypic matrix production while maintaining distinct cellular regions and phase-specific ECM deposition over time *in vitro* [206]. This phase-specific matrix heterogeneity was preserved in an *in vivo* subcutaneous implantation model in rats, and increased mechanical properties were observed in comparison with acellular scaffolds [205].

Various ceramics have been incorporated within different scaffolds in an effort to mimic the mechanical properties of this specialized interface. A gradient of calcium phosphate has been generated on gelatin-coated electrospun poly(caprolactone) by varying the immersion time in solution [207]. This produced a gradient of mechanical properties where increased mineralization yielded increased stiffness of the construct. Fibroblasts seeded on this gradient scaffold preferentially adhered to and proliferated on areas with higher mineral content. Another group has incorporated hydroxyapatite into PEG-based hydrogels for engineering of the bone-ligament interface. Cells adhered to and proliferated on these PEG-hydroxyapatite gels, and this construct was able to anchor with a fibrin matrix seeded with primary tendon fibroblasts [208].

Graded distribution of mineral deposition has also been achieved by seeding fibroblasts onto scaffolds containing a spatial distribution of retrovirus encoding the osteogenic transcription factor Runx2/Cbfa1 [209]. This gradient of immobilized retrovirus was generated by controlling the density of poly(L-lysine) deposition on collagen scaffolds. Controlling the spatial distribution of Runx2 resulted in patterns of osteoblastic differentiation and mineralized matrix deposition, forming a gradient of mechanical properties that was preserved upon *in vivo* implantation of the scaffold at an ectopic site.

11.4

Conclusions and Future Work

Significant progress has been made in improving the design and engineering of biomaterials for tendon/ligament tissue engineering. Researchers continue to develop a better understanding of cellular interactions with both synthetic and natural materials that are affected by structural organization, size-scale effects of microstructures within the scaffold, degradability and remodeling, and spatio-temporal presentation of biochemical and mechanical

11 cues. This improved understanding continues to inform design of novel biomaterials and protocols for tissue engineering.

Several challenges remain to be solved in order to successfully engineer tendon or ligament tissue. Many of the approaches discussed in this review still fail to fully replicate the mechanical properties of native tendon/ligament tissue, particularly with respect to elastic modulus, tensile strength, and viscoelastic characteristics. Increasingly, researchers are employing bio-inspired approaches to accomplish this feat by generating natural or synthetic fibers in an architectural configuration more reminiscent of native tissue. Future approaches will likely require the use of hybrid materials that incorporate the advantages of both natural and synthetic materials. A significant challenge remains with engineering a strong bond between mechanically dissimilar materials at the interfaces between engineered tendons/ligament and their skeletal and muscular counterparts. Progress has been made in engineering tissue interfaces with graded mechanical properties, though these constructs have not been optimized for tensile load bearing. Unification of approaches with braided scaffolds that allow better tensile load bearing will further replicate the complex mechanical properties of tendon tissue. Additionally, there remains a paucity of information with regard to the interactions of seeded cells with a complex set of cellular (cell–cell contacts), soluble (cytokines, growth factors) and insoluble (substrate stiffness, matrix topography/topology) cues presented all at once within the injured and healing joint capsule and by the biomaterial itself. Achieving the proper scaffold network topology, topography, and mechanical properties from the fiber to fascicle scale will require more sophisticated macroscale scaffold fabrication processes and may additionally rely on microscale biosynthetic and self-assembly approaches mediated by incorporated cells. On-demand release strategies must be developed for controlled spatial and temporal presentation of soluble morphogens and ECM ligands through covalent or physical incorporation into existing scaffolds. Mimicking the physiological microenvironment encountered during directed tissue development and healing will aid in directing the recruitment and actions of regenerative cells (progenitor and terminally differentiated) that work in concert to generate not only fibrous tissue, but also blood vessels and tissue interfaces necessary for a successful tendon or ligament.

As evidenced by some of the more recently developed biomaterials outlined in this review, our knowledge of how cells respond to biomaterials and the extracellular milieu encountered in the regenerative environment continues to grow at a rapid and exciting pace. Advancements continue to be made in engineering more complex materials to direct cell fate by presenting several cues in a controlled context as part of an instructive environment. New materials will likely work with and enhance the body's own mechanisms of repair, mobilizing endogenous or transplanted cells to reproduce complex tendons and ligaments. Although no single biomaterial approach outlined in this review has completely replicated the outstanding mechanical properties of native tendon and ligament tissue, their functional sophistication continues to develop and holds much promise for future tissue engineering strategies.

Acknowledgements This work was supported by an Aircast Foundation grant. We also would like to graciously thank Dr. Yongzhi Qiu, Mr. Derek M. Doroski, and Mr. Peter J. Yang for their contributions to the figures depicted in this review.

References

1. D.L. Butler, M. Dessler, and H. Awad. Functional tissue engineering: Assessment of function in tendon and ligament repair. In: Guilak F, Butler DL, Goldstein SA, Mooney DJ, editors. *Functional tissue engineering*. New York: Springer; 2003. p. 213–26
2. S. Woo, K. Hildebrand, N. Watanabe, J. Fenwick, C. Papageorgiou, and J. Wang. Tissue engineering of ligament and tendon healing. *Clin Orthop*. 1999; **367**(Suppl):S312–23.
3. M. Khatod, W.H. Akeson, and D. Amiel. Ligament injury and repair. In: Pedowitz RA, O'Connor JJ, Akeson WH, editors. *Daniel's knee injuries*. 2 ed. Philadelphia: Lippincott Williams and Wilkins; 2003. p. 185–201.
4. S.L. Woo, S.D. Abramowitch, R. Kilger, and R. Liang. Biomechanics of knee ligaments: Injury, healing, and repair. *J Biomech*. 2006; **39**(1):1–20.
5. C.T. Laurencin, and J.W. Freeman. Ligament tissue engineering: An evolutionary materials science approach. *Biomaterials*. 2005; **26**(36):7530–6.
6. R. Langer, and J. Vacanti. Tissue engineering. *Science*. 1993; **260**(5110):920–6.
7. B. MacArthur, and R. Oreffo. Bridging the gap. *Nature*. 2005; **433**(7021):19.
8. M. Khatod, and D. Amiel. Ligament biochemistry and physiology. In: Pedowitz R, O'Connor JJ, Akeson WH, editors. *Daniel's knee injuries*. 2 ed. Philadelphia: Lippincott Williams and Wilkins; 2003. p. 31–42.
9. P.V. Komi. Relevance of in vivo force measurements to human biomechanics. *J Biomech*. 1990; **23**(Suppl 1):23–34.
10. P.V. Komi, S. Fukashiro, and M. Jarvinen. Biomechanical loading of achilles tendon during normal locomotion. *Clin Sports Med*. 1992; **11**(3):521–31.
11. D.M. Doroski, K.S. Brink, and J.S. Temenoff. Techniques for biological characterization of tissue-engineered tendon and ligament. *Biomaterials*. 2007; **28**(2):187–202.
12. E.H. Chen, and J. Black. Materials design analysis of the prosthetic anterior cruciate ligament. *J Biomed Mater Res*. 1980; **14**(5):567–86.
13. F.R. Noyes, and E.S. Grood. The strength of the anterior cruciate ligament in humans and rhesus monkeys. *J Bone Joint Surg Am*. 1976; **58**(8):1074–82.
14. R.B. Martin, D.B. Burr, and N.A. Sharkey. Mechanical properties of ligament and tendon. In: Martin RB, Burr DB, Sharkey NA, editors. *Skeletal tissue mechanics*. New York: Springer; 1998. p. 309–46.
15. J.H. Wang. Mechanobiology of tendon. *J Biomech*. 2006; **39**(9):1563–82.
16. N.G. Shrive, G.M. Thornton, D.A. Hart, and C.B. Frank. Ligament mechanics. In: Pedowitz RA, O'Connor JJ, Akeson WH, editors. *Daniel's knee injuries*. 2 ed. Philadelphia: Lippincott Williams and Wilkins; 2003. p. 97–112.
17. A.P. Rumian, A.L. Wallace, and H.L. Birch. Tendons and ligaments are anatomically distinct but overlap in molecular and morphological features – A comparative study in an ovine model. *J Orthop Res*. 2007; **25**(4):458–64.
18. S.L. Woo, K. An, C. Frank, G. Livesay, A. Ma, J. Zeminski, et al. Anatomy, biology, and biomechanics of tendon and ligament. In: Buckwalter J, Einhorn T, Simon S, editors. *Orthopaedic basic science: Biology and biomechanics of the musculoskeletal system*. 2nd ed. Rosemont: American Academy of Orthopaedic Surgeons; 2000. p. 582–616.
19. F. Silver, J. Freeman, and G. Seehra. Collagen self-assembly and the development of tendon mechanical properties. *J Biomech*. 2003; **36**(10):1529–53.
20. M. Benjamin, and J. Ralphs. The cell and developmental biology of tendons and ligaments. *Int Rev Cytol*. 2000; **196**:85–130.
21. C.T. Laurencin, A.M. Ambrosio, M.D. Borden, and J.A. Cooper, Jr. Tissue engineering: Orthopedic applications. *Annu Rev Biomed Eng*. 1999; **1**:19–46.

22. C. McNeilly, A. Banes, M. Benjamin, and J. Ralphs. Tendon cells in vivo form a three dimensional network of cell processes linked by gap junctions. *J Anat.* 1996; **189**:593–600.
23. J. Ralphs, M. Benjamin, A. Waggett, D. Russell, K. Messner, and J. Gao. Regional differences in cell shape and gap junction expression in rat achilles tendon: Relation to fibrocartilage differentiation. *J Anat.* 1998; **193**(2):215–22.
24. J. Ralphs, A. Waggett, and M. Benjamin. Actin stress fibers and cell–cell adhesion molecules in tendons: Organisation in vivo and response to mechanical loading of tendon cells in vitro. *Matrix Biol.* 2002; **21**(1):67–74.
25. Z. Ge, J.C. Goh, and E.H. Lee. Selection of cell source for ligament tissue engineering. *Cell Transplant.* 2005; **14**(8):573–83.
26. T.W. Lin, L. Cardenas, and L.J. Soslowsky. Biomechanics of tendon injury and repair. *J Biomech.* 2004; **37**(6):865–77.
27. S.L. Woo, R.E. Debski, J. Zeminski, S.D. Abramowitch, S.S. Saw, and J.A. Fenwick. Injury and repair of ligaments and tendons. *Annu Rev Biomed Eng.* 2000; **2**:83–118.
28. V. Duthon, C. Barea, S. Abrassart, J. Fasel, D. Fritschy, and J. Menetrey. Anatomy of the anterior cruciate ligament. *Knee Surg Sports Traumatol Arthrosc.* 2006; **14**(3):204–13.
29. S. Fukuta, M. Oyama, K. Kavalkovich, F. Fu, and C. Niyibizi. Identification of types II, IX and X collagens at the insertion site of the bovine achilles tendon. *Matrix Biol.* 1998; **17**(1):65–73.
30. D. Suzuki, M. Takahashi, M. Abe, and A. Nagano. Biochemical study of collagen and its crosslinks in the anterior cruciate ligament and the tissues used as a graft for reconstruction of the anterior cruciate ligament. *Connect Tissue Res.* 2008; **49**(1):42–7.
31. B. Wang, W. Liu, Y. Zhang, Y. Jiang, W. Zhang, G. Zhou, et al. Engineering of extensor tendon complex by an ex vivo approach. *Biomaterials.* 2008; **29**(20):2954–61.
32. D. Butler, E. Grood, F. Noyes, and R. Zernicke. Biomechanics of ligaments and tendons. *Exerc Sport Sci Rev.* 1978; **6**:125–81.
33. L. Jozsa, M. Lehto, P. Kannus, M. Kvist, A. Reffy, T. Vieno, et al. Fibronectin and laminin in achilles tendon. *Acta Orthop Scand.* 1989; **60**(4):469–71.
34. I.F. Williams, K.G. McCullagh, and I.A. Silver. The distribution of types I and III collagen and fibronectin in the healing equine tendon. *Connect Tissue Res.* 1984; **12**(3–4):211–27.
35. F. Grinnell. Fibronectin and wound healing. *J Cell Biochem.* 1984; **26**(2):107–16.
36. K. Kadler, A. Hill, and E. Canty-Laird. Collagen fibrillogenesis: Fibronectin, integrins, and minor collagens as organizers and nucleators. *Curr Opin Cell Biol.* 2008; **20**:495–501.
37. S. Takahashi, M. Leiss, M. Moser, T. Ohashi, T. Kitao, D. Heckmann, et al. The RGD motif in fibronectin is essential for development but dispensable for fibril assembly. *J Cell Biol.* 2007; **178**(1):167–78.
38. F. Elefteriou, J.Y. Exposito, R. Garrone, and C. Lethias. Binding of tenascin-X to decorin. *FEBS Lett.* 2001; **495**(1–2):44–7.
39. M. Chiquet, A. Renedo, F. Huber, and M. Fluck. How do fibroblasts translate mechanical signals into changes in extracellular matrix production? . *Matrix Biol.* 2003; **22**(1):73–80.
40. R. Chiquet-Ehrismann, and R. Tucker. Connective tissues: Signalling by tenascins. *Int J Biochem Cell Biol.* 2004; **36**(6):1085–9.
41. R. Probstmeier, and P. Pesheva. Tenascin-C inhibits beta1 integrin-dependent cell adhesion and neurite outgrowth on fibronectin by a disialoganglioside-mediated signaling mechanism. *Glycobiology.* 1999; **9**(2):101–14.
42. M.Z. Ilic, P. Carter, A. Tyndall, J. Dudhia, and C.J. Handley. Proteoglycans and catabolic products of proteoglycans present in ligament. *Biochem J.* 2005; **385**(Pt 2):381–8.
43. K.G. Vogel. What happens when tendons bend and twist? Proteoglycans. *J Musculoskeletal Neuronal Interact.* 2004; **4**(2):202–3.

44. M. Campbell, A. Winter, M. Ilic, and C. Handley. Catabolism and loss of proteoglycans from culture of bovine collateral ligament. *Arch Biochem Biophys*. 1996; **328**(1):64–72.
45. N. Hey, C. Handley, C. Ng, and B. Oakes. Characterization and synthesis of macromolecules by adult collateral ligament. *Biochim Biophys Acta*. 1990; **1034**(1):73–80.
46. G.D. Pins, D.L. Christiansen, R. Patel, and F.H. Silver. Self-assembly of collagen fibers. Influence of fibrillar alignment and decorin on mechanical properties. *Biophys J*. 1997; **73**(4):2164–72.
47. J.H. Yoon, and J. Halper. Tendon proteoglycans: Biochemistry and function. *J Musculoskelet Neuronal Interact*. 2005; **5**(1):22–34.
48. S. Woo, D. Smith, K. Hildebrand, J. Zemininski, and L. Johnson. Engineering the healing of the rabbit medial collateral ligament. *Med Biol Eng Comput*. 1998; **36**(3):359–64.
49. P. Yang, and J. Temenoff. Engineering orthopaedic tissue interfaces. *Tissue Eng B Rev*. 2009; **15**(2):127–41.
50. M. Benjamin, and J. Ralphs. Fibrocartilage in tendons and ligaments – An adaptation to compressive load. *J Anat*. 1998; **193**(4):481–94.
51. J. Tidball. Force transmission across muscle cell membranes. *J Biomech*. 1991; **24**(Suppl 1): 43–52.
52. J. Trotter. Structure-function considerations of muscle-tendon junctions. *Comp Biochem Physiol A*. 2002; **133**(4):1127–33.
53. J. Tidball. Myotendinous junction injury in relation to junction structure and molecular composition. *Exerc Sport Sci Rev*. 1991; **19**:419–45.
54. T. Andriacchi, P. Sabiston, K. DeHaven, L. Dahners, S. Woo, C. Frank, et al. Ligament: Injury and repair. In: Woo S, Buckwalter J, editors. *Injury and repair of the musculoskeletal soft tissues*. Park Ridge: American Academy of Orthopaedic Surgeons; 1988. p. 103–28.
55. J. Hyman, and S. Rodeo. Injury and repair of tendons and ligaments. *Phys Med Rehabil Clin N Am*. 2000; **11**(2):267–88.
56. S. Thomopolous, G. Hattersley, V. Rosen, M. Mertens, L. Galatz, G. Williams, et al. The localized expression of extracellular matrix components in healing tendon insertion sites: An in situ hybridization study. *J Orthop Res*. 2002; **20**(3):454–63.
57. Y. Xu, and G. Murrell. The basic science of tendinopathy. *Clin Orthop Relat Res*. 2008; **466**(7):1528–38.
58. G. Vunjak-Novakovic, G. Altman, R. Horan, and D.L. Kaplan. Tissue engineering of ligaments. *Annu Rev Biomed Eng*. 2004; **6**:131–56.
59. S.A. Fenwick, B.L. Hazleman, and G.P. Riley. The vasculature and its role in the damaged and healing tendon. *Arthritis Res*. 2002; **4**(4):252–60.
60. R.H. Gelberman, C.R. Chu, C.S. Williams, J.G. Seiler, 3rd, and D. Amiel. Angiogenesis in healing autogenous flexor-tendon grafts. *J Bone Joint Surg Am*. 1992; **74**(8):1207–16.
61. S.H. Liu, R.S. Yang, R. al-Shaikh, and J.M. Lane. Collagen in tendon, ligament, and bone healing. A current review. *Clin Orthop Relat Res*. 1995; **318**:265–78.
62. M.A. Gomez. The physiology and biochemistry of soft tissue healing. In: Griffin LY, editor. *Rehabilitation of the injured knee*. 2nd ed. St. Louis: Mosby Company; 1995. p. 34–44.
63. G. Baer, and C. Harner. Clinical outcomes of allograft versus autograft in anterior cruciate ligament reconstruction. *Clin Sports Med*. 2007; **26**(4):661–81.
64. J. Carey, W. Dunn, D. Dahm, S. Zeger, and K. Spindler. A systematic review of anterior cruciate ligament reconstruction with autograft compared with allograft. *J Bone Joint Surg Am*. 2009; **91**(9):2242–50.
65. A. Krych, J. Jackson, T. Hoskin, and D. Dahm. A meta-analysis of patellar tendon autograft versus patellar tendon allograft in anterior cruciate ligament reconstruction. *Arthroscopy*. 2008; **24**(3):292–8.

66. R. Miller, and F. Azar. Knee injuries. In: Canale S, Beaty J, editors. *Campbell's Operative Orthopaedics*. Philadelphia: Mosby Elsevier; 2008. p. 2346–575.
67. K. Spindler, J. Kuhn, K. Freedman, C. Matthews, R. Dittus, and F.J. Harrell. Anterior cruciate ligament reconstruction autograft choice: Bone-tendon-bone versus hamstring: Does it really matter? A systematic review. *Am J Sports Med*. 2004; **32**(8):1986–95.
68. F.A. Petrigliano, D.R. McAllister, and B.M. Wu. Tissue engineering for anterior cruciate ligament reconstruction: A review of current strategies. *Arthroscopy*. 2006; **22**(4):441–51.
69. F. Barber. Should allografts be used for routine anterior cruciate ligament reconstructions? *Arthroscopy*. 2003; **19**(4):421.
70. D. Jackson, J. Corsetti, and T. Simon. Biologic incorporation of allograft anterior cruciate ligament replacements. *Clin Orthop Relat Res*. 1996; **324**:126–33.
71. G.H. Altman, R.L. Horan, H.H. Lu, J. Moreau, I. Martin, J.C. Richmond, et al. Silk matrix for tissue engineered anterior cruciate ligaments. *Biomaterials*. 2002; **23**(20):4131–41.
72. T. Funakoshi, T. Majima, N. Iwasaki, S. Yamane, T. Masuko, A. Minami, et al. Novel chitosan-based hyaluronan hybrid polymer fibers as a scaffold in ligament tissue engineering. *J Biomed Mater Res A*. 2005; **74**(3):338–46.
73. S. Guelcher, A. Srinivasan, J. Dumas, J. Didier, S. McBride, and J. Hollinger. Synthesis, mechanical properties, biocompatibility, and biodegradation of polyurethane networks from lysine polyisocyanates. *Biomaterials*. 2008; **29**(12):1762–75.
74. D.S. Torres, T.M. Freyman, I.V. Yannas, and M. Spector. Tendon cell contraction of collagen-GAG matrices in vitro: Effect of cross-linking. *Biomaterials*. 2000; **21**(15):1607–19.
75. C. Hwang, Y. Park, J. Park, K. Lee, K. Sun, A. Khademhosseini, et al. Controlled cellular orientation on PLGA microfibers with defined diameters. *Biomed Microdevices*. 2009; **11**(4):739–46.
76. K. Moffat, A. Kwei, J. Spalazzi, S. Doty, W. Levine, and H. Lu. Novel nanofiber-based scaffold for rotator cuff repair and augmentation. *Tissue Eng A*. 2009; **15**(1):115–26.
77. G. Schulze-Tanzil, A. Mobasheri, P.D. Clegg, J. Sendzik, T. John, and M. Shakibaei. Cultivation of human tenocytes in high-density culture. *Histochem Cell Biol*. 2004; **122**(3):219–28.
78. M. Chiquet, L. Gelman, R. Lutz, and S. Maier. From mechanotransduction to extracellular matrix gene expression in fibroblasts. *Biochim Biophys Acta*. 2009; **1793**(5):911–20.
79. Z. Feng, M. Ishibashi, Y. Nomura, T. Kitajima, and T. Nakamura. Constraint stress, microstructural characteristics, and enhanced mechanical properties of a special fibroblast-embedded collagen construct. *Artif Organs*. 2006; **30**(11):870–7.
80. D.R. Henshaw, E. Attia, M. Bhargava, and J.A. Hannafin. Canine ACL fibroblast integrin expression and cell alignment in response to cyclic tensile strain in three-dimensional collagen gels. *J Orthop Res*. 2006; **24**(3):481–90.
81. S. Joshi, and K. Webb. Variation of cyclic strain parameters regulates development of elastic modulus in fibroblast/substrate constructs. *J Orthop Res*. 2008; **26**(8):1105–13.
82. C.H. Lee, H.J. Shin, I.H. Cho, Y.M. Kang, I.A. Kim, K.D. Park, et al. Nanofiber alignment and direction of mechanical strain affect the ECM production of human ACL fibroblasts. *Biomaterials*. 2005; **26**(11):1261–70.
83. J. Cooper, J. Sahota, W. Gorum, J. Carter, S. Doty, and C. Laurencin. Biomimetic tissue-engineered anterior cruciate ligament replacement. *Proc Natl Acad Sci U S A*. 2007; **104**(9):3049–54.
84. J. Freeman, M. Woods, D. Cromer, L. Wright, and C. Laurencin. Tissue engineering of the anterior cruciate ligament: The viscoelastic behavior and cell viability of a novel braid-twist scaffold. *J Biomater Sci Polym Ed*. 2009; **20**(12):1709–28.
85. P. Vavken, and M.M. Murray. Translational studies in ACL repair. *Tissue Eng B*. 2010; **16**(1):5–11.

86. L.D. Bellincampi, R.F. Closkey, R. Prasad, J.P. Zawadsky, and M.G. Dunn. Viability of fibroblast-seeded ligament analogs after autogenous implantation. *J Orthop Res.* 1998; **16** (4):414–20.
87. K.G. Cornwell, B.R. Downing, and G.D. Pins. Characterizing fibroblast migration on discrete collagen threads for applications in tissue regeneration. *J Biomed Mater Res A.* 2004; **71** (1):55–62.
88. K.G. Cornwell, P. Lei, S.T. Andreadis, and G.D. Pins. Crosslinking of discrete self-assembled collagen threads: Effects on mechanical strength and cell–matrix interactions. *J Biomed Mater Res A.* 2007; **80**(2):362–71.
89. D. Deng, W. Liu, F. Xu, Y. Yang, G. Zhou, W. Zhang, et al. Engineering human neo-tendon tissue in vitro with human dermal fibroblasts under static mechanical strain. *Biomaterials.* 2009; **30**(35):6724–30.
90. E. Gentleman, A.N. Lay, D.A. Dickerson, E.A. Nauman, G.A. Livesay, and K.C. Dee. Mechanical characterization of collagen fibers and scaffolds for tissue engineering. *Biomaterials.* 2003; **24**(21):3805–13.
91. E. Gentleman, G.A. Livesay, K.C. Dee, and E.A. Nauman. Development of ligament-like structural organization and properties in cell-seeded collagen scaffolds in vitro. *Ann Biomed Eng.* 2006; **34**(5):726–36.
92. T. Tischer, S. Vogt, S. Aryee, E. Steinhäuser, C. Adamczyk, S. Milz, et al. Tissue engineering of the anterior cruciate ligament: A new method using acellularized tendon allografts and autologous fibroblasts. *Arch Orthop Trauma Surg.* 2007; **127**(9):735–41.
93. A. Caplan. Mesenchymal stem cells. *J Orthop Res.* 1991; **9**(5):641–50.
94. M. Pittenger, A. Mackay, S. Beck, R. Jaiswal, R. Douglas, J. Mosca, et al. Multilineage potential of adult human mesenchymal stem cells. *Science.* 1999; **284**(5411):143–7.
95. H.A. Awad, G.P. Boivin, M.R. Dressler, F.N. Smith, R.G. Young, and D.L. Butler. Repair of patellar tendon injuries using a cell–collagen composite. *J Orthop Res.* 2003; **21** (3):420–31.
96. D.L. Butler, and H.A. Awad. Perspectives on cell and collagen composites for tendon repair. *Clin Orthop Relat Res.* 1999; **367**(Suppl):S324–32.
97. G.H. Altman, R.L. Horan, I. Martin, J. Farhadi, P.R. Stark, V. Volloch, et al. Cell differentiation by mechanical stress. *FASEB J.* 2002; **16**(2):270–2.
98. J. Chen, G.H. Altman, V. Karageorgiou, R. Horan, A. Collette, V. Volloch, et al. Human bone marrow stromal cell and ligament fibroblast responses on RGD-modified silk fibers. *J Biomed Mater Res A.* 2003; **67**(2):559–70.
99. S. Cristino, F. Grassi, S. Toneguzzi, A. Piacentini, B. Grigolo, S. Santi, et al. Analysis of mesenchymal stem cells grown on a three-dimensional HYAFF 11-based prototype ligament scaffold. *J Biomed Mater Res A.* 2005; **73**(3):275–83.
100. H.W. Ouyang, S.L. Toh, J. Goh, T.E. Tay, and K. Moe. Assembly of bone marrow stromal cell sheets with knitted poly (l-lactide) scaffold for engineering ligament analogs. *J Biomed Mater Res B Appl Biomater.* 2005; **75**(2):264–71.
101. J. Moreau, D. Bramano, R. Horan K, D.L. Kaplan, and G. Altman. Sequential biochemical and mechanical stimulation in the development of tissue engineered ligaments. *Tissue Eng A.* 2008; **14**(7):1161–72.
102. J. Moreau, J. Chen, D. Kaplan, and G. Altman. Sequential growth factor stimulation of bone marrow stromal cells in extended culture. *Tissue Eng.* 2006; **12**(10):2905–12.
103. J.E. Moreau, J. Chen, D.S. Bramono, V. Volloch, H. Chernoff, G. Vunjak-Novakovic, et al. Growth factor induced fibroblast differentiation from human bone marrow stromal cells in vitro. *J Orthop Res.* 2005; **23**(1):164–74.
104. J.E. Moreau, J. Chen, R.L. Horan, D.L. Kaplan, and G.H. Altman. Sequential growth factor application in bone marrow stromal cell ligament engineering. *Tissue Eng.* 2005; **11**(11–12): 1887–97.

- 11
105. G.H. Altman, H.H. Lu, R.L. Horan, T. Calabro, D. Ryder, D.L. Kaplan, et al. Advanced bioreactor with controlled application of multi-dimensional strain for tissue engineering. *J Biomech Eng.* 2002; **124**(6):742–9.
 106. J. Chen, R.L. Horan, D. Bramono, J.E. Moreau, Y. Wang, L.R. Geuss, et al. Monitoring mesenchymal stromal cell developmental stage to apply on-time mechanical stimulation for ligament tissue engineering. *Tissue Eng.* 2006; **12**(11):3085–95.
 107. A. Engler, S. Sen, H. Sweeney, and D. Discher. Matrix elasticity directs stem cell lineage specification. *Cell.* 2006; **126**(4):677–89.
 108. M. Chicurel, C. Chen, and D. Ingber. Cellular control lies in the balance of forces. *Curr Opin Cell Biol.* 1998; **10**(2):232–9.
 109. D. Ingber. Tensegrity-based mechanosensing from macro to micro. *Prog Biophys Mol Biol.* 2008; **97**(2–3):163–79.
 110. P. Janmey, J. Winer, M. Murray, and Q. Wen. The hard life of soft cells. *Cell Motil Cytoskeleton.* 2009; **66**(8):597–605.
 111. X. Chen, X. Song, Z. Yin, X. Zou, L. Wang, H. Hu, et al. Stepwise differentiation of human embryonic stem cells promotes tendon regeneration by secreting fetal tendon matrix and differentiation factors. *Stem Cells.* 2009; **27**(6):1276–87.
 112. Y. Bi, D. Ehrichiou, T. Kilts, C. Inkson, M. Embree, W. Sonoyama, et al. Identification of tendon stem/progenitor cells and the role of the extracellular matrix in their niche. *Nat Med.* 2007; **13**(10):1219–27.
 113. M. Cheng, H. Yang, T. Chen, and O. Lee. Isolation and characterization of multipotent stem cells from human cruciate ligaments. *Cell Prolif.* 2009; **42**(4):448–60.
 114. Z. Yin, X. Chen, J. Chen, W. Shen, T. Hieu Nguyen, L. Gao, et al. The regulation of tendon stem cell differentiation by the alignment of nanofibers. *Biomaterials.* 2009; **31**(8):2163–75.
 115. J. Zhang, and J. Wang. Mechanobiological response of tendon stem cells: Implications of tendon homeostasis and pathogenesis of tendinopathy. *J Orthop Res.* 2009; **28**(5):639–43.
 116. S.J. Hollister. Porous scaffold design for tissue engineering. *Nat Mater.* 2005; **4**(7):518–24.
 117. L.E. Freed, F. Guilak, X.E. Guo, M.L. Gray, R. Tranquillo, J.W. Holmes, et al. Advanced tools for tissue engineering: Scaffolds, bioreactors, and signaling. *Tissue Eng.* 2006; **12**(12):3285–305.
 118. G.H. Altman, F. Diaz, C. Jakuba, T. Calabro, R.L. Horan, J. Chen, et al. Silk-based biomaterials. *Biomaterials.* 2003; **24**(3):401–16.
 119. T.J. Koob. Biomimetic approaches to tendon repair. *Comp Biochem Physiol A Mol Integr Physiol.* 2002; **133**(4):1171–92.
 120. S. Woo. Tissue engineering: Use of scaffolds for ligament and tendon healing and regeneration. *Knee Surg Sports Traumatol Arthrosc.* 2009; **17**(6):559–60.
 121. A. Vieira, R. Guedes, and A. Marques. Development of ligament tissue biodegradable devices: A review. *J Biomech.* 2009; **42**(15):2421–30.
 122. Y. Liu, H. Ramanath, and D.-A. Wang. Tendon tissue engineering using scaffold enhancing strategies. *Trends Biotechnol.* 2008; **26**(4):201–9.
 123. S. Kumbar, R. James, S. Nukavarapu, and C. Laurencin. Electrospun nanofiber scaffolds: Engineering soft tissues. *Biomed Mater.* 2008; **3**(3):1–15.
 124. Z. Ge, F. Yang, J. Goh, S. Ramakrishna, and E. Lee. Biomaterials and scaffolds for ligament tissue engineering. *J Biomed Mater Res A.* 2006; **77**(3):639–52.
 125. D. Hutmacher. Scaffold design and fabrication technologies for engineering tissues – State of the art and future perspectives. *J Biomater Sci Polym Ed.* 2001; **12**(1):107–24.
 126. S. Yang, K. Leong, Z. Du, and C. Chua. The design of scaffolds for use in tissue engineering. Part I: Traditional factors. *Tissue Eng.* 2001; **7**(6):679–89.
 127. G. Ryan, A. Pandit, and D. Apatsidis. Fabrication methods of porous metals for use in orthopaedic applications. *Biomaterials.* 2006; **27**(13):2651–70.

128. P. Bagnaninchi, Y. Yang, N. Zghoul, N. Maffulli, R. Wang, and A. El Haj. Chitosan micro-channel scaffolds for tendon tissue engineering characterized using optical coherence tomography. *Tissue Eng.* 2007; **13**(2):323–31.
129. C. Agrawal, and B. Ray. Biodegradable polymeric scaffolds for musculoskeletal tissue engineering. *J Biomed Mater Res.* 2001; **55**(2):141–50.
130. S. Yang, K. Leong, Z. Du, and C. Chua. The design of scaffolds for use in tissue engineering. Part II: Rapid prototyping techniques. *Tissue Eng.* 2001; **8**(1):1–11.
131. L. Moroni, J. de Wijn, and C. van Blitterswijk. Integrating novel technologies to fabricate smart scaffolds. *J Biomater Sci Polym Ed.* 2008; **19**(5):543–72.
132. B. Lanfer, F. Seib, U. Freudenberg, D. Stamov, T. Bley, M. Bornhauser, et al. The growth and differentiation of mesenchymal stem and progenitor cells cultured on aligned collagen matrices. *Biomaterials.* 2009; **30**(30):5950–8.
133. D. Zeugolis, G. Paul, and G. Attenburrow. Cross-linking of extruded collagen fibers – A biomimetic three-dimensional scaffold for tissue engineering applications. *J Biomed Mater Res A.* 2009; **89**(4):895–908.
134. D. Zeugolis, R. Paul, and G. Attenburrow. Extruded collagen-polyethylene glycol fibers for tissue engineering applications. *J Biomed Mater Res B.* 2007; **85**(2):343–52.
135. J. Guan, K. Fujimoto, M. Sacks, and W. Wagner. Preparation and characterization of highly porous, biodegradable polyurethane scaffolds for soft tissue applications. *Biomaterials.* 2005; **26**(18):3961–71.
136. H.A. Awad, D.L. Butler, M.T. Harris, R.E. Ibrahim, Y. Wu, R.G. Young, et al. In vitro characterization of mesenchymal stem cell-seeded collagen scaffolds for tendon repair: Effects of initial seeding density on contraction kinetics. *J Biomed Mater Res.* 2000; **51**(2):233–40.
137. E. Place, N. Evans, and M. Stevens. Complexity in biomaterials for tissue engineering. *Nat Mater.* 2009; **8**(6):457–70.
138. D. Williams. On the nature of biomaterials. *Biomaterials.* 2009; **30**(30):5897–909.
139. E. Place, J. George, C. Williams, and M. Stevens. Synthetic polymer scaffolds for tissue engineering. *Chem Soc Rev.* 2009; **38**(4):1139–51.
140. P. Ma. Biomimetic materials for tissue engineering. *Adv Drug Deliv Rev.* 2008; **60**(2):184–98.
141. W. Grayson, T. Martens, G. Eng, M. Radisic, and G. Vunjak-Novakovic. Biomimetic approach to tissue engineering. *Semin Cell Dev Biol.* 2009; **20**(6):665–73.
142. S. Badylak, D. Freytes, and T. Gilbert. Extracellular matrix as a biological scaffold material: Structure and function. *Acta Biomater.* 2009; **5**(1):1–13.
143. S. Guelcher. Biodegradable polyurethanes: Synthesis and applications in regenerative medicine. *Tissue Eng B.* 2008; **14**(1):3–17.
144. K. Webb, R.W. Hitchcock, R.M. Smeal, W. Li, S.D. Gray, and P.A. Tresco. Cyclic strain increases fibroblast proliferation, matrix accumulation, and elastic modulus of fibroblast-seeded polyurethane constructs. *J Biomech.* 2006; **39**(6):1136–44.
145. B. Cole, A. Gomoll, A. Yanke, T. Pylawka, P. Lewis, J. MacGillivray, et al. Biocompatibility of a polymer patch for rotator cuff repair. *Knee Surg Sports Traumatol Arthrosc.* 2007; **15**(5):632–7.
146. C. Bashur, R. Shaffer, L. Dahlgren, S. Guelcher, and A. Goldstein. Effect of fiber diameter and alignment of electrospun polyurethane meshes on mesenchymal progenitor cells. *Tissue Eng A.* 2009; **15**(9):2435–45.
147. P. Gunatillake, R. Mayadunne, and R. Adhikare. Recent developments in biodegradable synthetic polymers. *Biotechnol Annu Rev.* 2006; **12**:301–47.
148. L. Heckman, J. Fiedler, T. Mattes, M. Dauner, and R. Brenner. Interactive effects of growth factors and three-dimensional scaffolds on multipotent mesenchymal stromal cells. *Biotechnol Appl Biochem.* 2008; **49**(3):185–94.

- 11
149. H.H. Lu, J.A. Cooper, Jr., S. Manuel, J.W. Freeman, M.A. Attawia, F.K. Ko, et al. Anterior cruciate ligament regeneration using braided biodegradable scaffolds: In vitro optimization studies. *Biomaterials*. 2005; **26**(23):4805–16.
 150. L. Heckman, H. Schlenker, J. Fiedler, R. Brenner, M. Dauner, G. Bergenthal, et al. Human mesenchymal progenitor cell responses to a novel textured poly(L-lactide) scaffold for ligament tissue engineering. *J Biomed Mater Res B*. 2006; **81**(1):82–90.
 151. J.A. Cooper, Jr., L.O. Bailey, J.N. Carter, C.E. Castiglioni, M.D. Kofron, F.K. Ko, et al. Evaluation of the anterior cruciate ligament, medial collateral ligament, achilles tendon and patellar tendon as cell sources for tissue-engineered ligament. *Biomaterials*. 2006; **27**(13):2747–54.
 152. J.A. Cooper, H.H. Lu, F.K. Ko, J.W. Freeman, and C.T. Laurencin. Fiber-based tissue-engineered scaffold for ligament replacement: Design considerations and in vitro evaluation. *Biomaterials*. 2005; **26**(13):1523–32.
 153. J. Freeman, M. Woods, and C. Laurencin. Tissue engineering of the anterior cruciate ligament using a braid-twist scaffold design. *J Biomech*. 2007; **40**(9):2029–36.
 154. F. van Eijk, D. Saris, L. Creemers, J. Riesle, W. Willems, C. van Blitterswijk, et al. The effect of timing of mechanical stimulation on proliferation and differentiation of goat bone marrow stem cells cultured on braided PLGA scaffolds. *Tissue Eng A*. 2008; **14**(8):1425–33.
 155. F. van Eijk, D. Saris, N. Fedorovich, M. Kruyt, W. Willems, A. Verbout, et al. In vivo matrix production by bone marrow stromal cells seeded on PLGA scaffolds for ligament tissue engineering. *Tissue Eng A*. 2009; **15**(10):3109–17.
 156. J. Jenner, F. van Eijk, D. Saris, W. Willems, W. Dhert, and L. Creemers. Effect of transforming growth factor-beta and growth differentiation factor-5 on proliferation and matrix production by human bone marrow stromal cells cultured on braided poly lactic-co-glycolic acid scaffolds for ligament tissue engineering. *Tissue Eng*. 2007; **13**(7):1573–82.
 157. Z. Feng, Y. Tateishi, Y. Nomura, T. Kitajima, and T. Nakamura. Construction of fibroblast-collagen gels with orientated fibrils induced by static or dynamic stress: Toward the fabrication of small tendon grafts. *J Artif Organs*. 2006; **9**(4):220–5.
 158. N. Juncosa-Melvin, G. Boivin, M. Galloway, C. Gooch, J. West, and D. Butler. Effects of cell-to-collagen ratio in stem cell-seeded constructs for achilles tendon repair. *Tissue Eng*. 2006; **12**(4):681–9.
 159. N. Juncosa-Melvin, K. Matlin, R. Holdcraft, V. Nirmalanandhan, and D. Butler. Mechanical stimulation increases collagen type I and collagen type III gene expression of stem cell–collagen sponge constructs for patellar tendon repair. *Tissue Eng*. 2007; **13**(6):1219–26.
 160. N. Juncosa-Melvin, J. Shearn, G. Boivin, C. Gooch, M. Galloway, J. West, et al. Effects of mechanical stimulation on the biomechanics and histology of stem cell–collagen sponge constructs for rabbit patellar tendon repair. *Tissue Eng*. 2006; **12**(8):2291–300.
 161. C. Kuo, and R. Tuan. Mechanoactive tenogenic differentiation of human mesenchymal stem cells. *Tissue Eng A*. 2008; **14**(10):1615–27.
 162. L. McMahon, V. Campbell, and P. Prendergast. Involvement of stretch-activated ion channels in strain regulated glycosaminoglycan synthesis in mesenchymal stem cell-seeded 3D scaffolds. *J Biomech*. 2008; **41**(9):2055–9.
 163. V. Nirmalanandhan, M. Dressler, J. Shearn, N. Juncosa-Melvin, M. Rao, C. Gooch, et al. Mechanical stimulation of tissue engineered tendon constructs: Effect of scaffold materials. *J Biomech Eng*. 2007; **129**(6):919–23.
 164. V. Nirmalanandhan, M. Rao, M. Sacks, B. Haridas, and D. Butler. Effect of length of the engineered tendon construct on its structure–function relationships in culture. *J Biomech*. 2007; **40**(11):2523–9.
 165. V. Nirmalanandhan, J. Shearn, N. Juncosa-Melvin, M. Rao, C. Gooch, A. Jain, et al. Improving linear stiffness of the cell-seeded collagen sponge constructs by varying the components of the mechanical stimulus. *Tissue Eng A*. 2008; **14**(11):1883–91.

166. J. Shearn, N. Juncosa-Melvin, G. Boivin, M. Galloway, W. Goodwin, C. Gooch, et al. Mechanical stimulation of tendon tissue engineered constructs: Effects on construct stiffness, repair biomechanics, and their correlation. *J Biomech Eng.* 2007; **129**(6):848–54.
167. X. Cheng, U. Gurkan, C. Dehen, M. Tate, H. Hillhouse, G. Simpson, et al. An electrochemical fabrication process for the assembly of anisotropically oriented collagen bundles. *Biomaterials.* 2008; **29**(22):3278–88.
168. S. Liao, C. Chan, and S. Ramakrishna. Stem cells and biomimetic materials strategies for tissue engineering. *Mater Sci Eng C.* 2008; **28**(8):1189–202.
169. S. Hankemeier, C. Hurschler, J. Zeichen, M. van Griensven, B. Miller, R. Meller, et al. Bone marrow stromal cells in a liquid fibrin matrix improve the healing process of patellar tendon window defects. *Tissue Eng A.* 2009; **15**(5):1019–30.
170. S. Hankemeier, M. van Griensven, M. Ezechieli, T. Barkhausen, M. Austin, M. Jagodzinski, et al. Tissue engineering of tendons and ligaments by human bone marrow stromal cells in a liquid fibrin matrix in immunodeficient rats: Results of a histologic study. *Arch Orthop Trauma Surg.* 2007; **127**(9):815–21.
171. M.M. Murray, B. Forsythe, F. Chen, S.J. Lee, J.J. Yoo, A. Atala, et al. The effect of thrombin on ACL fibroblast interactions with collagen hydrogels. *J Orthop Res.* 2006; **24**(3):508–15.
172. M.M. Murray, S.D. Martin, and M. Spector. Migration of cells from human anterior cruciate ligament explants into collagen-glycosaminoglycan scaffolds. *J Orthop Res.* 2000; **18**(4):557–64.
173. M.M. Murray, and M. Spector. The migration of cells from the ruptured human anterior cruciate ligament into collagen-glycosaminoglycan regeneration templates in vitro. *Biomaterials.* 2001; **22**(17):2393–402.
174. H. Fan, H. Liu, S. Toh, and J. Goh. Anterior cruciate ligament regeneration using mesenchymal stem cells and silk scaffold in large animal model. *Biomaterials.* 2009; **30**(28):4967–77.
175. H. Fan, H. Liu, E. Wong, S. Toh, and J. Goh. In vivo study of anterior cruciate ligament regeneration using mesenchymal stem cells and silk scaffold. *Biomaterials.* 2008; **29**(33):3324–37.
176. R. Horan, I. Toponarski, H. Boepple, P. Weitzel, J. Richmond, and G. Altman. Design and characterization of a scaffold for anterior cruciate ligament engineering. *J Knee Surg.* 2009; **22**(1):82–92.
177. H. Liu, H. Fan, S. Toh, and J. Goh. A comparison of rabbit mesenchymal stem cells and anterior cruciate ligament fibroblasts responses on combined silk scaffolds. *Biomaterials.* 2008; **29**(10):1443–53.
178. H. Liu, H. Fan, Y. Wang, S. Toh, and J. Goh. The interaction between a combined knitted silk scaffold and microporous silk sponge with human mesenchymal stem cells for ligament tissue engineering. *Biomaterials.* 2008; **29**(6):662–74.
179. H. Liu, Z. Ge, Y. Wang, S. Toh, V. Sutthikhum, and J. Goh. Modification of sericin-free silk fibers for ligament tissue engineering application. *J Biomed Mater Res B.* 2007; **82**(1):129–38.
180. C. Craig, and C. Riekel. Comparative architecture of silks, fibrous proteins and their encoding genes in insects and spiders. *Comp Biochem Physiol B Biochem Mol Biol.* 2002; **133**(4):493–507.
181. J. Perez-Rigueiro, C. Viney, J. Llorca, and M. Elices. Mechanical properties of silkworm silk in liquid media. *Polymer.* 2000; **41**(23):8433–9.
182. P. Basile, T. Dadali, J. Jacobson, S. Hasslund, M. Ulrich-Vinther, K. Soballe, et al. Freeze-dried tendon allografts as tissue engineering scaffolds for Gdf-5 gene delivery. *Mol Ther.* 2008; **16**(3):466–73.
183. A. Chong, J. Riboh, R. Smith, D. Lindsey, H. Pham, and J. Chang. Flexor tendon tissue engineering: Acellularized and reseeded tendon constructs. *Plast Reconstr Surg.* 2009; **123**(6):1759–66.

- 11
184. J. Ingram, S. Korossis, G. Howling, J. Fisher, and E. Ingham. The use of ultrasonication to aid recellularization of acellular natural tissue scaffolds for use in anterior cruciate ligament reconstruction. *Tissue Eng.* 2007; **13**(7):1561–72.
 185. F. Li, H. Jia, and C. Yu. ACL reconstruction in a rabbit model using irradiated achilles allograft seeded with mesenchymal stem cells or PDGF-BB gene transfected mesenchymal stem cells. *Knee Surg Sports Traumatol Arthrosc.* 2007; **15**(10):1219–27.
 186. M. Mahirogullari, C. Ferguson, P. Whitlock, K. Stabile, and G. Poehling. Freeze-dried allografts for anterior cruciate ligament reconstruction. *Clin Sports Med.* 2007; **26**(4):625–37.
 187. H. Omae, C. Zhao, Y. Sun, K. An, and P. Amadio. Multilayer tendon slices seeded with bone marrow stromal cells: A novel composite for tendon engineering. *J Orthop Res.* 2009; **27**(7):937–42.
 188. P. Vavken, S. Joshi, and M. Murrari. TRITON-X is the most effective among three decellularization agents for ACL tissue engineering. *J Orthop Res.* 2009; **27**(12):1612–8.
 189. P. Whitlock, T. Smith, G. Poehling, J. Shilt, and M. van Dyke. A naturally derived, cyto-compatible, and architecturally optimized scaffold for tendon and ligament regeneration. *Biomaterials.* 2007; **28**(29):4321–9.
 190. J. Chen, C. Willers, J. Xu, A. Wang, and M. Zheng. Autologous tenocyte therapy using porcine-derived bioscaffolds for massive rotator cuff defect in rabbits. *Tissue Eng.* 2007; **13**(7):1479–91.
 191. T. Gilbert, A. Stewart-Akers, A. Simmons-Byrd, and S. Badylak. Degradation and remodeling of small intestinal submucosa in canine achilles tendon repair. *J Bone Joint Surg Am.* 2007; **89**(3):621–30.
 192. R. Liang, S. Woo, T. Nguyen, P. Liu, and A. Almarza. Effects of a bioscaffold on collagen fibrillogenesis in healing medial collateral ligament in rabbits. *J Orthop Res.* 2008; **26**(8):1098–104.
 193. T. Zantop, T. Gilbert, M. Yoder, and S. Badylak. Extracellular matrix scaffolds are repopulated by bone marrow-derived cells in a mouse model of achilles tendon repair. *J Orthop Res.* 2006; **24**(6):1299–309.
 194. C. Androjna, R. Spragg, and K. Derwin. Mechanical conditioning of cell-seeded small intestinal submucosa: A potential tissue-engineering strategy for tendon repair. *Tissue Eng.* 2007; **13**(2):233–43.
 195. S. Woo, Y. Takakura, R. Liang, F. Jia, and D. Moon. Treatment with bioscaffold enhances the fibril morphology and the collagen composition of healing medial collateral ligament in rabbits. *Tissue Eng.* 2006; **12**(1):159–66.
 196. K. Murphy, I. Mushkudiani, D. Kao, A. Levesque, H. Hawkins, and L. Gould. Successful incorporation of tissue-engineered porcine small-intestinal submucosa as substitute flexor tendon graft is mediated by elevated TGF-beta1 expression in the rabbit. *J Hand Surg Am.* 2008; **33**(7):1168–78.
 197. R. Abousleiman, Y. Reyes, P. McFetridge, and V. Sikavitsas. Tendon tissue engineering using cell-seeded umbilical veins cultured in a mechanical stimulator. *Tissue Eng A.* 2009; **15**(4):787–95.
 198. S. Badhe, T. Lawrence, F. Smith, and P. Lunn. An assessment of porcine dermal xenograft as an augmentation graft in the treatment of extensive rotator cuff tears. *J Shoulder Elbow Surg.* 2008; **17**(1 Suppl):35S–9S.
 199. D. Coons, and F. Barber. Tendon graft substitutes – Rotator cuff patches. *Sports Med Arthrosc Rev.* 2006; **14**(3):185–90.
 200. K. Derwin, A. Baker, R. Spragg, D. Leigh, and J. Iannotti. Commercial extracellular matrix scaffolds for rotator cuff tendon repair. *J Bone Joint Surg Am.* 2006; **88**(12):2665–72.
 201. M. Fini, P. Torricelli, G. Giavaresi, R. Rotini, A. Castagna, and R. Giardino. In vitro study comparing two collagenous membranes in view of their clinical application for rotator cuff tendon regeneration. *J Orthop Res.* 2007; **25**(1):98–107.

202. H. Fan, H. Liu, S. Toh, and J. Goh. Enhanced differentiation of mesenchymal stem cells co-cultured with ligament fibroblasts on gelatin/silk fibroin scaffold. *Biomaterials*. 2008; **29**(8):1017–27.
203. J. Hayami, D. Surrao, S. Waldman, and B. Amsden. Design and characterization of a biodegradable composite scaffold for ligament tissue engineering. *J Biomed Mater Res A*. 2009; **92**(4):1407–20.
204. Y. Kimura, A. Hokugo, T. Takamoto, Y. Tabata, and H. Kurosawa. Regeneration of anterior cruciate ligament by biodegradable scaffold combined with local controlled release of basic fibroblast growth factor and collagen wrapping. *Tissue Eng C*. 2008; **14**(1):47–57.
205. J. Spalazzi, E. Dagher, S. Doty, X. Guo, S. Rodeo, and H. Lu. In vivo evaluation of a multiphased scaffold designed for orthopaedic interface tissue engineering and soft tissue-to-bone integration. *J Biomed Mater Res A*. 2008; **86**(1):1–12.
206. J. Spalazzi, S. Doty, K. Moffat, W. Levine, and H. Lu. Development of controlled matrix heterogeneity on a triphasic scaffold for orthopedic interface tissue engineering. *Tissue Eng*. 2006; **12**(12):3497–508.
207. X. Li, J. Xie, J. Lipner, X. Yuan, S. Thomopolous, and Y. Xia. Nanofiber scaffolds with gradations in mineral content for mimicking the tendon-to-bone insertion site. *Nano Lett*. 2009; **9**(7):2763–8.
208. J. Paxton, K. Donnelly, R. Keatch, and K. Baar. Engineering bone-ligament interface using polyethylene glycol diacrylate incorporated with hydroxyapatite. *Tissue Eng A*. 2009; **15**(6):1201–9.
209. J. Phillips, K. Burns, J. Le Doux, R. Guldborg, and A. Garcia. Engineering graded tissue interfaces. *Proc Natl Acad Sci U S A*. 2008; **105**(34):12170–5.

Steven B. Nicoll

Contents

12.1	Introduction	344
12.2	Current Bone Grafting Materials	345
12.2.1	Demineralized Bone Matrix	346
12.2.2	Calcium Phosphate Ceramics and Bioactive Glasses	346
12.2.3	Natural and Synthetic Polymers	347
12.3	New Developments in Bone Grafting Materials	347
12.3.1	Self-Assembled Biomimetic Materials	348
12.3.2	Nanocomposite Scaffolds (Collagen)	349
12.3.3	Nanocomposite Scaffolds (Synthetics)	350
12.3.4	Nanocomposite Scaffolds (Natural Materials)	352
12.3.5	Microsphere-Based Scaffolds	353
12.3.6	Nanophase Ceramics and Material Properties/Processing	353
12.4	Future Directions	356
	References	357

Abstract Bone is the principal component of the skeletal system. It is comprised of an extracellular matrix that is characterized by a hierarchical and heterogeneous structure with features that span from the nanoscale to the macroscale and interact to perform the various functions of the tissue. For large defects, traditional therapies for bone repair include tissue grafts, which are limited by supply (autografts) and the potential for disease transmission (allografts). Alternatively, commercially available products used for bone reconstruction do not necessarily approximate the hierarchical nanoscale structure of the natural tissue. This chapter will focus on recent advances in the development of select biomimetic, self-assembled and nanocomposite materials for use in the repair and regeneration of osseous tissues.

Keywords Bone • Ceramic • Collagen • Composite • Hydroxyapatite • Polymer

S.B. Nicoll

Department of Biomedical Engineering, Grove School of Engineering, The City College of New York, Steinman Hall, Room 431, 160 Convent Avenue, New York, NY 10031, USA
e-mail: snicoll@ccny.cuny.edu

12.1

Introduction

Bone is a dynamic, vascularized hard tissue which serves many vital functions in vertebrates [1, 2]. As the principal component of the skeletal system, bone supports the weight of the body, allows for locomotion and protects the vital organs while also acting as a repository for various ionic species (i.e., calcium, phosphorous, magnesium, fluoride) which are essential for mineral homeostasis and other metabolic processes. Depending on the anatomical location, the structure and properties of bone can vary greatly. However, there are certain features that are common to all forms of bone. The inorganic mineral phase (50–70% by weight) consists of small, plate-like crystals (50 nm in length, 25 nm in width, and 2–5 nm in thickness) of a poorly crystalline, carbonate-substituted apatite, which contain vacancies and impurities and provides the high compressive strength associated with the tissue [3–6]. The organic matrix constitutes 20–40% of the weight and is comprised mostly of type I collagen (90%) which assembles into fibers (20–150 nm in diameter) that impart resistance to tensile and torsional forces. The noncollagenous proteins of the organic matrix consist of proteoglycans, glycoproteins, and γ -carboxyglutamic acid-containing proteins (i.e., osteocalcin) which determine structural organization, mediate cell attachment, and regulate mineralization [3, 4]. The native cell type responsible for bone matrix elaboration is the osteoblast, which originates from non-hematopoietic mesenchymal progenitor cells in the bone marrow [7].

The hierarchical structure of bone extends over multiple length scales. At the nanoscale (0.5–200 nm), the functional components are comprised of collagen fibrils embedded with calcium phosphate crystals and noncollagenous matrix proteins [8–11]. The major microstructural units (1–500 μm) are the osteons, which consist of concentric lamellae that surround Haversian canals (3–7 μm in diameter) and allow for blood and nutrient flow. At the macrostructural level, closely packed osteons further assemble into cortical (i.e., compact) bone, while a more loosely organized, porous matrix with concentric lamellae of collagen fibrils form cancellous (i.e., spongy) bone. The heterogeneous and anisotropic nature of the tissue gives rise to unique mechanical properties (Table 12.1) that have been difficult to replicate using engineered biomaterials [10–12].

As one of the few human tissues capable of regeneration, bone is able to naturally heal in response to injury. However, there are occasions in which bone healing must be augmented,

Table 12.1 Mechanical properties of cortical and cancellous bone [12]

Property	Cortical bone	Cancellous bone
Compressive strength (MPa)	100–230	2–12
Flexural, tensile strength (MPa)	50–150	10–20
Strain to failure (%)	1–3	5–7
Fracture toughness ($\text{MPa m}^{1/2}$)	2–12	–
Young's modulus (GPa)	7–30	0.5–0.05

such as in spinal fusion (arthrodesis) or for the treatment of fracture nonunions or skeletal deformities caused by infection, trauma, or tumor resection [13]. In such cases, osseous tissue repair is facilitated using bone grafts, accounting for over 600,000 procedures annually in the United States [14]. In order for a bone graft to successfully integrate into the native tissue, the material should be osteogenic, osteoinductive, and osteoconductive [15]. The gold standard for bone grafting is the autograft, which utilizes bone tissue harvested from another location in the patient's skeleton, most commonly from the iliac crest. Autogenous bone grafts contain progenitor or differentiated cells to promote osteogenesis, growth and differentiation factors that enable osteoinduction, and a three-dimensional matrix that allows for osteoconduction. However, the use of autografts has limitations, including availability, donor site morbidity, pain, infection, nerve damage, and hemorrhage [15–18]. Allografts, which are harvested from cadavers or other donors, are also used for bone grafting procedures. Allogeneic material is more readily available, but can result in disease transmission, immune response, and inferior mechanical and biological properties due to sterilization procedures [15].

Given the limitations associated with current bone graft technologies, considerable effort has been directed at developing viable alternatives for the restoration of osseous tissues. A number of natural and synthetic materials have been used in bone grafting procedures due to their abundant supply and ease of processing. Ideally, implementation of this strategy for bone tissue repair would incorporate the advantages of allografts and autografts. Specifically, engineered bone constructs should be readily available, and possess osteogenic, osteoinductive, and osteoconductive properties to promote functional integration with surrounding host tissue (i.e., osseointegration). A construct that could be developed *in vitro* or in the operating room just prior to implantation may circumvent the limitations of existing repair techniques and aid in the regeneration of damaged and diseased osseous tissues.

Presently, the commercially available products used for bone reconstruction are acellular materials (i.e., demineralized bone matrix, calcium-phosphate ceramics, resorbable polyesters, collagen) that do not necessarily approximate the hierarchical nanoscale structure of the natural tissue. As such, this chapter will focus on recent advances in the development of select biomimetic, self-assembled and nanocomposite materials for potential use in engineering living tissue equivalents for bone regeneration.

12.2 Current Bone Grafting Materials

From the perspective of materials design, a bone graft substitute should satisfy multiple criteria in order to ensure success in a clinical setting [19, 20]. Such materials should: (1) induce a minimal foreign body or immune response, (2) stimulate cell adhesion, osteogenic differentiation and bonding to bone, (3) provide an interconnected porous structure for cellular infiltration, vascularization and nutrient transport, (4) possess mechanical properties that approximate those of the host bone tissue, (5) degrade safely via controlled dissolution, (6) allow for fabrication in different formats and geometries for a range of applications, and (7) undergo sterilization without altering material properties. Several of these criteria have

12 been met by current products used for bone reconstruction. Nevertheless, there is still a need for new biomaterials with improved functionality and versatility.

12.2.1

Demineralized Bone Matrix

Demineralized bone matrix (DBM) is produced by the acid extraction of allograft bone, which removes the mineralized component and preserves type I collagen and noncollagenous proteins, including numerous growth factors [21, 22]. Commercially available DBM (Grafton, Osteotech; Accell, Integra Life Sciences), may be manufactured in many forms, including injectable gels, putty and flexible strips, all of which lack structural strength but possess osteoconductivity and osteoinductive agents. The osteoinductive ability of DBM to stimulate osseous tissue regeneration is dependent upon the activity of osteogenic growth factors, including bone morphogenic proteins (BMPs). DBM is considered “minimally manipulated” human allograft tissue by the Food and Drug Administration, with no mandated growth factor concentration or osteoinductive properties [23]. As a result, the various commercially available formulations of DBM exhibit a wide range of biologic functionality due to variations in BMP content associated with each preparation. In addition, DBM is also subject to the inherent shortcomings of allograft tissue (i.e., disease transmission).

12.2.2

Calcium Phosphate Ceramics and Bioactive Glasses

Hydroxyapatite (HA) is a major mineral component of calcified tissues [8, 9]. Synthetic HA ($\text{Ca}_{10}(\text{PO}_4)_6(\text{OH})_2$) and other calcium phosphates (i.e., β -tricalcium phosphate) have been used extensively in the clinical arena for bone repair applications due to their similarity with the mineral phase of the native tissue [24–26]. These materials possess excellent osteoconductive properties, as they support osteoblast adhesion and proliferation, and form strong bonds to adjacent hard and soft tissues, improving implant fixation. The resorption of calcium phosphate ceramics is dependent on the crystallinity of the lattice (i.e., less crystalline β -tricalcium phosphate degrades 3–12 times faster than HA), and can be tailored to match the rate of new bone matrix elaboration [27]. In addition, nanocrystalline bioceramics degrade more readily than conventional grain size calcium phosphates, allowing for further control over the dissolution rate [28]. Nanohydroxyapatite variants can be prepared by precipitation using emulsion, template and sol-gel techniques, but these methods rely on highly controlled parameters (reactant concentration, pH and temperature), which present technical challenges for reproducibility [29]. Existing commercial products range from cancellous bone void fillers composed of β -tricalcium phosphate (VITOSS, Orthovita) to HA and calcium carbonate bone graft substitutes (Pro Osteon, Biomet Osteobiologics). Although the various calcium phosphate ceramics have been used clinically for more than 2 decades, they are limited due to insufficient mechanical properties. Specifically, they possess high moduli and compressive strength but have a low fracture toughness and are

susceptible to brittle failure. Therefore, calcium phosphate ceramics have largely been used in non-load bearing applications (i.e., middle ear implants) and as bone fillers [30, 31].

Bioactive glasses have also been used for many years in powder form as bone defect fillers. The first bioactive glass developed by Hench and colleagues was in the $\text{Na}_2\text{O}-\text{CaO}-\text{SiO}_2-\text{P}_2\text{O}_5$ system and termed BioGlass[®] [32–34]. The primary advantage of such calcium and phosphorous-containing silica glasses is the rapid rate of surface reactivity, which leads to the formation of a carbonated HA on the material when exposed to biological fluids [32, 35, 36]. The initial surface reaction involves rapid ion exchange (Na^+ , Ca^{2+} , H^+ , H_3O^+) followed by a polycondensation reaction of surface silanols to produce a thick silica gel layer that provides nucleation sites for crystallization [34]. The resulting bone-like apatite is equivalent to the inorganic mineral phase of bone and bonds tightly to neighboring tissue. Bioactive glasses are also degradable and the ionic dissolution products have been shown to stimulate osteogenic differentiation and bone nodule formation [37]. However, as with the calcium phosphate ceramics, the bioactive glasses are compromised by brittle fracture behavior.

12.2.3

Natural and Synthetic Polymers

Polymers have been employed for bone tissue engineering applications because they possess physical properties that are similar to the fibrous proteins found in soft and hard connective tissues. Both natural and synthetic polymeric materials can be fabricated into defined geometries and formats (i.e., porous foams, dense plates) and modified chemically to modulate cell adhesion and degradation characteristics.

Collagen is the most widely used natural polymer for regenerative therapies owing to its biological properties favoring cell adhesion and differentiation [38]. Concerns exist over potential hypersensitivity reactions in patients as well as poor handling and weak mechanical properties [39]. As such, collagen is seldom used alone in bone repair strategies. Synthetic polymers for bone regeneration include polyfumarates, and the polyesters, poly(lactic acid), poly(glycolic acid) and polycaprolactone [40–42]. These resorbable materials offer versatile alternatives to natural polymers (i.e., collagen) and may be processed into three-dimensional scaffolds using techniques such as gas foaming, particulate leaching and phase separation to vary porosity, surface features and degradation rates [43]. Nevertheless, synthetic polymers often elicit inflammatory responses as a result of acidic degradation products and lack the bioactive, bone bonding properties of bioceramics.

12.3

New Developments in Bone Grafting Materials

Due to the limitations of existing bone graft substitutes, there has been a major effort to develop new materials that possess osteoinductive capabilities while also imparting sufficient mechanical properties to meet the demanding load-bearing requirements of native bone tissue. These approaches have focused on recapitulating the hierarchical nanoscale

structure and composition of bone using both natural and synthetic materials coupled with novel assembly and fabrication processes.

12.3.1

Self-Assembled Biomimetic Materials

The self-assembly of biomolecules is a well-characterized phenomenon in which molecules spontaneously organize under thermodynamic equilibrium conditions to form functional macromolecular structures stabilized by non-covalent interactions (i.e., hydrogen bonding, electrostatic interactions, van der Waals forces) [44, 45]. These macromolecular assemblies are often proteins that impart instructional cues to cells and provide mechanical functionality (i.e., collagen) or polynucleotides that encode genetic information (i.e., DNA, RNA). Studies investigating mechanisms of protein folding and self-assembly demonstrated that alternating amphiphilic peptide sequences are capable of aggregating and forming β -sheet secondary structures, depending on the presence of salts and pH [46, 47]. This knowledge has since been used for the rational design of water-soluble peptides comprised of alternating hydrophobic and hydrophilic amino acid residues that form soft hydrogels with changes in the ionic strength and/or pH of the aqueous solution [48].

Some of these new biomimetic peptide systems have been shown to promote osteogenesis and bone regeneration. For example, peptide RAD16-I (PuraMatrix™), with the amino acid sequence, AcNH-RADARADARADARADA-COONH₂ (Ac = Acetyl, R = Arginine, A = Alanine; D = Aspartic Acid), assembles into an anti-parallel β -sheet configuration that forms a nanofiber network that is structurally similar to type I collagen gels [49–51]. Three-dimensional RAD16-I hydrogel scaffolds support osteogenic differentiation of marrow-derived mesenchymal stem cells *in vitro*, as determined by the expression of alkaline phosphatase and osteocalcin (early and late bone differentiation markers, respectively) and by the deposition of a mineralized matrix [52]. Similarly, when used to fill small defects (3 mm) in mice calvaria, RAD16-I induced the expression of bone-related transcription factors (Osterix and Runx2) by cells in the vicinity of the defect, and resulted in the formation of a bony bridge with cortical bone medullary cavities [53]. Defects injected with Matrigel™ did not result in new bone formation bridging the defect site. Although RAD16-I does not contain any specific cell instructive motifs, the peptide has been covalently coupled to a 2-unit fibronectin binding sequence (PRGDSGYRGDS) and an osteopontin cell adhesion motif (DGRGDSVAYG) [54]. Such modified RAD16-I peptide scaffolds were shown to promote cell proliferation and osteoblastic differentiation by murine pre-osteoblast MC3T3-E1 cells *in vitro*.

Other self-assembling peptide networks exist that do not form the β -sheets characteristic of RAD16-I. A recently engineered peptide amphiphile relies on different mechanisms for assembly, with unique properties that are dictated by five distinct structural regions [55, 56]. These include: (1) a hydrophobic alkyl tail that provides amphiphilicity when combined with the peptide region, (2) four consecutive cysteine residues that form disulfide bonds when oxidized, (3) a flexible linker region of three glycine residues, (4) a single phosphorylated serine residue that interacts with calcium to direct mineralization, and (5) an RGD cell adhesion ligand. These peptide amphiphiles assemble into nanofibers that are

capable of nucleating HA crystals on their surfaces [55]. The crystallographic *c* axes of the HA crystals co-align with the long axes of the fibers, analogous to the nanoscale organization of collagen fibrils and HA crystals in bone. When placed in critical-size femoral defects in rats (5 mm gap), pre-assembled peptide amphiphilic nanofiber gels stimulated new calcified tissue formation which emanated from both ends of the defect, bridging the gap [57]. This regenerative response was linked to the presence of phosphorylated serine residues on the supramolecular nanofibers, as control matrices with non-phosphorylated serine residues exhibited significantly less bone volume after 4 weeks in vivo.

In addition to peptide-based biomimetic materials, self-assembled nanostructured scaffolds have also been developed from functionalized DNA base pair building blocks for bone regeneration applications. Helical rosette nanotubes (HRNs) comprised of the heterobicyclic base building block, Guanine[^]Cytosine (G[^]C), spontaneously self-assemble in aqueous solutions to form stable nanotubular architectures approximately 4 nm in diameter [58]. The G[^]C base unit possesses the Watson-Crick donor–donor–acceptor hydrogen bond (H-bond) array of guanine and the acceptor–acceptor–donor of cytosine. Under physiological conditions, these arrays assemble into six-membered rosette supermacrocycles that stack to form tubular structures stabilized by noncovalent interactions (i.e., H-bonds, hydrophobic effects), with a hollow core 11 Å in diameter [59]. At 60°C or when added to culture medium at body temperature, HRNs undergo a liquid to viscous gel phase transition that may be advantageous as an injectable therapy for treating bone fractures in situ. Studies have demonstrated that HRNs functionalized with the amino acid lysine (HRN-K) significantly enhanced osteoblast adhesion on titanium surfaces compared to uncoated Ti [58, 60]. It has also been reported that HRN-K embedded in biocompatible poly(2-hydroxyethyl methacrylate) (pHEMA) hydrogels promoted osteoblast adhesion and greatly decreased the polymerization time of the hydrogels [61]. Further, when the cell-adhesive RGDSK peptide was covalently attached to the G[^]C base, HRNs modified with RGDSK (HRN-RGD-K) and coated on pHEMA hydrogels resulted in a 200% increase in osteoblast adhesion relative to hydrogel controls without HRNs [62]. Moreover, osteoblast adhesion was greatly enhanced on HRN-coated hydrogels compared to poly-L-lysine and collagen-coated hydrogels. The increased osteoblast density on HRN hydrogels (HRN-RGD-K and HRN-K) was attributed to increased fibronectin adsorption as well as to the nanometric rosette features, which mimic the helical nanostructure of collagen in bone [61].

Although self-assembled systems have employed biomimetic processes to create materials conducive to osteoblast adhesion and mineralization, a lack of structural integrity and the ability to withstand the mechanical requirements for load bearing applications may limit the use of such scaffolds. Therefore, composites that recapitulate the nanoscale features and mechanical function of the collagen-apatite network have been explored for osseous tissue regeneration.

12.3.2

Nanocomposite Scaffolds (Collagen)

Bone is a natural composite with distinct organic (i.e., collagen) and inorganic (i.e., apatite crystals) phases that interact to impart unique physical and chemical properties to the tissue

(high strength, fracture and fatigue resistance, cell binding motifs) [11]. As a result, recent efforts to engineer bone replacements have attempted to mimic the composite nanostructure of the tissue by incorporating nanoscale crystals, particles and polymeric fibers [63]. The objective is to fabricate materials with functional properties that are superior to those of the individual components alone, and possess the appropriate porosity for nutrient transport and osseointegration (100–200 μm pore sizes) while maintaining strength and toughness as well as the ability to regulate bone cell function (e.g., adhesion, osteogenic differentiation).

A common approach is to design composite materials that integrate collagen and nanoparticulate HA, given the close similarity to the natural tissue composition [64]. For example, a nano-HA/collagen matrix was produced by precipitation of HA from an aqueous solution onto collagen sheets and convolved to form three-dimensional scaffolds [65]. These materials supported the outgrowth of cells from calvarial bone fragments, as extracellular matrix with proliferating cells was continuously produced at the interface between the bone fragments and the composite. The porous nano-HA/collagen matrix provided a microenvironment resembling that found *in vivo*, and cells within the composite eventually (by 21 days) acquired a three-dimensional, osteoblast-like polygonal shape.

More recent studies have attempted to recreate the nanofibrous structure of the collagenous extracellular matrix component of bone rather than use macroscale sponges or fibers. Scaffolds comprised of type I collagen nanofibers and nanocrystalline HA were produced using an electrospinning technique in which solutions of collagen and HA were drawn through a voltage gradient, forming jets that were collected layer-by-layer on a grounded aluminum target surface [66]. The diameter of the collagen nanofibers was 265 ± 0.64 nm and that of the collagen/HA nanofibers was 293 ± 1.45 nm. The crystalline HA (29 ± 7.5 nm) incorporated into the composite was embedded within the nanofibrous matrix of the scaffolds (Fig. 12.1). Human fetal osteoblasts cultured on the materials exhibited a 56% increase in mineralization after 10 days when seeded on collagen/HA constructs in comparison to collagen nanofiber meshes alone. These findings underscore the importance of the bioceramic constituent in modulating cellular behavior and suggest that electrospun collagen/HA nanofibrous scaffolds have potential for bone tissue engineering applications.

12.3.3

Nanocomposite Scaffolds (Synthetics)

Although collagen-based composites have shown promise as bone graft substitutes, collagen is not an ideal material component due to problems with sourcing, mechanical properties, and immunogenicity. As a result, a variety of synthetic polymers have been incorporated into nanocomposite scaffolds to supplement the collagenous phase and impart superior functional properties [67, 68]. Liao et al. used a freeze-drying technique to assemble collagen molecules and nanoparticulate HA into mineralized fibrils that were further dispersed into a poly(lactic acid) (PLA) matrix to provide additional mechanical strength and integrity [67]. The mineralized fibrils were approximately 6 nm in diameter and 300 nm in length while the pores within the composite scaffold ranged from 100 to 300 μm in size and formed an interconnected network. Increasing the PLA weight percent (wt%) of the construct (8, 10 and 12%) was found to improve the compressive strength,

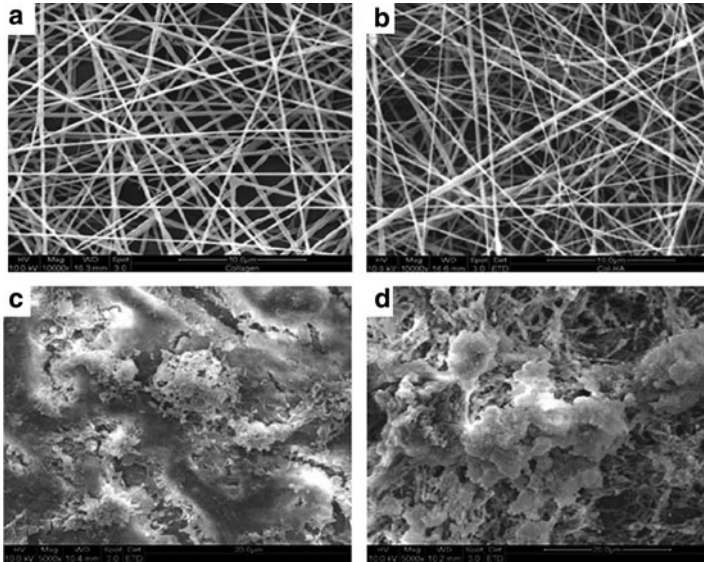


Fig. 12.1 Scanning electron micrographs of electrospun collagen (a) and collagen/hydroxyapatite (Col/HA) nanofibrous composites (b) for bone tissue repair. Human fetal osteoblasts exhibit enhanced mineral deposition on Col/HA scaffolds (d) in comparison to collagen nanofiber matrices (c) after 6 days in culture. Reprinted with permission from [66]

with the highest values (1.9 MPa) measured for the 12 wt% PLA composites. A similar dependence on PLA wt% for the compressive modulus was not observed, as the peak modulus of 47.3 MPa was determined for 10% PLA scaffolds. Overall, the values for the compressive strength and modulus were in the lower range of those of spongy bone. The materials were also shown to support rat calvarial osteoblast adhesion and matrix deposition. As such, the bioactivity coupled with the mechanical properties and the interconnected porosity indicate that the nano-HA/collagen/PLA composites may be useful for the repair or regeneration of cancellous bone.

Additional strategies have entirely replaced the collagenous phase of nanocomposite scaffolds with other polymeric materials rather than augment the existing nanostructured collagen-apatite network. For example, electrospun polycaprolactone (PCL) nanofibers and nanocrystalline HA (30.25 ± 4.43 nm) were fabricated into composite scaffolds and further surface-modified using oxygen plasma treatment to improve wettability [68]. PCL is a non-toxic, synthetic aliphatic polyester that is biocompatible and undergoes slow hydrolytic degradation into natural metabolites [69]. The fiber diameter, pore size and porosity of the nanofibrous PCL scaffolds were estimated to be 220–358 nm, 3–18 μ m, and 87% respectively, while values for the PCL/HA nanocomposites were 352–625 nm, 4–20 μ m, and 92%, respectively. The ultimate tensile strength of the PCL meshes was 3.37 MPa and that for the PCL/HA scaffolds was 1.07 MPa. Human fetal osteoblast cells cultured on surface-modified and unmodified PCL and PCL/HA nanofibrous scaffolds were shown to proliferate at a significantly higher rate on the surface-modified nanofibrous scaffolds. However,

12 mineralization was significantly increased only on PCL/HA nanofibrous scaffolds (both plasma treated and untreated), which appeared as mineral nodules synthesized by osteoblasts similar to the apatite of natural bone. Still, it is not clear how these nanocomposites would function under compressive loading, and the small pore size ($<20\ \mu\text{m}$) in comparison to scaffolds formed by freeze-drying or phase separation methods ($>100\ \mu\text{m}$) may be a barrier to osseointegration (although recent methods have been described using sacrificial layers to improve the pore structure of electrospun nanofibrous scaffolds [70]).

12.3.4

Nanocomposite Scaffolds (Natural Materials)

Aside from synthetic polymers (i.e., PLA, PCL), natural materials such as silk and chitosan have also been combined with nano-HA in place of collagen to form composites for bone regeneration. Silk from different sources (i.e., silkworm silk *Bombyx mori* and spider dragline silk *Nephila clavipes*) is an attractive natural material owing to its biocompatibility, slow degradation, and superior mechanical properties [71–74]. The Kaplan group has developed an approach whereby the biomimetic growth of calcium phosphate crystals on silk fibroin polymeric matrices (using both porous foams and electrospun nanofibrous scaffolds) is used to generate organic/inorganic composites [75, 76]. In one study, aqueous-derived silk fibroin scaffolds were prepared with the addition of polyaspartic acid during processing as a molecular recognition motif to enable subsequent nucleation and growth of apatite when soaked in a solution of CaCl_2 and Na_2HPO_4 [76]. While apatite nanoparticles were deposited on the scaffold walls in localized regions, there may not have been sufficient coverage to provide global stiffening, since the compressive strength (0.1–0.25 MPa) and modulus (1–3 MPa) were well below values for cancellous bone. Nevertheless, human mesenchymal stem cells cultured in osteogenic medium exhibited a significant increase in alkaline phosphatase activity and calcium deposition when seeded on premineralized silk fibroin composites in comparison to untreated scaffolds.

Chitosan is an amino polysaccharide derived from the structural biopolymer chitin, which is a principal component of crustacean exoskeletons, and has been shown to possess excellent biocompatibility [77]. Novel nanocomposite chitosan/HA scaffolds were prepared by combining an in situ co-precipitation synthesis approach with an electrospinning process [78]. Composites with an HA content of 30 wt% were first produced through a co-precipitation method in which chitosan was dissolved in a solution of H_3PO_4 and precipitated in an alkali suspension of CaOH_2 to obtain a homogenous dispersion of spindle-shaped HA nanoparticles (ca. $100 \times 30\ \text{nm}$) within the chitosan matrix. Using a small amount (10 wt %) of ultrahigh molecular weight poly(ethylene oxide) as a fiber-forming facilitating additive, electrospinning was then employed to form continuous chitosan nanofibers with diameters of $214 \pm 25\ \text{nm}$ and HA nanoparticles incorporated into the electrospun fibers. Human fetal osteoblasts cultured for up to 15 days on chitosan/HA nanofibrous scaffolds displayed significant mineral deposition compared with those without nanophase HA. The advantage of the biomimetic crystallization and co-precipitation strategies used in the fabrication of the silk and chitosan biopolymer/HA nanocomposites described here is that

these methods overcome the difficulties associated with nanoparticle agglomeration often encountered in the fabrication of composite materials.

12.3.5

Microsphere-Based Scaffolds

Another strategy for engineering scaffolds for bone reconstruction relies on the use of sintered microspheres to form bioactive composites with an interconnected porous structure. Specifically, degradable poly(lactide-*co*-glycolide) (PLGA) microspheres with a poorly crystalline calcium phosphate ceramic synthesized within the microspheres were fused together to form porous three-dimensional scaffolds for bone repair [79]. Careful manipulation of processing parameters resulted in scaffolds containing a nanocrystalline hydroxyapatite resembling that seen in bone. Varying the polymer/ceramic ratio of the microspheres and heating time of the composite produced a peak compressive modulus of 64.7 MPa, within the range of trabecular bone, using microspheres synthesized at 4°C, a high polymer/ceramic ratio, and a scaffold heating time of 90 min (at 90°C). A variation on this methodology was used to fabricate PLGA/45S5 bioactive glass (BG) microsphere composites using a water-oil-water emulsion technique [80]. 45S5 BG granules (<40 μm) were combined with PLGA to produce a bioactive and biodegradable composite substrate, while the addition of BG granules also served to reinforce and stiffen the polymeric matrix. The PLGA/BG scaffolds had an average porosity of 43% compared to 31% for PLGA microsphere matrices and the elastic modulus increased from 26.48 ± 3.7 MPa to 54.34 ± 6.08 MPa with the addition of BG as a reinforcement phase. Although the microspheres were much larger than the nanoscale particulates typically incorporated into composites for bone regeneration, a nanocrystalline apatite formed on the surface of the PLGA/BG scaffolds when they were immersed in simulated body fluid, a phenomenon that was not observed in PLGA controls. The BG-reinforced composites also supported cell adhesion (Fig. 12.2) and the expression of alkaline phosphatase and calcium phosphate nodule formation by seeded cells.

12.3.6

Nanophase Ceramics and Material Properties/Processing

The inclusion of nanophase ceramics (i.e., nanoparticulate HA) into composite bone graft substitutes has been well characterized in terms of their ability to enhance bone cell function in comparison to un-reinforced composites or those modified with conventional (microscale) particulates [81, 82]. However, nanophase bioceramics have also been shown to play an important role in improving the mechanical properties of polymer/ceramic nanocomposites. For example, Wei and Ma used a phase separation technique to produce nano-HA/poly(L-lactic acid) (PLLA) foam scaffolds with high porosity (>90%) and pore sizes of 50–100 μm [83]. The introduction of nano-HA particulates significantly increased the compressive modulus of the composites (from 4.3 to 8.3 MPa) when the content of nano-HA was increased from 10 to 50%. In comparison to composites produced using

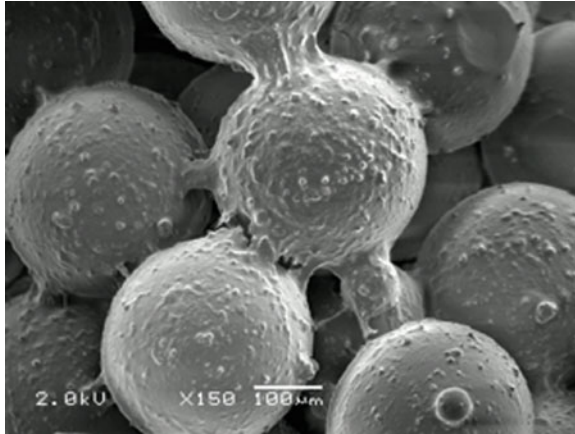


Fig. 12.2 Scanning electron micrograph of osteoblast and chondrocyte co-cultures seeded on sintered poly(lactide-*co*-glycolide)/45S5 bioactive glass microspheres (courtesy of Dr. Helen Lu, Columbia University)

conventional microscale HA particles, the nano-HA/PLLA scaffolds adsorbed significantly more proteins at high HA content (50–80%), which would be expected to enhance the cellular response to these materials. A related study used nanophase (67-nm diameter) and conventional (0.132- μm diameter) HA powder to fabricate HA/PLLA scaffolds by solvent casting in PLLA solutions of 30, 40 and 50 wt% [84]. The nanophase composites exhibited bending moduli at 40 and 50 wt% PLLA compositions that were significantly greater (1.5-fold) than corresponding scaffolds comprised of conventional HA. The values (0.54 ± 0.06 – 0.95 ± 0.09 GPa) were in the lower range of those reported for trabecular bone [85].

In order to achieve optimal functional (i.e., mechanical) properties, the particulate reinforcing phase of a composite material should be uniformly dispersed throughout the matrix. A variety of fabrication procedures have been utilized to produce nanocomposites for bone reconstruction with evenly distributed nanoparticulate phases. A recent study demonstrated that the choice of solvent can impact the dispersion of particles within a polymeric matrix. Particulates of 20% HA/80% β -TCP were dissolved together with PCL in either methylene chloride (MC) or a combination of dimethylformamide (DMF) and MC to electrospin PCL fibrous meshes infused with HA/ β -TCP [86]. The ceramic component of the PCL/HA/ β -TCP composites produced using the combination of DMF and MC as a solvent was more uniformly dispersed than in the fibrous meshes fabricated using MC alone. Moreover, the maximum tensile stress was significantly higher for composites fabricated from DMF and MC compared with scaffolds electrospun from MC (3.7 ± 1.0 MPa versus 1.9 ± 0.4 MPa, respectively). However, the average pore size of the meshes produced using the DMF and MC combination was only 7.0 ± 4.2 μm in contrast to the scaffolds fabricated using the MC solvent, with an average pore size of 79.6 ± 67 μm . As a result, human mesenchymal stem cells did not infiltrate into the composites electrospun using the DMF and MC solvent mixture.

Other methods have been employed to improve particulate dispersion that also enhance interfacial bonding between the matrix and the reinforcing phase. For instance, PLLA/nano-HA composites were fabricated in which the hydroxyl groups on the surface of the HA nanoparticles were chemically grafted to PLLA by ring opening polymerization of L-lactide in the presence of a catalyst, and the grafted nano-HA was further blended in a PLLA matrix [87]. Grafting allowed for a uniform distribution of nano-HA particles within the PLLA matrix and the strong tether to the molecular chains of PLLA improved the reinforcement effect of the HA nanoparticles. The grafted nano-HA/PLLA scaffolds exhibited a peak tensile strength (~75 MPa), bending strength (~125 MPa) and impact energy (~4.5 kJ/m²) at 4 wt% HA, all of which were significantly greater than values for PLLA/HA composites without grafting. These findings indicate that surface grafting may be used to enhance the mechanical properties of engineered PLLA-based scaffolds for bone regeneration.

Using a similar surface grafting approach, the Mikos group developed a novel photocrosslinked composite material comprised of poly(propylene fumarate) (PPF)/poly(propylene fumarate)-diacrylate (PPF-DA) and alumoxane nanofillers [88, 89]. The alumoxane particles were chemically modified with both a surfactant and a reactive functional group (to form acryloyl undecanoic amino acid-alumoxane) to facilitate dispersion and covalent interactions within the polymer. PPF/PPF-DA systems degrade via ester hydrolysis into the biocompatible products fumaric acid and propylene glycol, along with low quantities of acrylic acid and poly(acrylic acid-co-fumaric acid) [90]. The resulting nanocomposite material incorporating surface-modified alumoxane nanoparticles into the PPF/PPF-DA polymer demonstrated over a threefold improvement in flexural modulus (5.410 ± 0.460 GPa) compared with the polymer alone with only a 1 wt% loading of nanoparticles. These dramatic improvements in flexural properties may be attributed to the fine dispersion of nanoparticles into the polymer and increased covalent interaction between the polymer chains and the surface-modified nanoparticles. However, the flexural mechanical properties of these nanocomposites were only one-third of those measured for human cortical bone. In a follow-up study, PPF/PPF-DA composites with surface-modified alumoxane nanoparticles were implanted in the lateral femoral condyle of adult goats for 12 weeks [91]. Direct contact between the scaffolds and surrounding bone tissue was observed and the incorporation of alumoxane nanoparticles into the porous PPF/PF-DA scaffolds did not significantly alter *in vivo* bone biocompatibility or degradation.

In concurrent work, the same research group incorporated ultra-short single-walled carbon nanotubes (SWNTs) functionalized with dodecyl groups (Fig. 12.3) into porous PPF/(propylene fumarate)-diacrylate (PF-DA) scaffolds fabricated using a thermal-crosslinking particulate leaching technique to achieve pore volumes of 75–90% [92]. The functionalized SWNTs dispersed more uniformly into the composite scaffolds than unmodified SWNTs and augmented the mechanical properties of the composites, dependent upon the porosity. Specifically, the compressive strength (~0.3 MPa) and offset yield strength (~0.2 MPa) were significantly higher in PPF/PF-DA scaffolds with functionalized, ultra-short SWNTs at 80% porosity in comparison to un-reinforced PPF constructs. The PPF/PF-DA/SWNT composites were also osteoconductive as determined by their ability to support mesenchymal stem cell adhesion and proliferation *in vitro*. Still, these scaffolds did not exhibit osteoinductive properties consistent with nano-HA or BG-containing composite materials.

12.4 Future Directions

Advances in materials science and biomolecular engineering have resulted in the fabrication of novel biomaterials that mimic the nanostructured collagen-apatite network in native bone tissue. Although many of these newly developed materials may serve as suitable replacements for trabecular bone, their mechanical properties are not sufficient for the repair of cortical bone, as most scaffolds only achieve elastic moduli and compressive strength in the

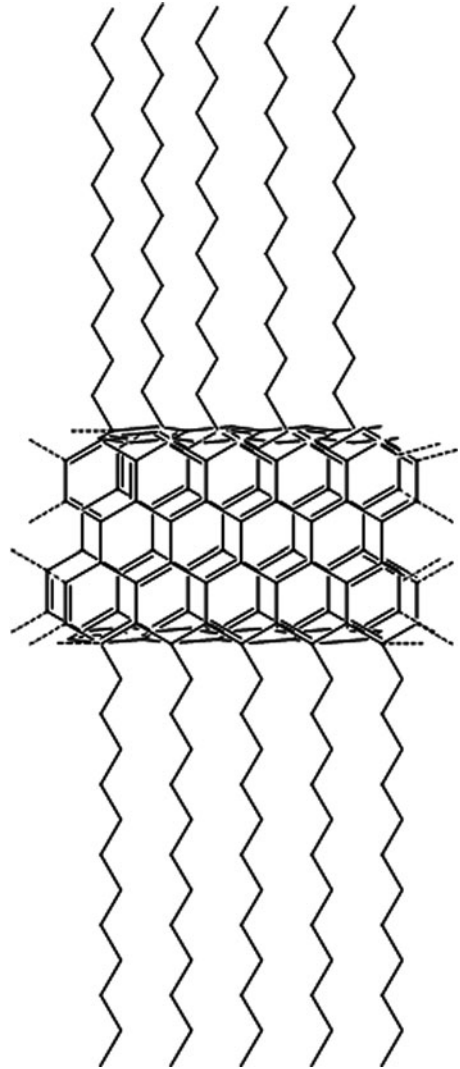


Fig. 12.3 Depiction of an ultra-short single-walled carbon nanotube functionalized with dodecyl groups to improve dispersion within polymeric matrices

low MPa range. The further use of surface functionalization and grafting techniques to facilitate nanoparticle dispersion and interfacial bonding may improve the performance of nanocomposite materials in load-bearing applications. It may also be possible to incorporate self-assembled amphiphilic structures on the surface of these more mechanically robust nanocomposite materials to control cellular adhesion and the deposition of mineralized matrix by neighboring cells.

Vascularization is another important aspect required for functional restoration of osseous tissues. Although many of the fabrication strategies presented in this chapter allow for the creation of an interconnected porous network, additional cues are necessary to stimulate blood vessel infiltration into the material. The incorporation of controlled release microspheres [93–95] and tethering of specific angiogenic growth factors, such as vascular endothelial growth factor [96], may be useful strategies for inducing neovascularization. Recently, sphingosine 1-phosphate, a bioactive phospholipid that modulates migration, proliferation, and survival in diverse cell types, including endothelial cells, has been shown to promote the formation of microvascular networks when incorporated into PLGA scaffolds [97]. This small molecule compound may be advantageous if used in concert with appropriate nanocomposite carrier materials to augment vascular remodeling and osseointegration of bone graft substitutes.

Ultimately, the mechanical properties and biological response to implantable materials for bone reconstruction are dictated by structural and physico-chemical interactions between the material constituents. Gaining a better understanding of these processes in the natural tissue may eventually lead to a new generation of constructs for osseous tissue regeneration.

Acknowledgements The author would like to thank Dr. Christopher Hee for helpful discussions during the preparation of this book chapter.

References

1. Baron R. Anatomy and ultrastructure of bone. In: Favus MJ, editor. *Primer on the Metabolic Bone Diseases and Disorders of Mineral Metabolism*. Lippencott Williams & Wilkins: Philadelphia, PA, 1999. p. 3–10.
2. Boskey AL. The organic and inorganic matrices. In: Hollinger JO, Einhorn TA, Doll B, Sfeir C, editors. *Bone Tissue Engineering*. CRC Press: Boca Raton, FL, 2005. p. 91–123.
3. Gehron Robey P, Bianco P, Termine JD. The cellular and biology and molecular biochemistry of bone formation. In: Coe FL, Favus MJ, editors. *Disorders of Bone and Mineral Metabolism*. Raven Press: New York, NY, 1992.
4. Lian JB, Stein GS, Canalis E, Gehron Robey P, Boskey AL. Bone formation: Osteoblast lineage cells, growth factors, matrix proteins, and the mineralization process. In: Favus MJ, editor. *Primer on the Metabolic Bone Diseases and Disorders of Mineral Metabolism*. Lippencott Williams & Wilkins: Philadelphia, PA, 1999. p. 14–29.
5. Boskey AL. Variations in bone mineral properties with age and disease. *J Musculoskelet Neuronal Interact* 2002;2:532–534.
6. Boskey A. Bone mineral crystal size. *Osteoporos Int* 2003;14:16–21.
7. Aubin JE. Advances in the osteoblast lineage. *Biochem Cell Biol* 1998;76:899–910.

8. Weiner S, Traub W. Organization of hydroxyapatite crystals within collagen fibrils. *FEBS Lett* 1986;206:262–266.
9. Weiner S, Traub W. Crystal size and organization in bone. *Connect Tissue Res* 1989;21:589–595.
10. Rho JY, Kuhn-Spearing L, Zioupos P. Mechanical properties and the hierarchical structure of bone. *Med Eng Phys* 1998;20:92–102.
11. Weiner S, Wagner HD. The material bone: structure mechanical function relations. *Annu Rev Mater Sci* 1998;28:271–298.
12. Hench LL, Wilson J. Introduction. In: Hench LL, Wilson JW, editors. *Introduction to Bioceramics*. World Scientific: Singapore, 1993. p. 1–24.
13. Einhorn TA, Lee CA. Bone regeneration: new findings and potential clinical applications. *J Am Acad Orthop Surg* 2001;9:157–165.
14. Weiss LE. Web watch. *Tissue Eng* 2002;8:167.
15. Khan SF, Cammissa FP, Sandhu HS, Diwan AD, Girardi FP, Lane JM. The biology of bone grafting. *J Am Acad Orthop Surg* 2005;13:77–86.
16. Fowler BL, Dall BE, Rowe DE. Complications associated with harvesting autogeneous iliac bone graft. *Am J Orthop* 1995;24:895–903.
17. Goulet J, Senunas L, DeSilva G, Greenfield M. Autogenous iliac crest bone graft: complications and functional assessment. *Clin Orthop Relat Res* 1997;339:76–81.
18. Vaccaro A. The role of the osteoconductive scaffold in synthetic bone graft. *Orthopedics* 2002;25(5 Suppl):s571–s578.
19. Jones JR, Ehrenfried LM, Hench LL. Optimising bioactive glass scaffolds for bone tissue engineering. *Biomaterials* 2006;27:964–973.
20. Hutmacher DW, Schantz JT, Lam CX, Tan KC, Lim TC. State of the art and future directions of scaffold-based bone engineering from a biomaterials perspective. *J Tissue Eng Regen Med* 2007;1:245–260.
21. Rihn JA, Kirkpatrick K, Albert TJ. Graft options in posterolateral and posterior interbody lumbar fusion. *Spine* 2010;35:1629–1639.
22. Pacaccio DJ, Stern SF. Demineralized bone matrix: basic science and clinical applications. *Clin Podiatr Med Surg* 2005;22:599–606.
23. Bae HW, Zhao L, Kanim LE, et al. Intervariability and intravariability of bone morphogenetic proteins in commercially available demineralized bone matrix products. *Spine* 2006;31:1299–1306; discussion 1307–1308.
24. Hee CK, Jonikas MA, Nicoll SB. Influence of three-dimensional scaffold on the expression of osteogenic differentiation markers by human dermal fibroblasts. *Biomaterials* 2006;27:875–884.
25. LeGeros RZ. Calcium phosphate-based osteoinductive materials. *Chem Rev* 2008;108:4742–4753.
26. LeGeros RZ. Properties of osteoconductive biomaterials: calcium phosphates. *Clin Orthop Relat Res* 2002;395:81–98.
27. LeGeros RZ. Biodegradation and bioresorption of calcium phosphate ceramics. *Clin Mater* 1993;14:65–88.
28. Nagano M, Nakamura T, Kokubo T, Tanahashi M, Ogawa M. Differences of bone bonding ability and degradation behavior *in vivo* between amorphous calcium phosphate and highly crystalline hydroxylapatite coating. *Biomaterials* 1996;17:1771–1777.
29. Venugopal J, Prabhakaran MP, Zhang Y, Low S, Choon AT, Ramakrishna S. Biomimetic hydroxyapatite-containing composite nanofibrous substrates for bone tissue engineering. *Philos Transact A Math Phys Eng Sci* 2010;368:2065–2081.
30. Dormer KJ, Bryce GE, Hough JV. Selection of biomaterials for middle and inner ear implants. *Otolaryngol Clin North Am* 1995;28:17–27.
31. Szpalski M, Gunzburg R. Applications of calcium phosphate-based cancellous bone void fillers in trauma surgery. *Orthopedics* 2002;25(5 Suppl):s601–s609.
32. Hench LL, Wilson J. Surface-active biomaterials. *Science* 1984;226:630–636.

33. Hench LL, Splinter RJ, Allen WC, Greenlee TK. Bonding mechanisms at the interface of ceramic prosthetic materials. *J Biomed Mater Res* 1971;2:117–141.
34. Hench LL. Bioceramics. *J Am Ceram Soc* 1998;81:1705–1728.
35. Matsuda T, Davies JE. The in vitro response of osteoblasts to bioactive glass. *Biomaterials* 1987;8:275–284.
36. Ducheyne P, Qiu Q. Bioactive ceramics: the effect of surface reactivity on bone formation and bone cell function. *Biomaterials* 1999;20:2287–2303.
37. Xynos D, Edgar AJ, Buttery LDK, Hench LL, Polak JM. Gene-expression profiling of human osteoblasts following treatment with the ionic products of Bioglass 45S5 dissolution. *J Biomed Mater Res* 2001;55:151–157.
38. Ramshaw JA, Peng YY, Glattauer V, Werkmeister JA. Collagens as biomaterials. *J Mater Sci Mater Med* 2009;20(Suppl 1):S3–S8.
39. DeLustro F, Dasch J, Keefe J, Ellingsworth L. Immune responses to allogeneic and xenogeneic implants of collagen and collagen derivatives. *Clin Orthop Relat Res* 1990;260:263–279.
40. Behraves E, Yasko AW, Engel PS, Mikos AG. Synthetic biodegradable polymers for orthopaedic applications. *Clin Orthop Relat Res* 1999;367 (Suppl):S118–S129.
41. Liu X, Ma PX. Polymeric scaffolds for bone tissue engineering. *Ann Biomed Eng* 2004;32:477–486.
42. Karp JM, Shoichet MS, Davies JE. Bone formation on two-dimensional poly(DL-lactide-co-glycolide) (PLGA) films and three-dimensional PLGA tissue engineering scaffolds in vitro. *J Biomed Mater Res A* 2003;64:388–396.
43. Ma PX, Choi JW. Biodegradable polymer scaffolds with well-defined interconnected spherical pore network. *Tissue Eng* 2001;7:23–33.
44. Whitesides GM, Boncheva M. Beyond molecules: self-assembly of mesoscopic and macroscopic components. *Proc Natl Acad Sci USA* 2002;99:4769–4774.
45. Whitesides GM, Grzybowski B. Self-assembly at all scales. *Science* 2002;295:2418–2421.
46. Seipke G, Arfmann HA, Wagner KG. Synthesis and properties of alternating poly(Lys-Phe) and comparison with the random copolymer poly(Lys 51, Phe 49). *Biopolymers* 1974;13:1621–1633.
47. Brack A, Orgel LE. Beta structures of alternating polypeptides and their possible prebiotic significance. *Nature* 1975;256:383–387.
48. Semino CE. Self-assembling peptides: from bio-inspired materials to bone regeneration. *J Dent Res* 2008;87:606–616.
49. Caplan MR, Schwartzfarb EM, Zhang S, Kamm RD, Lauffenburger DA. Control of self-assembling oligopeptide matrix formation through systematic variation of amino acid sequence. *Biomaterials* 2002;23:219–227.
50. Zhang S, Holmes T, Lockshin C, Rich A. Spontaneous assembly of a self-complementary oligopeptide to form a stable macroscopic membrane. *Proc Natl Acad Sci USA* 1993;90:3334–3338.
51. Zhao X, Zhang S. Fabrication of molecular materials using peptide construction motifs. *Trends Biotechnol* 2004;22:470–476.
52. Hamada K, Hirose M, Yamashita T, Ohgushi H. Spatial distribution of mineralized bone matrix produced by marrow mesenchymal stem cells in self-assembling peptide hydrogel scaffold. *J Biomed Mater Res A* 2008;84:128–136.
53. Misawa H, Kobayashi N, Soto-Gutierrez A, Chen Y, Yoshida A, Rivas-Carrillo JD, Navarro-Alvarez N, Tanaka K, Miki A, Takei J, Ueda T, Tanaka M, Endo H, Tanaka N, Ozaki T. PuraMatrix facilitates bone regeneration in bone defects of calvaria in mice. *Cell Transplant* 2006;15:903–910.
54. Horii A, Wang X, Gelain F, Zhang S. Biological designer self-assembling peptide nanofiber scaffolds significantly enhance osteoblast proliferation, differentiation and 3-D migration. *PLoS One* 2007;2:e190.

55. Hartgerink JD, Beniash E, Stupp SI. Self-assembly and mineralization of peptide-amphiphile nanofibers. *Science* 2001;294:1684–1688.
56. Hartgerink JD, Beniash E, Stupp SI. Peptide-amphiphile nanofibers: a versatile scaffold for the preparation of self-assembling materials. *Proc Natl Acad Sci USA* 2002;99:5133–5138.
57. Mata A, Geng Y, Henrikson KJ, Aparicio C, Stock SR, Satcher RL, Stupp SI. Bone regeneration mediated by biomimetic mineralization of a nanofiber matrix. *Biomaterials* 2010;31:6004–6012.
58. Chun AL, Morales JG, Webster TJ, Fenniri H. Helical rosette nanotubes: a biomimetic coating for orthopedics. *Biomaterials* 2005;26:7304–7309.
59. Fenniri H, Mathivanan P, Vidale KL, Sherman DM, Hallenga K, Wood KV, Stowell JG. Helical rosette nanotubes: design, self-assembly and characterization. *J Am Chem Soc* 2001;123:3854–3855.
60. Zhang L, Chen Y, Rodriguez J, Fenniri H, Webster TJ. Biomimetic helical rosette nanotubes and nanocrystalline hydroxyapatite coatings on titanium for improving orthopedic implants. *Int J Nanomedicine* 2008;3:323–333.
61. Zhang L, Ramsaywack S, Fenniri H, Webster TJ. Enhanced osteoblast adhesion on self-assembled nanostructured hydrogel scaffolds. *Tissue Eng* 2008;14:1353–1364.
62. Zhang L, Rakotondradany F, Myles AJ, Fenniri H, Webster TJ. Arginine-glycine-aspartic acid modified rosette nanotube-hydrogel composites for bone tissue engineering. *Biomaterials* 2009;30:1309–1320.
63. Rogel MR, Qiu H, Ameer GA. The role of nanocomposites in bone regeneration. *J Mater Chem* 2008;18:4233–4241.
64. Wahl DA, Czernuszka JT. Collagen-hydroxyapatite composites for hard tissue repair. *Eur Cell Mater* 2006;11:43–56.
65. Du C, Cui FZ, Zhu XD, de Groot K. Three-dimensional nano-HAp/collagen matrix loading with osteogenic cells in organ culture. *J Biomed Mater Res* 1999;44:407–415.
66. Venugopal J, Low S, Choon AT, Sampath Kumar TS, Ramakrishna S. Mineralization of osteoblasts with electrospun collagen/hydroxyapatite nanofibers. *J Mater Sci Mater Med* 2008;19:2039–2046.
67. Liao SS, Cui FZ, Zhang W, Feng QL. Hierarchically biomimetic bone scaffold materials: nano-HA/collagen/PLA composite. *J Biomed Mater Res B Appl Biomater* 2004;69:158–165.
68. Venugopal J, Low S, Choon AT, Kumar AB, Ramakrishna S. Electrospun-modified nanofibrous scaffolds for the mineralization of osteoblast cells. *J Biomed Mater Res A* 2008;85:408–417.
69. Li S, Vert M. Biodegradable polymers: polyesters. In: Mathiowitz E, editor. *Encyclopedia of Controlled Drug Delivery*. Wiley & Sons: New York, NY, 1999. p. 71–93.
70. Baker BM, Gee AO, Metter RB, Nathan AS, Marklein RA, Burdick JA, Mauck RL. The potential to improve cell infiltration in composite fiber-aligned electrospun scaffolds by the selective removal of sacrificial fibers. *Biomaterials* 2008;29:2348–2358.
71. Jin HJ, Fridrikh SV, Rutledge GC, Kaplan DL. Electrospinning Bombyx mori silk with poly(ethylene oxide). *Biomacromolecules* 2002;3:1233–1239.
72. Altman GH, Diaz F, Jakuba C, Calabro T, Horan RL, Chen J, Lu H, Richmond J, Kaplan DL. Silk-based biomaterials. *Biomaterials* 2003;24:401–416.
73. Horan RL, Antle K, Collette AL, Wang Y, Huang J, Moreau JE, Volloch V, Kaplan DL, Altman GH. In vitro degradation of silk fibroin. *Biomaterials* 2005;26:3385–3393.
74. Gosline JM, Guerette PA, Ortlepp CS, Savage KN. The mechanical design of spider silks: from fibroin sequence to mechanical function. *J Exp Biol* 1999;202:3295–3303.
75. Li C, Jin HJ, Botsaris GD, Kaplan DL. Silk apatite composites from electrospun fibers. *J Mater Res* 2005;20:3374–3384.
76. Kim HJ, Kim UJ, Kim HS, Li C, Wada M, Leisk GG, Kaplan DL. Bone tissue engineering with premineralized silk scaffolds. *Bone* 2008;42:1226–1234.

77. Singla AK, Chawla M. Chitosan: some pharmaceutical and biological aspects – an update. *J Pharm Pharmacol* 2001;53:1047–1067.
78. Zhang Y, Venugopal JR, El-Turki A, Ramakrishna S, Su B, Lim CT. Electrospun biomimetic nanocomposite nanofibers of hydroxyapatite/chitosan for bone tissue engineering. *Biomaterials* 2008;29:4314–4322.
79. Khan YM, Katti DS, Laurencin CT. Novel polymer-synthesized ceramic composite-based system for bone repair: an in vitro evaluation. *J Biomed Mater Res A* 2004;69:728–737.
80. Lu HH, El-Amin SF, Scott KD, Laurencin CT. Three-dimensional, bioactive, biodegradable, polymer-bioactive glass composite scaffolds with improved mechanical properties support collagen synthesis and mineralization of human osteoblast-like cells in vitro. *J Biomed Mater Res A* 2003;64:465–474.
81. Webster TJ, Ergun C, Doremus RH, Siegel RW, Bizios R. Enhanced functions of osteoblasts on nanophase ceramics. *Biomaterials* 2000;21:1803–1810.
82. Webster TJ, Ahn ES. Nanostructured biomaterials for tissue engineering bone. *Adv Biochem Eng Biotechnol* 2007;103:275–308.
83. Wei G, Ma PX. Structure and properties of nano-hydroxyapatite/polymer composite scaffolds for bone tissue engineering. *Biomaterials* 2004;25:4749–4757.
84. McManus AJ, Doremus RH, Siegel RW, Bizios R. Evaluation of cytocompatibility and bending modulus of nanoceramic/polymer composites. *J Biomed Mater Res A* 2005;72:98–106.
85. Keaveny TM, Hayes WC. Mechanical properties of cortical and trabecular bone. *Bone* 1993;7:285–344.
86. Patlolla A, Collins G, Arinze TL. Solvent-dependent properties of electrospun fibrous composites for bone tissue regeneration. *Acta Biomater* 2010;6:90–101.
87. Hong Z, Zhang P, He C, Qiu X, Liu A, Chen L, Chen X, Jing X. Nano-composite of poly(L-lactide) and surface grafted hydroxyapatite: mechanical properties and biocompatibility. *Biomaterials* 2005;26:6296–6304.
88. Horch RA, Shahid N, Mistry AS, Timmer MD, Mikos AG, Barron AR. Nanoreinforcement of poly(propylene fumarate)-based networks with surface modified alumoxane nanoparticles for bone tissue engineering. *Biomacromolecules* 2004;5:1990–1998.
89. Mistry AS, Cheng SH, Yeh T, Christenson E, Jansen JA, Mikos AG. Fabrication and in vitro degradation of porous fumarate-based polymer/alumoxane nanocomposite scaffolds for bone tissue engineering. *J Biomed Mater Res A* 2009;89:68–79.
90. He S, Timmer MD, Yaszemski MJ, Yasko AW, Engel PS, Mikos AG. Synthesis of biodegradable poly(propylene fumarate) networks with poly(propylene fumarate) – diacrylate macromers as crosslinking agents and characterization of their degradation products. *Polymer* 2001;42:1251–1260.
91. Mistry AS, Pham QP, Schouten C, Yeh T, Christenson EM, Mikos AG, Jansen JA. In vivo bone biocompatibility and degradation of porous fumarate-based polymer/alumoxane nanocomposites for bone tissue engineering. *J Biomed Mater Res A* 2010;92:451–462.
92. Shi X, Sitharaman B, Pham QP, Liang F, Wu K, Edward Billups W, Wilson LJ, Mikos AG. Fabrication of porous ultra-short single-walled carbon nanotube nanocomposite scaffolds for bone tissue engineering. *Biomaterials* 2007;28:4078–4090.
93. Jay SM, Saltzman WM. Controlled delivery of VEGF via modulation of alginate microparticle ionic crosslinking. *J Control Release* 2009;134:26–34.
94. Golub JS, Kim YT, Duvall CL, Bellamkonda RV, Gupta D, Lin AS, Weiss D, Robert Taylor W, Guldberg RE. Sustained VEGF delivery via PLGA nanoparticles promotes vascular growth. *Am J Physiol Heart Circ Physiol* 2010;298:H1959–H1965.
95. Ionescu LC, Lee GC, Sennett BJ, Burdick JA, Mauck RL. An anisotropic nanofiber/microsphere composite with controlled release of biomolecules for fibrous tissue engineering. *Biomaterials* 2010;31:4113–4120.

96. Leslie-Barbick JE, Moon JJ, West JL. Covalently-immobilized vascular endothelial growth factor promotes endothelial cell tubulogenesis in poly(ethylene glycol) diacrylate hydrogels. *J Biomater Sci Polym Ed* 2009;20:1763–1779.
97. Sefcik LS, Petrie Aronin CE, Wieghaus KA, Botchwey EA. Sustained release of sphingosine 1-phosphate for therapeutic arteriogenesis and bone tissue engineering. *Biomaterials* 2008;29:2869–2877.

Christopher J. Hunter

Contents

13.1	Introduction	364
13.2	Tissue Overview/Requirements	365
13.3	Review of Previous Work	369
13.3.1	Architecture	370
13.3.2	Biocompatibility	372
13.3.3	Bioactive Cues	373
13.3.4	Mechanical Function	374
13.3.5	Deliverability	375
13.4	Future Directions	376
13.4.1	Aligned/Microengineered Anisotropic Materials	377
13.4.2	Cell Adhesion and Targeted Signalling	377
13.4.3	Delivery Systems	378
13.4.4	The Ultimate Engineered Fibrocartilage: One Author's Guess	378
References	379

Abstract Fibrocartilage is a specialized tissue found in the intervertebral discs, the menisci of the knee and temporomandibular joint, and various symphyseal joints throughout the body. Its unique combination of tensile strength, compressive strength, and deformability makes it an ideal material for many structures, however a low intrinsic capacity for repair means that disease or damage can produce chronic debility. The fibrocartilages represent a significant challenge for tissue engineers. Biomaterials must be capable of withstanding significant mechanical stress while guiding formation of a complex microarchitecture. In this chapter, we will review the structure and biology of fibrocartilage and take a look at the biomaterial strategies that have been used. At present no material has satisfied all of the requirements for a successful tissue engineered therapy, however many promising developments have occurred.

Keywords Biomaterial • Biomechanics • Fibrocartilage

C.J. Hunter

Department of Mechanical and Manufacturing Engineering, Centre for Bioengineering Research and Education, McCaig Institute for Bone and Joint Health, University of Calgary, 2500 University Dr. NW, Calgary, AB, Canada T2N 1N4
e-mail: topherhunter@gmail.com

13.1 Introduction

Fibrocartilage is a ubiquitous structure, present anywhere a tough but flexible material is required for biomechanical function. Symphyseal joints are linked by fibrocartilage, while at least two articulating joints have a fibrocartilage bearing structure (the knee and the temporomandibular joint). As such, the fibrocartilage serves both connective (i.e. tensile) and bearing (i.e. tribological) purposes [1].

The primary distinguishing feature of all fibrocartilages is the blend of fibrous materials in a cartilaginous matrix. The fibers consist largely of collagen type I, while the matrix consists of other collagens plus proteoglycans. This structure acts very much like an engineered fiber-reinforced polymer, utilizing the tensile properties of the fibers and the compressive properties of the matrix. This yields a strong but flexible material for various joint structures.

Fibrocartilage disorders are a common source of musculoskeletal debility, including knee, low back, and orofacial pain (Table 13.1). The principal fibrocartilages involved in clinical diseases are the menisci of the knee, the meniscus of the temporomandibular joint (TMJ), and the intervertebral discs (IVDs).

Repair or replacement of these tissues is a relatively new concept. Until recently, treatment of meniscal damage was largely done via complete or partial meniscectomy (with no replacement of the excised tissues) or via total knee arthroplasty. Treatment of intervertebral disc damage was likewise via removal in the form of complete or partial discectomy with or without subsequent spinal fusion. The last decade has seen the appearance of total joint arthroplasty systems for the spine as well, thus allowing complete replacement of the joint. However arthroplasty of any joint is a significant surgery and represents a “no return” case for the patient; revisions and subsequent treatments are extremely limited. No matter what the treatment, the basic idea is to remove the offending fibrocartilage. With the advent of tissue engineering, one hopes that new treatment options may be possible. Even if the engineered tissue were only able to temporarily halt the progression of disease, it could delay the need for drastic arthroplasty procedures and significantly improve patient outcomes. However the technical challenges inherent in any tissue engineered system are substantial, and no less so in fibrocartilage.

The fibrocartilages represent a curious problem for the biomaterials scientist or tissue engineer. The repair structure must have tensile properties similar to ligament, compressive properties similar to cartilage, and strong adhesion to adjacent tissues (particularly for the IVD), yet it must remain pliable and tough. In this chapter, we will discuss the structure and

Table 13.1 Population incidence of fibrocartilage-related diseases

Joint	Incidence	References
Meniscus	18%	[2, 3]
TMJ	37.5%	[4]
IVD	30%	[5, 6]

function of fibrocartilages, the requisite features of biomaterials for tissue engineering, and the progress to date.

13.2

Tissue Overview/Requirements

Fibrocartilage is approximately 80% water, while the solid matrix contains dense collagen type I fibers embedded in a collagen type II ground substance with a low concentration of proteoglycan [7, 8]. Histologically, it appears as a dense tissue with organized bundles of fibrous matter, generally visible with hematoxylin and eosin or aniline blue stains [7, 9, 10]. The dominant cell type is generally referred to as fibrochondrocytes, distinguishing them from cells in hyaline articular cartilage. These spheroidal cells rest in individual lacunae, although occasional clonal groups can be found [11, 12]. The cells are typically described as strongly expressing collagen type I and aggrecan, lesser expression of collagen type II, and small amounts of various other molecules including elastin, collagen types II-VI, collagen type IX, versican, and biglycan [7–10]. However expression patterns change significantly over time, suggesting that the disease state of the individual may be of concern when designing a biomaterial substitute [10]. Fibrocartilage is found principally in the symphyses, intervertebral discs (IVDs), menisci, and temporomandibular joints (TMJs), though it is sometimes found as a repair tissue in the hyaline cartilage, and bears a strong resemblance to tissue in a fracture callus (Fig. 13.1).

Structurally, fibrocartilages are a fiber-reinforced composite material. The collagen fibers bear tensile load, while the cartilaginous ground substance bears compressive load. In this sense, the tissues are similar to steel-reinforced concrete or carbon fiber-reinforced epoxy. However unlike these engineered materials, fibrocartilage retains a substantial level of flexibility, allowing the tissue to deform under load. This is largely due to the poroelastic or viscoelastic behavior of the cartilage matrix. For a full description of cartilage mechanics in compression, see for example Lai and coauthors [13]. For present purposes, a brief qualitative discussion will suffice.

Articular cartilage and the nonfibrous matrix of fibrocartilage consist of a solid matrix and a fluid phase. Compaction of the solid phase is resisted by three key properties: viscous drag, electrostatic repulsion, and osmotic swelling. Viscous drag is generated as the fluid is expelled through the solid matrix. At a microstructural level the tissue is very complex, however we can consider it as acting like a sponge with geometrically complex pores. The fluid must navigate the twisting path out of the solid, and boundary-layer drag is generated by the solid-fluid interaction. Electrostatic repulsion is generated by the net negative charge of the solid phase. The solid matrix possesses a large fixed negative charge thanks to the sulphated glycosaminoglycans (sGAG) in the proteoglycans (particularly aggrecan, which contains by far the highest concentration of sGAG). These charges undergo mutual electrostatic repulsion, which swells the tissue and resists compression. Osmotic swelling is likewise generated by the fixed charges, which also attract positive ions from the surrounding synovial fluid, producing a net osmotic imbalance (the solute concentration inside the tissue is higher than that outside). This creates a further osmotic swelling pressure, which

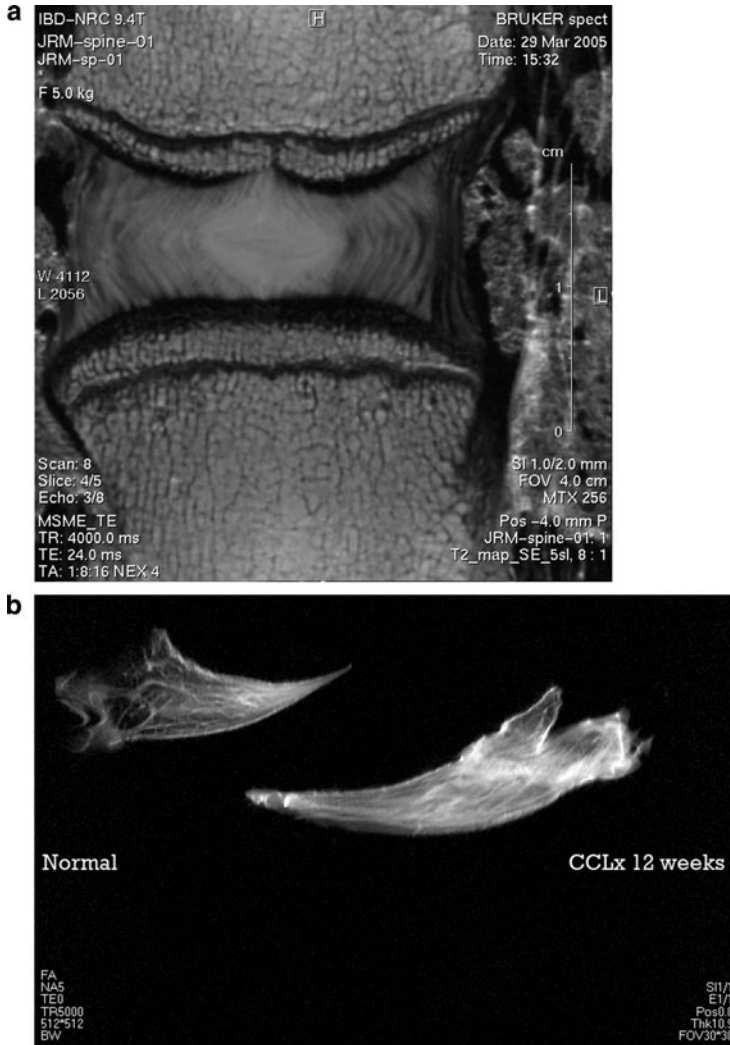


Fig. 13.1 9.4T T2-weighted MR microscopy of fibrocartilage reveals a complex architecture. **(a)** The intervertebral disc consists of an outer annulus fibrosus and an inner nucleus pulposus, with markedly different fibrous structure. **(b)** The menisci of the knee demonstrate both inhomogeneity and anisotropy, with a complex network of fibers (*upper left*: unoperated leg, *lower right*: 12 weeks after anterior cruciate ligament transection). Images courtesy of Dr. John Matyas, University of Calgary

further resists compression [13, 14]. Thus a viscoelastic mechanical response is generated by the complex interplay of various features. As we will see later, some biomaterials have attempted to replicate a variety of these features, but none have fully replicated the complexity of native tissue.

From a therapeutic perspective, the principal concerns of the biomaterials/tissue engineer are the fibrocartilages of the intervertebral discs, menisci, and temporomandibular joint, as these structures dominate the various pathologies involving fibrocartilage. All three share common features, but there are certain unique features to each tissue which present challenges to the tissue engineer.

The mechanical properties of fibrocartilage are complex. Each tissue demonstrates both regional variations and anisotropies, producing specialized mechanical structures for different joints. Each intervertebral disc consists of two primary regions: the outer annulus fibrosus (AF) and the inner nucleus pulposus (NP). The disc is anchored to adjacent cartilaginous endplates (similar to hyaline cartilage in structure and composition) via Sharpey's fibers, primarily originating in the AF [15]. The AF consists of overlapping concentric lamellae, with each successive lamella alternating collagen orientation approximately 45–60° from the spinal axis [16]. The NP of most mammalian adults is a loosely organized fibrocartilage with generally isotropic orientation (for a discussion of exceptions to this rule, see for example [17]). The NP contains more collagen type II, while the AF contains more collagen type I [16, 18]. Pathological degeneration most commonly presents as dehydration followed by tearing of the AF with subsequent herniation of the NP and/or reduction of disc height. These phenomena compromise the adjacent nerve roots and spinal cord, leading to chronic neurological involvement [19]. Current treatment options are quite limited, generally being either symptomatic (pharmaco- or physiotherapy) or invasive. The most common surgical options are partial discectomy (removal of herniated material) with or without vertebral fusion, fusion alone, or arthroplasty [20]. To date, no partial repair/replacement strategies have attained clinical effectiveness [21].

The menisci of the knee and TMJ are semicircular or ovoid, respectively, and form concavities to receive their articulations [12]. Both are thicker at their outer faces, where the collagen fibers are oriented circumferentially, and thin towards the central concavities, where the collagen fibers are oriented radially [22]. The menisci of the knee are anchored to the tibial plateau at the meniscal horns, with ligamentous material transitioning into Sharpey's fibers. The menisci of the TMJ are similarly attached to the capsular ligament and the adjacent bones [12]. Both menisci are predominantly composed of collagen type I. Pathology usually occurs in the form of tears along the fiber directions, though orthogonal ruptures are not uncommon. These tears can directly cause pain and discomfort, though more significant concerns focus around secondary joint instability, which can in turn induce osteoarthritis [23]. Treatment options include complete removal of the meniscus (though this is now uncommon practice), partial meniscectomy to remove the loose portion of the tissue, or suturing/stapling of the tear [24]. In more advanced cases where osteoarthritis of the adjacent cartilage has gone unchecked, total joint arthroplasty is the principal treatment option.

All fibrocartilages demonstrate anisotropy, though to varying degrees. This appears to be critical to mechanical function, as disruption of the architecture generally coincides with tissue degeneration and disease. The overlapping lamellae of the IVD contain obliquely oriented fibers to withstand both hoop stress and axial stress, while the different regions of the menisci contain variously oriented fibers to withstand local stresses. One might almost go so far as to suggest that a phenomenon similar to Wolf's Law may occur in fibrocartilage: collagen fibers orient with the local axis of stress.

The downside of anisotropy is that it can create weaker axes along which tears and fractures can propagate. Thus we note that all fibrocartilages have one dominant failure mode: tearing. To treat these events, we find two dominant treatment techniques: localized repair or en bloc replacement. In either case, functional repair/replacement of fibrocartilage will be challenging, as it will require the material to have adequate tensile and compressive stiffness as well as either low surface friction (in menisci and TMJ applications) or strong tissue integration (in the IVDs). If the device is designed for partial replacement of the tissue, adhesion to the adjacent fibrocartilage will also be essential.

Above all else, any fibrocartilage repair or replacement will have to serve a mechanical function. The fibrocartilages experience substantial forces during normal motion. Axial forces in the knee are estimated to range from 1.7 times body weight during a supine leg raise to 2.3 times body weight during walking [25], and up to three times body weight under impact activities such as jumping or falling [26]. The internal pressure of the IVD has been measured to range from 0.1 MPa when lying prone to 0.6 MPa when walking, and 2.3 MPa when lifting 20 kg by bending at the hips [27]. To withstand these forces, the fibrocartilages are exceptionally strong. However these properties vary significantly depending upon region and axis of loading, as seen in Table 13.2. The tissues also demonstrate significant toe regions and viscoelasticity, with dynamic moduli typically measured from 10 to 40 MPa and phase angles ranging from 16 to 20° [28]. It is notable that annulus fibrosus is both stronger and weaker than meniscus in the parallel and perpendicular directions, respectively. This may be due to the stronger alignment of annulus fibers, as even meniscal tissues retain a small amount of cross fibers in all regions, while the annulus demonstrates almost complete alignment in each lamella.

In the context of tissue engineering, these last points may be the most important. As we shall see, many attempts to engineer cartilages (fibrous or hyaline) have produced amorphous fibrocartilage. However while these efforts have generally attained appropriate

Table 13.2 Material properties of fibrocartilage

Tissue	Region	Axis	UTS (MPa)	Tensile modulus (MPa)
Meniscus (lateral/medial)	Central	Parallel to fibers	6.308/ 3.358	228.8/93.2
		Perpendicular to fibers	0.992/ 0.848	nd
	Anterior horn	Parallel to fibers	8.058/nd	159.1/159.6
		Perpendicular to fibers	0.803/nd	nd
	Posterior horn	Parallel to fibers	6.868/ 5.860	294.1/110.2
		Perpendicular to fibers	0.537/ 1.228	nd
Annulus fibrosus		Parallel to fibers	110	410
		Perpendicular to fibers	0.187	0.16

UTS ultimate tensile strength, nd no data available. Data derived from [28–30]

cellular phenotype and matrix expression, few if any have succeeded in replicating the intricate organization of the tissue, which is so essential to normal function.

13.3 Review of Previous Work

[A] man's reach should exceed his grasp, or what's a heaven for?
Robert Browning, 1812–1889

As of yet, no biomaterial, tissue engineered product, or prosthesis has truly replicated the function of any fibrocartilage. The lack of progress is not due to a shortage of ideas, though. A brief search of the patent literature indicates that this is a busy area of innovation: 1,668 patents are found under “artificial meniscus,” 857 under “prosthetic meniscus,” 2,964 under “artificial intervertebral,” 2,708 under “prosthetic intervertebral,” and 830 under “fibrocartilage.” Allograft treatments have been developed for menisci [31–33] and IVDs [34–36], though these procedures are relatively rare. Artificial menisci have been developed and are in various stages of clinical use, including Menaflex™ (formerly CMI®), Restore Orthobiologic Implant™, and Hyalograft C™. At least two artificial menisci have been developed for the TMJ, one being a silicone-based device and the other a Teflon-based device called Vitek TMJ, however the devices have been recalled by FDA and Health Canada, and there are various legal proceedings against the manufacturer [37–39]. In contrast, there are at least 18 artificial disc arthroplasty systems in various phases of commercial development and clinical trials. The most common clinical designs include: Bryan™, Prodisc™, and Maverick™, though many others are in use. Interestingly, while the three meniscus treatments listed above are all biomaterial scaffolds intended to interact with cells, the IVD treatments are all conventional arthroplasty devices lacking in cells or biological function. At present, the IVD biomaterials appear to be limited to research and development stages (see Table 13.4 for a summary of some common fibrocartilage biomaterials).

The general lack of success with biomaterial or tissue engineered therapies in the fibrocartilages should not be discouraging, however. The field is still new, and advancements at the research level are coming faster than ever. If anything, the mediocre performance of arthroplasty devices should suggest that biological function is essential to long-term efficacy of the implant. Let us turn now to consideration of how we may attain successful outcomes in tissue engineering.

One of the first attempts to develop a tissue engineered therapy in any orthopaedic tissue was in fibrocartilage. In 1988, Arnoczky and coauthors proposed using a fibrin clot to augment meniscal repairs. The clot was to act as a scaffold and chemoattractant for autologous cells, providing initial stability to the tear and supporting the growth of new repair tissue [40]. Numerous followup ideas have been proposed, but none have yet come to total fruition as a clinical therapy. However Arnoczky and others had pointed the way.

The ultimate goal of fibrocartilage tissue engineering is to achieve both initial mechanical stability and to allow the long-term formation of normal native tissues. In order to develop appropriate scaffolds, it is important to consider basic design principles such as

immunogenicity, biocompatibility, and method of delivery. Chan and Leong suggest that any biomaterial for tissue engineering should satisfy four key requirements: (1) provide adequate architecture to support and guide new tissue formation, preferably while degrading at a known rate; (2) be cell- and tissue-compatible to encourage cell adhesion and tissue formation; (3) provide bioactive cues and/or enhance delivery of growth factors; and (4) provide mechanical integrity to the implant site during healing and implant integration [41]. Other authors have suggested various other criteria, including deliverability, as important considerations [21]. Therefore a biomaterial for fibrocartilage engineering may need to be anisotropic with regional variations in mechanical properties, support adhesion and growth of fibrochondrocytes, provide appropriate signals via bound cell adhesion molecules and/or growth factors, withstand normal mechanical forces after implantation, and be deliverable in a clinically appropriate manner.

Numerous scaffolds have been proposed for fibrocartilage tissue engineering. Table 13.4 lists some of the candidate materials. To date, none have adequately addressed all of the design criteria. In general, these studies have focused largely on criteria (2), supporting cell adhesion, phenotype expression, and matrix secretion, while considerably less effort has been placed upon the other criteria.

13.3.1

Architecture

In order to restore the native tissue structure and function, we will very likely need to replicate at least some of the microarchitecture in our biomaterials; few isotropic materials have demonstrated the ability to form anisotropic tissues without substantial exogenous stimuli (such as mechanical stress). Therefore architectural support and guidance of new tissue formation will most likely require anisotropic biomaterials. If the designer chooses to induce such features in the biomaterial, then material choices become severely limited. For example, homogeneous hydrogels generally do not provide the requisite properties for either initial tissue mechanics or for guidance of new tissue formation. There have been some exciting attempts to produce architecture-mimicking materials, however few have progressed beyond a basic research stage.

Most fibrocartilage biomaterials have been either amorphous solids or isotropic fibrous scaffolds. These include Teflon, polyurethane, collagen, hyaluronan, agarose, alginate, and isotropic felts of polyglycolic acid (PGA) or poly lactic-co-glycolic acid (PLGA). In general, these studies have been designed to assess cell attachment, morphology, proliferation, and gene/protein expression. Most studies report production of collagen type II, despite the fact that type I is more common in fibrocartilage [42–45]. However small amounts of collagen type II are found in menisci and the inner IVD (particularly the nucleus pulposus) [46], so it is not entirely unreasonable to find some expression in engineered tissues.

Isotropic materials generally do not provide adequate structural guidance or mechanical support for the growing tissue. For example, fibrin gels typically exhibit a compressive stiffness around 3–15 kPa [47]. However some promising work in other tissues suggests

that mechanical stimulation may help to stimulate cell alignment and matrix stiffening. In particular, various studies by Nerem and colleagues have shown that cyclic mechanical stretch can improve the mechanical properties of collagen- and fibrin-based vascular constructs. Under cyclic distention, the vascular smooth muscle cells and/or mesenchymal stem cells elongate, align with the axis of circumferential strain, and condense the hydrogel matrix. The net results are constructs with morphological and mechanical properties similar to those of native vasculature [48–50]. There is some recent suggestion that a similar phenomenon may occur with engineered cartilage, though the results are relatively preliminary. In one notable study, annulus fibrosus cells placed in a type I collagen gel were cultured in a ring-shaped gel around a stiff mandrel. As the cells contracted the mesh, they presumably generated circumferential hoop stresses and aligned with the axis of stress [51]. Vanderploeg and colleagues found a similar phenomenon in fibrin gels, wherein cells aligned with the axis of uniaxial stretch [52]. Collectively, these studies suggest that anisotropy may be induced via exogenous signals, rather than biomaterial architecture. However such signals are generally slow to act, and therefore require extensive culture time *in vivo* prior to implantation. While not an absolute obstacle to clinical tissue engineering, this does pose problems for product development.

A handful of studies have investigated *in situ* performance of isotropic biomaterials. Porous Teflon materials had some initial success and were superior to untreated controls (with no meniscus whatsoever), but tended to generate foreign body responses, synovitis, and degradation particles [53, 54]. Polyurethanes likewise performed better than untreated controls, but elicited better biological response, with moderate cell invasion [55–58]. Interestingly, at least one study found regional variations in success rates, with the authors proposing that local vascularity may be an important predictor of outcome [58]. This may be of particular importance in the IVD, where vascularity is even lower than in the menisci. If so, various strategies may be required to overcome the low mass transport environment of the IVD. As of yet, very few methods have been proposed to overcome this issue.

Isotropic materials have found limited success, though the three existing meniscus products, Menaflex™, Restore Orthobiologic Implant™, and Hyalograft C™, fall in this category. Initial clinical findings with these products are promising, with generally positive outcomes at 5-year followup. The Restore Orthobiologic Implant received US FDA 510(k) clearance in 2007 to “reinforce soft tissue,” i.e. as a partial replacement to augment repair of tears [59]. The Menaflex implant likewise received 510(k) clearance in 2008 for replacement of the medial meniscus [60].

With the possible exceptions of Teflon and polyurethane, none of these scaffolds have provided adequate initial mechanical properties, nor have they produced engineered constructs with adequate mechanical properties for implantation. This could be solved by either extensive *in vitro* culture time (increasing costs and risk of contamination) or by using different biomaterials. Since the tissue’s own mechanical function appears to depend so heavily upon its anisotropic architecture, perhaps our biomaterials should attempt to mimic this structural feature.

A first step towards generating anisotropic biomaterials is to identify those substances that can be formed into fibrous structures. This significantly reduces the number of candidate materials. The list of fibrous biomaterials is relatively short, but includes such

diverse materials as polycaprolactone [61–64], poly(L-lactic) acid [65–67], polyglycolic acid [67–69], alginate [44], elastin [70, 71], and collagen [70–75] (though the latter two do not appear to have been used in fibrocartilage as of yet). The results are generally quite positive, though most studies are *in vitro* only, and *in vivo* performance data is quite limited. Fibrochondrocytes appear to adhere and proliferate well to these materials and express mRNA and protein for various extracellular matrix molecules, including the ubiquitous aggrecan and collagen types I and II. Most interestingly, the resulting tissue constructs often demonstrate cell and matrix alignment coincident with that of the original biomaterial [44, 61, 62, 65, 67, 76].

One major obstacle to fibrous biomaterials – and almost all homogeneous materials developed to date – is a low tensile strength. Compressive loading of the menisci or IVD generates substantial radial and circumferential stresses, which must be resisted by the material. Few if any biomaterials have obtained tensile strengths comparable to that of native fibrillar collagen. Among the strongest materials are poly (caprolactone) fabrics, with strength values ranging 1–25 MPa [77, 78], and polyglycolic acid fabrics, with strength values ranging 0.15–0.25 MPa [79]. However these materials undergo plastic deformation and creep failure when exposed to cyclic strain, limiting their use in engineering elastomeric tissues [80].

A relatively small number of studies have taken the next step and attempted to create anisotropic materials for fibrocartilage repair. In all three cases, poly (ϵ -caprolactone) nanofiber meshes were produced using electrospinning (which will be discussed later). The fibers were collected on a rotating mandrel during synthesis, producing a fabric mat of linearly oriented fibers. The resulting scaffolds were seeded with meniscal fibrochondrocytes or mesenchymal stem cells and cultured for up to 10 weeks *in vitro*. Total collagen and glycosaminoglycans content increased over time, with peak concentrations reaching 9.54 and 13.6 $\mu\text{g}/\text{mg}$, respectively, well below those of native tissue. Material testing revealed substantial anisotropy, with a tenfold change in tensile modulus and tensile strength through a 90° rotation [61, 62, 81].

To this authors' knowledge, only one group has attempted to replicate the gross architecture of the IVD. The isotropic nucleus pulposus was replicated using sodium alginate, while the anisotropic annulus fibrosus was replicated using isotropic PGA felt. Constructs were cultured both *in vitro* and *ex vivo* for up to 12 weeks, but the resulting mechanical and histochemical analyses revealed tissues which only superficially resembled the native IVD [67, 76]. Clearly we are still a long way from having a tissue engineered IVD, though progress is being made.

13.3.2

Biocompatibility

Fibrochondrocyte adhesion and biocompatibility appears to be a relatively straightforward issue. The tissues possess minimal vascularity or lymphatic access [46, 82], thus biocompatibility may not be a primary concern. In this regard, any material that passes ISO 10993 biocompatibility screening should be considered a candidate [83]. To date, all of the biomaterials used in fibrocartilage tissue engineering have passed basic biocompatibility

tests, though few have undergone rigorous testing per the ISO standard. From a regulatory standpoint, recall that no regulator approves materials (though Master Files are commonly kept, which demonstrate a basic safety level with a particular material composition). Only the final device undergoes regulatory review, and as such the designer should be cautious about placing too much hope on biocompatibility testing of individual materials.

13.3.3

Bioactive Cues

The list of potential bioactive cues is immense, and a comprehensive review of the subject is therefore beyond our current scope. Instead, a brief summary of the most common cues is illustrative (Table 13.3). Various growth factors have been explored, but the most common are bFGF, TGF- β 1, IGF-1, PDGF, and IL-1. The former four generally stimulate cell proliferation and matrix synthesis, while IL-1 elicits matrix catabolism. However few studies have investigated the simultaneous effects of these cytokines. Biological signals frequently combine in unpredictable or nonlinear fashions, so the separate effects of each molecule may not predict their combined effects. The anabolic growth factors elicit a similar response (increased synthesis of proteoglycan and collagen and increased proliferation), suggesting that they act at common points in the cytoplasmic signalling process. A visual inspection of the intracellular signalling pathways for each of these molecules (PowerPathways, Inc.) suggests that there are a few commonalities, including JNK, ERK 1/2, and ELK1, though none are shared between all four anabolic cytokines, and JNK is common with IL-1. Therefore it is likely that one or more of the growth factors affect fibrochondrocytes via unique signalling pathways, and they may have sympathetic or antagonistic effects when tested in combination. Only further testing will answer this urgent question.

Mechanical signals are likewise mixed; hydrostatic pressure and cyclic tension at physiologic ranges typically stimulates cell proliferation and matrix synthesis, while cyclic

Table 13.3 Selected bioactive cues in fibrocartilage engineering

	Factor	General effect	References
Growth factors	bFGF	Stimulatory	[84–89]
	TGF- β 1	Stimulatory	[84, 90–96]
	IGF-1	Stimulatory	[84, 97–101]
	PDGF	Stimulatory	[97, 100, 102]
	OP-1	Stimulatory	[103–105]
	IL-1	Inhibitory	[106–112]
Mechanical signals	Hydrostatic pressure	Stimulatory	[91, 93, 113–116]
	Cyclic compression	Inhibitory	[117]
	Cyclic tension	Stimulatory	[52]
Matrix signals	Hyaluronan	Stimulatory	[118, 119]
	RGD peptide	Stimulatory	[120]
	Fibronectin	Mixed	[121–123]

13 uniaxial compression may have an inhibitory effect, even possibly stimulating matrix catabolism [117]. This is in marked contrast to articular cartilage, where cyclic compression has long been understood to have a stimulatory effect [124–126].

Soluble and mechanical factors are not the only cues that can drive cell behavior. Matrix signals are the least understood, and probably merit the most attention from biomaterials scientists. Hyaluronan appears to have a strong stimulatory effect [118, 119], while fibronectin has a mixed effect upon matrix gene and protein expression [121–123]. Fibrochondrocytes express numerous integrins, including the $\alpha 1$, $\alpha 2$, $\alpha 5$, $\alpha 6$, αV , $\beta 1$, $\beta 3$, and $\beta 5$ subunits [127–130], plus cell adhesion molecules CD44 and CD105 [9]. These molecules produce a relatively “sticky” cell, capable of adhering to a wide variety of materials and surfaces. However one must remember that the recruitment of specific cell adhesion molecules can alter cell metabolism and phenotype; therefore selective adhesion may be a useful tool for fibrocartilage tissue engineering.

It is worth noting that many biomaterials lack any inherent capacity for cell adhesion. In particular, several of the hydrogels, including agarose, alginate, and PVA, are inert. Instead of directly binding cells, they encapsulate them in the hydrogel matrix. Therefore all bioactive cues come from either exogenous stimuli such as growth factors or from autocrine/paracrine signals created by the cells during tissue formation. This could be a positive feature of the material, as the tissue engineer potentially has much more direct control over the cell stimuli.

Several studies have attempted to manipulate the adhesive features of biomaterial surfaces, though few have worked in the specific area of fibrocartilage engineering [131]. In one notable study, Chang and coauthors investigated the effect of binding RGD to a silk scaffold for IVD tissue engineering. They found that while RGD did not affect cell attachment rates, it did alter cell morphology and increase expression of collagen type II and aggrecan mRNA [120]. This may be an important area of future investigation.

To make matters more complex, some biologically derived materials may contain bioactive signals, but often they are either uncharacterized or difficult to characterize. Collagen, for example, is not generally obtained as a normal intact protein. Instead, acid-solubilized protein is commonly used. This material consists of denatured collagen fibrils, which will undoubtedly present an abnormal signalling environment to cells. Porcine small intestinal submucosa (SIS) is derived from porcine gut, and contains a mixture of various extracellular matrix proteins, growth factors, cytokines, and other molecules [132, 133]. While the preparation appears to leave the various molecules relatively intact, the exact composition – or even batch-to-batch variability – is largely unpublished. For these reasons, one should use caution when opting for extracted biologically derived scaffolds; you may be dealing with significant unknown factors in your study.

13.3.4

Mechanical Function

Unless we are to propose extensive *in vitro* culture periods prior to implantation, adequate mechanical support will depend greatly upon the mechanical properties of the scaffold. If the material is to degrade, then it must do so at a compatible rate to the

new tissue formation. If not, then it must be compatible with the new tissue in the long-term.

Compressive and viscoelastic properties could be provided directly by the properties of the biomaterial's solid matrix, or by solid–fluid interactions. If we follow the general logic that biomimicry has the best chance of success, then a solid matrix with a large negative fixed charge density would appear to be a promising option. However no material to date has taken this tactic, perhaps because of the complex chemistry involved in fabricating such a nano-engineered material.

Another important consideration is anchorage of the implant to the surgical site. In the IVD, for example, even low-intensity activity generates substantial internal forces [27]. Thus an implant used to seal the ruptured annulus fibrosus, with a 1 cm² face, would have to withstand 60 N of ejection force when upright, and 230 N during heavy lifting. On a cylindrical implant 1cm deep, this translates to interfacial shear stress of 760 kPa and 2.9 MPa, respectively. In comparison, fibrin glue typically demonstrates shear strength around 2–10 kPa [134], far below that required in the IVD.

13.3.5

Deliverability

To date, very few studies have focused upon the deliverability of engineered fibrocartilages. Delivery of the menisci is relatively straightforward, as arthroscopic techniques have been developed and refined over several decades. Delivery of IVDs is more challenging, as the surgical procedures are varied, and the surgeon's visible window is often quite restricted (frequently a field of a few centimetres viewed and accessed through a 10–20 cm deep approach) [6]. Even something as simple as locating the correct surgical level can sometimes be challenging, particularly in overweight individuals [6]. This means that complex instrumentation is often required – see for example the detailed instruments developed for preparation, delivery, and positioning of various arthroplasty devices. Therefore special care should be taken in the initial design phase, in order to assure that reasonable delivery techniques will be available for the final product.

To take just one illustrative example, consider a two-phase hydrogel which is intended to be injected and polymerized in situ (such as fibrin). The injection needle would have to be placed into the disc from 10 to 20 cm away, then the polymer phases would be driven through a long needle or cannula into the disc. The risk of polymerization inside the delivery mechanism may prohibit mixing of the phases prior to injection, meaning that two cannulae will be required. Moreover, a substantial amount of material will be left inside the cannulae, effectively increasing waste and cost of the system.

It is clear that we need to give significant time and consideration to this complex issue. Even the best designed therapy will be useless if patients and surgeons are unwilling to adopt the time, morbidity, and complications inherent in a poorly designed delivery system (Table 13.4).

Table 13.4 Selected materials used in fibrocartilage repair and replacement

Material	Degradable?	Anisotropic?	Type	Example references/products
Alginate	Yes	Yes ^a	Biopolymer	[44, 67]
Bioglass	No	No	Glass-ceramic	[66, 135]
Chitosan/alginate/hyaluronate copolymer	Yes	No	Biopolymer	[136]
Collagen	Yes	Yes ^a	Biopolymer	Menaflex™ Restore orthobiologic implant [51, 137]
Hyaluronan	Yes	No	Biopolymer	Hyalograft C™ [65, 138, 139]
Poly(caprolactone) (PCL)	No	Yes	Polymer	[62, 66, 135, 140–142]
Polyglycolic acid (PGA)	Yes	Yes	Synthetic biopolymer	[67]
Poly(lactic acid) (PLA)	Yes	Yes ^a	Synthetic biopolymer	[66, 135, 143–146]
Poly(urethane)	No	No	Polymer	[55, 57, 58]
Poly(vinyl alcohol) (PVA)	No	No	Polymeric hydrogel	[147–149]
Scaffold-free	Yes	–	–	[42]
Silicone rubber	No	No	Polymer	[150]
Silk	No	Yes	Biopolymer	[120, 151]
Small intestinal submucosa	Yes	No	Mixed biopolymer	[152–159]
Teflon	No	No	Polymer	Vitek TMJ [53, 54, 160, 161]

^aAnisotropy of some materials is dependent upon the fabrication method chosen

13.4 Future Directions

The abdomen, the chest, and the brain will forever be shut from the intrusion of the wise and humane surgeon.

Sir John Eric Ericksen, British surgeon, appointed Surgeon-Extraordinary to Queen Victoria 1873

So the question stands: what next? Where do we go from here? History is full of predictions both astounding and ludicrous. Rather than try to predict the future direction of fibrocartilage biomaterials, let us summarize a few key areas, which may be worth studying in the near future.

13.4.1

Aligned/Microengineered Anisotropic Materials

As much as it pains me as a mechanical engineer, I feel strongly that mechanical stimulation alone will be insufficient to stimulate formation of adequate tissue architecture and properties. With every new study that is published, it appears more likely that micro- or nano-engineered materials with built-in anisotropy are the way to go. However the complexity of the architectures correlates directly to the difficulty in building it, so cost and effort may increase significantly. The worry is that these technologies will drive the engineered fibrocartilage beyond an acceptable range of cost-effectiveness; therefore improved fabrication technologies will also be required.

Several techniques have been developed to produce anisotropic biomaterials. Among the most promising are electrospinning and three-dimensional printing. Electrospinning is the technique used for most of the fibrous biomaterials mentioned earlier, with a few wet- or heat-spun materials. For a comprehensive review of electrospinning and the underlying theory, see various texts and papers [162–165]. In brief, the method involves extruding a thin stream of a charged polymer solution in a strong electromagnetic field. The field draws the fluid into a “Taylor Cone” with a final stream diameter ranging from micrometers to nanometers. By using a highly volatile solvent or a melt-spun material, the polymer is able to dry or cool by the time it hits a grounded target collector, forming extremely small fibers. One particular advantage of electrospinning is the potential to adjust the orientation of the ground to generate filaments with a preferential orientation. Various methods have been proposed, but spinning mandrels [61, 62] and parallel ground plates [166] are common. The spinning mandrel technique was used in the three published fibrocartilage studies [61, 62, 81], and has demonstrated promise. The greatest potential of electrospinning may be the ability to layer mats at various orientations. This can be achieved in various ways, including moving xy stages [167] or alternating ground electrodes [168]. This could lead to complex anisotropic structures, mimicking the native architecture of fibrocartilage. These structures would in turn hold great promise for tissue engineering applications.

Perhaps the optimum compromise will be a moderately structured material, which undergoes a brief period of mechanical stimulation *in vitro* prior to implantation. When linked to an appropriate physiotherapy regimen with light to moderate *in vivo* loading, this may provide adequate tissue properties for regenerative therapy.

13.4.2

Cell Adhesion and Targeted Signalling

As discussed earlier, we still have a very poor understanding of how cytokines, matrix signals, mechanical signals, and other environmental cues interact to influence the biology of fibrochondrocytes. Selective recruitment of cell adhesion molecules by the biomaterial, combined with bound or concentrated presentation of growth factors, may prove a powerful tool for fibrocartilage tissue engineering. This will require a large battery of parametric studies to investigate the (potentially nonlinear) combined effects of the various signals.

13 Several promising techniques have been developed for targeted cell adhesion and presentation of growth factors. For example, the previously mentioned technique of binding RGD domains can be used to enhance integrin binding. Polyethylene glycol (PEG) and polyethelene oxide (PEO) have also demonstrated the potential to bind various compounds, presenting a constitutive signal to nearby cells rather than the transient signal induced by free molecules [169, 170].

13.4.3

Delivery Systems

Delivery systems may require some optimization, particularly if the biomaterials or tissue engineered constructs are to be delivered in some unconventional manner. Direct implantation of an en bloc tissue replacement could use existing techniques for meniscectomy, discectomy, etc., but partial repairs could represent new delivery challenges. For example, percutaneous injection of in situ polymerizing biomaterials for IVD repair would require imaging techniques to validate needle position, instrumentation to remove the herniated disc tissue, and tracking methods to monitor biomaterial delivery and stability. Many of these techniques exist today, but may not be compatible with future biomaterials. Radiolucent biomaterials would not be trackable by fluoroscopy (the standard intraoperative imaging method), and some materials could require special site preparation to improve adhesion of the implant, requiring modified instrumentation.

13.4.4

The Ultimate Engineered Fibrocartilage: One Author's Guess

If I were pressured to hazard a prediction, I would suggest that the first truly functional engineered fibrocartilage will contain several key features. Firstly, the material will be a composite that mimics some of the native tissue's architecture. An electrospun polymer fiber assembly will be embedded into a hydrogel matrix possessing a negative fixed charge density. This combination will provide both architectural cues and initial mechanical stabilization for the growing tissue. Both will be biodegradable to facilitate regeneration of a native tissue. The construct will have various moieties bound to the fibrous and hydrogel matrix to facilitate cell adhesion and stimulate appropriate phenotypic expression. Many researchers and companies have expressed reservations about the use of exogenous growth factors, largely due to cost and contamination issues. However I doubt we will be able to completely avoid them, and some appropriate cytokines will be required, either bound to the matrix or delivered during a pre-implantation culture period. Finally, the construct will benefit from some controlled mechanical stimulation, either ex vivo prior to implantation or via well characterized postoperative physiotherapy.

Time will tell how (in)accurate my prediction turns out to be.

Fibrocartilage is a challenging tissue for the tissue engineer. Its structure and function present significant puzzles, and the literature is filled with unsuccessful attempts. Any biomaterial must provide mechanical stability, architectural and biological cues, be biocompatible,

and be deliverable in order to be a candidate. No material to date has achieved such lofty goals, but efforts continue unabated. These and many other challenges will need to be met before clinically effective engineered fibrocartilage can be developed. However there are numerous excellent research teams on the task, and it is very likely that new innovations will be coming soon.

Acknowledgements I gratefully acknowledge the support of the Alberta Heritage Foundation for Medical Research, the Alberta Ingenuity Fund, and the Natural Sciences and Engineering Research Council of Canada for their support.

Many thanks to Dr. John Matyas of the University of Calgary for sharing his MR images of the IVD and menisci.

References

1. Martini F, Bartholomew EF. *Essentials of anatomy & physiology*. 5th ed. San Francisco: Benjamin Cummings., 2009.
2. Englund M. Meniscal tear – a common finding with often troublesome consequences. *J Rheumatol* 2009 Jul;36(7):1362–1364.
3. Englund M, Guermazi A, Roemer FW, Aliabadi P, Yang M, Lewis CE, et al. Meniscal tear in knees without surgery and the development of radiographic osteoarthritis among middle-aged and elderly persons: The Multicenter Osteoarthritis Study. *Arthritis Rheum* 2009 Mar; 60(3):831–839.
4. Goncalves DA, Speciali JG, Jales LC, Camparis CM, Bigal ME. Temporomandibular symptoms, migraine, and chronic daily headaches in the population. *Neurology* 2009 Aug 25; 73(8):645–646.
5. Heliovaara M, Knekt P, Aromaa A. Incidence and risk factors of herniated lumbar intervertebral disc or sciatica leading to hospitalization. *J Chronic Dis* 1987;40(3):251–258.
6. Wiesel SW, International Society for Study of the Lumbar Spine. *The lumbar spine*. 2nd ed. Philadelphia: W. B. Saunders Co., 1996.
7. Buma P, Ramrattan NN, van Tienen TG, Veth RP. Tissue engineering of the meniscus. *Biomaterials* 2004 Apr;25(9):1523–1532.
8. Benjamin M, Ralphs JR. Biology of fibrocartilage cells. *Int Rev Cytol* 2004;233:1–45.
9. Verdonk PC, Forsyth RG, Wang J, Almqvist KF, Verdonk R, Veys EM, et al. Characterisation of human knee meniscus cell phenotype. *Osteoarthritis Cartilage* 2005 Jul;13(7):548–560.
10. Zhao CQ, Wang LM, Jiang LS, Dai LY. The cell biology of intervertebral disc aging and degeneration. *Ageing Res Rev* 2007 Oct;6(3):247–261.
11. Brindle T, Nyland J, Johnson DL. The meniscus: review of basic principles with application to surgery and rehabilitation. *J Athl Train* 2001 Apr;36(2):160–169.
12. Gray H, Pick TP, Howden R. *Anatomy, descriptive and surgical*. Rev. American, from the 15th English ed. New York: Bounty Books, 1977.
13. Lai WM, Hou JS, Mow VC. A triphasic theory for the swelling and deformation behaviors of articular cartilage. *J Biomech Eng* 1991 Aug;113(3):245–258.
14. Buschmann MD, Grodzinsky AJ. A molecular model of proteoglycan-associated electrostatic forces in cartilage mechanics. *J Biomech Eng* 1995 May;117(2):179–192.
15. Bell GR, Wiesel SW, Weinstein JN, Herkowitz HN, Dvorak J. *Anatomy of the lumbar spine: developmental to normal adult anatomy*. The Lumbar Spine. Philadelphia, PA: W.B. Saunders Company, 1996. p. 43–52.

16. Urban JP, Wiesel SW, Weinstein JN, Herkowitz HN, Dvorak J, Bell GR. Disc biochemistry in relation to function. *The Lumbar Spine*. Philadelphia, PA: W.B. Saunders Company, 1996. p. 271–281.
17. Hunter CJ, Matyas JR, Duncan NA. Cytomorphology of notochordal and chondrocytic cells from the nucleus pulposus: a species comparison. *J Anat* 2004 Nov;205(5):357–362.
18. Eyre DR, Muir H. Types I and II collagens in intervertebral disc. Interchanging radial distributions in annulus fibrosus. *Biochem J* 1976;157(1):267–270.
19. Helfet AJ, Gruebel Lee DM. Disorders of the lumbar spine: Arthur J. Helfet and David M. Gruebel Lee, with 14 guest authors. Philadelphia: Lippincott, 1978.
20. DePalma AF, Rothman RH. *The Intervertebral Disc*. Philadelphia, PA: W.B. Saunders Company, 1970.
21. Bron JL, Helder MN, Meisel HJ, Van Royen BJ, Smit TH. Repair, regenerative and supportive therapies of the annulus fibrosus: achievements and challenges. *Eur Spine J* 2009 Mar;18(3):301–313.
22. Wirth CJ. The meniscus – structure, morphology and function. *Knee* 1996;3(1–2):57–58.
23. Englund M. The role of the meniscus in osteoarthritis genesis. *Rheum Dis Clin North Am* 2008 Aug;34(3):573–579.
24. van Tienen TG, Hannink G, Buma P. Meniscus replacement using synthetic materials. *Clin Sports Med* 2009 Jan;28(1):143–156.
25. Taylor SJ, Walker PS, Perry JS, Cannon SR, Woledge R. The forces in the distal femur and the knee during walking and other activities measured by telemetry. *J Arthroplasty* 1998 Jun;13(4):428–437.
26. Mizrahi J, Susak Z. Analysis of parameters affecting impact force attenuation during landing in human vertical free fall. *Eng Med* 1982 Jul;11(3):141–147.
27. Wilke HJ, Neef P, Caimi M, Hoogland T, Claes LE. New in vivo measurements of pressures in the intervertebral disc in daily life. *Spine (Phila Pa 1976)* 1999 Apr 15;24(8):755–762.
28. Black J, Hastings GW. *Handbook of biomaterial properties*. 1st ed. London, New York: Chapman & Hall, 1998.
29. Bullough PG, Munuera L, Murphy J, Weinstein AM. The strength of the menisci of the knee as it relates to their fine structure. *J Bone Joint Surg Br* 1970 Aug;52(3):564–567.
30. Galante JO. Tensile properties of the human lumbar annulus fibrosus. *Acta Orthop Scand Suppl* 1967;100:101–191.
31. Hommen JP, Applegate GR, Del Pizzo W. Meniscus allograft transplantation: ten-year results of cryopreserved allografts. *Arthroscopy* 2007 Apr;23(4):388–393.
32. Lubowitz JH, Verdonk PC, Reid JB, 3rd, Verdonk R. Meniscus allograft transplantation: a current concepts review. *Knee Surg Sports Traumatol Arthrosc* 2007 May;15(5):476–492.
33. Kim JM, Bin SI. Meniscal allograft transplantation after total meniscectomy of torn discoid lateral meniscus. *Arthroscopy* 2006 Dec;22(12):1344–1350, e1341.
34. Luk KD, Ruan DK. Intervertebral disc transplantation: a biological approach to motion preservation. *Eur Spine J* 2008 Dec;17(Suppl 4):504–510.
35. Ruan D, He Q, Ding Y, Hou L, Li J, Luk KD. Intervertebral disc transplantation in the treatment of degenerative spine disease: a preliminary study. *Lancet* 2007 Mar 24;369(9566):993–999.
36. Skalli W, Dubouset J. Intervertebral disc transplantation. *Lancet* 2007 Mar 24;369(9566):968–969.
37. Friction JR, Look JO, Schiffman E, Swift J. Long-term study of temporomandibular joint surgery with alloplastic implants compared with nonimplant surgery and nonsurgical rehabilitation for painful temporomandibular joint disc displacement. *J Oral Maxillofac Surg* 2002 Dec;60(12):1400–1411; discussion 1411–1412.
38. Speculand B, Hensher R, Powell D. Total prosthetic replacement of the TMJ: experience with two systems 1988–1997. *Br J Oral Maxillofac Surg* 2000 Aug;38(4):360–369.

39. Mercuri LG. Considering total temporomandibular joint replacement. *Cranio* 1999 Jan;17(1):44–48.
40. Arnoczky SP, Warren RF, Spivak JM. Meniscal repair using an exogenous fibrin clot. An experimental study in dogs. *J Bone Joint Surg Am* 1988 Sep;70(8):1209–1217.
41. Chan BP, Leong KW. Scaffolding in tissue engineering: general approaches and tissue-specific considerations. *Eur Spine J* 2008 Dec;17(Suppl 4):467–479.
42. Aufderheide AC, Athanasiou KA. Assessment of a bovine co-culture, scaffold-free method for growing meniscus-shaped constructs. *Tissue Eng* 2007 Sep;13(9):2195–2205.
43. Henriksson HB, Svanvik T, Jonsson M, Hagman M, Horn M, Lindahl A, et al. Transplantation of human mesenchymal stem cells into intervertebral discs in a xenogeneic porcine model. *Spine (Phila Pa 1976)* 2009 Jan 15;34(2):141–148.
44. Shao X, Hunter CJ. Developing an alginate/chitosan hybrid fiber scaffold for annulus fibrosus cells. *J Biomed Mater Res A* 2007 Sep 1;82(3):701–710.
45. Neidlinger-Wilke C, Wurtz K, Liedert A, Schmidt C, Borm W, Ignatius A, et al. A three-dimensional collagen matrix as a suitable culture system for the comparison of cyclic strain and hydrostatic pressure effects on intervertebral disc cells. *J Neurosurg Spine* 2005 Apr;2(4):457–465.
46. Chevrier A, Nelea M, Hurtig MB, Hoemann CD, Buschmann MD. Meniscus structure in human, sheep, and rabbit for animal models of meniscus repair. *J Orthop Res* 2009 Sep;27(9):1197–1203.
47. Hunter CJ, Mouw JK, Levenston ME. Dynamic compression of chondrocyte-seeded fibrin gels: effects on matrix accumulation and mechanical stiffness. *Osteoarthritis Cartilage* 2004 Feb;12(2):117–130.
48. Seliktar D, Nerem RM, Galis ZS. Mechanical strain-stimulated remodeling of tissue-engineered blood vessel constructs. *Tissue Eng* 2003 Aug;9(4):657–666.
49. Seliktar D, Black RA, Vito RP, Nerem RM. Dynamic mechanical conditioning of collagen-gel blood vessel constructs induces remodeling in vitro. *Ann Biomed Eng* 2000 Apr;28(4):351–362.
50. Cummings CL, Gawlitta D, Nerem RM, Stegemann JP. Properties of engineered vascular constructs made from collagen, fibrin, and collagen-fibrin mixtures. *Biomaterials* 2004 Aug;25(17):3699–3706.
51. Bowles RD, Williams R, Zipfel W, Bonassar LJ. Self-assembly of aligned tissue engineered annulus fibrosus and IVD composite via collagen gel contraction. *Tissue Eng Part A* 2010 Apr;16(4):1339–1348.
52. Vanderploeg EJ, Imler SM, Brodtkin KR, Garcia AJ, Levenston ME. Oscillatory tension differentially modulates matrix metabolism and cytoskeletal organization in chondrocytes and fibrochondrocytes. *J Biomech* 2004 Dec;37(12):1941–1952.
53. Messner K. Meniscal substitution with a Teflon-periosteal composite graft: a rabbit experiment. *Biomaterials* 1994 Feb;15(3):223–230.
54. Messner K, Gillquist J. Prosthetic replacement of the rabbit medial meniscus. *J Biomed Mater Res* 1993 Sep;27(9):1165–1173.
55. de Groot JH, de Vrijer R, Pennings AJ, Klompmaker J, Veth RP, Jansen HW. Use of porous polyurethanes for meniscal reconstruction and meniscal prostheses. *Biomaterials* 1996 Jan;17(2):163–173.
56. Klompmaker J, Jansen HW, Veth RP, Nielsen HK, de Groot JH, Pennings AJ. Porous implants for knee joint meniscus reconstruction: a preliminary study on the role of pore sizes in ingrowth and differentiation of fibrocartilage. *Clin Mater* 1993;14(1):1–11.
57. Klompmaker J, Veth RP, Jansen HW, Nielsen HK, de Groot JH, Pennings AJ. Meniscal replacement using a porous polymer prosthesis: a preliminary study in the dog. *Biomaterials* 1996 Jun;17(12):1169–1175.
58. Klompmaker J, Veth RP, Jansen HW, Nielsen HK, de Groot JH, Pennings AJ, et al. Meniscal repair by fibrocartilage in the dog: characterization of the repair tissue and the role of vascularity. *Biomaterials* 1996 Sep;17(17):1685–1691.

59. FDA U. 510(k) premarket notification DePuy restore orthobiologic soft tissue implant. In: Affairs R, editor. Washington, DC, 2007.
60. FDA U. 510(k) premarket notification ReGen collagen scaffold (CS). In: Affairs R, editor. Washington, DC, 2008.
61. Li WJ, Mauck RL, Cooper JA, Yuan X, Tuan RS. Engineering controllable anisotropy in electrospun biodegradable nanofibrous scaffolds for musculoskeletal tissue engineering. *J Biomech* 2007;40(8):1686–1693.
62. Nerurkar NL, Elliott DM, Mauck RL. Mechanics of oriented electrospun nanofibrous scaffolds for annulus fibrosus tissue engineering. *J Orthop Res* 2007 Aug;25(8):1018–1028.
63. Wan Y, Feng G, Shen FH, Balian G, Laurencin CT, Li X. Novel biodegradable poly(1,8-octanediol malate) for annulus fibrosus regeneration. *Macromol Biosci* 2007 Nov 12;7(11):1217–1224.
64. Wan Y, Feng G, Shen FH, Laurencin CT, Li X. Biphasic scaffold for annulus fibrosus tissue regeneration. *Biomaterials* 2008 Feb;29(6):643–652.
65. Nesti LJ, Li WJ, Shanti RM, Jiang YJ, Jackson W, Freedman BA, et al. Intervertebral disc tissue engineering using a novel hyaluronic acid-nanofibrous scaffold (HANFS) amalgam. *Tissue Eng Part A* 2008 Sep;14(9):1527–1537.
66. Helen W, Merry CL, Blaker JJ, Gough JE. Three-dimensional culture of annulus fibrosus cells within PDLA/Bioglass composite foam scaffolds: assessment of cell attachment, proliferation and extracellular matrix production. *Biomaterials* 2007 Apr;28(11):2010–2020.
67. Mizuno H, Roy AK, Vacanti CA, Kojima K, Ueda M, Bonassar LJ. Tissue-engineered composites of anulus fibrosus and nucleus pulposus for intervertebral disc replacement. *Spine (Phila Pa 1976)* 2004 Jun 15;29(12):1290–1297; discussion 1297–1298.
68. Aufderheide AC, Athanasiou KA. Comparison of scaffolds and culture conditions for tissue engineering of the knee meniscus. *Tissue Eng* 2005 Jul–Aug;11(7–8):1095–1104.
69. Sha'ban M, Yoon SJ, Ko YK, Ha HJ, Kim SH, So JW, et al. Fibrin promotes proliferation and matrix production of intervertebral disc cells cultured in three-dimensional poly(lactic-co-glycolic acid) scaffold. *J Biomater Sci Polym Ed* 2008;19(9):1219–1237.
70. Buttafoco L, Kolkman NG, Engbers-Buijtenhuijs P, Poot AA, Dijkstra PJ, Vermes I, et al. Electrospinning of collagen and elastin for tissue engineering applications. *Biomaterials* 2006 Feb;27(5):724–734.
71. Boland ED, Matthews JA, Pawlowski KJ, Simpson DG, Wnek GE, Bowlin GL. Electrospinning collagen and elastin: preliminary vascular tissue engineering. *Front Biosci* 2004 May 1;9:1422–1432.
72. Rho KS, Jeong L, Lee G, Seo BM, Park YJ, Hong SD, et al. Electrospinning of collagen nanofibers: effects on the behavior of normal human keratinocytes and early-stage wound healing. *Biomaterials* 2006 Mar;27(8):1452–1461.
73. Buttafoco L, Kolkman NG, Poot AA, Dijkstra PJ, Vermes I, Feijen J. Electrospinning collagen and elastin for tissue engineering small diameter blood vessels. *J Control Release* 2005 Jan 3;101(1–3):322–324.
74. Shields KJ, Beckman MJ, Bowlin GL, Wayne JS. Mechanical properties and cellular proliferation of electrospun collagen type II. *Tissue Eng* 2004 Sep–Oct;10(9–10):1510–1517.
75. Matthews JA, Wnek GE, Simpson DG, Bowlin GL. Electrospinning of collagen nanofibers. *Biomacromolecules* 2002 Mar–Apr;3(2):232–238.
76. Mizuno H, Roy AK, Zaporojan V, Vacanti CA, Ueda M, Bonassar LJ. Biomechanical and biochemical characterization of composite tissue-engineered intervertebral discs. *Biomaterials* 2006 Jan;27(3):362–370.
77. Gaumer J, Prasad A, Lee D, Lannutti J. Structure-function relationships and source-to-ground distance in electrospun polycaprolactone. *Acta Biomater* 2009 Jun;5(5):1552–1561.
78. Kim YJ, Shin CH, Lee SI, Jang SH, Kim BS, Shin BY. Mechanical properties, biodegradability and weatherability of PCL/calcium carbonate composite. *J Korean Ind Eng Chem* 2000;11(3):276–284.

79. Klouda L, Vaz CM, Mol A, Baaijens FP, Bouten CV. Effect of biomimetic conditions on mechanical and structural integrity of PGA/P4HB and electrospun PCL scaffolds. *J Mater Sci Mater Med* 2008 Mar;19(3):1137–1144.
80. Webb AR, Yang J, Ameer GA. Biodegradable polyester elastomers in tissue engineering. *Expert Opin Biol Ther* 2004 Jun;4(6):801–812.
81. Baker BM, Mauck RL. The effect of nanofiber alignment on the maturation of engineered meniscus constructs. *Biomaterials* 2007 Apr;28(11):1967–1977.
82. Gray JC. Neural and vascular anatomy of the menisci of the human knee. *J Orthop Sports Phys Ther* 1999 Jan;29(1):23–30.
83. Gad SC. Safety evaluation of medical devices. 2nd ed. New York: M. Dekker, 2002.
84. Fox DB, Warnock JJ, Stoker AM, Luther JK, Cockrell M. Effects of growth factors on equine synovial fibroblasts seeded on synthetic scaffolds for avascular meniscal tissue engineering. *Res Vet Sci* 2010 Apr;88(2):326–332.
85. Narita A, Takahara M, Ogino T, Fukushima S, Kimura Y, Tabata Y. Effect of gelatin hydrogel incorporating fibroblast growth factor 2 on human meniscal cells in an organ culture model. *Knee* 2009 Aug;16(4):285–289.
86. Tumia NS, Johnstone AJ. Promoting the proliferative and synthetic activity of knee meniscal fibrochondrocytes using basic fibroblast growth factor in vitro. *Am J Sports Med* 2004 Jun;32(4):915–920.
87. Dahia CL, Mahoney EJ, Durrani AA, Wylie C. Intercellular signaling pathways active during intervertebral disc growth, differentiation, and aging. *Spine (Phila Pa 1976)* 2009 Mar 1;34(5):456–462.
88. Ellman MB, An HS, Muddasani P, Im HJ. Biological impact of the fibroblast growth factor family on articular cartilage and intervertebral disc homeostasis. *Gene* 2008 Aug 15;420(1):82–89.
89. Tsai TT, Guttapalli A, Oguz E, Chen LH, Vaccaro AR, Albert TJ, et al. Fibroblast growth factor-2 maintains the differentiation potential of nucleus pulposus cells in vitro: implications for cell-based transplantation therapy. *Spine (Phila Pa 1976)* 2007 Mar 1;32(5):495–502.
90. Wilson CG, Nishimuta JF, Levenston ME. Chondrocytes and meniscal fibrochondrocytes differentially process aggrecan during de novo extracellular matrix assembly. *Tissue Eng Part A* 2009 Jul;15(7):1513–1522.
91. Gunja NJ, Uthamanthil RK, Athanasiou KA. Effects of TGF-beta1 and hydrostatic pressure on meniscus cell-seeded scaffolds. *Biomaterials* 2009 Feb;30(4):565–573.
92. Gruber HE, Mauerhan D, Chow Y, Ingram JA, Norton HJ, Hanley EN, Jr., et al. Three-dimensional culture of human meniscal cells: extracellular matrix and proteoglycan production. *BMC Biotechnol* 2008;8:54.
93. Elder BD, Athanasiou KA. Synergistic and additive effects of hydrostatic pressure and growth factors on tissue formation. *PLoS One* 2008;3(6):e2341.
94. Pangborn CA, Athanasiou KA. Effects of growth factors on meniscal fibrochondrocytes. *Tissue Eng* 2005 Jul–Aug;11(7–8):1141–1148.
95. Chen WH, Lo WC, Lee JJ, Su CH, Lin CT, Liu HY, et al. Tissue-engineered intervertebral disc and chondrogenesis using human nucleus pulposus regulated through TGF-beta1 in platelet-rich plasma. *J Cell Physiol* 2006 Dec;209(3):744–754.
96. Gruber HE, Fisher EC, Jr., Desai B, Stasky AA, Hoelscher G, Hanley EN, Jr. Human intervertebral disc cells from the annulus: three-dimensional culture in agarose or alginate and responsiveness to TGF-beta1. *Exp Cell Res* 1997;235(1):13–21.
97. Gruber HE, Norton HJ, Hanley EN, Jr. Anti-apoptotic effects of IGF-1 and PDGF on human intervertebral disc cells in vitro. *Spine* 2000;25(17):2153–2157.
98. Gruber HE, Hoelscher GL, Ingram JA, Bethea S, Hanley EN. IGF-1 rescues human intervertebral annulus cells from in vitro stress-induced premature senescence. *Growth Factors* 2008 Aug;26(4):220–225.

99. Wang L, Lazebnik M, Detamore MS. Hyaline cartilage cells outperform mandibular condylar cartilage cells in a TMJ fibrocartilage tissue engineering application. *Osteoarthritis Cartilage* 2009 Mar;17(3):346–353.
100. Pratsinis H, Kleatsas D. PDGF, bFGF and IGF-I stimulate the proliferation of intervertebral disc cells in vitro via the activation of the ERK and Akt signaling pathways. *Eur Spine J* 2007 Nov;16(11):1858–1866.
101. Zhang R, Ruan D, Zhang C. Effects of TGF-beta1 and IGF-1 on proliferation of human nucleus pulposus cells in medium with different serum concentrations. *J Orthop Surg Res* 2006;1:9.
102. Tumia NS, Johnstone AJ. Platelet derived growth factor-AB enhances knee meniscal cell activity in vitro. *Knee* 2009 Jan;16(1):73–76.
103. Imai Y, Miyamoto K, An HS, Thonar EJ, Andersson GB, Masuda K. Recombinant human osteogenic protein-1 upregulates proteoglycan metabolism of human anulus fibrosus and nucleus pulposus cells. *Spine (Phila Pa 1976)* 2007 May 20;32(12):1303–1309; discussion 1310.
104. Masuda K, Imai Y, Okuma M, Muehleman C, Nakagawa K, Akeda K, et al. Osteogenic protein-1 injection into a degenerated disc induces the restoration of disc height and structural changes in the rabbit annular puncture model. *Spine (Phila Pa 1976)* 2006 Apr 1;31(7):742–754.
105. Masuda K, Takegami K, An H, Kumano F, Chiba K, Andersson GB, et al. Recombinant osteogenic protein-1 upregulates extracellular matrix metabolism by rabbit annulus fibrosus and nucleus pulposus cells cultured in alginate beads. *J Orthop Res* 2003 Sep;21(5):922–930.
106. McNulty AL, Guilak F. Integrative repair of the meniscus: lessons from in vitro studies. *Biorheology* 2008;45(3-4):487–500.
107. McNulty AL, Moutos FT, Weinberg JB, Guilak F. Enhanced integrative repair of the porcine meniscus in vitro by inhibition of interleukin-1 or tumor necrosis factor alpha. *Arthritis Rheum* 2007 Sep;56(9):3033–3042.
108. McNulty AL, Weinberg JB, Guilak F. Inhibition of matrix metalloproteinases enhances in vitro repair of the meniscus. *Clin Orthop Relat Res* 2009 Jun;467(6):1557–1567.
109. Wilusz RE, Weinberg JB, Guilak F, McNulty AL. Inhibition of integrative repair of the meniscus following acute exposure to interleukin-1 in vitro. *J Orthop Res* 2008 Apr;26(4):504–512.
110. Hoyland JA, Le Maitre C, Freemont AJ. Investigation of the role of IL-1 and TNF in matrix degradation in the intervertebral disc. *Rheumatology (Oxford)* 2008 Jun;47(6):809–814.
111. Le Maitre CL, Hoyland JA, Freemont AJ. Interleukin-1 receptor antagonist delivered directly and by gene therapy inhibits matrix degradation in the intact degenerate human intervertebral disc: an in situ zymographic and gene therapy study. *Arthritis Res Ther* 2007;9(4):R83.
112. Elfervig MK, Minchew JT, Francke E, Tsuzaki M, Banes AJ. IL-1beta sensitizes intervertebral disc annulus cells to fluid-induced shear stress. *J Cell Biochem* 2001;82(2):290–298.
113. Handa T, Ishihara H, Ohshima H, Osada R, Tsuji H, Obata K. Effects of hydrostatic pressure on matrix synthesis and matrix metalloproteinase production in the human lumbar intervertebral disc. *Spine* 1997;22:1085–1091.
114. Hutton WC, Elmer WA, Boden SD, Hyon S, Toribatake Y, Tomita K, et al. The effect of hydrostatic pressure on intervertebral disc metabolism. *Spine* 1999;24(15):1507–1515.
115. Hutton WC, Elmer WA, Bryce LM, Kozlowska EE, Boden SD, Kozlowski M. Do the intervertebral disc cells respond to different levels of hydrostatic pressure? *Clin Biomech* 2001;16(9):728–734.
116. Kasra M, Goel V, Martin J, Wang ST, Choi W, Buckwalter J. Effect of dynamic hydrostatic pressure on rabbit intervertebral disc cells. *J Orthop Res* 2003;21(4):597–603.
117. Imler SM, Doshi AN, Levenston ME. Combined effects of growth factors and static mechanical compression on meniscus explant biosynthesis. *Osteoarthritis Cartilage* 2004 Sep;12(9):736–744.

118. Haberstroh K, Enz A, Zenclussen ML, Hegewald AA, Neumann K, Abbushi A, et al. Human intervertebral disc-derived cells are recruited by human serum and form nucleus pulposus-like tissue upon stimulation with TGF-beta3 or hyaluronan in vitro. *Tissue Cell* 2009 Dec;41(6):414–420.
119. Alini M, Li W, Markovic P, Aebi M, Spiro RC, Roughley PJ. The potential and limitations of a cell-seeded collagen/hyaluronan scaffold to engineer an intervertebral disc-like matrix. *Spine (Phila Pa 1976)* 2003 Mar 1;28(5):446–454; discussion 453.
120. Chang G, Kim HJ, Kaplan D, Vunjak-Novakovic G, Kandel RA. Porous silk scaffolds can be used for tissue engineering annulus fibrosus. *Eur Spine J* 2007 Nov;16(11):1848–1857.
121. Aota Y, An HS, Homandberg G, Thonar EJ, Andersson GB, Pichika R, et al. Differential effects of fibronectin fragment on proteoglycan metabolism by intervertebral disc cells: a comparison with articular chondrocytes. *Spine (Phila Pa 1976)* 2005 Apr 1;30(7):722–728.
122. Anderson DG, Li X, Balian G. A fibronectin fragment alters the metabolism by rabbit intervertebral disc cells in vitro. *Spine (Phila Pa 1976)* 2005 Jun 1;30(11):1242–1246.
123. Anderson DG, Izzo MW, Hall DJ, Vaccaro AR, Hilibrand A, Arnold W, et al. Comparative gene expression profiling of normal and degenerative discs: analysis of a rabbit annular laceration model. *Spine (Phila Pa 1976)* 2002 Jun 15;27(12):1291–1296.
124. Grodzinsky AJ, Levenston ME, Jin M, Frank EH. Cartilage tissue remodeling in response to mechanical forces. *Annu Rev Biomed Eng* 2000;2:691–713.
125. Kim YJ, Sah RL, Grodzinsky AJ, Plaas AH, Sandy JD. Mechanical regulation of cartilage biosynthetic behavior: physical stimuli. *Arch Biochem Biophys* 1994 May 15;311(1):1–12.
126. Sah RL, Doong JY, Grodzinsky AJ, Plaas AH, Sandy JD. Effects of compression on the loss of newly synthesized proteoglycans and proteins from cartilage explants. *Arch Biochem Biophys* 1991 Apr;286(1):20–29.
127. Xia M, Zhu Y. Expression of integrin subunits in the herniated intervertebral disc. *Connect Tissue Res* 2008;49(6):464–469.
128. Nettles DL, Richardson WJ, Setton LA. Integrin expression in cells of the intervertebral disc. *J Anat* 2004 Jun;204(6):515–520.
129. Gilchrist CL, Chen J, Richardson WJ, Loeser RF, Setton LA. Functional integrin subunits regulating cell-matrix interactions in the intervertebral disc. *J Orthop Res* 2007 Jun;25(6):829–840.
130. Salter DM, Godolphin JL, Gourlay MS. Chondrocyte heterogeneity: immunohistologically defined variation of integrin expression at different sites in human fetal knees. *J Histochem Cytochem* 1995 Apr;43(4):447–457.
131. Macri L, Silverstein D, Clark RA. Growth factor binding to the pericellular matrix and its importance in tissue engineering. *Adv Drug Deliv Rev* 2007 Nov 10;59(13):1366–1381.
132. Badylak SF, Record R, Lindberg K, Hodde J, Park K. Small intestinal submucosa: a substrate for in vitro cell growth. *J Biomater Sci Polym Ed* 1998;9(8):863–878.
133. Voytik-Harbin SL, Brightman AO, Kraine MR, Waisner B, Badylak SF. Identification of extractable growth factors from small intestinal submucosa. *J Cell Biochem* 1997 Dec 15;67(4):478–491.
134. Silver FH, Wang MC, Pins GD. Preparation of fibrin glue: a study of chemical and physical methods. *J Appl Biomater* 1995 Fall;6(3):175–183.
135. Helen W, Gough JE. Cell viability, proliferation and extracellular matrix production of human annulus fibrosus cells cultured within PDLLA/Bioglass composite foam scaffolds in vitro. *Acta Biomater* 2008 Mar;4(2):230–243.
136. Hsu SH, Whu SW, Hsieh SC, Tsai CL, Chen DC, Tan TS. Evaluation of chitosan-alginate-hyaluronate complexes modified by an RGD-containing protein as tissue-engineering scaffolds for cartilage regeneration. *Artif Organs* 2004 Aug;28(8):693–703.
137. Sato M, Asazuma T, Ishihara M, Kikuchi T, Masuoka K, Ichimura S, et al. An atelocollagen honeycomb-shaped scaffold with a membrane seal (ACHMS-scaffold) for the culture of

- annulus fibrosus cells from an intervertebral disc. *J Biomed Mater Res A* 2003 Feb 1;64(2):248–256.
138. Tognana E, Borriore A, De Luca C, Pavesio A. Hyalograft C: hyaluronan-based scaffolds in tissue-engineered cartilage. *Cells Tissues Organs* 2007;186(2):97–103.
139. Burdick JA, Chung C, Jia X, Randolph MA, Langer R. Controlled degradation and mechanical behavior of photopolymerized hyaluronic acid networks. *Biomacromolecules* 2005 Jan–Feb;6(1):386–391.
140. Baker BM, Gee AO, Metter RB, Nathan AS, Marklein RA, Burdick JA, et al. The potential to improve cell infiltration in composite fiber-aligned electrospun scaffolds by the selective removal of sacrificial fibers. *Biomaterials* 2008 May;29(15):2348–2358.
141. Li WJ, Tuli R, Okafor C, Derfoul A, Danielson KG, Hall DJ, et al. A three-dimensional nanofibrous scaffold for cartilage tissue engineering using human mesenchymal stem cells. *Biomaterials* 2005 Feb;26(6):599–609.
142. Li WJ, Danielson KG, Alexander PG, Tuan RS. Biological response of chondrocytes cultured in three-dimensional nanofibrous poly(epsilon-caprolactone) scaffolds. *J Biomed Mater Res A* 2003 Dec 15;67(4):1105–1114.
143. Hsu SH, Chang SH, Yen HJ, Whu SW, Tsai CL, Chen DC. Evaluation of biodegradable polyesters modified by type II collagen and Arg-Gly-Asp as tissue engineering scaffolding materials for cartilage regeneration. *Artif Organs* 2006 Jan;30(1):42–55.
144. Badami AS, Kreke MR, Thompson MS, Riffle JS, Goldstein AS. Effect of fiber diameter on spreading, proliferation, and differentiation of osteoblastic cells on electrospun poly(lactic acid) substrates. *Biomaterials* 2006 Feb;27(4):596–606.
145. Kim K, Yu M, Zong X, Chiu J, Fang D, Seo YS, et al. Control of degradation rate and hydrophilicity in electrospun non-woven poly(D,L-lactide) nanofiber scaffolds for biomedical applications. *Biomaterials* 2003 Dec;24(27):4977–4985.
146. Li WJ, Laurencin CT, Catterson EJ, Tuan RS, Ko FK. Electrospun nanofibrous structure: a novel scaffold for tissue engineering. *J Biomed Mater Res* 2002 Jun 15;60(4):613–621.
147. Kobayashi M, Chang YS, Oka M. A two year in vivo study of polyvinyl alcohol-hydrogel (PVA-H) artificial meniscus. *Biomaterials* 2005 Jun;26(16):3243–3248.
148. Kobayashi M. A study of polyvinyl alcohol-hydrogel (PVA-H) artificial meniscus in vivo. *Biomed Mater Eng* 2004;14(4):505–515.
149. Kobayashi M, Toguchida J, Oka M. Development of an artificial meniscus using polyvinyl alcohol-hydrogel for early return to, and continuance of, athletic life in sportspersons with severe meniscus injury. II: animal experiments. *Knee* 2003 Mar;10(1):53.
150. Hartman LC, Bessette RW, Baier RE, Meyer AE, Wirth J. Silicone rubber temporomandibular joint (TMJ) meniscal replacements: postimplant histopathologic and material evaluation. *J Biomed Mater Res* 1988 Jun;22(6):475–484.
151. Chang G, Kim HJ, Vunjak-Novakovic G, Kaplan DL, Kandel R. Enhancing annulus fibrosus tissue formation in porous silk scaffolds. *J Biomed Mater Res A* 2010 Jan;92(1):43–51.
152. Le Visage C, Yang SH, Kadakia L, Sieber AN, Kostuik JP, Leong KW. Small intestinal submucosa as a potential bioscaffold for intervertebral disc regeneration. *Spine (Phila Pa 1976)* 2006 Oct 1;31(21):2423–2430; discussion 2431.
153. Bradley MP, Fadale PD, Hulstyn MJ, Muirhead WR, Lifrak JT. Porcine small intestine submucosa for repair of goat meniscal defects. *Orthopedics* 2007 Aug;30(8):650–656.
154. Cook JL, Fox DB, Malaviya P, Tomlinson JL, Farr J, Kuroki K, et al. Evaluation of small intestinal submucosa grafts for meniscal regeneration in a clinically relevant posterior meniscectomy model in dogs. *J Knee Surg* 2006 Jul;19(3):159–167.
155. Cook JL, Fox DB, Malaviya P, Tomlinson JL, Kuroki K, Cook CR, et al. Long-term outcome for large meniscal defects treated with small intestinal submucosa in a dog model. *Am J Sports Med* 2006 Jan;34(1):32–42.

156. Welch JA, Montgomery RD, Lenz SD, Plouhar P, Shelton WR. Evaluation of small-intestinal submucosa implants for repair of meniscal defects in dogs. *Am J Vet Res* 2002 Mar;63(3):427–431.
157. Cook JL, Tomlinson JL, Arnoczky SP, Fox DB, Reeves Cook C, Kreeger JM. Kinetic study of the replacement of porcine small intestinal submucosa grafts and the regeneration of meniscal-like tissue in large avascular meniscal defects in dogs. *Tissue Eng* 2001 Jun;7(3):321–334.
158. Gastel JA, Muirhead WR, Lifrak JT, Fadale PD, Hulstyn MJ, Labrador DP. Meniscal tissue regeneration using a collagenous biomaterial derived from porcine small intestine submucosa. *Arthroscopy* 2001 Feb;17(2):151–159.
159. Ledet EH, Jeshuran W, Glennon JC, Shaffrey C, De Deyne P, Belden C, et al. Small intestinal submucosa for annular defect closure: long-term response in an in vivo sheep model. *Spine (Phila Pa 1976)* 2009 Jun 15;34(14):1457–1463.
160. Schellhas KP, Wilkes CH, el Deeb M, Lagrotteria LB, Omlie MR. Permanent Proplast temporomandibular joint implants: MR imaging of destructive complications. *AJR Am J Roentgenol* 1988 Oct;151(4):731–735.
161. Heffez L, Mafee MF, Rosenberg H, Langer B. CT evaluation of TMJ disc replacement with a Proplast-Teflon laminate. *J Oral Maxillofac Surg* 1987 Aug;45(8):657–665.
162. Ratner BD. *Biomaterials science : an introduction to materials in medicine*. 2nd ed. Amsterdam, Boston: Elsevier Academic Press, 2004.
163. Doshhi J, Reneker DH. Electrospinning process and applications of electrospun fibers. *J Electrostat* 1995;35:151–160.
164. Hohman MM, Shin M, Rutledge G, Brenner MP. Electrospinning and electrically forced jets. I. Stability theory. *Phys Fluids* 2001 Aug;13(8):2201–2220.
165. Hohman MM, Shin M, Rutledge G, Brenner MP. Electrospinning and electrically forced jets. II. Applications. *Physics of Fluids* 2001 Aug;13(8):2221–2236.
166. Dalton PD, Klee D, Moller M. Electrospinning with dual collection rings. *Polymer* 2005 Jan 26;46(3):611–614.
167. Dalton PD, Joergensen NT, Groll J, Moeller M. Patterned melt electrospun substrates for tissue engineering. *Biomed Mater* 2008 Sep;3(3):034109.
168. Li D, Wang Y, Xia Y. Electrospinning nanofibers as uniaxially aligned arrays and layer-by-layer stacked films. *Adv Mater* 2004;16(4):361–366.
169. Yu L, Ding J. Injectable hydrogels as unique biomedical materials. *Chem Soc Rev* 2008 Aug;37(8):1473–1481.
170. Pai SS, Tilton RD, Przybycien TM. Poly(ethylene glycol)-modified proteins: implications for poly(lactide-co-glycolide)-based microsphere delivery. *AAPS J* 2009 Mar;11(1):88–98.

Contents

14.1	Introduction	390
14.2	Concepts in Liver Tissue Engineering	390
14.2.1	Liver Anatomy, Physiology and Diseases	390
14.2.2	Cell Source for Liver Tissue Engineering	393
14.2.3	Methods and Biomaterials for Ex Vivo Primary Hepatocyte Culture	396
14.3	Review of Previous Work of Liver Support Systems	399
14.3.1	Artificial/Bioartificial Liver	402
14.3.2	Hepatocyte Transplantation and Transplantable Liver Constructs	407
14.4	Future Directions	410
References	411

Abstract The development of liver support systems has been in intensive investigation for over 40 years. The main driving force is the shortage of donor organs for orthotopic liver transplantation. Liver cell transplantation and extracorporeal bioartificial livers (BAL) may bridge patients with end-stage liver diseases to successful orthotopic liver transplantation, support patients with acute liver failure to recover, and provide a curing method to patients with certain liver metabolic diseases. Another frontier of current liver tissue engineering is to construct many functional liver units in vitro for drug toxicity and metabolism screening. Much progress has been made, with several artificial liver dialysis devices on the market, a few BAL systems in clinical trials, and other in vitro micro-liver models in development. On the other hand, many lessons have been learned as well. In this chapter, we will focus on the review of advancement, challenges and the critical issues that have to be solved in the development of BAL systems and hepatic cell transplantation as well as in vitro micro-liver models from a tissue engineering perspective.

S. Wang (✉)

Department of Biomedical Engineering, ST-434, City University of New York, City College, 160 Convent Avenue, New York, NY 10031, USA
e-mail: shwang@ccny.cuny.edu

Keywords Artificial liver • Bioartificial liver • In vitro liver model • Liver tissue engineering

14.1 Introduction

Currently liver transplantation remains the only successful life-saving therapy to cure acute liver failure (ALF) or acute-on-chronic liver failure for patients with end-stage liver diseases. However, the shortage of donor organs, high cost of liver transplantation and the need for long-term immunosuppressive treatment are major limitations to whole or partial liver transplantation. According to UNOS (United Network for Organ Sharing) 2008 annual report [1], the number of patients active on the liver transplant waiting list has been stably over 12,000 since 2000. It was 15,786 in January 2010, but the number of liver transplantation procedures performed in the US in 2007 was only 6,489. Sixty-three percent of patients on the waiting list with active status had been waiting for more than one year (18% waiting for 1–2 years and 45% waiting for 2+ years). Death rate for the waiting list in 2006 was 113 per 1,000 patients. Graft survival for deceased donor liver transplantation was 90% at 3 months, 82% at 1 year, 68% at 5 years, and 53% at 10 years. Graft survival for living donor liver transplantation was 92% at 3 months, 85% at 1 year, 71% at 5 years, and 62% at 10 years. That means about 30% of patients with transplanted livers would need a second liver transplantation after 5 years and the number increases to about 40% for 10 years. In 2008, an estimated U.S. average first-year billed charge per liver transplant was \$523,400 [2]. The cost for the second transplantation is usually higher than the first one due to the more complicated patient conditions.

The development of liver support systems has been in intensive investigation for over 40 years. Many progresses have been made with a couple of artificial liver dialysis devices on market and some extracorporeal bioartificial livers (BAL) in clinical trials. On the other hand, many lessons have been learned as well. In this chapter, we will focus on the review of advancement, challenges and the critical issues that have to be solved in the BAL development from a tissue engineering perspective.

14.2 Concepts in Liver Tissue Engineering

14.2.1 Liver Anatomy, Physiology and Diseases

14.2.1.1 Anatomy and Histology of the Liver

The liver is the largest internal organ, weighing about 1.36 kg for an adult [3]. It located at the right-upper quadrant of the abdomen against the inferior surface of the diaphragm. The liver consists of two major lobes, left and right, and two minor lobes, caudate and quadrate.

The connective tissues divide the liver lobes into hexagon-shaped lobules with a portal triad at each corner and a central vein in the center of each lobule. Three vessels, the hepatic portal vein, hepatic artery and hepatic duct filled with secreted bile, are commonly located in triads. Hepatic cords composed with many layers of cuboidal hepatocytes radiate out from the central vein of each lobule. The spaces between the hepatic cords are fenestrated liver capillaries, hepatic sinusoids. The sinusoids are lined with very thin liver sinusoidal endothelial cells (LSEC) and hepatic phagocytic cells (Kupffer cells) [3]. Between hepatocytes and LSECs, the Space of Disse is a 1.4 μm wide basement membrane with extracellular matrix components of collagen I, III, IV and VI, fibronectin, laminin and proteoglycan [4]. Stellate cells, which are liver fibroblasts, are found in the Space of Disse around sinusoids and comparable to pericytes in other locations. Bile canaliculi, cleft-like lumens, lie between the hepatocytes at their apical and lateral sides within each cord.

Figure 14.1 is a schematic drawing of a hepatic sinusoid within hepatic cords coupled with blood and bile flow through the liver, heart and small intestine. Many of these basic units, hepatic sinusoids in between hepatic cords, stack around a central vein in a liver lobule. The conventional view regarding hepatic artery branches is that they carry oxygen-rich blood from the aorta to hepatic sinusoids. This blood supplies hepatocytes in the hepatic cords with oxygen. However, recently Dr. Eugenio Gaudio and his associates discovered that arterial blood from hepatic arteries goes first to peribiliary plexus, which is a capillary network wrapped around canal of Hering, and then their venous output goes to the sinusoids [5]. The blood coming from the small intestine in hepatic portal veins is nutrient-rich but oxygen-poor, so it supplies the hepatocytes with nutrients including growth factors and hormones. Blood in the sinusoids picks up plasma proteins, processed and waste molecules produced by the hepatocytes, and enters central veins which eventually

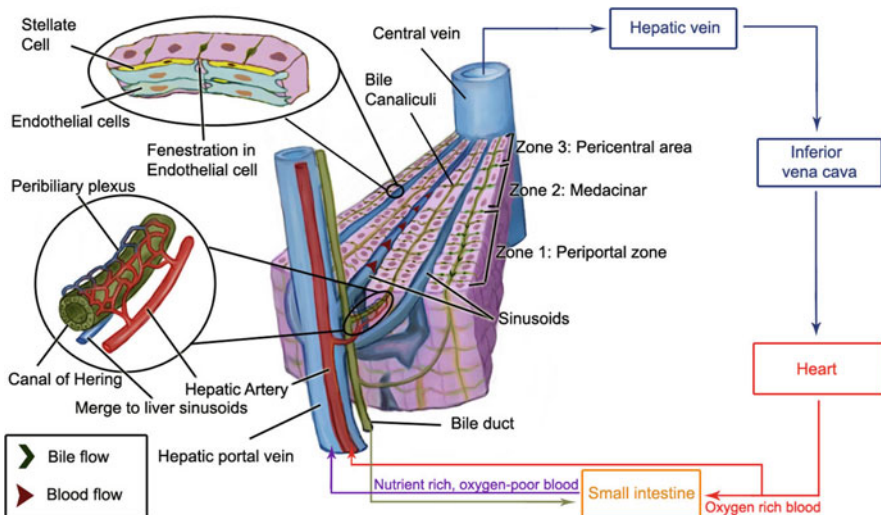


Fig. 14.1 The hepatic sinusoid and hepatic cord coupled with blood and bile flow through the liver, heart and small intestine

14 connect to inferior vena cava. Bile produced by hepatocytes enters bile canaliculi, which connect to canal of Hering, then hepatic ducts that carry bile out of the liver [3].

Hepatocytes along sinusoids exhibit striking morphologic, biochemical and functional differences based on their zonal locations shown in Fig. 14.1. The sizes of hepatocytes increase from Zone 1 to Zone 3 ranging from 20 μm to 35 μm . Cell proliferation is maximum at the periportal area (Zone 1) and negligible at pericentral area (Zone 3). There are dramatic differences in DNA content from Zone 1 to Zone 3 with periportal cells being diploid and a gradual shift to polyploid cells pericentrally. Even extracellular matrix components change from collagen III and IV, laminin, hyaluronic acid and chondroitin sulfate proteoglycan at Zone 1 to collagen I and III, fibronectin and heparin proteoglycan [6]. The sinusoidal structure of the liver is important for proper liver function. Loss of liver functions in the case of trauma or liver fibrosis is usually caused by damages to hepatic architecture.

14.2.1.2

Liver Physiology and Functions

Liver carries out important excretory and secretion functions, stores and digests nutrients, and detoxifies harmful chemicals. Here, we summarize them into six functions, bile production, sugar storage in the form of glycogen, nutrient inter-conversion among proteins, lipids and carbohydrates, detoxification (e.g. removing ammonia, a by-product of amino acid metabolism, and converting it to urea), phagocytosis, synthesis of many blood proteins (e.g. albumin, fibrinogen, globulin, heparin and clotting factors) and releasing them to blood circulation through the space of Disse and liver sinusoids [3]. The liver produces and secretes about 600–1,000 ml of bile per day while gallbladder can store about 40–70 ml of bile that is five to ten times more concentrated than that of freshly secreted bile. Bile contains no digestion enzymes but it neutralizes and dilutes stomach acid and emulsifies fat [3].

The main cell type of the liver that carries out most hepatic functions is the parenchymal cell, or hepatocyte, which makes up ~80% of hepatic volume or mass. The other 20% comprises extracellular spaces (e.g. sinusoidal lumina, Space of Disse, bile canaliculi) and the non-parenchymal cells including endothelial cells, Kupffer cells, lymphocytes and Stellate cells [7]. Zonal functions of hepatocytes along the sinusoids from periportal (Zone 1) to pericentral regions (Zone 3) are highly associated with the zonation of liver tissue histology. From Zone 1 to 3, the gradient of oxygen, growth factors and hormones is from 60–70 mmHg to 25–35 mmHg and from high to low respectively [4, 8]. This results in metabolic zonation including gradual change from gluconeogenesis to glycolysis for glucose metabolism, ureagenesis to glutamine synthesis for ammonia detoxification, and β -oxidation to liponeogenesis for lipid metabolism from Zone 1 to 3.

Currently, no liver support devices replicate normal biliary liver function. Functions of sugar storage, nutrient inter-conversion and phagocytosis are not an urgent need for end-stage liver patients. Thus, detoxification and/or blood protein synthesis are two major goals that bioengineers are trying to achieve in the field of liver tissue engineering.

14.2.1.3

Liver Diseases

Nonalcoholic fatty liver disease (NAFLD) is one of the most common chronic liver diseases in developed countries and recent literature suggests that mild to severe hepatic steatosis leads to nonalcoholic steatohepatitis [9, 10]. According to statistics from the Centers for Disease Control and Prevention, chronic liver diseases accounts for 27,555 lethalties, making it the 12th leading cause of death in the United States. The hallmark of NAFLD is dysregulation of hepatic lipid metabolism which often results in the metabolic syndrome [11]. The association of metabolic syndrome with NAFLD is due to various factors including obesity, insulin resistance, and cytokines released by adipose tissue [12]. The characteristic feature of NAFLD is steatosis which is often asymptomatic and involves accumulation of excessive triglycerides in hepatocytes [13]. Liver steatosis is a predisposing factor for fibrosis which often progresses to cirrhosis leading to the development of hepatocellular carcinoma (HCC) [14]. Fibrosis is characterized by the increased secretion and decreased degradation of extracellular matrix (ECM) components, especially collagen. The stellate cells of the liver are believed to be the main contributors of collagen secretion in fibrotic states by switching from a fat-storing phenotype to a myofibroblastic and collagen-producing phenotype. The progression of fibrosis leads to cirrhosis which is characterized by excessive scar formation and distortion of liver vasculature [15].

Alcohol liver disease (ALD) similar to NAFLD has the feature of fatty liver, dysregulation of lipid metabolism, inflammation, cirrhosis and hepatocellular carcinoma. ALD occurrence is closely correlated with the intake of alcohol; however, not all alcohol drinkers develop ALD and the pathogenesis of liver disease depends on the genetics and environment of the individuals [16].

Viral hepatitis is a common infection affecting 1.4 million people worldwide and has potentially severe outcomes including cirrhosis and hepatocellular carcinoma. Reports indicate that patients with hepatitis B virus (HBV) cirrhosis are suitable candidates for liver transplantation [17]. Interestingly, recent data suggests high prevalence of steatosis in patients with chronic hepatitis C [18].

Tissue engineering approaches can play a major role in both therapeutics development for these hepatic diseases and provide mechanistic understanding of the biology of these diseases and their interactions with drugs in a high throughput platform.

14.2.2

Cell Source for Liver Tissue Engineering

A unique characteristic of the liver is its regeneration ability *in vivo* after partial hepatectomy or injury induced by toxic agents or viruses. The standard partial hepatectomy removes two-third of the liver. The lost liver mass is restored by 5–7 days in rats [19] or 10–14 days in human [20]. However, hepatectomies with the resection of more than 80% of liver tissue do not obtain efficient regeneration and are related with high mortality [4]. It is generally accepted that 20–30% liver mass is preferable in liver supporting devices for Acute Liver Failure (ALF) patients using isolated hepatocytes because the cells in reality do

not have optimal functions in bioreactors [21]. In treatments using hepatocyte transplantation to cure certain metabolic diseases, transplantation of 10% liver mass would be sufficient to normalize the metabolic situation in many enzyme deficiencies [22, 23].

Assuming that human adult liver mass is about 1.4 kg and that there are about 140 million hepatocytes per gram of liver mass [24], this yields the need of about 3×10^{10} hepatocytes for cell transplantation using 10% liver mass or 6×10^{10} hepatocytes for a bioartificial liver containing 20% liver mass. Unlike liver in vivo, isolated primary hepatocytes, which are responsible for most of hepatic functions do not proliferate in ex vivo culture conditions. This causes one of the major obstacles in human liver tissue engineering, which is how to obtain a large quantity of functional hepatocytes. Thus, some bioartificial livers use porcine hepatocytes or human hepatoma cell lines despite the risks of transmission of zoonoses or tumorigenesis respectively. However, the current development in stem cell research, especially in hepatic stem cells and liver progenitor cells, opens up opportunities to grow a large amount of stem cells or progenitor cells ex vivo and then differentiate them into mature functional hepatocytes. Table 14.1 summarizes the different cell sources for human liver tissue engineering. Although infusion of bone marrow derived mesenchymal stem cells was tried to protect against experimental liver fibrosis in rats [25], the efficacy of extracted liver progenitors from bone marrow is extremely low. Currently,

Table 14.1 Current status of cell sources for human liver tissue engineering

Cell Type	Cell source	Hepatic functions	Risk of immune rejection	Other risks
Mature human hepatocytes	Scarce Rejected livers from organ donors (“beating heart donors”) Very little growth ex vivo	All hepatic functions	Mild	Very low
Human hepatoblasts and committed progenitors	Scarce Must obtain from fetal or neonatal livers 1 → 4 ~ 5k cells in 3 weeks ex vivo [28]	All hepatic functions after differentiation; Maturation takes time	Low	Very low
Human hepatic stem cells	Could be sufficient All age cadaveric livers due to ischemia tolerance of stem cells 1 → 40k cells in 3 weeks ex vivo [34]	All hepatic functions after differentiation; Maturation takes time	Low	Very low

(continued)

Table 14.1 (continued)

Cell Type	Cell source	Hepatic functions	Risk of immune rejection	Other risks
Human embryonic stem cells	Potentially unlimited due to excellent proliferation ex vivo	Partial hepatic functions after spontaneous/directed differentiation and purification	Low	Tumorigenesis
Human iPS cells	Potentially unlimited (individually tailored)	Partial hepatic functions after spontaneous/directed differentiation and purification	No	Tumorigenesis
Human hepatoma cell line	Unlimited	Reduced hepatic functions (e.g. C3A, HepaRG)	Mild	Potential of transmission of tumorigenic materials
Human immortalized hepatocytes	Unlimited	Hepatic function varies compared with primary mature cells (e.g. cBAL111, immortalized human fetal liver cell line [44])	Mild	Potential of transmission of tumorigenic materials
Porcine hepatocytes	Unlimited	Good functions initially	High	Potential of transmission of zoonoses (e.g. PERV)

the consensus is that fusion of bone marrow cells with liver cells provides much (if not all) of the effects [26, 27].

Polyloid adult hepatocytes do not proliferate in ex vivo cultures while one diploid adult hepatocyte can divide into about 130 daughter cells in 3 weeks under optimized culture conditions [28]. Limited growth was also reported when adult hepatocytes were cocultured at very low density almost reaching a single cell level initially on growth-arrested 3T3-J2 fibroblast feeder layers [29]. The early work on identification, isolation and growth of hepatic stem cells and progenitors had been limited due to (1) the costs and the difficulties in obtaining normal human liver tissue; (2) using centrifugal fraction protocols instead of multiparametric purification strategies including immunoselection; (3) non-optimized stem/progenitor cell culture conditions; and (4) using cultures containing both mature cells and progenitors. Mature hepatocytes produce soluble signals to inhibit the growth of progenitors [6]. A “cellular vacuum” is required for the progenitor proliferation ex vivo by separating

14 hepatic progenitors from adult hepatocytes and *in vivo* by selectively losing pericentral parenchymal cells [30], such as “oval cells” induction by oncogenic insults at pericentral end using hepatotoxin (e.g. carbon tetrachloride, CCL4) in liver injury models.

Hepatic stem cells in adult/pediatric human livers are present in the Canals of Hering, small ducts in Zone 1, with strong expression for cytokeratins (CK) 7 and 19 [31, 32]. The pioneering work of Strain identified that human hepatic progenitor cells also express CD117 (c-kit) [33]. Recently, using multiparametric flow cytometric sorting for cells with antigenic profiles negative for hematopoietic markers and positive for certain epithelial markers, two pluripotent progenitors (hepatic stem cells and hepatoblasts) and two unipotent progenitors (committed biliary and hepatocytic progenitors) from human fetal livers and from pediatric and adult human livers were isolated and identified [34]. All four populations are negative for hematopoietic markers (CD45, CD34, CD38, CD14, and glycophorin A), making them distinct from hepatocyte precursors from the bone marrow [35–37], and all share expression of epithelial cell adhesion molecule, EpCAM, cytokeratins 8, 18 and cadherin and CD133/1, also called prominin. The size of the EpCAM+ populations is 7–12 μm in diameter. The two pluripotent populations, the hepatic stem cells, and hepatoblasts, are distinguishable. Hepatic stem cells are N-CAM+ while hepatoblasts are ICAM+ with high expression of α -fetoprotein (AFP) and P450 7A. The hepatic stem cells are in the ductal plates of fetal and neonatal livers while hepatoblasts are the dominant parenchymal cell population in fetal and neonatal livers. However, the number of hepatoblasts decreases dramatically with age, so in adults they are found as single cells or small aggregates at the ends of the Canals of Hering. The numbers of the hepatoblasts are higher in diseased livers, especially cirrhotic livers. Mature liver cells are lost within about 1 h of death while hepatic stem cells can survive ischemia for 6–8 h, which means that hepatic stem cells can be obtained from livers of all age donors including living and deceased.

Huge progress in the differentiation of human embryonic stem cells (hESCs) to hepatocyte-like cells (HLCs) have been made by several groups in the past ten years [38–42]. However, the production of hESC-derived HLCs with all major liver functions remains a challenge [43]. In addition, there remains serious concerns of possible tumorigenesis potential of cells that don't fully commit to the liver lineage. Similar progress and concerns are shared in the field of producing HLCs from human induced pluripotent stem cells (iPSs). Thus, despite of their powerful potentials, the immediate application using hES/iPS derived hepatocytes is for drug screening and disease modeling.

14.2.3

Methods and Biomaterials for Ex Vivo Primary Hepatocyte Culture

14.2.3.1

Liver Tissue Culture

At the whole organ level, isolated perfused rat livers have been developed as an *in situ* model to study the liver synthetic ability of albumin and urea [45, 46], to test the drug toxicity *ex vivo* [47, 48], and to evaluate functional changes during injury and disease [49]. The isolated liver can be perfused with nutrition-rich medium through the portal vein

following the ligation of the hepatic artery [50]. This method can preserve the hepatic functions and architecture for a few hours, but only a single experiment can be performed on each liver. The high cost and significant variances in the results among individual isolated livers has hindered its wide applications [51].

The next technique developed to maintain functional liver tissue *ex vivo* is precision-cut liver slice culture. Liver slices from animal (e.g. rat, dog) and human livers to about 200 μm in thickness can be cultured for up to 3 days in a high-oxygen (70% vs. 20% of normal oxygen level) environment [52–54]. For years, liver slices have been used for studies of *in vitro* pharmaco-toxicology [55], inflammatory responses to bacteria [56], and hepatic metabolism of alcohol [57] and drugs (e.g. acetaminophen) [58]. Recently, the technique was used for *ex vivo* evaluation of antiviral therapy for chronic hepatitis C [59] and drugs for anti-liver-cancer [60] and anti-fibrosis treatments [61]. The main advantage of liver slice culture is that it can preserve the architecture and cell–cell heterotypic interactions in the liver. However, the hyper-physiological oxygen concentration required to maintain the liver slices in culture could significantly change hepatic metabolism, resulting in different responses compared to *in vivo* conditions. On the other hand, liver slices cannot be used for long-term *in vitro* liver toxicity and metabolic testing.

A recent development in liver tissue culture is the generation of hepatic organoids with preserved intrinsic tissue architecture from swine liver using mechanical dissociation [62]. These organoids may provide an alternative source for hepatic assist devices, *in vitro* disease modeling, and xenobiotic testing.

14.2.3.2

Methods and Biomaterials of Primary Mature Hepatocyte Culture

Over the past 50 years, a variety of methods of primary hepatocyte isolation have been explored. One milestone in this process was the introduction of enzymatic digestion [63]. It was furthered improved by using a one-step [64] and eventually a two-step perfusion via the portal vein [65], which dramatically enhanced the viability of isolated hepatocytes and has become the most commonly used hepatocyte isolation technique.

However, primary hepatocytes lose their phenotype rapidly after isolation under standard culture methods, maintaining liver-specific functions *in vitro* has been a major challenge. In 2D surface culture using traditional tissue culture dishes/plates, primary hepatocytes lose their cuboidal morphology and hepatic functions (e.g. albumin and urea synthesis) within a week after isolation. Cells dedifferentiate into fibroblast-like cells. Methods that can maintain the stable long-term functions of hepatocytes use different biomaterials and culture configurations, including (1) the collagen sandwich configuration [66–68], (2) 3-dimensional aggregate/spheroid culture induced by seeding on weakly adherent surfaces or soft gels such as poly HEMA coatings [69, 70], alginate sponges [71, 72], Matrigel [73, 74], self-assembling peptide hydrogel (PuraMatrix) [75], adipocyte-derived natural basement membrane extract (Adipogel) [76], or by preventing cell attachment to the substrate in suspension culture using spinner flasks [77], and (3) coculture with non-parenchymal cells including liver sinusoidal endothelial cells (LSEC) [7, 78, 79], 3T3-J2 fibroblasts to simulate stellate cell coculture [29, 80]. It was also reported that hepatocyte

14 coculture with Kuffer cells could more accurately mimic inflammatory responses similar to that seen in vivo [81, 82].

Hepatocytes under different culture configurations on different biomaterials show distinguishable morphologies. Figure 14.2 shows phase contrast images of four culture configurations, cuboidal single-layer hepatocytes in collagen sandwich, hepatocyte aggregates on Matrigel, hepatocyte spheroids on PuraMatrix, and coculture of LSEC with hepatocytes on PuraMatrix. The long-term hepatic functions (e.g. albumin and urea products, CYP450 activity) are compatible and high in cultures of collagen sandwich, Matrigel and PuraMatrix as well as Adipogel [75, 76]. The quick cell–cell contact after isolation in the aggregate/spheroid culture seems to provide a faster recovery from isolation stresses than that of collagen sandwich culture[75]. A detailed review about hepacyte culture techniques including the hepatocyte culture medium was presented by Nahmias et al. [83].

Two dimensional culture systems using the configuration of collagen sandwich or coculture can maintain the long-term hepatic phenotype and are robust and easy to maintain. However, they contain low cell numbers, and thus low functional capacity per

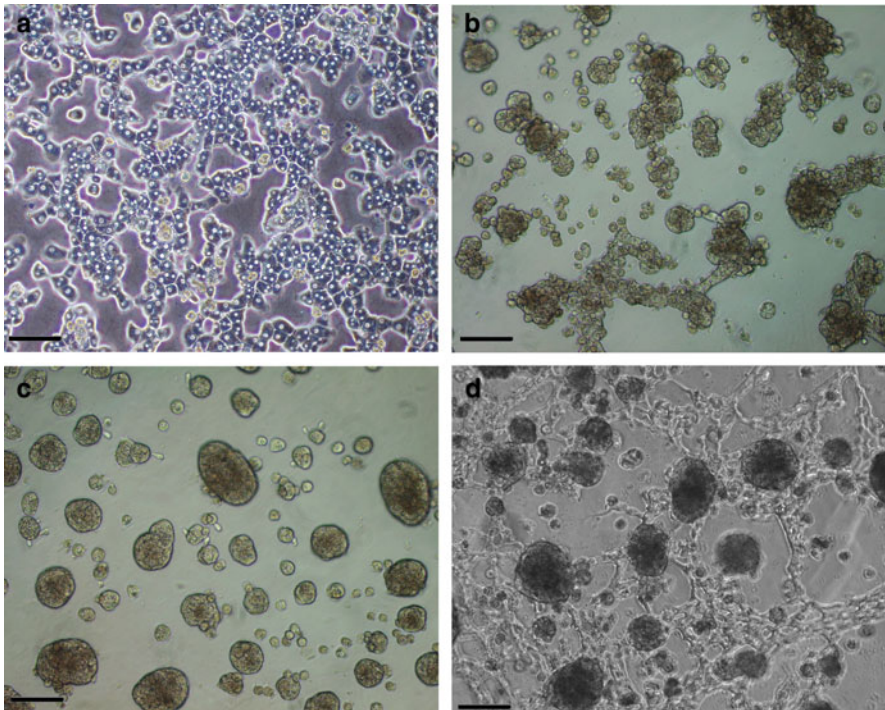


Fig. 14.2 Phase contrast images of primary rat hepatocyte culture and coculture configurations. (a) hepatocyte monolayer in collagen sandwich culture (day 3); (b) hepatocyte aggregates on Matrigel (day 3); (c) hepatocyte spheroids on self-assembling peptide hydrogel (PuraMatrix, day 3), (d) hepatocyte coculture with rat heart microvascular endothelial cells (RHME) seeded 10 days before hepatocyte seeding, stable hepatocyte spheroids formed within the network of tube-like structures preformed by 10 days culture of RHME cells. Scale bar is 100 μm

unit volume (typically $\sim 10^6$ cells/mL) and are difficult to adapt to a large-scale culture system. Nevertheless, the 2D hepatocyte culture systems have considerable potential as an *ex vivo* liver tissue model for *in vitro* liver toxicity screening and metabolism studies. One recent advance was to use micropatterned hepatocyte-3T3 cocultures for hepatitis C vaccine development [84]. This technology is being explored by a company, Hepregen, to develop a microliver platform for toxicity screening and drug discovery.

On the other hand, three dimensional culture methods are more amenable to scale-up and provide cells an opportunity to form a large number of intercellular contacts that help maintain their *in vivo* phenotype. Therefore, hepatic 3D aggregates/spheroid culture may provide feasible culture solution for bioartificial liver supporting systems. Although hepatocytes maintain long-term function on Matrigel, the potential tumorigenicity and immunogenicity, as well as poorly defined composition and potential batch-to-batch variation, of this material limits its use for *in vivo* therapeutic applications as well as for *in vitro* drug toxicity studies. Synthetic self-assembling peptide hydrogel, such as PuraMatrix, will be able to avoid the disadvantages of Matrigel in the *in vivo* applications and still provide the ability to achieve the similar hepatic functions in the *ex vivo* culture [75].

Another advance in the biomaterial development for liver tissue engineering has been the use of basement membrane extract secreted by primary human cells. Recent studies have shown that liver tissue derived extracellular matrix can maintain human hepatocyte function *in vitro* [85, 86]. One of the authors has recently reported the development of a novel adipocyte-derived natural basement membrane extract (BME) [76]. This new material termed Adipogel obviates disruption of protein-protein interactions; eases generating BME using a less cumbersome procedure, uses animal free extraction procedures and minimizes batch to batch variability, reduces the possibility of pathogen transmission, and retains the ability to modulate the supramolecular composition of the BME. Table 14.2 summaries biomaterials supporting primary hepatocyte culture *in vitro* partially or fully.

On the other hand, biomaterials have been in the development for drug delivery targeting antifibrosis [87]. Non-matrix primary hepatocyte sheets generated by culturing cells for 3 days on temperature-responsive polymer (PIPAAm) were detached and successfully transplanted subcutaneously in mice. Engraftment and formation of hepatic tissues was confirmed [88].

14.3

Review of Previous Work of Liver Support Systems

The rapid deterioration of liver functions in acute liver failure (ALF) results in coagulopathy and mental alteration (encephalopathy) in a patient without preexisting cirrhosis. Acute liver failure includes both fulminant hepatic failure (FHF) and subfulminant hepatic failure. Fulminant hepatic failure is used to describe the development of encephalopathy within 8 weeks of the onset of symptoms. Subfulminant hepatic failure patients have liver disease for up to 26 weeks before the development of hepatic encephalopathy. Patients with Wilson disease, hepatitis A and B, or autoimmune hepatitis may be included in spite of the possibility of cirrhosis if their disease has been active less than 26 weeks. Drug-related hepatotoxicity is the leading cause of acute liver failure in the United States. It has a very

Table 14.2 Biomaterials supporting primary hepatocyte culture

<i>Natural materials</i>	
Collagen Type I	Coating/single gel: monolayer, dedifferentiation and hepatic function decreasing, need non-parenchymal cells to maintain hepatic functions Sandwich culture: monolayer cuboidal morphology; high and long term basic hepatic functions (e.g. albumin, urea and CYP450)
Matrigel	Aggregates, high and long term hepatic functions
Alginate/chitosan	Spheroids (up to 100 μm in diameter), coculture with fibroblasts (NIH3T3) enhanced hepatic functions [89]
Alginate	Smaller spheroids and lower hepatic functions than that of alginate/chitosan sponge [89]
Adipogel	Soluble adipogel in medium on collagen single layer hepatocytes: enhanced albumin synthesis than that of collagen sandwich while urea and CYP450A1 are compatible Adipogel (top)/collagen (bottom) sandwich: compatible albumin and urea synthesis comparing to collagen sandwich, but lower CYP450A1
<i>Synthetic materials</i>	
PLLA	Hepatocyte-seeded PLLA disc with 95% porosity was tested in a pulsatile flow bioreactor. Cell spheroids were formed. Ammonia removal capacity and glycogen storage ability were demonstrated over 6 days [90]
PGLA	Cell morphology depends on the pore sizes, changing from big aggregates to spheroids then to smaller spheroids with pore sizes of 2.7, 16.5 and 67.4 μm , respectively. Hepatic functions were higher than collagen single gel culture but significantly lower than collagen sandwich culture [91]
Photosensitive-PEG	Hepatocytes alone in PEG had zero viability after one-day culture; co-encapsulation with 3T3-J2 fibroblast rescued the viability to ~50%; its potential usage in hepatocyte culture is in generating micoliver structures using microfabrication [92, 93]
PuraMatrix	Self-assembling peptide hydrogel (monomer sequence: Ac-(RADA) ₄ -CONH ₂); spheroids with the diameter of $80 \pm 21 \mu\text{m}$; compatible long term hepatic functions comparing to collagen sandwich or Matrigel culture

PLLA poly(L-lactic acid), *PGLA* poly(D,L glycolic-co-lactic acid), *PEG* poly(ethylene glycol)

high mortality, which is about 60–80% depending on the original cause and the clinical center/hospitals [21]. With improved intensive care, doctors have many artificial devices, such as artificial lung/ventilation, artificial heart, blood oxygenator, hemodialysis devices, heart-lung machine and aortic balloon pumping, to support their patients temporarily as a bridge to the next disease-curing step. However, there is still no artificial/bioartificial liver (BAL) in the intensive care unit to support ALF patients. The successful BAL that can support ALF patients and work as a bridge to liver transplantation has to be able to provide the detoxification function, hepatic synthetic and regulatory functions [94].

Despite functions of acute intervention and bridging to orthotopic liver transplantation that extracorporeal liver supporting systems can provide in the case of ALF or intoxication,

they may not be as desirable as intracorporeal systems (e.g. hepatocyte transplantation or transplantable constructs) in the treatment of many liver metabolic disorders, which require the correction of a small portion of the complex liver functions. In this case, the hepatocyte transplantation of 10% liver mass would be sufficient to reinstall the necessary metabolic functions in many enzyme deficient diseases [22]. Compared to whole liver transplantation, hepatocyte transplantation has some advantages, such as a lower mortality and morbidity due to the less invasive procedure, fewer consequences of graft loss due to the intact host liver with its own primary functions and vasculature, and less immunogenic reactions because allogenic hepatocytes may be engineered in vitro. Yet, hepatocyte transplantation shares the same major obstacle with BAL, which is the cell source for primary human hepatocytes. In addition, it has a big clinical challenge in how to transplant a sufficient cell mass without increasing portal hypertension and pulmonary dysfunction.

Nevertheless, significant progress has been made in the past 30 years in the AL/BAL development and its applications as well as clinical procedures of hepatocyte transplantation. Here we review several representative products that are FDA approved or under clinical trials or in preclinical research. They are summarized in Tables 14.3 and 14.4.

Table 14.3 Device design and current status of extracorporeal liver support systems

Device (company name)	Cell source and device configuration	Perfusion and treatment method	Current status
MARS (Gambro, Germany and Switzerland)	No cells; High-flux polysulfone dialyzer, 50 kDa cut-off; human albumin in dialysate	Whole blood 6 h/day up to 5 days;	FDA 510 (k) approval for drug overdoses and poisoning, June 2005 Completed Phase III for 70 patients with cirrhosis and HE Phase III in patients with FHF
Prometheus (Fresenius Medical Care, Germany)	No cells; polysulfone plasma separation filter (250 kDa cut-off, albumin permeable) connected to two toxin-absorber filters and dialysis circuit	Whole blood 6–8 h/day over 2–5 days	New clinical trial: the effect of prometheus on cerebral metabolism in acute liver failure
ELAD (Vital Therapies, La Jolla, CA)	Four hollow fiber cartridges with 300–400 g hepatoma derived C3A cells; Two cell filters in the plasma return line to patient for safety	Plasma in lumens of parallel fibers and cell aggregates in extracapillary spaces; Continuously for 3–30 days	Phase II clinical trial in patients with FHF with primary outcome measurement of 30-day transplant-free survival or bridge to transplant/recovery

(continued)

Table 14.3 (continued)

Device (company name)	Cell source and device configuration	Perfusion and treatment method	Current status
Hepa-Mate (previously HepatAssist, HepaLife Technologies, Boston, MA)	Two charcoal detoxification filters in series with a hollow fiber bioreactor with 7×10^9 cryopreserved porcine hepatocytes	Plasma in lumens of parallel fibers and cell aggregates on microcarriers in extracapillary spaces 6 h/day and up to 14 days	New Phase III clinical trial in patients with FHF without failed liver transplantation
MELS (Charité Virchow, Berlin, Germany)	Hemodialysis module in serial with a SPAD module followed by a hollow fiber bioreactor with 400–600 g human liver cells isolated from discarded cadaver livers	Plasma in lumens of interwoven fibers and cell aggregates in extracapillary spaces Continuous perfusion for 79 h on one patient	Finished Phase I clinical trial using porcine hepatocytes On-going Phase I clinical trial using human primary hepatocytes, 12 patients were treated.
AMC-BAL (Hep- Art, Amsterdam, Netherland)	Circularly wound polyester matrix around a polysulfone core with longitudinal hollow fibers for oxygen delivery and spacing between matrix; 10×10^9 porcine hepatocytes; A cell filter in the plasma return line for safety	No cell culture medium; plasma perfusion through hepatocytes attached on the polyester matrix surface Total duration of BAL treatment: 4–35 h in Phase I trials	Finished Phase I clinical trial Developing immortalized hepatic cell lines to replace the porcine hepatocytes as the cell source for the BAL

HE hepatic encephalopathy, *FHF* fulminant hepatic failure, *ELAD* extracorporeal liver assist device, *MELS* modular extracorporeal liver support, *SPAD* single pass albumin dialysis, *AMC* Amsterdam Medical Center

14.3.1

Artificial/Bioartificial Liver

14.3.1.1

Extracorporeal Artificial Liver: Blood Detoxification System

The idea behind an artificial liver is similar to a renal dialysis device, filtering out accumulated toxins in blood. However, in the blood of patients of liver failure, only some of the toxins accumulated are water soluble, while most are bound to blood proteins (e.g. albumin). There are two commercially available artificial liver devices, albumin dialysis

Table 14.4 Clinical studies of hepatocyte transplantation and outcomes

Liver disorder	Clinical study	Outcome
Chronic liver disease	At least eight patients including four children were reported in several studies; cell infusion was intrasplenic, intraportal or through hepatic artery.	Improved liver functions in all eight patients; bridged four patients to orthotopic liver transplantation (OLT) successfully; confirmed engrafted hepatocytes in spleen in two patients.
Acute liver failure	More than 15 patients including children were treated with liver cell infusion through splenic artery, portal vein or intraperitoneal cavity	Improved liver functions; extended survival time; full recovery in some patients without OLT; bridged to OLT successfully in some cases.
Inborn metabolic disease	OTC deficiency Newborn children received ~2–4 billion cells over 5–6 months period with immunosuppression followed by OLT	Temporary relief of hyperammonemia and protein intolerance; bridged to partial OLT successfully
	α 1-antitrypsin deficiency Two patients	Cirrhosis was found when cell infusion was performed, and subsequent OLT was operated
	Glycogen storage disease type 1a A 47-year-old patient received 2 billion cells with immunosuppression	Normal diet restored and could fast for 7 h without experiencing hypoglycaemia
	Infantile Refsum's disease A 4-year-old patient received 2 billion cells with immunosuppression	Decrease in total bile acids, dihydroxycoprostanic acid, and pipecholic acid; donor cell engraftment was confirmed
	Factor VII deficiency Two patients received 1–2 billion cells with immunosuppression	Temporary reduced the dose requirement of exogenous recombinant factor VII
	Crigler-Najjar syndrome type 1 At least three children age from 2 to 9 years old were treated with hepatic progenitor cells or hepatocytes with immunosuppression	In two cases, continuously reduced disorder was observed. In one case, only temporary benefit of cell transplantation was observed, and the patient received OLT later on

OTC Ornithine Transcarbamylase, *PFIC2* bile salt export protein deficiency

(Molecular Adsorbent Recirculating System, MARS) and fractionated plasma separation and adsorption (Prometheus).

The concept of albumin dialysis was introduced into the field of liver support devices by a research group at the University of Rostock in Germany [95]. In a MARS device, the blood circuit driven by the dialysis machine passes through the MARS FLUX dialyzer at a

median speed of 210 (170–500) mL/min before returning to the patient via the intravenous catheter. Thus, water-soluble and albumin-bound molecules of small molecular weight are removed from the blood by diffusion following a concentration gradient through the polysulfone membrane (50 kDa cut-off) into a standard dialysate solution containing 16.6% human albumin. The albumin containing dialysate itself is then filtered by a conventional dialyzer to remove unbound water-soluble molecules followed by activated charcoal column and ion exchange resin column to adsorb albumin-bound molecules. The purified albumin containing dialysate returns to MARS FLUX dialyzer to close the loop (Fig. 14.3a). Since 1999, the device has been commercially available throughout Europe and in a number of Asian countries. It is 510 (k) approved by the Food and Drug Administration (FDA) for drug overdoses and poisoning as of June 2005 in the US. Both preclinical and clinical trials on MARS proved a significant reduction of albumin-bound toxins (e.g. ammonia, bilirubin, bile acids, copper, short and middle chain fatty acids), neurological improvement and prolonged survival time [96, 97]. However, the impact of MARS on the survival of end-stage liver disease patients awaits the results of an on-going Phase III clinical trial in patients with fulminant and subfulminant hepatic failure. The primary outcome measure of this trial is patient survival at 6 months [98].

A simplified and alternative version of albumin dialysis is single pass albumin dialysis (SPAD). One preclinical study reported that MARS was the more effective kind of albumin dialysis than SPAD for the important substances like bile acids and that it was safer [99]. Nevertheless, Phase I and II clinical trials of SPAD are underway in patients with cirrhosis in France [100].

The idea of fractionated plasma separation and adsorption (FPSA) was published in 1999 [101]. Prometheus was more recently developed and commercialized in Europe and some Asian countries by Fresenius Medical Care in Germany. In a Prometheus system, a polysulfon filter with a cut-off of approximately 250 kDa is used in a dialyzer, AlbuFlow. Albumin and the protein bound toxins in plasma pass through AlbuFlow filter and then toxins are removed from the plasma by two adsorber filters. The filtered plasma combines with non-plasma portion of the blood and is filtered further by a conventional high-flux hemodialyzer (Fig. 14.3b). Detoxified blood returns to the patient via the intravenous

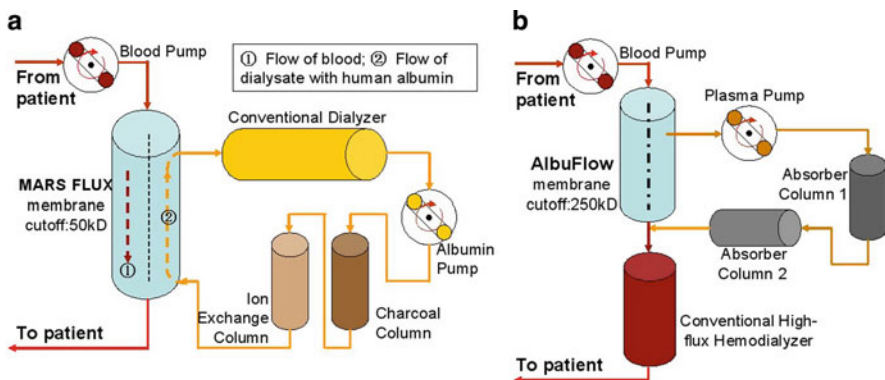


Fig. 14.3 Schematic drawing of (a) MARS and (b) Prometheus

catheter [102]. Initial studies have proven clinical use of Prometheus to be feasible and safe. Head-to-head comparisons of Prometheus and MARS have shown treatment with the former to be more efficient with respect to removal of most albumin-bound (e.g. bilirubin and ammonia) and water-solved markers (e.g. creatinine) [103, 104]. It is not known whether the observed greater detoxification capacity of Prometheus will translate into clinical benefit. In a recent randomized comparison of MARS and Prometheus, however, hemodynamic improvement was observed in response to MARS, but not Prometheus treatment [105]. In addition, patients' own blood albumin level was decreased after Prometheus treatment but not MARS [106]. A large randomized controlled trial investigating the effect of Prometheus on survival (HELIOS study) and on cerebral metabolism in acute liver failure has been conducted in Europe [107]. Nevertheless, liver/albumin dialysis must still be considered in the experimental stage because its contribution to improved patient survival has not been proven in large randomized trials.

14.3.1.2

Extracorporeal Bioartificial Liver (BAL)

One of major the liver functions, secretion or protein synthesis, can never be achieved in artificial liver support systems. In order to delivery hepatic synthetic and regulatory functions to patients with the end-stage liver diseases and bridge them to liver transplantation, several extracorporeal bioartificial liver support systems with primary porcine hepatocytes, immortalized hepatocytes or primary human hepatocytes are currently under clinical trials. Table 14.3 summaries the device design and current status of these extracorporeal liver support systems.

Hepa-Mate, previously known as HepatAssist, was the first BAL that went through clinical trials I, II and III. Phase I trials of HepatAssist in acute liver failure patients yielded promising results [108]. A pivotal Phase II/III prospective, randomized, controlled trial in 171 patients (86 control and 85 treated) with fulminant/subfulminant hepatic failure including 24 patients with primary nonfunction following failed liver transplant in 11 U.S. and 9 European medical centers was completed [109]. When 30-day survival was analyzed in the entire patient population, there was no difference between the control and HepatAssist-treated group. However, survival in fulminant/subfulminant hepatic failure patients, excluding those 24 patients with failed liver transplantation, was significantly higher in the BAL group compared with the control group. The company (HepaLife Technologies) has been planning a new Phase III clinical trial without the inclusion of failed liver transplant patients. Hepa-Mate consists of two charcoal detoxification filters in series with a polysulphone hollow fiber bioreactor (membrane pore size: 0.15–0.20 μm) with 7×10^9 cryopreserved porcine hepatocytes. Cells are cultured as aggregates on collagen coated dextran microcarriers in extracapillary spaces while plasma flow in lumens of parallel fibers. In its completed Phase II/III clinical trials, plasma perfusion was performed 6 h per day for 14 days unless a matching donor liver was located and the patient went on to liver transplantation. Porcine endogenous retrovirus (PERV) infection is a risk for using porcine hepatocytes in BAL. Twenty-eight patients in Phase I clinical trials of HepatAssist tested negative for PERV using polymerase chain reaction analysis of peripheral blood

mononuclear cells (PBMC) collected up to 5 years after treatment [110]. However, PERV infection remains a big concern and many European countries have banned the use of BAL that employ porcine hepatocytes. A recent *in vitro* study showed that primary human hepatocytes and endothelial cells were reproducibly infected by PERV originated from primary porcine hepatocytes within a BAL [111].

ELAD, Extracorporeal Liver Assist Device, avoided the PERV problem by using a liver cell line, C3A, derived from hepatoblastoma [112]. ELAD consists of four hollow fiber cartridges (120 kDa membrane cutoff) with ~100 g oxygenated C3A per cartridge. A cell filter (pore size: 0.45 μm) was added in the plasma return line to the patient's vein for safety in the modified version [113]. The ELAD device design is similar to Hepa-Mate but can be tailored for children by using 2–3 hollow fiber cartridges. Although hepatoma cells do not have the same high level of hepatic specific functions as primary hepatocytes, the feature of their easy *in vitro* maintenance allows the same ELAD device to be used for a much longer time than the BAL using primary hepatocytes. Currently, ELAD is under Phase II clinical trials in patients with FHF using primary outcome measurement of 30-day transplant-free survival or bridge to transplant/recovery [114].

MELS, Modular extracorporeal liver support, is an integrative BAL consisting of a bioreactor (CellModule) with primary human liver cells harvested from discarded human donor livers [115], a single-pass albumin dialysis unit (DetoxModule) presents human albumin for the removal of albumin-bound toxins in order to reduce the biochemical burden of the liver cells, and a hemodialysis unit (DialysisModule) provides for continuous venovenous hemofiltration if required in hepatorenal syndrome [116]. In the MELS liver bioreactor, polyether sulphone (PES) hollow fibers (400 kDa membrane cutoff) are interwoven instead of parallel. They contain three capillary systems. Two of these are used for counter directional flow perfusion of the cells with the patient's plasma and one capillary system enables integral oxygenation and carbon dioxide removal. Human liver cells (400–600 g) including parenchymal and nonparenchymal cells form tissue by spontaneous organization to aggregates immobilized to the surface of the capillaries. In their Phase I clinical trials using porcine hepatocytes, eight patients were successfully bridged to transplantation using continuous perfusion over a period of 8–46 h and were observed over at least 3 years with an organ and patient survival rate of 100% [117]. In one report using MELS with primary human liver cells, the perfusion was successfully performed for 79 h on a patient suffering from primary non-function of the transplant until a suitable organ became available [118]. Because of the ban of using porcine hepatocytes in many European countries, MELS is under clinical trial I using human primary hepatocytes.

AMC-BAL was developed at the Academic Medical Center (Amsterdam, Netherlands) 15 years ago. It consists of a circularly wound polyester matrix for porcine hepatocytes to attach with longitudinal polypropylene/polymethylpentane hollow fibers for oxygen delivery and to serve as spacers between the polyester matrix. Patients' plasma is in direct contact with hepatocytes through flow, and there is no flow of cell culture medium [119]. Its first clinical trials showed positive results in safety and efficacy in 12 ALF patients in Italy [120]. However, xenotransplantation legislation in many European countries prohibits the use of porcine hepatocytes in clinically applied BAL systems. The group has been developing a human-derived hepatocyte cell line as a biocomponent of BAL systems. Recently,

cBAL111 has been developed from immortalized human fetal liver cells and has been well characterized [44]. Although all hepatic functions were expressed in cBAL111, there was considerable variation in their levels compared with primary mature hepatocytes.

Bioartificial Liver Support System (BLSS) was originally developed in University of Pittsburgh Medical Center, and now is under development by Excorp Medical, Inc. Hybrid Bioartificial Liver (HBAL) has been under development at Nanjing University and its Drum Tower Hospital of Medical College in China. Both BLSS [121] and HBAL are BALs with the hollow fiber configuration with blood (BLSS)/plasma (HBAL) flow inside hollow fibers and porcine hepatocyte aggregates in the spaces between capillaries. In BLSS, cells are encapsulated in a collagen hydrogel. BLSS is under clinical trials I/II and HBAL is under clinical trial I [122, 123].

Comparison between different BALs that employ porcine hepatocytes, suggest that cell mass and bioreactor configuration (i.e. whether or not cells are in direct contact with patient's plasma without semipermeable membranes) affect the efficiency of toxic clearance. The total bilirubin and ammonia concentrations decreased by 29% and 23% respectively of the initial concentration in a study after HepaAssist treatment with 5×10^9 porcine hepatocytes [124], while the values were 44% and 31% respectively after AMC-BAL treatment with 10×10^9 porcine hepatocytes [120]. In AMC-BAL, the direct contact of patient plasma with porcine hepatocytes may contribute to its higher efficacy of detoxification. However, patient plasma provides an unfavorable environment for primary hepatocyte culture. In AMC-BAL, hepatic functions dropped to 80–90% after 3 days with 180 min perfusion each day, and 75% after 7 days [125]. Studies have shown that hepatic functions of hepatocytes exposed to plasma culture changed dramatically, and culture medium with insulin concentration above the physiological level resulted in fatty cells [126–128]. Recently developed, metabolic preconditioning methods that reduce the fat content in hepatocytes and perfused fatty liver may find strong applications in BALs [129].

14.3.2

Hepatocyte Transplantation and Transplantable Liver Constructs

In the case of some liver diseases (e.g. certain metabolic diseases) with primary undamaged liver functions and structure, replacement of a small fraction of the liver or a single liver function is more desirable than replacing the whole liver using an extracorporeal artificial/bioartificial liver. Hepatocyte infusion/injection through intraportal or intrasplenic routes has been investigated in both animal models and human patients. After injection, some of donor hepatocytes translocate and accumulate in the hepatic sinusoids, causing portal hypertension. Although the majority of these cells are washed away by blood, a portion of the cells can translocate into the space of Disse through the sinusoidal endothelium [130]. A transient disruption of gap and tight junctions between host hepatocytes eventually allows the engrafting of donor liver cells [131, 132]. Studies have shown that cell transplantation of no more than 10% liver mass usually did not cause complications, such as portal vein thrombosis and migration of cells to lungs leading to pulmonary embolism [133, 134]. However, less than 30% of the transplanted hepatocytes survive in the host liver [135]. Therefore, the major limitation of hepatocyte transplantation through the portal vein

14 or spleen is the number of engrafted donor cells can only reach about 3% of the host hepatocyte number without causing complications. How much hepatic function may improve from these 3% transplanted cells is debatable. However, since the host liver may provide the best microenvironment for the donor cells, the hope lies in the repopulation or proliferation of the engrafted donor cells if the cell transplantation method remains the same. On the other hand, the enhanced hepatic function(s) may be achieved by changing the cell transplantation method using tissue engineering of transplantable and engraftable liver tissue constructs with a much larger quantity of hepatocytes encapsulated in a biocompatible scaffold.

14.3.2.1

Clinical Hepatocyte Transplantation

Currently human liver cell transplantation has been tested in patients with chronic liver diseases like cirrhosis, in patients with acute liver failure, and in children with inborn metabolic liver diseases [136, 137]. Table 14.4 summarized the examples of clinical studies of liver cell transplantation and their outcomes.

Clinical trials of hepatocyte transplantation in patients with chronic liver diseases in general increased liver functions temporarily, such as controlling hyper-ammonemia, and could bridge the patients to orthotopic liver transplantation [138–140]. It was also reported in one patient that the total bilirubin and conjugated bilirubin started decreasing during the first month after cell infusion [141]. Because of the abnormality of liver architecture and scar tissue in end-stage liver disease patients, long term engrafting of transplanted hepatocytes is challenging.

Clinical trials of hepatocyte transplantation in patients with acute liver failure (ALF) gave more results that are positive. In one trial, three out of five patients who survived 48 h after hepatocyte transplantation (HT) had substantial improvement in encephalopathy scores, arterial ammonia levels, and prothrombin times. All three patients lived substantially longer than expected after liver cell infusion (12, 28, and 52 days) [142]. In two separate studies, two patients fully recovered without OLT after intraportal infusion of human hepatocytes (10^9 – 10^{10} cells) and immunosuppression of 4–12 months [143, 144]. In another study using fetal hepatocytes in transplantation, three out of seven patients fully recovered without OLT after liver cell infusion [145]. Despite these positive results, it should be realized that spontaneous survival rate is about 25% with drug induced or hepatitis B ALF patients due to improved intensive care [94]. Therefore, it is difficult to single out the positive effects of hepatocyte transplantation in the case of ALF patients.

On the other hand, data of the studies on patients with inborn metabolic diseases are easier to comprehend because the other primary liver functions are intact. There have been more than 14 children with inherited metabolic diseases who have undergone hepatocyte transplantation (HT) in various clinical trials to treat ornithine transcarbamylase deficiency [146, 147], α 1-antitrypsin deficiency [138, 148], glycogen storage disease type 1a [149], infantile Refsum's disease [150], factor VII deficiency [151], bile salt export protein deficiency (PFIC2, one patient in King's College, London, 2003) [152] and Crigler-Najjar

syndrome type 1 [153–155]. Although individual results are encouraging, different treatment protocols and the lack of a controlled study make it difficult to judge the overall significance of HT in the treatment of metabolic diseases [156].

14.3.2.2

Development of Transplantable Liver Tissue Constructs

The small number of hepatocytes permitted in direct cell infusion/injection without complications and the low percentage of engrafted donor cells motivated investigators to seek an alternative cell transplantation method using tissue engineering with three dimensional porous biomaterials.

Transplantable liver tissue constructs have been in development in rat models for over 15 years. The polymer matrix-based liver tissue could incorporate a larger number of hepatocytes from 20% of recipient's liver mass [157, 158] to the whole organ level [159]. Many types of porous polymers have been explored in the development of transplantable liver tissue engineering, including polyvinyl alcohol sponges [159], polylactic acid (PLA) or polylactic-co-glycolic acid (PLGA) [157], and polyglycolic acid (PGA). Due to the introduction of 3D matrix, the microenvironment for transplanted hepatocytes could be better controlled by defined growth factors [160] and extracellular components [73] to enhance the hepatic functions. Engineered liver tissue constructs have generally been subcutaneously implanted into the mesentery of rats. Thus, the problem of portal hypertension or pulmonary embolism caused by hepatocyte infusion could be avoided. In addition, the cell matrices could be easily removed if it is required.

Although long-term engraftment, cell proliferation in the matrix and hepatic functions of heterotopically transplanted hepatocytes have been shown in the glucuronyl-transferase-deficient Gunn rats [161] and vitamin C deficient ODS rats [158], the immediate cell survival rate was very low (~1%) 7 days after implantation and recovered to about 26% of the initial cell numbers in 2.5 months [157]. The possible solutions are prevascularization of the liver tissue constructs and the use of hepatocytes with higher proliferation ability, such as fetal liver cells. In a recent study, the transplantation of fibrin gel-immobilized fetal liver cells in a vascularized arterio-veno-venous (AV)-loop rat model was investigated [162]. The study showed that fibrin matrix allowed rapid blood vessel ingrowth from the AV-loop and thus engraftment of fetal liver cells was improved.

The major obstacle for translating successful animal data to human clinical trials using transplantable liver tissue constructs is perhaps the lack of a less invasive hepatotrophic stimulation method. Sufficient long-term stimulation of the transplanted hepatocytes is mandatory in clinical application of heterotopic hepatocyte transplantation. In many rat models, portocaval shunt operation was used as a standard technique for hepatotrophic stimulation. The development of efficient and noninvasive techniques for long-term hepatotrophic stimulation is essential for clinical applications of transplantable liver tissue constructs. In one study, it was reported that pancreatic islet cotransplantation in the matrix could result in a similar hepatocyte proliferation rate and albumin function compared to portocaval shunt operation over a month [163]. This is a much less invasive stimulation method.

14 The promising potential of hepatocyte-islet cotransplantation in matrix leads to the current Phase I clinical trial using a formaldehyde-free special matrix consisting of self-dissolving polymers with human autologous hepatocytic tissue and pancreatic tissue from liver resection and pancreatic biopsy, respectively [164]. The trial will be performed for enrolled patients with liver cirrhosis in Baermed Center for Abdominal Surgery, Zürich, Switzerland, and is currently in the patient recruiting stage.

14.4 Future Directions

It is evident from the above discussion that tissue engineering can have a far reaching impact in liver diseases. The major challenge is to develop strategies that can generate highly enriched functional lineage-specific progenitors or mature hepatocytes for cell transplantation in liver disease models and BAL supporting systems. Considering the utilization of attractive candidates of differentiated and undifferentiated hESCs/hiPSs for liver transplantation, further study of the distinct role of early and mature populations is warranted to determine which stage will ultimately provide the most benefit in animal disease models by ameliorating liver diseases. The development of stem cell transplantation therapy and testing the efficacy of such treatments in animal models would aid in preclinical development of therapeutics. In addition, hepatic stem cells isolated from human livers have a great immediate potential if the systematic cell expansion and storage can be established nationwide.

Another challenge is to generate natural/synthetic basement membrane matrices comprising ECM proteins, growth factors and biological activity for maintaining functional human hepatocytes for long term cultures. The cell secreted matrices hold tremendous potential because of various advantages, such as preservation of protein–protein interactions in their natural state, animal free extraction and reduction of pathogen transmission. On the other hand, synthetic self-assembling peptide hydrogels mimicking the functional motifs of ECM proteins is another promising direction for further exploration as matrices for liver tissue engineering.

A better understanding of host responses to hepatitis viruses and other inflammatory diseases can be done in a high-throughput platform in microscale cultures. More effort in this direction will provide an enhanced understanding of drug efficacy, drug–drug interactions and drug toxicity in liver diseases. Currently, there are no *in vitro* models for studying the mechanistic aspects of liver diseases under *in vitro* conditions. More efforts have to be made in studying human liver diseases using microscale tissue engineering and in the development of organotypic models in bioreactors. Once an organotypic model has been generated which mimics the hepatic tissue microenvironment and functionality, then it will aid in developing novel therapeutics for liver diseases.

Notably, the development of mechanistic understanding of immunomodulation of hepatocytes *in vitro* using bioreactor and microscale technology holds remarkable promise for drug screening and liver transplantation and may open new avenues for drug research and patient specific drug development.

Acknowledgements We appreciate Dr. Lola M. Reid for her kindness to share the slides of her keynote presentation, Endodermal Stem Cells and their Maturational Lineages, in the 2010 SPRBM (Society for Physical Regulation in Biology and Medicine) conference to Dr. Sihong Wang.

References

1. UNOS-Database, 2008 OPTN/SRTR Annual Report: Transplant Data, Chapter IV. Liver and Intestine Transplantation in the United States 1998–2007, http://optn.transplant.hrsa.gov/ar2008/Chapter_IV_AR_CD.htm?cp=5, January 2010.
2. Hauboldt RH, Hanson SG: 2008 U.S. Organ and tissue transplant cost estimates and discussion. Milliman Research Report, 2008.
3. Seely RR, Stephens TD, Tate P: Anatomy & physiology, seventh edition. New York: McGraw-Hill, 2006, p 903–908.
4. Arias IM, Boyer JL, Chrisari FV, Fausto N, Schachter D, Shafritz DA: The liver, biology and pathobiology, Fourth edition. Philadelphia: Lippincott Williams & Wilkins, 2001, p. 7–8.
5. Anastasi G, Cpitani S, Carnazza ML, Saverio C, Caro RD, Donato RF, Ferrario VF, Fonzi L, Franzì AT, Gaudio E, Geremia R, Lanza GG, Grossi CE, Manzoli FA, Mazzotti G, Michetti F, Miscia S, Mitolo V, Montella A, Orlandini G, Paparelli A, Renda T, Ribatti D, Ruggeri A, Sirigu P, Soscia A, Tredici G, Vitale M, Zaccheio D, Zauli G, Zecchi S: Trattato di anatomia umana (in italian), second edition. Milano, Italy: Arti Grafiche Salea, 2006.
6. Potten CS: Tissue stem cells. New York: Taylor & Francis, 2006.
7. Morin O, Goulet F, Normand C: Liver sinusoidal endothelial cells: Isolation, purification, characterization and interaction with hepatocytes. *Revis Biol Celular* 1988;15:1–85.
8. Allen JW, Bhatia SN: Formation of steady-state oxygen gradients in vitro: Application to liver zonation. *Biotechnol Bioeng* 2003;82:253–262.
9. Tiniakos DG, Vos MB, Brunt EM: Nonalcoholic fatty liver disease: Pathology and pathogenesis. *Annu Rev Pathol* 2010;5:145–171.
10. Stewart SF, Day CP: The management of alcoholic liver disease. *J Hepatol* 2003;38(Suppl 1): S2–13.
11. Duvnjak M, Tomasic V, Gomercic M, Smircic Duvnjak L, Barsic N, Lerotic I: Therapy of nonalcoholic fatty liver disease: Current status. *J Physiol Pharmacol* 2009;60(Suppl 7):57–66.
12. Yamamoto T, Yamaguchi H, Miki H, Shimada M, Nakada Y, Ogino M, Asano K, Aoki K, Tamura N, Masago M, Kato K: Coenzyme a: Diacylglycerol acyltransferase 1 inhibitor ameliorates obesity, liver steatosis, and lipid metabolism abnormality in KKA(y) mice fed high-fat or high-carbohydrate diets. *Eur J Pharmacol* 2010;640:243–249.
13. Cui W, Chen SL, Hu KQ: Quantification and mechanisms of oleic acid-induced steatosis in hepg2 cells. *Am J Transl Res* 2010;2:95–104.
14. Starley BQ, Calcagno CJ, Harrison SA: Nonalcoholic fatty liver disease and hepatocellular carcinoma: A weighty connection. *Hepatology* 2010;51:1820–1832.
15. Friedman SL: Hepatic stellate cells: Protean, multifunctional, and enigmatic cells of the liver. *Physiol Rev* 2008;88:125–172.
16. Gyamfi MA, Wan YJ: Pathogenesis of alcoholic liver disease: The role of nuclear receptors. *Exp Biol Med (Maywood)* 2010;235:547–560.
17. Samuel D, Feray C, Bismuth H: Hepatitis viruses and liver transplantation. *J Gastroenterol Hepatol* 1997;12:S335–S341.
18. Fierbinteanu-Braticevici C, Mohora M, Tribus L, Petrisor A, Cretoiu SM, Cretoiu D, Usvat R, Ionita L: Hepatocyte steatosis in patients infected with genotype 1 hepatitis C virus. *Rom J Morphol Embryol* 2010;51:235–242.

19. Higgins GM, Anderson RM: Experimental pathology of the liver. I. Restoration of the liver of the white rat following partial surgical removal. *Arch Pathol* 1931;12:186–202.
20. Michalopoulos GK, DeFrances MC: Liver regeneration. *Science* 1997;276:60–66.
21. Chamuleau RA: Future of bioartificial liver support. *World J Gastrointest Surg* 2009;1:21–25.
22. Asonuma K, Gilbert JC, Stein JE, Takeda T, Vacanti JP: Quantitation of transplanted hepatic mass necessary to cure the Gunn rat model of hyperbilirubinemia. *J Pediatr Surg* 1992;27:298–301.
23. Fiegel HC, Kaufmann PM, Bruns H, Kluth D, Horch RE, Vacanti JP, Kneser U: Hepatic tissue engineering: From transplantation to customized cell-based liver directed therapies from the laboratory. *J Cell Mol Med* 2008;12:56–66.
24. Sohlenius-Sternbeck AK: Determination of the hepatocellularity number for human, dog, rabbit, rat and mouse livers from protein concentration measurements. *Toxicol In Vitro* 2006;20:1582–1586.
25. Zhao DC, Lei JX, Chen R, Yu WH, Zhang XM, Li SN, Xiang P: Bone marrow-derived mesenchymal stem cells protect against experimental liver fibrosis in rats. *World J Gastroenterol* 2005;11:3431–3440.
26. Vassilopoulos G, Wang PR, Russell DW: Transplanted bone marrow regenerates liver by cell fusion. *Nature* 2003;422:901–904.
27. Wang X, Willenbring H, Akkari Y, Torimaru Y, Foster M, Al-Dhalimy M, Lagasse E, Finegold M, Olson S, Grompe M: Cell fusion is the principal source of bone-marrow-derived hepatocytes. *Nature* 2003;422:897–901.
28. Kubota H, Reid LM: Clonogenic hepatoblasts, common precursors for hepatocytic and biliary lineages, are lacking classical major histocompatibility complex class I antigen. *Proc Natl Acad Sci U S A* 2000;97:12132–12137.
29. Cho CH, Berthiaume F, Tilles AW, Yarmush ML: A new technique for primary hepatocyte expansion in vitro. *Biotechnol Bioeng* 2008;101:345–356.
30. Cho JJ, Malhi H, Wang R, Joseph B, Ludlow JW, Susick R, Gupta S: Enzymatically labeled chromosomal probes for in situ identification of human cells in xenogeneic transplant models. *Nat Med* 2002;8:1033–1036.
31. Saxena R, Theise N: Canals of hering: Recent insights and current knowledge. *Semin Liver Dis* 2004;24:43–48.
32. Theise ND, Saxena R, Portmann BC, Thung SN, Yee H, Chiriboga L, Kumar A, Crawford JM: The canals of hering and hepatic stem cells in humans. *Hepatology* 1999;30:1425–1433.
33. Strain AJ: Ex vivo liver cell morphogenesis: One step nearer to the bioartificial liver? *Hepatology* 1999;29:288–290.
34. Wauthier E, Schmelzer E, Turner W, Zhang L, LeCluyse E, Ruiz J, Turner R, Furth ME, Kubota H, Lozoya O, Barbier C, McClelland R, Yao HL, Moss N, Bruce A, Ludlow J, Reid LM: Hepatic stem cells and hepatoblasts: Identification, isolation, and ex vivo maintenance. *Methods Cell Biol* 2008;86:137–225.
35. Jiang Y, Jahagirdar BN, Reinhardt RL, Schwartz RE, Keene CD, Ortiz-Gonzalez XR, Reyes M, Lenvik T, Lund T, Blackstad M, Du J, Aldrich S, Lisberg A, Low WC, Largaespada DA, Verfaillie CM: Pluripotency of mesenchymal stem cells derived from adult marrow. *Nature* 2002;418:41–49.
36. Lagasse E, Connors H, Al-Dhalimy M, Reitsma M, Dohse M, Osborne L, Wang X, Finegold M, Weissman IL, Grompe M: Purified hematopoietic stem cells can differentiate into hepatocytes in vivo. *Nat Med* 2000;6:1229–1234.
37. Theise ND, Nimmakayalu M, Gardner R, Illei PB, Morgan G, Teperman L, Henegariu O, Krause DS: Liver from bone marrow in humans. *Hepatology* 2000;32:11–16.
38. Agarwal S, Holton KL, Lanza R: Efficient differentiation of functional hepatocytes from human embryonic stem cells. *Stem Cells* 2008;26:1117–1127.
39. Basma H, Soto-Gutierrez A, Yannam GR, Liu L, Ito R, Yamamoto T, Ellis E, Carson SD, Sato S, Chen Y, Muirhead D, Navarro-Alvarez N, Wong RJ, Roy-Chowdhury J, Platt JL, Mercer DF,

- Miller JD, Strom SC, Kobayashi N, Fox IJ: Differentiation and transplantation of human embryonic stem cell-derived hepatocytes. *Gastroenterology* 2009;136:990–999.
40. Cai J, Zhao Y, Liu Y, Ye F, Song Z, Qin H, Meng S, Chen Y, Zhou R, Song X, Guo Y, Ding M, Deng H: Directed differentiation of human embryonic stem cells into functional hepatic cells. *Hepatology* 2007;45:1229–1239.
 41. Duan Y, Catana A, Meng Y, Yamamoto N, He S, Gupta S, Gambhir SS, Zern MA: Differentiation and enrichment of hepatocyte-like cells from human embryonic stem cells in vitro and in vivo. *Stem Cells* 2007;25:3058–3068.
 42. Hay DC, Zhao D, Fletcher J, Hewitt ZA, McLean D, Urruticoechea-Uriguen A, Black JR, Elcombe C, Ross JA, Wolf R, Cui W: Efficient differentiation of hepatocytes from human embryonic stem cells exhibiting markers recapitulating liver development in vivo. *Stem Cells* 2008;26:894–902.
 43. Dalgetty DM, Medicine CN, Iredale JP, Hay DC: Progress and future challenges in stem cell-derived liver technologies. *Am J Physiol Gastrointest Liver Physiol* 2009;297:G241–G248.
 44. Deurholt T, van Til NP, Chhatta AA, ten Bloemendaal L, Schwartlander R, Payne C, Plevis JN, Sauer IM, Chamuleau RA, Elferink RP, Seppen J, Hoekstra R: Novel immortalized human fetal liver cell line, cbal111, has the potential to differentiate into functional hepatocytes. *BMC Biotechnol* 2009;9:89.
 45. Burke WT: Urea synthesis in the isolated perfused rat liver. *Biochem Biophys Res Commun* 1960;3:525–530.
 46. Gordon AH, Humphrey JH: Methods for measuring rates of synthesis of albumin by the isolated perfused rat liver. *Biochem J* 1960;75:240–247.
 47. McKindley DS, Chichester C, Raymond R: Effect of endotoxin shock on the clearance of lidocaine and indocyanine green in the perfused rat liver. *Shock* 1999;12:468–472.
 48. Palmen NG, Evelo CT, Borm PJ, Henderson PT: Toxicokinetics of dimethylacetamide (dmac) in rat isolated perfused liver. *Hum Exp Toxicol* 1993;12:127–133.
 49. Lee K, Berthiaume F, Stephanopoulos GN, Yarmush DM, Yarmush ML: Metabolic flux analysis of postburn hepatic hypermetabolism. *Metab Eng* 2000;2:312–327.
 50. Bessems M, t Hart NA, Tolba R, Doorschodt BM, Leuvenink HG, Ploeg RJ, Minor T, van Gulik TM: The isolated perfused rat liver: Standardization of a time-honoured model. *Lab Anim* 2006;40:236–246.
 51. Gores GJ, Kost LJ, LaRusso NF: The isolated perfused rat liver: Conceptual and practical considerations. *Hepatology* 1986;6:511–517.
 52. Martin H, Sarsat JP, Lerche-Langrand C, Housset C, Balladur P, Toutain H, Albaladejo V: Morphological and biochemical integrity of human liver slices in long-term culture: Effects of oxygen tension. *Cell Biol Toxicol* 2002;18:73–85.
 53. Lerche-Langrand C, Toutain HJ: Precision-cut liver slices: Characteristics and use for in vitro pharmacotoxicology. *Toxicology* 2000;153:221–253.
 54. Fisher RL, Gandolfi AJ, Brendel K: Human liver quality is a dominant factor in the outcome of in vitro studies. *Cell Biol Toxicol* 2001;17:179–189.
 55. Olinga P, Hof IH, Merema MT, Smit M, de Jager MH, Swart PJ, Slooff MJ, Meijer DK, Groothuis GM: The applicability of rat and human liver slices to the study of mechanisms of hepatic drug uptake. *J Pharmacol Toxicol Methods* 2001;45:55–63.
 56. Olinga P, Merema MT, de Jager MH, Derks F, Melgert BN, Moshage H, Slooff MJ, Meijer DK, Poelstra K, Groothuis GM: Rat liver slices as a tool to study LPS-induced inflammatory response in the liver. *J Hepatol* 2001;35:187–194.
 57. Zhao P, Kalhorn TF, Slattery JT: Selective mitochondrial glutathione depletion by ethanol enhances acetaminophen toxicity in rat liver. *Hepatology* 2002;36:326–335.
 58. Neyrinck A, Eeckhoudt SL, Meunier CJ, Pampfer S, Taper HS, Verbeeck RK, Delzenne N: Modulation of paracetamol metabolism by kupffer cells: A study on rat liver slices. *Life Sci* 1999;65:2851–2859.

59. Chang ML, Sung KF, Sheen IS, Lin SM, Yeh CT: A liver slice culture-based ex vivo assay to predict the outcome of antiviral therapy for chronic hepatitis C. *J Viral Hepat* 2009;16: 359–366.
60. Kern MA, Haugg AM, Eiteneuer E, Konze E, Drebbler U, Dienes HP, Breuhahn K, Schirmacher P, Kasper HU: Ex vivo analysis of antineoplastic agents in precision-cut tissue slices of human origin: Effects of cyclooxygenase-2 inhibition in hepatocellular carcinoma. *Liver Int* 2006;26:604–612.
61. van de Bovenkamp M, Groothuis GM, Meijer DK, Olinga P: Precision-cut fibrotic rat liver slices as a new model to test the effects of anti-fibrotic drugs in vitro. *J Hepatol* 2006;45: 696–703.
62. Irani K, Pomerantseva I, Hart AR, Sundback CA, Neville CM, Vacanti JP: Mechanical dissociation of swine liver to produce organoid units for tissue engineering and in vitro disease modeling. *Artif Organs* 2010;34:75–78.
63. Howard RB, Christensen AK, Gibbs FA, Pesch LA: The enzymatic preparation of isolated intact parenchymal cells from rat liver. *J Cell Biol* 1967;35:675–684.
64. Berry MN, Friend DS: High-yield preparation of isolated rat liver parenchymal cells: A biochemical and fine structural study. *J Cell Biol* 1969;43:506–520.
65. Seglen PO, Jervell KF: A simple perfusion technique applied to glucocorticoid regulation of tryptophan oxygenase turnover and bile production in the isolated rat liver. *Hoppe Seylers Z Physiol Chem* 1969;350:308–316.
66. Dunn JC, Tompkins RG, Yarmush ML: Long-term in vitro function of adult hepatocytes in a collagen sandwich configuration. *Biotechnol Prog* 1991;7:237–245.
67. Ryan CM, Carter EA, Jenkins RL, Sterling LM, Yarmush ML, Malt RA, Tompkins RG: Isolation and long-term culture of human hepatocytes. *Surgery* 1993;113:48–54.
68. Berthiaume F, Moghe PV, Toner M, Yarmush ML: Effect of extracellular matrix topology on cell structure, function, and physiological responsiveness: Hepatocytes cultured in a sandwich configuration. *FASEB J* 1996;10:1471–1484.
69. Landry J, Bernier D, Ouellet C, Goyette R, Marceau N: Spheroidal aggregate culture of rat liver cells: Histotypic reorganization, biomatrix deposition, and maintenance of functional activities. *J Cell Biol* 1985;101:914–923.
70. Tong JZ, Sarrazin S, Cassio D, Gauthier F, Alvarez F: Application of spheroid culture to human hepatocytes and maintenance of their differentiation. *Biol Cell* 1994;81:77–81.
71. Glicklis R, Shapiro L, Agbaria R, Merchuk JC, Cohen S: Hepatocyte behavior within three-dimensional porous alginate scaffolds. *Biotechnol Bioeng* 2000;67:344–353.
72. Maguire T, Davidovich AE, Wallenstein EJ, Novik E, Sharma N, Pedersen H, Androulakis IP, Schloss R, Yarmush M: Control of hepatic differentiation via cellular aggregation in an alginate microenvironment. *Biotechnol Bioeng* 2007;98:631–644.
73. Moghe PV, Berthiaume F, Ezzell RM, Toner M, Tompkins RG, Yarmush ML: Culture matrix configuration and composition in the maintenance of hepatocyte polarity and function. *Biomaterials* 1996;17:373–385.
74. Mitaka T: Reconstruction of hepatic organoid by hepatic stem cells. *J Hepatobiliary Pancreat Surg* 2002;9:697–703.
75. Wang S, Nagrath D, Chen PC, Berthiaume F, Yarmush ML: Three-dimensional primary hepatocyte culture in synthetic self-assembling peptide hydrogel. *Tissue Eng Part A* 2008;14:227–236.
76. Sharma NS, Nagrath D, Yarmush ML: Adipocyte-derived basement membrane extract with biological activity: Applications in hepatocyte functional augmentation in vitro. *FASEB J* 2010;24:2364–2374
77. Wu FJ, Friend JR, Hsiao CC, Zilliox MJ, Ko WJ, Cerra FB, Hu WS: Efficient assembly of rat hepatocyte spheroids for tissue engineering applications. *Biotechnol Bioeng* 1996;50:404–415.

78. Goulet F, Normand C, Morin O: Cellular interactions promote tissue-specific function, biomatrix deposition and junctional communication of primary cultured hepatocytes. *Hepatology* 1988;8:1010–1018.
79. Morin O, Normand C: Long-term maintenance of hepatocyte functional activity in co-culture: Requirements for sinusoidal endothelial cells and dexamethasone. *J Cell Physiol* 1986;129:103–110.
80. Bhatia SN, Yarmush ML, Toner M: Controlling cell interactions by micropatterning in co-cultures: Hepatocytes and 3t3 fibroblasts. *J Biomed Mater Res* 1997;34:189–199.
81. Hoebe KH, Witkamp RF, Fink-Gremmels J, Van Miert AS, Monshouwer M: Direct cell-to-cell contact between kupffer cells and hepatocytes augments endotoxin-induced hepatic injury. *Am J Physiol Gastrointest Liver Physiol* 2001;280:G720–G728.
82. Milosevic N, Schawalder H, Maier P: Kupffer cell-mediated differential down-regulation of cytochrome p450 metabolism in rat hepatocytes. *Eur J Pharmacol* 1999;368:75–87.
83. Nahmias Y, Berthiaume F, Yarmush ML: Integration of technologies for hepatic tissue engineering. *Adv Biochem Eng Biotechnol* 2007;103:309–329.
84. Ploss A, Khetani SR, Jones CT, Syder AJ, Trehan K, Gaysinskaya VA, Mu K, Ritola K, Rice CM, Bhatia SN: Persistent hepatitis c virus infection in microscale primary human hepatocyte cultures. *Proc Natl Acad Sci U S A* 2010;107:3141–3145.
85. Baptista PM, Orlando G, Mirmalek-Sani SH, Siddiqui M, Atala A, Soker S: Whole organ decellularization – a tool for bioscaffold fabrication and organ bioengineering. *Conf Proc IEEE Eng Med Biol Soc* 2009;2009:6526–6529.
86. Sellaro TL, Ranade A, Faulk DM, McCabe GP, Dorko K, Badyal SF, Strom SC: Maintenance of human hepatocyte function in vitro by liver-derived extracellular matrix gels. *Tissue Eng Part A* 2010;16:1075–1082.
87. Love RJ, Jones KS: Biomaterials, fibrosis, and the use of drug delivery systems in future antifibrotic strategies. *Crit Rev Biomed Eng* 2009;37:259–281.
88. Ohashi K, Yokoyama T, Yamato M, Kuge H, Kanehiro H, Tsutsumi M, Amanuma T, Iwata H, Yang J, Okano T, Nakajima Y: Engineering functional two- and three-dimensional liver systems in vivo using hepatic tissue sheets. *Nat Med* 2007;13:880–885.
89. Seo SJ, Kim IY, Choi YJ, Akaike T, Cho CS: Enhanced liver functions of hepatocytes cocultured with nih 3t3 in the alginate/galactosylated chitosan scaffold. *Biomaterials* 2006;27:1487–1495.
90. Torok E, Vogel C, Lutgehetmann M, Ma PX, Dandri M, Petersen J, Burda MR, Siebert K, Dullmann J, Rogiers X, Pollok JM: Morphological and functional analysis of rat hepatocyte spheroids generated on poly(L-lactic acid) polymer in a pulsatile flow bioreactor. *Tissue Eng* 2006;12:1881–1890.
91. Semler EJ, Ranucci CS, Moghe PV: Tissue assembly guided via substrate biophysics: Applications to hepatocellular engineering. *Adv Biochem Eng Biotechnol* 2006;102:1–46.
92. Tsang VL, Bhatia SN: Fabrication of three-dimensional tissues. *Adv Biochem Eng Biotechnol* 2007;103:189–205.
93. Underhill GH, Chen AA, Albrecht DR, Bhatia SN: Assessment of hepatocellular function within peg hydrogels. *Biomaterials* 2007;28:256–270.
94. Lee WM, Squires RH, Jr., Nyberg SL, Doo E, Hoofnagle JH: Acute liver failure: Summary of a workshop. *Hepatology* 2008;47:1401–1415.
95. Stange J, Mitzner S, Ramlow W, Gliesche T, Hickstein H, Schmidt R: A new procedure for the removal of protein bound drugs and toxins. *ASAIO J* 1993;39:M621–M625.
96. Hassanein TI, Tofteng F, Brown RS, Jr., McGuire B, Lynch P, Mehta R, Larsen FS, Gornbein J, Stange J, Blei AT: Randomized controlled study of extracorporeal albumin dialysis for hepatic encephalopathy in advanced cirrhosis. *Hepatology* 2007;46:1853–1862.
97. Stange J, Hassanein TI, Mehta R, Mitzner SR, Bartlett RH: The molecular adsorbents recycling system as a liver support system based on albumin dialysis: A summary of

- preclinical investigations, prospective, randomized, controlled clinical trial, and clinical experience from 19 centers. *Artif Organs* 2002;26:103–110.
98. Keyword “MARS”: Clinicaltrials.Org. <http://clinicaltrials.gov/>, retrieved in March 2010
 99. Peszynski P, Klammt S, Peters E, Mitzner S, Stange J, Schmidt R: Albumin dialysis: Single pass vs. Recirculation (mars). *Liver* 2002;22(Suppl 2):40–42.
 100. Keywords “Single Pass Albumin Dialysis”: Clinicaltrials.Org. <http://clinicaltrials.gov/>, retrieved in March 2010
 101. Falkenhagen D, Strobl W, Vogt G, Schrefl A, Linsberger I, Gerner FJ, Schoenhofen M: Fractionated plasma separation and adsorption system: A novel system for blood purification to remove albumin bound substances. *Artif Organs* 1999;23:81–86.
 102. Rifai K, Ernst T, Kretschmer U, Bahr MJ, Schneider A, Hafer C, Haller H, Manns MP, Fliser D: Prometheus – A new extracorporeal system for the treatment of liver failure. *J Hepatol* 2003;39:984–990.
 103. Evenepoel P, Laleman W, Wilmer A, Claes K, Kuypers D, Bammens B, Nevens F, Vanrenterghem Y: Prometheus versus molecular adsorbents recirculating system: Comparison of efficiency in two different liver detoxification devices. *Artif Organs* 2006;30:276–284.
 104. Krisper P, Haditsch B, Stauber R, Jung A, Stadlbauer V, Trauner M, Holzer H, Schneditz D: In vivo quantification of liver dialysis: Comparison of albumin dialysis and fractionated plasma separation. *J Hepatol* 2005;43:451–457.
 105. Laleman W, Wilmer A, Evenepoel P, Elst IV, Zeegers M, Zaman Z, Verslype C, Fevery J, Nevens F: Effect of the molecular adsorbent recirculating system and prometheus devices on systemic haemodynamics and vasoactive agents in patients with acute-on-chronic alcoholic liver failure. *Crit Care* 2006;10:R108.
 106. Krisper P, Stauber RE: Technology insight: Artificial extracorporeal liver support – How does prometheus compare with mars? *Nat Clin Pract Nephrol* 2007;3:267–276.
 107. Keyword “Prometheus”: Clinicaltrials.Org. <http://clinicaltrials.gov/>, retrieved in March 2010
 108. Mullon C, Pitkin Z: The hepatassist bioartificial liver support system: Clinical study and pig hepatocyte process. *Expert Opin Investig Drugs* 1999;8:229–235.
 109. Demetriou AA, Brown RS, Jr., Busuttill RW, Fair J, McGuire BM, Rosenthal P, Am Esch JS, 2nd, Lerut J, Nyberg SL, Salizzoni M, Fagan EA, de Hemptinne B, Broelsch CE, Muraca M, Salmeron JM, Rabkin JM, Metselaar HJ, Pratt D, De La Mata M, McChesney LP, Everson GT, Lavin PT, Stevens AC, Pitkin Z, Solomon BA: Prospective, randomized, multicenter, controlled trial of a bioartificial liver in treating acute liver failure. *Ann Surg* 2004;239:660–667.
 110. Pitkin Z, Mullon C: Evidence of absence of porcine endogenous retrovirus (perv) infection in patients treated with a bioartificial liver support system. *Artif Organs* 1999;23:829–833.
 111. Fruhauf JH, Mertsching H, Giri S, Fruhauf NR, Bader A: Porcine endogenous retrovirus released by a bioartificial liver infects primary human cells. *Liver Int* 2009;29:1553–1561.
 112. Ellis AJ, Hughes RD, Wendon JA, Dunne J, Langley PG, Kelly JH, Gislason GT, Sussman NL, Williams R: Pilot-controlled trial of the extracorporeal liver assist device in acute liver failure. *Hepatology* 1996;24:1446–1451.
 113. Millis JM, Cronin DC, Johnson R, Conjeevaram H, Conlin C, Trevino S, Maguire P: Initial experience with the modified extracorporeal liver-assist device for patients with fulminant hepatic failure: System modifications and clinical impact. *Transplantation* 2002;74:1735–1746.
 114. Keyword “ELAD”: Clinicaltrials.Org. <http://clinicaltrials.gov/>, retrieved in March 2010
 115. Sauer IM, Zeilinger K, Obermayer N, Pless G, Grunwald A, Pascher A, Mieder T, Roth S, Goetz M, Kardassis D, Mas A, Neuhaus P, Gerlach JC: Primary human liver cells as source for modular extracorporeal liver support – A preliminary report. *Int J Artif Organs* 2002;25:1001–1005.
 116. Sauer IM, Gerlach JC: Modular extracorporeal liver support. *Artif Organs* 2002;26:703–706.
 117. Sauer IM, Kardassis D, Zeilinger K, Pascher A, Gruenwald A, Pless G, Irgang M, Kraemer M, Puhl G, Frank J, Muller AR, Steinmuller T, Denner J, Neuhaus P, Gerlach JC: Clinical

- extracorporeal hybrid liver support – Phase I study with primary porcine liver cells. *Xenotransplantation* 2003;10:460–469.
118. Sauer IM, Zeilinger K, Pless G, Kardassis D, Theruvath T, Pascher A, Goetz M, Neuhaus P, Gerlach JC: Extracorporeal liver support based on primary human liver cells and albumin dialysis – treatment of a patient with primary graft non-function. *J Hepatol* 2003;39:649–653.
 119. van de Kerkhove MP, Poyck PP, Deurholt T, Hoekstra R, Chamuleau RA, van Gulik TM: Liver support therapy: An overview of the amc-bioartificial liver research. *Dig Surg* 2005;22:254–264.
 120. van de Kerkhove MP, Di Florio E, Scuderi V, Mancini A, Belli A, Bracco A, Dauri M, Tisone G, Di Nicuolo G, Amoroso P, Spadari A, Lombardi G, Hoekstra R, Calise F, Chamuleau RA: Phase I clinical trial with the amc-bioartificial liver. *Int J Artif Organs* 2002;25:950–959.
 121. Mazariegos GV, Patzer JF, 2nd, Lopez RC, Giraldo M, Devera ME, Grogan TA, Zhu Y, Fulmer ML, Amiot BP, Kramer DJ: First clinical use of a novel bioartificial liver support system (BLSS). *Am J Transplant* 2002;2:260–266.
 122. Chen Z, Ding YT: Functional evaluation of a new bioartificial liver system in vitro and in vitro. *World J Gastroenterol* 2006;12:1312–1316.
 123. Ding YT, Qiu YD, Chen Z, Xu QX, Zhang HY, Tang Q, Yu DC: The development of a new bioartificial liver and its application in 12 acute liver failure patients. *World J Gastroenterol* 2003;9:829–832.
 124. Samuel D, Ichai P, Feray C, Saliba F, Azoulay D, Arulnaden JL, Debat P, Gigou M, Adam R, Bismuth A, Castaing D, Bismuth H: Neurological improvement during bioartificial liver sessions in patients with acute liver failure awaiting transplantation. *Transplantation* 2002;73:257–264.
 125. van de Kerkhove MP, Poyck PP, van Wijk AC, Galavotti D, Hoekstra R, van Gulik TM, Chamuleau RA: Assessment and improvement of liver specific function of the amc-bioartificial liver. *Int J Artif Organs* 2005;28:617–630.
 126. Chan C, Berthiaume F, Lee K, Yarmush ML: Metabolic flux analysis of hepatocyte function in hormone- and amino acid-supplemented plasma. *Metab Eng* 2003;5:1–15.
 127. Chan C, Berthiaume F, Lee K, Yarmush ML: Metabolic flux analysis of cultured hepatocytes exposed to plasma. *Biotechnol Bioeng* 2003;81:33–49.
 128. Chan C, Berthiaume F, Washizu J, Toner M, Yarmush ML: Metabolic pre-conditioning of cultured cells in physiological levels of insulin: Generating resistance to the lipid-accumulating effects of plasma in hepatocytes. *Biotechnol Bioeng* 2002;78:753–760.
 129. Nagrath D, Xu H, Tanimura Y, Zuo R, Berthiaume F, Avila M, Yarmush R, Yarmush ML: Metabolic preconditioning of donor organs: Defatting fatty livers by normothermic perfusion ex vivo. *Metab Eng* 2009;11:274–283.
 130. Gupta S, Rajvanshi P, Lee CD: Integration of transplanted hepatocytes into host liver plates demonstrated with dipeptidyl peptidase IV-deficient rats. *Proc Natl Acad Sci U S A* 1995;92:5860–5864.
 131. Kumaran V, Joseph B, Bente D, Gupta S: Integrin and extracellular matrix interactions regulate engraftment of transplanted hepatocytes in the rat liver. *Gastroenterology* 2005;129:1643–1653.
 132. Wu YM, Joseph B, Berishvili E, Kumaran V, Gupta S: Hepatocyte transplantation and drug-induced perturbations in liver cell compartments. *Hepatology* 2008;47:279–287.
 133. Gupta S, Yerneni PR, Vemuru RP, Lee CD, Yellin EL, Bhargava KK: Studies on the safety of intrasplenic hepatocyte transplantation: Relevance to ex vivo gene therapy and liver repopulation in acute hepatic failure. *Hum Gene Ther* 1993;4:249–257.
 134. Rajvanshi P, Kerr A, Bhargava KK, Burk RD, Gupta S: Efficacy and safety of repeated hepatocyte transplantation for significant liver repopulation in rodents. *Gastroenterology* 1996;111:1092–1102.

135. Benedetti E, Kirby JP, Asolati M, Blanchard J, Ward MG, Williams R, Hewett TA, Fontaine M, Pollak R: Intrasplenic hepatocyte allotransplantation in dalmation dogs with and without cyclosporine immunosuppression. *Transplantation* 1997;63:1206–1209.
136. Strom SC, Bruzzone P, Cai H, Ellis E, Lehmann T, Mitamura K, Miki T: Hepatocyte transplantation: Clinical experience and potential for future use. *Cell Transplant* 2006;15 (Suppl 1):S105–S110.
137. Soto-Gutierrez A, Navarro-Alvarez N, Yagi H, Yarmush ML: Stem cells for liver repopulation. *Curr Opin Organ Transplant* 2009;14:667–673.
138. Strom SC, Chowdhury JR, Fox IJ: Hepatocyte transplantation for the treatment of human disease. *Semin Liver Dis* 1999;19:39–48.
139. Strom SC, Fisher RA, Thompson MT, Sanyal AJ, Cole PE, Ham JM, Posner MP: Hepatocyte transplantation as a bridge to orthotopic liver transplantation in terminal liver failure. *Transplantation* 1997;63:559–569.
140. Soriano HE: Liver cell transplantation: Human application in adults and children; Proceedings of falk symposium, hepatocyte transplantation, vol 126, Lancaster, UK: Kluwer Academic Publishers, 2002, pp 99–115.
141. Khan AA, Parveen N, Mahaboob VS, Rajendraprasad A, Ravindraprakash HR, Venkateswarlu J, Rao P, Pande G, Narusu ML, Khaja MN, Pramila R, Habeeb A, Habibullah CM: Management of hyperbilirubinemia in biliary atresia by hepatic progenitor cell transplantation through hepatic artery: A case report. *Transplant Proc* 2008;40:1153–1155.
142. Bilir BM, Guinette D, Karrer F, Kumpe DA, Krysl J, Stephens J, McGavran L, Ostrowska A, Durham J: Hepatocyte transplantation in acute liver failure. *Liver Transpl* 2000;6:32–40.
143. Fisher RA, Bu D, Thompson M, Tisnado J, Prasad U, Sterling R, Posner M, Strom S: Defining hepatocellular chimerism in a liver failure patient bridged with hepatocyte infusion. *Transplantation* 2000;69:303–307.
144. Schneider A, Attaran M, Meier PN, Strassburg C, Manns MP, Ott M, Barthold M, Arseniev L, Becker T, Panning B: Hepatocyte transplantation in an acute liver failure due to mushroom poisoning. *Transplantation* 2006;82:1115–1116.
145. Habibullah CM, Syed IH, Qamar A, Taher-Uz Z: Human fetal hepatocyte transplantation in patients with fulminant hepatic failure. *Transplantation* 1994;58:951–952.
146. Horslen SP, McCowan TC, Goertzen TC, Warkentin PI, Cai HB, Strom SC, Fox IJ: Isolated hepatocyte transplantation in an infant with a severe urea cycle disorder. *Pediatrics* 2003;111:1262–1267.
147. Puppi J, Tan N, Mitry RR, Hughes RD, Lehec S, Mieli-Vergani G, Karani J, Champion MP, Heaton N, Mohamed R, Dhawan A: Hepatocyte transplantation followed by auxiliary liver transplantation – A novel treatment for ornithine transcarbamylase deficiency. *Am J Transplant* 2008;8:452–457.
148. Strom SC, Fisher RA, Rubinstein WS, Barranger JA, Towbin RB, Charron M, Miele L, Pizarov LA, Dorko K, Thompson MT, Reyes J: Transplantation of human hepatocytes. *Transplant Proc* 1997;29:2103–2106.
149. Muraca M, Gerunda G, Neri D, Vilei MT, Granato A, Feltracco P, Meroni M, Giron G, Burlina AB: Hepatocyte transplantation as a treatment for glycogen storage disease type 1a. *Lancet* 2002;359:317–318.
150. Sokal EM, Smets F, Bourgois A, Van Maldergem L, Buts JP, Reding R, Bernard Otte J, Evrard V, Latinne D, Vincent MF, Moser A, Soriano HE: Hepatocyte transplantation in a 4-year-old girl with peroxisomal biogenesis disease: Technique, safety, and metabolic follow-up. *Transplantation* 2003;76:735–738.
151. Dhawan A, Mitry RR, Hughes RD, Lehec S, Terry C, Bansal S, Arya R, Wade JJ, Verma A, Heaton ND, Rela M, Mieli-Vergani G: Hepatocyte transplantation for inherited factor VII deficiency. *Transplantation* 2004;78:1812–1814.
152. Horslen SP, Fox IJ: Hepatocyte transplantation. *Transplantation* 2004;77:1481–1486.

153. Ambrosino G, Varotto S, Strom SC, Guariso G, Franchin E, Miotto D, Caenazzo L, Basso S, Carraro P, Valente ML, D'Amico D, Zancan L, D'Antiga L: Isolated hepatocyte transplantation for crigler-najjar syndrome type 1. *Cell Transplant* 2005;14:151–157.
154. Fox IJ, Chowdhury JR, Kaufman SS, Goertzen TC, Chowdhury NR, Warkentin PI, Dorko K, Sauter BV, Strom SC: Treatment of the crigler-najjar syndrome type I with hepatocyte transplantation. *N Engl J Med* 1998;338:1422–1426.
155. Khan AA, Parveen N, Mahaboob VS, Rajendraprasad A, Ravindrakrishna HR, Venkateswarlu J, Rao P, Pande G, Narusu ML, Khaja MN, Pramila R, Habeeb A, Habibullah CM: Treatment of crigler-najjar syndrome type 1 by hepatic progenitor cell transplantation: A simple procedure for management of hyperbilirubinemia. *Transplant Proc* 2008;40:1148–1150.
156. Meyburg J, Hoffmann GF: Liver cell transplantation for the treatment of inborn errors of metabolism. *J Inher Metab Dis* 2008;31:164–172.
157. Mooney DJ, Sano K, Kaufmann PM, Majahod K, Schloo B, Vacanti JP, Langer R: Long-term engraftment of hepatocytes transplanted on biodegradable polymer sponges. *J Biomed Mater Res* 1997;37:413–420.
158. Uyama S, Kaufmann PM, Kneser U, Fiegel HC, Pollok JM, Kluth D, Vacanti JP, Rogiers X: Hepatocyte transplantation using biodegradable matrices in ascorbic acid-deficient rats: Comparison with heterotopically transplanted liver grafts. *Transplantation* 2001;71:1226–1231.
159. Uyama S, Kaufmann PM, Takeda T, Vacanti JP: Delivery of whole liver-equivalent hepatocyte mass using polymer devices and hepatotrophic stimulation. *Transplantation* 1993;55:932–935.
160. Mooney DJ, Kaufmann PM, Sano K, Schwendeman SP, Majahod K, Schloo B, Vacanti JP, Langer R: Localized delivery of epidermal growth factor improves the survival of transplanted hepatocytes. *Biotechnol Bioeng* 1996;50:422–429.
161. Fiegel HC, Kneser U, Kluth D, Metzger R, Till H, Rolle U: Development of hepatic tissue engineering. *Pediatr Surg Int* 2009;25:667–673.
162. Fiegel HC, Prymachuk G, Rath S, Bleiziffer O, Beier JP, Bruns H, Kluth D, Metzger R, Horch RE, Till H, Kneser U: Foetal hepatocyte transplantation in a vascularized AV-loop transplantation model in the rat. *J Cell Mol Med* 2008;14:267–274.
163. Kaufmann PM, Kneser U, Fiegel HC, Pollok JM, Kluth D, Izbicki JR, Herbst H, Rogiers X: Is there an optimal concentration of cotransplanted islets of langerhans for stimulation of hepatocytes in three dimensional matrices? *Transplantation* 1999;68:272–279.
164. Keywords “Hepatocyte Matrix Implant”: [Clinicaltrials.Org. http://clinicaltrials.gov/](http://clinicaltrials.gov/), retrieved in March 2010.

Devang Odedra, Loraine Chiu, Lewis Reis, Fiona Rask, Katherine Chiang,
and Milica Radisic

Contents

15.1	Introduction	422
15.2	Cardiac Tissue Overview and Requirements for Successful Tissue Engineering	423
15.2.1	The Healthy Myocardium	423
15.2.2	Myocardial Infarction and Heart Failure	424
15.2.3	Current Clinical Treatment Methods	425
15.2.4	Emerging Treatment Options	425
15.2.5	The Requirements for Successful Myocardial Regeneration	426
15.3	Review of Previous Work	427
15.3.1	Cell Injection	427
15.3.2	In Vitro Cardiac Tissue Engineering	434
15.4	Future Directions	443
15.5	Summary	447
	References	448

Abstract This book chapter will explore the area of cardiac tissue engineering and biomaterials used for cardiac cell therapy. After describing the pathology of heart disease and presenting the motivation for pursuing tissue engineering for the heart, the chapter outlines some of the current clinical treatments used to correct the loss of function resulting from heart disease. Current collection of studies is then divided broadly into two sections: cell injection and engineered heart patches. Chemical modifications and biomolecule incorporation are examined for the cell injection studies. Types of scaffolds as well as cultivation techniques are discussed for the engineered heart patches. Finally, future directions in the field including finding a suitable cell source and increasing the vascularization of the patches are suggested.

Keywords Angiogenesis • Cardiomyocyte • Cell therapy • Heart • Heart failure • Hydrogel • Myocardial infarction • Regenerative medicine • Scaffold

M. Radisic (✉)

Institute of Biomaterials and Biomedical Engineering, University of Toronto, 164 College Street, Room 407, Toronto, ON, Canada M5S 3G9
e-mail: m.radisic@utoronto.ca

15.1 Introduction

Tissue engineering is a non-traditional field, born out of the crossing between life sciences, medicine, materials sciences and engineering. Y. C. Fung, a pioneer in biomechanics and bioengineering, first coined the term “tissue engineering” in 1985 [1]. The term was later officially introduced at a bioengineering panel meeting held by the National Science Foundation at Washington, DC in 1987 [2]. Later in 1988, the world of research saw the first scientific meeting devoted to tissue engineering, where the official definition of the term was unveiled: “the application of the principles and methods of engineering and the life sciences toward the fundamental understanding of structure/function relationships in normal and pathological mammalian tissues and the development of biological substitutes to restore, maintain, or improve functions” [2].

This definition outlines the variety of topics that a tissue engineer is involved in. A tissue engineer begins by first understanding the relationship between structure and function of cells, tissues and organs. The engineer then utilizes this understanding to develop biological substitutes that aid in remodeling. In this process, the tissue engineer needs to cycle through several roles that include a biologist, a material scientist, an engineer and a surgeon [3]. As a biologist, the tissue engineer must be familiar with the key molecular, chemical and cellular events that lead to tissue and organ formation. As a material scientist, the tissue engineer must study the native material properties of tissues and then design tissue substitutes to match these properties. As an engineer, the tissue engineer must develop systems to cultivate tissues in the laboratory and formulate models to predict the properties of tissues (e.g. mechanical properties) as a function of variables such as time. As a surgeon, the tissue engineer must study the interaction of the engineered tissue, once it is implanted into the body, with the surroundings and design strategies to minimize the immune response as well as maximize the integration of the tissue within the host tissue [4].

Interestingly enough, there are reports that suggest that tissue engineering was practiced even before the term was coined [5]. In 1858, Virchow’s suggestion that regeneration of tissues occurs through cell proliferation lead various researchers to focus on growing cells *in vitro*. Some of these researchers include Thiersch, who grew skin cells into granulating wounds in 1874 and Loeb, who was the first to report the growth of cells outside of human body in 1897. Later in 1916, Rous and Jones were able to separate cells through degradation of extracellular matrix proteins by trypsin. These studies steered the focus of the researchers towards expanding tissue-specific cells *in vitro*.

At a tissue engineering workshop held in 1988 at Tahoe City, there were reports of experimental work on the *in vitro* culture of T4 lymphocytes for cancer therapy, as well as indications of early clinical applications such as the use of cultured endothelial cell sheets in burn therapy [1]. Thirty-one papers were presented at the workshop, spanning the areas of vascular prostheses, infection caused by biomaterials, skin and connective tissues, and functional tissue transplant [1].

Since then, the field of tissue engineering has witnessed an exponential growth to finally arrive at its current booming stage, where it includes studies ranging from designing

artificial skin grafts to engineering functional heart tissues, which is the topic of this book chapter.

The classical tissue engineering approach involves incorporating living cells and biomolecules into a scaffold, which is then cultured in a bioreactor. This cultivation allows the engineered tissues to reach some degree of functionality in preparation for the implantation. The bioreactor cultivation step is often omitted in cases where immediate functionality is not required. Ideally, the cells proliferate within the scaffold, establish functional connections to one another and secrete extracellular matrix and necessary growth factors, finally leading to the development of a whole-tissue. Once this engineered tissue is implanted into the body, the scaffold further supports cell proliferation, survival and facilitates the infiltration of host vessels and cells while undergoing controlled degradation. The end result is that the scaffold fully biodegrades, leaving the originally implanted cells, fully integrated with the host architecture and restoring the lost function.

Today, a key challenge in tissue engineering is to grow thick tissues in laboratory in the absence of complex vasculature network that is available to cells in the body [6–8]. The lack of capillary network to provide blood supply limits the thickness of engineered tissues to 100–200 μm as cells do not receive adequate levels of nutrients, oxygen and waste removal [9, 10]. Furthermore, tissue engineering experiences many hurdles on the way such as cost, government regulations, ethics and acceptance by the general population [4]. The ultimate goal of tissue engineering is to augment or replace part of or entire organs such as bone, cartilage, liver, pancreas, heart and kidney. This will, in turn, lead to a decrease in the shortage of organ availability. As an added benefit, tissue engineering will provide models based on human body that can be effectively used to study and design new drugs [4].

15.2

Cardiac Tissue Overview and Requirements for Successful Tissue Engineering

In this book chapter, we will provide an overview of cardiac tissue engineering [11] with a specific focus on biomaterial scaffolds and hydrogels for cardiac tissue engineering. A variety of tissue engineering approaches that can be utilized to achieve the same goal, namely a beating piece of myocardium, will be described.

15.2.1

The Healthy Myocardium

The myocardium (cardiac muscle) is a highly differentiated tissue, ~ 1 cm thick in humans. It is composed of cardiac myocytes (CM), fibroblasts (FB), endothelial cells (EC) and smooth muscle cells (SMC). CMs comprise only 20–40% of the total cells in the heart but they occupy 80–90% of the heart volume [12]. The average cell density in the native rat myocardium is on the order of 5×10^8 cells/cm³ [13]. Morphologically, intact cardiac myocytes have an elongated, rod shaped appearance. Contractile apparatus of cardiac

myocytes consists of sarcomeres arranged in parallel myofibrils [14]. The cells are supported by a dense vasculature and an extracellular matrix that is rich in collagen and laminin. Electrical signals propagate through a three-dimensional syncytium formed by cardiomyocytes. Rapid impulse propagation is enabled by specialized junctions between cells, gap junctions, which are composed of different forms of connexin protein. The most abundant protein in ventricular cardiomyocytes is connexin-43. Groups of specialized cardiac myocytes (pace makers), fastest of which are located in the sinoatrial node, drive periodic contractions of the heart. Majority of the cardiomyocytes in the myocardium are non-pace maker cells and they respond to the electrical stimuli generated by pace maker cells. Excitation of each cardiac myocyte causes an increase in the amount of cytoplasmic calcium, which triggers mechanical contraction. The result is an electrical excitation leading to a coordinated mechanical contraction to pump the blood forward.

15.2.2

Myocardial Infarction and Heart Failure

Heart disease remains a leading cause of death among the population in North America, where myocardial infarctions (MI) are estimated to affect approximately eight million people [15]. MIs occur when there is a reduced blood supply to the heart, most commonly due to coronary artery blockage. These infarctions cause CM necrosis followed by edema and inflammation at the site of the infarct. Scar formation occurs during the following weeks and months with the proliferation of fibroblasts and deposition of collagen. During this period, biochemical and physical factors affect the myocardium and result in the remodeling of the ventricles, which adversely affects their function [16].

Remodeling activities include infarct expansion and ventricular dilation and expansion. Infarct expansion occurs early in the process, before the formation and stabilization of the scar, and results in the thinning and elongation of the non-contractile infarct. This process is attributed to the degradation of the collagen matrix as well as the activation of matrix metalloproteinases [16]. The ejection fraction of a patient, which is the fraction of total blood in the ventricle that can be pumped out in a heartbeat, is decreased in a manner that is proportional to the size and severity of the infarct. In order to compensate for this, the left ventricle (LV) expands to maintain the stroke volume, which is the volume of blood that a ventricle can pump out in a heartbeat [17]. This process increases wall stresses of the ventricle and can lead to ventricle enlargement. LV dilation can also be further affected by the biochemical stimuli of hypertrophic myocytes, which are present during the remodeling process [16]. Overall, the dilation of the ventricle has been shown to directly decrease patients' survival and may ultimately lead to congestive heart failure. The extent of remodeling is affected by the size of the infarct, how much the infarct heals and ventricular wall stresses.

There are currently no methods that can completely prevent these pathological events, however research is currently under way on the approaches that can stabilize the scar faster, reduce the expansion of the infarct, and decrease ventricular wall stresses that lead to further remodeling events. Treatments that limit the remodeling that occurs post infarction will improve the survival and quality of life of MI patients [18].

15.2.3

Current Clinical Treatment Methods

Routine clinical treatments attempt to prevent the pathological remodeling that occurs post infarction. These methods include both pharmacological methods that aim to inhibit remodeling pathways, as well as targeting the cause of MI, which is usually a blocked or partially blocked artery.

Reperfusion is a commonly used method that allows the flow of blood, and thus oxygen, back to the ischemic infarct. Several methods of reperfusion are used and these include thrombolysis, where a blood clot is broken down, and angioplasty, which widens a blocked blood vessel, among others. These methods have demonstrated beneficial effects including partially healing of the infarcted myocardium and limiting of LV remodeling [16, 19, 20].

In a study by Baks et al. patients treated with reperfusion within 6 h after acute MI were shown to have an infarct size reduced by 31% over the year, and they were also observed to have an increased ventricular wall thickness [21]. Although this method has shown significant improvements, the mechanism by which reperfusion benefits the myocardium is not fully understood. In addition, there are some injuries associated with reperfusion. It can cause a buildup of free oxygen radicals, calcium overloading of the cells, endothelial and microvascular dysfunction, as well as altered myocardial metabolism. These can all lead to irreversible cell damage or necrosis, and can have severe detrimental effects on patients [22].

There are also various pharmacological methods used to treat MI patients. Most of the drugs currently used clinically show only limited improvements on MI patients and many are under question as to the safety of the drug when used in the long term. The drugs nitroglycerin, diltiazem and verapamil contain organic nitrates and are vasodilators that restore blood flow to the site of infarction [23]. These drugs have been shown to have beneficial effects in the short term and mixed effects in the long term, with some concern that they may actually be harmful if used for over 24 h [16, 24]. Another drug, captopril, aims at inhibiting the growth factor angiotensin II, which has numerous negative effects on the myocardium, including CM hypertrophy. This drug contains inhibitors for enzymes that convert benign angiotensin I to harmful angiotensin II and studies have differing conclusions about the effectiveness of this drug [16, 25, 26].

None of the clinical methods currently used are effective at fully preventing infarct expansion and other remodeling processes. Patients affected by MI have no options for treatments that bring them back to full health, and thus the need for more effective clinical treatments is apparent.

15.2.4

Emerging Treatment Options

There are currently a variety of ideas for methods to attenuate the effects of MI, many of which are still in the preclinical stage. These methods include using cytokines to attract resident stem cells to the infarct [27], using insulin-like growth factors to protect native CMs, and inducing the differentiation of resident cardiac progenitors into CMs [28], among others. Another treatment approach that has undergone both preclinical and clinical trials is

cell injection. It has been shown that the delivery of various types of healthy cells to sites of infarction can improve the function of the heart and prevent further degeneration. The exact mechanism of improvement is still under debate but some researchers suggest that the transplantation of healthy cells results in the release of growth factors and other molecular signals. These help with angiogenesis, cell survival and with recruiting progenitors.

In general emerging approaches can be broadly divided into cell transplantation [29–31] and implantation of tissue engineered heart grafts, which are yet to be fully tested in clinical trials. The main distinction, as presented in this book chapter is that cell injection included application or recruitment of reparative cells to the site of injury, while in tissue engineering the cells are pre-organized into a functional tissue (i.e. one capable of contracting and propagating electrical signals). We believe that both approaches are viable treatment options, and that the choice of the appropriate regeneration strategy depends on factors such as time post-infarction and size of the affected area. Application of cells into the diseased tissue shortly after MI has the potential to minimize the formation of scar tissue and attenuate the pathological remodeling process. Tissue engineered cardiac patches may be more useful in later stages for the complete replacement of non-contractile areas. Tissue engineering may also provide living patches for repair of congenital malformations [29]. Both approaches will be presented in this book chapter, focusing on the properties of biomaterials utilized in those approaches.

15.2.5

The Requirements for Successful Myocardial Regeneration

In order to provide a functional cardiac patch, we must accurately mimic the structure of the native myocardium over several different length scales. At the centimeter scale, tissue engineering should yield a mechanically stable construct of clinically relevant thickness (~1 cm). This requirement is hampered by the diffusional limitations of oxygen supply encountered in most tissue culture vessels, coupled with the high metabolic demand of cardiomyocytes for oxygen (27.6 nmol/min/mg protein [32]). At the mm scale, the tissue should consist of elongated myofibers aligned in parallel, of the orientation angle that is changing along the thickness of the ventricle. At the mm scale, the tissue should also consist of high cell density (~ 10^8 cells/cm³) supported by the rich vasculature with intercapillary distance of ~20 μ m. At the nm scale, cells in the engineered cardiac tissue must be coupled by functional gap junctions and capable of electrical impulse propagation (e.g. 27 cm/s for a rat ventricle [33]) in order to prevent arrhythmia upon implantation. Finally, at the sub-cellular level (nm), the excitation-contraction machinery of individual cardiomyocytes must be functional.

Additionally, for true myocardial regeneration, both the vasculature and the beating cardiomyocytes need to be restored in the infarct zone. While neovascularization can be achieved by injection of various stem cells (e.g. from bone marrow), an autologous source of large numbers of cardiomyocytes currently cannot be obtained from sources such as bone marrow. Cardiomyocytes, in significant quantities (millions-a billion), can reliably be obtained from embryonic stem cells (ESC) or induced pluripotent stem cells (iPS).

15.3

Review of Previous Work

15.3.1

Cell Injection

15.3.1.1

Brief Overview of Cell Injection Studies

We provide here a brief overview of pre-clinical and clinical cell injection studies and for more information, we invite the reader to consult reviews devoted to this topic [30, 34–37]. The purpose of this section is to define limitations in cell injection procedures and motivate the use of biomaterials in enhancing the efficacy of the cell injection.

The first evidence that cell injection may be a viable therapeutic approach for MI came from the animal studies with injection of fetal or neonatal CMs. CM injection improved left ventricular function and ventricle thickness, thus attenuating pathological remodeling upon MI [38–41]. Injected CMs were demonstrated to integrate through gap junctions and intercalated discs with the host CMs [42]. Yet the enthusiasm generated by these studies was hampered when massive death of injected myocytes was demonstrated [43, 44]. In the search for a clinically relevant cell source, regeneration of MI in animal models was attempted by transplantation of skeletal myoblasts [45], ESC derived CMs [46–48], bone marrow derived mesenchymal stem cells (MSC) [49, 50] and hematopoietic stem (HS) cells [51–53] (reviewed in [30, 34]). Of these, only skeletal myoblasts and bone marrow mononuclear cells (BMMC, consisting of both HS and MSC) were pursued further in clinical trials. However, mature skeletal myoblasts do not express gap junction proteins, thus they are incapable of functionally integrating with the host myocardium. As a result, in the Phase I clinical trial of autologous skeletal myoblast transplantation arrhythmias occurred in four out of ten patients [54, 55]. The initial clinical studies with BMMC (reviewed in [31, 34]) indicated that BMMC transplantation was safe and that in some cases it contributed to the increase in left ventricular ejection fraction (LVEF) [56–58]. Recent meta-analysis demonstrated a significant, albeit low 3%, increase in LVEF as well as a significant reduction in infarct size (–5.6%) and end systolic volume (–7.4 ml) in patients treated by intracoronary cell injection after acute MI. Dose-response between injected cell volume and LVEF change was reported [59]. Although these studies are encouraging, modest improvements motivate investigation of new cell sources and new methods that increase survival and retention of injected cells. Most recently, a Phase I trial was initiated with the treatment of an acute MI patient using adult cardiac stem cells derived from his own cardiac biopsies (Marban et al, Cedars-Sinai Medical Center, newsbrief, July 01, 2009).

Several different routes of cell injection were utilized in the clinical studies described above. In patients with severe left ventricular dysfunction caused by MI and large non-viable hypokinetic/dyskinetic scars, skeletal myoblasts were injected into multiple sites across the scarred segments during standard coronary artery bypass grafting (CABG) [55]. CABG is an invasive procedure involving an open heart surgery. Cell injection in patients

with acute MI required a less invasive, non-surgical approach. In clinical trials, BMNC were injected in the left ventricle wall transendocardially via a NOGA-guided intraventricular catheter [58], or they were delivered into circulation by an intracoronary catheter with balloon occluder [56].

In most studies described above, the cells for myocardial regeneration were suspended in saline or culture medium followed by intramyocardial or coronary injection. The main challenges associated with that procedure were poor survival of the injected cells [43] and washout from the injection site [60]. According to some estimates, 90% of cells delivered through a needle leaked out of the injection site [38, 43]. In addition, a significant number of cells (~90%) died within days after injection [43, 44]. Thus developing improved delivery and localization methods (e.g. hydrogels) and effective anti-death strategies could significantly improve effectiveness of cell injection.

15.3.1.2

Injectable Biomaterials for Treatment of Myocardial Infarction

Over past 5 years, hydrogels have gained a significant attention as vehicles for delivery of reparative cells into the myocardium, due to their injectability and ability to control cross-linking chemistry. General requirements for a hydrogel to be used in myocardial regeneration are: (1) biocompatible, (2) biodegradable, (3) injectable, so that it can be applied with a syringe in a minimally invasive manner and (4) mechanically stable enough to withstand the beating environment of the heart. In addition, a biomaterial that can promote the attachment and survival of cells, and localize them at the infarction site, would address the current limitations of poor cell retention and survival.

Early studies relied on cell injection using natural hydrogels such as Matrigel [53, 61] or fibrin [62–64] reporting structural stabilization, reduced infarct size and improved vascularization upon injection of undifferentiated ESC [53, 61] or bone marrow cells [62–64]. Alginate alone was demonstrated to reduce pathological remodeling and improve function [65], initiating commercialization efforts of this hydrogel. A synthetic material, self-assembling peptide hydrogel (AcN-RARADADARARADADA-CNH) was also used, forming a nano-fibrous structure upon injection into the myocardium that promoted recruitment of endogenous ECs and supported survival of injected CMs [66]. Insulin-like growth factor-1 (IGF) bound to the self-assembling peptide was demonstrated to improve grafting and survival of CMs injected into MI [67]. Laflamme and Murry demonstrated that targeting of multiple pathways related to cell survival by encapsulating a number of biomolecules in Matrigel, significantly increased the survival and grafting of the human ESC-derived CM injected into infarcted rat hearts [68].

15.3.1.3

Natural and Synthetic Hydrogels of Relevance to Myocardial Cell Injection

Hydrogels are formed from a crosslinked network of hydrophilic polymers and are termed “hydrogels” since they have high water content. Despite this high affinity for water,

hydrogels maintain definite 3D structures that do not dissolve, due to their physical and chemical crosslinks [69]. Hydrogels have received a significant attention for tissue engineering applications due to this high water content and their biocompatibility [70]. The main types relevant for myocardial injection include those made from natural polymers, synthetic polymers as well as biomimetic hydrogels, i.e. synthetic polymers that contain biological activity [71].

Natural hydrogels are derived from natural sources and include proteins, and polysaccharides. The main advantages of these materials are that they have very low toxicity and high biocompatibility due to their natural origins [70]. The disadvantages of these materials are that their mechanical properties are generally not easy to tailor and xenogenic immune responses may also have to be considered.

Collagen and fibronectin are proteins found in the mammalian extracellular matrix (ECM) and they can form weak hydrogels, thus they are often used in cell culture. As both of these materials are natural proteins, they have amino acid domains that are recognized by the integrin receptors on the cells, which provides an advantage for cell attachment and survival within these hydrogels. Due to the weak nature of these hydrogels, modifications have to be made to increase the degree of their crosslinking [71]. Other disadvantages include their rapid degradation and large batch-to-batch variability, which affects their immunogenicity [72]. Gelatin is another natural polymer that has been investigated in the place of collagen. It is composed mostly of denatured collagen and thus retains its benefits with more stable mechanical properties. The main drawback is that it also has a variable composition [72]. Matrigel is a mixture of membrane proteins secreted by mouse tumor cells. It has also been investigated as an injectable hydrogel due to its ability to enhance cell adhesion and support cell growth. There are however issues related to its immunogenicity, safety in vivo and weak mechanical properties [72].

Alginate is a polysaccharide derived from brown seaweed that forms reversible ionic crosslinks in the presence of divalent cations such as calcium [71] to form a weak gel [63]. Hyaluronic acid (HA) is a glycosaminoglycan that is prevalent throughout the body. HA is associated with natural wound healing processes and retains this biological activity as a hydrogel [73]. A drawback is that this material requires various modifications in order to be able to crosslink into a hydrogel. Chitosan is a natural hydrogel derived from chitin, the most abundant organic molecule and main component in the exoskeletons of crustaceans, mollusks and insects. Chitosan is a linear polysaccharide that is obtained by de-acetylating chitin. The polysaccharide contains D-glucosamine units and N-acetyl-D-glucosamine groups linked by $\beta(1-4)$ glycosidic bonds [74]. The content of D-glucosamine determines the degree of deacetylation, which decreases the amount of N-acetyl-D-glucosamine units present. The degree of deacetylation can range from 30 to 90% and the molecular weight of chitosan ranges from 300 to over 1,000 kDa. The crystalline form of chitosan is soluble in dilute acids with pHs below 6, but becomes insoluble at pHs over 7. At lower pHs the amino groups on the glucosamine are protonated which allows for dissolution to occur. In general, chitosan can form a hydrogel in dilute acids due to the hydrogen bonds that are created between the polysaccharide chains [75]. In general, covalent modification of polysaccharides with bioactive peptides or proteins is required to support the attachment and phenotype of cardiovascular cells [76].

Specifically, we have modified chitosan with the peptide QHREDGS derived from angiopoietin-1, the peptide sequence implicated in the survival response of muscle cells cultivated in the presence of this growth factor [77]. The chitosan was rendered photo-crosslinkable by modification with azidiobenzoic acid (Az-chitosan) [78]. Neonatal rat heart cells cultivated on crosslinked films of Az-chitosan-QHREDGS attached, elongated and remained viable while they exhibited lower attachment levels and decrease in viability when cultivated on the chitosan substrates modified with the scrambled peptide sequence [79]. Interestingly, cells on Az-chitosan-QHREDGS were capable of resisting taxol induced apoptosis, while those on Az-chitosan-RGDS were not [79].

Synthetic hydrogels have the advantage of precisely defined compositions and mechanical properties that are generally easier to tailor. The major drawback coming with very diverse chemistries and compositions is that biodegradation products may be cytotoxic, depending on a specific hydrogel. The most commonly used synthetic hydrogel is polyethylene glycol (PEG). This material is nontoxic, non-immunogenic and has the added advantage of a US Food and Drug Administration approval. Modifications can be made in the block copolymer formations to make it degradable, and the rate of this can be tailored [70]. Synthetic hydrogels can be blended or covalently modified with natural materials such as proteins and peptides to incorporate bioactivity, and these gels are termed biomimetic hydrogels [71].

In general, the cells are first suspended in a liquid solution of the hydrogel to encapsulate them. An initiator or an initiating environment is then used to create crosslinks within the material to induce gelation. Therefore, the crosslinking conditions must be mild and reaction by-products non-cytotoxic in order to maintain cell viability. Commonly used crosslinking mechanisms in hydrogels used for cell encapsulation include radical chain polymerization and chemical crosslinking, which can be induced by thermal, redox and light exposing environments [71].

15.3.1.4

In Vivo Cardiac Tissue Engineering: Injection of Cells with Hydrogels

Injectable biomaterials give cells a temporary matrix while allowing for their placement to be localized at the sites of infarction with minimally invasive delivery methods. The cells can subsequently develop tissue and integrate with the host tissue *in vivo*. Thus, the injection with hydrogels *in vivo*, for the purpose of tissue regeneration is also referred to as *in vivo* tissue engineering.

The advantage of this method over pre-formed *in vitro* tissue is that the biomaterial can adapt to the structural environment and integrate with the myocardium in a more continuous manner, as it is injected in liquid form and gels *in situ* [61]. The delivery of this material is also less invasive. In addition, as the injectable biomaterial is in solution, pharmacological agents and growth factors can be more easily added [61]. Several *in vivo* studies have been completed using various injectable systems and all of them have shown some positive results for preventing the deterioration of the heart post MI.

In one study, bone marrow mononuclear cells were implanted into a fibrin matrix and then injected into rats subjected to cryoinjury to simulate a MI. The rats were assessed after 8 weeks and were found to have more tissue regeneration when treated with fibrin and cells although this tissue could not be identified as cardiac muscle. The material also degraded in this time frame and did not illicit an inflammatory response. Another positive result was that extensive neovascularization was also observed in the treated rats [64].

Christman et al. injected myoblasts into a commercial fibrin glue and injected this at the site of infarction in rats [63]. After 5 weeks, a significantly greater myoblast density was seen at the infarct site for the cells injected in fibrin glue, which showed that the gel resulted in better cell survival. These treated rats also had smaller infarcts and an increased number of microvessels within the scar.

Undifferentiated mouse embryonic stem cells were combined with Matrigel and injected into infarcted heart [80]. After 4 weeks, the cells survived in the biomaterial and showed some expression of connexin-43 between cells located where the biomaterial bordered the host myocardium. The mice treated with the biomaterial were also found to have better heart function, and thicker lateral and septal walls [80].

Zhang et al. studied the effect of injecting CMs in a mixture of collagen type I and Matrigel [81], the material used by Zimmerman et al. to create engineered heart tissue [82], in MI-induced rats. Positive connexin-43 staining was found in the cells in the biomaterial, and the biomaterial was also seen to improve the thickness and the function of the heart. The main drawback is that the material takes 1 h to gel, which could allow for significant cell loss, although no cell retention studies were conducted in these experiments.

Fetal CMs were suspended in an alginate scaffold, which was injected into rats with induced MIs. After 2 months the animals were studied and those treated with the biomaterial were found to have smaller end diastolic and systolic volumes as well as a smaller area of collagen scar at the site of the infarct [65].

A thermo-responsive chitosan based gel was prepared and injected into the infarcted hearts of rats with and without mouse ESCs, resulting in cell retention and 4 week graft size being significantly higher than PBS + ESC control. In addition, heart function (measured through echocardiography), wall thickness, and micro-vessel density were all higher in chitosan alone and chitosan + ESC groups than PBS + ESC control, with chitosan + ESC showing the greatest improvement 4 weeks after injection [83] (Fig. 15.1a–e).

A self-assembling peptide (RAD 16-II), originally developed by Zhang et al. was injected into the site of infarct in a rat MI model forming easily detectable nanofiber microenvironments that promoted endogenous EC recruitment, as well as (potential) myocyte progenitor recruitment [84] (Fig. 15.1f–g). The nanofiber hydrogel promoted survival and retention of neonatal CMs injected with the self-assembling peptide and even augmented the recruitment of endogenous cells [85].

Binding insulin-like growth factor-1 (IGF-1), a CM growth and differentiation factor, to the self-assembling peptide RAD16-II proved to be anti-apoptotic and increased cell growth in transplanted (injected) CMs and showed sustained, controlled, and targeted release of IGF-1 from the nanofibers for 28 days. Furthermore, improved systolic function was observed when CMs were injected with self-assembling RAD16-II tethered with IGF-1 in a rat MI study [67].

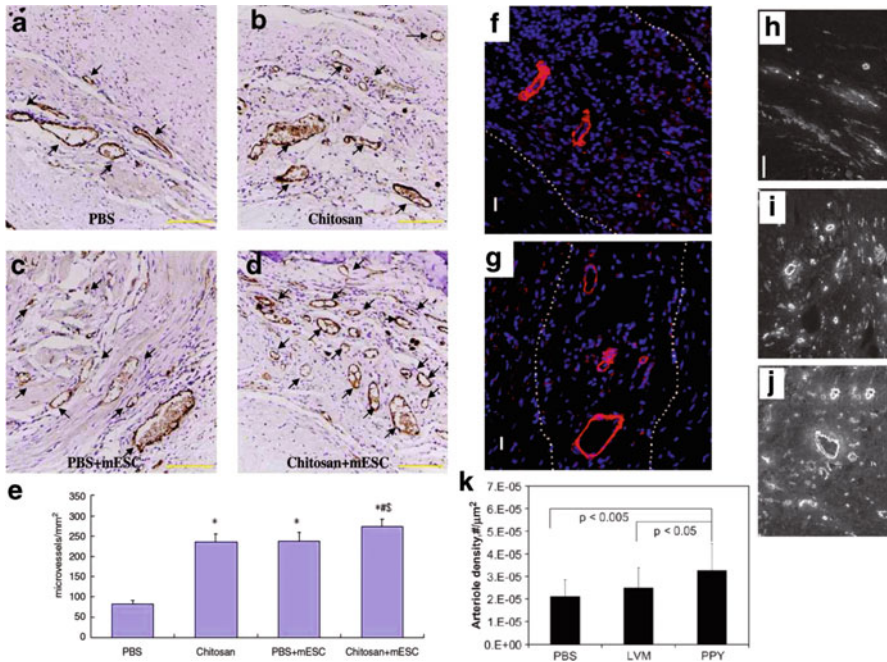


Fig. 15.1 Vasculogenesis in various injectable biomaterials with and without cells. (**a–d**) Microvessel density (*black arrows*) in the myocardial infarction sites 4 weeks after injection. (**a**) The microvessel density is low in phosphate buffered saline (PBS)-only group within the infarct area. (**b**) Chitosan-only injection can improve microvessel density. (**c**) Mouse embryonic stem cells (mESCs) injected in PBS also improved microvessel density. (**d**) mESCs injected in chitosan hydrogel improved microvessel density significantly. (**e**) Graph shows the statistical results (* $p < 0.01$ vs PBS only, # $p < 0.01$ vs. chitosan only, § $p < 0.01$ vs. PBS + mESCs). Scale bar, 100 μm [83]. (**f, g**) Smooth muscle cells populate the peptide microenvironment and form mature, vessel-like structures. (**f**) At 14 days after injection, the cells (blue = DAPI) in the microenvironment stained positively with an α -smooth muscle actin antibody (*red*) and showed features of organization. (**g**) At 28 days after injection, several arteriole-like structures were seen within the micro-environment in all samples. Scale bar, 10 μm [66]. (**h–k**) Increased arteriogenesis and myofibroblast infiltration in the infarct region. Arteriole staining was performed in the infarct area for PBS (**h**), LVM only (**i**), and LVM-PPy (**j**) treatment groups. Magnification is at $\times 10$. The bar represents 100 μm . (**k**) Graph shows means \pm SD for arteriole density [92].

15.3.1.5

Injection of Hydrogels Alone

Recent studies collectively indicate that an injection of hydrogel alone, without the reparative cells, may also attenuate pathological remodeling upon MI [65, 86–88]. For example, injection of alginate or collagen alone improved LV function and reduced cardiac remodeling post infarction [65, 89]. It is suspected that by changing the ventricular geometry and

mechanics, hydrogels reduce the elevated local wall stresses that have been implicated in pathological remodeling [90]. Finite element modeling of wall stresses indicated that upon injection of the material of elastic modulus 10–20 kPa in the infarct, the relationship between ejection fraction and the stroke volume/end-diastolic volume was improved. In addition, injections of the material in the border zone decreased end-systolic fiber stress proportionally to the volume and the stiffness of the injected material.

Ischemic mitral regurgitation (MR) is a common complication of coronary artery disease and relates to the displacement of the papillary muscles from ventricular distortion (post MI) and limits mitral closure due to apical tethering. An acute ischemic MR model was produced in sheep and a specially formulated poly-vinyl alcohol (PVA) polymer was injected into the myocardium under the papillary muscle forming an encapsulated, stable, and resilient gel. Supporting the infarcted myocardium and simultaneously repositioning the papillary muscles (to reduce apical tethering), injection of the PVA gel significantly decreased MR while not adversely affecting left ventricular function and mechanical properties, thereby presenting an alternate strategy for relieving acute ischemic MR vs. traditional surgical methods [91].

Two alginate biopolymers were modified to assess the therapeutic potential in rat MI models. Alginate modified with 0.025% v/v polypyrrole, a conductive polymer, injected into the infarct zone showed improved arteriogenesis at 5 weeks post treatment and significantly enhanced infiltration of myofibroblasts into the infarct area when compared to saline and alginate only controls [92] (Fig. 15.1h–k). Also, RGD conjugated alginate, and alginate alone, injected into the infarct zone showed improved LV function and increased arteriole density 5 weeks post injection when compared to BSA in PBS control [93]. Results from both studies again show the potential for non-cell based therapies to treat chronic heart failure. In addition, many of the above mentioned studies reviewed in Sect. 15.3.1.4 used a control group with just the acellular biomaterial and found that the material was able to produce some of the beneficial effects, but not all of those achieved with the cellular treatment.

We believe that properly tuning mechanical properties of a hydrogel and providing bioactive molecules, may offer new cell-free treatment options of myocardial infarction. The death of CM by necrosis and apoptosis peaks at 6 h upon acute MI [94]. However, the persistent and progressive loss of CM in neighboring areas of the infarct continues up to 60 days after the onset of MI. During this process, up to 35% of cells at the borders of subacute and old infarcts may become apoptotic [95], in comparison to only 1% in the remote regions of myocardium [96]. Studies in rats and dogs demonstrated that CM loss by apoptosis persists for 1–4 months upon MI, correlating with the progressive worsening of the pump function. Thus, developing hydrogels which specifically prevent apoptosis of the heart cells (e.g. QHREDGS peptide modified chitosan) may result in new treatment options in the future, where hydrogel injected alone in the border zone, without the reparative cells, would act to both mechanically stabilize the ventricle and prevent further apoptosis of cardiomyocytes.

For example, it was shown that EC induced CM protection post-infarction occurs through PDGF-BB signaling. Thus, binding PDGF-BB to the self-assembling nanofibers of RAD16-II hydrogel was evaluated as a potential therapeutic option. Sustained, targeted release of this signaling molecule to host myocardium was observed up to 14 days after

15 injection. Injection of nanofibers with PDGF-BB at the site of infarct in rats decreased CM death and preserved systolic function post MI, and showed (separately) a decrease in infarct size after ischemia/reperfusion [97].

Since the studies conducted thus far used different cell sources, hydrogels, animal models, delivery times post-infarction and experimental time frames, a direct comparison between the methods cannot be accurately achieved. While all reported studies have shown some form of improvement, complete myocardial regeneration has not been achieved. Perhaps, a valid question to be answered in the future is: What is the required level of myocardial regeneration in terms of survival and attenuation of symptoms? Complete regeneration is an ambitious goal that may not be required. Future studies must also increase their time frames, to better assess the long-term effects of these treatments.

Relative contribution of cells vs. the injected biomaterial to the attenuation of pathological remodeling also needs to be assessed and the mechanism by which various cells induce functional improvements needs to be elucidated. While with the injection of contractile cardiomyocytes, the expectation is that the cells will functionally couple to the host myocardium and contribute to contractile function, the same is not possible for non-cardiomyocytes. The exact mechanism by which non-myocytes impart the improvement in function and attenuation of pathological remodeling is still under debate but some researchers suggest that the transplantation of healthy cells results in the release of growth factors and other molecular signals, i.e. the paracrine effect. These help with angiogenesis, cell survival and recruitment of progenitors.

15.3.2

In Vitro Cardiac Tissue Engineering

Overall, three different cardiac tissue engineering approaches can be identified: (1) the seeding of cells onto preformed porous or fibrous scaffolds followed by bioreactor cultivation, (2) cultivation of cells encapsulated into hydrogels, and (3) a matrix-free approach that relies on cardiomyocyte self-assembly or stacking of confluent cell sheets. Since the first two approaches rely on the utilization of biomaterials to create a cell instructive microenvironment, they will be covered in more detail in this book chapter.

15.3.2.1

Cardiac Tissue Engineering Based on Biomaterial Scaffolds and Bioreactors

Scaffolds offer the advantage of control over their size, shape and mechanical properties. Scaffold structure alone can be effectively used to guide orientation of cardiomyocytes and yield anisotropic morphology similar to the native myocardium even in the absence of specific physical cues such as electrical or mechanical stimulation.

Porous Scaffolds

Three dimensional cardiac tissue constructs have been successfully cultivated in dishes using a variety of scaffolds amongst which collagen sponges have been widely reported. In the pioneering approach of Li and colleagues, fetal rat ventricular cardiac myocytes were expanded after isolation, inoculated into collagen sponges and cultivated in static dishes for up to 4 weeks [98]. The cells proliferated with time in culture and expressed multiple sarcomeres. Adult human ventricular cells were also used in a similar system, although they exhibited no proliferation [99].

Fetal cardiac cells were cultivated on porous alginate scaffolds in static 96-well plates. The cells formed spontaneously beating aggregates in the scaffold pores after 4 days in culture [100]. Cell seeding densities on the order of 10^8 cells/cm³ were achievable by using centrifugal forces during seeding [101]. Similarly, neonatal rat cardiomyocytes formed spontaneously contracting constructs when inoculated into collagen sponges (Tissue Fleece) within 36 h after seeding [102] and maintained their activity for up to 12 weeks. Furthermore, the contractile force could be increased upon addition of Ca²⁺ and epinephrine.

Fibrous Scaffolds

In a classical tissue engineering approach, fibrous polyglycolic acid (PGA) scaffolds were combined with neonatal rat cardiomyocytes and cultivated in spinner flasks and rotating vessels [103]. Scaffold consisted of non-woven PGA fibers 14 μ m in diameter and the scaffold porosity was high, at 97%. Being FDA-approved for biodegradable sutures, this material has an advantage from a clinical perspective. Neonatal rat or embryonic chick ventricular myocytes were seeded onto PGA scaffolds by placing a dilute cell suspension in the spinner flasks and mixing for three days (50 rpm) [103]. Constructs cultivated in well-mixed flasks exhibited significantly higher cellularity index and metabolic activity compared to the constructs cultivated in static flasks. After 1 week of culture, constructs seeded with neonatal heart cells contained a tissue-like region at the peripheries (50–70 μ m thick), which stained positive for tropomyosin and contained cells organized in multiple 3-D layers [104]. Electrophysiological studies conducted using a linear array of extracellular electrodes showed that the peripheral layer of the construct exhibited relatively homogeneous electrical properties and sustained macroscopically continuous impulse propagation on a centimeter-size scale [104]. Constructs containing cardiomyocytes that were enriched by preplating exhibited lower excitation threshold (ET), higher conduction velocity, higher maximum capture rate (MCR), and higher maximum and average amplitude of contraction.

PGA constructs cultivated in rotating bioreactors showed improved behavior, which can be attributed to the laminar flow conditions. The cells in the peripheral layer expressed tropomyosin and had spatial distribution of connexin-43 comparable to the neonatal rat ventricle. However, the expression levels of cardiac proteins connexin-43, creatine kinase-MM and sarcomeric myosin heavy chain were lower in rotating bioreactors cultivated constructs compared to the neonatal rat ventricle but higher than in the spinner flask

cultivated constructs [105]. It is important to note that the center of the constructs remained mainly acellular in both spinner flasks and rotating bioreactors due to diffusion limitations in oxygen and nutrient transport.

In the past 5 years, electrospun scaffolds have gained significant attention because of their attractive ability to control cell structure at sub-micron levels as well as offer control over mechanical properties, both of which are important for cell attachment and contractile function. Entcheva and colleagues synthesized oriented biodegradable non-woven poly(lactide) (PLA) scaffolds using electrospinning [106]. Neonatal rat cardiomyocytes were cultivated on these PLA matrices and exhibited remarkably well-developed contractile apparatus and electrical activity. Rockwood et al. grew primary cardiac ventricular cells on electrospun polyurethane scaffolds with either aligned or unaligned microfibers (Fig. 15.2a). After 2 weeks of culture, the cells were observed to organize according to the aligned fibres (Fig. 15.2b). In addition, the atrial natriuretic peptide (ANP) content of cultures grown on electrospun scaffolds was lower than cells grown on tissue culture flask, indicative of a more mature phenotype in these cells. The ANP content of cultures

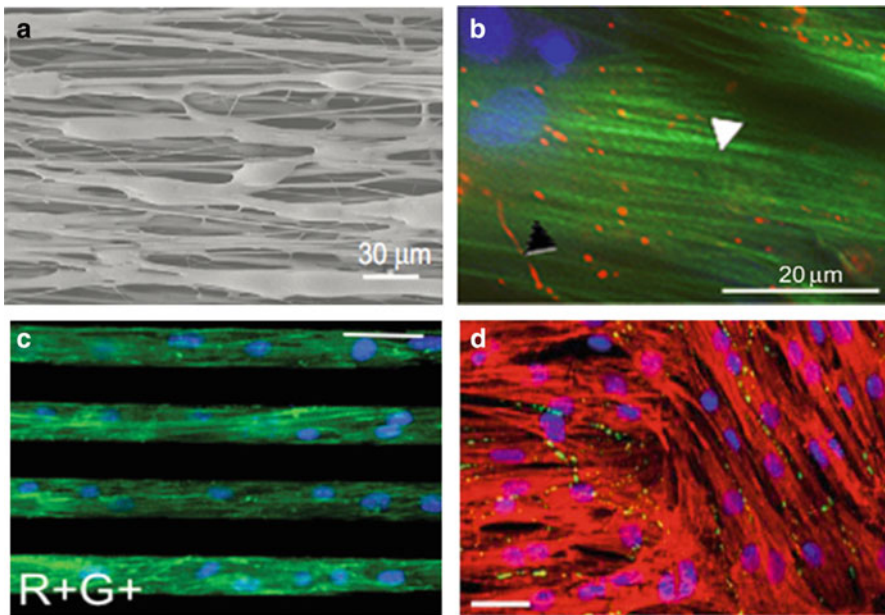


Fig. 15.2 Scaffolds for cardiac tissue engineering. (a) Electrospun polyurethane fibers synthesized by Rockwood et al. [107]. (b) Cardiomyocytes align to the fibres in (a). Connexin-43 gap junction have been stained as green [107]. (c) Cardiac progenitors derived from the red-positive and green-positive (R+G+) regions of the heart by Domian et al. are grown on fibronectin-patterned surfaces. R+G+ cells give rise to the maximum number of cardiomyocytes (labeled green with sarcomeric α -actinin), rather than differentiating into other types of cells such as smooth muscle cells (labeled red with smooth muscle myosin heavy chain). Blue indicates cell nuclei. Scale bar, 40 μ m [114]. (d) Aligned, cross-striated cardiomyocytes grown on the DTMRI/soft-lithography patterned fibronectin surfaces by Badie et al. Scale bar, 50 μ m. Red represents sarcomeric α -actinin, green represents connexin-43 and blue represents cell nuclei [116].

grown on aligned fibres was even lower than those grown on unaligned fibres. Hence, aligned fibres were able to induce cell alignment, as well as, shift their phenotype to a more mature stage [107].

In order to better understand the effect of scaffold properties on cell morphology, Fromstein et al. seeded embryonic stem cell-derived cardiomyocytes on collagen IV-coated scaffolds generated using two different techniques: thermally induced phase separation (TIPS) and electrospinning. Scaffolds generated with TIPS were thicker (1 mm) and exhibited a larger pore size (~20 μm). Scaffolds generated by electrospinning were thinner (~70 μm) and contained smaller pores (~5 μm). TIPS scaffolds promoted a rounded morphology for the seeded cardiomyocytes, whereas electrospun scaffolds demonstrated an elongated morphology. Despite the observed differences in the morphology, the cells on both scaffolds stained positively for cardiac markers (sarcomeric myosin heavy chain) and gap junctions (connexin-43), and were able to contract [108].

Thin Films and Microfabrication Approaches

A significant step towards a clinically useful cardiac patch was the cultivation of ES cell derived cardiomyocytes on thin polyurethane films. Cells exhibited cardiac markers (actinin) and were capable of synchronous macroscopic contractions [109]. The orientation and cell phenotype could further be improved by microcontact printing of extracellular matrix components (e.g. laminin) as demonstrated for neonatal rat cardiomyocytes cultivated on thin polyurethane and PLA films [110, 111].

We have used microfluidic patterning of hyaluronic acid on glass substrates to create thin (10–15 μm diameter) several millimeter long cardiac organoids that exhibited spontaneous contractions and stained positive for troponin I, a cardiac marker [112].

Freed and colleagues created an accordion-like scaffold using laser boring of 250 μm thick poly(glycerol sebacate) layer [113]. The accordion-like honeycomb was designed by overlapping two 200 by 200 μm squares at the angle of 45°. The pore-walls and struts were ~50 μm thick. The scaffolds were pretreated with cardiac fibroblasts followed by seeding of enriched cardiomyocytes. During pre-treatment, rotating culture was used, while static culture was used upon cardiomyocyte seeding. At the end of cultivation, the authors obtained contractile cardiac grafts with mechanical properties closely resembling those of the native rat right ventricle. In addition, the cells in the pores were aligned along the preferred direction.

In a recent study, Domian et al. identified distinct transcriptional signatures, including the expression of unique subsets of miRNAs, specific for the first and second heart fields in mouse embryos as well as embryonic stem cells. The mammalian heart is composed of a diversified set of muscle and nonmuscle cells that are differentiated from the progenitor cells in either first or second heart fields, or a combination of the two. Using the fluorescence profiles of progenitor cells governed by the expression of *Isl1*-dependent enhancer of the *Mef2c* gene or cardiac-specific *Nkx2.5* enhancer, the authors were able to isolate cells that had the maximum potential for differentiation into cardiomyocytes. These cells were able to align on micropatterned surfaces and were subsequently used to engineer beating muscular thin films *in vitro* that could be paced by field stimulation at 0.5 and 1 Hz [114] (Fig. 15.2c).

In another study, Feinberg et al. seeded a layer of neonatal rat ventricular cardiomyocytes on a polydimethylsiloxane membrane that could be detached from a thermo-sensitive poly (Isopropylacrylamide) layer at room-temperature. Called Muscular Thin Films, these cell-covered sheets could be designed to perform tasks such as gripping, pumping, walking and swimming by careful tailoring of the tissue architecture, thin-film shape and electrical-pacing protocol [115].

Badie et al. investigated yet another method to generate microstructure of heart tissue in vitro. The two-step method first involves imaging the heart using diffusion tensor magnetic resonance imaging (DTMRI). From the 3-D reconstructed image, a specific 2-D plane is chosen and the cardiac fibre directions on this plane are converted into soft-lithography photomasks, and later into fibronectin-coated polydimethylsiloxane sheets. Fibronectin patterns consisted of a matrix of $190 \mu\text{m}^2$ subregions, each comprised of parallel lines 11–20 μm -wide, spaced 2–8.5 μm apart and angled to match local DTMRI-measured fibre directions. By adjusting fibronectin line widths and spacing, cell elongation, gap junctional membrane distribution, and local cellular disarray were altered without affecting the cell direction (Fig. 15.2d). This approach enables the systematic studies of intramural structure-function relationships in both healthy and structurally remodelled hearts [116, 117].

Decellularized Native ECM Based Scaffolds

In a pioneering study, Taylor and colleagues utilized the ECM of the native rat heart as a scaffold for cardiac tissue engineering [118]. This approach enabled them to preserve the underlying geometry and create an ideal natural template for tissue engineering of the heart. The authors decellularized adult (12 weeks old) cadaveric Fisher rat hearts by coronary perfusion with detergents. In addition to ECM, the vasculature was also preserved and it was perfusable. The structure of the ventricles, atria, and heart valves were all preserved. Cardiomyocytes were then isolated from the neonatal rats and reseeded onto the structure. Vascular perfusion with the oxygenated media was provided via the peristaltic pump. In a subgroup of samples, rat aortic endothelial cells were injected into the patent aorta, in order to recellularize the vasculature. Macroscopic contractions were observed by day 4 of cultivation, while pump function of about 2.4 mmHg was generated at day 8 under electrical stimulation.

Badylak et al. implanted ECM derived from porcine urinary bladder into surgically created 2 cm^2 defect in the left ventricular free wall of dogs. Eight weeks following the implantation, the ECM patches showed higher regional systolic contraction compared to the control group where a material currently used for myocardial defects, Dacron, was implanted into the defects. Histological analysis suggested that cardiomyocytes accounted for about 30% of the remodeled tissue in the ECM scaffolds [119]. In a recent study, it was found that this improvement in the heart function can be attributed to an increase in the myocyte content in the ECM patches between week 2 and 8. The relationship between the myocyte content and the extent of mechanical function was observed to be linear. There was also some evidence (decrease in cardiomyocyte diameter and increase in the overall area occupied by cardiomyocytes over time) that suggested a possibility of cardiomyocyte proliferation in the patches [120].

Cultivation Systems

Perfusion: While the human ventricle is ~1–1.5 cm thick, viable grafts cultivated in dishes, spinner flasks and rotating vessels [103] are limited in thickness to ~150 μm due to the inability of diffusion to meet the oxygen demands of highly metabolically active cardiomyocytes at physiologic cell densities [121] (Fig. 15.3a, b). Since cardiac myocytes have a limited ability to proliferate, we developed a technique for seeding cells at high densities while maintaining cell viability [121]. Cell inoculation onto collagen sponges with Matrigel™ was immediately followed by medium perfusion with alternating direction of flow. These perfusion bioreactors provided convective-diffusive oxygen transport, thereby allowing cells to maintain aerobic cell metabolism. The constructs developed by this method exhibited high viability, density and spatially uniform distribution of cells, leading to improved contractile performance [121, 122]. Moreover, perfusion acted to remove dead cells from the environment, a task normally carried out by macrophages in healthy tissues in order to prevent secondary apoptosis.

In the native environment, tissues are vascularized by capillary networks ~20 μm apart to provide oxygen from the blood [123] (Fig. 15.3c). Hemoglobin, a natural oxygen carrier, acts to increase the oxygen carrying capacity of blood by 65 times. We used porous collagen and poly(glycerol sebacate) scaffolds in combination with biomimetic cultivation systems to develop functional contractile cardiac patches [9, 124] (Fig. 15.3d, f). In order to mimic the blood flow in native capillary, parallel array channeled scaffolds, pre-seeded with cardiac fibroblasts and inoculated with cardiomyocytes, were perfused with culture medium supplemented with perfluorocarbon (PFC), a synthetic oxygen carrier. Constructs showed more mature cell morphology, higher cell density and viability, and improved contractile properties, indicative of increased electrical coupling. Open channels were present throughout the construct (Fig. 15.3e), and mathematical modeling of the oxygen transport suggested that PFC particles acted as an oxygen reservoir in the culture medium [124] (Fig. 15.3f, g). Kofidis et al. supplied pulsatile flow to cardiomyocytes encapsulated in fibrin glue around a rat artery in vitro [125]. Dvir et al. designed a novel perfusion bioreactor that employs a distributing mesh upstream from the construct to provide homogeneous fluid flow and maximum exposure to perfusing medium [126]. This convective supply of oxygen led to increased cell viability in alginate scaffolds seeded with physiologically relevant cell [126].

Electrical stimulation: Excitation-contraction coupling is critical for development in the native heart. Consequently, it is essential that cells become electromechanically coupled and are capable of synchronously responding to electrical pacing signals [127]. Cardiac constructs prepared by inoculating collagen sponges with neonatal rat ventricular cells were electrically stimulated using supra-threshold square biphasic pulses (2 ms duration, 1 Hz, 5 V). The stimulation was initiated after 1–5 days after cell inoculation (3 day period was optimal) and applied for up to 8 days. Over only 8 days in vitro, electrical field stimulation led to cell alignment and coupling, increased amplitude of synchronous contractions by a factor of 7 and a remarkably high level of ultrastructural organization. Development of conductive and contractile properties of cardiac constructs was concurrent, with strong dependence on the initiation and duration of electrical

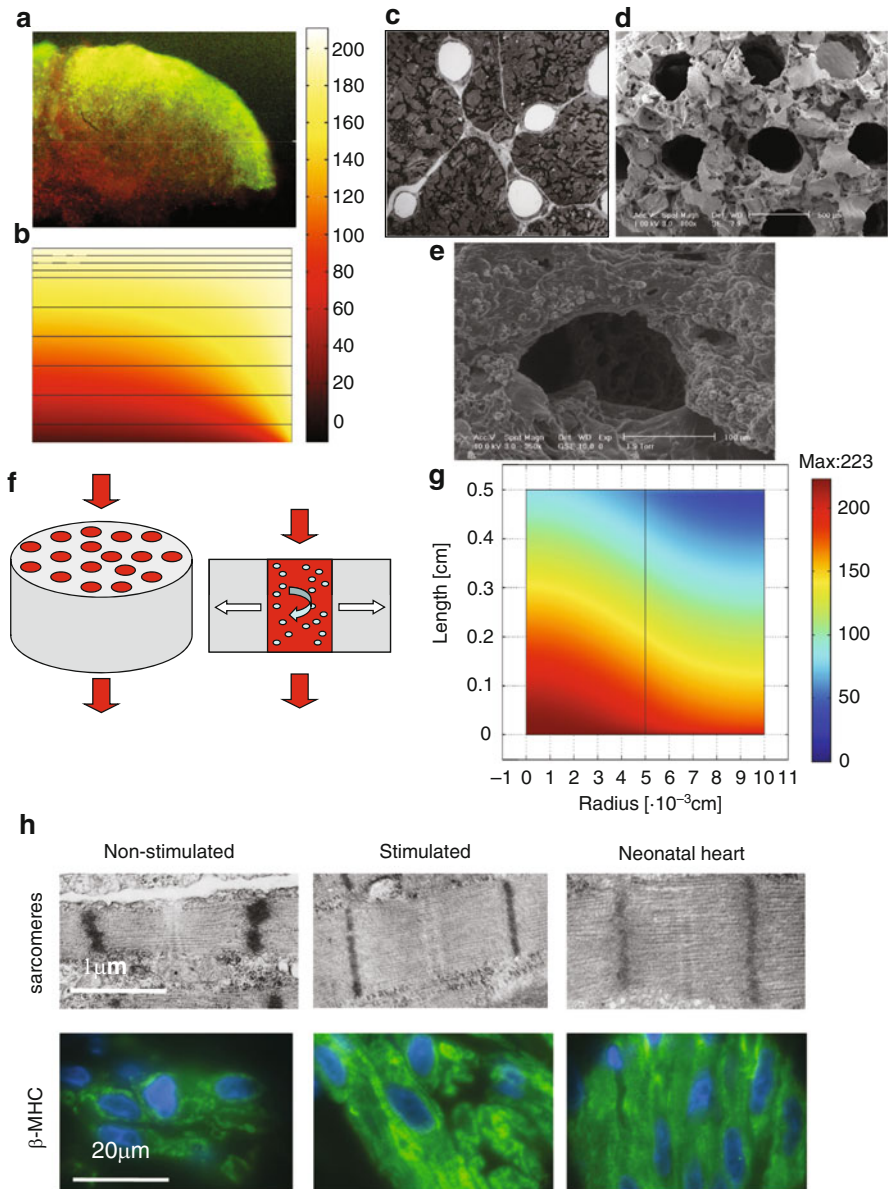


Fig. 15.3 Biomimetic approach to cardiac tissue engineering. **(a)** Cultivation of neonatal cardiomyocytes at high density 10^8 cells/cm³ in porous collagen scaffold results in uneven distribution of live cells. Live cells (*green*) are found at the periphery of the scaffold, while dead cells (*red*) are found in its interior. One half of scaffold cross-section is shown. **(b)** The distribution of live cells correlates to the oxygen concentration profile in the scaffold. **(c)** In the native heart, a dense capillary network provides oxygen and nutrients to the surrounding muscle fibers, cross-section shown. **(d)** A parallel array of channels of laser-bored within the poly(glycerol-sebacate) porous scaffolds, to mimic some aspects of the capillary network. **(e)** After cultivation of heart cells, a contractile construct is obtained and the channels remain open. **(f)** Perfusion of the channels with synthetic oxygen carriers ensures

stimulation. Aligned myofibers expressing cardiac markers (e.g. β -myosin heavy chain) were present in stimulated samples and neonatal heart (Fig. 15.3h). Stimulated samples had sarcomeres with clearly visible M, Z lines, H, I and A bands (Fig. 15.3h). In most cells, Z lines were aligned, and the intercalated discs were positioned between two Z lines. Mitochondria (between myofibrils) and abundant glycogen were detected. In contrast, non-stimulated constructs had poorly developed cardiac-specific organelles and poor organization of ultrastructural features.

Hence the *in vitro* application of a single, but key *in vivo* factor, progressively enhanced the functional tissue assembly and improved the properties of engineered myocardium at the cellular, ultrastructural and tissue levels.

15.3.2.2

Hydrogel Encapsulation and Mechanical Stimulation

Within the context of cardiac tissue engineering, disadvantages of the scaffolds that have been suggested to date include limited development of contractile force due to inherent stiffness of the scaffold, incomplete biodegradation, and poor cell alignment and morphology. Hydrogels, on the other hand, exhibit no mechanical or spatial restrictions. In a pioneering study, Eschenhagen et al. cast suspensions of embryonic chick cardiomyocytes in gels consisting of collagen I and culture medium into wells to generate spontaneously contracting engineered heart tissue (EHT) lattices [128]. Cyclic mechanical stretch was found to improve EHT structure and function. The EHTs exhibited elongated cell morphology and parallel organization. The forces of contraction ($\sim 2 \text{ mN/mm}^2$) were comparable to that of the native heart muscle [128].

In an improved setup, Zimmermann et al. cast encapsulated cells in circular molds and applied unidirectional phasic stretch. Mechanical loading was more equally distributed over the new circular geometry compared to previous square lattices [128, 129]. EHT displayed functional and morphological properties of differentiated heart muscle including highly organized sarcomeres arranged in myofibrils, specialized cell-junctions, T tubules and a well-developed basement membrane surrounding cardiomyocytes. In addition, primitive capillary formation was also observed [129].

In order to decrease the potential immunogenicity of their EHT, Zimmerman and colleagues discarded all xenogenic components from their culture [130]. This included cultivating the EHTs in serum-free and Matrigel-free conditions. Mixed heart cell populations rather than cardiomyocyte-rich populations were utilized, and the culture medium was supplemented with triiodothyronine and insulin [130]. Other studies have also established the need for

Fig. 15.3 (continued) that the entire tissue space around one channel received adequate supply of oxygen. (g) Oxygen concentration profile is shown for one half of the channel and tissue space surrounding the channel assuming 6.4 vol% of perfluorocarbon oxygen carrier in the culture medium. (h) Electrical field stimulation using suprathreshold pulses enables cultivation of engineered myocardium with highly differentiated cardiomyocytes, similar to those found in the native heart. Sarcomeres and staining for β -myosin heavy chain are shown.

15 nonimmunogenic media. Schwarzkopf et al. used autosppecies sera, in this case rat, for culturing of rat cardiomyocytes [131]. The metabolic activity of cells was significantly higher than cells cultivated in conventional culture medium with Fetal Bovine Serum.

In addition to engineering the patches of myocardium, Zimmermann and colleagues designed the first biological assist device [132]. The authors mechanically stimulated a hollow-spherical construct consisting of collagen I and neonatal rat cardiomyocytes until a beating pouch-like structure was created. The pouch was then placed over uninjured rat hearts in such a manner that the right and left ventricles were covered. Fourteen days after implantation, the pouch covered the epicardial surface of the heart and exhibited blood vessel ingrowth.

15.3.2.3

Matrix-Free Approaches

In a novel technology developed by Shimizu et al., contractile cardiac grafts were fabricated without the use of traditional matrix materials by stacking cell monolayers [133]. Surfaces coated with a temperature responsive polymer (poly-*N*-isopropylacrylamide), which is nonadhesive below 32°C, were used to culture layers of neonatal cardiomyocytes. Upon lowering of the temperature, pulsatile cell sheets detached spontaneously, while preserving cell junctions and adhesive proteins. These cell sheets were then stacked to form grafts. ECM produced by cells acted to adhere cell sheets together. Electrical and morphological communication between sheets was confirmed [133, 134]. This new cell sheet technology allows manipulation to form various graft shapes. A major limitation of this technology, however, is that the oxygen diffusion is constrained in the absence of a vascular network; graft thickness *in vitro* is limited to 3–4 cell layers only [134]. To overcome this limitation Shimizu et al. performed repeated transplantations of triple layered grafts into rat dorsal subcutaneous tissue, resulting in ~1 mm thick myocardium with well-organized vascular networks [135]. Complete graft vascularization was observed in constructs implanted over AV loops [135]. Although capable of generating a thick myocardium *in vivo*, this poly-surgery approach is not very clinically relevant due to the level of invasiveness required for multiple surgical interventions. Other matrix-free self-organization approaches include spontaneous wrapping of confluent monolayers around a poly(glycolic acid) string [136] and cultivation of myocardial spheroids from primary rat and mouse cardiac cell cultures via a refined hanging drop method [137].

15.3.2.4

Repair of Infarcted Myocardium Using Engineered Cardiac Tissue

The *in vivo* assessment of cardiac grafts is conventionally performed in rat infarction models mainly induced through two methods: cryoinjury [98] or left descending coronary artery (LAD) ligation [100]. In a pioneering study conducted by Li et al., neonatal rat cardiomyocytes seeded on collagen sponges were implanted onto damaged hearts of

Lewis rats [98]. After 5 weeks in vivo, cell survival and vascularization of constructs was measured. Leor et al. observed attenuation of the pathological remodeling process following implantation of cardiac grafts based on neonatal rat cardiomyocytes and porous alginate scaffolds onto injured myocardium of Sprague-Dawley rats [100]. Zimmermann et al. demonstrated integration and electrical coupling of a complex multi-loop graft to native myocardium in rats with LAD ligation. Functional improvement was suspected to be not merely a result of scar stabilization or paracrine effects. Functional integration of cardiac cell sheets to the heat-injured myocardium was also demonstrated [138].

15.4

Future Directions

Despite of the valuable achievements in the field of cardiac tissue engineering, there still remain several hurdles and challenges that need to be addressed. A central requirement is the identification of an appropriate human cell source, since adult cardiac myocytes are terminally differentiated and hence, cannot be sampled and proliferated for tissue engineering. Embryonic stem cells (ESC) are an attractive cell source because their differentiation leads to the generation of cardiomyocytes [29] at potentially unlimited quantities, and the resulting cells can graft with the host myocardium upon implantation [46, 139]. However, besides the ethical issues surrounding ESCs, there is a possibility that the presence of undifferentiated cells may lead to the formation of teratomas upon implantation [30]. Several recent studies report cultivation and implantation of cardiac grafts based on mouse and human embryonic stem cells [109, 140]. Recent evidence suggests that multipotent cardiovascular progenitors (is11+ or flk1+ or c-kit/Nkx2.5+), capable of giving rise to cardiomyocytes, endothelial cells and smooth muscle cells, can be selected and expanded from ESCs [141–143], thus potentially enabling the engineering of a multi-cell type cardiac tissue from a single cell source [141].

It has been reported that the heart may contain resident progenitor cells [144, 145]. Not only do these cells represent an excellent source of autologous cells, but they may enable detailed analysis of the process in cardiac cell lineage formation, tissue maturation and the development of disease [146]. However, it appears that there are multiple sub-populations that fit the description of a cardiac progenitor: c-kit+ [146], Sca-1 [147], and islet 1 (is11+) [144]. It remains to be determined whether these cells can be obtained from adult human biopsies and subsequently expanded in vitro.

Recently-introduced induced pluripotent stem (iPS) cells hold a great potential as they give rise to patient specific cells while avoiding the ethical issues surrounding ESCs [148]. It remains to be determined if cardiac patches can be engineered using iPS cells as a source of cardiomyocytes.

New and improved bioreactors will also need to be developed for large scale production of such cells ($>10^8$ cells/patient/patch). Careful consideration is required so that all non-human components (i.e. serum, Matrigel) during cultivation are replaced. Additionally, it will be

useful to generate different subtypes of human cardiomyocytes, with pacemaking-, atrial-, ventricular-, or Purkinje-like phenotypes, so that regenerative therapies can be extended over a wide range of heart diseases.

Besides finding a more suitable cell source, developing vasculature in thick patches to support cell survival in the deeper regions, remains a central issue in the field of cardiac tissue engineering [149]. A majority of the patches reported to date rely on diffusion for supplying the seeded cells with oxygen and nutrients. This limits the patch size to the maximum thickness that can be supplied with diffusion, about 100–200 μm , far from the clinically required thickness of ~ 1 cm [149]. Although, cell-seeding strategies to improve the cell distribution and survival within the patch, and medium perfusion strategies to ensure improved distribution of the nutrients to the cells have been reported, the key to circumvent this issue is to develop a vascular network within the patch prior to the implantation.

Endothelial cells (EC) are primarily involved in the development of vessel structures. It has been shown that ECs also support the survival and proliferation of CMs [150]. Hence, a viable option is to utilize ECs to develop the vascular network in the patch in order to prepare the patch for CM survival in later stages. Immobilized growth factors in combination with EC cell seeding represent an attractive option due to their long-lasting effects compared to soluble factors. Our lab has previously shown that immobilized vascular endothelial growth factor (VEGF), a key player in the migration, proliferation and assembly of ECs into vessels, on collagen scaffolds leads to improved EC survival and proliferation throughout the thickness of the scaffold [149]. We also demonstrated that covalent immobilization of VEGF and angiopoietin-1 enabled creation of tube-like structures in the scaffold *in vitro* [151] (Fig. 15.4a). These scaffolds were able to recruit endothelial cells in the chicken chorioallantoic membrane assay when the growth factors were freshly immobilized (Fig. 15.3b), as well as after aging the growth factor immobilized scaffolds in PBS for 28 days [151] (Fig. 15.3c). Currently, our lab is investigating the effects of scaffolds with immobilized growth factor gradients on EC migration and assembly (Odedra, Shoichet, Radisic in progress). Specifically, using microinjection and micropatterning methods, concentration gradients of VEGF, are created in the 3-D collagen scaffolds using the well-known carbodiimide chemistry. Strategies like this will bring us one step closer to the goal of creating engineered tissues that mimic the native tissues, by overcoming the challenge of cell-death in thick tissues and by providing the cells with vasculature-mediated nutrient and oxygen supply.

In addition, immobilization of growth factors on substrate surfaces could be applied to direct the differentiation of progenitor cells. Yamashita et al. previously reported that flk1+ cells derived from embryoid bodies after 3 days of spontaneous differentiation were in fact vascular progenitors and had the potential to further differentiate into endothelial and smooth muscle cell types with appropriate growth factor cues [152]. However, the soluble growth factors, only had the capability to control differentiation in a temporal manner. In order to control the spatial distribution of vascular cells on a surface, it is necessary to engineer the substrate surfaces with spatial control of growth factor presence (Fig. 15.4d). Tethered growth factors may also enhance cellular responses compared to the soluble growth factor conditions [153]. It is thought that growth factors tethered to substrate surfaces prevented

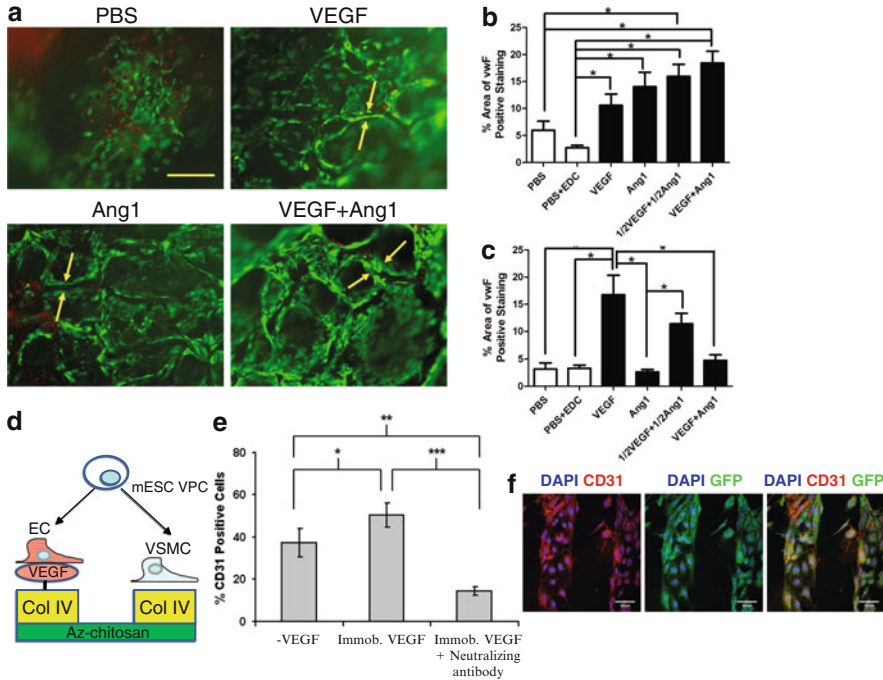


Fig. 15.4 Covalent immobilization of growth factors enables control of cell response on substrates for cardiovascular tissue engineering. VEGF and angiopoietin 1 were immobilized onto porous collagen scaffolds using carbodiimide chemistry. The control scaffolds were treated with PBS alone. **(a)** Live (green)/dead (red) staining of H5V endothelial cells after 7 days of cultivation demonstrated tube formation on growth factor immobilized scaffolds. Tubes were more pronounced on the VEGF +Ang1 scaffolds compared to the use of single growth factor alone. Scale bar 200 μ m. The cell-free growth factor scaffolds were implanted on top of the chorioallantoic membrane of a chick embryo. Three days later, the scaffolds were retrieved and the percent area staining for endothelial cell marker vonWillebrand factor was measured. **(b)** Implantation of a fresh scaffolds, immediately upon growth factor immobilization. **(c)** Implantation of a scaffold aged for 28 days in PBS after growth factor immobilization. **(d)** The principle of site-specific differentiation of Flk1+ vascular progenitor cells. Thin layer of photocrosslinked VEGF will render the entire surface non-cell adhesive. Islands of collagen IV will enable site-specific cell attachment. On some islands, VEGF is covalently tethered to collagen IV driving the differentiation towards endothelial cell lineage. **(e)** Immobilized VEGF drives differentiation towards CD31+ endothelial cells, while the application of VEGF neutralizing antibody abolishes the response. **(f)** The mESC derived vascular progenitors were engineered to express Flk1 (VEGF receptor 2) under control of GFP promoter. Immunostaining shows progenitors differentiated on the lanes of VEGF-collagen IV, co-staining positive for GFP (demonstrating the presence of VEGF receptor 2) and endothelial cell marker CD31. Scale bar 50 μ m.

internalization and degradation of the ligand/receptor complexes, which enabled prolonged signaling by the growth factors [153].

We previously described a strategy for site-specific differentiation by first covalently binding VEGF to Collagen IV, and subsequently micropatterning this VEGF-Collagen IV

solution onto a non-cell adhesive surface [154] (Fig. 15.4d). This allowed for differentiation of vascular progenitor cells into desired cell types within a confined area (Fig. 15.4e, f). We utilized the carbodiimide chemistry to covalently immobilize VEGF with Collagen IV molecules. The non-cell adhesive surface was first prepared with a thin layer of photocrosslinkable chitosan. Micro-contact printing stamps with 100 μm wide lanes were inked in the VEGF-Collagen IV immobilization solution, and the pattern was transferred to a surface coated with photocrosslinked chitosan. This micropatterning of differentiation cues was able to direct differentiation of embryoid body-derived flk1+ cells. After 3 days of culture on VEGF-patterned surfaces, approximately 55% of the cells were CD31+, indicating an endothelial cell lineage, which was comparable to conditions with soluble VEGF (Fig. 15.4f). These findings were further confirmed by blocking the engineered surface with neutralizing antibody against both soluble and immobilized VEGF. By neutralizing the VEGF, majority of the progenitor cells followed the default differentiation pathway into smooth muscle cells (Fig. 15.4e). In future studies, tethering of different growth factor cues, such as PDGF or Dkk, can be used to enhance differentiation towards smooth muscle or cardiomyocytes from a progenitor population.

Progress in this research field will inevitably be accelerated by the design of several new analytical techniques that allow real time monitoring of cell and tissue function to gain insight into the complex mechanisms of cardiogenesis and myocardial repair. Additionally, novel scaffolds and improved bioreactors capable of simultaneous application of multiple biochemical (e.g. growth factors) and physical (e.g. electrical, mechanical, perfusion) stimuli will be required. Bioreactor systems can also be used for rigorous studies of cardiac development and function to evaluate parameters such as the relative importance of each stimulus, when it should be applied and at what level. For these studies, we anticipate that microfluidic and BioMEMS (Micro-Electro-Mechanical Systems) techniques will be invaluable.

Engineered myocardium will be a useful tool to study the interactions among different cell populations within the heart during embryonic development and to learn the mechanisms by which transplanted cells promote cardiac repair. For example, we recently demonstrated that engineered myocardium allows the study of the differentiation and integration of ESC derived cardiomyocytes and progenitor cells in the cardiac environment *in vivo* [155]. With the availability of stem-cell derived human cardiomyocytes, the engineered heart tissue will become a useful model system for *in vitro* drug screening. In contrast to cultivating grafts of clinical size for cardiac repair, the basic pre-requisite for developing effective, high-throughput methods for pharmacological and developmental studies is the miniaturization of engineered tissue. We anticipate that advanced bioreactor technologies in conjunction with integrated microfluidic devices will facilitate this down-scaling.

A central question to the design of engineered cardiac tissue is whether native adult tissue structure needs to be reproduced exactly in order to achieve adequate function. The central dogma in tissue engineering is that sufficient function can be provided using simpler compositions and structures that can remodel and integrate into more complex structures upon implantation. Indeed, it is through this notion that clinically relevant tissue engineering therapies will emerge.

15.5 Summary

Myocardial Infarction (MI) affects about 8 million people in North America. During MI, a specific region in the heart experiences ischemia due to a fully or partially obstructed blood vessel, which compromises the oxygen supply to the region. The result is a rapid death of cells in this region, followed by pathophysiological remodelling and scar formation. Cardiovascular disease is the most significant cause of death worldwide. Drastic shortage of organs available for transplantation and limited improvements resulting from the reperfusion and pharmacological agents, motivate the need for an alternative and novel therapy. Cell injection and tissue engineering are amongst the emerging treatment options.

Biomaterials are critical as delivery vehicles for cell injection, or to act as scaffolds during *in vitro* cultivation of engineered cardiac tissues. Various natural, synthetic and biomimetic biomaterials have been studied for cell injection purposes with varying results. Natural materials such as collagen, gelatin, Matrigel and fibrin provide exceptional biocompatibility but lack in mechanical stiffness and exhibit high inter-batch variability. Hydrogels are especially attractive choice of biomaterial due to their high water content and biocompatibility. Natural hydrogels, like alginate and chitosan, have been used as biomimetic materials with some chemical modifications to enable cross-linking or augmented with biomolecules such as peptide sequences to enhance biological responses such as cell recruitment or attachment. Synthetic biomaterials, such as polyethylene glycol, have also been used as injectable biomaterials since they allow better control over physical and chemical properties compared to natural materials. A number of *in vivo* studies have been reported utilizing different combinations of biomaterials, cell type, and parameters such as the volume of cells and biomaterial injected and time course. Interestingly, in some studies the biomaterial alone was shown to lead to improved heart function. The exact mechanism behind the improvement following injection of biomaterial, either with cells or without, is not clearly known. The biomaterial serves to provide mechanically stabilize the scar as well as a transient environment for the cells to attach to and grow into.

The underlining approach for engineered heart patch involves seeding cells onto a biomaterial, culturing this tissue *in vitro* and then implanting the biomaterial onto the infarct. Porous scaffolds made of materials such as alginate and collagens have been used for this purpose with seeded cardiomyocytes. Fibrous scaffolds, such as woven polyglycolic acid or electrospun polyurethane, have also been explored for fabricating engineered heart patches especially due to their ability to align cells, as they are aligned in the native heart. Thin films, with precise micropatterned biomolecule distribution have been used to provide spatial control over cell morphology. Finally, decellularized scaffolds that contain only the extracellular components and intact vascular organization have been studied for their potential to support growth and integration of cells *in vivo*. Cultivation of these scaffolds *in vitro* is an important aspect of fabricating a functional heart patch and perfusion, electrical and mechanical stimulation bioreactors are required tools in this process. The *in vivo* results indicated that functional coupling of the engineered cardiac patch to the host myocardium is possible.

The field of cardiac tissue engineering is rapidly advancing. The quest for a suitable cell source is ongoing but is expected to reach a viable and ethically-accepted endpoint with the advent of induced pluripotent stem cells. On the other hand, strategies to guide the differentiation of currently used stem and progenitor cells in the *in vivo* infarct site itself will maximize the yields and minimize the undesired human interference associated when differentiating the cells *in vitro* before implantation. Finally, the challenge of increasing the vascularization of the patches *in vitro* continues to limit the cell distribution and survival in thick patches. However, with novel strategies such as immobilized growth factors, we are moving closer to mimicking the native environment *in vitro* and achieving the goal of reaching native-like vasculature.

Acknowledgements The work was supported by the Heart and Stroke Foundation of Ontario grant to Milica Radisic (NA 6077), NSERC Discovery grant, NSERC Strategic grant and an Early Researcher Award to Milica Radisic.

References

1. Black J. Western winter workshop on tissue engineering – Granlibakken, Tahoe-City, California, USA 26–29 February 1988. *Biomaterials*. 1988;9:379
2. Nerem RM, Sambani A. Tissue engineering: from biology to biological substitutes. *Tissue Eng*. 1995;1:3–13.
3. Caplan AI. Tissue engineering designs for the future: new logics, old molecules. *Tissue Eng*. 2000;6:1–8.
4. Griffith LG, Naughton G. Tissue engineering – current challenges and expanding opportunities. *Science*. 2002;295:1009–14.
5. van Winterswijk PJ, Nout E. Tissue engineering and wound healing: an overview of the past, present, and future. *Wounds*. 2007;19:277–84.
6. Laschke MW, Harder Y, Amon M, Martin I, Farhadi J, Ring A, et al. Angiogenesis in tissue engineering: breathing life into constructed tissue substitutes. *Tissue Eng*. 2006;12:2093–104.
7. Jiankang H, Dichen L, Yaxiong L, Bo Y, Hanxiang Z, Qin L, et al. Preparation of chitosan-gelatin hybrid scaffolds with well-organized microstructures for hepatic tissue engineering. *Acta Biomater*. 2009;5:453–61.
8. Yu HY, VandeVord PJ, Gong WM, Wu B, Song Z, Matthew HW, et al. Promotion of osteogenesis in tissue-engineered bone by pre-seeding endothelial progenitor cells-derived endothelial cells. *J Orthop Res*. 2008;26:1147–52.
9. Radisic M, Park H, Chen F, Salazar-Lazzaro JE, Wang Y, Dennis R, et al. Biomimetic approach to cardiac tissue engineering: oxygen carriers and channeled scaffolds. *Tissue Eng*. 2006;12:2077–91.
10. He JK, Li DC, Liu YX, Yao B, Lu BH, Lian Q. Fabrication and characterization of chitosan/gelatin porous scaffolds with predefined internal microstructures. *Polymer*. 2007;48:4578–88.
11. Dengler J, Radisic M. Tissue engineering approaches for the development of a contractile cardiac patch. *Future Cardiol*. 2007;3:425–34.
12. Nag AC. Study of non-muscle cells of the adult mammalian heart: a fine structural analysis and distribution. *Cytobios*. 1980;28:41–61.
13. Mandarin-de-Lacerda CA, Pereira LMM. Numerical density of cardiomyocytes in chronic nitric oxide synthesis inhibition. *Pathobiology*. 2000;68:36–42.
14. Severs NJ. The cardiac muscle cell. *Bioessays*. 2000;22:188–99.

15. Rosamund W, Flegal K, Furie K, Go A, Greenlund K, Haase N, et al. Heart Disease and Stroke Statistics – 2008 update: a report from the American Heart Association Statistics Committee and Stroke Statistics Subcommittee. *Circulation*. 2007;117:e25–146.
16. Sutton MG, Sharpe N. Left ventricular remodeling after myocardial infarction: pathophysiology and therapy. *Circulation*. 2000;101:2981–8.
17. McKay RG, Pfeffer MA, Pasternak RC, Markis JE, Come PC, Nakao S, et al. Left ventricular remodeling after myocardial infarction: a corollary to infarct expansion. *Circulation*. 1986;74:693–702.
18. Pfeffer MA, Braunwald E. Ventricular remodeling after myocardial infarction. Experimental observations and clinical implications. *Circulation*. 1990;81:1161–72.
19. Touchstone DA, Beller GA, Nygaard TW, Tedesco C, Kaul S. Effects of successful intravenous reperfusion therapy on regional myocardial function and geometry in humans: a tomographic assessment using two-dimensional echocardiography. *J Am Coll Cardiol*. 1989;13:1506–13.
20. Marino P, Zanolla L, Zardini P. Effect of streptokinase on left ventricular modeling and function after myocardial infarction: the GISSI (Gruppo Italiano per lo Studio della Streptochinasi nell'Infarto Miocardico) Trial. *J Am Coll Cardiol*. 1989;14:1149–58.
21. Baks T, van Geuns RJ, Biagini E, Wielopolski P, Mollet NR, Cademartiri F, et al. Effects of primary angioplasty for acute myocardial infarction on early and late infarct size and left ventricular wall characteristics. *J Am Coll Cardiol*. 2006;47:40–4.
22. Verma S, Fedak PW, Weisel RD, Butany J, Rao V, Maitland A, et al. Fundamentals of reperfusion injury for the clinical cardiologist. *Circulation*. 2002;105:2332–6.
23. Huang D, Zhang F, Qian J, Wang X, Ge J. Reversal of no-reflow/slow-flow. *Circulation*. 2008;118:S894.
24. Beltrame JF. Nitrate therapy in acute myocardial infarction: potion or poison? *Cardiovasc Drugs Ther*. 2008;22:165–8.
25. McMurray J, Solomon S, Pieper K, Reed S, Rouleau J, Velazquez E, et al. The effect of valsartan, captopril, or both on atherosclerotic events after acute myocardial infarction: an analysis of the Valsartan in Acute Myocardial Infarction Trial (VALIANT). *J Am Coll Cardiol*. 2006;47:726–33.
26. Braunwald E, Domanski MJ, Fowler SE, Geller NL, Gersh BJ, Hsia J, et al. Angiotensin-converting-enzyme inhibition in stable coronary artery disease. *N Engl J Med*. 2004;351:2058–68.
27. Orlic D, Kajstura J, Chimenti S, Limana F, Jakoniuk I, Quaini F, et al. Mobilized bone marrow cells repair the infarcted heart, improving function and survival. *Proc Natl Acad Sci U S A*. 2001;98:10344–9.
28. Welch S, Plank D, Witt S, Glascock B, Schaefer E, Chimenti S, et al. Cardiac-specific IGF-1 expression attenuates dilated cardiomyopathy in tropomodulin-overexpressing transgenic mice. *Circ Res*. 2002;90:641–8.
29. Soonpaa MH, Field LJ. Survey of studies examining mammalian cardiomyocyte DNA synthesis. *Circ Res*. 1998;83:15–26.
30. Laffamme MA, Murry CE. Regenerating the heart. *Nat Biotechnol*. 2005;23:845–56.
31. Dimmeler S, Zeiher AM, Schneider MD. Unchain my heart: the scientific foundations of cardiac repair. *J Clin Invest*. 2005;115:572–83.
32. Yamada T, Yang JJ, Ricchiuti NV, Seraydarian MW. Oxygen consumption of mammalian myocardial-cells in culture - measurements in beating cells attached to the substrate of the culture dish. *Anal Biochem*. 1985;145:302–7.
33. Sun LS, Legato MJ, Rosen TS, Steinberg SF, Rosen MR. Sympathetic innervation modulates ventricular impulse propagation and repolarisation in the immature rat heart. *Cardiovasc Res*. 1993;27:459–63.

34. Murry CE, Field LJ, Menasche P. Cell-based cardiac repair: reflections at the 10-year point. *Circulation*. 2005;112:3174–83.
35. Hansson EM, Lindsay ME, Chien KR. Regeneration next: toward heart stem cell therapeutics. *Cell Stem Cell*. 2009;5:364–77.
36. Chachques JC. Cellular cardiac regenerative therapy in which patients? *Expert Rev Cardiovasc Ther*. 2009;7:911–9.
37. Forrester JS, Makkar RR, Marban E. Long-term outcome of stem cell therapy for acute myocardial infarction: right results, wrong reasons. *J Am Coll Cardiol*. 2009;53:2270–2.
38. Muller-Ehmsen J, Peterson KL, Kedes L, Whittaker P, Dow JS, Long TI, et al. Rebuilding a damaged heart: long-term survival of transplanted neonatal rat cardiomyocytes after myocardial infarction and effect on cardiac function. *Circulation*. 2002;105:1720–6.
39. Reinecke H, Zhang M, Bartosek T, Murry CE. Survival, integration, and differentiation of cardiomyocyte grafts: a study in normal and injured rat hearts. *Circulation*. 1999;100:193–202.
40. Huwer H, Winning J, Vollmar B, Welter C, Lohbach C, Menger MD, et al. Long-term cell survival and hemodynamic improvements after neonatal cardiomyocyte and satellite cell transplantation into healed myocardial cryoinfarcted lesions in rats. *Cell Transplant*. 2003;12:757–67.
41. Li RK, Jia ZQ, Weisel RD, Mickle DA, Zhang J, Mohabeer MK, et al. Cardiomyocyte transplantation improves heart function. *Ann Thorac Surg*. 1996;62:654–60; discussion 60–1
42. Soonpaa MH, Koh GY, Klug MG, Field LJ. Formation of nascent intercalated disks between grafted fetal cardiomyocytes and host myocardium. *Science*. 1994;264:98–101.
43. Muller-Ehmsen J, Whittaker P, Kloner RA, Dow JS, Sakoda T, Long TI, et al. Survival and development of neonatal rat cardiomyocytes transplanted into adult myocardium. *J Mol Cell Cardiol*. 2002;34:107–16.
44. Zhang M, Method D, Poppa V, Fujio Y, Walsh K, Murry CE. Cardiomyocyte grafting for cardiac repair: graft cell death and anti-death strategies. *J Mol Cell Cardiol*. 2001;33:907–21.
45. Dorfman J, Duong M, Zibaitis A, Pelletier MP, Shum-Tim D, Li C, et al. Myocardial tissue engineering with autologous myoblast implantation. *J Thorac Cardiovasc Surg*. 1998;116:744–51.
46. Klug MG, Soonpaa MH, Koh GY, Field LJ. Genetically selected cardiomyocytes from differentiating embryonic stem cells form stable intracardiac grafts. *J Clin Invest*. 1996;98:216–24.
47. Etzion S, Battler A, Barbash IM, Cagnano E, Zarin P, Granot Y, et al. Influence of embryonic cardiomyocyte transplantation on the progression of heart failure in a rat model of extensive myocardial infarction. *J Mol Cell Cardiol*. 2001;33:1321–30.
48. Kehat I, Kenyagin-Karsenti D, Snir M, Segev H, Amit M, Gepstein A, et al. Human embryonic stem cells can differentiate into myocytes with structural and functional properties of cardiomyocytes. *J Clin Invest*. 2001;108:407–14.
49. Toma C, Pittenger MF, Cahill KS, Byrne BJ, Kessler PD. Human mesenchymal stem cells differentiate to a cardiomyocyte phenotype in the adult murine heart. *Circulation*. 2002;105:93–8.
50. Shake JG, Gruber PJ, Baumgartner WA, Senechal G, Meyers J, Redmond JM, et al. Mesenchymal stem cell implantation in a swine myocardial infarct model: engraftment and functional effects. *Ann Thorac Surg*. 2002;73:1919–25; discussion 26.
51. Orlic D, Kajstura J, Chimenti S, Jakoniuk I, Anderson SM, Li B, et al. Bone marrow cells regenerate infarcted myocardium. *Nature*. 2001;410:701–5.
52. Murry CE, Soonpaa MH, Reinecke H, Nakajima H, Nakajima HO, Rubart M, et al. Haematopoietic stem cells do not transdifferentiate into cardiac myocytes in myocardial infarcts. *Nature*. 2004;428:664–8.

53. Balsam LB, Wagers AJ, Christensen JL, Kofidis T, Weissman IL, Robbins RC. Haematopoietic stem cells adopt mature haematopoietic fates in ischaemic myocardium. *Nature*. 2004;428:668–73.
54. Hagege AA, Marolleau JP, Vilquin JT, Alheritiere A, Peyrard S, Duboc D, et al. Skeletal myoblast transplantation in ischemic heart failure: long-term follow-up of the first phase I cohort of patients. *Circulation*. 2006;114:1108–13.
55. Menasche P, Hagege AA, Vilquin JT, Desnos M, Abergel E, Pouzet B, et al. Autologous skeletal myoblast transplantation for severe postinfarction left ventricular dysfunction. *J Am Coll Cardiol*. 2003;41:1078–83.
56. Wollert KC, Meyer GP, Lotz J, Ringes-Lichtenberg S, Lippolt P, Breidenbach C, et al. Intracoronary autologous bone-marrow cell transfer after myocardial infarction: the BOOST randomised controlled clinical trial. *Lancet*. 2004;364:141–8.
57. Chen SL, Fang WW, Ye F, Liu YH, Qian J, Shan SJ, et al. Effect on left ventricular function of intracoronary transplantation of autologous bone marrow mesenchymal stem cell in patients with acute myocardial infarction. *Am J Cardiol*. 2004;94:92–5.
58. Perin EC, Dohmann HF, Borojevic R, Silva SA, Sousa AL, Mesquita CT, et al. Transendocardial, autologous bone marrow cell transplantation for severe, chronic ischemic heart failure. *Circulation*. 2003;107:2294–302.
59. Lipinski MJ, Biondi-Zoccai GG, Abbate A, Khianey R, Sheiban I, Bartunek J, et al. Impact of intracoronary cell therapy on left ventricular function in the setting of acute myocardial infarction: a collaborative systematic review and meta-analysis of controlled clinical trials. *J Am Coll Cardiol*. 2007;50:1761–7.
60. Reffelmann T, Kloner RA. Cellular cardiomyoplasty – cardiomyocytes, skeletal myoblasts, or stem cells for regenerating myocardium and treatment of heart failure? *Cardiovasc Res*. 2003;58:358–68.
61. Kofidis T, Lebl DR, Martinez EC, Hoyt G, Tanaka M, Robbins RC. Novel injectable bioartificial tissue facilitates targeted, less invasive, large-scale tissue restoration on the beating heart after myocardial injury. *Circulation*. 2005;112:1173–7.
62. Christman KL, Fok HH, Sievers RE, Fang Q, Lee RJ. Fibrin glue alone and skeletal myoblasts in a fibrin scaffold preserve cardiac function after myocardial infarction. *Tissue Eng*. 2004;10:403–9.
63. Christman KL, Vardanian AJ, Fang Q, Sievers RE, Fok HH, Lee RJ. Injectable fibrin scaffold improves cell transplant survival, reduces infarct expansion, and induces neovascularization in ischemic myocardium. *J Am Coll Cardiol*. 2004;44:654–60.
64. Ryu JH, Kim IK, Cho SW, Cho MC, Hwang KK, Piao H, et al. Implantation of bone marrow mononuclear cells using injectable fibrin matrix enhances neovascularization in infarcted myocardium. *Biomaterials*. 2005;26:319–26.
65. Landa N, Miller L, Feinberg MS, Holbova R, Shachar M, Freeman I, et al. Effect of injectable alginate implant on cardiac remodeling and function after recent and old infarcts in rat. *Circulation*. 2008;117:1388–96.
66. Davis ME, Motion JP, Narmoneva DA, Takahashi T, Hakuno D, Kamm RD, et al. Injectable self-assembling peptide nanofibers create intramyocardial microenvironments for endothelial cells. *Circulation*. 2005;111:442–50.
67. Davis ME, Hsieh PC, Takahashi T, Song Q, Zhang S, Kamm RD, et al. Local myocardial insulin-like growth factor 1 (IGF-1) delivery with biotinylated peptide nanofibers improves cell therapy for myocardial infarction. *Proc Natl Acad Sci U S A*. 2006;103:8155–60.
68. Laflamme MA, Chen KY, Naumova AV, Muskheli V, Fugate JA, Dupras SK, et al. Cardiomyocytes derived from human embryonic stem cells in pro-survival factors enhance function of infarcted rat hearts. *Nat Biotechnol*. 2007;25:1015–24.
69. Kopecek J. Hydrogel biomaterials: a smart future? *Biomaterials*. 2007;28:5185–92.

70. Peppas NA, Hilt JZ, Khademhosseini A, Langer R. Hydrogels in biology and medicine: From molecular principles to bionanotechnology. *Adv Mater.* 2006;18:1345–60.
71. Nicodemus GD, Bryant SJ. Cell encapsulation in biodegradable hydrogels for tissue engineering applications. *Tissue Eng Part B Rev.* 2008;14:149–65.
72. Jawad H, Lyon AR, Harding SE, Ali NN, Boccaccini AR. Myocardial tissue engineering. *Br Med Bull.* 2008;87:31–47.
73. Leach JB, Bivens KA, Patrick CW, Schmidt CE. Photocrosslinked hyaluronic acid hydrogels: natural, biodegradable tissue engineering scaffolds. *Biotechnol Bioeng.* 2003;82:578–89.
74. Suh JKF, Matthew HWT. Application of chitosan-based polysaccharide biomaterials in cartilage tissue engineering: a review. *Biomaterials.* 2000;21:2589–98.
75. Kim IY, Seo SJ, Moon HS, Yoo MK, Park IY, Kim BC, et al. Chitosan and its derivatives for tissue engineering applications. *Biotechnol Adv.* 2008;26:1–21.
76. Rowley JA, Madlambayan G, Mooney DJ. Alginate hydrogels as synthetic extracellular matrix materials. *Biomaterials.* 1999;20:45–53.
77. Dallabrida SM, Ismail N, Oberle JR, Himes BE, Rupnick MA. Angiotensin-1 promotes cardiac and skeletal myocyte survival through integrins. *Circ Res.* 2005;96:e8–24.
78. Yeo Y, Geng W, Ito T, Kohane DS, Burdick JA, Radisic M. Photocrosslinkable hydrogel for myocyte cell culture and injection. *J Biomed Mater Res B Appl Biomater.* 2007;81:312–22.
79. Rask F, Dallabrida SM, Ismail NS, Amoozgar Z, Yeo Y, Radisic M. Photocrosslinkable chitosan modified with angiotensin-1 peptide, QHREDGS, promotes survival of neonatal rat heart cells. *J Biomed Mater Res A.* 2010;95:105–17.
80. Kofidis T, de Bruin JL, Hoyt G, Lebl DR, Tanaka M, Yamane T, et al. Injectable bioartificial myocardial tissue for large-scale intramural cell transfer and functional recovery of injured heart muscle. *J Thorac Cardiovasc Surg.* 2004;128:571–8.
81. Zhang P, Zhang H, Wang H, Wei Y, Hu S. Artificial matrix helps neonatal cardiomyocytes restore injured myocardium in rats. *Artif Organs.* 2006;30:86–93.
82. Zimmermann WH, Melnychenko I, Wasmeier G, Didie M, Naito H, Nixdorff U, et al. Engineered heart tissue grafts improve systolic and diastolic function in infarcted rat hearts. *Nat Med.* 2006;12:452–8.
83. Lu W-N, Lü S-H, Wang H-B, Li D-X, Duan C-M, Liu Z-Q, et al. Functional improvement of infarcted heart by co-injection of embryonic stem cells with temperature-responsive chitosan hydrogel. *Tissue Eng Part A.* 2009;15:1437–47.
84. Zhang S, Holmes TC, DiPersio CM, Hynes RO, Su X, Rich A. Self-complementary oligopeptide matrices support mammalian cell attachment. *Biomaterials.* 1995;16:1385–93.
85. Davis ME, Motion JPM, Narmoneva DA, Takahashi T, Hakuno D, Kamm RD, et al. Injectable self-assembling peptide nanofibers create intramyocardial microenvironments for endothelial cells. *Circulation.* 2005;111:442–50.
86. Fujimoto KL, Ma Z, Nelson DM, Hashizume R, Guan J, Tobita K, et al. Synthesis, characterization and therapeutic efficacy of a biodegradable, thermoresponsive hydrogel designed for application in chronic infarcted myocardium. *Biomaterials.* 2009;30:4357–68.
87. Dobner S, Bezuidenhout D, Govender P, Zilla P, Davies N. A synthetic non-degradable polyethylene glycol hydrogel retards adverse post-infarct left ventricular remodeling. *J Card Fail.* 2009;15:629–36.
88. Leor J, Tuvia S, Guetta V, Manczur F, Castel D, Willenz U, et al. Intracoronary injection of in situ forming alginate hydrogel reverses left ventricular remodeling after myocardial infarction in Swine. *J Am Coll Cardiol.* 2009;54:1014–23.
89. Dai W, Wold LE, Dow JS, Kloner RA. Thickening of the infarcted wall by collagen injection improves left ventricular function in rats: a novel approach to preserve cardiac function after myocardial infarction. *J Am Coll Cardiol.* 2005;46:714–9.

90. Wall ST, Walker JC, Healy KE, Ratcliffe MB, Guccione JM. Theoretical impact of the injection of material into the myocardium: a finite element model simulation. *Circulation*. 2006;114:2627–35.
91. Hung J, Solis J, Guerrero JL, Braithwaite GJC, Muratoglu OK, Chaput M, et al. A novel approach for reducing ischemic mitral regurgitation by injection of a polymer to reverse remodel and reposition displaced papillary muscles. *Circulation*. 2008;118:S263–9.
92. Mihardja SS, Sievers RE, Lee RJ. The effect of polypyrrole on arteriogenesis in an acute rat infarct model. *Biomaterials*. 2008;29:4205–10.
93. Yu J, Gu Y, Du KT, Mihardja S, Sievers RE, Lee RJ. The effect of injected RGD modified alginate on angiogenesis and left ventricular function in a chronic rat infarct model. *Biomaterials*. 2009;30:751–6.
94. Anversa P, Cheng W, Liu Y, Leri A, Redaelli G, Kajstura J. Apoptosis and myocardial infarction. *Basic Res Cardiol*. 1998;93(Suppl 3):8–12.
95. Yaoita H, Ogawa K, Maehara K, Maruyama Y. Apoptosis in relevant clinical situations: contribution of apoptosis in myocardial infarction. *Cardiovasc Res*. 2000;45:630–41.
96. Olivetti G, Quaini F, Sala R, Lagrasta C, Corradi D, Bonacina E, et al. Acute myocardial infarction in humans is associated with activation of programmed myocyte cell death in the surviving portion of the heart. *J Mol Cell Cardiol*. 1996;28:2005–16.
97. Hsieh PCH, Davis ME, Gannon J, MacGillivray C, Lee RT. Controlled delivery of PDGF-BB for myocardial protection using injectable self-assembling peptide nanofibers. *J Clin Invest*. 2006;116:237–48.
98. Li R-K, Jia ZQ, Weisel RD, Mickle DAG, Choi A, Yau TM. Survival and function of bioengineered cardiac grafts. *Circulation*. 1999;100:II63–9.
99. Li RK, Yau TM, Weisel RD, Mickle DA, Sakai T, Choi A, et al. Construction of a bioengineered cardiac graft. *J Thorac Cardiovasc Surg*. 2000;119:368–75.
100. Leor J, Abouafia-Etzion S, Dar A, Shapiro L, Barbash IM, Battler A, et al. Bioengineered cardiac grafts: a new approach to repair the infarcted myocardium? *Circulation*. 2000;102:III56–III61.
101. Dar A, Shachar M, Leor J, Cohen S. Cardiac tissue engineering optimization of cardiac cell seeding and distribution in 3D porous alginate scaffolds. *Biotechnol Bioeng*. 2002;80:305–12.
102. Kofidis T, Akhyari P, Wachsmann B, Mueller-Stahl K, Boublik J, Ruhparwar A, et al. Clinically established hemostatic scaffold (tissue fleece) as biomatrix in tissue- and organ-engineering research. *Tissue Eng*. 2003;9:517–23.
103. Carrier RL, Papadaki M, Rupnick M, Schoen FJ, Bursac N, Langer R, et al. Cardiac tissue engineering: cell seeding, cultivation parameters and tissue construct characterization. *Biotechnol Bioeng*. 1999;64:580–9.
104. Bursac N, Papadaki M, Cohen RJ, Schoen FJ, Eisenberg SR, Carrier R, et al. Cardiac muscle tissue engineering: toward an in vitro model for electrophysiological studies. *Am J Physiol*. 1999;277:H433–44.
105. Papadaki M, Bursac N, Langer R, Merok J, Vunjak-Novakovic G, Freed LE. Tissue engineering of functional cardiac muscle: molecular, structural and electrophysiological studies. *Am J Physiol Heart Circ Physiol*. 2001;280:H168–78.
106. Zong X, Bien H, Chung CY, Yin L, Fang D, Hsiao BS, et al. Electrospun fine-textured scaffolds for heart tissue constructs. *Biomaterials*. 2005;26:5330–8.
107. Rockwood DN, Akins RE, Jr., Parrag IC, Woodhouse KA, Rabolt JF. Culture on electrospun polyurethane scaffolds decreases atrial natriuretic peptide expression by cardiomyocytes in vitro. *Biomaterials*. 2008;29:4783–91.
108. Fromstein JD, Zandstra PW, Alperin C, Rockwood D, Rabolt JF, Woodhouse KA. Seeding bioreactor-produced embryonic stem cell-derived cardiomyocytes on different porous, degradable, polyurethane scaffolds reveals the effect of scaffold architecture on cell morphology. *Tissue Eng Part A*. 2008;14:369–78.

109. Alperin C, Zandstra PW, Woodhouse KA. Polyurethane films seeded with embryonic stem cell-derived cardiomyocytes for use in cardiac tissue engineering applications. *Biomaterials*. 2005;26:7377–86.
110. McDevitt TC, Woodhouse KA, Hauschka SD, Murry CE, Stayton PS. Spatially organized layers of cardiomyocytes on biodegradable polyurethane films for myocardial repair. *J Biomed Mater Res A*. 2003;66:586–95.
111. McDevitt TC, Angello JC, Whitney ML, Reinecke H, Hauschka SD, Murry CE, et al. In vitro generation of differentiated cardiac myofibers on micropatterned laminin surfaces. *J Biomed Mater Res*. 2002;60:472–9.
112. Khademhosseini A, Eng G, Yeh J, Kucharczyk PA, Langer R, Vunjak-Novakovic G, et al. Microfluidic patterning for fabrication of contractile cardiac organoids. *Biomed Microdevices*. 2007;9(2):149–57.
113. Engelmayr GC, Jr., Cheng M, Bettinger CJ, Borenstein JT, Langer R, Freed LE. Accordion-like honeycombs for tissue engineering of cardiac anisotropy. *Nat Mater*. 2008;7:1003–10.
114. Domian IJ, Chiravuri M, van der Meer P, Feinberg AW, Shi X, Shao Y, et al. Generation of functional ventricular heart muscle from mouse ventricular progenitor cells. *Science*. 2009;326:426–9.
115. Feinberg AW, Feigel A, Shevkopylas SS, Sheehy S, Whitesides GM, Parker KK. Muscular thin films for building actuators and powering devices. *Science*. 2007;317:1366–70.
116. Badie N, Satterwhite L, Bursac N. A Method to replicate the microstructure of heart tissue in vitro using DTMRI-based cell micropatterning. *Ann Biomed Eng*. 2009;37(12):2510–21.
117. Badie N, Bursac N. Novel micropatterned cardiac cell cultures with realistic ventricular microstructure. *Biophys J*. 2009;96:3873–85.
118. Ott HC, Matthiesen TS, Goh SK, Black LD, Kren SM, Netoff TI, et al. Perfusion-decellularized matrix: using nature's platform to engineer a bioartificial heart. *Nat Med*. 2008;14:213–21.
119. Badylak SF, Kochupura PV, Cohen IS, Doronin SV, Saltman AE, Gilbert TW, et al. The use of extracellular matrix as an inductive scaffold for the partial replacement of functional myocardium. *Cell Transplant*. 2006;15(Suppl 1):S29–40.
120. Kelly DJ, Rosen AB, Schuldt AJ, Kochupura PV, Doronin SV, Potapova IA, et al. Increased myocyte content and mechanical function within a tissue-engineered myocardial patch following implantation. *Tissue Eng Part A*. 2009;15:2189–201.
121. Radisic M, Euloth M, Yang L, Langer R, Freed LE, Vunjak-Novakovic G. High-density seeding of myocyte cells for cardiac tissue engineering. *Biotechnol Bioeng*. 2003;82:403–14.
122. Radisic M, Yang L, Boublik J, Cohen RJ, Langer R, Freed LE, et al. Medium perfusion enables engineering of compact and contractile cardiac tissue. *Am J Physiol Heart Circ Physiol*. 2004;286:H507–16.
123. Korecky B, Hai CM, Rakusan K. Functional capillary density in normal and transplanted rat hearts. *Can J Physiol Pharmacol*. 1982;60:23–32.
124. Radisic M, Deen W, Langer R, Vunjak-Novakovic G. Mathematical model of oxygen distribution in engineered cardiac tissue with parallel channel array perfused with culture medium containing oxygen carriers. *Am J Physiol Heart Circ Physiol*. 2005;288:H1278–89.
125. Kofidis T, Lenz A, Boublik J, Akhyari P, Wachsmann B, Mueller-Stahl K, et al. Pulsatile perfusion and cardiomyocyte viability in a solid three-dimensional matrix. *Biomaterials* 2003;24:5009–14.
126. Dvir T, Benishti N, Shachar M, Cohen S. A novel perfusion bioreactor providing a homogeneous milieu for tissue regeneration. *Tissue Eng*. 2006;12:2843–52.
127. Radisic M, Park H, Shing H, Consi T, Schoen FJ, Langer R, et al. Functional assembly of engineered myocardium by electrical stimulation of cardiac myocytes cultured on scaffolds. *Proc Natl Acad Sci U S A* 2004;101:18129–34.

128. Eschenhagen T, Fink C, Remmers U, Scholz H, Wattochow J, Woil J, et al. Three-dimensional reconstitution of embryonic cardiomyocytes in a collagen matrix: a new heart model system. *FASEB J.* 1997;11:683–94.
129. Zimmermann WH, Schneiderbanger K, Schubert P, Didie M, Munzel F, Heubach JF, et al. Tissue engineering of a differentiated cardiac muscle construct. *Circ Res.* 2002;90:223–30.
130. Naito H, Melnychenko I, Didie M, Schneiderbanger K, Schubert P, Rosenkranz S, et al. Optimizing engineered heart tissue for therapeutic applications as surrogate heart muscle. *Circulation.* 2006;114:172–8.
131. Schwarzkopf R, Shachar M, Dvir T, Dayan Y, Holbova R, Leor J, et al. Autosppecies and post-myocardial infarction sera enhance the viability, proliferation, and maturation of 3D cardiac cell culture. *Tissue Eng.* 2006;12:3467–75.
132. Yildirim Y, Naito H, Didie M, Karikkineth BC, Biermann D, Eschenhagen T, et al. Development of a biological ventricular assist device: preliminary data from a small animal model. *Circulation.* 2007;116:116–23.
133. Shimizu T, Yamato M, Isoi Y, Akutsu T, Setomaru T, Abe K, et al. Fabrication of pulsatile cardiac tissue grafts using a novel 3-dimensional cell sheet manipulation technique and temperature-responsive cell culture surfaces. *Circ Res.* 2002;90:e40–8.
134. Shimizu T, Sekine H, Isoi Y, Yamato M, Kikuchi A, Okano T. Long-term survival and growth of pulsatile myocardial tissue grafts engineered by the layering of cardiomyocyte sheets. *Tissue Eng.* 2006;12(3):499–507.
135. Shimizu T, Sekine H, Yang J, Isoi Y, Yamato M, Kikuchi A, et al. Polysurgery of cell sheet grafts overcomes diffusion limits to produce thick, vascularized myocardial tissues. *FASEB J.* 2006;20:708–10.
136. Baar K, Birla R, Boluyt MO, Borschel GH, Arruda EM, Dennis RG. Self-organization of rat cardiac cells into contractile 3-D cardiac tissue. *FASEB J.* 2005;19:275–7.
137. Kelm JM, Ehler E, Nielsen LK, Schlatter S, Perriard JC, Fussenegger M. Design of artificial myocardial microtissues. *Tissue Eng.* 2004;10:201–14.
138. Furuta A, Miyoshi S, Itabashi Y, Shimizu T, Kira S, Hayakawa K, et al. Pulsatile cardiac tissue grafts using a novel three-dimensional cell sheet manipulation technique functionally integrates with the host heart, in vivo. *Circ Res.* 2006;98:705–12.
139. Zandstra PW, Bauwens C, Yin T, Liu Q, Schiller H, Zweigerdt R, et al. Scalable production of embryonic stem cell-derived cardiomyocytes. *Tissue Eng.* 2003;9:767–78.
140. Guo XM, Zhao YS, Chang HX, Wang CY, E LL, Zhang XA, et al. Creation of engineered cardiac tissue in vitro from mouse embryonic stem cells. *Circulation.* 2006;113:2229–37.
141. Kattman SJ, Huber TL, Keller GM. Multipotent flk-1+ cardiovascular progenitor cells give rise to the cardiomyocyte, endothelial, and vascular smooth muscle lineages. *Dev Cell.* 2006;11:723–32.
142. Wu SM, Fujiwara Y, Cibulsky SM, Clapham DE, Lien CL, Schultheiss TM, et al. Developmental origin of a bipotential myocardial and smooth muscle cell precursor in the mammalian heart. *Cell.* 2006;127:1137–50.
143. Ema M, Faloon P, Zhang WJ, Hirashima M, Reid T, Stanford WL, et al. Combinatorial effects of Flk1 and Tal1 on vascular and hematopoietic development in the mouse. *Genes Dev.* 2003;17:380–93.
144. Laugwitz KL, Moretti A, Lam J, Gruber P, Chen Y, Woodard S, et al. Postnatal is11+ cardioblasts enter fully differentiated cardiomyocyte lineages. *Nature.* 2005;433:647–53.
145. Moretti A, Caron L, Nakano A, Lam JT, Bernshausen A, Chen Y, et al. Multipotent embryonic is11+ progenitor cells lead to cardiac, smooth muscle, and endothelial cell diversification. *Cell.* 2006;127:1151–65.
146. Beltrami AP, Barlucchi L, Torella D, Baker M, Limana F, Chimenti S, et al. Adult cardiac stem cells are multipotent and support myocardial regeneration. *Cell.* 2003;114:763–76.

147. Oh H, Bradfute SB, Gallardo TD, Nakamura T, Gausin V, Mishina Y, et al. Cardiac progenitor cells from adult myocardium: homing, differentiation, and fusion after infarction. *Proc Natl Acad Sci U S A*. 2003;100:12313–8.
148. Takahashi K, Tanabe K, Ohnuki M, Narita M, Ichisaka T, Tomoda K, et al. Induction of pluripotent stem cells from adult human fibroblasts by defined factors. *Cell* 2007;131:861–72.
149. Shen YH, Shoichet MS, Radisic M. Vascular endothelial growth factor immobilized in collagen scaffold promotes penetration and proliferation of endothelial cells. *Acta Biomater*. 2008;4:477–89.
150. Narmoneva DA, Vukmirovic R, Davis ME, Kamm RD, Lee RT. Endothelial cells promote cardiac myocyte survival and spatial reorganization: implications for cardiac regeneration. *Circulation*. 2004;110:962–8.
151. Chiu LL, Radisic M. Scaffolds with covalently immobilized VEGF and Angiopoietin-1 for vascularization of engineered tissues. *Biomaterials*. 2010;31(2):226–41.
152. Yamashita J, Itoh H, Hirashima M, Ogawa M, Nishikawa S, Yurugi T, et al. Flk1-positive cells derived from embryonic stem cells serve as vascular progenitors. *Nature*. 2000;408:92–6.
153. Fan VH, Tamama K, Au A, Littrell R, Richardson LB, Wright JW, et al. Tethered epidermal growth factor provides a survival advantage to mesenchymal stem cells. *Stem Cells*. 2007; 25:1241–51.
154. Chiang CK, Chowdhury MF, Iyer RK, Stanford WL, Radisic M. Engineering surfaces for site-specific vascular differentiation of mouse embryonic stem cells. *Acta Biomater*. 2010;6: 1904–16.
155. Song H, Yoon C, Kattman SJ, Dengler J, Masse S, Thavaratnam T, et al. Regenerative Medicine Special Feature: interrogating functional integration between injected pluripotent stem cell-derived cells and surrogate cardiac tissue. *Proc Natl Acad Sci U S A*. 2010;107(8): 3329–34.

Biomaterials Approaches in Vascular Engineering: a Review of Past and Future Trends

16

Donny Hanjaya-Putra, Maureen Wanjare, and Sharon Gerecht

Contents

16.1	Introduction	458
16.1.1	The Importance of Vascularization	458
16.1.2	Cell Sources	459
16.1.3	Angiogenic Growth Factors	461
16.1.4	Scaffold Design	462
16.2	Concepts in Material Development and Tissue Requirements	463
16.2.1	Biomimetic Materials: A Lesson from Postnatal Angiogenesis	463
16.2.2	Natural and Synthetic Biomaterials	464
16.2.3	Cell Adhesion Regulates Vacuole Formation	466
16.2.4	Cell-Mediated Degradation Allows Lumen Formation	467
16.2.5	GFs and Oxygen Tension	468
16.2.6	Tube Stabilization by Prevascular Cells	469
16.2.7	Biomechanical Control Over Vascular Morphogenesis	470
16.3	Review of Previous Work	473
16.3.1	Hydrogels to Control Vascular Differentiation	473
16.3.2	Biomaterials for GFs and Gene Delivery	475
16.3.3	Biomaterials for Inducing Prevascularization	475
16.3.4	Microfabrication of Vascular Networks	478
16.4	Future Directions	478
	References	480

Abstract Creating functional vasculatures remains one of the fundamental challenges that must be addressed before large, complex tissue-engineered constructs can be used in clinical applications. Our current understanding of stem cell biology and vascular morphogenesis has allowed tissue engineers to design biomaterials that mimic the properties of native tissue and promote vascularization. Biomaterials approaches in

S. Gerecht (✉)

Department of Chemical and Biomolecular Engineering, Johns Hopkins Physical Sciences Oncology Center and Institute for NanoBioTechnology, Johns Hopkins University, Baltimore, MD 21218, USA
e-mail: gerecht@jhu.edu

tissue engineering include differentiation of vascular cells, delivery of angiogenic factors, *in vivo* and *in vitro* prevascularization, as well as microfabrication of complex vascular networks. This chapter will discuss the processes involved in vascular network assembly; these processes inspire the design of biomaterials to fit tissue vascularization. Previous work in this field will be described to allow discussion of the current state of the art and to provide insights into its future directions.

Keywords Endothelial cells (ECs) • Extracellular matrix (ECM) • Hydrogels • Smooth muscle cells (SMCs) • Vascular morphogenesis

16.1

Introduction

16.1.1

The Importance of Vascularization

A major purpose of tissue engineering is the therapeutic replacement of damaged organs or tissues with equivalent substitutes. Most tissues in the human body depend on the blood supply contained within blood vessels. Among its numerous functions, blood assists in the interstitial fluid exchange of nutrients, as well as in the delivery of oxygen to organs. Thus, in order to assimilate the different facets of tissue engineering within the body, the integration of blood must be considered. Vascularization involves the incorporation of blood as part of the tissue-engineered constructs and usually occurs spontaneously immediately after their implantation. Both the inflammatory wound-healing response and the hypoxic state of the implant contribute to this spontaneous vascularization [1]. The wound left by the surgical procedure induces an innate immune response, which results in the formation of fibrous tissues and microvasculature. At the same time, the encapsulated cells within the engineered tissue scaffold experience low oxygen tension, stimulating the release of angiogenic factors, such as VEGF [2]. Nonetheless, this spontaneous induction of vasculature is insufficient to supply the transplanted tissue with adequate oxygen and nutrients. Additional prevascularization within engineered constructs for skeletal muscle [3], cardiac patch [4–6], and skin graft have been reported to promote stem cell (SC) differentiation, to enhance the survival of the engineered constructs, and to facilitate their integration into host tissues. Clearly, additional strategies are required to induce vascularization within the engineered tissue constructs. Various vascular tissue engineering approaches endeavor to generate vascular networks within the engineered tissue constructs; these approaches encompass the differentiation of vascular cells, the delivery of angiogenic factors, *in vitro* and *in vivo* vascularization, as well as microfabrication of complex vascular networks. All of these approaches require a reliable source of vascular cells, angiogenic growth factors (GFs), and a scaffold design that serves as a temporary extra cellular matrix (ECM).

16.1.2

Cell Sources

Blood vessel formation occurs via either vasculogenesis or angiogenesis. Vasculogenesis takes place mainly in the embryo and involves the development of blood vessels *de novo* from the mesoderm layer. Angiogenesis involves the formation of blood vessels from an already established blood vessel network. The formation these blood vessels begins with the formation of nascent endothelial tubes by angiogenesis or vasculogenesis [7]. Most blood vessels are composed of endothelial cells (ECs) and supporting pericytes or vascular smooth muscle cells (SMCs), and fibroblasts. Endothelial cells form the inner surfaces of blood vessels; then, vascular smooth muscle progenitor cells are recruited to concentrically surround the endothelial layer [7]. Fibroblasts, primitive neuroectoderm-derived or mesodermally originated cells [8], are precursor cells that are able to make the ECM [8].

Vessel formation involves cell-to-cell communication, cell-to-matrix communication, and cytokine-regulated interaction [8]. Vascular tissue engineering also requires sources for ECs, vascular SMCs, and fibroblasts. Cells that have the potential to form networks of blood vessels are commonly infused into tissue constructs because of their potential to vascularize them (Fig. 16.1). For the most part, SCs do not have a predetermined fate; therefore, they are often used in vascularization. During the process of differentiation, SCs are induced by their microenvironment to form different types of cells in an organism. Advantages of using SCs include the ability to self-renew, the production of unaltered daughter cells, and the ability to provide specialized cell types. Additionally, cultured SCs often proliferate continuously, beyond the proliferating limit of primary cultured cells. SC sources are categorized as pluripotent SCs, multipotent SCs, and progenitor cells.

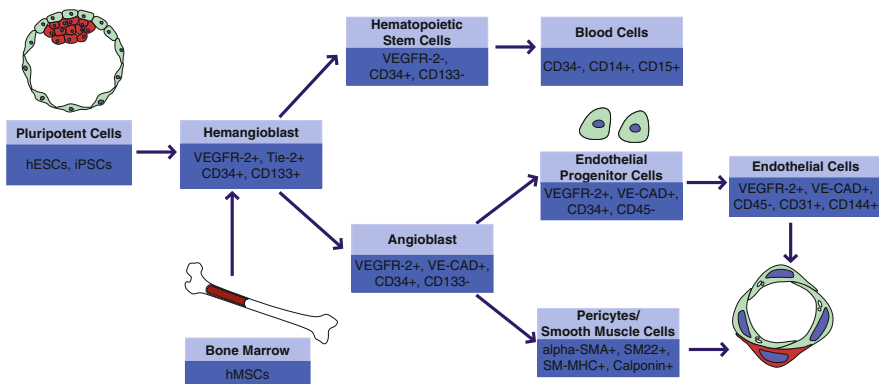


Fig. 16.1 Sources of cells for vascular engineering. Pluripotent cells, such as hESCs and iPSCs, can give rise to hemangioblast, which is precursor for both hematopoietic stem cells and angioblast. Vascular engineering utilizes endothelial cells and pericytes/smooth muscle cells to form stable and functional vascular networks

16.1.2.1

Embryonic Stems Cells and Induced Pluripotent Stem Cells

Pluripotent SCs have the ability to form all three germ layers of the body, i.e., the mesoderm, endoderm, and ectoderm. Pluripotent SCs can be derived from early embryos or induced from other SCs or terminally differentiated cells. Human embryonic SCs (hESCs) are derived from an embryo in its early stages as a blastocyst [9]. Hemangioblasts are cells from the mesoderm of the blastocyst that are precursors to blood islands [10]. In the embryo, hemangioblasts aggregate and migrate towards the yolk sack. In these aggregates, peripheral cells flatten and subsequently differentiate into ECs, while the cells located in the center of the hemangioblast aggregates differentiate into hematopoietic cells [11]. Vascular endothelial growth factor (VEGF) induces blood network formation of the hemangioblast cells by inducing migration, proliferation, and tube formation [10]. VEGF receptor 2 (VEGFR-2) is upregulated during early embryo development by VEGF [12], and has been considered the earliest differentiation marker for vascular cells [12, 13]. In vitro, vascular progenitor cells can be induced to differentiate into ECs and vascular SMCs with exposure to VEGF and platelet-derived growth factor (PDGF), respectively [13, 14]. We have recently reported a robust and efficient derivation of v-SMCs from hESCs using PDGF-BB and transforming growth factor-beta 1 (TGF- β 1) [15]. Induced pluripotent SCs (iPSCs) are derived by the transfer of transcription factors involved in pluripotency into adult stem cells or somatic cells. Induced pluripotent SCs maintain the developmental potential to differentiate into cell types from all three germ layers and could allow the generation of patient-specific pluripotent cells for regenerative medicine [16, 17]. Considerable research effort is focused on determining the sequential expression of vascular genes during differentiation, to elucidate the mechanism involved in vascular development, and to enable the derivation of vascular cells from a pluripotent population.

16.1.2.2

Mesenchymal Stem Cells

Mesenchymal SCs (MSCs) are multipotent SCs derived mainly from bone marrow or adipose tissue. Unlike pluripotent SCs, MSCs are easily isolated and expanded, and they differentiate into cell types of mesodermal lineages, including vascular cells [18]. VEGF and basic fibroblast growth factor (bFGF) have been shown to induce differentiation of bone marrow (BM) MSCs into vascular endothelium-like cells [19]. MSCs have also been shown to differentiate in vitro into SMCs and have been engineered to form blood vessel walls similar to native vessels [20]. Adipose tissue also represents a source of MSCs. The MSCs found in the stromal vascular portion of subcutaneous adipose tissue are known as processed lipoaspirate (PLA) cells. PLA cells secrete multiple blood vessels forming cytokines and GFs such as VEGF and hepatocyte growth factor (HGF) at bioactive levels [21]. The adipose-derived SCs are positive for endothelial and SC markers CD34, AC133, and ABCG2 [21]. An advantage of using adipose-derived SCs is that they represent a practical and abundant source of cells. Miranville et al. found that the stroma vascular fraction of adipose tissue contained CD34+/CD31- cells characteristic of endothelial progenitor

cells (EPCs) [21]. Traktuev et al. found that CD34 positive cells found in adipose tissue were resident pericytes that interacted with ECs (CD34+, CD31+, CD144+) [22]. The structural and functional interactions of the pericytes and the ECs played a role in vascular stabilization [22].

16.1.2.3

Progenitor Cells

Unlike SCs, progenitor cells differentiate into a predetermined cell type and are incapable of indefinite self-renewal. However, since progenitor cells are already committed toward a specific cell lineage, their differentiation into mature ECs is more easily attainable than directing the differentiation of ESCs or MSCs. Endothelial progenitor cells isolated from human peripheral blood and BM, are capable of differentiating into mature ECs in response to various stimuli, such as GFs, cytokines, and mechanical shear stresses [23]. Researchers have also demonstrated the isolation of EPCs from additional sources (besides the peripheral circulation and BM), including umbilical cord blood, liver tissue, or vascular walls themselves [24–27].

Recently, EPCs were redefined as endothelial colony-forming cells, which are rare circulating EPCs with robust proliferative potential and vessel-forming activity in vivo [28, 29]. The utilization of hEPCs to engineer blood vessels has mostly been investigated in the context of their ability to generate networks within scaffolds in vitro and to enhance network formation in vivo [30]. A recent study compared the formation and functions of tissue-engineered blood vessels generated by peripheral-blood- and umbilical-cord-blood-derived EPCs in a model of in vivo vasculogenesis. The study found that adult peripheral blood EPCs formed blood vessels that were unstable and regressed within 3 weeks. In contrast, umbilical cord blood EPCs formed normal functioning blood vessels that lasted for more than 4 weeks [24].

16.1.3

Angiogenic Growth Factors

The incorporation of GFs has been established as an effective method of promoting the formation of blood vessels. The major GFs important in vascularization include isoforms of VEGF, angiopoietins (Ang), PDGF, isoforms of fibroblast growth factor (FGF), TGF, HGF, and interleukin-8 (IL-8) [31].

The biological activity of VEGF, a homodimeric heparin-binding glycoprotein, is primarily focused on ECs during blood vessel formation [31]. VEGF has six isoforms, including VEGF₁₂₁, VEGF₁₆₅, VEGF₁₈₉, and VEGF₂₀₆ [31]. VEGF binds to two tyrosine kinase receptors, VEGF receptor-1 (VEGFR-1) and VEGF receptor-2 (VEGFR-2). EC migration and sprouting is upregulated by VEGF [31]. Seven days after implantation of cells in severe combined immunodeficiency mice, blood vessel density was experimentally observed to be an order of magnitude greater with the use of VEGF than with samples that

16 did not contain the GF [32]. VEGF is produced by many cell types, such as ECs, fibroblasts, and keratinocytes [31].

Angiopoietins are important partners of VEGF [31]. The angiopoietin-1 (Ang-1) and angiopoietin-2 (Ang-2) isoforms both bind to the receptor tie-2, and both are important in vascularization [31]. Ang-1 has the ability to phosphorylate the tie-2 receptor. Ang-2 is an antagonist of Ang-1 and cannot phosphorylate the tie-2 receptor [31]. Ang-2 blocks interactions between Ang-1 and tie-2. Ang-1 and VEGF are GFs specific for ECs. Ang-1 leads to the migration of ECs and the sprouting and formation of blood vessels in vitro [31]. Ang-2 is believed to have a role in destabilizing existing blood vessels [31].

PDGF stimulates the growth and movement of fibroblasts and SMCs [33]. The PDGF receptors are found mostly on ECs that occur in tube formation during angiogenesis [33]. During tissue repair, PDGF also assists with the formation of vascularized connective tissue [33]. The dual delivery of VEGF and PDGF B (PDGFB) in mouse hindlimbs was observed to produce a significantly higher proportion of mature blood vessels than the use of VEGF alone or PDGF alone [34].

The FGF family has 20 members. The first two of the GFs, FGF1 (acidic fibroblast growth factor or aFGF) and FGF2 (also known as bFGF), are important in blood network formation. Both bFGF and aFGF are single nonglycosylated polypeptides that have similar biological behaviors [31]. Both molecules interact with heparin sulfate proteoglycans in the ECM and are synthesized by inflammatory cells, dermal fibroblasts, and vascular ECs [31]. Both also support EC proliferation and migration during early stages of wound repair by clot formation and fibrin deposition [31]. They also induce EC differentiation [31].

TGF- β plays an important role in blood network formation by controlling cell proliferation, capillary tube formation, and ECM deposition [31]. Three isoforms of TGF- β (TGF- β 1, TGF- β 2, TGF- β 3) all bind to the same receptors and have the same biological responses in cell cultures, but they play distinct biological roles in vivo [31]. TGF- β is able to stimulate EC migration differentiation, tubule formation, and ECM deposition during blood network formation [31]. Additionally, it can induce blood network formation by indirectly recruiting inflammatory cells that release VEGF, PDGF, and FGF [31].

16.1.4

Scaffold Design

Three-dimensional (3D) scaffolds are used in vascularization because they imitate cells' natural surroundings. Additionally, scaffolds also provide a delivery vehicle for GFs and cells. Almost all tissue cells and blood vessels are surrounded by an ECM, a complex 3D fibrous meshwork [35]. The ECM contains different fibers that provide biochemical signals and sites for GFs storage. The ECM also serves as a scaffold, maintaining the structure of blood vessel wall shape and absorbing the mechanical forces generated by the pulsatile blood flow in the vessels [36]. The ECM around blood vessels is composed of three layers; the tunica intima, the tunica media, and the tunica adventitia. The EC layer of blood vessels is anchored on a basement membrane, which is the major component of the tunica intima [36]. The basement membrane contains network-organizing proteins, such as collagen IV, collagen XVIII, laminin, nidogen, entactin, and the proteoglycan perlecan. The tunica media

contains elastic tissue and vascular SMCs, while the tunica adventitia contains fibroelastic connective tissue [36]. Since the ECM surrounds cells and blood vessels *in vivo*, the incorporation of 3D scaffolds in tissue constructs is therefore essential in vascularization in order to emulate the body's ECM. Three-dimensional scaffolds are generated using either natural or synthetic polymers. Common natural polymers include collagen, gelatin, hyaluronate, glycosaminoglycan, chitosan, alginate, silk, fibrin, dextran, and Matrigel [35]. Common synthetic polymers include polyglycolic acid (PGA), polylactic acid (PLA), polylactic-co-glycolic acid (PLGA), poly-L-lactic acid (PLLA), poly-*ε*-caprolactone (PCL), polyethylene glycol (PEG), polyvinyl alcohol (PVA), polypropylene fumarate (PPF), and polyacrylic acid (PAA) [35]. Selection of materials for 3D scaffolds depends on biocompatibility, wettability, mechanical properties, and biodegradability. The natural ECM is a hydrated gel, and so hydrogels, which are networks of hydrophilic polymer chains, are commonly used as 3D scaffolds [35]. However, setbacks, such as weak cell adhesion caused by both the hydrophilicity of hydrogels and the lack of cell-binding motifs, arise when utilizing hydrogels [35]. Recent advances in biomaterials design has allowed the development of synthetic hydrogels which mimic the native ECM to direct vascular morphogenesis [37].

16.2

Concepts in Material Development and Tissue Requirements

16.2.1

Biomimetic Materials: A Lesson from Postnatal Angiogenesis

In contrast to vasculogenesis during embryonic development, postnatal angiogenesis occurs throughout adulthood, allowing the formation and regeneration of new blood vessels. More recent studies have suggested that adult neovascularization and therapeutic vascularization include postnatal vasculogenesis, angiogenesis, and arteriogenesis. BM-derived endothelial progenitor cells (EPCs) can mobilize to the site of vascularization in response to cytokines, tissue ischemia, and injury. This process involves a complex and co-regulated interaction between vascular cells and their surrounding environment. In recent decades, our understanding of neonatal angiogenesis has been vastly expanded, primarily due to well-defined *in vitro* models. The most common models are cultures of ECs in gels made of different ECM components, such as collagen, fibrin, fibronectin, and Matrigel. As part of the native tissue, these complex ECM architectures provide instructive physical and chemical cues that direct vascular morphogenesis, which involves several steps: (1) proteolytic degradation of basement membrane proteins by both soluble and membrane-bound MMPs, (2) cell activation, proliferation, and migration, (3) vacuole and lumen assembly into a tube with tight junctions at cell-cell contacts, (4) branching and sprouting, (5) synthesis of basement membrane proteins to support the formation of capillary tube networks, and (6) tube maturation and stabilization by pericytes (Fig. 16.2). It is evident that these complex processes require a delicate balance between various immobilized factors and soluble GFs, as well as endothelial and prevascular cell interactions. Since every step of vascular

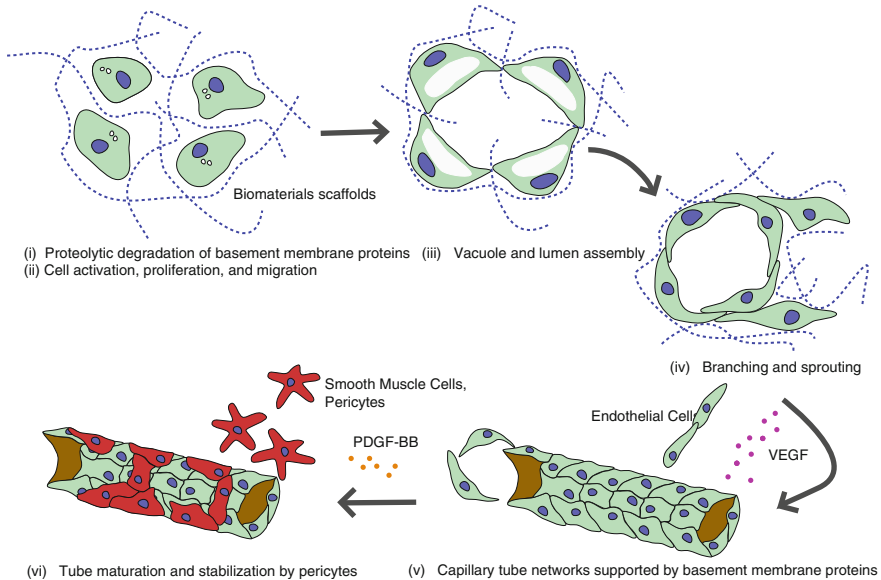


Fig. 16.2 Molecular regulation in vascular morphogenesis. Biomaterials scaffold for vascular engineering sought to support vascular morphogenesis, which involves several stages. (1) proteolytic degradation of basement membrane proteins by both soluble and membrane-bound MMPs, (2) cell activation, proliferation, and migration, (3) vacuole and lumen assembly into a tube with tight junctions at cell–cell contacts, (4) branching and sprouting to form complex vascular networks, (5) synthesis of basement membrane proteins to support the formation of capillary tube networks, and (6) tube maturation and stabilization by pericytes or smooth muscle cells

morphogenesis has a unique requirement, each of the cellular cues must be presented with the correct spatial and temporal context to allow vascular morphogenesis to progress. The challenge is to design synthetic biomaterials that capture those microenvironments which are conducive to the formation of vasculatures.

16.2.2

Natural and Synthetic Biomaterials

The choice of material is the first crucial step in designing constructs for vascular engineering. Naturally derived materials have major advantages such as having desired adhesive and degradation sites preferable to guide cellular cues and tissue remodeling, yet their mechanical properties are not easy to control [37]. The first type of natural biomaterial, are macromolecules that can be found abundantly in the body and include glycosaminoglycans (GAGs), glycoproteins, and proteoglycans. Depending on their spatial and temporal distribution throughout the body, various ECM components have different effects on promoting or inhibiting angiogenesis. For example, hyaluronic acid (HA) and fibronectin, which are major components of the embryonic ECM, have been shown to be vital regulators for

vascularization during embryogenesis [38]. In particular, fibronectin is a unique glycoprotein which contains cell adhesion and heparin-binding sites that synergistically modulate the activity of VEGF to enhance angiogenesis [39]. Various lineage studies have shown developmental abnormalities in embryonic hearts and vessels in fibronectin-null mice, suggesting its crucial role in mediating EC interactions [40, 41].

In contrast, the adult ECM consists mostly of laminin-rich basement membrane, which maintains the integrity of the mature endothelium, and interstitial collagen I, which promotes capillary morphogenesis [42]. Although collagen I is present during development, its role becomes increasingly important in postnatal angiogenesis after its reactive groups have been cross-linked to further stabilize the interstitial matrix [43]. Matrigel, isolated from cancer cells, is a solubilized basement membrane protein which is enriched in laminin and contains various GFs. Due to its biological properties, which mimic those of ECM, Matrigel has been used as a model to study both *in vitro* and *in vivo* angiogenesis. Within a few hours after seeding ECs on Matrigel, ECs are known to form capillary-like structures (CLSs), which mimic the process of *in vivo* angiogenesis. In vascular tissue engineering, Matrigel has been widely used to facilitate cell adhesion and to promote vascularization of tissue constructs [3–5]. Therefore, depending on the desired tissue microenvironments to be engineered (e.g., adult versus embryo and skin versus brain), the choice of material is crucial in promoting or inhibiting angiogenesis.

The second type of natural biomaterial are macromolecules that cannot be found in the body but can be easily isolated from plants (i.e., dextran and alginate) or animals (e.g., chitosan). Unlike the ECM components, these polysaccharides are inert and do not actively interact with cells; thus, they can be used as blank templates to engineer a cell-instructive scaffold to promote vascularization. In the absence of cell-adhesive ligands, the interactions between cells and these inert biomaterials are mediated primarily by adsorbed proteins through surface topography and hydrophilicity [44]. For instance, basic chemistry can be used to modify dextran, which is naturally resistant to protein adsorption and cell adhesion, into a bioactive scaffold for vascular tissue engineering with various VEGF release profiles [45]. Furthermore, introducing different functional groups into the sugar backbone alters the affinity and conformation of the adsorbed proteins, leading to enhanced integrin binding and cellular response [46].

Although this type of modification seems attractive, the approach still requires the addition of ECM components to facilitate their bioactivity, which raises many issues, such as a complex purification process, pathogen transfer, and immunogenicity. Therefore, a greater need exists to engineer a purely synthetic biomaterial which is xeno-free and instructive for vascular engineering. This synthetic biomaterial can be engineered from natural biomaterials (excluding ECM components), artificial protein polymers, self-assembling peptides, and synthetic polymers to form scaffolds which mimic the native ECM. For example, dextran and chitosan are natural biomaterials which have similar structures and do not possess any inherent cross-linking ability. However, a simple chemical modification, like introducing double bonds into the repeating unit, allows the cross-linking of these polysaccharides to form hydrogels. Alginate is another natural material which can be physically cross-linked by the addition of cations (i.e., Ca^{2+} or Mg^{2+}). Another option is to use a purely synthetic material, like PEG or PLGA. The pioneering work of the Hubbell research group turned PEG, a cell-resistant material, into instructive scaffolds for *in vivo*

16 vascularization [47, 48]. Furthermore, the synthetic material of choice must be biodegradable and biocompatible, and such physical properties as pore size, degradation kinetics, and elasticity, must be easily tunable to favor vascular morphogenesis. Instead of incorporating the ECM components to make it bioactive, certain synthetic peptides important for vascular morphogenesis can be incorporated into this inert synthetic material. The most common template is fibronectin, which contains binding domain arginine-glycine-aspartic acid (RGD), heparin-binding sites to regulate angiogenic GFs (VEGF, bFGF, etc.), and degradable sequences to allow vascular morphogenesis [42].

16.2.3

Cell Adhesion Regulates Vacuole Formation

Vascular cells sense their surrounding microenvironments through integrin receptors, which represent the first crucial step in vascular morphogenesis. Integrin is a transmembrane receptor which not only maintains cell adhesion to ECM but also controls cell proliferation, migration, differentiation, and cytoskeletal organization. Since blood vessels must be able to assemble in diverse tissue environments (e.g., adult versus embryo; and skin versus brain) which have different ECM components, it is evident that both β_1 and α_v integrins can support vascular morphogenesis. For example, $\alpha_1\beta_1$ and $\alpha_2\beta_1$ integrins control vascular morphogenesis in collagen-rich ECM, like adult tissue, while $\alpha_5\beta_1$ and $\alpha_v\beta_3$ integrins involve in fibronectin- and fibrin-rich ECM, like in embryonic tissue and healing wounds [42]. Regardless of the types of integrin involved, the binding of integrins onto RGD triggers several downstream signaling events mediated by Rho GTPase, particularly Rac1 and Cdc42 [49]. Extensive work by Davis and his colleagues has revealed the molecular mechanism that regulates this EC morphogenesis in fibrin and collagen gels. Fibrin hydrogels consist of polymerized fibrinogen, which, when thrombin is added, form nanometer scaled fibers that, to some extent, mimic those of ECM. Because they have binding sites for angiogenic GFs, fibronectin, and von Willebrand factor, fibrin hydrogels have been widely used to study the mechanism of angiogenesis in vitro [50, 51]. Using fibrin and collagen hydrogels as an in vitro angiogenesis model, Davis et al. showed that RGD-dependent pinocytotic events resulted in formation of vacuoles, which further coalesce into a developing lumen [52]. The model of highly dynamic vacuoles fusing into an open lumen has been further confirmed in vivo [53]. Consequently, in the context of engineering a synthetic biomaterial, both the amount of RGD and the method of presentation can determine the extent of vascular morphogenesis. The RGD-binding peptides ought to be presented at a level sufficient to facilitate cell binding and vacuole formation but not in excess, such as to inhibit branching and sprouting. Using an in vitro angiogenesis model, Folkman and Ingber were able to show that, when cultured on a moderate coating density that only partially resisted cell traction forces, ECs were able to retract and differentiate into branching capillary networks [54, 55]. High ECM density was saturated with RGD adhesion peptide, which allowed the cells to spread and proliferate, while low ECM density resulted in rounded and apoptotic cells. Interestingly, in medium ECM density, with the appropriate RGD adhesion peptide, ECs collectively retracted and differentiated into branching capillary networks with hollow tubular structures. It is evident that ECs exerted mechanical

forces on the surrounding ECM to create a pathway for migration and branching in forming vascular structures [56]. Hence, both the quantity of RGD peptide and the method of presentation within the engineered synthetic biomaterials determine the first morphogenetic event in angiogenesis.

16.2.4

Cell-Mediated Degradation Allows Lumen Formation

Scaffold degradation can control both structural integrity and temporal properties, which include the presentation of chemical and mechanical cues at various stages of angiogenesis. Ideally, the scaffold degrades over time to allow cellular infiltration, lumen formation, and ECM synthesis and distribution, all of which occur within 3–5 days in collagen and fibrin hydrogels. Through a comprehensive understanding of cell-mediated degradation in vascular morphogenesis, biomaterials properties (i.e., pore size, mechanics, and degradation profile) can be exploited to enhance tubulogenesis. Once ECs and the supporting prevascular cells are able to bind into the engineered scaffolds, they have to migrate and remodel their surrounding ECM in order to form, stabilize, and induce regression of the vascular networks. Matrix metalloproteinase (MMP), a family of zinc-dependent endopeptidases, digest specific ECM components and activate other type of MMPs and GFs in order to control angiogenesis [57]. Soluble MMPs are secreted as proenzymes, which can be activated by multiprotein complexes of membrane type-MMPs (MT-MMPs) and urokinase plasminogen activator (u-PA) to localize matrix degradation to the close vicinity of the cells [58]. For instance, circulating VEGF induced the expression of MMP-9 in BM, which resulted in mobilizing endothelial and mast progenitor cells to the site of vascularization, further increasing the expression of VEGF [59]. At this initial stage of vascularization, MMPs mediated the breakdown of basement membrane, exposing quiescent EC to collagen-I and fibrin-enriched interstitial matrix, which resulted in EC proliferation, invasion, and migration. We and others have shown that MT1-MMP activates pro-MMP-1, -2, and -9, which enable EC migration and tube morphogenesis in collagen [60, 61], fibrin [62], and hyaluronic acid/gelatin hydrogels [63]. In order for the intracellular vacuoles to coalesce into a lumen, ECs require adhesive ligands for traction [37] and utilize MT1-MMP to create physical spaces which facilitate the directed migration of cells to align with neighboring cells [56, 60, 64]. Unlike ECM components, that inherit these proteolytic degradation sites, most synthetic biomaterials are designed to degrade by ester hydrolysis, a process which is uncommon *in vivo*. Therefore, ECs can only invade this synthetic scaffold if the minimal pore size is larger than the cell diameter (e.g., a soft self-assembling peptide) [65] or if the scaffold bears an MMP-degradable sequence [66]. The Hubbell research group has pioneered this approach by incorporating an MMP-degradable sequence as a cross-linker into PEG scaffolds to promote vascular healing and therapeutic angiogenesis [67, 68]. When grafted *in vivo*, ECs were able to invade, remodel, and vascularized this MMP-sensitive scaffold [67, 69]. Hence, incorporating MMP-degradable peptides is essential to direct vascular morphogenesis in 3D synthetic biomaterials.

16.2.5

GFs and Oxygen Tension

A complex series of soluble GFs are needed to recruit and differentiate vascular progenitor cells, as well as to orchestrate the process of tube formation and stabilization. The challenge is to design synthetic biomaterials to deliver these regulatory factors with controllable pharmacokinetics. During embryogenesis, the earliest blood vessels originate from a mesoderm lineage and differentiate into hemangioblasts in response to bFGF and VEGF. Then, VEGFR-2⁺ cells can further differentiate into either ECs or SMCs in the presence of VEGF or PDGFB, respectively [13]. VEGF, a key angiogenic factor, stimulates EC survival, migration, and proliferation [70]. In the early stage of angiogenesis, VEGF and bFGF have been shown to synergistically stimulate EC sprouting and tube assembly [52]. Since VEGF has a half-life of less than 90 min in the circulation [71] and a narrow therapeutic concentration range, which if exceeded can cause leaky and unstable capillary walls [72], designing synthetic biomaterials with the right temporal and spatial presentation of VEGF is crucial for angiogenesis [73]. One strategy is to design a cell-demanded release of VEGF by chemically immobilizing VEGF with an MMP-degradable sequence within the scaffold. Two weeks after implantation, grafted scaffolds were found to be highly vascularized, indicating that host vascular cells remodeled the scaffolds and formed vascular networks in response to the sustained release of VEGF [67].

In the next step in angiogenesis, tube stabilization is regulated by GFs secreted by both ECs and prevascular cells. A nascent blood vessel secretes PDGFB to promote the proliferation, migration, and recruitment of mural cells. Once recruited, mural cells secrete Ang1 to suppress EC apoptosis, coordinate vascular polarity, and promote vessel stabilization. TGF- β , Ang2, and placental-like growth factor (PLGF) are also known to further induce ECM production, growth arrest, vessel stabilization, and maturation. Hence, the concept guiding the design of materials should be to deliver VEGF in tandem or sequentially with other GFs [44]. The work of the Mooney research group elegantly captured this dynamic balance between tube formation and stabilization. Due to the different affinities for alginate hydrogels, encapsulated VEGF and PDGF showed distinct release kinetics profiles that can be used therapeutically to form mature blood vessels supported by SMCs and to restore cardiac function in a rat model of myocardial infarction [74]. A recent study has improved this strategy by immobilizing the GFs within the scaffolds [75]. Covalent immobilization can prolong GF bioactivity by protecting against cellular inactivation and receptor/ligand complex internalization, and can better control local vascularization within the scaffolds. One week after implantation, mature and stable blood vessels were found in collagen gel with covalently immobilized VEGF and Ang-1 [75].

Another consideration in designing synthetic biomaterials is the distribution of oxygen along the scaffolds. Oxygen is much less able to diffuse across a thick scaffold and tissue than across stirred medium in a bioreactor. Consequently, cells encapsulated inside scaffolds will have different affinities toward oxygen than those distributed around the perimeter of the scaffolds. Vascular cells, and in particular ECs, are known to have a molecular mechanism to compensate for lower oxygen consumption. Hypoxia-inducible factor-1 α (HIF-1 α) is a transcription factor which is selectively stabilized under physiological oxygen tension

(20%) and which becomes activated under hypoxic conditions (3–5%) [76]. HIF-1 α plays a critical role in both angiogenesis and vasculogenesis by mediating the hypoxia-induced production of VEGF and other angiogenic cytokines/GFs – such as stromal-derived factor 1 (SDF1), stem cell factor, placental GF, angiopoietin 1 and 2, and PDGF-BB – which are involved both in the local activation of ECs and the mobilization and recruitment of EPCs, MSCs, and other BM-derived angiogenic cells [77–80]. Hence, a precise control over the oxygen gradient across tissue-engineered constructs could, in turn, enhance vascularization.

16.2.6

Tube Stabilization by Prevascular Cells

The next step in angiogenesis is tube stabilization, which is tightly controlled by the interaction between ECs and mural cells, such as pericytes in capillaries and SMCs in arteries. Once a nascent tube has been established, MMP activity must be inhibited to avoid prolonged matrix degradation, tube leakage, and vascular regression. The adventitia region of blood vessels is enriched not only by the supporting ECM but also by fibroblasts, which can migrate and differentiate into pericytes through heterotypic interaction with ECs [81–83]. The D'Amore research group has intensively studied the interaction between ECs and 10T1/2 mesenchymal precursor cells through PDGF and TGF- β signaling, that mediates pericyte and SMC differentiation [82]. In addition to secreting Ang-1 to act on the Tie-2 receptor on ECs, these pericytes also secrete tissue inhibitor matrix complex-3 (TIMP-3) to inhibit MT-MMPs, MMPs, and VEGF-R2, which will stop EC invasion and morphogenesis [42, 60, 84, 85]. These EC-pericyte interactions further induce ECs to secrete TIMP-2 – which inhibits MT-MMPs, MMPs, and disintegrin – and metalloproteinases (ADAMs) to stabilize tube assembly. To capture this delicate balance, synthetic biomaterials ought to integrate both MMP-degradable sequences, to allow vascular morphogenesis, and nonproteolytic degradable sequences, to support vascular stabilization and structural integrity prior to *in vivo* implantation.

Moreover, coculture of ECs and prevascular cell precursors is also required to form a stable blood vessel within the engineered scaffolds. A coculture of human umbilical vein ECs (HUVECs) and 10T1/2 mesenchymal precursor cells in a fibronectin-collagen gel scaffold has been shown to form a long-lasting blood vessel *in vivo* [24, 86, 87]. A similar approach has been used to coculture HUVECs and embryonic fibroblasts into porous PLGA/PLLA scaffolds coated with Matrigel to induce vascularization in skeletal muscles [3] and in cardiac constructs [4, 5]. These perivascular cell precursors are suggested to play a vital role in forming stable blood vessels in three ways: (1) secreting ECM to direct vascular morphogenesis, (2) supporting vessel walls by differentiation into SMCs, and (3) expressing angiogenic factors to support EC survival. Collectively, these studies suggest that such perivascular cell precursors as 10T1/2 mesenchymal precursor cells and embryonic fibroblasts are active partners of ECs in forming stable and functional vessels within the engineered tissue construct.

16.2.7

Biomechanical Control Over Vascular Morphogenesis

It has become increasingly evident that the biomechanical properties of ECM, such as matrix orientation and mechanics, play a profoundly influential role in controlling vascular morphogenesis. Due to its versatility and mechanical properties (i.e., cross-linking density, pore sizes, and topography), ECM has powerful features that can be exploited to further direct vascularization.

16.2.7.1

Matrix Orientation

Native ECM provides an instructive template for ECs and perivascular cells to orient, interact, and organize into tubular structures. Perivascular cells, such as fibroblasts, are primarily responsible for laying down ECM components in early embryogenesis and continue to do so throughout adulthood. Various studies using fibroblast-derived matrix have revealed the 3D complexity of these ECM networks [88–90]. A recent study by Soucy and Romer showed that a fibroblast-derived matrix alone is sufficient to induce HUVECs to undergo vascular morphogenesis independent of any angiogenic factors. Further colocalization analyses suggested that fibronectin with a distinct structure and organization was uniquely distributed among other secreted matrix components, such as collagen, tenascin-C, versican, and decorin. Cell matrix adhesions and MT1-MMP activity were reported to orient and localize within this fibrous fibronectin, which is indicative of integrin-mediated vascular morphogenesis [91]. The unique orientation, organization, and nanotopography of fibrous fibronectin represent features that can be integrated into synthetic scaffolds. Synthetic polymers, like PLGA and PCL, can be electrospun to produce various fiber sizes with micro- to nanoscale features that resemble fibrous fibronectin. We have previously shown that surface nanotopography enhanced the formation of CLSs *in vitro* [92]. When grown on 600 nm width grooves, EPCs showed reduced proliferation and enhanced migration, but no changes in expression of EC markers. Moreover, after 6 days of culture, EPCs organized into superstructures along the nano grooves, in significant contrast to EPCs grown on planar surfaces (Fig. 16.3). The addition of Matrigel further induced the formation of CLSs with enhanced alignment, organization, and tube length compared to a flat surface. This underscores the increasingly important role of nanotopography in guiding and orienting vascular assembly. When integrated into the tissue-engineered construct – for instance, using filamentous scaffold geometry [93] and micropatterning [94] – the orientation and structure of the engineered vasculature can be controlled.

16.2.7.2

Matrix Mechanics

Changes in ECM mechanics can lead to focal changes in GF availability [54, 75], drive capillary morphogenesis [95], and stimulate angiogenesis *in vivo* [96]. By altering matrix

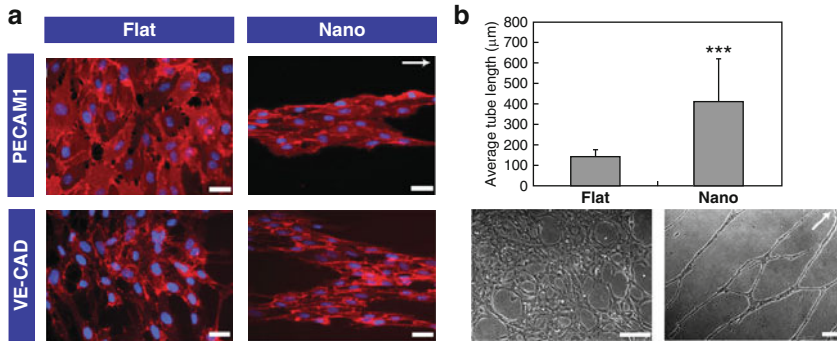
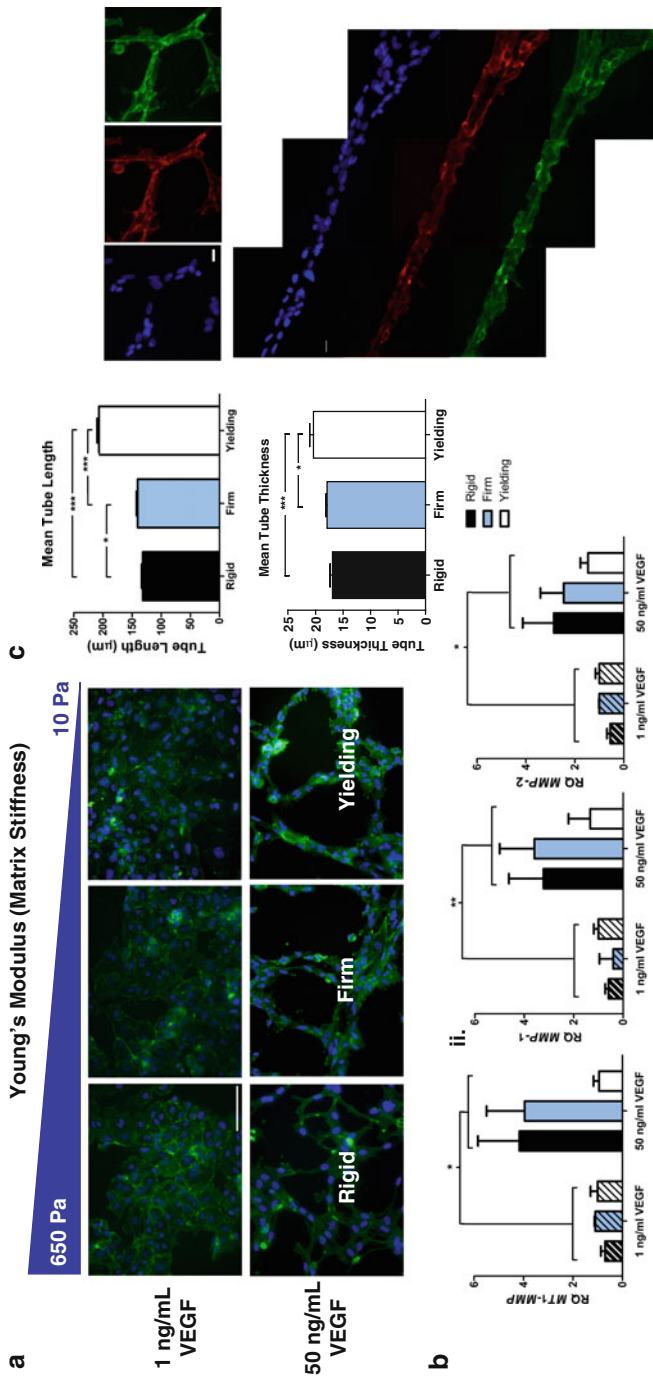


Fig. 16.3 Requirement for synthetic ECM – topography. **(a)** Nanotopography induces the formation of supercellular band structures in long-term EPC culture. EPCs cultured on flat substrates began forming confluent layers of cells after 6 days of culture. In contrast, EPCs cultured on nanotopography began to form supercellular band structures aligned in the direction of the features (as indicated by the *arrow*) after 6 days of culture. These morphological differences are evident through staining of PECAM-1 and VE-CAD. *Scale bars* are 50 μm . **(b)** Organized capillary tube formation in vitro. Capillary-like structures (CLSs) were induced by the addition of Matrigel after 6 days. EPCs cultured on flat substrates (*lower left*) formed low-density unorganized structures, while EPCs cultured on nanotopographic substrates (*lower right*) formed extensive networks of organized structures with (*upper panel*) longer average tube lengths than EPCs cultured on flat substrates ($***p < 0.001$). The direction of the linear nanotopographic features is indicated by the *arrow*. *Scale bars* are 200 μm . Printed with permission [92]

adhesivity and mechanics, Ingber and Folkman illustrated how FGF-stimulated ECs can be switched between growth and differentiation during angiogenesis. Recently, biomechanical cues from the ECM and signals from GF receptors have been implicated as regulating the balance of activity between TFII-I and GATA2 transcription factors, which govern the expression of VEGFR2 to instigate angiogenesis [97]. Matrix stiffness not only regulates cell response to soluble GFs, but also cell morphogenesis during angiogenic sprouting. The tip of a new capillary sprout has been found to become thinner, primarily due to MMP activity, to locally degrade the basement membrane proteins. This region, with a high rate of ECM turnover and a thin basement membrane, becomes more compliant and stretches more than the neighboring tissue. Consequently, the decrease in matrix stiffness changes the balance of forces across cell integrin receptors, increases cell tension, and results in cytoskeletal arrangement to form branching patterns that are characteristic of all growing vascular networks [95]. We and others have shown that a decrease of matrix stiffness in collagen gels [98, 99], fibrin gels [100, 101], self-assembling peptides [65], and HA hydrogels [63] resulted in an increase of capillary branching, elongated tubes, and enlarged lumen structures. On a relatively compliant matrix, EPCs do not have to produce as many MMPs in order to degrade, exert mechanical tension, and contract the matrix for vascular morphogenesis to occur. On the other hand, on a stiffer matrix, EPCs have to produce more MMPs to overcome the extra mechanical barriers; even then, this local decrease in substrate stiffness cannot support vascular morphogenesis (Fig. 16.4) [63]. This model also



explains the rapid appearance of large functional vessels in granulation tissue as a response to the wound healing mechanism [96]. Soon after the engineered vascularized tissue construct has been implanted *in vivo*, the process of wound healing begins with an initial inflammation reaction, the deposition of fibrin matrix, and an immediate reaction from the host's immune system [102]. Together with neutrophils and macrophages, activated fibroblasts appear in the wound within 2–3 days after surgery. These activated fibroblasts differentiate into myofibroblasts that express α -smooth muscle actin (α -SMA), which is responsible for secreting ECM components and contracting the surrounding tissue. Recently, fibroblast invasion has been shown to result in a compliant, contracted matrix, which is responsible for the large vascularization found at the site of implantation [96]. In light of this, the cross-linking density of a synthetic biomaterial, which in turn controls matrix stiffness, can be easily manipulated to vary GF availability and to direct vascularization. Collectively, these findings highlight the relevance of engineering a synthetic scaffold with mechanical elasticity suiting the specific needs of tissue vascularization.

16.3

Review of Previous Work

16.3.1

Hydrogels to Control Vascular Differentiation

16.3.1.1

Alginate

Alginate is a polyanionic copolymer derived from sea algae and has 1,4-linked β -D-mannuronic (M) and α -L-guluronic (G) residues [103]. The M and G residues vary in proportion and distribution along a polymer chain [103]. The polymer is biocompatible and forms hydrogels when exposed to such multivalent cations as calcium and barium ions. Hydrogels are formed when the multivalent ions and the carboxylic acid group on the alginate backbone form ionic bonds [103]. When used for cell immobilization and microencapsulation, alginate hydrogels typically have small pores in the nanometer range in order to prevent cell movement out of the hydrogel [103]. Calcium-binding alginate polymers have been used in the encapsulation and transplantation of pancreatic cells with the retention of normal function and with greater viability than nonencapsulated transplants *in vivo* in animal models [104, 105]. Human embryonic SCs have also been encapsulated; however, differentiation is nonspecific after transplantation in mice [106]. As a consequence of their biocompatibility and their ability to entrap cells, alginate scaffolds are readily used for vascularization. For successful vascularization, alginate scaffold pores should be interconnected and large enough to incorporate the ingrowth of blood vessels after implantation (i.e., on the order of several hundred micrometers in size) [1]. In alginate scaffolds with 90% porosity and pore sizes ranging from 50 to 200 μm , we observed hESCs aggregation and formation of embryoid bodies after 48 h

16 [107]. Alginate did not hinder differentiation, because embryoid bodies derived from the scaffolds differentiated into all three germ layers [107]. Evidence of vasculogenesis within scaffolds has also been reported, with the observation of the formation of voids and tubelike structures and with the majority of cells positive for the CD34 marker [107].

Experimentally, delivery of the bFGF encapsulated in 3D scaffolds accelerated vascularization after the implantation of the scaffolds in the mesenteric membrane of the rat peritoneum [108]. Lambert et al. observed that alginate scaffolds containing encapsulated bFGF had nearly four times more capillary ingrowth after implantation compared to alginate scaffolds not containing bFGF [108].

16.3.1.2

Hyaluronic Acid/Hyaluronan

HA, or hyaluronan, makes up a major part of the ECM in connective tissues, and the human body is estimated to contain 20 g of HA [109]. HA is ubiquitously distributed and facilitates cells adhesion, proliferation, motility, and morphogenesis [38, 110–112]. HA is a glycosaminoglycan composed of a nonsulfated polysaccharide of (1-b-4) D-glucuronic acid and (1-b-3) N-acetyl-D-glucosamine [109]. The carboxylic and hydroxyl groups make the HA molecule easy to modify. HA chains are semiflexible in solution and, consequently, HA is a useful space-filling molecule with the ability to deform [109]. Cells can be encapsulated in HA-based scaffolds using photopolymerization, i.e., the use of light to initiate the formation of cross-linked HA hydrogel networks [113]. Advantages of HA scaffolds include biocompatibility and noninvasive implantation of prepolymer constructs by exposure to low intensity visible or ultraviolet light [113]. We previously reported that HA matrices support self-renewal of hESCs and direct their vascular differentiation [114].

16.3.1.3

Dextran

Dextran is a polysaccharide derived from bacteria and degraded by dextranase. Dextran coatings limit cell adhesion and spreading [115]. Dextran-based hydrogels are biocompatible and are comparable to the synthetic polymer PEG [115]. Dextran hydrogels can be generated by physical or chemical cross-linking by covalent attachment of polymerizable groups. Hydrogels developed from methacrylated dextran and PEG produce macropores in the gels ranging from 10 to 120 μm , which is preferable for cell migration [116]. Acrylated dextran hydrogels that can encapsulate cells have also been developed [117]. Ferreira et al. conducted a vascularization study in which hESCs were encapsulated in a dextran-based hydrogel using microencapsulated VEGF₁₆₅ and a tethered RGD peptide [118].

16.3.2

Biomaterials for GFs and Gene Delivery

It is well established that the stimulation of new vessel formation *in vivo* can be achieved by delivering angiogenic factors, either as GF proteins or via gene transfer, directly to the targeted site. This strategy, also known as therapeutic angiogenesis, can be integrated into engineered tissue constructs to stimulate different stages of blood vessel formation and to enhance their vascularization after implantation. At the first stage, VEGF and bFGF can induce the mobilization, recruitment, and activation of EPCs to undergo vascular morphogenesis [56, 59, 63, 82, 119]. The delivery dosages of these GFs must be tightly controlled to enhance angiogenesis without creating vascular leakage, hypotension, and hemorrhage [120]. Therefore, a more promising approach delivers a cocktail of angiogenic molecules – such as VEGF, PlGF, Ang-1, PDGF, and TGF- β – involved in vessel formation and stabilization [120]. The methods of delivering VEGF, whether dual versus sequential release or soluble versus immobilized with other combinations of GFs, could strongly affect the degree of vascularization [73–75]. Sequential delivery of VEGF and PDGF in alginate hydrogels induced mature vascular networks in a hindlimb ischemia model [34]. Covalently immobilized VEGF and Ang-1 in collagen gel increased vascular ingrowth into the scaffolds [75]. Coupling GFs with MMP-degradable peptides could turn a synthetic polymer into bioactive scaffolds to promote vascularization [67, 68]. In addition to the delivery of GFs to directly stimulate angiogenesis, various strategies have focused on delivering small transcription factors, such as HIF-1 α [121], sonic hedgehog homolog (SHH) [122], or bone morphogenetic protein (BMP)-2, -4, or -6 [123], all of which induce surrounding cells to secrete angiogenic GFs. Particularly, gene delivery has been explored to generate populations of cells that constitutively express either VEGF or a stabilized form of HIF-1 α . Since it lacks the oxygen-sensitive degradation domain present in the native form, the stabilized form of HIF-1 α is able to translocate to the nucleus to initiate a hypoxic response involving upregulation of angiogenic GFs under normoxic conditions. When packed within fibrin hydrogels and applied to a dermal wound model, the stabilized form of HIF-1 α was able to enhance angiogenesis and produce a mature vessel *in vivo* [124]. Nonviral delivery of GFs and angiogenic-inducing genes represents a powerful approach in inducing vascularization in tissue-engineered constructs.

16.3.3

Biomaterials for Inducing Prevascularization

Although therapeutic vascularization using GFs and gene delivery have proven effective, they have a few associated problems [120]. First, this strategy relies heavily on vessel ingrowth from the host, which quite often is neither rapid nor sufficient to support the engineered tissue constructs. Second, finding the minimum number of molecules necessary and delivering them with the right release pharmacokinetics remains a challenging

16 problem. Third, the delivered factors, such as HIF-1 α , SHH, and BMP, might harm the engineered tissue construct. Consequently, an alternative strategy which can be used both *in vivo* and *in vitro* is required to induce prevascularization of the engineered tissue constructs.

16.3.3.1

In Vivo Prevascularization

This strategy seeks to utilize the body as a bioreactor for the engineering of a vascularized tissue construct. In order to induce *in vivo* prevascularization, the engineered tissue construct must be implanted into a region that is enriched in blood vessels, such as the omentum. Attached to the greater curvature of the stomach, the omentum comprises adipose tissue interspersed compact tissue containing lymphocytes, macrophages, and hematopoietic cells. Vascularization of tissue constructs implanted in the omentum occurs as a result of the presence of high concentrations of VEGF and bFGF within this region. When compared to other organs, the omentum has been reported to have a ten- to hundredfold higher concentration of VEGF, which is responsible for the recruitment of endothelial progenitor cells during angiogenesis [125]. Kim et al. used the omentum to culture canine cells *in vivo* [126]. After 1 week, the canine cells seeded on porous PLGA proliferated in the canine omentum: the cell-polymer constructs maintained their original dimensions, and the formation of multicell layered structures containing abundant blood vessels was observed [126]. This strategy could even be extended to induce vascularization of a complex construct, such as cardiac graft. Recently, Dvir et al. used a porous alginate scaffold seeded with neonatal cardiomyocytes (CMs) in a mixture of Matrigel with pro-survival and angiogenic factors, such as IGF-1, VEGF, and SDF-1. Once tissue organization was achieved, the engineered cardiac graft was transplanted into the omentum, a blood-vessel enriched membrane, for further maturation and vascularization. A sustained release of angiogenic factors was able to attract ECs and perivascular cells, resulting in a highly vascularized engineered cardiac graft. When explanted and then transplanted onto an infarcted heart, the graft was able to integrate into the host myocardium. However, this strategy requires the implantation to the omentum region, an invasive procedure which is not practical for clinical application. Alternatively, *in vivo* prevascularization can be induced using arteriovenous (AV) loops to connect the host blood vessel with the tissue-engineered construct. A vein or synthetic graft is used to form a shunt loop between an artery and vein and is enclosed within the scaffolds to be vascularized [127–129]. When integrated into fibrin hydrogel [127], collagen-GAG hydrogel [130], and Matrigel [131], this AV loop culture chamber was able to induce perfused vascular networks within 7–10 days. Utilizing this AV loop approach with neonatal CMs seeded into Matrigel, Morrissett et al. were able to obtain a highly vascularized graft 2 mm in thickness [131]. Similarly, this approach has been applied successfully to induce vascularization in cardiac [131], bone [132], and skeletal tissue [133]. Although this approach can yield perfused and functional vascular networks, it requires two separate surgeries: first to implant the construct at the vascularization site and second to implant the vascularized construct into the final defect site. In addition, many cells may die during the first implantation, due to a limited supply of oxygen and nutrients coupled with the slow process of *in vivo*

vascularization. Hence, this approach can be improved by inducing *in vitro* vascularization prior to implantation [2].

16.3.3.2

In Vitro Prevascularization

Introducing vascularization *in vitro* prior to implantation of the engineered tissue constructs has gained interest recently due to its versatility and its utility for integration into various tissue-engineered constructs. The basic principle of this strategy is to provide the right culture conditions and microenvironment *in vitro* to induce ECs to form stable and functional vascular networks. A combination of coculture cells, GF cocktails, and biomimetic biomaterials is required to orchestrate this intricate process of vascular morphogenesis (as reviewed in the Sect. 16.2). Due to its angiogenic features, ECM components – like fibronectin, collagen, and Matrigel – have been widely used as the materials of choice to induce *in vitro* vascularization. As a proof of concept, *in vitro* prevascularization was first reported using a triculture of human keratinocytes, human dermal fibroblasts, and HUVECs in a collagen hydrogel scaffold to reconstruct prevascularized skin [134]. The ability of fibroblasts to secrete a large amount of human ECM in the 3D scaffolds and the ability of keratinocytes to secrete VEGF are responsible for the spontaneous formation of capillary networks [135]. Upon implantation, these engineered networks can then anastomose to the ingrowing host vasculature and supply the constructs with nutrients and oxygen. Since the host vasculature does not need to grow into the entire construct, this approach could speed up the vascularization process from weeks to days. The prevascular network in a skin construct could anastomose to the host vasculature within 4 days, compared to 14 days for a nonprevascularized construct [135]. Moreover, with the proper perfusion method, this strategy could enhance the survival and functionality of the tissue-engineered constructs. Levenberg et al. utilized a triculture of myoblasts, HUVECs, and mouse embryonic fibroblasts (MEFs) to engineer a vascularized skeletal muscle. A porous scaffold of PLGA/PLLA was used to provide structural integrity to the constructs, while the tricultured cells were mixed with Matrigel, which facilitated cell adhesion and vascular morphogenesis. Prevascularization was shown to increase blood perfusion and survival of the engineered constructs [3]. A similar approach has been used to prevascularize more complex tissue constructs, like cardiac grafts. Once implanted, the engineered cardiac graft must not only be fully anastomosed and perfused, but must also synchronize with the electrical syncytium of the existing myocardium. Lesman et al. have reported that prevascularized cardiac constructs were able to induce CM maturation into elongated and multinucleated myotubes which contained gap junctions and organized anisotropically [5, 6]. These findings were supported by other studies that linked vascularization and tissue differentiation [120], which is crucial in engineering a complex and highly vascularized organ.

Another crucial aspect of engineering a prevascularized construct *in vitro* is the source of ECs and prevascular cells. Human pluripotent SCs can be differentiated into vascular progenitor cells using hydrogels (as discussed in Sect. 16.3.1). Similarly, a more clinically relevant cell source, marrow-derived stem cells, like EPCs, can form functional blood vessels (as reviewed in Sect. 16.1.2) and can be stabilized by pericytes derived from

MSCs. Coculture of EPCs and MSCs in a Matrigel plug was able to induce robust and functional networks [136]. After 4 weeks of implantation, a coculture with 20% EPCs and 80% MSCs was shown to exhibit superior vessel density with patent vascular networks. In response to PDGF, MSCs migrated into ECs and differentiated into SMCs by expressing myocardin and SM22 α [87]. These findings add to the growing body of evidence showing the role of mesenchymal prevascular cells in supporting stable and long-lasting functional vasculatures [86, 87].

16.3.4

Microfabrication of Vascular Networks

Recent technology in microfabrication and biodegradable microfluidics allow the design of complex vascular networks. Vacanti and Borenstein pioneered the concept of engineering a vasculature using a microelectromechanical system (MEMS). To mimic the natural vasculature, as well as oxygen and nutrient delivery, these capillary networks can be perfused and endothelialized. Traditionally, etching and lithographic techniques are used to produce a desired polydimethylsiloxane cast with micron-sized precision. To fit various tissue needs, 3D scaffolds with complex vascular microchannels can be produced by subsequently stacking single-layer microfluidic networks, with consideration for oxygen limitations [137, 138]. Biodegradable and biocompatible elastomers, such as poly(glycerol sebacate) (PGS) [137], and natural protein biopolymers, such as silk fibroin [139, 140], have been explored to form 3D scaffolds with complex vascular microchannels. More recent technologies involve direct-write assembly [141], laser-guided direct writing [142], and soft lithography [143], which can be applied to various hydrogels, including alginate, collagen, and fibrin. A soft lithography technique was used to fabricate microfluidic channel networks within cell-encapsulated calcium alginate hydrogel [144]. Two independent networks were incorporated into the hydrogel, maintaining steady-state gradients throughout the hydrogels for both reactive and nonreactive solutes. As a result, the diffusion of molecules, cell viability, and metabolic activity could be quantitatively measured. A similar approach has been used to micropattern collagen and gelatin gels to produce micron-sized cavities, which could be seeded with ECs within a fibroblast-seeded hydrogel to form a rudimentary vascularized tissue [145]. Collectively, these approaches allow the fabrication of complex vascular networks with precise control over oxygen and nutrient transport – essential to the design and engineering of a vascularized tissue construct.

16.4

Future Directions

Creating functional vasculatures remains one of the most fundamental challenges to be addressed before large tissue-engineered constructs can be used in clinical applications [1, 63, 120]. Recent developments in biomaterials that have allowed multiple strategies for improving vascularization include using biomaterials for the differentiation of vascular

cells, GF delivery, and *in vivo* and *in vitro* prevascularization, as well as microfabrication of complex vascular networks. While each strategy has unique advantages, at present it is unclear which method will work best to improve *in vivo* vascularization. For clinical application, delivering angiogenic factors is the simplest method that has proven effective at restoring blood flow in ischemic and other disease models [71, 74]. However, this strategy relies mainly on vessel ingrowth from the host vasculature – a time-consuming process which may not be suitable when rapid vascularization is needed to support and integrate the tissue-engineered constructs.

Various studies have shown that both *in vivo* and *in vitro* prevascularization within tissue-engineered constructs can improve the survival, integration, and functionality of the newly implanted constructs [3–6]. While *in vivo* prevascularization resulted in mature, organized, and perfused vasculatures, this strategy required multiple surgeries, which are deemed impractical for future clinical use. On the other hand, *in vitro* prevascularization has not been able to fully duplicate the *in vivo* process that used the body as bioreactor. Despite efficient *in vitro* induction of vasculatures, vessel perfusion and functionality remain major problems for *in vivo* integration. Moreover, to facilitate cell adhesion and promote vessel morphogenesis, most studies utilized ECM components (e.g., collagen, fibrin, and Matrigel), which are irrelevant for clinical use. Therefore, the current challenge is to design a synthetic biomaterial which can capture the biological complexity of native tissue: to differentiate vascular progenitor cells into functional vascular cells and to induce their morphogenesis into vascular networks and their integration into the host vasculature. Since each stage of vascular cell differentiation and morphogenesis has unique molecular regulators, these synthetic biomaterials ought to have precise temporal and spatial controls to mimic the native tissue [37]. At first, biomaterials should be able to maintain the self-renewal and undifferentiated state of SCs; then, only when needed, the scaffold trigger cells to differentiate into vascular cells. Much progress in biomaterials design has been made in controlling vascular cell differentiation, both through physical constraints (i.e., porosity) [107] and GF delivery (i.e., soluble and immobilized) [114, 118]. Next, the scaffold ought to induce vascular morphogenesis by controlling RGD ligand density, cell-demanded degradation, and GF profiles. Recent innovations in biomaterials design have created scaffolds sensitive to light [114], pH [146], temperature [147], and cytokines [148], which can be integrated to control vascular morphogenesis. Of particular interest, light-sensitive hydrogels can be used to create scaffolds with distinct cross-linking density to promote and inhibit the spreading and migration of cells [149]; these scaffolds, in turn, can be used to pattern complex vascular networks. Since vascular morphogenesis is sensitive to tissue stiffness [63], orientation [92], and polarity [150, 151], creating elasticity, GFs, and an oxygen gradient along the 3D scaffold could also induce vascular assembly into a tube [152]. The recent invention of photodegradable hydrogels, whose mechanical and chemical properties are controllable during the timescale of cellular development [153], could in turn be useful to promote various stages of vascular assembly. Combined with other strategies (e.g., angiogenic delivery and microfabrication of GFs), GF presentation and oxygen tension within a novel biomaterials design could be quantitatively modeled to control prevascularization of the tissue-engineered constructs.

Once implanted, the prevascularized tissue must be perfused with blood and connected to the host vasculature. At this stage, biomaterials should be able to attract an immune

16 response and stimulate the ingrowth of the host vasculature. Blood perfusion into the scaffolds could happen by the spontaneous ingrowth of the host vasculature or with the help of microsurgery, using the AV loop approach. The functionality of the newly formed vessels must be tested not only through histology analysis but, more importantly, through vessel perfusion and their ability to restore blood flow in disease models [1, 120]. Despite the great progress made in the field, engineering functional vascularized tissue constructs remains a challenge for biomaterials design. An integrated approach that incorporates the strength of each strategy could provide a real solution in the near future.

Acknowledgements We would like to acknowledge funding from the AHA-Scientist Development grant, National Institute of Health grant U54CA143868, and a March of Dimes-O'Conner Starter Scholar award.

References

1. Rouwkema, J., N.C. Rivron, and C.A. van Blitterswijk, *Vascularization in tissue engineering*. Trends in Biotechnology, 2008. **26**(8): p. 434–441.
2. Laschke, M.W., et al., *Angiogenesis in tissue engineering: breathing life into constructed tissue substitutes*. Tissue Engineering, 2006. **12**(8): p. 2093–2104.
3. Levenberg, S., et al., *Engineering vascularized skeletal muscle tissue*. Nature Biotechnology, 2005. **23**(7): p. 879–884.
4. Dvir, T., et al., *Prevascularization of cardiac patch on the omentum improves its therapeutic outcome*. Proceedings of the National Academy of Sciences of the United States of America, 2009. **106**(35): p. 14990–14995.
5. Caspi, O., et al., *Tissue engineering of vascularized cardiac muscle from human embryonic stem cells*. Circulation Research, 2007. **100**(2): p. 263–272.
6. Lesman, A., et al., *Transplantation of a tissue-engineered human vascularized cardiac muscle*. Tissue Engineering Part A, 2010. **16**(1): p. 115–125.
7. Hungerford, J.E., et al., *Development of the aortic vessel wall as defined by vascular smooth muscle and extracellular matrix markers*. Developmental Biology, 1996. **178**(2): p. 375–392.
8. Drake, C.J., J.E. Hungerford, and C.D. Little, *Morphogenesis of the first blood vessels*. Annals of the New York Academy of Sciences, 1998. **857**: p. 155–179, Morphogenesis: cellular interactions.
9. Gerecht-Nir, S. and J. Itskovitz-Eldor, *The promise of human embryonic stem cells*. Best Practice & Research. Clinical Obstetrics & Gynaecology, 2004. **18**(6): p. 843–852.
10. Patan, S., *Vasculogenesis and angiogenesis as mechanisms of vascular network formation, growth and remodeling*. Journal of Neuro-Oncology, 2000. **50**(1): p. 1–15.
11. Ribatti, D., *Hemangioblast does exist*. Leukemia Research, 2008. **32**(6): p. 850–854.
12. Yamashita, J., *Differentiation and diversification of vascular cells from embryonic stem cells*. International Journal of Hematology, 2004. **80**(1): p. 1–6.
13. Yamashita, J., et al., *Flk1-positive cells derived from embryonic stem cells serve as vascular progenitors*. Nature, 2000. **408**(6808): p. 92–96.
14. Bai, H. and Z.Z. Wang, *Directing human embryonic stem cells to generate vascular progenitor cells*. Gene Therapy, 2007. **15**(2): p. 89–95.
15. Vo, E., et al., *Smooth-muscle-like cells derived from human embryonic stem cells support and augment cord-like structures in vitro*. Stem Cell Reviews and Reports, 2010. **6**(2): p. 237–247.

16. Yu, J., et al., *Induced pluripotent stem cell lines derived from human somatic cells*. *Science*, 2007. **318**(5858): p. 1917–1920.
17. Takahashi, K., et al., *Induction of pluripotent stem cells from adult human fibroblasts by defined factors*. *Cell*, 2007. **131**(5): p. 861–872.
18. Pittenger, M., et al., *Multilineage potential of adult human mesenchymal stem cells*. *Science*, 1999. **284**(5411): p. 143–147.
19. Liu, D., X. Li, and Z. Zhang, *Differentiation of human bone marrow mesenchymal stem cells into vascular endothelium-like cells induced by vascular endothelial growth factor and basic fibroblast growth factor in vitro*. *Journal of Clinical Rehabilitative Tissue Engineering Research*, 2008. **12**(47): p. 9216–9220.
20. Gong, Z. and L.E. Niklason, *Small-diameter human vessel wall engineered from bone marrow-derived mesenchymal stem cells (hMSCs)*. *The FASEB Journal*, 2008. **22**(6): p. 1635–1648.
21. Miranville, A., et al., *Improvement of postnatal neovascularization by human adipose tissue-derived stem cells*. *Circulation*, 2004. **110**(3): p. 349–355.
22. Traktuev, D.O., et al., *A population of multipotent CD34-positive adipose stromal cells share pericyte and mesenchymal surface markers, reside in a periendothelial location, and stabilize endothelial networks*. *Circulation Research*, 2008. **102**(1): p. 77–85.
23. Asahara, T., et al., *Isolation of putative progenitor endothelial cells for angiogenesis*. *Science*, 1997. **275**(5302): p. 964–966.
24. Au, P., et al., *Differential in vivo potential of endothelial progenitor cells from human umbilical cord blood and adult peripheral blood to form functional long-lasting vessels*. *Blood*, 2008. **111**(3): p. 1302–1305.
25. Cherqui, S., et al., *Isolation and angiogenesis by endothelial progenitors in the fetal liver*. *Stem Cells*, 2006. **24**(1): p. 44–54.
26. Grenier, G., et al., *Resident endothelial precursors in muscle, adipose, and dermis contribute to postnatal vasculogenesis*. *Stem Cells*, 2007. **25**(12): p. 3101–3110.
27. Zengin, E., et al., *Vascular wall resident progenitor cells: a source for postnatal vasculogenesis*. *Development*, 2006. **133**(8): p. 1543–1551.
28. Mead, L.E., et al., *Isolation and characterization of endothelial progenitor cells from human blood*. *Current Protocols in Stem Cell Biology*, 2008. **Chapter 2**.
29. Yoder, M.C., et al., *Redefining endothelial progenitor cells via clonal analysis and hematopoietic stem/progenitor cell principals*. *Blood*, 2007. **109**(5): p. 1801–1809.
30. Wu, X., et al., *Tissue-engineered microvessels on three-dimensional biodegradable scaffolds using human endothelial progenitor cells*. *American Journal of Physiology. Heart and Circulatory Physiology*, 2004. **287**(2): p. H480–H487.
31. Jie, L., Z. Yan-Ping, and S.K. Robert, *Angiogenesis in wound repair: angiogenic growth factors and the extracellular matrix*. *Microscopy Research and Technique*, 2003. **60**(1): p. 107–114.
32. Smith, M.K., et al., *Locally enhanced angiogenesis promotes transplanted cell survival*. *Tissue Engineering*, 2004. **10**(1–2): p. 63–71.
33. Nomi, M., et al., *Principals of neovascularization for tissue engineering*. *Molecular Aspects of Medicine*, 2002. **23**(6): p. 463–483.
34. Richardson, T.P., et al., *Polymeric system for dual growth factor delivery*. *Nature Biotechnology*, 2001. **19**(11): p. 1029–1034.
35. Lee, J., M.J. Cuddihy, and N.A. Kotov, *Three-dimensional cell culture matrices: state of the art*. *Tissue Engineering Part B: Reviews*, 2008. **14**(1): p. 61–86.
36. Eble, J.A. and S. Niland, *The extracellular matrix of blood vessels*. *Current Pharmaceutical Design*, 2009. **15**: p. 1385–1400.
37. Lutolf, M.P. and J.A. Hubbell, *Synthetic biomaterials as instructive extracellular micro-environments for morphogenesis in tissue engineering*. *Nature Biotechnology*, 2005. **23**(1): p. 47–55.

- 16
38. Toole, B.P., *Hyaluronan: from extracellular glue to pericellular cue*. Nature Reviews. Cancer, 2004. **4**(7): p. 528–539.
 39. Wijelath, E.S., et al., *Heparin-II domain of fibronectin is a vascular endothelial growth factor-binding domain: enhancement of VEGF biological activity by a singular growth factor/matrix protein synergism*. Circulation Research, 2006. **99**(8): p. 853–860.
 40. Francis, S.E., et al., *Central roles of alpha5beta1 integrin and fibronectin in vascular development in mouse embryos and embryoid bodies*. Arteriosclerosis, Thrombosis, and Vascular Biology, 2002. **22**(6): p. 927–933.
 41. Astrof, S., D. Crowley, and R.O. Hynes, *Multiple cardiovascular defects caused by the absence of alternatively spliced segments of fibronectin*. Developmental Biology, 2007. **311**(1): p. 11–24.
 42. Davis, G.E. and D.R. Senger, *Extracellular matrix mediates a molecular balance between vascular morphogenesis and regression*. Current Opinion in Hematology, 2008. **15**(3): p. 197–203.
 43. Robins, S.P., *Biochemistry and functional significance of collagen cross-linking*. Biochemical Society Transactions, 2007. **35**(5): p. 849–852.
 44. Place, E.S., N.D. Evans, and M.M. Stevens, *Complexity in biomaterials for tissue engineering*. Nature Materials, 2009. **8**(6): p. 457–470.
 45. Sun, G., et al., *Functional groups affect physical and biological properties of dextran-based hydrogels*. Journal of Biomedical Materials Research Part A, 2010. **93**(3): p. 1080–1090
 46. Keselowsky, B.G., D.M. Collard, and A.J. García, *Integrin binding specificity regulates biomaterial surface chemistry effects on cell differentiation*. Proceedings of the National Academy of Sciences of the United States of America, 2005. **102**(17): p. 5953–5957.
 47. Ehrbar, M., et al., *Cell-demanded liberation of VEGF121 from fibrin implants induces local and controlled blood vessel growth*. Circulation Research, 2004. **94**(8): p. 1124–1132.
 48. Ehrbar, M., et al., *Endothelial cell proliferation and progenitor maturation by fibrin-bound VEGF variants with differential susceptibilities to local cellular activity*. Journal of Controlled Release, 2005. **101**(1–3): p. 93–109.
 49. Davis, G.E., W. Kon, and A.N. Stratman, *Mechanisms controlling human endothelial lumen formation and tube assembly in three-dimensional extracellular matrices*. Birth Defects Research. Part C, Embryo Today: Reviews, 2007. **81**(4): p. 270–285.
 50. Zhou, X., et al., *Fibronectin fibrillogenesis regulates three-dimensional neovessel formation*. Genes & Development, 2008. **22**(9): p. 1231–1243.
 51. Janmey, P.A., J.P. Winer, and J.W. Weisel, *Fibrin gels and their clinical and bioengineering applications*. Journal of the Royal Society Interface, 2009. **6**(30): p. 1–10.
 52. Bayless, K.J. and G.E. Davis, *The Cdc42 and Rac1 GTPases are required for capillary lumen formation in three-dimensional extracellular matrices*. Journal of Cell Science, 2002. **115**(6): p. 1123–1136.
 53. Kamei, M., et al., *Endothelial tubes assemble from intracellular vacuoles in vivo*. Nature, 2006. **442**(7101): p. 453–456.
 54. Ingber, D.E. and J. Folkman, *Mechanochemical switching between growth and differentiation during fibroblast growth factor-stimulated angiogenesis in vitro: role of extracellular matrix*. The Journal of Cell Biology, 1989. **109**(1): p. 317–330.
 55. Folkman, J., C.C. Haudenschild, and B.R. Zetter, *Long-term culture of capillary endothelial cells*. Proceedings of the National Academy of Sciences of the United States of America, 1979. **76**(10): p. 5217–5221.
 56. Davis, G.E. and C.W. Camarillo, *Regulation of endothelial cell morphogenesis by integrins, mechanical forces, and matrix guidance pathways*. Experimental Cell Research, 1995. **216**(1): p. 113–123.
 57. Rundhaug, J.E., *Matrix metalloproteinases and angiogenesis*. Journal of Cellular and Molecular Medicine, 2005. **9**(2): p. 267–285.

58. Van Hinsbergh, V.W.M., M.A. Engelse, and P.H.A. Quax, *Pericellular proteases in angiogenesis and vasculogenesis*. Arteriosclerosis, Thrombosis, and Vascular Biology, 2006. **26**(4): p. 716–728.
59. Urbich, C. and S. Dimmeler, *Endothelial progenitor cells: characterization and role in vascular biology*. Circulation Research, 2004. **95**(4): p. 343–353.
60. Stratman, A.N., et al., *Endothelial cell lumen and vascular guidance tunnel formation requires MT1-MMP-dependent proteolysis in 3-dimensional collagen matrices*. Blood, 2009. **114**(2): p. 237–247.
61. Chun, T.H., et al., *MT1-MMP-dependent neovessel formation within the confines of the three-dimensional extracellular matrix*. The Journal of Cell Biology, 2004. **167**(4): p. 757–767.
62. Collen, A., et al., *Membrane-type matrix metalloproteinase-mediated angiogenesis in a fibrin-collagen matrix*. Blood, 2003. **101**(5): p. 1810–1817.
63. Hanjaya-Putra, D., et al., *Vascular endothelial growth factor and substrate mechanics regulate in vitro tubulogenesis of endothelial progenitor cells*. Journal of Cellular and Molecular Medicine, 2009. DOI: 10.1111/j.1582-4934.2009.00981.x
64. Sage, E.H. and R.B. Vernon, *Regulation of angiogenesis by extracellular matrix: the growth and the glue*. Journal of Hypertension, 1994. **12**(10): p. S145–S152.
65. Sieminski, A.L., et al., *The stiffness of three-dimensional ionic self-assembling peptide gels affects the extent of capillary-like network formation*. Cell Biochemistry and Biophysics, 2007. **49**(2): p. 73–83.
66. Lutolf, M.P., et al., *Synthetic matrix metalloproteinase-sensitive hydrogels for the conduction of tissue regeneration: engineering cell-invasion characteristics*. Proceedings of the National Academy of Sciences of the United States of America, 2003. **100**(9): p. 5413–5418.
67. Zisch, A.H., et al., *Cell-demanded release of VEGF from synthetic, biointeractive cell ingrowth matrices for vascularized tissue growth*. The FASEB Journal, 2003. **17**(15): p. 2260–2262.
68. Seliktar, D., et al., *MMP-2 sensitive, VEGF-bearing bioactive hydrogels for promotion of vascular healing*. Journal of Biomedical Materials Research. Part A, 2004. **68**(4): p. 704–716.
69. Zisch, A.H., M.P. Lutolf, and J.A. Hubbell, *Biopolymeric delivery matrices for angiogenic growth factors*. Cardiovascular Pathology, 2003. **12**(6): p. 295–310.
70. Ferrara, N., H.P. Gerber, and J. LeCouter, *The biology of VEGF and its receptors*. Natural Medicines, 2003. **9**(6): p. 669–676.
71. Fischbach, C. and D.J. Mooney, *Polymers for pro- and anti-angiogenic therapy*. Biomaterials, 2007. **28**(12): p. 2069–2076.
72. Von Degenfeld, G., et al., *Microenvironmental VEGF distribution is critical for stable and functional vessel growth in ischemia*. The FASEB Journal, 2006. **20**(14): p. 2657–2659.
73. Silva, E.A. and D.J. Mooney, *Effects of VEGF temporal and spatial presentation on angiogenesis*. Biomaterials, 2010. **31**(6): p. 1235–1241.
74. Hao, X., et al., *Angiogenic effects of sequential release of VEGF-A165 and PDGF-BB with alginate hydrogels after myocardial infarction*. Cardiovascular Research, 2007. **75**(1): p. 178–185.
75. Chiu, L.L.Y. and M. Radisic, *Scaffolds with covalently immobilized VEGF and Angiopoietin-1 for vascularization of engineered tissues*. Biomaterials, 2010. **31**(2): p. 226–241.
76. Semenza, G.L., *HIF-1 and human disease: one highly involved factor*. Genes & Development, 2000. **14**(16): p. 1983–1991.
77. Bosch-Marce, M., et al., *Effects of aging and hypoxia-inducible factor-1 activity on angiogenic cell mobilization and recovery of perfusion after limb ischemia*. Circulation Research, 2007. **101**(12): p. 1310–1318.
78. Lee, K., et al., *Anthracycline chemotherapy inhibits HIF-1 transcriptional activity and tumor-induced mobilization of circulating angiogenic cells*. Proceedings of the National Academy of Sciences of the United States of America, 2009. **106**(7): p. 2353–2358.

79. Lee, K., et al., *Acridflavine inhibits HIF-1 dimerization, tumor growth, and vascularization*. Proceedings of the National Academy of Sciences of the United States of America, 2009. **106** (42): p. 17910–17915.
80. Abaci, H.E., et al., *Adaptation to oxygen deprivation in cultures of human pluripotent stem cells, endothelial progenitor cells, and umbilical vein endothelial cells*. American Journal of Physiology. Cell Physiology, 2010. **298**(6): p. C1527–C1537.
81. Hirschi, K.K. and P.A. D'Amore, *Pericytes in the microvasculature*. Cardiovascular Research, 1996. **32**(4): p. 687–698.
82. Hirschi, K.K., S.A. Rohovsky, and P.A. D'Amore, *PDGF, TGF- β , and heterotypic cell-cell interactions mediate endothelial cell-induced recruitment of 10T1/2 cells and their differentiation to a smooth muscle fate*. The Journal of Cell Biology, 1998. **141**(3): p. 805–814.
83. Hirschi, K.K. and M.W. Majesky, *Smooth muscle stem cells*. Anatomical Record. Part A Discoveries in Molecular, Cellular, and Evolutionary Biology, 2004. **276**(1): p. 22–33.
84. Davis, G.E. and W.B. Saunders, *Molecular balance of capillary tube formation versus regression in wound repair: role of matrix metalloproteinases and their inhibitors*. The Journal of Investigative Dermatology. Symposium Proceedings, 2006. **11**(1): p. 44–56.
85. Saunders, W.B., et al., *Coregulation of vascular tube stabilization by endothelial cell TIMP-2 and pericyte TIMP-3*. The Journal of Cell Biology, 2006. **175**(1): p. 179–191.
86. Koike, N., et al., *Tissue engineering: creation of long-lasting blood vessels*. Nature, 2004. **428**(6979): p. 138–139.
87. Au, P., et al., *Bone marrow derived mesenchymal stem cells facilitate engineering of long-lasting functional vasculature*. Blood, 2008. **111**(9): p. 4551–4558.
88. Soucy, P.A. and L.H. Romer, *Endothelial cell adhesion, signaling, and morphogenesis in fibroblast-derived matrix*. Matrix Biology, 2009. **28**(5): p. 273–283.
89. Sorrell, J.M., M.A. Baber, and A.I. Caplan, *A self-assembled fibroblast-endothelial cell coculture system that supports in vitro vasculogenesis by both human umbilical vein endothelial cells and human dermal microvascular endothelial cells*. Cells, Tissues, Organs, 2007. **186**(3): p. 157–168.
90. Sottile, J. and D.C. Hocking, *Fibronectin polymerization regulates the composition and stability of extracellular matrix fibrils and cell-matrix adhesions*. Molecular Biology of the Cell, 2002. **13**(10): p. 3546–3559.
91. Romer, L.H., K.G. Birukov, and J.G. Garcia, *Focal adhesions: paradigm for a signaling nexus*. Circulation Research, 2006. **98**(5): p. 606–616.
92. Bettinger, C.J., Z. Zhang, S. Gerecht, J. Borenstein, and R. Langer, *Enhancement of in vitro capillary tube formation by substrate nanotopography*. Advanced Materials, 2008. **20**: p. 99–103.
93. Gafni, Y., et al., *Design of a filamentous polymeric scaffold for in vivo guided angiogenesis*. Tissue Engineering, 2006. **12**(11): p. 3021–3034.
94. Igarashi, S., J. Tanaka, and H. Kobayashi, *Micro-patterned nanofibrous biomaterials*. Journal of Nanoscience and Nanotechnology, 2007. **7**(3): p. 814–817.
95. Ingber, D.E., *Mechanical signaling and the cellular response to extracellular matrix in angiogenesis and cardiovascular physiology*. Circulation Research, 2002. **91**(10): p. 877–887.
96. Kilarski, W.W., et al., *Biomechanical regulation of blood vessel growth during tissue vascularization*. Nature Medicine, 2009. **15**(6): p. 657–664.
97. Mammoto, A., et al., *A mechanosensitive transcriptional mechanism that controls angiogenesis*. Nature, 2009. **457**(7233): p. 1103–1108.
98. Sieminski, A.L., R.P. Hebbel, and K.J. Gooch, *The relative magnitudes of endothelial force generation and matrix stiffness modulate capillary morphogenesis in vitro*. Experimental Cell Research, 2004. **297**(2): p. 574–584.
99. Deroanne, C.F., C.M. Lapierre, and B.V. Nusgens, *In vitro tubulogenesis of endothelial cells by relaxation of the coupling extracellular matrix-cytoskeleton*. Cardiovascular Research, 2001. **49**(3): p. 647–658.

100. Stephanou, A., et al., *The rigidity in fibrin gels as a contributing factor to the dynamics of in vitro vascular cord formation*. *Microvascular Research*, 2007. **73**(3): p. 182–190.
101. Kniazeva, E. and A.J. Putnam, *Endothelial cell traction and ECM density influence both capillary morphogenesis and maintenance in 3-D*. *American Journal of Physiology. Cell Physiology*, 2009. **297**(1): p. C179–C187.
102. Singer, A.J. and R.A.F. Clark, *Cutaneous wound healing*. *The New England Journal of Medicine*, 1999. **341**(10): p. 738–746.
103. Eiselt, P., et al., *Porous carriers for biomedical applications based on alginate hydrogels*. *Biomaterials*, 2000. **21**(19): p. 1921–1927.
104. Lim, F. and A.M. Sun, *Microencapsulated islets as bioartificial endocrine pancreas*. *Science*, 1980. **210**(4472): p. 908–910.
105. Figliuzzi, M., et al., *Biocompatibility and function of microencapsulated pancreatic islets*. *Acta Biomaterialia*, 2006. **2**(2): p. 221–227.
106. Dean, S.K., et al., *Differentiation of encapsulated embryonic stem cells after transplantation*. *Transplantation*, 2006. **82**(9): p. 1175–1184.
107. Gerecht-Nir, S., et al., *Three-dimensional porous alginate scaffolds provide a conducive environment for generation of well-vascularized embryoid bodies from human embryonic stem cells*. *Biotechnology and Bioengineering*, 2004. **88**(3): p. 313–320.
108. Perets, A., et al., *Enhancing the vascularization of three-dimensional porous alginate scaffolds by incorporating controlled release basic fibroblast growth factor microspheres*. *Journal of Biomedical Materials Research. Part A*, 2003. **65**(4): p. 489–497.
109. Almond, A., *Hyaluronan*. *Cellular and Molecular Life Sciences*, 2007. **64**(13): p. 1591–1596.
110. Dickinson, L.E., et al., *Functional surfaces for high-resolution analysis of cancer cell interactions on exogenous hyaluronic acid*. *Biomaterials*, 2010. **31**(20): p. 5472–5478.
111. Liu, D., et al., *Expression of hyaluronidase by tumor cells induces angiogenesis in vivo*. *Proceedings of the National Academy of Sciences of the United States of America*, 1996. **93**(15): p. 7832–7837.
112. Toole, B.P., T.N. Wight, and M.I. Tammi, *Hyaluronan-cell interactions in cancer and vascular disease*. *The Journal of Biological Chemistry*, 2002. **277**(7): p. 4593–4596.
113. Burdick, J.A., et al., *Controlled degradation and mechanical behavior of photopolymerized hyaluronic acid networks*. *Biomacromolecules*, 2004. **6**(1): p. 386–391.
114. Gerecht, S., et al., *Hyaluronic acid hydrogel for controlled self-renewal and differentiation of human embryonic stem cells*. *Proceedings of the National Academy of Sciences of the United States of America*, 2007. **104**(27): p. 11298–11303.
115. Stephen, P.M. and S. John, *Immobilized RGD peptides on surface-grafted dextran promote biospecific cell attachment*. *Journal of Biomedical Materials Research*, 2001. **56**(3): p. 390–399.
116. Lévesque, S.G., R.M. Lim, and M.S. Shoichet, *Macroporous interconnected dextran scaffolds of controlled porosity for tissue-engineering applications*. *Biomaterials*, 2005. **26**(35): p. 7436–7446.
117. Ferreira, L., M.H. Gil, and J.S. Dordick, *Enzymatic synthesis of dextran-containing hydrogels*. *Biomaterials*, 2002. **23**(19): p. 3957–3967.
118. Ferreira, L.S., et al., *Bioactive hydrogel scaffolds for controllable vascular differentiation of human embryonic stem cells*. *Biomaterials*, 2007. **28**(17): p. 2706–2717.
119. Darland, D.C. and P.A. D'Amore, *TGF β is required for the formation of capillary-like structures in three-dimensional cocultures of 10T1/2 and endothelial cells*. *Angiogenesis*, 2001. **4**(1): p. 11–20.
120. Jain, R.K., *Molecular regulation of vessel maturation*. *Nature Medicine*, 2003. **9**(6): p. 685–693.
121. Dery, M.A., M.D. Michaud, and D.E. Richard, *Hypoxia-inducible factor 1: regulation by hypoxic and non-hypoxic activators*. *The International Journal of Biochemistry & Cell Biology*, 2005. **37**(3): p. 535–540.

122. Pola, R., et al., *The morphogen Sonic hedgehog is an indirect angiogenic agent upregulating two families of angiogenic growth factors*. *Nature Medicine*, 2001. **7**(6): p. 706–711.
123. Deckers, M.M., et al., *Bone morphogenetic proteins stimulate angiogenesis through osteoblast-derived vascular endothelial growth factor A*. *Endocrinology*, 2002. **143**(4): p. 1545–1553.
124. Trentin, D., et al., *Peptide-matrix-mediated gene transfer of an oxygen-insensitive hypoxia-inducible factor-1 α variant for local induction of angiogenesis*. *Proceedings of the National Academy of Sciences of the United States of America*, 2006. **103**(8): p. 2506–2511.
125. Zhang, Q.-X., et al., *Vascular endothelial growth factor is the major angiogenic factor in omentum: mechanism of the omentum-mediated angiogenesis*. *The Journal of Surgical Research*, 1997. **67**(2): p. 147–154.
126. Suh, S., et al., *Use of omentum as an in vivo cell culture system in tissue engineering*. *ASAIO Journal*, 2004. **50**(5): p. 464–467.
127. Lokmic, Z., et al., *An arteriovenous loop in a protected space generates a permanent, highly vascular, tissue-engineered construct*. *The FASEB Journal*, 2007. **21**(2): p. 511–522.
128. Mian, R., et al., *Formation of new tissue from an arteriovenous loop in the absence of added extracellular matrix*. *Tissue Engineering*, 2000. **6**(6): p. 595–603.
129. Cassell, O.C., et al., *The influence of extracellular matrix on the generation of vascularized, engineered, transplantable tissue*. *Annals of the New York Academy of Sciences*, 2001. **944**: p. 429–442.
130. Manasseri, B., et al., *Microsurgical arteriovenous loops and biological templates: a novel in vivo chamber for tissue engineering*. *Microsurgery*, 2007. **27**(7): p. 623–629.
131. Morritt, A.N., et al., *Cardiac tissue engineering in an in vivo vascularized chamber*. *Circulation*, 2007. **115**(3): p. 353–360.
132. Kneser, U., et al., *Engineering of vascularized transplantable bone tissues: induction of axial vascularization in an osteoconductive matrix using an arteriovenous loop*. *Tissue Engineering*, 2006. **12**(7): p. 1721–1731.
133. Bach, A.D., et al., *A new approach to tissue engineering of vascularized skeletal muscle*. *Journal of Cellular and Molecular Medicine*, 2006. **10**(3): p. 716–726.
134. Black, A.F., et al., *In vitro reconstruction of a human capillary-like network in a tissue-engineered skin equivalent*. *The FASEB Journal*, 1998. **12**(13): p. 1331–1340.
135. Tremblay, P.L., et al., *In vitro evaluation of the angiostatic potential of drugs using an endothelialized tissue-engineered connective tissue*. *The Journal of Pharmacology and Experimental Therapeutics*, 2005. **315**(2): p. 510–516.
136. Melero-Martin, J.M., et al., *Engineering robust and functional vascular networks in vivo with human adult and cord blood-derived progenitor cells*. *Circulation Research*, 2008. **103**(2): p. 194–202.
137. Bettinger, C.J., et al., *Microfabrication of poly (glycerol-sebacate) for contact guidance applications*. *Biomaterials*, 2006. **27**(12): p. 2558–2565.
138. Fidkowski, C., et al., *Endothelialized microvasculature based on a biodegradable elastomer*. *Tissue Engineering*, 2005. **11**(1–2): p. 302–309.
139. Bettinger, C.J., et al., *Silk Fibroin Microfluidic Devices*. *Advanced Materials* (Deerfield Beach, Fla.), 2007. **19**(5): p. 2847–2850.
140. Altman, G.H., et al., *Silk-based biomaterials*. *Biomaterials*, 2003. **24**(3): p. 401–416.
141. Therriault, D., S.R. White, and J.A. Lewis, *Chaotic mixing in three-dimensional microvascular networks fabricated by direct-write assembly*. *Nature Materials*, 2003. **2**(4): p. 265–271.
142. Nahmias, Y., et al., *Laser-guided direct writing for three-dimensional tissue engineering*. *Biotechnology and Bioengineering*, 2005. **92**(2): p. 129–136.
143. Cho, H., et al., *How the capillary burst microvalve works*. *Journal of Colloid and Interface Science*, 2007. **306**(2): p. 379–385.
144. Choi, C.H., et al., *Generation of monodisperse alginate microbeads and in situ encapsulation of cell in microfluidic device*. *Biomedical Microdevices*, 2007. **9**(6): p. 855–862.

145. Golden, A.P. and J. Tien, *Fabrication of microfluidic hydrogels using molded gelatin as a sacrificial element*. Lab on a Chip, 2007. **7**(6): p. 720–725.
146. Park, T.G. and A.S. Hoffman, *Synthesis and characterization of pH- and or temperature-sensitive hydrogels*. Journal of Applied Polymer Science, 1992. **46**(4): p. 659–671.
147. Sun, G.M., X.Z. Zhang, and C.C. Chu, *Formulation and characterization of chitosan-based hydrogel films having both temperature and pH sensitivity*. Journal of Materials Science. Materials in Medicine, 2007. **18**(8): p. 1563–1577.
148. Klumb, L.A. and T.A. Horbett, *Design of insulin delivery devices based on glucose sensitive membranes*. Journal of Controlled Release, 1992. **18**(1): p. 59–80.
149. Khetan, S., C. Chung, and J.A. Burdick, *Tuning hydrogel properties for applications in tissue engineering*. Conference Proceedings : Annual International Conference of the IEEE Engineering in Medicine and Biology Society. IEEE Engineering in Medicine and Biology Society. Conference, 2009. **1**: p. 2094–2096.
150. Chung, S. and D.J. Andrew, *The formation of epithelial tubes*. Journal of Cell Science, 2008. **121**(21): p. 3501–3504.
151. Lubarsky, B. and M.A. Krasnow, *Tube morphogenesis: making and shaping biological tubes*. Cell, 2003. **112**(1): p. 19–28.
152. Lutolf, M.P., *Biomaterials: spotlight on hydrogels*. Nature Materials, 2009. **8**(6): p. 451–453.
153. Kloxin, A.M., et al., *Photodegradable hydrogels for dynamic tuning of physical and chemical properties*. Science, 2009. **324**(5923): p. 59–63.

Erin Lavik

Contents

17.1	Introduction	490
17.2	The Tissues in Question and How They are Damaged	490
17.3	Technologies in Clinical Use and in Clinical Trials	491
17.3.1	Nerve Grafts: Autografts and Allografts	491
17.3.2	Decellularized Nerve grafts	493
17.3.3	Tubes and Conduits	494
17.3.4	Cellular Therapies	494
17.3.5	Pharmacological Therapies	496
17.4	Neural Tissue Engineering	497
17.4.1	Early Approaches: Leveraging the Regeneration Seen in the PNS	497
17.4.2	Leveraging the Regeneration Seen in the Neonate to Promote Repair in the Adult	498
17.4.3	Polymers for SCI More Broadly	500
17.5	Future Directions	502
17.5.1	The Role of Collaborations in Achieving These Goals	502
17.6	What We Have Not Covered	503
	References	503

Abstract Biomaterials have played a role in the nervous system as drug delivery vehicles and scaffolds. The nervous system, both the peripheral and central, are capable of repair and regeneration when the appropriate environment is presented and this suggests that biomaterials could fundamentally change treatment following injury and disease by building a permissive environment for repair. Yet, when engineers have used materials particularly as scaffolds, one of the most striking findings is how similar many of their results have been across types of materials and approaches. Clearly, there is much still to learn. Part of that learning process comes from looking at what has succeeded

E. Lavik
 Case Western Reserve University, Room 309, Wickenden Building, 10900 Euclid Avenue,
 Cleveland, OH 44106-7207, USA
 e-mail: Erin.lavik@case.edu

in the clinic and using that to design the next generation of translatable approaches to treatment.

Keywords Drug delivery • Nerve grafts • Stem cells • Translation

17.1

Introduction

As scientists who spend our time making and testing polymers, it seems obvious that we should look at the role polymers play in nerve repair and regeneration. Long defects do not regenerate effectively in the peripheral nervous system (PNS), and there is even less repair and remodeling in the central nervous system (CNS). In both cases, though, there is evidence that building a new environment can promote repair. Our materials have the power to build new environments. We have the right tools, and a challenge that needs a solution. So, we build new environments, and we promote repair. It seems like a clear path forward, and celebration seems imminent.

If there is such a simple formula, we have not found it yet. But, there are things to celebrate and learn from in the field, and there are paths that are hopeful. There are also a lot of caveats along the way, and we need to be cognizant of them as well. We also need to remember our goal: to promote recovery and improvement in people. The technologies we develop need to be amenable to the surgeons and their current techniques and approaches, and they need to be safe and effective enough that patients will want to use them. Taking new approaches in the field from the idea to the patient is an incredibly collaborative and tough enterprise, but it is the one that matters. Success at the bench is not enough.

I asked one of my colleagues, a neurosurgeon, what drives him to do research? I think I expected him to say something about his passion for science or the like. He told me that he was tired of walking into the ER and having to tell patients he had nothing to help them. He needed new tools.

The purpose of the field of neural tissue engineering is to assist in developing those tools. Both in the clinic and at the bench, materials are a critical part of our toolkit and allow us to modify the environment through scaffolding to guide repair, supports to augment or direct cellular function, and as drug delivery vehicles.

17.2

The Tissues in Question and How They are Damaged

Neurons are the cells that carry the electrical signals throughout the nervous system. Each has a nucleus called a cell body or soma, and extends axons, or neurites which form synapses with other neurons. The nervous system can be broken down into the central nervous system (CNS) and the peripheral nervous system (PNS). The CNS includes the

brain, spinal cord, optic nerve, retina, and the olfactory bulb. The PNS includes the remaining portions of the nervous system. The cell bodies of the neurons are all within the CNS. The axons of the neurons exist both within the CNS as well as in the PNS. The neural components of the PNS involve the axons and synapses.

Glia are all the non-neural cells of the neural system, and include oligodendrocytes, astrocytes, and microglia in the CNS. Oligodendrocytes produce the myelin sheaths which insulate the axons of the neurons. Their equivalent within the PNS are the Schwann cells. Schwann cells differ from oligodendrocytes in that they surround and myelinate individual axons, whereas oligodendrocytes extend processes to myelinate several axons. Since there are fewer cells responsible for myelination in the CNS, more efficient packing of axons is possible [1]. Astrocytes are involved in potassium ion and neurotransmitter concentration regulation, as well as in nutritional support for the neurons. They play a pivotal role in forming the blood–brain barrier. The microglia are phagocytic cells that respond to infection and injury in the CNS.

The PNS can be damaged through trauma leading to the crushing or severance of axons. There is significant regeneration in the PNS of the axons if the damage is not too extensive [2]. The rule of thumb in the field is that axons can regenerate up to 1 cm [3]. Beyond this, regeneration and recovery is typically very limited and requires intervention. The axons of the PNS can also be damaged through drug regimes including chemotherapy and diseases including diabetes which can lead to peripheral neuropathy [4]. In cases such as this, it would be attractive to have interventions that not only promote repair but also halt the degeneration.

While axons within the PNS exhibit regeneration when the damage is limited, there is little endogenous axonal regeneration or repair in the region of the CNS [5]. Damage to the CNS can occur as the result of trauma including spinal cord injury (SCI) and traumatic brain injury (TBI), as well as strokes and a myriad of diseases including Huntington's, Amyotrophic lateral sclerosis (ALS), Parkinson's and Alzheimer's disease (Fig. 17.1).

Neuroprotection and neural repair are approaches that have the potential to ameliorate aspects of these conditions, and neural tissue engineering may help to provide tools for these approaches.

17.3 Technologies in Clinical Use and in Clinical Trials

17.3.1 Nerve Grafts: Autografts and Allografts

When a nerve is severed or crushed, the first approach is to trim the damaged components and suture the nerve end to end. However, when the damage is significant, this may not be possible. In cases where nerve repair is pursued at later time points after an injury, there is often retraction of the nerve ends and the tension applied can exacerbate the damage and lead to poor outcomes [6]. The first approach, then, is to remove a nerve segment from another region and perform an autograft. However, there are limited numbers of nerves than

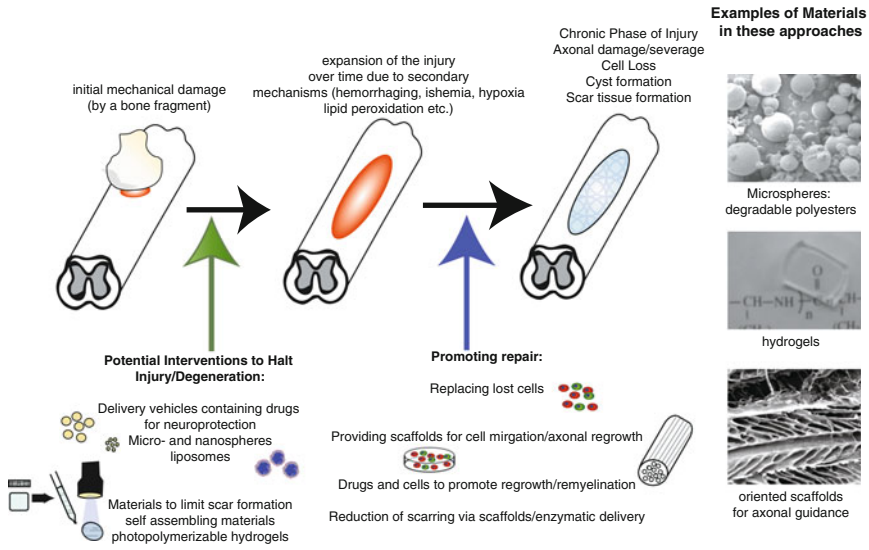


Fig. 17.1 Schematic outlining the phases of spinal cord injury, some of the points of intervention, and some of the interventions that have been pursued. The initial mechanical injury is followed by an injury cascade that leads to further degeneration. In the acute phase post injury, interventions have focused on limiting injury. These interventions, in particular, must be minimally invasive, and ideally, would be delivered systemically and immediately following injury before substantial degeneration has occurred. Targeted interventions (such as nanoparticles or liposomes) may be attractive carriers of neuroprotective drugs in this phase. Materials such as self assembling ones have been shown to reduce injury and lead to better outcomes [124] and may also have a role. In the chronic phase, approaches to treatment often focus on repairing the tissue that is present, for example by promoting remyelination of spared axons, or trying to build new tissue. Spinal cord injury often leads to a cystic cavity at the center of the injury, and materials have long been thought to be suitable for scaffolds across the cyst. Successful therapy will most likely require multiple interventions such as providing a scaffold and digesting scar tissue

can be harvested, and in many cases, autografts are not possible [7]. The next option is using allografts, nerve grafts from donors, typically cadavers [6].

Both autografts and allografts contain Schwann cells which are capable of endocytosing debris and remyelinating the regenerating axons. When either graft is used, the graft itself experiences Wallerian degeneration leading to the loss of the axonal segments in the grafts, and Schwann cells promote the formation of tubes called bands of Bungner which support regenerating axons [7]. The major difference with an allograft is the immunological mismatch between the graft and host [6]. For allografts to be successful, immunosuppression of the host is required [6]. Without immunosuppression, the graft Schwann cells die limiting the efficacy of the grafts [8]. Even with immunosuppression, there is turnover from donor to host Schwann cells in the graft, but properly timed dosing leads to temporary residence of donor Schwann cells and more regenerating fibers. The need for temporary immunosuppression is one of the major concerns with allografts.

Nerve grafts have been used clinically primarily in the PNS. However, nerve grafts have been used following CNS injury to bridge from above the CNS injury to specific peripheral targets such as the bladder to try and improve specific functions [9]. There have also been reports regarding the use of nerve bridges to bridge the lesion following SCI [10, 11]. The number of patients is extremely small in these reports (a single case in each publication) and the goal in each was to demonstrate surgical feasibility and safety. There have been more patients studied, but with limited presentation in scientific settings. In 1996, a group published an approach using nerve grafts to bridge the lesion in a full transection rodent model of SCI [12]. The lead author, H. Cheng, followed up the paper with a poster about the clinical results of the procedure in ten patients [13], but the results have not been published. The poster suggested that there may be been modest improvements, but the pre- and post-treatment assessments were not always the same for each individual making it impossible to know whether there were benefits to the approach.

17.3.2

Decellularized Nerve grafts

While nerve grafts are clinically extremely useful, the limited autografts and immunosuppression associated with allografts have driven clinical development of alternative, complementary therapies. This is where biomaterials begin to find a footing, although the first ones are biologically derived biomaterials. Allografts are essentially a scaffold. The Schwann cells in them die, and host cells replace them. Can one build a scaffold that is everything in the allograft besides the cells? The caveat to this is that the death of the donor cells may play an important role in stimulating repair, but if one can obtain some of the benefits of allografts without using immunosuppression, one may have an important approach for patients where immunosuppression is ill advised. The approach is to take the allografts and remove all of the cellular components through a decellularization process.

Decellularized grafts involve treatment with either detergents, repeated freeze-thaw cycles, or a combination of the two approaches to remove the cellular components while maintaining the extracellular matrix (ECM) [14]. This is not a simple thing. One has to balance removing cells with preserving the ECM. Harsh detergents will remove the cells effectively and alter the ECM making it less well suited to supporting axonal extension. Gentle methods may not remove all of the cells. Once the approach is optimized, the ECM scaffolding can support the ingrowth of cells and axons, and it has been shown to be an effective scaffold for axonal regeneration in the PNS [15].

The Avance nerve grafts by AxoGen Inc. are based on decellularized nerve grafts and are sold in lengths up to 50 mm for the repair of nerve discontinuities. They have approval by the FDA as a Human Cellular and Tissue-based product. The attraction of this approach is that it avoids the immune response to the Schwann cells, and the theory is that since the decellularizing process maintains the ECM, the host Schwann cells can migrate into the graft efficiently and build a permissive environment for regeneration [16]. They are less effective than autografts especially over long gaps, but they provide an alternative treatment.

17.3.3

Tubes and Conduits

The decellularized nerve grafts still involve the potential risks associated with human tissue products. The next step are more purely materials-based systems. The clinical alternatives available include porous collagen tubes, the Integra NeuraGen system [3, 17], and silicone tubes [18–20]. The porous collagen tubes have been used in the clinical setting and results are comparable to silicone tubes [21, 22]. Both can promote limited repair. The thought with the silicone tubes is that they contain and concentrate the growth factors produced after the injury which may augment repair while impeding the ingrowth of scar tissue. Likewise, the collagen tubes are thought to impede scar tissue while facilitating transport.

Essentially, in each step, we move further away from the biological system and closer to a synthetic system with the advantages and disadvantages associated with each. In general, the biological approach gives the best results, but the synthetic systems avoid immunosuppression, are readily available, and lead to functional improvements for patients.

17.3.4

Cellular Therapies

There are a number of clinical trials throughout the world looking at using cells to promote repair or recovery in the CNS. Olfactory ensheathing cells (OECs) have drawn a great deal of interest and ire. OECs are glial or supporting cells within the olfactory bulb. They are intimately associated with the olfactory neurons which are one of the few neural cell types that are constantly replenished and replaced through a patient's lifetime. OECs are thought to play an important role in directing the integration, differentiation and synaptogenesis of the new neurons of the olfactory bulb [23]. They also promote the regeneration of axons from the PNS into the CNS which makes them extremely intriguing for the regeneration community since regeneration is very limited in the CNS [5]. OECs lie at the interface between the PNS and CNS. There are a set in the olfactory epithelium of the PNS and a set in the olfactory nerve layer of the CNS [23] and these may have distinct functions [24]. OECs can be isolated from patients olfactory bulbs but there are a host of questions that arise as to which OECs are isolated, whether they can be expanded, and if so, which ones expand preferentially, and what are the most promising phenotypes [25].

Nonetheless, there are a number of human trials involving the administration of different flavors of OECs. One of the largest and most controversial is the trial in China by Dr. Huang. The trial has involved more than 400 patients with SCI and 100 with amyotrophic lateral sclerosis (ALS) who received OECs. Dr. Huang and his colleagues published a paper in 2003 documenting some of the findings from 171 patients [26]. In the paper, the OECs are cited as being cultured from the glomerular layer of fetal olfactory bulbs. OECs are present in the olfactory nerve layer of the CNS which is adjacent to the glomerular layer [23]. It is assumed that these are the cells isolated, but without further details as to the isolation or characterization procedures, it is hard to know the specific nature of the cells used.

In 2006, Dobkin, Curt, and Guest wrote a summary of seven of the patients who received transplants [27]. The seven patients studied had already decided to have the transplants and agreed to pre- and post-surgical follow-ups with the authors. The majority of patients felt they had some, limited improvements, but the authors note that these improvements could not be quantified with the standard scales used for spinal cord injury, in particular, the American Spinal Cord Injury Association (ASIA) tools. At least five of the patients had serious complications from the procedures including meningitis, confusion, and gastrointestinal bleeding.

Much has been written about Dr. Huang and his procedures [28–30] with warnings to patients that the procedures have not been shown to exhibit demonstrable improvements and involve significant complications. It is also the largest study of its kind, and even if the procedure shows no benefit, it would be helpful for the results to be made available so one can learn from what has been encountered during the procedures. The study has stimulated the call to develop clearer guidelines for clinical trials for SCI [31], as well as the development of China SCINet which aims to continue to do large patient studies but with greater planning for the trials, more robust follow up after the treatments, and better dissemination of the findings [32].

OECs have been studied in clinical settings by other groups on a smaller scale. In 2008, an Australian group published their findings from administration of OECs in six patients with complete SCI [33]. They used the ASIA testing and imaging modalities to assess pre- and post-operatively. They compared the treated patients to a control group who did not receive the surgery and followed patients for 3 years. The OECs were autologous which is one of the potential attractions of OECs, and the study showed no impact on olfaction from the biopsies to obtain cells. There were no functional motor differences as a result of the treatment, but the patients did appear to exhibit small improvements in sensory function although the authors note that quantification of such function is more difficult to assess.

In the U.S., the major cell based trial has been the Stem Cells Inc. trial for Batten disease, a rare liposomal storage disorder, in the group of disorders known as neuronal ceroid lipofuscinosis (NCL) [34]. Batten disease is an orphan disease affecting less than 200,000 people in the U.S., and the trial involved delivering neural stem cells which have been shown in a rodent model of Batten disease to replace the enzyme that is not produced in patients which leads to the lipid build up that affects neuronal function and leads to death. The disease is a childhood disorder, and most children die in their teens [35]. Phase I has been completed with patients tolerating the procedure and no reported adverse events thus far [34], but bioethicists question the appropriateness of a trial in children when there is likely to be no benefit to them [36].

There are a number of things to consider with these cell-based therapies. The first is that most of the cells die very soon after transplantation. This has been seen in many animal models, and it is assumed to be conserved in humans. Cells can have dramatic impacts on a transient basis, but if one's goal is to use the cells as a drug delivery vehicle or as a functional component of a tissue, then one needs to address cell survival. The second is that even when told by many different authorities in the field that these approaches may not have any benefit to the patients, the patients and their families are seeking out these trials. There are few therapies available for a large number of neurological injuries and diseases. There is a strong need and desire for therapies.

17.3.5

Pharmacological Therapies

Biology makes drug therapies in the nervous system exceptionally challenging. The nervous system is protected by the blood–brain barrier which includes the blood–spinal cord barrier and blood–retina barriers as well [37]. Typical routes of administration including oral and intravenous delivery often do not lead to relevant concentrations of the drug of interest in the neural tissue. After injury, and as a result of many diseases of the CNS, the barrier can become leaky [38–40]. However, transport across the barrier, even when it is disrupted, can be limited. As a result, many of the therapies pursued using traditional delivery vehicles have been limited by the substantial doses needed to have a neurological impact. These doses can often lead to significant side effects and call into question the cost-benefit ratio of the approaches as has been the case in some of the steroid approaches to treating injury including methylprednisolone following SCI [41, 42].

As a result, alternative approaches that deliver drugs directly to the nervous system have been used. One of the most well known drug delivery products in the nervous system is the Gliadel wafer. The Gliadel wafer is a polyanhydride based polymer that delivers *bis*-chloronitrosourea (BCNU), a chemotherapy agent, over three weeks [43] and is implanted following resection of the primary tumor in glioblastoma multiforme (GBM), one of the most deadly brain cancers due to their malignant nature. The FDA approved it in 1996. In a paper on 10 years of use of the Gliadel wafer, the authors report similar incidences of complications and median survival time of 13.5 months with the wafer with 20% surviving 2 years [44]. As a point of comparison, 10% of the patients who received radiotherapy following surgery, a common treatment paradigm, survived 2 years or more [45].

Other well known pharmacological interventions for neurological disorders include the delivery of glial cell line derived neurotrophic factor (GDNF) for Parkinson's disease. In this trial, patients received a pump with catheters into the putamen of the brain to deliver GDNF to reduce the death of dopaminergic neurons associated with the progression of Parkinson's [46]. The trial was discontinued in 2004 much to the ire of patients who formed advocacy groups to lobby for GDNF and sought to sue Amgen, the maker of the GDNF in the studies [47]. In 2006, Lang et al. published that in a second trial, there were no benefits, and there was significant toxicity with 10% of the patients making antibodies to GDNF [48].

This is a very brief overview of some of the approaches being taken on the pharmaceutical front. There are excellent reviews of some of the ongoing trials in SCI [42], ALS [49], and stroke [50, 51] as a starting point to gaining insight into the current state of trials and therapeutic approaches involving pharmaceuticals. The majority of drugs currently being tried for neurological injuries and disease are previously approved for other conditions and have a strong record of safety. One of the challenges of developing new drugs for the nervous system is many of the conditions affect relatively small numbers of people and the investment required to develop the drugs is tremendous.

17.4 Neural Tissue Engineering

Clearly, drugs, drug delivery paradigms, cells, and scaffolds can and do play roles clinically in treating disorders and diseases of and injuries to the nervous system. What role, then, can neural tissue engineering play? Using drug delivery, cellular therapy and polymer science, we can begin to build new environments. Repair is possible in both the PNS and CNS with a permissible environment [52, 53]. So, how do we build this environment?

It will depend on the tissue and injury or disease state. To focus the remainder of the discussion, we will concentrate on neural tissue engineering strategies for SCI since there are a number of different approaches that provide a coherent sense of how the field is moving and how the next set of approaches fit with what is currently in the clinic and clinical trials.

17.4.1 Early Approaches: Leveraging the Regeneration Seen in the PNS

As noted before, axons in the CNS exhibit very little regeneration while the PNS, in comparison, exhibits substantial regenerative capacity. Within the PNS, a number of scaffolds have been seen to promote regeneration, and following from this, many groups have used scaffolds to create an environment that is permissive for repair and regeneration following SCI. Techniques involving carbon fibers [54], collagen [55], and Matrigel, an ECM substitute derived from mouse sarcoma, in poly(acrylonitrile): poly(vinylchloride) (PAN/PVC) tubes [56–63] have been studied with respect to axon extension and guidance in the spinal cord. The logic in the Schwann cells/guidance tube approach is to build the more regenerative environment of the PNS within the CNS.

The Bunge group at the Miami Project to Cure Paralysis has pursued the use of guidance tubes seeded with Schwann cells in Matrigel to promote the regeneration of axons in the spinal cord. First, Xu et al. [59] showed that axon regeneration was greatly improved when Schwann cells were seeded into a guidance tube filled with Matrigel as compared with just the guidance tube and Matrigel alone. Extending this work, Xu et al. [60] showed that the ingrowth of CNS axons was virtually doubled by the introduction of the neurotrophins, NT-3 and BDNF, and the treatment stimulated the regeneration of the axons associated with the vestibulospinal and raphespinal tracts, which are important in motor control. Chen et al. [64] in a related study, found that similar results could be achieved with the same grafts and the introduction of methylprednisolone.

In the above studies, the distal end of the guidance tube was blocked, and only ingrowth was studied. However, in more recent work, the Bunge group used a guidance tube which was open on both ends and repeated the initial study using Schwann cells. They found that the axons formed a bridge across the transection, but exhibited no ingrowth into the distal end of the spinal cord [62].

The lack of ingrowth into the distal end of the cord is not surprising based on the understanding of the inhibitory nature of the damaged white matter [65, 66]. However, these inhibitory effects appear to be quite complicated. While regeneration in very limited lesions such as the transection of the corticospinal tract has been achieved using IN-1 has been achieved [66–68] even in a chronic injury model [69], the antibody appeared to be incapable of producing a similar response in the larger injury model. Introduction of the antibody to the myelin inhibitory protein, IN-1, in this model induced sprouting of the corticospinal tract, but no ingrowth into the distal end of the cord [56].

Ingrowth into the spinal cord from implants is clearly extremely challenging but not impossible. While there is much to inhibit ingrowth, there is evidence that the CNS, even the white matter, can support regeneration. Davies et al. [70] showed that axons could regenerate in uninjured white matter. They further showed axons regenerated not only in uninjured white matter but in degenerating white matter of the spinal cord [71]. It appears that the injury site itself is inhibitory, but if axons traverse the injury site, they may regenerate beyond the injury. Glial scar formation occurs, even in severe spinal cord injury, after the initial impact during the secondary injury processes [72]. Some of the ECM components produced by astrocytes after injury that form the glial scar are inhibitory to repair including the chondroitin sulfate proteoglycans [73–75]. If one can overcome the inhibitory environment of the injury site and suppress glial scar formation, at least temporarily, one may be able promote regeneration and functional recovery.

In fact, building on the combinatorial approach using a scaffold, Schwann cells, and growth factors, and adding OECs and chondroitinase ABC to digest the inhibitory chondroitin sulfate proteoglycans, the Bunge group has promoted some functional recovery and regeneration following SCI [76, 77]. It is clear that one can use a scaffold-based system, and in a combinatorial manner, modify the environment to promote repair.

17.4.2

Leveraging the Regeneration Seen in the Neonate to Promote Repair in the Adult

In contrast to the limited capacity for repair in the adult, the neonatal spinal cord exhibits significant endogenous regeneration following SCI [78]. Several groups have sought to use the capacity of younger tissue to promote repair by grafting fetal tissue following SCI. The grafts have been shown to be permissive substrates for axonal growth [79], and augmentation of the growth and some functional recovery has been achieved with the addition of neurotrophic factors [80, 81]. Fetal tissue holds promise for treating a variety of diseases of and injuries to the CNS, but beyond the controversy regarding its use, it is an extremely limited supply, and a large amount of tissue may be needed for a single viable transplant. In Parkinson's disease, for example, it takes six fetuses to provide enough viable tissue for one transplant because 90–95% of the neurons in the transplant die shortly after grafting [82]. While much may be learned from fetal transplants, an alternative must be sought to create a truly viable treatment. Therefore, it may be wise to consider what may be learned from the neonate and applied to developing new treatment approaches.

17.4.2.1

Neural Progenitor and Stem Cells

Neonatal tissue has a large number of neural progenitor cells (NPCs) or what some call neural stem cells (NSCs) which can replace lost cells and remyelinate axons [83]. NPCs and NSCs can be expanded following isolation, avoiding the fundamental limitation of fetal tissue. NPCs have shown the capacity to replace cells lost to injury [84, 85] and disease [86–88] and, in some cases, restore some function [89, 90]. Neural progenitors have been found to form multipolar neurons in a healthy spinal cord but only bipolar neurons when injected after transection of the cord [91]. It was hypothesized the cell–cell contacts are essential for differentiation into complex morphologies. Other work has suggested that NPCs are capable of forming neurons, even motor neurons, following injury [92]. Following a crush model of SCI, NPCs have been seen to become glia but not neurons [93]. The formation of glia may be an important aspect of regeneration. Not only can they insulate the axons and provide the appropriate supporting structures and trophic factors, but it has been shown that glia appear to be essential to the formation of functional synaptic connections for developing neurons [94]. Remyelination following spinal cord injury has also been shown to lead to functional improvement [95–97].

The key questions for using NPCs in the spinal cord are how to improve their survival and direct their differentiation. The environment following injury is potentially a challenging one into which to transplant progenitor cells [98, 99]. The critical issue, then, is how to work with or alter that environment. Altering or building an environment that augments the behavior of promising cell types including NPCs is the playing field on which those in the neural tissue engineering community thrive.

17.4.2.2

Polymers and NPCs

Polymer scaffolds have been shown to improve the survival [100] and differentiation [101, 102] of progenitor cells. By choosing a polymer system that promotes survival and differentiation as the foundation for building growth factor delivery and surface molecule presentation into the environment, one may be able to achieve much more robust survival and differentiation of NPCs and harness their capacity for repair.

However, before one starts building onto the scaffold, one may be able to choose a scaffold that in itself influences NPC behavior. Scaffolds based on collagen and Matrigel may be attractive for engineering many tissues since they contain components or are the basis of the extracellular matrix of most tissues, with the striking exception being the ECM of the CNS which is based on hyaluronic acid (HA) network functionalized with a range of proteoglycans [103]. NPCs make those proteoglycans while their differentiated progeny down regulate them [104] meaning that NPCs can stick to unmodified HA but their progeny will not. As NPCs differentiate in these materials, expressing more mature markers, the mature cells do not attach unless the HA gels are modified with other molecules to promote attachment [105].

The scaffold can play an important role in NPC behavior, and that has been demonstrated using both architectural cues as well as mechanical cues to influence NPC migration and differentiation. Electrospun scaffolds based on degradable polymers have been shown to promote elongation of NPCs and subsequent differentiation into neuronal phenotypes, particularly when the fibers are aligned [106–109]. In vivo, the architecture has been shown to guide axons making them attractive candidates for repair.

The caveat to the oriented nano- and microfiber scaffolds is that they must be made and then implanted. From a translational point of view, this is very challenging. There are cysts that form in the spinal cord following injury, and many, including myself, have wondered whether one might be able to remove scar tissue and implant a scaffold, but it is clear from many, many conversations with neurosurgeons, that they do not want to do something like this for fear that it will exacerbate injury. Thinking back to the complications involved in some of the cell delivery trials, even the delivery of cells following SCI which involved limited invasiveness runs the risk of infection and other complications. Removing tissue has a much higher potential set of complications including further damage.

In light of this, many groups have moved to systems that can be set or gelled in place. The majority of these have been based on hydrogels consisting of HA, poly(ethylene glycol) (PEG), collagen, peptides, or some combination of all of these. Hydrogels have drawn a great deal of interest in the nervous system due to their high biocompatibility, mechanical properties which parallel those of soft tissues, and their ability to be injected as a liquid which gels in situ [110].

One of the major limitations of hydrogels until recently was that their properties, including their mechanical and chemical properties, could not be easily tailored. A number of crucial steps have now been made which permits the necessary modifications and tailoring required to build well-controlled microenvironments for the CNS. Several groups have synthesized libraries of hydrogels and investigated the role of the materials properties on NPC differentiation [111–116]. One of the interesting findings that appears to be conserved between the different groups and materials studied is that a modulus that is close to what is estimated to be brain tissue stiffness (approximately 3,000–5,000 Pa [117]) seems to be optimal for promoting neuronal differentiation of NPCs.

17.4.3

Polymers for SCI More Broadly

17.4.3.1

Scaffolds for Guidance and Inhibition of Scar Tissue

Both polymer scaffolds which are made and implanted and those which gel in situ have been studied for their ability to reduce the formation of scar tissue and promote axonal guidance following SCI. To promote axon guidance, groups have used scaffolds as diverse as carbon fibers [54], collagen modified with peptides [118, 119], PLGA [120], hydrogel guidance tubes [121, 122], and fibrin gels [123]. Most of these were done in some flavor of a

transection model where a cavity was made and the material placed in the site. It is striking in that with this very diverse set of materials, there are only small differences in outcomes. Most supported sprouting of axons into the injury site, but there was rarely much regeneration, and when seen, it typically seemed to involve small numbers of fibers. However, all of these materials seemed to have an important impact on the spinal cord environment. In every case where it was characterized, a reduction in glial scarring was seen. This is a huge step in promoting repair.

The big question becomes what happens when these materials are introduced in a more minimally invasive manner following a more clinically applicable crush or contusion spinal cord injury. Is glial scarring still reduced? The answer, gratefully, seems to be yes. A number of groups have started to administer materials that gel in situ following contusion injuries. Tysseling-Mattiace et al. have shown that administration of a hydrogel based on self assembling peptides one day post injury reduces glial scarring and increases neurite outgrowth and sprouting [124]. Wolery et al. saw a similar outcome with a collagen gel based system [125]. Both groups reported better functional outcomes with the administration of their respective polymers.

17.4.3.2

Delivering Growth Factors

Materials may be able to help build a more permissive environment for repair and healing. To augment this, several groups have started to look at these materials as drug delivery vehicles as well. A number of growth factors are upregulated in the neonate following injury which exhibits regeneration that are not seen in the adult at the concentrations and duration seen in the neonate [52, 53]. These factors include GDNF, brain-derived neurotrophic factor (BDNF), and neurotrophic-3 (NT-3). If one can emulate the presentation of one or more of these growth factors, one may be able to promote repair. Drug delivery technology provides a means to replicate the temporal delivery profiles of growth factors identified in the neonate in the adult spinal cord following injury.

Gels and materials delivering NT-3 have been shown to promote more robust sprouting and axonal elongation in a number of models coupled with improved functional outcomes in some of the work [126, 127]. Likewise, delivery of BDNF has also led to improved outcomes [128–131]. GDNF has also been correlated with more outgrowth [132].

This is a far from complete list, but the key point is that the materials can have an impact, and the combination of materials and growth factors leads to better outcomes. We have not begun to look at dosing or the impact of delivery time, but it is impressive how much has been achieved with relatively simple systems. Part of the current discussion in the field is what level of success is necessary to justify considering translating the findings. With the side effects seen in the GDNF-Parkinson's trial, it is clear that a positive effect and exceptional safety testing are needed before considering the potential clinical application.

17.5

Future Directions

If our goal is to develop new approaches for people, we need to start at the end and figure out for the condition we hope to treat exactly what is and is not possible from the patient's and physician's perspectives. We also need to be cognizant of how the FDA might receive the technology and to that end, many officials at the FDA advocate talking to them early and often if one thing one's technology might have clinical value.

One of the fundamental challenges of tissue engineering approaches is that they are often multicomponent systems with polymers, cells, and drugs involved. Such combination systems have been more challenging to get approved because of their complexity and the number of branches of the FDA that are likely to be involved. They also scare potential investors, which limits one's options for raising the tremendous capital needed to pursue new therapies. The ideal system is a simple one, but the reality is that for a number of complex neurological conditions, successful treatment is likely to involve a combination system.

Nonetheless, there are significant inroads being made into developing and testing new therapies based on single component systems in the nervous system whether they are cellular, pharmacological, or scaffold-based systems. We can learn from everything that has been done in the clinic and target our research to the most translatable technologies with the greatest chance of success. There have been tremendous steps forward clinically with relatively simple approaches.

Biomaterials can have tremendous impact in focal injuries and insults including stroke, SCI, and TBI. They can modulate the environment dramatically, especially when introduced acutely after injury. That is not to say that cells will not improve the results. They will, but the big question right now is what cells for which indication. With the advent of iPS cells and new insights into stem cell microenvironments broadly, we can begin to see how some of these technologies, if successful, might be able to be translated.

For more diffuse disorders, some of the technologies that combine imaging with local delivery are tremendously exciting. The blood–brain barrier is still a formidable challenge, but some of the targeting paradigms are starting to look like they may be able to make it through [133–138].

17.5.1

The Role of Collaborations in Achieving These Goals

I have a colleague who believes an MD/PhD in neuroscience is the perfect person to tackle these challenges. It seems unlikely to this author that any one person, no matter how gifted, is the solution. The successes thus far have been based on intense collaborations and a certain amount of courage to try new approaches. The systems we are tackling are tremendously complex. We are more likely to be successful if we bring our diverse expertise

together and share our different perspectives and insights. There is no perfect person for this work, only great groups who work well together.

17.6 What We Have Not Covered

This chapter covers only a small part of the greater field. We have not looked at the role of remyelination in disease and injury processes, the role of embryonic stem cells, the contribution of angiogenesis to building neural tissue, or the role of other technologies that can work in a synergistic fashion such as electrical stimulation approaches. All of these have tremendous clinical potential and some are in or very close to clinical trials.

There are huge challenges in promoting protection and repair in the nervous system. There are at least as many potential approaches. By working together and leveraging the successes of each approach, we can and will develop new therapeutic paradigms.

Acknowledgements I am grateful to Andrew Shoffstall who read drafts of this chapter and offered suggestions and insights.

References

1. Whittemore S. Lecture at the Kentucky Trust for Spinal Cord Regeneration Conference, 1997.
2. Chen ZL, Yu WM, Strickland S. Peripheral regeneration. *Annu Rev Neurosci* 2007;30:209–233.
3. Chang AS, Yannas IV. Peripheral Nerve Regeneration. In: Smith B, Adelman G, editors. *Neuroscience Year, Supplement to the Encyclopedia of Neuroscience*, 1992. p. 125–126.
4. Malik RA. Current and future strategies for the management of diabetic neuropathy. *Treat Endocrinol* 2003;2(6):389–400.
5. Beattie MS, Bresnaan JC, Komon J, Tovar CA, Meter MV, Anderson DK, et al. Endogenous repair after spinal cord contusion injuries in the rat. *Exp Neurol* 1997;148:453–463.
6. Siemionow M, Sonmez E. Nerve allograft transplantation: a review. *J Reconstr Microsurg* 2007;23(8):511–520.
7. Mackinnon SE, Dellon A. *Surgery of the Peripheral Nerve*. New York: Thieme Medical Publishers, 1988.
8. Midha R, Mackinnon SE, Becker LE. The fate of Schwann cells in peripheral nerve allografts. *J Neuropathol Exp Neurol* 1994;53(3):316–322.
9. Livshits A, Catz A, Folman Y, Witz M, Livshits V, Baskov A, et al. Reinnervation of the neurogenic bladder in the late period of the spinal cord trauma. *Spinal Cord* 2004;42(4):211–217.
10. Tadie M, Liu S, Robert R, Guiheneuc P, Pereon Y, Perrouin-Verbe B, et al. Partial return of motor function in paralyzed legs after surgical bypass of the lesion site by nerve autografts three years after spinal cord injury. *J Neurotrauma* 2002;19(8):909–916.
11. Oppenheim JS, Spitzer DE, Winfree CJ. Spinal cord bypass surgery using peripheral nerve transfers: review of translational studies and a case report on its use following complete spinal cord injury in a human. *Experimental article. Neurosurg Focus* 2009;26(2):E6.
12. Cheng H, Cao Y, and Olson, L. Spinal Cord Repair in Adult Paraplegic Rats: Partial Restoration of Hind Limb Function. *Science* 1996;273:510-513.

13. Huang W, Chuang T, Liao K, Shih Y, Lee L, Cheng H. Prospective Study of Nerve Repair in Patients with Chronic Cervical Spinal Injury. Washington, DC: Society for Neuroscience, 2005.
14. Gilbert TW, Sellaro TL, Badylak SF. Decellularization of tissues and organs. *Biomaterials* 2006;27(19):3675–3683.
15. Hudson TW, Zawko S, Deister C, Lundy S, Hu CY, Lee K, et al. Optimized acellular nerve graft is immunologically tolerated and supports regeneration. *Tissue Eng* 2004;10(11–12): 1641–1651.
16. Whitlock EL, Tuffaha SH, Luciano JP, Yan Y, Hunter DA, Magill CK, et al. Processed allografts and type I collagen conduits for repair of peripheral nerve gaps. *Muscle Nerve* 2009;39(6):787–799.
17. Chamberlain LJ, Yannas IV, Hsu HP, Strichartz G, Spector M. Collagen-GAG substrate enhances the quality of nerve regeneration through collagen tubes up to level of autograft. *Exp Neurol* 1998;154(2):315–329.
18. Lundborg G, Rosen B, Dahlin L, Holmberg J, Rosen I. Tubular repair of the median or ulnar nerve in the human forearm: a 5-year follow-up. *J Hand Surg Br* 2004;29(2):100–107.
19. Dahlin LB, Lundborg G. Use of tubes in peripheral nerve repair. *Neurosurg Clin N Am* 2001;12(2):341–352.
20. Dahlin LB, Anagnostaki L, Lundborg G. Tissue response to silicone tubes used to repair human median and ulnar nerves. *Scand J Plast Reconstr Surg Hand Surg* 2001;35(1):29–34.
21. Wangenstein KJ, Kalliainen LK. Collagen Tube Conduits in Peripheral Nerve Repair: A Retrospective Analysis. *Hand (N Y)* 2009 Nov 24.
22. Meyer RA, Bagheri SC. A bioabsorbable collagen nerve cuff (NeuraGen) for repair of lingual and inferior alveolar nerve injuries: a case series. *J Oral Maxillofac Surg* 2009; 67(11):2550–2551.
23. Barnett SC. Olfactory ensheathing cells: unique glial cell types? *J Neurotrauma* 2004; 21(4):375–382.
24. Au WW, Treloar HB, Greer CA. Sublaminar organization of the mouse olfactory bulb nerve layer. *J Comp Neurol* 2002;446(1):68–80.
25. Kawaja MD, Boyd JG, Smithson LJ, Jahed A, Doucette R. Technical strategies to isolate olfactory ensheathing cells for intraspinal implantation. *J Neurotrauma* 2009;26(2):155–177.
26. Huang H, Chen L, Wang H, Xiu B, Li B, Wang R, et al. Influence of patients' age on functional recovery after transplantation of olfactory ensheathing cells into injured spinal cord injury. *Chin Med J (Engl)* 2003;116(10):1488–1491.
27. Dobkin BH, Curt A, Guest J. Cellular transplants in China: observational study from the largest human experiment in chronic spinal cord injury. *Neurorehabil Neural Repair* 2006; 20(1):5–13.
28. Cyranoski D. Patients warned about unproven spinal surgery. *Nature* 2006;440(7086):850–851.
29. Judson H. The problematical Dr. Huang Hongyun. *Technol Rev* 2005;5(1):1–5.
30. Chew S, Khandji AG, Montes J, Mitsumoto H, Gordon PH. Olfactory ensheathing glia injections in Beijing: misleading patients with ALS. *Amyotroph Lateral Scler* 2007;8(5): 314–316.
31. Fawcett JW, Curt A, Steeves JD, Coleman WP, Tuszynski MH, Lammertse D, et al. Guidelines for the conduct of clinical trials for spinal cord injury as developed by the ICCP panel: spontaneous recovery after spinal cord injury and statistical power needed for therapeutic clinical trials. *Spinal Cord* 2007;45(3):190–205.
32. Cyranoski D. Chinese network to start trials of spinal surgery. *Nature* 2007;446(7135):476–477.
33. Mackay-Sim A, Feron F, Cochrane J, Bassingthwaight L, Bayliss C, Davies W, et al. Autologous olfactory ensheathing cell transplantation in human paraplegia: a 3-year clinical trial. *Brain* 2008;131(Pt 9):2376–2386.
34. Taupin P. HuCNS-SC stemcells. *Curr Opin Mol Ther* 2006;8(2):156–163.

35. Cooper JD. Moving towards therapies for juvenile Batten disease? *Exp Neurol* 2008;211(2): 329–331.
36. Martin RA, Robert JS. Is risky pediatric research without prospect of direct benefit ever justified? *Am J Bioeth* 2007;7(3):12–15.
37. Abbott NJ, Ronnback L, Hansson E. Astrocyte-endothelial interactions at the blood–brain barrier. *Nat Rev Neurosci* 2006;7(1):41–53.
38. Rite I, Machado A, Cano J, Venero JL. Blood–brain barrier disruption induces in vivo degeneration of nigral dopaminergic neurons. *J Neurochem* 2007;101(6):1567–1582.
39. Zlokovic BV. The blood–brain barrier in health and chronic neurodegenerative disorders. *Neuron* 2008;57(2):178–201.
40. Zünkeler B, Carson R, Olson J, Blasberg R, DeVroom H, Lutz R, et al. Quantification and pharmacokinetics of blood–brain barrier disruption in humans. *J Neurosurg* 1996;85(6): 1056–1065.
41. Bracken MB, Shepard M, Holford T, Leosummers L, Aldrich E, Fazl M, et al. Administration of methylprednisolone for 24 or 48 hours or tirilazad mesylate for 48 hours in the treatment of acute spinal cord injury. Results of the Third National Acute Spinal Cord Injury Randomized Controlled Trial. *JAMA* 1997;277:1597–1604.
42. Hawryluk GW, Rowland J, Kwon BK, Fehlings MG. Protection and repair of the injured spinal cord: a review of completed, ongoing, and planned clinical trials for acute spinal cord injury. *Neurosurg Focus* 2008;25(5):E14.
43. Dang WB, Daviau T, Ying P, Zhao Y, Nowotnik D, Clow CS, et al. Effects of GLIADEL(R) wafer initial molecular weight on the erosion of wafer and release of BCNU. *J Control Release* 1996;42(1):83–92.
44. Attenello FJ, Mukherjee D, Dato G, McGirt MJ, Bohan E, Weingart JD, et al. Use of Gliadel (BCNU) wafer in the surgical treatment of malignant glioma: a 10-year institutional experience. *Ann Surg Oncol* 2008;15(10):2887–2893.
45. Stupp R, Hegi ME, Mason WP, van den Bent MJ, Taphoorn MJ, Janzer RC, et al. Effects of radiotherapy with concomitant and adjuvant temozolomide versus radiotherapy alone on survival in glioblastoma in a randomised phase III study: 5-year analysis of the EORTC-NCIC trial. *Lancet Oncol* 2009;10(5):459–466.
46. Gill SS, Patel NK, Hotton GR, O'Sullivan K, McCarter R, Bunnage M, et al. Direct brain infusion of glial cell line-derived neurotrophic factor in Parkinson disease. *Nat Med* 2003; 9(5):589–595.
47. GDNF poses troubling questions for doctors, drug maker. Toxicity, negative outcome raise doubts. *Ann Neurol* 2006;59(3):A5–6.
48. Lang AE, Gill S, Patel NK, Lozano A, Nutt JG, Penn R, et al. Randomized controlled trial of intraputamenal glial cell line-derived neurotrophic factor infusion in Parkinson disease. *Ann Neurol* 2006;59(3):459–466.
49. Corcia P, Meininger V. Management of amyotrophic lateral sclerosis. *Drugs* 2008;68 (8):1037–1048.
50. Al-Shahi Salman R. Haemostatic drug therapies for acute spontaneous intracerebral haemorrhage. *Cochrane Database Syst Rev* 2009(4):CD005951.
51. Wardlaw JM, Murray V, Berge E, Del Zoppo GJ. Thrombolysis for acute ischaemic stroke. *Cochrane Database Syst Rev* 2009(4):CD000213.
52. Nakamura M, Bregman BS. Differences in neurotrophic factor gene expression profiles between neonate and adult rat spinal cord after injury. *Exp Neurol* 2001;169(2):407–415.
53. Widenfalk J, Lundstromer K, Jubran M, Brene S, Olson L. Neurotrophic factors and receptors in the immature and adult spinal cord after mechanical injury or kainic acid. *J Neurosci* 2001;21(10):3457–3475.
54. Khan T, Dauzvardis M, Sayers S. Carbon filament implants promote axonal growth across the transected rat spinal cord. *Brain Res* 1991;541:139–145.

55. Marchand R, Woerly S. Transected spinal cords grafted with *in situ* self-assembled collagen matrices. *Neuroscientist* 1990;36:45–60.
56. Guest JD, Hesse D, Schnell L, Schwab ME, Bunge MB, Bunge RP. Influence of IN-1 antibody and acidic FGF-fibrin glue on the response of injured corticospinal tract axons to human Schwann cell grafts. *J Neurosci Res* 1997;50:888–905.
57. Guest JD, Rao A, Olson L, Bunge MB, Bunge RP. The ability of human Schwann cell grafts to promote regeneration in the transected nude rat spinal cord. *Exp Neurol* 1997;148:502–522.
58. Ramón-Cueto A, Cordero MI, Santos-Benito FF, Avila J. Functional recovery of paraplegic rats and motor axon regeneration in their spinal cords by olfactory ensheathing glia. *Neuron* 2000;25:425–435.
59. Xu XM, Guénard V, Kleitman N, Bunge MB. Axonal regeneration into Schwann cell-seeded guidance channels grafted into transected adult rat spinal cord. *J Comp Neurol* 1995;351:145–160.
60. Xu XM, Guénard V, Kleitman N, Aebischer P, Bunge MB. A combination of BDNF and NT-3 promotes supraspinal axonal regeneration into Schwann Cell grafts in adult rat thoracic spinal cord. *Exp Neurol* 1995;134:261–272.
61. Gautier SE, Oudega M, Frago M, Chapon P, Plant GW, Bunge MB, et al. Poly(α -hydroxyacids) for application in the spinal cord: resorbability and biocompatibility with adult rat Schwann cells and spinal cord. *J Biomed Mater Res* 1998;42:642–654.
62. Xu XM, Chen A, Guénard V, Kleitman N, Bunge MB. Bridging Schwann cell transplants promote axonal regeneration from both the rostral and caudal stumps of the transected adult rat spinal cord. *J Neurocytol* 1997;26:1–16.
63. Xu X, Zhang S-X, Li H, Aebischer P, Bunge M. Regrowth of axons into the distal spinal cord through a Schwann-cell-seeded mini-channel implanted into hemisectioned adult rat spinal cord. *Eur J Neurosci* 1999;11:1723–1740.
64. Chen A, Xu XM, Kleitman N, Bunge MB. Methylprednisolone administration improves axonal regeneration into Schwann cell grafts in transected adult rat thoracic spinal cord. *Exp Neurol* 1996;138:261–276.
65. Schwab ME, and Caroni, P. Oligodendrocytes and CNS myelin are nonpermissive substrates for neurite growth and fibroblast spreading *in vitro*. *J Neurosci* 1988;8:2381–2393.
66. Schnell L, Schwab ME. Axonal regeneration in the rat spinal cord produced by an antibody against myelin-associated neurite growth inhibitors. *Nature* 1990;343:269–272.
67. Brosamle C, Huber AB, Fiedler M, Skerra A, Schwab ME. Regeneration of lesioned corticospinal tract fibers in the adult rat induced by a recombinant, humanized IN-1 antibody fragment. *J Neurosci* 2000;20:8061–8068.
68. Bregman BS, Kunkel-Bagden E, Schnell L, Dai HN, Gao D, Schwab ME. Recovery from spinal cord injury mediated by antibodies to neurite growth inhibitors. *Nature* 1995;378:498–501.
69. Meyenburg Jv, Brosamle C, Metz GAS, Schwab ME. Regeneration and sprouting of chronically injured corticospinal tract fibers in adult rats promoted by NT-3 and the mAb IN-1, which neutralizes myelin-associated neurite growth inhibitors. *Exp Neurol* 1998;154:583–594.
70. Davies SJ, Fitch MT, Memberg SP, Hall AK, Raisman G, Silver J. Regeneration of adult axons in white matter tracts of the central nervous system. *Nature* 1997;390:680–683.
71. Davies SJA, Goucher DR, Doller C, Silver J. Robust regeneration of adult sensory axons in degenerating white matter of the adult rat spinal cord. *J Neurosci* 1999;19:5810–5822.
72. Osterholm JL. The pathological response to spinal cord injury. *J Neurosurg* 1974;40:5–33.
73. Properzi F, Asher R, Fawcett J. Chondroitin sulphate proteoglycans in the central nervous system: changes and synthesis after injury. *Biochem Soc Trans* 2003;31(2):335–336.
74. Rhodes K, Fawcett J. Chondroitin sulphate proteoglycans: preventing plasticity or protecting the CNS? *J Anat* 2004;204(1):33–48.
75. Silver J, Miller JH. Regeneration beyond the glial scar. *Nat Rev Neurosci* 2004;5(2):146–156.

76. Pearse DD, Pereira FC, Marcillo AE, Bates ML, Berrocal YA, Filbin MT, et al. cAMP and Schwann cells promote axonal growth and functional recovery after spinal cord injury. *Nat Med* 2004;10(6):610–616.
77. Fouad K, Schnell L, Bunge MB, Schwab ME, Liebscher T, Pearse DD. Combining Schwann cell bridges and olfactory-ensheathing glia grafts with chondroitinase promotes locomotor recovery after complete transection of the spinal cord. *J Neurosci* 2005;25(5):1169–1178.
78. Saunders NR, Kitchener P, Knott GW, Nicholls JG, Potter A, Smith TJ. Development of walking, swimming and neuronal connections after complete spinal cord transection in the neonatal opossum *Monodelphis domestica*. *J Neurosci* 1998;18:339–355.
79. Jakeman LB, Reier PJ. Axonal projections between fetal spinal cord transplants and the adult rat spinal cord: a neuroanatomical tracing study of local interactions. *J Comp Neurol* 1991;307:311–334.
80. Bregman BS, McAtee M, Dai HN, Kuhn PL. Neurotrophic factors increase axonal growth after spinal cord injury and transplantation in the adult rat. *Exp Neurol* 1997;148:475–494.
81. Coumans J, Lin TT-S, Dai H, MacArthur L, McAtee M, Nash C, et al. Axonal regeneration and functional recovery after complete spinal cord transection in rats by delayed treatment with transplants and neurotrophins. *J Neurosci* 2001;21:9334–9344.
82. Barinaga M. Fetal neuron grafts pave the way for stem cell therapies. *Science* 2000;287:1421–1422.
83. Gage FH. Mammalian neural stem cells. *Science* 2000;287:1433–1438.
84. Nishida A, Takahashi M, Tanihara H, Nakano I, Takahashi JB, Mizoguchi A, et al. Incorporation and differentiation of hippocampus-derived neural stem cells transplanted in injured adult rat retina. *Invest Ophthalmol Vis Sci* 2000;41(13):4268–4274.
85. Kurimoto Y, Shibuki H, Kaneko Y, Ichikawa M, Kurokawa T, Takahashi M, et al. Transplantation of adult rat hippocampus-derived neural stem cells into retina injured by transient ischemia. *Neurosci Lett* 2001;306(1–2):57–60.
86. Isacson O, Deacon TW, Pakzaban P, Galpern WR, Dinsmore J, Burns LH. Transplanted xenogenic neural cells in neurodegenerative disease models exhibit remarkable axonal target specificity and distinct growth patterns of glial and axonal fibres. *Nat Med* 1995;1:1189–1194.
87. Castilho R, Hansson O, Brundin P. Improving the survival of grafted embryonic dopamine neurons in rodent models of Parkinson's disease. *Prog Brain Res* 2000;127:203–231.
88. Armstrong RJE, Tyers P, Jain M, Richards A, Dunnett SB, Rosser AE, et al. Transplantation of expanded neural precursor cells from the developing pig ventral mesencephalon in a rat model of Parkinson's disease. *Exp Brain Res* 2003;151(2):204–217.
89. Ogawa Y, Sawamoto K, Miyata T, Miyao S, Watanabe M, Nakamura M, et al. Transplantation of in vitro-expanded fetal neural progenitor cells results in neurogenesis and functional recovery after spinal cord contusion injury in adult rats. *J Neurosci Res* 2002;69(6):925–933.
90. Pluchino S, Quattrini A, Brambilla E, Gritti A, Salani G, Dina G, et al. Injection of adult neurospheres induces recovery in a chronic model of multiple sclerosis. *Nature* 2003;422(6933):688–694.
91. Onifer SM, Cannon AB, Whittemore SR. Altered differentiation of CNS neural progenitor cells after transplantation into the injured adult rat spinal cord. *Cell Transplant* 1997;6:327–338.
92. Park K, Liu S, Flax J, Nissim S, Stieg P, Snyder E. Transplantation of neural progenitor and stem cells: developmental insights may suggest new therapies for spinal cord and other CNS dysfunction. *J Neurotrauma* 1999;16:675–687.
93. Cao Q, Zhang YP, Howard RM, Walters WM, Tsoulfas P, Wittemore SR. Pluripotent stem cells engrafted into the normal or lesioned adult rat spinal cord are restricted to a glial lineage. *Exp Neurol* 2001;167:48–58.
94. Pflieger FW, Barres BA. Synaptic efficacy enhanced by glial cells in vitro. *Science* 1997;277:1684–1687.

95. Liu S, Qu Y, Stewart TJ, Howard MJ, Chakraborty S, Holekamp TF, et al. Embryonic Stem Cells Differentiate into Oligodendrocytes and Myelinate in Culture and After Spinal Cord Transplantation. *Proc Natl Acad Sci U S A* 2000;97:6126–6131.
96. Jeffery ND, Crang AJ, O'Leary MT, Hodge SJ, Blakemore WF. Behavioral Consequences of oligodendrocyte progenitor cell transplantation into experimental demyelinating lesions in the rat spinal cord. *Eur J Neurosci* 1999;11:1508–1514.
97. Akiyama Y, Honmou O, Kato T, Uede T, Hashi K, Kocsis JD. Transplantation of clonal neural precursor cells derived from adult human brain establishes functional peripheral myelin in the rat spinal cord. *Exp Neurol* 2001;167:27–39.
98. Einstein O, Ben-Menachem-Tzidon O, Mizrahi-Kol R, Reinhartz E, Grigoriadis N, Ben-Hur T. Survival of neural precursor cells in growth factor-poor environment: implications for transplantation in chronic disease. *Glia* 2006;53(4):449–455.
99. Okano H, Ogawa Y, Nakamura M, Kaneko S, Iwanami A, Toyama Y. Transplantation of neural stem cells into the spinal cord after injury. *Semin Cell Dev Biol* 2003;14(3):191–198.
100. Tomita M, Lavik E, Klassen H, Zahir T, Langer R, Young MJ. Biodegradable polymer composite grafts promote the survival and differentiation of retinal progenitor cells. *Stem Cells* 2005;23(10):1579–1588.
101. Silva GA, Czeisler C, Niece KL, Beniash E, Harrington DA, Kessler JA, et al. Selective differentiation of neural progenitor cells by high-epitope density nanofibers. *Science* 2004;303(5662):1352–1355.
102. Yang F, Murugan R, Wang S, Ramakrishna S. Electrospinning of nano/micro scale poly (ϵ -lactic acid) aligned fibers and their potential in neural tissue engineering. *Biomaterials* 2005;26(15):2603–2610.
103. Matthews RT, Kelly GM, Zerillo CA, Gray G, Tiemeyer M, Hockfield S. Aggrecan glycoforms contribute to the molecular heterogeneity of perineuronal nets. *J Neurosci* 2002;22(17):7536–7547.
104. Kabos P, Matundan H, Zandian M, Bertolotto C, Robinson ML, Davy BE, et al. Neural precursors express multiple chondroitin sulfate proteoglycans, including the lectican family. *Biochem Biophys Res Commun* 2004;318(4):955–963.
105. Pan L, Ren Y, Cui F, Xu Q. Viability and differentiation of neural precursors on hyaluronic acid hydrogel scaffold. *J Neurosci Res* 2009;87(14):3207–3220.
106. Cao H, Liu T, Chew SY. The application of nanofibrous scaffolds in neural tissue engineering. *Adv Drug Deliv Rev* 2009;61(12):1055–1064.
107. Carlberg B, Axell MZ, Nannmark U, Liu J, Kuhn HG. Electrospun polyurethane scaffolds for proliferation and neuronal differentiation of human embryonic stem cells. *Biomed Mater* 2009;4(4):45004.
108. Yao L, O'Brien N, Windebank A, Pandit A. Orienting neurite growth in electrospun fibrous neural conduits. *J Biomed Mater Res B Appl Biomater* 2009;90(2):483–491.
109. Wang HB, Mullins ME, Cregg JM, Hurtado A, Oudega M, Trombley MT, et al. Creation of highly aligned electrospun poly-L-lactic acid fibers for nerve regeneration applications. *J Neural Eng* 2009;6(1):016001.
110. Anseth KS, Metters AT, Bryant SJ, Martens PJ, Elisseeff JH, Bowman CN. In situ forming degradable networks and their application in tissue engineering and drug delivery. *J Control Release* 2002;78(1–3):199–209.
111. Hynes SR, Rauch MF, Bertram J, Lavik EB. A library of tunable poly(ethylene glycol)/poly-L-lysine hydrogels to investigate the materials cues that influence neural stem cell differentiation. *J Biomed Mater Res A* 2009;89(2):499–509.
112. Ma W, Fitzgerald W, Liu QY, O'Shaughnessy TJ, Maric D, Lin HJ, et al. CNS stem and progenitor cell differentiation into functional neuronal circuits in three-dimensional collagen gels. *Exp Neurol* 2004;190(2):276–288.

113. Teixeira AI, Duckworth JK, Hermanson O. Getting the right stuff: controlling neural stem cell state and fate in vivo and in vitro with biomaterials. *Cell Res* 2007;17(1):56–61.
114. Banerjee A, Arha M, Choudhary S, Ashton RS, Bhatia SR, Schaffer DV, et al. The influence of hydrogel modulus on the proliferation and differentiation of encapsulated neural stem cells. *Biomaterials* 2009;30(27):4695–4699.
115. Saha K, Keung AJ, Irwin EF, Li Y, Little L, Schaffer DV, et al. Substrate modulus directs neural stem cell behavior. *Biophys J* 2008;95(9):4426–4438.
116. Jiang FX, Yurke B, Firestein BL, Langrana NA. Neurite outgrowth on a DNA crosslinked hydrogel with tunable stiffnesses. *Ann Biomed Eng* 2008;36(9):1565–1579.
117. Engler AJ, Sen S, Sweeney HL, Discher DE. Matrix elasticity directs stem cell lineage specification. *Cell* 2006;126(4):677–689.
118. Woerly S, Pinet E, de Robertis L, Van Diep D, Bousmina M. Spinal cord repair with PHPMA hydrogel containing RGD peptides (NeuroGel (TM)). *Biomaterials* 2001;22(10):1095–1111.
119. Woerly S, Doan VD, Sosa N, de Vellis J, Espinosa-Jeffrey A. Prevention of gliotic scar formation by NeuroGel (TM) allows partial endogenous repair of transected cat spinal cord. *J Neurosci Res* 2004;75(2):262–272.
120. Teng YD, Lavik EB, Qu X, Park KI, Ourednik J, Zurakowski D, et al. Functional recovery following traumatic spinal cord injury mediated by a unique polymer scaffold seeded with neural stem cells. *Proc Natl Acad Sci U S A* 2002;99(5):3024–3029.
121. Tsai EC, Dalton PD, Shoichet MS, Tator CH. Synthetic hydrogel guidance channels facilitate regeneration of adult rat brainstem motor axons after complete spinal cord transection. *J Neurotrauma* 2004;21(6):789–804.
122. Tsai EC, Dalton PD, Shoichet MS, Tator CH. Matrix inclusion within synthetic hydrogel guidance channels improves specific supraspinal and local axonal regeneration after complete spinal cord transection. *Biomaterials* 2006;27(3):519–533.
123. Johnson PJ, Parker SR, Sakiyama-Elbert SE. Fibrin-based tissue engineering scaffolds enhance neural fiber sprouting and delay the accumulation of reactive astrocytes at the lesion in a subacute model of spinal cord injury. *J Biomed Mater Res A* 2010;92(1):152–163.
124. Tysseling-Mattiace VM, Sahni V, Niece KL, Birch D, Czeisler C, Fehlings MG, et al. Self-assembling nanofibers inhibit glial scar formation and promote axon elongation after spinal cord injury. *J Neurosci* 2008;28(14):3814–3823.
125. Woerly S, Doan VD, Evans-Martin F, Paramore CG, Peduzzi JD. Spinal cord reconstruction using NeuroGel implants and functional recovery after chronic injury. *J Neurosci Res* 2001;66(6):1187–1197.
126. Piantino J, Burdick JA, Goldberg D, Langer R, Benowitz LI. An injectable, biodegradable hydrogel for trophic factor delivery enhances axonal rewiring and improves performance after spinal cord injury. *Exp Neurol* 2006;201(2):359–367.
127. Taylor SJ, McDonald JW, Sakiyama-Elbert SE. Controlled release of neurotrophin-3 from fibrin gels for spinal cord injury. *J Control Release* 2004;98(2):281–294.
128. Jain A, Kim YT, McKeon RJ, Bellamkonda RV. In situ gelling hydrogels for conformal repair of spinal cord defects, and local delivery of BDNF after spinal cord injury. *Biomaterials* 2006;27(3):497–504.
129. Park J, Lim E, Back S, Na H, Park Y, Sun K. Nerve regeneration following spinal cord injury using matrix metalloproteinase-sensitive, hyaluronic acid-based biomimetic hydrogel scaffold containing brain-derived neurotrophic factor. *J Biomed Mater Res A* 2010;93(3):1091–1099.
130. Patist CM, Mulder MB, Gautier SE, Maquet V, Jerome R, Oudega M. Freeze-dried poly(D, L-lactic acid) macroporous guidance scaffolds impregnated with brain-derived neurotrophic factor in the transected adult rat thoracic spinal cord. *Biomaterials* 2004;25(9):1569–1582.
131. Stokols S, Tuszynski MH. Freeze-dried agarose scaffolds with uniaxial channels stimulate and guide linear axonal growth following spinal cord injury. *Biomaterials* 2006;27(3):443–451.

132. Iannotti C, Li HY, Yan P, Lu XB, Wirthlin L, Xu XM. Glial cell line-derived neurotrophic factor-enriched bridging transplants promote propriospinal axonal regeneration and enhance myelination after spinal cord injury. *Exp Neurol* 2003;183(2):379–393.
133. Kurakhmaeva KB, Djindjikhshvili IA, Petrov VE, Balabanyan VU, Voronina TA, Trofimov SS, et al. Brain targeting of nerve growth factor using poly(butyl cyanoacrylate) nanoparticles. *J Drug Target* 2009;17(8):564–574.
134. Ren T, Xu N, Cao C, Yuan W, Yu X, Chen J, et al. Preparation and therapeutic efficacy of polysorbate-80-coated amphotericin B/PLA-b-PEG nanoparticles. *J Biomater Sci Polym Ed* 2009;20(10):1369–1380.
135. Denora N, Trapani A, Laquintana V, Lopedota A, Trapani G. Recent advances in medicinal chemistry and pharmaceutical technology – strategies for drug delivery to the brain. *Curr Top Med Chem* 2009;9(2):182–196.
136. Patel MM, Goyal BR, Bhadada SV, Bhatt JS, Amin AF. Getting into the brain: approaches to enhance brain drug delivery. *CNS Drugs* 2009;23(1):35–58.
137. Tiwari SB, Amiji MM. A review of nanocarrier-based CNS delivery systems. *Curr Drug Deliv* 2006;3(2):219–232.
138. Roney C, Kulkarni P, Arora V, Antich P, Bonte F, Wu A, et al. Targeted nanoparticles for drug delivery through the blood-brain barrier for Alzheimer's disease. *J Control Release* 2005 28;108(2–3):193–214.

Nivedita Sangaj and Shyni Varghese

Contents

18.1	Introduction	512
18.2	Biochemical Cues	513
18.2.1	ECM-Derived Biomaterials	513
18.2.2	Natural Polymers	518
18.2.3	Hybrid Materials	519
18.2.4	Functionalization with Biochemical Cues	520
18.2.5	Synthetic Biomaterials	523
18.2.6	Biomaterials as a Reservoir of Growth Factors	525
18.2.7	Biomaterials for Immunomodulation	526
18.3	Biophysical Cues	527
18.3.1	Mechanical Properties of Biomaterials	527
18.3.2	Biomaterials for Micro- and Nano-Scale Cues	528
18.4	Two-Dimensional Cultures Versus Three-Dimensional Cultures	530
18.5	Conclusion and Future Directions	531
	References	532

Abstract Stem cell engineering has enormous potential to study developmental processes, disease progression, drug screening, and to provide new therapeutics. The interaction of stem cells with their microenvironment plays an important role in determining the stem cell fate. One of the most important environmental factors is the extracellular matrix, which defines the biochemical and biophysical niche from which the stem cells receive various regulatory signals. Artificial matrices based on natural and synthetic materials have been developed to direct stem cell fate such as proliferation and differentiation. Some of these approaches are being currently explored clinically and other more sophisticated multi-functional biomimetic materials with defined properties are currently under development. In this chapter we discuss some of the recent trends in the development of biomaterials and their applications in directing self-renewal and differentiation of stem cells.

S. Varghese (✉)

Department of Bioengineering, University of California, San Diego, 9500 Gilman Drive, La Jolla, CA 92093-0412, USA

e-mail: svarghese@ucsd.edu

Keywords Biomaterials • Differentiation • ECM • Microenvironment • Self-renewal • Stem cells

18.1 Introduction

Stem cells are characterized by their ability to self-renew, proliferate without phenotypic alteration, and differentiate into tissue specific progeny [1]. The normal homeostasis and repair of native tissues are maintained by the stem cells residing within the adult tissues, which expeditiously replace the dysfunctional ones. These characteristics render them the most promising cell source for regenerative medicine ranging from cell therapy to functional tissue/organ replacements. Although the ability of stem cells to differentiate and contribute to tissue repair offers great potential to treat various debilitating diseases, before such an approach can be translated from the “bench to the bed side”, many fundamental biological and engineering challenges need to be surmounted. Some of these challenges include *ex vivo* expansion of stem cells without phenotypic and karyotypic alterations, controlled and efficient differentiation into the targeted cell/tissue, and integration with the host tissue upon transplantation. Each of these aspects requires development of defined culture conditions that involve matrices with defined material and interfacial properties, and defined medium components. To this end, research in biomaterials and stem cell engineering has made many advances. Some of these advancements have led to clinical and preclinical trials (<http://www.clinicaltrials.org>). Advances in biomaterials have focused on developing temporary tissue replacements and devising strategies to regulate cellular functions so as to promote their growth and/or differentiation both *in vitro* and *in vivo*. In this chapter, we will be discussing these advancements in the context of stem cell engineering and regenerative medicine.

The cell/tissue culture techniques developed for nerve fiber by Ross Harrison in 1907 have been considered as a paradigm shift in medicinal engineering laying the foundation to *in vitro* cell and tissue cultures [2]. Since then, numerous studies have focused on developing various *in vitro* cell culture environments to direct cellular functions such as growth, differentiation, and structural organization. The optimal cell culture system should be able to regulate proliferation and tissue/lineage specific differentiation of stem cells efficiently and reproducibly in a spatial and temporal manner. In native tissue, cells are surrounded by multi-functional extracellular matrices and the chemical and physical signaling arising from the microenvironment plays a pivotal role in maintaining the tight regulation of various cellular activities [3]. Figure 18.1 depicts the various functions of native ECM. Such a multifunctional and dynamic nature of the extracellular matrix (ECM) presents a challenge in creating artificial matrices that recapitulate the spatio-temporal characteristics of native ECM.

Biomaterials play a central role in the pursuit to develop well-defined and robust *in vitro* artificial matrices. This includes both naturally-derived and synthetic materials. Many of the material developmental methods integrate principles from biochemistry, material science,

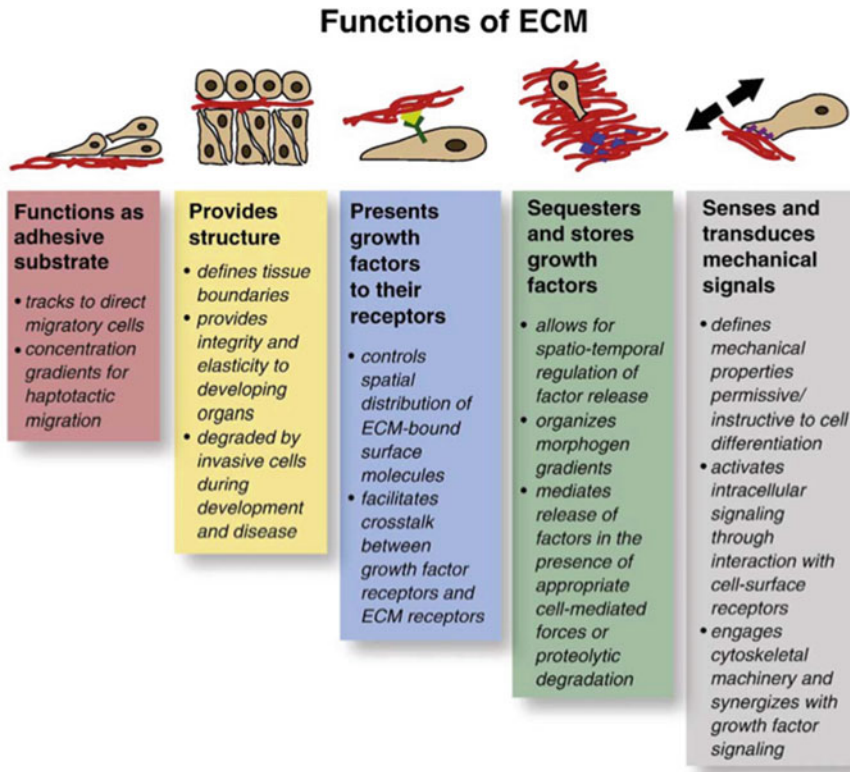


Fig. 18.1 Multifunctional ECM and its interaction with cells [3] (Reprinted from Rozario et al., *Develop Biol* 2010;341:126–140 with permission from Elsevier)

biology, biophysics, engineering, and polymer sciences [4–6]. Such artificial matrices would have enormous applications in regenerative medicine as excellent model systems for dissecting cellular functions, signaling pathways, disease progression, and tissue morphogenesis and as scaffolds for tissue and cell engineering. The specific focus of this chapter is to examine various biophysical and biochemical cues of the biomaterials (or scaffolds) that influence stem cell proliferation and differentiation.

18.2 Biochemical Cues

18.2.1 ECM-Derived Biomaterials

ECM, which surrounds the cells in native tissue, is a well-hydrated structure of various proteoglycans and proteins in most of the tissues. Due to their inherent ability to mediate

cell attachment and undergo cell-mediated degradation, ECM-derived materials have been extensively explored to support the *in vitro* growth of stem cells. Some of the early and continuously explored approaches for mimicking the tissue specific environment involve utilization of decellularized tissues as scaffolds for controlling the tissue specific differentiation of progenitor/stem cells [7–9]. This is mainly due to the tissue specific biochemical cues that the decellularized matrix offers in addition to the geometry and structure. A recent study by Ott et al. demonstrated that decellularized whole hearts maintaining the geometry, ECM structure and composition, and vascular architecture not only supported differentiation of neonatal cardiac cells but also resulted in the formation of functional tissue (beating heart) [7]. Decellularized native tissues have also been adapted to engineer anatomically shaped bone grafts from adult stem cells such as bone marrow derived mesenchymal stem cells (MSC) [8]. Here the complex architecture of the temporomandibular joint (TMJ) condylar bone was generated from decellularized trabecular bone using digitized clinical images. The human mesenchymal stem cells (hMSC) seeded within the decellularized tissue underwent osteogenic differentiation resulting in neo-bone tissue when the MSC-laden decellularized tissue was cultured in a bioreactor with interstitial flow of culture medium.

Adapting a similar approach, physicians in Spain have recently carried out a successful trachea replacement, which restored the functionality of the respiratory tract of a 30-year-old woman suffering from end-stage airway disease. This was achieved by decellularizing the donor trachea along with removing major histocompatibility complex (MHC) antigens from the tissue using detergent enzymatic procedures, followed by recellularizing the decellularized tissue with autologous cells such as epithelial cells and MSC-derived chondrocytes. Utilization of autologous cells limited the immune response and thereby the associated complications [9]. Although using decellularized tissue to direct tissue specific differentiation of progenitor/stem cells is very attractive, the approach is limited due to the lack of donor tissues, associated donor site morbidity (when harvested from the patient/or a living donor), immunological response to allografts and xenografts, and the specialized techniques required to decellularize the tissue while preserving ECM composition, geometry and vascularization. The biggest obstacle however could be the availability of the donor tissue.

The limitations posed by the donor tissue can, however, be partially addressed using tissue engineering approaches. Indeed there exist few reports demonstrating the possibility of directing tissue specific differentiation of stem cells using tissue engineered ECM. Datta et al. have examined the potential of *in vitro* engineered osteogenic ECM to induce osteogenic differentiation of MSC [10, 11]. The tissue engineered ECM was generated by differentiating the osteoblastic cells *in vitro* for 12 days and decellularizing the neo-ECM by rapid freeze-thaw cycling. The ECM that was laid down by the osteoblastic cells promoted osteogenic differentiation of rat MSC. Beyond promoting differentiation, the tissue engineered bone-like ECM also promoted cell proliferation [10]. In addition to demonstrating the *in vitro* effect, the same research group also evaluated the performance of decellularized tissue engineered ECM *in vivo* [11]. Although the implant was found to be vascularized, no bone formation was observed *in vivo*. Additionally, the implant was infiltrated with fibroblasts and fat cells from the host.

In another study, Hoshiba et al. employed tissue engineered ECM to understand the stage specific changes in ECM on regulating stem cell differentiation [12]. This study was

motivated by the fact that in native tissue, ECM undergoes constant remodeling to regulate various stages of cellular/tissue morphogenesis. To examine the stage specific effect of ECM on proliferation and differentiation of stem cells, the authors adapted ECM laid down by hMSC *in vitro*. The ECM from stage specific osteogenic differentiation was determined based on the duration of differentiation in osteogenic inducing culture where ECM after 1 and 3 weeks were identified as early and late stages of osteogenesis, respectively. Although the tissue engineered “osteogenic-ECM” supported the adhesion and proliferation of newly seeded MSC, they exhibited a differential effect on the osteogenic differentiation of these cells. The early stage osteogenic ECM promoted the osteogenic differentiation of newly seeded hMSC as compared to late stage osteogenic ECM. In contrast, expression for PPAR γ – an adipogenic marker was higher in hMSC cultured on late stage osteogenic ECM.

One of the most widely used ECM-derived biomaterials for *in vitro* cell culture is Matrigel (invented almost 2 decades ago), which is extracted from mouse tumors and is available commercially from BD Biosciences. It is a multi-component, highly hydrated ECM based matrix enriched with laminin and collagen, thereby anticipated to resemble the complex extracellular environment found in many soft tissues [13]. The utilization of Matrigel as an *in vitro* artificial matrix for cell culture has been an invaluable tool for stem cell and matrix biologists in understanding cell behavior within complex multi-component systems [14]. Matrigel has extensively been used for *in vitro* stem cell culture, and is found to support self-renewal of pluripotent stem cells such as embryonic stem cells (ESC) and induced pluripotent stem cells (iPSC) in the absence of feeder cells [14].

Besides such multi-component ECM-based materials, single component ECM materials are also widely used for *in vitro* stem cell culture. Indeed, the first successful feeder-free culture of human embryonic stem cells (hESC) was realized by employing cell culture dishes functionalized with ECM proteins such as laminin [14]. While Matrigel and laminin-coated plates supported self-renewal of hESC (H1, H7, H9, and H14), the fibronectin and collagen type IV-coated plates could not support the undifferentiated state of hESC. A combination of Matrigel and conditioned medium from mouse embryonic fibroblasts (MEF) supported *in vitro* growth of hESC up to 130 population doublings without introducing any karyotypic changes. In contrast, similar culture on gelatin-coated culture plates showed a spontaneous differentiation.

Harnessing the beneficial effects of ECM to support *in vitro* self-renewal of pluripotent stem cells, Brafman et al. have employed a cellular microarray to identify the ECM components that support self-renewal of hESC [15]. Strikingly, their finding demonstrated an interesting aspect of embryonic stem cells: cell dependent outcome! Brafman et al. observed that the responses of two cell lines (Hues 9 and Hues 10) were different to each ECM components or certain combinations of ECM components, although both cell lines were derived by the researchers under almost similar culture conditions [16]. The Authors studied the effect of individual and combinations of ECM components (collagen I, collagen III, collagen IV, collagen V, laminin and fibronectin) on proliferation and pluripotency of hESC in MEF conditioned medium as well as in defined medium. In conditioned medium, no single component supported proliferation with retained pluripotency. Higher cell proliferation was observed only in the presence of either laminin or fibronectin in combination with other ECM components. Among all components, only laminin showed positive effects on both proliferation and pluripotency of ESC. Of the various combinations studied, a combination of collagen

I, collagen IV, laminin and fibronectin showed better proliferation than any individual component or combination of ECM components or even Matrigel in conditioned medium.

Further, the same combination of ECM was studied in defined medium with and without growth factors. In the absence of conditioned medium, ESC showed reduced proliferation and pluripotency reinstating the fact that soluble components in the presence of ECM components are required for proliferation of cells with their retained differentiating ability. In defined medium the aforementioned ECM combination supported both proliferation and pluripotency of ESC. However, the presence of growth factors such as bone morphogenic protein 4 (BMP-4) and retinoic acid (RA) in defined medium reduced the pluripotency of ESC. Further, this ECM combination showed proliferation and pluripotency of ESC for long term culture (up to ten passages) in both conditioned and defined medium supplemented with basic fibroblast growth factor (bFGF).

In another study, Braam et al. have demonstrated that proliferation of hESC in mTeSR1 medium was supported by only Matrigel and purified vitronectin as compared to other tested ECMs such as fibronectin, laminin and collagen IV. However, in the presence of MEF conditioned medium all the tested ECM components supported attachment and proliferation of hESC [17]. Based on the beneficial effect of vitronectin, the authors have evaluated the effect of recombinant vitronectin on ex vivo expansion of ESC. All of the three tested hESC lines (HES2, HUES1, HESC-NL3) showed proliferation on vitronectin without any change in their karyotype for up to five passages. Further, these ESC showed differentiation to all three germ lines when supplemented with appropriate growth factors. The above mentioned studies suggest a synergistic role of cells, soluble factors and extracellular matrix components in maintaining self-renewal of hESC in vitro.

Interestingly, a recent study by Miyazaki et al. showed that beyond the type of proteins, the exact isoform of the protein can be a decisive factor in cellular response [18]. There are at least 15 types of laminin isomers and each interacts with a specific type of integrin. Miyazaki et al. first evaluated the major integrin expressed by hESC on laminin using recombinant human laminin (rhLM), and found that hESC mainly expressed $\alpha 6\beta 1$, which is in agreement with other reports [16]. Although integrin $\alpha 6\beta 1$ is known to bind to different isoforms of laminin (such as laminin-111, -332, and -511), the hESC (KhES-1, KhES-2, and KhES-3) showed different responses in adhesion and proliferation on these three rhLMs. hESC proliferated on these three isoforms of laminin for several passages while maintaining pluripotency. However, the cell proliferation was predominantly more on laminin -332 as compared to -511 and -111.

Conversely, in the case of mouse embryonic stem cells (mESC), laminin-511 isoform supported multiple passages (39 passages) of mESC in an undifferentiated state. In contrast, mESC cultured on laminin-332, which is shown to support hESC, showed proliferation without maintaining pluripotency [19]. The mESC retained self-renewal capacity while maintaining pluripotency on laminin-511 even in the absence of cell–cell contact at lower cell density, indicating that the mere contact of cells with laminin-511 (cell–matrix interaction) was sufficient for supporting self-renewal of mESC. This differential cell response of mESC and hESC to laminin isoforms reinstates the fact the conditions supporting mESC may not be sufficient for hESC. One of the major differences identified between mESC and hESC is that in contrast to mESC that can maintain in vitro self-renewal in presence of leukemia inhibitor factor (LIF) without any feeder layer support, hESC require

support from feeder layers (or conditioned medium from feeder cells along with ECM support) to maintain their *ex vivo* self-renewal.

It is evident from the aforementioned studies that the engagement of integrin adhesion receptors with the extracellular matrix plays an important role in determining the stem cell fate. Report by Hayashi et al. further supports the importance of cell surface integrins in regulating self-renewal of ESC using ECM components [20]. In their study, mESC cultured on fibronectin and laminin showed spread morphology and underwent differentiation into ectoderm lineage even in the presence of LIF. Interestingly, mESC on fibronectin and laminin expressed integrin $\beta 1$ complex formation, and by blocking such integrin complex formation the authors were able to reverse the matrix-induced differentiation of mESC.

In addition to providing adhesive surfaces for proliferating cells, ECM components also play an important role in directing the differentiation of stem cells. For instance, laminin molecules are known to play an important role in the formation and migration of neural cells. Ma et al. reported laminin as a key ECM molecule that enhances the neural progenitor generation and proliferation, and it promotes differentiation of hESC to neurons in a dose dependent manner [21]. These authors compared the embryoid bodies (EBs) plated on poly-D-lysine, poly-D-lysine/fibronectin, poly-D-lysine/laminin, type I collagen and Matrigel in the presence of soluble factors that support neural differentiation. All of the substrates supported the differentiation, albeit at varying degrees. However, neural differentiation was greater on laminin and laminin rich Matrigel. The observed laminin or Matrigel supported neural differentiation of ESC was mainly mediated by integrin $\alpha 6 \beta 1$ engagement.

In addition to laminin, other ECM proteins have also been extensively used for supporting *in vitro* cell culture and one of the extensively used ECM components is collagen. Collagen is the most abundant insoluble fibrous protein found in the body and it is a major component of tissues where the structural integrity and mechanical strength are required. In native tissue, collagen is assembled via electrostatic interaction among various amino acid groups [22].

Beyond using as a coating for tissue culture plates and synthetic scaffolds, collagen gels have been extensively used as a three dimensional support for *in vitro* cell culture. Collagen gels are prepared by altering the temperature or pH, which results in physical gels, where the networks are formed through secondary interactions devoid of any chemical crosslinks. In addition to supporting the adhesion and proliferation of cells, collagen is also known to support differentiation of stem cells, e.g., chondrogenesis of bovine MSC in three dimensional scaffolds based on collagen type I, collagen type II and alginate showed upregulation of chondrogenic genes in collagen type II gels [23]. MSC cultured on collagen type I in presence of TGF- β and dexamethasone showed osteoinduction as well as chondroinduction while with collagen type II the differentiation was more towards chondrogenesis. In another study, neuronal progenitor cells encapsulated within collagen I gels showed proliferation and differentiation into all three major neuronal lineage cells (neurons, astrocytes and oligodendrocytes) [24]. Collagen type IV is reported to induce differentiation of mESC and hESC into mesodermal lineage [25, 26]. Collagen type IV is shown to support derivation of Flk⁺ cell from embryonic stem cells with more than 95% efficiency [27]. Such derived Flk1⁺ cells were further differentiated into both endothelial and mural cells.

Another extensively used protein-based scaffold for cell culture is silk. Silk is a naturally-derived protein produced by silk worms and various spiders. Silk has exceptionally

high fiber strength, toughness and elasticity. Silk fibroin shows a combination of superior mechanical properties in fibrous form, bioactivity, low inflammation and hydrolytic stability due to its hydrophobic nature, making it a good candidate as cell culture scaffolds for directing their differentiation [28]. Additionally, the amino acid moieties present on silk fibroin can be used to conjugate various peptides and growth factors to induce tissue specific or differentiation pathway specific signaling within the scaffold. Its versatility to fabricate scaffolds in desired forms has been exploited for studying the chondrogenesis of MSC and its application for engineering multiple tissues such as vascular graft, skin, bone, cartilage, ligament, etc.

So far we have discussed the application of ECM proteins on stem cell growth and differentiation. Similar to ECM proteins, the polysaccharides present in the ECM also play an important role in maintaining various cellular activities. One of the extensively studied polysaccharides is hyaluronic acid. Hyaluronic acid (HA) is a nonsulfated glycosaminoglycan (GAG) and contributes to various physiological processes such as angiogenesis, cell migration, inflammation regulation, and resilience of cartilage. HA is also known to play a crucial role in early embryonic development. Hydroxyl and carboxyl groups present in HA have been used to create functionalized HA precursors. Modified HA containing functional groups such as thiols, methacrylates, aldehydes and divinyl sulfone can be used to form hydrogels. Gerecht et al. used methacrylated hyaluronic acid based hydrogel for self-renewal of hESC in a three-dimensional environment, where photopolymerization was used to encapsulate hESC (H9, H11 and H1) colonies within the HA hydrogels [29]. hESC maintained their undifferentiated state in the presence of MEF conditioned medium for up to 20 days. These HA supported undifferentiated ESC can be easily released by treatment with hyaluronidase (an enzyme that degrades HA) without inducing any detrimental effect to the encapsulated hESC. Additionally, the HA-supported ESC maintaining their undifferentiated state could be differentiated into endothelial lineage by culturing them in the presence of endothelial growth medium.

HA-based hydrogels have also been extensively used for regulating differentiation of stem cells, vocal chord augmentation, and wound healing [30]. Harnessing the ability of HA materials to interact with MSC, Chung et al. utilized HA hydrogels to promote chondrogenic differentiation of hMSC [31]. A comparative study analyzing the effect of HA hydrogels on promoting osteogenic differentiation of goat MSC showed about 30% cells positive for alkaline phosphatase in HA hydrogels as against 5% positive cells in polyglycerol hydrogels [32].

18.2.2

Natural Polymers

Naturally derived polysaccharides that are used extensively for cell culture include chitosan, alginate, and agarose. Due to the structural similarity of chitosan to the GAG found in ECM of native tissues such as articular cartilage, it has been explored for application in cartilage engineering [33]. Another widely used biomaterial is alginate derived from seaweed. Alginate based scaffolds have been used due to its mild gelling conditions, its interconnected porous structure and consequently better diffusion. For

instance, calcium alginate porous scaffolds have been found to support the proliferation of encapsulated mESC and their differentiation into pancreatic cells when cultured in supplemented mediums [34].

18.2.3

Hybrid Materials

While offering a wide range of advantages, the ECM derived biomaterials also pose some limitations in terms of modifying their mechanical properties, varying composition depending upon their source, obtaining them in purified forms and in sufficient quantity, cost effectiveness, processing them into three dimensional structures, their immunogenicity if they are of animal origin, patient-to-patient varying enzymatic degradation level, and thus difficulty in customizing to meet the requirements of the target experiment. As compared to natural biomaterials, synthetic materials offer varied options in tunability of structural composition, mechanical properties, architecture, degradability etc. Further, the reduced batch-to-batch variation in the quality, higher scalability, absence of immunogenicity due to non-animal sources, and amenity to numerous fabrication techniques open up wide options for scaffold preparation and their potential applications. However, lack of bioactivity of synthetic materials is the major deterrent for their application as scaffolds and is circumvented by combining them with natural materials in multiple ways such as blending, coating or chemical conjugation.

Hybrid materials containing components of both natural and synthetic materials exhibit combined advantages of both the systems. For instance, ECM-based materials offer biocompatibility, adhesion and biological signals, while synthetic materials offer advantages in terms of structural, mechanical, and chemical properties. Depending upon the nature of the ECM incorporated, the encapsulated cells exhibit different morphologies, which could have significant influence on determining their growth and differentiation. Figure 18.2 shows the effect of poly(ethylene glycol) (PEG)-based hybrid hydrogels containing various ECM molecules on the morphology of encapsulated cells. Such hybrid materials are extensively used to promote stem cell differentiation both in the presence and absence of differentiation inducing soluble factors. For instance, incorporation of chondroitin sulfate (CS), an ECM component of cartilage, into PEG hydrogel was found to induce the chondrogenesis of hMSC [35]. Similarly, chondrogenic differentiation of hMSC was observed when cells were cultured in serum free media on scaffolds having cob-web like mesh structures based on collagen and poly (lactic-co-glycolic acid) [36]. Both these studies have observed improved cell aggregation within these scaffolds leading to enhanced chondrogenesis.

Benoit et al. have employed heparin-functionalized PEG hydrogels to promote osteogenic differentiation of hMSC [37]. The functional ability of heparin-based hydrogels to support osteogenic differentiation was primarily attributed to their ability to bind to proteins such as fibronectin and BMP-2, which in turn promoted cell-material interactions. In another study, chitosan functionalized with various GAG molecules (heparin, heparin sulfate, dermatan sulfate, chondroitin 4-sulfate, chondroitin 6-sulfate, and hyaluronic acid) was employed to identify biomaterials that can support growth and tissue specific differentiation of MSC [38]. GAG-functionalized chitosan materials were found to promote proliferation of

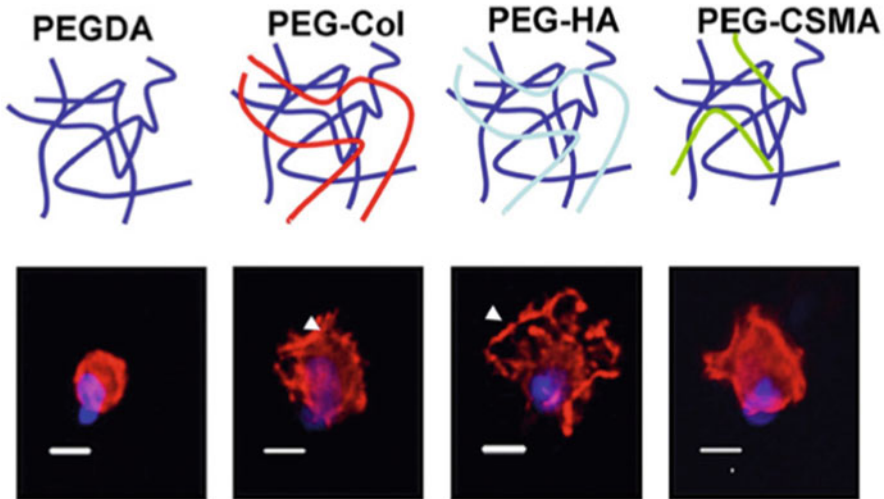


Fig. 18.2 Incorporation of ECM components into PEG hydrogels resulted in distinct cellular morphology as seen by actin (*red*) and DAPI (*blue*) staining. Scale bar: 10 μm [4] (Reprinted from Hwang et al., *Adv Drug Deliv Rev* 2008;60:199–214 with permission from Elsevier)

MSC as compared to tissue culture plates and unmodified chitosan surfaces and the growth rates of MSC increased with increasing GAG components on the culture surfaces.

18.2.4

Functionalization with Biochemical Cues

Another approach to impart biological cues and cell adhesive groups onto synthetic matrices is functionalizing them with cell recognizing bioactive motifs, such as small molecular weight peptides. The advantages of peptides over proteins are that the former is small molecular weight and can be manufactured with conformational stability, and can be functionalized easily. Incorporation of small molecular weight peptides is sufficient to engage the cell surface receptors and activate various biochemical pathways to control various cellular activities such as adhesion, proliferation, survival, and differentiation [39]. For example, incorporation of tri-amino acid sequence arginine-glycine-aspartic acid (RGD) commonly found in most of the ECM has been widely used to improve the cell–matrix interactions [39, 40]. Adhesion of cells to their extracellular matrix is a fundamental process in governing stem cell fate and commitment. Nuttleman et al. have shown that RGD-functionalized PEG hydrogels improve the survival of encapsulated hMSC [40]. In contrast, hMSC within the bioinert PEG hydrogels undergo apoptosis due to lack of cell–matrix interactions.

Similarly, poly(*N*-isopropyl acrylamide)-co-acrylic acid (poly(NIPAM-co-AAc)) hydrogels containing RGD motifs have been shown to support self-renewal of hESC (HSF-6 hESC cell line) for a short period of time (~5 days) in the presence of MEF conditioned

medium [41]. The hESC on these PNIPAM-based hydrogels containing higher concentrations of RGD moieties (105–150 μM) showed morphology similar to ESC grown on MEF. Beyond RGD peptides, these PNIPAM-based hydrogels also contain MMP-13 cleavable Gln-Pro-Gln-Gly-Leu-Ala-Lys moieties. In a recent study, Lee et al. have devised a three dimensional (3D) artificial matrix functionalized with integrin binding peptides to support self-renewal of mESC in vitro in a 3D environment [42]. By employing these artificial matrices, the authors have demonstrated the importance of simultaneous signaling of different integrins $\alpha 5\beta 1$, $\alpha v\beta 1$, $\alpha 6\beta 1$, and $\alpha 9\beta 1$ in maintaining self-renewal of mESC.

In another study, Dedra et al. have screened a number of laminin-derived peptides to identify candidates that can support hESC growth given that the laminin can support in vitro growth of ESC [43]. Their studies demonstrate that only a few laminin-derived peptides support the proliferation and self-renewal of ESC (H1 and H9 cell lines) without inducing differentiation. Of the various peptides studied to identify the critical receptor-ligand pair for maintaining self-renewal of the ESC, the RNIAEIKDI sequence with high density was found to support the adhesion and proliferation of ESC while maintaining their undifferentiated state.

In a recent study, Alberti et al. used immobilized LIF to support self-renewal of mESC, where the LIF immobilized materials supported pluripotency of mESC for a short culture time (~2 weeks or six to eight passages) in the absence of diffusible LIF molecules [44]. The LIF molecules were immobilized by covalently attaching them directly onto poly (octadecene-alt-maleic anhydride) (POMA) or through PEG based spacer arms on POMA. The effect of immobilized LIF on the ESC was compared with LIF noncovalently attached by deposition on ECM coated on POMA hydrogel. The immobilized LIF showed activation of signaling pathways (STAT3 and MAPK) in a dose-dependent manner, and the mode of LIF presentation (LIF adhered to the underlying biomaterial via chemical attachment versus physical adsorption) did not affect their functional properties.

In addition to promoting self-renewal or differentiation of stem cells, biomaterials have also been employed to deliver progenitor cells into compromised tissues. In vivo transplantation of cells is limited by the death of most transplanted cells and/or their poor engraftment with the host tissue. Hill et al. recently demonstrated a biomaterial based approach to circumvent these limitations [45]. The approach involved transplanting progenitor cells within a synthetic biomaterial (alginate scaffolds functionalized with G_4RGDSP), which promote viability and proliferation of the embedded cells without promoting their terminal differentiation. In addition to peptide functionalization, the scaffold also contained growth factors relevant to muscle tissue formation. The migration of cells to the host tissue from the scaffold is dependent upon the scaffold porosity and it cannot be achieved by using a hydrogel system (especially non-degradable). Therefore, in this study, the authors used macroporous alginate scaffolds with open interconnected pores. Such a material-based reservoir of progenitor cells allowed the migration of the transplanted cells to the host tissue, and promoted skeletal muscle regeneration.

Beyond supporting self-renewal and proliferation of stem cells, peptides have been used to promote differentiation of stem cells. For instance, Silva et al. have demonstrated that self-assembled nanofibers encoded with laminin epitope IKVAV selectively promote neuronal differentiation of neural progenitor cells [46]. Similarly, PEG hydrogels decorated with collagen mimetic peptides (CMP) have been shown to promote chondrogenic

differentiation of MSC [47]. Collagen mimetic peptides having a specific amino acid sequence of $-(\text{Pro-Hyp-Gly})_x-$, which form a triple helix structure akin to native collagens, and thereby represent both chemical and physical characteristics of collagens peptides have been shown to exhibit strong affinity towards both native and denatured type 1 collagen.

A number of studies have shown enhanced chondrogenesis of adult stem cells in RGD-functionalized biomaterials [48, 49]. Studies by Hwang et al. have shown that PEG hydrogels functionalized with RGD peptides support chondrogenic differentiation of ESC [48]. However, recently emerging studies suggest that the role of RGD is not as direct as it was thought to be earlier. RGD mediated cell–matrix interactions promote the survival and commitment of MSC, however, its persistence can limit the terminal differentiation of differentiating MSC [49]. Manipulation of the material properties by cleaving the RGD, however, promotes the complete differentiation of MSC undergoing chondrogenesis.

Salinas et al. have modified PEG hydrogels with two peptide motifs, RGD and KLER, for promoting chondrogenic differentiation of hMSC. The KLER sequence is a binding site of decorin protein and is known to bind to collagen type II matrix [50]. PEG hydrogels containing both KLER and RGD moieties were found to promote the chondrogenic differentiation of encapsulated MSC compared to hydrogels containing only RGD.

RGD functionalized PEG hydrogels have also been shown to promote osteogenesis of MSC, while soluble RGD peptides inhibited such differentiation [51]. Similarly, Shin et al. have demonstrated enhanced osteogenic differentiation of rat MSC in oligo(poly(ethylene glycol) (fumarate)) (OPF) hydrogels functionalized with RGD sequences even in the absence of β -glycerolphosphate and dexamethasone, osteogenic inducing soluble factors [52]. It was suggested that the interaction between RGD peptides and cell surface integrins activated intracellular pathways, triggering osteogenic differentiation akin to that seen when cells are exposed to osteogenic inducing factors such as dexamethasone. This is supported by other studies indicating that selective activation of integrins can trigger osteogenic differentiation of progenitor cells [53].

Hsiung et al. have recently reported an enhanced osteogenic differentiation of hMSC in alginate gels in presence of cyclic RGD over linear RGD. The improved differentiation is mainly attributed to the enhanced cell surface integrin-ligand binding offered by the cyclic RGD [54]. A number of studies have examined the role of hydroxyapatite (HAp) binding peptides for regulating osteogenic differentiation of stem cells [55]. For tethered peptide (e.g., RGD) sequences on scaffolds, clustering of peptides, their density, number of peptide per cluster, and cluster size can have effect on the integrin-mediated cellular processes [56].

Functionalizing synthetic biomaterials with peptide sequences can also be used to impart cell responsive degradability to biomaterials [57]. Biodegradation of ECM *in vivo* is mediated by matrix metalloproteinases (MMP), enzymes linked on the cell surface. Conjugation of PEG scaffolds with MMP-sensitive GPQGWGQ peptide along with cystine peptide for adhesion of cells was found to emulate the cell migration and cell invasion [57, 58]. Additionally, photolabile linkages have been used to release peptide on demand for chondrogenesis of hMSC [59].

In addition to functionalizing the synthetic materials with peptide groups, coating the synthetic materials with ECM components to improve adhesivity has been extensively used for supporting the proliferation and differentiation of stem cells. Levenberg et al. used Matrigel and fibronectin to improve the adhesivity of porous scaffolds based on a blend of

poly (lactic-co-glycolic acid) (PLGA)/polylactic acid (PLLA) [60]. The ESC (H9) cultured on these scaffolds underwent differentiation into ectodermal, mesodermal and endodermal lineages responding to the differentiation inducing soluble factors. Both fibronectin and Matrigel supported adhesion, proliferation, and viability of hESC. When implanted in SCID mice the scaffold supported hESC continued to differentiate and formed organized tissues. Additionally, the transplanted hESC-laden PLGA/PLLA was found to anastomose with the host vasculature. In a similar study by Lee et al. three dimensional poly (lactide-co-glycolic acid) scaffolds were conferred bioactive by coating with laminin. Differentiated hESC seeded on this scaffold and transplanted between liver lobules in SCID mice showed complex tissue formation in vivo and expressed various ECM proteins characteristics of multiple lineages [61].

18.2.5

Synthetic Biomaterials

In the absence of any cell recognizing moieties, adhesion of stem cells to synthetic biomaterials is often governed by non-specific protein adsorption. A variety of material properties (such as functional groups, charge density, roughness, mechanical properties, and hydrophobicity) can play pivotal roles in determining the extent and type of protein adsorbed onto the synthetic biomaterials from the surrounding culture conditions (soluble factors, serum, etc). Beyond modulating the protein adsorption, the chemical and physical properties of the materials can also regulate the conformation of adsorbed proteins, which in turn play a significant role in the engagement of cell surface integrins. Such differential adsorption of ECM components from culture medium and/or protein conformations can have significant effects on their ability to direct stem cell differentiation.

In a recent study, Phillips et al. investigated the effect of functional groups of the biomaterials on differentiation of MSC using self-assembled monolayer (SAMs) on ω -functionalized alkanethiols on gold substrates [62]. SAMs having different functional groups such as $-\text{CH}_3$, $-\text{OH}$, $-\text{COOH}$, $-\text{NH}_2$, varied in their hydrophobicity (thereby wettability). The SAMs presenting different terminal groups not only differed in the amount of fibronectin adsorption but also modulated their conformation differentially. These self-assembled monolayers having different functional groups exhibited varying differentiation potential of MSC. SAMs with $-\text{NH}_2$ functional groups promoted osteogenic differentiation, while $-\text{OH}$ functionalized surfaces promoted adipogenic differentiation.

Benoit et al. have used a similar approach wherein PEG chains were tethered with small molecules having different functional groups, to direct differentiation of MSC [63]. Functional groups were introduced on PEG chains by incorporating monomers like methacrylic acid ($-\text{COOH}$), 3,3,4,4-tetrafluorobutyl methacrylate ($-\text{F}$), ethylene glycol methacrylate phosphate ($-\text{PO}_4$), t-butyl methacrylate ($-\text{butyl}$) and 2-amino methacrylate ($-\text{NH}_2$). hMSC showed osteogenic and adipogenic differentiation in PEG hydrogels containing phosphate and t-butyl functional groups, respectively, when cultured in growth medium. The observed trend in differentiation of hMSC within PEG matrices with different functional groups in the absence of any differentiating media is attributed to altered cell-matrix interaction owing to the specific functional groups that induce the pathways for production of phenotype-specific

molecules. In an alternative mechanism, the final differentiation can also be a result of the nucleated sequestering of cell-secreted molecules by functionality on the matrix. The functional group-directed differentiation was observed both in the two-dimensional (2D) environment where the hMSC were plated on hydrogel discs and 3D environment where the cells were encapsulated within the hydrogel.

Chastain et al. used two different materials viz. PLGA and PCL to modulate the preferential adsorption of ECM proteins from serum and demonstrated that depending upon the adsorbed protein the material showed differential effect on osteogenic differentiation of hMSC [64]. The authors showed that the adhesion of MSC onto PCL was mediated by vitronectin, while adhesion of MSC onto PLGA was mediated by type-1 collagen. Interestingly, hMSC cultured on PLGA scaffold expressed more osteocalcin when compared to those cultured on PCL, indicating the role of surface characteristics of the matrix and specificity of integrin binding in differentiation.

Similarly, manipulation of spacer length used to conjugate amines on the surface was found to alter the adhesion and proliferation of human hematopoietic stem/progenitor cells (hHSPC) [65]. Amination of grafted polyacrylic acid on polyether sulfone nanofibrous scaffolds with amines having different methylene chain lengths was found to result in differential adhesion and colony size of hHSPC. Amines containing two and four methylene units showed better cell proliferation as compared to hexamethylene amine based spacers in cytokine supplemented culture. In the absence of serum or specific cell adhesion ligands, observed cell adhesion on aminated surfaces is believed to be mediated by CD34+ antigens via electrostatic polar interactions.

Researchers have also been increasingly investigating the ability of synthetic biomaterials to support self-renewal and proliferation of ESC in vitro. Studies by Harrisona et al. have shown that proliferation of mESC increased with an increase in the hydrophilicity of the surface of poly(α -hydroxy esters) [66]. Surface hydrophilicity of various polymers such as polylactide, polyglycolic acid and poly(lactide-co-glycolide) was altered by treating with KOH. The increased cell proliferation was attributed to the increased adsorption of serum factors, which can act as an intermediate cell binding protein.

There exists a number of tissue engineered organs that were created with the help of synthetic biomaterial-based three dimensional structural supports. One of the first tissue engineered organs is human cartilage, and it was achieved by seeding chondrocytes onto a synthetic biodegradable PLGA/PLLA-based template shaped as a human ear. The cell-laden scaffold was then implanted into subcutaneous pockets of athymic mice [67]. Specimens harvested after 12 weeks showed the in vivo cartilage tissue formation and maintenance of the implant structure. Adapting a similar approach, Atala et al. have tissue engineered functional bladders, where the cells isolated via biopsy were seeded within a biodegradable scaffold made of polyglycolic acid and collagen and cultured in vitro [68]. Similarly, vascularized bone grafts for critically-sized mandible defects were generated using synthetic structural supports and MSC from the patient [69]. This was achieved by creating a titanium mesh cage recapitulating the size and shape of the mandibular defect. The cage was filled with bone mineral blocks containing human bone morphogenic protein and the patient's bone marrow. The filled titanium mesh cage was then implanted inside the latissimus dorsi muscle of the patient. After 7 weeks of in vivo culture, the tissue engineered mandible was used to treat the patients' mandibular defect. Figure 18.3 shows tissue

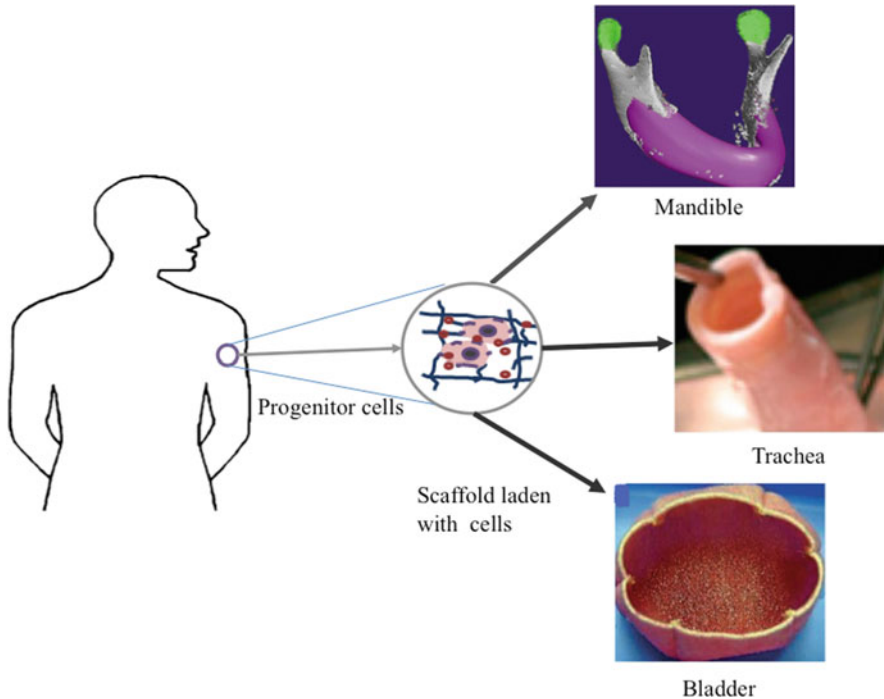


Fig. 18.3 Tissue engineered human organs using progenitor cells with scaffolds based on natural and synthetic matrices [9, 68, 69] (Reprinted from Macchiarini et al., *The Lancet*, 2008;372: 2023–2030, Atala et al., *The Lancet*, 2006; 367: 1241–1246, Warnket et al., *The Lancet*, 2004, 364, 766–770 with permission from Elsevier)

engineered organs based on both natural and synthetic materials and stem cells. Aforementioned examples demonstrate the applicability of synthetic materials in regenerative medicine and also the immense opportunity to explore them for therapeutics.

18.2.6

Biomaterials as a Reservoir of Growth Factors

In addition to being a structural support, ECM components also function as a reservoir of growth factors and cytokines and coordinate their spatio-temporal release. Biomaterials have been extensively used to regulate growth factor signaling for stem cells, and most of the initial efforts were focused on protecting the bioactive agents (by encapsulation) and achieving their prolonged availability (by slow and/or controlled release) [70]. In such cases, the release of bioactive agents is achieved through diffusion, degradation, or differential swelling responding to the external cues such as temperature or pH. Studies have shown that the release of retinoic acid from PLGA microspheres can direct the differentiation of pluripotent cells into neurons [71]. Carpenedo et al. have used a similar approach to

control homogeneous and organized differentiation of EBs of mESC [72]. Since the stem cell growth and differentiation involve a complex cascade of events engaging multiple growth factors, researchers have also utilized the sequential release of growth factors to regulate stem cell differentiation [73].

Mercado et al. grafted recombinant human morphogenic protein (rhBMP) on self-assembled nanoparticles based on poly (lactide fumarate) and poly(lactide-co-glycolide fumarate) such that rhBMP is released concurrent with the layer-by-layer degradation of the matrix [74]. After 14 days of incubation with rat MSC, both types of nanoparticles containing rhBMP induced equivalent mineralization as directly added rhBMP in growth media. Similarly, a porous scaffold based on elastase-sensitive polyurethane urea nanofibers containing insulin-like growth factor (IGF-1) encapsulated in poly(lactide-co-glycolide) microspheres was found to support growth of hMSC even under hypoxia/nutrient starving conditions [75]. In this study, IGF-1 showed a triphasic release profile with retained bioactivity for up to 4 weeks.

In contrast to microencapsulation where the availability of growth factor is dependent upon the degradation and diffusion kinetics, tethering growth factor onto the biomaterial ensures its availability in a desired orientation similar to that observed in ECM. Fan et al. have demonstrated that the surfaces functionalized with epidermal growth factor (EGF) promote spreading and survival of human telomerase reverse transcriptase immortalized hMSC (hTMSC) in culture [76]. Additionally, the tethered EGF increased the number of hMSC colonies formed, unlike soluble EGF [77].

In addition to the above discussed approaches, researchers have employed the inherent ability of ECM components to bind to various proteins and growth factors to promote biological activity in synthetic material-based artificial matrices [37]. For instance, PEG biomaterials were modified with heparin moieties to module growth factor binding. Heparin, a highly sulfated glycoaminoglycan, contains binding domains for various growth factors such as bFGF and BMP-2. Benoit et al. showed a sustained release of bFGF (up to 5 weeks) from heparin domains. In another study, Benoit et al. made use of fluvastatin release from PEG hydrogel scaffolds in order to activate release of BMP-2 from encapsulated hMSC, thereby stimulating osteogenic differentiation of these cells [78].

18.2.7

Biomaterials for Immunomodulation

One of the biggest challenges in transplantation of cells is immunorejection as the transplanted cells have to overcome the barrier of secreted pro-inflammatory cytokines as a response to the injury. The secreted cytokines further recruit more immune cells and activate apoptotic pathways. As a preventive mechanism for such immunorejection by the host cells, biomaterials are incorporated with immunomodulatory mechanisms. Various functionalizing and encapsulation approaches have been explored for effective delivery of antigens for cytosolic delivery [79]. Isolating the transplanted cells using semi-permeable biomaterials has been conventionally used to protect the transplanted cells from the host immune system. However, often when encountered by soluble pro-inflammatory cytokines, the transplanted cells fail to perform.

To isolate the transplanted cells from such soluble pro-inflammatory cytokines, Lin et al. used cytokine-antagonizing PEG hydrogels, where the peptides having high selectivity and affinity for pro-inflammatory cytokine-tumor necrosis factor (TNF α) blocked their interaction with the cell surface receptors [80]. Here, PEG hydrogels were modified with a peptide mimic WP9QY derived from TNF α -receptor binding site that binds to TNF α so strongly that it inhibits TNF α from binding to the cell surface receptors. Differentiating rat pheochromocytoma (PC12) cells encapsulated within PEG-RGD-WP9QY scaffolds showed higher viability as compared to PEG-RGD scaffolds. Similarly, mouse pancreatic islet cells encapsulated within PEG-RGD-WP9QY did not show any difference in insulin secretion or metabolic activity when incubated in an environment containing high levels of TNF α . In another study, affinity peptide-functionalized (WKNFQT1) PEG hydrogels were formulated to modulate the activity of monocyte chemotactic protein 1 (MCP-1). This chemokine is known to generate the chemotaxis of monocytes, dendritic cells, and memory T cells [81].

18.3 Biophysical Cues

18.3.1 Mechanical Properties of Biomaterials

As discussed earlier, the ECM provides a structural support to the cells and acts as a template for their growth with multifunctional characteristics of providing biochemical cues. In addition to the biochemical cues, they also provide biomechanical cues (static and/or dynamic) to the embedded cells. In recent years, stiffness of the biomaterials has been employed as a knob to regulate cell shape, which in turn plays an important role in phenotype determination [82]. For instance, Engler et al. showed that the tissue specific differentiation of stem cells (here MSC) can be achieved by culturing them on substrates having stiffness comparable to that of the native tissue [83]. Similarly, a number of studies have shown the effect of material stiffness on proliferation and tissue specific differentiation of progenitor cells [84–87].

Wang et al. demonstrated stiffness dependent cellular response of hMSC using an injectable hydrogel based on modified gelatin [88]. The cell proliferation was found to increase with the decrease in the stiffness of the materials. Further, hydrogels with lower stiffness showed higher neurogenesis in the absence of any growth factor. Evans et al. studied the effect of biomaterial stiffness on the differentiation of mESC (TG2 α E14) using poly(dimethyl siloxane) (PDMS) matrices plasma treated and covalently coated with collagen I to facilitate cell adhesion [89]. Their study demonstrated an upregulation of mesendoderm markers of mESC with increasing stiffness of the PDMS material from 41 kPa to 2.7 MPa, and the effect was independent of cell density. They also showed substrate stiffness dependent osteogenic differentiation of the mESC. Studies by Battista et al. showed limited proamniotic cavity formation of differentiating EBs within collagen

18 type 1 gels (three-dimensional environment) having an elastic modulus of 34 Pa as compared to that of 16 Pa [90].

A recent study by Winter et al. has shown that hMSC become quiescent on ECM-coated acrylamide hydrogels having an elastic modulus of 250 Pa [91]. These quiescent cells however further undergo adipogenic differentiation upon exposure to adipogenic inducing soluble factors, thus indicating the maintenance of their differentiating potential. Rowland et al. have demonstrated the effect of a combination of ECM components along with substrate stiffness on modulating differentiation of hMSC using acrylamide hydrogels coated with various ECM components [92]. A significant difference in cell shape with response to the ECM components was observed for the same substrate stiffness. Further, the osteogenic differentiation was more prominent on stiffer matrices. However, the expression of transcription factor Runx2 varied with the type of the adhesive ECM component used to coat the acrylamide gels. Taken together cell shape and differentiation pattern, the authors concluded that a combination of biochemical and biomechanical cues arising from the extracellular environment is required for stem cell differentiation.

Hydrogels based on PEG and poly-L-lysine (PLL) showed differential interaction with neural stem cells depending upon the mechanical and chemical properties of the surface [93]. Particularly hydrogels having modulus of 3,500–5,000 Pa – equivalent to brain tissue, showed higher cell migration and differentiation. In a range of hydrogels prepared by varying the molecular weights and mole ratios of PEG/PLL, the neuronal differentiation was found to increase with the increase in molecular weight of PLL and this effect is attributed to the increased cell interactions with an increase in the surface charge of PLL. In another study, the effect of dynamic elasticity of the matrix on differentiation of the cells is studied by using photolabile crosslinks in PEG based hydrogels whose elasticity can be manipulated by controlling the photodegradation [94].

In addition to static mechanical cues, cells respond to dynamic mechanical cues. The cellular response to dynamic mechanical cues has been exploited to culture them in bioreactors to induce a physicochemical microenvironment for promotion of cell proliferation and uniform tissue development [95]. However, dynamic mechanical cues are beyond the scope of this topic and hence will not be discussed.

18.3.2

Biomaterials for Micro- and Nano-Scale Cues

One of the characteristics of native tissue is its hierarchical organization over different length scales ranging from nano- to macro-scale. Depending upon the composition and intermolecular interactions, the ECM molecules can differ in their organization, thus presenting differential topological cues to the cells. Advancements in biomaterial technologies, such as micro and nanofabrication techniques have enabled the development of structures with nano- and micro-topologies to modulate various cellular functions such as adhesion, alignment, shape, and differentiation. A recent study by Yim et al. has shown nano-topography induced changes in focal adhesion, and cytoskeletal organization of hMSC. These cytoskeletal changes significantly influenced the viscoelastic properties of the cells [96].

In another study, the same authors have shown that hMSC, when cultured on Collagen I coated PDMS substrates with nanoscale grooves of 350 nm width, showed alignment and differentiation to a neuronal lineage in the presence of neuron inducing factors [97]. Similarly, adult rat hippocampal progenitor cells cultured on micropatterned biomaterial surfaces modified with laminin showed preferred alignment in the direction of the groove (13 μm width \times 4 μm height) as compared to its non-grooved counterparts and showed improved neuronal differentiation [98]. Gerecht et al. have evaluated the response of hESC towards substrates with nanotopography by employing fibronectin-coated PDMS with line gratings [99]. The ESC cultured on these substrates exhibited elongation and alignment and reduced cell proliferation. In addition, authors also observed organization and polarization of cytoskeletal proteins that could be reversed with the aid of exogenous supplementation of actin disrupting agents.

In an interesting study by Dalby et al. the effect of nano-topographical cues on the osteogenic differentiation of hMSC was examined in the absence of osteo-promoting soluble factors using nano-featured poly(methyl methacrylate) (PMMA) substrates with varying symmetry and degrees of disorder [100]. MSC cultured on disordered surface showed higher aggregation and osteogenic potential than on the highly ordered or randomly patterned surfaces. Researchers have also developed self-assembling oligopeptides as artificial matrices with nanoscale cues [46, 101]. These self-assembled nanofiber-based matrices have been shown to support growth and differentiation of a variety of cells.

Electrospinning has been used to impart micro or nano topologies to biomaterials, where the electrospun fibers mimic the fibrillar structure of ECM. Additionally, the long fibrillar structure induces alignment of the cells and directionality to the growing cells. Electrospinning has recently gained a lot of attention due to its attractive features, such as greater control over fiber geometry, flexibility in choice of the polymers, and higher surface to volume ratio of the resultant fibers for cell attachment. Dang et al. reported the myogenic differentiation of hMSC on thermally responsive electrospun hydroxyl butyl chitosan nanofibers [102]. After 2 weeks of culturing, hMSC showed aligned cytoskeleton and nuclei on electrospun fibers of hydroxyl butyl chitosan with and without incorporated collagen I, whereas there was an absence of any preferential alignment on similar hydroxyl butyl chitosan film. These hMSC with aligned fiber topography and elongated nuclear shape on culturing in growth medium showed upregulation of myogenic gene expression.

Electrospun materials have also been used to direct differentiation of MSC into other lineages. Li et al. used electrospun polycaprolactone nanofiber for multilineage differentiation of hMSC to adipogenic, chondrogenic and osteogenic differentiation by culturing in suitable media [103]. In another study, the same authors found that chondrocytes cultured on nanofibrous PLLA scaffold showed higher proliferation and retained morphology as compared to microfibrillar PLLA scaffold, which demonstrates the different biological activities of the cell varying with the dimensionality of the fibers [104]. In a similar study by Shih et al. electrospun reconstituted type I collagen nanofibers were found to support the proliferation of hMSC while maintaining their potency for osteogenic differentiation [105].

In yet another approach to mimic ECM morphology, Smith and coworkers prepared PLLA nanofibers by phase separation methods and compared with PLLA films for osteogenic differentiation of mESC [106]. Matrices based on nanofibers of average

18 diameter 50–500 nm and a porosity of 93% showed enhanced spreading and attachment of ESC. These ESC, when cultured in osteogenic medium, showed increased differentiation towards bone tissue formation as indicated by the extent of mineralization and expression of osteocalcin. The differentiation of mESC to mesodermal and osteogenic lineage is attributed to the higher amount of serum protein adsorbed on nanofibrous scaffolds as compared to films.

In addition to creating nano-sized moieties during the fabrication, inclusion of nanomaterials during scaffold preparation has been explored to elicit favorable cellular responses. Nanomaterials show unique surface properties such as surface energy, surface wettability, surface chemistry and topography due to higher surface area and roughness. Jan et al. reported the use of single wall carbon nanotube (SWNT) based materials for the differentiation of mouse embryonic cortical neurospheres and neural stem cells (NSC) [107]. In a study by MacCullen et al. multiwall carbon nanotube (MWNT) encapsulated within nanofibrous porous polylactic acid (PLA) scaffolds showed improved proliferation and longitudinally aligned aggregation of hMSC as compared to similar nanofibers without MWNT [108].

In a novel way to control the undifferentiated state of hESC, Mohr et al. developed a microwell culture technique [109]. This process was used to develop EBs with controlled sizes that could be maintained in an undifferentiated state for a long time. The constrained geometry to control the colony size was defined by PDMS based microwells functionalized with self-assembled monolayers of alkanethiols to resist the protein adsorption. Uniform aggregate size and shape of EBs are believed to support the reproducible differentiation of hESC. Confined geometry of the microwells ensures the cell–cell signaling and colony aggregation required for survival and self-renewal of EBs. These microwell cultured ESC could be passaged further with retained pluripotency.

18.4

Two-Dimensional Cultures Versus Three-Dimensional Cultures

Most of the *in vitro* studies involving stem cells are carried out on 2D tissue culture plates coated with ECM components, or employing 2D biomaterial disks. These *in vitro* cultures do not mimic the physiological environment of the cells and may potentially introduce culture dependent artifacts. The physiological environment of a cell in a living organism has a three-dimensional architecture of varying length scales (nano-, mesoscopic-, micro-, and macro scale). In a classic study, Cukierman et al. demonstrated the differential expression of cell surface integrins depending upon whether the fibroblasts were cultured in a 2D environment or 3D environment [110]. Compared to 2D, fibroblasts in 3D displayed enhanced cellular activities (motility and proliferation) and narrowed integrin usage. Similarly, studies involving cancer cells indicate that 3D cultures providing cell–matrix and cell–cell interactions could be a powerful tool in cancer research [111].

Significant differences were found in the differentiation profile of ESC when cultured in a 3D environment versus 2D [112–114]. For instance, the expression of aggrecan in chondrogenesis of ESC was found to vary in 2D and 3D culture under similar conditions

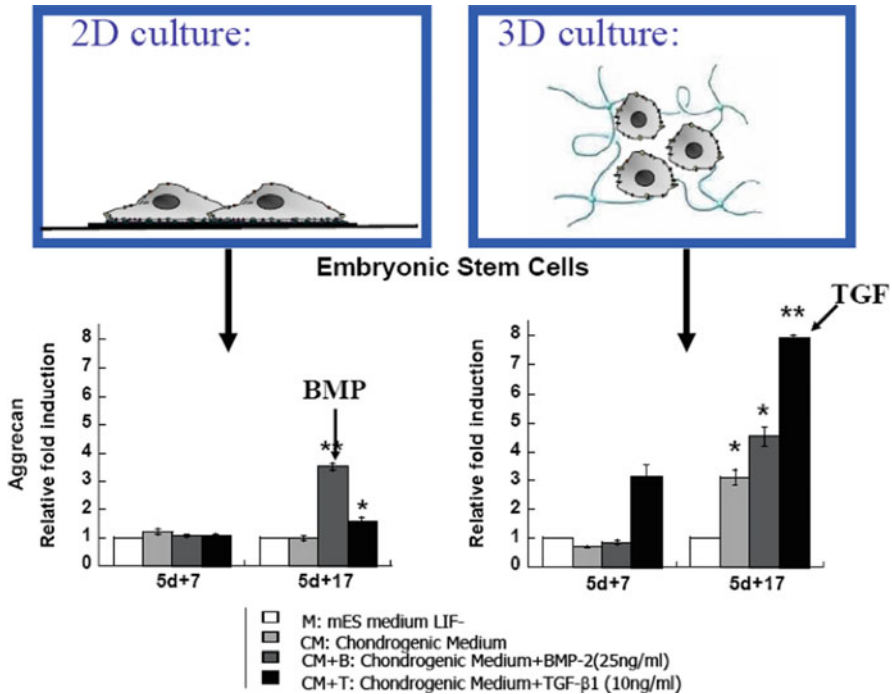


Fig. 18.4 ESC culture in 2D and 3D environment and relative expression of aggrecan under different conditions [4] (Reprinted from Hwang et al., *Adv Drug Deliv Rev* 2008; 60:199–214 with permission from Elsevier)

as shown in Fig. 18.4 [4]. A report by Levenberg et al. showed that a fibronectin-coated 3D scaffold supported hESC differentiation and their 3D structure formation compared to their 2D counterparts (fibronectin coated culture plate). They also observed a similar finding when compared to cells on Matrigel with cells on a Matrigel imbided 3D scaffold [60].

18.5

Conclusion and Future Directions

Although some of the discussed successful cell based therapeutics demonstrate potential, there exist reports that illustrate the challenges associated with stem cell therapeutics. A recent report in *PLoS Medicine* describes the outcome of a boy who was treated with human fetal neural stem cells [115]. A boy suffering from ataxia telangiectasia (AT) was treated with intracerebellar and intrathecal injections of human fetal neuronal stem cells. However, 4 years after his first stem cell transplantation a glio-neuronal brain tumor of stem cell origin was found in the recipient's brain. This reinstates the need to dissect the important environmental factors, which will solely control lineage/tissue specific

differentiation of stem cells, while preventing uncontrolled proliferation and heterogeneous differentiation of stem cells. This also indicates the need to well characterize the stem cells and to generate new tools to study them *in vitro*.

Although advancements in biomaterials have enabled creation of synthetic material based artificial matrices with precise structural and functional properties, the development of multi-functional materials that can simultaneously provide multiple dynamic biochemical and mechanical cues to the embedded cells is still a challenge. Development of such composite systems will be a key component in the development of next-generation, biologically-inspired materials. Harnessing the principle of stimuli-responsive biomaterials could lead to the development of artificial bioactuating systems for stem cell engineering.

Ongoing challenges remain in controlling the material properties of biomaterial-based artificial matrices spatially and temporally. Major advances have been made in creating responsive materials and many of them require exogenous interference. It would be advantageous to create materials that can undergo dynamic changes responding to the cellular activities mimicking the native tissue remodeling. The combination of material science, development biology, and systems analysis might be a powerful tool in understanding matrix-mediated tissue morphogenesis in multiple scales.

Engineering hierarchical tissues from stem cells requires multiple signals in a spatially controlled manner. This could be achieved by creating anisotropic biomaterials with spatially and temporally graded structural, chemical, and mechanical regulatory cues so as to control the tissue specific differentiation. One of the biggest challenges in biomaterial-stem cell interactions is its context dependency; cellular response to a single biomaterial varies depending upon the cell type, soluble factors, and culture conditions. Recently, high throughput screening approaches have been used to identify cell–material interactions in the presence of various growth factors and soluble factors, as well as physical cues to evaluate the effect of culture conditions on stem cell fate [116]. Interdisciplinary approaches involving material science and stem cell biology not only open up possibilities for translation but also provides a platform to learn more about the underlying mechanism and the role of cell–matrix interactions on stem cell fate and morphogenesis.

Acknowledgement We apologize to many of our colleagues whose deserving work could not be included in this chapter due to constraint of length.

References

1. Fuchs E, Tumber T, Guasch G. Socializing with neighbors: Stem cells and their niche. *Cell* 2004;116:769–778.
2. Dawes-Hoang RE, Wieschaus EF. Cell and development biology – A shared past, an intertwined future. *Dev Cell* 2001;1:27–36.
3. Rozario T, DeSimone DW. The extracellular matrix in development and morphogenesis: A dynamic view. *Dev Biol* 2010;341:126–140.
4. Hwang NS, Varghese S, Elisseeff J. Controlled differentiation of stem cells. *Adv Drug Deliv Rev* 2008;60:199–214.

5. Griffith LG, Swartz MA. Capturing complex 3D tissue physiology *in vitro*. *Nat Rev Mol Cell Biol*, 2006;7:211–214.
6. Place ES, Evans ND, Stevens MM. Complexity in biomaterials for tissue engineering. *Nat Mater* 2009;8:457–470.
7. Ott HC, Matthiesen TS, Goh S-K, Black L, Kren SM, Netoff TI, Taylor DA. Perfusion-decellularized matrix: Using nature's platform to engineer a bioartificial heart. *Nat Med* 2007;14:213–221.
8. Grayson WL, Fröhlich M, Yeager K, Bhumiratana S, Chan ME, Cannizzaro C, Wan LQ, Liu XS, Guo XE, Vunjak-Novakovic G. Engineering anatomically shaped human bone grafts. *Proc Natl Acad Sci USA* 2010;107:3299–3304.
9. Macchiarini P, Jungebluth P, Go T, Asnaghi MA, Rees LE, Cogan TA, Dodson A, Martorell J, Bellini S, Parnigotto PP, Dickinson SC, Hollander AP, Mantero S, Conconi MT, Birchall MA. Clinical transplantation of a tissue-engineering airway. *Lancet* 2008;372:2023–2030.
10. Datta N, Pham QP, Sharma U, Sikavitsas VI, Jansen JA, Mikos AG. *In vitro* generated extracellular matrix and fluid shear stress synergistically enhance a 3D osteogenic differentiation. *Proc Natl Acad Sci USA* 2006;103:2488–2493.
11. Pham, QP, Kasper FK, Mistry AS, Sharma S, Yasko AW, Jansen JA, Mikos AG. Analysis of the osteoconductive capacity and angiogenicity of an *in vitro* generated extracellular matrix. *J Biomed Mater Res A* 2009;88:295–303.
12. Hoshiba T, Kawazoe N, Tateishi T, Chen G. Development of stepwise osteogenesis-mimicking matrices for the regulation of mesenchymal stem cell functions. *J Biol Chem* 2009;284:31164–31173.
13. Kleinman HK, McGarvey ML, Liotta LA, Robey PG, Tryggvason K, Martin GR. Isolation and characterization of type IV procollagen, laminin, heparin sulfate proteoglycans from the EHS sarcoma. *Biochemistry* 1982;21:6188–6193.
14. Xu C, Inokuma MS, Denham J, Golds K, Kundu P, Gold JD, Carpenter MK. Feeder-free growth of undifferentiated human embryonic stem cells. *Nat Biotechnol* 2001;19:971–974.
15. Brafman DA, Shah KD, Felner T, Chien S, Willert K. Defining long-term maintenance conditions of human embryonic stem cells with arrayed cellular microenvironment technology. *Stem Cells Dev* 2009;18:1141–1154.
16. Cowan CA, Klimanskaya I, McMahon J, Atienza J, Witmyer J, Zucker JP, Wang S, Morton CC, McMahon AP, Powers D, Melton DA. Derivation of embryonic stem-cell lines from human blastocysts. *N Engl J Med* 2004;350:1353–1356.
17. Braam SR, Zeinstra L, Litjens S, Oostwaard DW-V, Brink SVD, Laake LV, Lebrin F, Kats P, Hochstenbach R, Passier R, Sonnenberg A, Mummery CL. Recombinant vitronectin is a functionally defined substrate that supports human embryonic stem cell self-renewal via $\alpha v \beta 5$ integrin. *Stem Cells* 2008;26:2257–2265.
18. Miyazaki T, Futaki S, Hasegawa K, Kawasaki M, Sanzen N, Hayashi M, Kawase E, Sekiguchi K, Nakatsuji N, Suemori H. Recombinant human laminin isoforms can support the undifferentiated growth of human embryonic stem cells. *Biochem Biophys Res Commun* 2008;375:27–32.
19. Domogatskaya A, Rodin S, Boutaud A, Tryggvason K. Laminin-511 not -332, -111 or -411 enables mouse embryonic stem cell self-renewal *in vitro*. *Stem Cells* 2008;26:2800–2809.
20. Hayashi Y, Furue MK, Okamoto T, Ohnuma K, Myoishi Y, Fukuhara Y, Abe T, Sato JD, Hata R-I, Asashima M. Integrins regulate mouse embryonic stem cell self-renewal. *Stem Cells* 2007;25:3005–3015.
21. Ma W, Tavakoli T, Derby E, Serebryakova Y, Rao MS, Mattson MP. Cell-extracellular matrix interactions regulate neural differentiation of human embryonic stem cells. *BMC Dev Biol* 2008;8:90 (1–13)

22. Svendsen KH, Koc MHJ. X-ray diffraction evidence of collagen molecular packing and crosslinking in fibrils of rat tendon observed by synchrotron radiation. *EMBO J* 1982;1: 669–674.
23. Bosnakovski D, Mizuno M, Kim G, Takagi S, Okumura M, Fujinaga T. Chondrogenic differentiation of bovine bone marrow mesenchymal stem cells (MSCs) in different hydrogels: Influence of collagen type II extracellular matrix on MSC chondrogenesis. *Biotechnol Bioeng* 2006;93:1152–1163.
24. Ma W, Fitzgerald W, Liu Q, O’Shaughnessy TJ, Maric D, Lin HJ, Alkon DL, Barker JL. CNS stem and progenitor cell differentiation into functional neuronal circuits in three-dimensional collagen gels. *Exp Neurol* 2004;190:276–288.
25. Pöschl E, Schlötzer-Schrehardt U, Brachvogel B, Saito K, Ninomiya Y, Mayer U. Collagen IV is essential for basement membrane stability but dispensable for initiation of its assembly during initial development. *Development* 2004;131:1619–1628.
26. Schenke-Layland K, Angelis E, Rhodes KE, Heydarkhan-Hagvall S, Mikkola HK, MacLellan WR. Collagen IV induces trophoectoderm differentiation of mouse embryonic stem cells. *Stem Cells* 2007;25:1529–1538.
27. Yamashita J, Itoh H, Hirashima M, Ogawa M, Nishikawa S, Yurug T, Naito M, Nakao K, Nishikawa S-I. Flk-positive cells derived from embryonic stem cells serve as vascular progenitors. *Nature* 2000;408:92–96.
28. Wang Y, Kim H-J, Vunjak-Novakovic G, Kaplan DL. Stem cell based tissue engineering with silk biomaterials. *Biomaterials* 2006;27:6064–6082.
29. Gerecht S, Burdick JA, Ferreira LS, Townsend SA, Langer R, Vunjak-Novakovic G. Hyaluronic acid hydrogel for controlled self-renewal and differentiation of human embryonic stem cells. *Proc Natl Acad Sci USA* 2007;104:11298–11303.
30. Kutty JK, Webb K. Mechanomimetic hydrogels for vocal fold lamina propria regeneration. *J Biomater Sci Polym Ed* 2009;20:737–756.
31. Chung C, Burdick JA. Influence of three dimensional hyaluronic acid microenvironments on mesenchymal stem cell chondrogenesis. *Tissue Eng* 2009;15:243–254.
32. Fedorovich NE, Oudshoorn MH, Geemen DV, Hennink WE, Alblas J, Dhert WJA. The effect of photopolymerization on stem cells embedded in hydrogels. *Biomaterials* 2009;30: 344–353.
33. Ragetly GR, Griffon DJ, Lee H, Fredericks LP, Gordon-Evans W, Chung YS. Effect of chitosan scaffold microstructure on mesenchymal stem cell chondrogenesis. *Acta Biomater* 2010;6:1430–1436.
34. Wang N, Adams G, Buttery L, Falcone FH, Stolnik S. Alginate encapsulation technology supports embryonic stem cell differentiation into insulin-producing cells. *J Biotechnol* 2009;144:304–312.
35. Varghese S, Hwang NS, Canver AC, Theprungsirikul P, Lin DW, Elisseeff J. Chondroitin sulfate based niches for chondrogenic differentiation of mesenchymal stem cells. *Matrix Biol* 2008;27:12–21.
36. Chen G, Liu D, Tadokoro M, Hirochika R, Ohgushi H, Tanaka J, Tateishi T. Chondrogenic differentiation of human mesenchymal stem cells cultured in a cobweb-like biodegradable scaffold. *Biochem Biophys Res Commun* 2004;322:50–55.
37. Benoit DSW, Durney AR, Anseth KS. The effect of heparin-functionalized hydrogels on three-dimensional human mesenchymal stem cell osteogenic differentiation. *Biomaterials* 2007;28:66–77.
38. Uygun BE, Stojisih SE, Matthew HWT. Effects of immobilized glycosaminoglycans on the proliferation and differentiation of human mesenchymal stem cells. *Tissue Eng* 2009;15A: 3499–3512.
39. Bacakova L, Filova E, Rypacek F, Svorcik V, Stary V. Cell adhesion on artificial materials for tissue engineering. *Physiol Res* 2004;53 (Suppl 1):S35–S45.

40. Nuttelman CR, Tripodi MC, Anseth KS. Synthetic hydrogel niches that promote hMSC viability. *Matrix Biol* 2005;24:208–218.
41. Li YJ, Chung EH, Rodriguez RT, Firpo MT, Healy KE. Hydrogels as artificial matrices for human embryonic stem cell self-renewal. *J Biomed Mater Res A* 2006;79:1–5.
42. Lee ST, Yun JI, Jo YS, Mochizuki M, Vlies A, Kontos S, Ihm JE, Lim JM, Hubbell JA. Engineering integrin signaling for promoting embryonic stem cell self-renewal in a precisely defined niche. *Biomaterials* 2010;31:1219–1226.
43. Derda R, Li L, Orner BP, Lewis RL, Thomson JA, Kiessling LL. Defined substrates for human embryonic stem cell growth identified from surface arrays. *ACS Chem Biol* 2007;2:347–355.
44. Alberti K, Davey RE, Onishi K, George S, Salchert K, Seib FK, Bornhäuser M, Pompe T, Nagy A, Werner C, Zandstra PW. Functional immobilization of signaling protein enables control of stem cell fate. *Nat Methods* 2008;7:645–650.
45. Hill E, Boonthekul T, Mooney DJ. Regulating activation of transplanted cells controls tissue regeneration. *Proc Natl Acad Sci USA* 2006;103:2494–2499.
46. Silva GA, Czeisler C, Krista L, Niece KL, Beniash E, Harrington DA, Kessler JA, Stupp SI. Selective differentiation of neural progenitor cells by high-epitope density nanofibers. *Science* 2004;303:1352–1355.
47. Lee HJ, Yu C, Chansakul T, Hwang NS, Varghese S, Yu SM, Elisseeff JH. Enhanced chondrogenesis of mesenchymal stem cells in collagen mimetic peptide-mediated microenvironment. *Tissue Eng* 2008;14:1843–1851.
48. Hwang NS, Varghese S, Zhang Z, J Elisseeff J. Chondrogenic differentiation of human embryonic stem cell-derived cells in arginine-glycine-aspartate modified hydrogels. *Tissue Eng* 2006;12:2695–2706.
49. Salinas CN, Anseth KS. The enhancement of chondrogenic differentiation of human mesenchymal stem cells by enzymatically regulated RGD functionalities. *Biomaterials* 2008;29:2370–2377.
50. Salinas CN, Anseth KS. Decorin moieties tethered into PEG networks induce chondrogenesis of human mesenchymal stem cells. *J Biomed Mater Res A* 2009;90:456–464.
51. Yang F, Williams CG, Wang D, Lee H, Manson PN, Elisseeff JH. The effect of incorporating RGD adhesive peptide in polyethylene glycol diacrylate hydrogel on osteogenesis of bone marrow stromal cells. *Biomaterials* 2005;26:5991–5998.
52. Shin H, Temenoff JS, Bowden GC, Zygorakis K, Farach-Carson MC, Yaszemski MJ, Mikos AG. Osteogenic differentiation of rat bone marrow stromal cells cultured on Arg-Gly-Asp modified hydrogels without dexamethasone and β -glycerol phosphate. *Biomaterials* 2005;26:3645–3654.
53. Kundu AK, Khatiwala CB, Putnam AJ. Extracellular matrix remodeling, integrin expression, and downstream signaling pathways influence the osteogenic differentiation of mesenchymal stem cells on poly(lactide-co-glycolide) substrates. *Tissue Eng* 2009;15A:273–283.
54. Hsiong SX, Boonthekul T, Huebsch N, Mooney DJ. Cyclic arginine-glycine-aspartate peptides enhance three dimensional stem cell osteogenic differentiation. *Tissue Eng* 2009;15A:263–272.
55. Lee JS, Lee JS, Murphy WL. Modular peptides promote human mesenchymal stem cell differentiation on biomaterial surfaces. *Acta Biomater* 2010;6:21–28.
56. Palecek SP, Loftus JC, Ginsberg MH, Lauffenburger DA, Horwitz AF. Integrin-ligand binding properties govern cell migration speed through cell-substratum adhesiveness. *Nature* 1997;385:537–540.
57. Lutolf MP, Raeber JP, Zisch AH, Tirelli N, Hubbell JA. Cell-responsive synthetic hydrogels. *Adv Mater* 2003;15:888–892.
58. Lutolf MP, Lauer-Fields JL, Schmoekel HG, Metters AT, Weber FE, Fields GB, Hubbell JA. Synthetic matrix metalloproteinase-sensitive hydrogels for the conduction of tissue regeneration: Engineering cell-invasion characteristics. *Proc Natl Acad Sci USA* 2003;100:5413–5418.

59. Kloxin AM, Kasko AM, Salinas CN, Anseth KS. Photodegradable hydrogels for dynamic tuning of physical and mechanical properties. *Science* 2009;324:59–63.
60. Levenberg S, Huang NF, Lavik E, Rogers AB, Itskovitz-Eldor J, Langer R. Differentiation of human embryonic stem cells on three dimensional polymer scaffolds. *Proc Natl Acad Sci USA* 2003;100:12741–12746.
61. Lee JG, Lim SA, Croll T, Williams G, Lui S, Cooper-White J, McQuade LR, Mathiyalagan B, Tuch BE. Transplantation of 3D scaffolds seeded with human embryonic stem cells: Biological features of surrogate tissue and teratoma-forming potential. *Regen Med* 2007;2:289–300.
62. Phillips JE, Petrie TA, Creighton FP, Garcia AJ. Human mesenchymal stem cell differentiation on self-assembled monolayers presenting different surface chemistries. *Acta Biomater* 2010;6:12–20.
63. Benoit DSW, Schwartz MP, Durney AR, Anseth KS. Small functional groups for controlled differentiation of hydrogel-encapsulated human mesenchymal stem cells. *Nat Mater* 2008;7: 816–823.
64. Chastain SR, Kundu AK, Dhar S, Calvert JW, Putnam AJ. Adhesion of mesenchymal stem cells to polymer scaffolds occurs via distinct ECM ligands and controls their osteogenic differentiation. *J Biomed Mater Res A* 2006;78:73–85.
65. Chua K-N, Chai C, Leeb P-C, Ramakrishna S, Leong KW, Mao H-Q. Functional nanofibers scaffolds with different spacers modulate adhesion and expansion of cryopreserved umbilical cord blood hematopoietic stem/progenitor cells. *Exp Hematol* 2007;35:771–781.
66. Harrison J, Pattanawong S, Forsythe JS, Gross KA, Nisbet DR, Behc H, Scott TF, Trounson AO, Mollard R. Colonization and maintenance of murine embryonic stem cells on poly (α -hydroxy esters). *Biomaterials* 2004;25:4963–4970.
67. Cao Y, Vacanti JP, Paige KT, Upton J, Vacanti CA. Transplantation of chondrocytes utilizing polymer-cell construct to produce tissue-engineered cartilage in the shape of a human ear. *Plast Reconstr Surg* 1997;100:297–302.
68. Atala A, Bauer SB, Soker S, Yoo JJ, Retik AB. Tissue-engineered autologous bladders for patients needing cytoplasty. *Lancet* 2006;367:1241–1246.
69. Wamke PH, Springer ING, Wiltfang J, Acil Y, Eufinger H, Wehmöller M, Russo PAJ, Bolte H, Sherry E, Behrens E, Terheyden H. Growth and transplantation of a custom vascularized bone graft in a man. *Lancet* 2004;364:766–770.
70. Lin C-C, Metters AT. Hydrogels in controlled release formulations : Network design and mathematical modeling. *Adv Drug Deliv Rev* 2006;58:1379–1408.
71. Newman KD, McBurney MW. Poly (D,L lactic-co-glycolic acid) microsphere as biodegradable microcarriers for pluripotent stem cells. *Biomaterials* 2004;25:5763–5771.
72. Carpenedo RL, Bratt-Leal AM, Marklein RA, Seaman SA, Bowen NJ, McDonald JF, McDevitt TC. Homogeneous and organized differentiation within embryoid bodies induced by microsphere-mediated delivery of small molecules. *Biomaterials* 2009;30: 2507–2515.
73. Borselli C, Storrie H, Benesch-Lee F, Shvartsman D, Cezar C, Lichtman JW, Vandenburgh HH, Mooney DJ. Functional muscle regeneration with combined delivery of angiogenesis and myogenesis factors. *Proc Natl Acad Sci USA* 2010;107:3287–3292.
74. Mercado AE, Ma J, He X, Jabbari E. Release characteristics and osteogenic activity of recombinant human bone morphogenic protein-2 grafted to novel self-assembled poly(lactide-co-glycolide fumarate) nanoparticles. *J Control Release* 2009;140:148–156.
75. Wang F, Li Z, Tamama Z, Sen CK, Guan J. Fabrication and characterization of pro-survival growth factor releasing, anisotropic scaffolds for enhanced mesenchymal stem cell survival/growth and orientation. *Biomacromolecules* 2009;10:2609–2618.
76. Fan VH, Au A, Tamama K, Littrell R, Richardson LB, Wright JW, Wells A, Griffith LG. Tethered epidermal growth factor provides a survival advantage to mesenchymal stem cells. *Stem Cells* 2007;25:1241–1251.

77. Marcantonio NA, Boehm CA, Rozic RJ, Au A, Wells A, Muschler GF, Griffith LG. The influence of tethered epidermal growth factor on connective tissue progenitor colony formation. *Biomaterials* 2009;30:4629–4638.
78. Benoit DS, Collins SD, Anseth KS. Multifunctional hydrogels that promote osteogenic human mesenchymal stem cell differentiation through stimulation and sequestering of bone morphogenic protein 2. *Adv Funct Mater* 2007;17:2085–2093.
79. Hubbell JA, Thomas SN, Swartz MA. Materials engineering through immunomodulation. *Nature* 2009;462:449–460.
80. Lin C-C, Metters AT, Anseth KS. Functional PEG-peptide hydrogels to modulate local inflammation induced by the pro-inflammatory cytokine TNF α . *Biomaterials* 2009;30:4907–4914.
81. Lin C-C, Boyer PD, Aimetti AA, Anseth KS. Regulating MCP-1 diffusion in affinity hydrogels for enhancing immune-isolation. *J Control Release* 2010;142:384–391.
82. Ingber DE. Cellular mechanotransduction: Pulling all the pieces together again. *FASEB J* 2006;20:811–827.
83. Engler AJ, Sen S, Sweeney HL, Discher DE. Matrix elasticity directs stem cell lineage specification. *Cell* 2006;126:677–689.
84. Khatiwala CB, Kim PD, Peyton SR, Putnam AJ. ECM compliance regulates osteogenesis by influencing MAPK signaling downstream of RhoA and ROCK. *J Bone Miner Res* 2009;24:886–898.
85. Saha K, Keung AJ, Irwin EF, Li Y, Little L, Schaffer DV, Healy KE. Substrate modulus directs neural stem cell behavior. *Biophys J* 2008;95:4426–4438.
86. Banerjee A, Arha M, Choudhary S, Ashton RS, Bhatia SR, Schaffer DV, Kane RS. The influence of hydrogel modulus on the proliferation and differentiation of encapsulated neural stem cells. *Biomaterials* 2009;30:4695–4699.
87. Teixeira AI, Ilkhanizadeh S, Wigenius JA, Duckworth JK, Inganäs O, Hermanson O. The promotion of neuronal maturation on soft substrates. *Biomaterials* 2009;30:4567–4572.
88. Wang L-S, Chung JE, Chan PP-Y, Kurisawa M. Injectable biodegradable hydrogels with tunable mechanical properties for the stimulation of neurogenesis differentiation of human mesenchymal stem cells in 3D culture. *Biomaterials* 2010;31:1148–1157.
89. Evans ND, Minelli C, Gentleman E, LaPointe V, Patankar SN, Kallivretaki M, Chen X, Roberts CJ, Stevens MM. Substrate stiffness affects early differentiation events in embryonic stem cells. *Eur Cell Mater* 2009;18:1–14.
90. Battista S, Guamieri D, Borselli C, Zeppetelli S, Borzacchiello A, Mayol L, Gerbasio D, Keene DR, Ambrosio L, Netti PA. The effect of matrix composition of 3D constructs on embryonic stem cell differentiation. *Biomaterials* 2006;26:6194–6207.
91. Winer JP, Janmey PA, McCormick ME, Funaki M. Bone marrow-derived mesenchymal stem cells become quiescent on soft substrates but remain responsive to chemical or mechanical stimuli. *Tissue Eng* 2009;15:147–154.
92. Rowlands AS, George PA, Cooper-White JJ. Directing osteogenic and myogenic differentiation of MSCs : Interplay of stiffness and adhesive ligand presentation. *Am J Physiol Cell Physiol* 2008;295:1037–1044.
93. Hynes SR, Rauch MF, Bertram JP, Lavik EB. A library of tunable poly(ethylene glycol)/poly(L-lysine) hydrogels to investigate the material cues that influence neural stem cell differentiation. *J Biomed Mat Res A* 2008;89:499–509.
94. Kloxin AM, Benton JA, Anseth KA. In site elasticity modulation with dynamic substrates to direct cell phenotype. *Biomaterials* 2010;31:1–8.
95. Burdick JA, Vunjak-Novakovic G. Engineered microenvironments for controlled stem cell differentiation. *Tissue Eng* 2009;15:205–219.
96. Yim EKF, Darling EM, Kulangara K, Guilak F, Leong KW. Nanotopography-induced changes in focal adhesions, cytoskeletal organization and mechanical properties of human mesenchymal stem cells. *Biomaterials* 2010;31:1299–1306.

97. Yim EKF, Pang SW, Leong KW. Synthetic nanostructures inducing differentiation of human mesenchymal stem cells into neuronal lineage. *Exp Cell Res* 2007;313:1820–1829.
98. Recknor JB, Sakaguchi DS, Mallapragada SK. Directed growth and selective differentiation of neural progenitor cells on micropatterned polymer substrates. *Biomaterials* 2006;27:4098–4108.
99. Gerecht S, Bettinger CJ, Zhang Z, Borenstein JT, Vunjak-Novakovic G, Langer R. The effect of actin disrupting agents on contact guidance of human embryonic stem cells. *Biomaterials* 2007;28:4068–4077.
100. Dalby MJ, Gadegaard N, Tare R, Andar A, Riehle MO, Herzyk P, Chris DW, Wilkinson CDW, Oreffo RO. The control of human mesenchymal stem cell differentiation using nanoscale symmetry and disorder. *Nat Mater* 2007;6:997–1003.
101. Gelain F, Hori A, Zhang A. Designer self-assembling peptide scaffolds for 3-D tissue cell cultures and regenerative medicines. *Macromol Biosci* 2007;7:544–551.
102. Dang JM, Leong KW. Myogenic induction of aligned mesenchymal stem cell sheets by culture on thermally responsive electrospun nanofibers. *Adv Mater* 2007;19:2775–2779.
103. Li W-J, Tuli R, Huang X, Laquerriere P, Tuan RS. Multi-lineage differentiation of human mesenchymal stem cells in a three-dimensional nanofibrous scaffolds. *Biomaterials* 2005;26:5158–5166.
104. Li W-J, Jiang YJ, Tuan RS. Chondrocyte phenotype in engineered fibrous matrix is regulated by fiber size. *Tissue Eng* 2006;12:1775–1784.
105. Shih Y-R, Chen C-N, Tsai S-W, Wang YJ, Lee OK. Growth of mesenchymal stem cells on electrospun type I collagen nanofibers. *Stem Cells* 2006;24:2391–2397.
106. Smith LA, Liu X, Hu J, Wang P, Ma PX. Enhancing osteogenic differentiation of mouse embryonic stem cells by nanofibers. *Tissue Eng* 2009;15:1855–1864.
107. Jan E, Kotov NA. Successful differentiation of mouse neural stem cells on layer-by-layer assembled single-walled carbon nanotube composite. *Nano Lett* 2007;7:1123–1128.
108. McCullen SD, Stevens DR, Roberts WA, Clarke LI, Bernack SH, Gorga RE, Lobo EA. Characterization of electrospun nanocomposite scaffolds and biocompatibility with adipose-derived human mesenchymal stem cells. *Int J Nanomedicine* 2007;2:253–263.
109. Mohr JC, de Pablo JJ, Palecek SP. 3-D microwell culture of human embryonic stem cells. *Biomaterials* 2006;27:6032–6042.
110. Cukierman E, Pankov R, Stevens DR, Yamada KM. Taking cell–matrix adhesions to the third dimension. *Science* 2001;294:1708–1712.
111. Abbott A. Biology's new dimension. *Nature* 2003;424:870–872.
112. Hwang NS, Kim MK, Sampattavanich S, Baek JH, Zhang Z, Elisseeff J. Effects of three-dimensional culture and growth factors on chondrogenic differentiation of murine embryonic stem cells. *Stem Cells* 2006;24:284–291.
113. Tanaka H, Murphy CL, Murphy C, Kimura M, Kawai S, Polak JM. Chondrogenic differentiation of murine embryonic stem cells: Effect of culture conditions and dexamethasone. *J Cell Biochem* 2004;93:454–462.
114. Liu H, Jian LJ, Roy K. Effect of 3D scaffold and dynamic culture condition on the global gene expression profile of mouse embryonic stem cells. *Biomaterials* 2006;27:5978–5989.
115. Amariglio N, Hirshberg A, Scheithauer BW, Cohen Y, Loewenthal R, Trakhtenbrot L, Paz N, Koren-Michowitz M, Waldman D, Leider-Trejo L, Toren A, Constantini S, Rechavi G. Donor-derived brain tumor following neural stem cell transplantation in an ataxia telangiectasia patient. *PLoS Med* 2009;6:221–231.
116. Yang F, Mei Y, Langer R, Anderson DG. High throughput optimization of stem cell microenvironments. *Comb Chem High Throughput Screen* 2009;12:554–561.

Part III

Concepts in Biomaterial Translation and Product Development

Benjamin A. Byers and Dolores Baksh

Contents

19.1	Introduction	542
19.2	Conceptualization and Preclinical Activities	542
19.3	Development and Design Control: Engineering Rigor and Quality Systems Implementation	548
19.3.1	Applying Design Controls	548
19.3.2	Design and Development Planning	550
19.3.3	Design Inputs	551
19.3.4	Design Outputs	551
19.3.5	Design Review	552
19.3.6	Design Verification	552
19.3.7	Design Validation	553
19.3.8	Design Transfer	554
19.3.9	Design Changes	556
19.3.10	Design History File	556
19.4	Regulatory Strategy and Evidence Generation	556
19.5	Marketing, Commercialization and Post-market Surveillance	559
	References	560

Abstract The total product life cycle (TPLC) provides a framework by which medical device companies incorporate international regulatory guidelines and best practices to translate product concepts, including novel biomaterial therapeutics, into clinical and commercial reality. The TPLC emphasizes continuity between all phases of a medical product's lifetime, including Concept/Feasibility, Design/Development, Validation, Commercialization/Production, Post-Market Surveillance/Support. This product development cadence evolves through definition of the unmet clinical need and market opportunity, application of design control methodologies, consideration of manufacturability and scalability, and execution of the evidence generation and regulatory strategies. Throughout each of these activities, design controls are leveraged to promote cross-functional engagement of

B.A. Byers (✉)

New Product Development, DePuy Mitek, a Johnson & Johnson Company, 325 Paramount Dr, Raynham, MA 02356, USA
e-mail: bbyers@its.jnj.com

19 sales and marketing, research and development, quality assurance, regulatory affairs, operations and finance to ensure the medical device will provide a safe and efficacious solution for patients and surgeons.

Keywords Design controls • Product development • Total product life cycle

19.1 Introduction

Effective translation of next generation biomaterials into safe and efficacious clinical solutions for patients and surgeons merits an overview of several key aspects of the product development pathway, including definition of the unmet clinical need and market opportunity, review of design control methodologies, consideration of manufacturability and scalability, and discussion of the evidence generation (preclinical and clinical studies) and regulatory strategy processes. In the context of the biomaterial technologies and future directions illustrated in previous chapters, the objective of the current overview is to provide perspective of these cornerstones of product development within the scope of the total product life cycle (TPLC).

The Food and Drug Administration's (FDA) Center for Devices and Radiological Health (CDRH) typically provides regulatory oversight for medical devices and biomaterials to be marketed in the United States. CDRH has provided its TPLC strategic vision which emphasizes interdependent connectivity of all phases of a product's development from inception to obsolescence (Fig. 19.1). In general, the biomedical device industry manages product commercialization through a matrix of activities embodying this TPLC model that meshes with international regulatory requirements to ensure the highest quality assurance is incorporated into the various phases of a medical device's lifetime. Biomedical device companies establish a governance structure that meets their business needs and permits prudent concurrent engineering throughout product development. Typical phases of the development process are often segmented into Concept/Feasibility, Design/Development, Validation, Commercialization/Production, Post-Market Surveillance/Support.

19.2 Conceptualization and Preclinical Activities

As the name implies, the Concept/Feasibility stage equates to the discovery phase of the product life cycle, in which as few as one but typically several ideas or concepts are prototyped and evaluated with an incubator mentality. Due to its preliminary nature, the concept phase receives limited quality and regulatory oversight and largely parallels the bench-top, in vitro and preclinical in vivo studies conducted in academic laboratories to characterize the potential functionality and efficacy of novel biomaterial solutions.

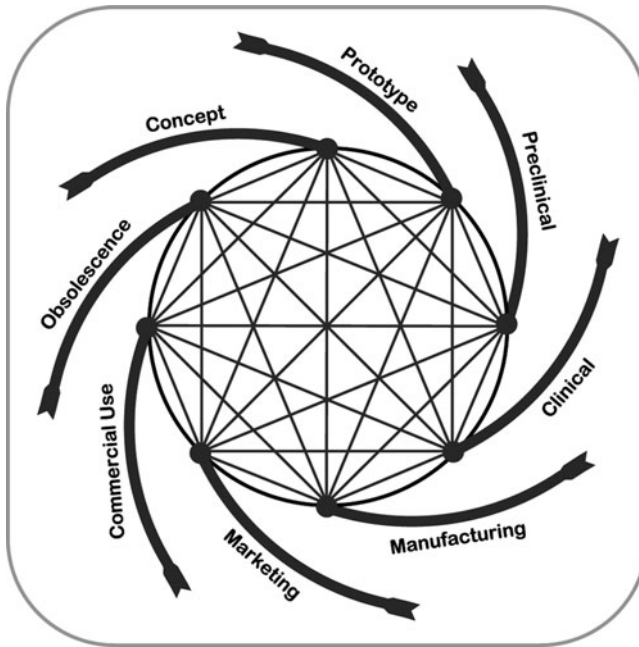


Fig. 19.1 Total product life cycle (TPLC) model detailed by the FDA's Center for Devices and Radiological Health Source: FDA Center for Devices and Radiological Health

Ultimately, based on their preclinical outcomes and the company's strategic marketing prioritization, promising concepts are funneled into subsequent phases of the product life cycle addressed in later sections of this overview.

Some of the most critical aspects of the TPLC occur in the concept phase, including definition of the unmet clinical need, identification of user needs (surgeon and/or patient), analysis of the market opportunity and competitive landscape, and intellectual property protection of ideas to provide a competitive advantage. It follows that even informal incorporation of these principles into academic research significantly enhances the probability that innovative materials and/or product concepts can progress into clinical and commercial reality whether through university incubators or industry licensing and partnership.

Appreciation for the unmet clinical need that a novel biomaterial may address is of paramount importance in defining its value and marketability. Significant due diligence is required to clearly define the unmet need, and the potential inputs are broad, including interfacing with surgeons/clinicians and/or societies of medical professionals, reviewing peer-reviewed literature and ongoing clinical trials [1], comprehensive understanding of the current and future trends of the industry and the treatment paradigm for the target indication, evaluating potentially competitive products and companies operating in or near the indication of interest, and even engaging reimbursement experts (health technology assessors for insurance companies and hospitals or independent consultants in the field). Synthesis of this market research data will not only substantiate (or possibly refute) the perceived unmet

clinical need, but more clearly define who will use it, what supportive evidence must be generated, who will ultimately be willing to pay for it, and how much it is worth. Given the clinical indication targeted, identifying materials or products currently marketed for that indication provide a basis to establish whether a new material solution will ultimately be categorized with clinical utility (1) similar to that already provided by marketed products (or a “me-too” product), (2) *incrementally* evolves existing therapies, (3) *substantially* improves the treatment paradigm or (4) *transformationally* impacts either the mode of implantation (delivery) or healing (repair and/or regeneration) in an entirely new and potentially game-changing manner [2]. Due to the maturity of biomaterials in medicine, medical device companies have immense options to leverage pre-existing biomaterials with long and proven histories of clinical safety and efficacy, including natural (collagen, hyaluronan, fibrin), synthetic (polylactides, polyglycolides, polycaprolactones, polydioxanones), and inorganic materials (hydroxapatite, tricalcium phosphate). In some instances, this historical data serves as a rather formidable barrier to entry for novel biomaterials lacking a well-established safety profile and clinical adoption. While it is likely that the greatest commercial value of a new biomaterial product would ultimately be realized from new in-class, transformational biomaterials, factors such as freedom to operate, market size and growth rate, development lead time, competitive landscape, and evidence generation and regulatory filing requirements coalesce to underpin true valuation. Depending upon the clinical indication, there may be tangible commercial advantage to new solutions which offer incremental or substantial improvements to the form or function of existing materials that have well-accepted and proven clinical track records in the same or alternate indications. Further, while transformational innovation is enticing based on the potential financial windfall from a new in-class biomaterial therapy, these technologies are typically accompanied by significant costs (both real and opportunity) and may add considerable risk to a company’s strategic business plan. It follows that more risk averse companies may prefer to mitigate product development risk by devoting resources to incremental or substantial product improvements to ensure long term stability and viability of their business entity.

Once the target unmet clinical need is clearly defined, scoping the user needs ensures the proper inputs will be taken into account as the form, fit and function of the biomaterial therapy are developed. User needs are aptly summarized as capturing the requirements of all stakeholders that interface with the product and eventually evolve into the product specifications. Primary stakeholders are the patient that will be receiving the therapeutic biomaterial and the clinical team, including the surgeon and operating room (OR) staff that will be handling and delivering it to the site of repair or participating in the surgery or procedure. At the highest level, user needs are qualitative product attributes obtained during preliminary market research and validated continuously throughout the product development process. Key attributes that are important to the patient are focused on those related to safety and efficacy of the biomaterial, including biocompatibility, quantity and chemical identity of degradation bi-products if the material is bioresorbable, resorption mechanism and profile relative to the therapeutic requirements for the specific indication, and the three-dimensional architecture and surface chemistry given the interaction with host cells. In addition to these therapeutic attributes required for clinical success in their patients, surgeon users and OR staff are conscious of the material’s intraoperative integrity to support handling and manipulation, mode of delivery and function of supporting devices that

facilitate placement, method and durability of fixation in the site of repair, product sterility, packaging and presentation to the sterile field. Evaluating and incorporating these and many other product attributes into the design process at the concept phase will facilitate more robust clinical solutions and dramatically increase the probability that the final product will address the complete scope of user needs.

A firm understanding of the competitive landscape, market opportunity and growth rate provides substantial value both initially and throughout the product development process. It is of unequivocal significance to know and understand the competition's trends and tendencies in both the past and present to more reliably predict the future path to ensure that a new product concept remains a viable candidate for market penetration, creation and even leadership. Additionally, it is likely that competitors are pursuing broad and potentially insurmountable intellectual property protection for their own products and indications. While it is ideal to be exclusive and grow alone in a particular clinical indication, a large target market still provides opportunity for multiple players to participate and drive growth. In certain cases, competition and an evolving treatment paradigm can be a significant ally to new product development efforts for several reasons, including reinforcing the sense of urgency, maintaining customer focus and elevating the design rigor to ensure the highest caliber product will reach and meet the customers' needs more effectively than the competition.

Independent of whether novel biomaterial solutions are categorized as incremental, substantial or transformational or whether they are conceptualized in academia or industry, robust intellectual property (IP) protection of new ideas is of paramount importance to value and commercial potential. Ideally, the patent or patent suite protecting a specific technology will provide both *exclusivity*, indicating the owner has the right to exclude or prevent others from using the intellectual property, and *freedom to operate*, meaning there is absence of third-party IP rights that impede a patent owner's progress toward achieving their desired commercial goal [3]. Thorough review of the current IP landscape for the biomaterial formulation/composition of matter and specific method or application(s), including a geographical review in all markets being considered for the commercialization of the technology, is critical to defining the IP valuation of a specific biomaterial solution. The IP review process facilitates identification of the competitive landscape or, depending upon the inventor's position and the intellectual property maturity of the space, the partnership landscape. For example, patent claim(s) that provide an owner with focused exclusivity but without freedom to operate due to third party coverage in the space may have limited commercial value in isolation. However, value may be created through partnership or licensing the patent to the third party with freedom to operate in the indication of interest. Clearly, the breadth and depth of the claims and geographical coverage that provide the broadest exclusivity and freedom to operate only serve to enhance a biomaterial or product's value to the inventor. While novel chemical species and biomaterial formulations may be more straightforward to protect; freedom to operate in the target indication(s) must receive adequate due diligence early in the IP and patenting process. Furthermore, depending upon the specific market opportunities, a novel material that is capable of being leveraged as a platform technology for multiple indications may provide substantial commercial value relative to a material that is restricted to a single clinical indication. Finally, the desire to publish and present new

and perhaps groundbreaking scientific data at the first opportunity must be carefully balanced with the challenges that public disclosure could propagate later in the patenting process. It is important to ensure that proper invention disclosures have been filed prior to sharing information in a public forum.

The previous concept phase deliverables largely detail collection of data that indicate how a new product *should* perform in the target indication in order to effectively meet the user needs. The final critical aspect of feasibility research is demonstration that the product concept actually *does or has strong potential to* address those user requirements to be a viable commercial product. A thorough, well designed preclinical test plan is essential to demonstrating feasibility and advancing a product concept into subsequent stages of development. Initial evaluations typically include relevant in vitro biological and biomechanical analyses to demonstrate the material has the proper chemical and physical characteristics to function in the target indication. When practical, physical performance testing should be performed with appropriately recognized standards established by organizations such as the American Society for Testing Materials (ASTM) [4]. Biomaterial scaffolds designed to serve as matrices for cellular based repair are typically screened for their ability to support cell adhesion, division and/or differentiation to support native matrix deposition. Depending upon their intended use, relevant physical characteristics such as porosity, pore size and pore connectivity, and mechanical attributes, including compressive or tensile strength, of a biomaterial are characterized to demonstrate their capability to support not only their in vivo requirements post-implantation but also intraoperative handling and fixation during the surgical procedure. In parallel with mechanical integrity studies of the native biomaterial, analysis of the mode and rate of degradation in both structure and mechanical properties is also typically evaluated for biodegradable materials in the scope of in vitro aging and degradation studies. Simulated use studies to evaluate the intended delivery and fixation methods are also essential to thoroughly understand the intraoperative performance of a new biomaterial solution. For example, if the material is to be delivered in liquid form and subsequently cured on demand in situ, constraints of the surgical technique envisioned for delivery of the material should be well understood early in the concept phase. If the target indication is one typically performed in a salinated environment, including arthroscopic knee, shoulder or hip surgery, the concept may extend far beyond development of the flowable biomaterial itself and also include novel delivery instrumentation that promotes delivery in a fluid milieu. Equally important is evaluation of the intended fixation methodology to be leveraged for retaining the biomaterial at the site of repair, including the use of natural or synthetic adhesives, bioresorbable or permanent sutures or tissue staples, or an entirely novel fixation technique.

Depending upon the ability to leverage predicate clinical data, preclinical animal studies may also be required to demonstrate safety and efficacy of the product. As discussed later, biocompatibility testing to establish safety and toxicity commensurate with the intended use and exposure duration of a biomaterial is required. Under certain circumstances predicate data can be leveraged; however, formulation variants or new material combinations likely necessitates completion of new testing of the proposed material. Preclinical safety and efficacy studies are generally viewed as critical supportive

data for any biomaterial product regulated under Investigational Device Exemption (IDE) status by FDA [5]. When readily available in peer-reviewed literature, it is desirable to leverage well characterized and commonly accepted animal models. If model development is necessary, prudent and methodical characterization of the new model will likely be required in support of any future regulatory filings. Independent of the indication, a properly designed efficacy study will have measurable outputs and be statistically powered to detect differences between the study group and a relevant control over a clinically relevant post-operative follow-up period. Importantly, the control arm(s) of a study may range broadly to consist of a sham procedure, empty lesion/defect or, perhaps more appropriately, the current standard of care for the indication. Given moral standards imposed on human clinical studies and the increasing relevance of comparative effectiveness, it is unlikely that a sham surgical procedure would be approved by the FDA as a comparator in a human clinical study provided an established standard of care exists. It is therefore prudent to adopt this rigorous approach when designing even early stage preclinical animal studies. Studies comparing to sham or “no treatment” may provide an unrealistically low efficacy threshold, and therefore present business risk in that they do not establish the baseline efficacy offered by the current standard of care. Inclusion of a standard of care comparator may raise the efficacy bar for a new material, but this approach potentially limits development risk by revealing deficiencies in a new product’s therapeutic prospects early in the development life cycle. A multi-species preclinical data set is also value added, as demonstrating efficacy in multiple species will significantly strengthen an IDE application. The formal transition between “proof of concept” preclinical animal studies and more advanced preclinical evaluations intended to support FDA filings is often difficult to predict, so it is encouraged to conduct preclinical studies in compliance with Good Laboratory Practices (GLP) for Nonclinical Studies [6]. In summary, developing a high caliber preclinical strategy that incorporates sound experimental design, appropriate comparators, measurable outputs and relevant endpoints into the earliest stages of preclinical animal work can dramatically reduce development time and improve decision-making capabilities. Additionally, a more robust preclinical data package will enhance any IDE application.

As demonstrated by this overview, the Concept/Feasibility stage is clearly much more than conjuring up a good idea and conducting a few ad hoc experiments to demonstrate that it may have some clinical promise. In commercial reality, the Concept phase is the foundation that the product development cycle builds upon going forward. A rigorous and detailed approach at the earliest stages of innovation will undoubtedly improve a product’s robustness and ability to exceed all anticipated user needs as well as those attributes that are sometimes “accidentally” identified as the design matures during later phases of development and is validated with additional surgeon user feedback. Although the timing and level of evidence required to officially charter a concept project into the next stage varies across the biomedical device industry, at some critical juncture a decision point arises, and a project will either be terminated or the feasibility data and business case develops in which identified risks have been sufficiently mitigated to justify commitment of additional resources and the Concept project transitions to the Development phase.

19.3

Development and Design Control: Engineering Rigor and Quality Systems Implementation

Once a product concept translates into the Design/Development pipeline, international standards provide a framework in which companies conduct, monitor and document the cadence of activities associated with the design and manufacture of the medical device. Specifically, the United States Food and Drug Administration (FDA) has published the Quality System Regulation (QSR) [7] and the European Union observes the International Organization for Standardization (ISO) 13485:2003 [8] to ensure the highest quality assurance practices are used in the design and manufacture of medical devices.

The intent of this section is to provide a brief but non-comprehensive overview of the critical aspects of the medical device design control framework as highlighted in the regulations (Fig. 19.2) [9]. Depending upon the ultimate classification of the product by FDA, additional regulations may apply, including those applicable to drugs and/or biologics. Per FDA guidelines, specific application of these regulations is the responsibility of the company based on the scope of the product they are developing. Simply stated, design controls are a series of checks and balances that focus on routine and thorough review of the design throughout the development process to ensure the design addresses the user needs and design requirements and that the project is properly resourced to execute on the development plan. The development life cycle has been portrayed in a waterfall model (Fig. 19.3) which prompts review and cross-functional approval of the design at multiple phases of the design and development process, including evaluation of the processes by which the device is to be manufactured. While the regulations can be over interpreted as burdensome, in reality, they provide an operational framework that, when executed properly, can actually reduce a company's financial risk and expedite development of safe and efficacious medical devices [10]. As an example, identifying the need for and implementing a critical design or formulation change or manufacturing optimization earlier in development is likely to be significantly less costly than when a product is already marketed.

19.3.1

Applying Design Controls

Per FDA regulations, medical devices are stratified into three categories (Class I, II or III) based on their complexity and extent to which they pose patient risk with regulatory oversight increasing from Class I to III [11]. Class I devices (tongue depressors, examination gloves, hand-held surgical instruments, etc.) present minimal potential for harm to the user and are subject to general controls, including good manufacturing techniques and appropriate labeling. Most Class I devices are exempt from FDA pre-notification requirements. Class II devices are generally categorized as non-invasive (infusion pumps, electrically powered endo/arthroscopes, needles and suture material, etc.) and require additional controls typically including premarket notification 510(k). Legal marketing of a substantially



Fig. 19.2 Summary of the components of the design control framework. Source: 21 CFR Part 820, Subpart C, Section 820.30

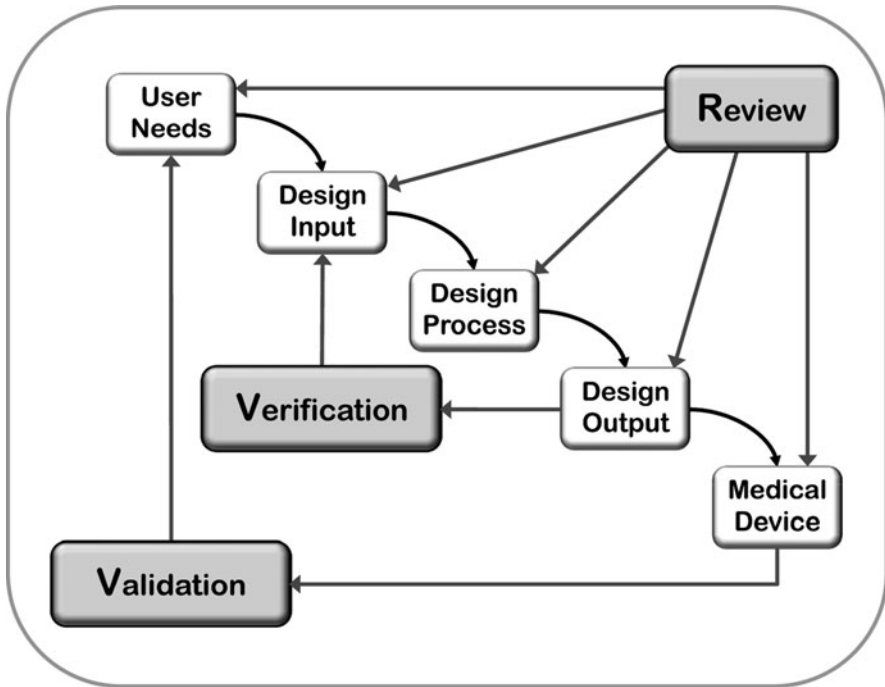


Fig. 19.3 Design control applied through waterfall process (used with permission of the Medical Devices Bureau, Health Canada)

equivalent or “predicate” device in the U.S. may result in some biomaterial therapies being rated as Class II devices. Class III devices (drug-eluting stents, heart valves, orthopaedic implants with growth factors, etc.) are viewed as higher risk devices or lack an equitable pre-existing comparator for a 510(k) application. Manufacturers of Class III medical devices are required to demonstrate safety and efficacy in the target patient population and obtain premarket approval (PMA) prior to commercialization. Design controls must be observed by medical device manufacturers of select Class I and all Class II and III devices.

19.3.2

Design and Development Planning

The focal aspects of design control ensure cross-functional engagement of sales and marketing, research and development, quality assurance, regulatory affairs, operations (manufacturing and supply chain) and finance to navigate the product development life cycle. Based on the diversity of the project team and breadth of requirements to develop a product, it is imperative to implement an effective plan to guide the team’s activities.

While the project plan will provide a baseline estimate as to how long it will take to complete the design control deliverables, the most significant objective of the plan is to ensure the project is adequately resourced, demonstrate cross-functional ownership and establish alignment for the deliverables detailed in the plan. It follows that a more rigorous planning process typically leads to fewer questions on action item ownership and execution later in development as well as more accurate forecasting of the launch timeline. Importantly, the future can never be predicated, and design or manufacturing challenges are certain to present themselves throughout the product development life cycle. It is critical to continually update the project plan as the scope of the development process evolves and to maintain cross-functional approval and alignment as development progresses.

19.3.3

Design Inputs

Design inputs are the foundation of the design and design control process and are initially derived (*or output*) from the series of activities previously discussed in the Concept/Feasibility phase, including the user needs, market need and reimbursement potential, and performance characteristics obtained in laboratory or preclinical testing. Accurate and thorough scoping of the design inputs will improve the efficiency and reliability of the design and development process. In addition to the natural safety and effectiveness attributes established in the product performance requirements, physical size and shape, stability, biocompatibility, sterilization, packaging, storage, intraoperative handling and delivery, and required regulations and standards must all be identified early on for implantable biomaterial therapies. Design inputs should be specific and measurable product performance specifications. Creating “wish list”, ambiguous and/or conflicting design inputs may establish requirements that the device is unable to attain or send the project team back into a loop to resolve open design inputs [9].

19.3.4

Design Outputs

As noted above, the first design outputs originate from the work conducted in the feasibility phase to form the initial design inputs of the development phase. Ultimately, it is the primary role of the project team to demonstrate that the design outputs meet the design input requirements to ensure a safe and efficacious device is marketed. The outputs of the design establish specific acceptance criteria that are approved by the design team and ultimately verified through inspection or testing, including product specifications, component and assembly level drawings and tolerances, raw material specifications, risk analyses, packaging and labeling, manufacturing specifications and procedures and results of device testing. Detailed documentation of the team’s activities evaluating the design will ensure that each design input is traceable to an output, thereby demonstrating that all design inputs are satisfied by the design.

19.3.5 Design Review

Formal design reviews are opportunities to review the status of a design at key phases of the product development life cycle. The foremost intent of the design review is to identify potential issues or risks with a design at each phase before it advances to later stages of development in which additional human and financial resources will be committed to the development effort. This checks and balances system is highlighted in the waterfall diagram model (Fig. 19.3) that illustrates the recurring review process throughout the product development life cycle; however, it is necessary to emphasize that the intent of the design review and design control process in general is not to entirely compartmentalize the different phases of product development and that prudent concurrent engineering should be employed whenever relevant risks have been mitigated.

Typically, design reviews occur under the oversight of an independent individual or team with relevant technical expertise to thoroughly evaluate the merits of the design. The independent review team evaluates all aspects of the device development to assess risk and ensure the design outputs meet the design inputs established for the design. Depending upon the complexity of the design and manufacturing process, the independent design review team may be populated with multiple cross-functional roles. After all, a medical device is more than just a single design engineer's responsibility, so limiting a design review to only one technical research and development design reviewer may not fully capitalize on the opportunity to review the other critical program requirements such as manufacturability or quality assurance documentation. While most cross-functional teams operate in an open, effective environment where critical information flows readily, preparation for and execution of the design review also allows the project team to review and share all information and reflect on previous activities to identify potential gaps in the verification process.

19.3.6 Design Verification

Design verification is the mechanism to confirm that the design outputs satisfy the design inputs. Verification testing can be fairly broad in scope, incorporating inspection, functional performance testing under nominal and or extreme conditions of the design or manufacturing processes, risk analysis, biocompatibility, evaluations of conformance to regulations and standards, packaging evaluations and compatibility with the intended sterilization process.

Acceptance criteria and sampling plans established in design output procedures and protocols correlate to the risk analyses conducted. The failure-modes effects analysis (FMEA) is a summary of all potential failure modes associated with a device, subassemblies or components and serves as a foundation for the design verification test plan. Naturally, the greater the risk of a potential failure mode, the more robust the design controls (inspection, testing, etc.) must be to ensure the product is extremely well characterized to mitigate risk of that failure mode occurring in the field. For example, if a biomaterial has a specific compressive strength specification, the components of the FMEA, including the severity,

projected occurrence and/or design controls in place to detect a potential failure to meet this specification can be leveraged to establish risk-adjusted acceptance criteria for the design output. Design verification puts the test plan in action by conducting functional testing to demonstrate that the biomaterial will perform as expected at the necessary confidence and reliability levels to mitigate risk of a particular failure occurring. Risk-adjusted statistical techniques can be applied to both variable (quantitative) and attribute (pass/fail) specifications. Continuing the example of compressive strength, the closer the actual compressive strength of the biomaterial is to the specification or the greater the variation observed within or across different manufacturing lots of product, the more testing a design team must complete to confidently demonstrate that the compressive strength will always meet the specification. It follows that a sufficiently robust design should provide adequate confidence and reliability, such that the nominal compressive strength of the material exceeds the specification by an acceptable statistical margin.

In the context of the current review of next generation biomaterials, the criticality of biocompatibility certainly merits specific consideration. Through its Blue Book Memorandum #G95-1, FDA currently recognizes ISO 10993 [12] as the appropriate series of standards for biocompatibility conformance. Biocompatibility confirms that the safety and toxicity of the biomaterial is acceptable for the intended use such that the biomaterial will not produce adverse effects locally or systemically, be carcinogenic, or adversely affect reproduction or development. The scope of testing to confirm acceptable biocompatibility is a function of the tissue type(s) (blood, soft tissue, bone, etc.) the device will be contacting as well as the duration of exposure. This requirement and potential risks associated with new biomaterial formulations are the basis for many medical device companies continuing the propagation and development of biomaterials with a proven history of clinical safety and biocompatibility. Regardless, next generation biomaterial compositions will be developed, and they are to be tested for biocompatibility on a product representative of the “finished good”, incorporating all of the raw materials and potential additives of the manufacturing process as well as the terminal sterilization process. This ensures no adverse interactions result from the sterilization mode. The scope of the testing requirements are a function of the intended use and duration of exposure of the biomaterial, including acute, sub-acute and chronic toxicity; irritation to skin, eyes and mucosum; sensitization; hemocompatibility; genotoxicity; carcinogenicity; and effects on reproduction and development. Requirements can further escalate for specific indications, including neurotoxicity or immunotoxicity. Once the scope of testing is identified, biocompatibility testing should be conducted in partnership with clinical research organizations that have a proven, credible history of implementing these well-established models with proper positive and negative controls run in parallel. Further, these studies should be conducted in accordance with GLP techniques.

19.3.7

Design Validation

Design validation establishes that the design meets the user needs and intended use requirements and is evaluated once design verification has been completed. The principal activity of design validation is confirming the device performs as expected under the

19 conditions anticipated and in the hands of those that will actually use the device in the clinical setting. To achieve this objective, the FDA's expectation is that manufacturers confirm that initial production batches are evaluated under actual or simulated use conditions. It is anticipated that design validation will occur later in the development timeline such that product evaluated is produced to be representative of the actual long term manufacturing process. It is preferred that these manufacturing processes would have been previously validated to ensure product evaluated is truly representative of that to be produced on a routine basis. As with all phases of product testing, documenting the source of product used for the validation in the approved protocols and reports is critical, as is an appropriate rationale should the validation occur with product from any other source than the routine manufacturing process.

Under the most basic validation strategy, an accepted and qualified in vitro test could be leveraged to demonstrate conformance to the user needs; however, it is more common to perform simulated use testing in a cadaver setting. This strategy ensures the clinician, surgeon and associated staff are unpackaging, handling, preparing, and implanting the biomaterial device in a manner consistent with how it is intended to be used in the clinical setting. This simulated use testing is conducted in accordance with the instructions for use (IFU) that is published to document the surgical technique and indications for which the device is intended, and all supporting surgical instruments, delivery systems, etc. should be included in the evaluation. It follows that design validation activities again prompt review of the risk analyses, both design and procedural, to adequately document newly identified risks that arise in the hands of the intended user. As is expected due to their full engagement with the product being developed, design engineers and project team members become experts with the biomaterial device and/or procedural technique, and by default, failure modes may not be adequately understood until the product is handled by someone less familiar with the product's attributes and intended use(s).

19.3.8

Design Transfer

Once design validation is complete, the next phase of the design control process is design transfer. Quite simply, as the name implies, this step of the process involves the "transfer" of the product from the design phase to manufacturing. This is addressed in the Production and Process Controls Section of the QSR [13]. It only makes business sense that companies devote sufficient due diligence to the manufacturing process to ensure that a product can be made efficiently, reproducibly, and affordably. Proper manufacturing controls combined with rigorous quality oversight and inspection of manufactured goods, ensure that medical devices meet the design intent and will be safe for the patient. Additionally, medical device companies operate under the objective to establish acceptable profit margins in order to reinvest into the research and development pipeline and grow the business, so product cost relative to the intended sales price is always a key input to the design and manufacturing process.

It is understood that a considerable amount of time is often required to bring manufacturing facilities on-line, and more complex devices may require significantly more manufacturing resources to develop and qualify the manufacturing processes. As a

result, it is often a prudent business decision to fully engage the manufacturing personnel as early in the design process as possible to partner in the design engineering effort and ensure that the final design is indeed manufacturable over the expected lifetime of the product. While this practice of concurrent engineering in the design control process may add additional costs and resource requirements to the project in the short term, it can save considerable time and investment and mitigate risk that the perfect design can never be manufactured. As with design controls, process control and validation centers on documentation and approval for all steps of the manufacturing process, and all operators conducting the manufacturing processes must be adequately and continuously trained. The intent of process validation is to ensure the product is made consistently with the highest quality assurance. When possible, all aspects/steps of the manufacturing process should be validated. Process validations typically identify an acceptable process “window” or range for parameters that will yield a final product that consistently meets the design requirements. In real world manufacturing, process parameters cannot be so constrained that consistent manufacturing is unachievable. This is an especially important aspect to consider for new biomaterial formulations. Even at the earliest phases of chemical synthesis, it is imperative to establish an understanding as to the process variables which impact the attributes of the finished good, including time, temperature, catalyst, reactor volume and source, shelf-life and purity of the raw materials, etc. Clearly, if biomaterial synthesis is not repeatable or scalable, the probability of commercial success is severely limited.

While the most critical aspect, manufacturing the product is only one challenge of the manufacturing process validation. Additional requirements to be addressed during the development process that are transferred to manufacturing include packaging and sterilization. Implantable biomaterials must be distributed in a format that maintains their sterility and integrity/stability under the potentially extreme conditions observed during transit and storage. Further, the packaging configuration must be intuitive for the end user to open and extract the device or implant. Special processes such as drying and sealing may also be required to ensure environmental factors such as moisture do not prematurely degrade biodegradable polymers susceptible to hydrolytic cleavage. Ideally, a finished good biomaterial will be stored at or near room temperature such that it can be stocked in distribution centers and hospital/surgical center storage requirements at minimal cost. Consideration should be given to special storage and shipping conditions in the event the product must be shipped and maintained in a cold environment. While still a viable option, these constraints will complicate the supply chain and likely add undesirable cost to the product. Finally, the sterilization mode could have a significant impact on the manufacturing and packaging processes. Due to cost implications of aseptic processing, it may be preferable to sterilize a product post-manufacture using ethylene oxide (EtO), gamma irradiation or electronic beam (E-beam). As detailed in the design verification section above, it is critical to confirm that the sterilization process selected is compatible with the device and does not adversely impact the physical properties or functional performance of the components and/or final assembly or configuration of the medical device. As with the assembly and process validations that are conducted for a device, packaging and sterilization validations are also required to demonstrate that these processes adequately mitigate risks identified in the failure-mode effects analysis. Specifically, the sterilization cycle must ensure and the packaging must maintain product sterility, and the impact of the sterilization process itself

should not introduce additional issues, such as EtO residuals or chemical reactions resulting from the irradiation process that could compromise biocompatibility.

19.3.9

Design Changes

It is to be expected that a design or biomaterial will evolve during the development life cycle, as even the most thorough feasibility and prototyping and rigorous project planning and risk analyses do not always capture every failure mode. Significant information is obtained throughout development as production tooling is manufactured and parts are inspected, assembled and tested. In fact, thorough design verification testing could demonstrate the occurrence of new failure modes that were not predicted based on prototypes. Design changes are managed through the design control process, and relevant design verification and validation and process validations must be repeated, documented and approved appropriately. It is important for quality assurance and regulatory affairs to review the scope of the design change in the context of previous regulatory submissions to understand whether additional filings are necessary to inform FDA of the design change.

19.3.10

Design History File

The design history file serves as a complete record of evidence that design control was followed during the development process, including cross-functional approval of all the iterations/versions of documents required under the design control system, such as the development plan, design inputs and specifications, design outputs, design verification and validation, drawings and documentation of the design reviews that occurred throughout development.

In summary, the components of design controls are intended as a series of checks and balances that guide the product development team through routine and thorough reviews of the design throughout the development process to ensure the device is safe, performs as intended and is manufactured with high quality standards. Documentation generated under this framework serves to demonstrate that appropriate rigor is being imparted during the design process and that cross-functional approvals are being obtained at strategic points throughout development.

19.4

Regulatory Strategy and Evidence Generation

A product's regulatory strategy, whether 510(k) [14] for Class II and select Class I devices or PMA [15] for Class III devices, is typically scoped early in development. The device classification is a function of the intended use, indications for use and risk posed by the

device, and the FDA publishes a classification database and corresponding classification regulations to assist manufacturers in the identification of the appropriate classification of their device. The regulatory filings and clinical evaluations required in association with either regulatory path are also defined in the regulations. As noted above, Class II devices must demonstrate substantial equivalence to a predicate device and typically leverage prior clinical safety and efficacy data of the predicate, as only a small fraction of 510(k) premarket notifications require clinical evidence to support marketing clearance. Clinical evaluation of Class III devices is regulated under the FDA's Investigational Device Exemption (IDE). An IDE permits the investigational device to be used in a clinical study in order to collect safety and effectiveness data required in support of a PMA application or, as needed, a 510(k) submission. Once approved by the FDA, clinical study protocols are routed to local Institutional Review Boards (IRB) that monitor clinical evaluation activities and patient welfare at specific hospitals and/or surgery centers. Once these approvals are obtained, a clinical study can be conducted on the investigational device. Typical clinical evaluations of medical devices are comprised of a pilot study, which evaluates safety in a limited patient population for the target indication, and the pivotal study, which assesses safety and effectiveness in a much larger patient population intended to receive the device. If a combination product (medical device plus a drug and/or biologic) is regulated by an agency other than CDRH, the clinical study structure may follow that of a drug or biologic and consist of three phases, including Phase I, II and III [16]:

Phase I Trials: Initial studies to determine the metabolism and pharmacologic actions of drugs in humans, the side effects associated with increasing doses, and to gain early evidence of effectiveness; may include healthy participants and/or patients.

Phase II Trials: Controlled clinical studies conducted to evaluate the effectiveness of the drug for a particular indication or indications in patients with the disease or condition under study and to determine the common short-term side effects and risks.

Phase III Trials: Expanded controlled and uncontrolled trials after preliminary evidence suggesting effectiveness of the drug has been obtained, and are intended to gather additional information to evaluate the overall benefit–risk relationship of the drug and provide an adequate basis for physician labeling.

Independent of the clinical path followed, manufacturers must demonstrate their adherence to design controls in the development of the investigational device and ensure that robust risk analyses have been completed at each phase. Employing rigorous clinical trial design, execution, monitoring and follow-up is critical to assessing the clinical potential of a new biomaterial therapy. Clinical trial design must incorporate an appropriate comparator, which typically is noted as the clinical standard of care for the target indication. Relevant inclusion and exclusion criteria must be established to ensure the target patient population will enable the sponsor to draw appropriate safety and effectiveness conclusions. Clinical endpoints for the study groups range broadly, including survival, patient reported outcomes (PROs) for pain, function and quality of life, functional performance or activity-based tests, diagnostic imaging, etc. As detailed in the preclinical section earlier, the clinical study design must be powered to detect clinically meaningful differences between the study groups at relevant post-operative time points. Ultimately, the clinical study outcomes should enable the sponsor to assess the

19 “comparative effectiveness” of a candidate biomaterial or device relative to the standard of care by evaluating the safety and efficacy profiles as well as the impact on the surgical procedure time or degree of invasiveness in the context of the differential cost of the two therapies. While positive clinical outcomes are necessary to attain regulatory approval, demonstrating a health care cost benefit relative to a well-established standard of care will be a key driver in supporting reimbursement efforts with insurers and hospitals to facilitate adoption of a novel biomaterial solution.

Historically, biomaterials have been regulated by CDRH as devices; however, an important point to emphasize as introduced in the discussion on clinical trial design is that more complex devices, such as biomaterials impregnated with active drugs or biologics, are classified as combination products by FDA. Regulation of these products is determined by the FDA Office of Combination Products (OCP), which functions to develop guidance and regulations for combination products and assign an FDA center to have primary jurisdiction for the regulatory oversight of the combination product. The OCP defines combination products to include [17]:

- (1) A product comprised of two or more regulated components, i.e., drug/device, biologic/device, drug/biologic, or drug/device/biologic, that are physically, chemically, or otherwise combined or mixed and produced as a single entity.
- (2) Two or more separate products packaged together in a single package or as a unit and comprised of drug and device products, device and biological products, or biological and drug products.
- (3) A drug, device, or biological product packaged separately that according to its investigational plan or proposed labeling is intended for use only with an approved individually specified drug, device, or biological product where both are required to achieve the intended use, indication, or effect and where upon approval of the proposed product the labeling of the approved product would need to be changed, e.g., to reflect a change in intended use, dosage form, strength, route of administration, or significant change in dose; or
- (4) Any investigational drug, device, or biological product packaged separately that according to its proposed labeling is for use only with another individually specified investigational drug, device, or biological product where both are required to achieve the intended use, indication, or effect.

A manufacturer pursues a Request for Designation (RFD) [18] to formally identify the agency with jurisdiction over the combination product to determine whether the clinical evaluation will be conducted as an Investigational Device Exemption (IDE) or Investigational New Drug (IND) [19]. OCP assigns primary jurisdiction to an agency, including CDRH, the Center for Biologics Evaluation and Research (CBER) or the Center for Drug Evaluation and Research (CDER), based on the primary mode of action (PMOA) of the combination product. The PMOA is defined as “the single mode of action of a combination product that provides the most important therapeutic action of the combination product.” In the event the PMOA has yet to be defined by the manufacturer or FDA at the time a designation is requested, jurisdiction is ultimately defined based on FDA experience with similar products. Additionally, the scope of marketing application(s), PMA, Biologic License Application (BLA) [20] and/or Priority New Drug Applications (NDA) [21] for

combination products are defined once OCP assigns a lead Center that will have primary jurisdiction over the combination product. Typically, most combination products require only a single market application for the product's approval, clearance or licensure; however, FDA may also determine that two applications are necessary based on the product.

19.5

Marketing, Commercialization and Post-market Surveillance

Once a design has completed development, exited design control through successful design transfer and corporate management approval, and the requisite regulatory approval (510(k) or PMA) has been attained, it is then marketed and commercialized. The scope of the market introduction can range from a limited to full market launch. Limited launches enable companies to restrict the use of a new product to a controlled number of surgeon customers in order to obtain preliminary market feedback while controlling initial product inventory levels. Companies may perform post market studies to pursue peer-reviewed publications in support of reimbursement activities. Independent of the execution of post marketing clinical studies, it is the responsibility of all medical device manufactures to develop a risk management plan and post marketing surveillance strategy to monitor, document and more importantly resolve customer complaints related to the quality and performance of the device or any product safety concerns. These activities are expected to continue throughout a product's post market lifetime to ensure high product quality and customer satisfaction is maintained. While a post market surveillance program is required by regulators of medical device manufacturers, it quite simply makes sound business sense to confirm that the product continues to meet the user needs and design intent as product use and number of users expands over time. It follows that the company takes responsibility to respond and resolve product issues with an appropriate strategy.

This overview highlighted many of the key components of the medical device development process in the context of the Total Product Life Cycle. By design, the TPLC is intended to provide continuity and connectivity between the earliest stages of the concept phase through obsolescence of a medical device. As a device obsolesces and is replaced with a next generation solution, one that hopefully provides enhanced performance or improved ease of use or offers additional features, it is imperative for project teams and their company's design control system to implement a feedback loop in which the experiences and lessons learned throughout a product's development and total life cycle are fully leveraged as primers in the concept phase of future design iterations and multi-generational product platforms. It is the obligation of each development team to document and share lessons learned, including successes and more importantly, temporary setbacks and challenges overcome, such that future development efforts can be even more successful and timely. Finally, each component of this overview, including concept and early stage feasibility, product development through design control principles, evidence generation and regulatory strategy and commercialization and post market surveillance, are all critical pieces of an extremely complicated process influenced continuously by changes in business

objectives; entry and exit of competition; release of new regulations, guidance or standards; management and project team turnover; and design and manufacturing challenges. In the end, however, with rigorous planning, a keen focus on design and process excellence through design and process control, and adaptability to change, a project team can successfully navigate these challenges to deliver medical device and biomaterial solutions that offer safe and effective solutions for patients.

References

1. <http://www.clinicaltrials.gov/>
2. Foster RN, Kaplan S. Creative destruction: why companies that are built to last underperform the market, and how to successfully transform them. New York: Currency; 2001
3. Fenton GM, Chi-Ham C, Boettiger S. Freedom to operate: the law firm's approach and role. In: Krattiger A, Mahoney RT, Nelson L et al. editors. Executive guide to intellectual property management in health and agricultural innovation: a handbook of best practices. Oxford, UK: MIHR and Davis, USA: PIPRA; 2007. Available from: <http://www.ipHandbook.org>
4. <http://www.astm.org/>
5. Code of Federal Regulations Title 21 Part 812 (Investigational device exemptions). Available from: <http://www.fda.gov/>
6. Code of Federal Regulations Title 21 Part 58 (Good laboratory practice for nonclinical laboratory studies). Available from: <http://www.fda.gov/>
7. Code of Federal Regulations Title 21 Part 820 (Quality system regulation). Available from: <http://www.fda.gov/>
8. ISO 13485:2003 (Medical devices – quality management systems – requirements for regulatory purposes). Available from: <http://www.iso.org/iso/home.html>
9. Code of Federal Regulations Title 21 Part 820 Subpart C (Quality system regulation – design controls). Available from: <http://www.fda.gov/>
10. Teixeira MB, Bradley R. Design controls for the medical device industry. Boca Raton: CRC Press; 2003
11. Code of Federal Regulations Title 21 Part 860 (Medical device classification procedures). Available from: <http://www.fda.gov/>
12. ISO 10993. Available from: <http://www.iso.org/iso/home.html>
13. Code of Federal Regulations Title 21 Part 820 Subpart G (Quality system regulation – production and process controls). Available from: <http://www.fda.gov/>
14. Code of Federal Regulations Title 21 Part 807 Subpart E (Establishment registration and device listing for manufacturers and initial importers of devices – premarket notification procedures). Available from: <http://www.fda.gov/>
15. Code of Federal Regulations Title 21 Part 814 (Premarket approval of medical devices). Available from: <http://www.fda.gov/>
16. <http://clinicaltrials.gov/ct2/info/glossary>
17. Code of Federal Regulations Title 21 Part 3.2(e) (Product jurisdiction – definitions – combination products). Available from: <http://www.fda.gov/>
18. Code of Federal Regulations Title 21 Part 3.7 (Product jurisdiction – request for designation). Available from: <http://www.fda.gov/>

19. Code of Federal Regulations Title 21 Part 312 (Investigational new drug application). Available from: <http://www.fda.gov/>
20. Code of Federal Regulations Title 21 Parts 600, 601 and 610 (Regulations regarding BLAs for therapeutic biological products). Available from: <http://www.fda.gov/>
21. Code of Federal Regulations Title 21 Part 314 (Applications for FDA approval to market a new drug or an antibiotic drug). Available from: <http://www.fda.gov/>

About the Editors



Dr. Jason A. Burdick is an Associate Professor in the Department of Bioengineering at the University of Pennsylvania, USA. He obtained his undergraduate degree in Chemical Engineering at the University of Wyoming (1998) and his PhD in Chemical Engineering at the University of Colorado (2002). He began his position at Penn after postdoctoral work (2003–2005) at the Massachusetts Institute of Technology. The focus of work in his laboratory is the development of biodegradable polymers for applications in tissue engineering and drug delivery. Much of this work focuses on the engineering of cartilage tissues, including articular cartilage and the knee meniscus, as well as biomaterial approaches to attenuate outcomes after myocardial infarction. Additionally, much of this work is focused on using material cues to alter stem cell

behavior, including with spatial and temporal control. He has received several research awards, including a K22 Scholar Development and Career Transition Award from the National Institutes of Health, a Fellowship in Science and Engineering from the David and Lucille Packard Foundation, an Early Career Award from the Wallace H. Coulter Foundation, and a CAREER Award from the National Science Foundation. Additionally, his work is supported by funding from the National Institutes of Health and the Department of Veterans' Affairs. He has published over 80 peer-reviewed papers and is on the editorial boards of the *Journal of Biomedical Materials Research A*, *Biomacromolecules*, and *Tissue Engineering*.



Dr. Robert Mauck is an Assistant Professor of Orthopaedic Surgery and Bioengineering at the University of Pennsylvania, USA. He obtained his undergraduate degrees in Biochemistry and Biomedical Engineering at Columbia University (1998), and completed his PhD at Columbia in the Cellular Engineering and Musculoskeletal Biomechanics Laboratories (2003). After postdoctoral studies (2003–2005) at the National Institutes of Health in the Cartilage Biology and Orthopaedics Branch, Dr. Mauck developed a new research program in the McKay Orthopaedic Research Laboratories at the University of Pennsylvania. His group focuses on the engineering of musculoskeletal tissues, with a particular interest in restoring articular cartilage, the knee meniscus, and the intervertebral disc. Dr. Mauck's team uses rigorous mechanical and molecular analyses to characterize native tissue structure and function and employs this information to enhance the functional properties of engineered constructs through focused technology development. Specifically, this work employs adult mesenchymal stem cells, custom mechanobiologic culture conditions, and novel cell scaffolding technologies. His work is supported with funding from the National Institutes of Health, the Veterans' Administration, as well as several private foundations. Dr. Mauck was awarded the 2008 ISSLS Prize in Biomechanics and the 2009 YC Fung Young Investigator Award from the ASME. Dr. Mauck has published more than 65 manuscripts in the field of tissue engineering and regenerative medicine and is on the editorial board of the journal *Tissue Engineering*.